Zhao-Yin Wang
Joseph H.W. Lee
Charles S. Melching

River Dynamics and Integrated River Management

TSINGHUA
UNIVERSITY PRESS

Springer

Zhao-Yin Wang
Joseph H. W. Lee
Charles S. Melching

**River Dynamics and Integrated
River Management**

Zhao-Yin Wang
Joseph H. W. Lee
Charles S. Melching

River Dynamics and Integrated River Management

With 645 figures

TSINGHUA
UNIVERSITY PRESS

Springer

Authors:

Zhao-Yin Wang
State Key Laboratory of Hydroscience
and Engineering
Tsinghua University
Beijing 100084, China
E-mail: zywang@tsinghua.edu.cn

Joseph H. W. Lee
Hong Kong University of Science and Technology
Hong Kong, China
E-mail: jhwlee@ust.hk

Charles S. Melching
Environmental Consultant
Greenfield, Wisconsin 53221
E-mail: steve.melching17@gmail.com

Preface

In 1994, Dr. E. Plate and I initiated the Sino-German cooperation research on unsteady sediment transportation (known as GESINUS), which was supported by VW-Foundation and DFG of Germany and National Natural Science Foundation of China (NSFC). The bilateral cooperation achieved important results and shifted my main research interest from fluvial rivers to mountain rivers. The idea to study and write a book on integrated river management came to my mind when I found that the sedimentation problems in the lower reaches of rivers were essentially caused by riverbed incision in upstream reaches.

The writing of this book began in 1997 when Dr. G. Klaassen invited me to teach a short course in the IHE Delft with the main contents of the course focused on the Yellow River training and management and the Three Gorges Project on the Yangtze River in China. The notes from this short course have become the main contents of Chapters 6 and 7 of this book. In the same year I took part in a western China investigation organized by the Central Government, one of the themes was greening the mountains and hills and beautifying the landscape. To answer the question "if the bare hills in arid and semi-arid areas can be vegetated?" I studied the dynamic relations among vegetation development, soil erosion, and various stresses on the vegetation and established the theory and model of vegetation-erosion dynamics, which has become the main contents of Chapter 2. During the process of developing the model a discussion with Dr. J. B. Thornes was very constructive.

To study riverbed incision and control strategies my research group established field experimental stations on the Xiaojiang River in Yunnan, Mianyuan River in Sichuan, and East River in Guangdong. The results from the field investigations and field experiments at these sites have become the main contents of Chapter 3. I began to study debris flow in 1984 and visited the Dongchuan Debris Flow Observation and Research Station every year, where I witnessed debris flows. Dr. Z. Kang worked in the station for 20 years and was among my research partners. The great Wenchuan Earthquake occurred on May 12, 2008 and rekindled my research interest in landslides and debris flows. My research group studied landslides, avalanches, and debris flows in the earthquake area in the period 2008-2010, during which Dr. P. Cui supported us with valuable ideas and convenient access to data. The results from these studies enriched the contents of Chapter 4.

The main concepts of sediment transportation and fluvial processes in Chapter 5 are from Dr. Ning Chien. It was under the guidance of Dr. Ning Chien that I started my research in the field of sedimentation, especially hyperconcentrated flows. I worked with him for seven years with sincere and deeply friendly feelings. I was deeply saddened when he passed away in 1986. I here express a few words of both my grief and fond memories of my dearest professor.

I have collaborated with Dr. J.H.W. Lee on several research projects since 1999. We studied river ecology and the eutrophication and algal blooms in the Bohai Sea and Hong Kong waters. The discussion between us on various issues on the river management, especially deltaic and coastal processes, elicited valuable ideas for integrated river management. Dr. Lee contributed Chapter 8, which makes the book more complete.

Dr. Ben Yen, Dr. Tai Wai Soong, Dr. C. S. Melching, and I initiated Sino-U.S. cooperation on environmental sediment research in 1999. During my visits to the U.S. I contacted the Federal Interagency Stream Restoration Working Group and discussed stream restoration with various members of this group. The discussion was very constructive for writing Chapter 10. Since then my research team began to study aquatic ecology. In 2003, I was granted a research project from the Ministry of Science and Technology to study the ecology of Yangtze River, and in 2007 I was granted a research project from the NSFC to

study benthic invertebrates. The research results from these projects have become the main contents of Chapter 10.

Dr. C. S. Melching made great contributions to this book. He has visited China and collaborated with my research group every year since 2004. We worked together on sediment transportation, aquatic ecology, and water quality and published quite a few papers. Dr. Melching gave me valuable ideas for stream ecology and contributed Chapter 9. Moreover, he polished the English of all chapters several times. It is due to his efforts the English of book is at the international standard.

In the period from 2005 to 2010 my research group conducted several experiments on the Diaoga River and the Jiangjia Ravine in Yunnan, and the Mianyuan River in Sichuan and performed field investigations and measurement in the Yalutsangbu, Yellow, East, and Songhua rivers to search for methods of integrated river management for geological hazard mitigation, erosion and sedimentation control, and ecological restoration. Both theoretical and technical results were obtained and they have become the main contents of Chapter 11.

The style of the book is such that it should readily useable as a textbook for graduate students and also as a reference book for scientists and engineers. There were several versions of the book beginning from 2003, which were printed at Tsinghua University as a textbook for graduate and Ph.D. students. The main contents of the book were also used as a textbook at the University of Hongkong, IHE Delft, Bari University, and UNESCO training courses organized by the International Research and Training Center on Erosion and Sedimentation. I have been working as the Chief Editor of the International Journal of Sediment Research since 1996 and an Associate Editor of the International Journal of River Basin Management (IAHR). The experience of journal editor helped me to access new research results, which was helpful for completion of the book. Finally, it is a pleasant duty to express thanks to all my immediate collaborators over the years, who have contributed in different ways to the creation of this book.

Zhao-Yin Wang
May 2014, Beijing

Contents

Introduction

All land is part of a watershed or river basin and the water, which flows over it and through it, shapes all landscapes. Figure 1 shows the landscape sculptured by erosion in Greece and the very dry land in Egypt. Indeed, rivers are such an integral part of the land that in many places it would be as appropriate to talk of riverscapes as it would be of landscapes. Rivers are much more than merely water flowing to the sea. Rivers carry downhill not just water, but just as importantly sediments, dissolved minerals, the nutrient-rich detritus of plants and animals. Their ever-shifting beds and banks and the groundwater below are all integral parts of rivers. Even the meadows, forests, marshes and backwaters of floodplains can be seen as part of the rivers—and the rivers as part of them.

(a)   (b)

Fig. 1   (a) The landscape sculptured by erosion in Greece; and (b) River flow is the main force for development of geomorphology even in the very dry Egypt

The main **functions of rivers** are draining floods, supplying drinking water, maintaining ecology, irrigating farmland, transporting sediment, supplying power, providing habitat for fishes, assimilating wastewater, and providing navigation. Humans exploit the resources of rivers by constructing dams and water-diverting channels, developing navigation channels, and harvesting fishes, which result in changes in the river hydrology, runoff, sediment transport, riparian and stream habitats, and water quality.

Watersheds start at mountain peaks and hilltops. Snowmelt and rainfall wash over and through the high ground into rivulets, which drain into fast-flowing mountain streams. As the streams descend, tributaries and groundwater add to their volume and they become rivers. As they leave the mountains, rivers slow and start to meander and braid, seeking the path of least resistance across widening valleys with alluvial floors laid by millennia of sediment-laden floods. Eventually rivers will flow into a lake or ocean. Where the river carries a heavy sediment load and the land is flat, the alluvial sediments may form a delta. Estuaries, the places where the fresh water of rivers mixes with the ocean's salt water, are among the most biologically productive parts of rivers and of seas. Most of the world's fish catch comes from species that are dependent for at least part of their lifecycle on a nutrient-rich estuarine habitat.

Figure 2 shows the components of a river system, materials transported and the aspects affected by the rivers and transported materials. Rivers can be recognized as mountain rivers, alluvial rivers, and estuaries. A **mountain river** is the most upstream part of the river, including the river source and the upstream tributaries of the river, where the river system flows through mountainous areas and the flow is confined by mountains. Usually the channel bed of a mountain river is composed of gravel. Mountain rivers receive most of the sediment, nutrient-rich detritus of plants and animals, dissolved materials, and usually more than half of the water. For a large river the upstream reaches compose the input-part of the river and are closely affected by the watershed or drainage area. Erosion control and vegetation development are the most challenging tasks for researchers and watershed managers. Erosion induced landslides and debris flows are disastrous in the upstream reaches. Mountain rivers are quite often incised rivers and degradation of the channel bed causes many problems. Therefore, erosion control and vegetation development over the watershed, landslides and debris flows, and control of channel bed incision are major topics of mountain river studies.

River   Transported materials   Affected

Over land flow areas;
Mountain rivers:
Alluvial rivers;
Reservoirs;
Estuary

Water; Sediment;
Nutrient; Dissolved
materials, Adsorbed
materials

Landscape;
Environment;
Ecology;
Human society
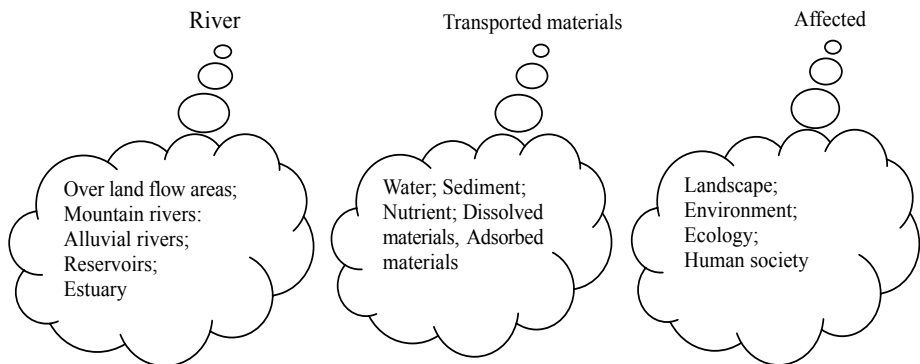
Fig. 2 River system, transported materials, and aspects affected by rivers and the transported materials

An **alluvial river** is defined as a river with its boundary composed of the sediment previously deposited in the valley, or a river with erodible boundaries flowing in self-formed channels. Over time the stream builds its channel with sediment it carries and continuously reshapes its cross section to obtain depths of flow and channel slopes that generate the sediment-transport capacity needed to maintain the stream channel. Alluvial rivers are mostly perennial streams and the channel bed is composed mainly of sand and silt. A large river usually originates from mountains and flows over floodplains before it pours into the ocean, therefore, it is a mountain river in its upper reaches and an alluvial river in its lower reaches. Many alluvial rivers are large rivers or flat-land sections of large rivers, such as the lower reaches of the Yellow River and the middle and lower reaches of the Yangtze River. These alluvial rivers are confined within the valley defined by human constructed or artificially reinforced levees. The river morphology and river patterns depend mainly on the sediment transportation and deposition. Rivers are the main source of water resources for agriculture, urban use, and industry. River floods are major natural disasters accounting for 1/3 of the total loss due to natural hazards. The quality of river water is important for human health. Flood and sediment transportation are natural processes in these rivers and water diversion, channelization, and navigation are human disturbance to the rivers. Thus, sediment transportation, water resources development and flood defense are the most important issues in the alluvial river management.

The **estuary** is the connection part of a river with the water body (lake, sea, or ocean) into which it flows, including the river mouth, a river section affected by the tide, and the water body area affected by the river flow. Sediment is deposited for land creation and very often a delta develops in the area. In

recent years, the need for sustainable development of coastal cities and marine resources has given rise to challenging environmental problems. Examples include the environmental impact assessment of dredging and sludge/spoil dumping and the transport and transformation of nutrients and heavy metals at the sediment-water interface. Urban development including large-scale land reclamation and population growth induced increase in sewage discharge puts the estuary ecosystem under stress. Red Tide is a phenomenon in which the seawater is discolored by high algal biomass. Some algal species produce potent toxins, which accumulate in shellfish that feed on those algae, resulting in poisoning in human consumers. There has been a significant expansion of red tide episodes and impacts throughout the world over the last several decades. Very unusual red tides have occurred in the Bohai, East China, and south China seas in the past decades. Delta and coastal processes, eutrophication, and algal blooms are the major challenges for the management of estuaries.

A variety of **river-uses** was the driving force of societal development in the past and now is even more important in economic and cultural development. Rivers, and the rich variety of plants and animals which they sustain, provided hunter-gatherer societies with water for drinking and washing, and with food, drugs and medicines, dyes, fibers, and wood. Farmers reap similar benefits as well as, where needed, irrigation for their crops. For pastoral societies, who graze their herds over wide areas of often parched plains and mountains, perennial vegetation along the banks of rivers provides life-sustaining food and fodder during dry seasons and droughts. Towns and cities use and misuse rivers to carry away their wastes. Rivers also served as roadways for commerce, exploration, and conquest. The role of rivers as the sustainers of life and fertility is reflected in the myths and beliefs of a multitude of cultures.

Many countries have taken an increasing interest in **river dynamics and integrated river management** coordinating various sectors of river issues. A developing country, like China, now strongly emphasizes the goal of flood control, water resources development, and protecting environment in addition to reducing poverty by supporting efficient and sustainable development of agriculture and light industries. Water is acknowledged to have a significant impact on the economic development potential of individuals, through agriculture, water supply and sanitation, public health, power generation, flood mitigation, etc. In addition, water sustains ecological systems, which also have economic value, and in turn generate a healthy hydraulic system. Poor people can improve their welfare by having access to water. In turn, people who are wealthier and better educated are better able under stress conditions to make cautious use of water, thus, not pre-empting the next generation from having similar benefits from the same water system.

Integrated river management aims at reconciling the provision of safety to the people dwelling by the river and sustainable use of the land and water. It also aims at making water use economically productive, socially equitable, and environmentally sustainable. These goals can be achieved in principle in many ways, but the fact that the water system is characterized by important externalities and unusually high transaction costs (as compared to the power sector, for instance) limits the options for workable institutional arrangements. It is attractive to concentrate on a hydrographically coherent region such as a river basin, catchment, or drainage or *polder* area, as all key actors and all decision-making can be brought under one purview.

Where water users have managed to put their common long-term interest ahead of their desire for quick personal gain, and, thus, engaged in collective action, 'catchment based' water management has been practiced in many places around the world. For integrated river management, one has to understand the whole river system very well, including all issues of a river, and all aspects of the natural and human-impacted system and their interconnections.

In China, there are more than 50,000 rivers each with a catchment area larger than 100 km^2, including more than 1,500 rivers with a catchment area larger than 1,000 km^2. Most of the rivers are located in the eastern and southern parts of the country. The seven most important rivers are the Songhua, Liaohe,

Haihe, Yellow, Huaihe, Yangtze, and Pearl Rivers.

Chapter 1 of this book summarizes the basic concepts and major issues of river management in China, providing a base for the book. Chapter 2 discuss erosion, vegetation and presents the vegetation-erosion dynamics model. Chapter 3 describes the phenomena and impacts of channel bed incision, with emphasis on management strategies for mountain rivers. Chapter 4 discusses landslide and debris flow and related management strategies. Chapter 5 provides a conceptual framework of alluvial rivers, including sediment transportation and fluvial processes. Chapter 6 describes flood defense and fluvial river management strategies with the Yellow River as an example. Chapter 7 discusses the impacts of impoundments on rivers, including dam construction and dam removal, sedimentation and strategies. The Three Gorges Project on the Yangtze River is discussed in detail as an example. Chapter 8 presents the issues, laws and management strategies of estuaries. Chapter 9 presents the basic knowledge of water quality management. Chapter 10 introduces the main theories of river ecology and methods of ecological assessment and restoration. Chapter 11 presents new theories and practices of integrated river training and management, including the principles of river training, methods of sediment budget, artificial step-pool system for incision and debris flow control and ecological improvement.

Readers may learn the basic knowledge of all aspects of rivers from this book, which pays no attention to the mathematical details of technical description but focuses on comprehensive and modern concepts and new methods of river management. Researchers may also obtain inspiration from the discussions such as the relation between resistance and channel stability, ecological functions of step-pool system, the relation between the habitat diversity and biodiversity, and vegetation-erosion dynamics. These discussions and many new concepts may shed light on the study of river dynamics and management.

1 Basic Concepts and Management Issues of Rivers

Abstract
Basic concepts are introduced in this chapter to help the readers understand the contents of the other chapters in this book. The water cycle and modes of stream network development, Horton's laws, sediment and sediment load, and various river patterns are defined and presented. Concepts of the water environment and stream ecology are briefly introduced. The major river management issues, such as water resources management, flood defense, reservoir management, river bed incision and geological disasters, erosion control, and river uses are also discussed.
Key words
Water cycle, Stream order, Sediment load, River patterns, Ecology, Management issues

1.1 Basic Concepts

1.1.1 Hydrological Cycle

Precipitation is the water falling over the land from the atmosphere primarily in the form of rain and snow. Precipitation can return to the atmosphere; move into the soil; or run off the earth's surface into a stream, lake, wetland, or other water body. More than half of the precipitation falling over the land of China evaporates to the atmosphere rather than being discharged as stream flow to the oceans. This "short-circuiting" of the hydrologic cycle occurs because of the two processes, interception and transpiration. A portion of precipitation never reaches the ground because it is intercepted by vegetation and other natural and constructed surfaces. The amount of water intercepted in this manner is determined by the amount of interception storage available on the above-ground surfaces.

Transpiration is the diffusion of water vapor from plant leaves to the atmosphere. Unlike intercepted water, which originates from precipitation, transpired water originates from water taken in by the roots of plants. **Evaporation of soil moisture** is, however, a much slower process due to the capillary and osmotic forces that keep the moisture in the soil and the fact that vapor must diffuse upward through soil pores to reach surface air at a lower vapor pressure. When calculating the hydrologic budget of a watershed the transpiration from vegetation and the evaporation from the soil typically are considered together as evapotranspiration.

Infiltration—Close examination of the soil surface reveals millions of particles of sand, silt, and clay separated by channels of different sizes. These macropores include cracks, "pipes" left by decayed roots and wormholes, and pore spaces between lumps and particles of soil. Water is drawn into the pores by gravity and capillary action. Gravity is the dominant force for water moving into the largest openings, such as worm or root holes. Capillary action is the dominant force for water moving into soils with very fine pores. Infiltration is the term used to describe the movement of water into soil pores. The infiltration rate is the amount of water that soaks into soil over a given length of time. The maximum rate at which water infiltrates into a soil is known as the soil's **infiltration capacity**.

Ground water—The size and quantity of pore openings also determines the movement of water within the soil profile. Gravity causes water to move vertically downward. This movement occurs easily through larger pores. As pores reduce in size capillary forces eventually take over and cause water to move in any direction. Water will continue to move downward until it reaches an area completely saturated with water, the phreatic zone or zone of saturation. The top of the phreatic zone defines the **ground water table or phreatic surface**. In mountainous area the channels are incised very deep and lower than the phreatic

surface of the neighboring hills, ground water flows through rock pores and the channel banks into the river, as shown in Fig. 1.1. This part of ground water returning to the rivers keeps the stream flow perennial and relatively stable.
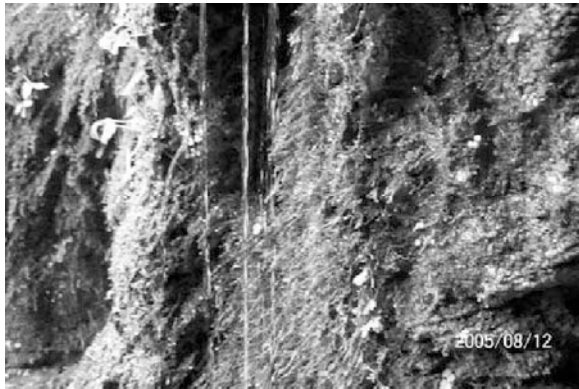
Fig. 1.1 Ground water flows though rock pores and channel banks into the stream (Chexi Creek near the Three Gorges of the Yangtze River)

If rainfall intensity is less than infiltration capacity, water infiltrates into the soil at a rate equal to the rate of rainfall. If the rainfall rate exceeds the infiltration capacity, the excess water either is detained in small depressions on the soil surface or travels down slope as **surface runoff** (Fig. 1.2). Factors that affect runoff processes include climate, geology, topography, soil characteristics, and vegetation. Average annual runoff ranges from zero (desert) to more than 1 meter in China. The surface runoff gathers and flows in streams or rivers, and finally pours into the ocean. Runoff discharge (or discharge) is the volume of water flowing across a section of the stream per time and usually the unit of discharge is cubic meters per second (m^3/s or cms in some literature).
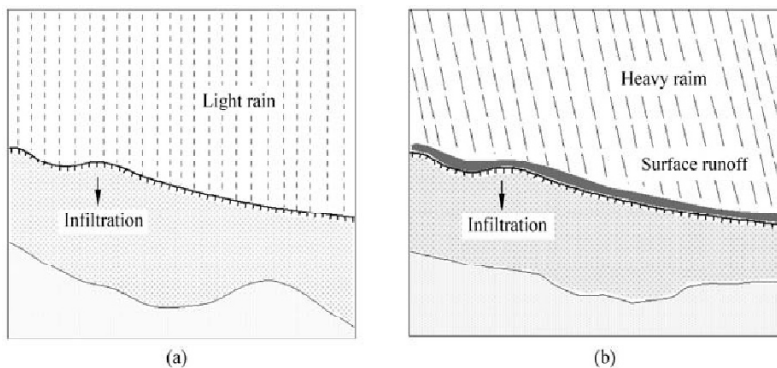
Fig. 1.2 (a) No surface runoff for light rain; (b) Surface runoff occurs when rainfall intensity exceeds the infiltration capacity

1.1.2 Drainage Network

The drainage network occupies only a small part of a drainage basin, but it has been the subject of great geomorphic and hydrologic interest, especially since the publication of Robert Horton's paper on drainage network in 1945. The techniques developed by Horton for quantitative description of a drainage network

opened the study and understanding of this complex geomorphic system. Horton's approach to network description was applied and expanded by the "Columbia School" of A. N. Strahler and his students, and many studies of drainage basins and stream networks have followed the lead of Horton and Strahler.

Stream ordering—Horton (1945) developed a method of classifying, or ordering, the hierarchy of natural channels within a watershed, and the modified system of Strahler (1957) is probably the most popular today. Horton-Strahler's stream ordering system is portrayed in Fig. 1.3(a). The uppermost channels in a drainage network (i.e., headwater channels with no upstream tributaries) are designated as the first-order streams down to their first confluence. A second-order stream is formed below the confluence of two first-order channels. Third-order streams are created when two second-order channels join, and so on. In the figure the intersection of a channel with another channel of lower order does not raise the order of the stream below the intersection (e.g., a fourth-order stream intersecting with a second-order stream is still a fourth-order stream below the intersection). Within a given drainage basin, stream order correlates well with other basin parameters, such as drainage area or channel length. Consequently, knowing what order a stream is can provide clues concerning other characteristics such as which longitudinal zone it resides in and relative channel size and depth.

The stream ordering method by Horton and Straheler is very useful for theoretical analysis but not practically useful for engineering studies because one cannot identify the first order streams in a watershed. In engineering practice the channels are ordered in the following method as shown in Fig. 1.3(b): the channels flowing into the stem river, which flows into the ocean, are the first order tributary of the river; the channels flowing into one of the first order tributaries are the second order tributary; and the channels flowing into one of the second order tributaries are the third order tributary; etc..

(a)   (b)
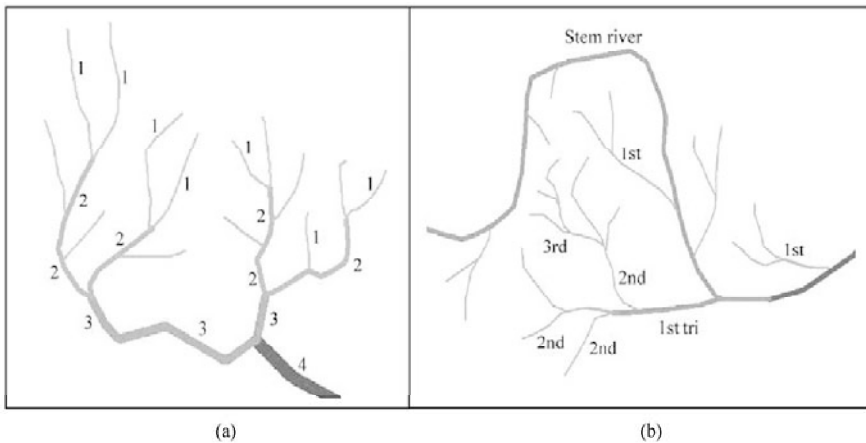
Fig. 1.3 Stream orderings in a drainage network (a) Horton-Strahler's stream ordering system; (b) Engineering stream ordering system

Horton's Laws Horton (1945) pioneered quantitative studies of river morphology by introducing his laws of stream number, N_m, stream length, L_m, stream area, A_m, and stream slope, s_m; i.e.,

$$N_\omega = Ae^{-B\omega} \tag{1.1}$$

$$L_\omega = Ce^{D\omega} \tag{1.2}$$

$$s_\omega = Ee^{-F\omega} \tag{1.3}$$

$$A_\omega = Ge^{H\omega} \tag{1.4}$$

where ω = stream order; N_ω = number of ω-th order streams; L_ω = length of ω-th order streams; s_ω = slope of ω-th order streams; and A_ω = drainage area of ω-th order stream; and A, B, C, D, E, F, G, H = constants. These empirical laws were not derived from basic theories in physics or other fundamental theories. However, the validity of these equations have been independently verified and accepted as the basic laws in river morphology. An example of Horton's laws is shown in Fig. 1.4 for the Rogue River basin in Oregon (Yang, 1971).
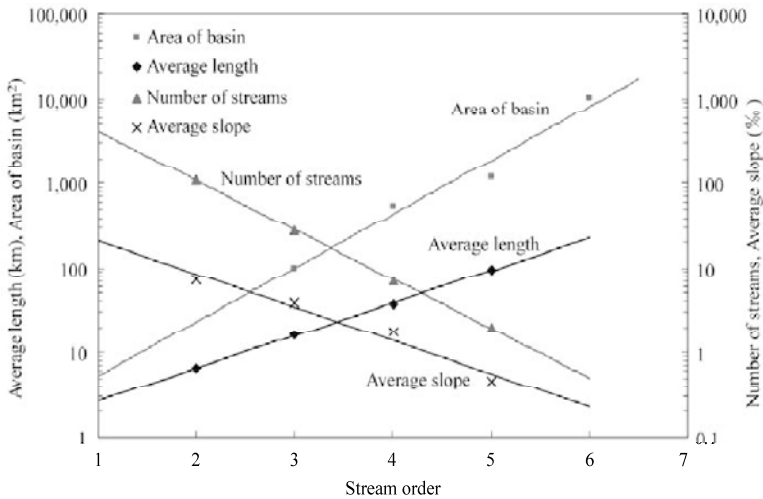
Fig. 1.4　An example of Horton's laws for the Rogue River basin (after Yang, 1971)

Model of network growth—Horton (1945) not only pioneered the quantitative description and analysis of channel networks and established "laws" of network composition, but he also proposed a model of network growth by overland flow. Horton suggested that on a steep, newly exposed surface a series of parallel rills develop and that, with time, cross-grading and micro-piracy among these rills produce an integrated dendritic network (Fig. 1.5 Model A). A second model of network growth is the headward growth type (Howard, 1971), in which the drainage network develops fully at the edge of an undissected area (Fig. 1.5 Model B). As growing headward and bifurcate, the channels fill the space available and form a fully developed dendritic network. In the third model suggested by Glock (1931), the drainage area is rapidly subdivided by channels and the addition of tributaries then fills the available space (Fig. 1.5 Model C).

Among the three models of network growth, one extreme is the Horton model (Fig. 1.5 Model A), in which parallel channels develop almost instantaneously over the surface, and the final pattern of the network progressively emerges by internal changes (capture) and replacement of the initial pattern of rills. This model occurs only in very small drainage area, generally smaller than 1 km^2. At the other extreme is the headward-growth model in which a "wave of dissection" (Howard, 1971; Schumm, 1956) can be envisioned at the tips of first-order channels, which is the active zone of network headward growth (Fig. 1.5 Model B). As this wave progresses into the undissected basin, the fingertip channels lengthen and bifurcate, leaving behind a channel system that is almost fully developed. In this developed portion of the network few additions or losses of channels occur during the continued extension of the network. The significant feature of this model is that the network is almost fully developed as the wave of dissection passes a particular point. This model may occur in large drainage areas, for instance, 1000 km^2. The third model (Fig. 1.5 Model C) lies between the two extremes and occurs in drainage areas smaller than 100 km^2.
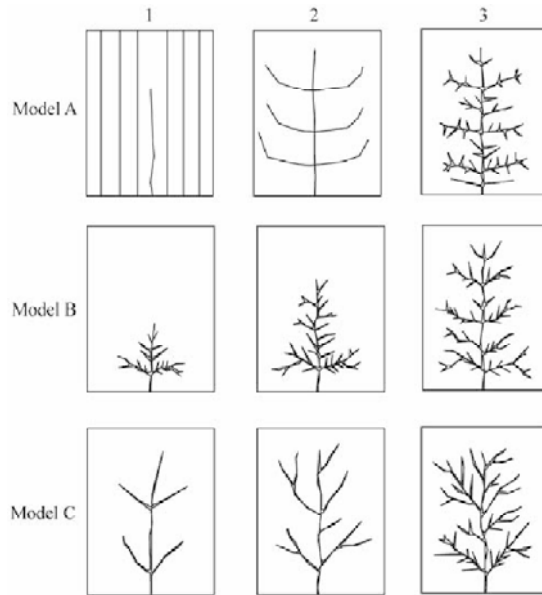
Fig. 1.5 Models of drainage network growth: Model A—Replacement of parallel rills by an angular dendritic pattern; Model B—Expansion by slow headward growth into available area; Model C—Extension of rapidly growing, long channels that block out drainage areas. Tributaries are added subsequently to fill in drainage networks (after Schumm et al., 1987)

Figure 1.6 shows an example of the development of B-type channel network on the Loess Plateau in North China. The channel network is developing from a deep-cut river valley toward the undissected flat plateau. In this case the fingertip channel has space to freely develop its shape. Figure 1.7(a) shows a developing C-type channel networks in the upper reaches of the Yangtze River in Yunnan Province, and Fig. 1.7(b) shows a developed B-type channel networks in the same area. Channel bed incision and various erosions are the main drives of the network growth.

Fig. 1.6 Development of B-type channel network on the Loess Plateau in North China. The channel network is developing from a deep-cut river valley toward the undissected flat plateau

(a)

(b)

Fig. 1.7 C-type channel networks in the upper reaches of the Yangtze River in Yunnan Province: (a) Developing network; (b) Developed network (See color figure at the end of this book)

Random growth model—Leopold and Langbein (1962) proposed a random walk model, in which a matrix or grid coordinate scheme is used within which the network grows. Each grid element represents a unit length of possible growth. Figure 1.8 shows the homework of a student with the random growth model. The length of a stream from initiation to its joining with another stream has a minimum limit, which is dependent on separation or cell size, and the actual length of an individual link is, therefore, a function of the cell size in the matrix. The square cell represents the unit area required to support a unit length of channel. Rainfall over each unit area creates the minimum runoff, the direction of the runoff is determined by a random number. According to the topography of China the probabilities of the flow direction are selected as follows:

West-East $P = 0.5$; East-West $P = 0.1$; North-South $P = 0.2$ and South-North $P = 0.2$

In Fig. 1.8 an arrow represents the flow direction on each cell. The arrow direction is determined with random numbers generated by the computer. For instance, if the random number is in the range of 0–5,000, the flow direction is from west to east; if the number is in the range of 5,001–7,000, the flow direction is from north to south; if the number is in the range of 7,001–8,000, the flow direction is from east to west; and if the number is in the range of 8,001–9,999, the flow direction is from south to north. Two neighboring

arrows, if they are not in opposite directions, may connect to form a first order stream. Two first-order streams meet at the confluence and form a second-order stream, and so on. There are two fifth order rivers flowing from west to east, as shown in Fig. 1.8. There are a few close circles with arrows rotating anticlockwise or clockwise, which are interpreted as riparian lakes.
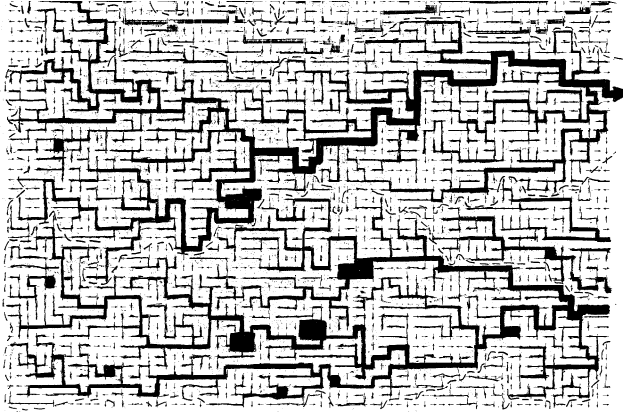
Fig. 1.8 Homework of a student with the random walk model

Despite all these efforts at simulation, Howard (1971) commented that "the random growth models simulate many of the characteristics of natural stream systems, but it remains uncertain to what extent inferences may be drawn about the processes responsible for natural stream systems." He also suggested that although natural stream systems appear to exhibit numerical relations nearly identical to those of topologically random channel networks, the relevant geomorphic processes are deterministic and the apparent randomness arises from independent variation of a large number of factors, such as microclimate and lithology (Abrahams, 1984). It has also been demonstrated that networks developed by strict rules of growth are similar to those generated by random processes, which caused Stevens (1974) to conclude that "randomness can appear regular and regularity random."

Minimum stream power theory—Yang (1971) proposed the minimum stream power theory, which is very useful for river researchers. From thermodynamics, the entropy Φ is defined as

$$\Phi = \int \frac{\mathrm{d}E}{T} \tag{1.5}$$

where E = total thermal energy per unit mass; and T = absolute temperature used to measure thermal energy. The entropy concept and thermal dynamic laws can be applied to a non-thermal system if the energy in that system can be measured by a positive parameter. Yang (1971) considered potential energy the only useful energy available to a river system, and elevation can be used to measure the potential energy in a river system. When a unit mass or weight of water flows downstream, it releases its potential energy, converts it into kinetic energy, and then uses it for erosion and sediment transport. Yang defined the entropy of a river system as

$$\Psi = \int \frac{\mathrm{d}H}{Z_m} \tag{1.6}$$

where H = total potential energy per unit weight of water; and Z_m = elevation measured from mean sea level for an m-th order system. Similar to the absolute temperature T in a thermal system, Z_m is a positive parameter which can be used to measure potential energy per unit weight of water in a river system.

The entropy in the u-th order river is

$$\Psi_u = \int \frac{\mathrm{d}H_u}{Y_u} = k\int \frac{\mathrm{d}Y_u}{Y_u} \tag{1.7}$$

where H_u = average potential energy in the u-th order river; Y_u = average total fall or change of elevation in the u-th order river; and k = a conversion factor between potential energy and elevation. The distribution of potential energy per unit weight of water in a river system is directly proportional to its elevation. The probability that a particular amount of potential energy will be lost in the u-th order river is

$$p_u = \frac{H_u}{H} = \frac{Y_u}{Z_m} \tag{1.8}$$

Substituting Eq. (1.8) into Eq. (1.7)

$$\Psi_u = k\int \frac{\mathrm{d}p_u}{P_u} = k\ln p_u + c_u \tag{1.9}$$

In which c_u is a constant. The total entropy of a system is equal to the sum of the entropy of each part.

$$\Psi = \sum_{u=1}^{m} \Psi_u = k\sum_{u=1}^{m} \ln p_u + c \tag{1.10}$$

In which $c=c_1+c_2+\cdots+c_m$. According to Lewis and Randall (1961), the most likely distribution of energy in a system under dynamic equilibrium condition is that the entropy of the whole system is a maximum, i.e.,

$$\sum_{u=1}^{m} \ln p_u = \text{maximum} \tag{1.11}$$

From the definition of the probability, $\sum_{u=1}^{m} p_u = 1$. The entropy reaches its maximum value as the water head evenly distributed, i.e.,

$$p_1 = p_2 = \cdots = p_m \tag{1.12}$$

According to Prigogine (1967), during the evolution toward a stationary state, the rate of entropy production per unit mass or weight should be a minimum compatible with external constraints.

$$\frac{\mathrm{d}Y}{\mathrm{d}t} = \text{minimum}$$

which can be expressed as

$$\frac{\mathrm{d}Y}{\mathrm{d}t} = \frac{\mathrm{d}Y}{\mathrm{d}x}\frac{\mathrm{d}x}{\mathrm{d}t} = sV = \text{minimum} \tag{1.13}$$

In which x is the distance along the flow direction, s is energy slope, V is velocity. Integration of Eq. (1.13) yields

$$\int sV\mathrm{d}A = Qs = \text{minimum} \tag{1.14}$$

In which $\mathrm{d}A$ is the differential of wet area, Q is the discharge, and s is riverbed slope, which is equal to the energy slope in steady flows.

Define a stream power $P = \gamma Qs$, Eq. (1.14) can be rewritten as:

$$P = \gamma Qs = \text{minimum} \tag{1.15}$$

In which γ is the specific weight of water.

Equation (1.15) states Yang's law of least rate of energy expenditure that during the evolution toward its equilibrium condition, a river will adjust or choose its course of flow in such a manner that the rate of potential energy expenditure per unit mass or weight of water is a minimum. The minimum value depends on the constraints applied to the system (Yang, 1972).

Mechanism of merging of streams—According to the minimum stream theory, the river network develops to reach the minimum stream power per distance. Two parallel u-th order streams transporting water at discharges Q_1 and Q_2 merge to form a $(u+1)$-th order stream. The $(u+1)$-th order stream is more meandering and transports water with discharge equal to the sum of Q_1 and Q_2. The difference of stream power between the $(u+1)$-th order stream and the two u-th order streams is:

$$\Delta P = \gamma Qs - \gamma(Q_1 s_1 + Q_2 s_2) \qquad (1.16)$$

in which s is the slope of the larger stream, s_1 and s_2 are the slopes of the smaller streams. Replace the slopes s_1 and s_2 with the average slope of the u-th order stream, s_u, and replace the slope s with the average slope of the $(u+1)$-th order stream, Eq. (1.16) becomes

$$\Delta P = \gamma(Q_1 + Q_2)(s_{u+1} - s_u) \qquad (1.17)$$

From Eq. (1.3) s_{u+1} is smaller than s_u, thus ΔP must be negative. Therefore, the stream power becomes smaller as the two streams merge into a larger stream. In general, small streams always merge into larger ones to minimize the stream power.

1.1.3 Sediment

Three primary geomorphic processes affect rivers, i.e., ① erosion, the detachment of soil particles; ②sediment transport, the movement of eroded soil particles in flowing water; and ③ sediment deposition, settling of eroded soil particles to the bottom of a water body. In these processes sediment plays undoubtedly the main role. The following section introduces the main concepts of sediment and sediment transportation.

Sediment is defined as the solid particles found in a deposit after transportation by flowing water, wind, wave, glacier, and gravitational action. **Sediment discharge** is defined as the mass or volume of sediment passing a stream cross section in a unit of time. The typical units for sediment discharge is tons per second or per day. To differentiate various types of particles, sediment is subdivided into groups. For a long time, various kinds of terminology have been used for the different sizes of sediment particles.

Sediment classification—Attenberg made his classification at the beginning of the nineteenth century. It was approved by the International Association for Soil Sciences in 1927 as the standard in soil analysis, and it has been widely adopted in European countries. Most American geologists use Wentworth's classification (Wentworth, 1922). In 1947 the American Geophysical Union drew up a new standard for sediment classification (Subcommittee on Sediment Terminology, 1947). This standard is based on the same groups that Wentworth used. The only difference is that each group was subdivided, so that the denomination of classes is more complete. Classification of sediment in hydraulic engineering in China followed that applied in the former Soviet Union. Some divergence remains between this classification and those in European countries and the United States. This book uses the Chinese classification. Two classifications of sediment are given in the following:

Chinese classification:

    Boulder (> 200 mm)   >   **Cobble** (20 – 200 mm)   >   **Gravel** (2 – 20 mm) >

    Sand (0.05 – 2 mm)   >   **Silt** (0.005 – 0.05 mm)   >   **Clay** (<0.005 mm)

Attenberg's classification

    Boulder (> 200 mm)   >   **Cobble** (20–200 mm)   >   **Gravel** (2 – 20mm) >

    Coarse Sand (0.2 – 2 mm) >   **Fine sand** (0.02 – 0.2 mm)   >   **Silt** (0.002 – 0.02mm) >

    Clay (<0.002 mm)

Despite the several classifications of sediment used in various countries, they have some points in common. Most of the intervals for the sediment groups are unequal, because the sizes cover such a wide range. Stone blocks and fine clay particles differ by a factor of more than a million. Evidently, the

classification of sediment size must follow a geometric scale; i.e., an appropriate ratio between neighboring groups must be taken. For the Atterberg and the Chinese classification, the ratio is 10, and for the American Geophysical Union classification the ratio is 2. In connection with this aspect, sieve openings for granulometry also follow a certain ratio. For example, the sizes of the openings in the Tailor sieves follow the ratio of $2^{0.25}$. The grain sizes such as 0.005, 0.05, and 2 mm are used as demarcations of sediment groups because sediment particles larger and finer than these tend to show quite different characteristics, as shown in Table 1.1 (Ruhin, 1957).

Table 1.1 Relation between particle diameter and sediment properties (after Chien et al., 1998)

Terminology and size (mm)	Phenomena of sediment movement				Fall velocity-diameter relation			Composition of sediment deposits			Method of size analysis			
	Bed load	Suspended load	Focculation	Brownian movement	$\omega=f(D^{0.5})$	$\omega=f(D^{0.5-2})$	$\omega=f(D^2)$	Fragment of rocks	Fragment of minerals	Clay minerals	Direct measurement	Sieve settling	Settling	Centrifugal settling
Boulder (100−200)														
Cobble (10−100)														
Gravel (2−10)														
Sand (0.05−2)														
Silt (0.05−0.005)														
Clay (<0.005)														

Note: D is diameter of particles and ω is the fall velocity of a single particle in water

Sediment is the product of weathering of rocks, and thus, is closely related to lithology. Figure 1.9 shows different sediments from the areas with different lithologic compositions. In the upper reaches of the East River, which is a tributary of the Pearl River in China, most of the drainage area is composed of granite. Feldspar in the granite changed into kaolinite in the process of weathering, which results in quartz and mica particles and fine kaolinite particles (Fig. 1.9(a)). There are few gravel, cobbles and boulders in this area. In the Xiaojiang watershed, the rocks consist of metamorphic rocks, including phylite, layer stone, mud stone, and sand stone. Weathering of these rocks generates solid particles with various sizes from clay to boulders. Figure 1.9(b) shows the sediment deposits of debris flow in the area. In the limestone area in Dali in Yunnan Province in South China the rock is weathered mainly by dissolution by rainfall containing CO_2. In the process no granular material is produced. Therefore, there is a very thin layer of soil on the hills and very poor vegetation may develop in this area (Fig. 1.9(c)). Generally speaking, granite produces boulders, coarse sand and small amount of clay; limestone produces boulders, cobbles and gravel; shale produces clay and silt; sandstone produces boulders, cobbles, gravel and sand; and metamorphic rocks produces various sizes of sediment.

Size distribution—Sediment refers usually not to individual particles but rather to a mixture with innumerable particles of different sizes, shapes, and mineral compositions. Although sediment particles are not cemented together to form an entity, many properties pertinent to sediment manifest themselves mainly through the existence of an ensemble of sediment particles. **Size distribution** of sediment particles, including the degree of uniformity, reflects directly the properties of parent rocks and the intensity of the sorting process by river flow; it is also closely related to the amount of sediment transported. The most useful method to describe the size distribution of sediment is the cumulative size- frequency curve, in which sediment size (its logarithm) is taken as the ordinate, and the percentage by weight of sediment

particles that is finer than the given size is taken as the abscissa. Cumulative size distribution curves are shown on a logarithmic-probability scale in Fig. 1.10.
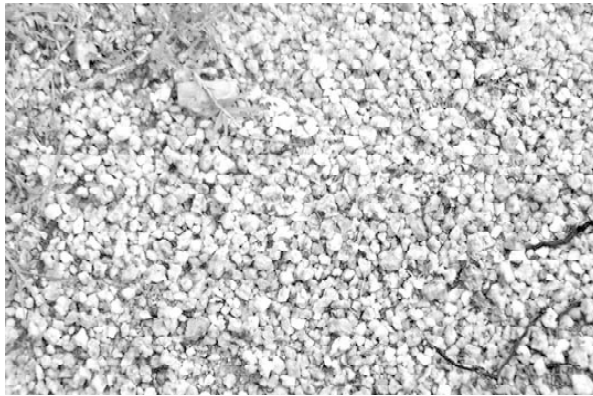
(a)

(b)

(c)

Fig. 1.9 (a) Weathering of granite produces quartz, feldspar and mica particles in the upper reaches of the East River in Guangdong in South China; (b) Weathering of metamorphic rocks in the Xiaojiang watershed produces various particles from clay to boulders; (c) Weathering of limestone produces few granular particles in Dali in Yunnan (See color figure at the end of this book)
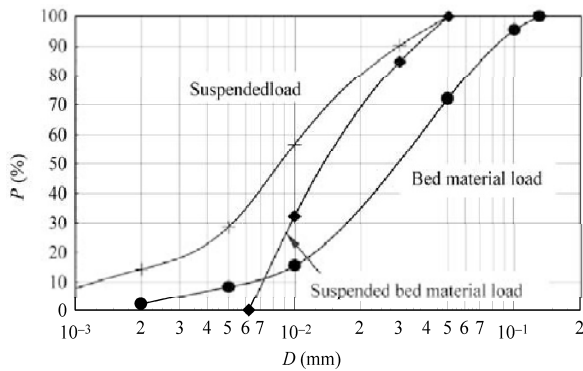
Fig. 1.10   Size distribution curves of sediments: The abscissa is the cumulative percentage of particles finer than the corresponding diameter on the ordinate (*D*-coordinates) (after Wang et al., 2001)

Size distribution curves can reflect distinguishing features of sediment samples, but such curves may not be convenient to use in the quantitative descriptions and comparisons of one example with another. Therefore scientists have proposed the use of a variety of characteristic parameters to describe features of the sediment size distribution and to carry out statistical analyses based on those parameters. The most useful parameter is the **median diameter D_{50}** which is the value on the ordinate of the point on the accumulative curve corresponding to the 50% on the abscissa. The **sorting coefficient** defined by $(D_{84}/D_{16})^{0.5}$ is also often used to represent the uniformity of the sediment mixture.

1.1.4   Sediment Loads and Bed Forms

Sediment loads are the sediments carried by the flow or the sediments in motion. Sediment loads can be classified according to their patterns of motion as contact load (rolling or sliding), saltation load, suspended load, and laminated load. In these, contact load, saltation load, and laminated load all belong to the category of bed load.

1.1.4.1   Bed Load

Figure 1.11 shows various patterns of motion of sediment load and their relation with the bed. The particles on the bed are subjected to drag force by the flow and slide or roll forward making contact with the bed frequently. These particles are called **contact load.** If the flow velocity is high, the force acting on the bottom surface of the particle is enlarged because the particle has moved a small distance away from the bed, and the bottom surface area on which the static pressure acts increases. Therefore, the lift force becomes much greater. In other words, the particle experiences an abrupt increase in the lift force at the instant of rolling away from the bed. Consequently, it may jump into the flow from the bed. As the particle rises to some height, the effect of the increasing horizontal velocity component of the particle is greater than the effect of the flow velocity, and the relative movement between the particle and the flow begins to reduce. In general, as the particle reaches its highest point, its velocity is close to the local flow velocity. From this point, the particle descends. Particles moving in such a way produce what is called **saltation load.** Contact load and saltation load are bed load (Chien et al., 1998).

If the saltation height of a particle is large, the particle gains much momentum from the flow, and it may rebound after it falls down and strikes the bed. In some cases the particle does not only rebound, but it may also induce other bed particles that it hits to jump into flow. The height of particle saltation is proportional to the density difference between the particles and the fluid. The natural sand particles usually have the same density (2.65 g/cm³). Since the density of water is more than 800 times larger than that of
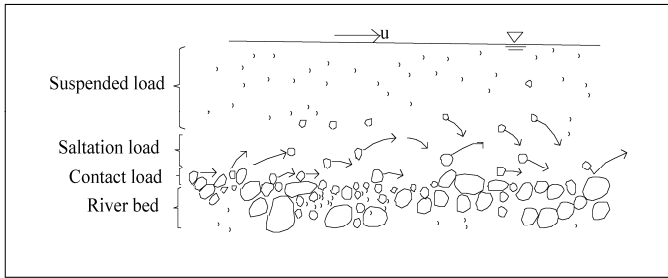
Fig. 1.11   Various sediment loads in stream flows

air at room temperature, the height of saltation in wind is about 800 times larger than that in water flow if the particles jump from the bed at same initial velocity. The difference is of profound significance. For movement of wind-blown sand, particles jump quite high and gain much more energy from the wind. And when they fall on the bed they splash more particles into the flow. The chain reaction results in a sharp increase in the rate of sediment transportation soon after sand motion is initiated in desert. Although the saltation load in flowing water is more important than the contact load, the height of saltation is usually only a few times the particle diameter in water flow, and the kinetic energy it possesses when falling back down onto the bed is not enough to induce such chain reactions.

If the drag force of the flow is extremely high a **laminated load** motion may occur. As the surface of the riverbed is neither compact nor impermeable, and is composed of granular materials, the shearing force of the flow may transmit into the bed. If the resistance of the surface layer of the bed due both to the submerged weight of the particles resting on the bed surface and to the extra pressure exerted by the saltation load and contact load, is not sufficient to overcome the shearing stress acting on that layer, the layer next to the surface is bound to move. The motion may penetrate into the bed gradually, following a progressive increase in stream power. Since the grains are closely packed in the bed, they can move only in layers, and in the process of movement, the moving bed is dilated to a certain extent so as to attain more freedom of mobility. There is no turbulence within the layers because the shear between layers checks the development of turbulent eddies (Wang and Qian, 1987). Laminated load motion was first observed in flume experiments and debris flows (Wang and Qian, 1985). Recently, the author observed laminated load motion in a mountain stream on the Yunnan-Guizhou Plateau. The bed slope of the stream is around 0.09. In flood season numerous layers of bed sediment were initiated and moved in layers as laminated load motion. The laminated load particles are relatively uniform with diameter about 1–5 mm. The average velocity is only about 0.5 m/s but the sediment transporting capacity is extremely high. Laminated load motion is a special form of bed load motion with an extremely high intensity.

1.1.4.2   Suspended Load

Flows at high velocity are turbulent and have eddies of various sizes. If a particle jumping from the bed enters such an eddy, it may be carried far away from the bed. In order to carry a particle, the size of the eddy must be much larger than the particle and its upward velocity component must be higher than the fall velocity of the particle. If an eddy is of about the same size as a particle, the particle is liable to fall out of the eddy; hence, the eddy would no longer affect the movement of the particle. On the contrary, if an eddy is much greater than a particle, the eddy may carry the particle for a long time. And by the time the particle falls out of the eddy, it may already have been carried into the region of the main flow. Obviously, the transport of suspended particles is mainly the effect of large-scale eddies. These particles, carried by eddies and moving downstream at the same velocity with the flow, are called the suspended load, as shown in Fig. 1.11. Suspension of particles takes a certain amount of energy from the turbulent

flow. Hence, the existence of suspended load reduces the turbulence intensity.

As shown in Fig. 1.12, the concentration distribution of suspended load is heterogeneous, with a negative concentration gradient. The coarser the sediment, the more heterogeneous is the distribution. In steady turbulent flow, the amount of sediment carried by eddies from the lower layer into the upper layer per time is proportional to the concentration gradient. The sediment falling down from the upper layer into the lower layer is the product of concentration, S_v, and the fall velocity, ω. If the concentration distribution is in equilibrium, the following equation results:

$$\varepsilon_y \frac{dS_v}{dy} + S_v \omega = 0 \tag{1.18}$$

in which ε_y is the diffusion coefficient of sediment and y is the position in the vertical direction. Many researchers have assumed

$$\varepsilon_y = \kappa U_* y \frac{h-y}{h} \tag{1.19}$$

in which $\kappa = 0.41$ is the von Karman constant, $U_* = \sqrt{gsR}$ is the shear velocity, R is the hydraulic radius of the flow and is equal to the average depth (h) in wide river channel, and g is the acceleration due to gravity Substituting Eq. (1.19) into Eq. (1.18) and integrating yields the vertical concentration profile of suspended load

$$\frac{S_v}{S_{va}} = \left(\frac{h-y}{y} \cdot \frac{a}{h-a} \right)^z \tag{1.20}$$

in which a is the elevation from the bed of a reference point, S_{va} is the concentration at the point, and Z is given by

$$Z = \frac{\omega}{\kappa U_*} \tag{1.21}$$

is a dimensionless number called the **Rouse Number**.
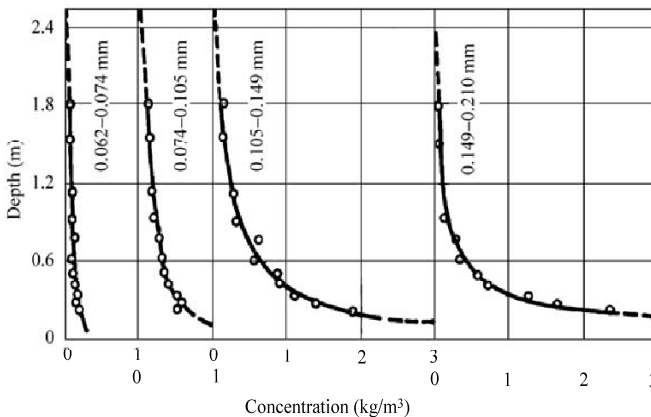
Fig. 1.12   Concentration profiles of different sizes of suspended sediment in a natural river compared with the theoretical formula (Eq. (1.20)) (after Wang et al., 2001)

1.1.4.3   Bed Material Load and Wash Load

Einstein, Anderson and Johnson (1940) analyzed a number of size distribution curves of sediment samples and found that the ratios of fine to coarse sediment in the channel bed and that for the sediment

in motion are quite different. Sediment in the channel bed is composed of much more coarse and much less fine sediment than is the moving sediment. The fine sediment in the flow is not saturated to its capacity and the rate of transport depends only on the amount contained in the oncoming flow. Thus, the amount of coarse sediment carried by the flow depends on the sediment transport capacity and exhibits a well defined relation with the discharge of water. In contrast, the concentration of fine sediment depends only on the supply of the sediment from an upstream reach and shows no obvious correlation with the discharge. Because coarse sediment always exchanges with bed material during transport it is called "bed material load". In contrast, fine sediment, eroded and washed from upland watersheds that has been transported through the channel over a long distance and is scarcely ever deposited in the channel, is called "wash load". Wash load always moves as suspended load.

Wash load refers to the sediment washed away through the channel without any exchange with the bed sediment and plays no role in the river morphological process. Wash load concentration is normally a function of supply; i.e., the stream can carry as much wash load as the watershed and banks can deliver. Bed material load is composed of the sediment of size classes found in the streambed. Bed material load moves along the streambed by rolling, sliding, or jumping, and may be periodically entrained into the flow by turbulence, where it becomes a portion of the suspended load. Bed material load is hydraulically controlled and can be computed using sediment transport equations.

The previously defined terms can be combined in a number of ways to give the total sediment load in a stream. However, it is important not to combine terms that are not compatible. For example, the suspended load and the bed material load are not complimentary terms because the suspended load may include a portion of the bed material load, depending on the energy available for transport. The total sediment load is correctly defined by the combination of the following terms:

$$\text{Total Sediment Load} = \text{Bed Material Load} + \text{Wash Load}$$

or

$$\text{Total Sediment Load} = \text{Bed Load} + \text{Suspended Load}$$

or

$$\text{Total Sediment Load} = \text{Bed Load} + \text{Suspended Bed Material Load} + \text{Wash Load}$$

What is the criterion for distinguishing bed material load and wash load? Einstein suggested using D_5 of the bed sediment as the critical diameter. Sediment carried by the flow finer than D_5 is wash load and those coarser are bed material load. Partheniades (1977) employed 0.06 mm as a critical diameter to differentiate bed material load and wash load, because for sediment finer than 0.06 mm the cohesive force among particles is important and coarser sediment is cohesionless. Some researchers have suggested that the criterion for differentiating bed material load and wash load should include not only sediment size but also flow intensity. Wang and Dittrich (1992) analyzed the rate of sediment transport in the Yellow River at high concentrations under different flow intensities and found that sediment much coarser than 0.06 mm may wash downstream for several hundreds of kilometers without exchange with the bed sediment. Thence they proposed that the bed load, suspended bed material load, and wash load could be identified as follows:

$$\text{Bed Load} > Z = 3 > \text{Suspended Bed Material load} > Z = 0.06 > \text{Wash Load} \tag{1.22}$$

In such a way the three kinds of load can be identified using the Rouse number. Table 1.2 lists the main features and differences of the bed material load and wash load.

1.1.4.4   Bed Forms

Bed forms are wave-like regularities found on the bed of a stream that are related to flow characteristics. They are given names such as "dunes," "ripples," and "antidunes." They are related to the transport of

Table 1.2 Main features of bed material load and wash load

Features	Bed material load	Wash load
Origin	Soil erosion in watershed	Soil erosion in watershed
Direct origin	River bed upstream	Sediment yield in watershed
Composition of bed material	Main portion of the bed material usually does not change except for heavily sediment-laden rivers	On the bed surface, changing with incoming amount and flow intensity
Composition of moving sediment	A small portion of the moving sediment	Main portion of the moving sediment
Patterns of movement	Bed load and suspended load	Suspended load
Transport rate	Determined from the flow intensity and less correlated with incoming sediment, but for heavily sediment laden rivers depending also on the incoming sediment	Determined mainly from the incoming sediment
Relation between flow and sediment transport	Relation established on basis of mechanics and may be estimated by sediment transport capacity formulas	Relations based on watershed characteristics, determined by measured or empirical data
Significance	Transport rate determines bed stability	Transport rate determines rate of reservoir deposition
Criterion	Coarser than D_5 of the bed material; Rouse number Z larger than 0.06	Finer than D_5 of the bed material; Rouse number Z smaller than 0.06

sediment and they interact with the flow because they change the roughness of the stream bed. An analog to stream bed forms is desert sand dunes. In alluvial rivers with the bed consisting of sand and silt, various bed forms may develop. At low flow velocity over an initially flat stationary bed, no sediment moves; but once the flow velocity reaches a certain value, some particles are set in motion. Finally, **ripples** with a regular shape form. The longitudinal cross sections of ripples usually are not symmetrical. The upstream face is long and has a gentle slope, and the downstream face is short and steep. Ripples are the smallest of the bed configurations.

With increasing flow velocity, the **dunes** develop with triangular profile that advance downstream due to net deposition of particles on the steep downstream slope. Dunes move downstream at velocities that are small relative to the stream flow velocity. The size of a dune is closely related to the water depth. Dunes in large rivers can be kilometers long and several meters high. They may be less than half a meter in other rivers. If the velocity continues to increase, the bed form develop into **antidunes**. Antidune is a type of bed configuration that is in phase with the wave on the water surface, and these two waves interact strongly. Antidunes move upstreamward is symmetrical in shape, like a surface wave.

In mountainous area the stream bed consists of boulders and cobbles. There is no ripples and dunes but a **step-pool system** may developed, which occurs in high-gradient (>3%−5%) mountain streams with alternating steps and pools having a stair-like appearance (Chin, 1999). The step-pool system occurs usually on a stream with bed materials consisting of particles with diameters differing by several orders of magnitude with the largest diameter on the same order as the water depth. Cobbles and boulders generally compose the steps, which alternate with finer sediments in pools to produce a repetitive, staircase like longitudinal profile in the stream channel.

1.1.5 River Patterns

Meandering rivers—Natural river is rarely straight. **Sinuosity** is defined as the ratio of the channel centerline length to the length of the valley centerline. If the sinuosity is over 1.3, the stream can be considered meandering. Figure 1.13 shows a typical meandering river, which is a tributary of the Yellow

River, flowing on the Qinghai-Tibet Plateau of China. In the picture a new oxbow lake is forming. Its upstream end which has been cut off from the river and the lower end is still connecting with the river. Most natural rivers are meandering river.

Fig. 1.13   A typical meandering river with oxbow lake (tributary of the Yellow River) on the Qinghai-Tibet Plateau

Straight rivers—A straight river is often a straight reach of a river. The straight reach is usually not long. Channelization of rivers and construction of levees make rivers straight. Even where the channel is straight it is usual for the thalweg, or line of maximum depth, to wander back and forth from near one bank to the other. Opposite the point of greatest depth there is usually a bar or an accumulation of mud along the bank, and these bars tend to alternate from one side of the channel to the other. Figure 1.14 shows a straight section of the lower East River in south of China. Channelization and hardened banks made the channel straight.

Fig. 1.14   Channelization and hardened banks made the lower East River a straight river

Braided and anabranching rivers—Braided rivers have separated channels divided by bars. Bars, which divide the stream into separate channels at low flow, are often submerged at high flow. If the bars have been stabilized by vegetation and the multiple channels are stable, the river is classified in some literatures into anabranching river. Figure 1.15(a) shows a braided river in the Lhasa River, which is a tributary of the Yalutsangbu River. Figure 1.15(b) shows an example of anabranching river in the lower reaches of the Minjiang River, the famous Dujiangyan irrigation project is shown in the picture. Several channels in the

reach are separated by vegetated islands. The islands are composed of gravel, sand and soils. Although not as frequent as single-thread channels, braided channels occur in a wide range of environments, from proglacial to semi-arid and at large range of scales, from the small streams on sandy beaches to the largest continental rivers.

<div align="center">(a)   (b)</div>
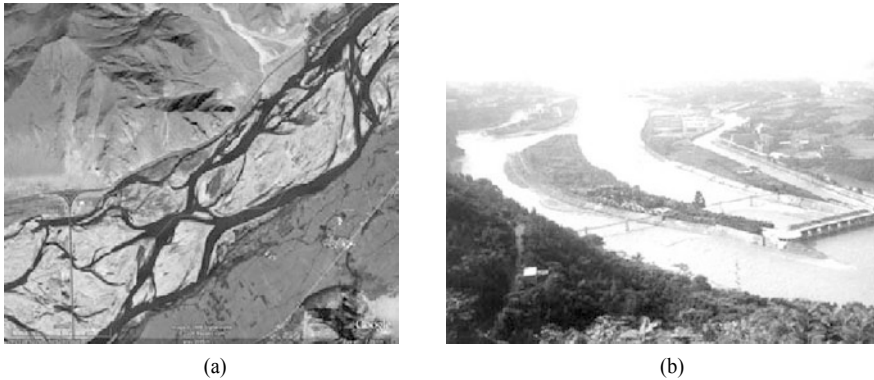
Fig. 1.15 (a) Braided channels of the Lhasa River on the Qinghai-Tibet Plateau; (b) Anabranching channels of the Minjiang River, the famous Dujiangyan irrigation project is shown in the picture

Wandering rivers—A wandering river is defined as a river with an unstable channel. A wandering river carries a heavy sediment load and the discharge and sediment-carrying capacity are unsteady. A wandering river is usually associated with river aggradation. There are sand bars in the river channel but usually the stream flow remains in one channel during one period of time and flows in another channel during a second period of time. This is different from the braided rivers, in which the stream flows in multiple channels simultaneously. One important feature of a wandering river is the high speed of migration of the main stream channel.

The lower Yellow River is a wandering river with bed material mainly composed of silt and fine sand of median diameter of about 0.02 mm. The sediment is very erodible. Bank erosion occurs at one side, meanwhile sediment deposition occurs at the other side of the channel. Figure 1.16 shows the wandering motion of the Yellow River section upstream of Zhengzhou in the periods of 1960–1964 and 1981–1985 (Wang et al., 2001). In the period of 1980–1985, hyperconcentrated floods occurred and the river channel wandered at high speed and the riverbed was silted up. At the Luocunpo cross section, the stream channel moved southward more than 5 km in the period of 1984–1985.

Anastomosing river—Schumm (1968) first introduced the concept of anastomosing river for describing multiple channel system with straight, meandering or braided reaches. Knighton and Nanson (1993) described it as a system of multiple channels separated by islands, which are usually excised from the continuous floodplain and which are related to the size of the channels. Smith and Smith (1980) used the term "anastomosing river" for an interconnected network of low gradient, relatively deep and narrow, straight to sinuous channels with stable banks composed of fine grained sediment (silt/clay) and vegetation. Wang (2000, 2002) analyzed the characteristics of anastomosing rivers and indicated that anastomosing river is a result of development of channels on floodplain and braided river is a result of development of bars and small islands on rivers. Ni et al. (2000) studied the transformation of anastomosing river and braided river or meandering river. However, anastomosing river has not got its position in the conventional classification of river patterns. In fact, many Chinese rivers, especially in northeastern China, are anastomosing river. Figure 1.17 shows a satellite image of the anastomosing Mudanjiang River in
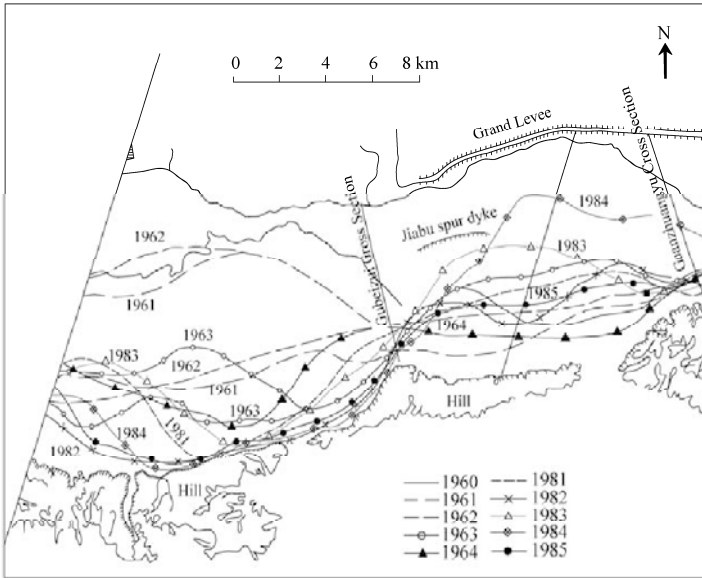
Fig. 1.16 Wandering channel of the lower Yellow River during the periods 1960–1964 and 1981–1985. The high speed of migration of the channel can be seen by identifying the curves of the channels of the consecutive years

Northeast China. On the flat plane land the river bifurcates into two or more channels and merge again after traveling a long distance. The characteristics of the river are in accordance with the description of Smith and Smith (1980).

Fig. 1.17 Anastomosing channels of the Mudanjiang River in Northeast China (Satellite image from the Google Earth)

1.1.6 Morphological and Hydraulic Features

Channel slope—Channel slope or gradient is measured as the difference in elevation between two points in the stream divided by the stream length between the two points. Channel slope directly impacts flow velocity, shear stress, and stream power. Since these attributes drive the geomorphic processes of erosion, sediment transport, and sediment deposition, channel slope becomes a controlling factor for channel shape and pattern.

   Knickpoint is a term to describe a location in a river or channel where there is a sharp change in

channel slope, such as a waterfall or a quake lake, resulting from differential rates of erosion above and below the knickpoint. Differential rates of erosion can be resulted from a change in the lithology of the river channel and bed structures. The river, having gained more potential energy due to gravity, will then proceed to work the knickpoints out of its system by either erosion (in the case of waterfalls) or deposition (in the case of quake lakes) in order for the river to reattain its smooth concave graded profile. In the southwesten China almost all streams have knickpoints, which are resulted mostly from landslide dams. The knickpoints consist of not bed rocks but step-pool system.

Longitudinal bed profile of alluvial rivers—For alluvial rivers the bed materials consist mainly of sand (or silt). The longitudinal profile is usually concave upward. As described previously in the discussion of dynamic equilibrium, streams adjust their profiles and patterns to try to minimize the time rate of expenditure of potential energy, or stream power, present in flowing water. The concave upward shape of a stream's profile appears to be due to adjustments a river makes to help minimize stream power in the downstream direction. Stream power has been defined as the product of discharge and slope. Since stream discharge typically increases in the downstream direction, slope must decrease in order to minimize stream power. The decrease in slope in the downstream direction results in the concave up longitudinal profile.

According to the minimum stream power theory, the morphology of fluvial rivers develops to reach the minimum stream power (Yang, 1983). This can be described by the following equation:

$$\frac{dP}{dx} = \frac{d}{dx}(\gamma s Q) = \gamma \left(Q \frac{ds}{dx} + s \frac{dQ}{dx} \right) = 0 \tag{1.23}$$

in which P is the stream power, γ is the specific weight of water, s is the riverbed slope, and x is the distance along the river course. For most rivers, the discharge increases along its course due to the inflow from tributaries; thus, the term sdQ/dx is positive. According to Eq. (1.23), the term Qds/dx must be negative, or the slope of the riverbed decreases along its course; so that rivers exhibit concave riverbed profiles.

Most longitudinal profiles of streams are concave upward. As described previously in the discussion of dynamic equilibrium, streams adjust their profiles and patterns to minimize the time rate of expenditure of potential energy, or stream power, present in flowing water. The concave upward shape of a stream's profile appears to be due to adjustments a river makes to help minimize stream power in a downstream direction. The decrease in slope in a downstream direction results in the concave longitudinal profile.

Figure 1.18 shows the distributions of annual average discharge and average water stage along the course of the Yangtze River. Following the increase in the discharge, the slope of the water surface, which in fact represents the average bed slope, becomes gentler. The bed profile is then a concave shape.
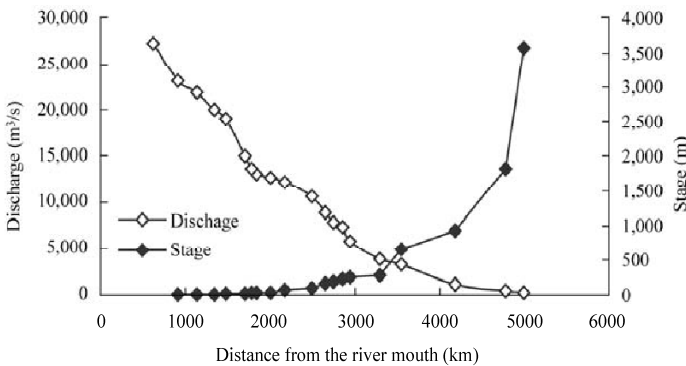
Fig. 1.18 Distribution of annual average discharge and average stage, which represents the longitudinal bed profile of the river, along the course of the Yangtze River

Sinuosity—Sinuosity is not a profile feature, but it does affect stream slope. Sinuosity is the stream length between two points on a stream divided by the valley length between the two points. For example, if a stream is 2,700 m long from point A to point B, and if the valley length distance between those two points is 1,000 m, that stream has a sinuosity of 2.7. A stream can increase its length by increasing its sinuosity, resulting in a decrease in slope.

Channel cross sections—Figure 1.19 presents the type of information that should be recorded when collecting stream cross-sectional data. In stable alluvial streams, the high points on each bank represent the top of the bankfull channel. Channel cross sectional data need to include enough points to define the channel related with a portion of the floodplain on each side.
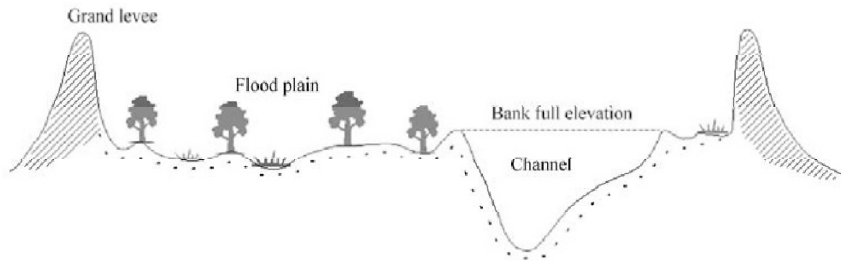
Fig. 1.19 Typical channel cross section

Resistance and velocity—Channel slope and roughness are important factors in determining stream flow velocity. Flow velocity is used to help predict what discharge a cross section can convey. As discharge increases, either flow velocity, flow area, or both must increase. Roughness plays an important role in streams. It helps determine the depth or stage of flow in a stream reach. As flow velocity slows in a stream reach due to roughness, the depth of flow has to increase to maintain the volume of flow that entered the upstream end of the reach. This is the concept known as flow continuity. Typical roughness along the boundaries of the stream includes: sediment particles of different sizes; bed forms; bank irregularities; the type, amount, and distribution of living and dead vegetation; and other obstructions. Roughness generally increases with increasing particle size. The shape and size of instream sediment deposits, or bed forms, also contribute to roughness.

1.1.7 Chemical Features

Scientists have been able to define several interdependent cycles for many of the common dissolved constituents in water. Central among these cycles is the behavior of oxygen, carbon, and nutrients, such as nitrogen (N), phosphorus (P), sulfur (S), and smaller amounts of common trace elements.

The total concentration of all dissolved ions in water, also known as **salinity**, varies widely. Precipitation typically contains only a few parts per thousand (ppt) of dissolved solids, while the salinity of seawater averages about 35 ppt.

pH, alkalinity, and acidity—The acidic or basic (alkaline) nature of water is commonly quantified by the negative logarithm of the hydrogen ion concentration, or pH. A pH value of 7 represents a neutral condition; a pH value less than 5 indicates moderately acidic conditions; a pH value greater than 9 indicates moderately alkaline conditions. Many biological processes, such as reproduction, cannot function in acidic or alkaline waters.

Dissolved oxygen—Dissolved oxygen (DO) is a basic requirement for a healthy aquatic ecosystem. Most fish and aquatic insects "breathe" oxygen dissolved in the water column. Some fish and aquatic organisms are adapted to low oxygen conditions, but most sport fish species, such as trout and salmon,

suffer if DO concentrations fall below a concentration of 3 to 4 mg/L. Larvae and juvenile fish are more sensitive and require even higher concentrations of DO (USEPA, 1997). Many fish and other aquatic organisms can recover from short periods of low DO in the water. However, prolonged episodes of depressed DO concentrations of 2 mg/L or less can result in "dead" water bodies.

Water absorbs oxygen directly from the atmosphere, and from plants as a result of photosynthesis. The ability of water to hold oxygen is influenced by temperature and salinity. Water loses oxygen primarily by respiration of aquatic plants, animals, and microorganisms. Due to their shallow depth, large surface exposure to air, and constant motion, undisturbed streams generally contain an abundant DO supply. However, external loads of oxygen-demanding wastes or excessive plant growth induced by nutrient loading followed by death and decomposition of vegetative material can deplete oxygen.

Oxygen may be produced in stream by aquatic plants. Through photosynthesis, plants capture energy from the sun to fix carbon dioxide into reduced organic matter as follows:

$$6CO_2 + 6H_2O + 36ATP = C_6H_{12}O_6 + 6O_2 \qquad (1.24)$$
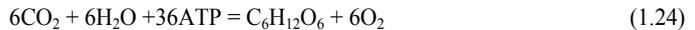
where 36 ATP reflects the light energy necessary for photosynthesis.

Note that photosynthesis produces oxygen. Plants utilize their simple photosynthetic sugars and other nutrients (notably nitrogen [N], phosphorus [P], and sulfur [S] with smaller amounts of several common and trace elements) to operate their metabolism and to build their structures. Most animal lifes depend on the release of energy stored by plants in the photosynthetic process. This process is known as respiration and consumes oxygen. The actual process of respiration involves a series of energy converting oxidation-reduction reactions. This defines the biological oxygen demand.

Sediment oxygen demand (SOD) represents the oxygen demand of respiration of organisms in the sediment and the benthic decomposition of organic material. The demand for oxygen by sediment and benthic organisms can, in some instances, be a significant fraction of the total oxygen demand in a stream. This is particularly true in small streams. The effects may be particularly acute during low-flow and high-temperature conditions, as microbial activity tends to increase with increased temperature.

Nutrients—In addition to carbon dioxide and water, aquatic plants (both algae and higher plants) require a variety of other elements to support their bodily structures and metabolism. Just as with terrestrial plants, the most important of these elements are nitrogen and phosphorus. Additional nutrients, such as potassium, iron, selenium, and silica, are needed in smaller amounts and generally are not limiting factors to plant growth. When these chemicals are limited, plant growth may be limited. However, excessive growth of algae and other aquatic plants instream can result in nuisance conditions and the depletion of DO during nonphotosynthetic periods by the respiration of plants and decay of dead plant material can create conditions unfavorable to aquatic life.

Phosphorus in freshwater systems exists in either a particulate phase or a dissolved phase. Both phases include organic and inorganic fractions. The organic particulate phase includes living and dead particulate matter, such as plankton and detritus. Inorganic particulate phosphorus includes phosphorus precipitates and phosphorus adsorbed to particulates. In the aquatic environment, nitrogen can exist in several forms—dissolved nitrogen gas (N_2), ammonia and ammonium ion (NH_3 and NH_4^+), nitrite (NO_2^-), nitrate (NO_3^-), and organic nitrogen as proteinaceous matter or in dissolved or particulate phases. The most important forms of nitrogen in terms of their immediate impacts on water quality are the readily available ammonia ions, nitrites, and nitrates. Only a few life-forms (for example, certain bacteria and bluegreen algae) have the ability to fix nitrogen gas from the atmosphere. Most plants can use nitrogen only if it is available as ammonia (NH_3, commonly present in water as the ionic form ammonium, NH_4^+) or as nitrate (NO_3^-).

Toxic chemicals—Toxic organic chemicals (TOC) are synthetic compounds that contain carbon, such as polychlorinated biphenyls (PCBs) and most pesticides and herbicides. Many of these synthesized

compounds tend to persist and accumulate in the environment because they do not readily break down in natural ecosystems. Some of the most toxic synthetic organics, DDT and PCBs, have been banned from use in the United States for decades yet continue to cause problems in the aquatic ecosystems of many streams. The chemical industry has produced many useful organic chemicals: plastics, paints and dyes, fuels, pesticides, pharmaceuticals, and other items of modern life. These products and their associated wastes and byproducts can interfere with the health of aquatic ecosystems.

Degradation—Synthetic organic compounds (SOC) can be transformed into a variety of degradation products. Ultimate degradation, or mineralization, results in the oxidation of organic carbon to carbon dioxide. Major transformation processes include photolysis, hydrolysis, and oxidation-reduction reactions. The latter are commonly mediated by biological systems.

Photolysis refers to the destruction of a compound by the energy of light. The energy of light varies inversely with its wavelength. Long-wave light lacks sufficient energy to break chemical bonds. Short wave light (x-rays and gamma rays) is very destructive; fortunately for life on earth, this type of radiation largely is removed by the upper atmosphere. Light near the visible spectrum reaches the earth's surface and can break many of the bonds common in SOC.

Oxidation-reduction reactions are what fuels most metabolism in the biosphere. SOC are generally considered as sources of reduced carbon. In such situations, what is needed for degradation is a metabolic system with the appropriate enzymes for the oxidation of the compound. A sufficient supply of other nutrients and a terminal electron acceptor are also required.

1.1.8   River Ecology

Ecology is the science of studying the relations among different organisms and the relations between organisms and their environment.

Terrestrial ecosystems—The biological community of a stream corridor is determined by the characteristics of both terrestrial and aquatic ecosystems. The terrestrial ecosystem is composed of biological communities living or growing on land (the watershed). Terrestrial ecosystems are fundamentally tied to processes within the soil. The ability of a soil to store and cycle nutrients and other elements depends on the properties and microclimate (i.e., moisture and temperature) of the soil, and the soil's community of organisms.

Terrestrial plant communities—These plant communities in the watershed are a valuable source of energy for the biological communities, provide physical habitat, and moderate solar energy fluxes to and from the surrounding aquatic and terrestrial ecosystems. Given adequate moisture, light, and temperature, the vegetative community grows in an annual cycle of active growth/production, senescence, and relative dormancy. The growth period is the product of incidental solar radiation, which drives the photosynthetic process through which inorganic carbon is converted to organic plant materials.

The distribution and characteristics of vegetative communities are determined by climate, water availability, topographic features, and the chemical and physical properties of the soil, including moisture and nutrient content. The characteristics of the plant communities directly influence the diversity and integrity of the faunal communities. Plant communities that cover a large area and that are diverse in their vertical and horizontal structural characteristics can support far more diverse faunal communities than relatively homogenous plant communities, such as meadows. As a result of the complex spatial and temporal relation that exist between **floral and faunal communities**, current ecological characteristics of these communities reflect the recent historical (100 years or less) physical conditions of the landscape.

The quantity of terrestrial vegetation, as well as its species composition, can directly affect stream channel characteristics. Root systems in the streambank can bind bank sediments and moderate erosion processes. Trees and smaller woody debris that fall into the stream can deflect flows and induce erosion

at some points and deposition at others. Thus, woody debris accumulation can influence pool distribution, and the formation of microhabitats for aquatic communities.

The sensitivity of animal communities to vegetative characteristics is well recognized. Numzerous animal species are associated with particular plant communities, many require particular developmental stages of those communities (e.g., old-growth,) and some depend on particular habitat elements within those communities (e.g., snags). The structure of streamside plant communities also directly affects aquatic organisms by providing inputs of appropriate organic materials to the aquatic environment and providing cover along banks, and by influencing instream habitat structure through inputs of woody debris (Gregory et al. 1991).

Plant communities can be viewed in terms of their **internal complexity,** including the number of layers of vegetation and the species comprising each layer; competitive interactions among species; and the presence of detrital components, such as litter, downed wood, and snags. Species and age composition of vegetation structure also can be extremely important. The quality and vigor of the vegetation can affect the productivity of fruits, seeds, shoots, foots, and other vegetative features. Poorer vigor can result in less food and fewer consumers (wildlife).

Plant communities are dynamic and change over time. The differing regeneration strategies of particular vegetation types lead to characteristic patterns of **plant succession** following disturbances in which pioneer species well-adapted to bare soil and plentiful light are gradually replaced by longer-lived species that can regenerate under more shaded and protected conditions.

Terrestrial fauna—Stream corridors are used by wildlife more than any other habitat type (Thomas et al. 1979) and are a major source of water to wildlife populations. The faunal composition of a stream corridor is a function of the interaction of food, water, cover, and spatial arrangement (Thomas et al. 1979). Stream corridors offer the optimal habitat for many forms of wildlife because of the proximity to a water source and an ecological community that consists primarily of hardwoods in many parts of the U.S., which provide a source of food, such as nectar, catkins, buds, fruit, and seeds (Harris 1984).

The spatial distribution of vegetation is also a critical factor for wildlife. The linear arrangement of streams results in a maximized edge effect that increases species richness because a species can simultaneously access more than one cover (or habitat) type and exploit the resources of both (Leopold 1933). Edges occur along multiple habitat types including the aquatic, riparian, and upland habitats. Forested connectors between habitats establish continuity between forested uplands that may be surrounded by unforested areas. These act as feeder lines for dispersal and facilitate repopulation by plants and animals. Thus, connectivity is very important for retaining biodiversity and genetic integrity on a landscape basis.

Reptiles and amphibians—Nearly all amphibians (salamanders, toads, and frogs) depend on aquatic habitats for reproduction and overwintering. While less restricted by the presence of water, many reptiles are found primarily in stream corridors and riparian habitats. Thirty-six of the 63 reptile and amphibian species found in west-central Arizona in the U.S. were found to use riparian zones. In the Great basin, 11 of 22 reptile species require or prefer riparian zones (Ohmart and Anderson, 1986).

Birds—Birds are the most commonly observed terrestrial wildlife in riparian corridors. Bird species richness reflects the vegetative diversity and width of the river corridor. Over half of these breeding birds are species that forage for insects on foliage (e.g. vireos, warblers) or species that forage for seeds on the ground (e.g. doves, orioles, grosbeaks, and sparrows). Next in abundance are insectivorous species that forage on the ground or on trees (e.g. thrushes, and woodpeckers).

Mammals—The combination of cover, water, and food resources in riparian areas makes them desirable habitat for large mammals such as deer, moose, and elk that can use multiple habitat types. Other mammals depend on riparian areas in some or all of their range.

Hoover and Wills (1984) reported 59 species of mammals in cottonwood riparian woodlands of Colorado,

the U.S., second only to pinyon-juniper among eight other forested cover types in the region. Fifty-two of the 68 mammal species found in west-central Arizona, the U.S., in Bureau of Land Management inventories use riparian habitats. Stamp and Ohmart (1979) found that riparian areas had a greater diversity and biomass of small mammals than adjacent upland areas.

Aquatic ecosystems and aquatic habitat—The biological diversity and species abundance in streams depend on the diversity of available habitats. Naturally functioning, stable stream systems promote the diversity and availability of habitats. A stream's cross-sectional shape and dimensions, its slope and confinement, the grain-size distribution of bed sediments, and even its planform affect aquatic habitat. Under less disturbed situations, a narrow, steep-walled cross section provides less physical area for habitat than does a wider cross section with less steep sides, but may provide more biologically rich habitat in deep pools compared to a wider, shallower stream corridor. A steep, confined stream is a high-energy environment that may limit habitat occurrence, diversity, and stability.

Habitat—Habitat is a term used to describe an area where plants or animals (including people) normally live, grow, feed, reproduce, and otherwise exist for any portion of their life cycle. Habitats provide organisms or communities of organisms with the necessary elements of life, such as space, food, water, and shelter. Under suitable conditions often provided by stream corridors, many species can use the corridor to live, find food and water, reproduce, and establish viable populations. Habitat increases with stream sinuosity. Uniform sediment size in a streambed provides less potential habitat diversity than a bed in which many grain sizes are represented. Habitat subsystems occur at different scales within a stream system (Frissell et al. 1986). The grossest scale, the stream system itself, is measured in thousands of meters, while segments are measured in hundreds of meters and reaches are measured in tens of meters. A reach system includes combinations of debris dams, boulder cascades, rapids, step/pool systems, pool/riffle sequences, and or other types of streambed forms or "structures," each of which could be 3 m or less in scale. Frissell's smallest scale habitat subsystem includes features that are 0.3 m or less in size. Examples of these microhabitats include leaf or stick detritus, sand or silt over cobbles or other coarse material, moss on boulders, or fine gravel patches.

Wetlands—Wetlands is a general term used to describe areas, which are neither fully terrestrial nor fully aquatic. Wetlands are lands where saturation with water is the dominant factor determining the nature of soil and vegetation development. The International Union for the Conservation of Nature and Natural Resources organized an international conference for wetland protection in Ramsar in 1971 and the member states signed the Convention on Wetlands of International Importance Especially as Waterfowl Habitat, which is known as Ramsar Wetland Convention. China has become a member state since 31 July 1992. As shown in Fig. 1.20 wetlands are defined by the wetland convention as areas of marsh, everglade, fen, peatland and swamp, where natural or artificial, permanent or temporary, with water that is static of flowing, fresh, brackish or salt, including areas of marine water, the depth of which at low tide does not exceed six meters (www.ramsar.org).

The minimum essential characteristics of a wetland are recurrent, sustained inundation or saturation at or near the surface and the presence of physical, chemical, and biological features that reflect recurrent sustained inundation or saturation. Common diagnostic features of wetlands are hydric soils and hydrophytic vegetation. These features will be present except where physicochemical, biotic, or anthropogenic factors have removed them or prevented their development (National Academy of Sciences, 1995). Wetlands may occur in streams, riparian areas, and floodplains of the stream corridor. Wetlands are transitional between terrestrial and aquatic systems where the water table is usually at or near the surface or the land is covered by shallow water (Cowardin et al., 1979). For vegetated wetlands, water creates conditions that favor the growth of hydrophytes-plants growing in water or on a substrate that is at least periodically deficient in oxygen as a result of excessive water content (Cowardin et al., 1979) and promotes the

development of hydric soils—soils that are saturated, flooded, or ponded long enough during the growing season to develop anaerobic conditions in the upper part (National Academy of Sciences, 1995).
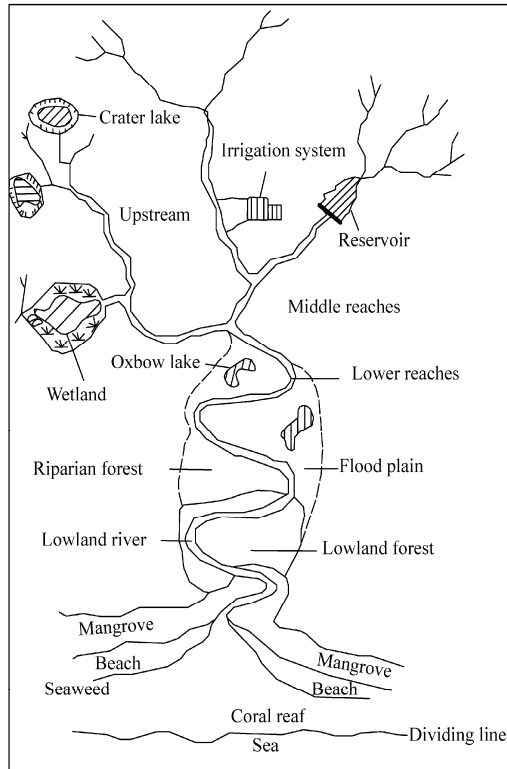
Fig. 1.20   Wetlands defined in Ramsar Wetland Convention

Wetland functions include fish and wildlife habitat, water storage, sediment trapping, flood damage reduction, water quality improvement/pollution control, and ground water recharge. Wetlands have long been recognized as highly productive habitats for threatened and endangered fish and wildlife species. Wetlands provide habitat for 60 to 70 percent of the animal species federally listed in the U.S. as threatened or endangered (Lohoefner, 1997).

Mangroves—Mangroves are a diverse group of plants, which have been able to exploit a habitat of inter tidal zones. There are 55 species of mangroves in 10 families. The largest mangrove forests are in Bangladesh and Nile Delta. China has mangrove forests in Guangxi and Hainan Provinces and the Pearl River delta. The last few decades have seen a rapid growth of interest in the mangrove ecosystems. This is due, on the one hand, to the perception that mangrove ecosystems are valuable resources, and, on the other hand, due to vested economic interests. Mangroves are remarkable tropical plants that grow with their roots partly or wholly submerged in seawater. They make tidal forests in the tropical and subtropical zones, and these rainforests, referred to as "mangal," straddle the abrupt interphase between sea and land. They are economically important because they are a source of timber. The bark of mangroves are materials for production of red dye, therefore, they are named red tree in Chinese. Mangroves also protect shorelines from wave damage and provide a nursery for many commercial fish. To the scientist they offer an interesting opportunity to study organisms that adapt to both marine and terrestrial environments

(Tomlinson, 1986).

Mangroves are exposed to saltwater inundation, low oxygen levels around their roots, high light and temperature conditions, and periodic tropical storms. Despite these harsh conditions, mangroves may form luxuriant forests, which have significant economic and environmental value throughout the world—they provide coastal protection and underpin fisheries and forestry operations, as well as a range of other human activities. The red mangrove has tangled, reddish roots. The mangrove appears to be standing or walking on the surface of the seawater with muddy bed, and therefore, has a nickname of working tree.

Mangroves can only live on muddy coast and not able to grow on sand beaches. Reproduction in red mangroves is primarily accomplished through embryo production. Mangroves have floating seeds that germinate while still attached to the mother plant. An embryo may be embedded in the mud as it falls and thus, it soon germinates. Figure 1.21 shows a mangrove forest in Deep Bay in the Pearl River estuary with embryo attached on the mother tree in the left picture and seedling of mangrove growing on the muddy coastal beach in the right picture.

(a)   (b)
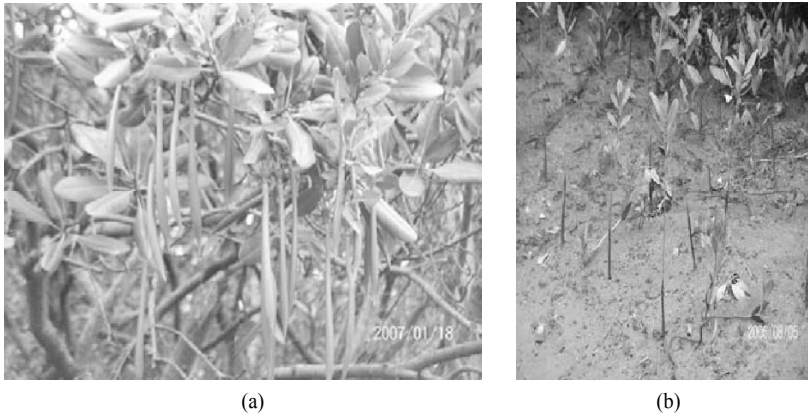
Fig. 1.21 (a) Mangrove forest in the muddy Deep Bay in the Pearl River estuary; (b) Seedling of mangroves growing on the muddy beach

Riparian area—Riparian areas are the areas contiguous to and affected by surface and subsurface hydrological features of perennial or intermittent lotic and lentic water bodies (rivers, streams, lakes, and drainage ways). Riparian areas have one or both of the following characteristics: ① distinctly different vegetative species than adjacent areas; and ② species similar to adjacent areas but exhibiting more vigorous or robust growth forms. Riparian areas are usually transitional between wetland and upland.

Aquatic plants—Aquatic plants usually consist of algae and mosses attached to permanent stream substrates. Rooted aquatic vegetation may occur where substrates are suitable and high currents do not scour the stream bottom.

Benthic invertebrate—The benthic invertebrate community of streams may contain a variety of biota, including bacteria, protists, rotifers, bryozoans, worms, crustaceans, aquatic insect larvae, mussels, clams, crayfish, and other forms of invertebrates. Aquatic invertebrates are found in or on a multitude of microhabitats in streams including plants, woody debris, rocks, interstitial spaces of hard substrates, and soft substrates (gravel, sand, and muck). Generally speaking, there are more benthic invertebrates in gravel bed than a sand bed. Figure 1.22 shows some species of macro-invertebrates from gravel bed streams. Invertebrate habitat at all vertical strata including the water surface, the water column, the bottom surface, and deep within the hyporheic zone.
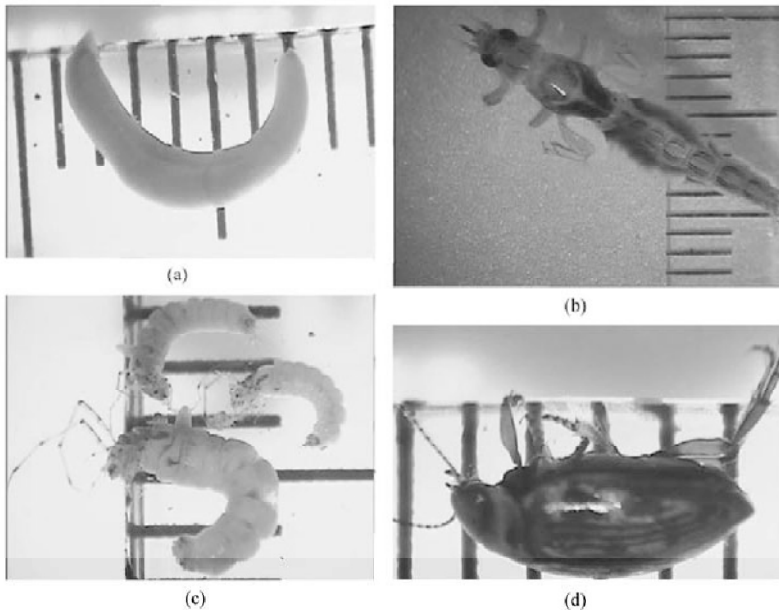
Fig. 1.22 Some species of benthic macro-invertebrates living in gravel bed rivers: (a) leech (*Hirudinea*); (b) mayfly (*Ephemeridae*); (c) caddis fly (*Trichoptera*); and (d) *Dytiscidae*

Fish—Fish are ecologically important in the stream ecosystems because they are usually the largest vertebrates and often are the apex predator in the aquatic systems. The numbers and species composition of fish in a given stream depends on the geographic location, evolutionary history, and such intrinsic factors as physical habitat (current, depth, substrates, riffle/pool ratio, wood snags, and undercut banks), water quality (temperature, DO, suspended solids, nutrients, and toxic chemicals), and biotic interactions (exploitation, predation, and competition).

Indicator species—Landres et al. (1988) defined an indicator species as an organism whose characteristics (e.g., presence or absence, population density, dispersion, reproductive success) are used as an index of attributes or environmental conditions of interest, which are difficult, inconvenient, and expensive to measure for other species. Ecologists and management agencies have used aquatic and terrestrial indicator species as assessment tools for many years. In many cases benthic invertebrates are selected as indicator species for assessment of river ecology. The assumptions implicit in using indicators are that if the habitat is suitable for the indicator it is also suitable for other species and that wildlife populations reflect habitat conditions.

Ecological stress—Ecological stresses are defined as the disturbances that bring changes to river ecosystems. The ecological stresses are natural events or human-induced activities that occur separately or simultaneously. Either individually or in combination, the ecological stresses have the potential to alter the structure and impair the ability of the river ecosystem to perform key ecological functions. A stress occurring within or adjacent to a river typically produces a causal chain of effects, which may permanently alter one or more characteristics of a stable system.

Stream restoration—According to the U.S. National Research Council (NRC, 1992), restoration should involve the return of a given ecosystem to a state approximating that in which it existed prior to disturbances. Restoration of the impaired river ecosystem is necessary for most of the worldrivers.

1.2   Major River Management Issues

1.2.1   Water Resources

Water resources refer to available or possibly available water sources that possess adequate quantity and utilizable quality and may be utilized in a specific location for a specific purpose. Only the available water sources (such as river runoff) and waters in water bodies either on the surface or in groundwater aquifers, which take part in hydrological cycle activities, are considered and counted for quantitative statistics. China has enormous water resources but they are unevenly distributed in space and in time. In per capita terms, China's water resources are about 75% of the Asian average, and 35% of the world average. The total volume of annual runoff is 2.7 trillion m^3, equivalent to about 45% of the precipitation corresponding to a depth of 284 mm over the land area. About 65% of the country's territory lies in catchments of rivers flowing to the sea, and 35% in inland, landlocked basins. About 27% of natural runoff flows into neighboring countries, mainly in the southwest and the northeast boundary rivers. The Ertix River in the far northwest flows north to join the Ob River in Siberia. About 0.6% of the total runoff flows into China from other countries. Glaciers store about 5.1 trillion m^3. Annual melt-water is about 2% of the combined discharge of the inland rivers. Groundwater recharge is about 0.83 trillion m^3 although most of this represents water transformed into river flows under natural conditions and is thus already accounted for by river runoff. Excluding such double counting, the net total water available (surface water plus groundwater) is 2.8 trillion m^3, and the net additional contribution of groundwater is about 0.1 trillion m^3. This is mainly rainfall infiltration on the plains since groundwater in mountainous areas is almost wholly accounted for in base flows which are included in river flows.

The water resources distribution in China is very non-uniform, with the south-east of the country wet and north-west dry. Figure 1.23 shows the 10 water resources zones of China and the inflow and outflow of moisture across the north, east, south, and west borders. The main moisture supply is from the south of
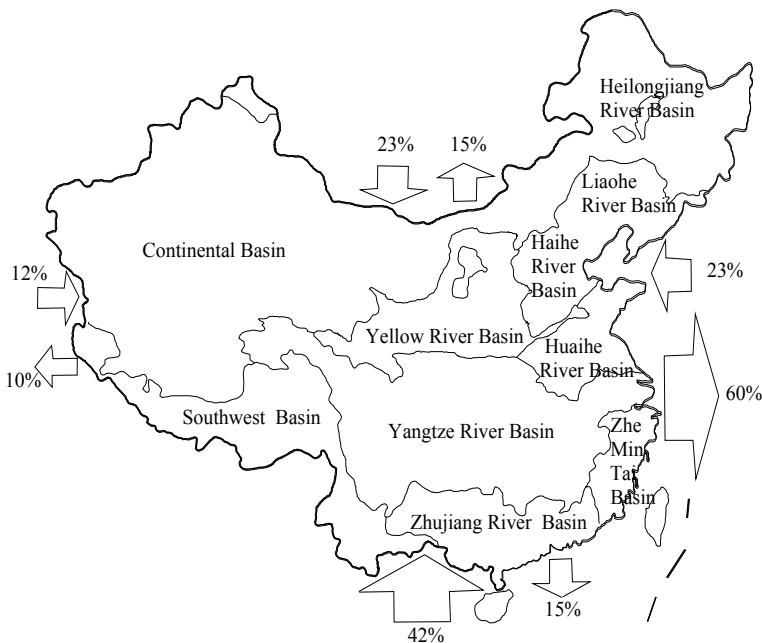
Fig. 1.23   Inflow and outflow of moisture to China and the 10 water resources zones of China

the country, which consists of 42% of the total moisture inflow and the main moisture outflow is across the east border, which is 60% of the total outflow. Therefore, the main moisture flow path over China is from the south border to the east border, which makes the southeasten China wet. Only 10%–23% of the moisture inflow and outflow are across the west and north borders. Thus, the precipitation in north and west China is much less than in south and east China. The average precipitation in the southeast of China is about 2,000 mm, and the highest precipitation takes place at the China-India boundary, which is about 5,000 mm. In the zone south of the Yangtze River the precipitation is about 1,000 mm. In the zone from the Yangtze River to Qingling and the lower Yellow River, it is about 800–900 mm. Further to the north the precipitation reduces to 400–600 mm. precipitation is even less to the northwest. The lowest precipitation occurs in the Turpan basin with average annual rainfall of only 7.1 mm. The reason to make the water resources availability even worse is the non-uniform distribution of rainfall over time. In south China the maximum 4 month precipitation is about 60% of the annual precipitation while in north China the value is 80%. The inter-year variation, defined as the maximum annual precipitation over the minimum annual precipitation is larger than 8 in the northwestern China, 3–4 northeastern china and 2–3 south China.

The surface runoff is mainly transported in the 7 major rivers listed in Table 1.3. In the Pearl River basin the water resources per capita is more than 4000 m^3, but the value is only 260 m^3 in the Haihe-Luanhe River basin.

Table 1.3 Water resources of major rivers in China and comparison with the world average (after Chen, 1991)

River basin	Runoff (10^9 m^3)	Population (million)	Farmland (10^6 ha)	Water/p (m^3/p)	Water/ha (m^3/ha)
Pearl River	336	83	4.7	4,097	71,670
Yangtze River	951	380	23.4	2,505	40,575
Songhua River	74	52	10.4	1,451	7,110
Yellow River	66	93	12.2	716	5,430
Huaihe River	62	142	12.3	439	5,055
Liaohe River	15	34	4.4	435	3,345
Haihe-Luanhe Rivers	29	110	11.3	262	2,550
World average (1987)*	38,830	5,000	1,500	7,766	25,887
World average (1996)*	38,830	5,770	1,500	6,730	25,887
World average (2006)*	38,830	6,480	1,500	5,995	25,887

Note: The total ground water of China is 872 billion m^3;
* Data source: the Ministry of Water Resources of China.

The development of the economy and urbanization has been increasing the water demand very quickly in the past two decades. The number of cities in China increased from 295 in 1984 to 640 in 1995, in the same period the urban population increased from 140 to 400 million. The water consumption per person also increases quickly following the enhancement of the living standards. For the last twenty years, the rapid expansion in urban water supply systems has been evident, both in terms of the increase in the number of urban systems and cities served and in the water supplied for both residential and industrial purposes. In 1996, 95% of the non-agricultural residents living within city boundaries were connected to an urban system, with coverage falling to 85% in the northeast provinces of Heilongjiang, Jilin and Inner Mongolia. However, only 25% of the agricultural residents in the areas defined as urban are served by water systems.

The Water Law of the People's Republic of China stipulates that: "in the development and utilization of water resources, the domestic water demands of urban and rural inhabitants shall be satisfied first,

while agricultural and industrial water demands as well as navigation requirements shall also be considered and taken care of." From the early 1950s to the late 1970s, while the total water use in China increased by four times, the urban water use and industrial water use (inclusive of thermal power water use) increased by eight and twenty-two times respectively. The quality of urban water sources is required to meet the Standards for Environmental Quality of Surface Water and the quality of municipal tap water to meet the Standards for Domestic Drinking Water in China. The mutual relation between water supply and drainage not only lies in the necessity of rationally and timely draining of wastewater, which is equivalent to 60% to 70% of water supply, but also in the necessity of reusing a certain amount of the wastewater after being properly treated. More than two thirds of the cities draw their supplies or part of their supplies from groundwater in the country, and about one fourth of the national public water supply capacity comes from groundwater. Urban water supply is the main purpose of water resources development.

The total water demand of the country is 530 billion m^3 at present. It will increase to 1100 billion m^3 in 2040, thence the water demand will remain at that level. At present, about 500 billion m^3 of water are used. The speed of water resources development will lag behind the increasing water demand. The amount of water shortage will increase from 30 billion m^3 to 100 billion m^3. Inter-basin water transfer projects are the main strategy to ease the water shortage. Seven short distance inter-basin water transfer projects have finished, including the Luanhe-Tianjin water transfer project, the Yellow River-Qingdao project, and the Biliuhe-Dalian project. The long distance inter-basin water transfer projects from the Yangtze River to north China have been launched. The total capacity of the three routes—the east route from Yangzhou to Tianjin, the middle route from Danjiangkou to Beijing, and the west route from the upper reaches and the tributaries of the Yangtze River to the Yellow River is 40–50 billion m^3. Water shortage can only be partly eased but not solved by these transfers. New strategies are needed.

1.2.2 Flooding

Several devastating floods have occurred worldwide in the 1990s, with a long list of flood events each killing more than a thousand people or causing material losses in excess of one billion U.S. dollars (Kundzewicz, 1997). A number of extreme floods of exceptional severity have occurred in the 1990s. A 100-year flood occurred on the Rhine River with stage at Cologne at 10.69 m just 13 months after the previous one in 1993 with stage at the same place 10.63 m. The 1993-flood on the Mississippi river has been regarded as the most devastating flood in the modern history of the United States. Flood records on the main stem of the Mississippi were broken at several observation stations by up to 1.2 m. In St. Louis, Missouri, the previous record stage was exceeded for more than three weeks. In China, five flood events killing over 1,000 persons each occurred in the period 1990–1998, and according to the Munich Reinsurance (Munich Re, 1999) there have been 24 flood events in the world that caused total losses in the excess of one billion U.S. dollars each. The highest flood losses of the order of more than 20 billion U.S. dollars were recorded in 1996 and 1998. The 1998 floods on the Yangtze River, Songhua River and Nenjiang River and the 1996 floods on the Yellow River and Haihe River were highest events in terms of flood stage, economic loss, and the impact on the environment, society, and flood control strategies.

The flood losses in China quickly increased in the 1990s. Figure 1.24 shows the flood losses in 1991–1999 compared with the average annual loss in the 1980s (Cheng, 2002). In the 1990s the flood loss (8 Yuan = 1 U.S. dollar) is much higher than the flood loss in the 1980s. In 1996 and 1998 the flood losses were over 200 billion Yuan. One reason for the ever-increasing flood loss is the development of the economy, the other reason is the increasing flood hazard.

As shown in Fig. 1.25 the high flood risk areas in China are mainly the areas surrounding the lower Yellow River and the middle and lower Yangtze River, the Haihe River basin, the Huaihe River basin, and the Songhua River and Nenjiang River basins. These areas are densely populated and have been rapidly
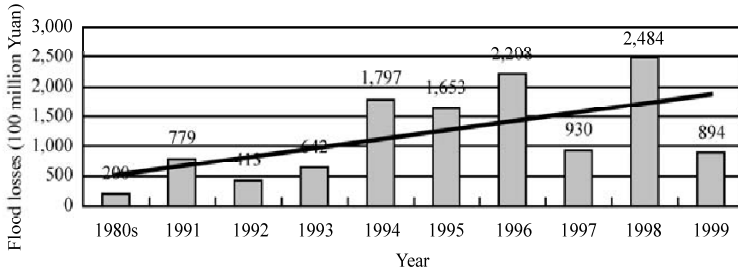
Fig. 1.24   Flood losses in 1991–1999 compared with the average annual loss in the 1980s (after Cheng, 2002)
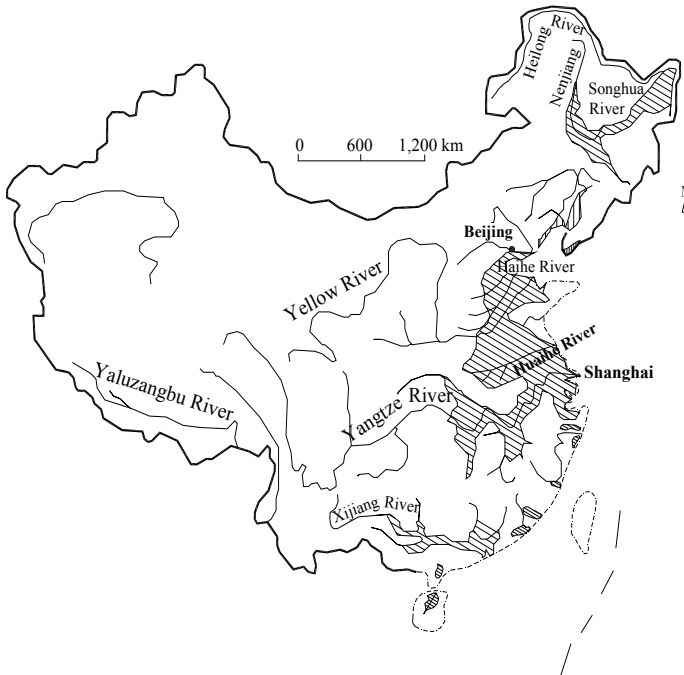
Fig. 1.25   Major rivers and high flooding risk areas (shaded areas) in China

industrialized, therefore, the potential flood damage costs are high. The climate of China is mainly monsoon type and rainstorm floods occur in the summer. The precipitation concentrates within a few months and results in well defined flood and low flow seasons. For instance, the flood season is from late June to September for the Yangtze River, from July to August for the Yellow River, from the mid of July to August for the Haihe River and from August to September for the Songhua and Nenjiang Rivers. The rainfall intensity in China is high, therefore, the peak discharge is high. Figure 1.26 shows the highest flood discharge of various scales of the drainage areas in China compared with those of the world highest values. The recorded peak discharges are nearly equal to the highest in the world. With the high peak discharge and short flood season, the floods of Chinese rivers are difficult to predict and control (Luo and Luo, 1996).

The 2005 flood on the West River, the 1998 floods on the Yangtze and Songhua Rivers, and the 1996 floods on the Yellow and Haihe Rivers indicate a trend of increasing flood disasters. Figure 1.27 shows that a 100-year flood that hit Wuzhou on the West River basin in Southern China in 2005. Flood water flowed over the levee and flooded the residences and the commercial areas of the city. The flood loss was great.
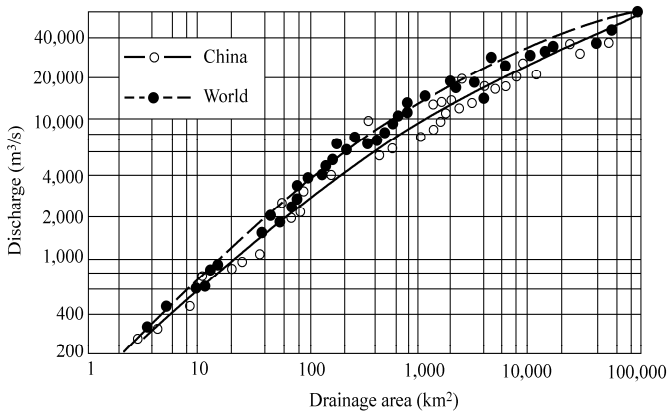
Fig. 1.26 The highest flood discharge of rivers as a function of drainage area in China compared with rivers throughout the world (after Luo and Luo, 1996)

Not only huge flood but also small flood may cause great loss. Figure 1.28 shows people escaping from the flooded floodplain of the Yellow River, which is in Henan Province near Zhengzhou, during the 1996 flood. The flood discharge was 7,860 m^3/s, which was only a 2-year flood. About 2.41 million people were affected by the flood and 800 million U.S. dollars were lost. The main causes of the high flood disaster were the abnormal high stage and low conveyance capacity of the channel due to sedimentation. In the lower reaches the river flood plain is confined between the grand levees of the Yellow River. Rapid economic development and population growth lead to extensive invasion into the river floodplain. Although the total amount of annual sediment deposition in the lower Yellow River was reduced, the amount of sediment deposition in the main channel was increased. Consequently, the channel cross section became smaller, and the water conveying capacity of the river channel was greatly reduced.
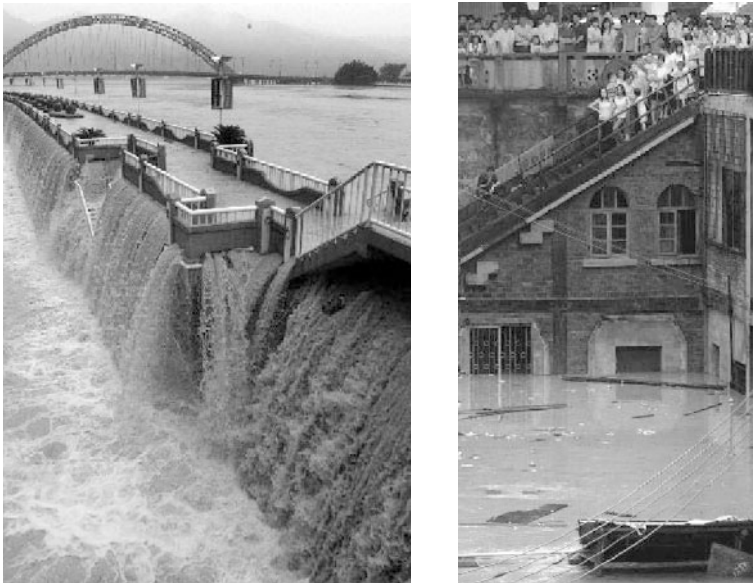
Fig. 1.27 A 100-year flood hit the Wuzhou City in the West River basin in 2005

Fig. 1.28 People escaping from the flooded floodplain at Changyuan, which is in Henan Province near Zhengzhou during the 1996 flood period

In 1998 a rare flood occurred on the Yangtze River, which resulted in serious flood damages and affected 8 million people. Heavy rainfalls occurred in the area in the summer of 1998 in the wake of the strongest El Nino phenomenon of the century, which reached its maximum at the end of 1997 and ended in May 1998. Meteorologists have hypothesized that this phenomenon increased the snow accumulation in Europe and on the Qinghai-Tibet Plateau. Because more snow accumulated, the monsoon was delayed and the major rain belt was shifted to the South, and more rain fell in the Yangtze River Valley.

The recurrence period of the 1998 flood is only 8 years in terms of the crest flood discharge and the recurrence period is about 100 years in terms of flood volume (Ministry of Water Resources, 1999). During the flood, one levee breach occurred at Jiujiang City on the Yangtze River and it was closed in several days. The cities and main railways and highways were not affected by the flood. The flood caused 1,075 polder levee breaches, inundated 321,000 ha of land. The death toll was 2,292, most of which were the victims of flash floods and debris flows in the mountains.

The flood disasters in recent years exhibit new features different from the traditional flood disasters. In summary, flood disasters in China are more frequent than in earlier times because increasing population pressure and economic development are changing the river regime, and the flood control system has not matched the change (Cheng, 2002). The disastrous flood on the Yangtze River in 1998 is a result of abnormal heavy rainfall, but the extremely high flood stage is due to less flood diversion, reduced regulation capacity of riparian lakes, and channel sedimentation. The Yangtze River also experienced higher stages at lower flows in the 1998 flood compared with the 1954 flood. New river management and flood control strategies are needed to meet the challenge of flooding.

1.2.3 Soil Erosion

Environmental health encompasses the maintenance and quality of the natural resources: soil, water, air, and biota. According to preliminary statistics compiled for the world, the annual erosion of surface soil from river basins amounts to 60 billion tons, of which 17 billion tons are discharged into the oceans. In the process, as much as 5 to 7 million ha of farms are annually ruined. Moreover, aeolian erosion of bare lands has intensified desertification after depriving the ground of good top soil. Eroded soil contains nitrogen, phosphorous, and other nutrients that deposit in lakes and reservoirs contaminating the waters resulting in eutrophication and other biological as well as chemical processes.

China is a country suffering severe erosion, with 1.82 million km^2 subject to water erosion, 1.88 million km^2 subject to aeolian erosion, and 1.25 million km^2 subject to glacial erosion. In other words, more than

46% of the territory of the country are being eroded. Parts of the territory of China are overlaid with loess; these include the southern part of the northeastern China and the southeast part of the northwestern China. The loess widely spreads over the Yellow River basin extending from the east of Qinghai Province in the west and the relics of the Great Wall in the north to Qinling Mountain in the south and the coastal region in the east. The loess is quite uniform in its textural lack of granular structure, and it is bound together mainly by calcium sulphate that is highly soluble and apt to be leached and eroded by rainfall. In addition, with a porosity ratio as high as 40%, loess is characterized by well-developed vertical joints that are susceptible to erosion and weathering. Over history, most of the vegetation in the basin has been destroyed and the erosion process has been aggravated. The severe soil erosion has not been brought entirely under control over the basin, although great efforts have been devoted to soil conservation. According to preliminary statistics, annual soil loss in the middle Yellow River basin amounts to 3,700 $t/yr.km^2$, on average, which is about 27.5 times the average annual rate throughout the world of 134 $t/yr.km^2$. Enormous amounts of sediment are eroded from the basin and flow through mountain creeks and streams to the river, producing a sediment concentration that is higher than in almost any other part of the world. Figure 1.29 shows the Loess Plateau consisting of very erodible soil.

Fig. 1.29   Soil erosion in the Loess Plateau of central China bring a huge amount of sediment to the lower reaches of the Yellow River (See color figure at the end of this book)

The total soil volume eroded from the Yellow River basin is about 2.3 billion tons per year. Comparably, the total soil volume eroded from the Yangtze River basin is about 2.2 billion tons per year. From 1950 to 1996, the Chinese people had improved 0.7 million km^2 of the land susceptible to water-erosion, but in the mean time, the total land susceptible to water-erosion has increased from 1.16 million km^2 to 1.82 million km^2. As a result the untreated land susceptible to water-erosion remains at 1.13 million km^2 (Wang, 2000). The main causes for the increase of land susceptible to water-erosion are deforestation, overgrazing, harvest of medical herbs, slope tillage, development of mining and urbanization. For instance, people in the Xiaojiang watershed on the Yunnan-Guizhou Plateau of China cut trees and burned the wood for iron and copper production in 1958. The forest cover was reduced from 23% to 18% due to logging and the erosion rate was almost doubled. In the Yangtze River basin alone, the area of steep slope land people are still plowing is more than 11 million ha. The Shenfu-Dongsheng coal mining removed 162 million tons of soil in the period 1998–2000, and thus, greatly intensified the erosion rate.

Erosion causes many problems. More than 5 billion tons of fertile soil are lost every year due to erosion,

in which the amount of nitrogen, phosphorus and potassium in the eroded soil is about 50 million tons, which is much higher than the annual national production of fertilizer (30 million tons). The farmland deteriorates and grain production also is reduced by erosion. Moreover, the nutrients are transported with the sediment into the environmental waters and causes eutrophication and red tide. More than 240 harmful algal blooms occurred in the 1990s, causing huge economic losses. Erosion exerts the highest ecological stress on the vegetation cover. In the northern part of the Loess Plateau, the vegetation can hardly develop because the extremely intensive erosion carries off the topsoil on which the vegetation relies. In the areas with vegetation, such as the upper reaches of the Yangtze River, erosion damages and destroys the vegetation and scars the land surface.

Erosion from the upper reaches provides the rivers with too much sediment that causes sedimentation of the channels and high flood risks. For instance, the Yellow River is notorious for its frequent avulsions and flooding disasters. The main reason is the heavy sediment load from the erosion of the Loess Plateau. The Yellow River sediment causes not only the siltation of the lower channel reaches of the river itself, but also the shrinkage of the mouths of drainage channels of the Haihe River drainage system. Figure 1.30 shows that the silt drifting from the Yellow River mouth under the action of tidal currents is deposited at the New Ziya River mouth, which is one of the major drainage channels of the Haihe River Drainage System. The channel is silted up by 6 m and the discharge capacity of the channel has reduced by 60% (Hu et al., 1999).

The main erosion control strategies applied in China are building sediment barriers in gullies and terracing the sloped farmland in the arid and semi-arid areas; building sediment-check dams and reforesting the hills in the wet areas; and comprehensive reclamation of small river basins in both arid and wet areas. Comprehensive reclamation of small basins is the main strategy applied in the Loess Plateau. The area is arid and semi-arid and, therefore, reforestation alone is difficult to achieve the objective of erosion control. People built many sediment barriers and created productive warped farmland. Terraced fields enclosed with borders 20 cm high may trap almost all rainfall water and greatly reduce erosion. Impounding water with dam on rivers provides water for drinking, irrigation, and reforestation. People plant grass on the slope and trees around the fields and roads. As a result, the sediment fed into the rivers by erosion from the Loess Plateau has been greatly reduced since 1984 (Gu, 1994).

Fig. 1.30 The silt drifting from the Yellow River mouth under the action of tidal currents is deposited at the New Ziya River mouth. The channel is silted up by 6 m and the discharge capacity of the channel has reduced by 60% (See color figure at the end of this book)

Reforestation is effective in wet areas (the southern China, for example) if mass movement of soil is controlled by multiple check dams. The success of reforestation relies more on the agricultural policy than technology. The change of ownership from community to private households has incited incentives for farmers toward reforestation since the 1980s. After the 1998-flood on the Yangtze River state-funded reforestation projects in the upper Yangtze River watershed sped up. Reforestation has been successful in many watersheds. Nevertheless, in mountainous areas people are still burning wood for cooking and heating. Planting shrubs and fast-growing trees in selected zones to provide the local people fuel wood is an effective measure to protect the forest.

1.2.4   Riverbed Incision and Geological Disasters

Riverbed incision is defined as continuous bed erosion and bed-level lowering. Mountain rivers either were or are incised rivers. Alluvial rivers may also experience a shot period of bed incision. Riverbed incision may be caused by tectonic motion, meanders cutoff, stream caption, dam construction, channelization and many other causes. Geologic and geomorphic causes require many years to develop a response, whereas climatic and hydrologic variability, animal grazing, and human activities can have a more immediate impact. Figure 1.31(a) shows the stream bed incision in the upper Yangtze River (Jinsha River) in the southwestern China. The rising Qinghai-Tibet Plateau increases the stream slope and bed erosion. The plateau has deeply incised by the river by more than 2,000 m. Figure 1.31(b) shows an incised section of the Yunzhong River, which is a tributary of the Hutuo River in Hebei Province in North China. Impoundment of a reservoir trapped sediment and released clear water, which resulted in several meters bed incision in the downstream reach of the reservoir.

(a)   (b)

Fig. 1.31   (a) The upper Yangtze River in the southwestern China incised the Qinghai-Tibet Plateau by more than 2,000 m; (b) Impoundment of a reservoir on the Yunzhong River caused channel bed incision in a downstream reach by several meters

Almost all geological hazards are associated with river bed incision. Channel bed incision increases bank slope and causes bank failures, landslides and debris flows. Moreover, bed incision of a river propagates to its tributaries and gullies. Finally all slopes become steeper and more serious soil erosion occurs. A persistence of landslide events occur in the actively incising river gorges on the eastern margin of the Qinghai-Tibet Plateau. The direct causes of the landslide events were rainstorm and earthquake, while the essential cause of the events was river bed incision. The Wenchuan earthquake on May 12, 2008 triggered several hundreds of large scale landslides on numerous rivers, which were all incised rivers. Figure 1.32(a) shows a huge avalanche on the deeply incised Kangding River on the east margin of the

Qinghai-Tibet Plateau, which was triggered by an earthquake (Ms 7.5) in 1955. Figure 1.32(b) shows a landslide dam triggered by the Wenchuan earthquake (Ms 8.0) on the Zongqu Ravine in Maoxian, Sichuan on May 12, 2008. The Zongqu Ravine was deeply incised and the slopes are very steep. Although the ravine is not close to the epicenter but the landslide occurred because of bed incision makes the slopes unstable.

(a)   (b)
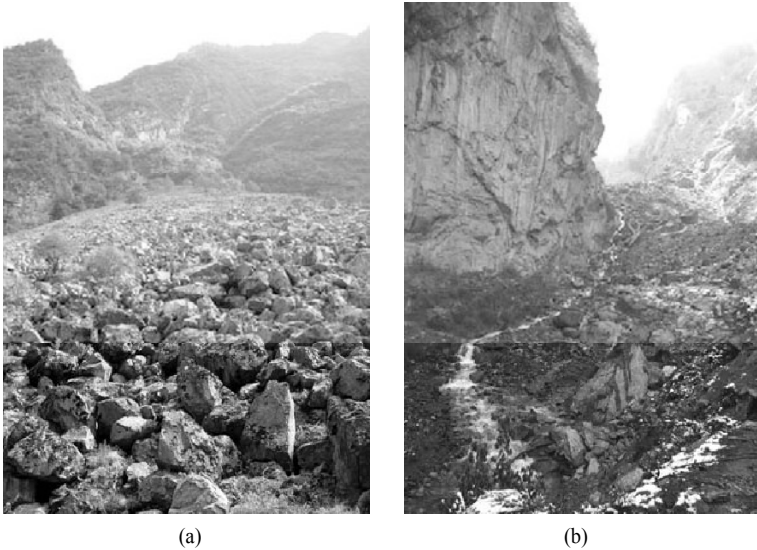
Fig. 1.32   (a) A huge avalanche on the deeply incised Kangding River on the eastern margin of the Qinghai-Tibet Plateau, which was triggered by an earthquake (Ms 7.5) in 1955; (b) A landslide triggered by the Wenchuan earthquake created a 70 m high landslide dam on the Zongqu Ravine in Maoxian, Sichuan on May 12, 2008

The eastern margin of the Qinghai-Tibet Plateau is one of the world's broadest and most dramatic transient landscapes that has been deeply incised by major rivers and their tributaries (Clark et al., 2006). Major rivers start at high elevations over 4,000 m, where they are slightly incised into the relict landscape, and transition into rapidly incising, high-relief, dissected gorges with steep hillslopes (Ouimet et al., 2007). Hillslopes, following incision, display zones of adjustment with steepest values in the lowermost reaches of individual basins. These observations highlight the transient response of rivers to rapid incision on trunk streams as waves of landscape adjustment propagate upstream and up hillslopes.

The Dadu River and Yalong River are major tributaries of the Yangtze River, both over 1,000 km in length. The Dadu and Yalong rivers have each experienced catastrophic landslide damming events within the past 250 years that were triggered by large earthquakes (>Ms 6.0) (Tianchi, 1990; Dai et al., 2005). Accounts from the example on the Dadu River indicate as many as 100,000 deaths were caused by the downstream flooding associated with initial dam failure, making it one of the most disastrous events ever resulting from a landslide dam breach (Dai et al., 2005). Recent catastrophic events such as these have also been documented in the Min River gorge to the east of the Dadu and in the main Yangtze River gorge to the west of the Yalong, indicating that landslide damming is a widespread and ongoing phenomenon in all river gorges on the eastern margin (Tianchi, 1990; Chai et al. 2000). The dynamic coupling between river incision and landslide dam can significantly influence the evolution of fluvial landscapes. An important feedback exists within rapidly incising landscapes, where hillslope erosion, following incision, slows or stops river incision by covering the bed with larger volumes of sediment or coarser grain sizes of sediment than annual floods can transport downstream.

1.2.5 Pollution and Eutrophication

Most of the rivers are also used to carry wastewater discharged from communities and industry. The river water is polluted and the river environment is damaged. Following the enhancement of people's living standards, the water consumption per capita has increased by several times in the past 30 years. The urban sewage discharge has also increased by 400% between 1980 and 2000, although the treatment and recycling of wastewater has also increased in the same period. Figure 1.33 shows the annual wastewater discharge from towns and cities. The industrial wastewater discharge slightly has reduced since 1990 because of the efforts for pollution control and the increasing rates of wastewater treatment and recycling. Nevertheless, urban sewage discharge has increased by doubling on average each 4 years and the trend is still continuing. The annual sewage discharge was over 22 billion tons in 1998.
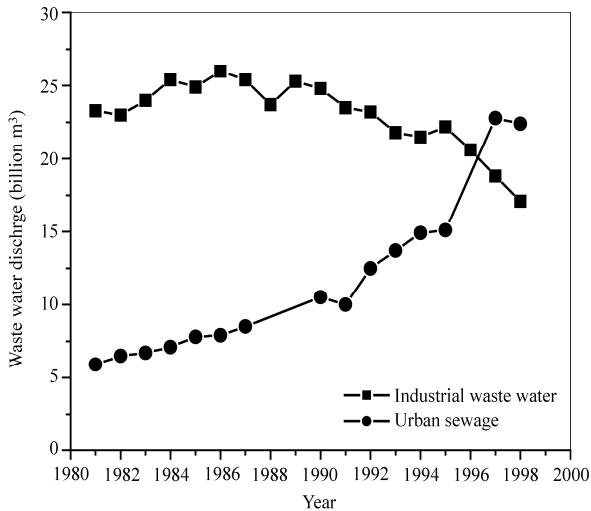
Fig. 1.33 Industrial wastewater and urban sewage discharges into Chinese rivers and seas in the period 1980–2000 (Wang et al., 2001)

The wastewater and sewage are partly discharged into the rivers without any treatment. Heavy metals, toxic materials, and nutrients in the wastewater and sewage pollute the rivers. The Huaihe River water had been using for drinking before the 1990s. In the 1980s, the river was polluted by the wastewater from numerous paper mills and chemical factories. Fish in the river were poisoned and the people dwelling by the river, for instance the residents in Bengbu, have had to dig deep wells and buy bottled water for drinking. The tap water, which is from the river, can only be used for washing toilets. The same story has occurred in the Weihe River, which is the largest tributary of the Yellow River. The river water is so seriously polluted that the water quality is worse than Class-V of the national water quality standards. Figure 1.34 shows the dirty water of the river. The river is seriously polluted and all fish have been killed. The bad odor of the water can be smelled many kilometers off. The Weihe River directly pour into the Yellow River and pollutes the Yellow River water.

The ecological system adjacent to rivers and in the waters connecting the rivers is affected by the pollution. Eutrophication has been a focal point of social attention since the 1980s. Algal blooms are a result of eutrophication of lakes and seas. The phenomenon of water discoloration, irrespective of the causative organism, has been called a red tide. The red tide algae, produces copious amounts of sticky mucus during its peak abundance, the mucus coats the gills of fish and shellfish, and causes them to

suffocate. Some harmful algae, like dinoflagellate, also produce toxic material and may transfer the toxic to humans through the food web. The 1998 red tide in the Bohai Sea of China spread over a 50 thousand km^2 area, killing many fish and causing $80 million in losses.

Fig. 1.34   Pollution causes the bad odor the Weihe River water and kills all fish (See color figure at the end of this book)

Algal blooms rarely occurred in seas near China before the 1980s because the nutrients supply was not sufficient. Eutrophication due to intensified human activities in recent decades has released the nutrient constraint and red tide has occurred quite often. Figure 1.35 shows the number of red tide events per decade from the 1950s to 1990s. Almost no red tides occurred in the 1950s and 1960s but the number of red tide events increased in an explosive way to more than 240 events in the 1990s. Comparing Fig. 1.35 with Fig. 1.33 it can be seen that the red tide events follow almost the same growth curves of urban population and sewage discharge. The growth curves exhibit the same law with a turning point about 1980, when the economy of China took off. There is no doubt that the high frequency of red tide events is a result of extremely high rates of fertilizer usage and wastewater discharge, which are in turn the results of the high speed of economic development and industrialization of china. If the trend continues, most of sea life in the seas near China will be extinct and the seas will become seas of death.
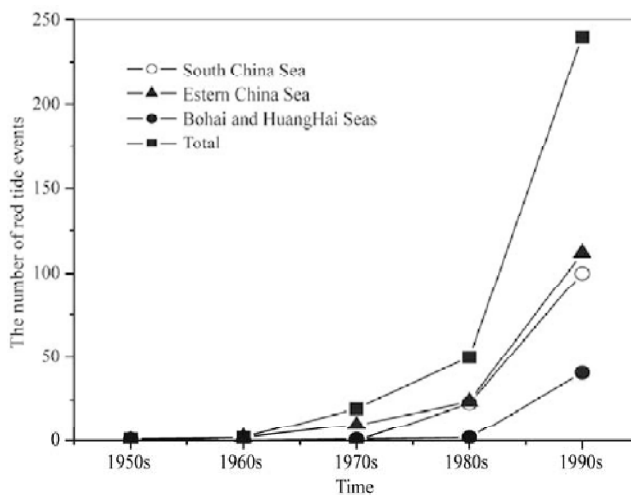
Fig. 1.35   The number of red tide events per decade occurring in the seas near China in the period of the 1950s–1990s

1.2.6 Reservoir Management

In the past decades, China had watched marvelous economic wonders and accelerated dam construction. Most Chinese rivers have been impounded for the purposes of flood control, power generation, water supply, irrigation, and/or navigation. On the Yellow River 11 major reservoirs were constructed in 1957–1993. They are from upstream down the river: Longyangxia Reservoir, Lijiaxia Reservoir, Liujiaxia Reservoir, Yanguoxia Reservoir, Bapanxia Reservoir, Qingtongxia Reservoir, Sanshenggong Reservoir, Wanjiazhai Reservoir, Tianqiao Reservoir, Sanmenxia Reservoir, and   Xiaolangdi Reservoir. The total capacity of the reservoirs is 55.8 billion m^3, equal to the annual runoff of the whole watershed. More than 10 billion of sediment has been trapped by the reservoirs reducing the total amount of sediment deposited in the lower Yellow River.

The Xiaolangdi Reservoir is used to supply water to Henan, Shandong, and Hebei Provinces, and also used to regulate water and sediment. The capacity for trapping sediment is 7 billion m^3. It is predicted that the sediment from the Loess Plateau can be trapped by the reservoir for at least 20 years, and, therefore, the lower Yellow River will be scoured and the flood risk will then be eased. Moreover, the reservoir is also used to create artificial floods to scour the lower reaches of the channel.

Impoundment of rivers causes many problems. For instance, the Sanmenxia Reservoir was impounded in 1960. The confluence of the Weihe River flowing into the Yellow River is in the backwater region of the reservoir. The high pool level caused sediment deposition at the river mouth followed by serious retrogressive sedimentation. The ground water table raised and the flood discharge capacity of the Weihe River greatly reduced due to sedimentation in the channel. The ancient city of Xian is endangered by the reduced channel capacity. At present, hydraulic engineers are discussing decommissioning of Sanmenxia Reservoir (not removing the dam but opening all the outlets and maintaining the pool at the lowest level as before the dam construction). Figure 1.36 shows the Yellow River at Sanmenxia dam- the Three Gate Gorges before the dam construction and the dam (a) and the Sanmenxia Dam impounded in 1960. The reservoir lost 6 billion m^3 of its capacity in just 10 years of operation due to sedimentation.

| (a) | (b) |
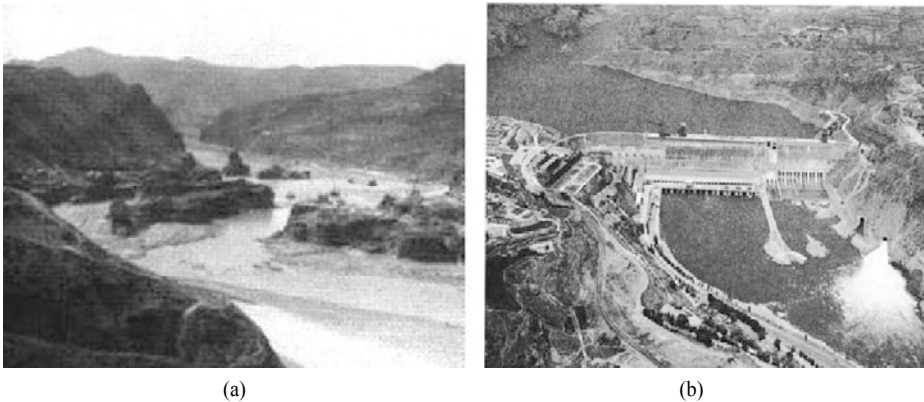
Fig. 1.36 (a) The Yellow River at Sanmenxia – the three gates gorges before the construction of the dam; (b) The Sanmenxia Dam, which was the first dam on the Yellow River completed in 1960 and reconstructed two times to mitigate the sedimentation of the reservoir (YRCC, 2001)

For small reservoirs (less than 100 million m^3 capacity) the percentage of capacity loss due to sedimentation is even higher. The major strategies to control sedimentation and restore the capacity of the reservoirs are: storing the clear water and discharging the turbid water; flushing by drawdown and flushing by emptying the reservoir; dredging, and making use of density currents.

For reservoirs on rivers with high sediment concentration and low water runoff drawdown flushing and empty flushing are applied. Low-level outlets are open in the flood season to drawdown or empty the reservoirs and create riverine flows along the impounded reaches, which scour and release the sediment deposited in the reservoirs. Retrogressive erosion is induced by drawdown and empty flushing, which may extend the flushing far upstream of the dam. The Hengshan Reservoir on the Changyuan River in the Shanxi Province is a gorge type small reservoir with a capacity of about 13 million m^3. The area is arid and there is almost no flow in the non-flood seasons. The reservoir was used to store water during the flood season and provide water for irrigation in the non-flood seasons. It was silted up quickly in the first 8 years of operation and 30% of the capacity was lost due to sedimentation. Then, the reservoir was emptied for flushing of sediment in the flood seasons of 1974 and 1979. Consequently, about 2 million m^3 of its capacity was regained.

The Three Gorges Project (TGP) on the Yangtze River is the largest reservoir in China with the highest power generation capacity in the world. Problems and strategies related to the project are discussed in Chapter 7.

1.2.7   River Uses

1.2.7.1   Hydro-Power

By the end of 1999, the total installed capacity for hydropower in the country amounted to 70,000 MW with an annual energy output of 210 trillion Wh, which ranked second and third among all the countries in the world, respectively. There are about 220 large- and medium-sized hydropower stations either completed or under construction at present, in which 20 have an installed capacity of more than 1,000 MW, 37 have an installed capacity of more than 500 MW; and 53 have a dam higher than 100 m. (IWHR, 2000)

During the 1950s, the first large-sized hydropower station, Xin'anjiang was constructed, with a dam height of 102 m and an installed generating capacity of 662.5 MW. After that a cascade of hydropower development was carried out for the medium and small rivers of Xinfeng in Guangdong province, Zhexi in Hunan province, Yili in Yunnan province, Maotiao in Guizhou province and Yongding in Beijing.

During the 1960s, a number of large- and medium-sized hydropower projects were constructed, such as Liujiaxia in Gansu province (installed capacity 1,160 MW), Danjiangkou in Hubei province (900 MW), Zhexi in Hunan province (447.5 MW), and Yunfeng on the Yalu River (400 MW). During the 1970s, the hydropower projects of Fengtan in Hunan province (400 MW) in Liaoning Province, Bikou in Gansu province (330 MW), Gongzui in Sichuan province (700 MW), and Qingtongxia on the Yellow River (272 MW) were constructed.

During the 1980s, construction of hydropower projects was carried out on an even larger scale. The Wujiangdu in Guizhou province (630 MW), Baishan in Jilin province (900 MW), Longyangxia in Qinghai province (1,280 MW), Dongjiang in Hunan province (500 MW) and Gezhouba on the Yangtze River in Habei province (2,715 MW) were completed and put into operation. (IWHR, 2000)

During the 1990s, the improvement of managerial institution for the development of hydropower resources greatly accelerated the development of hydropower and the construction periods for the main structures of large-sized hydropower stations were generally reduced by 1-2 years in comparison with the past, with the examples including the Lubuge, Guangxu I, Shuikou, Geheyan, Yantan, Manwan, Wuqiangxi, Lijiaxia, Tianhuangping, Shisanling, Lianhua, Ertan, and Tianshengqiao Hydropower Projects. The construction of pumped-storage power stations also saw great progress, and the completed ones include the Guangzhou Project in Guangdong province (2,400 MW), Shisanling Project in Beijing (800 MW), and the Tianhuangping (1,800 MW) and Xikou Projects in Zhejiang province (80 MW).

In China, the total installed capacity rose from 65.9 GW in 1980 to 236.5 GW in 1996 and 254.2 GW in 1997, a rate of increase that lagged behind that of gross domestic product (GDP) although still a relatively

high net increase. The installed capacity of hydropower makes up about 25% of the total installed capacity with large hydropower stations each with the capacity of larger than 250 MW being about 50% of the total hydro in both installed capacity and annual energy output. The share of hydropower has tended to decline relative to the total power capacity and output. Most of large thermal power stations are located at the coal mine heads in the northern China (Shanxi, Hebei, Henan, and Shaanxi Provinces), though some are also located near load centers such as Shanghai and Guangzhou. Most of the large hydropower stations are located in remote mountainous regions in the upper reaches of the Yellow River, Yangtze River, and the rivers of the southwest. In each region, the share of hydropower varies greatly, being particularly low in the northern and eastern China, and significantly higher in the northwest, central southern, and Fujian and Sichuan provinces. The Three Gorges Project, currently under construction, will add 17,800 MW by 2007. Nevertheless, only 17% of the total exploitable hydro-power resources of China have been exploited. Dam construction in China is still in the developing stage. This is different from developed countries, where people are discussing decommissioning of dams.

1.2.7.2 Irrigation

China is a large agricultural country. Irrigation and drainage play a very important role in the agricultural production. The country may be divided into five categories of areas: very humid, humid, semi-humid, semi-arid, and arid. The country may also be divided into three different zones based on the different requirements of irrigation/drainage for agricultural crops, that is, a perennial irrigation zone with less than 400 mm of mean annual precipitation, an unstable irrigation zone with mean annual precipitation between 400 mm and 1,000 mm, and a rice irrigation zone with more than 1,000 mm of mean annual precipitation. The perennial irrigation zone covers most parts of northwest china and the upper and middle reaches of the Yellow River, composing 45% of the land area of the whole country. The unstable irrigation zone covers mainly the lower reaches of the Yellow River, the Huaihe and Haihe River basins and northeast China, where the irrigation requirement index (crop water requirement met by irrigation) may be as high as 50% or even higher in a dry year. The rice irrigation zone covers the middle and lower reaches of the Yangtze River, the Pearl and Minjiang River basins and part of southwest China.

Chemical fertilizers and irrigation are usually the main measures to enhance agricultural production. The use of fertilizer has reached its maximum in China and further increases will not affect the production. Increase in the area of irrigation will be the main strategy to enhance agricultural production. China is planning to increase the area of irrigation by 83%–122% in 50 years. Table 1.4 shows the projection of the development of irrigation areas in the main river basins.

1.2.7.3 Inland Navigation

The cost of inland navigation is usually only 1/3 of railway and 1/10 of highway costs. The Yangtze River, the Huaihe River, the Grand Canal, and the Pearl River are the main inland navigation channels of China. In the Yangtze River and its tributaries the total length of navigation channels is 70,000 km, the value is 20,000 km in the Huaihe River, 1,035 km in the Grand Canal, and 14,100 km in the Pearl River. Nevertheless, the length of channel with water depth over 2.5 m, in which a 1,000 ship may navigate, is less than 5,000 km. Canalization of rivers, construction of harbors and ship locks, and digging canals will promote inland navigation.

1.2.8 Ecological Restoration and Integrated River Management

Environment protection and ecological restoration have become very popular in China. Restoration of the impaired stream ecosystem is necessary for most of the worldrivers. Ecological restoration involves the return of a given ecosystem to a state approximating that in which it existed prior to disturbances and ecology protection implies maintaining the organisms and their environment unchanged.

Table 1.4 Projection of the development of irrigation areas in river basins

Basins	High development			Low development		
	Irrigation area (million ha)			Irrigation area (million ha)		
	2010	2030	2050	2010	2030	2050
Songhua-Liaohe	6.5	7.5	7.7	6.2	6.7	6.7
Haihe	7.4	7.6	7.7	7.4	7.5	7.5
Huaihe	10.4	10.7	10.8	10.5	10.6	10.7
Yellow	5.4	5.8	6.0	5.4	5.6	5.7
Yangtze	15.1	15.6	15.8	15.0	15.3	15.2
Pearl	4.5	4.6	4.7	4.4	4.5	4.5
SE Rivers	1.9	2.0	2.0	1.9	1.9	1.9
SW Rivers	0.8	0.9	0.9	0.8	0.8	0.9
Inland Rivers	4.7	4.9	4.9	4.3	4.6	4.6
The North	34.5	36.5	37.0	33.7	35.1	35.3
The South	22.4	23.1	23.4	22.1	22.5	22.5
Total average	56.9	59.5	60.4	55.8	57.6	57.8

Source: Ministry of Water Resources of China

River training and river uses have resulted in many rivers "dead". For instance water diversion in the middle and lower reaches of the Yellow River caused the river dried out in the period of 1972–1998. Flow cut-offs have occurred in 19 years in the period 1972–1998. Another example is the pollution of the Yongding River near Beijing since the construction of the Guanting Reservoir and numerous small reservoirs in the upstream reaches. Figure 1.37 shows the Yanghe River, which is a tributary of the Guanting Reservoir. Almost all fresh water is diverted for the irrigation and urban use and only sewage and waste water discharged from urban areas and industries is flowing in the river. The water is so seriously polluted that all fish and most of the macro-invertebrates have been extinct and only a few very tolerant species of invertebrates can be found from the river.

Fig. 1.37 Seriously polluted water in the Yanghe River, which is a tributary of the Yongding River and flows into the Guanting Reservoir

In river management, the decision makers often put the economic benefits before the ecological protection. For instance, Shanghai has a problem of land shortage and has been reclaiming the wetland in the East Chongming Shore in the Yangtze River estuary to ease the land shortage. Figure 1.38 shows the agricultural development from the wetland in the East Chongming Shore in several phases (left) and the

levees constructed in 2001 to separate the land from water (right). The development of agriculture has caused reduction in wetland area and number of wild animals.

(a)   (b)
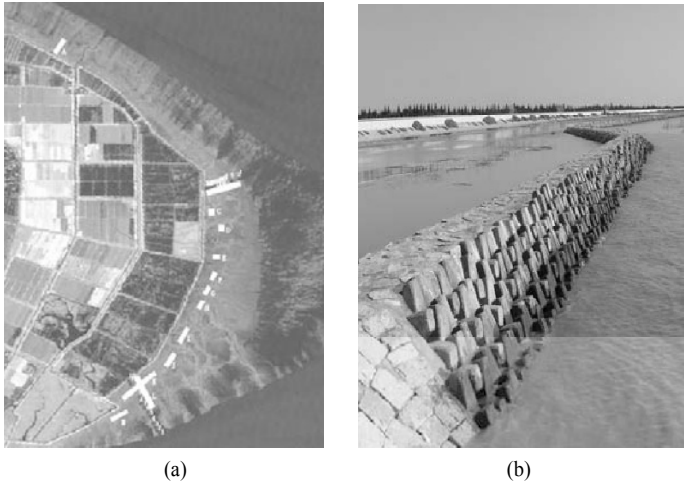
Fig. 1.38 (a) Agricultural development from the wetland in the East Chongming Shore in the Yangtze River mouth in several phases; (b) The levees constructed in 2001 to separate the land from water (right)

There are also examples of ecological protection in China. Figure 1.39 shows the wood path in the Jiuzhai Creek in Sichuan in west China. The creek has become well known in its beautiful landscape and attracted more than 2 million visitors every year. The managers have done a great effort to protect the environment and ecology. The wood trails lead to all tourism attractions in the park. The river water is only for drinking-use. The natural ecology is well protected although it receives millions of visitors every year.

Fig. 1.39 The wood path for visitors in the Jiuzhai Creek (Sichuan basin in the western China) to protect the environment and ecology

The river management is not integrated. Most of dams are operated to achieve the highest power generation without consideration of stream ecology. And the managers of water resources just meet the water demands and take no consideration of fluvial process. Sediment transportation in rivers causes many problems, such as the reservoir sedimentation, flood stage rising, and impairment of stream ecology. But sediment is a resources for land creation in river mouth and the main factor to maintain coastal equilibrium.

Integrated river management is needed to coordinate the upper, middle and lower reaches and the river estuary, economic benefit and ecological restoration, and environment for sustainable development. For this purpose the managers are required to understand all problems and management strategies for river development.

Review Questions

1. What are the major functions of rivers?
2. What is integrated river management?
3. Create a river network by applying the random walk model and clearly state all your assumptions.
4. Name various types of sediments and sediment loads and explain the difference between them.
5. What is water cycle?
6. What are the main river patterns?
7. What are the main chemical features of a river?
8. What are the main pollution concerns for rivers?
9. Please state the relevant concepts of a river ecosystem.
10. Explain the mechanism of merge of rivers with the minimum stream power theory.
11. What are the major issues in river management in China?
12. What are the reasons for the southeastern China to be wet and the northwestern China to be dry?
13. What are the major strategies to ease water shortage?
14. What are the main reasons for increases in flood loss?
15. What are the consequences of soil erosion?
16. What is red tide and why has the number of the red tide events increased so fast in recent decades?
17. What are the main sectors of river ecology?
18. What are the main problems in impounded rivers and how can they be solved?

References

Abrahams A.D., 1984. Channel networks: a geomorphological perspective. Water Resource Res, 20(2), 161–168

Alaerts G.J., Hartvelt F.J.A. and Patorni F.M., 1999. Water sector capacity building: Cancepts and instruments, A.A. Bakema, Rotterdam

Chai H.J., Liu H.C., Zhang Z.Y. and Xu Z.W., 2000. The distribution, causes and effects of damming landslides in China. Journal of the Chengdu University of Technology, 27(3), 302–307 (in Chinese)

Chen J.Q., 1991. Water resources in China. In Qian Z.Y. (Ed): Water conservancy in China. Water Resources and Hydro-Power Press, 1–42 (in Chinese)

Cheng X.T., 2002. Change of flood control situation and adjustments of flood management strategies in China. In Wu B.S., Wang Z.Y. et al. (Ed): Flood defence 2002. Science Press New York Ltd, 98–106

Chien N., Wan Z.H. and McNown J., 1998. Mechanics of Sediment Movement. ASCE Press, United States

Chien N., Wan Z.H. and McNown J., 1998. Mechanics of Sediment Movement, ASCE Press, New York

Chin A., 1999. The morphologic structure of step-pool in mountain streams. Geomorphology, l27, 191–204

Ciccacci S., D'Alessandro L., Fredi P. and Lupia P.E., 1992. Relation between morphometric characteristics and denudation processes in some drainage basins of Italy. Zeitschrift fuer Geomorphologic, N.F. 36–1, 53–67

Clark M.K., Royden L.H., Whipple K.X., Burchfiel B.C., Zhang X. and Tang W., 2006. Use of a regional relict landscape to measure vertical deformation of the eastern Tibetan Plateau. Journal of Geophysical Research, 111, F03002, doi: 10.1029/2005JF000294

Cowardin L.W., V.Carter, F.C., Golet, and E.T. LaRoe. 1979. Classification of wetlands and deep water habitats of the United States. U.S. Fish and Wildlife Service, Washington, DC.

Dai, F.C., Lee, C.F., Deng, J.H. and Tham, L.G. 2005. The 1786 earthquake-triggered landslide dam and subsequent darn-break flood on the Dadu River, Southwestern China. Geomorphology, 65, 205-221. Doi:10.1016/j.geomorph.2004.08.011.

Einstein H.A., Anderson A.G. and Johnson J.W., 1940. A distinction between bed load and suspended load in natural streams. Transaction of American Geophysical Union, Pt. 2, 628–633

Frissell C.A., Liss W.L., Warren C.E. and Hurley M.D., 1986. A hierarchical framework for stream habitat classification: Viewing streams in a watershed context. Environmental Management, 10, 199–214

Glock W., 1931. The development of drainage systems: A synoptic view. Geographical Review, 21, 475–482

Gregory S.V., Swanson F.J., McKee W.A. and Cummins K.W., 1991. An ecosystem perspective on riparian zones. Bioscience, 41, 540–551

Gu W.S., 1994. Basic situation and law of water and sediment variation in the Yellow River basin and discussion of the measures for controlling soil loss. Soil and Water Conservation in China, 7, 8–14 (in Chinese)

Hallegraeff G.M., 1993. A review of harmful algal blooms and their apparent global increase. Phycologia, 32(2), 79–99

Harris L.D., 1984. The fragmented forest. University of Chicago Press, Chicago, Illinois

Hoover R.L. and Wills D.L. (eds), 1984. Managing forested lands for wildlife. Colorado Division of Wildlife, Denver

Horton R.E., 1945. Erosional development of streams and their drainage basins: hydrophysical approach to quantitative morphology. Geological Society of America Bulletin, 56, 275–370

Howard A.D., 1967. Drainage analysis in geological interpretation. Bull Amer Assoc Petroleum Geologists, 51(11), 2246–2259

Hu S.X., Wang Z.Y. and Ding P.X., 1999. Shrinkage of the estuarine channels of the Haihe drainage system and its influences on flood hazard. International Journal of Sediment Research, 14, (2) 65–76

IWHR (China Institute of Water Resources & Hydropower Research). 2000. Large dam construction in China. Beijing: China Water Power Press.

Kinner D.A. and Moody J.A., 2005. Drainage networks after wildfire. International Journal of Sediment Research, 20(3), 194–201

Kirchner J.W., 1993. Statistical inevitability of Horton's laws and the apparent randomness of stream channel networks. Geology, 21, 591–594

Knighton A.D. and Nanson G.C., 1993. Anastomosis and the continuum of river pattern. Earth Surface Process and Landforms, 18, 613–625

Kundzewicz Z.W., 1997, Floods in perspective-setting the stage. Proc. European Expert Meeting on the Oder Flood 1997.

Landres P.B., Verner J. and Thomas J.W., 1988. Ecological uses of vertebrate indicator species: a critique. Conservation Biology, 2, 316–328

Leopold A., 1933. The conservation ethic. Journal of Forestry, 31, B-16 Stream Corridor

Leopold L.B. and Langbein W.B., 1962. The concept of entropy in landscape evolution. US Geological Survey, Professional Paper, N, 500-A

Lewis G.N. and Randall M., 1961. Thermodynamics. 2nd edition, revised by Pitzer K.S. and Brewer L. McGraw-Hill, New York, 91–92

Liu H. and Wang Z.Y., 2008. Relationship between river network pattern and environmental conditions. Journal of Tsinghua University (Sci &Tech), 48 (9), 1408–1412 (in Chinese)

Lohoefner, 1997. Personal communication. Deputy Chief, Division of Endangered Species, US Fish and Wildlife Service, Arlington, VA

Luo C.Z. and Luo J.X., 1996. Major flood disasters in China. China Bookstore (in Chinese)

Ministry of Water Resources of China, 1999. 1998 floods in China. Water and Hydropower Press (in Chinese)

Munich Re., 1999. Flooding and Insurance. Munich Reinsurance Company, Munich, 79

National Academy of Sciences, 1995. Wetlands: characteristics and boundaries. National Academy Press, Washington, DC

National Research Council (NRC), 1992. Restoration of aquatic ecosystems: science, technology, and public policy. National Academy Press, Washington, DC

Ni J.R., Wang S.J. and Wang G.Q., 2000. River patterns and special and temporal transformation modes. International Journal of Sediment Research, 4, 357–370

Ohmart R.D. and Anderson B.W., 1986. Riparian habitat. In Inventory and monitoring of wildlife habitat, ed. Cooperrider A.Y., Boyd R.J. and Stuart H.R., U.S. Department of the Interior, Bureau of Land Management Service Center, Denver, Colorado, 169–201

Ouimet W.B., Whipple K.X., Royden, L.H., Sun Z.M. and Chen Z.L., 2007. The influence of large landslides on river incision in a transient landscape: Eastern margin of the Tibetan Plateau (Sichuan, China). Geological Society of America Bulletin, 119(11/12), 1462–1476; doi: 10.1130/B26136.1

Partheniades E., 1977. Unified View of Wash Load and Bed Material Load. Journal of Hydraulic Division, Proceeding of American Society of Civil Engineers, 103(HY9), 1037–1058

Prigogine I., 1967. Introduction to Thermodynamics of Irreversible Process. Third edition, John Wiley, New York.

Qian Z.Y., 1991. Water Conservancy in China. Water Resources and Hydro-Power Press (in Chinese)

Ruhin A.B., 1957. On the Properties and Classification of Clastic Sediment. Selected Papers in Geology (translated from Russian), 33–48 (in Chinese)

Schumm H.A., 1968. Speculation concerning of paleohydrologic controls of terrestrial sedimentation. Geological Society of American Bulletin, 79, 1573–1588

Schumm S.A., Mosley M.P. and Weaver W.E., 1987. Experimental fluvial geomorphology. John Willey & Sons.

Schumm S.A., 1956. The evolution of drainage systems and slopes in badlands at Perth Amboy, New Jersey. Geological Society of American Bulletin, 67, 597–646

Shreve R.L., 1966. Statistical law of stream numbers. J. Geol. 74, 17–37

Smith D.G. and Smith N.D., 1980. Sedimentation in anastomosed rivers system: example from alluvial valleys near Banff Alberta. Journal of Sediment Petrology, 50, 157–164

Stamp N. and Ohmart R.D., 1979. Rodents of desert shrub and riparian woodland habitats in the Sonoran Desert. Southwestern Naturalist, 24, 279

Stankiewicz J., 2005. Fractal river networks of southern Africa. South African Journal of Geology, 108, 333–344

Stevens P.S., 1974. Patterns in nature. Atlantic Monthly Press, Boston

Strahler A.N., 1957. Quantitative analysis of watershed geomorphology. American Geophysical Union Transactions, 38, 913–920

Subcommittee on Sediment Terminology, 1947. Report of the subcommittee on sediment terminology, American Geophysical Union. Transition of American Geophysic Union, 28(6), 936–938

Thomas J.W. (ed.), 1979. Wildlife habitat in managed forests: the Blue Mountain of Oregon and Washington. Ag. Handbook 553. U.S. Department of Agriculture Forest Service

Tianchi L., 1990. Landslide management in the mountain areas of China: ICIMOD Occasional Paper No. 15, Kathmandu, Nepal.

Tomlinson B.P., 1986. The botany of mangroves Cambridge: Cambridge University Press. London

United States Environmental Protection Agency (USEPA). 1997. The quality of our nation's water: 1994. EPA841R95006. U.S. Environmental Protection Agency, Washington, DC

Wang S.J. and Yin S.P., 2000. Discussion on the classification of anastomosing and braided rivers. Dixueqianyuan, 7, 79–86 (in Chinese)

Wang S.J., 2002. Comparison of development and stability of two river patterns with multiple channels. Diqiuxuebao, 23(1), 89–93 (in Chinese)

Wang X.K., Li D.X. and Xu S.T., 2001, Experimental study on sedimentation in excavated trench under the action of tidal flow. International Journal of Sediment Research, 16(2), 184–188

Wang Z.Y. and Liang Z.Y., 2000. Dynamic characteristics of the Yellow River mouth. Earth Surface Process and Landforms, 25, 765–782

Wang Z.L., 2000. General Situation of soil and water loss and integrated control in China. Journal of Catastrophology, 15(3), 18–25 (in Chinese)

Wang Z.Y. and Dittrich Andreas., 1992. A study on problems in suspended sediment transportation. Proceedings of the 2-nd International Conference on Hydraulics and Environmental Modeling of Coastal, Estuarine and River Waters, Ashgate, England, 467–478

Wang Z.Y. and Qian N., 1985. Experimental study of motion of laminated load. Scientia Sinica (English Version), Ser. A, 28(1), 102–112

Wang Z.Y. and Qian N., 1987. Laminated load: Its development and mechanism of motion. International Journal of Sediment Research, 2, 102–124

Wang Z.Y. and Wu Y.S., 2001. Sediment removing capacity and river motion dynamics. International Journal of Sediment Research, 16(2), 105–115

Wentworth C.K., 1922. A scale of grade and class terms for clastic sediments, Journal of Geology, 30, 373–392

Yang C.T., 1972. Unit stream and sediment transport. ASCE Journal of the Hydraulics Division, 18(HY10), 1805–1826

Yang C.T., 1971. Potential energy and stream morphology. Water Resources Research, 7(2), 311–322

Yang C.T., 1983. Minimum rate of energy dissipation and river morphology. In Proceedings of Symposium on Erosion and Sedimentation. Colorado State University, Fort Collins, Colorado, 3.2–3.19

YRCC (Yellow River Conservancy Commission), 2001. Yellow River Century. Yellow River Press (in Chinese)

2 Vegetation-Erosion Dynamics

Abstract

In a broad sense, all rivers develop from rills and gullies in the process of erosion. Erosion is classified according to agents causing erosion into water erosion, wind erosion, gravity erosion, glacier erosion and cultural erosion. Water erosion occurs in different forms: splash erosion, sheet erosion, rill erosion, gully erosion and channel erosion. Grain erosion is defined as the phenomenon of breaking down of bare rocks under the action of sun exposure and temperature changes, detachment of grains by wind, flow of grains down the slope under the action of gravity, and accumulation of eroded material at the toe of the mountain forming a deposit fan. Vegetation is the most important factor affecting the erosion process and development of rills. Vegetation, fluvial-geomorphic processes and landforms are inextricably interconnected parts of the landscape. Vegetation-erosion dynamics studies the laws of evolution of watershed vegetation under the action of various ecological stresses. Vegetation and erosion are a pair of competing and mutually interacting aspects of a watershed. For a watershed, vegetation and erosion may reach an equilibrium state if the circumstances remain unchanged for a long period of time. However, the equilibrium may not be stable. Ecological stresses, especially human activities, may disturb the balance and initiate a new cycle of dynamic processes. Studies considering both geomorphology and vegetation in the watershed are uncommon yet may provide important information regarding geomorphological and ecological processes.

Key words

Agents of erosion, Water erosion, Ecological stresses, Vegetation-erosion dynamics, Riparian vegetation

2.1 Erosion

2.1.1 Agents of Erosion

According to Columbia Encyclopedia (Columbia University, 2000): erosion is generally defined as the processes by which the surface of the earth is constantly being worn away. In other words erosion means the detachment and removal of solid particles from their original place. Erosion is distinguished from weathering, which is defined as the process of chemical or physical breakdown of the minerals in the rocks, although the two processes may occur concurrently (Halsey et al, 1998; Wikipedia, 2009). According to preliminary statistics compiled for the world, the annual erosion of surface soil from river basins amounts to 60 billion tons, of which 17 billion tons are discharged into the oceans. In the process, as much as 5 million to 7 million ha of farms are annually ruined. Eroded soil contains nitrogen, phosphorous, and other nutrients that deposit in lakes and reservoirs contaminating the waters resulting in eutrophication and other biological as well as chemical processes.

The principal erosion agents are gravity, running water, glaciers, and wind. Human activity is also an agent of erosion. Erosion overlaps with detachment of solid particles from the rock and mass movement, or, the transfer of solid material down slopes. Weathering is also included as an erosive process. Over the surface of the planet, the average rate of erosion is about 0.02 mm/yr. In some places the rate is much higher, and in others it is greatly lower (Columbia University, 2000).

Erosion may be classified according to the erosion agents as water erosion, gravitational erosion, glacial erosion, and wind erosion (eolian erosion). Water is the substance most readily associated with erosion. Water erosion is also the most important form of erosion for river management. Various types of water erosion are discussed in the next section of this chapter.

Gravity erosion—Gravity plays an important role in all forms of erosion. Gravity erosion itself is the

mass movement of landslide, avalanche, slumping and surface creep, as material is moved from higher elevations to lower elevations under the action of gravity. In small scale erosion, gravity may cause a rock to drop from a height, such that it falls to the ground and breaks into pieces. Large scale gravitational erosion includes slope creep, avalanche, and landslide. Avalanche, landslide, and debris flow are discussed in Chapter 3. Slump is a gravitational erosion of solid material slipping down along a curved slope surface, which occurs when the slope becomes too steep, and the base material cannot support the rock and soil above. A curved scar is left where the slumped materials originally rested. Creep is the movement of rock and sediment slowly shifting downhill, which is caused by gravity alone. Creep is extremely slow and would be difficult to see without a lot of measurements over time.

Glacier erosion—A glacier is a moving mass of ice of large volume on the land surface. It moves by gravity, as a consequence of its extraordinary weight. A glacier steadily moves forward, carrying pieces of rock, soil, and vegetation with it. Under certain conditions, a glacier may have a layer of melted water surrounding it, which greatly enhances its mobility. In a wet and warm maritime climate a glacier moves at a speed of about 300 m/yr. By contrast, in the dry, exceptionally cold, inland climate of Antarctica, the Meserve Glacier moves at a speed of just 3 m/yr (www.answer.com). Figure 2.1 shows the Hailuo Gully Glacier on Gongga Mountain on the east margin of the Qinghai-Tibet Plateau. The glacier has eroded the gully bed and banks and carries a lot of solid material on its surface flowing down the gully at a speed of 170 m/yr to 350 m/yr.

Fig. 2.1   The Hailuo Gully glacier on the Gongga Mountain on the east margin of the Qinghai-Tibet Plateau has eroded the gully bed and carries a lot of solid material on its surface (See color figure at the end of this book)

Freezing and thawing also causes erosion. Changes in temperature and moisture cause expansion and contraction of materials, as when water seeps into a crack in a rock and then freezes, expanding and splitting the rock. The solid particles detached from the rock deposit on the hillside at an angle approximately equal to the angle of repose of the grains. Figure 2.2(a) shows the rock erosion resulting from freezing and thawing on a 4700 m high mountain at Luhuo on the Qinghai-Tibet Plateau. Figure 2.2(b) shows the fans of deposits or eroded sediment at the toe of the Rocky Mountains in Canada resulting from freezing and thawing. The sediment from the freezing and thawing erosion is relatively uniform with a median diameter around one centimeter.

Shattering erosion—As a consequence of freezing and thawing shattering erosion of rocks and underlying stratified talus deposits has been reported from temperate upland environments as well as cold environments worldwide (Saas and Krautblatter, 2007). Stratified scree deposits with rich fine

sediment are not confined to areas which experience or formerly experienced a periglacial climate and prior glaciation, but also occur in vegetated upland environments (Garcia-Ruiz et al., 2001; Curry and Black, 2002). Usually shattering erosion is found in high mountains with elevations of 1200–4000 m (Saas and Krautblatter, 2007; Matsuoka, 2008). But it is also found in south Wales at 650–770 m (Harris and Prick, 2000). The lithology of the weathering rocks are limestone, dolostone, marls, and sandstone (Curry and Black, 2002; Turner and Makhlouf, 2002; Saas and Krautblatter, 2007). Only a few data have been obtained about the rate of shattering erosion because it is very slow. Thirteen years of observations in the southeastern Swiss Alps found that shattering erosion occurred at an average rate about 0.1 mm/yr with significant spatial and inner-annual variations (Matsuoka, 2008). The freeze-thaw cycle is the main agent for shattering erosion. A five-year study in the Japanese Alps revealed that the shattering rate of rocks was much higher in the freeze-thaw period from October to next May than in the frost-free period from June to September (Matsuoka, 1990).

Shattering erosion in high mountains, especially the particle movement on slopes, has caused some problems to highways. Some studies have been done on the movement of grains on the slopes and protection of the highways from the deposition of grains. The deposits are called stratified scree deposits or alpine scree slopes in some literature (Hetu et al., 1995). Chinese researchers studied the structure of grain deposit fans, repose angles, and stability of the fan (Wang et al., 2007a, 2007b and 2007c). This research focused on the velocity distribution of grain flow on the slope and the pressure exerted on the protection walls of highways by the deposit fan. Other researchers studied the critical initiation of slump of grain deposits on slope (Chang et al., 2006).

(a)   (b)
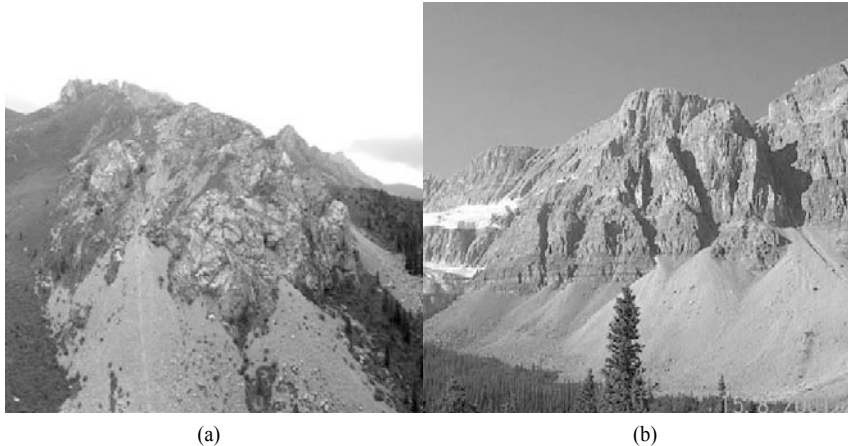
Fig. 2.2   (a) Freezing and thawing of rocks resulted in rock erosion on a 47,00 m high mountain at Luhuo on the Qinghai-Tibet Plateau; (b) Eroded sediment resulting from freezing and thawing deposits at the toe of the Rocky Mountains in Canada

Wind erosion is the result of sand movement by the wind. There are two main effects. First, wind causes small particles to be lifted, and, therefore, moved to another region. Second, these suspended particles may impact on solid objects causing erosion by abrasion. Wind erosion generally occurs in areas with little or no vegetation, often in the areas where there is insufficient rainfall to support vegetation. Sand dunes in deserts are the most common example of wind erosion. Wind erosion of bare lands has intensified desertification by depriving the ground of good top soil. Wind erosion is referred to as eulian erosion, the name being a reference to Aeolus, the Greek god of the winds encountered in Homer's *Odyssey*.

Wind has a greater frictional component when the wind carries sand, every grain of which is like a cutting tool. In some desert regions the bases of rocks or cliffs have been sandblasted, leaving a mushroom-shaped formation. Figure 2.3 shows mushroom-shaped rocks resulting from wind erosion in the Arches National Park of the U.S.

Fig. 2.3   Mushroom-shaped rocks resulting from wind erosion in the Arches National Park of the U.S.

   Cultural erosion—Human activities also cause or intensify soil erosion, which is termed cultural erosion. When land is disturbed by construction activities, soil erosion increases from 2 to 40,000 times the pre-construction erosion rate (Wang and Wang, 1999). Erosion rates from construction sites are typically 10 to 20 times those from agricultural lands and they can be 100 times as high. Wolman and Schick (1967) found sediment yields on an open construction site in Maryland of 49,200 t/km^2 compared to 380 t/km^2 in a stable urban area nearby. Goldman et al. (1986) found that in the San Francisco Bay Area the average rate of erosion for non-construction land uses (grazing, agriculture, forests, etc.) was about l,780 t/(km^{2}yr), whereas the erosion rate from construction sites was 11,600 to 15,700 t/(km^{2}yr) and sometimes higher. Erosion rates from construction sites typically were 20 times the average erosion rates of non-construction land uses. Although a wide variation in erosion rates is reported in the literature, it is clear that construction causes a large increase in erosion.

   Erosion removes the smaller and less dense constituents of topsoil. These constituents, clay and fine silt particles and organic material, hold nutrients that plants require. The remaining subsoil is often hard, rocky, infertile, and dry. Thus, reestablishment of vegetation is difficult and the eroded soil produces less growth. In the management of rivers, people can control erosion by planting vegetation that holds the soil, by carefully managing and controlling land usage, and by lessening the slope angle in places where gravity tends to erode the soil.

2.1.2   Water Erosion

2.1.2.1   Types of Water Erosion

Flowing water is the main agent causing erosion. Water erosion is the most important erosion for river management. Water erosion is essentially a two-part process. One part is the loosening of soil particles

caused largely by raindrop impact. The other part of the process is the transportation of soil particles, largely by flowing water. The primary erosion locations are overland slopes, gullies, agricultural areas, mining operations, and construction sites. Various forms of water erosion are related to river management and can be controlled by planting vegetation:

Splash erosion—When vegetative cover is stripped away, the soil surface is directly exposed to raindrop impact. On some soils, a very heavy rain may splash as much as 22,400 t/km^2 of soil (Buckman and Brady, 1969). If the soil is on a slope, gravity will cause the splashed particles to move downhill. When raindrops strike bare soil, the soil aggregates are broken up. Fine particles and organic matter are separated from heavier soil particles. This pounding action destroys the soil structure. A hard crust often forms when the soil dries. This crust inhibits water infiltration and plant establishment, and runoff and future erosion are thereby increased. Splash erosion is closely related to raindrop size. Large raindrops have a much greater impact than small raindrops.

Sheet erosion—Sheet erosion is caused by shallow "sheets" of water flowing over the soil surface (Fig. 2.4). These very shallow moving sheets of water are seldom the detaching agent, but the flow transports soil particles that have been detached by raindrop impact. The shallow surface flow rarely moves as a uniform sheet for more than a few feet before concentrating in the surface irregularities (VSWCC, 1980).

Ril1 erosion—Rill erosion begins when shallow surface flow starts to concentrate in low spots in the soil surface (Fig. 2.4). As the flow changes from sheet flow to deeper flow in these low areas, the velocity and turbulence of flow increase. The energy of this concentrated flow is able to both detach and transport soil particles. This action begins to cut tiny channels called rills. Rills are small but well-defined channels that are at most only several to several tens cm deep (VSWCC, 1980).

Gully erosion—Gully formation is a complex process that is not fully understood. Some gullies are formed when runoff cuts rills deeper and wider or when the flows from several rills come together and form a large channel. Gullies can enlarge in both uphill and downhill directions. Water flowing over the headwall of a gully causes undercutting. In addition, large chunks of soil can fall from a gully headwall in a process called mass-wasting. This soil is later carried away by storm water runoff. A heavy rain can transform a small rill into a major gully almost overnight (Reader, 1975; Goldman et al., 1986). Figure 2.5 shows the rills being developing into gullies due to rainstorm erosion. Once a gully is created, it is very difficult to stop it from growing, and it is costly to repair.
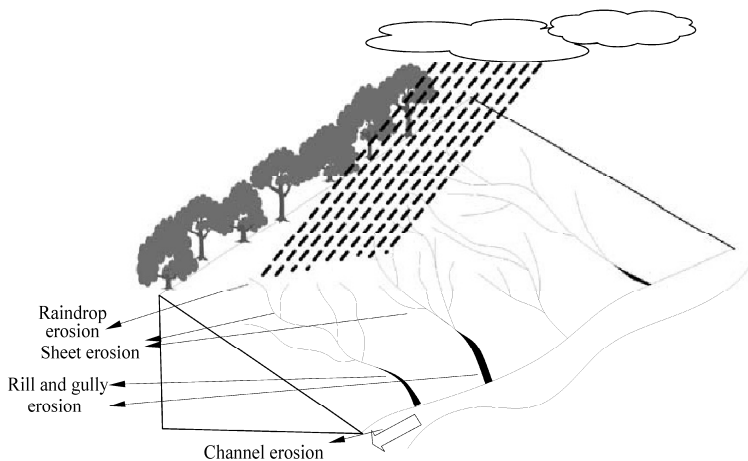
Fig. 2.4   Types of water erosion

Fig. 2.5 Rills developing into gullies due to rainstorm erosion

Channel erosion (bank erosion)—Channel erosion occurs when bank vegetation is disturbed or when the volume or velocity of flow in a stream is increased. Natural streams have adjusted over time to the quantity and velocity of runoff that normally occur in the watershed. The vegetation and rocks lining the banks are sufficient to prevent erosion under these steady-state conditions. However, when a watershed is altered by removing vegetation, by increasing the amount of impervious surfaces, or by paving tributaries, stream flows are changed also. Typical changes are an increase in the peak flow during storms and an increase in stream velocity. The changing flow may scour the banks and causes bank collapse, as shown in Fig. 2.6. Repair of eroded stream banks is difficult and costly. Erosion often occurs at stream bends and at constrictions, such as those where bridges cross a stream. Erosion may also begin at the point where a storm drain or culvert discharges into a stream. In the section with hardened banks the flow scours the channel bed and causes channel incision.

Fig. 2.6 Channel erosion and collapse of vegetative banks and hardened banks on the Charlooze River in Iran, which was caused by floods (See color figure at the end of this book)

2.1.2.2 The Principal Factors Affecting Water Erosion

Principal factors affecting erosion are climate, soil characteristics, topography and ground cover.

Climate—Climate affects erosion potential both directly and indirectly. In the direct relation, rain is the driving force of erosion. Raindrops dislodge soil particles, and runoff carries the particles away. The erosive power of rain is determined by rainfall intensity (inches or millimeters of rain per hour) and droplet size. For example, Meyer (1971) reported that where annual rainfall is 760 mm, raindrop impact energy over a 2.6 km^2 area is equivalent to nearly 10,000 tons of TNT annually. Table 2.1 shows the kinetic energy of rainfall of various intensities. The table shows that 6 mm raindrops falling from a cloudburst have over 2,000 times as much kinetic energy per unit time as a drizzle with l-mm raindrops. A highly intense rainfall of relatively short duration can produce far more erosion than a long-duration storm of low intensity. Also, storms with large raindrops are much more erosive than misty rains with small droplets. Though yearly rainfalls over 2,540 mm commonly occur in the Pacific northwest of the U.S., storms in that area tend to have low intensity with a very fine droplet size, and, thus, erosion is not severe (Gray and Leiser, 1982; Lull, 1959).

Table 2.1   Kinetic energy of rainfalls of various intensities and droplet sizes (after Gray and Leiser, 1982; Lull, 1959)

Rainfall	Intensity (mm/hr)	Median diameter (mm)	Fall velocity (m/s)	Drops per area per time drops/ (m^2·s)	Kinetic energy J/ (m^2·hr)
Fog	0.127	0.01	0.003	67,425,135	5.896*10^{-7}
Mist	0.051	0.1	0.213	27017	1.159*10^{-3}
Drizzle	0.254	0.96	4.115	151	2.160
Light rain	1.016	1.24	4.785	280	11.632
Moderate rain	3.81	1.60	5.700	495	61.896
Heavy rain	15.24	2.05	6.706	495	342.537
Excessive rain	40.64	2.40	7.315	818	1,087.011
Cloudburst	101.6	2.85	7.894	1,216	3,165.584
Cloudburst	101.6	4.00	8.900	441	4,025.210
Cloudburst	101.6	6.00	9.296	129	4,388.617

The indirect relation between climate and erosion is subtle. The yearly pattern of rainfall and temperature by and large determines both the extent and the growth rate of vegetation. As will be seen later, vegetation is the most important form of erosion control. Climates with relatively mild year-round temperatures and frequent, regular rainfall (as in the southeastern the U.S. and the British Isles) are highly favorable to plant growth. Vegetation grows rapidly and provides a complete ground cover, which protects the soil from erosion. A cleared land can be greened easily if the revegetation is properly done.

In erosive areas the cycle of soil freeze and thaw exacerbates soil erosion. Soil particles and rocks may be detached because water in the pores and interstices of rocks swell as it is frozen. Figure 2.7 shows the soil erosion caused by soil freeze and thaw in the Xizhao Gully on the Loess Plateau in China. The rocks in the area are formed in Tertiary material and are loosely bonded. Water penetrates into the rock interstices and breaks the rocks when it is frozen. The erosion rate of rocks in the area is as high as 2-10 mm per year.

The Sierra Nevada, Cascade Range, and dry climates, such as the vast desert areas of the southwestern United States and the Loess Plateau in the northwestern China, are far less favorable for plant growth, and, thus, are much more susceptible to erosion. In each of those climatic extremes, the natural vegetation requires a very long period of time to become established. It lives in a fragile balance with its environment. Because the climate is so harsh, it is very difficult to reestablish any plant cover that is disturbed. Rainfall is

Fig. 2.7　Soil erosion caused by freeze and thaw in the Xizhao Gully on the Loess Plateau of China

very infrequent in deserts; but when it does occur, it is typically very intense. Erosion rates often are high because there is little ground cover to protect the soil. In cold climates the growing season is very short. Plant reestablishment is a difficult and costly process. Even with the best of efforts, success cannot be assured (White and Franks, 1978).

Soil Characteristics—The following four soil characteristics are important in determining soil erodibility: ① texture; ② organic matter content; ③ structure; and ④ permeability. Soil texture refers to the sizes and proportions of the particles making up a soil. Sand, silt, and clay are the three major classes of soil particles. Soils high with sand content are said to be coarse-textured. Because water readily infiltrates into sandy soils, the runoff, and consequently the erosion potential, is relatively low. Soils with a high content of silts and clays are said to be fine textured or heavy. Clay, because of its stickiness, binds soil particles together and makes a soil resistant to erosion. However, once the fine particles are eroded by heavy rain or fast-flowing water, they will travel great distances before settling. Typically, clay and fine silt particles will settle in a large, calm water body, such as a bay, lake, or reservoir, at the down stream end of a watershed. Thus, silty and clayey soils are frequently the worst water polluters. Soils that are high in silt and fine sand and low in clay and organic matter are generally the most erodible (Mills and Clar, 1976; VSWCC, 1980).

Organic matter consists of plant and animal litter in various stages of decomposition. Organic matter improves soil structure and increases permeability, water-holding capacity, and soil fertility. Organic matter in an undisturbed soil or in mulch covering a disturbed site reduces runoff and, consequently, erosion potential. Mulch on the surface also reduces the erosive impact of raindrops. Mulching can accelerates re-establishment of grass vegetation. Figure 2.8(a) shows straw mulch placed on an area disturbed in the construction of a rain garden in the Marquette University campus. Two weeks late the grass re-established itself through the straw, as shown in Fig. 2.8(b).

Soil structure is the arrangement of soil particles into aggregates. A granular structure is the most desirable one. Soil structure affects the soil's ability to absorb water. When the soil surface is compacted or crusted, water tends to run off rather than infiltrate. Erosion hazard increases with increased runoff. Loose, granular soils absorb and retain water, which reduces runoff and encourages plant growth. Soil permeability refers to the ability of the soil to allow air and water to move through the soil. Soil texture and structure and organic matter all contribute to permeability. Soils with high permeability produce less runoff at a lower rate than soils with low permeability, which minimizes erosion potential. The higher

(a)   (b)

Fig. 2.8   (a) Mulching with straw on a disturbed rain garden in the Marquette University campus, the U.S.; (b) two weeks late the grass re-established itself through the straw

water content of a permeable soil is favorable for plant growth, although it may reduce slope stability in some situations.

By identifying erodible soil types early in the planning process, the site planner can know what portions of the site require the most diligent erosion control efforts. Mulching and vegetating exposed soils and minimizing the area of exposure of highly erodible soils are effective techniques for preventing soil movement. Sediment control structures, such as sediment basins, that prevent sediment from being washed off sites may also be necessary, since some soil movement is inevitable.

Topography—Slope length and slope steepness are critical factors in erosion potential, since they determine in large part the velocity of runoff. The energy (and, thus, the erosive potential) of flowing water increases with the square of the velocity. Long, continuous slopes allow runoff to build up momentum. The high velocity runoff tends to concentrate in narrow channels and produce rills and gullies. The shape of a slope also has a major bearing on erosion potential. The base of a slope is more susceptible to erosion than the top, because runoff has more momentum and is more concentrated as it approaches the base. Constructing a convex slope magnifies this problem, whereas a concave slope reduces it. Leaving a relatively flat area at the base of a slope not only reduces erosion but also allows sediment from the upper portions of the slope to settle out.

Slope orientation can also be a factor in determining erosion potential. In northern latitudes, south-facing slopes are hotter and drier than other slope orientations. In drier climates, vegetation is sparser on such slopes and reestablishment of vegetation there may be relatively difficult. Conversely, northern exposures tend to be cooler and moister; but they also receive less sun, which results in slower plant growth.

Ground cover—The term "ground cover" refers principally to vegetation, but it also includes some other surface structures placed by nature and humans (such as mulches, jute netting, wood chips, and crushed rock). If the soil consists of some flake shape particles the particles may form a tile structure to protect the soil against splash erosion. Figure 2.9(a) shows tile structure on the slope in the Xiaojiang River basin in southern China, where the rate of water erosion is extremely high.

It is no doubt that vegetation is the most effective form of erosion control. No man-made products can approach it in long-term durability and effectiveness. Vegetation shields the soil surface from the impact of falling rain, slows the velocity of runoff, holds soil particles in place, and maintains the soil's capacity to absorb water. Figure 2.9(b) shows the role of vegetation in protecting the soil from erosion in a mountainous area in central China. The role of vegetation and the dynamic interaction between vegetation and erosion are discussed in detail in the following section.
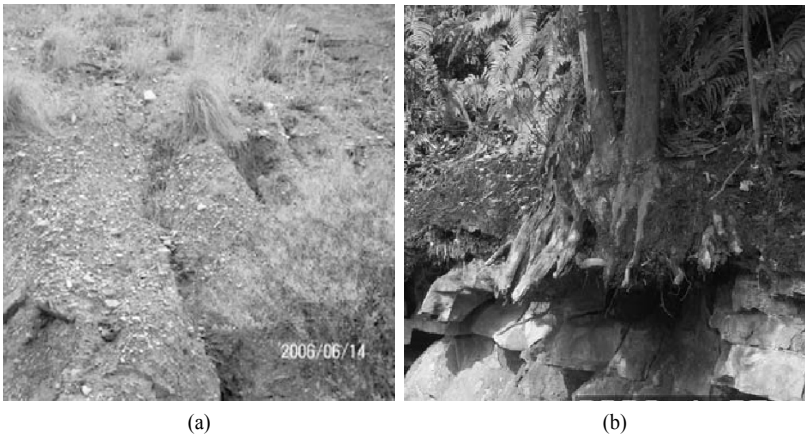
(a)   (b)

Fig. 2.9 (a) Tile structure on the slope in the Xiaojiang River basin in southern China; (b) Vegetation cover protecting the soil from various erosion (See color figure at the end of this book)

2.1.3 Grain Erosion and Control Strategy

Grain erosion is a unique type of erosion that occurred intensively in the dry valleys in Yunan, especially in Sichuan after the Wenchuan Earthquake, which occurred at the Longmenshan fault on May 12, 2008, in China. Grain erosion is defined as the phenomenon of breaking down of bare rocks under the action of sun exposure and temperature changes, detachment of grains by wind, flow of grains down the slope under the action of gravity, and accumulation of eroded material at the toe of the mountain forming a deposit fan. The grains, 0.1–200 mm in diameter, jump and hit against the mountain slope surface and cause detachment of slope debris or rock surface, which results in further erosion. Bare rocks were cause by avalanches, landslides, and human activities. Grain erosion of bare rocks is much (100–1000 times) more intensive than shattering erosion. Rock fall, bank failure, avalanche and landslide resulted in bare rocks in mountainous areas, especially the mountainous areas experiencing riverbed incision. Human activities, such as highway construction and mining, also cause bare rocks. Mass movements triggered by the Wenchuan Earthquake have left a huge area of bare rocks (Wang et al., 2009b). Erosion of rocks has been occurring in the form of grain detachment and movement. The erosion is extremely intense. A surface layer of 3–50 cm of the bare rocks has been eroded one year after the earthquake.

The grain particles are removed from the parent rocks by wind or tremors, and they roll, slide, or saltate down and scour the slope like a water flow，then accumulate at the toe of the mountain and form a deposit fan. It is difficult to classify such a type of erosion into weathering, shattering erosion, slope erosion, wind erosion, or gravity erosion. Different from other erosion types the solid particles have rather uniform size and the detachment and movement are generally in single grain or multiple grains. Thus, such a type of erosion is named **grain erosion** and the flow of grains on slopes is named **grain flow**.

Grain erosion also occurred before the Wenchuan Earthquake in dry valleys with poor vegetation. Dry valleys have two unique features, which may be used as diagnostic characteristics: ① deeply incised valley on a plateau; and ② significantly higher temperatures and evaporation rates and lower precipitation than the surrounding area on the plateau. The Jinsha River valley (upper Yangtze River), the upper Minjiang River valley, and the Xiaojiang River valley are dry valleys. The Xiaojiang River is a small tributary of the Jinsha River in Yunnan Province. Rockfalls, avalanches, slope slumps, small scale landslides, or human activities resulted in bare rocks on slopes in the dry valley. Grain erosion has been occurring on the bare rocks for more than ten years. The problem was not given paid much attention before the Wenchuan Earthquake because the area of grain erosion was small.

In general a grain erosion site consists of three parts: grain erosion surface at the top, grain flow section in the middle, and a deposit fan at the toe of the slope, as shown in Fig. 2.10 (Wang et al., 2009b). The rock surface of grain erosion has a slope angle in the range of 45°–60°. There is no vegetation on the erosion surface. The detached particles roll or flow through a section, which has a slope angle of about 40°. The deposit fan has an angle of about 35°, which is equal to the angle of repose of the granular material.

In the grain flow section the particles rolled and jumped down the slope. At each step a particle hit against the slope material, thus, the grain flow scoured the slope to form a channel. The channel has an angle of about 40° and the channel bed consists of relatively uniform sediment. Occasionally, particles fall onto the grain flow section from the grain erosion surface and initiate numerous particles rolling and saltating along the "path". Sometimes a layer of grains flows down the section, during which most of the particles slide and roll. The grain flow cuts the slope and forms a flume-like granular movement path.

Figure 2.11(a) shows a 2 m deep channel of a grain flow section on the bank of the Xiaobaini Ravine (a tributary of the Xiaojiang River), which is about 50 m long with a slope of 42°. Figure 2.11(b) shows several grain erosion sites along the Minjiang River near Wenchuan. Avalanches induced by the Wenchuan Earthquake have left many bare rocks along the Minjiang River. Intensive grain erosion has been occurring, especially in the dry season from March to June in 2009. The grains are much finer than the avalanche deposit. A part of the grain erosion deposit has been carried away by the river flow. Figure 2.11(c) shows a grain erosion site on the north bank of the upper Jiangjia Ravine, which provided a lot of loose solid material for debris flows. Figure 2.11(d) shows the vegetation damaged by grain erosion and grain flow along Jiuzhai Creek, which is a famous tourist attraction because of its beautiful landscape and vegetation. The grain flow section is 800 m long. The lithology consists of limestone and the grains generated from the erosion have a mean diameter of about 10 cm. The grains jump down the slope and hit against the trees. Most trees on the grain flow path have been killed.
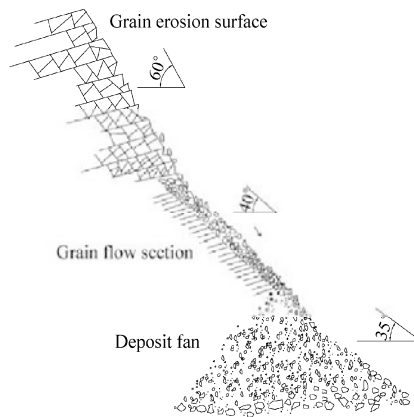
Fig. 2.10   Schematic diagram of a grain erosion site

Grain erosion has caused flying stones that have injured humans. Most of the highways in western Sichuan province are constructed along rivers. People have repaired or reconstructed highways that were damaged or destroyed by the earthquake. All highways were reopened before the one year anniversary of the Wenchuan earthquake. Nevertheless, due to the continual grain erosion, particles with a diameter from 1 cm to 20 cm roll and saltate down the slope potentially falling on cars and humans. The authors of this paper have witnessed that the windshield of a car was broken and the driver was seriously injured by a flying stone. Grain erosion has caused many highways to become so called "flying stone sections", especially

the highway along the Minjiang River. The highway managers have hired many people to monitor the flying stones and issue warning signals. The highways are occasionally closed because of these flying stones.

Grain erosion provides plenty of solid materials for mass movements. The deposit fans consist of uniform and loose solid materials and have high slope. Rainfall with an intensity of more than 20 mm/day triggers mass movements of the grains. These mass movements behave like debris flows but the distance of movement is, however, much shorter than normal debris flows, and in general travel distance is only several tens to one hundred meters. With water in the interstices of particles, which plays the role of lubrication, the grains move down the slope to streams or highways. Such a mass movement is called slope debris flow. The slope debris flow carries a lot of grains into rivers or deposits the grains on highways, causing blockage of highway transportation or local sedimentation on the riverbed. Figure 2.12(a) shows slope debris flow sediment deposited on the highway along the Mianyuan River. A rainfall of intensity of 47 mm/day initiated the slope debris flow, which carried sediment from the grain erosion deposit fan for a short distance from the high slope to the highway. The highway transportation was cut off for a few months by numerous slope debris flows. The angle of the debris flow deposit was about 15 degrees, much higher than normal debris flow deposit. A lot of grain erosion occurred along the Minjiang River. Figure 2.12(b) shows that a grain erosion deposit caused local sedimentation in the Minjiang River and changed the flow regime. The aquatic ecosystem was impacted by the sedimentation. Fish and benthic invertebrates lost their habitat due to the sedimentation.
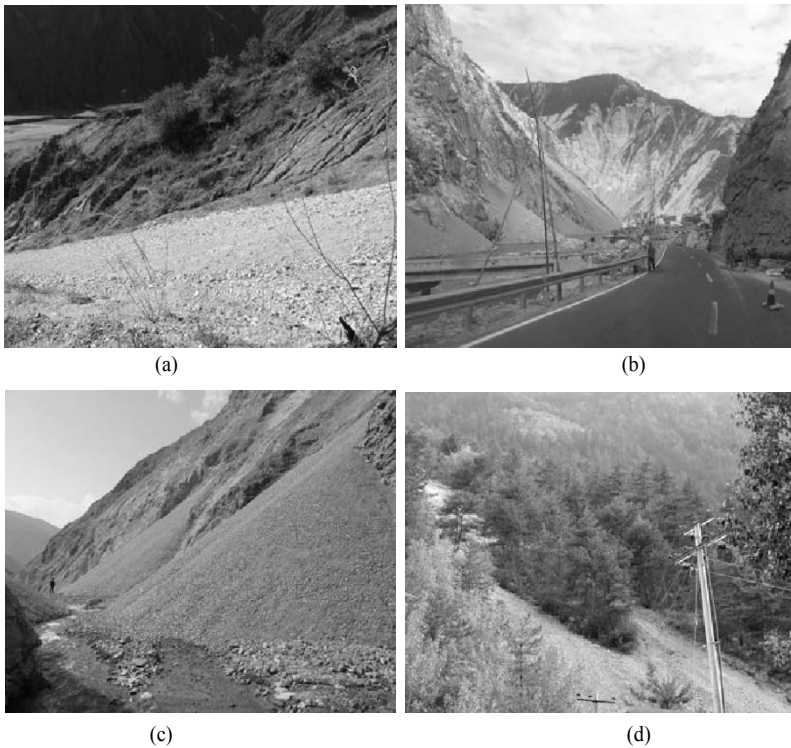
(a)   (b)

(c)   (d)

Fig. 2.11 (a) Grain flow in the Xiaobaini Ravine scoured the bank slope to form a 2 m deep 42° slope channel; (b) Several grain erosion sites along the Minjiang River near Wenchuan; (c) Grain erosion on the north bank of the upper Jiangjia Ravine, in Yunnan, China; (d) Grain flow on the slope of Jiuzhai Creek, which has killed many trees (See color figure at the end of this book)

(a)   (b)

Fig. 2.12   (a) A slope debris flow sediment deposit on the highway along the Mianyuan River; (b) Grain erosion deposit causing local sedimentation in the Minjiang River

Grain erosion occurs as a result of expansion and contraction due to temperature change and breakdown of rocks under the action of sunshine. The new bare rocks are very vulnerable to erosion. Without the protection of vegetation cover or a layer of soil on the surface, bare rocks are acted on by the radiation from the sun and temperature change. The exposure to weathering and the cycle of expansion during the day and contraction in the night causes fissures and breaks down the rocks. Figure 2.13(a) shows cracking bare limestone due to exposure to weathering and temperature change along the Mianyuan River. The limestone is fragile and a surface layer about 10 cm thick was broken. The surface layer of the rock is further broken down into grains. Wind or tremors caused the grains to roll down the slope. Figure 2.13(b) shows a layer of grain erosion deposit covering an avalanche deposit fan along the Minjiang River near Wenchuan. The grain erosion occurred on granite rock and the grains are generally finer than the grains in limestone areas. The grains are very uniform in size with a median diameter of about 1 cm. As a comparison the avalanche deposit beneath the grain layer is much more non-uniform consisting of stones of several meters and fine particles less than 1 mm. Because the grains from grain erosion are uniform in size and regular in shape people have mined the grains for building materials at some grain erosion sites with access to transportation facilities.

(a)   (b)

Fig. 2.13   (a) Bared limestone is cracked and broken down due to insolation and temperature change; (b) A layer of grain erosion deposit covered on an avalanche deposit fan on the Minjiang River near Wenchuan

   Grain erosion has occurred mainly in granite, limestone, and metamorphic rocks. The grains produced due to grain erosion in the limestone area was relatively coarse with diameter between 10–200 mm, grains in the granite area were finer with diameter between 5–30 mm; while in the metamorphic rock area the grain diameter varied in a large range from 0.1–300 mm. Figure 2.14 shows the size distributions of grain erosion deposits from the Minjiang River (granite rock), Jiuzhai Creek (limestone), and Xiaojiang River (phyllite rocks), in which GE represents grain erosion. Minjiang 1 and Minjiang 2 are two grain erosion sites along the Minjiang River near Wenchuan. Jiangjia and Dabaini Ravines are two tributaries of the Xiaojiang River. As a comparison the size distributions of landslides on the Shiting and Qingzhu Rivers, which are not far from Mianyang, are shown in the figure as well. The two landslides were triggered by the Wenchuan earthquake and caused thousands of casualties. The range of the size distributions of solid particles in the landslide deposits has 6 orders of magnitude from 0.01 mm to 10 m, whereas the grain erosion deposit has diameters within 2 orders of magnitude for granite and limestone and 3 orders of magnitude for metamorphic rocks. Relatively uniform grain size and lack of large stones are common features of grain erosion which is much different from those of landslides and avalanches.
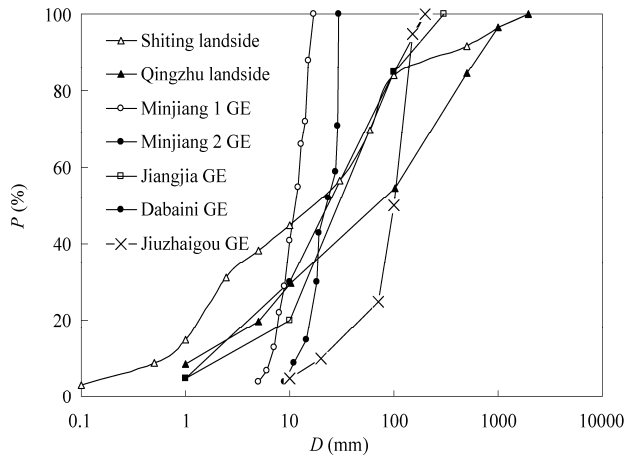
Fig. 2.14   Size distributions of grain erosion deposits (GE represents grain erosion)

   Exposure to weathering is the main agent for grain erosion, which may be proved by the following phenomena. The rocks on the Minjiang River became bare after the avalanches on May 12, 2008 triggered by the earthquake. Until early March 2009, grain erosion along the Minjiang River occurred only at several sites with limited areas. From March to June, the Minjiang River experienced the strongest sun exposure and driest season. During this time grain erosion developed very quickly with the area of grain erosion almost doubled. In general, the grain erosion on the south-facing bank of rivers is much more intense than that on the north-facing bank. Figure 2.15 shows the grain erosion on the south-facing bank and rill erosion (water erosion) on the north-facing bank of the Chaqing Gully along the Xiaojiang River. The lithology (phyllite) and rainfall on the two banks are the same but the sun exposure on the north-facing bank is much weaker than on the south-facing bank, therefore, grain erosion occurs on the south-facing bank and water erosion occurs on the north-facing bank. These phenomena prove that sun exposure weathering is the most important agent for grain erosion.

   Shattering erosion is mainly caused by freeze-thaw cycles and has very different characteristics. It was found that north-facing slopes have more intense erosion than south-facing slopes in semiarid northeastern Arizona canyons (Burnett et al, 2000; Halsey et al, 1998).

(a)   (b)

Fig. 2.15 Grain erosion occurs on the south-facing bank (a) while rill erosion (water erosion) occurs on the north-facing bank (b) of a small stream (See color figure at the end of this book)

A surface layer of bare rocks was broken down into grains due to sun exposure and temperature change. Over time a certain thickness of the surface layer of the rocks has been broken down into grains. Wind detached the grains from the rock and triggered grain flow. The amount and size of grains removed by wind is a function of wind speed. An experiment was done to study the relation of the amount and size of grains blown down with wind speed. Because grain erosion occurs at quite high elevations or on dangerous cliffs in the earthquake area, the experiment was done in the Xiaojiang River basin where grain erosion occurs on relatively small mountains. The lithology at the experiment sites is metamorphic rock consisting mainly of phyllite. The grains of a surface layer of rocks were blown down with bellows and batteries, which were transported to the mountain slopes along the Chaqing Gully by donkeys. The wind speed was measured with a rotational wind velocity meter. The bellows had a square nozzle of 10×10 cm^2. A Blast of wind with a maximum speed of 20 m/s acted on the bare rock surface and the grains blown by the wind were collected with a bag and weighed with a balance. For each experiment an area of 1 m^2 of the bare rock surface was acted on by the wind at a given wind speed for 10 min. Figure 2.16 shows the experimental results.

As shown in Fig. 2.16(a) the amount of grains blown down by wind in the four experiments had a consistent relation with wind speed and was proportional to the fourth power of wind speed. The size of the largest grain blown down from the bared rock was proportional to the wind speed (Fig. 2.16(b)), that is:

$$E_b = R_1 U^4 ; \quad D_m = R_2 U \tag{2.1}$$

in which U is the wind speed (m/s), E_b is the amount of the grains blown down by wind per time per square meter of bare rocks (g/min·m^2), and D_m is the diameter of the largest grain blown down by wind in (mm), R_1 is a constant and is equal to 0.00625, R_2 is a constant and is equal to 1.0. A wind with a speed of 20 m/s blew 1 kg of grain per minute away from one square meter of the bare rock with a maximum grain size of 20 mm. The bellows used in the experiment can only generate winds of speeds equal to or less than 20 m/s. In the gully, however, natural winds of maximum speed over 35 m/s were measured with the wind velocity meter. The amount and size of grains blown down by wind can certainly be larger than those from the experiment.

The amount of grains blown down by wind depends on the wind speed and also on the cumulative time of weathering before the wind. In the experiment a wind speed of 20 m/s continued for 40 minutes, and the amount of grains blown down by the wind per time reduced with time, as shown in Figure 2.16(c). Four measurements, each lasting 10 minutes, were made during the experiment of wind acting on 1 m^2

for 40 minutes. At the same wind speed the amount of grains blown down by wind per time reduced from 1,000 g/m²min in the first 10 minutes to only 100 g/m²·min in the fourth 10 minutes because after the grains on the top surface were removed the remaining grains were not readily detached from the rock. No general laws for the size of largest grains blown down by wind were found. It seems that the grain size increased from 20 mm to 45 mm, and, then, it reduced to about 25 mm as shown in Fig. 2.16(d).
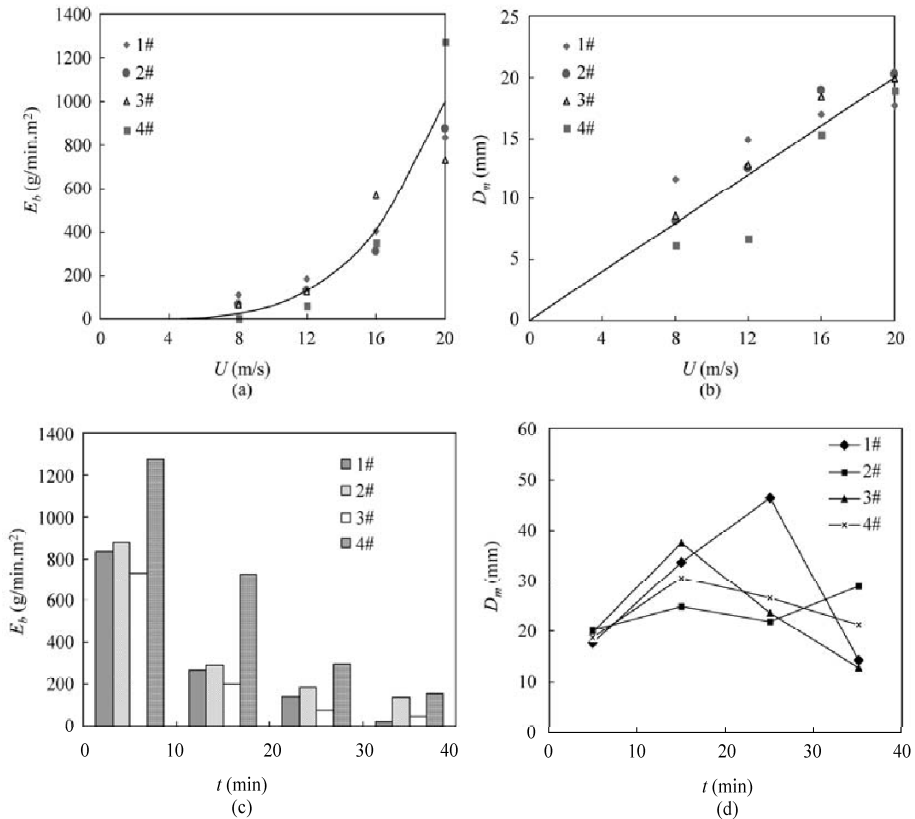
Fig. 2.16 (a) Amount of grains blown by wind from 1 m² of rock surface per time as a function of the wind speed; (b) The largest grain size blown by wind as a function of wind speed; (c) Reduction with time of the amount of grains blown down by wind from 1 m² of rock surface per time in consecutive experiments; (d) Variation of the largest size of blown grains in consecutive experiments (Wang et al., 2010)

The rate of grain erosion blown by wind per area per time in Fig 2.16 represents a high instantaneous rate of grain erosion. The annual rate of grain erosion, however, depends on the frequency of high speed winds, rate of sun weathering, and the action of temperature change. In general, the bare rock may be eroded by several to several tens of centimeters per year, depending on the lithology, location, local weather, and winds. As shown in Fig. 2.13(b) the depth of the grain erosion deposit on the avalanche deposit fan, which could be easily identified by its uniform size, was measured with a scale at two or three places. The average depth of the grain erosion deposit multiplied by the surface area of the fan was the volume of grains eroded from each grain erosion site in the past year. The area of grain erosion of the bare rock surface was measured with laser range meters, which have a maximum error of 1m. The bare rock surfaces were generally larger than 100 m in length and width, therefore, the maximum relative error

was less than 1%. The rate of grain erosion of rocks was obtained by dividing the volume of grains over the surface area of bare rock. The same measurement was also performed for 9 grain erosion sites in the Xiaojiang River basin. The rate of grain erosion of bare rocks along on the Minjiang River was between 3 to 53 cm/yr, with an average rate of grain erosion of about 17 cm/yr. The rate of grain erosion in the Xiaojiang River basin was only 1.1–4.6 cm/yr, with an average rate of about 2.8 cm/yr (Wang et al., 2010). The rate of grain erosion in the earthquake area was much higher than in the Xiaojiang River basin because the bare rocks in the earthquake area were fresh. The rate of grain erosion will gradually reduce if even no control strategies are taken. Compared with the shattering erosion the rate of grain erosion was more than 1000 times higher.

Studies have been devoted to the particle movement in the grain flow section and strategies have been suggested to control the grain flows (Wang et al., 2007a,b,c; Xu et al., 2007). The proposed control strategies were engineering measures for protection of highways, such as concrete sealing, protection walls, and removing grain deposits with machines (Xu et al., 2007). These strategies are aimed at controlling the movement of grains rather than controlling the erosion on the bare rocks. Nevertheless, grain flow control is not essential for mountain hazard control. If the grain erosion is not controlled any grain flow control structure will finally fail to control grain flow. Thus, essentially no control has been achieved. Moreover, some engineering measures worsened the damage to highways (Sun et al., 2006).

The essential cause of grain erosion is devegetation and exposure of bare rocks to weathering and temperature change. Therefore, an essential strategy to control erosion is revegetation. Several studies have been done on the interactions between moisture, lithobiontic organisms, and rock weathering. Some researchers simply assumed that the organic weathering replaces inorganic processes and paid attention to the rates of bioerosion while little attention was paid to the role of erosion control played by a particular species (Naylor et al., 2002). Only a few studies have attempted to identify bioprotection of lichens during weathering processes recently (Carter and Viles, 2003, 2005). Yet there is little consensus over whether rates of lichen-mediated weathering are slower than rates of a abiotic weathering of otherwise identical rock surfaces (Lee, 2000). In fact, epilithic organisms can tremendously change microclimate. The canopy temperature of cushion vegetation in the Alps could be 27℃ and relative humidity could be 98%, while the air temperature is 4℃ and relative humidity is only 40% (Korner 2003). Scientists also conducted field experiments and concluded that the epilithic lichen retains moisture and reduces thermal stress on the surface of limestone effectively (Carter and Viles, 2003).

It was found from field investigations that if a thin layer of lichen and moss grow on the rock surface, the weathering and temperature change are mitigated and cannot directly act on the rock, and no grain erosion occurs. The bare rock experienced grain erosion. Wind with a speed of 20 m/s from the experimental bellows blew down more than 9 kg of grains in 10 minutes from $1m^2$ of rock surface. When the same wind acted on another rock surface, on which there was a thin layer of moss and lichen, however, no grains were blown down. The moss and lichen layer was only about 1 mm thick, but it effectively protected the rock from the direct action of sun and temperature change.

An experiment was done at Xiaomuling, which is a grain erosion site along the Mianyuan River. Spores of five moss species were collected from local and neighboring areas and mixed with a clay suspension. The clay material was collected from fine sediment deposits on the floodplains of the Mianyuan River and the clay particles were finer than 0.01 mm. The concentration of clay suspension was 265 kg/m^3. The collected sporophyls were smashed with a machine. The clay suspension had a certain concentration of the smashed sporophyls to have a sufficient amount of spores per liter of clay suspension. The experimental plots were more than 100 m high above the Mianyuan River. Local farmers were hired to carry the clay suspension with moss spores up to the mountain and pour down the suspension onto the bare rock surface at several plots.

Several rainstorms occurred after the experiment. Rain washed a part of the clay suspension down to the lower part of the bare rock, which helped to spread the moss spores to a large area of the rock surface. Figure 2.17(a) shows the grain erosion site at Xiaomuling on the Mianyuan River. Figure 2.17(b) shows the clay suspension layer with moss spores. Two moss species had germinated on the rock surface after one month of the experiment. Two months later the experimental plots had become green with a thin layer of moss growing, as shown in Fig. 2.17(c). Because rainstorms spread the clay suspension to the lower part of the rocks, the area of greened rock surface was larger than the rock surface with clay cover at the beginning of the experiment. Only two species of moss: *Rhizomnium sp.* and *Grimmia sp.* successfully germinated on the rock surface. Both of the species were collected from local vegetated rocks.
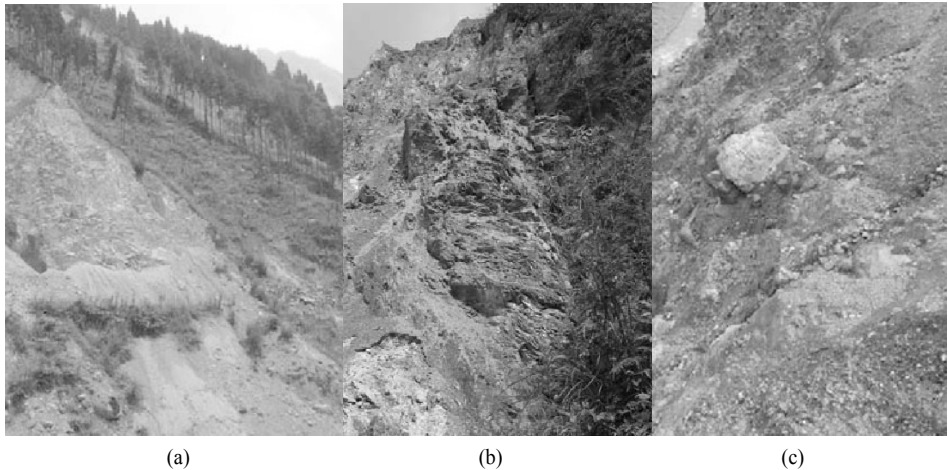
<div>
(a) (b) (c)
</div>

Fig. 2.17 (a) Grain erosion site at Xiaomuling on the Mianyuan River, Sichuan; (b) Clay suspension with moss spores was splashed on the Xiaomuling grain erosion rock; (c) Two months later the rock surface was green and grain erosion was controlled (See color figure at the end of this book)

Selection of moss species is important for the success of the vegetation restoration. However, the clay suspension with moss spores must be poured onto the top part of the local bare rock. If only a lower part of the bare rock is covered with clay suspension and it is revegetated, while the grain erosion on the upper part continues, the grains falling from upper part may destroy or bury the newly greened lower rock surface. The grain erosion rock surfaces in the Minjiang River valley are rather high and very dangerous for humans to climb up. Helicopters may be used to pour the clay suspension with moss spores onto the top of the bare mountains in order to quickly control grain erosion and revegetate the bare mountains.

2.2　Vegetation

2.2.1　Various Vegetations

Generally, vegetation affects the fluvial process and the development of the drainage network, including the channel incision process. In the past century human activities have resulted in deforestation in many countries. Extensive loss of vegetation cover in the watershed can decrease infiltration and increase runoff, leading to higher flood peaks and additional runoff volume. Where reduced cover increases overland flow and reduces infiltration, additional water may flow more rapidly into stream channels, producing a more "flashy" stream system. Reductions in base flow and increases in storm flow can result in a formerly

perennial stream becoming intermittent or ephemeral. Restoration of vegetation in the watershed has become one of the main tasks of management of the river ecosystem.

Basically, vegetation development needs water, soil, and suitable temperatures. In nature, vegetation develops almost everywhere, on the mountains and in river valleys, even deserts and glaciers. Figure. 2.18(a) shows the vegetation on the glacier near Banff in Canada. The trees may grow in only 1–2 months in summer, when the soil temperature is over $0°C$. Most of the trees have an age over 1,000 years although the trunk diameter of the trees is only several tens of centimeters. Figure 2.18(b) shows the trees in the Sinai Peninsula in Egypt, where the climate is very dry and rain several years.

(a)

(b)

Fig. 2.18   (a) Vegetation in the glacier near Banff in Canada. Most of the trees have an age over 1,000 years; (b) Trees in the Sinai Peninsula in Egypt, where the climate is very dry and rain several years

Development of the vegetation cover in mountainous or hilly areas depends on the local climate, precipitation, soil texture, parent material, topography, soil erosion, types of land-use, and human activities. Among them, soil erosion is the most important natural factor and human activities are the most vital non-natural factor affecting the vegetation. Kosmas et al. (2000) studied the effect of land parameters on vegetation and erosion on the island of Lesvos, Greece. The island is divided into semi-arid and sub-humid zones. Low rainfall combined with high evapotranspiration demands in the semi-arid zone has significantly affected vegetation performance and the degree of erosion.

Vegetation cover increases with increasing rainfall and soil depth. In the area with insufficient soil, the thickness of the soil layer determines the average height of vegetation. Essentially, the weight of the roots of a plant and the soil grasped by the roots must be greater than the weight of the over ground part of the plant. Figure 2.19 shows the vegetation on the north part of Taihang Mountain in the northern China. This area is covered mainly with dolomite limestone. The rock is weathered mainly by dissolution by rainfall containing CO_2. In the process no granular material is produced. Therefore, there is a thin layer of soil on the mountain and poor vegetation may develop in this area.

Fig. 2.19 There is a very thin layer of soil on the north part Taihang Mountain in the northern China. Only a few species of shrubs can grow in this area, and, thus, the vegetation is poor

In many places, human activities have completely or partly changed the vegetation. According to the extent of impact of human activities the vegetation may be classified into primitive vegetation, reforested vegetation, and domestic vegetation. **Primitive vegetation,** such as virgin forest, has not been disturbed by human activities. The floral community usually consists of complex species composition. Most of the primitive vegetation in the world has been destroyed by forest fire, logging, and other natural disasters and human activities. There are only several plots of primitive vegetation in high mountainous areas. Figure 2.20 shows a primitive forest in the Jiuzhai basin in western Sichuan, China.

Fig. 2.20 Primitive vegetation in the Jiuzhai basin in western Sichuan, China

Reforested vegetation—To accelerate development of new vegetation humans plant trees in mountainous areas throughout the world. The dominant species of wood are planted by humans, which consist of a few selected species; but the under-story community develops under the natural conditions and consists of local species, which results in a complex system of **reforested vegetation**. Figure 2.21 shows an example of the reforested vegetation in Calcutta, India. The woods were planted by humans but the lower layer of the vegetation consists of shrubs, grasses, and liana developed naturally. In general, reforested vegetation conforms to the natural environment and it may sustain if humans discontinue the artificial disturbance.

Fig. 2.21 Reforested vegetation in Calcutta, India. The wood was planted by humans but the lower layer of the vegetation consisting of shrubs, grasses, and liana developed naturally

Domestic vegetation is a different concept from reforested vegetation. In the process of urbanization, various plants have been planted and acclimated to beautify people's living environment. Thus, domestic vegetation has developed around cities. Such kinds of vegetation have adjusted to the human stresses (irrigation, pesticides, wind protection, etc.) and it will not sustain if humans discontinue management. This is a phenomenon of yield. Of course, a crop field is a kind of domestic vegetation. Figure 2.22 shows the domestic vegetation around a living area planted to beautify the environment in Sharm El Shrek on the Sinai Peninsula in Egypt. There is almost no rain in the areas and the vegetation relies on irrigation by humans. The water is desalinized seawater from the Red Sea.

Fig. 2.22 Domestic vegetation around a living area in Sharm El Shrek on the Sinai Peninsula in Egypt, for which a sprinkler system distributes desalinized seawater from the Red Sea

Vegetation succession is defined as the process of an initial pioneer suite of plants established in the early stage of colonization of bare land, which consists mainly of herbaceous species that require high amounts of light, being replaced gradually by a suite of plants, which consists of woods, shrubs, and grasses that tolerate low light or closed canopy situations. There are four types of vegetation succession associated with river management, i.e. ① reforestation of forests removed by different stresses, such as logging, forest fire, and volcanic eruption; ② colonization and development of the plant community on land newly created by sedimentation, such as bars or islands in a river channel; ③ vegetation development on blown sand dunes with humans disturbance; and ④ vegetation development on landslide and avalanche deposits. Figure 2.23 shows a vegetation succession from a pioneer suite consisting of lichen and grasses (a), to a suite consisting of shrubs and grasses (b), and finally to a complex suite consisting of woods, shrubs and grasses (c) on the Yunnan-Guizhou Plateau in southwestern China.

Riparian vegetation—While watershed vegetation affects the long-term development of the river network, riparian vegetation exerts more direct and short term effects on the degradation and aggradation of the river channel. Riparian vegetation may be defined as the vegetation growing on fluvial surfaces that are inundated or saturated by the dominant or bank-full discharge (Hupp and Osterkamp, 1996). Woody vegetation may be removed or damaged by degrading channel processes, and, in turn, may substantially ameliorate degrading conditions and play a critical role in the initiation and character of channel recovery processes. Most floodplains, riverine wetlands, river channel banks, and in-channel features potentially support riparian vegetation; only terraces with flood return intervals exceeding about 3 years do not typically support riparian assemblages (Nilsson et al., 1989). Intact riparian zones are recognized as critical features in the landscape for maintenance of biodiversity. They are 'the most diverse, dynamic, and complex biophysical habitats on the terrestrial portion of the Earth' (Naiman et al., 1994). In temperate areas, the riparian zone supports more species of plants than any other habitat. In western North America, riparian zones comprise less than 1% of the total land area, yet 80% of terrestrial vertebrate species are dependent upon them for at least part of their life cycle (Miller et al., 1995). In North America and Europe, more than 80% of riparian corridors have disappeared in the last 200 years (Naiman et al., 1992). Because channel incision promotes the development of terraces that are infrequently flooded, incision potentially has a substantial role in altering, damaging, or destroying much of the riparian zone world-wide.

Watershed vegetation—Vegetation in a watershed is the most important factor affecting surface runoff and soil erosion. Vegetation and erosion are a couple of competing and mutually interacting aspects of a watershed. In the northern part of the Loess Plateau of China, the vegetation hardly develops because the extremely high rate of erosion tears away the topsoil, on which the vegetation relies. In areas with vegetation, such as the upper reaches of the Yangtze River, erosion damages and destroys the vegetation and scars the land surface. Erosion causes not only soil loss but also loss of water and nutrients. Kosmas et al. (1998) found that under semi-arid climatic conditions water vapor adsorption by the soil could be more than the water received from rainfall. They measured that from February to August. 1996, a total amount of 226 mm of water vapor was adsorbed by the soil, while the total rainfall was only 179 mm in the same period. Soil erosion reduces this adsorbed water, which is important for vegetation development. The total organic carbon in soil is about 1,550 billion, plus 1,200 billion of C in oil, gas, and coal (Schapenseel and Pfeiffer, 1998). On average, the world's rivers annually transport about 0.5 billion tons of organic carbon to the oceans. This transport, in general, is equally distributed between dissolved and particulate fractions of the river load (Spitzy and Ittekkot, 1991). A significant fraction of the transported carbon is finally oxidized and emitted into the atmosphere. A principal off-site environmental impact is due to the disruption of the global carbon cycle, resulting in an erosion-induced efflux of about 1.14 billion t/yr from soil to the atmosphere (Lal and Kimble, 1998). The influence of the efflux on the climate is considerable.

(a)

(b)

(c)

Fig. 2.23   Vegetation succession from a pioneer suite consisting of lichen and grasses (a), to a suite consisting of shrubs and grasses (b), and finally to a complex suite consisting of woods, shrubs and grasses on the Yunnan-Guizhou Plateau in southwestern China (c)

Vegetation control erosion—Vegetation is the most effective form of erosion control and it is also self-healing. Vegetation reduces erosion by ① adsorbing the impact of raindrops, ② reducing the velocity and scouring power of runoff, ③ reducing the runoff volume by increasing the percolation into the soil, ④ binding soil with roots, and ⑤ protecting the soil from wind erosion (Goldman et al., 1986). On the Loess Plateau of China the Wangjiagou Gully has a well-established forest that has trapped sediment and, therefore, the gully bed has risen 5 m in 120 years (Li, 1993). Investigations into many small watersheds

on the Loess Plateau demonstrate that 40% vegetation cover may reduce the soil erosion by 62%, and 54% vegetation cover may reduce erosion by 80% (Li and Zhang, 1997). A study indicates that the soil erosion the Loess Plateau is inversely proportional to the density of the vegetation cover. The sediment yield reduces to nearly zero if the forest cover is higher than 60% (Wang and Wang, 1999).

   Estimating rate of erosion with vegetation—Vegetation may be used for estimation of the erosion rate. Rill and gully erosion are the main patterns of upland erosion. It is estimated that more than 60% of sediment yield results from rill and gully erosion. The rate of rill and gully erosion can be estimated by the following method: select newly eroded rills or gullies on slopes with vegetation, as shown in Fig. 2.24. The trees on the banks of the gully are very useful for the erosion estimation. Tree-ring sampling is performed to estimate the age of plants on the gully banks and the depth of the gully erosion is measured directly from the tree elevation to the gully bed. The rate of the gully erosion may be calculated by dividing the depth of the gully by the age of the plants. This method is based on the assumption that vegetation and rills or gullies develop on the slope simultaneously, and the plants grow up while the rills and gullies erode.

Fig. 2.24   Trees on the gully banks used to estimate the rate of gully erosion (See color figure at the end of this book)

   Modeling of vegetation development—Many efforts have been made to model vegetation dynamics. Svirezhev (1999) studied the development of vegetation patterns (grass or forest) under climatic and anthropogenic stresses. Three fundamentally different approaches to the solution of the problem have been proposed. The first one is based on the assumption that climatic factors such as temperature, precipitation, etc., are the factors which best define the allocation of different plant communities around the world. The approach has been used to investigate the geographical distribution of the main biomes under prospective climatic changes at a global scale (Monserud et al., 1993). The second approach is based on the description of physiological growth processes and their dependence on local climatic parameters, and it mainly operates with the global carbon cycle. The third approach is an attempt to apply dynamic models using either mathematical ecology or mathematical evolutionary genetics. Introducing $p(x, y, t)$ and $q(x, y, t) = 1 - p$ to represent the probabilities of the vegetation pattern being forest and grass, respectively, Svirezhev (1999) presented a simple model to calculate the probability of the vegetation of an area being grass or forest.

   Maley and Brenac (1998) analyzed the pollen record from the Lake Barombi Mbo and found that the vegetation is naturally dynamic with pollen concentration varying from 1,000–50,000 per gram of deposit following climate change and other stresses. Pedersen (1998) introduced a conceptual model of the process of tree mortality responding to ecological stresses. To simulate short and long-term stresses the model

predicts changes in tree vigor. The results also suggest a mechanism by which short-term environmental stresses affect tree physiology prior to death. Mulligan (1998) examined the impact of climatic variability on hydrology and vegetation cover using the PATTERN ecosystem model. An examination of the variability of soil erosion which results from this variable hydrology and vegetation cover indicates the temporally erratic nature of erosion events, the tendency for most erosion to occur during infrequent extreme events, and the dynamic response of erosion to climatic variability. The results also indicate the dependence of erosion on the type of vegetation cover and vegetation response to climatic variability. Thornes (1985) proposed a model of the geomorphologic process considering the rate of change of vegetation. The differential equations of vegetation and erosion are coupled and the influence of wild animals is modeled.

2.2.2 Ecological Stresses on Vegetation

Ecological stress—While the vegetation harmonizes itself with the environment, it suffers various ecological stresses. Ecological stress is defined as any kind of disturbance, natural or non-natural, on the vegetation development, which may change the vegetation cover or affect the evolution process of vegetation. Soil erosion is the most important natural ecological stress and human activities are the non-natural ecological stress. Conversely the development of vegetation cover affects the soil erosion with the interaction, following a law of dynamics. For a watershed, vegetation and erosion may reach an equilibrium state if the circumstances remain unchanged for a long period of time.

Generally speaking, vegetation suffers from various ecological stresses, including erosion, forest fire, drought, windstorm, grazing, air pollution, logging, acid rain, and reforestation. Human activities, including mining, road construction, logging, and reforestation, exhibit the most direct, and in many cases, the strongest ecological stresses on the vegetation. Drought is the most potent natural ecological stress reducing the vigor of vegetation, which may eventually cause mortality of vegetation because most of the dead trees experienced vigor reduction prior to mortality. Bussotti and Ferretti (1998) studied the impact of air pollution on a forest in Europe and found that air pollution reached the concentration likely to have adverse effects on forest vegetation. Ozone has been proven to cause foliage injury in a variety of native forest species in different countries. Obvious declines of vegetation related to environmental factors are: ① the deterioration of some coastal forests due to the action of polluted sea spray; ② the deterioration of reforestation projects, especially conifers mainly due to the poor ecological compatibility between species and site; and ③ the decline of deciduous oaks due to the interaction of climate stresses and pests and diseases. Catastrophic wind causes damage and fall of trees. Clinton and Baker (2000) studied the forest tree-fall due to storms and pit and mound topography resulting from catastrophic wind in the U.S. Wind has caused large-scale forest disturbance.

Natural stresses—Among the many natural ecological stresses that disturb structure and functions of vegetation are erosion, drought, storm, floods, hurricanes, tornadoes, fire, lightning, salinization of soil, volcanic eruptions, earthquakes, insects and disease, landslides, temperature extremes, and grazing. For instance, erosion damages the vegetation on the slope of the Yunnan-Guizhou Plateau of China (Fig. 2.25(a)); salinization of soil may kill the shrubs, grass, and trees (Fig. 2.25(b)); and an earthquake induced landslide destroyed the vegetation on the Jiufener Mountain in Taiwan, China in 1999 (Fig. 2.25(c)); insects killed trees (Fig. 2.25(d)); a heavy snow broke trees and almost killed a forest on the Zhangjiajie Mountain (Fig. 2.25(e)); and a forest fire cleared the vegetation in the upper reaches of the East River watershed in Guangdong Province in southern China (Fig. 2.25(f)). For the latter case most of the roots are still alive and new vegetation is quickly developing.

Natural disturbances are sometimes agents of regeneration and restoration. Certain species of riparian plants, for example, have adapted their life cycles to include the occurrence of destructive, high-energy

disturbances, such as alternating floods and droughts. In general, riparian vegetation is resilient. A flood that destroys a mature cottonwood forest also commonly creates nursery conditions necessary for the establishment of a new forest (Brady et al., 1985), thereby increasing the riparian system.
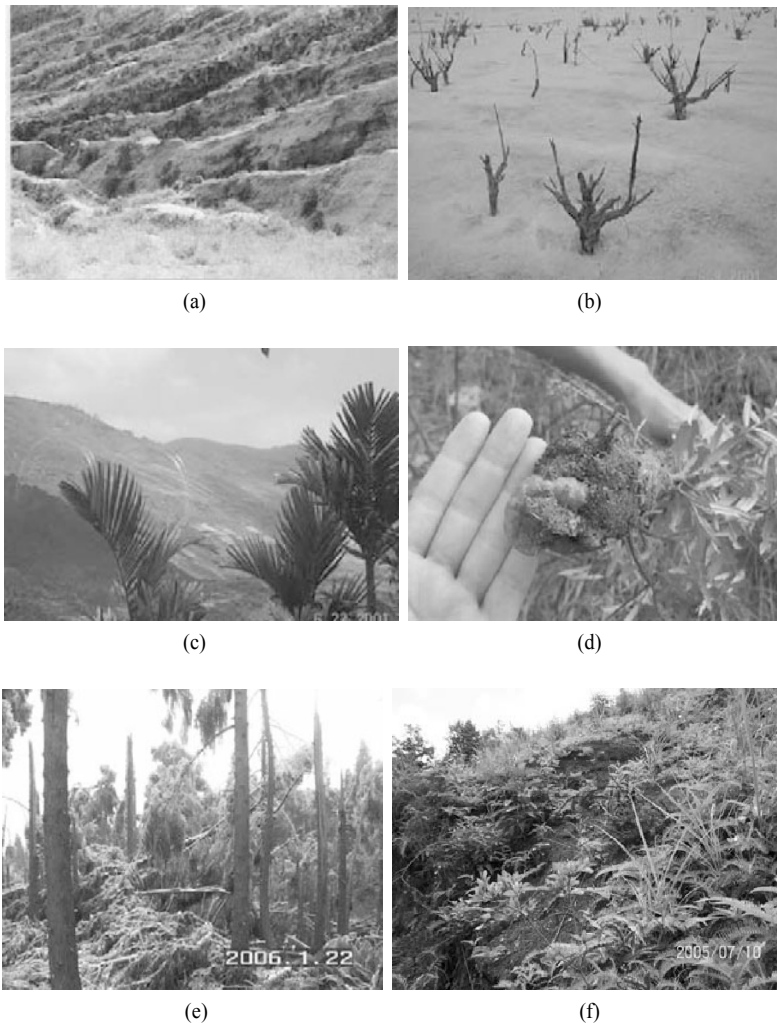
Fig. 2.25   Various natural stresses on vegetation: (a) Soil erosion damages the vegetation on a slope of the Yunnan-Guizhou Plateau of China. (b) Soil salinization has resulted in the mortality of shrub vegetation on the Yellow River delta; (c) An earthquake-induced landslide destroyed the vegetation in Taiwan, China in 1999; (d) Insects killed trees; (e) Heavy snow broke trees on Zhangjiajie Mountain; and (f) A forest fire cleared the vegetation in the upper reaches of the East River in southern China (See color figure at the end of this book)

Human-induced ecological stresses are exerting ever-increasing impacts on vegetation. The human-induced stresses include land use change, agriculture, urbanization, air pollution, sewage and industrial waste contamination, husbandry, logging, reclamation, mining, road construction, and afforestation. Figure 2.26 shows the effect of mining (a), road construction (b), agriculture (c), and husbandry (d) on vegetation.

(a)　　　　　　　　　　　　　　　　　　(b)

(c)　　　　　　　　　　　　　　　　　　(d)
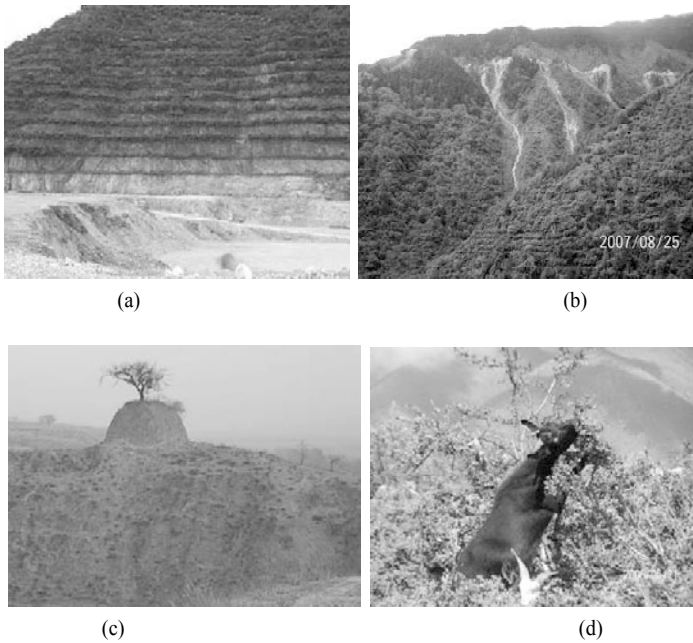
Fig. 2.26 (a) Effect of quarrying on vegetation. To mitigate the effect of quarrying on the vegetation workers transport soil to the quarry face and plant grasses to green the quarry; (b) Road construction causing forest damage; (c) Farmers reclaim the slope land for agriculture and some trees have been removed; (d) Goats eat buds and leaves of shrubs, intense grazing impairs vegetation

Mining—Exploration, extraction, processing, and transportation of coal, minerals, sand and gravel, and other materials have had and continue to have a profound effect on vegetation. Surface mining methods include strip mining, open-pit operations, placer mining, and hydraulic mining. Such mining activity has frequently resulted in destruction of vegetation. In some cases today, mining operations still disturb most or all of entire watersheds. Mining can often remove large areas of vegetation at the mine site, transportation facilities, processing plant, tailings piles, and related activities. Reduced shade can increase water temperatures enough to harm aquatic species. Loss of cover vegetation, poor-quality water, changes in food availability, and disruption of migration can have serious effects on terrestrial wildlife. Species composition may change significantly. Transportation, staging, loading, processing, and similar activities cause extensive changes to soils including loss of top-soil and soil compaction. Direct displacement for construction of facilities reduces the number of productive soil acres in the watershed, as does covering of productive soil by materials such as tailings. These activities decrease infiltration, increase runoff, accelerate erosion, and increase sedimentation

Water and soils are contaminated by acid mine drainage (AMD) and the materials used in mining. Acid mining drainage, formed from the oxidation of sulfide minerals like pyrite, is widespread. Many hard rock mines are located in iron sulfide deposits. Upon exposure to water and air, such deposits undergo sulfide oxidation with attendant release of iron, toxic metals (lead, copper, zinc), and excessive acidity. Mercury was often used to separate gold from the ore; therefore, mercury was also lost into streams. Present-day miners using suction dredges often find considerable quantities of mercury still resident in streambeds. Current heap-leaching methods use cyanide to extract gold from low-quality ores. This poses a special risk if operations are not carefully managed. Toxic runoff or precipitates can kill

streamside vegetation or can cause a shift to species more tolerant of mining conditions. This affects habitat required by many species for cover, food, and reproduction.

Farming—An obvious human stress disturbing vegetation is the conversion of natural areas to farmland, resulting in the removal of native riparian and upland vegetation. Producers often crop as much productive land as possible to enhance economic returns; therefore, native vegetation is sacrificed to increase arable acres. As the composition and distribution of vegetation are altered, the interactions between vegetation structure and function become fragmented. Vegetation removal can result in sheet and rill as well as gully erosion, reduced infiltration, increased upland surface runoff and transport of contaminants, increased soil erosion, unstable stream channels, and impaired habitat.

Agricultural drainage, which allows the conversion of wetland soils to agricultural production, lowers the water table. Tile drainage systems concentrate ground water discharge to a point source, in contrast to diffuse natural discharges. Subsurface tile drainage systems and drainage ditches constitute a landscape scale network of disturbances. Underground water supplies have diminished at an alarming rate in the areas surrounding cities and towns. These practices have eliminated or fragmented habitat.

Tillage and soil compaction interfere with the soil's capacity to partition and regulate the flow of water in the landscape, increase surface runoff, and decrease the water-holding capacity of soils. Tillage also often aids in the development of a hard pan, a layer of increased soil density and decreased permeability that restricts the movement of water into the subsurface. This results in changes in surrounding vegetation. Pesticides and nutrients (mainly nitrogen, phosphorous, and potassium) applied during the growing season can leach into ground water or flow in surface water, either dissolved or adsorbed to soil particles.

Logging—Vegetation is a key factor influencing the bio-communities of the watershed. Forest thinning includes the removal of either mature trees or immature trees to provide more growth capability for the remaining trees. Final harvest removes mature trees, either singularly or in groups. Both activities reduce vegetative cover. Tree removal decreases the quantity of nutrients in the watershed since approximately one-half of the nutrients in trees are in the trunks. In stream nutrient levels can increase if large limbs fall into streams during harvesting and decompose. Conversely, when tree cover is removed, there is a short-term increase in nutrient release followed by long-term reduction in nutrient levels. Logging of trees can reduce availability of cavities for wildlife use and otherwise alter the biological system as the tree cover is removed. Loss of habitat for fish, invertebrates, aquatic mammals, amphibians, birds, and reptiles can occur. Removal of topsoil, soil compaction, and equipment and log skidding can result in long-term loss of productivity, decreased porosity, decreased soil infiltration, and increased runoff and erosion. Soil disturbance by logging equipment can have a direct physical impact on habitat for a wide variety of amphibians, mammals, fish, birds, and reptiles, as well as physically harm wildlife. Loss of cover, food, and other needs can be critical. Sediment produced for logging areas can clog fish habitat.

Husbandry—Vegetation is stressed by husbandry, or grazing of domestic livestock, primarily cattle and sheep. Grass vegetation is particularly attractive to livestock. Unless carefully managed, livestock can overuse these areas and cause significant disturbance. The primary impacts that result from grazing of domestic livestock are the loss of vegetative cover due to its consumption or trampling from the presence of livestock. Reduced vegetative cover can increase soil compaction and decrease the depth of and productivity of topsoil. Reduced cover of mid-story and over-story plants decreases shade and increases water temperatures.

Trampling, trailing, and similar activities of livestock physically impact soil moisture content by compaction, varying markedly with soil type and moisture content. Very dry soil is seldom affected, while very wet soils may also be resistant to compaction. Moist soils are typically more subject to compaction

damage. Compaction of soils by grazing animals can cause increased soil bulk density, reduced infiltration, and increased runoff. Loss of capillarity reduces the ability of water to move vertically and laterally in the soil profile. Reduced soil moisture content can reduce site capacity for lowland plant species and favor upland species. Excessive trailing can result in gully formation and eventual channel extension and migration. Unmanaged grazing can significantly impair vegetation. Figure 2.26(d) shows trees damaged by the goats. Heavy husbandry impairs vegetation.

Recreation—The amount of impact caused by recreation depends on soil type, vegetation cover, topography, and intensity of use. Various forms of foot and vehicular traffic associated with recreational activities can damage riparian vegetation and soil structure. All-terrain vehicles, for example, can cause increased erosion and habitat reduction. At locations, reduced infiltration due to soil compaction and subsequent surface runoff can result in increased sediment loading to a stream (Cole and Marion, 1988). Both concentrated and dispersed recreation can cause disturbance and ecological change. Camping, hunting, fishing, boating, and other forms of recreation can cause disturbances to vegetation and bird colonies. Motorcycles and horses cause far more damage to vegetation and trails than do pedestrians.

2.2.3 Classification of Stresses

The degree of vegetation development may be represented by the coverage of trees and shrubs, the thickness of vegetation (height of trees shrubs and grasses) and the vigor of the trees, biomass per unit area, and age and health of the plants. In the view of controlling erosion, binding soil with roots and shelter of plants are a highly effective function of vegetation, therefore, the mass of the plant roots per unit area and cover of vegetation are meaningful parameters. However, the mass of plant roots is difficult to measure and the measurement may damage the plants. Thus, the density of vegetation cover (vegetation cover for simplification) and vigor typically are applied to represent the state of vegetation development. The vegetation cover is defined as the percentage of the area with trees and shrubs in the entire area. The vigor of trees is dynamic responding to the impact of various stresses and is an important indicator if the instantaneous state of the vegetation is studied.

Long-term stresses—Ecological stresses, natural or human-induced, can be classified into: ① long-term stresses, such as erosion, air pollution, and grazing; ② short-term stresses, such as drought, pests and diseases, and acid rain; and ③ instant stresses, such as a volcano eruption, forest fire, logging and wind storms. Vigor reduction and mortality of vegetation may result from short-term stress (e.g., drought) acting on trees that have been predisposed to injury by long-term ecological stresses (e.g., air pollution).

Long-term ecological stresses, for instance, the stress resulting from air pollution can be mathematically expressed by:

$$A_\tau = a_1 Po_1 + a_2 Po_2 + a_3 Po_3 + ... \tag{2.2}$$

In which Po_1, Po_2, and Po_3 are the concentrations of pollutant 1, pollutant 2, and pollutant 3; and $a_1, a_2,$ and a_3 are impact factors of the pollutants on the vegetation. Here long-term implies the period during which the present vegetation developed.

Short-term stress, such as drought, impacts the vegetation temporarily (one year or several years) but more intensively.

$$P_\tau = \frac{P - P_e}{P_e} \tag{2.3}$$

in which P is the precipitation in a year, and P_e is the vegetation water demand. The vegetation water demand can be estimated by using an ecological method or a hydrologic method. The former calculates the water demand according to the plant species of the vegetation. The later assumes that the vegetation

water demand is proportional to the soil water received from precipitation, which equals the long-term average precipitation minus the average runoff depth. If the precipitation is more than the vegetation water demand, the stress is positive and vegetation growth and vigor will be promoted. If drought occurs, the stress is negative and the vegetation will suffer.

Instant stresses—For the instant ecological stress, a step function $\Delta(t)$ and an impulse function $\delta(t)$ are applied and given as follows

$$\Delta(t_0) = \begin{cases} 0 & \text{if} \quad t \le t_0 \\ 1 & \text{if} \quad t > t_0 \end{cases} \tag{2.4}$$

and

$$\delta(t_0) = \frac{d\Delta(t_0)}{dt} = \begin{cases} 0 & \text{for} \quad t \ne t_0 \\ 1 & \text{for} \quad t = t_0 \end{cases} \tag{2.5}$$

The instant ecological stresses can be mathematically expressed with the δ-function.

$$f_\tau = K_{inst}\delta(t_0) \tag{2.6}$$

in which K_{inst} is a coefficient representing the reduction of vegetation due to the instant stress occurring at time t_0. For instance, the eruption of the Mount St. Helens volcano in the U.S in 1980 exerted an extremely high but instant stress on the forest vegetation of more than ten thousand square kilometers of the neighboring area. The forest vegetation cover was totally destroyed and the area was changed into bare mountains and hills. Figure 2.27 shows the bare hills 13 years after the eruption of the volcano. The vegetation had not recovered yet after a long period of time. This process can be then, without consideration of other stresses, simply be described by the equation:

$$\frac{dV}{dt} = -K_{inst}\delta(1980) \tag{2.7}$$

in which V is the vegetation cover; t is time, $K_{inst} = 0.8 \text{ yr}^{-1}$ because the vegetation was about 0.8 before the eruption and it was totally destroyed by the eruption of the volcano. After integration the vegetation process is obtained

$$V(t) = \begin{cases} 0.8 & \text{before} \quad 1980 \\ 0.0 & \text{after} \quad 1980 \end{cases}$$

The stress resulting from logging can also be expressed by an impulse function. For instance, the vegetation cover of the Xiaojiang watershed on the Yunnan-Guizhou Plateau of China was reduced by 5% due to logging in 1958. People cut the trees and burned the wood for iron and copper production. The stress on the vegetation is then

$$f_\tau = K_{inst}\delta(1958) \tag{2.8}$$

in which $K_{inst} = 0.05 \text{ yr}^{-1}$. The ecological stress by catastrophic wind can be expresses in the same way.

Reforestation has become the artificial ecological stress with the most positive influence. Usually it is a continuous effort and is expressed with a continuous function. Assume the rate of the reforestation is maintained at $V_R(t)$, the stress is then

$$F_\tau = V_R(t) \tag{2.9}$$

Of course, the recently planted trees do not behave immediately like mature trees. But as long as the reforestation is continuously maintained, and the trees planted in the past years grow up, the expression by Eq. (2.9) of the stress resulting from reforestation is correct.

Mortality and vigor stresses—Ecological stresses are classified into mortality stresses and vigor stresses for modeling of the dynamic process. The watershed vegetation has the following ecological functions:

control of soil erosion-including rainfall and surface runoff erosion and wind erosion; habitat, and primary productivity. For instance, the roots and fallen leaves from the shrubs and grass on the Maousu Desert in Northwestern China result in surface crusting of the sand dunes, which protects the desert from wind erosion and fixes the sand dunes. In general, the ecological function of vegetation depends on the density of vegetation cover and the vigor of vegetation.

Fig. 2.27   The mount St. Helens Volcano erupted in 1980 and destroyed the forest vegetation cover. The picture was taken in 1993. The mountains and hills of the area were still bare 13 years after the eruption of the volcano

The ecological functions of vegetation are a function of vegetation cover, vigor, and functional index:

$$F = V \cdot V_g^{\ \xi} \tag{2.10}$$

in which F = functional capability of vegetation, V = fraction of vegetation cover, V_g = vigor of vegetation, ξ = the functional index. The value of ξ is different for different ecological functions. The functions of wind erosion control, habitat, and primary productivity depend highly on the vigor of vegetation, and the value of ξ is large. In this case both vigor stress and mortality stress are important. For rainfall and surface runoff erosion, however, vegetation controls the erosion mainly by its root system, in which the vigor of vegetation plays a less important role, and the value of ξ is small. In this case, the mortality stresses are mainly considered and vigor stresses are omitted.

Vegetation is composed of trees, shrubs, and grass, which may overlap with each other. In hilly areas, the roots of grass are not as strong as those of tree forests to resist flowing water and protect gully banks and the overland slope from erosion. The vigor of vegetation may be represented by the density of foliage and branches, the biomass production per unit area, or age and health of the plants. It can be measured by the ratio of the seasonal biomass production per area to the biomass production of the vegetation subjected to no stresses. The vigor reduces to zero if the vegetation is impaired, and dies because of ecological stresses. Compared with vegetation cover, the vigor of vegetation is much more dynamic and always fluctuates under the impacts of ecological stresses.

Mortality stress is defined as the stresses directly causing mortality of vegetation. Volcano eruption, forest fire, and logging are mortality stresses. Debris flow and landslide, in some cases, also cause mortality.

Vigor stress is defined as the stresses causing only vigor reduction. Drought, pollution, grazing, insects and diseases, windstorm, and flooding are a few examples of vigor stresses. Drought is the most important vigor stress. If the vegetation suffers continuing drought the vigor of the vegetation may greatly reduce or even reduce to zero. Under the action of vigor stresses, vegetation will adjust itself to fit the stressed environment. If the vigor stresses are strong and impact the vegetation for a long time, the vigor of the vegetation may reduce to zero. If the stresses are removed before the vegetation perishes, the impaired vegetation can recover in a short period of time. The capability of self-healing is termed **resilience.** The vegetation in warm and wet area exhibits high resilience because the precipitation, climate, and soil favor quick vegetation recovery.

The following theorems describe vigor stresses:

(1) The vigor of vegetation is represented by the parameter V_g, which varies in the range of 1 to 0. $V_g=1$ implies the perfect function of vegetation in photosynthesis, erosion control, providing habitat and primary productivity for the bio-community, wind reduction, interception of dust and raindrops, increasing percolation into the soil, etc., and $V_g=0$ represents death of the trees and zero ecological functions.

(2) Vigor of vegetation reduces if vigor stresses act on the vegetation, i.e., $V_g<1$. The vegetation may recover if the stresses are removed.

(3) The speed of vigor recovery depends on the structure of vegetation, or on the resilience of the vegetation. The resilience r_e is a function of the composition of the species of the vegetation, the climate, precipitation, and the soil composition.

(4) If vigor stresses act on the vegetation for a long period of time the vigor of vegetation may reduce to zero, which results in mortality.

Both mortality and vigor stresses are negative because they cause reduction of vigor or death of vegetation. Reforestation and nursing enhances the cover and vigor of vegetation, and is a positive stress. They are not included in the mortality and vigor stresses.

In some cases, the vegetation has developed under very harsh ecological conditions and the development has taken a long period of time under no external stresses. The resilience of such a vegetation is usually very low or zero. Any strong stress, vigor stress or mortality stress, acting on the vegetation may kill the vegetation. Such a kind of vegetation is called vulnerable vegetation. For instance, the forest in the glacier near Banff in Canada and the trees in Sina; Peninsula in Egypt, shown in Fig. 2.18, cannot recover if the vegetation is destroyed by a forest fire or logging.

The grassland on the Qinghai-Tibet Plateau of China has developed over quite a long period of time because the temperature and precipitation are low. A part of it was damaged by human harvesting of medicinal herbs (roots of the grass). It could not recover even if the stresses are reduced or removed. In the Maousu Desert in northwest China, people have stopped the motion of sand dunes by planting straw and dry grass to form a framework, as shown in Fig. 2.28(a). Planting shrubs in the desert is not a difficult job, but to assist the shrubs to survive wind storms is not so easy. Figure 2.28(b) shows the human care for protection of shrubs to resist wind. After a long period of time the human efforts have resulted in nice vegetation cover on the desert, as shown in Fig. 2.28(c). After a long period of continuous effort the dunes are greened by grass and shrubs and a surface crust has formed on the desert, which can resist against wind erosion. Nevertheless, the vegetation is vulnerable. If any stress by human activities damages the vegetation, it cannot recover by natural processes. Human and animal traffic can damage the crust. If the sand dunes are moved by wind, the vegetation can be quickly destroyed, as shown in Fig. 2.28(d).

(a)

(b)

(c)

(d)

Fig. 2.28 (a) In the Maousu Desert in northwestern China, people have stopped the motion of sand dunes by planting straw and dry grass to form a framework; (b) Protection of shrubs to resist wind; (c) A nice vegetation cover has developed on the desert; and (d) A surface crust formed on the desert, which can resist against wind erosion. Human and animal traffic can damage the crust

2.3   Vegetation-Erosion Dynamics

Vegetation-erosion dynamics is a new interdisciplinary science, studying the laws of evolution of watershed vegetation under the action of various ecological stresses (Wang et al., 2003a). Different from other stresses, soil erosion not only impacts the vegetation but also is affected by the vegetation. Vegetation and erosion are a pair of competing and mutually interacting aspects of a watershed. In nature, the development of vegetation cover and variation of soil erosion affect each other, following a dynamic law. For a watershed, vegetation and erosion may reach an equilibrium state if the circumstances remain unchanged for a long period of time, as shown in Fig. 2.29. However, the equilibrium may not be stable. Ecological stresses, especially human activities, may disturb the balance and initiate a new cycle of dynamic processes.

Fig. 2.29   Vegetation and erosion may reach an equilibrium state, if the circumstances remain unchanged for a long period of time (See color figure at the end of this book)

The vigor of trees is dynamic responding to the impact of various stresses and is an important indicator if the instantaneous state of the vegetation is studied. For the functions of wind erosion control, habitat, and primary production of vegetation, both the vegetation cover and vigor are important and must be considered in any dynamic model. For rainfall and runoff erosion control, vigor is not important and only the vegetation cover need be studied and modeled.

2.3.1   Differential Equations

The vegetation cover is a function of the mortality stresses, soil erosion, and human activities. Different from other stresses, soil erosion not only impacts the vegetation but also is affected by the vegetation. In sediment engineering, erosion usually is quantitatively represented by E, the rate of sediment eroded from a unit area per year. In general, the existing vegetation favors vegetation development due to the effects of canopy cover providing shadow and propagation of mature vegetation, but erosion destroys the vegetation cover. Therefore, the rate of change of vegetation is proportional to the vegetation but inversely proportional to the erosion rate. The dynamics of the vegetation under the action of ecological stresses is described by the following differential equation:

$$\frac{dV}{dt} = aV - cE - K_{\text{inst}}\delta(t_0) + V_R \tag{2.11}$$

Where V is the fraction of vegetation cover, and a and c are parameters, the third term on the right hand side represents the mortality stresses which are usually instant stresses. The fourth term V_R represents the human stresses, which may be positive (reforestation) or negative (deforestation). In the equation, a is

a parameter representing the effect of shadow and propagation with dimensions [time^{-1}] and units (yr^{-1}). The value of a depends on the precipitation, soil, and species composition of the vegetation and must be determined using field data. The parameter c represents the damage to vegetation by erosion, with dimensions [area/mass] and units (km^2/t). The value of c depends on soil texture and the species composition of the vegetation. If the soil is thin and erosion may seriously impair the vegetation, the value of c is large.

It must be noted that the erosion rate in the equation is a moving average value over a certain period of time because the erosion rate fluctuates following rainfall and runoff, but the vegetation is affected by the long-term action of erosion, which is represented by an average rate of erosion. For instance, the averaging period may be 10 years, then the moving average value of the erosion rate is attributed to the year in the center of the averaged range of years. For example, the average from the 1st to 10th year is plotted at the 6th year, the value for the 7th year is the average from the 2nd to 11th year, and so on. E in the equations is not a fluctuating parameter but a rather smooth function of time, as shown in Fig. 2.30. The Anjiagou Gully located in Dingxi County of Gansu Province is in the watershed of the Donghe River, which is a tributary of the Zuli River on the Loess Plateau of China. The annual runoff, the rate of erosion, and the moving average rate of erosion over a 10-year period for the Anjiagou Gully are shown in Fig. 2.30. The rate of erosion fluctuates with variation in runoff but the moving average of erosion reflects only the trend of variation. The rate of erosion in Eq. (2.11) is the moving average value of erosion but is still called the rate of erosion for convenience.
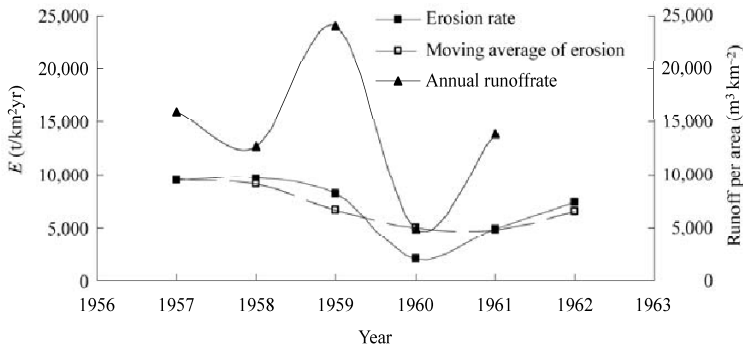
Fig. 2.30 Variation of the annual runoff, the annual rate of erosion, and the moving average rate of erosion of the Anjiagou Gully in Gansu Province, China

If $K_i \delta(t_0)$, E, and V_R are known as functions of time and the parameters a and c are determined, the vegetation development under the action of the stresses can be determined. Nevertheless, the rate of erosion E is usually not given because it depends, in turn, on the vegetation, therefore, one more equation is needed to solve for V and E. Thornes (1985) proposed coupled differential equations for the vegetation-erosion processes. The equation for erosion is applied and revised here by introducing the impact of human activities on erosion:

$$\frac{dE}{dt} = bE - fV + E_R \tag{2.12}$$

in which b and f are parameters to be determined with field data, E_R represents the impact of human activities on erosion, including the increase of erosion due to mining, road construction, land-use change, and agriculture; and the reduction of erosion by the application of soil conservation measures, such as terrace field replacing slope tillage, structures controlling slope erosion, and sediment-trapping dams. The

parameter b represents the effect of increasing erosion by removing topsoil in the process of erosion, and the parameter f represents the effect of vegetation controlling erosion. Figure 2.31 shows that once the top soil is removed the slope suffers from accelerating soil erosion in a red soil area in southern China.

Combining Eqs. (2.12) and (2.11) the coupled differential equations for the vegetation-erosion interaction under the action of ecological stresses are obtained as (Wang et al., 2003a)

$$\left.\begin{array}{l}\dfrac{dV}{dt} - aV + cE = -K_{inst}\delta(t_0) + V_R \\[3mm] \dfrac{dE}{dt} - bE + fV = E_R\end{array}\right\} \qquad (2.13)$$

In the equations, the dimension of patameter b is $[1/\text{time}^{-1}]$ with the units yr^{-1}, the dimensions of f and E_R are $[\text{mass}/(\text{area·time}^2)]$ with the units of $\text{t}/(\text{km}^2\text{yr}^2)$. The parameters a, c, b, and f are important and they are functions of climate, precipitation, soil, topography, and morphology. For any watershed or area the parameters can be determined by applying a trial and error method and using data on vegetation, erosion, and human activities.

Fig. 2.31 A slope suffers from accelerating soil erosion because the top soil is removed in a red soil area in southern China (See color figure at the end of this book)

The differential equations are non-homogeneous and linear and may be solved theoretically as follows:

$$V = c_1 e^{m_1 t} + c_2 e^{m_2 t} + e^{m_1 t} \int \left[e^{-m_1 t} e^{m_2 t} \int e^{-m_2 t} \left(\frac{dV_\tau}{dt} - bV_\tau - cE_\tau \right) dt \right] dt \qquad (2.14)$$

$$E = c_1 \frac{a - m_1}{c} e^{m_1 t} + c_2 \frac{a - m_2}{c} e^{m_2 t} + e^{m_1 t} \int \left[e^{-m_1 t} e^{m_2 t} \int e^{-m_2 t} \left(\frac{dE_\tau}{dt} - aE_\tau - fV_\tau \right) dt \right] dt \qquad (2.15)$$

in which

$$\left.\begin{array}{l}V_\tau = -K_{inst}\delta(t_0) + V_R \\[2mm] E_\tau = E_R\end{array}\right\} \qquad (2.16)$$

The exponents m_1 and m_2 are given as follows:

$$m_{1,2} = \frac{1}{2}\left[(a+b) \pm \sqrt{(a+b)^2 - 4(ab - cf)}\right] \qquad (2.17)$$

c_1 and c_2 are integration constants to be determined by the boundary conditions. For any watershed if the ecological stresses are known the vegetation and erosion processes can be theoretically described by Eqs. (2.14) and (2.15).

It must be noted that the vegetation cover V in the differential equations is calculated in different ways for different erosions because different erosions can be controlled by different types of vegetation. Figure 2.32(a) shows that herbaceous vegetation on the Qinghai-Tibet Plateau completely controls splash erosion and sheet erosion but does not control gully erosion. Figure 2.32(b) shows that herbaceous vegetation in the Xiaojiang River basin on the Yunnan-Guizhou Plateau controls rill erosion. Figure 2.32(c) shows that shrubs and trees in Lixian County on the Loess Plateau control gully erosion. Nevertheless, not all erosion can be controlled by vegetation. Figure 2.32(d) shows that well developed complex vegetation consisting of trees, shrubs, and grasses on the Chenyoulan River in Taiwan, China could not control bank failure, which was caused by channel erosion during the flood on August 8, 2009. Several buildings fell into the river and one building was suspended on the cliff.
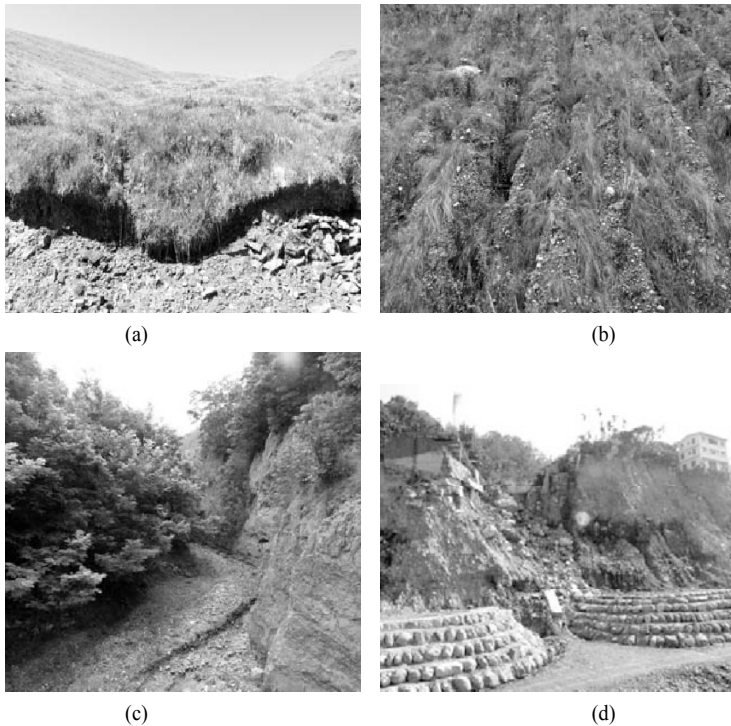
Fig. 2.32   (a) Herbaceous vegetation on the Qinghai-Tibet Plateau controls splash and sheet erosions but not gully erosion; (b) Herbaceous vegetation in the Xiaojiang River basin controls rill erosion; (c) Shrubs and trees on the Loess Plateau control gully erosion; (d) Channel erosion caused bank failure on the Chenyoulan River in Taiwan, China (See color figure at the end of this book)

In the differential equations, the vegetation cover, V, is the coverage ratio of vegetation consisting of grasses for studying the vegetation-erosion dynamics in the Qinghai-Tibet Plateau because there is no intensive gully erosion and rill and sheet erosions are the main type of erosion in the area. Whereas for studying the vegetation-erosion dynamics in the Xiaojiang River basin, where gully erosion is intensive and is the dominant erosion type, the value of V in the differential equations is the vegetation cover of trees and shrubs. Herbaceous vegetation is not counted in this case because grasses cannot control gully erosion.

2.3.2   Application of Vegetation-Erosion Dynamics

The vegetation-erosion dynamics model is first applied to the Loess Plateau and Yunnan-Guizhou Plateau

in western China. The Anjiagou watershed is on the Loess Plateau with elevation in the range of 1,900–2,250 m above the sea level, and has a drainage area of 9.06 km². There are many gullies in the watershed with a distribution density of 3.14 km/km². The gullies are 30–50 m deep. The annual precipitation is 427 mm, of which 60% occurs in July, August, and September. The annual pan evaporation is 1,526 mm and annual average temperature is 6.3℃. The soil is composed of gray desert soil, spodosol, and loamy soil. The gully bed and gully slope are covered with halogenic soil. The rate of soil erosion was as high as 10,000 t/(km²·yr) and the vegetation cover was only 5.7% before the 1950s, when erosion control projects were launched. The erosion control and reforestation of the watershed were performed in three phases (Ye, 1986; Li, 1986; Zhang et al., 1986): ① From the mid 1950s to the mid 1960s, the local people terraced the sloping farmland, and planted trees and grass on the bare hills and slopes. They constructed 4 sediment-trap dams in the late 1950s. ② From the mid 1960s to the late 1970s, the reforestation effort was interrupted but the construction of terraced farm fields continued. ③ From the late 1970s to the 1980s, reforestation was intensified and the construction of terraced fields continued. In the meantime, a project of comprehensive watershed management was conducted to speed up the erosion control and greening of the landscape. In the late 1970s, other 3 sediment-trap dams were completed.

Land-use change in the watershed was mainly to farmland, forest, and wasteland, among them farmland was changed from sloped land to forest and terraced fields and the wasteland was greened into forest and grassland. Data on land-use change, reforestation, rate of erosion, and the sediment amount trapped by the dams during the period 1950–1990 were collected. The sediment trap dams raised the gully bed and reduced the bed slope and bank slope. Even if the dams have been filled with sediment they still are effective in stabilizing the slopes and promoting vegetation development. The area of reforestation by planning trees, shrubs, and grass per year is divided over the total area of the watershed, yielding the value of V_r. The value of E_r consists of two parts: the reduction in erosion resulting from by changing the sloped land into terraced fields and from sediment trap dams. The first part is calculated as the ratio of the area of terraced fields each year to the total area of the watershed multiplied by the sediment-yield per year. And the second part is obtained by taking the differential of the cumulative sedimentation curve of the dams divided by the total area.

Because V_r and E_r are not constants and cannot be described with a simple mathematical function, the solution, Eqs. (2.14) and (2.15) cannot simply be applied, but rather Eq. (2.13) must be solved numerically. The four parameters for the Anjiagou watershed were determined as follows:

$$a = 0.001(1/\text{yr}), \quad c = 0.0000018(\text{km}^2/\text{yr}), \quad b = 0.01(1/\text{yr}), \quad f = 400(\text{t}/(\text{km}^2 \cdot \text{yr}^2)) \tag{2.18}$$

For each parameter, a trial-and-error method was used to compare the computed result with the data. The trial-and-error method was performed many times for every adjustment of each parameter until the best-fitting value of the parameter was obtained. Because the vegetation cover V is defined in the domain [0, 1], and the erosion rate E is in the domain [0,∞), the value of vegetation cover is taken as $V = 0$ if the calculation yields $V < 0$; and $V = 1$ if the calculation yields $V > 1$; and the erosion rate is taken as $E = 0$ if the calculation yields $E < 0$.

Figure 2.33(a) shows the computed and measured development process of vegetation cover and Fig. 2.33(b) shows the variation of the rate of erosion for the Anjiagou watershed. The computed curves closely follow the real processes, implying that the theoretic model is able to simulate the complex and dynamic evolution processes of vegetation and erosion.

The Xiaojiang River is a tributary of the Yangtze River that begins on the northeastern Yunnan-Guizhou Plateau of China. The elevation is in the range of 1,100–4,344 m above the sea level. Dongchuan City is located in the middle and lower reaches of the river with a drainage area of 1,881 km². It is located in the semi-tropical zone with the average temperature over 20℃. The annual precipitation is 688 mm in the middle and lower reaches and over 1,000 mm in the upper reaches. The drainage area has active tectonic

motions and the rocks have been cut into small pieces. The area was covered with well-growing forest but the forest cover was damaged due to copper mining and metallurgical industries over the past 400 years. Erosion rates as high as 13,000 t/(km^2·yr) and debris flow occur very often in its 107 tributary gullies. Because of soil erosion the vegetation cover deteriorated from more than 40% to less than 10% in the past century. In the 1950s the vegetation cover was about 25% but deforestation and logging for the copper and steel production in 1958 cut the vegetation by 5%. From that time the vegetation cover continued to reduce due to the high rate of erosion. Since the late 1970s, however, people have made a great effort to green the hills by reforestation but only limited results have been achieved. In the 1990s the reforestation effort was intensified and the vegetation cover turned from reducing to increasing. The lead author of this book has made field investigations in the area during the high erosion rate period in summer since 1998 and collected data on reforestation, land-use change, rate of erosion, and erosion control.
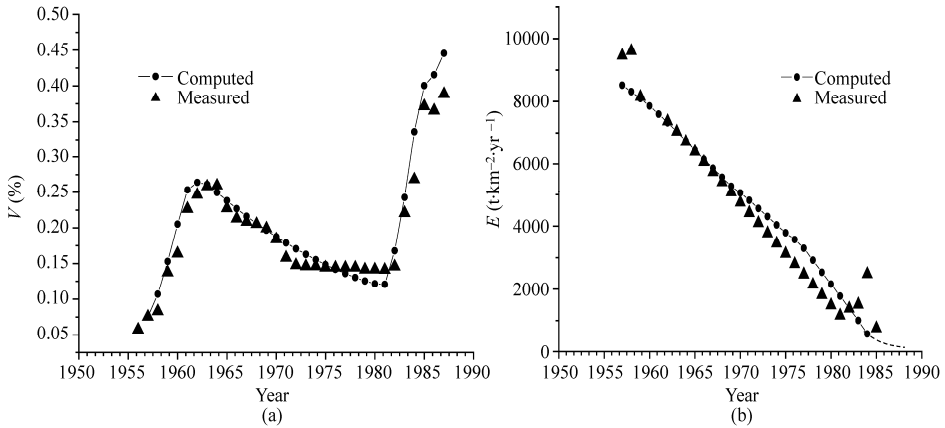
Fig. 2.33 (a) Computed and measured development process of vegetation cover (V) and (b) computed and measured rate of erosion (E) for the Anjiagou watershed in China (Wang et al., 2003b)

The parameters a, c, b, and f were determined by applying a trial-and-error method for the Xiaojiang watershed as follows:

$$a = 0.03(1/\text{yr}), \quad c = 0.000005(\text{km}^2/\text{yr}), \quad b = 0.054(1/\text{yr}), \quad f = 200 \ (\text{t}/(\text{km}^2\cdot\text{yr}^2)) \tag{2.19}$$

The main ecological stresses on the vegetation are logging and reforestation. From the 1950s to 1970s human activities exhibited minor influence on the vegetation and erosion, except for the intensive logging reducing 5% of the forest cover in 1958. Since 1979 humans has reforested the hills at a rate of 1% annually, and, in the meantime, humans has accelerated erosion, adding 60 t/(km^2·yr^2) per year, due to road construction, mining, and other activities. Such an impact is reinforced year by year. Thus, the functions $V_\tau(t)$ and $E_\tau(t)$ are:

$$\left. \begin{array}{l} V_\tau(t) = -K_{\text{inst}}\delta(1958) + V_{\tau_0}\Delta(1979)e^{n(t-t_0)} \\ E_\tau(t) = E_{\tau_0}\Delta(1979)e^{n(t-t_0)} \end{array} \right\} \tag{2.20}$$

in which $K_{\text{inst}} = 0.05 \ \text{yr}^{-1}$, $V_{\tau_0} = 0.01 \ \text{yr}^{-1}$, $n = 0.1$, $E_{\tau_0} = 60 \ (\text{t}/(\text{km}^2\cdot\text{yr}^2))$, and $\Delta(1979)$ is the step function with step at 1979. Substituting Eq. (2.20) into Eqs. (2.14) and (2.15) the following theoretical solution is obtained:

$$V(t) = c_1 e^{m_1 t} + c_2 e^{m_2 t} - K_{\text{inst}}\Delta(1958) + \Delta(1979)\frac{V_{\tau_0}(n-d) - cE_{\tau_0}}{(n-a)(n-d) - cf}e^{n(t-t_0)} \tag{2.21a}$$

$$E(t) = c_1 \frac{a - m_1}{c} e^{m_1 t} + c_2 \frac{a - m_2}{c} e^{m_2 t} + \Delta(1979) \frac{-fV_{\tau_0} + (n-a)E_{\tau_0}}{(n-a)(n-d) - cf} e^{n(t-t_0)} \tag{2.21b}$$

in which t is the time in years from the initiation of this study (1954 in this case) and $t - t_0$ is the time from 1979, m_1 and m_2 are given by Eq. (2.17), and c_1 and c_2 are determined by the initial conditions.

The solution of the vegetation-erosion dynamics, given by Eq. (2.19), provides the evolution process of vegetation and erosion, as shown in Fig. 2.34. The theoretical solution agrees well with the measured data. The values of the parameters shown in Eq. (2.19) are for the Xiaojiang watershed and they are the climate, soil, and morphology and are independent of the human caused stresses. Therefore, the values can be applied to sub-watersheds within the area, within which the climate, morphology, and soil composition are the same but the human caused stresses may be quite different from those on the Xiaojiang watershed as a whole.
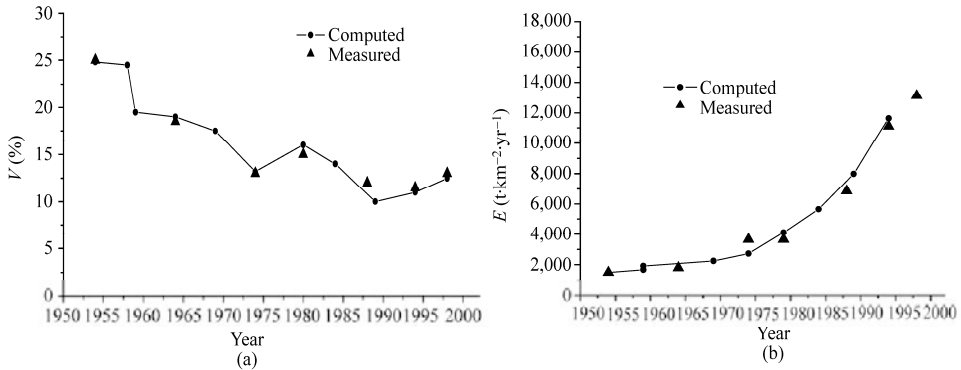
Fig. 2.34 Theoretical solution for the variation of (a) vegetation (V) and (b) erosion rate (E) for the Xiaojiang watershed in comparison with measured data (after Wang et al., 2003a)

The Heishuihe River is a tributary of the Xiaojiang River. It is 3.9 km long with drainage area of 9.94 km^2. In this watershed debris flow has occurred frequently and the erosion rate was high in the 1960s and 1970s. The watershed was selected as a demonstration area of an intensive erosion control and reforestation project. The vegetation cover was only 7.6% and the soil erosion rate was 7,243 t/(km^2·yr) before 1978 when the intensive erosion control project started. The major strategies of the project were reforestation and controlling erosion with check dams. The hills and slopes were reforested at a rate of 4% per year, and the erosion rate was reduced by the construction of a series of dams by 650 t/(km^2·yr) every year. After 20 years the watershed changed its landscape completely. The vegetation cover increased to 70% and the erosion rate is reduced to less than 200 t/(km^2·yr).

The development of vegetation and variation of erosion can be described directly by the theoretical solution of the vegetation-erosion dynamics, in which the values of a, c, b, and f are directly taken from Eq. (2.19). The stresses are constant $V_\tau(t) = 0.04\,\mathrm{yr}^{-1}$, $E_\tau(t) = -650$ (t/km^2·yr^2). In this case the stresses are

$$V_\tau(t) = V_{\tau_0}, \qquad E_\tau(t) = E_{\tau_0} \tag{2.22}$$

Substituting Eq. (2.22) into Eqs. (2.14) and (2.15), and integrating yields

$$V(t) = c_1 e^{m_1 t} + c_2 e^{m_2 t} - \frac{bV_{\tau_0} + cE_{\tau_0}}{ab - cf} \tag{2.23a}$$

$$E(t) = c_1 \frac{a - m_1}{c} e^{m_1 t} + c_2 \frac{a - m_2}{c} e^{m_2 t} - \frac{fV_{\tau_0} + aE_{\tau_0}}{ab - cf} \tag{2.23b}$$

in which $V_{\tau_0} = 0.04$ yr^{-1}, $E_{\tau_0} = -650$ t/km^{2}yr^2, and c_1 and c_2 are determined by the initial conditions: $V(t = 1978) = 0.076$, and $E(t = 1978) = 7,243$ t/km^{2}yr.

The values of the parameters a, c, b, and f are the same as those given by Eq. (2.19) because the Heishuihe watershed is in the watershed of the Xiaojiang River and the climate, morphology, and soil compositions are the same. Equation (2.23) provides the theoretical solution of the vegetation and erosion processes, as shown in Fig. 2.35. The theoretical curves agree well with the measurements. During the first 10 years the vegetation cover developed slowly but the development accelerated during the second 10 years.
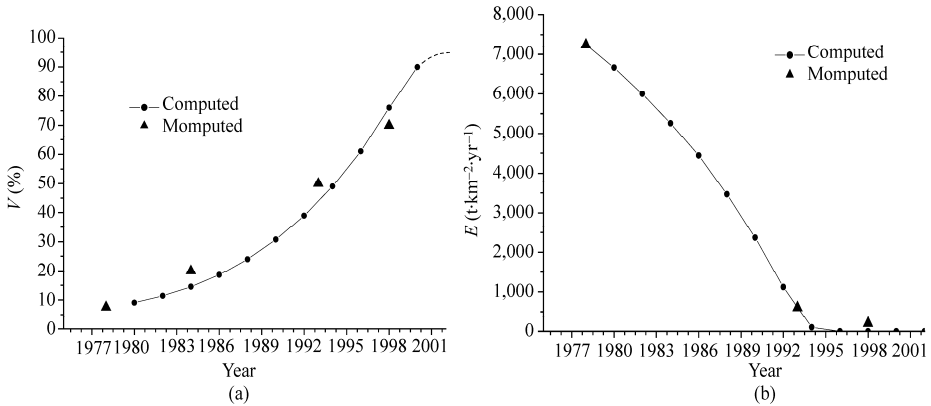
Fig. 2.35   Comparison of the theoretical curves calculated with the same parameters as for the parent Xiaojiang watershed with the real development process of (a) vegetation cover and (b) erosion rate for the Heishuihe watershed (after Wang et al., 2003a)

Another example is the Shengou watershed near the suburbs of Dongchuan City. This small watershed experienced extremely high rates of erosion and degradation of vegetation in the 1950s–1970s. Debris flow damaged the farm fields and factories, and even invaded the downtown of the city many times. The erosion rate was 8,000 t/km^{2}yr and the vegetation cover was only 6% in the 1970s. The government launched the erosion control and reforestation project in 1976. People constructed more than 200 check dams and planted trees to green the hills at a rate of 4% per year. The erosion rate was reduced by 700 t/km^{2}yr every year. After 20 years the vegetation cover increased to 60% and the erosion rate reduced to less than 150 t/km^{2}yr. No debris flow occurred anymore.

The ecological stresses and the solution of the vegetation-erosion equations are the same as those for the Heishuihe watershed but only the values of the initial conditions and the coefficients of the stresses are different, they are:

$$V(t = 1976) = 0.06, \quad E(t = 1976) = 8,000 \text{ t/km}^2\text{yr} \quad V_{\tau_0} = 0.04 \text{ yr}^{-1}, \quad E_{\tau_0} = -700 \text{ t/km}^2\text{yr}^2.$$

The values of the parameters a, c, b, and f are the same as those given by Eq. (2.19). Figure 2.36 shows the comparison between the theoretical solution and the measurements. The agreement of the theory and data proves again that the vegetation-erosion dynamics is a powerful tool for prediction of the vegetation evolution of areas of known, regionally consistent climate, morphology, and soil composition. Again the result shows slow development of the vegetation cover in the first 10 years but much faster development in the second 10 years, implying the effort of reforestation and erosion control must be a long-term strategy for effective improvement of the vegetation.

The agreement between the data and the theoretical curves proves that the parameters a, c, b, and f are independent of the stresses and initial conditions. Once the parameters are determined for a watershed or

an area, they can be directly applied to the sub-watersheds or neighboring areas with the same climate, topography, soil, and vegetation composition.
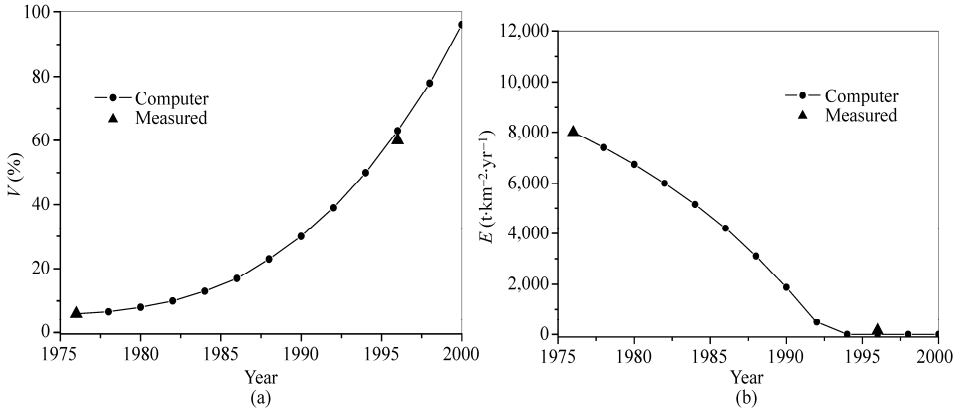
Fig. 2.36 Comparison of the theoretical curves calculated with the same parameters as for the parent Xiaojiang watershed with the real development process of (a) vegetation cover and (b) erosion rate for the Shengou watershed (after Wang et al., 2003a)

2.3.3 Vegetation-Erosion Chart

The vegetation-erosion chart is used to discuss the development trends of vegetation and erosion in the case of no human-caused stresses. If the stress terms are zero, Eqs. (2.14) and (2.15) can be rewritten as:

$$\left.\begin{array}{l} V' = aV - cE \\ E' = bE - fV \end{array}\right\} \tag{2.24}$$

in which $V' = \dfrac{\mathrm{d}V}{\mathrm{d}t}, E' = \dfrac{\mathrm{d}E}{\mathrm{d}t}$, which are expressed as functions of V and E. V' and E' may be positive or negative, therefore, the $V-E$ plane: $V \in [0,1], E \in [0,\infty)$ can be divided into three zones by the two lines $V' = 0, E' = 0$, or

$$E = \frac{a}{c}V; \quad E = \frac{f}{b}V \tag{2.25}$$

If the values of a, c, b, and f are known，the two lines are given by Eq. (2.25) and the vegetation-erosion chart can be developed.

Figure 2.37 shows the vegetation-erosion chart for the Xiaojiang watershed, in which the values of a, c, b, and f are from Eq. (2.19). The three zones are:

Zone A: $\mathrm{d}V/\mathrm{d}t < 0$, $\mathrm{d}E/\mathrm{d}t > 0$. In this zone the vegetation cover is deteriorating and the erosion rate is increasing. The larger the zone is, the more difficult for the vegetation to develop. The size of Zone A depends on the value of $\max\left\{\dfrac{a}{c}; \dfrac{f}{b}\right\}$, the larger the value, the smaller the zone.

Zone C: $\mathrm{d}V/\mathrm{d}t > 0$, $\mathrm{d}E/\mathrm{d}t < 0$. In this zone the ecological system is developing toward complete vegetation cover and zero erosion rate. A large Zone C favors stable vegetation. The size of the zone depends on the value of $\min\left\{\dfrac{a}{c}; \dfrac{f}{b}\right\}$, the larger the value, the larger the zone. For a watershed in this zone, a forest may be logged to a certain extent (not bringing the system over the lower line) and the vegetation may recover after a period. The period of recovery depends on the ecological resilience.
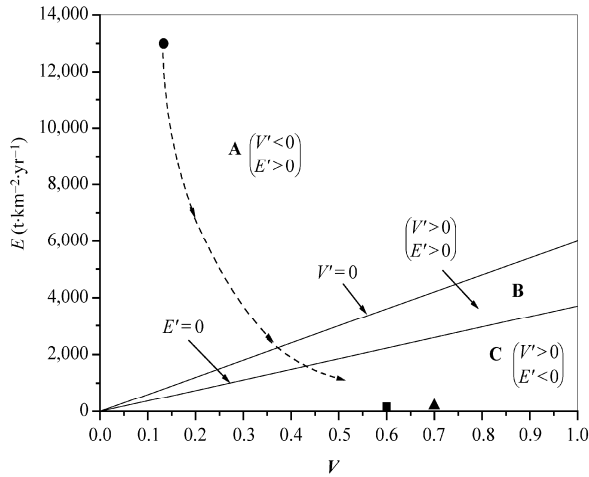
Fig. 2.37   Vegetation-erosion chart for the Xiaojiang watershed and its sub-watersheds (●- Xiaojiang watershed in the 1990s; ▲- Heishuihe watershed in the 1998; ■- Shengou watershed in the 1996) (after Wang et al., 2003a)

Zone B: $dV/dt > 0$, $dE/dt > 0$. In this zone the vegetation cover is in an unstable state. Both vegetation and erosion are increasing. If erosion increases faster or human caused stresses lead to deforestation and erosion continues to increase the ecological system may enter Zone A. If vegetation increases faster or human controls are applied to erosion, such as reforestation of the hills the ecological system may enter Zone C.

The vegetation-erosion chart is exclusively resolved by the parameters a, c, b, and f, which are determined by long-term measurement of the vegetation and erosion variation. The parameters are constant and universal for the areas of the same climate, topography, soil, and vegetation compositions. If the values of the parameters a and f are large, the system in most cases is in the Zone C developing toward perfect vegetation. If the values of c and b are large, the system in most cases is in Zone A developing toward poor vegetation and high rates of erosion.

The three points in Fig. 2.37 indicate the state of the vegetation and erosion for the Xiaojiang watershed and the Heishuihe and Shengou sub-watersheds. The ecological systems of the Heishuihe and Shengou watersheds moved from Zone A to Zone C thanks to 20 years of effort of intensified reforestation and erosion control. Now, they are developing toward perfect vegetation. Nevertheless, the Xiaojiang watershed as a whole is still in Zone A and exhibits the development trend toward poor vegetation, which can offset, to a certain extent, the human effort for improvement of the vegetation. The dashed curve in the figure shows the suggested route for moving the system into Zone C. First, erosion control must be performed to reduce the erosion rate by 60–80%, thus the system is moved into Zone B. Then the development trend of $V'>0$ may support reforestation projects moving the system into Zone C. Erosion control is very important in the area for re-vegetating the hills. Mere planting of trees and shrubs do not work well for greening land subject to high erosion.

Similarly, the vegetation-erosion chart for the Anjiagou watershed on the Loess Plateau is prepared using the values of the parameters given by Eq. (2.18), as shown in Fig. 2.38. There is no Zone B but rather a Zone D, in which $V'<0, E'<0$. The ecological system in Zone D also is unstable, because both vegetation and erosion are reducing. If the vegetation reduces faster than erosion the system may enter into the Zone A and if erosion reduces faster than vegetation the system may enter into the Zone C.

The Zone C in the chart is very small and the Zone D is large. The tangent of the line $E'=0$ is high, implying high effectiveness of vegetation in controlling erosion. On the other hand, the line $V'=0$ is almost horizontal, which suggests that erosion control helps little for vegetation development. Thus, in
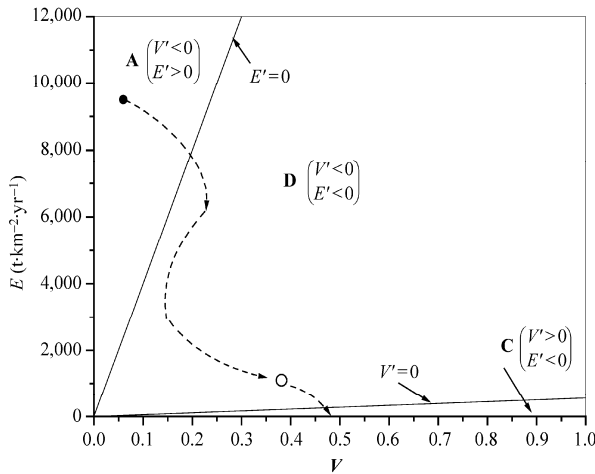
Fig. 2.38 Vegetation-erosion chart for the Anjiagou watershed on the Loess Plateau of China (●-before 1956; ○-in 1988; → route of the vegetation development and erosion reduction) (after Wang et al., 2003b)

the Loess Plateau the most effective way to control erosion is to increase the vegetation cover, to move the system from the Zone A into the Zone D. Thence the system will move in the direction of erosion reduction but also vegetation reduction. Humans can further increase the vegetation cover by planting trees and reduce erosion by engineering strategies. The dashed curve shows the route of watershed management and vegetation development. Unfortunately, Zone C is too small to stable vegetation development. Human effort is always needed to maintain a stable or increasing vegetation cover. For the Anjiagou watershed, although reforestation and erosion control have been continued for more than 30 years, the rate of erosion has been reduced by 90%, and the vegetation cover has increased by 8 times, the state of the system still is in Zone D. It is possible for the system to return to Zone A if the vegetation is not carefully protected. To move the system into Zone C, both reforestation and erosion control must be continued.

From the vegetation-erosion dynamics and the vegetation-erosion chart the following can be concluded. ① Vegetation is affected by various stresses. The stresses can be mathematically expressed, based on which the coupled differential equations of vegetation-erosion dynamics are established. ② Four parameters a, c, b, and f in the equations are determined using field data and a trial and error method. ③ The theoretical solution of the coupled differential equations has been compared with the real development processes of vegetation and erosion in the Anjiagou watershed on the Loess Plateau and the Xiaojiang watershed and its sub-watersheds on the Yunnan-Guizhou Plateau. The theoretical curves agree well with the field measurements of the real processes. ④ Simplifying from the coupled differential equations and using the four parameters the vegetation-erosion chart can be developed, with which one can predict the development trend of the vegetation and erosion, and suggest the most effective strategy to permanently improve the landscape. ⑤ On the Yunnan-Guizhou Plateau with relatively high precipitation and temperature, vegetation can develop well if erosion is controlled and the vegetation is stable after improvement. On the dry and cold Loess Plateau, vegetation can effectively control erosion but erosion reduction exhibits low effectiveness on vegetation development. Vegetation in the area is not stable and management is always needed to maintain the vegetation.

In general the vegetation of a watershed or an area may exist in three states, i.e., vegetation-developing and erosion-reducing, vegetation-deteriorating and erosion-increasing, and the transitional state between the two. Human activities may change a watershed from one state into another, the effort required depends on the distance from the present position to the destination position on the vegetation-erosion chart.

Figure 2.39(a) shows the vegetation status in Zone A in Wudu County in the upper reaches of the Jialing River where the vegetation has been destroyed erosion is severe and debris flow occurs often. Figure 2.39(b) shows the vegetation status in Zone C in Guangyuan City in the upper reaches of the Jialing River, which is only about 200 km distance from Wudu County. The vegetation has been preserved and erosion is controlled by the vegetation. The two states in the figure are relatively stable and disturbances by humans can hardly change them.

(a)

(b)

Fig. 2.39   (a) Vegetation-erosion status in Zone A in Wudu County in the upper reaches of the Jialing River; (b) Vegetation-erosion status in Zone C in Guangyuan City (about 200 km distance from Wudu County) in the upper reaches of the Jialing River

Determination of values of the four parameters a, c, b, and f is difficult for areas or watersheds without long term data of soil erosion and vegetation. Because the four parameters depend mainly on climate, soil, and topography, Wang and Wang (2007) collected data from 13 small watersheds on the loess plateau. They applied the vegetation-erosion dynamics equations to the areas and obtained the values of the four parameters for the Eq. (2.14) for best agreement with the data. The geographical locations of the 13 small watersheds are shown in Fig. 2.40 and the basic features and the values of the parameters a, c, b, and f for the 13 watersheds are listed in Table 2.2.
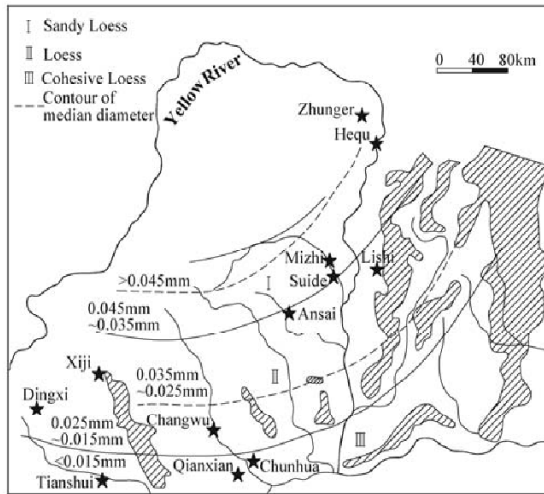
Fig. 2.40 Geographical locations of the 13 small watersheds in the Loess Plateau used to evaluate the vegetation-erocess dynamics model

Table 2.2 The four parameters in the vegetation-erosion differential equations and climatic, topographical, and soil characteristics of 13 small watershed on the Loess Plateau

Watershed	County	P (mm)	T (°C)	s	D_{50} (mm)	a (1/yr)	c ($10^{-6}km^2/t$)	b (1/yr)	f (t/(km^2.yr^2))
Chuanzhang	Zhunger	400.0	7.2	0.172	0.046	0.0010	1.90	0.033	450
Nanqugou	Hequ	462.9	6.8	0.708	0.044	0.0010	1.30	0.030	450
Zhuanyaogou	Hequ	447.5	8.8	0.695	0.042	0.0015	1.30	0.025	450
Yulingou	Mizhi	451.6	8.5	0.780	0.038	0.0015	1.40	0.021	470
Wangmaogou	Suide	513.0	10.0	0.836	0.036	0.0020	1.50	0.015	510
Zhifanggou	Ansai	549.1	8.8	0.680	0.034	0.0022	1.70	0.014	500
Wangjiagou	Lishi	506.1	8.8	0.412	0.032	0.0020	1.75	0.020	470
Anjiagou	Dingxi	427.4	6.3	0.398	0.022	0.0010	1.70	0.014	480
Huangjiaercha	Xiji	402.2	5.8	0.323	0.029	0.0010	2.00	0.015	480
Wangdonggou	Changwu	584.1	8.3	0.462	0.02	0.0020	1.80	0.019	380
Nihegou	Chunhua	600.6	9.5	0.368	0.014	0.0030	1.50	0.012	350
Zaozigou	Qianxian	590.0	10.9	0.202	0.012	0.0045	1.10	0.011	300
Luergou	Tianshui	574.1	11.0	0.661	0.011	0.0040	1.32	0.014	400

Note: P is the annual precipitation; T is the annual average temperature; s is the average slope; and D_{50} is the median diameter of the soil.

Table 2.2 shows that the value of a increases with the precipitation and temperature. In general the existing vegetation favors vegetation development and parameter a is positive due to the effect of canopy cover providing shade and propagation of mature vegetation. But this effect is limited by low precipitation and low temperature. In arid and semi-arid areas there is not enough water for vegetation development, the parameter a is small. In cold areas plants grow very slowly and the parameter a is small. Soil and topography do not affect the value of a obviously. parameter c represents the area of vegetation damaged by soil erosion, or, vegetation-damage caused by one ton of soil erosion. The erosion layer on the Loess

Plateau is thick and the *c* value is small. In a hilly area with slope debris in the suburbs of Beijing and the in Xiaojiang watershed, one ton of soil erosion may cause a larger area of vegetation-damage, and the *c* value is large. Parameter *b* represents the effect of increasing erosion by removing topsoil in the process of erosion. The surface of the hilly area with slope debris near Beijing is composed of various particles with a wide range of size and erosion cannot penetrate down, therefore, the value of *b* is small. In the Xiaojiang watershed and on the Loess Plateau, the vegetation protects the soil from erosion. Once the top layer is eroded the erosion may further penetrate down to the erodible soil. Therefore, the value of *b* is large. Parameter *f* represents the effect of vegetation controlling erosion, which is large for the Loess Plateau.

A correlation analysis is performed with the data in Table 2.2. The result indicates that parameter *a* depends mainly on the precipitation and annual average temperature; and parameter *c* depends mainly on the slope and the median diameter of the soil. Figure 2.41 shows parameter *a* as a function of the precipitation and annual average temperature, and parameter *c* as a function of the slope and the median diameter of the soil. In the varying ranges of the precipitation, temperature, slope, and soil size, the two parameters can be preliminarily determined with the diagrams. The parameters *b* and *f* cannot be clearly expressed as functions of the climatic, morphological, and soil conditions of the watershed from the correlation analysis with the available data. More work is needed to establish empirical formulas for parameters *b* and *f*. If, however, parameters *a* and *c* are predetermined for a watershed according to the precipitation, temperature, slope, and soil size, parameters *b* and *f* can be easily determined with data.
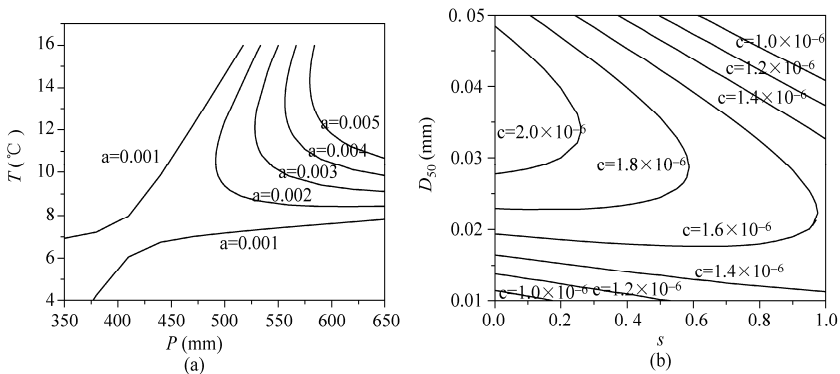
Fig. 2.41   For the loess plateau (a) Parameter *a* as a function of the annual precipitation and annual average temperature; and (b) Parameter *c* as a function of the slope and the median diameter of the soil

2.3.4   Application of Vegetation-Erosion Chart

Effective strategies for restoration of watershed vegetation and erosion control can be found by analyzing the vegetation erosion chart.

2.3.4.1   Loess Plateau

The geographical range of the Loess Plateau is N 33°43'–N 41°16'、E 100°54'–E 114°33'. It extends from Taihang Mountain in the east to the Helan Mountain in the west and from the Qingling Mountain in the south to the Great Wall in the north. The total area is about 480,000 km². The annual precipitation varies in the range of 200–700 mm, with the highest precipitation in the southeastern part and lowest precipitation in the northwestern part. More than 60% of the rainfall occurs in June, July, August and September (Tang, 2004). The Loess Plateau is divided into four areas according to climate, topography, soil, morphology, and soil erosion: Area I is a sandy and hilly area along the Great Wall, as shown in Fig. 2.42; Area II is

the east loess hilly and gully area; Area III is the west loess hilly and gully area; and Area IV is Loess Plateau gully area, which is located in the southeasternmost of the Loess Plateau.
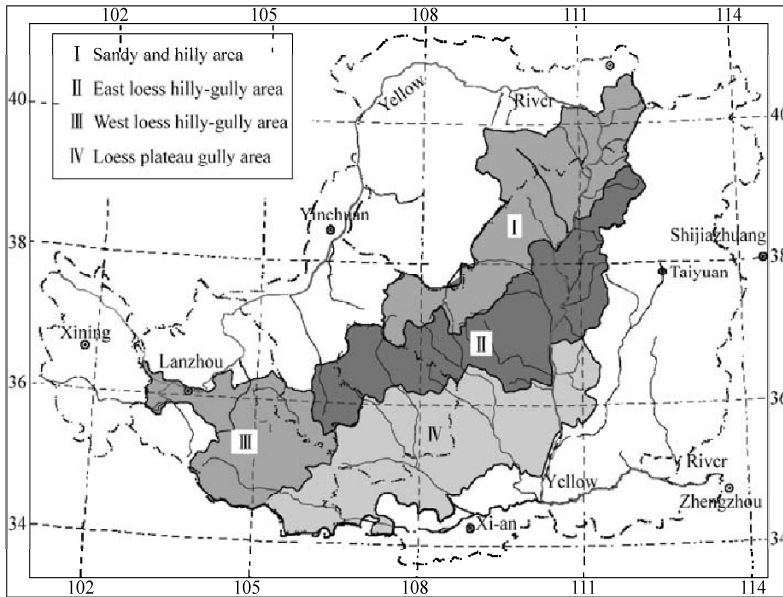
Fig. 2.42 Zoning of the Loess Plateau in the Yellow River basin (after Wang and Wang, 2007)

According to the data of vegetation and erosion for the four areas, the parameters *a, c, b,* and *f* are determined with the diagrams in Fig. 2.41 and using the method of trial and error, as listed in Table 2.3. With the values of the parameters the vegetation-erosion charts are worked out, as shown in Fig. 2.43. The four vegetation-erosion charts show that for the sandy and hilly area along the Great Wall, and the west and east loess hilly and gully areas, Zone C is very small and the points of present status are far from Zone C. It is almost impossible to develop a sustainable vegetation having capacity of self-restoration. Only by intensive soil erosion control and reforestation projects on very small watersheds can vegetation be improved. Even when vegetation is developed a certain amount of human management is still necessary because Zone C is very small and the vegetation has no capacity of self-restoration.

Table 2.3 Average values of *a, c, b,* and *f* for the four areas in the Loess Plateau and the present vegetation cover and erosion

No	Zone	Parameters				Present vegetation and erosion	
		$a \times 10^3$ (1/yr)	$c \times 10^6$ (10^{-6}km²/t)	$b \times 10^2$ (1/yr)	f (t/(km².yr²))	V	E (t·km^{-2}·a^{-1})
I	Sandy and hilly area along the Great Wall	1–1.5	1.3–1.9	2.5–3.3	450–470	0.293	11,500
II	East loess-hilly and gully area	1.5–3	1.5–1.8	1.4–2.1	470–520	0.380	11,000
III	West loess hilly and gully area	1–2	1.7–2.0	1.4–1.5	450–490	0.309	5,400
IV	Loess Plateau gully area	2–4.5	1.1–1.8	1.1–1.8	300–400	0.440	3,500

For the plateau-gully area in the southeastern most part of the Loess Plateau, the vegetation can be permanently improved because Zone C is relatively large, which means the vegetation has a capacity of
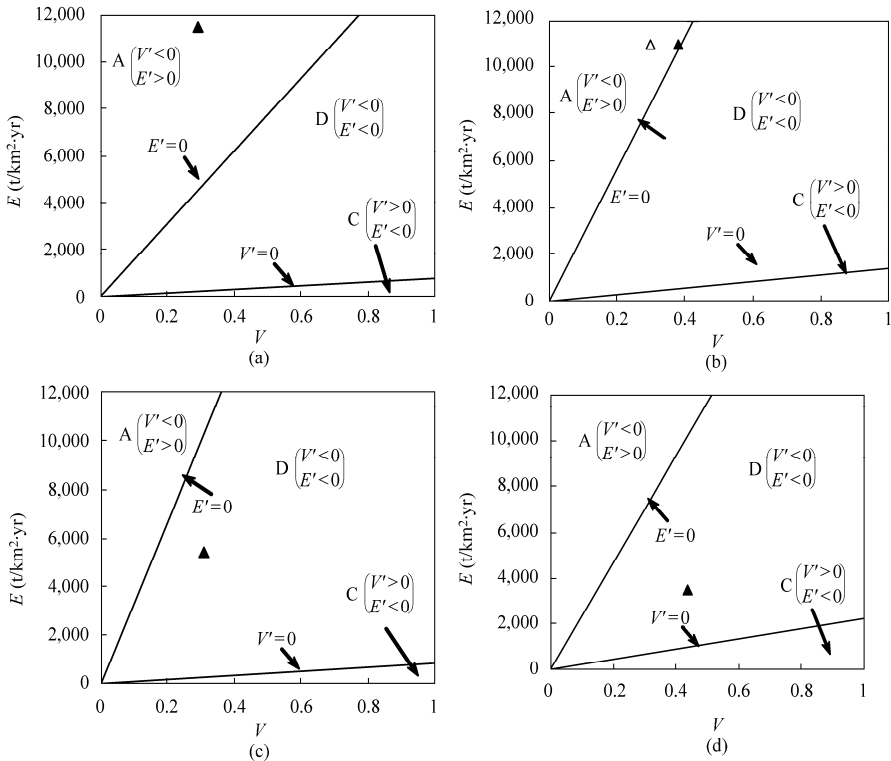
Fig. 2.43   Vegetation-erosion charts for the four areas in the Loess Plateau in China: (a) Area I- Sandy and hilly area along the Great Wall; (b) Area II- East loess-hilly and gully area; (c) Area III- West loess hilly and gully area; (d) Area IV- Loess Plateau gully area (▲- Present status of vegetation and erosion; Δ- Present status of vegetation and erosion in Area II excluding Yan-an city)

self-restoration. The main strategy is intensive reforestation. Once a relatively high vegetation cover has been achieved the vegetation is self sustainable and human management is only needed to avoid deforestation. For other three dry and cold areas (Areas I–III) in the Loess Plateau the strategies of watershed management should be as follows: ① Planting trees to reduce erosion. The straight line $E' = 0$ is steep, thus, reforestation may easily move the status point into the Zone D, in which the erosion rate may automatically reduce. ② Managing artificial vegetation carefully. Because Zone C is small, vegetation is not stable even when the vegetation has been greatly improved and erosion has been reduced. Management is always needed to maintain the vegetation. Neither reforestation nor erosion control are effective for further vegetation development. Reforestation can be applied as an effective strategy to control erosion but vegetation development must rely on human effort.

2.3.4.2   The Yangtze River Basin

The Yangtze River is 6,300 km long and has a drainage area of 1.80 million km^2. From the source to Yichang (Three Gorges Dam site) is the upper reach, from Yichang to Hukou (Poyang Lake mouth) is the middle reach, from Hukou to Datong is the lower reach, and below Datong is the estuary. There are 562,000 km^2 of land experiencing soil erosion in the upper reaches of the river. The annual sediment yield from the upper Yangtze River basin is 2.2 billion tons (Tang, 2004). Glacial erosion occurs in the Qinghai-Tibet Plateau and serious rainfall erosion occurs in the Yunnan-Guizhou Plateau. For

vegetation-erosion analysis the upper Yangtze River basin is divided into three areas according to climate, topography, soil, morphology, and soil erosion and vegetation: Qinghai-Tibet plateau, hot and dry valleys, and Yuannan-Guizhou-Sichuan area, as shown in Fig. 2.44.

On the Qinghai-Tibet Plateau, the annual average temperature is only $-4.2℃$ at the Tuotuohe meteorological station, which results in low evaporation. Vegetation may slowly develop and mainly is herbaceous. The Jinsha River valley and many tributary valleys on the Yuannan-Guizhou Plateau are dry and hot valleys, where the annual average temperature is about $20℃$, and monthly average rainfall from December to April is less than 10 mm, which results in poor vegetation. In the summer from June to September, the monthly rainfall is more than 120 mm, which causes high soil erosion. Splash erosion, sheet erosion, and rill erosion are moderate but gully erosion is extremely intensive. The sediment eroded from the area is composed of clay, silt, sand, gravel, cobbles, and boulders. More than 50% of the sediment load in the Yangtze River are from the Jinsha River basin. On the Yunnan-Guizhou Plateau and in the Sichuan basin, it is warm and wet. The average annual precipitation is about 1,000 mm and annual average temperature is about $18℃$. Vegetation develops well and soil erosion is low.
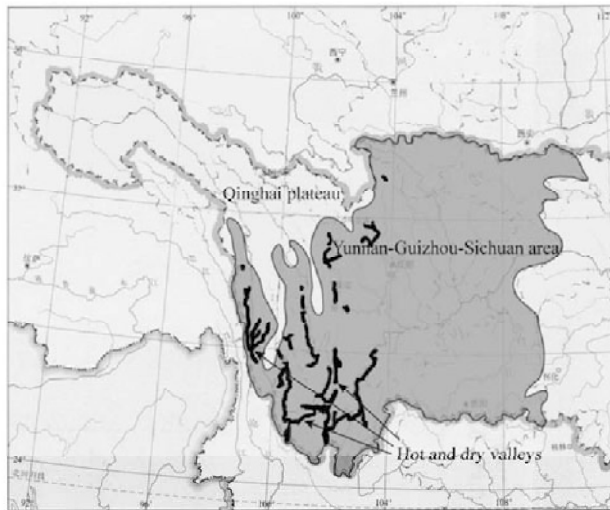
Fig. 2.44 Zoning of the upper Yangtze River basin for vegetation-erosion analysis

Using the data of vegetation and erosion rate measured in the Mengzong Watershed on the Qinghai-Tibet Plateau, the four parameters are determined as follows:

$$a = 0.001(1/t); c = 0.0000014(km^2 / yr); b = 0.01(1/ yr); f = 190(t / km^2 yr^2) \tag{2-26}$$

With the values of the parameters the vegetation-erosion chart for the Qinghai-Tibet Plateau is developed, as shown in Fig. 2.45(a). The chart has a very small Zone C and a large Zone D. The vegetation is vulnerable and has no capacity of self-restoration. If the vegetation on the Qinghai-Tibet Plateau is destroyed, it is very difficult to restore. Therefore, the main management strategy for the area is careful protection of the vegetation.

In the hot and dry valleys the vegetation is poor and the soil erosion is intense. The four parameters are determined with data as follows:

$$a = 0.017 - 0.03(1/ yr); \quad c = 0.000002 - 0.000005(km^2 / t);$$
$$b = 0.045 - 0.054(1/ yr); \quad f = 200 - 350(t / km^2 yr^2) \tag{2.27}$$

The *c* value is relatively large, *b* value is very large, and *f* value is small, which implies that soil erosion may seriously impair the vegetation and deforestation may substantially increase soil erosion. Figure 2.45(b) shows the vegetation erosion chart for the hot and dry valleys, in which there is a relatively large Zone C, a large Zone A and very small Zone B. The points representing the current status of vegetation and erosion are mostly in the Zone A. Although the current vegetation is very poor, if soil erosion is controlled, a new vegetation may develop. The watershed may move into Zone C. The new vegetation will have a relatively high capacity of self-restoration, and it will have a moderate resilience and may sustain a certain intensity of ecological stresses.

The strategies for vegetation restoration for the hot and dry valleys should be as follows. ① Making use of limited sources for reforestation of small watersheds, as has been done for the Heshuihe and Shengou watersheds. If limited resources of labor, funds, and materials are used for the whole area, the vegetation may be improved more or less and erosion can be reduced to a certain extent after a period of continued reforestation. Despite some reforestation effort the status point in the chart may still be in Zone A. If the efforts for reforestation and erosion control are not continued, the vegetation may deteriorate and the erosion rate may increase again. Only if necessary the resources are used for a small watershed will the status point in the chart be moved into Zone C in a not long period of time. Thence, the vegetation will perfect itself. In this way all small watersheds can be greened one by one. ② Controlling erosion before planting trees. Erosion control is more important than planting trees for the hot and dry valleys at the beginning stage of because the present status point is far for Zone C. By terracing the slopes and constructing check dams in gullies, the erosion rate can be reduced below 5,000 t/km²yr. Then, reforestation will be more effective. ③ Allowing limited husbandry and selected logging as fuel and fodder. For a watershed whose status point in the chart is in the Zone C, limited husbandry and logging may be allowed. Vegetation in Zone C is stable and limited logging cannot badly impair the vegetation.

On the Yunnan-Guizhou Plateau and in the Sichuan Basin it is warm and wet and the slope is gentle. Therefore, the rate of soil erosion is low and vegetation develops well. The four parameters are determined with data as follows:

$$a = 0.01 - 0.024(1/a); \quad c = 0.000001 - 0.000005(km^2/t);$$
$$b = 0.01 - 0.03(1/a); \quad f = 250 - 400(t/km^2a^2) \tag{2.28}$$

Figure 2.45(c) shows the vegetation-erosion chart for the Yunnan-Guizhou Plateau and the Sichuan Basin, which has a rather large Zone C, a large Zone A, and a moderate Zone D. The points of current status for Yunnan (Kunming), Guizhou (Guiyang), and Sichuan Provinces are in Zone C. The point for Chongqing is in Zone D but very close to Zone C. The vegetation in the area may sustain moderate logging. The main management strategy is to avoid any large scale of deforestation.

2.3.4.3   Mountainous Area with Slope Debris in North China

This area includes the mountainous and hilly areas in Hebei Province, Beijing, and Tianjin. The annual average temperature is about 10℃ and the annual precipitation is about 600 mm. The soil layer is thin. Human activities act as a very strong stress on the vegetation, both negative (deforestation) and positive (reforestation). The four parameters are determined as follows:

$$a = 0.006 - 0.009(1/a); \quad c = 0.000004 - 0.0000045(km^2/t);$$
$$b = 0.003 - 0.005(1/a); \quad f = 180 - 210(t/km^2a^2) \tag{2.29}$$

Figure 2.46 shows the vegetation-erosion chart for the area, which has a very large Zone D, a small Zone A, and a small Zone C. The vegetation in the area is not stable and may be changed by human activities to a large extent.
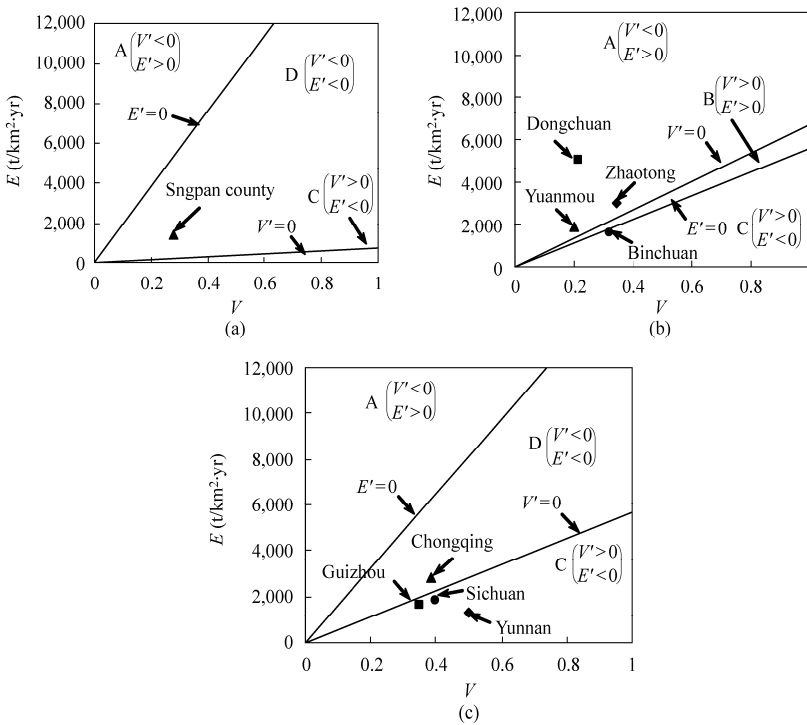
Fig. 2.45 Vegetation-erosion charts for the upper Yangtze River basin: (a) Qinghai-Tibet Plateau; (b) Hot and dry valleys; (c) The Yunnan-Guizhou Plateau and the Sichuan Basin
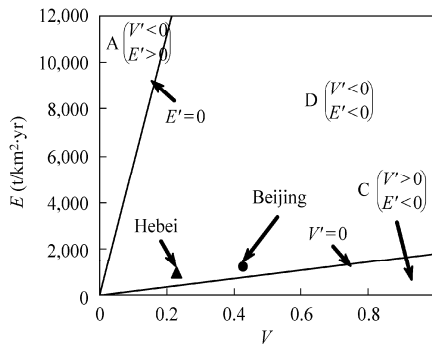
Fig. 2.46 Vegetation-erosion chart for the mountainous and hilly area in north China

2.3.4.4 Red Soil Area in South China

The red soil area in south China includes Guangdong, Guangxi, Jiangxi, and Fujian provinces in China. It is very wet and warm. Generally the vegetation develops well and limited erosion occurs in the area. For instance, Huizhou may be a representative area for the red soil area, which is located in Guangdong Province, southern China. The annual precipitation is 2,000 mm and annual average temperature is 25℃. There was high density of vegetation cover before the 1960s. In the 1970s and 1980s human activities and poor management resulted in severe deforestation and many hills became bare and the rate of

soil erosion was nearly 8,000 t/km²yr. An experimental research station was established in 1978 and experiments of reforestation were performed in the area. In selected experimental plots, trees were planted in the first 4 years and grasses, shrubs, liana, and bamboo grew quickly in the following years. The vegetation develops with time and the rate of soil erosion reduces with time as shown in Fig. 2.47(a)–(d). An experimental plot is used as a comparison, in which no trees are planted and the plot is closed for natural development of vegetation. The variation in vegetation and erosion of the comparison plot is shown in Fig. 2.47(e)–(f).
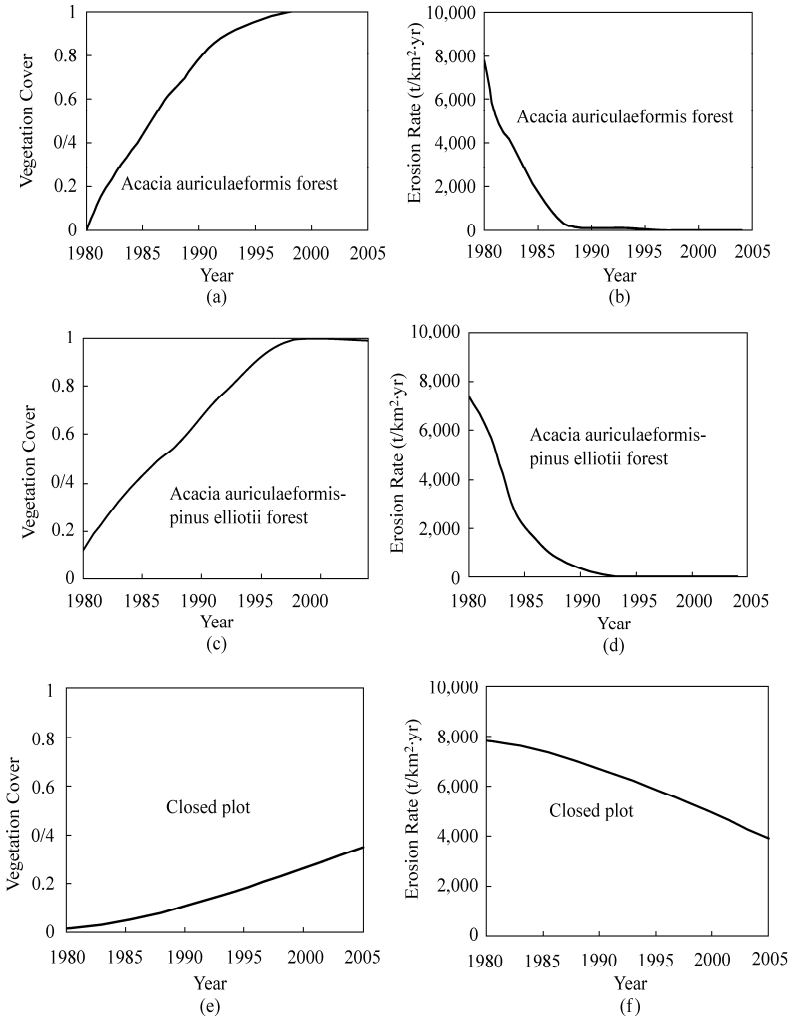
Fig. 2.47 Comparison of the vegetation development and the erosion reduction of reforested plots by planting Acacia Mangium (a) and (b) and Acacia Mangium and Pine (c) and (d) with a plot, which is closed for natural development of vegetation (e) and (f) for Huizhou, Guangdong Province, south China

The differential equations of vegetation-erosion dynamics are applied to the Huizhou area, and the parameters of a, c, b, and f are determined with the data from the experiment plots as follows:

$$a = 0.06(1/\text{yr}), \quad c = 0.000005(\text{km}^2/\text{t}), \quad b = 0.01(1/\text{yr}), \quad f = 500 \text{ (t/(km}^2\cdot\text{yr}^2)) \qquad (2.30)$$

The vegetation and erosion chart for this area is developed as shown in Fig. 2.48. The straight line $E' = 0$ is steep and Zone C is very large. The point of the vegetation-erosion status in 1978 is in Zone A. Planting trees and control of erosion moved the point into Zone C. Thence, the vegetation develops automatically and the vegetation community develops from simple wood to a complex community consisting of different species, including grasses, shrubs, liana, woods and bamboo.
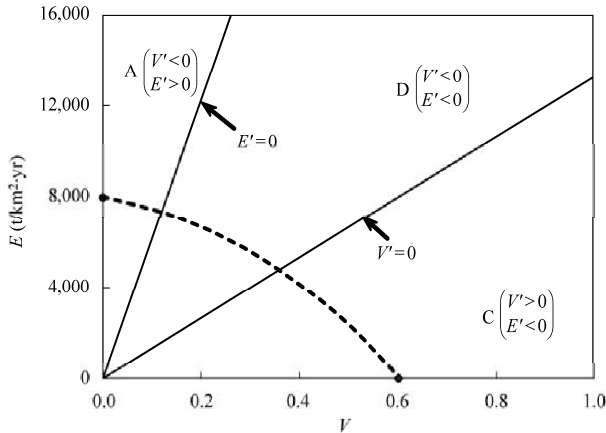
Fig. 2.48   Vegetation-erosion chart for Huizhou area in Guangdong Province, southern China

From Eq. (2.24) it can be calculated that the rate of vegetation development may be accelerated from $dV/dt = 0.002$ (yr^{-1}) to $dV/dt = 0.014$ (yr^{-1}) if the reforestation area is increased from 20% to 40% for erosion rate equal to 2,000 t/km^{2}yr. In other words, the rate of vegetation development may be increased by 7 times if the area of tree-planting is increased by 2 times. In general, the vegetation succession from pioneer species well-adapted to bare soil and plentiful light to longer-lived species that can regenerate under more shaded and protected conditions takes about a century. Planting dominant tree species in the area accelerated the plant succession. It takes only 24 years to develop a vegetation consisting of a complex plant community including long-lived wood species and grasses and shrubs accustomed to shaded and protected conditions. The time of vegetation development is shortened by 75%.

Figure 2.49 (b) shows the development process of the vegetation cover of woods, grasses, shrubs, liana, and bamboo in 1981–2004. Only tree planting was performed in the beginning period in 1981–1984. In the following years, the vegetation cover and the species composition of the vegetation developed automatically. All species of shrubs, liana, bamboo and some wood are local species and develop naturally. Figure 2.49(a) shows the comparison of the closed plot, in which only herbaceous and some shrubs species, which are well-adapted to bare soil and plentiful light, have been developed.

Figure 2.50 shows the pictures of the two cases, in the experimental plot the trees of Acacia Mangium have well grown and the natural species have also developed within the forest. In the comparison plot only some grasses and shrubs can grow under the conditions of bare soil and plentiful light after 24 years of natural development.

Legend

Woods
- ☐ Acacia auriculaeformis
- ▨ Ailanthus altissima
- ■ Cinnamomum camphora
- ▨ Scheffera actinophylla
- ■ Sapium discolor
- ▨ Others

Herbage
- ▨ Dicranopteris pedata
- ▨ Melinis minutiflora
- ▨ Miscanthus floridulus
- ▨ Gahnia tristis
- ▨ Scleria hookeriana

- ▨ Imperata cylindrica
- ▨ Blechnum orientale
- ☐ Melastoma dodecandrum
- ▨ Setaria viridis
- ▨ Helicteres angustifolia
- ▨ Eremochloa ciliaris
- ▨ Eriachne pallescens
- ▨ Scirpus subcapitatus
- ▨ Bulbostylis barbata
- ▨ Exacum
- ▨ Eleusine indica
- ▨ Eragrostis poaeoides
- ▨ Lycopodium Cernuum
- ▨ Dianella ensifolia

- ▨ Ischaemum barbatum
- ▨ Cymbopogon goeringii
- ▨ Others

Shrubs and bamboo
- ▨ Rhodomyrtus tomentosa
- ▨ Baeckea frutescens
- ▨ Melastoma candidum
- ▨ Lantana camara
- ▨ Cleridendrun fortunatum
- ▨ Psychotria rubra
- ▨ Prunus mume
- ▨ Bambusa stenostachya

- ▨ Xylosma congestum
- ▨ Syzygium jambos
- ▨ Aglaia odorata
- ▨ Others

Liana
- ▨ Rhododendron simsii
- ▨ Lygodium japonicum
- ▨ Smilax china
- ▨ Zanthoxylum nitidum
- ▨ Fructus Zanthoxyli Planispini
- ▨ Smilax china
- ▨ Others

Fig. 2.49   (a) Development of vegetation in a closed plot, in which only herbaceous and some shrubs species have been developed; (b) Development process of vegetation cover consisting of woods, grasses, shrubs, liana, and bamboo in 1981–2004 in an experimental plot by planting Acacia Mangium, which has accelerated plant succession.

Fig. 2.50   Comparison of the vegetation consisting of woods, grasses, shrubs, liana, and bamboo in an experimental plot by planting Acacia Mangium (a) with the vegetation in a closed plot consisting of only herbaceous and some shrubs species (b) (See color figure at the end of this book)

2.4   Riparian Vegetation

Riparian vegetation, by definition, is controlled in both form and species distribution by fluvial-geomorphic forms and processes, which, in turn, are products of prevailing hydrologic conditions. Riparian vegetation, channel form, and streamflow are mutually adjusted features of the bottomland landscape; alteration of one will result in compensating adjustment of the others. Severe degradation of the channel typically removes most of the riparian zone from the influence of fluvial processes for all but the highest flows. The influence of the riparian zone on fluvial processes and aquatic biota is, likewise, substantially reduced, which usually leads to deterioration of aquatic ecosystems and water quality. Although some research has been conducted on the use of vegetation to mitigate the effects of channel incision (Shields et al., 1993 and 1995), substantially less research has been devoted to the description and interpretation of the role that riparian vegetation plays during incision and subsequent recovery. The basic organization and content of this section is patterned after Hupp (1988), but the authors have integrated much of the recent literature to the basic discussion of concepts and applications.

2.4.1   Zoning of Riparian Vegettion
In equilibrated fluvial systems characteristic vegetation species and patterns have adapted to the prevailing environmental processes associated with particular fluvial landforms (Ma et al., 2006; Hack and Goodlett, 1960; Zimmermann and Thom, 1982). Interdisciplinary (fluvial-geomorphic and plant ecological) approaches clearly show that riparian vegetation is an integral part of an equilibrated fluvial system. Moreover, during natural geomorphic recovery from degradation, invasive or ruderal plants may play an important and sometimes critical role in the re-establishment of equilibrium conditions (Osterkamp and Costa, 1987; Hupp, 1992; Friedman et al., 1996a). Hickin (1984) listed five ways in which vegetation affects fluvial geomorphology:

(1) by creating flow resistance on most fluvial surfaces;

(2) by increasing bank strength through root mass development;

(3) by increasing sedimentation on channel bars;

(4) by providing large woody debris (LWD) that may affect numerous hydraulic processes, including debris jams, flow deflection, and bank armoring; and

(5) by increasing sediment deposition and stability on banks and other low fluvial surfaces.

All of these effects can be seen along streams, particularly during channel recovery following incision (Hupp, 1992; Fetherston et al., 1995; Diehl, 1997).

Specific riparian plant species grow on specific fluvial landforms. The typical landforms that may be found along alluvial streams are shown in Fig. 2.51. Some species may be restricted to only one landform, others may occur on two adjacent landforms, and still others may occur on most fluvial landforms (Fig. 2.51). The likelihood of a given species vigorously growing on a particular landform is a function of the suitability of the site for germination and establishment, and the ambient environmental conditions at the site that permit persistence at least until reproductive age. The distribution pattern may be limited by the tolerance of a species to a specific disturbance or stress regime, as well as by tolerance for other more diffuse interactions including competition, for which one set of factors drives the limits at one extreme, while another set drives the limits at the other extreme. In fluvial systems, the distribution of vegetation across landforms may be driven largely by the tolerance of species to specific geomorphic processes at the severe end of a stress-equilibrium relation and by competition with other riparian species at the other end. In temperate regions, where water is abundant, vegetation distribution can be related to the distribution of fluvial landforms (Hupp and Osterkamp, 1985). In arid and semi-arid environments, bare sites for colonization are relatively abundant, but water availability is limiting. Thus, in dry climates, vegetation

patterns may be strongly influenced by surface floods and ground-water levels (Zimmermann, 1969; Friedman et al., 1996b).
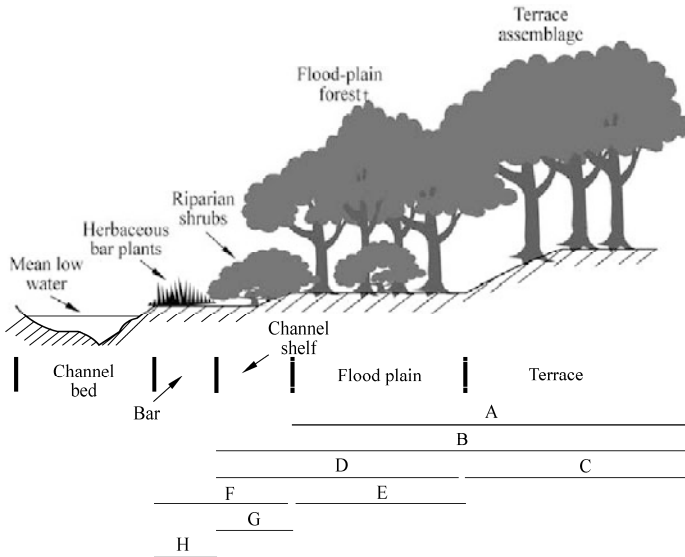
Fig. 2.51   Distribution of typical riparian plant communities in relation to fluvial landforms. Idealized individual species distributions are shown in bars A through H; for example, species A typically grows on floodplains and terraces and is restricted on lower fluvial surfaces (after Hupp, 1992)

The following descriptions and definitions (from Hupp and Osterkamp, 1996) are for the typical fluvial landforms found along most streams from temperate to semi-arid regions. The term bottomland refers to all fluvial generated landforms and the vegetation they support. These landforms occur as terraces high in the valley section and, in descending order, proceed through floodplain, various riparian features including riverine wetlands, channel bars, to the channel bed (Fig. 2.51). Alluvial streams impacted by channel incision will be dominated by fluvial processes during the recovery period. The recovery process (unaided by human restoration) may require decades to centuries (Hupp, 1992).

Table 2.3   Fluvial-landforms and their relations with vegetation type, flow duration (i.e., percentage of time the landforms are inundated), and flood frequency (Hupp and Osterkamp, 1996)

Fluvial landform	Vegetation type	Flow duration	Flood frequency
Channel bar	Largely absent	About 40%	
Channel shelf	Riparian shrubs	5%–25%	
Floodplain	Floodplain forest		1–3 years
Terrace	Terrace assemblage		>3 years

The channel bed is the surface that is wholly or partly covered by flows below mean annual discharge. Thus, at least part of the channel bed is inundated at all times. Channel bars (Fig. 2.51, Table 2.3) occur in the active-channel part of the valley section and are the lowest prominent geomorphic feature higher than, but within, the active-channel bed. The level of the channel bar generally corresponds to a stage slightly higher than the low-flow water stage. The channel shelf, a bank feature, is a horizontal to gently sloping surface (Fig. 2.51, Table 2.3). The channel shelf is best developed along relatively steep-gradient

reaches. The level of the channel shelf along many perennial streams approximates the level of the mean annual discharge. Floodplains (Fig. 2.51, Table 2.3) are the flat surfaces that are flooded, on average, once per 1-3 years. The water elevation just necessary to reach the floodplain is termed bankfull stage. Terraces may occur for a number of reasons (Howard et al., 1968), however, most represent former floodplains and may be at various levels above the modern floodplain (Fig. 2.51, Table 2.3). Channel incision typically renders once active floodplains to terraces through degradation. The likelihood of terrace inundation is always less than that of the floodplain, with the frequency of terrace inundation less than once every 3 years.

Figure 2.52 shows the riparian vegetation by a small river in the U.S. The roots of the riparian forest increase the roughness and reduce bank erosion.

Fig. 2.52 Riparian forest by a small river in the U.S. The roots of the riparian forest increase the roughness and reduce bank erosion

Research in forested areas over the past two decades has shown lLWD in and along the channel to be an important element of fluvial-geomorphic form and process. Most streams, even those in semi-arid environments, naturally support woody riparian vegetation. Meandering, avulsion, braiding, and changes in channel width along forested, low-gradient channels may be controlled at least in part by LWD. LWD may buttress portions of the channel slowing flow in the lee of the obstruction, thus enhancing sediment deposition (Osterkamp and Costa, 1987).

2.4.2 Role of Vegetation in Fluvial Process

2.4.2.1 Degradation

Many mountainous streams in China are degrading channels. Even for those that have achieved equilibrium many causes may induce channel degradation or aggradation. Any natural or human induced causes that change the channel gradient or supply of sediment from the drainage basin in an equilibrated fluvial system may cause channel aggradation or degradation. Woody riparian vegetation typically does not become established on the active channel bed of perennial streams (Hupp and Osterkamp, 1985). Thus, initial bed degradation does not directly affect riparian vegetation. However, as degradation increases bank heights, the roots of plants growing above the bed may significantly increase bank stability along

banks that would otherwise fail (Thorne, 1990). Roots, growing below the bed of ephemeral channels, may act as natural grade-control structures in degrading systems and limit headcut migration (Germanoski and Ritter, 1988).

Once degradation increases bank heights past a critical threshold (shear stresses in excess of material strength), however, mass wasting of the banks occurs regardless of riparian vegetation, toppling vegetation down the bank slope on failure blocks (Simon and Hupp, 1987 and 1992). This failed woody vegetation sometimes re-establishes on the lower bank slope (Hupp, 1992) or may contribute to the LWD load of the stream. In both cases this vegetation may ultimately ameliorate degrading conditions by increasing channel roughness, promoting flow deflection, and adding coarse material (LWD), thus decreasing flow velocity and subsequent erosion (Gregory and Gurnell, 1988; Shields et al., 1994; Fetherston et al., 1995).

If the channel gradient is near equilibrium, riparian vegetation and large woody debris may facilitate sediment trapping and initiate aggrading conditions and the recovery process (Simon and Hupp, 1992). Drift or LWD may be generated along incised channels in greater quantities than along non-degraded streams. Diehl (1997) notes that channelized and subsequently incised streams generate abundant LWD because increased bank heights promote bank failure in forested riparian surfaces

The effects of degrading channels on riparian vegetation, particularly below dams, has been summarized by Williams and Wolman (1984). They note that the extent of riparian vegetation below the floodplain elevation increases after dam closure, most likely due to regulation of peak flows. The reduction of peak flows and sediment trapping behind dams, however, limits the production of coarse sediment and the creation of mid-channel bars and islands necessary for some riparian species to establish (Scott et al., 1996). Thus, species diversity may decrease and community composition may change after dam closure (Baker, 1989; Stromberg and Patten, 1992; Nilsson and Jansson, 1995). Comprehensive establishment of riparian vegetation on bars and islands along the North Platte River, Nebraska, occurred after several dam closures early last century; this vegetation establishment promotes the coalescence of islands and bars and threatens critical habitat for sandhill cranes. Collier et al. (1996) observed that the steady reduction of both springtime flows and total annual flow have allowed the encroachment of cottonwood (Populus), elm (Ulmus), and willow (Salix) on bare sand bars and islands.

Vegetation on former floodplains along incised channels may be adversely affected by degradation as a result of water stress from lowered water tables. Johnson et al. (1976) attributed a post-dam decrease in several floodplain species along the Missouri River, in part, to a reduction in high flows that formerly delivered nutrients and maintained a higher water table. Along these same reaches, Reilly and Johnson (1982) correlated a substantial decrease in the growth rate of many surviving floodplain species with the near elimination of over-bank flooding and lowered floodplain water tables following dam closure.

2.4.2.2   Aggradation

Channel evolution is a complex response punctuated by geomorphic thresholds (Schumm, 1973). One of these thresholds, the regime shift from bed degradation to bed aggradation, signals the beginning of the recovery cycle following channel incision. The shift from general degradation to general aggradation reflects a regime shift from a regime dominated by vertical processes (erosion) associated with non-equilibrium incision to a regime dominated by lateral processes (point-bar development and meander initiation and extension) consistent with equilibrated conditions (Schumm et al., 1984; Harvey and Watson, 1986; Simon, 1989; Hupp and Simon, 1991).

Channel banks may not achieve equilibrium conditions coincident with the establishment of channel-bed equilibrium. If the channel bed has degraded past a critical bank-height threshold, bank failure and subsequent bank widening may continue until bank angles are reduced to a stable form (Simon and Hupp, 1987; Hupp and Simon, 1991). Sustained accretion on the low parts of bank surfaces is coincident with,

and facilitated by, the establishment of dense woody vegetation (Hupp and Simon, 1991; Hupp, 1992). The woody vegetation on recently stabilized banks and floodplains increases soil strength through root development and reduces flow velocity by increasing surface roughness (Williams and Wolman, 1984; Hupp and Simon, 1991; Shields et al., 1993 and 1995). This vegetated depositional area expands from low on the bank slope, and depending on the magnitude of prior degradation, may ultimately extend to the former floodplain elevation.

Many rivers are now channelized and the riparian vegetation experiences devastation and recovery. The amount of vegetation cover, age of the riparian plants, and species richness varies with the stage of channel recovery after channelization (Fig. 2.53; Simon and Hupp, 1987). Vegetation cover is high during stage I and stage III where it occurs above the limit of channelization; here the mature riparian vegetation has not been affected by channel incision. For channelized reaches, cover is lowest in stage II, the construction stage, during which woody vegetation typically is removed, and in stage IV where numerous bank failures remove woody plants and preclude the establishment of new vegetation (Fig. 2.53). Cover and number of species increase from late stage IV through stage VI. The age of the woody plants through the course of channel evolution closely matches the trends in cover for obvious reasons. Trends in the number of species (or species richness) also match those of cover and age. The greater site stability of riparian areas in stages I and III may promote greater species richness, while severe instabilities in stage IV and early stage V preclude all but the most vigorous, ruderal species.
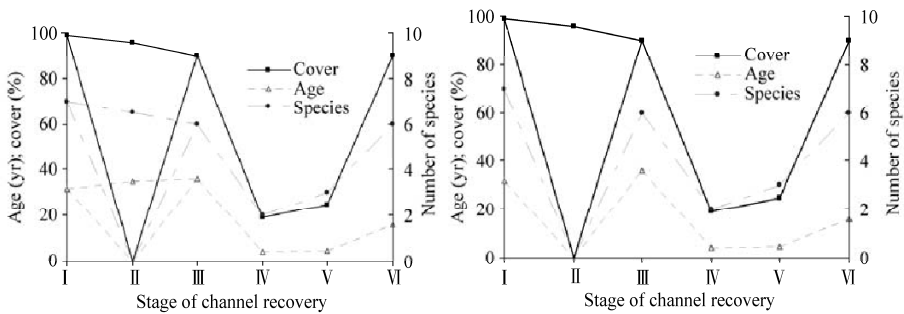
Fig. 2.53   Age, cover, and numbers of species as functions of the stage of channel degradation and recovery (after Simon and Hupp, 1987)

2.4.2.3   Large woody debris (LWD)

Wallerstein et al. (1997) found LWD induced sedimentation exceeded LWD induced scour, thus the overall effect of debris jams is grade control and accelerated sedimentation, promoting stable channel features that may trigger the onset of recovery. They also offer a classification of debris jams based on debris length L and channel width (Fig. 2.54) that may be used as a conceptual model to evaluate types of LWD along incised channels. The use of artificially placed LWD has been shown to increase channel stability along incised channels, whereas removal of LWD increased degradation (Shields and Gippel, 1995).

Vegetation patterns seemingly develop largely in response to surface-stability conditions, accretion tolerance, inundation tolerance, and, for some species, light availability. For example, three distinct suites of vegetation were identified as recovery vegetation along incised channels in west Tennessee (Hupp and Simon, 1991; Hupp, 1992), which develop in succession beginning near the end of stage IV through stage VI (Fig. 2.53) of the Simon and Hupp (1987) model of channel evolution, matching the ameliorating conditions during the recovery period. The initial pioneer suite (Suite l, Table 2.4) of riparian plants establish late in stage IV or early in stage V and are hardy, fast-growing plants dispersed in late spring,

Underflow jam
L>W
Local bed & bank scour
limited backwater
sedimentation

Dam jam
L=W
Backwater pools and
log-steps.
Sediment wedge formation,
and plunge scour

Deflector jam
0.5W<L<W
Flow deflection,bed
scour and bank erosion.
Local channel widening
bar development in the
lee of jams

Parallel/bar head jam
L<0.5W
Bank toe protection
sepecially in apex of bends.
Accelerates incipient bar
growth

Increasing watershed ared/discharge

Fig. 2.54 Impacts of the large woody debris on fluvial processes (*L* is the length of the woody debris; and *W* is the channel width) (after Wallerstein et al., 1997) (See color figure at the end of this book)

Table 2.4 Summary of pioneer, intermediate, and hardwood species suites and their characteristics, which occur during the recovery period after channel incision in west Tennessee (after Hupp, 1992, revised)

Vegetation succession	Pioneer species (Suite 1)	Intermediate species (Suite 2)	Hardwood species (Suite 3)
Time	Late Stage IV	Stage V	Stage VI
Species	Salix nigra, Betula nigra, Acer negundo, Platanus occidentalis, Populus dehoides	Carpinus caroliniana, Fraxinus pennsylvanica, Taxodium Populus dehoides, Nissa aquatica	Quercus lyrata, Q. nigra, Q. pagadofolia, Q. phellos, Fagus grandifolia
Bank stability	Ruderal, unstable sites	Stable conditions	Mature, stable conditions
Light requirements	Shade intolerant	Moderately shade tolerant	Shade tolerant
Plant life cycle	Fast-growing, short-lived plants	Slow-growing, long-lived plants	Slow-growing, long-lived plants
Reproduction	Extensive asexual reproduction	Rare asexual reproduction	Rare asexual reproduction
Seed life	Abundant short-lived seeds	Long-lived seeds	Short-lived seeds
Seed dispersal	Wind and/or water dispersal	Wind and/or water dispersal	Animal dispersal
Seed timing	Seed release in late spring	Seed release in late summer	Seed release in late summer/fall

a time that coincides with lowered stream flow elevations exposing fresh surfaces for establishment. These species tolerate moderate to high amounts of mass wasting and accretion and generally require high amounts of light. Additionally, upland ruderal species may establish high on the former floodplain and its banks, where overbank flows have been eliminated, or nearly so, because of the degraded channel. A second intermediate suite (Suite 2, Table 2.4) of riparian vegetation establishes late in the recovery period (late in stage V) and generally requires stable banks, low amounts of accretion, and tolerates low

light or closed canopy situations. A final suite of hardwood vegetation (Suite 3, Table 2.4), typical of undisturbed systems, may establish on the new floodplain after complete recovery to a meandering channel and the development of natural levees. Although the exact species involved in recovery (Table 2.4) will vary from region to region, it is reasonable to assume that the characteristics of the suites along many recovering incised channels will be similar.

2.4.3 Dendrogeomrophic Evidence of Evolution of Incised Rivers

Dendrogeomorphology is the study of geomorphic processes through the use of dendrochronologic (tree ring) analysis (Shroder, 1980; Shroder and Butler, 1987). Tree ring analysis may be used to estimate the rate of channel widening, bank and floodplain accretion, and the timing of vegetation establishment (stability) on various fluvial surfaces (Hupp, 1987). The mechanism of radial growth is well documented in the botanical literature. The annual increment of tree growth has been the basis of many studies using tree rings in documentation of the magnitude and frequency of important hydrologic and geomorphic events. Trees and saplings growing on bank surfaces may also be tilted or scarred during mass wasting or may be partly buried during bank or floodplain accretion. Thus, increment cores or cross sections collected from riparian trees can be aged and crossdated to determine the timing of geomorphic events. When stem age data are combined with measurements of failure-block width or burial depth, the rates of channel widening and bank accretion, respectively, may be estimated. Figure 2.55 shows the types of botanical evidence of geomorphic events including floods and mass wasting (Hupp,1988).
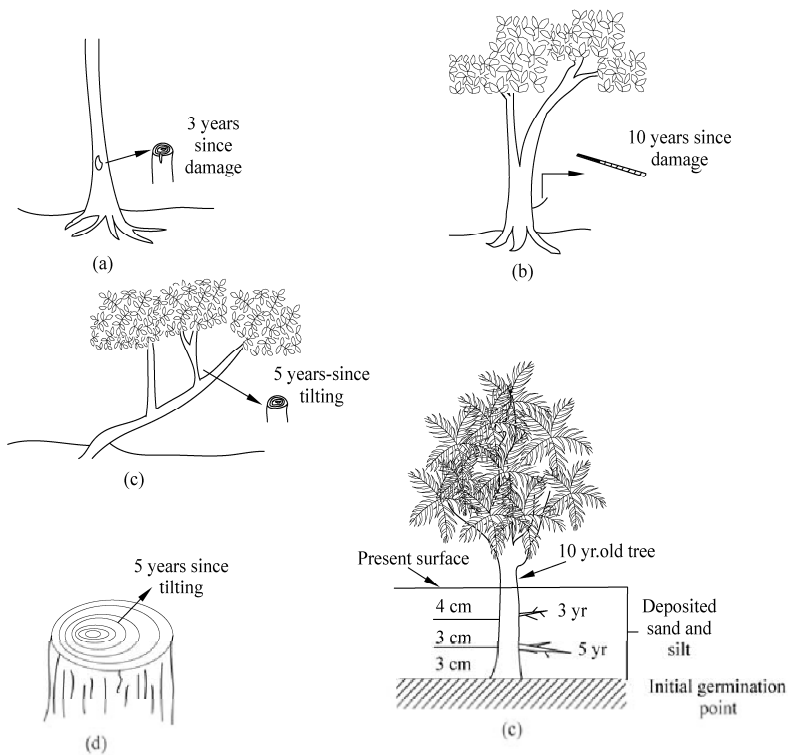
Fig. 2.55 Types of botanical evidence of geomorphic events: (a) Corrasion scar; (b) split base sprouts; (c) Sprouts from tilted parent; (d) Eccentric growth; and (e) Generalized buried sapling, showing age and depth of sediment deposition (after Hupp, 1988)

At least five basic types of botanical evidence of geomorphic events are useful, as shown in Fig. 2.55 (Sigafoos, 1964; Hupp, 1988): ① corrasion scars; ② adventitious sprouts; ③ eccentric growth; ④ secondary roots, and ⑤ buried sapling with adventitious roots showing ages and depth of sediment deposition. Corrasion scars and sprouts from tilted parent stems yield accurate (usually within one year) dates of bank failure. Increment cores or cross sections are taken through scars or at the base of tilt sprouts to determine when the trees were impacted. Figure 2.56(a) shows sprouts from a tilted parent stem of a tree by a small river in central China. The sprouts are about 6 months old, from which it is estimated that a flood event occurred 6 months ago and caused the bank erosion and the tree tilted. Figure 2.56(b) shows a dying tree in the Xiaojinchuan River in Sichuan Province, which explains that there was a relative stable vegetative island in the river that had existed for several tens of years. A major event occurred recently and the island was scoured away. It is estimated that the flood was an major event with high sediment-removal capacity.

(a)   (b)
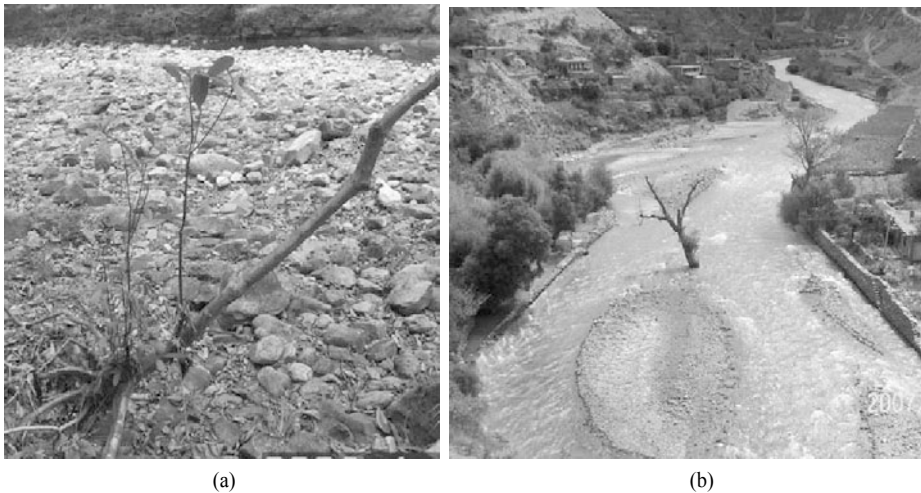
Fig. 2.56   (a) Sprouts from tilted parent stem of a tree by a small river in central China. It is estimated that a flood event occurred 6 months ago and caused the bank erosion and the tree tilted; (b) A dying tree in the Xiaojinchuan River in Sichuan Province, which indicates that there was a relatively stable vegetated island in the river.

Eccentric growth often occurs when a stem is tilted off centre and is easily determined from cross sections by noting where relatively concentric ring formation abruptly shifts to eccentric ring formation. Eccentric ring patterns provide accurate dates of tilting, often to the season of occurrence. Estimates of channel widening are made first by determining the ages of stem deformations associated with bank failure, and then subsequently measuring the width of the slump block or the distance between affected stems and the present top-bank edge (Fig. 2.57). Slump blocks of varying ages and entrained woody plants provide a history of recent bank failure along a given reach.

Sediment carried by high water may be deposited around the bases of riparian trees and saplings growing on various fluvial geomorphic surfaces. Buried trunks, branches, and adventitious roots permit estimates of the sediment accretion rate. A rate of accretion may be estimated (Fig. 2.55) by digging the ground adjacent to buried stems to the depth of their original root collar (germination point), coring the stem for age determination, and subsequently dividing the depth of burial by stem age.

Over the last 25 years or so, there has been a substantial increase in the amount of plant ecological and fluvial-geomorphic research on the role vegetation in geomorphic form and process and vice versa.
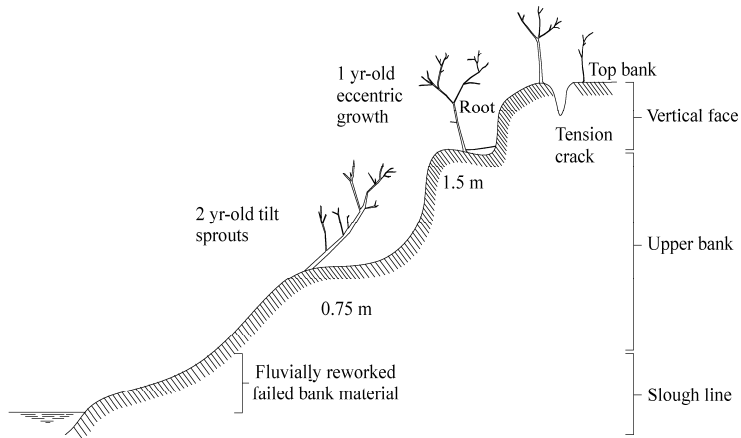
Fig. 2.57 Botanical evidence of events of bank cross section widening of a degraded channel. Bank forms are indicated on the right (after Hupp, 1987)

However, much of this integrated research has remained in more academic circles rather than reaching the applied sector, excepting some excellent biotechnical approaches to streambank stabilization. Several directions for future applied and basic research should be fruitful; a few are now offered. Dendrogeomorphic approaches to assessing the impact and long-term effects of channel incision offer a relatively inexpensive, yet relatively accurate methodology that has yet to come into widespread use. The effect vegetation has on bank stability (root strength versus surcharge) has received little quantitative study. The role vegetation plays in affecting channel roughness, flow velocity, and sediment deposition rate and location has only recently been appreciated and there are yet but few quantitative studies.

Review Questions

1. Answer the following questions

    (a) What are main agents of erosion?

    (b) Why grain erosion became important after a great earthquake?

    (c) What are the ecological functions of vegetation? What are the major stresses on vegetation?

    (d) Why is erosion a special stress? How are the ecological stresses classified? List the vigor stresses and mortality stresses.

    (e) What will happen if a vigor stress acts on the vegetation?

    (f) What is vulnerable vegetation? Give an example.

    (g) What does vegetation-erosion dynamics study and what problems can be solved with knowledge of the dynamics?

    (h) What is riparian vegetation? How does riparian vegetation affect fluvial geomorphology?

    (i) State the process of degradation and recovery of streams with woody riparian vegetation and the general variation of the vegetation, including number of species, cover, and age of the vegetation in the process.

    (j) What is dendrogeomorphology? What are the basic types of botanical evidence used in the dendrogeomorphology?

    (k) A bank failure occurred about 3–5 years ago, explain how can you estimate the accurate time of the bank failure with the dendrogeomorphic approaches.

2. From collected data the values of the parameters of the vegetation-erosion dynamics model were obtained as follows: $a = 0.02$ (1/yr); $c = 0.00001$ (km^2/t); $b = 0.05$ (1/yr); $f = 50$ (t/km^{2}yr^2). Work out the vegetation-erosion chart. At present, the vegetation cover is $V = 5\%$ and sediment yield by erosion is $E = 4,000$ (t/km^{2}yr). Indicate the location of the vegetation-erosion status on the chart, and suggest an efficient strategy of vegetation improvement and erosion control (Accurate figures of reforestation and erosion reduction are not required).

3. As shown in the lower diagram in the Figure the floodplain has been experiencing a siltation process over the past 10 years. Analyze the diagram ad state the sedimentation process.
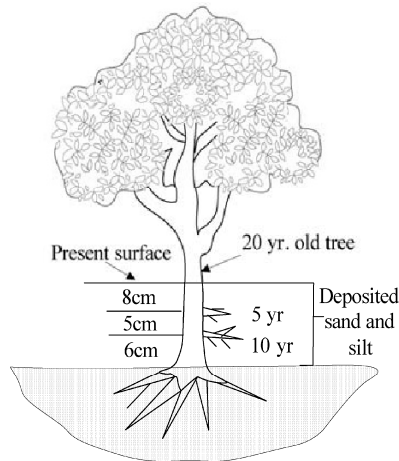
References

Baker W.L., 1989. Macro and micro-scale influences on riparian vegetation in western Colorado. Annals of the Association of American Geographer, 79, 65–78

Brady W., Patton D.R. and Paxson J., 1985. The development of southwestern riparian gallery forests. In: Riparian ecosystems and their management: reconciling conflicting uses. USDA Forest Service General Technical Report RM-120, Rocky Mountain Forest and Range Experiment Station, Fort Collins, Co, 39–43

Buckman H.O. and Brady N.C., 1969. The Nature and Properties of Soils. The Macmillan Company, New York

Burnett B.N., Meyer G.A. and McFadden L.D., 2000. Aspect-related microclimatic influences on slope forms and processes, northeastern Arizona. Journal of Geophysical Research - Part F - Solid Earth, 113(F3), 2–9

Bussotti F. and Ferretti M., 1998. Air pollution, forest condition and forest decline in southern Europe: An overview. Environmental Pollution, 101, 49–65

Carter N.E.A. and Viles, H.A., 2003. Experimental investigations into the interactions between moisture, rock surface temperatures and an epilithic lichen cover in the bioprotection of limestone. Building and Environment, 38(9-10), 1225–1234

Carter N.E.A. and Viles, H.A., 2005. Bioprotection explored: The story of a little known earth surface process. Geomorphology, 67(3–4), 273–281

Chang X., Wu G. and Guo Q., 2006. Formation of sand-sliding slope and its controlling countermeasure. Highway, 1, 89–91 (in Chinese)

Clinton B.D. and Baker C.R., 2000. Catastrophic windthrow in the southern Appalachians: Characteristics of pits and mounds and initial vegetation responses. Forest Ecology and Management, 126, 51–60

Cole D.N. and Marion J.L., 1988. Recreation impacts in some riparian forests of the eastern United States. Environmental Management, 12, 99–107

Collier M., Webb R.H. and Schmidt J.C., 1996. Dams and rivers. A primer on the downstream effects of dams. U.S. Geological Survey Circular 1126, 1–96

Columbia University, 2000. Columbia Encyclopedia, Columbia University Press, New York

Curry A.M. and Black R., 2002. Structure, sedimentology and evolution of rockfall talus in Mynydd Du, South Wales. Proceedings of the Geologists' Association, 114, 49–64

Diehl T.H., 1997. Drift in channelised streams. In: Management of Landscapes Disturbed by Channel Incision, Wang, S.S.Y., Langendoen, E.J. and Shields, F.D. Eds., University of Mississippi, Oxford, Ms, 139–144

Fetherston K.L., Naiman R.J. and Bilby R.E., 1995. Large woody debris, physical process, and riparian forest development in montane river networks of the Pacific Northwest. Geomorphology, 13, 133–144

Friedman J.M., Osterkamp W.R. and Lewis W.M., 1996a. Channel narrowing and vegetation development following a Great Plains flood. Ecology, 77, 2167–2181

Friedman J.M., Osterkamp W.R. and Lewis W.M., 1996b. The role of vegetation and bed-level fluctuations in the process of channel narrowing. Geomorphology, 14, 341–351

Garcia-Ruiz J.M., Valero-Garces B., et al., 2001. Stratified scree in the central spanish pyrenees: palaeoenvironmental implications. Permafrost and Periglacial Processes, 12(3), 233–242

Germanoski D. and Ritter D.F. 1988. Tributary response to local base level lowering below a dam. Regulated Rivers Research and Management, 2, 11–24

Goldman S.J., Jackson K. and Bursztynske T.A., 1986. Erosion & sediment control handbook. McGraw-Hill Book Company, New York

Gray D.H. and Leiser A.J., 1982. Biotechnicai slope protection and erosion control. Van Nostrand Reinhold, New York

Gregory K.L. and Gurnell A.M., 1988. Vegetation and river channel form and process. In: Biogeomorphology. Viles H.A. (ed.), Basil Blackwell, Oxford, 11–42

Hack J.T. and Goodlett J.C., 1960. Geomorphology and forest ecology of a mountain region in the central Appalachians. U.S. Geological Survey Professional, Pp.347

Halsey D.P., Mitchell D.J. et al., 1998. Influence of climatically induced cycles in physical weathering. Quarterly Journal of Engineering Geology and Hydrogeology, 31, 359–367

Harris S.A. and Prick A., 2000. Conditions of formation of stratified screes, Slims River valley, Yukon Territory: A possible analogue with some deposits from Belgium. Earth Surface Processes and Landforms, 25(5), 463–481

Harvey M.D. and Watson C.C., 1986. Fluvial processes and morphological thresholds in incised channel restoration. Water Resources Bulletin, 22, 359–368

Hetu B., Vansteijn H. et al., 1995. Role of dry grain flows in the formation of a certain type of stratified scree. Permafrost and Periglacial Processes, 6(2), 173–194

Hickin E.J., 1984. Vegetation and river channel dynamics. Canadian Geographer, 28, 111–126

Howard A.D., Fairbridge R.W. and Quinn J.J., 1968. Terraces, fluvial introduction. In: The encyclopaedia of geomorphology. Fairbridge, R.W. (ed.), Reinhold, New York, 1117–1123

Hupp C.R. and Osterkamp W.R., 1985. Bottomland vegetation distribution along Passage Creek, Virginia, in relation to fluvial landforms. Ecology, 66, 670–681

Hupp C.R. and Osterkamp W.R., 1996. Riparian vegetation and fluvial geomorphic processes. Geomorphology, 14, 277–295

Hupp C.R. and Simon A., 1991. Bank accretion and the development of vegetated depositional surfaces along modified alluvial channels. Geomorphology, 4, 111–124

Hupp C.R., 1987. Determination of bank widening and accretion rates and vegetation recovery along modified West Tennessee streams. In: Proceedings of the international symposium on ecological aspects of tree-ring analysis. DOE CONF-8608144, 224–233

Hupp C.R., 1988. Plant ecological aspects of flood geomorphology and paleoflood history. In: Baker V.R., Kochel R.C. and Patton P.C. (ed.), Flood Geomorphology, John Wiley and Sons, New York, 335–356

Hupp C.R., 1992. Riparian vegetation recovery patterns following stream channelisation: A geomorphic perspective. Ecology, 73, 1209–1226

Johnson W.C., Burgess R.L. and Keammerer W.R., 1976. Forest overstory vegetation and environment on the Missouri River floodplain in North Dakota. Ecological Monographs, 46, 59–84

Korner C., 2003. Alpine Plant Life: Functional plant ecology of high mountain ecosystems. Springer Press

Kosmas C., Danalatos N.G. and Gerontidis S.t., 2000. The effect of land parameters on vegetation performance and degree of erosion under Mediterranean conditions. Catena, 40, 3–17

Kosmas C., Danalatos N.G., Poesen J. and Van Wesemael B., 1998. The effect of water vapour adsorption on soil moisture content under Mediterranean climatic conditions. Agricultural Water Management, 36(2), 157–168

Lal R. and Kimble J.M., 1998. Soil conservation for mitigating the greenhouse effect. In: Towards sustainable land use. Catena Verlag GmbH, 185–192

Lee M.R., 2000. Weathering of rocks by lichens: Fragmentation, dissolution and precipitation of minerals in a microbial microcosm. Environmental Mineralogy: Microbial interactions anthropogenic influences. Contaminated Land and Waste Management, 9, 77–107

Li B., 1986. The integrated management of the Anjiagou watershed. Collection of reports of experimental results on soil and water conservation, research institute of Dingxi soil and water conservation, Gansu Province, 20-35 (in Chinese)

Li M. and Zhang, L., 1997. On the function of vegetation on the watershed management of the middle reaches of the Yellow River, Proc. 3rd cross-strait workshop on hydro-science and technology. China Institute of Water Resources and Hydro-Power Research, 793–802 (in Chinese)

Li Z., 1993. On the function of stabilizing slope and erosion control of forest. Sediment Research, No.1 (in Chinese)

Li F.K., Dietrich W.E. and Trush W.J., 1995. Downstream ecological effects of dams; A geomorphic perspective. Bioscience, 45, 183–192

Lull H.W., 1959. Soil compaction on forest and range lands. U.S. Department of Agriculture Miscellaneous Publication 768, Washington, D.C

Ma X.B., Wang Z.Y., Cheng D.S. and Deng J.Q., 2006. Diversity evaluation of riparian vegetation in middle reaches of the East River. Journal of Hydraulic Engineering, 37(3), 348–353 (in Chinese)

Maley J. and Brenac P., 1998. Vegetation dynamics, palaeoenvironments and climatic changes in the forests of western Cameroon during the last 28,000 years. B.P. Review of Palaeobotany and Palynology, 99, 157–187

Matsuoka N., 1990. The rate of bedrock weathering by frost action - Field-measurement and a predictive model. Earth Surface Processes and Landforms, 15(1), 73–90

Matsuoka N., 2008. Frost weathering and rockwall erosion in the southeastern Swiss Alps: Long-term (1994-2006) observations. Geomorphology, 99(1–4), 353–368

Meyer, C.D. 1971. Soil erosion by water on upland areas. In River Mechanics Vol. II, ed. H.W. Shen, pp.27.1±27.5. Privately published, Fort Collins, Colorado.

Miller J.R., Schulz T.T., Hobbs N.T., Wilson K.R., Schrupp D.L. and Baker W.L., 1995. Changes in the landscape structure of a southeastern Wyoming riparian zone following shifts in stream dynamics. Biological Conservation, 72, 371–379

Mills T.R. and Clar M.L., 1976. Erosion and sediment control in surface mining in the eastern U.S. U.S. Environmental Protection Agency. Washington, D.C

Monserud R.A., Denissenko O.V. and Tchebakova N.M., 1993. Comparison of siberan paleovegetation to current and future vegetation under climate change. Climate Research, 3, 143–159

Mulligan M., 1998. Modelling the geomorphologic impact of climatic variability and extreme events in a semi-arid environment. Geomorphology, 24, 59–78

Naiman R.J., Beechie T.J., Benda L.E., Berg D.R., Bisson P.A., MacDonald L.H., O'Connor M.D., Olson P.L. and Steel E.A., 1992. Fundamental elements of ecologically healthy watersheds in the Pacific northwest coastal ecoregion. In: Watershed Management. Springer-Verlag, New York, 127–188

Naylor L.A., Viles H.A., et al., 2002. Biogeomorphology revisited: looking towards the future. Geomorphology, 47(1), 3–14

Nilsson C., Grelsson G., Johansson M., et al., 1989. Patterns of plant species richness along riverbanks. Ecology, 70, 77–84

Nilsson C. and Jansson R., 1995. Floristic differences between riparian corridors of regulated and free-flowing boreal rivers. Regulated Rivers: Research and Management, 11, 55–66

Osterkamp W.R. and Costa J.E., 1987. Changes accompanying an extraordinary flood on a sandbed stream. In: Catastrophic Flooding, Mayer L. and Nash D. (ed.), Allen and Unwin, Boston, 201–224

Pedersen B., 1998. Modeling tree moretality in response to short and long term environmental stresses. Ecological modelling, 105, 347–351

Reader B.J., 1975. Inc., Michigan soil erosion and sedimentation control guidebook. Michigan department of natural resources. Bureau of Water Management, Lansing, MI

Reilly P.W. and Johnson, W.C., 1982. The effects of altered hydrologic regime on tree growth along the Missouri River in North Dakota. Canadian Journal of Botany, 60, 2410–2423

Saas O. and Krautblatter M., 2007. Debris flow-dominated and rockfall-dominated talus slopes: Genetic models derived from GPR measurements. Geomorphology, 86(1–2), 176–192

Schapenseel H.W. and Pfeiffer E.M., 1998. Impacts of possible climate change upon soils, some regional consequences. In: Towards Sustainable Land Use. Catena Verlag GmbH, 194–208

Schumm S.A., 1973. Geomorphic thresholds and complex response of drainage systems. In: Fluvial Geomorphology. Morisawa M. (ed.), State University of New York, Binghamton, 299–310

Schumm S.A., Harvey M.D. and Watson C.C., 1984. Incised channels: morphology, dynamics and control. Water Resources Publications, Littleton, CO

Scott M.L., Friedman J.M. and Auble G.T., 1996. Fluvial processes and the establishment of bottomland trees. Geomorphology, 14, 327–339

Shields F.D., Knight S.S. and Cooper C.M., 1995. Use of biotic integrity to assess physical habitat degradation in warmwater streams. Hydrobiologia, 312(3), 191–208

Shields F.D., Cooper, C.M. and Knight S.S., 1993. Initial habitat response to incised channel rehabilitation. Aquatic Conservation Marine and Freshwater Ecosystems, 3, 93–103

Shields F.D. and Gippel C.J., 1995. Prediction of effects of woody debris removal on flow resistance. Journal of Hydraulic Engineering, 121, 341–354

Shields F.D., Knight S.S. and Cooper C.M., 1994. Effects of channel incision on base flow stream habitats and fishes. Environmental management, 18, 43–57

Shroder J.F., 1980. Dendrogeomorphology: Review and new techniques of tree-ring dating. Progress in Physical Geography, 4, 161–188

Shroder J.F. and Butler D.A., 1987. Tree-ring analysis in the earth sciences. In: Proceedings of the international symposium on ecological aspects of tree-ring analysis. DOE CONF- 8608144, 186–212

Sigafoos R.S., 1964. Botanical evidence of floods and flood-plain deposition. U.S. Geological Survey Professional, 485-A, 1–35

Simon A. and Hupp C.R., 1992. Geomorphic and vegetative recovery processes along modified stream channels of West Tennessee. U.S. Geological Survey Open-File Report, 91–502

Simon A. and Hupp C.R., 1987. Geomorphic and vegetative recovery processes along modified Tennessee streams: An interdisciplinary approach to disturbed fluvial systems. In: Forest Hydrology and Watershed Management. IAHS Publication, 167, 251–262

Simon A., 1989. A model of channel response in disturbed alluvial channels. Earth Surface Processes and Landforms, 14, 11–26

Spitzy A. and Ittekkot V., 1991. Dissolved and particulate organic matter in rivers. In: Ocean Margin Processes in Global Change. Mantoura R.F.C., Martin J.M., Wollast R. (ed.), John Wiley, Chichester, 5–17

Stromberg J.C. and Patten D.T., 1992. Response of Salix lasiolepis to augmented stream flows in the upper Owens River. Madrono, 39, 224–235

Sun H., Shang Y. and Lu Q., 2006. Formative mechanism and control countermeasure of sand-sliding slope. Journal of Natural Disaster, 15(4), 28–32 (in Chinese)

Svirechev Y.M., 1999. Simplest dynamic model of the global vegetation pattern. Ecological Modelling, 124, 131–144

Tang K.L., 2004. Water and soil conservation in China. Science Press, Beijing (in Chinese)

Thorne C.R., 1990. Effects of vegetation on riverbank erosion and stability. In: Vegetation and erosion. Thornes J.B. (ed.), John Wiley and Sons, Chichester, England, 123–144

Thornes J.B., 1985. Environmental systems-patttens, processes and evolution. In: Horizon in physical geography. Gregory K.J. and Clark J., (ed.), Macmillan, 27–46

Turner B.R. and Makhlouf I., 2002. Recent colluvial sedimentation. In: Jordan: fans evolving into sand ramps. Sedimentology, 49(6), 1283–1298

Virginia Soil and Water Conservation Commission (VSWCC), 1980. Virginia erosion and sediment control handbook, Richmond, VA

Wallerstein N., Thorne C.R. and Doyle M.W., 1997. Spatial distribution and impact of large woody debris in northern Mississippi. In: Management of Landscapes Disturbed by Channel Incision, Wang S.S.Y., Langendoen E.J. and Shields F.D. (ed.), University of Mississippi, Oxford, Ms, 145–150

Wang F.X. and Wang Z.Y., 2007. Zoning and management strategies for the Loess Plateau based on vegetation-erosion dynamics. Journal of Tsinghua University (Science and Technology), 47(12), 2119–2122 (in Chinese)

Wang X.D. and Wang Z.Y., 1999. Effect of land use change on runoff and sediment yield. International Journal of Sediment Research, 14(4) 37–44

Wang Z.Y., Cui P. and Wang R.Y., 2009a. Mass movements triggered by the Wenchuan Earthquake and management strategies of quake lakes. International Journal of River Basin Management, 7(1), 1–12

Wang Z.Y., Liu D.D. and Shi W.J., 2009b. Grain erosion induced by the Wenchuan Earthquake and its control. Science of Soil and Water Conservation, 7(6), 1–8 (in Chinese)

Wang Z.Y., Shi W.J. and Liu D.D., 2010. Continual erosion of bared rocks after the Wenchuan Earthquake and control strategies. Journal of Asian Earth Sciences (Accepted)

Wang Z.Y., Wang G.Q. and Gao J., 2003a. A dynamic model of vegetation-erosion process. Journal of Environmental Sciences, 23(1), 98–105 (in Chinese)

Wang Z.Y., Wang G.Q., Li C.Z. and Wang F.X., 2003b. Preliminary study on the vegetation - erosion dynamics and its application. Sciencia Sinica, Series D, 8, 1–11

Wang C., Que Y., Li X. and Zhang X., 2007a. Movement characteristics and dynamical numerical analysis of sand-sliding slope composed by granular clastics: Part II of sand-sliding slope series. Rock and Soil Mechanics 28(2), 219–223 (in Chinese)

Wang C., Que Y., Xu J. and Li X., 2007b. Equation of motion and soil pressure for sand-sliding slope composed by granular clast: Part III of sand-sliding slope series. Rock and Soil Mechanics 28(7), 1299–1303 (in Chinese)

Wang C., Zhang X., Que Y. and He S., 2007c. Formation and basic characteristics of sand-sliding clastslope composed of granular clasts: Part I of sand-sliding slope series. Rock and Soil Mechanics 28(1), 29–35 (in Chinese)

White C.A. and Franks A.L., 1978. Demonstration of erosion and sediment control technology, lake tahoe region of california, final report, california state water resources control board. U.S. Environmental Protection agency, Cincinnati

Wikepedia, 2009. http://en.wikipedia.org/wiki/Erosion

Williams G.P. and Wolman M.G., 1984. Downstream effects of dams on alluvial rivers. U.S. Geological Survey Professional Paper, Pp. 1286

Wolman M.G. and Schick A.P., 1967. Effects of construction on fluvial sediment, urban and suburban areas of Maryland. Water Resources Research, 3, 451–464

Xu J., Wang C., He S., Zhang X. and Zhou I., 2007. Sheet pile wall's techniques for stabilization of 610 sand-sliding slope composed of granular clast. Research of Soil and Water Conservation, 14(3), 315–317 (in Chinese)

Ye Z.O., 1986. Investigation and analysis of erosion control in the Anjiagou watershed. Collection of reports of experimental results on soil and water conservation. Research Institute of Dingxi Soil and Water Conservation. Gansu Province, 8–16 (in Chinese)

Zhang F., Li D.G. and Wan T.C., 1986. Analysis on the experiments integrated management of the Anjiagou Watershed and the effects on soil erosion reduction. Collection of of reports of experimental results on soil and water conservation. Research Iinstitute of Dingxi Soil and Water Conservation. Gansu Province, 44–53 (in Chinese)

Zimmermann R.C. and Thom B.G., 1982. Physiographic plant geography. Progress in Physical Geography, 6, 45–59

Zimmermann R.C., 1969. Plant ecology of an arid basin, Tres Alamos-Redington area, southeastern Arizona. U.S. Geological Survey Professional, 485-D

3   Mountain Rivers and Incised Channels

Abstract

An incised river is defined as a river that is experiencing bed-level lowering. From the viewpoint of geomorphological process, mountain rivers either were or are incised rivers. Large rivers may be incised rivers in the upper reaches, but fluvial rivers in the lower reaches. The development of channel incision in mountainous areas depends on the rainfall, watershed vegetation, and soil and rock compositions. Incision may cause landslides, debris flows, and riverbed scour and in conjunction with bank erosion, provides sediment to the flow. A step-pool system is a geomorphologic phenomenon occurring in high-gradient mountain streams with alternating steps and pools. Cobbles and boulders generally compose the steps, which alternate with finer sediments in pools to produce a repetitive, staircase like longitudinal profile in the stream channel. The tight interlocking of particles in steps gives them an inherent stability that only extreme floods are likely to disturb. Step-pool system maximizes the resistance, and, thus, controls riverbed incision. A bedrock channel has bedrock exposed along the channel bed or walls for at least approximately half its length, or has bedrock limits to the magnitude and location of bed scour and bank erosion during floods. Bedrock channels most commonly occur in regions of high topographic relief. Relief may be a product of recent tectonic uplift, as in the Himalayan Mountains of central Asia. The exposed bedrock implies that the channels may be particularly sediment-starved during floods and subjects to long term incision. The causes and evolution process of incised rivers and control strategies of channel bed incision are also discussed in this chapter.

Key words

Mountain rivers, Step-pool system, Riverbed incision, Bedrock channel, Incision control strategies

3.1   Incised Rivers

3.1.1   Riverbed Incision

At the most fundamental level, without incision there is no channel. In a broad sense, therefore, one can consider channel incision as a requirement of denudation, drainage-network development, and landscape evolution (Darby and Simon, 1999). Channel incision has been and is a major concern of river managers because it disrupts transportation, destroys agricultural land, threatens adjacent structures, drastically alters environmental conditions, and produces sediment that causes further problems downstream. Therefore, the causes of channel incision have been a topic of great interest because a better understanding of the phenomenon could lead to prevention.

The most dramatic channel incision occurs on the east margin of the Qinghai-Tibet Plateau. Geologically, the Indian Plate moves northward at a rate of 5 cm/yr and collides with the Eurasian Plate, resulting in the uplift of the Himalaya mountains and the Qinghai-Tibet Plateau (Wikipedia, 2011). The Qinghai-Tibet Plateau has become the highest plateau in the world and is referred to as the third pole of the earth. Uplift of the plateau resulted in accelerated fluvial incision because of the remarkable increase in stream bed slope at its margin. The fluvial incision into the plateau margin in response to tectonic motion resulted in isolating remnants of the original plateau surface. These remnants of the plateau surface can be used as reference surfaces against which to evaluate the impact of lateral erosion since uplift. The high loads of sediment carried by the tributary streams of the Yellow, Yangtze, and Lancang rivers on the plateau indicate rapid rates of denudation in the catchments.

Rapid fluvial incision into bedrock has been interpreted to reflect a tectonic uplift of similar magnitude,

thereby sustaining topographic equilibrium. In uplifting mountain belts, an end-member scenario can be formulated in which the rate of bedrock uplift is matched by the rate of stream incision and valley lowering (Hovius and Stark, 2006). The slopes steepen until topographic elements become unstable and collapse, producing rock falls, avalanches, and landslides. Tectonic uplift has been found to be responsible for the abandonment of valleys, formation of deep and incised river valleys, highly irregular longitudinal profiles of channels, and the varying number and tilting of terraces. Among these features, deep valleys formed by the incision of rivers with high flow velocity are a prominent characteristic of active, uplifting mountain areas. On a large scale, the ridge-valley landscape of the entire Qinghai-Tibet Plateau was formed by the mechanism of intensive incision.

The continuous rising of the Qinghai-Tibet Plateau has resulted in steep slopes and several active faults including the Longmenshan Fault where a great earthquake, known as the Wenchuan Earthquake, occurred on May 12, 2008. River-bed incision has dominated the fluvial process in the area. The frequent landslides on threshold hill-slopes is one means of relief adjustment to fluvial bedrock incision. Besides the rate of rock uplift and incision intensity, the characteristics of the underlying rock are another controlling factor. Limestone usually has great permeability, thus allowing rainfall to infiltrate to the subsurface and reducing incisions on the surface (Hovius and Stark, 2006). Rocks with lower permeability, but vulnerable to weathering, usually are more prone to mass wasting; for example, the granite in the lower Minjiang River. Observations have revealed that steady incision during low and intermediate flow conditions leads to channel bed lowering while significant channel widening occurs during big floods. Crucially, such floods help transmit the effect of the accumulated thalweg lowering to adjacent hill slopes. Deep landscape dissection has produced high-relief, narrow river gorges, and threshold hill-slopes that frequently experience large landslides, making the entire region highly susceptible to quake lake formation. The quake lakes and their management play an important role in the morphological process and reclamation of the land in the earthquake area.

Of course, channel incision occurs mainly in mountainous rivers. However, incision may also occur in channels of relatively gentle slope. Because of dense population and infrastructure channel incision in an in habited plane area is more disastrous, although the incision is in much smaller scale than that on the Qinghai-Tibet Plateau margin. For example, rapid urbanization and the resulting increase in peak flows from a watershed can result in substantial channel incision in urban areas threatening homes, roads, and other infrastructure, serious incision problems have resulted in the bluffs near Lake Michigan in the Chicago and Milwaukee areas in the U.S. Release of clear water from a reservoir also may cause incision of the downstream reaches, and channelization of a river may cause continuous scour of the channel bed (Wang, 1999). The Sanmenxia Reservoir began filling with water in 1960 and released clear water beginning in September 1960. A 400 km long reach was scoured when the reservoir released water at a rate of 1,000 m^3/s and an 800 km reach along the riverbed was scoured when the released discharge was over 2,000 m^3/s (Yang et al., 1994). From September 1960 to October 1964, the released clear water from the reservoir scoured 2 billion tons of sediment from the bed of the lower Yellow River. The incision of the riverbed endangered bridge piers and exposed oil pipelines, which were buried beneath the riverbed. The Dashi River is located to the north of Qinhuangdao, with bed sediment mainly composed of sand and gravel. An oil pipeline from the Daqing oil field to Qinhuangdao crossed the river. A 1,126 m long pipe section was buried 2 m beneath the bed. A reservoir with a storage capacity of 70 million m^3 was built 3 km upstream of the river-pipeline crossing. The reservoir released a discharge of 4,250 m^3/s, equal to the 100-year flood, in the summer of 1984. The riverbed was seriously scoured and the oil pipe was exposed to the flow and was broken. A large amount of oil was discharged into the river, which resulted in serious environmental pollution.

The middle reaches of the Mississippi River were shallow and unstable. American engineers began to

train the river by the end of the 19th century. Then the river was channelized by dykes and groins and the main channel of the river was scoured 2 m (Stevens et al., 1975). The Rhine River was channelized by German engineers in the 19th century. It has become a human-controlled straight waterway. Sediment was trapped by dams and weirs in the upstream reaches and tributaries. Consequently, flood flow scoured the riverbed. The ground water table in the zone by the river was then reduced by 1-2 m and the navigation conditions of the river channel were worsened. In order to prevent channel bed incision, German engineers have had to feed gravel to the river at a rate about 170,000 t/yr since 1978 and the strategy has proved successful (Kuhl, 1992). Incision control strategies will be discussed in detail in Section 4.8.

Table 3.1 lists the incised channels on the basis of size and location. Rills are small channels that form on steep slopes (Fig. 3.1(a)). They are ephemeral because they can be obliterated seasonally by frost action or by the ploughing of fields. They are of little concern except that they increase stream turbidity, and they can deepen and become permanent gullies. Gullies are incised channels that form where there was no existing channel. They form on valley sides (Fig. 3.1(b)) and on valley floors. Entrenched streams are existing channels that have become incised. Figure 3.1(c) shows a stream in the upper Yangtze River basin in Sichuan Province, which is developing into an entrenched stream in a process of channel incision. Composite incised channels are composed of reaches that are gullies, as defined above, and reaches that are entrenched streams. Depending upon the design and construction, a channelized stream can also be a composite incised channel. Figure 3.1(d) shows the Grand Canyon of the Colorado River, U.S.. It is a composite incised channel, showing the different varieties of valley-floor gullies. Scarps are formed by erosion. Headcut occurs in the tributary gullies. The incision of the valley floor forms terraces. Rill erosion is still occurring on the floor and the rills will eventually develop into gullies and integrate into the drainage network.

Table 3.1   Incised channels in different scales (based on Schumm et al., 1984)

Incised channels	Notes
Rill	Very small (centimeters) ephemeral channel on steep slopes
Gully	A relatively deep (meters) incised channel that formed where there was no pre-existing channel. There are valley-side gullies and valley-floor gullies which can be continuous or discontinuous
Entrenched stream	Incision of an existing channel produces a deep unstable channel such as a mountain stream experiencing continuous incision.
Composite incised river	A complex river system with incised main stem river and tributary channels (the middle reaches of the Yellow River for example)

Incised streams are disturbed ecosystems. Although Brookes (1988) refers to the effects of channelized streams on stream ecology, the same can be said for incised stream systems in general:"...habitat diversity and niche potential are reduced, and, the quality and functions of the species occupying the system are changed."

Sediment produced from incised channel systems impacts local and downstream water quality. Populations of fish and benthic macro-invertebrates (a measure of water quality) are severely impacted in incised channels (Brookes, 1988). Mobile, unstable streambeds destroy spawning habitats and pool-riffle sequences. Bank failures result in loss of riparian vegetation cover, higher water temperatures, and increased turbidity. Changes in bed-material composition, or complete burial of gravel substrates by aggradation, also cause destruction of aquatic habitat. Because the cover provided by riparian vegetation is lost by mass failure of channel banks, populations of mammals and birds are also reduced along incised stream corridors (Carothers and Johnson, 1975; Possardt and Dodge, 1978; Barclay, 1980).

Channel incision may cause many problems in navigation. Lowering of local ground water tables as a result of incision can also have far-reaching effects on floodplain and wetland flora and fauna.
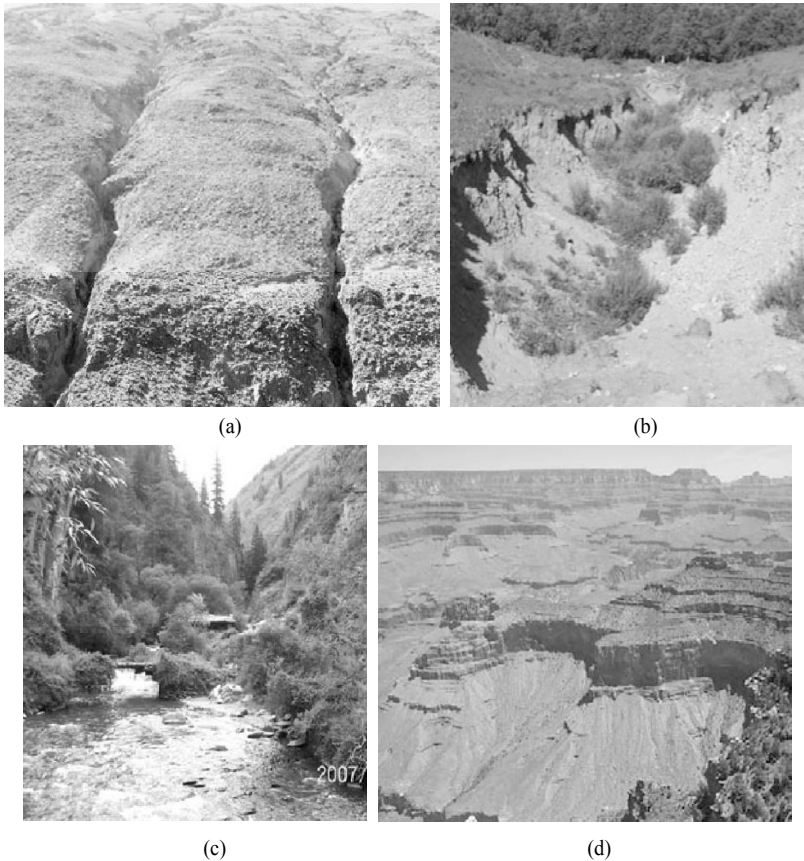
Fig. 3.1 (a) Rills developed on slope by erosion on the bank slope of the Yalutsangbu River; (b) A gully developed from rills in the Yongding River basin; (c) A stream in the upper Yangtze River basin in Sichuan Province developing into an entrenched stream in a process of channel incision; (d) The Grand Canyon of the Colorado River, U.S. is a composite incised channel (See color figure at the end of this book)

Incised channel systems pose particular challenges to engineers, managers, and planners because they are extremely dynamic. Since incised channels convey flows that are even more erosive than the same flow within a non-incised channel, river crossings and other in-stream structures must be able to cope with the maximum amount of morphological change that is likely to occur during the design life of the structure. It is also essential to investigate the effects that a structure is likely to have on channel processes. For example, various types of grade-control structures have been successfully used to arrest the upstream propagation of knickpoints and ensuing degradation. It has been found, however, that if the structure ponds water as a dam, resulting in sediment deposition upstream from the structure, a new wave of degradation is induced by clear-water flows downstream (Simon and Darby, 1997c). In alluvial reaches that are actively widening, maintenance of cross-section shapes at bridges is often counterproductive. The narrower section at the bridge can cause backwater effects during high flows, resulting in a hydraulic drop through the bridge opening and the development of enormous scour holes downstream. These scour

holes ultimately migrate back upstream through the bridge opening, posing a threat to the stability of the bridge and threatening public safety.

Trees and tree branches delivered to incised channels by bank failures often become trapped on the upstream sides of bridge piers and abutments. Accumulation results in trapping of additional debris and the redirection of flows. Secondary flows result in scour around piers and abutments, undercutting of bank toes, and slab failures. Large woody debris and its effects have been cited as a cause for bridge failures in incised channels (Robbins and Simon, 1983; Melville and Dongol, 1992; Wallerstein and Thorne, 1996; Hupp, 1997). On the other hand, large woody debris may mitigate the channel incision by creating high resistance and trapping sediment. Figure 3.2 shows large woody debris deflecting the flow in a tributary stream of the Yalong River in Sichuan, China, which results in sedimentation mitigation of channel incision.

Fig. 3.2   Large woody debris mitigates incision in a tributary stream of the Yalong River in Sichuan

In field investigations the diagnostic feature of incised rivers is the "V"-shape channel. If the lower banks have higher slope than upper banks the river experienced accelerating incision in the past decades and is of particular danger of bank failures or landslides. The banks of incised rivers are mostly at the critical slope, which means that a slight increase in bank slope may cause bank failures or even landslides. On incised rivers the bank slope may be higher than 30°. In some cases it may be as high as 45°. Lithologic characters are the most important factor for the bank slopes. Limestone, granite and sandstone support high slopes but shale, antigorite and phyllite can only sustain low slopes. Poor vegetation is associated with reduced slope. Figure 3.3(a) shows the incised Liwu River in Taiwan, China with "V" shape valley. The bank slope is so steep and unstable that rainstorms often cause bank failures and landslides. Because bank failures bring a lot of sediment into the river the sediment concentration in the river is quite high. Figure 3.3(b) shows a bank failure due to incision on a river in Sichuan.

3.1.2   Causes of Incision

The causes of channel incision are numerous and they can be grouped into six categories (Table 3.2) that at least partly reflect the different time and space scales at which formative processes operate (Darby and Simon, 1999). Geologic and geomorphic causes may require many years to develop a response, whereas climatic and hydrologic variability, animal grazing, and human activities can have a more immediate impact. For example, a wetter climate (C2) will increase discharge (D1), and increased rainfall intensity (C3) will increase peak discharge (D2). Also, there is feedback from human and animal activities to hydrologic controls. For example, human activities, 1, 3, 4, 5, 13, 14, and 15 will modify water discharge and sediment loads.

Fig. 3.3 (a) The upper reaches of the Liwu River in Taiwan, China; (b) Bank failure due to incision on a small stream in Sichuan (See color figure at the end of this book)

Table 3.2 Causes of incised channels (after Darby and Simon, 1999)

Category	Causes	Studies
A. Geologic	A1. Uplift	Burnett and Schumm (1983), Wang et al. (2009)
	A2. Subsidence	Ouchi (1985)
	A3. Faulting	Keller and Pinter (1996), Mayer (1985), Ouimet et al. (2007)
	A4. Lateral tilt	Reid (1992)
B. Geomorphologic	B1. Stream capture	Shepherd (1979), Galay (1983)
	B2. Base-level lowering	Begin et al. (1980)
	B3. Meander cutoffs	Winkley (1994), Love (1992)
	B4. Avulsion	Kesel and Yodis (1992), Schumm et al. (1996)
	B5. Lateral channel shift	LaMarche (1966), Galay (1983)
	B6. Cliff retreat	Schumm and Phillips (1986)
	B7. Sediment storage (increased gradient)	Patton and Schumm (1975), Trimble (1974), Mead et al. (1990), James (1991), Vandeaele et al. (1996)
	B8. Mass movement	Martinson (1986), Rodolfo (1989), Ohmori (1992)
	B9. Groundwater sapping	Higgins (1990), Jones (1997)
C. Climatic	C1. Drier	Knox (1983), Graf (1983), Hall (1990)
	C2. Wetter	Knox (1983), Graf (1983), Bull (1991)
	C3. Increased intensity	Knox (1983), Balling and Wells (1990)
D. Hydrologic	D1. Increased discharge	Burkard and Kostachuk (1995)
	D2. Increased peak discharge	Macklin et al. (1992)
	D3. Decreased sediment load	Lane (1955), James (1991)
E. Animals	E1. Grazing	Alford (1982), Graf (1983), Prosser and Slade (1994)
	E2. Tracking	Trimble and Mendel (1995)
F. Humans	F1. Dam construction	Williams and Wolman (1984)
	F2. Sediment diversion	Galay (1983)
	F3. Flow diversion	Maddock (1960)
	F4. Urbanization	Morisawa and LaFlure (1979)
	F5. Dam removal, failure	Galay (1983)
	F6. Lowering lake levels	Born and Ritter (1970), Galay (1983)
	F7. Meander cutoff	Lagasse (1986), Winkley (1994)
	F8. Underground mining	Goudie (1982)
	F9. Groundwater and petroleum withdrawal	Lofgren (1969), Goudie (1982), Prokopovich (1983)
	F10. Sand and gravel mining	Harvey and Schumm (1987)
	F11. Dredging	Lagasse (1986)
	F12. Roads, trails, ditches	Burkard and Kostachuk (1995), Gellis (1996)
	F13. Channelization	Schumm el al. (1984), Simon (1994)
	F14. Deforestation	Macklin et al. (1992)
	F15. Fire	Laird and Harvey (1986), Heede et al. (1988)

Table 3.3 uses the reference codes of Table 3.2 to categorize the various causes by their effect and by the type of incision, respectively, which is either upstream or downstream progressing or both (Galay, 1983). The most common example of downstream progressing incision occurs downstream from large dams. One can also group the causes into those that increase energy and those that decrease the resistance of the surface or channel. For example, anything that causes steepening of the channel increases stream power and a stream's ability to incise. All of the geologic, geomorphic, climatic, and hydrologic causes with the exception of B8 and B9 fall into the category of increased energy. In contrast, animal causes reduce resistance by removing vegetation and channelizing flow. The human causes combine both effects with the effect of increasing energy by increasing or concentrating flow (F3, F4, F12, F13, F14, F15) by increasing gradient (F5, F6, F7, F8, F10, F11), and/or by decreasing sediment loads (F1, F2, F10, F11). A single cause can produce either a gully or an entrenched stream or both, and the effect of the incision can either propagate upstream or downstream or both.

Table 3.3   Effects and types of incision

Formation of a new channel (gully)	Deepening of existing channel (entrenched channel)	Downstream progressing	Upstream progressing
A1, A2, A3, A4	A1, A2, A3		A1, A2, A3, A4
B2, B4, B6, B7, B8, B9	B1, B2, B3, B5, B6, B8	B4, B8	B1, B2, B3, B4, B5, B6, B7, B8, B9
C1, C2, C3	C2, C3	C1, C2, C3	C1, C2, C3
D1, D2, D3	D1, D2, D3	D1, D2, D3	D1, D2, D3
E1, E2			E1, E2
F3, F4, F8, F9, F12, F14, F15, F16	F1, F2, F3, F4, F5, F6, F7, F8, F9, F10, F11, F13, F14, F15	F1, F2, F3, F4, F10, F11, F12, F14, F15	F3, F4, F5, F6, F7, F8, F9, F10, F11, F12, F13, F14, F15

3.1.2.1   Geological Causes

Uplift, subsidence, and faulting all modify the slope of the valley floor and channel gradient. For example, channel incision should occur on the downstream steeper part of uplift and at the upstream steeper side of subsidence and where a stream crosses from the up-thrown to the down-dropped portions of a fault. If the uplift is a dome, gullies can form a radiating pattern. Lateral tilt of a valley floor can cause avulsion and the development of a new channel, and lateral fault displacement can also cause stream incision and gullies.

The 921 earthquake in Taiwan (September 21, 1999) was caused by tectonic motion. The tectonic motion generated a huge fault, and caused lateral tilt of river valleys. Figure 3.4 shows that the left side of a river in Taiwan, has risen up and the right side of the river has settled down by 8 m due to the tectonic motion. Erosion and incision of the channel bed was induced thereafter. The magnitude of the resulting incision depends on the amount of deformation and the ability of a channel to adjust to the altered slope by increasing its sinuosity (Schumm, 1985).

According to the British Geological Survey, the Indian Plate moves northward at a rate of 5 cm/year (Chen and Gavin, 2008). Its collision with the Eurasian Plate has resulted in the uplift of the Himalaya and the Qinghai–Tibetan plateau, and associated earthquake activity. The rate of horizontal movement is about 5 cm/yr at Himalaya, 4 cm/yr in the source area of the Lancang and Yangtze Rivers, to about 2 cm/yr at the Qilian Mountain. As a result the Himalaya rises at a rate of 21 mm/yr while the Qilian Mountains rise at a rate of 5 mm/yr. The Sichuan basin, located to the east of the plateau, is stationary. This pronounced variability in the rates of horizontal movement has resulted in many active faults and river bed incision of almost all rivers on the east margin of the plateau.
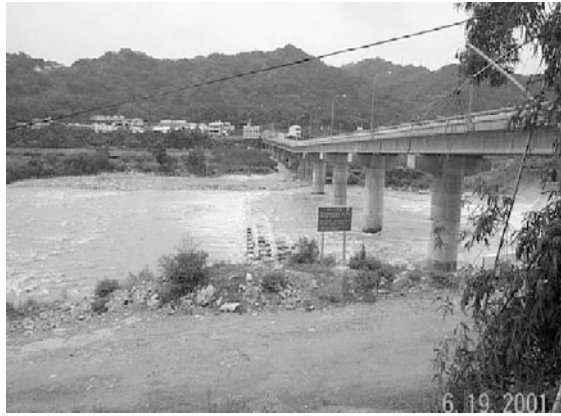
Fig. 3.4 A broken bridge illustrating the lateral tilt of the river valleys caused by the 921 earthquake in Taiwan (September 21, 1999)

The streams in the area are incised channels and the bank slopes are so steep that slope failures readily occur during rainstorm and earthquake events. The rising plateau has increased the gradient of rivers and caused dramatic changes to stream networks. In general the rivers flows from northwest to southeast are strengthened and extended but the rivers in an opposite direction are reduced in length or eliminated. Asymmetry of stream networks is then evident in watersheds on the margin of the plateau. Figure 3.5 shows the stream network of the Xihanshui River (the upstream area of the Jialing River) on the northeastern margin of the plateau. All large tributaries join the river from the northwestern side, creating a very asymmetrical stream network. More than 90% of the drainage area is on the western side of the river. This situation is repeated for many stream networks at the margins of the Qinghai-Tibetan Plateau.
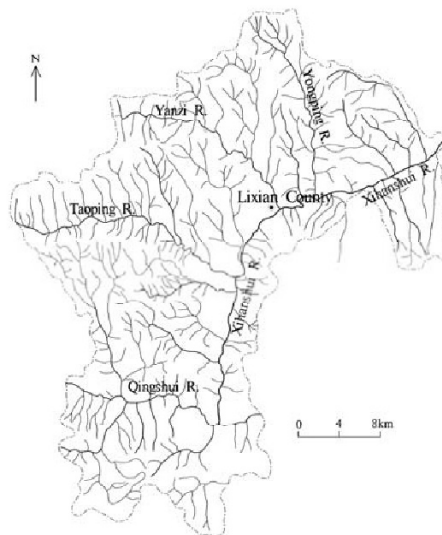
Fig. 3.5 Asymmetrical distribution of tributaries and drainage area of the Xihanshui River

3.1.2.2 Geomorphic Causes

Geomorphic causes of incision for the most part involve an increase in gradient. For example, stream capture, base-level lowering, meander cutoffs, avulsion, cliff retreat, sediment storage, and lateral shift of

a main channel can cause a local steepening of the channel gradient and incision. It has been demonstrated, for example, that sediment deposition and storage in valleys and on alluvial fans eventually leads to steeper gradients and the formation of discontinuous gullies (Fig. 3.1) and alluvial-fan trenches (Schumm et al., 1984), when a threshold of slope stability or stream power is exceeded. Cliff retreat and lateral channel shift can shorten and, therefore, steepen the affected channels.

Other processes, such as mass movement, can produce incision. Mudflows and debris flows are capable of erosion and channel enlargement, and when a landslide delivers large amounts of sediment to a valley floor, this deposit will eventually be eroded and become incised by the existing stream. In addition, where groundwater emerges from a sloping surface, a channel can be produced that extends back toward a drainage divide or to the source of the groundwater.

3.1.2.3 Climatic and Hydrologic Causes

Climatic and hydrologic causes of incision are closely related, and perhaps they should not be separated in Table 3.2. Nevertheless, it is possible to think of a climate change that alters vegetation. A change to a drier climate can reduce vegetation cover and produce higher sediment loads and higher peak discharges. A change to a wetter climate can increase vegetative cover, which reduces sediment loads and increases mean annual runoff. These climatic changes produce hydrologic changes that cause incision. Climatic fluctuations also may produce hydrologic responses, such as major floods, periods of increased discharge, and changes in sediment loads, without greatly affecting vegetative cover.

3.1.2.4 Human and Animal Causes

Human activity of a variety of types is known to cause channel incision. These causes can be grouped into four effects as follows: decreased sediment loads, increased annual discharge and peak discharge, flow concentration, and increased channel gradient. Decreased sediment loads can be caused by dam construction, sediment mining, urbanization, diversion of sediment into another channel such as a canal, and gravel mining and dredging. Flow can be concentrated with the effect of increasing stream power by gravel mining and dredging, urbanization, roads, trails, ditches, channelization, and by flow constriction by dikes. Gradient can be increased by dam removal, lowering of water levels in lakes and reservoirs, meander cutoffs, mining, withdrawal of fluids and hydro-compaction, gravel mining, dredging, and channelization.

Figure 3.6(a) shows sediment mining from the Lishui River in Hunan Province, China. Sediment demand for building materials has been increasing due to economic development and urbanization in China. There are no laws to control sediment mining from rivers. Consequently, the total amount of sediment mining in many places is much more than the annual coarse sediment load (bed load). As a result the channel bed has incised down by several to twenty meters.

Channelization has become an important cause of bed and bank erosion. Figure 3.6(b) shows that channelization of the Charlooz River in Iran causing channel incision, which endangered the banks and a nearby road. The banks are hardened and smoothened, therefore, high velocity current may flow near the banks and cause erosion of the bank toe. The river channel is narrowed and straightened because of urban construction. The flow velocity is enhanced, which caused river bed incision and bank collapse, as shown in the figure.

It has been argued long that overgrazing has produced the great arroyos of the southwestern U.S. Whether or not this is true, weakening of vegetation cover by grazing can produce channel incision. Tracking of animals also decreases infiltration rates, which in turn increases runoff both on hill slopes and in the trails.

(a)

(b)
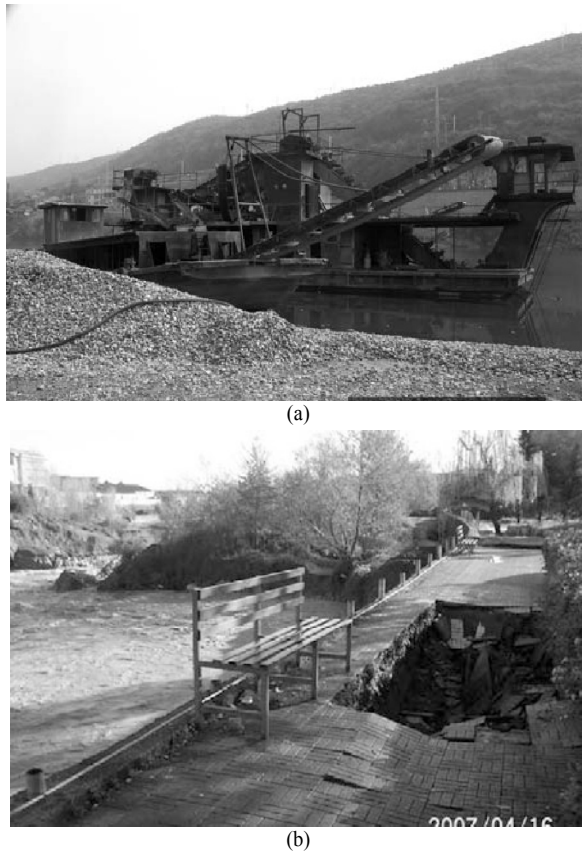
Fig. 3.6 (a) Sediment mining from the Lishui River in Hunan Province, China; (b) Channelization of the Charlooz River in Iran causing channel incision, which endangered the banks and a nearby road

3.1.3   Evolution process of Incised River

3.1.3.1   Channel Incision

The incision of the river channel indicates a period of vertical instability or disequilibrium by degradation. Lane (1955) suggested degradation occurs if

$$Qs > kQ_s D_{50} \tag{3.1}$$

where Q is the channel-forming discharge ($m^3 s^{-1}$), s is the channel gradient, k is a coefficient, Q_s is the unit bed-material discharge ($m^2 s^{-1}$), and D_{50} is the median grain size of the bed material (m). Figure 3.7 shows the factors affecting channel degradation or aggradation and their dynamic relations.

The bankfull discharge of non-incised, stable streams is generally accepted to be in the range of the 1-2 year recurrence interval flow (Wolman and Leopold, 1957; Williams, 1978). As degradation progresses, discharge capacity increases and the channel is able to pass progressively larger volumes of water within its enlarged cross section. The frequency of floodplain inundation is, therefore, reduced to less than the 1 to 2-year recurrence interval and the floodplain becomes a terrace. This has important implications for the geomorphic effectiveness of moderate and high recurrence-interval flows, which would have previously spilled out over the floodplain, dissipating flow energy. In an incised system, such flows are constrained within the deeper, narrower cross section and exert higher shear stresses, transporting

more sediment than the same flow (same recurrence-interval flow) prior to degradation (Simon, 1992; Simon and Darby, 1997a). The dominant discharge, defined by magnitude-frequency analysis of long-term sediment-discharge rates (Wolman and Miller, 1960; Andrews, 1980; Thorne et al., 1993; Andrews and Nankervis, 1995) may, therefore, be quite distinct in incised versus non-incised rivers. This has serious implications for morphological analyses and design tools which are based on regime relations (Leopold and Maddock, 1953; Hey and Thorne, 1986) or other methods, which rely on specification of the bankfull or dominant discharge (Rosgen, 1996). Particular care must, therefore, be exercised in identifying the level of the bankfull discharge, and determining whether the discharge at that level actually represents the dominant flow.
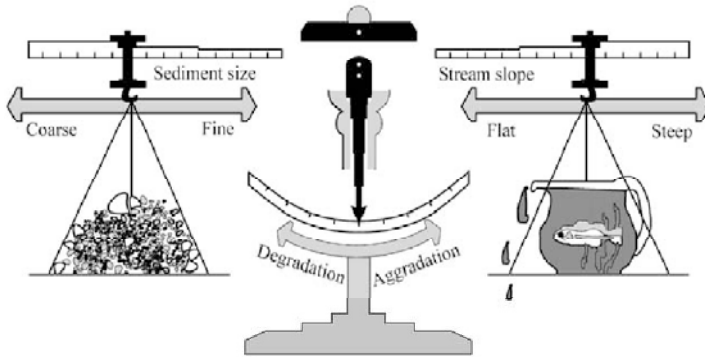
Fig. 3.7 Factors affecting channel degradation or aggradation. The channel incision (or siltation) is determined by the stream's energy, slope, and flow of water in balance with the size and quality of the sediment particles (after FISRWG, 1997)

3.1.3.2 Bank Erosion

An important characteristic of incised alluvial channels is the role of bank erosion and channel-width adjustment. Depending on the strength of the bank materials, increases of bank heights and angles resulting from incision may be sufficient to trigger mass movement under gravity (Daniels, 1960; Thorne et al., 1981; Little et al., 1982; Schumm et al., 1984; Simon and Hupp, 1986; Simon, 1989, 1992; Darby and Thorne, 1996; Simon and Darby, 1997a). A common feature of the response of incised channels is, therefore, the sudden switching of the locus of channel instability from deepening to widening. Rates of channel widening in incised channels range over several orders of magnitude; from less than 0.01 m yr^{-1} in bedrock canyons, to less than 1.0 m yr^{-1} in cohesive stream bank materials, to as much as 100 m yr^{-1} in non-cohesive stream bank materials.

The bank heights of incised channels are greater than those prior to incision, and the upper bank surfaces are wetted less frequently by rises in stage. Bank failure may occur during the receding limb of a flood as shown in Fig. 3.8. The onset of widening by mass movement processes results in distinguishable bank morphologies (Simon, 1989), which in turn depend on the type and mode of bank failure. Planar failures are generally associated with very steep banks and with the formation of tension cracks, which develop at the ground surface and extend downward. Rotational failures occur along the highest banks with shallower angles and tend to occur later in the adjustment sequence. Slab failures are characterized by the toppling of an upper bank mass after undercutting of the lower part of the bank by fluvial action (Thorne, 1990) or by pore pressure induced pop-out failures (Bradford and Piest, 1980; Simon and Darby, 1997b). Figure 3.9 shows a bank failure due to bed incision of the Liujia Ravine in Lixian county of Gansu Province. A recent flood scoured the river bed by about one meter and the banks became very

unstable and the bank failure occurred.
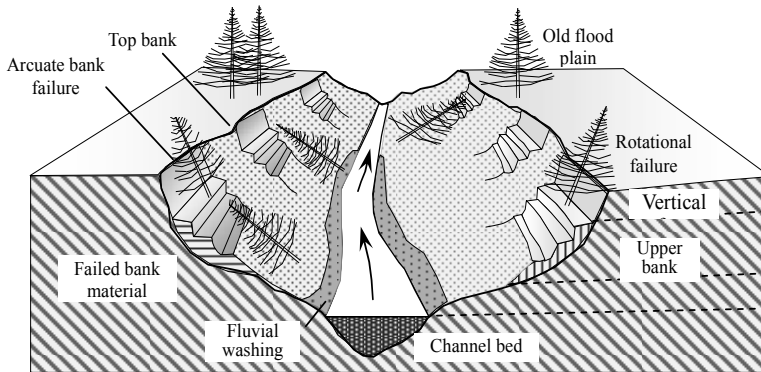
Fig. 3.8　Schematic illustration showing the morphological features of a typical incised river channel (after Darby and Simon, 1999)

Fig. 3.9　Bank failure during the process of stream bed incision of the Liujia Gully in Lixian, Gansu (See color figure at the end of this book)

Channel widening is an extremely important process in accelerating the recovery of incised streams because it acts to reduce flow depth, available shear stress, and sediment-transport capacity for a given discharge. Together with the input of volumes of hydraulically controlled sediment from eroding banks, these processes act as a feedback mechanism to reduce the rate of bed degradation. This helps to promote establishment of a more stable longitudinal profile through aggradation downstream. Predictive analyses, such as numerical models of incised channels, that ignore channel widening run the serious risk of biasing estimates of future channel changes or stable morphologies (Darby and Thornes 1996; Simon and Darby, 1997a).

3.1.3.3　Evolution of Incised Channels
In general, the morphological process of incised rivers goes through four stages as shown in Fig. 3.10(a) Rapid degradation of the channel bed ensues as the channel begins to adjust after tectonic motion. The valley takes a narrow "V" form. There is little space for humans to reclaim the hill slopes; (b) Degradation

continues and the river valley widens. Because degradation flattens the channel gradient, the available stream power for a given discharge reduces with time. Concurrently, bank heights increase and bank angles steepen, which induces bank failures and successive landslides. Especially during earthquakes, many rockfalls, avalanches, and landslides occur, causing the valley to broaden laterally. The valley takes a broad "V" form in this stage. Because the valley becomes wider and the bank slopes gentler, humans can reclaim the hill slopes, build houses, plant crops, and construct roads and highways; (c) As degradation migrates further upstream, aggradation becomes the dominant trend in previously degraded sites, because the flatter gradient cannot transport the increased sediment loads emanating from upstream. The river bed becomes flat and the valley takes a "U" form. The valley becomes safer for humans to reclaim and live in than in Stage 2; (d) Attainment of a new dynamic equilibrium takes place through ① bank widening and the consequent flattening of bank slopes, and knickpoint establishment through landslide occurrence, quake lake formation, or in some cases dam construction by humans, ② sediment deposition and bed structure development, and the establishment and proliferation of riparian vegetation that adds roughness elements, enhances bank accretion, and reduces the stream power for a given discharge, and ③ flow energy consumption at knickpoints and bed-gradient reduction in the reaches upstream of the knickpoints.

Figure 3.11(a) shows an example of a tributary of the Minjiang River in stage 1. In this stage, deeply incising rivers often create a landform called an inner gorge at the interface between hill slopes and river channels. An inner gorge is characterized by a convex break in the hill-slope gradient, and lined by hill-slope toes significantly steeper than those of upper valley flanks. Thus, the hill slope is divided into the upper slope and the inner gorge wall (Korup., 2006). Figure 3.11(b) shows an example of the Dajinchuan River in Sichuan in stage 2. Figure 3.11(c) shows an example of the Kuaihe River in the upper Yangtze River basin in stage 3. Figure 3.11(d) shows an example of an upstream reach of the Dahu River in Sichuan in stage 4. The valley is wide and flat. Several knickpoints consume energy and the gradient between the knickpoints is low. The valley takes a broad "U" form, which is suitable for humans to live and facilitates the best stream ecology.
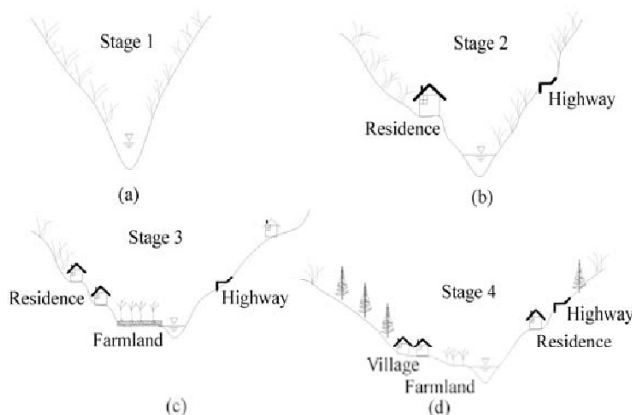
Fig. 3.10   Four stages of the morphological process of incised rivers.（a）Rapid degradation stage showing a narrow "V" form valley; (b) degradation and widening stage showing a broad "V" form valley; (c) widening and resiltation stage, showing a "U" form valley; and (d) equilibrium stage showing a broad "U" form valley

3.1.3.4   Riparian Vegetation

In many incised stream systems, riparian vegetation plays an important role in flow and near-bank hydraulics, bank stability, and stream habitat. In humid environments, the sequence of processes and
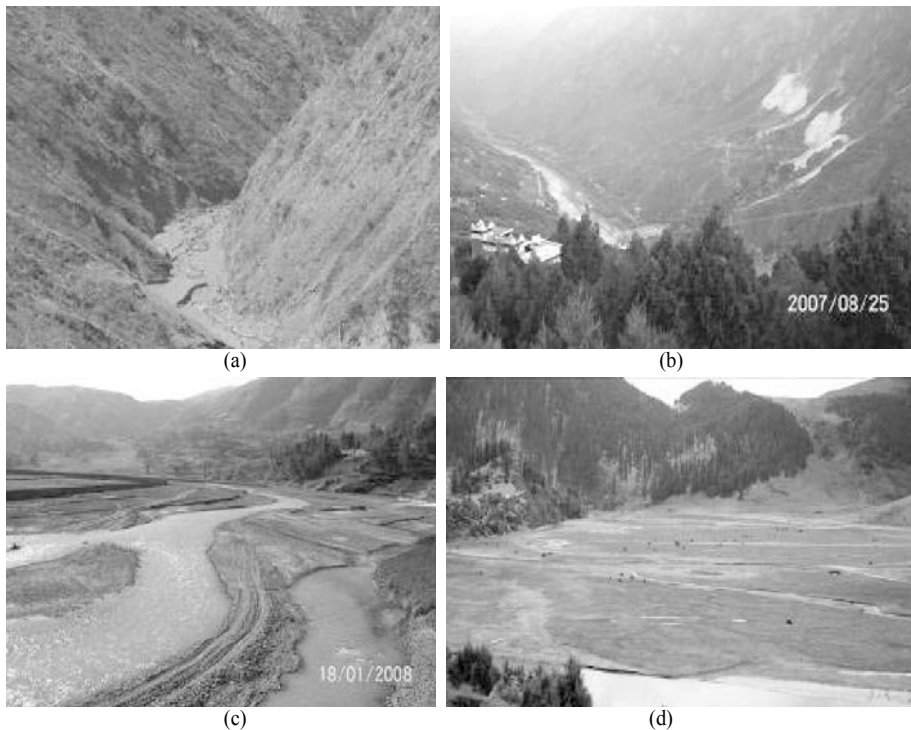
Fig. 3.11 (a) A tributary of the Minjiang River in the rapid degradation stage; (b) the Dajinchuan River in the degradation and widening stage; (c) the Kuaihe River in the upper Yangtze River basin in the aggradation and widening stage; (d) an upstream reach of the Dahu River in the equilibrium stage (See color figure at the end of this book)

forms associated with the evolution of incised channels is accompanied by related changes in the character and quantity of riparian vegetation (Hupp and Simon, 1991; Hupp, 1992; Simon and Hupp, 1992; Hupp, 1997). Riparian vegetation may be directly removed by a disturbance or by mass failures during channel adjustment. Re-establishment of woody vegetation on the banks of incised channels generally occurs initially on low-bank surfaces and is accompanied by reworking of failed materials and fluvial deposition (Simon and Hupp, 1986; Hupp and Simon, 1991). This is an indication that relative stability is returning to the stream bank as vegetation extends upslope with time.

Vegetation increases flow resistance on bank surfaces and can result in locally reduced velocities and enhanced deposition. In contrast, vegetation either germinated in situ, or delivered with a failure block to a low-bank position, can cause eddying, flow deflection, and basal erosion of bank toes of the opposite bank or bar. Riparian vegetation also has a variety of effects on the shearing resistance of stream banks through its effects on root reinforcement (Wu and McKinnell, 1976), permeability (Collison and Anderson, 1996), and pore-pressure distributions (Huck et al., 1970), and increases in shear strength due to increased suction. Figure 3.12 shows the riparian vegetation by a small river in the Mississippi River drainage basin resisting bank erosion with the roots of the trees bonding the bank soil. Reinforcement of the shearing resistance of stream banks by roots is of course limited to the rooting depth of the riparian vegetation. Field studies have shown that roots with diameters greater than 15 to 20 mm do not greatly contribute to increased shear strength (Coppin and Richards, 1990). Large roots are better treated as soil anchors (Gray and Leiser, 1982). The effects of riparian vegetation on deep-seated rotational or other failures where the failure-plane depth exceeds the rooting depth is, therefore, limited to creating a

surcharge by increasing the normal force on the potential failure plane. The varying effects of vegetation on incised stream bank stability have not been addressed in detail although Abernathy and Rutheford (1998) provide a review of research in North America, Europe, and Australia.

Techniques and results for tropical cut slopes, which are characterized by deep, heterogeneous profiles may prove useful in analyzing incised channel banks (Anderson et al., 1996; Collison and Anderson, 1996). A modified version of the combined slope hydrology-stability model CHASM (Anderson and Kemp, 1991) may be particularly useful for testing the role of riparian vegetation on the stability of banks in incised streams.

Fig. 3.12   The riparian vegetation by a small river in the Mississippi River drainage basin resists bank erosion with the roots of the trees bonding the bank soil

3.2   Bedrock Channels

3.2.1   Incision Rate of Bedrock Channels

A bedrock channel may be defined as one for which morphology and gradient are directly controlled by bedrock (Wohl, 1998). A bedrock channel has bedrock exposed along the channel bed or walls for at least approximately half its length, or has bedrock limits to the magnitude and location of bed scour and bank erosion during floods. Bedrock exposure along at least half the channel length suggests that alluvium does not accumulate to a depth at which the active channel is formed entirely in alluvium. The presence of bedrock as channel boundaries during large discharges will facilitate different patterns of hydraulics, sediment transport, and channel morphology than those common along alluvial channels. Bedrock-constrained valley walls may limit floodplain development so that bedrock channels have low-flow and high-flow portions. A bedrock channel may also have a bedrock surface into which a low-flow inner channel is incised, thus, having inner channel flow in the dry season and high (flood plain) flow in flood season (Figure 3.13).

Bedrock channels most commonly occur in regions of high topographic relief. Relief may be a product of recent tectonic uplift, as in the Himalayan Mountains of central Asia, or the Colorado Plateau of the southwestern U.S. High topographic relief in a drainage basin tends to produce high stream gradients, and, thus, the potential for high sediment transport capacity and flow energy per unit of discharge. The exposed bedrock implies that the channels may be particularly sediment-starved during floods.

Flood flows along channels incised into highly weathered, soft, or thinly bedded or jointed rocks result

in substantial channel incision via abrasion, flaking, or plucking of bedrock. An example of bedrock channel incision is the middle reaches of the Yellow River, as shown in Figure 3.14(a). The channel bed is composed of thin-layered limestone. The heavy sediment load carried by the flow makes the flow more abrasive and the flow has cut an inner channel up to 40 m deep. Figure 3.14 (b) shows the bare bedrock bed of the Jinghe River, a tributary of the Weihe River in China. The bed cross section exhibits a V-shape, which is similar to the second type in Fig. 3.13.
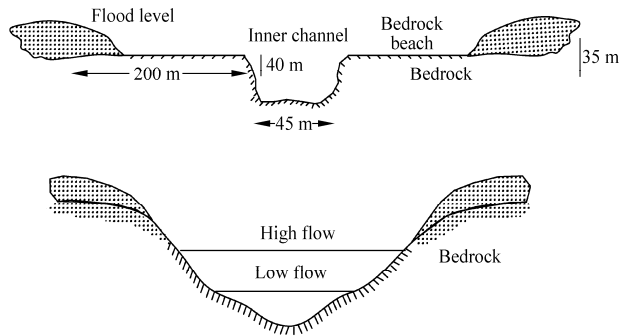
Fig. 3.13 Schematic illustration of U-shape and V-shape channels of low-flow and high-flow morphologies present along bedrock channels (after Wohl, 1992)

(a)

(b)

Fig. 3.14 (a) Bed rock channel in the middle reaches of the Yellow River; (b) Bed rock channel of the Jinghe River with a V-shaped cross sections (See color figure at the end of this book)

Bedrock channels tend to be incised below the surrounding slopes and uplands. Because bedrock channel incision commonly occurs over the course of centuries to millennia, channel instability resulting from bed incision is not as widespread a problem among bedrock channels as among alluvial channels. However, there are conditions under which rapid bedrock channel incision may create hazards. As listed in Table 3.4 the average rate of bedrock channel incision ranges from 0.5 to 1000 mm/kyr, depending on the bedrock, the flow in the channel, and the bed gradient.

Table 3.4   Published long-term average rates of bedrock channel incision (after Schumm and Chorley, 1983; and Wohl and Grodek, 1994)

Rate (cm kyr^{-1})	Lithology	Location	Drainage area (km^2)	Climate tectonics	Time range of incision	Source
9	granite, andesite	Sierra Nevada, California, U.S.	35,000	arid, uplift	Pliocene-Quaternary	Huber, 1981
30	sedimentary	Colorado, U.S	11,800	semiarid, uplift	Miocene-Quaternary	Larson et al., 1975
7	metamorphic	Colorado, U.S.		semiarid, uplift	Pliocene-Quaternary	Scott, 1975
45–130	sedimentary	Nahal Zin, Israel	1,540	hyperarid, uplift	Quaternary	Goldberg, 1976; Schwarcz et al., 1979; Yair et al., 1982
10	sedimentary	Nahal Paran, Israel	3,600	hyperarid, uplift	Quaternary	Wohl and Grodek, 1994
30	basalt, limestone	Utah, U.S.	9,900	semiarid, uplift	Quaternary	Hamblin et al., 1981
9.5	sedimentary	Arizona, U.S.	68,500	semiarid, uplift	Quaternary	Rice, 1980
23–25	basalt	Jalisco, Mexico		arid, uplift	Pliocene-Quaternary	Righter, 1997
15	suggested average rate of bedrock channel incision in middle latitudes					Pitty, 1971
25–47	sedimentary	Utah, U.S.	115,000	semiarid, uplift	Quaternary	Harden and Colman, 1989
1,000	igneous and metamorphic	Pakistan	260,000	semiarid, uplift	Quaternary	Leland et al., 1995
60,000	shale and fine sand stone	Taiwan, China		Wet and tropical	20th–21st century	Fourth River Department, 2006
70–180	sedimentary	California, U.S.	655	Mediterranean, uplift	Holocene	Merritts et al., 1994
<25	sedimentary, intrusive igneous	California, U.S.	10–20	Mediterranean, uplift	Quaternary	Rosenbloom and Anderson, 1994
0.5–8	basalt	Kauai, Hawaii U.S.	0.1–90	seasonal tropical to semiarid, uplift	Pliocene-Quaternary	Seidl et al., 1994
40–100*	basalt	Kauai, Hawaii U.S.	0.1–90	seasonal tropical to semiarid, uplift	Pliocene-Quaternary	Seidl et al., 1997
50–690	sedimentary	Montana, U.S.	1,420	humid temperate, uplift	Quaternary	Foley, 1980

(Continued)

≤1,000	mudstone	Japan	0.15–0.4	humid temperate, uplift	Quaternary	Mizutani, 1996
5.7	limestone	New Guinea	0.02	humid tropical, uplift	Quaternary	Chappell, 1974
≤1.57*	sedimentary	Ontario, Canada	686,000	humid temperate, passive	Quaternary	Tinkler et al., 1994
0.5–3	basalt, metamorphic	southeastern Australia	20–400	humid temperate, passive	Miocene-Quaternary	Young and McDougall, 1993
300	basalt, sedimentary	Svalbard, Norway		subpolar, passive	Quaternary	Budel, 1982.
2.7	carbonates, crystalline rocks	Virginia, U.S.		humid temperate, passive	Quaternary	Granger et al., 1997

* Symbol denotes knickpoint migration upstream

The Jinghe River, in the Loess Plateau of China, carries a huge amount of sediment and flows into the Weihe River. The annual sediment load/water ratio is as high as 140 kg/m^3. Because the sediment is fine and there is no bed sediment, the bedrock is exposed to the flow and the bed is incised at a rate of about 5 mm/kyr.

Very fast incision rate occurs on the bed rock composed shale and fine sand stone. Figure 3.15 shows the bed rock channel of the Cho-shui River in Taiwan. The Chichi Barrage was constructed on the river in 1999 for water diversion and irrigation. Sediment was trapped in the reservoir, which caused more than 50% of capacity loss of the reservoir. The released clear water from the barrage scoured the river bed and carried the bed sediment away. The bare rock exposed directly under the action of the erosion and flow scouring. In the meantime sediment mining also caused bed rock exposure. The bed rock composed mainly of shale and fine sand stone which were deposited in Tertiary. A very intensive channel bed incision occurred in the past decade. A 16 km long bed rock channel was incised down by about 6 m (Fourth River Department, 2006). The deepest incision depth was 25 m measured in 2006. The rate of bed rock incision was as high as 0.6 m per year.

Fig. 3.15 Bed rock channel downstream of the Chichi Barrage of the Cho-shui River in Taiwan experiencing extremely high incision rate

3.2.2 Incision Processes of Bedrock Channels

The bedrock channel is eroded by three processes: corrosion, corrasion, and cavitation. Corrosion refers

to chemical weathering and solutions that may directly erode the bedrock, as in carbonate lithologies, or, more commonly, may weaken the bedrock and render the substrate more susceptible to erosion by corrasion and cavitation (Carling and Grodek, 1994). Very few estimates have been published of direct chemical weathering in channels. Most chemical erosion rates are averaged across a basin, and, thus, incorporate groundwater and soil processes, or are obtained from rock faces exposed on hill slopes, buildings, or tombstones. Generalized estimates for drainage basins range from 0.005 to 0.2 mm yr^{-1} for carbonates and shales and 0.7 mm yr^{-1} for evaporites (Lerman, 1988). In one of the few studies that quantified in-channel chemical erosion, Smith et al. (1995) measured rates of $0.022 - 0.200$ mm yr^{-1} in carbonate terrains of eastern Australia. Figure 3.16 shows a bedrock channel in the Three Gorges area of the middle reaches of the Yangtze River, which is suffering from chemical corrosion. The channel bed is composed of limestone and is likely to be eroded by corrosion. The rate of the corrosion is estimated at about a few cm/kyr.

Fig. 3.16   The limestone bedrock channel of a stream in the Three Gorges area of the middle reaches of the Yangtze River is suffering from chemical corrosion

Corrasion is abrasive weathering of bedrock by clusters moving along the channel as bed load. Partly because it is very difficult to separate erosion caused by abrasion from erosion caused by other processes, and partly because rates of bedrock channel erosion are commonly slow relative to the duration of most field studies, no published rates of bedrock channel erosion caused solely by abrasion are available The most rapid rates of abrasion probably occur during turbulent floods with large and fairly coarse sediment loads, along channels of weakly resistant bedrock. Channels likely to be dominated by corrasional erosion have numerous potholes, longitudinal grooves, knickpoints, and similar erosional features along the channel bed and walls. The bedrock channel of the Yangtze River near the Gezhouba Dam exhibits a lowest point of elevation of -10 m, $60 - 70$ m lower than the surrounding bed elevation. The main cause of the incision is abrasion of bed load particles against the relatively soft bedrock.

Perhaps corrasion is the most important process associated with fast bedrock channel incision. Figure 3.17(a) shows the bedrock channel of the Lijiang River in Guangxi, China. The beautiful landscape in the area was firstly sculpted by the corrosion process but the bed rock channel is eroded mainly by corrasion induced by gravel movement on the bed. Figure 3.17(b) shows the incised bedrock channel of a tributary of the Jinsha River (upper Yangtze River). The bed rock channel has been incised down by about 20 m mainly due to corrasion. Figure 3.17(c) shows the parallel corrosion slots because of bed load movement on the bedrock of the Jinsha River. During the flood season gravel bed load was

transported in the river. Particles slid or jumped over the bedrock channel and hit against the bedrock, which cause the bedrock corrasion.

Cavitation occurs when velocity fluctuations in a flow induce pressure fluctuations that cause the formation and implosion of vapor bubbles. The shock waves generated by implosion can weaken bedrock and pit the rock surface. Under sustained high flows, the erosive potential of this process can be phenomenal. During 1983, discharges up to 900 m^3 s^{-1} through the spillway at Glen Canyon Dam on the Colorado River, U.S., generated cavitation that within days eroded pools up to 10 m deep and 6 m long in a stair step configuration down the 12.5 m diameter concrete-lined spillway (Eckley and Hinchliff, 1986).

Corrosion, corrasion and cavitation may occur simultaneously in the process of bedrock channel incision. In most cases remarkably little is known about the actual processes by which bedrock channels are eroded. Quantitative experimental studies using both cohesive silt and clay substrates in flumes, and actual rock and sediment for estimating abrasion rates, would be extremely useful.
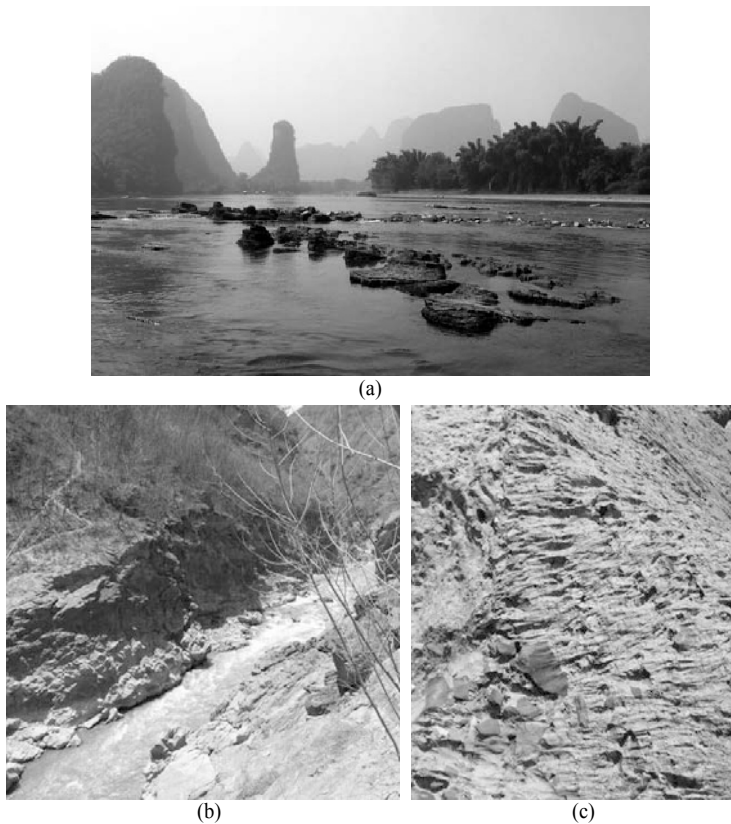
(a)

(b)   (c)

Fig. 3.17 The bedrock channel of the Lijiang River is eroded by corrasion induced by gravel movement on the bed; (b) Bedrock channel of a tributary of the Jinsha River has been incised down by about 20 m mainly due to corrasion; (c) Parallel corrasion slots on bedrock of the Jinsha River (See color figure at the end of this book)

The surface of bedrock channel can be rough, which creates high resistance and consume the flow energy. Figure 3.18 shows the rough bed of the Black River in Shaanxi. The bedrocks are scoured into a bedrock step-pool system. The high resistance of bedrock structure controls the bed incision and stabilizes the channel bed. A section of such bedrock channel becomes a knickpoint of the river.

Fig. 3.18 Rough bedrock of the Black River in Shaanxi

3.2.3 Knickpoints

A high gradient of a section of bedrock channel may take the form of vertical or undercut waterfalls several meters in height, or they may be short, steep sections of channel called knickpoints Bedrock channels may also have downstream variability in gradient as a result of knickpoints. Knickpoints are commonly most well developed in layered or jointed rocks; and are generally regarded as disequilibrium features that either migrate upstream, erode toward a lower angle, or otherwise change in form or location fairly quickly relative to the evolution of the stream channel. Knickpoints, are, thus, commonly regarded as evidence of channel instability in the form of headcut migration. Figure 3.19(a) shows the famous Kettle Waterfall in the middle reaches of the Yellow River in China. The fall is a knickpoint formed in the channel. The knickpoint migrates upstream at a rate about $0.5 - 0.7$ m/yr. The knickpoint is maintaining a nearly vertical face as it migrates upstream.

The classic theory for a process of knickpoint retreat in stepped headcuts was first proposed by Gilbert (1896, 1907) for Niagara Falls. This theory featured undercutting by erosion of less resistant strata due to turbulence and abrasion in the plunge pool, creating an increasingly unstable cap rock that eventually failed (Tinkler et al., 1994). However, the plunge pool at Niagara Falls is not undercut below the water level, and the role of plunge pool erosion in knickpoint retreat remains unclear. Subsequent studies have described knickpoints for which pothole erosion at the lip is an important component of headward retreat (Bishop and Goldrick, 1992). The Kettle Waterfall on the Yellow River retreats due to the erosion caused by the turbid water. It occurs often that many circle holes develop around the knickpoint, which are called potholes. The mechanism of the development of potholes is yet to be studied. Potholes were observed at the water fall. Figure 3.19(b) shows the pothole around the Kettle Waterfall. Figure 3.20 shows developing potholes around a small knickpoint on a mountain stream in the Xiangjiang River Basin in Hunan Province, China.

Knickpoints are the sites of the greatest concentration of energy dissipation along the course of a stream. Most investigators have assumed that knickpoints retreat fairly rapidly, and have concentrated on the mechanisms and rates of knickpoint retreat. Shear stress is highest just above and at the knickpoint face (Gardner, 1983). Knickpoint retreat is proportional to discharge, and is a function of the balance between the rate of downward wear on the steep reach and the rate of backward wear on the knickpoint face, and of knickpoint height (Holland and Pickup, 1976). Very few actual measurements exist for rates of bedrock knickpoint retreat. Exceptions come from the well-dated Niagara Falls region and from Hawaii. Radiocarbon ages of clam shells at Niagara Falls suggest that the 46-m-high falls migrated very slowly $(0.05 - 0.70$ m yr$^{-1})$ along the narrow gorge section at Niagara Glen from 10,500 to 5,500 yr BP,

when upper Great Lakes water bypassed the site (Tinkler et al., 1994). Prior to that interval, river discharge and recession rates were similar to those at present (1.57 m yr^{-1}), and similar rates resumed after 5,200 yr BP.

(a)

(b)

Fig. 3.19 (a) The Kettle Waterfall is a Knickpoint of the bedrock channel in the middle reaches of the Yellow River; (b) Potholes at the Kettle Waterfall on the Yellow River

Fig. 3.20 Developing potholes around a small knickpoint on a mountain stream in the Xiangjiang River Basin in Hunan Province, China

3.3 Bed Structures Resisting Incision

3.3.1 Step-pool Systems

A step-pool system is a geomorphologic phenomenon occurring in high-gradient ($>3 - 5\%$) mountain streams with alternating steps and pools having a stair-like appearance (Chin, 1999). The step-pool system usually occurs on a stream with bed materials consisting of particles with diameters differing by several orders of magnitude with the largest diameter on the same order as the water depth. Cobbles and boulders generally compose the steps, which alternate with finer sediments in pools to produce a repetitive, staircase like longitudinal profile in the stream channel, as shown in Fig. 3.21.
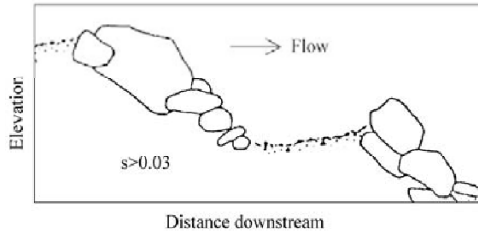
Fig. 3.21   Staircase-like longitudinal profile of a step-pool system in high gradient stream channels

A step-pool system develops usually in small mountain streams with a several meters wide channel. Figure 3.22(a) shows the step-pool system in a small ravine in the upper Yangtze River basin, which has a channel width of only 2 m. Large stones play an important role in the development of a step-pool system. In relative large streams with high gradients, step-pool systems may develop if there are huge stones. Figure 3.22(b) shows the step-pool system on the Xiaojinchuan River in Sichuan Province, which has a channel width of several tens of meters. The large stones have a diameter of more than 5 m. The structure developed after a landslide and long term erosion. The step-pool system causes a water head reduction of more than 50 m and composes a knickpoint of the Xiaojinchuan River.

The tight interlocking of particles in steps gives them an inherent stability that only extreme floods are likely to disturb, which suggests that step-pools are a valid equilibrium form, especially when coupled with their apparent regularity and their role in satisfying the extreme condition of resistance maximization. Step-pool systems also develop in many mountain streams in China, such as the Yuzixi and Zagunao rivers, tributaries of the Minjiang River and the Jiuzhai Creek in Sichuan Province, the Qingshui River in Guizhou Province, and the Shengou Ravine and tributaries of the Xiaojiang River in Yunnan Province.

There are many research results on the hydraulic features of regular step-pool systems. The step-pool system affects not only flow resistance but also sediment transport, which in flume experiments occurs as a series of waves linked to the underlying bed morphology (Whittaker, 1987, Rosport, 1994). Their role as energy dissipaters can be impaired when pools become filled with sediment (Whittaker and Jaeggi Martin, 1982), for then there is an increase in velocity and erosive capability, reactions that are opposite to the original formation of mechanism the step-pool system. The bed adjustment in a step-pool system in Leinbach, Germany shows the function of increasing flow resistance (Ergenzinger, 1992). The large boulders in the steps act as a framework tightly interlocking the structure resulting in considerable stability. Given the need for one or more keystones, the development of a step is strongly influenced by local sediment supply and transport conditions. The pools between steps provide storage sites for finer bed material.

Step-pool morphology can be characterized by two variables: step wavelength L and step height H_s, so that H_s/L is an index of step steepness and bears a close relation to the loss of head per unit length of

(a)

(b)

Fig. 3.22 (a) Step-pool system in a small ravine in the upper Yangtze River basin (b) Step-pool system on the Xiaojinchuan River in Sichuan, China

channel (Abrahams et al., 1995). Pool-pool or step crest-step crest spacing has an average of $2-4$ stream widths in two Oregon streams and is also rather variable because of an uneven distribution of bedrock outcrops and boulder deposits along the channels (Grant et al., 1990). Step structure appears to be better defined and more regular on steeper slopes (Judd and Peterson, 1969; Whittaker, 1987; Chin, 2002; Grant et al., 1990; Wohl and Grodek, 1994), which implies that, if step height is controlled by the largest particles an increase in the bed slope must be accommodated by more closely spaced steps.

The flow over the boulders forming each step is supercritical (Froude number, $Fr > 1$) and changes to sub-critical ($Fr < 1$) in the pool, causing a considerable amount of energy dissipation through turbulent mixing (Hayward, 1980; Whittaker and Jaeggi Martin, 1982). In addition, energy is expended as a result of the form drag exerted by the large particles that make up the steps. Thus, step-pool systems have an important resistance role, which is of particular significance in mountain streams where alternative forms of energy dissipation, such as lateral adjustment, are inhibited by the narrowness of the valleys, and where the large amounts of potential energy generated by the steep slopes could otherwise lead to extreme erosion.

A step-pool system is the best ecologically sound riverbed pattern in mountain streams. Large fishes may swim up through the steps and small fishes may swim up against low velocity in the gaps between

the stones. The shallow and deep waters and high and low velocities of flows provide high diversity of habitat for a high diversity of species. The pools provide refuge for juvenile fishes and in dry years may preserve water and serve as oases for faunal species.
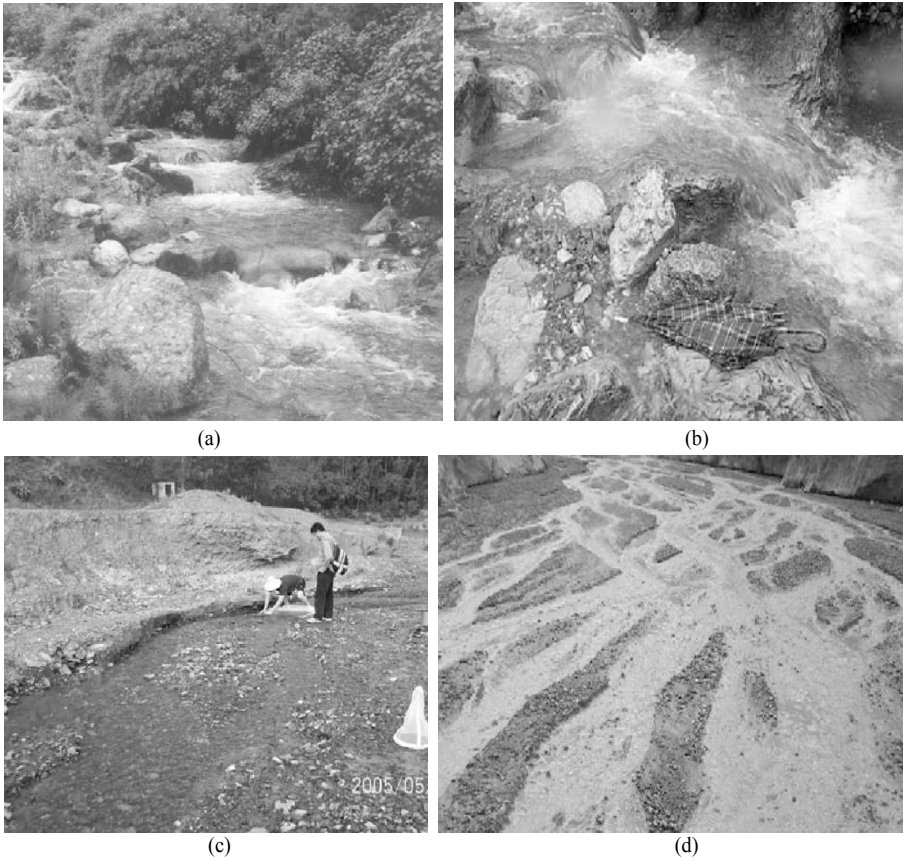
(a)   (b)   (c)   (d)

Fig. 3.23   (a) A step-pool system develops in a high gradient stream channel- Shenggou Creek; (b) Step—pool causes hydraulic jumps; (c) No step-pool system in the Jiangjia Ravine, which is about 16 km from Shengou Creek; (d) No step-pool system in the Xiaobaini Ravine (8 km away from Shengou Creek) (See color figure at the end of this book)

A step-pool system develops in the process of channel incision, in cases of insufficient sediment supply from upstream. For instance, a step-pool system developed in Shengou Creek in the past 30 years after extensive erosion control and reforestation projects were implemented in the drainage area of the creek. Before 1976 debris flows frequently occurred in Shengou Creek, and there were no step-pool systems. Slope and gully erosion provided enough sediment to the stream and heavy sediment transportation and poor vegetation cover dominated the river basin. Riparian vegetation has developed and sediment transportation has sharply reduced in the past decades thanks to the efforts of erosion control and reforestation projects. Thus, sediment-starved flows have scoured the channel bed and step-pool systems have developed. Figure 3.23(a) and (b) show the streambed morphology of Shengou Creek. As a comparison, the Jiangjia Ravine, also a tributary of the Xiaojiang River, is only 17 km from Shengou Creek. Erosion has not been controlled in the Jiangjia Ravine watershed and bed load is transported by the stream flow. The streambed is still silting up as a result of too much sediment load

from upstream. There is no step-pool system in the Jiangjia Ravine, as shown in Fig. 3.23(c). The Xiaobaini Ravine flows into the Xiaojiang River from the opposite side (left side) and is 8 km from Shengou Creek. Bed load motion and suspended load transportation are present in the stream. The bed sediment consists mainly of gravel and sand. Although it has the same climate and bed sediment composition as Shengou Creek, no step-pool system is present in the ravine, as shown in Fig. 3.23(d).

Shatford Creek is an eastward flowing tributary of Shingle Creek, in the Okanagan Valley of British Columbia, Canada. Zimmermann and Church (2001) investigated the creek and reported the features of step-pools in the creek. Four sections were selected each about 60 m in length. In each reach steps reflect the location of key boulders. Figure 3.24 shows the longitudinal profiles of these reaches. Reach 1 is dominated by rapids and lacks large boulders, therefore, the peak-flow water line is more linear in Reach 1 than in any of the other reaches (Fig. 3.24(a)). Reach 2 has a highly variable bed profile. At the 19-m point of the reach, the channel is split around a large tree and a few large boulders and at the 32-m point the channel goes through a tight bend, as shown in Fig. 3.24(b). Reach 3 is the steepest and has the narrowest channel, largest boulders, and lowest mean velocity (Fig. 3.24(c)). Reach 4 has the clearest, continuous set of step-pools. However, the heights of the steps and depths of the pools are highly variable (Fig. 3.24(d)). The step at the 23-m point of the reach is composed of two large boulders, about 2 m in diameters each, which rest beside each other.
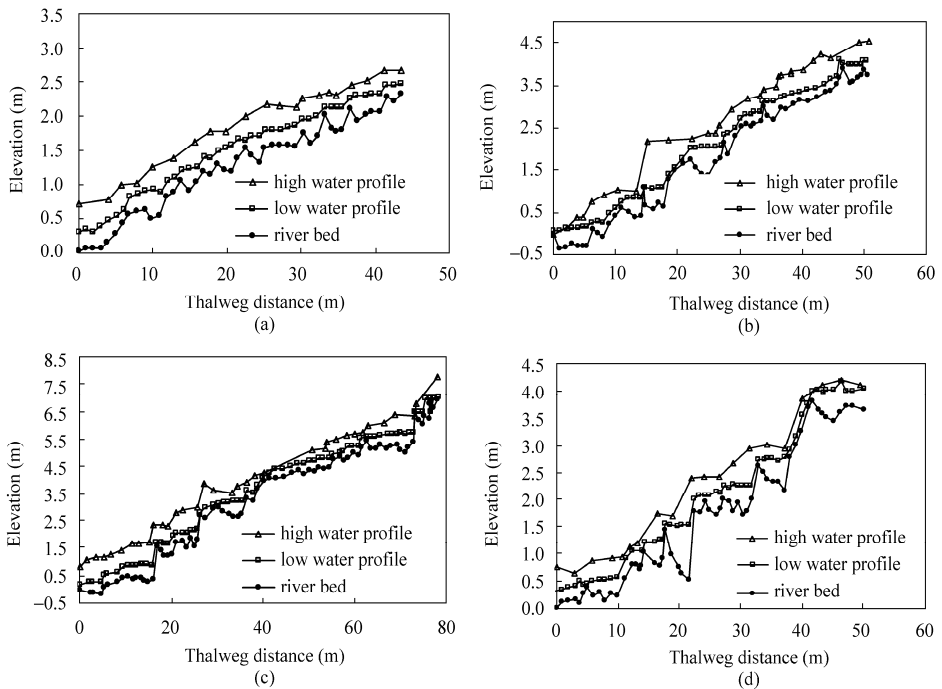
Fig. 3.24 The longitudinal profiles of four reaches of Shatford Creek British, Columbia, Canada. (a) Poorly developed step-pool system in Reach 1 because of lacks large boulders; (b) Highly variable bed profile in Reach 2; (c) Steepest and narrowest channel in Reach 3 with a developed step-pool system; (d) Clearest and continuous set of step-pools in Reach 4

Rosport (1997) reported that the length of a regular step-pool system increases with the average discharge. Whittaker (1987) suggested that the length of a regular step-pool system, or the distance

between two steps or two pools, L, is inversely proportional to the average slope of the stream, S:

$$L = 0.31s^{-1.19} \qquad (3.2)$$

where L is in meters. The decrease in step length is rapid as the slope increases up to about 0.15. The influence of bed slope on the adjustment of step-pool morphology is further illustrated by a relation between the average step steepness (H_s/L) and slope obtained by Abrahams et al. (1995) from field and laboratory data;

$$H_s / L \sim 1.5s \qquad (3.3)$$

This relation indicates that the average elevation loss due to steps is about 1.5 times the average elevation loss along a reach, which implies that about one third of the step height is the result of pool scour (Knighton, 1984).

Wohl and Thompson (2000) measured the vertical velocity profiles of flow in a small mountain channel with step-pool bed forms. The results suggest that locations downstream from bed-steps are dominated by wake turbulence from mid-profile shear layers. Locations upstream from steps, at steps, and in runs are dominated by bed-generated turbulence. Adverse pressure gradients above and below steps may enhance turbulence generation, whereas favorable pressure gradients at steps suppress turbulence. The wake-generated turbulence leads to higher energy dissipation in step-pool reaches relative to more uniform-gradient reaches. The bed-generated turbulence that predominates at step lips and upstream from steps, and in runs, is analogous to the turbulence that dominates riffles and runs in pool-riffle channels. The wake-generated turbulence in step-pools is also analogous to the shear associated with lateral eddies in larger pools, except that in step-pools the shearing occurs primarily at mid-profile and across the channel rather than throughout the profile and along the channel margins.

Wang et al. (2009) measured the velocity distributions in the pool section and step section of Shengou Creek with a current meter. Shengou Creek is located in the upper reaches of the Yangtze River basin in southwestern China, and there is a fully developed step-pool system on the creek. Measurements were done at the step-lips, in the pools, and in reaches of normal run. Roller eddies occur immediately downstream of the step making it difficult to measure the velocity profile. The velocity profiles in the pools were measured at a distance of 1.5 m from the steps. Figure 3.25 shows the velocity profiles measured at a step-lip, 1.5 m downstream of the step in the pool section, and 2 m above the step where the flow is almost in a normal run. The step is about 0.7 m high. The points in the figure are the mean
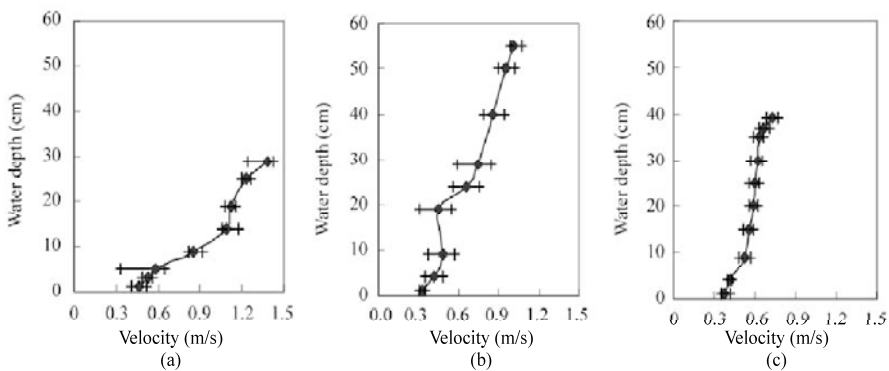
Fig. 3.25 Velocity profiles measured in Shengou Creek: (a) profile at a step-lip, where the water depth is 0.32 m; (b) profile 1.5 m downstream of the step in a pool where the water depth is 0.61 m; (c) profile 2 m above the step, where the water depth is 0.42 m. The range of "+——+" shows the variation range of the mean velocity at the measurement point, which indicates the intensity of fluctuation of velocity

value of velocity and the crosses are the minimum and maximum values of velocity. The results support the conclusions of Wohl and Thompson (2000) that the bed-generated turbulence predominates at step lips and upstream from steps and in runs. The pool section is dominated by wake-generated turbulence. The shearing occurs primarily at mid-profile and across the channel rather than throughout the profile, even at a distance of 1.5 m downstream from the step.

Although steps composed of boulders are the most common type, they can also form in bedrock (Hayward, 1980; Wohl and Grodek, 1994). In this case the steps consist of rocks and there are gravel and fine material in the pools. Figures 3.26(a) and 3.26(b) show bedrock step pool systems in steep mountain streams. The step pool systems in bed rock channels function similarly in energy consumption and resistance maximization as those in gravel bed channels. The flow velocity in the channel with step-pools is effectively reduced and the impact and risk of flash flood are mitigated. Step-pool systems have been reported from a wide range of humid and arid environments (Chin, 2002), and analogous forms have even been observed in supraglacial streams (Knighton, 1984). They, thus, appear to be a fundamental element of steep fluvial systems.

(a)   (b)
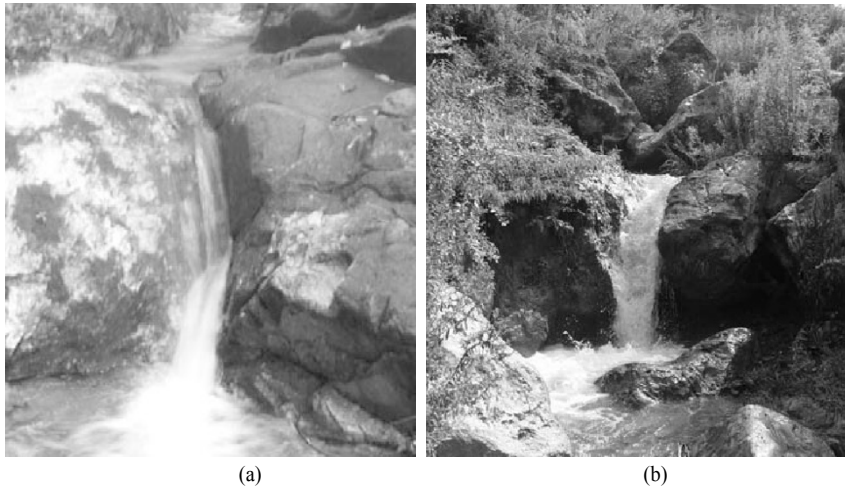
Fig. 3.26   (a) A step pool on a bedrock channel in Hong Kang; (b) A bed rock step-pool system in a steep mountain stream in southwestern China

Step-pool systems can also form through accumulation of large woody debris in heavily forested catchments (Keller and Swanson, 1979). In this case the steps consist of large woody debris and there are fine materials in the pools. Figure 3.27 shows a step-pool system in the Jiuzhai Creek in northern Sichuan. The step-pool system is developed on a landslide dam on which good vegetation has already developed. Large woody debris form the steps and created high resistance, which protects the landslide dam from erosion.

3.3.2   Development of a Step-Pool System

3.3.2.1   Development Degree of a Step-Pool System
The most important hydraulic feature of step-pool systems is the extremely high bed roughness, which maximizes the resistance and reduces the flow velocity. To represent the bed roughness of a step-pool system a parameter, S_P, is introduced, which may be used to describe the development degree of a step-pool system:

$$S_P = \frac{length\text{-}of\text{-}thalweg}{length\text{-}of\text{-}straight\text{-}line} - 1 \tag{3.4}$$

The length-of-thalweg is the total length of the curved bed surface with boulders or gravel along the thalweg, and the length-of-straight-line is the length of a straight line from the beginning point to the end point of the measured bed section. For a flat bed with fine sediment, $S_P = 0$. For beds with step-pools, sand dunes, or other bed structures, S_P is larger than 0.

Fig. 3.27   A step-pool system on a landslide dam in the Jiuzhai Creek in northern Sichuan

Wang et al. (2009) designed an instrument and measured the development degree of a step-pool system, S_P. The instrument, shown in Fig.3.28(a), consists of thirty measuring rods with a space of 5 cm between them placed on a horizontal aluminum steel frame that may slide down onto the bed surface. The upper ends of the rods describe the bed profile in front of a screen. Moving the frame along the thalweg of the stream and each time taking a picture, the bed profile along the thalweg can be measured. The S_P value is then calculated by the following formula:

$$S_P = \frac{\sum_{i=1}^{m} \sqrt{(R_{i+1} - R_i)^2 + 5^2}}{\sqrt{[5(m-1)]^2 + (R_m - R_1)^2}} - 1 \tag{3.5}$$

in which R_i is the reading of the upper end of the measuring rods on the screen in cm, and m is the total number of the readings, which is generally larger than 300. Figure 3.28(b) shows the measurement of S_P with the instrument in the Yigong Tsangbu River in Tibet. For a stream without step-pools S_P is smaller than 0.1. If a step-pool system is well developed the value of S_P may larger than 0.3. For extremely developed step-pool on steep slope the value of S_P can be as large as 0.5. Only for very huge step-pool systems composed of huge stones with diameter of larger than 10-20 m the value of S_P can reach 1.0.

With the specially designed instrument, the bed profile of the thalweg and the development degree of a step-pool system, S_P, in the streams were measured. Figure 3.29 shows the measured bed profiles of the thalweg of Shengou Creek, Fork Gully, and the Jiangjia Ravine, which are located in the upper reaches of the Yangtze River basin in southwestern China. Shengou Creek, the Jiangjia Ravine, and Fork Gully are tributaries of the Xiaojiang River on the Yunnan-Guizhou Plateau in southern China, which flows into the upstream reach of the Yangtze River. The elevation in Fig. 3.29 shows the relative elevation along the course for each stream not the elevation above sea level. Figure 3.29 clearly shows that Shengou

Creek has the best developed step-pool system and has the largest bed roughness. Fork Gully is developing a step-pool system and the bed roughness is between that of the Jiangjia Ravine and Shengou Creek. The Jiangjia Ravine has no step-pool system and the roughness and resistance are small. Field investigations found that the height of steps depends on the size of the largest particles (Wohl et al., 1997). In general both the height and the number of steps per length increase with the bed slope. Closer spacing of steps often occurs with steeper slopes in response to an increase in the number of large particles. If sufficient time is given for a step-pool system to develop, the S_P value increases with the average bed slope.
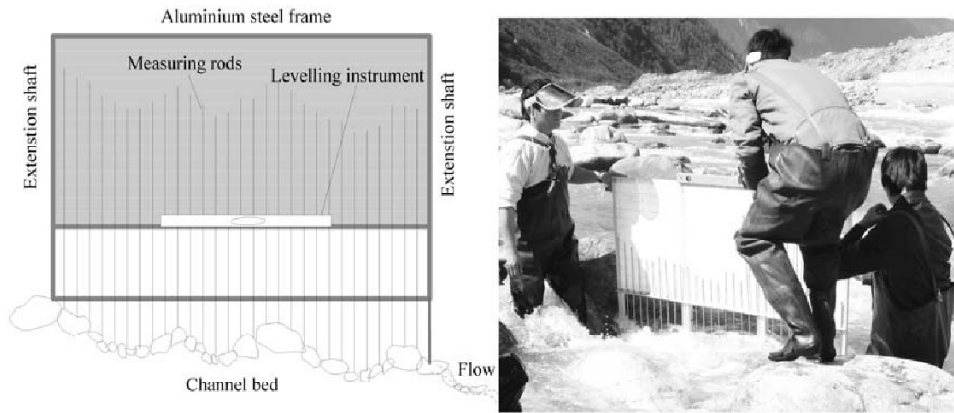
Fig. 3.28 (a) Instrument for measuring the development degree of step-pool system; (b) Measurement of the S_P value on the Yigong Tsangbu landslide dam
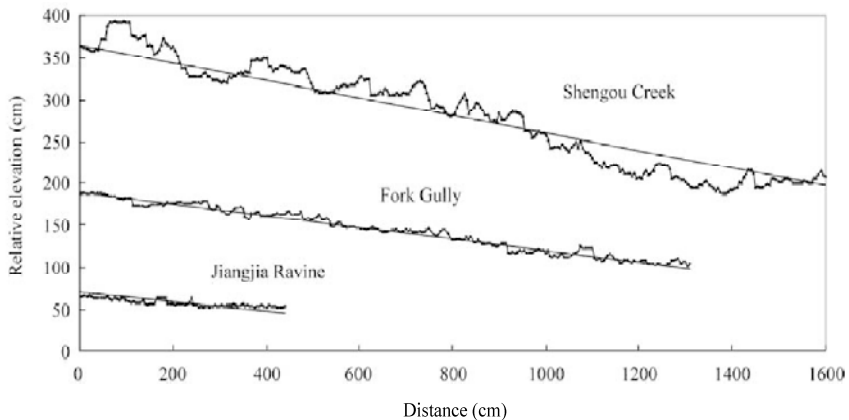
Fig. 3.29 Thalweg profiles of Shengou Creek, Fork Gully, and the Jiangjia Ravine

Figure 3.30 shows the S_P value as a function of average bed slope, s, in which the triangles are measured in mountain streams including Shengou Creek, the Jiangjia and Xiaobani ravines, and Fork Gully, and the black points are the results from a laboratory experiment, which is discussed in the following section. In general, the development degree of a step-pool system increases with the average bed slope. Two straight lines are shown in the figure roughly describing the trends for the mountain

streams and the experiments. The line for the mountain streams is much steeper than the line for the experiments. One reason for the difference is that there are big boulders in the streams but the size of big particles in the experiment is confined by the material used. The higher the bed slope, the greater is the flow energy needing to be consumed per length of the channel. To maintain a stable channel, step-pools are needed to consume the flow energy in the case of high bed slopes. Therefore, the development degree of step-pools is proportional to the bed slope.
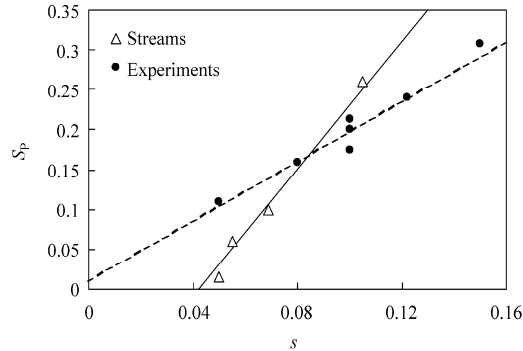
Fig. 3.30 Development degree of a step-pool system, S_P, as a function of the average bed slope

3.3.2.2 Experimental Studies

Many experimental studies have been conducted on the development of step-pool systems (Rosport, 1994; Grant et al., 1990). An experiment was done in a Plexiglas tilting flume 5-m long, 8-cm wide, and 20-cm high (Wang et al., 2004). The slope was in the range of 0.05-0.15 and water discharge varied from 0.1 l/s to 1.5 l/s. The discharge was measured with a triangular notch weir at the entrance. Three size distributions of gravel and sand mixtures were used in the experiments, as shown in Fig. 3.31. The difference between the gravel and sand mixtures lies in the existence of some large gravel and cobbles. For each experiment, a 10-cm thick layer of the sand-gravel mixture was initially put in the flume and formed a flat channel bed. Clear water at a given discharge flowed and scoured sediment from the channel bed. Gradually a relatively stable step-pool system developed and the erosion rate reduced to a minimum. The flow depth increased and flow velocity decreased following the development of the step-pool system.
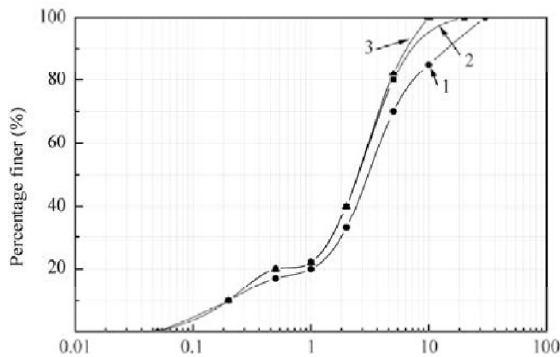
Fig. 3.31 Size distributions of sand-gravel mixtures used in the experiments on step-pool formation (after Wang et al., 2004)

The channel bed developed into three kinds of bed form in different cases. In the first case, the flow power was small but the clear water flow could remove the fine bed materials. Only coarse particles remained in the top layer of the bed, and, thus, an armor layer had developed, which might resist the shear stress of the flow. The roughness of the bed became larger and the velocity reduced. In the second case, not many cobbles and large gravel were present in the bed material. The flow might remove the coarsest particles as well, and the armor layer had been destroyed. The moving particles formed dunes that generated form drag, which caused reduction in the flow velocity. In the third case, cobbles and large gravel were present in the bed material, and the flow power was high enough to remove all individual particles. However, the largest particles acted as keystones and prevented other large and small particles from moving. A sequence of frameworks of tightly interlocking structures developed on the channel bed. The interlocking structures exhibited an inherent stability, which could resist the assaults of the flow and composed the steps. Behind the steps the bed was scoured into pools. The flow over the steps was supercritical, and it changed to subcritical in the pools. Hydraulic jumps formed in the pools, which functioned as energy dissipation pools and greatly reduced the flow velocity. Thus, the step-pool system obviously increased the resistance and the flow depth, which was of particular significance for the stability of the channel bed. The form drag and the hydraulic jumps consumed a large amount of flow energy, which otherwise could lead to extreme erosion.

Figure 3.32 shows the development process of the step-pool system: (a) an armor layer formed in a

(a)

(b)

(c)

(d)
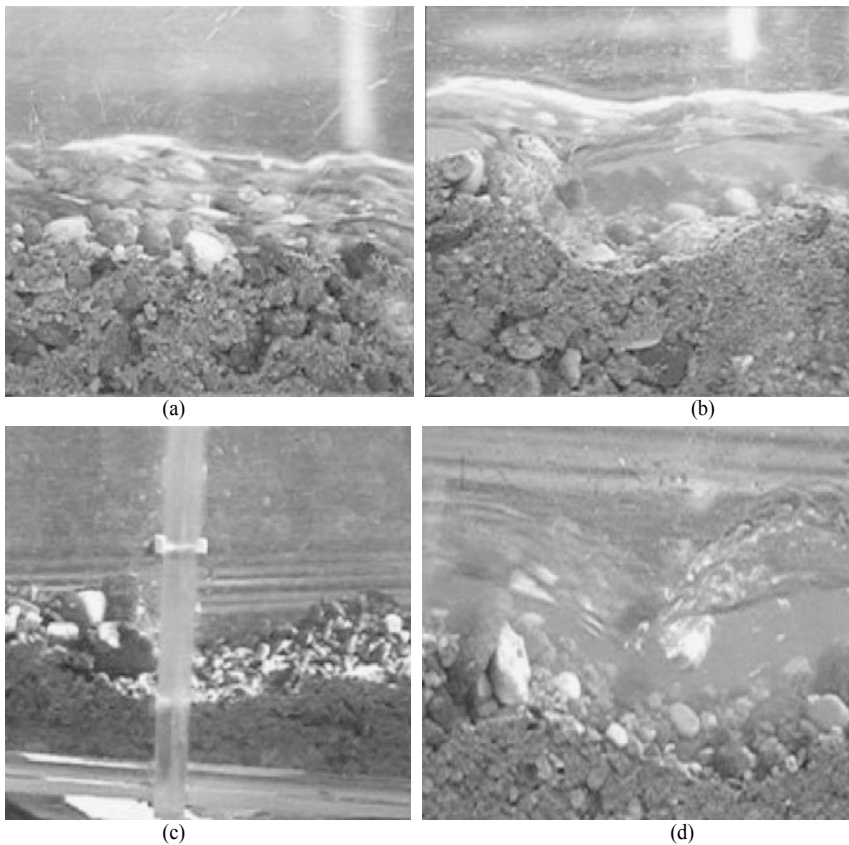
Fig. 3.32 Development process of a step-pool system: (a) armor layer; (b) step-pool; (c) dry bed-form after the experiment; and (d) hydraulic jump at a step-pool section

flow of low stream power; (b) in flows of high stream power the channel bed developed into step-pools; (c) dry bed-form after the experiment; and (d) a hydraulic jump at a step-pool section.

Table 3.5 lists Manning's roughness coefficient n and the rate of bed load transportation during different stages of bed form development, in which the hydraulic radius was measured directly from the average depth; the average velocity was calculated from the discharge and average depth; Manning's roughness coefficient, n, was calculated using Manning's formula, which represents the resistance of the bed to the flow; and the rate of bed load transportation per width was measured using a sediment trapping basket at the downstream end of the flume, which is, in fact, the rate of erosion from the channel bed per time in the case of no sediment supply from the entrance.

Table 3.5 Manning's roughness coefficient n and rate of bed load transportation during different stages of bed form development

No	Hydraulic radius R (cm)	Average velocity U (m/s)	Manning's roughness n	Rate of bed load transport per width g_b (kg/min.m)	Stage of bed form development
1	0.87	0.718	0.0186	15.0	Developing
2	1.25	0.500	0.0341	5.4	Developing
3	0.96	0.651	0.0219	12.3	Armor layer
4	1.28	0.488	0.0354	4.6	Armor layer
5	1.53	0.408	0.0477	0.73	Step-pool system
6	1.66	0.377	0.0547	0.04	Step-pool system
7	1.64	0.377	0.0545	0.05	Step-pool system

During the developing stage (Stage Ⅰ in Fig. 3.33) the channel bed was eroded by the flow and the measured rate of bed load transportation was high. Manning's roughness coefficient, n, varied with the adjustment of the bed form. In the second stage (Stage Ⅱ) an armor layer formed after a period of erosion and the resistance became larger because the bed surface was rough. In the meantime the rate of bed erosion and sediment transportation to the downstream end was reduced. The armor layer could not remain long because the sediment-starved flow initiated motion of the individual coarse particles. These coarse particles were stopped by some even bigger particles and accumulated there building a structure. More particles overlapped and formed steps at several places. The flow over the steps scoured the
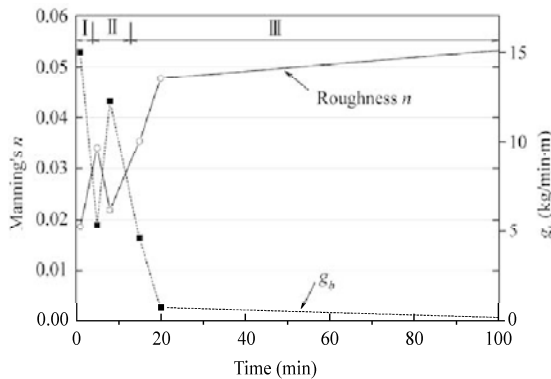
Fig. 3.33 Variation of Manning's roughness coefficient, n, and the rate of sediment transportation per width, g_b, during the three stages of channel bed development for a step-pool system

sections downstream of the steps and dug them into pools. The resistance increased further, and, thus, the erosion reduced. Finally the roughness reached its maximum and the channel bed became stable (Stage Ⅲ). The rate of sediment transportation to the downstream end decreased to nearly zero.

The development of a step-pool system needs a period of time under natural conditions, depending on the bed sediment composition, incoming sediment load, and hydrological features of the stream. Artificial step-pool systems obtained by simply placing boulders and cobbles together to form steps at a regular spacing may speed up the process. In one experiment in the flume, large gravel was put into the flume to form rough artificial steps. Then, clear water flows through the channel and the step-pool system gradually developed. The time needed for maturity of the step-pool system is only one fifth of the time for the natural development process. Much less sediment was eroded from the bed during the artificial process than that in the natural development process.

A step-pool system stabilizes the streambed because the steps maximize the flow resistance, consume the flow energy and protect the streambed from erosion (Whittaker and Jaeggi Martin, 1982; Abrahams et al., 1995). Thus, an explanation of why step-pool systems develop and why they have a particular morphology can be couched in terms of their effect on energy dissipation. In the experiments, the step-pool system developed, and, then the bed became stable. In mountain streams in the Cascades of Washington state, the resistance caused by step-pool systems composes more than 90%, and the grain resistance and channel form drag make up less than 10% of the total (Curran and Wohl, 2003). Because the resistance caused by step-pool systems makes up the main resistance of the flow, Manning's roughness coefficient, n, is a function of the development degree of the step-pool system.

Figure 3.34 shows Manning's roughness coefficient n from the experiments and field investigations as a function of S_P. In general, Manning's roughness coefficient n increases with the step-pool development degree, S_P. However, Manning's roughness coefficient n from the field investigations increases with S_P at a much higher rate than that from the experiments. There are backflow areas and three dimensional large eddies in the streams, which consume a lot of energy. In the flume experiments, however, the width is uniform and no backflow areas and large scale eddies may develop. At the same S_P value for the thalweg profile, the resistance is smaller in the experiments than that in the streams.
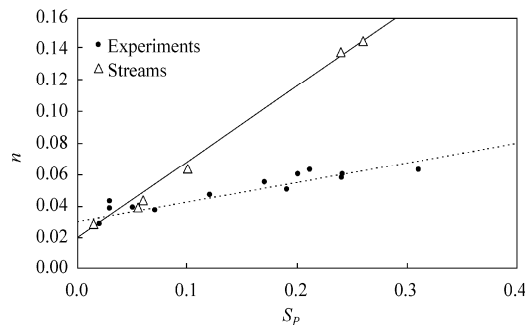
Fig. 3.34 Manning's roughness coefficient n as a function of the development degree of the step-pool system S_P

Wang et al. (1999) proposed a concept of river bed inertia: if the channel bed scour by flows is regarded as a kind of accelerating motion of the bed, the sediment carrying capacity of the flow is a "positive force" and the incoming sediment load is a "negative force", the resistance to the bed scour is defined as the "channel bed inertia". Only if the "positive force" is balanced by the "negative force" or the channel bed inertia is infinity, the river bed remains undeformed. Details of the concept are discussed

in Chapter 5. The river bed inertia can be calculated with the formula:

$$I_b = \gamma_s (1-p) \frac{g_{b*} - g_{bin}}{S_r}$$
(3.6)

where p is the porosity, $\gamma_s(1-p)$ is the dry weight of the bed material, S_r is the scour rate of the channel bed in weight per area per time, g_{b*} is the bed load carrying capacity of the flow, or the rate of bed load transport by the flow when in equilibrium, g_{bin} is the rate of bed load carried by the flow at the entrance of the studied reach. For a given composition of bed material, the bed inertia I_b is regarded as a constant. Small bed inertia implies that the bed deforms quickly with the change of flow and has low stability. If the bed inertia is large, the bed responds mimimally to the flow changes. The riverbed inertia depends on the development degree of the bed structure and composition of the bed material. If there is no structure, the river bed inertia increases with the sorting coefficient of bed material, D_{90}/D_{10}.

The development of a step-pool system enhances the river bed inertia. Figure 3.35 shows the channel bed inertia of the Jiangjia Ravine and Fork Gully in comparison with the experimental results as a function of D_{90}/D_{10}, where the subscript indicates the percentage of the particles smaller than this diameter For the Jiangjia Ravine, the bed load carrying capacity is equal to 0.759 kg/s.m for a flow with hydraulic radius of 0.08 m. A field experiment was done by closing a branch of the stream and cutting bed load transportation from upstream, thus, creating a clear water flow of a hydraulic radius of 0.08 m in a single channel section. All sediment collected in the downstream end of the section was scoured from the section. The measured scour rate of bed sediment from the section was on average 0.01 kg/sm². The riverbed inertia calculated with Eq. (3.6) equals to 141 t/m². The water flowing in Fork Gully is from fountain springs. The scour rate was measured at 6.6×10^{-5} kg/s·m in a flow with hydraulic radius of 0.055 m. The river bed inertia calculated equals 17,000 t/m². In Shengou and Jiuzhai creeks, the water depth is large but the flow cannot scour sediment from the bed because the step-pool system protects the bed sediment from erosion. In other words, the scour rate is zero for almost all flow conditions. For instance, the step-pool system has developed in the middle and lower reaches of Shengou Creek in 2001. The creek has not eroded down in the period 2001-2007. Only the sediment load from upper reaches may have partly been transported through the middle and lower reaches in the period. For most cases the scour rate is zero, therefore, the riverbed inertia is infinite.
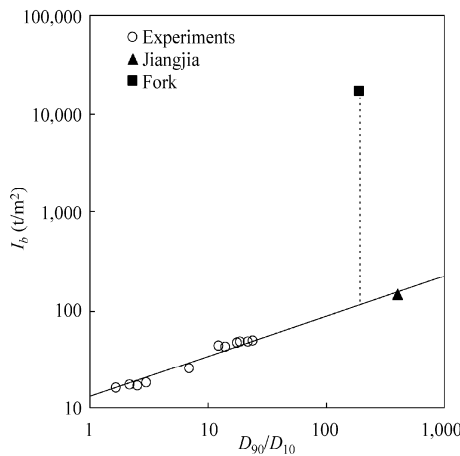
Fig. 3.35   Riverbed inertia, I_b as a function of the sorting coefficient D_{90}/D_{10} for channel beds without a step-pool system and with a developing step-pool system

In the experiments, no step-pools could develop if there is no gravel larger than 1/8 times of the channel width. Sediment with size distribution 1,2, or 3 in Fig. 3.31 were used to study the mechanism of step-pool development and results show that only several step-pools developed with size distribution 3, and continuous step-pool systems developed well with size distributions 1 and 2.

Incoming sediment load from the upstream entrance negatively affects the development of step-pools. In a few experiments sediment was supplied to the flow from the entrance of the flume. The sediment load reduced or even stopped the development of step-pools. In fact, the step-pool system develops as a result of bed erosion. If the incoming sediment load is equal to or greater than the sediment-carrying capacity of the flow, there is no bed erosion, and, hence, step-pools cannot develop. The same conclusion has been obtained from field investigation in the Xiaojiang watershed on the Yunnan Plateau, China.

From the laboratory experiments and field investigations it has been learned that the development of step-pools requires: ①high channel bed slope, generally in the range of 3%－20%; ②small width/depth ratio; ③non-uniform sediment composition; and ④sediment-starved flow and channel bed erosion. Analyzing the data the following empirical formula has been obtained to estimate the degree of development of the step-pool system:

$$S_P = \alpha S \left(\frac{D_{max}}{D_{50}} - b \right)^m \left(1 - \frac{g_{bin}}{g_b} \right) + c \tag{3.7}$$

in which D_{max} is the maximum diameter of the bed materials，g_{bin} and g_b are the incoming bed load from upstream and bed-load carrying capacity of the flow. The coefficient α, the constant b and c, and the exponent m may have different values in different streams and should be determined with data.

Experiments and field investigations have proved that the development of step-pool systems increases the flow resistance, consumes the flow energy, and protects the streambed from erosion. The results of flume experiments have extended this role in suggesting that step-pool systems not only increase flow resistance but also maximize it (Whittaker and Jaeggi Martin, 1982; Abrahams et al., 1995). Their innovative experiments and field observations led Abrahams et al. (1995) to conclude that step-pool systems, evolve towards a state of maximum resistance because that implies maximum stability. Thus, an explanation of why step-pool systems develop and why they have a particular morphology can be couched in terms of their effect on energy dissipation. Moreover, step-pools may provide high diversity of habitats for aquatic bio-communities. The flows over the steps adsorb oxygen from the air and increase the concentration of dissolved oxygen, which is important for the aquatic ecosystem.The experiments indicated that the resistance of step-pools is high for low flow depths and low for high flow depths. If the flow depth is less than the height of the steps, the flow over the steps jumps into the pools and causes turbulent eddies and a hydraulic jump. If the flow depth is high, the steps are submerged under water, the flow skims over the steps, no hydraulic jumps result, and the energy dissipation is less (Curran and Wohl, 2003). Following the increase in the relative depth the function of energy dissipation of step-pools reduces and the resistance then becomes smaller and smaller. In most cases the flow depth is less than the step height and hydraulic jumps occur in the pool sections. The function of energy dissipation of step-pools is closely related to the hydraulic jumps. The flow is supercritical in the step sections and becomes subcritical in the pool sections. The hydraulic jump makes the flow change from supercritical to subcritical and during the jump the flow energy is dissipated. A lot of turbulent eddies are produced and air bubbles are mixed with water in the jumps.

In summary, a step-pool system develops when the streambed undergoes erosion. If the flow power is small, fine particles are removed and coarse particles remain and form an armor layer, which creates, high grain resistance. If the flow power is high and all particles can be removed by the flow, the moving particles form dunes, which generate form drag. If there are cobbles and large gravel, the largest particles

act as keystones in the development of steps. Behind the steps the bed is scoured into pools. The flow over the steps is supercritical, and the flow is subcritical in the pools. The resistance is maximized by the development of the step-pool system. The development degree of step-pools is proportional to the streambed slope. If the incoming sediment load is equal to or more than the sediment-carrying capacity of the flow, no bed erosion occurs and, hence, no step-pools form. The rate of energy dissipation resulting from step-pools is a function of S_P. The higher is S_P, the larger is the rate of energy dissipation. The step-pool system increases the resistance and flow depth, reduces the shear stress, and protects the streambed from erosion. A step-pool system not only stabilizes the streambed but also provides ecologically sound habitats for the aquatic bio-community. The flow over the steps adsorbs oxygen and increases the concentration of dissolved oxygen, which is important for the aquatic ecosystem.

3.3.3 Other Types of Bed Structures

River bed configurations in natural streams are shaped by varying flows; at competent flows the least stable particles move into more stable positions to create structured bed forms. The step-pool system is the strongest bed structure resisting channel incision. Other commonly occurring bed structures in high gradient small mountain streams are ribbing structures occurring in less high gradient middle sized mountain streams, and star-studded boulders, bank stones, and pebble clusters occurring in low slope large mountain rivers. The additional mechanical strength of the bed structures is results from three sources: ① grain-to-grain contact involving intergranular friction; ② particle interlock; and ③ shelter, especially of the particles in the wake tail. The structures reduce the lift and drag forces acting on the particles in the lee side of the structures (Reid, 1992). These structures function in resisting channel incision and stabilizing the channel bed.

3.3.3.1 Ribbing Structures

In streams with slopes in the range 0.5% – 3% ribbing structures often develop, enhancing the flow resistance and mitigating channel incision. Figure 3.36 shows typical ribbing structures. Cobbles and boulders overlap with each other and form ribs extending out from the banks. The structure exhibits high stability and enhances high resistance against the flow, thus, protecting the banks and channel bed from erosion. Figure 3.37 shows two bridges on a tributary of the East River in Guangdong Province, southern China. The comparison shows the effect of channel incision control provided by ribbing structures. In the downstream section of the river without ribbing structures the channel bed is eroded down by about 2 m

(a)	(b)

Fig. 3.36 (a) Ribbing structure in the Yuzixi River, a tributary of the Minjiang River; (b) Ribbing structure developed in a tributary of the East River in southern China

and the bridge is endangered by the incision (left picture). In the upstream section with ribbing structures (the ribbing structure is shown in Fig. 3.37(b)) the channel bed remains stable, no channel incision occurred, and the bridge is safe. The two sections are only 6 km apart and the flow discharge is the same.

The Balan River is a tributary of the Songhua River in northeastern China. The bed slope is about 0.5% – 1% and ribbing structures have developed on the bed. The ribbing structures are composed of cobbles, gravel, and some boulders, as shown in Fig. 3.38. The structures have successfully controlled channel incision and the channel bed is stable.
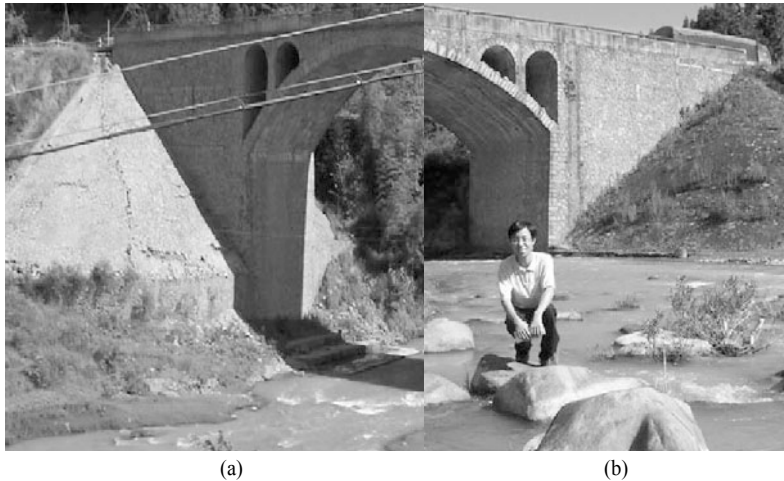
(a)   (b)

Fig. 3.37 (a) In a section of a tributary of the East River without ribbing structures the channel bed is eroded down by about 2 m and the bridge is endangered by the incision; (b) In a section of the same stream with ribbing structures the channel bed remains stable (See color figure at the end of this book)

Fig. 3.38 Ribbing structures in the Balan River, which is a tributary of the Songhua River in northeastern China. The ribbing structure is composed of cobbles, gravel, and some boulders

3.3.3.2 Star-Studded Boulders

In mountain streams with gradient of 0.5% – 1% a bed structure of star-studded boulders develops, which consists of a series of sections with high bed gradient with star-studded boulders and supercritical flows between two sections with gentle slope and sub-critical flows. In the Balan River, there are several reaches with star-studded boulders. Many boulders with diameters around 0.5 – 1.5 m are scattered on the channel bed. These boulders distribute on the channel bed randomly, and they emerge from the whole

channel including the deepest part of the channel, as shown in Fig. 3.39. The randomly distributed boulders on the channel bed create a high and uniform resistance throughout the channel bed, and, thus, consume the energy of the flow and form a stable channel bed. The reaches with the star-studded boulders are about 200 – 500 m long, and there are reaches 0.5 – 3 km long with a gravel bed and deep water between every two reaches with the star-studded boulders. The slope in the reaches with the star-studded boulders is about two times of the slope of the reaches with a gravel bed. Figure 3.39 shows two reaches with star-studded boulders.

Fig. 3.39   Two reaches with the star-studded boulders in the Balan River in northeastern China

3.3.3.3   Bank Stones

Bank stones structures are simple self-developed structures of incised rivers for protection of the banks. Figure 3.40(a) shows the bank stone structure on the Dadu River in Sichuan Province. Boulders of diameter larger than 1 m line on the two side of the channel and increase the bank roughness. Thus, the flow velocity is reduced near the banks and high velocity current cannot assault the banks. The bank stones structure effectively controls bank erosion and protects the Danba County Town. Figure 3.40(b) shows the bank stones in the 200 m wide Jialing River, a tributary of the Yangtze River in southwestern China. Boulders and stones are transported from the nearby tributaries and gullies and line the banks. The structure reduces the current velocity and enhances the stability of the channel.

3.3.3.4   Boulder and Cobble Clusters

Boulder and cobble clusters are accumulations of sediment on either (or both) the lee and the stoss side of an obstacle clast in rivers with poorly sorted sediments (Wittenberg, 2002a). These bed forms are considered to develop periodically during the falling stage of high flow events under rapid turbulent flow. Cluster bed forms are the most prevalent type of small-scale bed forms in gravel-bed rivers and contribute to roughness properties and the enhanced bed stability. Figure 3.41(a) shows the boulder clusters in the Baohe River, a tributary of the Hanjiang River and Fig. 3.41(b) shows the cobble clusters with a shape of a diamond in the Golden Whip Brook in the Xiangjiang River basin in Central China.

Sear (1992) and Sohag (1993) used a dynamic penetrometer to set bed stability criteria in relation to the bed strength exerted by different structural arrangements of bed particles. Sear (1996) found that clusters, especially obstacle clasts, wake and stoss accumulations, are among the most resistant configurations of a gravel riverbed to entrainment. Shear stress required to entrain clustered sediments is higher than that required for entraining open bed particles (Brayshaw, 1985; Reid., 1992; James, 1993;

(a)

(b)

Fig. 3.40 (a) Bank stones structure on the Dadu River, which protects the Danba County Town; (b) Bank stones structure on the Jialing River (See color figure at the end of this book)
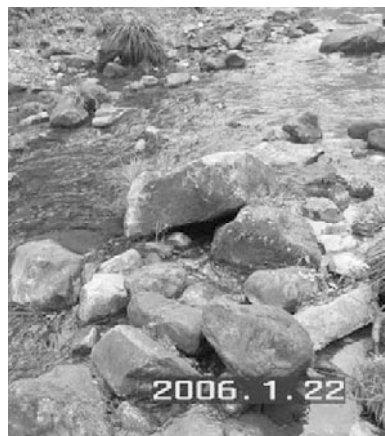
(a)   (b)

Fig. 3.41 (a) Pebble clusters in the Baohe River, a tributary of the Hanjiang River showing a shape like the alignment of wide geese; (b) Cobble clusters in the Golden Whip Brook in the Xiangjiang River basin in Central China, showing a diamond shaped cluster

Hassan and Church, 2000). Consequently, the overall transport distance of clustered sediments is less than unconstrained particles (Laronne and Carson, 1976; Brayshaw, 1985; Reid., 1992). Since pebble clusters may occupy 10－50 percent of the river bed (Hassan and Reid, 1990; Reid., 1992; Wittenberg, 2002b) their role in influencing equilibrium conditions on riverbeds, and, hence, channel sections, cannot be ignored.

Wittenberg and Newson (2005) took a morphological approach to interpreting the initiation and movement of gravel, using particle tracing to determine the movement of individual cluster particles over a range of flood event magnitudes and durations. The experiment was carried out on the River South Tyne, UK, in 1996. They used flow hydrographs measured nearby and also benefited from previous studies of historical development, channel morphology, and sediment transport at the same site. More than 30 clusters were monitored over a seven-month period during which a flood with a peak discharge of 183 m³/s occurred. The clusters occupied 7－16 percent of the bed，as shown in Fig. 3.42. Changes occurred at each element of the cluster: stoss, obstacle, and wake. Wake particles are transported most easily. Four processes were common: ①scouring and removal of cluster particles; ②aggregation of particles due to deposition processes, ③*in-situ* modifications, namely dislodgement, without major replacement or transportation; and ④formation of new bed forms.
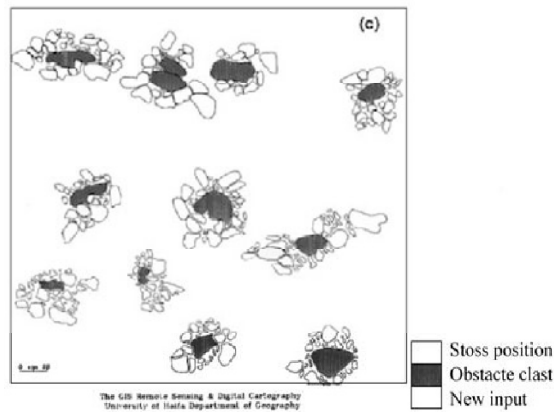
Fig. 3.42   Spatial distribution of clusters (after Wittenberg and Newson, 2005)

At the cluster scale, stoss and wake particles moved for the relatively short distances for flows that were insufficient to dislodge the obstacle clasts. *Random movement* of stoss particles occurred for distances of less than 1 m and most of the wake particles were entrained. Nonetheless, similar-sized wake particles and stoss particles exhibited different transport distances. Wake particles moved further downstream compared to stoss particles of the same size. The movement length of a single clast is limited and generally ceases when the clast is entrapped by an adjacent cluster. The bed area covered with clusters does not exhibit profound changes; also, neither the surface grain size distribution, nor the structure of the main bed forms altered.

3.4   Environmental Impacts and Control Strategies of Riverbed Incision

3.4.1   Environmental Impacts

The most disastrous consequence of riverbed incision is increased bank slopes and landslides. Channel degradation may affect the stability of slopes. The case of the Fier River, a tributary of the upper Rhine

River, is spectacular. With incision exceeding 10 m, landslides were generated on hillslopes due to both modification of aquifer drainage and footslope destabilization by channel degradation. This example illustrates negative effects on human activities, especially when landslides occur in urbanized areas affecting roads and houses. The relation between landslide and riverbed incision will be discussed in Chapter 4.

The most far-reaching influence of channel incision is soil erosion. In fact stream channel incision is the essential cause of bank erosion, rill erosion, and slope erosion. Channel incision increases stream slope, bank slope, and instability of watershed slope. The increased soil erosion and sediment yield may cause a new cycle of fluvial processes of the river. The process may last for a century or a longer period of time. Over history the Yellow River scoured the channel down to the bedrock in the middle reaches, which reduced the base level of all tributaries from the Loess Plateau. Most of these tributaries have not reached equilibrium and headward channel erosion, bank erosion, and gully erosion are still continuing after centuries. Figure 3.43 shows the eroded gullies in the loess plateau and headward erosion.

Fig. 3.43 Eroded gullies in the Loess Plateau and headward erosion, which are essentially caused by channel incision of rivers on the plateau

The Xiaojiang River in Yunnan was an incised river and experienced a high rate of bed incision because its confluence with the Jinsha River was suddenly scoured down around a million years ago. The incision propagated upstream and propagated into its tributaries. The Jiangjia Ravine is a tributary of Xiaojiang River. The incision caused soil erosion in its watershed, which has become the most serious erosion land in the Xiaojiang River basin. In a recent period the upper Jiangjia Ravine experienced an accelerate incision, which caused gravitational erosion and a new cycle of slope soil erosion. Figure 3.44(a) shows the incised upper Jiangjia Ravine. The ravine was incised down and there is no bed structure to resist the incision because the lithology consists mainly of shale, which was broken due to tectonic motion. Thus the lower part of the ravine banks is very steep. Serious gravitational erosion occurred, as shown in Fig. 3.44(b). Bank failures and landslides occurred and destroyed the pine forest, which was developed on the slope before the accelerated incision and the new cycle of erosion.

The direct and short-term impacts of channel incision are listed in Table 3.6, including damage to human structures, and impacts on aquatic and riparian ecosystems. This review is not intended to be comprehensive, rather examples are cited only to illustrate the trends summarized from the literature.

Obviously, many of the effects listed are closely related, and others might choose to organize them differently, but the review presented here should provide a systematic overview of the environmental effects of channel incision.

(a)   (b)

Fig. 3.44   (a) Incised upper Jiangjia Ravine; (b) Bank failures and landslides destroyed the pine forest at the upper end of the Jiangjia Ravine (See color figure at the end of this book)

Table 3.6   Review of environmental, ecological, and societal impacts of channel incision (after Bravard et al., 1999)

Effects on channel geometry, structures, and riparian vegetation	Environmental, ecological, and societal impacts	Location and references
Narrowing of active channel, decreased width/depth ratio	Reduced area of aquatic habitat and altered channel margin habitat; Reduced bed surface for infiltration and groundwater recharge. Concentration of flow and increased shear stress lead to further incision	Bear River, California (James, 1991); Cache Creek, California (Northwest Hydraulics consultants, 1995); Southeast France (Bravard et al., 1997)
Channel simplification and abandonment of multiple channels	Loss of habitat diversity. Impoverishment of fish community. Reduced length of channel margin habitat	northern Mississippi (Shields et al., 1994)
Modification of bank morphology	Bank erosion and subsequent channel widening and instability, loss of agricultural land, and infrastructure. Change in bank configuration reduces opportunity for seedling establishment downstream.	northern Mississippi (Thorne, 1997) Iowa (Lohnes, 1997); Marias River, Montana (Rood and Mahoney, 1995)
Increased sediment transport to downstream from erosion of bed and banks	Aggradation of downstream reaches	Wooler Water, UK (Sear and Archer, 1998)
Loss of gravel bars	Loss of habitat, reduced biodiversity	Isar and Lech Rivers, Bavaria, Germany (Reich, 1991, 1994)
Armoring (coarsening of substrate)	Loss of spawning gravels for fish	Sacramento River, California (Parfitt and Buer, 1980); Garonne River, France (Beaudelin, 1989)
Exposure of bedrock	Loss of spawning gravels and hyporheic habitats, Loss of groundwater, Barrier to fish migration	Ardeche and Dr6me Rivers (Landon and Piegay, 1994)

(Continued)

Undermining hill slopes	Trigger landslides, which deliver large quantities of sediment to the channel	Fier River, France (Bravard et al., 1997)
Undermining of bridges	Loss or costly repair of bridges	Colorado (Lane, 1955); Tujunga Wash, California (Scott, 1973); Arizona (Bull and Scott, 1974); Apenine rivers, Italy (Tagliavini, 1978); Stony Creek, California (Kondolf and Swanson, 1993); Loire River, France (Gasowski, 1994); Cache Creek, California (Northwest Hydraulics consultants, 1995); western Iowa (Lohnes, 1997); Arroyo Passajero, California (Leclerc et al., 1997); Wooler Water, UK (Sear and Archer, 1998); Arno River, Italy (Billi et al., 1997); Kaoping River, Taiwan (Kondolf, 1997)
Undermining of dikes and embankments	Loss or costly repair	Otaki River, New Zealand (Soil and Water, 1985); Arve River, France (Peiry, 1993; Blanc et al., 1989); Drome River, France (Landon et al., in press)
Undermining of pipeline crossings	Loss or costly repair	San Luis Rey River, Califronia (PBGS., 1994) Arroyo Passajero, California (Leclerc et al., 1997)
Reduced filtering of water into water supply intakes	Reduced water quality, potentially increased treatment expense	Russian River, California (Marcus, 1992) Mad River, California (Lehre et al., 1993)
Lowering of alluvial water table	Loss of alluvial groundwater storage. Dewatering and loss of hyporheic habitat in river banks. Dewatering roots of riparian vegetation and/or prevention of new plants establishing, modification of tree growth and transpiration (e.g., poplar); Drainage of formerly saturated active channel, permitting establishment of riparian forests. Dewatering of floodplain wetlands and former channels, converting vegetation and invertebrate communities. Modification of water physico-chemistry	southeast Australia (Eyles, 1977); Enza River, Italy (Tagliavini, 1978); Missouri River (Reilly and Johnson, 1982); Zimbabwe (Whitlow, 1985); Ain River, France (Roux, 1986; Pautou and Girel, 1986; Marston et al., 1995); Rhone River, France (Pautou, 1988); Southwestern U.S. (DeBano and Schmidt, 1989); Rhone River, France (Creuzé des Cha.telliers and Reygrobellet, 1990); Drome River, France (SOGREAH, 1991); Laboratory (Rood and Mahoney 1995); Russian River, California (Sonoma County, 1992); Lake County, California (Lake County, 1992)

The incision of the channel bed enhances the river capacity to discharge flood flow. The enhanced channel capacity typically leads to more rapid transmission of floodwaters downstream. While this reduces flood risk on-site and upstream, it increases flood hazard downstream because flood peaks are no longer attenuated by channel and floodplain storage. Beaudelin (1989) showed that the travel time of similar flood waves on the Garonne River decreased from 19 to 10 hours between Toulouse and Castelsarrazin (60 km) from 1950 to the late 1980s as a result of incision, increasing flood risks downstream.

Channel incision can result in the loss of gravel bars, and, consequently, the loss of habitat and biodiversity. It was reported that on the Isar and Lech Rivers in Bavaria (Reich, 1991, 1994), incision of the riverbed caused the loss of the plants Myricaria germanica, as well as the birds that prefer these plants for habitat. The encroachment of willow thickets and pine forest has reduced the number and area of pioneer habitats, isolating areas of open gravel bars (i.e., creating gaps in this once continuous habitat), and increasing the upstream to downstream distance between habitats, which has modified colonization

dynamics of species. The length of gaps between the gravel bars along the Isar River was 80 to 100 m in 1925, but 100 to 1,500 m in 1985. As a result, a grasshopper species is endangered due to a lack of large gravel bars and the large gaps between bars.

With increased shear stress, the incised reach may become armored as smaller, more mobile gravel is exported downstream, leaving only larger, less mobile particles in the reach (Livesey, 1965). One consequence is the loss of spawning habitat for fish such as the Alosa fallax in the upper Garonne River, sturgeon in the lower Garonne (Beaudelin, 1989), and chinoot salmon in the Sacramento River in California (Parfitt and Buer, 1980). Bed gravel may completely disappear, leaving bedrock exposed. This eliminates not only spawning habitat but also refuge and hyporheic habitat for juvenile fish, invertebrates, and microorganisms between large particles in the bed. Exposure of bedrock can create knickpoints, which can be barriers to the upstream migration of fish. Incision of the Fier River, France, in the 1970s, exhumed a 6 m high limestone outcrop that blocks migration of salmonids.

Incision has come to public attention mostly through impacts on human structures and the high costs of repair or replacement. Bridges have been extensively affected by channel incision throughout the world on large rivers and small tributaries. Even in the lower reaches of the Yellow River, which has for a long period of time plagued people with serious sedimentation, local incision has caused bridge piles exposure due to the impoundment of the Xiaolangdi Dam, as shown in Fig. 3.45(a). The same story occurred on the Weihe River, the largest tributary of the Yellow River. Figure 3.45(b) shows a bridge on the river at Baoji. A flood scoured the river bed by 2 m and a buried part of the bridge piers is exposed.

In western Iowa, incision-related damage to bridges between 1916 and 1992 was estimated at 1.1 billion US dollars (Lohnes, 1997). The California Department of Transportation estimated that 1% of the 12,000 bridges over water in the state are severely threatened by scour, mostly related to incision resulting from gravel mining.

Municipal and industrial water supply intakes are often located within alluvial gravels below the riverbed to benefit from the filtering effects of the gravel. Many such intakes have been exposed, or the filtering effects of gravel have been reduced, by incision and loss of overlying bed material (Lehre et al., 1993; Florsheim and Goodwin, 1995). Flood protection embankments are also vulnerable to undercutting by channel incision.

(a)   (b)

Fig. 3.45   (a) Exposed bridge piles on the lower Yellow River due to release of clear water from the Xiaolangdi Reservoir eroding the channel bed; (b) A buried part of the bridge piers is exposed due to incision on the Weihe River at Baoji

Incision typically lowers the alluvial water table, because the channel determines the level down to which the alluvial groundwater drains. As the channel lowers, the alluvial water table migrates downward as well. Lowering of the alluvial water table directly results in loss of groundwater storage. In some cases, wells can be lowered and water pumped from greater depths, increasing water costs significantly. Along the lower Drome River an estimated 6×10^6 m^3 of groundwater storage has been lost because of incision of 3 to 5 m since 1960 (SOGREAH, 1991). Similarly, along a 18 km reach of the Enza River, Italy, an estimated 1.4×10^6 m^3 of groundwater storage was lost in 25 years due to incision (Tagliavini, 1978).

Fig. 3.46 Dying riparian forest in northeastern China. Incision has resulted in a drop of the water table below the root zone of the trees

Lowering of the alluvial water table can induce profound ecological and landscape changes, including the loss of riparian vegetation as the water table and capillary fringe drop below the root zone of riparian plants. In northeast China, lowering of the water table by channel incision induced extensive mortality of juvenile woods (Fig. 3.46). The character of the landscape can change as riparian corridors disappear from desert landscapes.

3.4.2 Incision Control Strategies

3.4.2.1 Control Strategies

Channel incision essentially results from high flow velocity and insufficient bed load. Therefore, there are two kinds of strategies to control incision: ①enhance the bed resistance to reduce the flow velocity; and ②increase bed load. Humans can intervene and prevent channel incision by utilizing a variety of channel stabilization procedures. Channel deepening may cease as a result of geologic controls or geomorphic changes, but climatic, hydrologic, and animal changes will probably only change the rate at which the channel evolves. Table 3.7(a) provides a review of control strategies enhancing resistance, and Table 3.7(b) lists the strategies to increase bed load. They are not comprehensive but rather the table presents a framework through which the reader can approach the problem of remediation of the effects of incision.

The process of incision can cause the channel to encounter bedrock and resistant alluvium. This material will greatly reduce or halt incision, and the concentration of coarse sediments can cause armoring of the channel bed, which can halt incision. In addition, the type of sediment in the alluvial valley

Table 3.7   Strategies to control riverbed incision (after Bravard et al., 1999)

(a) Control incision with structures

Strategies	Potential benefits	Location and reference
Preservation of quake lakes	Creation of knickpoint and stabilization of stream profile	Dadu River at the east margin of the Qinghai-Tibet Plateau (Ouimet et al., 2007); Tributaries of the Fujiang, Tuojiang, Minjiang, and Jialing rivers in the Wenchuan earthquake area in southwestern China (Wang et al., 2009)
Weirs	Control downward cutting of the bed	Giffre River (SOGREAH, 1988); Arve River (Peiry et al., 1994); Rhone River (Klingeman et al., 1994, 1998); western Iowa (Lohnes, 1997); Northern Mississippi (Mendrop and Little, 1997); southwestern U.S. (Debano and Schmidt, 1989)
Spur dikes	Increase channel stability	Rhone River (Klingeman et al., 1994, 1998)
Drop pipe structures	Control head cut migration	Yazoo Basin, Mississippi (Smiley et al., 1997)
Bank protection	Prevent outflanking	
Channel widening	Reduce unit stream power and shear stress	Emme River, Switzerland (Jaeggi, 1989)
Compound channel creation	Reduce unit stream power and shear stress	Miller Creek, California (Haltiner et al., 1996)
Beaver re-establishment	Dams control slope and trap sediment	western U.S. and Cooper Creek, Idaho (Marston, 1994)
Restriction of grazing	Enhance riparian vegetation	western U.S. (Platts and Nelson, 1989; Chaney et al., 1990)
Channel armoring		Streams in Germany (Kern, 1994)
Channel relocation		Danube River, Germany (Kern, 1992)
Weirs, spur dikes, drop pipe structures	Improve aquatic habitat	Twentymile Creek, Mississippi (Shields and Hoover, 1991); northwest Mississippi (Shields et al., 1993,1995a); Goodwin Creek, Mississippi (Cooper et al., 1997); Yazoo Basin, Mississippi (Smiley et al., 1997)

(b) Control incision by increasing bed load supply

Strategies	Potential benefits	Location and reference
Supply bed load from upstream	Hill slope destabilization or landslide reactivation	Drome River (Piegay et al., 1997)
Supply bed load from floodplain	Dike destruction and/or streamway preservation	Ainive, France (Bravard et al., 1990); Russian River, California (Florsheim and Goodwin, 1995); Drome River (Piegay et al., 1996a); southeastern France (Piegay et al., 1996b); Loire River, France (Bazin and Gautier, 1996)
Increasing bed load by artificial input (gravel dumping)		Rhine River, Germany (Kuhl, 1992); Danube River, Austria (Golz, 1994); Rhone River (Klingeman et al., 1994, 1998); Meuse River, Netherlands (Klassan et al., 1998);
Increase bed load by land use approaches		Southwestern U.S. (DeBano and Schmidt, 1989); western USA (Chaney et al., 1990)
Floodplain excavation	Improve connectivity between groundwater, floods, and ecological units	southwestern Germany (Kern, 1992); Sweden (Petersen et al., 1992); Rhone River (Piegay et al., 1997b)
Abandoned channel excavation		Rhone River (Henry and Amoros, 1995)
Artificial groundwater supply		Rhone River (Stroffek et al., 1996; Fruget and Michelot, 1997)

fill can significantly affect the process of channel incision and adjustment. For example, it was determined that channels incising into cohesive sediments (silts and clays) deepen rapidly, whereas channels incising into sandy sediments widen rapidly and deepen much less. Hence, natural control of incised-channels is primarily sedimentological, which influences the rate, type, and magnitude of incised-channel evolution.

Bed load motion plays an important role in resisting channel incision. Coarse sediment particles, like gravel, slide or move by saltation on the bed, applying a grain pressure on the stationary bed materials. The pressure is known as the dispersive pressure defined by Bagnold (1954). It may balance the lift force or suction force of the flow, which is the main mechanism of scouring of bed materials. With enough bed load moving on the bed, the channel bed is not scoured and the channel incision is, therefore, stopped.

For cost-effective control of incising channels, timing is most important and, therefore, it is an important variable in any scheme to control an incised channel and to reduce sediment load. Figure 3.47 shows, in general, how incised channel drainage density (length of incised channels per unit area) changes with time and how sediment yield follows this trend. In a drainage basin that contains incising channels, sediment production increases as the length of incising channels increases (Fig. 3.47, Times 1 to 4). However, at Time 4, the maximum, headward growth of the incised channels has ended, and they begin to stabilize between Times 4 and 7. By understanding this cycle of channel incision from initial stability (Time 1) to renewed stability (Time 8) it is possible to select times when channel control practices will be most effective. For example, when incision is just commencing (Times 1 and 2) or when channels are almost stabilized (Times 6, 7, and 8) control measures will be most successful in preventing incision and finally stabilizing the channels, but at Times 6, 7, and 8, the most cost effective action would be to do nothing. At Times 3, 4, and 5, control will be difficult and expensive.
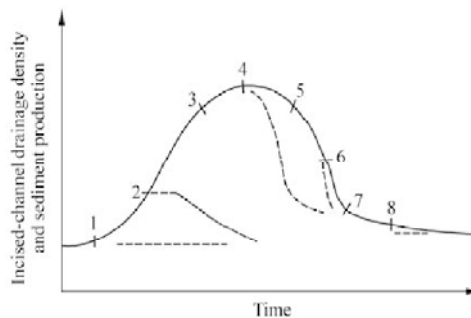
Fig. 3.47   Hypothetical changes of sediment production and incised channel (gully) drainage density at eight times during incised channel evolution. Dashed lines indicate the effect of gully control structures at various times during channel evolution (after Schumm, 1999)

3.4.2.2   Knickpoints

Natural knickpoints (e.g. waterfalls) and artificial knickpoints (e.g., dams) control stream bed incision. Korup and Montgomery (2008) studied the bed incision of the Tsangpo River and concluded that the knickpoints developed from quake lakes created by glacial landslides inhibit channel bed incision. Natural knickpoints may be created by the rivers that cross a sharp lithologic contrast (i.e., weak rock type to strong) in the form of waterfalls, by transient river response to upstream migration of incision in modes of detachment-limited bedrock river incision (Whipple and Tucker, 2002), or by large scale landslides damming streams.

Channel incision of numerous streams on the eastern margin of the Qinghai-Tibet Plateau has produced high-relief, narrow river gorges, and threshold bank hillslopes. The bank slope is so unstable that many

large landslides have occurred during earthquakes or rainstorms. A stable landslide dam stabilizes and blocks a river valley, either initially or after some degree of catastrophic failure and dam-outburst flood erosion. Step-pool system developed on landslide deposits consisting of a high percentage of large (>1 m) boulders often lead to the formation of stable landslide dams and knickpoints.

A landslide dam creates a quake lake or barrier lake on the stream. Once upstream lake levels reach the top of the landslide dam and water flows over the landslide deposits and erosion-resistant boulders armor the channel bed as finer material is washed away. This process condenses the original landslide material to a smaller mass composed of large boulders, stabilizing the landslide dam, and protecting the top of the initial deposit from further erosion. These large boulders are not easily moved in even large floods, and serve to roughen the bottom of the channel. There is often an evidence of advanced fluvial sculpting of boulders, which attests to long periods of boulder stability (Ouimet et al., 2007). Upstream of landslide dams, river gradients are low, and fine-grained lake sediments and alluvial gravels accumulate. The abrupt change in slope associated with the transition from upstream, low-gradient fills to steep, dramatic rapids through the landslide deposits creates significant knickpoints with a drop in elevation of up to 100- to 300-m (Korup, 2006). The integrated effects of large landslides on river channels completely prohibit rivers from eroding their bed and incising over the length of the landslide mass and associated fill deposits.

The period of local non-incision continues for the entire duration of a landslide dam event, from the emplacement of the dam to complete incision through landslide deposits and some portion of the associated upstream fill. During this time, the long-term evolution of the river profile and landscape evolution are affected in two main ways: ①downstream reaches continue to incise, while landslide reaches do not, and ②upstream reaches fill and the whole profile upstream becomes flatter.

The Gesudza He, a tributary of the Dadu River, is dominated by landslide dams, boulder rapids, and impounded alluvial fills for 40 km upstream of its confluence with the Dadu River main stem (Fig. 3.48). The most dramatic of these landslide dams occurs 15 km upstream from the confluence with the Dajin Chuan, with a 150 m drop through the rapids caused by the landslide deposits. Field surveys show nicely the characteristic drop in channel width and increase in channel slope across the landslide mass where the channel is armored by the large boulders. The same conditions occurred in the Dajin Chuan and Xiaojin Chuan rivers, which are also upstream tributaries of the Dadu River. At 17 km of the Xiaojin Chuan and 20 km of the Dajin Chuan, respectively, upstream from the confluence, landslide dams created two knickpoints, which effectively controlled the retrogressive erosion and channel incision of the two rivers.

Large knickpoints at the margin of the Qinghai-Tibet Plateau range in elevation from $1,000-4,000$ m. The total water head of a large knickpoint can be as large as several hundred meters. The Hutiaoxia (i.e., Tiger Leaping Gorge) landslide and avalanche dam on the Jinsha River has a water head of 213 m. Several large knickpoints at Hutiaoxia, Deqin, and Mangkang are shown along the longitudinal profile of the Jinsha River in Fig. 3.49. The Hutiaoxia landslide and avalanche dam created a large barrier lake (Fig. 3.50). Although the discharge of the river was so high to about 4,000 m^3/s the water surface in the barrier lake was as smooth as a mirror because of the huge depth and low flow velocity. The lake traps all bedload and a large portion of the suspended load. The lake has not yet been filled. A step-pool system with huge hydraulic jumps has developed downstream of the barrier lake, consuming most of the flow energy and protecting the river bed from incision.

The large knickpoints may totally change patterns of fluvial processes and river morphology. The upper Yellow River was an incised stream with many deep-gorge sections. Knickpoints developed from landslide dams stopped the incision and formed high gradient reaches in the longitudinal profile. Figure 3.51 shows the bed profile of the upper Yellow River from the source (Erlin Lake) to Longyangxia Dam—the
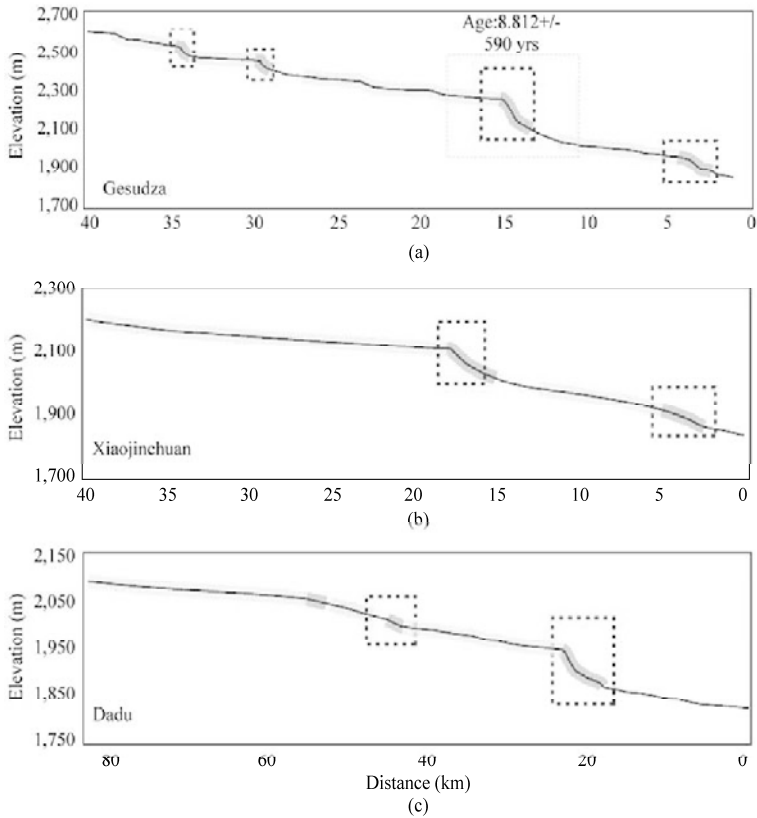
Fig. 3.48 River bed profiles of the Gesudza, Xiaojin Cuan, and Dajin Chuan Rivers, showing the knickpoints developed from landslide dams (after Ouimet et al., 2007)
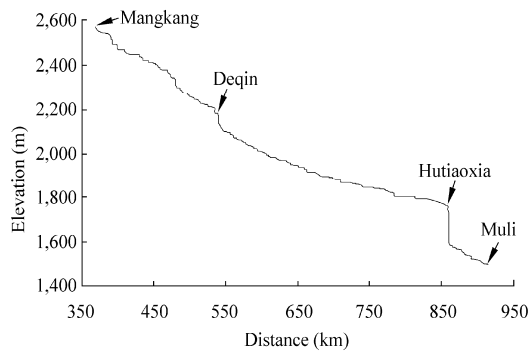
Fig. 3.49 Bed profile of the Jinsha River showing the large knickpoints at Hutiaoxia (Leaping Tiger Gorge), Deqin and Mangkang

uppermost large dam on the river. Two large knickpoints are evident: immediately downstream of Dari County town and downstream of Kesheng Town. Several landslide dams, with large barrier lakes upstream, characterize these knickpoints. These barrier lakes have been filled with sediment. Figure 3.51 (b) shows a part of the Kesheng knickpoint, which consists of several landslide dams and barrier lakes. The
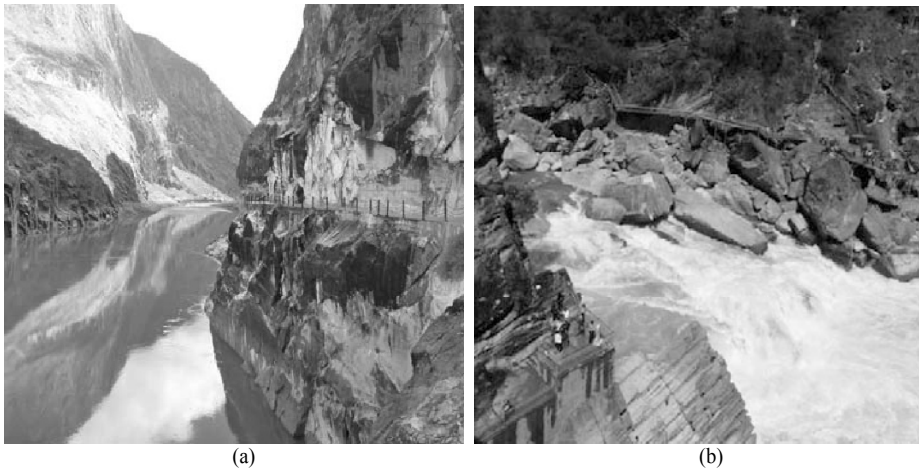
Fig. 3.50 (a) Hutiaoxia barrier lake; (b) Part of the step-pool system on the Hutiaoxia landslide dam (See color figure at the end of this book)

transition from landslide dams into large knickpoints has greatly influenced river profiles and landscape evolution. The longitudinal bed profile of the Yellow River in the 1,400 km long reach is very unusual, with a convex upward curve caused by the two large knickpoints. Harkins et al. (2007) reported a similar phenomenon for tributaries of the Yellow River. Downstream reaches are steep but incision is controlled by step-pool systems. Upstream reaches have adjusted to a new, unchanging base level.
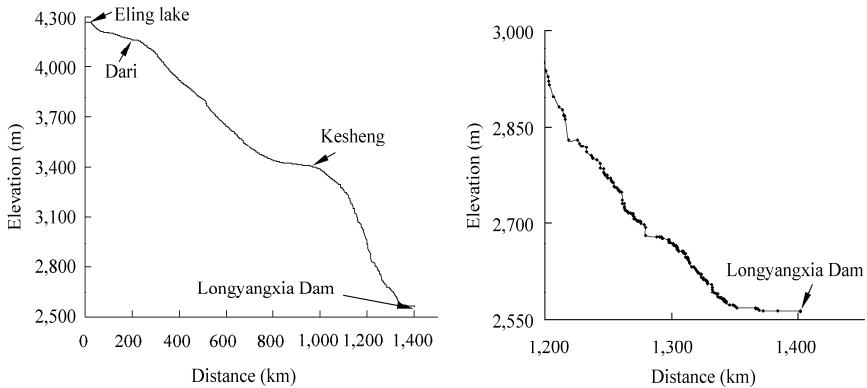
Fig. 3.51 (a) Bed profile of the Yellow River from the source (Erlin Lake) to Longyangxia Dam; (b) Part of the Kesheng knickpoint consisting of several landslide dams and barrier lakes

Long term aggradation following the knickpoint formation has resulted in wide and shallow cross sections in upstream areas, whereas the landslide dam section itself is narrow and deep. The distribution of channel processes, and resulting river morphologies, have adjusted to these damming events. Localized aggradation upstream of knickpoints has brought about a transition from vertical bed evolution to horizontal fluvial process. Reduction in slope and accumulation of fine-grained sediments has facilitated the development of anabranching and braided channel planforms (e.g. just upstream of Dari, see Fig. 3.52).

Fig. 3.52 Satellite image of the anabranching channels upstream of the Dari knickpoint

Several or even hundreds of landslide dams often occurred simultaneously on a reach of an incised mountain river, which were triggered by one great earthquake. The potential energy of bank failure and the slope erosion were greatly reduced and sediment yield from the watershed was reduced nearly to zero. In this case the quake lakes may be preserved for long term and become beautiful landscapes. The Tiger Leaping Gorge lake on the Jinsha River is an examples.

Figure 3.53 shows the bed profile of the Jiuzhai Creek in Sichuan. The creek was an incised mountain stream with average slope of about 4% where intensive landslide activities occurred. More than 100 landslides have created 118 quake lakes and 12 water falls 20,000 years ago. The slope of the spillway channels on the landslide dams is as high as 20% and the deepest lake has an average water depth of more than 80 m. All the landslide dams and quake lakes have been preserved. The preservation of the dams and lakes stopped stream bed incision and stabilized the stream. These landslide dams have become knickpoints controlling the bed incision of the stream. Such system has super-stability and remains stable under extra-ordinary stresses. No more landslides occurred on the Jiuzhai Creek during the Songpan Earthquake in 1976 (Ms 7.2, i.e., magnitude 7.2 in Richter scale), which was only 70 km from Jiuzhai. The Wenchuan earthquake in 2008 (Ms 8.0) had no influence on the Jiuzhai Creek.
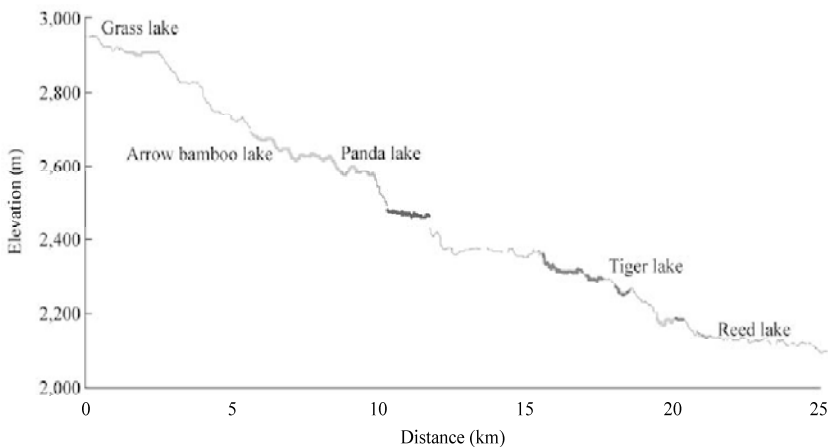
Fig. 3.53 Profile of the Jiuzhai Creek and locations of the landslide dams and lakes

Figure 3.54 shows a landslide dam, the beautiful quake lake, and vegetated step-pool system on the dam of the Jiuzhai Creek. The Jiuzhai Creek has become the most attractive tourist destination in Sichuan. The landslide dams and quake lakes created multiple habitats for riparian and aquatic ecology. Different physical conditions support different bio-communities, and diversified physical conditions may support diversified bio-communities. The landslide dams and quake lakes in the Jiuzhai Creek provide diversified habitats for different species and have the best ecosystems. Samples of benthic invertebrates were taken from the Jiuzhai Creek and 60 other mountain streams in China. The Jiuzhai Creek is among the best mountain streams, which have the highest taxa richness and high abundance.

(a)　　　　　　　　　　　　　　　　(b)
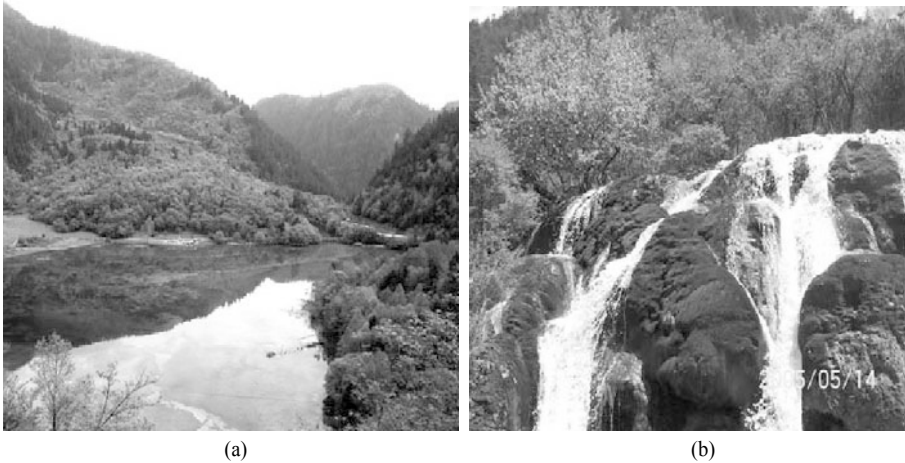
Fig. 3.54 (a) A landslide dam and a quake lake on the Jiuzhai Creek; (b) Beautiful vegetation on the landslide dam

3.4.2.3 Incision Control with Structures

The simplest form of an incision control structure consists of non-erodible material across the channel to form a hard point. These structures are often referred to as rock sills, or bed sills. These types of structures are generally most effective in small stream applications and where the drop heights are generally less than about 1 m. A series of rock sills, each creating a head loss of about 0.6 m, was used successfully on the Gering Drain in Nebraska (Stufft, 1965). The design concept is shown in Fig. 3.55.
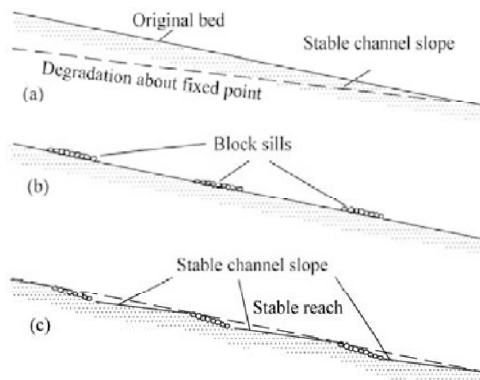
Fig. 3.55 Channel stabilization with rock sills (after Whittaker and Jaeggi, 1986)

Construction of bed sills is sometimes accomplished by simply placing the rock along the streambed to act as a hard point to resist the erosive forces within the degradation zone. In other situations, a trench may be excavated across the streambed and then filled with rock. A critical component in the design of these structures is ensuring that there is a sufficient volume of non-erodible material to resist the general bed degradation, as well as any additional local scour at the structure. This is illustrated in Fig. 3.56, which shows a riprap control structure designed to resist both the general bed degradation as well as any local scour that may be generated at the structure. In this instance, the riprap section must have sufficient mass with an acceptable thickness to fill and protect the anticipated scour hole depth.
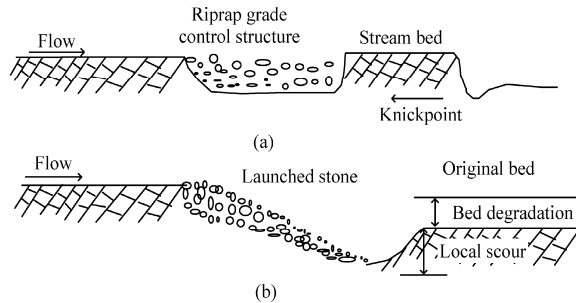
Fig. 3.56 (a) A riprap control structure with sufficient launch stone to handle anticipated scour and (b) the riprap structure in response to bed degradation and local scour

In the case of the sloping riprap drop structures used by the Denver Urban Drainage and Flood Control District, an impervious clay fill is used in conjunction with a lateral cutoff wall (McLaughlin Water Engineers, Ltd., 1986). This design is illustrated in Fig. 3.57. A significant feature that distinguishes the sloping riprap structure from the other structures is the pre-formed, rock protected, scour hole. A scour hole is a natural occurrence downstream of any drop whether it is a natural overfall or a human-made structure. The lateral extent of the scour hole must also be considered to ensure that it does not become so large that the structure is subject to being flanked. With many simple grade control structures in small stream applications, very little, if any, attention is given to the design of a stilling basin or pre-formed scour hole. The erosion is allowed to form the scour hole. However, at higher flow and drop situations, a pre-formed scour hole protected with concrete, riprap, or some other erosion resistant materials is usually required to dissipate energy and to eliminate uncertainties in the size and location of the resultant scour hole. This scour hole serves as a stilling basin for dissipating the energy of the plunging flow.

Weirs are widely used to control channel incision. In effect, weirs act as artificial bedrock outcrops, boulder clusters, or large organic debris in the channel bed. They do not solve the incision problem downstream in cases of sediment starved flows or increased shear stress resulting from channel confinement; rather they physically control the downward cutting of the riverbed in one reach. As shown in Fig. 3.58, the bed profiles of the Giffre River in France measured in 1912 and 1988 show how weirs control the downward cutting of the riverbed. Such solutions may induce fish habitat degradation by blocking migration and increasing reaches with very low slopes. In some cases, installation of weirs in an incising channel can improve aquatic habitat, partially restoring some of the habitat values lost in the process of channel incision. However, their greatest utility is probably the prevention of upstream incision.

DeBano and Schmidt (1989) also illustrated that weirs can raise the water table and favor riparian vegetation recolonization in a desert area (Fig. 3.59). On Twentymile Creek, Mississippi, U.S. weirs

designed to create stable scour holes and a low-flow channel with vegetated banks resulted in more diversified substrate and a greater low-flow channel depth, leading to increased fish abundance and diversity (Shields and Hoover, 1991). Specifically, installation of spur dikes on alternate banks contributed to creation of stable pool/riffle habitats, with increased woody debris related habitat and greater carbon input to the channel.
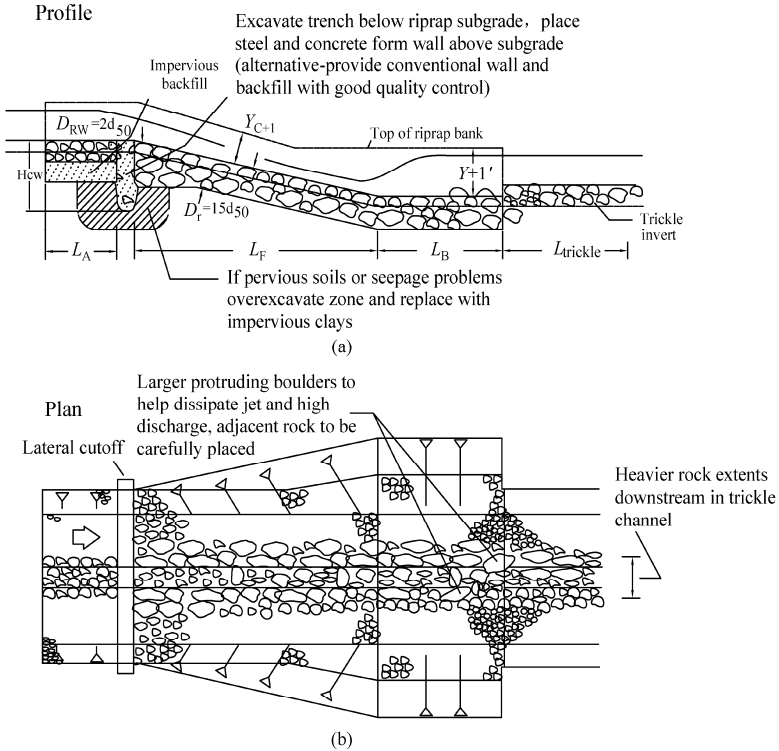
Fig. 3.57 Sloping drop grade control structure with pre-formed riprap lined scour hole (after McLaughlin Water Engineers, Ltd., 1986)
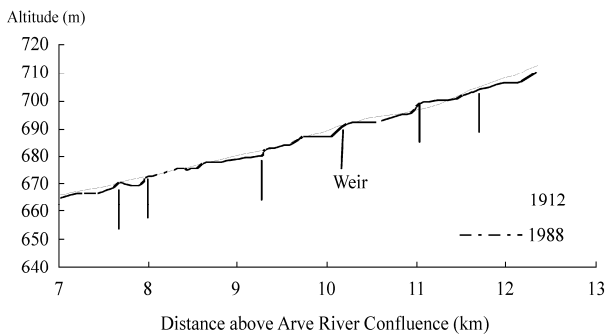
Fig. 3.58 Bed profiles of the Giffre River in France measured in 1912 and 1988. The arrows indicate the location of the weirs (after Bravard et al., 1999)
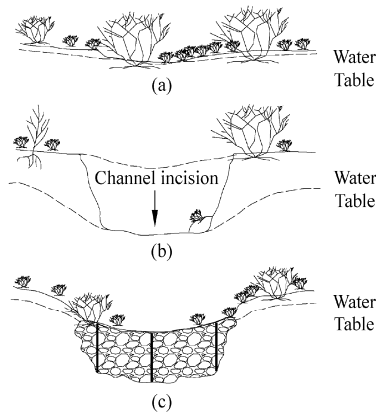
Fig. 3.59 Channel degradation and riparian forest disappearance along streams from semi-desert areas of the western United States. Weirs are used to raise the water table and rehabilitate a riparian buffer strip (after DeBano and Schmidt, 1989)

3.4.2.4 Artificial Step-pool System

In most cases channel incision cannot be controlled. And in many cases, the control structures induce some negative effects. Therefore, remedial strategies are more practical and environmentally sound. One strategy is to create a step-pool system or an armored bed that will resist entrainment, and, thus, prevent incision. Figure 3.60(a) shows the artificial step-pool system on an incised river in Taiwan, China applied to protect a bridge (50 m from the front step). The piers of the bridge are endangered by incision of the channel. Huge stones of diameter up to 2 m were placed on the river bed to form steps. The flow velocity is reduced and the bridge scour is stopped. In Germany many rivers are incised by sediment-starved flows. The government spent 40 million Euros to construct the artificial step-pools on the Mangfall River (Fig. 3.60(b)), which have effectively controlled incision of the channel, although the step-pools have been partly broken by a flood. The riprap steps look natural and form no barrier to fish migration.

When incision results from channel confinement and increased unit stream power, the channel may be modified to reduce unit stream power, basically by reducing gradient or increasing width. The incision control structures discussed above, of course, can reduce gradient by concentrating the river's fall in discrete, controlled steps. The channel gradient can also be reduced by artificially increasing the channel's sinuosity. Width can be increased by mechanically enlarging the channel, or by permitting the river to erode its banks, thereby contributing to the bed load sediment supply as well.

Another strategy to reduce bed shear stress from channel confinement in incised channels is to excavate a new, lower floodplain adjacent to the low-flow channel at a level that will frequently flood. Such "compound" channels have other benefits, because riparian vegetation can be established on the floodplain, increasing habitat value, and the low-flow channel can be permitted to erode its banks and migrate within the compound channel (Haltiner et al., 1996). This approach had been applied to the Meuse River in the Netherlands (Klassan et al., 1998)

3.4.2.5 Bed Load Supply

Artificial step-pools can be used on small and high slope streams, but would probably not be applicable for large rivers with high unit stream power where even coarse particles are likely to be mobilized (Kern, 1997). In this case bed load supply is effective to control incision. As shown in Fig. 3.61, on the Rhine River below the Barrage Iffezheim, an annual average of 170,000 t of sand and gravel are dumped on the river bed from barges to compensate for trapping of bed load by upstream dams (Kuhl, 1992). Key factors

(a)

(b)

Fig. 3.60 (a) A step-pool system, composed of huge stones of diameter up to 2 m effectively mitigates the incision, which endangered the Beifeng Bridge near Taichong; (b) The Mangfall River—a tributary of the Inn River in Germanyr—is protected with artificial step-pools

for the effectiveness of the strategy are the size composition of the sediment fed to the river, and the location and time of dumping. It has been proved that the strategy stopped the incision of the channel not only in the section of dumping but also in the reaches downstream. Similar approaches have been tested in the Danube River below Vienna (Go1z, 1994).

On the Drome River, the sediment budget is in disequilibrium as a result of upland afforestation, which has reduced bed load supply from the catchment, gravel extraction from the channel, and protection of alluvial banks from erosion. River managers have decided, on an experimental basis, to permit sediment from a large landslide to be transported downstream (rather than remove it as would be the standard procedure now) to augment bed load supply to incised downstream reaches (Piegay et al., 1997b). Bed load supply can also be increased by permitting the river to erode its banks upstream. It may require decades before the increased supply to the upper reaches has an effect downstream, but monitoring of the effects is likely to provide extremely useful information for evaluating such strategies elsewhere in the future. With elimination of most upstream gravel supply on the Sacramento River (because of dam construction and gravel mining), bank erosion was an extremely important source of

gravel to the channel, and concerns about the impact on the gravel supply were raised in response to recent proposals to expand bank protection along the river.
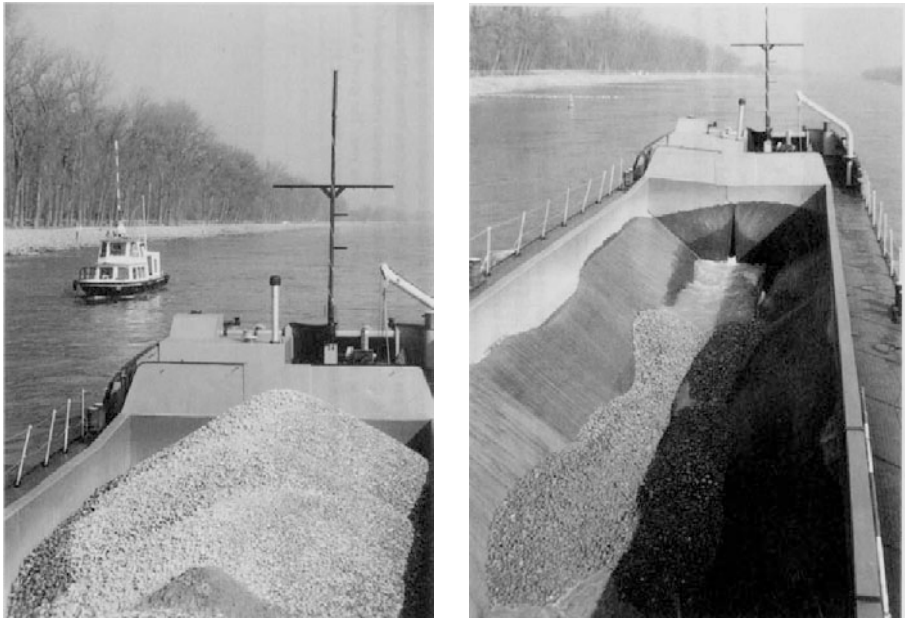
Fig. 3.61   A bottom-dump scow loaded with a sand-gravel mixture is dumping gravel onto the Rhine River bed downstream of the Iffezheim Dam to mitigate the incision of the river (after Kuhl, 1992).

In many cases, the root causes of incision are changes in runoff or sediment generation at the watershed scale. In many European rivers, afforestation and small dam construction in the late 19th century reduced the delivery of sand and gravel to the channel, causing incision, which was later exacerbated by gravel mining and further dam construction (Bravard et al., 1997).

In the cases where the incision has proceeded so far that it cannot be reversed, or where the factors causing the incision cannot be controlled, the most practical approach may be to accept the incision and simply mitigate the effects as best as possible. Because of the environmental effects of lowered water tables, efforts have been made to restore alluvial water tables even if the bed elevation cannot be restored. Along the Gardon River, France, an impermeable dike was buried at depth in the floodplain to dam groundwater, and to restore moisture conditions in the riparian floodplain. In the riparian forest along the Rhone River, a permeable canal has been proposed (Fruget and Michelot, 1997; Stroffek et al., 1996) to supply the forest with water.

In the mountain rivers where the bed surface contains large blocks and boulders the natural resistance against bed erosion is relatively high. Large, isolated boulders induce local energy losses. If the big concrete components are selectively added to the bed surface, then the natural resistance can be increased by taking into account the contribution of the components, which are already in place. For extreme flows this contribution may be insufficient, and the components with individual masses of 10 to 40 t are required. As a result, they have to be manufactured on the spot. While the fact that these elements are made of concrete may not please environmental purists, the application of heavy concrete elements rather than high check dams leaves the low flow conditions in an almost natural state. It is argued that this technique is also a major contribution to river restoration. Such techniques set up hidden training structures which

180

become effective only in extreme events, and shape the channel for normal floods with a more flexible technique, and in particular respect the natural planform alignment.

Review Questions

1. Explain under what conditions the channel incision occurs?.
2. What are the main causes of river channel incision?
3. What are the naturally developed bed structures that resist channel incision?
4. Under what conditions can the step-pools develop?
5. If the step-pools develop in a river, what are the features of the river?
6. Explain the functions of the knickpoints in morphological processes.
7. What environmental and societal effects may be induced by channel incision?
8. How can people control the incision?
9. You are a manager of an incised river, work out a plan to mitigate the impacts of channel incision on environment and ecology.
10. Explain the landscape development during the channel incision process, provide some examples.

References

Abernathy B. and Rutherford I.D., 1998. Where along a river's length will vegetation most effectively stabilise stream banks? Geomorphology, 23, 55–75

Abrahams A.D., Li G. and Atkinson J.F., 1995. Step-pool stream: Adjustment to maximum flow resistance. Water Resources Research, 31(10), 2593–2602

Alford J.J., 1982. San Vicente arroyo. Annals of the Association of American Geographers, 72, 398–403

Anderson M.G. and Kemp M.J., 1991. Towards an improved specification of slope hydrology in the analysis of slope instability problems in the tropics. Progress in Physical Geography, 15, 29–52

Anderson M.G., Collison A.J.C., Hartshorne D.M., Lloyd D.M. and Park A., 1996. Developments in slope hydrology-stability modeling for tropical slopes. In: Advances in hillslope processes, Anderson M.G. and Brooks S.M. (eds.), John Wiley & Sons, Chichester, England, 799–821

Andrews E.D., 1980. Effective and bankfull discharges of streams in the Yampa River Basin, Colorado and Wyoming. Journal of Hydrology, 46, 311–330

Andrews E.D. and Nankervis J.M., 1995. Effective discharge and the design of channel maintenance flows for gravel-bed rivers. In: Natural and Anthropogenic Influences in Fluvial Geomorphology, Costa J.E., Miller A.J., Potter K.W. and Wilcock P.R. (eds.), American Geophysical Union, Washington, DC, 151–164

Bagnold R.A. 1954. Experiments on a gravity free dispersion of large solid spheres in a Newtonian fluid under shear. Proceedings of the Royal Society London, 225A, 49–63

Balling R.C. and Wells S.G., 1990. Historical rainfall patterns and arroyo activity within the Zuni River drainage basin. New Mexico, Annals of the Association of American Geographers, 80, 603–617

Barclay J.S., 1980. Impact of stream alterations on riparian communities in south-central oklahoma, report FWS/OBS-80/17, office of biological services, fish and wildlife service. U.S. Department of the Interior, Washington, DC

Bazin P. and Gautier E., 1996. Un espace de liberte pour la Loire et l`Allier: de la determination a la gestion. Revue de Geographie de Lyon, 71, 377–385 (in French)

Beaudelin P., 1989. Conséquences de l'exploitation de granulats dans la Garonne. Revue de Géographie des Pyrénées et du Sud-Ouest, 4, 603–616 (in French)

Begin Z.B., Meyer D.F. and Schumm S.A., 1980. Knickpoint migration in alluvial channels due to base level lowering. Journal of the Waterways and Ports Division, 106, 369–388

Billi P., Rinaldi M. and Simon A., 1997. Disturbance and adjustment of the Arno River, Central Italy. I. Historical perspectives the last 2000 years. In: Management of landscapes disturbed by channel incision, Wang S.Y., Langendoen E.J. and Shields F.D. (eds.), University of Mississippi, Oxford, ms, 505–600

Bishop P. and Goldrick G., 1992. Morphology, processes and evolution of two waterfalls near Cowra, New South Wales. Aus tralian Geographer, 23, 116–121

Blanc X., Pinteur F. and Sanchis T., 1989. Consequences de 1'enfoncement du lit de l'Arve sur les berges et les ouvrages, bilan general des transports solides sur le cours d'eau. La Houille Blanche, 3–4, 226–230 (in French)

Born S.M. and Rittcr D.F., 1970. Modern terrace development near Pyramid Lake, Nevada, and its geologic implications. Geological Society of America Bulletin, 81, 1233–1242

Bradford J.M. and Piest R.F., 1980. Erosional development of valley-bottom gullies in the upper midwestern United States. In: Thresholds in geomorphology, Coates D.R. and Vitek J.D. (eds.), George Allen and Unwin, Boston, 75–101

Bravard J.P., Amoros C., Pautou G., Bornette G., Bournaud M., Creuze D., Chatelliers M., Gibert J., Peiry J.L., Perrin J.F. and Tachet H., 1997. River incision in south-east France: morphological   phenomena and ecological effects. Regulated Rivers: Research and Management, 13, 1–16

Bravard J.P., Franc O., Landon N., Large J.L. and Peiry J.L., 1990. La basse vallee de I'Ain: Etude geomorphologique. Report. Agence de Vau Rhone Mediterranee Corse (in French)

Bravard J.P., Kondolf G.M. and Piegay H., 1999. Environmental and societal effects of channel incision and remedial strategies, In: Incised Rivers, Darby S.E. and Simon A. (eds.), John Wiley and Sons, Chichester/New York

Brayshaw A.C., 1985. Bed microtopography and entrainment thresholds in gravel bed rivers. Geological Society of American Bulletin, 96, 218–223

Brookes A., 1988. Channelized Rivers: Perspectives for environmental management. John Wiley and Sons, Ltd., Chichester, U.K.

Budel J., 1982. Climatic Geomorphology (translated by L. Fischer and D. Buschc). Princeton University Press, Princeton, NJ

Bull W.B., 1991. Geomorphic Responses to Climate Change. Oxford University Press, Oxford

Bull W.B. and Scott K.M., 1974. Impact of mining gravel from urban stream beds in the southwestern United States. Geology, 2, 171–174

Burkard M.B. and Kostaschuk R.A., 1995. Initiation and evolution of gullies along the shoreline of Lake Huron. Geomorphology, 14, 211–219

Burnett A.W. and Schumm S.A., 1983. Alluvial river response to neotectonic deformation in Louisiana and Mississippi. Science, 222, 49–50

Carling P.A. and Grodek T., 1994. Indirect estimation of ungauged peak discharges in a bedrock channel with reference to design discharge selection. Hydrological Processes, 8, 497–511

Carothers S.W. and Johnson R.R., 1975. The effects of stream channel modifications on birds in the southwestern United States. In: symposium on stream channel modification. Harrisonburg, VA, 60–70

Chaney E., Elmore W. and Platts W.S., 1990. Livestock grazing on western riparian areas. US Environmental Protection Agency, Washington, DC

Chappell J., 1974. The geomorphology and evolution of small valleys in dated coral reef terraces, New Guinea. Journal of Geology, 82, 795–812

Chen J., Gavin H., 2008. Finite Fault Model of the May 12, 2008 Mw 7.9 Eastern Sichuan, China Earthquake. United States Geological Survey–National Earthquake Information Center. http://earthquake.usgs.gov/, Retrieved 2008-05-15.

Chin A., 1999. The morphologic structure of step-pool in mountain streams. Geomorphology, l27, 191–204

Chin A., 2002. The periodic nature of step-pool mountain streams. American Journal of Science, 302, 144–167

Collison A.J.C. and Anderson M.G., 1996. Using a combined slope hydrology/stability model to identify suitable conditions for landslide prevention by vegetation in the humid tropics. Earth Surface Processes and Landforms, 21, 37–747

Cooper CM., Testa S. and Shields F.D., 1997. Invertebrate response to physical habitat changes resulting from rehabilitation efforts in an incised unstable stream. In: management of landscapes disturbed by channel incision,Wang S.S.Y., Langendocn E.J. and Shields F.D. (eds.), University of Mississippi, Oxford, MS, 887–892

Coppin N.J. and Richards I.G., 1990. Use of vegetation in civil engineering. Construction Industry Research and Information Association (CIRIA), London

Creuzé des Chatelliers M. and Reygrobellet J.L., 1990. Interactions between geomorphological processes, benthic and hyporeic communities: First results on a by-passed canal of the French upper Rhône River. Regulated Rivers:

Research and Management, 5, 139–158

Curran J.H. and Wohl E.E., 2003. Large woody debris and flow resistance in step-pool channels, Cascade Range, Washington. Geomorphology, 51(1–3), 141–157

Daniels R.B., 1960. Entrenchment of the willow drainage ditch, Harrison County, Iowa. America Journal of Science, 258, 161–176

Darby S.E. and Simon A., 1999. Incised river channels: processes forms, engineering and management. John Wiley and Sons, Chichester/New York

Darby S.E. and Thorne C.R., 1996. Numerical simulation of widening and bed deformation of straight sand-bed rivers. Journal of Hydraulic Engineering, 122(2), 184–193

De J.C., 1991. A re-appraisal of the significance of obstacle clasts in the cluster bedform dispersal. Earth Surface Processes and Landforms, 16(8), 737–744

DeBano L.F. and Schmidt L.J., 1989. Improving Southwestern Riparian Areas Through Watershed Management. U.S. Department of Agriculture, Forest Service, Fort Collins,CO

Eckley M.S. and Hinchliff D.L., 1986. Glen Canyon Dam's quick fix. Civil Engineering, 56, 46–48

Ergenzinger P., 1992. Riverbed adjustment in a step-pool system in Lainbach, upper Bavaria. In: sediment transport in gravel-bed rivers, Thorne C.R., Bathurst J.C. and Hey R.D. (eds.), Wiley, 415–430

Eyles R.J., 1977. Changes in drainage networks since 1820, southern tablelands, NSW. Australian Geographer, 13, 377–386

Federal Interagency Stream Restoration Working Group, 1997. Stream Corridor Restoration. The National Technical Information Service, U.S.

Florsheim J. and Goodwin P., 1995. Russian River Enhancement Plan: geomorphology and hydrology. Californian Coastal Conservancy, Oakland, CA

Foley M.G., 1980. Bed-rock incision by streams: Summary. Geological Society of America Bulletin, Part II, 91, 577–578

Fourth River Department, 2006. Study on channel bed variations and related regulation strategies for the reach downstream of Chi-Chi weir in Cho-shui River, Zhongxing University, MOEAWRA0950321

Fruget J.F. and Michelot J.L., 1997. Derives cologiques et gestion du milieu fluvial rhodanien. Geocarrefour, 72, 35–48 (in French)

Galay V.J., 1983. Causes of riverbed degradation. Water Resources Research, 19, 1057–1090

Gardner T.W., 1983. Experimental study of knickpoint and longitudinal profile evolution in cohesive, homogeneous material. Geological Society of America Bulletin, 94, 664–672

Gasowski Z., 1994. L'enfoncement du lit de la Loire. Revue de Geographic de Lyon, 69, 41–46 (in French)

Gellis A.C., 1996. Gullying at the Petroglyph National Monument, New Mexico. Soil and Water Conservation, 51, 155–159

Gilbert G.K., 1896. Niagara Falls and their history. National Geographical Monographs, 1, 203–236

Gilbert G.K., 1907. Rate of recession of Niagara Falls. U.S. Geological Survey Bulletin, 306

Goldberg P., 1976. Upper Pleistocene geology of the Avdat/Aqev area. In: Prehistory and Paleoenvironments in the Central Negev, Israel. Vol. 1, The Avdat/Aqev Area, Marks, A.E. (ed.), Southern Methodist University Press, Dallas, 25–55

Golz E., 1994. Bed degradation, nature, causes and countermeasures. Water Science and Technology, 29, 325 − 333

Goudie A., 1982. The Human Impact, MIT Press, Cambridge, MA

Graf W.L., 1983. The arroyo problem-palaeohydrology and palaeohydraulics in the short term. In: Background for palaeohydrology, Gregory K.J. (ed.), John Wiley and Sons, Chichester, England

Granger D.E., Kirchner J.W. and Finkel R.C., 1997. Quaternary downcutting rate of the New River, Virginia, measured from differential decay of cosmogenic ^{26}A1 and ^{10}Be in cave-deposited alluvium. Geology, 25, 107–110

Grant G.E., Swanson F.J. and Wolman M.G., 1990. Pattern and origin of stepped-bed morphology in high gradient streams, Western Cascades, Oregon. Geological Survey of America Bulletin, 102, 340–352

Gray D.H. and Leiser A.J., 1982. Biotechnical slope protection and erosion control. Van Nostrand Reinhold, New York

Hall S.A., 1990. Channel trenching and climatic change in the southern US Great Plains. Geology, 18, 342–345

Haltiner J.P., Kondolf G.M. and Williams P.B., 1996. Restoration approaches in California. In: river channel restoration. guiding principles for sustainable projects, Brookes A. and Shields F.D (eds.), John Wiley and Sons,

Chichester, England, 291–330

Hamblin W.K., Damon P.E. and Bull W.B. 1981. Estimates of vertical crustal strain rates along the western margins of the Colorado Plateau. Geology, 9, 293–298

Harden D.R. and Colman S.M., 1989. Geomorphology and quaternary history of canyonlands, southeastern Utah. In: geological society of america field trip guide. 1988, Holden G.S., (ed.), Colorado School of Mines Professional Contribution 12, 336–369

Harkins N., Kirby E., Heimsath A., Robinson R. and Reiser U., 2007. Transient fluvial incision in the headwaters of the Yellow River, northeastern Tibet, China. Journal of Geophysical Research, Earth Surface, 112, F3

Harvey M.D. and Schumm S.A., 1987. Response of Dry Creek, California, to land use change, gravel mining and dam closure. International Association of Hydrologists Scientific Publication, 165, 451–460

Hassan M.A. and Church M., 2000. Experiments on surface structure and partial sediment transport. Water Resources Research, 36, 1885–1895

Hassan M.A. and Reid I., 1990. The influence of microform bed roughness elements on flow and sediment transport in gravel bed rivers. Earth Surface Processes and Landforms, 15(8), 739–750

Hayward J.A., 1980. Hydrology and stream sediments in a mountain catchment, Ph. D. thesis, Univ. of Canterbury, Christchurch, New Zealand

Heede B.H., Harvey M.D. and Laird J.R., 1988. Sediment delivery linkages in a chaparral watershed following a wildfire. Environmental Management, 12, 349–358

Henry C.P. and Amoros C., 1995. Restoration ecology of riverine wetlands: II. An example in a former channel of the Rhone River. Environmental Management, 19(6), 903–913

Hey R.D. and Thorne C.R., 1986. Stable channels with mobile gravel beds. Journal of Hydraulic Engineering, 112(8), 671–689

Higgins C.G., 1990. Gully development. Geological Society of America Special, Pp, 252

Holland W.N. and Pickup G., 1976. Flume study of knickpoint development in stratified sediment. Geological Society of America Bulletin, 87, 76–82

Hovius N. and Stark C.P., 2006. Landslides from Massive Rock Slope Failure. The Netherlands: Springer

Huber N.K., 1981. Amount and timing of late cenozoic uplift and tilt of the central Sierra Nevada, California-evidence from the upper San Joaquin River Basin. U.S. Geological Survey Professional, Pp, 1197

Huck M.G., Klepper B. and Taylor H.M., 1970. Diurnal variations in root diameter. Plant Physiology, 45, 529–530

Hupp C.R., 1992. Riparian vegetation recovery patterns following stream canalization: A geomorphic perspective. Ecology, 73, 1209–1226

Hupp C.R., 1997. Riparian vegetation, channel incision, and ecogeomorphic recovery. In: Management of Landscapes Disturbed by Channel Incision, Wang S.S.Y., Langendoen E.J. and Shields F.D. (eds.), University of Mississippi, Oxford, MS, 3–11

Hupp C.R. and Simon A., 1991. Bank accretion and the development of vegetated depositional surfaces along modified alluvial channels. Geomorphology, 4, 111–124

Jaeggi M., 1989. Channel engineering and erosion control. In: Alternatives in regulated rivers management, CRC Press, Gore J.A. and Petts G.E. (eds.), Boca Raton, FL, 163–184

James A.L., 1991. Incision and morphologic evolution of an alluvial channel recovering from hydraulic mining sediment. Bulletin of the Geological Society of America, 103, 723–736

James C.S., 1993. Entrainment of spheres-An experimental study of relative size and clustering effects. International Association of Sedimentologists. Special Publication 17, Blackwell, Oxford, 3–10

Jones J.A.A., 1997. Subsurface flow and subsurface erosion. In: Process and Form in Geomorphology, Stoddart D.R. (ed.), Routledge, London, 74–120

Judd H.E. and Peterson D.F., 1969. Hydraulics of large organic debris on channel, Utah Water Research Lab. Utah State University, Logan, Report PRWG, 17–6

Keller E.A. and Pinter N., 1996. Active Tectonics, Prentice-Hall, Upper Saddle River, NJ

Keller E.A. and Swanson F.J., 1979. Effects of large organic material on channel form and fluvial processes. Earth Surface Processes and Landforms, 4, 361–380

Kern K., 1992. Restoration of lowland rivers: The German experience. In: Lowland Floodplain Rivers, Carling P.A. and Petts G.E. (eds.), John Wiley and Sons, Chichester, England, 279–287

Kern K., 1994. Lessons from ten years experience in rehabilitating rivers and streams in Germany. In: Proceedings of the First International Conference on Guidelines for Natural Channel Systems, Shrubsole D. (ed.), Canadian Water Resources Association, Cambridge, Ontario, 219–232

Kern K., 1997. Restoration of incised channels: Large rivers. In: Management of Landscapes Disturbed by Channelizasion, Wang S.S.Y., Langendoen E.J. and Shields F.D., (eds.), University of Mississippi, Oxford, MS, 673–678

Kesel R.H. and Yodis E.G., 1992. Some effects of human modifications on sand-bed channels in southwestern Mississippi. USA. Environmental Geology and Water Science, 20, 93–104

Klassan G.J., Lambeek J., Mosselman E., Duizendstra H.D. and Nieuwenhuijzen M.E., 1998. Re-naturalization of the Meuse River in the Netherlands. In: Gravel Bed Rivers in the Environment, Klingeman P.C., Beschta R., Komar P. and Bradley J. (eds.), Water Resources Publications, Littleton, Co, 655–674

Klingeman P.C., Bravard J.P. and Giuliani Y., 1994. Les impacts morphodynamiques sur le Rhone en Chautagne (France). Revue de Geographic de Lyon, 1, 73–87 (in French)

Klingeman P.C., Bravard J.P., Giuliani Y., Olivier J.M. and Pautou G., 1998. Hydropower reach by-passing and dewatering impacts in gravel-bed rivers. In: Gravel Bed Rivers in the Environment, Klingeman P.C., Beschta R., Komar P. and Bradley J. (eds.), Water Resources Publications, Littleton, Co, 313–344

Knighton D., 1984. Fluvial Forms and Process. Edward Arnold, London

Knox J.C., 1983. Responses of river systems to Holocene climates. In: Late-Quaternary Environments of the United States, Wright H.E. (ed.), University of Minnesota Press, Minneapolis, 26–41

Kondolf G.M., 1997. Hungry water: Effects of dams and gravel mining on river channels. Environmental Management, 21, 533–551

Kondolf G.M. and Swanson M.L., 1993. Channel adjustments to reservoir construction and in stream gravel mining, Stony Creek, California. Environmental Geology and Water Science, 21, 256–269

Korup O., 2006. Rock-slope failure and the river long profile. Geology, 34 (1), 45–48

Korup O. and Montgomery D.R., 2008. Tibetan Plateau river incision inhibited by glacial stabilization of the Tsangpo gorge. Nature, 455, 786–789

Kuhl D., 1992. 14 years of artificial grain feeding in the Rhine downstream the barrage Iffezheim. In: Proceedings, 5th International Symposium on River Sedimentation, Karlsruhe, Germany, 1121–1129

Lagasse P.F., 1986. River response to dredging. Journal of the Waterways and Ports, 112, 1–14

Laird J.R. and Harvey M.D., 1986. Complex response of a chaparral drainage basin to fire. International Association of Hydrologists Scientific Publication, 159, 165–183

Lake County., 1992. Lake county aggregate resource management plan, lake county planning department. Resource Management Division, Lakeport, CA

LaMarche V.C., 1966. An 800-year history of steam erosion as indicated by botanical evidence. U.S. Geological Survey Professional Paper, 550-D, 83–86

Landon N. and Piégay H., 1994. L'incision de deux affluents sub-médilerranéens du Rhône: la Drôme et l'Ardéche. Revue de Géographic de Lyon, 69, 63–72

Landon N., Piegay H. and Bravard J.P., 1998. The Drome River incision (France): From assessment to management. Landscape and Urban Planning, 43 (1), 119–131

Lane E.W., 1955. The importance of fluvial morphology in hydraulic engineering. Proceedings of the American Society of Civil Engineers, 81(745), 1–17

Laronne J.B. and Carson M.A., 1976. Interrelationship between bed morphology and bed-material transport for a small, gravel-bed channel. Sedimentology, 23, 67–85

Larson E.L., Ozima M. and Bradley W.C., 1975. Late Cenozoic basic volcanism in northwestern Colorado and its implications concerning tectonism and the origin of the Colorado River system. In: Cenozoic History of the Southern Rocky Mountains, Curtis B.F. (ed.), Geological Society of America Memoir, 144, 155–178

Leclerc R.F., MacArthur R.C. and Galay V.J., 1997. Arroyo incision due to tectonism and land subsidence, Arroyo Pasajero, California. In: Management of Landscapes Disturbed by Channel Incision, Wang S.S.Y., Langendoen E.J. and Shields F.D. (eds.), University of Mississippi, Oxford, MS, 589–594

Lehre A., Klein R.D. and Trush W., 1993. Analysis of the effects of historic gravel extraction on the geomorphic character and fisheries habitat of the lower mad river, humboldt county, california, appendix to the draft program environmental impact report on gravel removal from the lower mad river, Department of Planning, County of

Humboldt, Eureka, CA

Leland J.F., Reid M.R., Burbank D.W., Finkel R.C. and Caffee M., 1995. [10]Be and [26]A1 exposure ages from bedrock river-cut terraces in northern Pakistan: Implications for incision and uplift rates. EOS Transactions, 76, F685

Leopold L.B. and Maddock T., 1953. The hydraulic geometry of stream channels and some physiographic implications. U.S. Geological Survey Professional Paper, 252, 1–57

Lerman A., 1988. Weathering rates and major transport processes: An introduction. In: Physical and chemical weathering in geochemical cycles, Lerman A. and Meybeck M. (eds.), Kluwer Academic Publications, Dordrecht, The Netherlands, 1–10

Little W.C., Thorne C.R. and Murphey J.B., 1982. Mass bank failure analysis of selected Yazoo Basin streams. Transactions of the American Society of Agricultural Engineers, 25, 1321–1328

Livesey R.H., 1965. Channel armoring below Fort Randall Dam. USDA Miscellaneous Publication 1970, 461−470

Lofgren B.E., 1969. Land subsidence due to the application of water. Engineering Geology, II, 271–303

Lohnes R.A., 1997. Stream channel degradation and stabilization: The iowa experience. In: Management of landscapes disturbed by channelizasion, Wang S.S.Y., Langendoen E.J. and Shields F.D. (eds.), University of Mississippi, Oxford, MS, 35–41

Love D.W., 1992. Rapid adjustment of the Rio Puerco to meander cutoff: Implications for effective geomorphic processes, crossing thresholds and timing of events. New Mexico Geological Society Guidebook, 43rd Field Conference, San Juan Basin, IV, 399–405

Macklin M.G., Rumsby B.T. and Heap T., 1992. Flood alluviation and entrenchment: Holocene valley-floor development and transformation in the British uplands. Geological Society of America Bulletin, 104, 631–643

Maddock T., 1960. Erosion control on five mile creek, Wyoming. International Association of Hydrologists Scientific Publication, 53, 170–181

Marcus L., 1992. Status Report: Russian River resource enhancement plan. California Coastal Conservancy, Oakland, CA

Marston R.A., 1994. River entrenchment in small mountain valleys of the Western USA: Influence of beaver, grazing and clearcut logging. Revue de Geographic de Lyon, 69, 11–16

Marston R.A., Girel J., Pautou G., Piegay H., Bravard J.P. and Arneson C., 1995. Channel metamorphosis, floodplain disturbance and vegetation development: Ain River, France. Geomorphology, 13, 121–131

Martinson H.A., 1986. Channel adjustments after passage of a lahar. In: Proceedings of the Fourth Federal Interagency Sedimentation Conference, Las Vegas, Nevada, 5, 143–152

Mayer L., 1985. Tectonic geomorphology of the basin and range Colorado Plateau boundary in Arizona. In: Tectonic Geomorphology, Morisawa M. and Hack J.T. (eds.), Allen and Unwin, Boston, 235–259

McLaughlin Water Engineers, Ltd. 1986. Evaluation of and design recommendations for drop structures in the Denver Metropolitan Area. A report prepared for the Denver Urban Drainage and Flood Control District by McLaughlin Water Engineers, Ltd

Mead R.H., Yuzyk T.R. and Day T.J., 1990. Movement and storage of sediment in rivers of the United States and Canada. In: Surface Water Hydrology: The Geology of North America, Wolman M.G. and Riggs H.C. (eds.), Geological Society of America, Washington, DC, 255–280

Melville B.W. and Dongol D.M., 1992. Bridge pier scour with debris accumulation. Journal of Hydraulic Engineering, 118, 1306–1310

Mendrop K.B. and Little P.E., 1997. Grade stabilization requirements for incised channels. In: management of landscapes disturbed by channel incision, Wang S.S.Y., Langendoen F.J. and Shields F.D. (eds.), University of Mississippi, Oxford, MS, 223–228

Merritts D.J., Vincent K.R. and Wohl E.E., 1994. Long river profiles, tectonism, and eustasy: A guide to interpreting fluvial terraces. Journal of Geophysical Research, 99(B7), 14031–14050

Mizutani T., 1996. Longitudinal profile evolution of valleys on coastal terraces under the compound influence of eustasy, tectonism and marine erosion. Geomorphology, 17, 317–322

Morisawa M. and LaFlure E., 1979. Hydraulic geometry, stream equilibrium and urbanization. In: adjustments of the fluvial system, Rhodes D.D. and Williams G.P. (eds.), Kendall-Hunt, Dubuque, IA, 333–350

Northwest Hydraulics Consultants, 1995. Cache creek streamway study, unpublished report to yolo county community development agency, Woodland, CA

Ohmori H., 1992. Dynamics and erosion rate of the river running on a thick deposit supplied by a large landslide.

Zeischrift für Geomorphologie, 36, 129–140

Ouchi S., 1985. Response of alluvial rivers to slow active tectonic movement. Geological Society of America Bulletin, 96, 504–515

Ouimet W.B., Whipple K.X., Royden L.H., Sun Z.M. and Chen Z.L., 2007. The influence of large landslides on river incision in a transient landscape: Eastern margin of the Tibetan Plateau (Sichuan, China). Geological Society of America Bulletin, 119 (11/12), 1462–1476

Parfitt D. and Buer K., 1980. Upper sacramento river spawning gravel study, california department of water resources, Northern Division, Red Bluff, CA

Parsons Binkerhoff Gore and Storrie, Inc, 1994. River management study: Permanent protection of the San Luis Rex River aqueduct crossings, Report to San Diego County Water Authority

Patton P.C. and Schumm S.A., 1975. Gully erosion northwestern Colorado: A threshold phenomenon. Geology, 3, 83–90

Pautou G., 1988. Perturbations anthropiques et changements de végétation dans les systèmes fluviaux. L'organisation du paysage fluvial rhodanien entre Genève et Lyon. Documents de Cartographie Ecologique, XXXI, 73–96 (in French)

Pautou G. and Girel J., 1986. La vegetation de la basse plaine de 1'Ain: organisation spatiale et evolution. Documents de Cartographie Ecologique, XXIX, 147–160 (in French)

Peiry J.L., 1993. L'ingenieur et la riviere dans la vallee de l'Arve (Haute-Savoie) et ses consequences sur la dynamique fluviale contemporaine. In: Le fleuve et ses Metamorphoses, Piquet F. (ed.), Didier Erudition, Paris, 245–255 (in French)

Peiry J.L., Salvador P.G. and Nouguier F., 1994. L'incision des rivieres des Alpes du Nord: Etat de la question. Revue de Geographic de Lyon, 69, 47–56 (in French)

Petersen R.C., Petersen L.B. and Lacoursiere J., 1992. A building block model for stream restoration. In: River Conservation and Management, Boon P.J., Calow P. and Petts G.E. (eds.), John Wiley and Sons, Chichester, England, 293–310

Piegay H., Barge O. and Landon N., 1996a. Streamway concept applied to river mobility/human use conflict management. In: Rivertech'96: New/Emerging Concept for Rivers, Maxwell W.H.C., Preul H.C. and Stout G.E. (eds.), IWRA, Chicago, IL, 681–688

Piegay H., Barge O., Bravard J.P., Landon N. and Peiry J.L., 1996b. Comment delimiter l'espace de liberie des rivieres. In: L'eau, L'homme et la Nature, Societe Hydrotechnique de France, Paris, 275–284 (in French)

Piegay H., Joly P., Foussadier R., Mourier V. and Pautou G., 1997. Principes de rehabilitation des marges du Rhone a partir d'indicateurs geomorphologiques, phyto-ecologiques et batrachologiques, le cas du Rhone court-circuite de Pierre-Benite. GeoCarrefour, 72, 7–22 (in French)

Pitty A.F., 1971. Introduction to Geomorphology, Methuen, London

Platts W.S. and Nelson R.L., 1989. Characteristics of riparian plant communities and streambanks with respect to grazing in northeastern Utah. In: Practical approaches to riparian resource management, an Educational Workshop, Gresswell R.E. (ed.), Billings, MT, 73–81

Possardt E.E. and Dodge W.E., 1978. Stream channelization impacts of songbirds and small mammals in Vermont. Wildlife Society Bulletin, 6, 18–24

Prokopovich N.P., 1983. Neotectonic movement and subsidence caused by piezometric decline. Bulletin of the Association of Engineering Geologists, 20, 393–404

Prosser I.P. and Slade C.J., 1994. Gully formation and the role of valley-floor vegetation, southeastern Australia. Geology, 22, 1127–1130

Reich M., 1991. Grasshoppers (Orthoptera, saltatoria) on alpine and dealpine riverbanks and their use as indicators for natural floodplains dynamics. Regulated Rivers. Research and Management, 6, 333–339

Reich M., 1994. Les impacts de l'incision des rivieres des Alpes bavaroises sur les communautes terrestres du lit majeur. Revue de Geographie de Lyon, 69, 25–30 (in French)

Reid J.B., 1992. The Owens River as a tiltmeter for Long Valley Caldera, California. Journal of Geology, 100, 353–363

Reilly P.W. and Johnson W.C., 1982. The effects of altered hydrologic regime on tree growth along the Missouri River in North Dakota. Canadian Journal of Botany, 60, 2410–2423

Rice R.J., 1980. Rates of erosion in the Little Colorado valley, Arizona. In: Timescales in Geomorphology, Cullingford

R.A., Davidson D.A. and Lewin J. (eds.), Wiley, Chichester, 317–331

Righter K., 1997. High bedrock incision rates in the Atenguillo River Valley, Jalisco, western Mexico. Earth Surface Processes and Landforms, 22, 337–343

Robbins C.H. and Simon A., 1983. Man-induced channel adjustment of Tennessee streams. U.S. Geological Survey Water-Resources Investigations Report 82–4098. Pp 129, 71 fig, 5 tab, 38 ref.

Rodolfo K.S., 1989. Origin and early evolution of lahar channel at Mabinit, Mayon Volcano, Philippines. Geological Society of America Bulletin, 101, 414–426

Rood S.B. and Mahoney J.M., 1995. River damming and riparian Cottonwoods along the Marias River. Montana Rivers, 5, 195–207

Rosenbloom N.A. and Anderson R.S., 1994. Hillslope and channel evolution in a marine terraced landscape, Santa Cruz, California. Journal of Geophysical Research, 99(B7), 14013–14029

Rosgen D.L., 1996. Applied River Morphology. Wildland Hydrology, CO

Rosport M., 1994. Stability of torrent beds characterised by step-pool textures. International Journal of Sediment Research, 9(3), 124–132

Rosport M., 1997. Hydraulics of steep mountain streams. International Journal of Sediment Research, 12(3), 99-108

Roux A.L., 1986. Recherches Inierdisciplinaires sur les Ecosystemes de la Basse Plaine de Vain (France): Potentialites Evolutives et Gestion, Documents de Cartographic Ecologique XXIX, Universite J. Fourier, Grenoble (in French)

Schumm S.A., 1985. Patterns of alluvial rivers. Annual Review of Earth and Planetary Sciences, 13, 5–27

Schumm S.A., 1999. Causes and control of channel incision, In: Incised Rivers, Darby S.E., and Simon A. (eds.), John Wiley and Sons, Chichester/New York

Schumm S.A. and Chorley R.J., 1983. Geomorphic controls on the management of nuclear waste. U.S. Nuclear Regulatory Commission, NUREG/CR–3276, Washington, DC

Schumm S.A. and Phillips W., 1986. Composite channels of the Canterbury Plain, New Zealand: A Martian analog. Geology, 14, 326–329

Schumm S.A., Erskine W.D. and Tilleard J., 1996. Morphology, hydrology and evolution of the anastomosing Ovens and King Rivers, Australia. Geological Society of America Bulletin, 108, 1212–1224

Schumm S.A., Harvey M.D. and Watson C.C., 1984. Incised Channels: morphology, dynamics and control. Water Resources Publications, Littleton, CO

Schwarcz H.P., Blackwell B., Goldberg P. and Marks A.E., 1979. Uranium series dating of travertine from archaeological sites, Nahal Zin, Israel. Nature, 277, 558–560

Scott G.R., 1975. Cenozoic surfaces and deposits in the southern Rocky Mountains. In: Cenozoic history of the Southern Rocky Mountains, Curtis B.F. (ed.), Geological Society of America Memoir 144, 227–248

Scott K.M., 1973. Scour and fill in Tujunga Wash a fanhead valley in urban southern California 1969. U.S. Geological Survey Professional Paper 732–B

Sear D.A., 1992. Impact of hydroelectric power release on sediment transport processes in pool-riffle sequences. In: Dynamics of Gravel Bed Rivers, Billi P., Hey R.D., Thorne C.R. and Tacconi P. (eds.), Wiley, Chichester, England, 629–650

Sear D.A., 1996. Sediment transport in riffle-pool sequences. Earth Surface Processes and Landforms, 21, 147–164

Sear, D.A. and Archer, D. 1998. Effects of gravel extraction on stability of gravel-bed rivers: the Wooler water, Northumberland, UK., In: Beschta P.C., Komar R.L., Bradley P.D. and Klingeman J.B., Editors, Gravel-Bed Rivers in the Environment, Water Resources Publications LLC, Highlands Ranch, CO, United States 1998, 415–432

Seidl M.A., Dietrich W.E. and Kirchner J.W., 1994. Longitudinal profile development into bedrock; an analysis of Hawaiian channels. Journal of Geology, 102, 457–474

Seidl M.A., Finkel R.C., Caffee M.W., Hudson G.B. and Dietrich W.E., 1997. Cosmogenic isotope analyses applied to river longitudinal profile evolution: Problems and interpretations. Earth Surface Processes and Landforms, 22, 195–209

Shepherd R.G., 1979. River channel and sediment responses to bedrock lithology and stream capture, Sandy Creek drainage, central Texas. In: Adjustments of the Fluvial System, Kendall-Hunt, Rhodes D.D. and Williams G.P. (eds.), Dubuque, IA, 255–275

Shields F.D., Cooper C.M. and Knight S.S., 1993. Initial habitat response to incised channel rehabilitation. Aquatic Conservation: Marine and Freshwater Ecosystems, 3, 93–103

Shields F.D., Cooper C.M. and Knight S.S., 1995a. Experiment in stream restoration. Journal of Hydraulic Engineering, 121, 494–502

Shields F.D. and Hoover J.J., 1991. Effects of channel restabilization on habitat diversity, Twentymile Creek, Mississippi. Regulated Rivers. Research and Management, 6, 163–181

Shields F.D., Knight S.S. and Cooper C.M., 1994. Effects of channel incision on base flow stream habitats and fishes. Environmental Management, 18, 43–57

Simon A., 1989. A model of channel response in disturbed alluvial channels. Earth Surface Processes and Landforms, 14, 11–26

Simon A., 1992. Energy, time, and channel evolution in catastrophically disturbed fluvial systems. In: Geomophic Systems: Geomorphology, Phillips J. P. and Renwick W.H. (eds.), 5, 345–372

Simon A., 1994. Gradation processes and channel evolution in modified west Tennessee streams: Process, response and form. U.S. Geological Survey Professional Paper, 1470

Simon A. and Darby S.E., 1997a. Process-form interactions in unstable sand-bed river channels: a numerical modeling approach. Geomorphology, 21, 85–106

Simon A. and Darby S.E., 1997b. Bank erosion processes in two incised meander bends: goodwin creek, Mississippi. In: management of landscapes disturbed by channel incision, Wang S.S.Y., Langendoen E.J. and Shields F.D. (eds.), University of Mississippi, Oxford, MS, 256–261

Simon A. and Darby S.E., 1997c. Disturbance, channel evolution, and erosion rates: hotophia reek, Mississippi. In: management of landscapes disturbed by channel incision, Wang S.S.Y., Langendoen E.J. and Shields F.D. (eds.), University of Mississippi, Oxford, MS, 476–481

Simon A. and Hupp C.R., 1986. Channel evolution in modified Tennessee channels. In: proceedings of the fourth federal interagency sedimentation conference march 24–27, Vol. 2, U.S. Government Printing Office, Washington, DC, 5-71 to 5–82

Simon A. and Hupp C.R., 1992. Geomorphic and vegetative recovery processes along modified stream channels of West Tennessee. U.S. Geological Survey Open-File Report, 91–502

Smiley P.C., Cooper C.M., Kallies K.W. and Knight S.S., 1997. Assessing habitats created by installation of drop pipes. In: management of landscapes disturbed by channel incision, Wang S.S.Y., Langendoen E.J. and Shields F.D. (eds.), University of Mississippi, Oxford, MS, 35–41

Smith D.I., Greenaway M.A., Moses C. and Spate A.P., 1995. Limestone weathering in eastern Australia. Part I: Erosion rates. Earth Surface Processes and Landforms, 20, 451–463

Sogreah., 1988. Schema d'amenagement du haut Giffre, etude de la revision du schema. Syndicat intercommunal a vocations multiples du haut Giffre, Report (in French)

Sogreah., 1991. Etude de diagnostic de la nappe de la basse vallée de la Drôme. Direction Départementale de l'Equipemcnt de la Drôme, report and maps (in French)

Sohag M.A., 1993. Sediment tracing, bed structure and morphological approaches to sediment transport estimates in a gravel-bed river: The River South Tyne, Northumberland, UK. PhD Thesis, University of Newcastle upon Tyne

Soil and Water., 1985. Attacks on the otaki - gravel or grants. Soil and Water Magazine, National Water and Soil Conservation Authority, Wellington, New Zealand, 22, 2–14

Sonoma County, 1992. Sonoma county aggregate resources management plan and environmental impact report. Prepared by EIP Associates for Sonoma County Planning Department, Santa Rosa, CA

Stevens M.A., Simons D.B. and Schumm S.A. 1975. Man-induced changes of middle Mississippi River. Journal of the Waterways, Harbors and Coastal Engineering Division, 101, 119–133

Stroffek S., Amoros C. and Zylberblat M., 1996. La logique de rehabilitation physique appliquee un grand fieuve: le Rhone. Revue de Geographie de Lyon, 71, 287–296

Stufft W.A., 1965. Erosion control to Gering Valley. ASCE, Hydraulics Division Conference, Tucson, AZ

Tagliavini S., 1978. Le modificazioni geomorphologiche ed idrogeologiche conseguenti all'attivita estrattiva nella conoide del torrente Enza. In: proceedings of the conference on attivita estrattiva dei materiali inerti da costruzioni. Effetti sugli Arnbienti e Risorse Alternative (in Italian)

Thorne C.R., 1990. Effects of vegetation on riverbank erosion and stability. In: vegetation and erosion, Thornes J.B. (ed.), John Wiley and Sons, Chichester, England, 123–144

Thorne C.R., 1997. Fluvial processes and channel evolution in the incised rivers of north-central Mississippi. In: management of landscapes disturbed by channel incision, Wang S.S.Y., Langendoen E.J. and Shields F.D. (eds.), University of Mississippi, Oxford, MS, 23–34

Thorne C.R., Murphey J.B. and Little W.C., 1981. Bank stability and bank material properties in the bluffline streams of northwest Mississippi. Appendix D, Report to the Corps of Engineers, Vicksburg District under Section 32 Program, Work unit 7, USDA-ARS Sedimentation Laboratory, Oxford, Mississippi

Thorne C.R., Russell A.P.G. and Alam M.K., 1993. Planform pattern and channel evolution of the Brahmaputra River, Bangladesh. In: Braided Rivers, Best J.L. and Bristow C.S. (eds.), Geological Society of London, 257–276

Tinkler K.J., Pengelly J.W., Parkins W.G. and Asselin G., 1994. Postglacial recession of Niagara Falls in relation to the Great Lakes. Quaternao Research, 42, 20–29

Trimble S.W., 1974. Man-induced Soil Erosion on the Southern Piedmont 1700 – 1970. Soil Conservation Society, Ankeny, IA

Trimble S.W. and Mendel A.C., 1995. The cow as a geomorphic agent: A critical review. Geomorphology, 13, 233–253

Vandeaele W., Posesen J., Govers G. and Van Wesemael B., 1996. Geomorphic threshold conditions for ephemeral gully incision. Geomorphology, 16, 161–173

Wallerstein N. and Thorne C.R., 1996. Impact of in-channel organic debris on fluvial process and channel form in unstable channel environments. In: proceedings of the sixth federal interagency sedimentation conference, Las Vegas. U.S. Government Printing Office, Washington, DC, 11–32 to 11–38

Wang Z.Y., 1999. Experimental study on scour rate and channel bed inertia. Journal of Hydraulic Research, 27–47

Wang Z.Y., Xu J. and Li C.Z., 2004. Development of step-pool sequence and its effects in resistance and stream bed stability. International Journal of Sediment Research, 19(3), 161–171

Wang Z.Y., Cui P. and Wang R.Y., 2009. Mass movements triggered by the Wenchuan Earthquake and management strategies of quake lakes. International Journal of River Basin Management, 7(4), 391 – 402

Wang Z.Y., Melching, C.S., Duan, X.H. and Yu, G.A., 2009. Ecological and hydraulic studies of step-pool systems. ASCE Journal of Hydraulic Engineering, 135(9), 705–717

Wang Z.Y., 1999, Experimental study on scour rate and channel bed inertia. Journal of Hydraulic Research, IAHR, 37(1), 17–38

Whitlow J.R., 1985. Dambos in Zimbabwe: A review. Zeitschrift fur Geomorphologie Supplementband, 52, 115–146

Whittaker J. and Jaeggi Martin N.R., 1986. Bockschwellen, Mitteilungen der Versuchsanstalt fur Wasserbau, Hydrologie und Glaziologie Nr. 91, an der Eidgenossischen Technischen Hochschule Zurich, (in German)

Whittaker J.G. and Jaeggi Martin N.R., 1982. Origin of step-pool system in mountain streams. Journal of hydraulic Engineering, (HY6), 758–773

Whittaker J.G., 1987. Sediment transport in step-pool streams. In: Sediment Transport in Gravel-Bed Rivers. Thorne C.R., Bathurst J.C. and Hey R.D. (eds.), Wiley, Chichester, 545-579Wikipedia., 2008, 2008 Sichuan earthquake, http://en.wikipedia.org/wiki/Wenchuan_earthquake

Williams G.P. and Wolman M.G., 1984. Downstream effects of dams on alluvial rivers. U.S. Geological Survey Professional Paper, 1286

Wikepedia, 2011. http://en.wikipedia.org/wiki/Indian_plate, 2011.

Williams G.W., 1978. Bankfull discharge of rivers. Water Resources Research, 14, 1141–1154

Winkley B.R., 1994. Response of the lower Mississippi River to flood control and navigation improvements. In: The variability of large alluvial Rivers, Schumm S.A. and Winkley B.R. (eds.), American Society of Civil Engineers, New York, 45–74

Wittenberg L., 2002a. Structural patterns and bed stability of humid temperate, Mediterranean and semi-arid gravel bed rivers. PhD thesis, University of Newcastle upon Tyne

Wittenberg L., 2002b. Structural patterns in coarse gravel river beds: Typology, survey and assessment of the role of grain size and river regime. Geografiska Annaler, 84A(1), 25–37

Wittenberg L. and Newson M.D. 2005. Particle clusters in gravel-bed rivers: An experimental morphological approach to bed material transport and stability concepts. Earth Surface Processes and Landforms, 30, 1351–1368

Whipple K.X. and Tucker G.E. 2002. Implications of sediment-fl ux dependent river incision models for landscape evolution. Journal of Geophysical Research, 107(B2), 20

Wohl E., Madsen. and Lee M., 1997. Characteristics of log and clast bed-steps in step-pool streams of northwestern Montana. U.S. Geomorphology, 20, 1–10

Wohl E.E., 1992. Bedrock benches and boulder bars: Floods in the Burdekin Gorge of Australia. Geological Society of America Bulletin, 104, 770–778

Wohl E.E., 1998. Incised bedrock channels, In: Incised Rivers, Darby S.E. and Simon A. (eds.), John Wiley and Sons

Wohl E.E. and Grodek T., 1994. Channel bed-steps along Nahal Yael, Negev Desert, Israel. Geomorphology, 9, 117–126

Wohl E. and Thompson D. 2000: Velocity characteristics along a small step-pool channel. *Earth Surf. Processes Landforms*, 25, 353–367

Wolman M.G. and Leopold L.B., 1957. River flood plains: Some observations on their formation. U.S. Geological Survey Professional Paper, 282-C, 87–107

Wolman M.G. and Miller J.P., 1960. Magnitude and frequency of forces in geomorphic process. Journal of Geology 68, 54–74

Wu T.H. and McKinnell W.P., 1976. Strength of tree roots and landslides on Prince of Wales Island, Alaska. Canadian Geotechnical Journal, 16, 19–33

Yair A., Goldberg P. and Brimer B., 1982. Long term denudation rates in the Zin-Havarim badlands, northern Negev, Israel. In: Badland Geomorphology and Piping, Bryan, R. and Yair, A. (eds.), Geo Books, Norwich, England, 279–291

Yang Q.A., Long Y.Q. and Miao F.G., 1994. Operational Studies of Sanmenxia Project on the Yellow River, Henan People's Press (in Chinese)

Young R.W. and McDougall I., 1993. Long-term landscape evolution: Early Miocene and Modern rivers in southern New South Wales, Australia. Journal of Geology, 101, 35–49

Yu C.Z., 1994. Hydraulics, Vol. II, Educational Press of China (in Chinese)

Zimmermann A. and Church M., 2001. Channel morphology, gradient profile and bed stresses during flood in a step-pool channel. Geomorphology, 40, 311–327

4 Debris Flows and Landslides

Abstract

A landslide is a mass movement occurring on steep slopes under the action of gravity. Debris flow is a distinct type of mass movement commonly triggered by intense rainfall and/or melting snow on steep hill slopes. It differs from landslide in its "flowing" feature. Flow means relative movement in numerous layers of the medium, whereas a slide occurs only along one or several interfaces or beds. The main causes of landslides and avalanches are earthquakes and rainstorms. Disaster chains are initiated by landslides and avalanches. Great landslides resulted in barrier lakes. The stability of a landslide dam depends on the development degree of the step-pool system in the spillway channel on the landslide dam and the highest stream power of flow. Preserved landslide dams may develop into a knickpoint and become a key factor for river pattern establishment and river stability.

Debris flows have buried towns, villages, highways, railways, and farmland, broken bridges and dammed rivers; caused casualties and impaired habitats. Debris flow is extremely unsteady, which is initiated on steep slopes, flows down gullies, and deposits at the mouth of debris flow gullies. Debris flows are classified into pseudo-one-phase debris flows and two-phase debris flows. There is no obvious relative movement between the solid particles and liquid in pseudo-one-phase flow and there is relative movement between the solid phase and liquid phase in two phase debris flow. Pseudo-one-phase debris flows are very non-Newtonian and are characterized by the striking phenomena of intermittent flow, the "bed-paving process," low resistance and drag reduction, extremely high super-elevation at bends, and well-mixed deposit materials. Two-phase debris flows are composed of stones and gravel as the solid phase and the fluid mixture of water and low concentrations of clay and sand as the liquid phase. They exhibit high, steep heads consisting of rolling, colliding, large gravel, which distinguishes two-phase debris flows from a normal torrential flood. The liquid phase is mostly Newtonian.

Debris flows and landslides are serious challenges in management of mountain rivers. However, they are especially disastrous in China and Japan where the high population and high percentage of mountainous land result in a dangerous mixture. This chapter focuses on the description of the basic characteristics, consequences, and control strategies of debris flows and landslides.

Key words

Landslide, Disaster chains, Landslide dam, Barrier lake, Debris flow control strategies, Hazard mitigation

4.1 Disasters Caused by Landslides and Debris Flows

4.1.1 Landslides

A landslide is a mass movement occurring on steep slopes under the action of gravity. Landslides occur in two thirds of the mountainous areas of China, especially in northwestern and southwestern China. More than 120 million dollars were lost due to landslides and avalanches every year before the 1990s (NFH and IMH, 1994).

Landslides and similar mass movements can be classified according to their movement types, scales, and material of the sliding body. Four types of mass movements can be recognized: 1) topple; 2) rockfall; 3) avalanche; and 4) landslide. Topple is the phenomenon of rock column detachment due to freezing-thawing of water in the interstices of rocks. Rockfall is the phenomenon of a few huge rocks falling from a cliff or steep slope. An avalanche is the collapse of a cliff and slope under the action of gravity triggered by earthquake or rainstorm. A landslide is the mass movement of rock and soil down a slope

along one or several sliding beds under the action of gravity. In many publications these mass movements are all called landslides.

Figure 4.1 shows the four types of mass movement in mountain areas with high bank slope: (a) Topple—detachment of columns of rock along the Juma River near Beijing; (b) Rockfall—a huge stone fell from a steep slope along the Juma River; (c) Avalanche—mass movement of broken rocks down the bank slope of the Minjiang River triggered by the Wenchuan Earthquake in 2008; (d) Landslide—movement of slope debris and rocks induced by the Wenchuan Earthquake along the Qingzhu River in Sichuan, China. Avalanche and landslide are the most important mass movements and the general term of landslides means these two mass movements in the literature and this book.

<table>
<tr><td>(a)</td><td>(b)</td></tr>
<tr><td>(c)</td><td>(d)</td></tr>
</table>
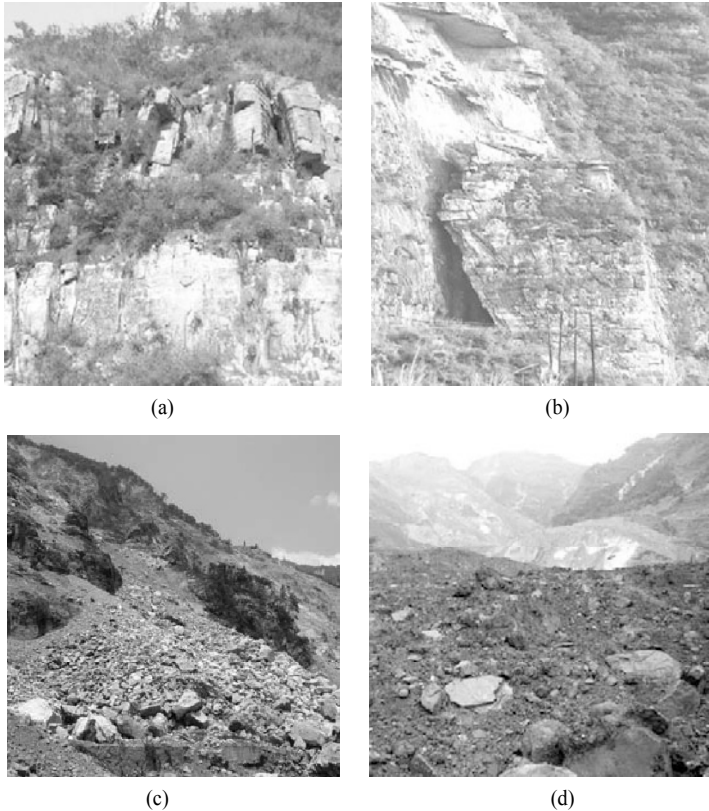
Fig. 4.1 Different types of mass movements: (a) topple; (b) rockfall; (c) avalanche; (d) landslide (See color figure at the end of this book)

Earthquake is often the direct cause of landslides. There have been many examples of earthquake-induced avalanches and landslides. The 1999 Chi-Chi earthquake in Taiwan, China, induced landslides in the Tachia catchment. The subsequent rainfall events associated with the passage of typhoons have led to a significant increase in the area affected by landslides. As a result, the sediment production rate was still increasing four years after the earthquake event (Lin et al., 2005). The relation between the magnitude of an earthquake and the intensity of landslides has been studied. It was found that the minimum earthquake magnitude needed generate a landslide is M = 4.3 ± 0.4 on the moment magnitude scale (Malamud et al., 2004).

Compared with storm-triggered landslides, the earthquake-triggered avalanches and landslides mobilize much coarser sediment. The storm-triggered landslides primarily result from local pore water pressure gradients and are likely to be most pronounced in the shallow subsurface. Seismic ground motion affects local stress fields well below the topographic surface and may trigger a relatively large number of deep-seated, bedrock-involved avalanches and landslides. Such mass movements are likely to produce coarse debris with diameters of up to several meters. The mobilized sediment is, therefore, difficult to transport by river flow. A large volume of mobilized debris deposits at places where the potential for onward transport is low. Because seismic ground motion is strongest at ridge crests (Geli et al., 1988), earthquake-induced avalanches and landslides often cluster around high points and deposit debris on hillslopes rather than on channel floors (Hovius and Stark, 2006).

The landslides may also be classified according to the type of motion into rotational landslides and translational landslides. Figure 4.2 shows a rotational landslide occurring on the Liujia Gully in the Xihanshui Basin in Gansu, China. The sliding body moved along a curved bed. The upper part moved almost vertically downward, left a chair-back shaped concavity. The lower part moved toward the river channel and formed a convex slope. The chair-form is a diagnostic feature of rotational landslides. Figure 4.2(b) shows a translational landslide occurring in the Xiaojiang watershed in Yunnan, China. The sliding body moved along a planar slip surface for several hundred meters.

(a)

(b)
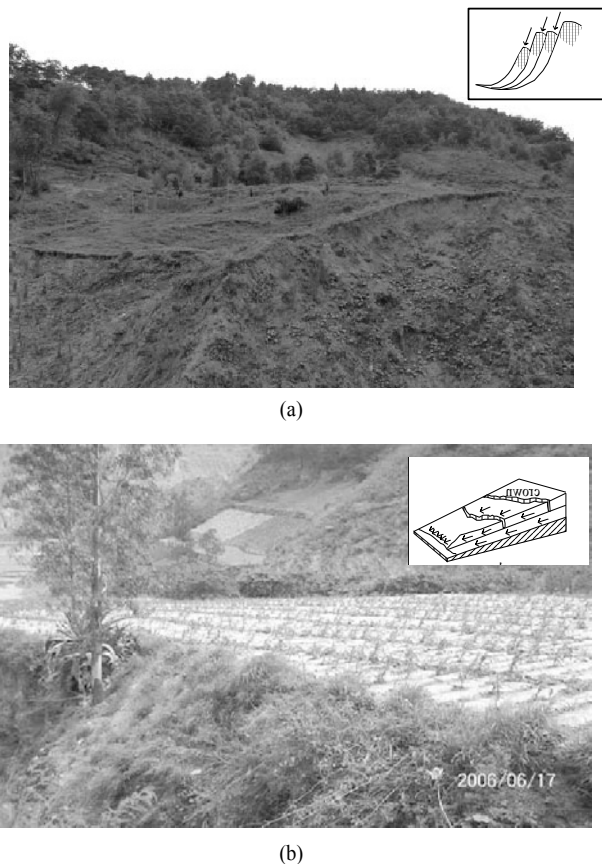
Fig. 4.2   (a) A chair-form rotational landslide on the Liujia Gully in the Xihanshui River basin in Gansu Province in western China; (b) A translational landslide in the Xiaojiang watershed

Landslides also are classified according to their scale into: huge landslides with a volume of sliding material over $10^8\,m^3$, large scale landslides with volume between $10^6\,m^3$ and $10^8\,m^3$, middle scale landslide with volume between $10^4\,m^3$ and $10^6\,m^3$, and small scale landslides with a volume less than $10^4\,m^3$. Rockfalls are usually in the small scale, and avalanches and rockslides are in the middle and small scales. Only the translational and rotational landslides are in the large and huge scales.

Landslides are also classified according to their causes into earthquake landslides, rainstorm landslides, congelifraction avalanches, liquefaction landslides, reservoir-induced landslides, highway landslides, and mining landslides. Rainfall induced landslides occur widely in hilly and mountainous areas. According to the water content of the sliding body, landslides are classified into dry landslides, unsaturated landslide, and saturated landslides. Landslides also are classified by materials into rock landslides, semi-solid landslides, and soil landslides.

China is a country with a vast territory of mountains. Landslides and avalanches occur throughout the mountainous areas. Figure 4.3 shows the distribution of landslides and debris flows in China (NFH and IMH, 1994), in which the different shadowed areas are debris flow areas with different types of debris flows and the locations of black points are the sites of landslides. Frequent and disastrous landslides occur in areas with active tectonic and stream erosion areas. These areas cover two thirds of the mountainous areas of China, especially northwestern and southwestern China. Many landslides have occurred along the upper reaches of the Yangtze River and at the edge of the Qinghai-Tibet Plateau.
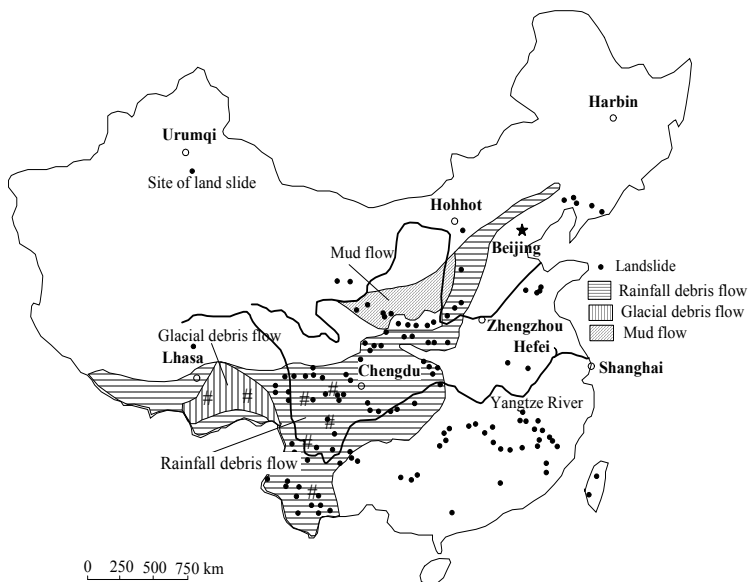
Fig. 4.3   Distribution of landslides and debris flows in China (The different shadowed areas are debris flow areas with different types of debris flows and the locations of black points are the sites of landslides) (after NFH and IMH, 1994)

Huge and large scale landslides are triggered by earthquakes or rainstorms. But some small scale landslides result from human activities, such as disposal of mining debris, deforestation, and construction on slopes. Swanston (1999) analyzed the relation between landslides and timber harvest. Forest harvest operations in southeastern Alaska have influenced both the frequency and size of landslide events. Southeastern Alaska is characterized by naturally steep slopes, shallow soils, and a thick, old-growth forest cover. Precipitation ranges from 1,524 and 5,080 mm a year. Because of high soil permeability,

drainage is primarily by subsurface flow with little or no overland flow. During major storm periods, high soil moisture levels and local areas of saturation are produced on slopes, greatly increasing the unstable character of the surface materials. Under these conditions, landslide is a dominant process of soil erosion and sediment transport. In the early 1960's, prior to large scale harvest activities, 1,374 failures occurred at forested sites scattered over the Tongass National Forest south. Most failures occurred in unique topographic situations and appeared to be directly linked to initiation by temporary water table development during high intensity storms (Swanston, 1969). Of the natural (undisturbed) failures identified in this early survey, 87% were of the debris avalanche/debris flow type (Varnes, 1978).

In 1960 and 1961 the forest experienced large-scale logging. An aerial photographic survey of landslides occurring between 1963 and 1983 in forested terrain in the Tongass National Forest provided region-wide data on landslide type, frequency, distribution, and general relations to harvest activities. This survey involved the location, typing, and terrain characterization of all post-1962 landslides greater then 77 m^3 (100 yd^3) in initial failure volume (Varnes, 1978). The post-logging landslide activity showed rate 4 times the natural rate following the first clear-cut harvesting on a major scale in southeastern Alaska.

4.1.2   Debris Flows

Debris flow is a distinct type of mass movement commonly triggered by intense rainfall and/or melting snow on steep hill slopes. It differs from landslide in its "flowing" feature. Flow means relative movement in numerous layers of the medium but a slide occurs only along one or several interfaces or beds. Although great efforts have been made in the study of the mechanism of motion, considerable ambiguity persists concerning the initiation and motion of debris flows. Debris flow is turbulent because of its high flow velocity in some circumstances and is laminar due to its high viscosity in other cases. Debris flow is extremely unsteady, which is initiated on steep slopes, flows down gullies, and deposits at the mouth of debris flow gullies.

Debris flow is a widely distributed and frequently occurring hazard in mountainous regions of China. Chinese people call the phenomenon "dragon", because of its power and irresistible nature. Debris flow is very disastrous because it carries an extremely high concentration of sediment load and big rocks. Mechanical properties of debris flow depend highly on the concentration and composition of the solid material. Debris flows are classified into mudflow, mud-rock flows and water-rock flow according to the composition of the solid materials. The mud-rock flow, consists of mud and stones. The size of the solid particles ranges from clay finer than 0.001 mm to boulders of several or tens of meters in diameter. Clay particles make up a certain proportion of the total amount of sediment, generally about 3–5%. The flocculent structure of clay particles has a great effect on the dynamic properties and transport capacity, and causes the flow to experience some unique phenomena. Mudflow often takes place on the Loess Plateau in China. Water-rock flow mainly occurs in marble, dolomite, limestone, and conglomerate rock areas or partly in granite mountain areas. The solid material in water-rock flow is mainly composed of coarse sand, gravel, and boulders. Debris flow can also be classified into glacial debris flow and rainfall debris flow according to their genesis.

It is more important to classify debris flow according to its dynamic characteristics. So that debris flows are classified into pseudo-one phase debris flows and two-phase debris flows (Wang et al., 1999). Pseudo-one phase debris flows are further classified into viscous debris flows, subviscous debris flows, and low viscous debris flows. Pseudo-one phase debris flow is non-Newtonian, has a large yield stress, and exhibits laminar flow and intermittent features in many cases. In two-phase debris flows the solid phase consists of gravel and boulders and the liquid phase consists of water with clay and silt in suspension, sometimes also sand and fine gravel are in suspension. There is obvious relative movement between the solid phase and the liquid phase. The two types of debris flows are discussed in detail later.

Debris flow occurs often as a consequent mass movement after landslides. Thus, debris flow and landslide are related in a causal chain of morphological processes. The 1999 Chi-Chi earthquake in Taiwan, China, induced many landslides in the Tachia catchment. The subsequent rainfall events led to a significant increase in the debris flow events, and as a result, four years after the earthquake event, the sediment production rate was still increasing. After the Chi-Chi earthquake, over 20,000 landslides totaling approximately 113 km^2 had occurred. Consequently, a great deal of loose sediment was produced, which in turn promoted heavy debris flows during subsequent typhoons and heavy rains. The most outstanding example was a severe debris flow hazard causing the deaths of more than 240 people during Typhoon Toraji on July 30, 2001 (Lin et al., 2005).

The Wenchuan earthquake occurred in Sichuan province, China on May 12, 2008 and triggered a huge scale and several tens of large scale landslides, which yielded a huge amount of sediment. The sediment deposited on the gully bed and slopes, or even dammed streams creating quake lakes. The loose materials resulting from the landslides are likely to be removed by flowing water and transported in debris flows. A large scale landslide occurred on the Huoshigou Gully in Chongzhou County on May 12, 2008, which has yielded several million tons of sediment in the gully. Several days later a heavy rain triggered a debris flow, which scoured the landslide deposit and dug a 30–40 m deep channel, as shown in Fig. 4.4(a). The debris flow carried extremely high sediment concentration into the Anzi River and sediment deposited on the bed. About 2 km along the channel bed of the river was silted up by 4-9 m, as shown in Fig. 4.4(b).

(a)

(b)

Fig. 4.4 A large scale landslide occurred on the Huoshigou Gully in Chongzhou County, which was triggered by the Wenchuan Earthquake on May 12, 2008: (a) A flood flow scoured the landslide deposit by 30–40 m and developed into a debris flow; (b) The debris flow carried sediment into the Anzi River and resulted in 4–9 meters of sedimentation on the bed (See color figure at the end of this book)

Debris flow occurs mainly in Sichuan, Yunnan, and Tibet. More than 800 counties in these provinces (about 40% of the total) have recorded debris flows and more than 60 towns were damaged by debris flows. According to a preliminary investigation, there are more than 10,000 debris flow gullies throughout the country. Rainfall debris flow frequently occurs in Yunnan, Sichuan, and Gansu provinces. The Xiaojiang watershed in Yunnan Province has a drainage area of 3,220 km^2. There are 107 debris flow gullies in the area. More than 100, sometimes more than 2,000 events of rainfall debris flows take place in the area and more than 2×10^7 tons of solid material is carried into the Xiaojiang River annually. Among these debris flow gullies the Jiangjia Ravine is the most notorious. More than 10 events of debris flow take place in the gully every year and 28 events of debris flow were recorded in 1965. The upstream gully bed is cut down 2–3 m per year and the incision causes debris flows every year, whereas the mouth of the gully aggrades 1.36 m annually due to deposition of the debris. It is no wonder that the Xiaojiang watershed is called a museum of debris flow. In the middle reach of the Bailong River in Gansu Province almost all gullies are debris flow gullies. There are 10 debris flow gullies per kilometer along the river on average.

Glacial debris flow takes place mainly on the Qinghai-Tibet Plateau. The Guxiang gully in the plateau is a large glacial debris flow gully. Several tens of glacial debris flows occur there annually. A glacial debris flow of extremely large scale occurred in the gully in 1953. The maximum depth of the debris flow was estimated at 40–95 m and the maximum discharge was estimated as 28,600 m^3/s. About 10 million m^3 of solid material was transported by the debris flow.

The Loess Plateau is located in the middle reaches of the Yellow River, which is covered by a layer of Quaternary loess deposits with a maximum depth of 400 m. The loess soil is liable to be eroded and the plateau is cut by an uncountable number of gullies. Mudflows with silt concentrations up to 1,600 kg/m^3 occur in the gullies every year. The mudflows are very viscous and non-Newtonian. In many cases the mudflows were laminar.

Debris flow shows obvious periodicity. The occurrence of very active debris flow lasts 50–70 years. Overlapping on the long period are 6-year, 11-year, and 22-year short periods. The 1960s and 1980s were two active periods of debris flow. Debris flows took place simultaneously in Tibet, Sichuan, Gansu, Sha-anxi, Liaoning, and Jilin provinces in 1981. In Sichuan Province alone 61 counties were hit by debris flows. Figure 4.5 shows the 6-year and 11-year periods of occurrence of debris flow events in the Jiangjia Ravine near Kunming in Yunnan Province in southwest China. It also shows that the annual amount of sediment transportation is proportional to the number of debris flow events.
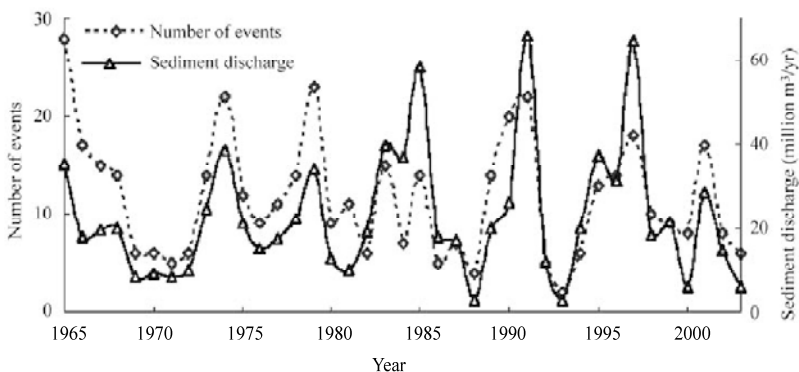
Fig. 4.5 Periodic occurrence of debris flow events and annual volume of sediment transportation in the Jiangjia Ravine near Kunming in Yunnan Province in southwest China (He et al., 2003)

4.1.3 Landslide Disasters

4.1.3.1 Landslide Events

More than 30 large-scale landslides occurred along the Sichuan-Tibet Highway in the 1960s. The landslides blocked the highway more than 1,500 days. A landslide damming the Palongzangbu River created the Ranwu Lake, at 3,990 m above the sea level, it is 26 km long and 1-2 km wide. A landslide at the Layue section of the highway in 1966 with a sliding volume of over 20 million m^3 destroyed 5 km highway and the highway route had to be changed. From June to August 1966, 648 landslides occurred in the Guxiang Gully in Tibet Autonomous Region and provided abundant solid material for large-scale debris flows. Dongjiu Village is located by the Lulang River and the Sichuan-Tibet Highway. A heavy rainstorm triggered a landslide in September 1991. The sliding body thrust into and dammed the Lulang River. The river water was forced to scour the highway destroying it (NFH and IMH, 1994).

In the Three-Gorges area of the Yangtze River evidence of 404 landslides and avalanches has been observed with a total volume of 3 billion m^3, which dammed the river and stopped navigation in the channel many times. Figure 4.6 shows the distribution of large-scale landslides and rock avalanches along the Yangtze River near the Three Gorges Dam. Many villages and towns are located in the old landslide areas or even on the sliding bodies. Landslides threaten the people there. Most of the landslides are bedrock landslides occurring in strata of classic rocks with weak intercalation. There are a few landslides in surface deposits. They were partly or completely revived old landslides in bedrock. The Liyutuo landslide is located in Wushan County, on the left bank of the Yangtze River, as shown in Fig. 4.6. The volume of its remains is about 10 million m^3. In September 1979, a rainfall that lasted for more than 10 days triggered superficial landslides on the front part of the landslide deposit with a volume of 0.78 million m^3. Soon afterwards, several open cracks appeared near the rear margin and the east lateral border of the old landslide deposit (SCST and MGMR, 1988).
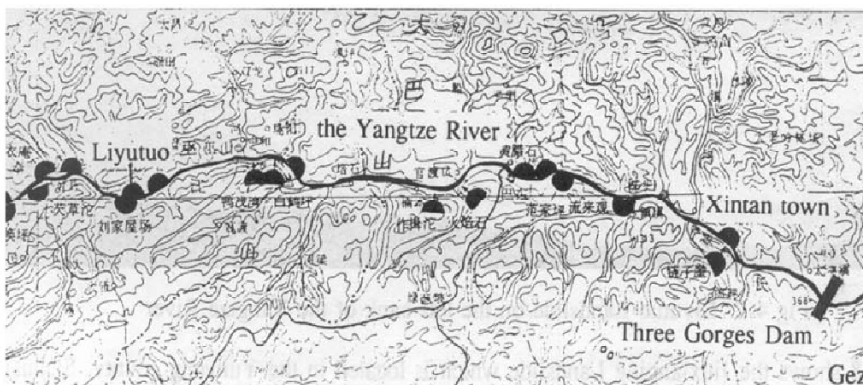
Fig. 4.6 Distribution of large-scale landslides and rock avalanches along the reaches of the Yangtze River upstream of the Three Gorges Dam

The Xintan landslide occurred in 1985. It was a large-scale landslide that attracted attention from the whole country. Figure 4.7 shows the sliding body of the Xintan Landslide before and after sliding. The town of Xintan was located on the left side of the Yangtze River in Xiling Gorge, about 37 km upstream from the Three Gorges Dam site. At 3:45 on June 12, 1985 a sliding body 50 m thick, 2,000 m long and 200-700 m wide with the town of Xintan on it collapsed and slid into the Yangtze River. The total volume of the sliding body was 30 million m^3 and more than 2 million m^3 thrust into the river. The Town

of Xintan on the sliding body disappeared. The sliding body induced huge waves, the first more than 90 m high and the second 50 m high. The waves destroyed 13 steel ships and 64 wooden boats. Ten people on board were killed and 8 were missing (HLIG, 1985).

(a)   (b)
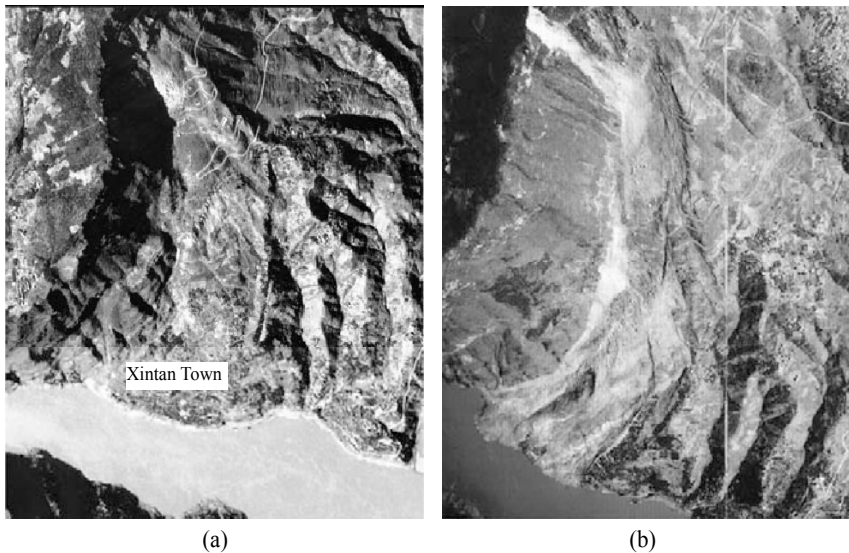
Fig. 4.7   The Xintan Landslide occurred in 1985 on the left side of the Yangtze River near the Three Gorges Dam: (a) before sliding; (b) after sliding. (after SCST and MGMR, 1988)

Landslide is the major geological disaster in Hong Kong. Figure 4.8 shows the annual landslide fatalities in Hong Kong from 1948–1996. In terms of landslides, 1972 was the most disastrous year with 150 landslide caused deaths.
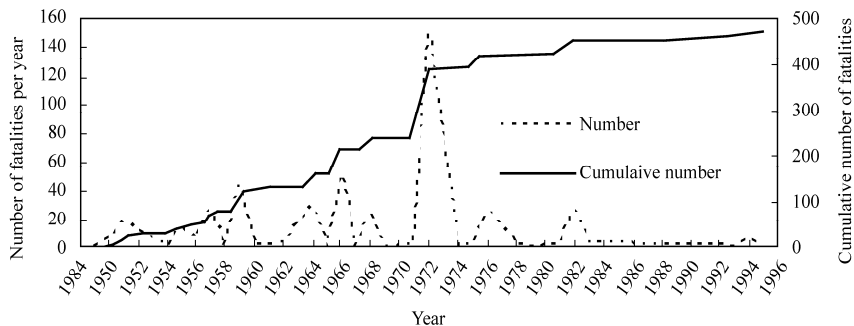
Fig. 4.8   Annual landslide fatalities in Hong Kong in the period 1948–1996. Landslides in 1972 claimed 150 lives and caused great economic loss (after Wang, 1999)

4.1.3.2   Disaster Chains

The great Wenchuan Earthquake (Ms 8.0) occurred on May 12, 2008 and killed about 100,000 people. The earthquake caused numerous landslides and avalanches on streams. According to the China Geological Survey, 1,701 landslides and 1,844 rock avalanches occurred triggered by the earthquake (Cui, 2009). Another report gave much higher numbers of landslides and avalanches, with a total number

of more than 15,000 (Yin, 2008). The zone with a high density of landslides (more than 10% of the surface area) stretches for 240 km along the Longmenshan fault, on which the Wenchuan Earthquake occurred, and the width of this zone varies from 25-30 km wide in the southwestern section of the fault to 3-5 km wide in the northeastern section of the fault.

Several disaster chains have been initiated by the Wenchuan Earthquake, and each of the disaster chains consists of several episodes (Xu et al., 2010). The disaster chain is defined as a chain of disastrous events; each event is the main cause of the next event. Four types of disaster chains have been identified. In the first chain, landslide created a quake lake, which was followed by a flood caused by landslide dam failure and very intensive fluvial processes. The last episode of the chain is loss of habitats and destruction of aquatic bio-communities. The Tangjiashan and Huoshigou landslides initiated such a type of disaster chain. The second chain consisted of a huge landslide burying a drainage system, debris flows, and development of new drainage system and intensive fluvial processes. The Wenjiagou landslide initiated such a type disaster chain. The third chain consisted of avalanches, grain erosion (intensive erosion of bare rocks due to exposure to weathering and temperature change), slope debris flows, and flying stones. Many such disaster chains occurred on the mountains by the Minjiang River from Yingxiu to Wenchuan. The fourth chain has only two episodes: the first episode was avalanches during the earthquake at elevations between 100 and 800 m from the riverbed, and the second episode was new avalanches and rock falls due to increased slope angle in the high mountains (400-1500 m from the riverbed).

1) Chain 1: Landslide—dam failure flood—intensive fluvial process—loss of habitats
Chain 1 consists of four disastrous events: 1) a landslide occurring almost at the same time of the earthquake and formation of a landslide dam on rivers; 2) landslide-dam failure after a short period of storage of river water (10-60 days) and subsequent flooding; 3) intensive sediment movement and fluvial processes in the downstream reaches; and 4) loss of aquatic habitats and dramatic reduction of fish and macro-invertebrate species.

The most precarious of quake lakes triggered by the Wenchuan Earthquake was the Tangjiashan quake lake on the Jianjiang River that was formed by a huge landslide from Tangjiashan Mountain. The volume of the sliding body was about 20.37 million m^3 and the landslide dam was 612 m long (across the river), 803 m wide (along the river), and 82–124 m high. It mainly consisted of quaternary deposits and clastic rocks. The total storage capacity of the quake lake was about 316 million m^3. There was a high risk of dam-break flooding when 200 million m^3 of water had stored in the lake. A spillway was dug on the dam and then the water began releasing through the spillway. To help the water scour the spillway bed to a low level, large boulders were removed by explosions. The elevation of the spillway channel on the dam was eroded down from 740 m to 714 m, and the channel bed was cut wider from about 10 m to 100 m (Fig. 4.9(a)). The lake water volume reduced from 246 million to 86 million m^3. Although the peak discharge rate was 6420 m^3/s during the course of channel cutting and lake-water draining, no casualties or damage were caused by the draining flood. The dam draining flood carried a lot of sediment to the downstream reaches and an intensive fluvial process was initiated. The downstream reach was silted up by 20 m and intensive sedimentation and erosion occurred in 2008 and 2009. A 20 m thick sedimentation layer was scoured by floods in 2008 and 2009 and a new channel formed in the river (Fig. 4.9(b)).

The second example of disaster chain 1 was initiated by the Huoshigou landslide. The Huoshigou Ravine is a second-order tributary of the Minjiang River in Chongzhou, near Chengdu. It was a straight river with very steep slopes and good riparian vegetation before the earthquake. The Huoshigou landslide was a high-speed and long-distance landslide, which created an extremely huge air cushion and air waves with strong and destructive impact during its movement (Zhang, et al, 2008). Hundreds of houses were buried and 39 people were killed by the landslide.

(a)

(b)

Fig. 4.9 (a) Lake water flows through the enlarged spillway from the Tangjiashan quake lake and scours the landslide dam on May 31, 2008; (b) Sedimentation and new channel in the downstream reach of the Tangjiashan quake lake (Nov. 2009)

The landslide created a small quake lake with a capacity of 75,000 m^3. Witnesses stated that the landslide moved down along the ravine and was obstructed at the Calabash Mouth, a very narrow section of the ravine. Thus, the solid materials piled up and formed a dam. The dam was composed of very fine and loosely deposited materials. During a rainstorm, the water level in the quake lake rose sharply and soon caused dam failure on May 13, 2008. Two more rainstorms occurred on May 14 and 17, 2008, which resulted in floods and scouring of the dam. A "V" shape channel with a depth of more than 50 m and bank slope angle of 38° was scoured through the dam.

Three large scale debris flows carried a huge amount of solid materials to the downstream reaches and created a 2–30 m thick sedimentation layer in a section of about 7 km of the river. The sediment deposit was scoured again by flood, and intensive fluvial processes occurred in the section. Figure 4.10 shows the location of the landslide occurrence, the sliding area, the area of landslide deposits, the quake lake and the deposits of debris flows.
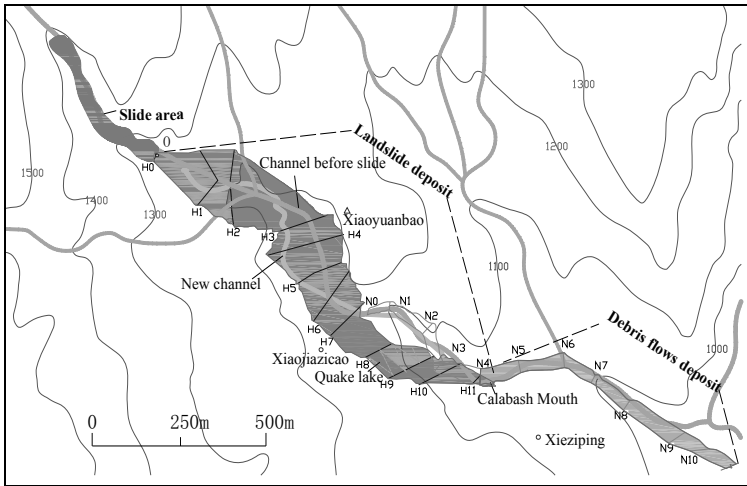
Fig. 4.10 Huoshigou Gully landslide and the initiated disaster chain

Figure 4.11 shows the longitudinal profiles of the river pre-, post-, and one year after the earthquake. The longitudinal profile and cross-sections before the earthquake were obtained from a 1960s topographic map with a scale of 1:50,000. By using the map and the measured cross sections, the volumes of the landslide deposits and debris flows deposits were calculated. The volume of the landslide deposit was 7.21 million m^3, and the volume of the debris flow deposit was 1.25 million m^3. The debris flow caused an intensive fluvial process, which in turn caused habitat loss and dramatic reduction of biodiversity in the downstream reaches. Two samples of benthic invertebrates were taken in the river reaches affected and unaffected by the debris flows about ten months after the earthquake. The sampling area, flow velocity, and substrates were similar at the two sites. The species were identified under a microscope. In the unaffected reach sixteen families or genus were found including several very intolerant species, such as Corydalidae, Rhyacophilidae, and Goeridae. In the affected reach, however, only seven families or genus were found. The biodiversity was much lower due to the intensive fluvial process.
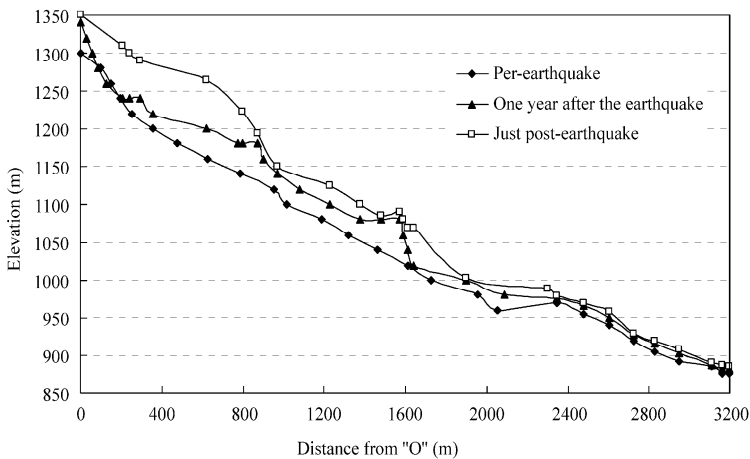
Fig. 4.11 Longitudinal profiles of the Huoshigou Ravine channel pre-and postf-earthquake, and one year after the earthquake

2) Chain 2: Landslide—debris flows—new drainage system—intensive fluvial process

Chain 2 consists of four disastrous events: 1) a huge landslide at the time of the earthquake and burial of the entire drainage system; 2) debris flows in the first and second flood seasons; 3) development of a new drainage system in the first few years after the earthquake; and 4) incision of the new channels and intensive fluvial processes.

An example of disaster chain 2 was initiated by the Wenjiagou landslide during the Wenchuan Earthquake. The Wenjiagou Ravine is a tributary of the Mianyuan River and is located in Qingping Township, which was 3.25 km long with a drainage area of 12.31 km^2. All of the gullies in the drainage area were incised with depths of more than 100 m and bank slopes of 30–50. The Wenjiagou landslide began from a high elevation and slid very fast along the ravine to the confluence with the Mianyuan River. The total volume of landslide deposit was about 81.6 million m^3 (Sichuan Geological Engineering Corporation, 2009). The landslide buried the Wenjiagou Ravine and its tributaries underneath landslide debris with a thickness of 20–180 m. Thirty-four houses were buried, and more than 80 people were killed by the landslide. The landslide deposit consists of loose solid materials with different sizes.

The Wenjiagou Ravine was not a debris flow gully and there was no debris flow in the past 100 years before the earthquake. The landslide provided plenty of loose materials for debris flow. Almost all rainstorms with an intensity higher than 30 mm/day triggered debris flows in 2008. A large debris flow after a rainstorm with an intensity of 88 mm/day on Sep. 22–24, 2008 transported 0.9 million m^3 of sediment to the ravine mouth, burying roads, houses and farmland. The debris flows scoured the landslide deposit and formed a "V" shaped channel with a depth of 50 m. About 1.7 million m^3 of sediment has been removed from the landslide deposit by the debris flows, and about 1 million m^3 of sediment has been carried to the ravine mouth.

A new drainage system was developing in the process of scouring and debris flows. Figure 4.12 shows the landslide and the new gully that was developed on the landslide deposit. Figure 4.13 shows the longitudinal profiles of the Wenjiagou Ravine before the earthquake, after the landslide in May 2008, and after new drainage development in 2009. Very intensive channel bed incision occurred on the new Wenjiagou Ravine. Because the banks of the new gully were very steep, incision of the gully bed caused collapse of the banks. Consequently, more debris flows took place. In the meantime, the sediment carried into the Mianyuan River also caused intensive fluvial processes.

3) Chain 3: Avalanches—grain erosion—slope debris flow

The Wenchuan Earthquake triggered numerous avalanches and rock falls along streams. The avalanches have left a great area of bare rocks (Wang et al., 2009a). The newly exposed rocks are fragile and easily broken down under the action of sunshine and temperature change. Intensive grain erosion has been occurring since the exposure, details of grain erosion are discussed in Chapter 2. The rate of grain erosion of bare rocks on the Minjiang River was between 3 to 53 cm/yr, with an average of about 17 cm/yr (Wang et al., 2010a).

Grain erosion caused slope debris flows and generated flying stones, which caused damage to cars and injured humans. Grain erosion resulted in a lot of loose and uniform particles depositing with high slopes. Rainfall with an intensity of more than 20 mm/day triggers mass movements of the grains. These mass movements behave like debris flows but the distance of the movement is, however, much shorter than normal debris flows, and in general travels only several tens to one hundred meters. This mass movement is called slope debris flow. It carries a lot of grains into rivers or deposits the grains on highways, causing blockage of highway transportation or local sedimentation on the riverbed.
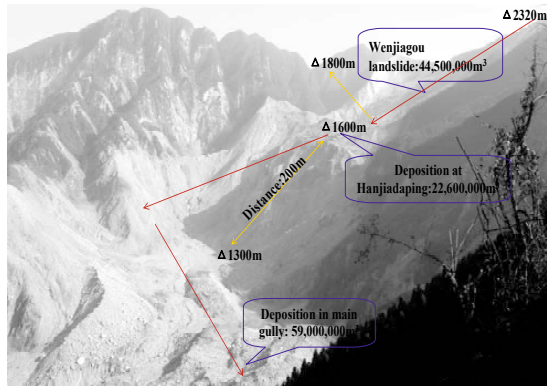
(a)

(b)

Fig. 4.12 (a) Wenjiagou landslide (after Sichuan Geological Engineering Corporation, 2009); (b) New Wenjiagou Gully is developing on the deposits of the landslide (See color figure at the end of this book)
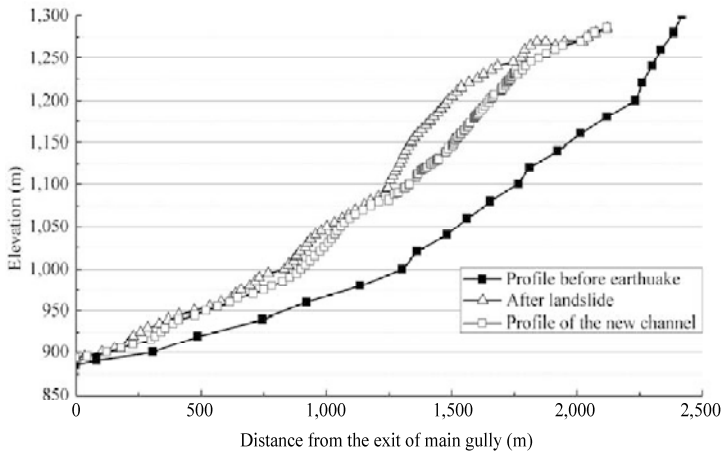
Fig. 4.13 Longitudinal profiles of the main channel before the earthquake, after the landslide in May 2008, and after the new drainage development in 2009

4) Chain 4: Avalanches—new avalanches

Chain 4 consists of only two disastrous events: avalanches during the earthquake, which mainly occur at an elevation near the riverbed; and new avalanches at higher elevations. More than 90% of the avalanches directly triggered by the Wenchuan Earthquake occurred in an elevation range of 100-800 m above the riverbed. The avalanches increased the slope of the upper part of the mountains.

Many avalanches were triggered by the Wenchuan Earthquake on the Minjiang and Yuzixi rivers, where the lithology was mainly granite. The Yuzixi River is a tributary of the Minjiang River, which flows into the Minjiang River at Yingxiu. The density of avalanches was so high along the two rivers that about 50% of the valley slopes (0-500 m from the riverbed) were covered by avalanches. Figure 4.14(a) shows the area percentage of avalanches on the valley slopes along the river from the mouth at Yingxiu to Qicenglou. The percentage was measured with laser range meters. Figure 4.14(b) shows the riverbed profile before the earthquake, which was obtained from DEM data measured in the 1960s; the riverbed after the avalanches in 2008, which was measured using GPS receivers; and elevations of avalanches, which were measured by using laser range meters. The avalanches created many small quake lakes and enhanced the bed elevation by several tens of meters at different places. The avalanches mostly occurred at elevations between 100 and 600 m from the riverbed.
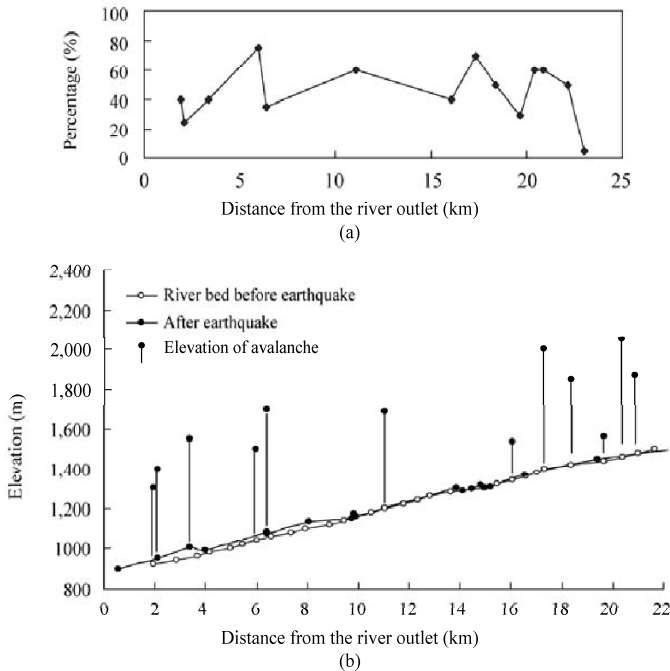
Fig. 4.14   (a) Area percentage of avalanches on the valley slopes along the Yuzixi River; (b) Riverbed profile before the earthquake, after the avalanches, and the elevation of the avalanches

On the Minjiang River, the upper part of the mountains (400-1500 m from the riverbed) lost the support of the lower part due to the avalanches below. The slopes of the upper mountains increased or even some parts became suspended. Moreover, the earthquake caused the rocks to be cracked and broken. In the following years, new avalanches occurred when rainstorms or tremors occurred. In 2009, such avalanches occurred at the Chediguan Bridge on the Minjiang River and Zongqugou Ravine, a tributary of the Minjiang River.

The highway from Dujiangyan to Wenchuan was seriously damaged by the earthquake and was reconstructed and reopened before the one-year anniversary of the earthquake. The Chediguan Bridge is a key bridge crossing the Minjiang River. The bridge was broken by new avalanches from the right bank of the Minjiang River (N31°18'05.9", E103°27'59.1") at 4:40 in the morning of July 25, 2009 (Beijing Time). In fact, this event was the second episode of the disaster chain. The Wenchuan Earthquake caused many avalanches on the slopes with elevations of 100–400 m from the riverbed at this place. Consequently, rocks at higher elevations became unstable. Consecutive rock falls occurred from elevations of about 400 m in the afternoon of July 24, 2009, as shown in Fig. 4.15(a). In the morning of July 25, 2009, an avalanche occurred from elevations of 500-600 m. A huge stone of more than 200 tons fell down and broke the third pier of the Chediguan Bridge, causing more than 60 m of the bridge to collapse. Five trucks and a van dropped into the Minjiang River, six people were killed and 12 injured. Transportation was cut off for two weeks (http://bbs.3608.com/showtopic-247080-1.html).

Figure 4.15(b) shows a side view the cross-section of the avalanches. The banks are so steep because the riverbed has been incising for centuries due to the fluvial process of the minjiang River. The slope angle of the right bank is 40°–50°, which is higher than any repose angle of solid materials. The avalanches during the earthquake increased the slope in the upper part of the bank. Thus, new avalanches occurred and caused the tragedy.
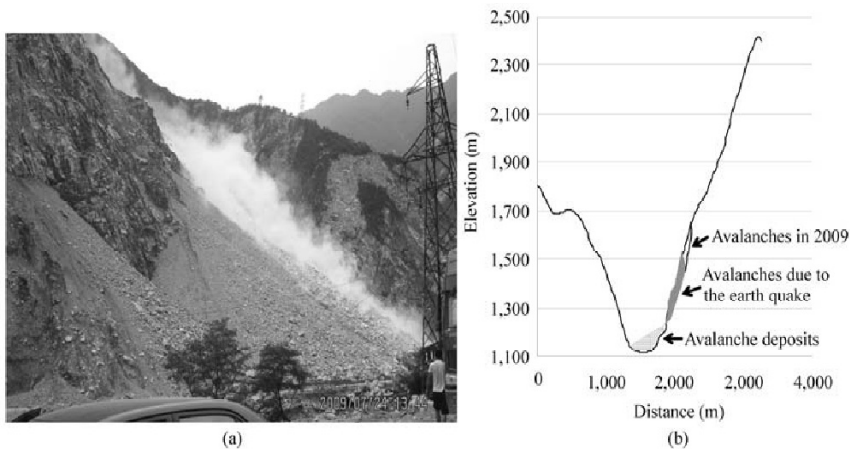
Fig. 4.15 Small scale avalanches and rock falls at Chediguan on July 24, 2009; (b) Side view of the Chediguan avalanche (on July 25, 2009)

A similar event occurred at the Zongqugou Ravine, a deeply incised tributary of the Minjiang River near Maoxian. The lithology was mainly composed of limestone which was easily cracked by the earthquake. The bank slopes, especially the left bank, were also in the range of 40-50° before the earthquake (as shown in Fig. 4.16). The Wenchuan Earthquake caused avalanches and rock falls from the elevations of 400~800 m. Huge stones with diameters of 1-15 m dropped into the Zongqugou Ravine and formed a quake lake with a capacity of about 200,000 m^3. In March 2009, an avalanche occurred at high elevations (>800 m) and several huge stones larger than 10 m of diameter fell down and hit against on the quake lake dam. The dam was partly broken and a small dam failure flood occurred, which caused no casualties.

5) Attenuation factor

In the four disaster chains, the time of occurrence of each disaster episode is longer than that of the previous episode. Figure 4.17 shows the estimated time of occurrence of various disasters. Landslides and

avalanches occurred almost simultaneously with the earthquake. Landslide dam failure floods occurred about 10–60 days after the landslides. The Chi-Chi Earthquake in Taiwan, China on Sep. 21, 1999, caused an unusually high frequency of debris flows and intensive fluvial processes in about 10 years after the earthquake (Lin et al., 2008). The impacts on ecology are mainly caused by the intensive fluvial process and last for about a decade. Soil erosion and grain erosion intensified by the earthquake may last for 100 years (Koi et al., 2008; Lin et al., 2008). New avalanches occurred due to the increased slope and cracked rocks. The time of occurrence of the avalanches in high elevations is estimated to be within 10 years. Vegetation development may mitigate the risk of avalanches in high elevations.
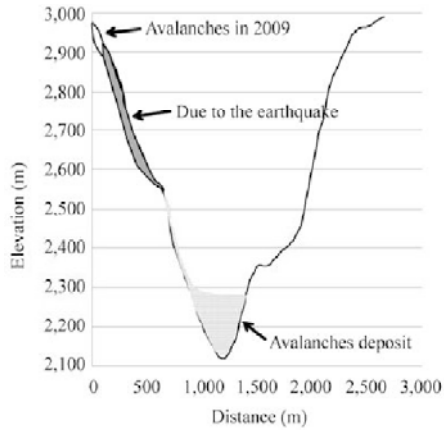
Fig. 4.16   Side view of the Zongqugou avalanches
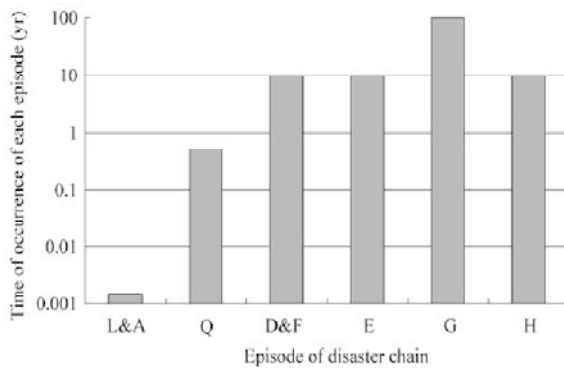
Fig. 4.17   Estimated time of occurrence of various disasters: L&A: Landslides and avalanches; Q: Failure of quake lake dam; D&F: Debris flows and intensive fluvial processes; E: Impacts on ecology; G: Erosion, especially grain erosion; H: New avalanches at high elevations

In the four disaster chains, the intensity of each disaster episode is lower than that of the previous episode. There is attenuation along the disaster chain. If the magnitude of the geological disaster is evaluated using volumes of mass movement the attenuation factor can be defined as the ratio of the volume of mass movement in one episode of a chain to the volume of the mass movement in the previous episode. For instance, in the Huoshigou disaster chain, the volume of the landslide was 7.21 million m^3, but the volume of all debris flows was 1.25 million m^3. Thus, its attenuation factor is 0.17.

In the Wenjiagou disaster chain, the total volume of the landslide was 81.6 million m^3, and mass

movement in debris flows was about 6.2 million m^3. Moreover, debris flow will continue to occur in future. Thus, the attenuation factor would be about 0.08. In chain 3, the attenuation factor may be calculated with the area of rocks on which avalanches and grain erosion occurred. On the Minjiang River from Caopo to Wenchuan, grain erosion occurred on about 30% of the bare rock surface. In other words, the attenuation factor for avalanches and grain erosion was about 0.3. In chain 4, the new avalanches occurred only at several places. The ratio of areas with new avalanches was very small. In conclusion the intensity of disasters attenuates from one episode to the next episode. If the attenuation factor is defined as the ratio of the volume of mass movement in one episode to that of the previous episode, the attenuation factor varied in the range of 0.08–0.3.

4.1.4 Debris Flow Disasters

4.1.4.1 Burying Cities and Towns
Debris flows have brought disasters to cities, towns, and villages. Records show that about 100 cities and towns have been hit by debris flows, such as Hanyuan, Luding, Derong, Xichang, Nanping, Luhuo, and Jinchuan in Sichuan Province; Dongchuan, Qiaojia, Nanjian, Deqin, and Yangbi in Yunnan Province; Jiangzi, Yadong, Basu, Dingri, Suoxian, and Dingqing in Tibet Autonomous Region; and Lanzhou, Wudu, Wenxian, and Lixian in Gansu Province. A huge scale of debris flow occurred in the suburbs of the Xichang in Sichuan Province in 1891, it damaged 5 streets and caused more than 1,000 casualties.

On July 8, 1984, a debris flow was triggered in the Guanmiao Ravine, Nanping County in Sichuan Province. The debris flow carried 60 huge stones of diameter 5–10 m and 430 stones of diameter 2–5 m and rushed down to the county town with a velocity of 9.2 m/s. It cut away half of a three story building and destroyed a 1 m thick concrete wall of a prison. Boulders, rocks, gravel, and silt buried the street.

Rain continued from August 18 to 20, 1978, in the Pingshan County of Hebei Province, which is located on the east slope of Taihang Mountain. The soil was saturated with water. Finally, a strong rainstorm with an intensity of 400 mm in 4 hours on August 20 initiated a debris flow in the evening. The debris flow carried 12 million m^3 of solid material and rushed into the Niujuangou at high speed. The head of the debris flow was 13 m high. The whole village was flattened and more than 20 people were killed.

In the watershed of the Daying River in Yunnan Province, there are 116 debris flow gullies. The Lianghe is located in the downstream fan of two debris flow gullies. Two debris flows occurred in 1975 and buried the long distance bus terminal and the Lianghe High School. A debris flow in 1977 rushed into the town of Jiubao, and destroyed 100 houses and killed 1 person. In 1968 a terrible debris flow occurred in the Nanhuai River (a tributary of the Daying River) and washed 3 villages away killing 97 people. More than 200 ha of farmland and several sections of the highway were buried.

In Xide County in Sichuan Province, the town of Hongmo was flattened by a debris flow in 1967. All buildings and houses were destroyed and 80 people were killed. The town residents had to resettle in neighboring areas. On July 10, 1988, a debris flow from Huaying Mountain buried the town of Xikou, Ma-an-ping village, the Xikou cement factory and the No.12 coal mine. Gravel and silt buried many buildings, transportation facilities, and 221 people. On May 27, 1984, a debris flow from the Heishan Gully buried the Yinmin copper mine in Dongchuan, Yunnan Province. The mine stopped production for half a month and lost a million dollars.

4.1.4.2 Cutting Railways and Highways
Debris flows have brought disasters to railways by burying railway tracks and stations, damaging railway structures, derailing trains, killing passengers, and cutting off transportation. There are 1,368 debris flow gullies along the railways in China. Two hundred and ninety-two debris flow disasters have happened in the past years and 41 railway stations were buried. Railway transportation was stopped for 7,500 hours between 1950 and 1990 (Shen et al., 1991).

On July 7, 1959, and August 5, 1979, rainstorms initiated debris flows in the Bayan and Samalong canyons by the Qinghai-Tibet Railway. Debris flows destroyed several bridges, blocked several culverts, damaged several hundred meters of railway tracks, buried 27 houses, overturned a freight train, and killed 17 people in 1979. The railway was cut off for two days. On July 20, 1964, a mudflow was initiated by a rainstorm in gullies of Gaolan Mountain, in the southern suburbs of Lanzhou, Gansu Province. The mudflow damaged a small bridge and carried and unloaded 250,000 m^3 of silt, sand, and gravel to the Lanzhou Railway Hub. Twenty-five days latter, another mudflow from the Naoding Gully buried the Chengguanying Station (near the Lanzhou station) again. The mudflows stopped rail traffic for 34 hours.

In 1969, a debris flow from the Puwei Gully destroyed shelters of construction workers for the Chengdu-Kunming Railway and caused 23 casualties. In the same year, a debris flow from the Shamalada Gully killed 40 workers who were constructing the railway. In 1974, a debris flow from Erduluku Gully buried the Aidai Railway Station and killed two people. On July 12, 1978, a rainstorm in the Baoji-Tianshui area triggered landslides in the Caizi Gully (with a catchment area 0.4 km^2) and the Mitang Gully (0.5 km^2). The landslides soon transformed into mud flows and rushed to the Lanzhou-Lianyungang railway. The mud flows damaged a bridge, blocked a 2.25 m arch culvert, destroyed 80 houses, and buried the Railway with 200,000 m^3 of sediment. The debris on the railway was 4 m high and 360 hours were spent to remove it.

On July 9, 1981, a debris flow with an 8 m high head flowed from a gully to the Chengdu-Kunming railway at velocity of 13.2 m/s. It carried rocks with diameters of several meters and the density of the mixture was estimated at 2.32 t/m^3. The debris flow damaged the 110 m long Liziyida Bridge at the Dadu River of the Chengdu-Kunming Line. A pier and an abutment were destroyed. The No. 422 passenger train crashed and overturned and 300 passengers were killed. More than 5 million dollars were lost and the railway was blocked for 384 hours. On August 21, 1981, a long duration rainstorm initiated torrential floods and 45 debris flows carrying huge amounts of sediment in the Baoji-Luoyang area. The debris flows buried 5 railway stations and sections of railway tracks, damaged 8 bridges, silted 4 tunnels, and blocked several culverts along the Baoji-Luoyang Railway line. The rail traffic was stopped for 2 months. In Taiwan, debris flows cause cutoff of highways quite often. Figure 4.18 shows a highway bridge destroyed by a debris flow in Hualian County in Taiwan Province, China (Zhang, 2006). Debris flows often have cut off railway transportation. Recently a debris flow buried the mountain railway and blocked a train on June 11, 2006 (China Times, June 11, 2006).

Fig. 4.18   A debris flow destroyed a highway bridge in Hualian County in Taiwan Province, China (after Zhang, 2006)

There are 341 debris flow gullies along the Sichuan-Tibet Highway. More than 1,300 debris flows blocked, buried, and destroyed the highway in the past 30 years. Debris flows destroyed 17 of the 48 bridges

along the highway, and damaged or blocked 200 culverts. Highway transportation was stopped for more than 1,500 days. Annual cost resulting from debris flow was more than 1 million dollars. In 1985, a huge scale debris flow occurred in the Peilong Gully, which is located in the Bomi-Dongjiu section of the highway. The debris flow destroyed several hundred meters of the highway and overturned more than 80 vehicles including trucks, buses, and cars. The highway was then blocked for more than 6 months (Wu et al., 1993).

4.1.4.3 Damming Rivers

Many debris flow gullies are perpendicular to main river channels. Debris flow carries a huge amount of solid materials to the confluence with the main river and often dams the main river channel. Sometimes the debris dam is high and a barrier lake is formed. The retained water inundates farmland, roads, highways, and villages upstream from the debris dam. When the debris bar is broken, a more serious catastrophe can be caused to the downstream area.

It is recorded that debris flows from the Baishui Gully in Yunnan Province dammed the Yangtze River two times. Debris flows from the Hailuo Gully dammed the Longchuan River, a tributary of the Yangtze River three times. On July 18, 1984, a debris flow from the Guanmiao Ravine of Nanping County, Sichuan Province, dammed the Bailong River. The debris dam was broken after 30 minutes and a torrential flood was generated. The flood carried the sediment downstream and destroyed villages, many houses, farmland, and highways. The flood also resulted in aggradation and incision of the downstream channel.

Debris flows from the Jiangjia Gully dammed the Xiaojiang River for 48 days in 1919, 40 days in 1937, 30 days in 1949, 19 days in 1954, 78 days in 1961, 98 days in 1964, and 90 days in 1968. The dammed river water inundated 600 ha of farmland, highway, and railway. Figure 4.19(a) shows the debris flow deposit, which dammed the Xiaojiang River for 2 weeks. Figure 4.19(b) shows the Yangtze River, which is almost dammed by the debris flow deposit from the Xiaojiang River.

(a)

Fig. 4.19 (a) A debris flow deposit dammed the Xiaojiang River; (b) The upper Yangtze River (Jinsha River) is almost dammed by a debris flow deposit from the Xiaojiang River

Debris flow could also result in the river moving from its original location to a new channel. The Xiaojiang River was a meandering river. Since the last century the watershed has become a very active debris flow area. Debris flows have carried a lot of sediment into the river, and, therefore, accelerated the siltation of the channel. The river then changed from a meandering into a wandering river. Debris flow also has caused quick sedimentation of reservoirs.

4.1.4.4   Degrading Environment

Debris flow may cut the gully bed by 3–5 m, sometimes by more than 10 m, and carry 0.1–10 million m^3 of solid material to downstream rivers or hill slope fans. The intensive erosion causes instability of the slope, collapse of the gully banks, and destroys the slope vegetation. The gravel, boulders, and cobbles carried by debris flow deposit in the gully mouth and cover grassland and farmland there. The mouth is then changed into a sea of stone. Debris flow transports a lot of sediment into the downstream rivers and makes the sediment concentration high and the water quality bad.

Debris flow may destroy forests and result in an enlarged diurnal temperature difference and wind intensification. Debris flow areas become drier in the dry season and suffer from more intense rainstorms in the wet season. The groundwater table lowers because it is recharged less due to less detention time of rainfall on the surface and in surface runoff flows. Farmland is destroyed by debris flow and then the farmers have to plough the slope land speeding up slope erosion. Debris flow may also change the landscapes. Figure 4.20 shows that a debris flow buried and scoured farmland by the Jiangjia Ravine in southern China in 2008.

Fig. 4.20   A debris flow buried and scoured farmland by the Jiangjia Ravine in southern China in 2008

4.2   Effects of Landslides on Rivers

4.2.1   Essential Cause of Landslides

4.2.1.1   Riverbed Incision

The continuous rising of the Qinghai–Tibet Plateau has resulted in steep slopes and several active faults around the margin of the plateau, including the Longmenshan Faults where the Wenchuan Earthquake

occurred in 2008. At the east margin of the plateau river-bed incision has dominated the fluvial processes. The slope of the stream banks increases with channel bed incision and is in a threshold state. Any further increase in slope due to incision and disturbances from earthquakes or rainstorms may result in landslides. Deep landscape dissection has produced high-relief, narrow river gorges, and threshold hill-slopes that frequently experience large landslides, making the entire region highly susceptible to quake lake formation. The landslide dams and their management are important in the morphological process. Essentially, incision created the conditions necessary for landslide occurrences, but landslide dams and resulting quake lakes in turn slowed or stopped river bed incision.

The essential cause of avalanches and landslides is the riverbed incision no matter if they are triggered directly by earthquake or rainstorm. As shown in Fig. 4.21, as the river cuts into the bed below the sliding surface, the sliding body loses the support of the sediment and rock at the toe of the sliding body and the sliding body slides along the slip surface into the river. If the river bed was not incised to the depth of the slip surface then the landslide would not occur. From the viewpoint of river training and management, some landslides might be prevented if the riverbed incision were controlled.
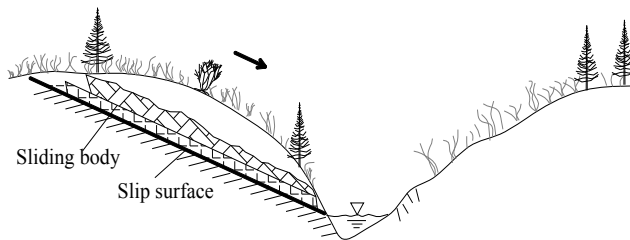
Fig. 4.21 A stream cutting the bed below the slip surface and causing a landslide

4.2.1.2 A Simple Model of Landslides

The stability of the sliding body and the critical condition for landslide formation can be simply explained using Fig. 4.22, in which W is the weight of the loading per area of the slip surface, U stands for the uplift force resulting from pore groundwater pressure in the soil, α is the angle of the inclined slip surface, $\tan\phi'$ is the frictional coefficient, and τ_y is the yield strength of the material. Landslide will occur if:

$$W\sin\alpha > \tau_y + (W - U)\cos\alpha\tan\phi' \tag{4.1}$$

This method is appropriate in cases of translational landslides on gentle slopes and in homogeneous soils. An earthquake may reduce the yield strength and the frictional coefficient suddenly and trigger many landslides in a very short time.
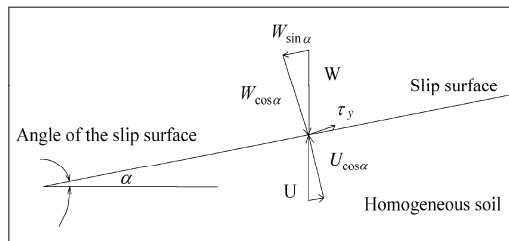
Fig. 4.22 Stability of a sliding body and the critical condition for translational landslide on a gentle slope in homogeneous soils

The model (Eq. 4.1) implies that an increase in loading, for instance due to rainfall and or supply of water to the soil; an increase in the angle of the slip surface, for instance due to stream incision and erosion of the toe of the sliding body; reduction in the yield strength, for instance during earthquake, and reduction in the frictional coefficient, may result in landslides.

Seismic waves cause not only sudden reduction in the yield strength of the slip surface, but also cause a sudden increase in pore pressure. Using real seismic waves, the possible seismic loadings on the sliding surface due to the seismic excitation during earthquake have been studied. Through a newly developed ring shear apparatus, the seismic loadings were applied successfully to the soils on the sliding surface to mimic the seismic response of soil during an earthquake (Wang et al., 2007). Figure 4.23 shows the result of a seismic simulation test, in which the normal stress is equal to W, or the weight of loading per area. It reveals that due to the seismic loading, a certain amount of excess pore-water pressure was built up within the saturated sliding surface, which led to the failure of the slope (Wang et al., 2007). As the pore pressure increases to about 0.5 times of the normal stress, the shear resistance reduces sharply. As the pore pressure increases to nearly equal to the normal stress, the shear resistance reduces to zero and displacement increases quickly (sliding occurs). After failure, high excess pore-water pressure was generated with an increase of shear displacement. This finally resulted in a great reduction in the shear resistance and rapid movement.
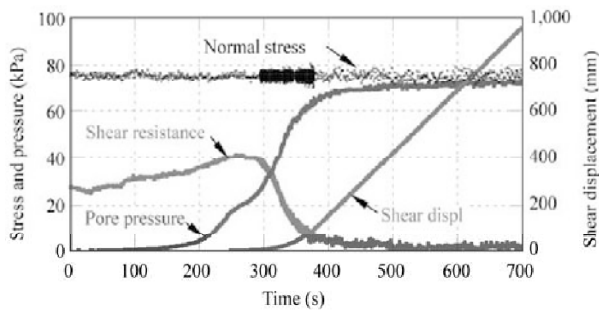
Fig. 4.23 Result of seismic simulation test - Due to the seismic loading, a certain amount of excess pore-water pressure was built up within the saturated sliding surface, which led to the failure of the slope (after Wang et al., 2007)

4.2.2 Landslide Dams

4.2.2.1 Removal and Preservation of Landslide Dams

Large landslides often create landslide dams. Landslide dams may fail, be removed or be preserved. In the past, humans could do nothing on the landslide dams, which failed or remained naturally depending on the composition of landslide debris and on the flow discharge of the rivers. At Tianshan Mountain, which is shared by China, Kazakhstan, Uzbekistan, Kyrgyzstan, and Tajikistan, the Sarez Earthquake triggered the Usoi landslide with a volume of 2.2 billion m^3. The landslide blocked the Murgab River with the highest landslide dam in the world (500–600 m high), forming Sarez Lake, in 1911 (Gaziev, 1984). Almost one century has passed and Sarez Lake is still storing water and the water level is rising at a rate of 18.5 cm/year (Schuster and Alford, 2004). The risk of dam failure is increasing following the increasing water level and the safety of the dam has attracted world wide attention.

Some researchers have concluded that landslide dams will inevitably fail, probably due to channel erosion during a flood. Many landslide dams fail within 1 year or less (Costa and Schuster, 1988; Schuster, 2000). Becker et al. (2007) have the same opinion and they indicated that no landslide dams formed in large rivers on the West Coast in the central Southern Alps had survived to the present day. For example,

Buller River dams formed during 1929 and 1968 earthquakes failed within days or weeks of formation during floods or high normal flow (Hancox et al., 1997). If a landslide dam fails it induces catastrophic outburst floods and debris flows following rapid dam failure. One of the earliest historic accounts of a landslide dam-break flood has been described by Hegan et al. (2001) and IGNS (2003) for Waimatai Stream near Waihi in New Zealand.

Nevertheless, Korup (2004b) indicated that the failure theory is in fact not true. Korup et al. (2006) found large rockslides and rock avalanches that blocked rivers in the late Pleistocene to Holocene were preserved in the Himalayas, the Tien Shan, and the New Zealand Southern Alps despite rates of uplift and erosion of up to 10 mm/year. These natural dams controlled fluvial response on 10^1–10^4 year timescales and the rockslide dammed lakes had persisted up to ten thousand years before being drained or filled. Nicoletti and Parise (2002) analyzed the stability of seven landslide dams in southeastern Sicily. These landforms were part of a set of 146 landslides in this area, which were considered to be stable. Southeastern Sicily consists of a plateau (the Hyblaean Mountains) incised by canyons and surrounded by lower lands. The landslide dams involved six rock slides and one rock fall, which were triggered by an earthquake. Landslide volume ranged from about 0.5 to 34 million m^3. With reference to Crozier and Pillans (1991) classification of landslide lakes, all cases show a main valley lake, and back and supra lakes were sporadically present. One damming was attributable to the 1693 earthquake with certainty; another of the dammings, to the same earthquake with high probability. Although the seven dams were stable and no failures had occurred, five dams were reincised to some extent.

Humans manage landslide dams in two ways: removal or preservation. Landslide dams triggered by earthquakes were regarded as dangerous because massive amounts of water were pooling up at a very high rate behind the landslide dams, which might eventually fail and result in dam break flooding, potentially endangering the lives of thousands of people in the downstream reaches. To eliminate the risk of dam break flooding, humans removed the landslide dams using explosives. Thus, the water volume stored in the quake lakes was released and the pool level was reduced to a minimum, so that the flood risk downstream was minimized. This strategy has been applied to landslide dams where there was a high population density in the downstream reaches. Humans are used to having everything under control. The landslide dams are naturally formed structures. The composition, structure, and physical forces within landslide dams are not well understood. Therefore, people are predisposed to remove the landslide dams.

Removal of landslide dams is not a good strategy for long term management of incised mountain rivers. Only if the stability of a landslide dam is low and a dam failure flood poses a threat to the downstream reaches, the removal strategy must be applied. On the other hand, preservation of a landslide dam has the potential to inhibit channel incision and is the best management strategy in most cases. Safran et al. (2008) used a 1-D finite difference model of longitudinal profile evolution to explore the implications of such processes for long-term (10^6 yr) incision patterns and morphologic development, and concluded that the morphologic signature of landslide dams is context-dependent but can be significant; correct genetic interpretation of longitudinal profile morphology may hinge on recognizing such effects. Ouimet et al. (2007) explored a probabilistic, numerical model to provide a quantitative framework for evaluating how landslides influence bedrock river incision and landscape evolution within the Dadu and Yalong river catchments. Stable, gradually eroding landslide dams create mixed bedrock alluvial channels with spatial and temporal variations in incision, ultimately slowing long-term rates of river incision, thereby reducing the total amount of incision occurring over a given length of river. Therefore, preservation of landslide dams may reduce new landslide hazard on incised mountain streams (Wang et al., 2009a).

Landslide dams and quake lakes are a feedback within the natural system. The landslide dams may form knickpoints on the river bed profile and initiate extensive and prolonged aggradation upstream.

They act as a primary control on channel morphology and longitudinal river profiles, inhibiting incision and further preventing the complete adjustment of rivers to regional tectonic forcing. The feedbacks among hillslope processes are prevalent throughout this landscape and are characteristic of transient landscapes on the eastern margin of the Qinghai–Tibet Plateau.

In general sedimentation begins to occur in quake lakes once the lakes are formed. Over time the quake lakes will be filled with sediment. The river banks become more stable even during earthquakes. Figure 4.24(a) shows the bed profile of the Shenxi Ravine. Three landslide dams (N1, N2, and N3) formed more than 1,000 years ago (by estimation with sedimentation rate) and the three lakes have been filled up. The landslide dams were stable because they consisted of a lot of boulders and a step-pool system has developed very well. The three barrier lakes lost their capacity due to sedimentation. There was only a 30 m section behind the N2 dam, which stored water with a depth of about 0.5 m. The river bed had been raised by 200 m, which greatly reduced the risk of potential landslides. This stream is just at the Yingxiu-Beichuan Fault. During the Wenchuan Earthquake on May 12, 2008, tectonic motion caused the left side (northwestern side) of the Shenxi Ravine to rise by 4 m. Figure 4.24(b) shows a highway along the ravine, which was tilted and broken by the earthquake. Nevertheless, no landslides or avalanches occurred on the stream. The mountains are still green, which is very different from other stream basins. Within a 30 km distance from the Longmenshan Fault, almost all mountains were bared due to landslides and avalanches triggered by the earthquake (Wang et al., 2009a). The extraordinary stability of the Shenxi Ravine is mainly due to the three preserved landslide dams.
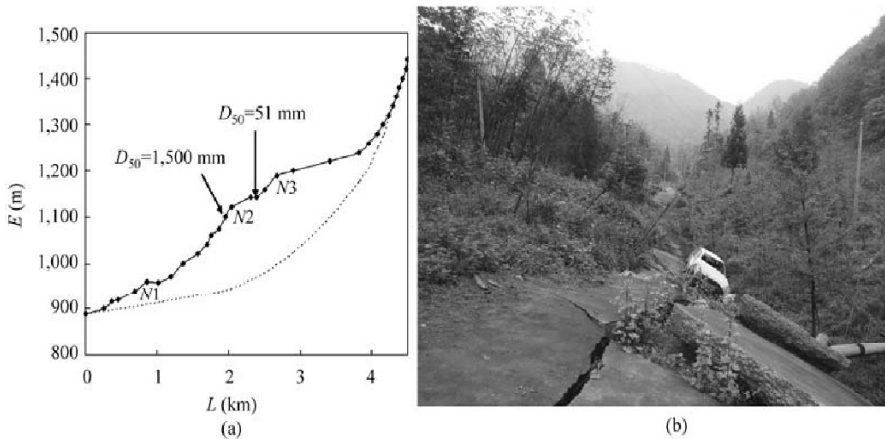
Fig. 4.24 (a) Bed profiles of the Shenxi Ravine, showing three landslide dams and filled lakes; (b) Tilted and broken highway along the Shenxi Ravine during the Wenchuan Earthquake (See color figure at the end of this book)

The incising rivers can be seen as wounds on the surface of the Earth, and landslide dams and quake lakes can be regarded as scabs formed to allow these wounds heal by themselves. The landslide dams control channel bed incision and reduce the risk of new landslides, improve the stream ecology, and create beautiful landscape. If the risk of dam failure is not high and the safety of humans is not threatened by the quake lakes, the landslide dams and quake lakes should be stabilized rather than be removed. If a landslide dam that persists for more than 10 years is assigned the "stable" status class, a statistical inventory of 232 landslide dams and quake lakes showed that only 37% of all landslide dams appear to have failed (Korup, 2004a and 2004b). This result indicates that preservation of quake lakes is not only possible, but may also be a major strategy for quake lake management.

4.2.2.2 Preservation Ratio

No landslide dam has been completely removed by a dam break outburst flood and very few landslide dams have been completely preserved. Naturally, as the water level in a quake lake reaches the lowest part of the top of the landslide dam the water flow scours the loose material and forms a spillway channel. The top of the landslide dam is scoured by the flow and, in the meantime, erosion-resistant boulders overlap and construct a step-pool system on the spillway. The most important hydraulic feature of step-pool systems is the extremely high bed roughness, which maximizes the resistance to the flow and causes the highest energy consumption, and, thus, protects the bed from being scoured (Strom and Papanicolaou, 2007). Details of step-pool systems is given in Chapter 4.

The scouring process reduces the original landslide dam material to a smaller mass composed of boulders and cobbles, stabilizing the dam and protecting the top of the initial deposit from further erosion. The step-pool system is not easily moved in even large floods, and serves to maximize the roughness of the channel (Wang et al., 2004; Maxwell and Papanicolaou, 2001). Finally, the spillway channel becomes a narrow and steep reach cutting through the landslide dam, but with a step-pool system to consume the flow energy. Thus, the height of the preserved part of the dam is lower than the original landslide dam height.

The preservation ratio of a landslide dam, R, is defined as:

$$R = \frac{H_{preserved}}{H_{original}} \tag{4.2}$$

in which $H_{preserved}$ is the dam height after the formation of the spillway channel and scouring; $H_{original}$ is the original landslide dam height. A landslide dam is regarded as preserved if the value of R is larger than 0.9; as half-preserved if the value of R is between 0.5 and 0.9; and as failed if the value of R is smaller than 0.5. The ratio reduces in the first one or two years after the formation of the landslide dam and quickly becomes stable after a major flood.

Three Diexi Lakes on the Minjiang River were created by landslides during the Diexi Earthquake (Ms 7.5) in 1933. The lakes partly failed 45 days after the dam's formation. The dam failure flood killed 2,500 people (Sichuan Seismological Bureau, 1983). Nevertheless, about two thirds of the dams have been preserved. They are half-preserved dams. Figure 4.25(a) shows the upper Diexi landslide dam, the spillway channel, and the upper and lower lakes. The lakes have a maximum water depth of 98 m although quite a lot of the lakes' capacity has been lost due to sedimentation in the past 76 years. Figure 4.25(b) shows the Shibangou landslide dam formed during the Wenchuan Earthquake on the Qingzhu River in Qingchuan County. The top part of the dam was removed by explosives in June 2008 in order to restore a highway and mines in the quake lake. More than half of the dam height is preserved, therefore, it is a half-preserved dam.
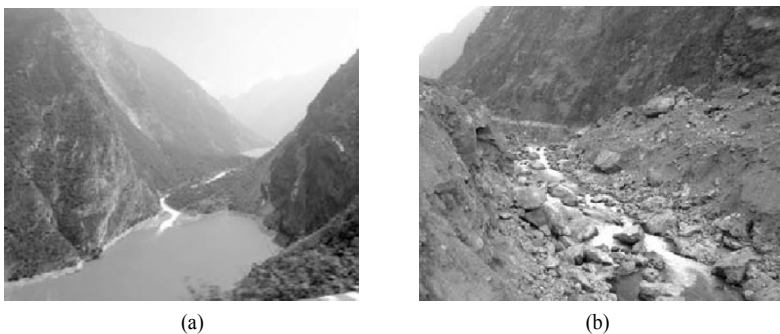
| (a) | (b) |

Fig. 4.25   (a) Spillway channel on the Diexi landslide dam, and the upper and lower lakes on the Minjiang River; (b) Half-preserved Shibangou landslide dam on the Qingzhu River in Qingchuan County (See color figure at the end of this book)

4.2.2.3 Stability of Landslide Dams

Wang et al. (2010b) studied the stability of landslide dams by field investigations. Figure 4.26 shows the study area. The landslide dams triggered by the Wenchuan earthquake are mostly around the Longmenshan Faults (dashed lines in the lower map). Tectonic motion and uplift of the Qinghai-Tibet Plateau have caused 73 earthquakes on the plateau and its margins over 267 years in the Qing Dynasty (SSB-FU, 1983). Numerous landslide dams triggered by the earthquakes have failed, remained, or been partly-preserved, and have already developed into knickpoints. To study the long term stability of landslide dams and their influence on fluvial processes, landslide dams that occurred in ancient times on the plateau and its margin also were investigated. Figure 4.26 shows the rivers and locations of 91 landslide dams created during the Wenchuan Earthquake around the Longmenshan Faults (National Panel of Wenchuan Earthquake, 2008), and ancient landslide dams (failed or preserved) on the Jinsha River, Yarlong Tsangpo, Yigong Tsangpo, Yalong River, source reach of the Yellow River, and Jiuzhai Creek on the Qinghai–Tibetan Plateau.
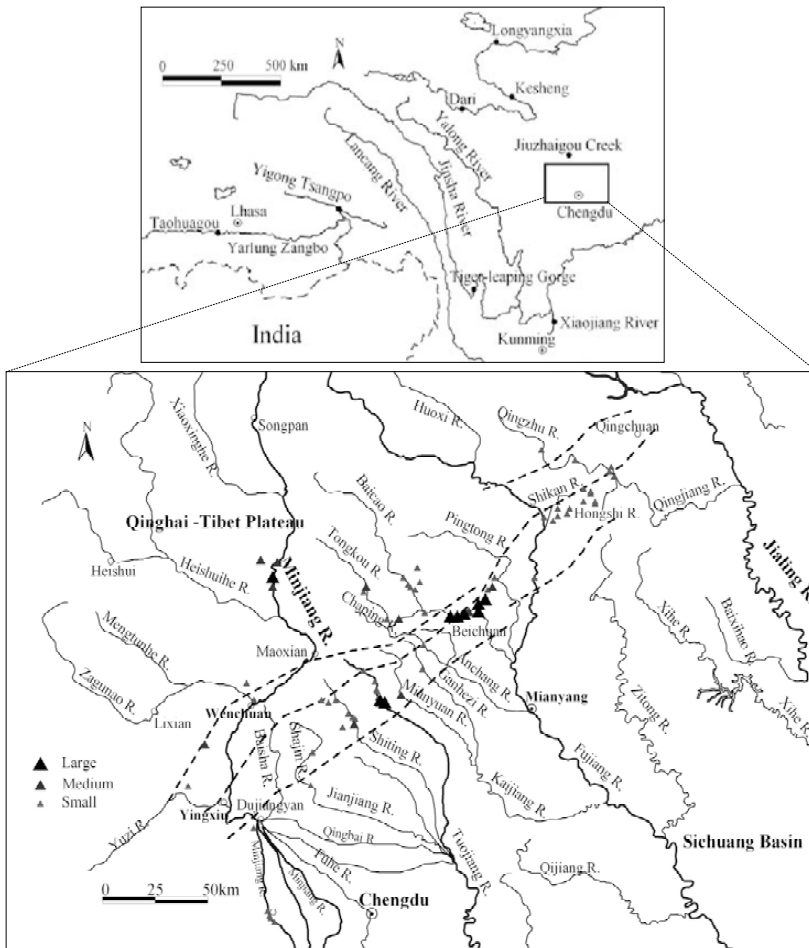
Fig. 4.26 Study area and landslide dams created by earthquakes around the Longmenshan Faults (dashed lines) and on the Qinghai-Tibet Plateau

The stability of a landslide dam depends directly on the development degree of the step-pool system, S_P, in the spillway channel on the landslide dam. The definition and measurement of the S_P value are given in Chapter 3. Except for the development degree of the step-pool system on the spillway channel, the stream power of flow is the most important factor. For small streams with a peak flood discharge less than 30 m³/s the preservation ratio of landslide dams, R, is well related with S_p, the development degree of the step-pool system. Eight field investigations were done to the landslide dams in the Wenchuan Earthquake area in 2008 and 2009. S_P and R were measured with the special instrument and GPS receivers and laser range meters (Wang et al., 2010a or b). Figure 4.27 shows R as a function of S_P. The preservation ratio, R, linearly increases with S_P. If S_P is larger than 0.45, the preservation ratio R equals 1, i.e. the landslide dams may be completely preserved. On the other hand, if S_P is smaller than 0.27, R is smaller than 0.5, i.e. the landslide dam may fail.
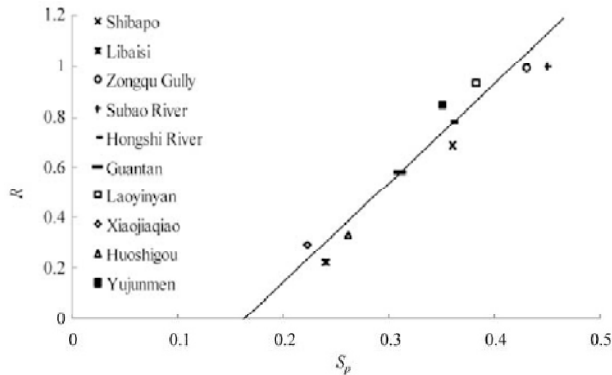
Fig. 4.27 Preservation ratio of landslide dams, R, as a function of the development degree of step-pool system, S_p, for small streams

Figure 4.28 shows the Yujunmen barrier lake on the Mianyuan River in Sichuan (left) and a step-pool system on the spillway channel (right). The lake was created by a landslide which was triggered by the Wenchuan Earthquake on May 12, 2008. The top part of the landslide dam was removed by humans in order to reduce the lake water level for constructing a highway along the lake. Two floods scoured the spillway channel and rearranged the stones to form the step-pool system. The S_P value was measured at 0.37 and the preservation ratio was about 0.88.

Fig. 4.28 Yujunmen barrier lake on the Mianyuan River in Sichuan (left) and a step-pool system on the spillway channel on the Yujunmen landslide dam (right) (See color figure at the end of this book)

For large rivers with flood discharge higher than 30 m³/s, however, the stability of a landslide dam depends not only on the development of a step-pool system, but also on the stream power of the flood flow. The S_P value of step-pool systems on the landslide dam for preserved, half-preserved, and failed landslide dams, created by the landslides during the Wenchuan Earthquake or other landslides that occurred a long time ago (10 years to 1,000 years), was measured with the instrument previously described. The width of the channel, and the height and length of the landslide dams were measured with the GPS receivers and laser range meters. The flood flow discharge was collected from the nearest hydrological stations. Sediment samples were taken for size distribution analysis. In most cases the flow in the central zone of the channel was not accessible or very dangerous to measure. The S_P value was measured near the banks. An experiment was conducted in a dry channel, where the water was diverted for power generation. The measurements with the special instrument proved that the measured S_P value near the banks during the low flow season was very close to that in the central flow zone of the channel. The error is less than 5% (Liu, 2009). Most of the measurements of the S_P value were performed near the banks, where the measurement was not so dangerous.

The stream power is given as follows:

$$P = \gamma Q s \tag{4.3}$$

in which q is the flood discharge, s is the bed gradient, and γ is the specific weight of water. The stream power per width is very useful, which is given as follows:

$$p = \gamma q s \tag{4.4}$$

in which q is the flood discharge per channel width.

Figure 4.29 shows the relation of the S_P value of the step-pool system on the channel with the stream power per width. Except for the landslide dams created by the Wenchuan Earthquake in 2008, the failed and preserved landslide dams on rivers in the Qinghai-Tibet Plateau were also measured. The Yigong Tsangpo landslide dam occurred in April 2000 and failed in June 2000. The landslide dam lake had a huge capacity of about 3 billion m³. The dam failure flood resulted in an extremely high discharge. The Taohuagou Landslide occurred on the Yarlong Tsangpo, which almost completely failed. The two landslide dams have high, S_P values but the preservation ratio is low because the flow had very high stream power.
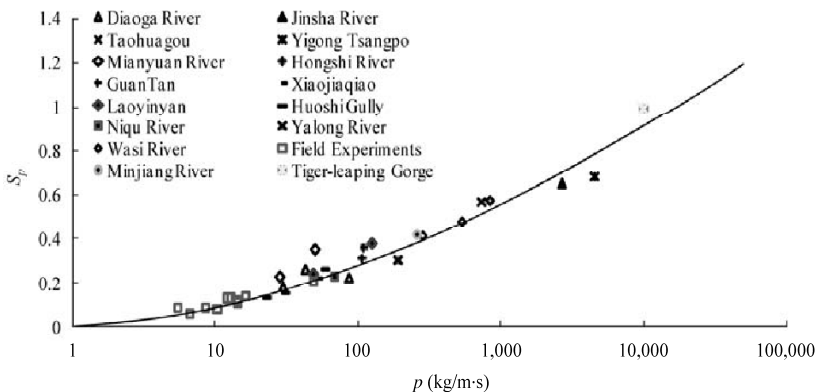
Fig. 4.29   Development degree of step-pool system, S_P, as a function of unit stream power, P, for stabilized channels on landslide dams

All the measurements were performed on the stabilized channels of the landslide dams. In general, a step-pool system developed following scouring and development of the spillway channel. Boulders and cobbles were rearranged to form structures and reached maximum stability during the scouring. Finally the step-pool system was so well developed that flood flows could not scour the bed material. The stream power of the flow and the energy consumption by the step-pool system reached equilibrium, which is represented by the curve in Fig. 4.29. If the S_P value of the channel on a landslide dam was smaller than the value of the curve, the channel would incise down. The S_P value increased following the incision and finally reached a value around the curve. If the S_P value was higher than the curve the landslide dam would be stable and the preservation ratio would be the final preservation ratio of the landslide dam.

The development of a step-pool system and the preservation ratio of landslide dams depend on a number of factors, most important of which are the size of the original landslide deposit, the percentage of large boulders within that deposit, and the geometry of the valley (Costa and Schuster, 1988). The failure risk of the landslide dams soon after the earthquake depends on the size composition of landslide materials, the width of the dam and the water head of the lake. If a landslide dam is mainly composed of fine materials such as soil and fine gravel, it is likely that the materials are soon flushed away by the overspill flow and the landslide dam collapses. If a landslide dam is composed of stones of different sizes, including big boulders, a strong step-pool system may develop and the quake lake is stabilized. If a landslide dam is composed of much fine materials, and also many big stones, the time needed for the step-pool structures in the spillway to develop and stabilize the dam would be long, during which the risk of dam failure is high. Figure 4.30 shows the size distributions of the original landslide deposits, in which the symbols of preserved and half-preserved landslide dams are black solid points and those of failed landslide dams are hollow points. All landslide dams with original material consisting of at least 10% of boulders larger than 1m have been preserved or half-preserved. For size distributions with a high percentage of large boulders, a strong step-pool system may soon develop with a minimum incision of the spillway channel; thus, the dam may be preserved. Therefore, the percentage of large boulders is of the greatest importance for the final stabilization of the landslide dams.
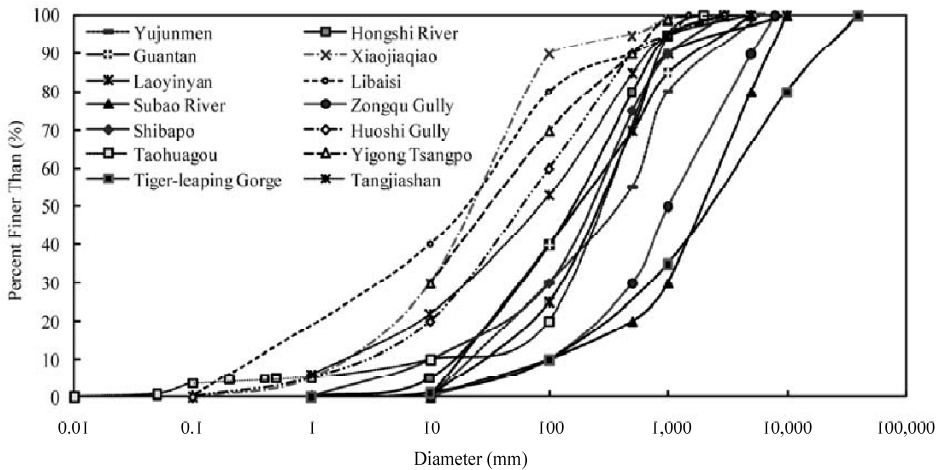
Fig. 4.30 Size distributions of original landslide deposits of failed landslide dams (hollow points) and preserved and half-preserved landslide dams (black solid points)

4.3   Mechanisms of Debris Flows

4.3.1   Pseudo-One-Phase and Two-Phase Debris Flows.

Debris flows may be classified into pseudo-one-phase debris flows and two-phase debris flows. Pseudo-one-phase debris flow occurs if there is a large portion of clay, silt and sand. In pseudo-one-phase debris flows, water and solid particles make up a fluid mixture, in which gravel, cobbles and even boulders are moving with the surrounding clay, silt and sand suspension. There is no visible relative movement between the solid particles and suspension. Viscous and sub-viscous debris flows are pseudo-one-phase flow. The pseudo-one-phase debris flows can be approached by employing a constitutive equation. Johnson (1970) and Yano and Daido (1965) postulated that debris flow material behaves as a homogeneous viscoplastic continuum. Many scientists have employed their models to study pseudo-one-phase debris flows (Julien and Lan, 1991; Iverson and Denlinger, 1987). Pseudo-one-phase debris flow has a plug in velocity profiles, which explains that the upper part of the flow moving at a uniform velocity like a solid plug. Pseudo-one-phase debris flow can develops from a continuous flow into an intermittent flow composed of a series of roll waves (Wang et al. 1990; Wang, 2002). Because the loose solid materials in dry valleys have a large portion of fine and cohesive particles, the debris flows are mostly pseudo-one-phase debris flow and often develop into intermittent flows (Kang et al., 2004).

Two-phase debris flow occurs if the fractions of clay, silt and sand in the solid materials are little. In two-phase debris flows boulders, cobbles and gravel compose the solid phase and water or suspension of clay, silt and sand is the liquid phase (Wang et al., 1999). Typical two-phase debris flows exhibit a high, steep head consisting of rolling boulders. There is obvious relative movement between the liquid phase and the solid phase and solid particles collide with each other, which consumes a lot of energy. The debris flows in the Wenchuan earthquake area were mostly two-phase debris flow and some were pseudo-one-phase debris flow.

Bagnold (1956, 1954) made the most prominent early efforts to construct a theory that accounts for particle collisions. The core of the theory is the concept of dispersive force. The theory postulates the debris is a mixture of a dilatant fluid but shear stress is generated mainly by collision between particles. Scientists have employed this model to study two-phase debris flows (Takahashi, 1981; Savage and McKeown, 1983). Two-phase debris flows, even with very high concentration of solid materials, were not very killing because the velocity is not so high. Large pseudo-one-phase debris flows, however, were extremely disastrous because the velocity was high and people had no time to escape even a warning signal was issued as the debris flow was detected in the upstream section.

Figure 4.31(a) and (b) shows the deposits of a pseudo-one-phase debris flow in the Jiangjia Ravine. The pseudo-one-phase debris flow mixture looks like concrete. Figure 4.31(c) shows the deposits of a two-phase debris flow in the Doufu Ravine in the Xiaojiang River basin in Yunnan. The two-phase debris flow picture was taken just two days after the debris flow event. Stones and gravel deposited in the gully and the liquid continued flowing down after unloading of the coarse grains. Therefore, the gully surface is covered with stones and gravel.

The debris flows in Sichuan, southwesten China, are mostly two-phase debris flow, because the solid materials in the area consist of a lot of boulders, cobbles and gravel. Sand, silt and clay made up only a small portion of the loose solid materials. In the two-phase debris flows cobbles and boulders collide with each other and consume most of the flow energy. The velocity of the two-phase debris flows was much smaller than pseudo-one-phase debris flows. Figure 4.31 (d) shows the deposit of a two-phase debris flow occurring in the Zoumaling Gully in the Mianyuan River basin in Sichuan in 2008. About 90% of the solid phase was cobbles and boulders with a median diameter about 0.4 m. The liquid phase was suspension of silt and clay. The velocity of the debris flow was estimated at only about 1.5 m/s

because it stricken against but was not able to destroy the three story building, which was just located on the path of the debris flow at the gully mouth. Local farmers told the authors that the velocity of the debris flow was about walk speed of humans. It was due to the low velocity the debris flow was not very killing.
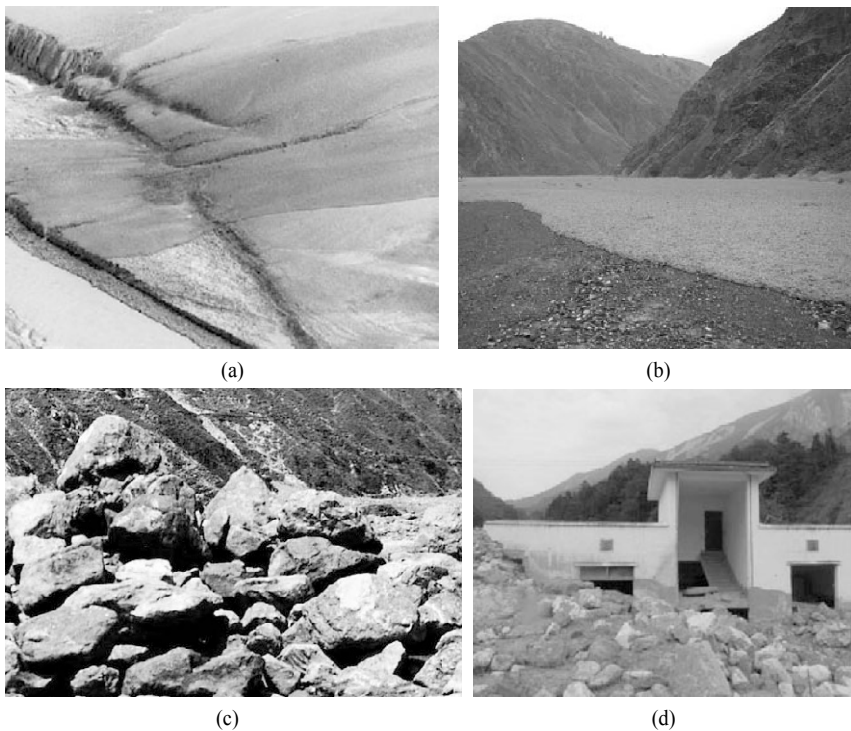
(a)   (b)

(c)   (d)

Fig. 4.31 (a) Deposits of a pseudo-one-phase debris flow in the Jiangjia Ravine on the Yunnan-Guizhou Plateau of China; (b) Pseudo-one-phase debris flow mixture looks like concrete; (c) Deposits of a two-phase debris flow in the Doufu Ravine; (d) Deposit of a two-phase debris flow in the Zoumaling Gully in the Mianyuan River basin in Sichuan in 2008. A building in the gully was not destroyed by the debris flow because the velocity was low (See color figure at the end of this book)

As a comparison pseudo-one-phase debris flows had extremely high velocity and were very disastrous, such as the large volume debris flow occurring in Zhouqu county on Aug. 7, 2010. There was no relative movement between the solid particles and liquid within the debris flow and the flow energy only consumed at the boundaries. The pseudo-one-phase debris flow had extremely high velocity. It was reported that the highest velocity of a pseudo-one-phase debris flow in Peru was as high as 81 m/s (Browning, 1973). Such a high velocity was not directly measured. In the Jiangjia Ravine in Yunnan, southern China, the velocity of pseudo-one-phase debris flow was measured with a double radar velocimeter, which received high frequency radio waves reflected from the head of debris flows. The highest velocity was measured at 26.8 m/s (Kang et al., 2004).

Pseodo-one-phase debris flow is a rheological flow. A rheological or constitutive equation relating stress and strain is needed for the debris flows because the flow exhibit non-Newtonian behavior. For the two-phase debris flows rheological equation is not enough to describe the flow behavior because there is relative movement between the two phases and energy exchange between the two phases. Nevertheless, some scientists simply use rheological equation to describe two-phase debris flows.

In the past decades much effort has been made to develop the constitutive equations and various models have been proposed on the bases of the visoplastic and dilatant models, for the pseudo-one-phase and two-phase debris flows (Julien and Lan, 1991; McTigue, 1982; Iverson and Denlinger, 1993, Shen and Ackermann, 1982). The models were applied to study the velocity profiles of debris flows. The idea to use a constitutive equation is to balance the shear stress created by the shear flow with the driving shear created by gravity on the slope. Then a velocity distribution can be obtained if all the parameters and the coefficients are known.

For pseudo-one-phase debris flow Johnson and Rohm (1970) and Yano and Daido (1965) postulated that debris flow material behaves as a homogeneous viscoplastic continuum. Many scientists have applied this model to study pseudo-one-phase debris flow (Chen, 1988; Shen and Ackermann, 1982). With the constitutive equation of a viscoplastic fluid they explained the velocity profile with a plug of laminar flow that is often observed in mudflows and viscous debris flows. The viscoplastic model can also interpret the striking phenomenon of debris flow waves. Wang et al. (1990) and Wang (2001) experimentally and theoretically studied the development of a viscoplastic fluid from continuous flow into intermittent debris flow composed of a series of waves. They derived differential equations indicating that the yield strength is the essential factor affecting the instability and development of the waves. Figure 4.32 shows the stress-strain rate relation of the viscoplastic model and the dilatant model.

For two-phase debris flows Bagnold (1956) and Takahashi (1978, 1980, 1981) made the most prominent early effort to construct a theory that accounts for particle interactions. The central feature of their theory is the concept of grain flow dispersive stress, which was originally introduced by Bagnold (1954). The theory postulates that the debris flow is a dilatant fluid but the shear stress is generated mainly by the collision between the particles (Fig. 4.32). Scientists have applied this model to study two-phase debris flows (Savage, 1984, Savage and McKeown, 1983). The theory provides the mechanism of supporting force for the movement of gravel and stones, a velocity profile distinct from that of water flow, and high resistance of debris flow, and seems to provide an explanation for the segregation of large and small particles that lead to the debris flow head consisting of large stones and to inverse grading in debris flow deposits.
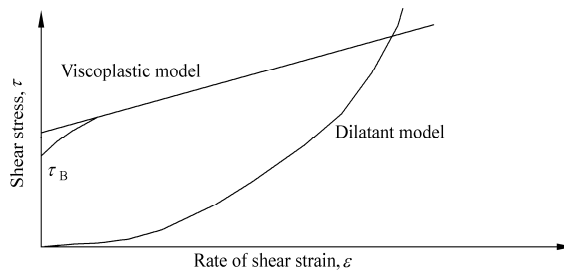
Fig. 4.32 The stress-strain rate relation of the viscoplastic model and the dilatant model for debris flows

Shortcomings exist in both the viscoplastic and dilatant models. The viscoplastic model does not work well for the resistance of pseudo-one-phase debris flow. The model predicts the debris flow velocity to be much lower than the flow of water because the viscosity and the yield shear stress of the debris mixture is much greater than water. In fact, the velocity of pseudo-one-phase debris flows in the Jiangjia Ravine, Yunnan Plateau of China, is sometimes even higher than the flow of water. The debris flow is composed of high concentrations of fine material and the flow appears to be laminar, which means that the resistance can be represented by the viscosity if it is really a kind of viscoplastic fluid. On the contrary, drag reduction occurs in pseudo-one-phase debris flows and the rate of drag reduction is as high as 60% (Wang et al., 2001). In other words, pseudo-one-phase debris flows move at 2 times higher velocities

than water in the same gully. The results indicate that the resistance of debris flow cannot be approached using the viscoplastic constitutive equations.

For the dilatant model of two-phase debris flow, an essential shortcoming is the omission of the interaction between the two phases and identification of different roles of different materials in the debris flow. The constitutive equation can be applied only if all parts of the flow behave the same rheologically, which is not true for most debris flows. Another important shortcoming of the theories is neglecting the unsteadiness of the flow. In unsteady flow, the shear stress is not balanced by the driving force and the inertia or the kinetic energy of the flow plays a role in the motion, especially at the initiation stage, and in maintaining the motion for a distance in a region of very gentle slope.

Debris flow normally occurs in gullies and rivers, which have drainage areas of 1–100 km^2. If plenty of loose solid materials are available on a slope the so called slope debris flow may occur on a slope which has an extremely small drainage area. Slope debris flow is defined as the phenomenon that a high-concentration mixture of debris and water flows down the slopes for a short distance and then stops at the toe of the slope (often at highways and river banks). The slope debris flow is very different from the normal debris flows and is discussed in this chapter as well.

4.3.2 Mechanisms of Two-Phase Debris Flows

4.3.2.1 Initiation of Two-Phase Debris Flows

Debris flow is often initiated during channel bed erosion by rainstorm floods flowing down the gullies. The initiation of two-phase debris flows was studied experimentally in a tilting flume 10 m-long and 50 cm-wide with glass-sided walls (Wang, 2002; Wang and Zhang, 1989). Five kinds of gravel were used for the experiments with diameters ranging from 5–10 mm to 50–90 mm. The liquid phase was a suspension of water and clay with a concentration of about 100 kg/m^3. Before the experiments the gravel was put on the bed forming a mobile bed 20 cm deep. Then, clear water or the clay suspension flowed down the flume from the upstream entrance. The water content, gravel concentration, size distribution, and the rate of gravel transport were obtained by analyzing the samples. The initiation and movement of the debris flows were observed by two video-cameras from the top and the glass side-walls of the flume.

As shown in Fig. 4.33 if the slope of the flume bed was small or the discharge of the liquid phase was small, no debris flow was initiated. In this case water flowed over the bed and individual particles were carried by the flow, in the motion of normal bed load (Fig. 4.33(a)). The front was low and propagated down the slope at a relatively high velocity. There were no or very few particles in the front. The gravel concentration was only 0-80 kg/m^3. The velocity of the flow was higher than that of the debris flow and the front velocity was close to the surface velocity of the main flow because a much smaller number of particles was carried by the flow and much less energy was consumed by the solid phase. This is the normal bed load-laden flow.

As the slope and the discharge of the liquid phase increased and became large, however, particles were removed from the bed and rolled in the front of the flow (Fig. 4.33(b)). Individual particles move faster than the front, and thence more and more particles moved to the front, forming a head consisting of rolling particles (Fig. 4.33(c)). Particles in the head collided with each other and with the bed, consuming a lot of energy, therefore, the head moved at a lower velocity than the liquid and particles in the main flow. The particles in the main flow caught up with and rolled over the head. The head became so high as to be several times the diameter of the large stones and stopped growing. The head rolled down the flume like a bulldozer (Fig. 4.33(d)). Particles in the head collided with each other and made noise. A high concentration of particles, up to 1,100–1,600 kg/m^3, was carried down the flume with the head. This is debris flow. Many debris flows in nature are initiated by storm rainfall and turbulent runoff and exhibit the same physical pattern as in the experiments.
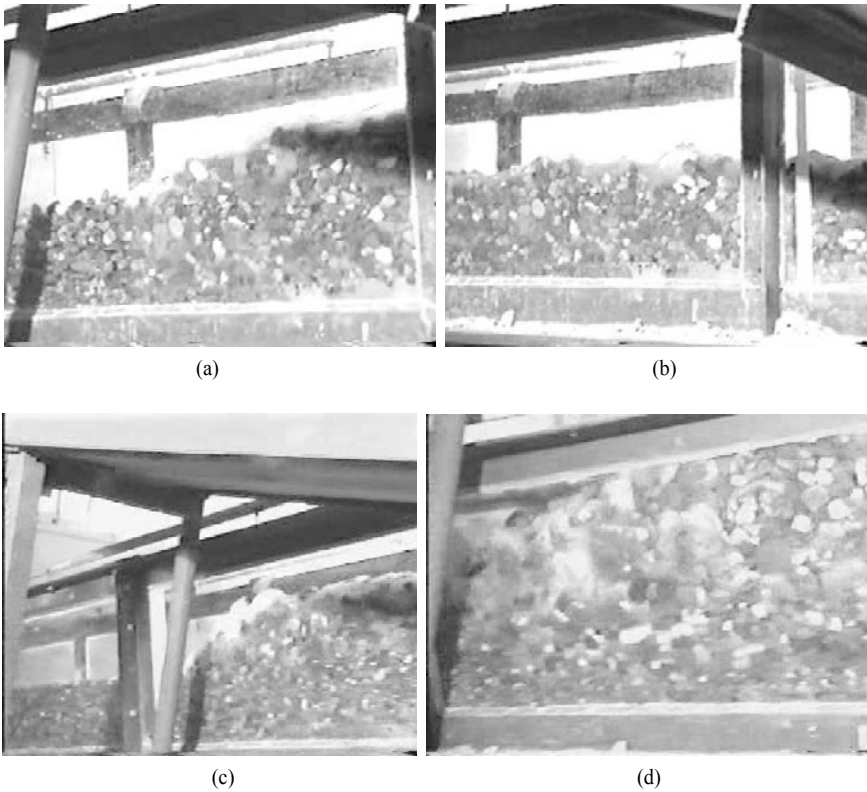
Fig. 4.33 (a) Normal bed load-laden flow at low slope and low discharge; (b) Initiation of a head with rolling particles; (c) High concentration of particles in the head; (d)Debris flow head rolls down like a bulldozer (after Wang et al., 2005)

In two-phase debris flows, the solid particles always collide with each other during motion. Collision and abrasion make the particles round and smooth. Figure 4.34 shows stones with a round shape and smooth surface from the two-phase debris flow deposit in the Diaoga Ravine, a tributary of the Xiaojiang River in Yunnan Province of China. Local people use these stone spheres for decoration in front of their houses.

Fig. 4.34 Spherical stones with smooth surface from the two-phase debris flow deposit in the Diaoga Ravine, a tributary of the Xiaojiang River in Yunnan Province of China

4.3.2.2 Critical Bed Gradient for Initiation of Debris Flow

There is a critical bed gradient, s_c, below which no debris flow can be initiated for a given bed gravel composition. The coarser the bed materials, the higher is the critical slope. Figure 4.35 shows the critical slope as a function of the median diameter of the bed material, which is mathematically expressed as:

$$s_c = 0.024D_{50}^{2/3} \tag{4.5}$$

in which D_{50} is the median particle diameter in millimeters. From Eq. (4.5) it can be determined that debris flow may be initiated on a gentle slope if the bed material is not coarse. Field data have proven that in most cases a gully is a debris flow gully if its slope is greater or a non-debris flow gully if its slope is smaller than the critical value given by Eq. (4.5). In other words, for a gully with a given slope, it can become a debris flow gully if there is plenty of fine gravel on the bed, or it is a non-debris flow gully if the bed material is coarse.

Takahashi (1978, 1980) presented a model of the initiation of debris flow. From his model debris flow can be initiated if the shear stress of the flow is greater than the shear resistance of a layer of debris deposits. The layer then will slide down the slope and move with the flowing liquid, therefore, debris flow develops as a result of the mixture of the solid deposit and the liquid. Takahashi (1978, 1980) found the critical slope for debris flow development to be about $14.3°$ or $s_c = \tan 14.3° = 0.23$. Takahashi's model can be applied to landslides and the debris flows developing from landslides but not to the debris flow resulting from bed erosion caused by a torrential flood. The critical slope for a flood-caused debris flow is smaller than that given by the shear stress model. The median diameter of bed materials of the Jiangjia Gully is about 5–12 mm. Equation (4.5) gives a critical slope of about 0.13. The slope of the upstream portion of the gully is about 0.15 and there are plenty of loose solid deposits in the area. Therefore, debris flows often occur in the gully if the rainfall intensity is higher than 0.5 mm/min.
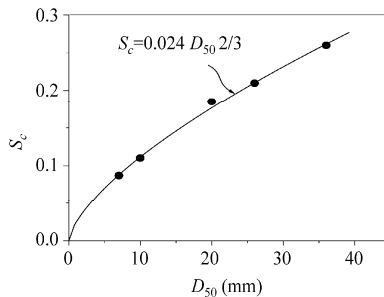
Fig. 4.35 Critical slope for initiation of debris flow as a function of the median diameter of bed material (after Wang et al., 2005)

4.3.2.3 Height of Debris Flow Head

Generally, the head grows at the beginning of the debris flow development and then reaches an equilibrium height. Figure 4.36 shows the growth process of the debris flow head following the propagation down the flume, in which L is the distance from the entrance and h_d is the height of the debris flow head. Miyazawa (1998) obtained similar results from debris flow experiments with gravel of diameter of 5–10 mm.

The experiments of Wang et al. (2005) also revealed that debris flow can be triggered only if the incoming flow discharge is sufficiently high even if the bed gradient is over the critical value. If, however, a debris flow is triggered, the front head is high and steep. The height of the debris flow head depends mainly on the size of the gravel in the debris flow. The height of the debris flow head in the
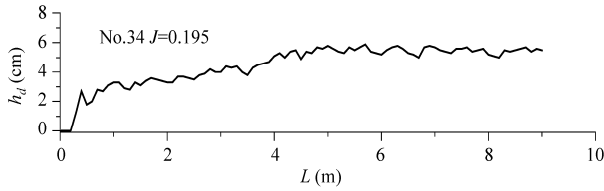
Fig. 4.36   Growth process of the debris flow head (L = the distance from the entrance, h_d = the height of the debris flow head)

experiment with gravel of median diameter 7.3 mm was only 4 cm. Whereas the head height of a debris flow occurring in a debris flow gully with a median diameter of about 200 mm of gravel was about 1.2 m. The head height of debris flow is proportional to the size of gravel, as shown in Fig. 4.37.   An empirical relation between h_d and D_{50} can be mathematically formulated as:

$$h_d = 5.5D_{50} \tag{4.6}$$

It was observed that the water content in the head was low, and sometimes only dry particles moved in the very front of the head. The velocity of the liquid phase and the particles in the following part of the head was higher than the moving speed of the head. The instantaneous velocity of small particles was measured to be higher than that of large particles. Two paradoxes were observed: (1) the small particles exhibit high velocity but move slower, large particles exhibit low velocity but move faster; (2) particles in the head consume a lot of kinetic energy due to collisions with each other and between the moving particles and the bed, therefore, the movement of the head is subjected to an extremely high resistance, but the debris flow head grows and remains flowing.
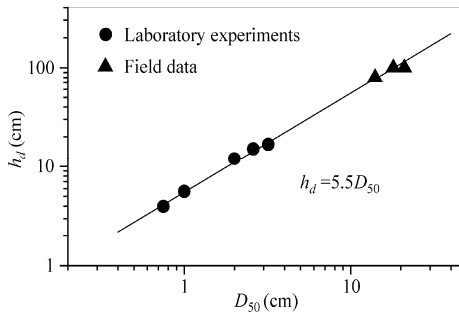
Fig. 4.37   Height of debris flow head (h_d) as a function of the median diameter of gravel (D_{50})

4.3.2.4   Stone Street

Two-phase debris flows always exhibit a high, steep, and noisy front composed of large stones. Collisions of big stones make noise and consume a lot of energy. Hence, the resistance to the movement of the front is high and the velocity of the stones in the front part is lower than those behind. The mechanism of the low-velocity head and high velocity of the following flow has been explained by Wang and Zhang (1990) and Wang (2002). The average velocity of large particles in two-phase debris flows is higher than small particles. More and more stones finally move to the front of the debris flow. Because more and more stones come to the front some stones have to go to the two sides of the gully where the driving force is smaller and the resistance due to collision with the banks is larger. The stones stop at the two sides of the gully and form a stone street. Figure 4.38 shows the stone street in a debris flow gully in the Xiaojiang River basin, in which big stones clearly exhibit two lines on the two sides of the gully. No big stones are

present in the central part of the channel because after has the front has passed, the rear of the debris flow deposit left in the center of the gully, consists of small particles.

Fig. 4.38   "Stone street" phenomenon of two-phase debris flow in the Xiaojiang River basin in Yunnan Province, China

4.3.2.5   Velocity and Velocity Profiles

From the two-phase debris flows experiments, Wang (2001) obtained the following formula for the velocity of debris flow head:

$$u_d = 2.96 \frac{\gamma_s - \gamma}{\gamma_s} \frac{q}{C_{vd} h_d \left[1 - 20J + 12.6 \frac{\gamma_s - \gamma}{\gamma_s} \right]} \tag{4.7}$$

In which, u_d is the velocity of debris flow head, q is discharge of water per width, h_d is the height of debris flow head, C_{vd} is the ratio of volume of solid particles to that of debris flow, which is obtained by measurement. The formula is useful for debris flows consisting of gravel, cobbles, boulders, and very limited concentrations of clay and silt.

The velocity profiles of solid particles were analyzed by digitizing the video record of the debris flow experiments. In the experiments, a rolling head moved down the flume and following the head was the main flow. Figure 4.39 shows the velocity profiles in the head and the main flow of two experiments Nos. 15 and 17. The particle velocity profiles of the main flow are similar to the grain velocity profile of debris flow experiments by Tsubaki et al. (1983). It is striking that the velocity profiles of the particles in the head are quite different from those in the main flow (Fig. 4.39). Particles in the head move at a much lower velocity than those at the same relative elevation in the main flow. The particle's velocity in the main flow is about 2 times those in the head. The shapes of the profiles also are different. The head profiles are nearly linear and those of the main flow are more curved.

The mechanism of the velocity difference between the particles in the head and the main flow is perhaps that the particles in the main flow receive energy from the flowing liquid and accelerate to a high velocity. They catch up with the head and collide with and transfer their energy to the particles in the head, then decrease in velocity. The concentration of particles in the head is much higher than that in the main flow. A lot of energy is consumed by collisions between the particles and with the bed, so that the head is subjected to great resistance and moves at a much lower velocity.
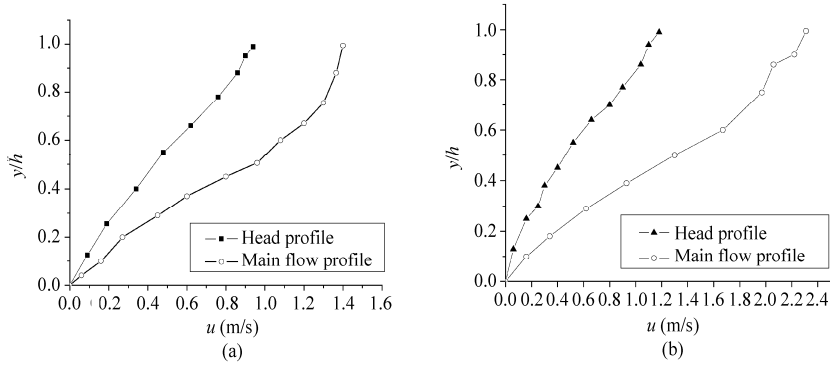
Fig. 4.39   (a) Velocity profiles of particles in the head and the main flow of experiment No. 15; (b) Velocity profiles of particles in the head and the main flow of experiment No. 17 (after Wang et al., 2005)

4.3.2.6   Mechanism of Larger Particles Concentrating in the Front Head

Experimental observation also has found that the head is composed mainly of large particles. One can reason that large particles move at higher velocities than small particles and thence concentrate in the head. Many people have accepted the theory that the dispersive force is proportional to the particle diameter to the power of 2, and, thus, big particles are raised to the upper layer, so that the large particles finally concentrate in the front of the head. In fact the weight of the particles is proportional to the diameter to the power of 3, which tends to move big particles down to the bed. The instantaneous velocity of small particles is higher but the average velocity is lower than for large particles. Figure 4.40 shows the velocity profiles of particles in the head, the velocity profile of large particles ($d = 40$–60 mm) in the main flow, and the velocity profile of small particles ($d = 10$ mm) in the main flow of the experiment. The velocity of small particles is higher than the velocity of large particles in the upper flow and lower in the lower flow.
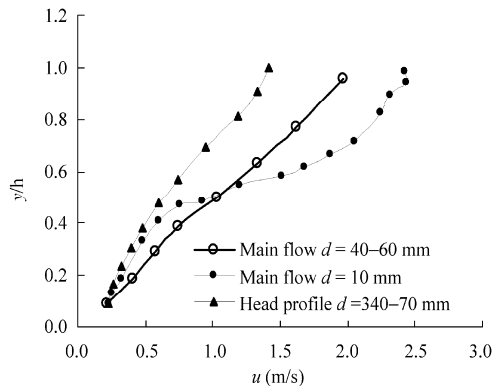
Fig. 4.40   Velocity profile of particles in the head and velocity profiles of large and small particles in the main flow of the experiment (after Wang et al., 2005)

A small particle accelerates under the action of the liquid flow and moves faster than the large particles. It hits a large particle in front of it and transfers its kinetic energy to the large particle by the collision. Then the small particles stop moving and fall down on the bed. The phenomenon is seen for many small particles. Following the movement of the debris flow down the flume more and more small particles fall

down and accumulate on the bed. Thus, a layer of small particles is seen between the stagnant bed and the moving particles, as shown in Fig. 4.41. On the other hand, the large particles receive energy from the small particles and move at a stable velocity and finally move to the head. This fact indicates that the theory of a dilatant model for the large stones in the head is not correct. In the dilatant theory, large particles move faster because the dispersive force is proportional to D^2, large particles are subjected to large lifting dispersive force and hence rise to the surface of the flow where the velocity is high. Therefore, large particles move faster and finally concentrate in the debris flow head. This theory is not correct. Large particles move "faster" and catch up with the head because they move continuously but small particles stop and fall down after moving for a distance and colliding with large particles.

Fig. 4.41   A layer of small particles between the bed and the moving particles

4.3.2.7   Resistance of Two-phase Debris Flows

The resistance of debris flow is usually represented by Manning's roughness coefficient, n. Figure 4.42 shows Manning's n values for debris flows calculated with the following formula:

$$n = \frac{1}{u_d} h_d^{2/3} s^{1/2} \tag{4.8}$$

in which u_d is the average velocity, h_d is the height of the head of the debris flow. Figure 4.42 shows Manning's roughness n as a function of the median diameter of the bed gravel. For the same bed material, the resistance of for debris flow is about 10 times higher than that of normal sediment-laden flow. In normal sediment-laden flow particles move with the liquid, rolling or moving by saltation over the bed. In debris flow, particles collide with each other and with the bed so that a supporting force - the so-called dispersive force is created. The collisions consume a lot of energy and create a great resistance to flow.
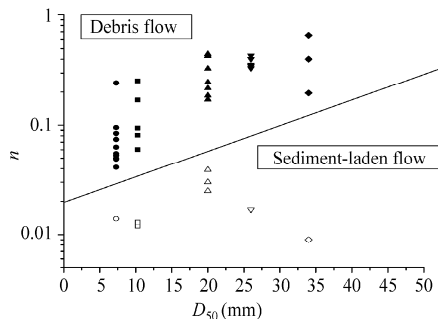
Fig. 4.42   Manning's roughness coefficient n as a function of the median diameter of the bed gravel

Therefore, two-phase debris flow exhibits extremely high resistance compared with normal sediment-laden flow. The resistance of debris flow increases with the diameter of the solid material because collisions among bigger particles consumes more energy and creates higher flow resistance.

4.3.3 Phenomena and Mechanisms of Pseudo-one-Phase Debris Flows

4.3.3.1 Development of Pseudo-one-Phase Debris Flows

Pseudo-one-phase debris flow often occurs in the Xiaojiang watershed on the Yunnan-Guizhou Plateau. The solid materials are fine and consist of clay, sand, and gravel. The Dongchuan Debris Flow Observation and Research Station further classifies the pseudo-one-phase debris flows into viscous debris flow if the density of the mixture is higher than 1.9 g/cm^3 (generally between 1.9–2.3 g/cm^3), subviscous debris flow if the density is between 1.6–1.9 g/cm^3, and low viscous debris flow if the density is lower than 1.6 g/cm^3. Kang (1985a) reported that debris flow in the Jiangjia Ravine occurs during or after rainstorms in summer and typically begins with a torrential flood. Following erosion of the gully bed the flood develops into a flow with a high solids concentration in 10–20 minutes. The concentration of solid material reaches 100–160 kg/m^3, or and the density of the flowing mixture is about 1.1 g/cm^3. Then the flow develops further into a low-viscous and subviscous debris flow in a short time and the density of the flowing mixture increases from 1.1 g/cm^3 to 1.9 g/cm^3. The highlight of the process is the formation of an intermittent viscous debris flow when the density reaches 1.9–2.3 g/cm^3. A series of debris flow waves rush downstream one after another. This process lasts 2–3 hours in general, during which 80-100 waves pass through the channel. Each wave lasts only about 20–30 seconds. Between the waves the mixture stopped flowing for 1–5 min. Then the flow transforms into sub-viscous debris flow and low-viscous debris flow following dilution of the mixture.

4.3.3.2 Intermittence of Viscous Debris Flow

Figure 4.43 shows the intermittent process of a viscous debris flow (Kang, 1985a or b). One can see from the figure that the discharge and velocity are intermittent and the velocity of the debris flow wave was as high as 8 m/s. The viscous debris flow develops into a series of roll waves as the specific weight increases to 1.8 g/cm^3 or the weight concentration of solids reaches 1,280 kg/m^3. Each wave exhibits a front head composed of large gravel and stones, a body with relatively uniform depth and surface velocity, and a rear of small depth, as shown in Fig. 4.44. Between two waves there is no-flow but still a solid-liquid mixture.
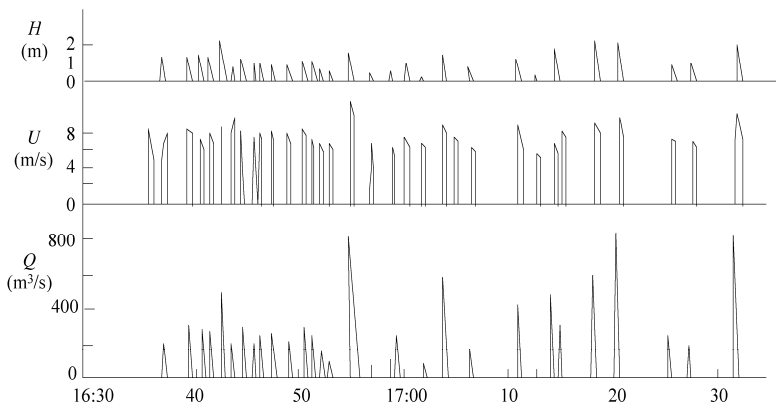
Fig. 4.43 A typical viscous debris flow process in the Jiangjia Ravine from 16:30 to 17:30 (after Kang, 1985a). H = the depth, Q = discharge, and U = propagation velocity of the debris flow wave measured at the Dongchuan Station

The matrix of the viscous debris flow consists of water, silt, and clay. The concentration of silt and clay is high, and, therefore, the matrix exhibits non-Newtonian features and yield stress. The development of the intermittent wave pattern is related to the yield strength of the matrix and Froude number (Details are given later).
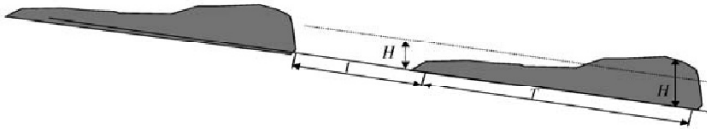
Fig. 4.44   Viscous debris flow develops into a series of roll waves

4.3.3.3   Roll Waves

Wang and his collaborators studied experimentally and theoretically the mechanism of the development of roll waves (Wang et al., 1990; Wang, 2002). The experiments were done in a flume of 26-m long and 50-cm wide, using clay suspensions as the flowing medium, which is a viscous-plastic fluid and behaves similarly to a viscous debris flow. The roll waves generally developed as follows: a slight fluctuation in velocity occurred as clay suspension flowed in the flume, then some ripples appeared on the surface. The ripples grew into waves as they propagated downstream, and more ripples formed at the same time. Sometimes the waves grew so large that their maximum discharges were more than double the incoming discharge, and the residual mud stopped moving after the waves passed. The roll waves stopped growing when they reached a certain amplitude. The growth process is shown in Fig. 4.45 and a fully developed roll wave has the form shown in Fig. 4.46, in which the streamlines of the flow are seen by a viewer moving with the wave.
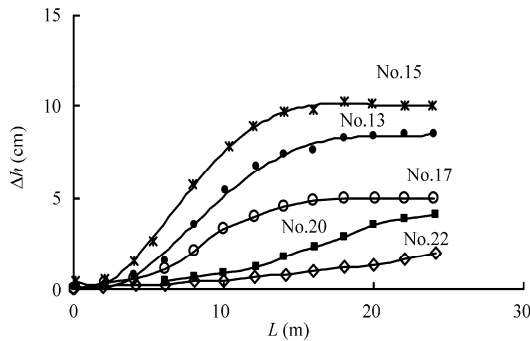
Fig. 4.45   Wave height, Δh, increases with the distance, L, down the slope. Ripples may grow into waves if the yield stress, τ_y, is large. The waves stopped growing when they reached a certain amplitude (after Wang, 2002)

The wave always propagates more rapidly than the flow between waves. A portion of the mud moves upward like a fountain under the extrusion of the wave as it was caught by the wave. Then it divides into two parts, one part flowing forward at a velocity $2u$ (where u is the speed of the wave) and forming a rolling front and the other part flowing at a velocity less than u that gradually lags behind the wave.

Wang (2002) studied the mechanism of the development of the roll waves and derived the following equation by applying the Bingham model and the de Saint Venant equations:

$$\frac{\mathrm{d}}{\mathrm{d}t}(\Delta u) = \frac{1}{2\rho_m h}\left[\frac{\tau_B}{\sqrt{(gh)}} - \frac{\eta}{d}(1 - Fr)\right]\Delta u \tag{4.9}$$

where Δu is the initial perturbation in velocity, τ_B is the yield shear stress, η is the rigidity coefficient, h is the flow depth, g is the acceleration of gravity, ρ_m is the density and d is the thickness of the shearing layer, and Fr is the Froude number of the flow. The derivation of the equation is given in Appendix 1 of this Chapter.
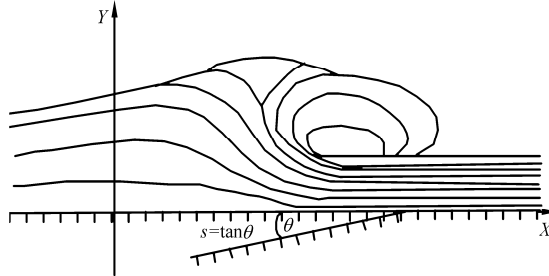
Fig. 4.46   A fully developed roll wave. The streamlines are seen by a viewer moving with the wave. A part of the mud moves upward like a fountain under the extrusion of the wave. Then it divides into two parts, one part flows forward and other part flows at a velocity less than the wave speed and gradually lags behind the wave (after Wang et al., 1990)

If the fluid has a large yield stress and the Froude number is larger than one, the flow will be very unstable and quickly develops into roll waves. Many viscous debris flows in the Jiangjia Ravine are examples of such flows (Kang, 1985b). If the Froude number is smaller than one but the rigidity coefficient, η, is small and the yield stress is large, the flow also is unstable and develops into wave flow. Some unstable hyperconcentrated flows in the tributaries of the Yellow River are examples of this type of flow. Whereas if the yield stress is small and η is large, a non-Newtonian flow is stable at low Froude numbers, e.g., flows of crude oil and lava are stable because magma has an extremely high rigidity coefficient.

In pseudo-one-phase debris flows, the development of roll waves is essentially due to the yield stress of the debris mixture. Normalizing the two terms on the right hand side of Eq. (4.8) with the acceleration of gravity, g, as follows, Wang (2002) defined two dimensionless numbers, S_y and S_{vis}, to represent the effects of yield stress and viscosity:

$$S_y = \frac{\tau_B}{g\rho_m h} \tag{4.10a}$$

$$S_{vis} = \frac{\eta u}{g\rho_m h d} \tag{4.10b}$$

It may be derived from the theory of motion that the any perturbation of the flow depth may develop into a large wave if S_y is large. The growth rate of the perturbation wave height per distance is given as follows:

$$\frac{\Delta h}{L} = \frac{\tau_B}{2\gamma_m h} = \frac{1}{2}S_y \tag{4.11}$$

Equation (4.11) explains that the larger is the yield stress and the smaller is the flow depth, the higher will be the growth rate of the perturbation wave. The measured growth processes in the experiments are shown in Fig. 4.47, which shows that the growth rate of waves is proportional to S_y, agreeing with the theoretical conclusion. Nevertheless, the exact growth rate of the perturbation waves is smaller because the assumption of $\eta = 0$ used for deriving Eq. (4.11) is not true.

In summary, pseudo-one-phase debris flows or flows of other non-Newtonian fluids may develop into roll waves essentially due to the yield stress of the fluid. 1) The free-surface is unstable and roll waves

may develop even at constant incoming flow rate if S_y is much larger than S_{vis}; and 2) the free surface is stable if S_y is smaller than S_{vis}. The growth rate of wave height depends on the parameter S_y. The larger is the parameter S_y, the higher the growth rate and the higher the waves.
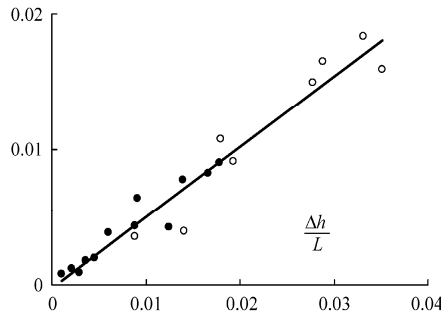
Fig. 4.47   Growth rate per distance of the wave height $\Delta h/L$ as a function of the dimensionless parameter $\tau_B/2\,Y_m h$

4.3.3.4   Bed-Paving Process

Pseudo-one-phase debris flow often develops into a series of waves. When a wave flows through a channel, a layer of water-sediment mixture deposits is stuck on the channel bed. The flow wave becomes smaller and smaller because of the loss of volume of the mixture. when it finally stops it forms a paved path with a layer of water-sediment mixture. Then another wave follows. This process is termed the "bed-paving process" by Chinese researchers. In the Jiangjia Ravine, the average paving distance of a wave is about 50 m.

Pseudo-one-phase debris flow has a yield stress, and flows down an inclined channel only if its depth exceeds a critical value, H_0. When a pseudo-one-phase debris flow wave passes through an open channel, a tail section with a depth less than H_0 stops moving under action of the yield stress. The wave, therefore, becomes shorter and shorter and finally rests on the channel bed. As long as the matrix of the debris flow exhibits a yield stress, the first few debris flow waves pave the way and then the following waves can flow through the channel.

A wave flowing over a channel paved with a debris mixture resulting from the foregoing waves, may lose a part of its volume (rear part) if its velocity is low, or in other cases it may gain in volume by taking a part of the mixture from the bed if its velocity is high. A debris flow wave can grow or shrink depending on the thickness of the debris mixture layer previously deposited on the channel bed. This brings about a great difficulty in predicting the debris flow discharge. Figure 4.48 shows the variation of discharge of a debris flow wave along the flowing course in the Little Almakinca River in Russia. The discharge was less than 20 m³/s and increased to 150 m³/s after traveling 4 km. It reduced from 150 m³/s to about 60 m³/s after traveling 0.4 km farther, and then it increased to about 230 m³/s in another 1.6 km of travel.
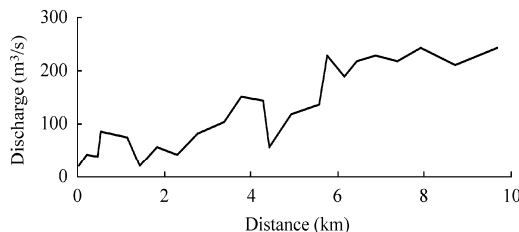
Fig. 4.48   Variation of a debris flow discharge along the Little Almakingka River

4.3.3.5   High Superelevation at Bends and Climbing Ascending Slopes

Some unique characteristics of pseudo-one-phase debris flow are extremely high superelevation at bends and climbing ascending slopes. Table 4.1 presents measured superelevations of pseudo-one-phase debris flows in Japan and the U.S. (Sieyama and Woemoto, 1981; Pierson, 1986). As a comparison, the table also lists the calculated superelevations of flowing water. One can see from the table that the measured superelevation of debris flow was as much as several meters to several tens of meters, greater than the calculated value for flowing water. Moreover, pseudo-one-phase debris flow can climb a gentle ascending slope, and sometimes can even climb over little hills. When a debris flow wave encounters a towering obstacle in the flow course, the front will rise up to a certain height. Figure 4.49(a) shows the extremely high superelevation marked by debris flow mud at a bend of the Jiangjia Ravine in the Xiaojiang Watershed in Yunnan Province of China; and Figure 4.49(b) shows debris flow deposits on a hill composed of several layers of large stones and fine solid materials in the Chaqing Gully in the Xiaojiang watershed.

Table 4.1   Superelevation of pseudo-one-phase debris flow (Sieyama and Woemoto, 1981; Pierson, 1986)

Location	Rc (m)	U (m/s)	B (m)	ΔH_d (m)	ΔH_w (m)
Yakitakai	442	5	13.5	2.6	0.08
	212	5	20.0	4.0	0.24
	74	5	13.0	3.4	0.43
	94	5	15.0	3.5	0.40
Miaokao Plateau	365	17	110.1	50.0	8.90
Mount St. Helens			70.0	20.0	

Note: Rc = the radius of the curvature at the bend, U = velocity of the flow, B = width of the channel; ΔH_d = supperelevation of debris flow (measured); ΔH_w = calculated supperelevation of water flow
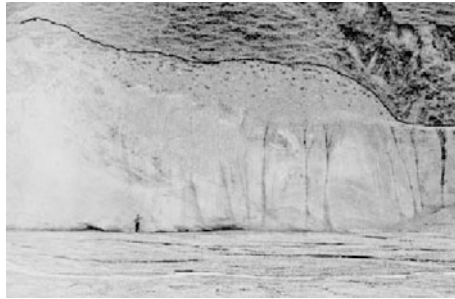
(a)

(b)

Fig. 4.49   (a) Extremely high superelevation of debris flow in a bend of the Jiangjia Ravine; (b) Ancient debris flow deposits on a hill in the Chaqing Gully, Xiaojiang watershed

The extremely high superelevation of debris flow is disastrous and causes casualties very often because people pay less attention to the risk of debris flow if their houses are located on high slopes. Figure 4.50 shows a building on a slope of the Qiongshan Gully in the upper Dadu River basin, which was destroyed by a debris flow that occurred at about 11 pm July 15, 2003. The head of the debris flow climbed on the slope of more than 15 m smashing the building and killed 51 people, when they had a party in the building (Chen et al., 2004).

Fig. 4.50   A debris flow in the Qiongshan Gully in the upper Dadu River basin climbed on a slope of more than 15 m and smashed a building killing 51 people in 2003

4.3.3.6   Bimodal Grain Size Distribution

Many debris flows have a bimodal grain size distribution. Figure 4.51(a) shows the measured granulometric curves of debris flow in the Liuwan Gully, northwest China. In the figure p is the frequency density of grains of diameter D. Each curve in the figure has two peak values in the frequency density. The first peak is located at $D = 0.01 - 0.1$ mm and the second one is located at $D = 2 - 40$ mm.
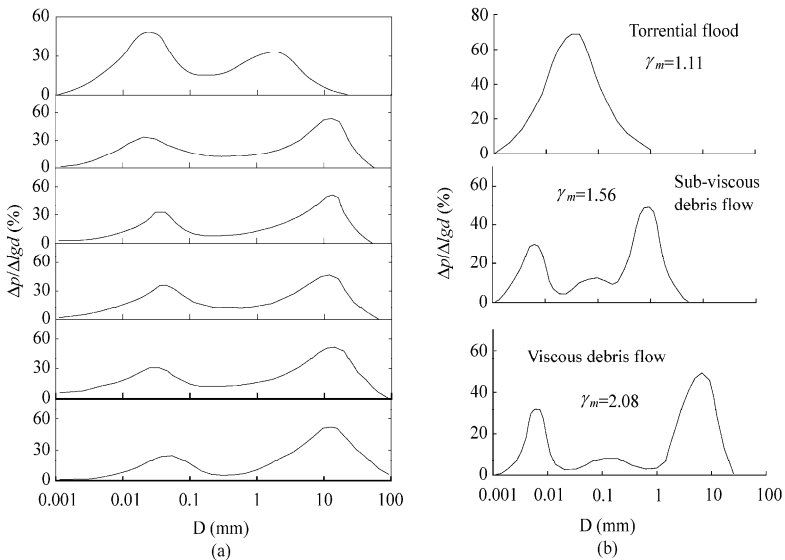
Fig. 4.51   (a) Bimodal grain size distribution of debris flow in the Liuwan Gully; (b) Grain size distributions of torrential flood, sub-viscous debris flow and viscous debris in the Jiangjia Ravine (after Kang, 1985b)

Characteristics of the grain size distribution are, of course, closely related to the supply conditions of sediment in the watershed. On the other hand, the grain size distribution is also affected by the selectivity of the movement pattern to solid grains, Figure 4.51(b) shows the grain size distributions in a debris flow development process from torrential flood low-viscous debris flow, viscous debris flow that occurred in the Jiangjia Ravine (Kang, 1985b). Suspended load dominates in the torrential flood and the size distribution had only one peak of frequency density. In sub-viscous and viscous debris flows, however, neutrally buoyant load dominates, adding one peak of much coarser grain size to the lower peak of finer particles.

4.3.3.7 Sorting of Debris Flow Deposits

Generally speaking, deposits from pseudo-one-phase debris flows consisting of clay, sand, and gravel, are a well mixed mixture of various particles. In the Bailong River, the thickness of debris flow deposits is as much as 30–50 m. The profile of the deposit shows huge stones and gravels mixed together with sand and clay (Li and Deng, 1985). But two-phase debris flows occasionally bring about inverse grading of the deposit (upward coarsening deposit), which is quite different from sedimentation in rivers. Such a unique sorting is a characteristic of deposits of two-phase debris flows, in which there is little clay and silt.
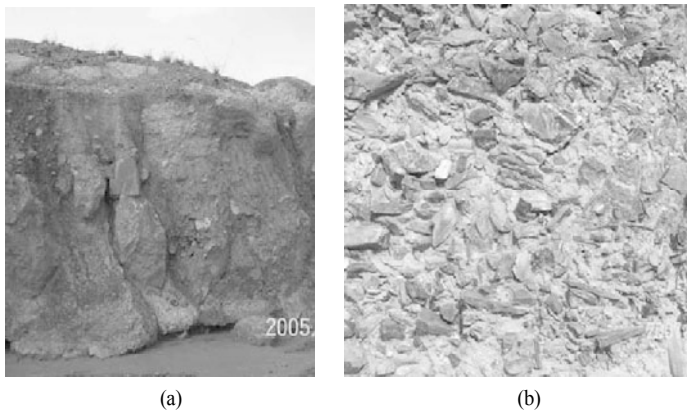
| (a) | (b) |

Fig. 4.52 (a) Viscous debris flow deposits in the Dabaini Ravine in the Xiaojiang watershed; (b) Viscous debris flow deposits in a debris flow gully in the Bailong River basin in Gansu Province (See color figure at the end of this book)

Deposits from low-viscous debris flows usually are positive graded (upward fining), and deposits from viscous and subviscous debris flows are well mixed. In general, deposits from debris flows usually are well mixed, but sometimes may be inverse graded, or positive graded. Figure 4.52 shows the viscous debris flow deposit in the Dabaini Gully in the Xiaojiang watershed on the Yunnan-Guizhou Plateau (a); and viscous debris flow deposit in a debris flow gully in the Bailong River basin in Gansu Province (b). Large stones and fine materials are well mixed, which implies that solid material with different sizes moved together during viscous debris flows.

4.3.3.8 Serious Degradation and Aggradation

Debris flow often results in great degradation in the upstream and serious aggradation at the mouth of the gully. For instance, in the upstream of the Bomi-Guxiang Gully in Tibet, the gully bed was cut down 140–180 m in the period 1954–1963, or 16 m annually (Deng, 1985). It was observed that degradation of the debris flow gully resulted mainly from retrogressive erosion as debris flow occurred. In a debris flow in the Guxiang Gully in 1964, a 1-m-bed drop moved upstream at a speed of 1 m/min. Sometimes debris flow brings about another type of erosion wherein large stones in the surge head dig a ditch into the bed

and push forward. Debris flow also caused serious bank erosion due to its high velocity and shear force, and even causes movement of the debris flow channel.

As debris flow carries a huge amount of debris to the mouth of the gully, the solid particles will deposit because of a sudden reduction of the channel slope. A huge fan-shaped stone-sea appears and sometimes the deposit dams rivers. The rate of aggradation also is quite high. It is estimated that more than 1.15×10^8 tons of solid material accumulated and the bed rose 16 m in the mouth area of the Guxiang Gully in the period 1953–1965.

Figure 4.53 shows the aggradation and degradation of the Jiangjia Ravine in the periods 1957–1985 and 1957–2002 (He et al., 2003). Gully erosion is the main type of erosion, which produces 75–83% of the total sediment yield from the ravine. The eroded sediment from the upstream reaches was transported in debris flows and deposited in the downstream reaches of the ravine. The gully bed aggraded by more than 40 m in the period of 1957–2002. A huge amount of sediment is stored in the downstream reaches and the mouth of the ravine. The same story has occurred in numerous debris flow gullies. All the mouths of the debris flow gullies along the Xiaojiang River have been silted up by several tens of meters in the past 50 years.
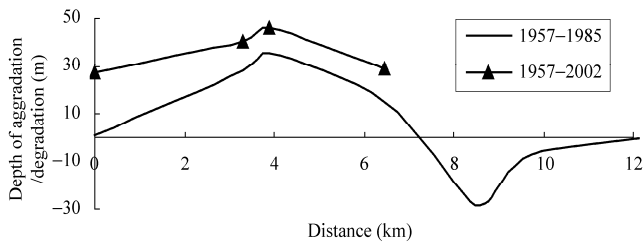
Fig. 4.53   Aggradation (+) and degradation (–) of the Jiangjia Ravine in the periods 1957–1985 and 1957–2002 as a function of distance from the ravine mouth (after He et al., 2003)

The Dongchuan Debris Flow Observation and Research Station of the Chinese Academy of Sciences is on the Jiangjia Ravine. The first observation tower was 30 meters higher than the channel bed in the 1970s. Aggradation of the debris flow channel endangered the observation tower, as shown in Fig. 4.54(a) and people had to give up the tower and build a new one on much higher ground in the 1990s. The channel bed silted up and approached to the tower base. In 2009 the observation tower fell into the ravine due to direct assult of flow at the tower base, as shown in Fig. 4.54(b).

(a)   (b)

Fig. 4.54   (a) Aggradation of the debris flow channel endangered the original observation tower on the Jiangjia Ravine in 2006; and (b) The tower fell into the ravine due to direct assault of flow at the tower base in 2009

4.3.3.9 Resistance and Drag Reduction in Pseudo-one-Phase Debris Flows

The resistance of a two-phase debris flow is much larger than for the flow of water. However, the resistance of a pseudo-one-phase debris flow is sometimes lower than for the flow of water. Wang et al. (1999), assisted by the Dongchuan Debris Flow Observation and Research Station, measured the roughness of clear water flow in the Jiangjia Ravine, collected the resistance of pseudo-one-phase debris flows, and compared them, as shown in Fig. 4.55. The resistance of debris flow is less than half that for clear water flow which means that the velocity of debris flow in the gully is higher than 2 times that of clear water flow at the same flow depths. This result implies a striking drag reduction in debris flow. There must be a special mechanism resulting in the drag reduction.
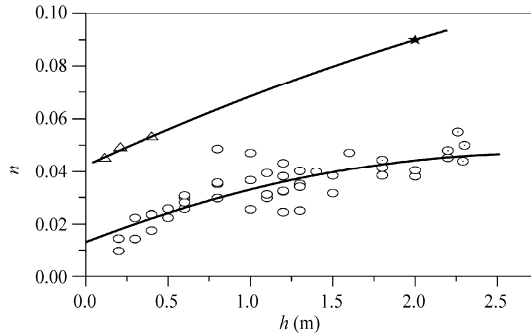
Fig. 4.55 The Manning resistance coefficient, n, of clear water flows and pseudo-one-phase debris flows as a function of flow depth, h, in the Jiangjia Ravine, Xiaojiang watershed on the Yunnan-Guizhou Plateau of China

Drag reduction is a focal point of research by scientists and hydraulic engineers, and sediment induced drag reduction has been reported in the recent years. Chanson (1994) reported drag reduction resulting from sediment and air bubbles. Wang et al. (1998) studied the resistance and drag reduction of hyperconcentrated flow over rough boundaries and found that the drag reduction is due to the turbulence suppressing effect of high concentrations and the smoothing of the boundary. Many parameters have been proposed to represent resistance resulting from debris flow and none of them has been successfully applied to a specific flow.

If the pseudo-one-phase debris flow is homogenous and laminar, the resistance can be represented by its rheological parameters such as viscosity and yield strength (Johnson and Rahn, 1970; Yano and Daido, 1965). Despite the much higher viscosity, the yield stress of debris flow means extremely higher resistance rather than drag reduction. If the flow is turbulent, the resistance resulting from turbulent stress mostly dominates the flow and there is no theoretical formula for the estimation of the resistance. The shape of the channel and the bed form also contribute to the complexity of the problem. Hydraulic engineers have applied the Manning roughness coefficient, n, to represent the resistance to the flow and experience has been accumulated in the estimation of the roughness.

The drag reduction in debris flow is so obvious and is an important phenomenon receiving little attention. The discharge of a debris flow gully, such as the Jiangjia and Dabaini gullies, is several times higher than that of the Xiaojiang River into which they pour. Drag reduction is a cause of the extremely high discharge.

The mechanism of the drag reduction is probably a result of the bed paving process. Figure 4.56 shows a comparison of the bed surface before and after the bed paving process. The bed surface is obviously smoother after the paving process. Another mechanism of drag reduction is due to air bubbles in the debris mixture. Figure 4.57 shows the holes left by air bubbles in a debris flow deposit in a debris flow gully in the Bailong River basin in Wudu County in Gansu Province.

(a)

(b)

Fig. 4.56 Comparison of the bed surfaces before (a) and after (b) the bed paving process. The bed surface is much smoother after the bed paving process and the resistance is, therefore, reduced (See color figure at the end of this book)
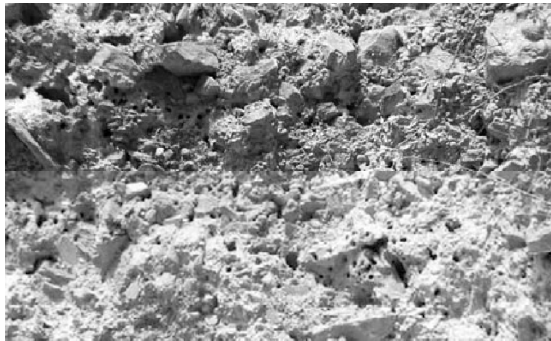
Fig. 4.57 The holes left by air bubbles in a debris flow deposit in a debris flow gully in the Bailong River basin in Wudu County, Gansu Province, in west China

Figure 4.58 shows the relation of the ratio of drag reduction with the concentration of air bubbles, in which the concentration of air bubbles, C_g, is the ratio of the volume of air bubbles to the total volume of the mixture. The ratio of drag reduction is defined as

$$R_D = (n_w - n_d)/n_w \tag{4.12}$$

where n_d is the roughness of debris flow calculated with Eq. (4.8) and n_w is the roughness of water flow.

The ratio of drag reduction in pseudo-one-phase debris flow is as high as 60%. The air bubbles play a role of cushing, which reduces the resistance. It is clearly shown that the concentration of air bubbles enhances the ratio of drag reduction. About 30% of the drag reduction can be attributed to the effect of the air cushing.
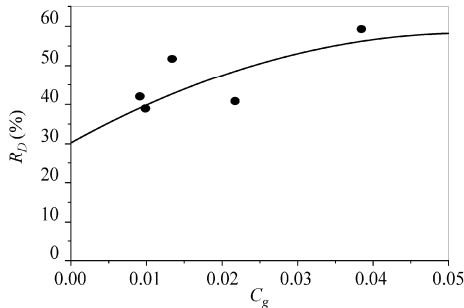
Fig. 4.58   The relation of the ratio of the drag reduction (R_D) with the concentration of air bubbles (C_g) (C_g is the ratio of the volume of air bubbles to the total volume of the mixture)

4.3.4   slope Debris Flows

4.3.4.1   Slope Debris Flows

Slope debris flow occurs if there are plenty of loose solid materials on the slope. High intensity rainfall triggers mass movements of the loose solid materials down the slope. These mass movements behave like debris flows but the distance of movement is, however, much shorter than normal debris flows, and in general travels only several tens to one hundred meters. Such a mass movement is called a slope debris flow. In general, slope debris flows occur on steep slopes without apparent drainage area and streams. This is different from the normal debris flows that flow in gullies with a certain drainage area.

Slope debris flows occur at piled gangue deposit and grain erosion deposit fans, the latter has been discussed in Chapter 2. Figure 4.59 shows a slope debris flow at a gangue deposit of a gold mine on a mountain slope in Lixian County, Gansu Province of China. A huge amount of gangue deposit was piled on the mountain slope Fig. 4.59(a), which had a relatively uniform size distribution with median diameter of about 20 mm. The slope of the deposit was equal to the repose angle (about 32°). Heavy rainfal caused slope debris flows (b). The slope debris flow traveled only 60 m and deposited at gengle slopes.

Fig. 4.59   (a) Gangue deposit of a gold mine on a mountain slope in Lixian County, Gansu Province; (b) A slope debris flow on the gangue deposit which was initiated by heavy rainfall (See color figure at the end of this book)

4.3.4.2　Slope Debris Flows after the Wenchuan Earthquake

A lot of slope debris flows occurred after the Wenchuan Earthquake because thousands of avalanches and landslides triggered by the earthquake resulted in a huge amount of loose solid materials on slopes. An investigation of slope debris flows and measurements of 19 slope debris flows were performed from June to August 2009 (Li et al., 2010). Figure 4.60 shows the earthquake area and the location of the 19 slope debris flows in the Mianyuan and Minjiang river basins. Figure 4.61 shows a slope debris flow that occurred at Xiaogangjian on August 26, which blocked the only highway from Hanwang to Qingping. During the rainfall with an intensity of about 90 mm/d on July 17, 2009, several tens of slope debris
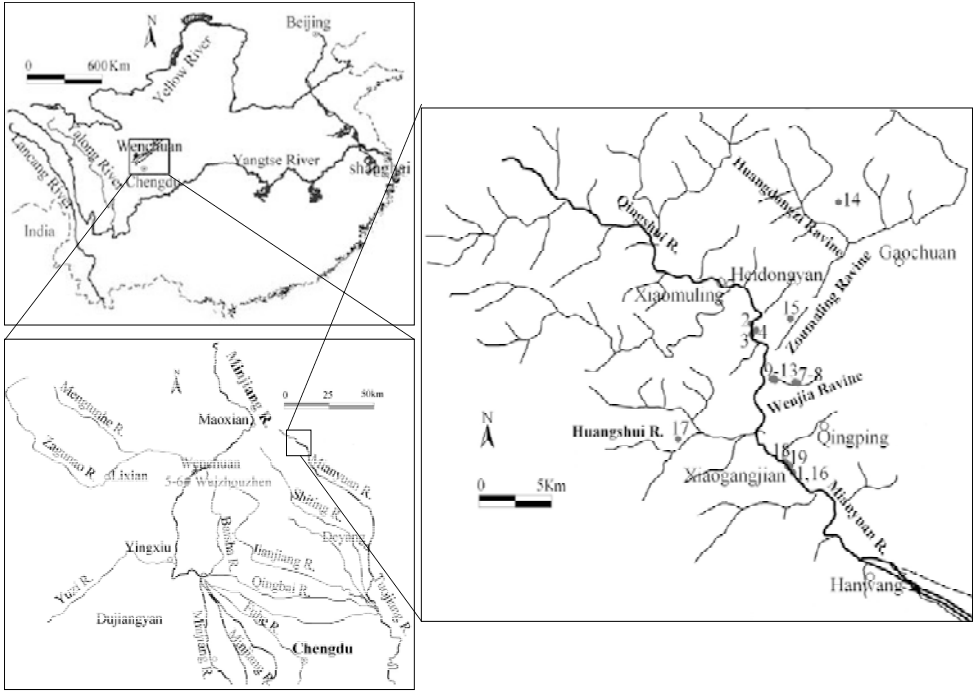
Fig. 4.60　Wenchuan Earthquake area and the locations of the 19 slope debris flows

(a)   (b)

Fig. 4.61　(a) Slope debris flow at Xiaogangjian along the Mianyuan River; (b) Slope debris flow at Xiaomuling along the Mianyuan River (See color figure at the end of this book)

flows occurred along the Mianyuan River between Heidongyan and Hanwang. The distance between twoslope debris flows was only several tens of meters. The slope debris flows moved slowly and traveled for a distance of only several tens of meters. Thus, slope debris flows caused no casualties but caused great damage to highways and rivers.

4.3.4.3 Slope Debris Flows Are Two-phase Debris Flow

Slope debris flows are generally two-phase debris flows because there included very little of clay and silt. Figure 4.62 shows that size distribution of some of the 19 slope debris flows in the Wenchuan Earthquake area. The particles finer than 1mm were less than or much less than 10% of the total solid materials. The median diameter was between 20–200 mm for the debris flow deposits. There was only 1–2% of clay and silt in the solid materials. Collisions between solid particles consume a lot of energy and, therefore, the velocity of slope debris flow was very low. The velocity of the slope debris flows was calculated at only several centimeters per second with Eq. (4.7). The slope debris flows traveled for a distance of only several tens of meters. The low velocity resulted in the short travel distance and high slope of deposit.
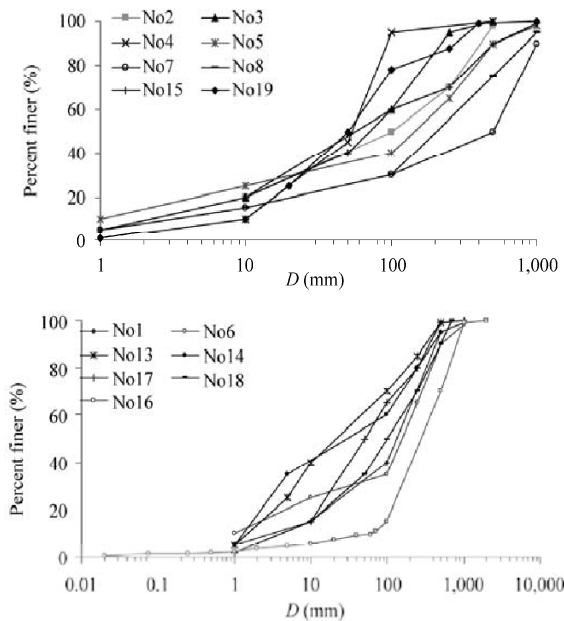
Fig. 4.62 Cumulative size distribution of some of the 19 slope debris flow deposits in the Wenchuan Earthquake area

4.3.4.4 Deposits of Slope Debris Flows

Most of the slope debris flows consisted of two parts: formation section and deposit. The formation section was in fact at the deposit of an avalanche or the deposit fan of grain erosion, which had a high slope with an average value of about 38°. The head of the deposit of a slope debris flow took the form of a "tongue." The volume of deposits varied and depended on the scale of the slope debris flow. The surface slope of slope debris flow deposits ranged from 6° to 21° with an average value of about 10°. The slope of the deposits is much higher than for normal debris flow in gullies. If a slope debris flow occurred on a long slope, there was a flow section between the formation section and the deposit. The surface slope of the flow section was lower than that the formation section, but higher than that of the deposit.

Figure 4.63 shows the deposit slope of debris flows as a function of drainage area for slope debris flows in the earthquake area and normal debris flows in the Jiangjia Ravine in Yunnan (Kang, 1996). The

slope of the debris flow deposits in the Jiangjia Ravine was about 5°, and the slope of the slope debris flow deposit was about 10°.
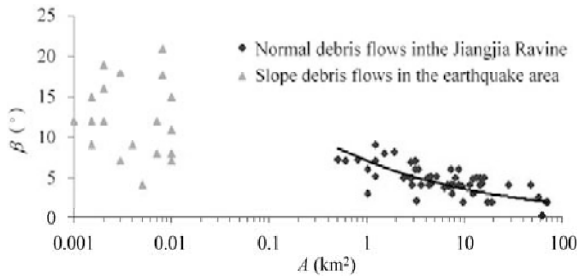
Fig. 4.63 Deposit slope β of slope debris flows in the Wenchuan Earthquake area and of normal debris flows in the Jiangjia Ravine as a function of the drainage area

4.3.4.5 Low Water Content in Slope Debris Flows

All water in the slope debris flows was from local rainfall because there was a very small drainage area. Water and small amounts of clay and silt mixed into a liquid, which plays the role of lubricant among the coarse particles instead of as a carrier. The concentration of total solid materials in the slope debris flows was very high. Measured solid concentrations by weight for slope debris flows were 83–91%. Because surface runoff was not needed for triggering slope debris flows the rainfall intensity to trigger slope debris flow was much smaller than the rainfall for initiating normal debris flows. The statistics of the 19 slope debris flow revealed that a rainfall intensity higher than 20 mm/day may trigger a single slope debris flow; a rainfall intensity higher than 30 mm/day may trigger several slope debris flows simultaneously; and a rainfall intensity higher than 90 mm/day may trigger a group of slope debris flows simultaneously. Because the water content in slope debris flows was very low collisions between solid particles were intense and the velocity was very low. The travel distance of slope debris flow was only several tens of meters.

4.4 Mitigation of Landslide and Debris Flow Hazards

4.4.1 Mitigation of Landslide Hazards

The Xintan Landslide (Fig. 4.7) was very hazardous but did not cause a great disaster thanks to accurate prediction. Xintan Town has recorded more than 20 landslides in 1,000 years. A landslide in 1030 was triggered by an earthquake and dammed the Yangtze River for 20 years. In 1559 a landslide destroyed a village and killed 300 people. The old sliding body slid again in 1936 and destroyed 20 houses. In 1958 a sliding body with a volume of 30,000 m^3 moved again and killed 2 people and destroyed a factory. In 1964 a landslide with a volume of 100,000 m^3 occurred. In the period after 1964 a series of small-scale landslides have occurred in the Xintan area.

The prediction of the landslide on 12 June 1985 was very successful. Figure 4.64 illustrates the Xintan monitoring system, which has detected creeping of the sliding body since 1982. Movement of the sliding body intensified in 1983 and at a few observation points the system measured 1–7 m of displacement from July 1984 to November1985. On 9–11 June 1985, many cracks appeared on the slope, hot air emitted from the ground and villagers heard abnormal noise from the ground. Scientists predicted a large-scale landslide 24 hours before the event on 11 June. Because of the accurate prediction all 1,371 people living in the town were evacuated and great casualties were avoided (HLIG, 1985).

Some engineering measures have been taken to control landslides and avalanches. In the Three Gorges reaches of the Yangtze River, drainage systems have been improved to reduce the water content of the soil and concrete walls were constructed to reduce the risk of landslides. Figure 4.65(a) shows a drainage system on a landslide body in the upper Yangtze River basin installed to lower the groundwater table and Fig. 4.65(b) shows concrete walls installed to stabilize a sliding body.
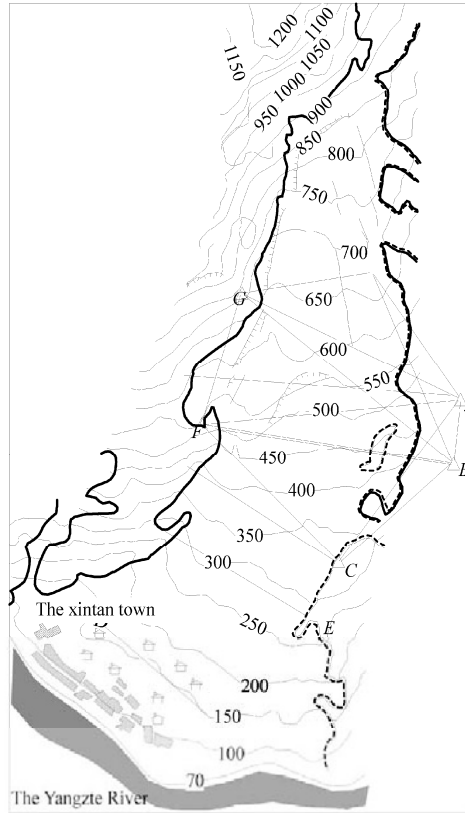
Fig. 4.64   The monitoring system used for prediction of the Xintan Landslide of 12 June 1985

Fig. 4.65   (a) A drainage system on a landslide body in the upper Yangtze River basin installed to lower the groundwater table; and (b) Concrete walls installed to stabilize a sliding body

In Hong Kong the government has been increasing the budget for landslide control since the mid 1990s. Figure 4.66 shows the annual budget and expenditure for landslide control in the period 1977–2000. The money was used to build anti-landslide structures. Figure 4.67 is a schematic of anchors and concrete piers used for stabilizing slopes and protecting highways.
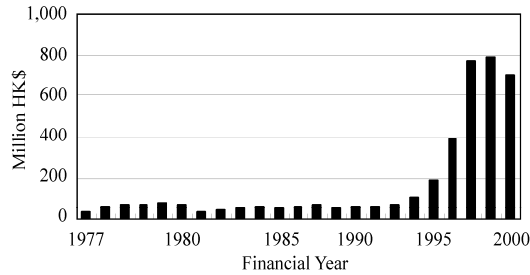
Fig. 4.66   Annual budget for landslide control in Hong Kong in the period 1977–2000
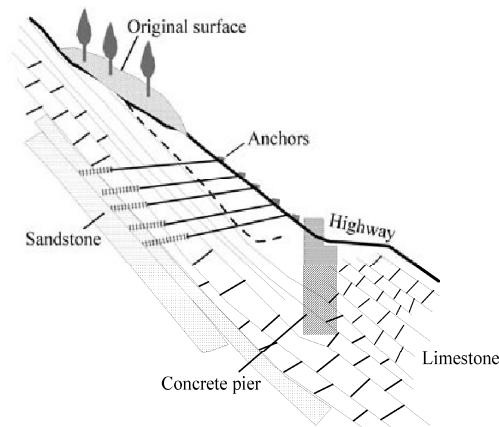
Fig. 4.67   Schematic of anchors and concrete piers used for stabilizing slopes and protecting highways

Figure 4.68(a) shows the steep slope in the campus of the University of Hong Kong has been stabilized with numerous anchors. These anchors bind the surface rocks with the deep rock, which effectively controls rock falls and avalanches. Figure 4.68(b) shows the concrete piers for landslide control in Danba in Sichuan Province of China. The county town is located on the banks of the Dadu River and the risk of landslide is high due to the very steep slope. Drainage systems, piers, and anchors have been constructed to reduce the risk of landslides throughout china and in mountainous areas world wide.

4.4.2   Prediction and Warning of Debris Flow

4.4.2.1   Prediction of Debris Flow
Prediction of debris flow remains in the development stage. An important routine for prediction of rainstorm debris flows is to relate rainfall intensity in 10 min and the antecedent rainfall to debris flow. Chen (1985) analyzed data of nearly one hundred rain storms and tens of debris flows in the watershed of the Jiangjia Ravine in the Xiaojiang watershed on the Yunnan-Guizhou Plateau of China. The main results obtained are shown in Fig. 4.69, where I_{10} is 10 min rainfall intensity, or the maximum rainfall

(a)

(b)

Fig. 4.68   (a) Anchors stabilizing the slope in the campus of the University of Hong Kong; (b) Concrete piers for landslide control in Sichuan Province of China
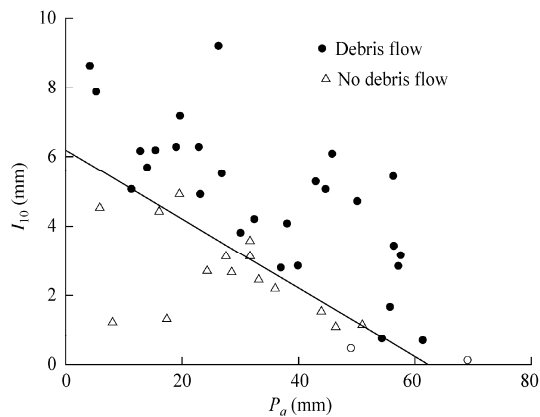
Fig. 4.69   Critical 10 min. rainfall intensity, I_{10}, and antecedent rainfall index, P_a, for triggering debris flows in the Jiangjia Ravine, Xiaojiang watershed on the Yunnan-Guizhou Plateau of China (after Chen, 1985)

in 10 min P_a is a factor of accumulated precipitation in the past 20 days and is given by the following formula:

$$P_a = P_0 + 0.8P_1 + 0.8^2 P_2 + 0.8^3 P_3 + \cdots + 0.8^{20} P_{20} \tag{4.13}$$

in which P_0 is the rainfall just before the most intense 10-min. rainfall, P_i is the rainfall on the day i-days before the current day. Figure 4.69 shows that debris flow occurs if:

$$10.33 \, I_{10} + P_a > 62 \text{ mm} \tag{4.14}$$

The analysis also indicates that if P_a is smaller than 30 mm and I_{10} is larger than 4 mm, gusty and short-time debris flow occurs, whereas if P_a is larger than 60 mm and I_{10} is less than 2 mm, low-viscous debris flow occurs. By combining Eq. (4.14) and rainstorm forecasting, debris flow in that area can be predicted. The same method and the criterion I_{10} are applied for prediction of debris flow in other debris flow gullies in China.

4.4.2.2 Warning System

Many detection and warning systems have been developed for protecting railways, highways, bridges, factories and mines from debris flows. These detection and warning systems work based on different principles. For instance, vibration detectors receive vibration induced by debris flow and transmit a warning signal to the protected objects. Debris flow level detectors can send warning signals to the protected objects when a debris flow is over a given stage. These warning systems are working in many debris flow areas, and they have successfully sent warning signals to railways, bridges, and towns and have saved people's lives and property.

The UJ-2 type ground sound wave probe and warning system was developed by the Chengdu Institute of Mountain Hazards Studies in 1984. The system can automatically work for 3 months powered by batteries. The system was tested in 1984–1985 and successfully sent warning signals of 12 debris flows to the protected areas 2.8 km downstream. The signals arrived at the protected object 8 minutes ahead of the debris flow. The system worked well but the warning time is not long. The warning devices may be installed on rock walls of debris flow gullies, concrete levees, dams or dykes, and buried in the channel bed. Figure 4.70 shows a ground sound wave probe installed on a dam.

Fig. 4.70　A ground sound wave probe installed on a dam

VI-1 type and DFT-3 type debris flow stage probes and warning systems were developed by Shanghai Changning Science Association. The systems sent signals to the protected objects when a debris flow was over a critical stage. The signals arrived at the protected object 8 minutes ahead of the debris flow head.

4.4.3 Debris Flow Control Engineering

Debris flow-control engineering has a long history in China. People dwelling in debris flow areas built dams

and dredged floodways to avoid or reduce debris flow disasters several hundred years ago. Engineering measures to control debris flow are:

4.4.3.1 Diversion Works

Diversion channels and guide-ways are constructed to divert floods from the upstream of a debris flow gully, and reduce discharge of floods and the kinetic energy of the flow so that debris flow is prevented or reduced in scale. The Xinkang amianthus mine in Sichuan Province built a tunnel to divert water from the upstream of the Dahong Gully to a river. The capacity of the tunnel was 190 m^3/s, equivalent to the 20- year flood of the gully. The flood discharge of the gully was substantially reduced by the tunnel and no debris flow has occurred in the past 20 years. Figure 4.71 shows the diversion channels at the Niwan Gully and the Jiangjia Ravine. The Niwan channel diverts debris flow from the Niwan Gully to the Bailong River and protects farmland from being buried by debris. The Jiangjia Channel diverts debris flow to a debris siltation basin and then to the Xiaojiang River. Hence, damming of the Xiaojiang River is avoided. Figure 4.72 shows debris flow-guiding channels in a debris flow gully in the Xiaojiang River basin, which has successfully guided debris flows to the Xiaojiang River and protected the village and farmland on the fan. The ribs on the guiding channel create resistance and consume the energy of debris flows, and, therefore, reduce the destructive force of the debris flows.
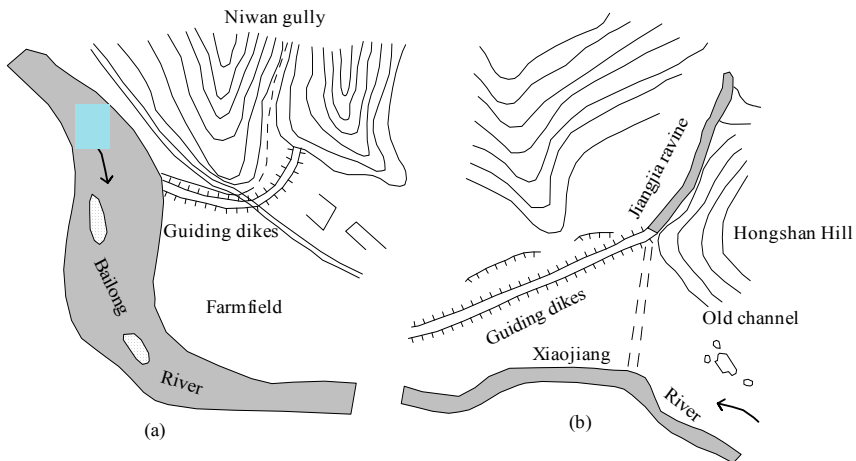
Fig. 4.71 (a) Diversion channel at the Niwan Gully, which diverts debris flows and protects farmland. (b) A channel diverts debris flow to a debris siltation basin, protecting the Xiaojiang River from damming

4.4.3.2 Dams and Dam Cascades

Dams and dam cascades on a debris flow gully have been built to trap debris and effectively check debris flow. Daqiao Creek, a tributary of the Xiaojiang River was a very active debris flow gully. Five detention dams were built over 7 km along the gully. These dams considerably reduced solid material transported into the Xiaojiang River. Nowadays lattice dams are widely used because they can trap large boulders carried by the debris flow and reduce harmfulness. Lattice dams also have much longer life spans because they silt up at a low speed. Figure 4.73(a) shows the debris flow control dam cascade on the Houshan Ravine of Heishui County, Sichuan Province (Kang, 1996). Each dam is 3–5 m high and 10–20 m wide. They function to check debris flow and protect each other. Figure 4.73(b) shows the comb frame dam on a debris flow gully in the Cho-Shui River basin in Taiwan, China. The dam trapped big stones but released water and silt downstream.

Fig. 4.72   Debris flow-guiding channels on a debris flow gully in the Xiaojiang River basin
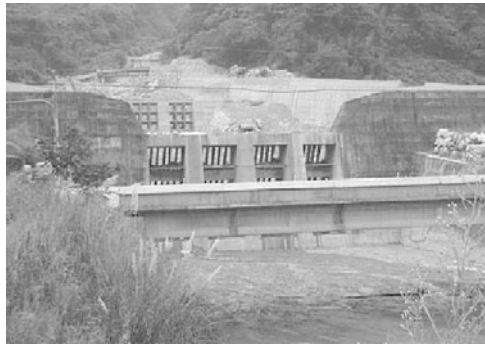
(a)

(b)

Fig. 4.73   (a) Debris flow control dam cascade on the Houshan Ravine of Heishui County, Yunnan Province, China (after Kang, 1996); (b) Comb frame dam on a debris flow gully in Taiwan, China (See color figure at the end of this book)

Debris flows carry a lot of sediment and fill the reservoirs very quickly. Bed load particles roll or jump over the dam crest and cause abrasion. Figure 4.74(a) shows a check dam on the Diaoga River in the Xiaojiang River basin, which was constructed 30 years ago. The dam has been cut into a groove one meter wide and 4.5-m deep by the bed load movement. The rate of abrasion of the dam was as high as 0.15 m/yr. Moreover, the flow over the spillway is energetic and causes local scour of the dam base,

which may result in dam failure. Figure 4.74(b) shows a filled dam on a small debris flow gully by the Jinsha River. The dam was scoured by the falling flow from the dam crest. The dam may soon fail although the reservoir had been filled.

Several energy-dissipation structures have been applied: (1) an auxiliary dam with a height of 1/3–1/4 the main dam height at a distance of 2 times the main dam height downstream from the main dam dissipates the flow energy and protects the main dam from serious local scour. Sometimes two or three auxiliary dams are necessary; (2) a underground concrete wall stabilizes the gully bed downstream from the dam; (3) in narrow gullies a curved gravity dam resists the local scour; and (4) a protection apron protects the bed from scour. If the main dam is high and the flow discharge is large the auxiliary dam may also suffer from dam base scour. In this case two or three auxiliary dams are necessary. The second auxiliary dam is lower than the first auxiliary dam and the third is even lower. Figure 4.75 shows three auxiliary dams downstream of a main dam on a debris flow gully in Ningnan County in Sichuan Province, China, which protect the main dam from flow scour and control debris flow.

(a)   (b)
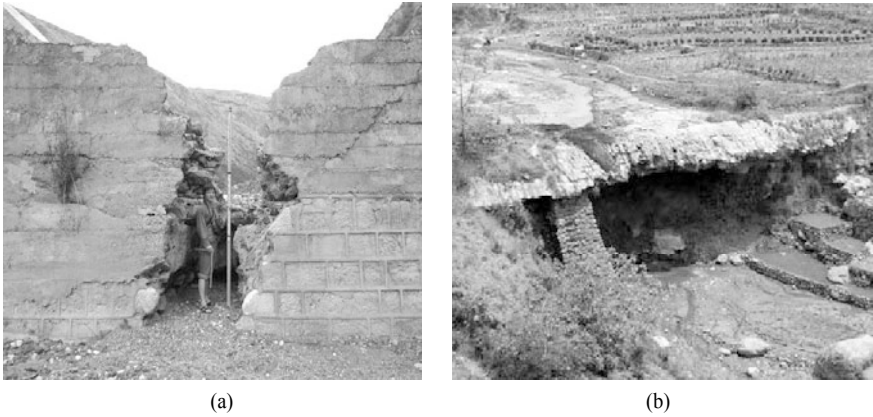
Fig. 4.74   (a) A check dam on the Diaoga River has been cut into a groove one meter wide and 4.5-m deep by bed load movement; (b) A dam on a small debris flow gully by the Jinsha River was scoured by the falling flow

Fig. 4.75   Three auxiliary dams downstream of a main dam on a debris flow gully in Ningnan County, Sichuan Province

4.4.3.3 Flume

To build a flume across a railway or highway is an effective measure and is widely used in China. In Gansu Province alone there are 25 flumes, which guide debris flow over highways or railways and consequently protect the highways and railways from damage from debris flow. Figure 4.76 shows a debris flow flume over the highway at Wudu County in Gansu Province, which has successfully protected the highway from being buried by debris flow deposits.

(a)

(b)

Fig. 4.76　(a) Debris flow flume over the highway at Wudu County in Gansu Province; (b) The flume has successfully protected the highway from being buried by debris flow deposits

4.4.3.4 Slope Stabilization

To build terraces on the slope where debris flow is initiated may stabilize the slope and control debris flow. Figure 4.77 shows the terrace structure constructed for control of the debris flow in the Dengqian River in Yunnan Province. The terraces are 3,700-m long and 2 m wide. Orchard and forest are developed on the terraces and slope. The terraces have effectively reduced slope erosion and controlled debris flows.

4.4.3.5 Ecological Measures for Debris Flow Control

Reforestation is an ecological measure for thoroughly controlling debris flow. In Nanpin County, Sichuan Province, for example, people stopped ploughing and growing crops on slope-land and reforested and
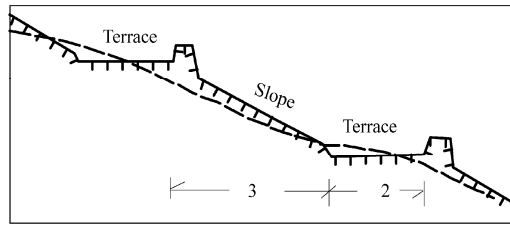
Fig. 4.77 Terraces on slopes mitigate debris flow disasters

planted grass on these slopes. This effectively reduced debris flow disasters. Building soil-retaining structures at key locations is necessary for preventing landslides and debris flows. It also benefits the formation of a protective cover of vegetation. In some areas people hammered willow trunks into the gully bed, with 1 m underground and 0.5 m above ground. Sediment carried by debris flows is trapped by the willow piles. Following sediment deposition in front of the willows piles the willow grew up and became strong. Willow forests might grow from the debris flow gully and debris flow can be controlled. Figure 4.78 shows that debris flow control dams and reforestation of the hills as the comprehensive debris flow control strategy in the Shengou drainage basin have changed the debris flow gully into a forest park in Dongchuan in Yunnan Province.

Fig. 4.78 Debris flow control dams and reforestation of the hills used as the comprehensive debris flow control strategy in the Shengou drainage basin have changed the debris flow gully into a forest park of the Dongchuan City; Yunnan Province

4.4.4 Reclamation of Landslides and Debris Flow Fans

Landslides occur on steep mountains with deeply incised streams. There is a lack of flat land or gentle slope land in the mountainous areas. Landslides created flat or gentle slope land, which may be reclaimed for agriculture, residence and urban construction. Figure 4.79(a) shows a landslide deposit on the Xiaojiang River, which has been reclaimed for agriculture and village. The potential energy of the slope was released during the landslide and the risk of new sliding is low. Figure 4.79(b) shows the Dongchuan city town on a huge landslide deposit. The landslide occurred a thousand years ago. The landslide deposit is stable. A city with a population of a half million has developed on the landslide deposit. Many new buildings are under construction.
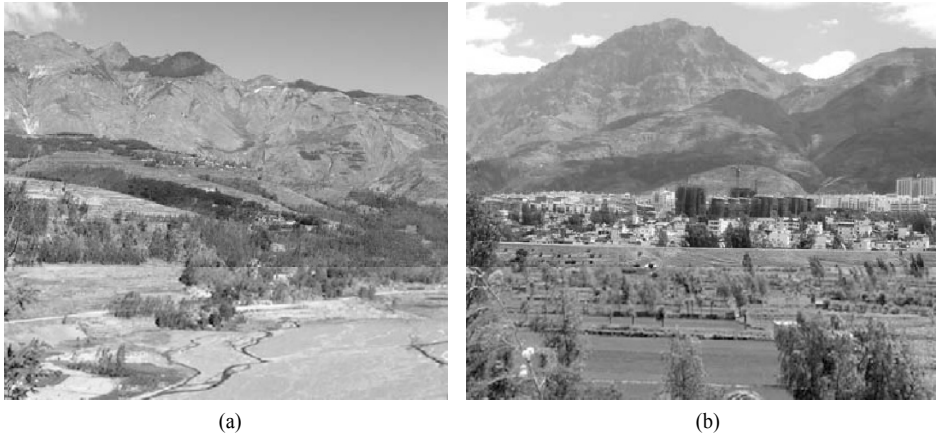
<div align="center">(a)　　　　　　　　　　　　　　　　　　(b)</div>

Fig. 4.79　(a) Agriculture and village on a landslide deposit by the Xiaojiang River; (b) The Dongchuan city town on a huge landslide deposit in Yunnan, China (See color figure at the end of this book)

Debris flows transport a huge amount of sediment to the gully mouths, or confluence with rivers. In general the rivers have much smaller bed gradient than the debris flow gullies. Therefore, most of the sediment can not be carried downstream by the river flow and rather deposits at the gully mouth to form debris flow fans. Figure 4.80 shows a debris flow fan at the Awangxiaohe Ravine, which flows into the Xiaojiang River. The Awangxiaohe Ravine was a debris flow gully. The debris flow fan is flat and fertile. Local people have reclaimed the land for agriculture and township construction. Nowadays, the Awangxiaohe town has becomes a center for residence, education and market.

Fig. 4.80　A new town developed on the Awangxiaohe debris flow fan in the Xiaojiang River basin (See color figure at the end of this book)

Appendix

Mathematical derivation and explanation for the phenomenon of roll waves

Pseudo-one-phase debris flow can be simulated with the Bingham model

$$\tau = \tau_B + \eta\varepsilon \tag{4.A1}$$

in which τ is the shear stress of the flow, τ_B is the yield shear stress of the fluid, η is the rigidity coefficient (called Bingham viscosity by some researchers), and ε is the shear rate, which is equal to the velocity gradient in laminar flow.

For unsteady open channel flow, the de Saint Venant equations (one-dimensional continuity equation and momentum equation) are

$$\frac{\partial h}{\partial t} + u\frac{\partial h}{\partial x} + h\frac{\partial u}{\partial x} = 0 \tag{4.A2}$$

$$\frac{\partial u}{\partial t} + u\frac{\partial u}{\partial x} + g\frac{\partial h}{\partial x} = gJ - \frac{\tau_0}{\rho_m h} \tag{4.A3}$$

where u is the cross sectional average velocity, τ_0 is the shear stress of the flow acting on the bed, or the resistance of the bed to the flow, h is the depth of flow, J is energy slope, which is equal to bed gradient s in steady uniform flows, ρ_m is the density of the flowing mixture, x is the distance along the flowing course, g is the acceleration of gravity, and t is time. Applying the method of characteristics, the two partial differential equations can change into two groups of normal differential equations in which one group follows the C1-family of characteristic curves

$$\frac{dx}{dt} = u + \sqrt{(gh)} \tag{4.A4}$$

$$\frac{d}{dt} = (u + 2\sqrt{(gh)}) = gJ - \frac{\tau_0}{\rho_m h} \tag{4.A5}$$

and another group follows the C2-family of characteristic curves

$$\frac{dx}{dt} = u - \sqrt{(gh)} \tag{4.A6}$$

$$\frac{d}{dt} = (u - 2\sqrt{(gh)}) = gJ - \frac{\tau_0}{\rho_m h} \tag{4.A7}$$

In steady uniform flow, the velocity u and the depth h are constants, and the frictional resistance must then be equal to the tractive force, i.e.

$$gJ = \frac{\tau_0}{\rho_m h} \tag{4.A8}$$

If a perturbation induces increments Δu, $\Delta(2\sqrt{(gh)})$ and $\Delta(\tau_0/(\rho_m h))$, then Eq. (4.A5) becomes

$$\frac{d}{dt}(u + 2\sqrt{(gh)} + \Delta u + \Delta(2\sqrt{(gh)})) = gJ - \frac{\tau_0}{\rho_m h} - \Delta\left(\frac{\tau_0}{\rho_m h}\right) \tag{4.A9}$$

Subtracting Eq. (4.A5) from Eq. (4.A9) yields

$$\frac{d}{dt}(\Delta u + \Delta(2\sqrt{(gh)})) = -\Delta\left(\frac{\tau_0}{\rho_m h}\right) \tag{4.A10}$$

Equation (4.A10) is called a perturbation equation along the C1-family of characteristic curves (Wang,

257

2002). Similarly, the perturbation equation along the C2-family of characteristic curves is

$$\frac{d}{dt}(\Delta u - \Delta(2\sqrt{(gh)})) = -\Delta\left(\frac{\tau_0}{\rho_m h}\right) \tag{4.A11}$$

In a steady laminar flow of a Bingham fluid, the shear stress τ_0 is given by (4.A1):

$$\tau_0 = \tau_B + \eta\varepsilon \tag{4.A12}$$

Figure 4.A1 shows the general velocity distribution of Bingham flow in an open channel. The upper part is a plug in which the fluid flows at a uniform velocity u_p, which is nearly equal to the average velocity. Only in the zone near the bed does the velocity vary, from zero to u_p. The thickness of the layer is assumed to be δ. The velocity gradient, therefore, is roughly u/δ, and

$$\frac{d}{dt}(\Delta u + \Delta(2\sqrt{gh})) = -\Delta\left(\frac{\tau_B}{\rho_m h} + \eta\frac{u}{\rho_m h\delta}\right) \tag{4.A13}$$
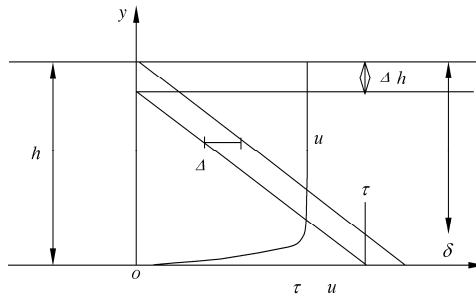
Fig. 4.A1   Velocity distribution of non-Newtonian open channel flow for a Bingham fluid

As shown in Fig. 4.A2, a perturbation that occurs at point $A(x,t)$ in the $x-t$ plane will propagate along the characteristic curves AB and AC. For any point B on the $C_1{}^1$ characteristic curve that passes through the point $A(x,t)$, a characteristic curve $C_2{}^2$ intersects the $C_1{}^1$ curve at point B. There is a relation between Δu and $\Delta(2\sqrt{(gh)})$ at point B (i. e. any point on the $C_1{}^1$ characteristic curve).
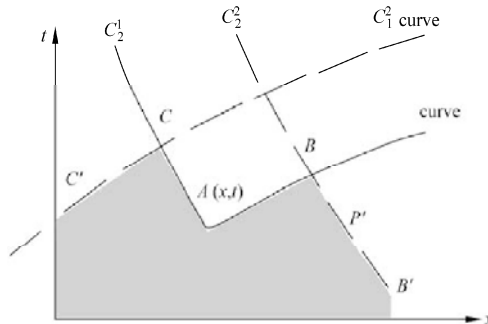
Fig. 4.A2   Characteristic curves on the $x-t$ plane (The abscissa is the x-axis and the ordinate is the time t-axis). If a perturbation occurs at the point A, it propagates downstream along the $C_1{}^1$ curve and upstream along the $C_2{}^1$ curve

The area below the curves CAB is undisturbed. The initial perturbation has no effect on the area, and the velocity u and depth h remain constant. Integration of Eq. (4.A11) along the $C_2{}^2$ characteristic curve yields

$$\Delta u - \Delta(2\sqrt{gh})) = \int_{B'}^{B} -\Delta\left(\frac{\tau_0}{\rho_m h}\right) dt \tag{4.A14}$$

Point P' is always in the undisturbed area as it moves from B' to a point near B, and $\Delta(\tau_0/\rho_m h)$ is zero in the process of integration except at point B. Since $\Delta(\tau_0/\rho_m h)$ is not infinite at B, Eq. (4.A14) gives

or

$$\Delta u - \Delta(2\sqrt{(gh)}) = 0 \tag{4.A15}$$

$$\Delta u = \Delta(2\sqrt{(gh)})$$

For a low discharge of mudflow, the average velocity is small. If the yield stress of the mud is large, the second term on the right hand side of Eq. (4.A13) is negligible, and the equation can be rewritten as

$$\frac{d}{dt}\left(\sqrt{\frac{g}{h}}\,\Delta h\right) = -\frac{1}{2}\Delta\left(\frac{\tau_B}{\rho_m h}\right) = \frac{1}{2}\frac{\tau_B}{\rho_m h^2}\Delta h \tag{4.A16}$$

In the process of deriving Eq. (4.A16) and Eq. (4.A15) and the following formulas

$$\Delta(2\sqrt{(gh)}) = \frac{d}{dh}(2\sqrt{(gh)})\Delta h = \sqrt{(gh)}\Delta h \tag{4.A17}$$

$$\Delta\left(\frac{\tau_B}{\rho_m h}\right) = \frac{d}{dh}\left(\frac{\tau_B}{\rho_m h}\right)\Delta h = -\frac{\tau_B}{\rho_m h^2}\Delta h \tag{4.A18}$$

have been used.

The integration of Eq. (4.A16) yields

$$\frac{\Delta h}{\Delta h_0} = e^{\frac{\tau_B}{2\sqrt{(gh)}\rho_m h}t} \tag{4.A19}$$

where Δh_0 is the initial perturbation in depth.

Equation (4.A19) indicates that the initial perturbation Δh_0 will grow, and the larger the yield stress τ_B and the smaller the mud depth h, the faster the wave will grow. After a perturbation   develops into a roll wave, the continuities of velocity and depth no longer hold, thence Eq. (4.A19) does not hold true. Therefore, the wave height cannot grow indefinitely.

If the average velocity u and the rigidity coefficient η are large and the yield stress is small, the second term on the right hand side of Eq. (4.A13) is much larger than the first one, and Eq. (4.A13) may be rewritten as

$$\frac{d}{dt}(\Delta u) = -\frac{1}{2}\Delta\left(\frac{\eta u}{\rho_m h\delta}\right) \tag{4.A20}$$

in which Eq. (4.A18) has been used. Since

$$\Delta\left(\frac{\eta u}{\rho_m h\delta}\right) = \frac{\partial}{\partial u}\left[\frac{\eta u}{\rho_m h\delta}\right]\Delta u + \frac{\partial}{\partial h}\left[\frac{\eta u}{\rho_m h\delta}\right]\Delta h = \frac{\eta u}{\rho_m h\delta}\left(\frac{\Delta u}{u} - \frac{\Delta h}{h}\right) = \frac{\eta}{\rho_m h\delta}(1 - Fr)\Delta u \tag{4.A21}$$

Equation (4.A20) can be rewritten as

$$\frac{d}{dt}(\Delta u) = -\frac{\eta}{2\rho_m h\delta}(1 - Fr)\Delta u \tag{4.A22}$$

or after integration

$$\frac{\Delta u}{\Delta u_0} = e^{-\frac{\eta(1-Fr)}{2\rho_m h\delta}t} \tag{4.A23}$$

where Δu_0 is the initial perturbation in velocity, and $Fr = u / \sqrt{(gh)}$ is the Froude number. Equation (4.A23) proves that in a high velocity flow of low yield stress, as long as $Fr < 1$, the perturbation in velocity Δu_0 always decreases, hence, the flow is stable.

Equations (4.A19) and (4.A23) give the results for the two extreme cases. In the general case, both terms on the right hand side of Eq. (4.A13) should be taken into account. Then

$$\frac{\mathrm{d}}{\mathrm{d}t}(\Delta u) = \frac{1}{2\rho_m h} \left[\frac{\tau_B}{\sqrt{gh}} - \frac{\eta}{\delta}(1 - Fr) \right] \Delta u \tag{4.A24}$$

If the fluid has a large yield stress and the Froude number is larger than one, the flow will be very unstable and quickly develops into roll waves. Many pseudo-one-phase debris flows in the Jiangjia Ravine are examples of such flows (Kang, 1985a). If the Froude number is smaller than one but the rigidity coefficient η is small and the yield stress large, the flow also is unstable and develops into wave flow. Some unstable hyperconcentrated flows in the tributaries of the Yellow River are examples of this type of flow. Whereas if the yield stress is small and η is large, a non-Newtonian flow is stable at low Froude number, e.g., flows of lava are stable because magma has an extremely high rigidity coefficient.

Review Questions

1. Where do landslides or debris flows occur in China? What disasters can debris flows and landslides cause?

2. What is the essential cause of landslides? Why?

3. What disaster chains have been initiated by landslides and avalanches?

4. Under what conditions should a landslide dam be removed?

5. Under what conditions should a landslide dam be preserved? Why?

6. List the main phenomena of pseudo-one-phase debris flows and explain simply the mechanisms of the phenomena.

7. List the main phenomena of two-phase debris flows and explain simply the mechanisms of the phenomena.

8. What are the main strategies to control landslides and debris flows?

9. Why do large particles concentrate in the debris flow head even though small particles have higher instantaneous velocities than large particles?

10. Why do viscous debris flow develop into roll waves?

11. Why does drag reduction occur in viscous debris flows?

References

Bagnold R.A., 1954. Experiments on a gravity free dispersion of large solid spheres in a Newtonian fluid under shear. Proceedings of the Royal Societyof London, Series A, Mathematical and Physical Sciences, 225(1160), 49–63

Bagnold R.A., 1956. The flow of cohesionless grains in fluids. Philosophical Transactions of the Royal Society of London, Series A, 249 (964), 235–297

Becker J.S., Johnston D.M., Paton D., Hancox G.T., Davies T.R., McSaveney M.J. and Manville V.R., 2007. Response to landslide dam failure emergencies: Issues resulting from the October 1999 Mount Adams landslide and dam-break flood in the Poerua River. Westland, New Zealand. Natural Hazards Review, 8(2), 35–42

Browning J.M., 1973. Catastrophic rock slide in Mount Huascaran North-Central Peru, May 31, 1970. The American Association of Petroleum Geologists Bull, 57(7), 1335–1341

Chanson H., 1994. Drag reduction in open channel flow by aeration and suspended load. Journal of Hydraulic Research. 32(1), 87–101

Chen C.L., 1988. Generalized viscoplastic modeling of debris flow. Journal of Hydraulic Engineering, 114, 237–258

Chen J., 1985. A Preliminary analysis of the relation between debris flow and rainstorm at the Jiangjia Gully of Dongchuan in Yunnan. Memoirs of Lanzhou Institute of Glaciology and Cryopedology, Chinese Academy of Sciences, 4, 88–96

Chen N.S., Cao Y.C. and Li D.F., 2004. Conflux process analysis of disastrous debris flow in the Qiongshan Racine Gully, Danba County, Sichuan Province. Journal of Natural Disasters 13(3), 104–108

Costa J.E., and Schuster R.L., 1988. The formation and failure of natural dams. Geological Society America Bulletin, 100, 1054–1068

Crozier M.J. and Pillans B.J., 1991. Geomorphic events and landform response in south-eastern Taranaki, New Zealand. Catena, 18, 471–487

Cui P., Chen X.Q., Zhu Y.Y., Su F.H., Wei F.Q., Han Y.S., Liu H.J. and Zhuang J.Q., 2009. The Wenchuan Earthquake (May 12, 2008), Sichuan Province, China, and resulting geohazards. Natural Hazards (in Chinese)

Deng Y., 1985. A preliminary approach to the geologic and geomorphologic effect of debris flow. Memoirs of Lanzhou Institute of Glaciology and Cryopedology, 4, 241–250

Gaziev E., 1984. Study of the Usoi landslide in Pamir, procedings 4th Intornational Symposium. on Landslides, Toronto, 1, 511–514

Geli L., Bard P.Y. and Jullien B., 1988. The effect of topography on earthquake ground motion: A review and new results. Bulletin of the Seismological Society of America, 78, 42–63

Hancox G.T., Perrin N.D. and Dellow G.D., 1997. Earthquake induced landsliding in New Zealand and implications for MM intensity and seismic hazard assessment. Client Rep of. No. 43601B. Institute of Geological and Nuclear Sciences, Wellington, New Zealand

He Y.P., Sun E.Z. and You Y., 2003. Monitoring of sedimentation and erosion of the Jiangjia Ravine. Study report for the key NSFC and research project, No. 49831010 (in Chinese)

Hegan B.D., Johnson J.D., Stevens C., 2001. Landslide risk from the Hipaua Geothermal Area near Waihi Village at the southern end of Lake Taupo. Engineering in Hazardous Terrain, Proceedings, New Zealand Geotechnical Society Symposium, Christchurch, 439–448

HLIG (Hubei Landslide Investigation Group), 1985. Prediction of the Xintan landslide. Bulletin of Soil and Water Conservation, 5, 1–8

Hovius N. and Stark C.P., 2006. Landslides from massive rock slope failure. The Netherlands, Springer

IGNS (Institute for Geological and Nuclear Sciences), (eds.), 2003. GeoNet News, 2, Lower Hutt, 8

Iverson R.M. and Denlinger R.P., 1987. The physics of debris flows-a conceptual assessment. Beschta R.L. et al. (ed.), Erosion and Sedimentation in the Pacific Rim, IAHS Publication, 165, 155–165

Iverson R.M. and Denlinger R.P., 1993. The physics of debris flow-A conceptual assessment, In Beschita et al. (edit): Erosion and Sedimentation in the Pacific Rim, IAHS Publication, 165, 155–165

Johnson A., 1970. Physical processes in geology. California, USA. Freeman Cooper & Company

Johnson A.M. and Rohm P.H., 1970. Mobilization of debris flows: Zeitschrift fur Geomorphologie Supplementband, 9, 168–186

Julien P.Y. and Lan Y., 1991. Rheology of hyperconcentrations. Journal of Hydraulic Engineering, 117, (3) 346–353

Julien P.Y. and Lan Y., 1991. Rheology of hyperconcentrations. Journal of Hydraulic Engineering, 107, 346–353

Kang Z.C., 1985a. A velocity analysis of viscous debris flow at Jiangjia Gully of Dongchuan in Yunnan. Memoirs of Lanzhou Ins. of Gla. and Cryo, 4 (in Chinese)

Kang Z.C., 1985b. Characteristics of the flow patterns of debris flow at Jiangjia Gully in Yunnan. Memoirs of Lanzhou Institute of Glaciology and Cryopedology, 4, 97–100 (in Chinese)

Kang Z.C., 1996. Debris Flow Fazards and Their Control in China. Science Press of China, Beijing (in Chinese)

Kang Z.C., Lee C.F., Ma A.N. and Ruo J.T., 2004. Debris flow studis in China. China Science Press, Beijing (in Chinese)

Koi T., Hotta N., Ishigaki I. and Matuzaki N., 2008. Prolonged impact of earthquake induced landslides on sediment yield in a mountain watershed: The Tanzawa region, Japan. Geomorphology, 101, 692–702

Korup O., 2004a. Landslide-induced river channel avulsions in mountain catchments of southwest New Zealand. Geomorphology, 63, 57–80

Korup O., 2004b. Geomorphometric characteristics of New Zealand landslide dams, Engineering Geology, 73, 13-35

Korup O., Strom A. and Weidinger J., 2006. Fluvial response to large rock-slope failures: Examples from the Himalayas, the Tien shan, and the southern Alps in New Zealand. Geomorphology, 78(1–2), 3–21

Li H. and DengY., 1985. Distribution and deposit features of debris flow in China. Memoirs of Lanzhou Institute of Glaciology and Cryopedology, 4, 251–255

Li Y.F., Wang Z.Y., Shi W.J. and Wang X.Z., 2010. Slope debris flows in the Wenchuan Earthquake area. submitted to the Journal of Mountain Science

Lin J.C., Jen C.H., Petley D.N., Rossen N.J. and Dunning S.A., 2005. On the response of the fluvial system to extensive earthquake-triggered landslides. Geophysical Research Abstracts, Vol. 7

Lin W.T., Lin C.Y., Tsai J.S. and Huang P.H., 2008, Eco-environmental changes assessment at the Chiufenershan landslide area caused by catastrophic earthquake in Central Taiwan. Ecological Engineering, 33(3–4), 220–232

Liu H.X., 2009. Research on the distribution of streambed structures and their influence on fluvial morphology. Tsinghua University, PhD dissertation, 136 (in Chinese)

Malamud B. D., Turcotte D.L., Guzetti F. and Reichenbach P., 2004. Landslides, earthquakes and erosion. Earth and Planetary Science Letters, 229, 45–59

Maxwell A.R. and Papanicolau A.N., 2001. Step-pool morphology in high-gradient streams. International Journal of Sediment Research, 16, 380–390

McTigue D.F., 1982. A nonlinear constitutive model for granular material. Journal of Applied Mechanics, Transactions, ASME, 49(6), 291–296

Miyazawa N., 1998. Flow behavior of head of stone debris flow on unsaturated erodible bed, river sedimentation-theory and application, Jayawadena A.W., Lee J.H.W. and Wang Z.Y. (eds.), Balkema A.A. Publishers, Rotterdam, 295–301

National Panel of Wenchuan Earthquake, 2008. Atlas of geological and earthquake disasters of the Wenchuan Earthquake. Beijing: Sinomaps Press (in Chinese)

NFH and IMH (National Flood Control Headquarters and Chengdu Research Institute of Mountainous Hazards), 1994. flash floods, debris flows and landslides and control strategies. Science Press of China

Nicoletti P.G. and Parise M., 2002. Seven landslide dams of old seismic origin in southeastern Sicily (Italy). Geomorphology, 46, 203–222

Ouimet W.B., Whipple K.X., Royden L.H., Sun Z.M. and Chen Z.L., 2007. The influence of large landslides on river incision in a transient landscape: Eastern margin of the Tibetan Plateau (Sichuan, China). GSA Bulletin, 119(11–12), 1462–1476

Pierson T.C., 1986. Flow behavior of channelized debris flow, Mount St. Helens, Washington. In: Hillslope Processes. Abrahams, Boston, Allen and Unwin, eds., 269–296

Safran E.B., Peden D., Harrity K., Anderson S.W., O'Connor J.E., Wallick R., House P.K., Ely L., 2008. Impact of landslide dams on river profile evolution. American Geophysical Union, Fall Meeting, abstract #H54D-03

Savage S.B., 1984. The mechanics of rapid granular flows. Advances in Applied Mechanics, 24, 289–366

Schuster R.L. and Alford D., 2004. Landslide dam and lake Sarez, Pamir Mountains. Tajikistan, Environmental and Engineering Geoscience, 10(2), 151–168, SCST and MGMR (State Commission of Science and Technology and Ministry of Geology and Mineral Resources of China), 1988. Landslide and Rockfalls of Yangtze Gorges, Tai Dao Publishing Ltd., Beijing (in Chinese and English)

Schuster R.L., 2000. Outburst debris-flows from failure of natural dams. In: Debris-Flow Hazards Mitigation: Mechanics, Prediction, and Assessment. Wieczorek G. and Naeser N. (eds.), Balkema, Rotterdam, The Netherlands, 29–42

Shen H.H. and Ackermann N.L., 1982. Constitutive relationships for fluid-solid mixtures. Journal of the Engineering Mechanics Division, ASCE, 748–763

SCST (State Commission of Science and Technology), People's Republic of China & MGMR (Ministry of Geology and Mineral Resources), People's Republic of China. 1988. Landslides and Rockfalls of Yangtze Gorges. Tai Dao Translation & Production Ltd, Hongkong.

Shen S.C., Zhang M., Li F.X., Zhu C.H., Chen G.X. and Wang J.Y., 1991. Debris flow along railways in china. Proceedings International Symposium on Debris Flow and Flood Disaster Protection, A1–A19

Sichuan Geological Engineering Corporation, 2009. Emergency geological prospecting project for 5.12 earthquake and earthquake-triggered disasters: Exploration, feasibility study, design reports of the Wenjiagou Gully, (in Chinese)

Sichuan Seismological Bureau, 1983. The Diexi Earthquake in 1933. Chengdu: Sichuan Science and Technology Press (in Chinese)

SSB-FU (State Seismological Bureau and Fudan University), 1983. Atlas of the Historical Earthquakes in China—The Qing Dynasty Period. Beijing: Sinomaps Press, (in Chinese)

Strom K.B. and Papanicolaou A.N., 2007. ADV measurements around a cluster microform in a shallow mountain stream. Journal of Hydraulic Engineering, 133(12), 1379-1389

Swanston D.N., 1969. Mass wasting in coastal Alaska. U.S. Department of Agriculture Forest Service Research Paper PNW-83, 15

Swanston D.N., 1999. Landslide response to timber harvest in southeast Alaska, Proceedings, 7th Federal Interagency Sedimentation Conference

Sieyama T. and Woemoto S., 1981. Characteristics of debris flow at bends. Journal of Civil Eng, (5)

Savage S.B. and McKeown S., 1983. Shear stress developed during rapid shear of dense concentrations of large spherical particles between concentric cylinders. Journal of Fluid Mechanics, 127, 453–472

Takahashi T., 1978. Mechanical characteristics of debris flow. Journal of the Hydraulics Division, ASCE, 104, 1153–1169

Takahashi T., 1980. Debris flow on prismatic open channel. Journal of the Hydraulics Division, ASCE, 106(3), 381–386

Takahashi T., 1981. Debris flow, Ann. Rev. Fluid Mech, 13, 57–77

Tsubaki T., Hashimoto H. and Suetsugi T., 1983. Interparticles stresses and characteristics of debris flow. Journal of Hydroscience and Hydraulic Engineering, 1(2), 67–82

Varnes D.J., 1978. Slope movement types and processes. In: Landslides-Analysis and Control, National Academy of Sciences Transportation Research Board Special Report No. 176. Schuster R.L. and Krizek R.J. (eds.), 12–33

Wang G., Sassa K. and Fukuoka H., 2007. A flowslide in the 2003 Sanriki-Minami Earthquake. Japan Proceedings 4th International Conference on Debris Flow and Disaster Mitigation, Armsterdam

Wang Z.Y. and Zhang X.Y., 1989. Experimental study of initiation and laws of motion of debris flow. Acta Geographica Sinica, 44(3), 291–301

Wang Z.Y. and Zhang X.Y., 1990. Initiation and Laws of Motion of Debris Flows. Hydraulic/Hydrology of Arid Land, ASCE. New York, 596–601

Wang Z.Y., 1999. Mountainous hazards in China. German IDNDR-Series 18, German Committee for International Decade for Natural Disaster Reduction, 1–48

Wang Z.Y., 2001. Experimental study on debris flow head and the energy theory. Journal of Hydraulic Engineering, 3, 21–29 (in Chinese)

Wang Z.Y., 2002. Free surface instability of non-Newtonian laminar flow. Journal of Hydraulic Research, 40(4), 449–460

Wang Z.Y., 2002. Free surface instability of non-newtonian laminar flows. Journal of Hydraulic Research, IAHR. 40(4), 449–460

Wang Z.Y., Cui P. and Wang R.Y., 2009a. Mass movements triggered by the Wenchuan Earthquake and management strategies of quake lakes. International Journal of River Basin Management, 7(1), 1–12

Wang Z.Y., Cui P. and Yu B., 2001. The mechanism of debris flow and drag reduction. Journal of Natural Disasters, 10(3), 37–43 (in Chinese)

Wang Z.Y., Cui P., Yu G.A. and Zhang K., 2010b. Stability of landslide dams and development of knickpoints. submitted to the Journal of Environmental Geology

Wang Z.Y., Larsen P., Nestmann F. and Dittrich A., 1998. Resistance and drag reduction of hyperconcentrated flows over rough boundaries. Journal of Hydraulic Engineering, 1, 1–9 (in Chinese)

Wang Z.Y., Shi W.J. and Liu D.D., 2010a. Continual erosion of bared rocks after the Wenchuan Earthquake and control strategies. Journal of Asian Earth Sciences (accepted)

Wang Z.Y., Wai O.W.H. and Cui P., 1999. Field investigation on debris flows. International Journal of Sediment Research, 14(4), 10–23

Wang Z.Y., Wai Onyx W.H. and Cui P., 1999. Field investigation on debris flows. International Journal of Sediment Research, N14(4), 10–23

Wang Z.Y., Xu J. and Li C.Z., 2004, Development of step-pool sequence and its effects in resistance and stream bed stability. International Journal of Sediment Research, 19(3), 161–171

Wang Z.Y., Lin B.N. and Zhang X.Y., 1990. Instability of non-newtonian fluid flow. Mechanica Sinica, 3, 266–275

Wany Z.Y., Wang G.Q. and Liu C., 2005, Viscous and Two-phase Debris Flows in Southern China's Yunnan Plateau. Water International, 30(1), 14–23

Wu J.S., Tian L.Q., Kang Z.C., Zhang Y.F. and Liu J., 1993. Debris Flow and Its Comprehensive Control. Science Press of China

Xu M.Z., Wang Z.Y., Qi L.J. and Liu L., 2010. Disaster chains initiated by the Wenchuan Earthquake. submitted to the Journal of Environmental Geology

Yano K. and Daido A., 1965. Fundamental study on mudflow. Bulletinl Disaster Prevention Research Institute, Kyoto Univ, Japan, 14, part 2, 69–83

Yin Y.P., 2008. Researchs on the geo-hazards triggered by Wenchuan Earthquake, 2008, Sichuan. Journal of Engineering Geology, 16(4), 3–12 (in Chinese)

Zhang Y.S., Lei W.Z., Shi J.S., Wu S.R. and Wang X.L., 2008. General characteristic of 5.12 earthquake-induced geoharzards in Sichuan. Journal of Geomechanics, 14(2), 109–116 (in Chinese)

Zhang, D.J., 2006. Debris flow and debris flow control in Taiwan. Technical Report, Disaster Control Center of Gaoyuan Technical University (in Chinese)

5 Sediment Movement in Alluvial Rivers

Abstract

Sediment is transported by river flow in the forms of suspended load and bed load. The fluvial process is a result of sediment deposition and erosion. Flood, avulsion and sediment transportation and deposition are the natural processes in alluvial rivers and water diversion, channelization, and navigation are human disturbances to rivers. The fluvial process is the macroscopic view and long-term consequence of sediment movement. This chapter introduces the basic knowledge of sediment movement and fluvial processes, paying attention to the fall velocity of sediment particles, flow resistance, bed forms, and the rate of sediment transportation, hyperconcentrated floods, river patterns, and unsteady sediment transportation. This knowledge is useful for alluvial river management.

Key words

Hydraulics, Sediment load, Fluvial processes, Hyperconcentrated flows, Meandering river, Braided river

5.1 Hydraulics

5.1.1 Hydrograph

Streams flow out of mountainous areas and pour into flat-land sections of a river, which extend on the plain between the estuary and the mountains. The flat-land sections of large rivers, such as the lower reaches of the Yellow River and the middle and lower reaches of the Yangtze River, are alluvial rivers. An alluvial river is defined as a river with its boundary composed of the sediment previously deposited in the valley, or a river with erodible boundaries flowing in self-formed channels. Over time the stream builds its channel with sediment it carries and continuously reshapes its cross section to obtain depths of flow and channel slopes that generate the sediment-transport capacity needed to maintain the stream channel. Alluvial rivers are mostly perennial streams and the channel bed is composed mainly of sand and silt. Alluvial rivers are lowland rivers flowing through areas that often are densely populated. Many alluvial rivers are confined within a channel defined by human constructed or artificially reinforced levees.

Flows in a river may range from no flow to flood flows in a variety of time scales. On a broad scale, historical climate records reveal occasional persistent periods of wet and dry years. Many rivers in the U.S., for example, experienced a decline in flows during the "dust bowl" decade in the 1930s. Unfortunately, the length of record regarding wet and dry years is short (in geologic time), making it difficult to predict broad-scale persistence of wet or dry years. Seasonal variations of stream flow are more predictable, though somewhat complicated by persistence factors. Because design work requires using historical information (period of record) as a basis for designing for the future, flow information is usually presented in a probabilistic format. Two formats are especially useful for planning and designing stream corridor restoration: (1) *Flow duration*—the percentage of time over which a given flow discharge was equaled or exceeded; (2) *Flow frequency*—the probability a given flow discharge will be exceeded (or not exceeded) in a year.

Figure 5.1 presents an example of a flow frequency expressed as a series of probability curves. The graph displays months on the *x*-axis and a range of mean monthly discharges on the *y*-axis. The curves indicate the probability that the mean monthly discharge will be smaller than the value indicated by the curve. For example, in January, there is a 90% chance that the discharge will be smaller than 9,000 m³/s. Stage is the water surface elevation recorded relative to some horizontal elevation datum, usually sea level. Stage records are valuable for the definition of high and low water levels. The record of stage is

called the stage hydrograph, it can often be translated into flow rate (discharge) units. A stage recorder can be as simple as a ruler along a bridge or other structures. It can be read periodically but it usually is automatically recorded. The automation is achieved by using a water float, pressure sensor, or change in electric resistance caused by water contact (Wanielista, 1990).

Discharge (or flow rate) is calculated by measuring the flow velocity. Current meters are revolution counting meters that convert angular velocity to linear velocity and consist of a propeller or cup wheel, a revolution counter, shaft, and ruder. If the depth of the flow is over 0.6 m, the U.S. Geological Survey recommends that the average velocity for the section can be estimated as the average of the velocities measured at 0.2 and 0.8 times the total depth of the watercourse. If the depth is less than 0.6 m, the U.S. Geological Survey recommends that the velocity at 0.6 times the depth of the watercourse can be presumed to represent the average velocity for that section of the stream. Once the average velocity for a section is determined, the flow rate can be determined by multiplying the average velocity and the cross-sectional area (Rantz et al., 1982).
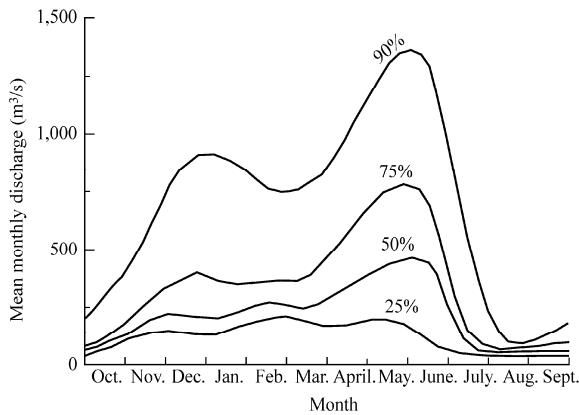
Fig. 5.1 An example of monthly probability curves. The curves indicate the probability that the mean monthly discharge will be smaller than the value indicated by the curve

For a stable channel section, the discharge exhibits a good relation with stage in a form of curves, which is called a stage-discharge relationship. Figure 5.2 shows the stage-discharge relation curve for the Longchuan Hydrological Station on the East River in south China. With the curve the fluctuating discharge during a flood can be estimated by recording stage variation. If sedimentation or erosion occurs in the section and neighboring reaches the stage-discharge relation can change and the discharge should be measured with current meters.
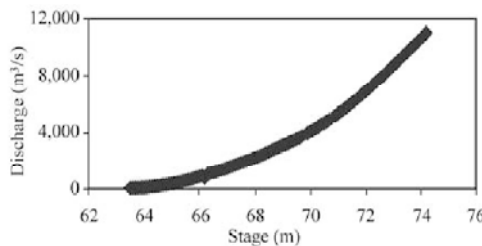
Fig. 5.2 Stage-discharge relation curve based on 20 years data for the Longchuan Hydrological Station on the East River in south China

A hydrograph is a graph of flow discharge versus time. It is typically a plot but can be a listing of flow rate versus time for a specific river. Figure 5.3 shows the discharge hydrograph of a flood in 2005 at the Longchuan Station on the East River, which shows the flood consisting of 3 parts: a rising limb, a crest segment or peak discharge, and a recession curve or falling limb.
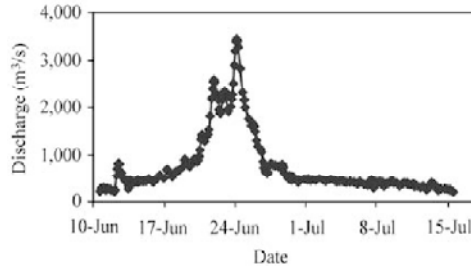
Fig. 5.3   Hydrograph of a flood in 2005 at the Longchuan Station on the East River, which shows a rising limb (from June 10 to June 20), a crest segment (from June 20 to June 26), and a recession or falling limb (from June 20 to July 15)

5.1.2   Open Channel Flows

Laminar flow and turbulent flow—Open channel flows may be laminar or turbulent, subcritical or supercritical, depending on the Reynolds number and Froude number. The phenomena of laminar flow and turbulent flow can still be best illustrated by the classical experiment of Reynolds, as shown in Fig. 5.4. At the beginning of the experiment, the tank is full of clear water that had been allowed to stand completely still for some time; the valve is then opened slightly and water begins to flow through the tube. At the same time a dye solution is injected at the entrance to reveal the pattern of flow. At low velocities the dye solution follows a distinct straight line as it passes through the pipe. It does not mix with surrounding flow layers (a). This is laminar flow. At a higher velocity, the line of dye begins to waver (b). With still further increasing velocity, the line breaks up and the dye solution diffuses over the entire cross section of the tube, completely losing its original appearance (c). This is called turbulent flow.
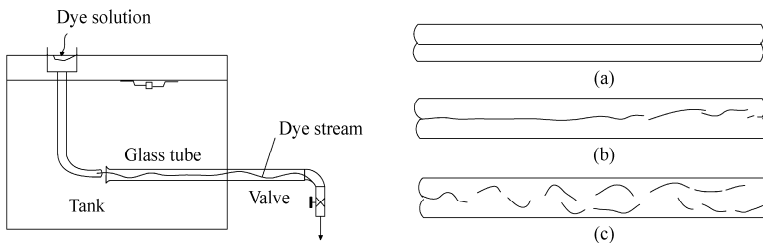
Fig. 5.4   Experiment of Reynolds. (a) Laminar flow; (b) Transitional flow; and (c) Turbulent flow

For laminar flow the following relation between shear stress, τ, and velocity gradient, $\dfrac{du}{dy}$ is well known.

$$\tau = \mu \frac{du}{dy} = v\rho \frac{du}{dy} \tag{5.1}$$

in which μ and v are the coefficients of dynamic viscosity and kinematical viscosity for the fluid, respectively, ρ is the density of the fluid, u is the velocity in the x-direction and y is the direction normal to the flow boundary. This is Newton's Law and a fluid that follows the law is called a Newtonian Fluid.

Inertial force acting on a unit water volume is proportional to $\rho U^2/L$, where U is the average velocity over the cross section and L is a representative dimension that usually taken to be the diameter of pipe (in pipe flow). The viscous force, behaving as an internal force binding the water molecules, can reduce their fluidity and attenuate a disturbance. The viscous force acting on a unit water volume is proportional to $\mu U/L^2$. The turbulence phenomenon essentially depends on the balance between these two forces. The ratio of the inertial force to the viscous force acting on a unit volume of water constitutes a dimensionless number called the Reynolds number (Re):

$$Re = Ud/v \tag{5.2}$$

in which d is the diameter of a pipe. In the experiments conducted by Reynolds, the flow was laminar if the Reynolds number was less than about 2,000, and it always became turbulent if the Reynolds number exceeded a value in the range 10,000–12,000, and the flow is in a transitional range if the Reynolds number is between the two values. Later researchers found that laminar flow could be maintained for Reynolds numbers as high as 50,000 for very smooth pipes and very quiescent initial conditions.

Define the hydraulic radius, R, as the ratio of the cross sectional flow area, A, to the wetted perimeter P, which is given for a pipe flow by:

$$R = \frac{A}{P} = \frac{\frac{1}{4}\pi d^2}{\pi d} = \frac{1}{4}d \tag{5.3}$$

According to the definition the hydraulic radius for an open channel flow is, assuming a simple river channel with a rectangular cross section, given by:

$$R = \frac{A}{P} = \frac{Bh}{B+2h} \approx h \tag{5.4}$$

in which B is the width of the channel, h is the depth of the flow, and $B \gg h$. For alluvial rivers, the width is usually a hundred times larger than the depth, and, therefore, the hydraulic radius is approximately equal to the average water depth. Applying Eqs. (5.2)–(5.4) the Reynolds number for an open channel flow is given by:

$$Re = \frac{Ud}{v} = \frac{4Uh}{v} \tag{5.5}$$

With this definition the critical values for laminar and turbulent flows are the same for an open channel flow as for a pipe flow.

For water flows in alluvial rivers, the Reynolds number exceeds 12,000 and is always turbulent. Only for hyperconcentrated flows, which the kinematical viscosity may be 100–1,000 times larger than that of clear water, the flow may be laminar.

Turbulent flow consists of numerous eddies of various sizes. In order to explain how local disturbances can induce eddies, one can envision a surface of separation in a non-viscous fluid with different velocities on the two sides of the surface, as shown in Fig. 5.5(a). If the streamlines on the separation surface are deformed or bent for some reason, as shown in Fig. 5.5(b), the velocity is higher, and the pressure lower, at places where the streamlines are more concentrated. The situation is just the opposite where streamlines are more widely dispersed. As a consequence, the bending of streamlines is intensified, as shown in Fig. 5.5(c). Ultimately eddies are produced, as shown in Fig. 5.5(d). In alluvial rivers, not only does the flow separate from dune crests, but it also produces local small-scale separations in the flow around individual protruding sediment particles, and eddies can form at any of these separation surfaces. Furthermore, the velocity gradient in open channel flow is generally large near the boundary. Hence, the entire perimeter of a river bed is a source of turbulence.
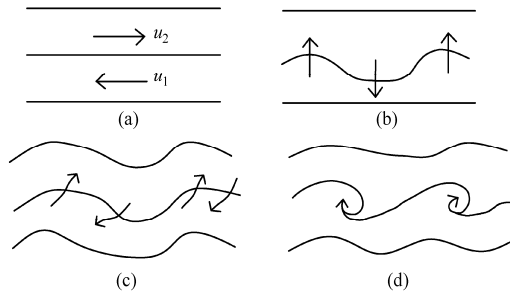
Fig. 5.5   Sketch of vortices evolving due to velocity gradient (after Qian and Wan, 1983)

Subcritical and supercritical flows—In open channel flow, the gravitational force is important. The ratio of the inertial force to the gravitational force is the Froude number. The weight of water in a unit volume is $\gamma = \rho g$. Then the Froude number is given by

$$Fe = U / \sqrt{gh} \tag{5.6}$$

in which h is the average depth of the river flow and g is the acceleration due to gravity.

If the Froude number is larger than 1, an open channel flow is supercritical. In a supercritical flow any surface wave cannot propagate upstream and standing waves appear on the water surface. The water depth is determined by discharge and local bed resistance, and is not affected by downstream conditions. On the contrary, an open channel flow is subcritical if the Froude number is smaller than 1. In a subcritical flow surface waves may propagate upstream and no standing waves form on the water surface. The water depth is affected by discharge, local bed resistance, and downstream conditions. Flows in small mountain streams are generally supercritical and flows in large rivers are subcritical. The middle and lower reaches of large rivers are alluvial rivers with large discharge and low gradient, in which the flow is subcritical. Figure 5.6(a) shows supercritical flow in a mountain stream and the standing waves, and Fig. 5.6(b) shows subcritical flow in the Jinsha River, in which waves generated by a navigating boat are moving on the water surface.
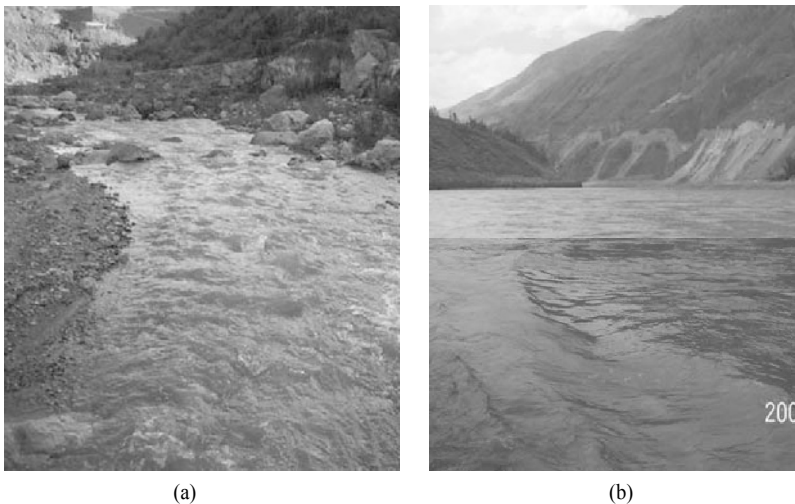
Fig. 5.6   (a) Supercritical flow in a mountain stream, in which there are some standing waves; (b) Subcritical flow in the Jinsha River, in which waves generated by a navigating boat are moving on the water surface (See color figure at the end of this book)

5.1.3 Velocity Profile

Velocity profile—The foregoing reasoning helps us understand the mechanism of momentum exchange between adjacent layers in a moving fluid. In Fig. 5.5(c), the adjacent surface area is A_0, the relative velocity between adjacent layers is u' and the fluctuating cross-current velocity is v. If this cross-current velocity were uniformly distributed over the surface A_0, then the mass transported from the lower layer B to the upper layer A per unit of time would be $\rho v' A_0$. If the particles thus transported into layer A become thoroughly mixed with particles already in layer A and are brought to move axially with the velocity of layer A, the momentum exchange exerts a shear force F on the surface of layer A in the direction of the motion:

$$F = \rho \, A_0 u' v' \tag{5.7}$$

The shear stress per unit area would then be

$$\tau = F / A_0 = \rho \, u' v' \tag{5.8}$$

In reality u' and v' vary continuously at any point within the flow, and the shear stress τ is proportional to the average value of the product of u' and v, $\tau = \rho \, \overline{u' v'}$. In a river, the velocity generally increases with distance from the bed. If the direction of u' is taken as positive when it coincides with the flow direction, and the direction of v' is positive when it is directed upward from the bed, then the sign of u' is always opposite to that of v'. For such a system, the preceding equation should be rewritten as:

$$\tau = -\rho \, \overline{u' v'} \tag{5.9}$$

This is the conventional form for turbulent shear stress. Since the nineteenth century, much of the study concerning turbulence has been an attempt to transform the pattern of velocity fluctuation into a function of the time-averaged velocity and the consequent establishment of a relation between the distribution of velocity and stress.

In 1925 Prandtl first simulated the momentum exchange on a macro-scale in an effort to explain the mixing phenomenon induced by turbulence in water flow; and, he, thus, established the mixing-length theory for turbulent flow. He assumed

$$v' \sim u' = l \frac{du}{dy} \tag{5.10}$$

where l is called the Prandtl mixing length. Then Eq. (5.9) can be written as

$$\tau = \rho \, l^2 \frac{du}{dy} \left| \frac{du}{dy} \right| \tag{5.11}$$

In analogy to the equation for laminar flow, the equation is rewritten as

$$\tau = \eta_t \frac{du}{dy} \tag{5.12}$$

in which

$$\eta_t = \rho \, l^2 \left| \frac{du}{dy} \right|$$

is called the eddy viscosity. If the Reynolds number of the flow is not much larger than its critical value, so that turbulent and viscous effects are both important, the shear between fluid layers is the sum of the shears due to turbulence and viscosity, i.e.

$$\tau = (\mu + \eta_t) \frac{du}{dy} \tag{5.13}$$

Just as there is a difference in concept between the average free path of air molecules and the mixing length of turbulent flow, so is there a difference between the eddy viscosity and the dynamic viscosity; the latter is a property of the fluid, and has nothing to do with location in the flow, whereas the former is not a constant, but rather varies with both location and local velocity.

In most turbulent flows, the shear stress results mainly from momentum exchange, and Eq. (5.12) can be written as

$$\tau = \varepsilon_m \frac{d(\rho u)}{dy}$$

in which

$$\varepsilon_m = l^2 \left| \frac{du}{dy} \right| \tag{5.14}$$

is called the momentum exchange coefficient, which is similar to the kinematical viscosity in the laminar flow. The momentum exchange coefficient is actually the product of the mixing length and the root-mean-square of the fluctuation in velocity.

In turbulent open channel flow, if the flow is steady and uniform, the velocity profile follows an empirical velocity distribution, which is known as the velocity-defect law:

$$\frac{u_m - u}{U_*} = -\frac{1}{\kappa} \ln \frac{y}{h} \tag{5.15}$$

in which $U_* = \sqrt{\tau_0 / \rho} = \sqrt{gRs}$ is called the shear velocity, τ_0 is the shear stress at the bed, s is bed slope; κ is the von Karman constant ($=0.41$), and u_m is the maximum velocity in the profile and can be roughly taken as the velocity at the water surface. The formula can be applied to both rough and smooth boundaries if the flow is turbulent.

For river flow, the boundary is always rough, and the velocity distribution in a region near the bed, $y/h<0.2$, is given by

$$\frac{u}{U_*} = \frac{1}{\kappa} \ln \frac{y}{k_s} + A_r \tag{5.16}$$

where k_s is the equivalent sand grain roughness (roughness height), and $A_r = 8.5$.

In steady open channel flow, the distribution of gravitational shear stress is

$$\tau = \tau_0 (1 - y / h) \tag{5.17}$$

By applying the velocity distribution formula the distribution of eddy viscosity can be obtained as follows:

$$\eta_t = \rho \varepsilon_m = \frac{\tau_0 (1 - y / h)}{\dfrac{du}{dy}} = \rho \kappa U_* y \left(1 - \frac{y}{h} \right) \tag{5.18}$$

Bursting process—Studies in the 1960s and 1970s indicated that turbulence is not as random as was initially believed. Space related and time-related orderly motions do exist in turbulent flows. These motions can be called a quasi-cyclic process. They result from events that are repeated in time and in space but are not strictly periodical. The two most striking events, which are observed near the boundary, are (1) the lift-up of low-speed streaks from near the boundary, and (2) the "sweep" of high-speed fluid toward the boundary.

The intermittently lifted low-speed streaks leave the boundary and penetrate the main flow region. Figure 5.7 (a) is a sketch of the ejection of low-speed streaks as observed by dye injection. The main part

of the observed low-speed streak is indicated by the arrows shown in the figure. Initially, the low-speed streak migrates slowly downstream as a whole, and drifts slowly outward. This stage persists over some distance. But once the low-speed streak attains a critical distance from the boundary, it moves rapidly outward as it moves downstream. The critical distance is not fixed as it varies in the statistical sense. The trajectory of the ejected fluid, as measured by Kline et al. (1967), is shown in Fig. 5.7(b) and (c). In the figure, x is in the flow direction, and y is perpendicular to the boundary. The shaded area denotes the distribution density of the fluid ejected at a time t and reaching the location x (or y). Although the individual trajectories vary considerably, the average trajectory is rather stable; also, its average value coincides with its mode. The low-speed streak enters the region of main flow with a longitudinal velocity that is much lower than that of the surrounding fluid. Hence, on the plot of instantaneous longitudinal velocity profile, an inflection point appears at the place reached by the low-speed streak. Velocity profiles with inflection points are often unstable, and can induce flow oscillations further downstream. Such oscillations can be detected in the third picture in Fig. 5.7 (a). The region where the oscillation first appears is in the range of $y^+ = 8$ to 12 (in which y^+ is the dimensionless distance from the boundary, v is the kinetic viscosity). The oscillation amplifies quickly. After some 3 to 10 periods, this flow structure collapses, and an even more chaotic motion appears. The collapse usually happens in the region $10 < y^+ < 30$. Some researchers have suggested that the low-speed streaks rise even to the region $y^+ > 100$. The fourth and fifth pictures in Fig. 5.7 (a) show the twisting and ultimate collapse.
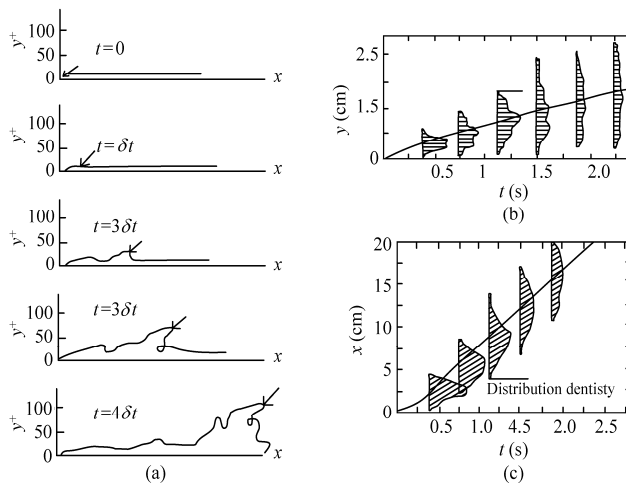
Fig. 5.7 (a) Dye streak breakup as seen from the side, (b) Trajectory of ejected eddies in the y direction and (c) Trajectory of ejected eddies in the x direction (Kim et al., 1971)

Another striking feature near the boundary, in addition to the ejection of low-speed streaks, is the "sweep" of high-speed fluid from the main flow region onto the boundary. Grass (1971) demonstrated the "sweep" phenomenon by means of sediment particles (diameter 0.1 mm) moving on a smooth bed. In the experiment, the bed was painted black, and the sediment particles were white. Coming from the main flow region and reaching the boundary, the high-speed fluid carried away all the sediment particles, and uncovered a path along the black bed. The sediment particles moved downstream with a little lateral diffusion. Offen and Kline (1974) conducted other experiments focusing attention on the inherent correlation between uplift of the low-speed streak from the wall and sweep of the high-speed fluid. Not only did they inject a dye solution and place a platinum wire close to the boundary, they also injected a dye solution

into the main flow region where the velocity profile was logarithmic. They observed two characteristic features. ① Before almost every uplift of a low-speed streak and the appearance of an oscillation at the boundary, a disturbance originating in the main flow region occurred just upstream. Originating in the logarithmic velocity distribution region, i.e., usually in the range of $20 < y+ < 200$, the disturbance possessed an eddy-like flow pattern with a mean motion toward the wall. The oscillation in the boundary region was always located downstream of that disturbance. ② The low-speed streak grew and was gradually lifted up. At the end of the growth stage of the oscillating low-speed streak, the mutual action of the fluid in the streak and the fluid in the logarithmic region induced another large eddy-like structure. This eddy system grew downward toward the boundary, and a disturbance in the main flow region formed that moved toward the boundary. Thus. inducing another uplift and oscillation of a low-speed streak at a location further downstream.

The momentum of the faster water is transmitted to the slower boundary water. In doing so, the faster water tends to roll up the slower water in a spiral motion. It is this shearing motion, or shear stress, that also moves bed particles in a rolling motion downstream. Particle movement on the channel bottom begins as a sliding or rolling motion, which transports particles along the streambed in the direction of flow.

5.1.4　Bed Forms

5.1.4.1　Development of Bed Forms

Stream channels and their floodplains are constantly adjusting to the stream power and sediment supplied by the watershed. Channel response to changes in water and sediment load may occur at differing times and locations, requiring various levels of energy expenditure. Daily changes in stream power and sediment load result in frequent adjustment of bed forms and roughness in many streams with movable beds. Streams also adjust periodically to extreme high and low-flow events. Similarly, long-term changes in runoff or sediment yield from natural causes, such as climate change, wildfire, etc., or human causes, such as cultivation, overgrazing, or rural-to-urban conversions, may lead to long-term adjustments in channel cross section and planform that are frequently described as channel evolution. Stream channel response to changes in stream power and sediment load has been described qualitatively in a number of studies (e.g., Lane, 1955; Schumm, 1977).

In alluvial rivers with the bed consisting of sand and silt, various bed forms may develop. While sediment is being transported, the bed load particles move collectively in all sorts of ways along the riverbed. Their motion in turn can cause changes in the configuration of the riverbed in accordance with the variation of the sediment transport rate. The collective movement of large quantities of sediment particles on the bed is called bed form movement.

With low rates of flow over an initially flat stationary bed, as shown in Fig. 5.8 (a), no sediment moves; but once the flow velocity reaches a certain value, some particles are set in motion. Soon after that, a few particles may gather on the bed and form a small ridge; this ridge gradually moves downstream and tends to increase in length. Finally, the ridges connect and ripples with a regular shape form, as shown in Fig. 5.8(b) (Chien et al., 1998).

The longitudinal profile of ripples usually is not symmetrical. The upstream face is long and has a gentle slope, and the downstream face is short and steep. The former is generally 2–4 times as long as the latter. The height of ripples is usually between 0.5 and 2 cm; the highest ripple is not more than 5 cm. The wave lengths normally do not exceed 30 cm, and they are usually within the range of 1 to 15 cm.

Ripples are the smallest of the bed configurations. They are related to the physical parameters near the river bed and have little correlation with the water depth. Their occurrence is the result of the unstable viscous layer near the boundary. They can form in both shallow and deep water. In plan, they either are

parallel to each other, or have a shape like fish scales. With an increase of the flow velocity, the plan form of the ripples gradually develops from straight lines to curves and then to a pattern like fish scales, symmetrical or unsymmetrical. Figure 5.9(a) shows the parallel ripples and Fig. 5.9(b) shows the fish scales ripples in the Liuhe River, which is a tributary of the Liaohe River in China. The sand diameter is about 0.5 mm and the ripples are about 1– 4 cm high and 10 – 40 cm long.

(a) Flat bed

(b) Ripples

(c) Dunes

(d) Transitional dunes are going to disppear

(e) Flat bed

(f) Antidunes
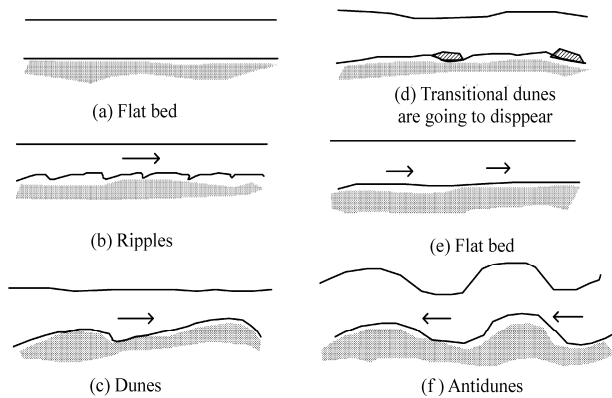
Fig. 5.8 Development of the bed forms following increase in flow intensity (after Chien et al., 1998)

(a)   (b)
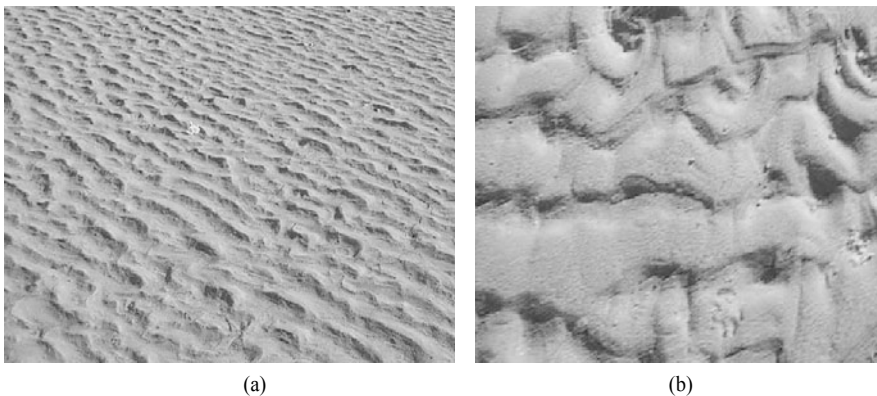
Fig. 5.9 (a) Parallel ripples about 1-2 cm high and 10–20 cm long; (b) Fish scales ripples about 2–4 cm high and 20–40 cm long, in the Liuhe River which is a tributary of the Liaohe River in northeastern China

With increasing flow velocity, ripples develop further and eventually become dunes (Fig. 5.8(c)). The size of a dune is closely related to the water depth. Figure 5.10 shows that the heights and lengths of dunes vary significantly in different rivers. Dunes in large rivers can be kilometers long and several meters high, such as in the Mississippi River and the Yangtze River. They may be less than half a meter in other rivers, like the Volga River. The dunes move at different speeds, varying from 1 m/day (Volga River) to 100 m/day (the Yellow River).

Figure 5.11 shows the sand dunes on the bed of the Songzi River, which is a distributary of the middle reaches of the Yangtze River and diverts flood water from the Yangtze River into Tongting Lake. The bed material consists of fine sand with diameter around 0.1 mm. The sediment is rather uniform. The dunes are 0.5–1 m high and 10–30 m long. Compared with ripples sand dunes are rather irregular in shape.
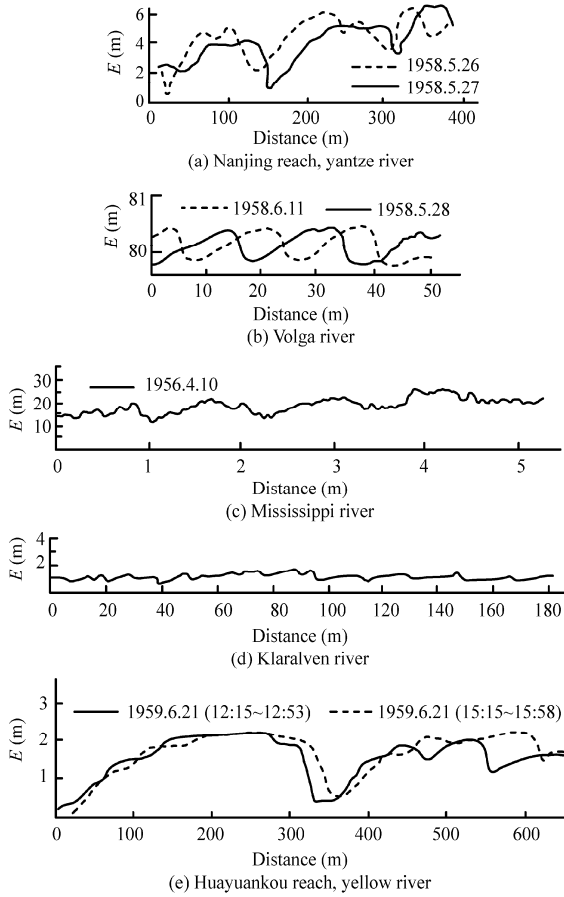
Fig. 5.10 Various scales of the heights and lengths of dunes in the Mississippi, Yangtze, Volga, and Yellow rivers (after Qian and Wan, 1983)

Fig. 5.11 Sand dunes (0.5–1 m high and 10–30 m long) on the bed of the Songzi River in the middle reaches of Yangtze River basin (See color figure at the end of this book)

Sand dunes on the river bed and in sand desert look similar. Figure 5.12 shows the sand dunes in the Kubuqi desert in northwest China. The sand has a median diameter around 0.2 mm and the dunes are about 10 m high and 50–100 m long.
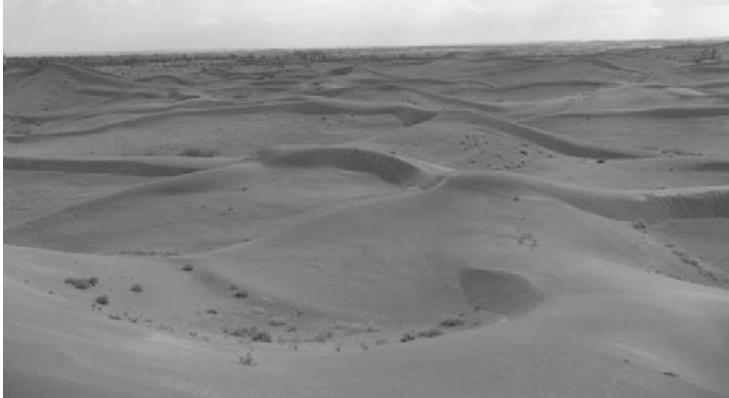
Fig. 5.12 Sand dunes (10 m high and 50 m long) in the Kubuqi Desert in northwest China (See color figure at the end of this book)

If the flow velocity is raised progressively, the dune pattern changes in plan from straight lines to curves; it then has a shape like a moon crescent. The dimension of the straight ridge in the transverse direction is larger than that along the streamwise direction. Stripe dunes often occur on beaches on the inner bank of a river bend, and they stretch downstream towards the outer side of the bend. The direction of the flow near the bed, which brings sediment to the inner side, is perpendicular to the ridge lines of the dunes; the latter form a larger angle with the direction of the surface flow. If the amplitude of a sand wave is large compared to the water depth, the sand wave can affect the water surface. The water surface is usually lower near the dune peak. Many waves of small amplitude form in this vicinity, and they occasionally make what looks, from a distance, like a stripe on the surface. This stripe reflects, in fact, the location of the ridge line of the dune. People living near the lower Yellow River call this phenomenon "Lianzishui" (Chien et al., 1998). If the ratio of the dune height to the water depth is large enough, the vortex that originates in the separation region downstream of the dune peak is strong enough to carry a high concentration of sediment up to the water surface, it then has the appearance of water at its boiling point.

If the dune reaches a certain height and the flow velocity is then increased further, the dune decays; its wave length increases and its height gradually decreases to the form shown in Fig. 5.8(d). With still further increase in velocity, the bed becomes flat again (Fig. 5.8(e)). Figure 5.13(a) is a plot of the dune height against the depth of water in the Hankou section of the Yangtze River. The maximum height occurs if the water stage is 21.5 m. If the water stage is below this level, the dune height increases gradually with the discharge or with the water stage; and if the stage is above it, the dune height decreases. If the water stage is 24.5 m or more, the riverbed is flat again.

The sediment transport rate is quite large in the second flat bed phase. If the velocity continues to increase, the flow approaches or becomes supercritical (Froude number, Fr>1), and the bed form develop into antidune (Fig. 5.8(f)). Antidune is a type of bed configuration that is in phase with the wave on the water surface, and these two waves interact strongly. The differences between antidunes and dunes are as follows: the shape of a dune is non-symmetrical, and the streamlines of the flow separate at the dune peak; in contrast, an antidune is symmetrical, more like a surface wave, the streamlines are almost parallel to the river bed and no separation occurs. If antidunes form, the water surface also undulates; this process is

called "Gan" in the Yellow River, in order to distinguish it from wind-induced surface waves. With dunes, the bed configuration does not correspond with the surface wave; the surface wave and the bed configuration are out of phase.
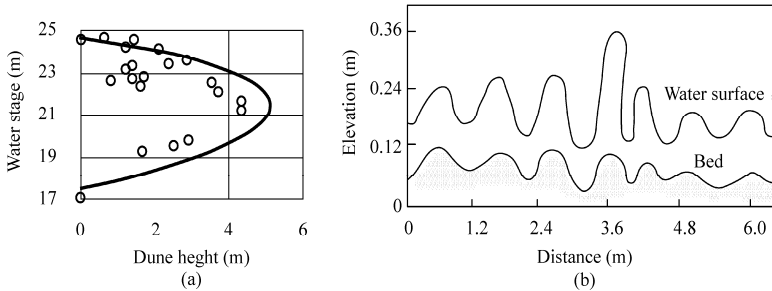
Fig. 5.13   (a) The height of dunes varying with the water stage measured at the Hankou Hydrological Station of the Yangtze River; (b) A general picture of antidunes (after Chien et al.,1998)

Antidunes can move either in the same direction as the flow, as do ripples and dunes, or in the opposite direction, this is the reason for the phenomenon is named anti-dune. The former is called a "downstreamward antidune" and the latter is called an "upstreamward antidune." Antidunes often form in shallow flows that are moving at high velocities. The amplitude of an antidune is comparatively large. The flow must climb the upstream or rising side of the antidune, and usually drops part of its sediment load there. On the downstream side of the peak, the flow possesses surplus energy and can entrain sediment from the bed. As a consequence, even though the movement and transport of every particle is in the direction of the flow, the sand wave as a whole profile, generally moves upstream.

The direction of individual antidune movement should not be confused with the direction of movement of a series of sand waves. Although the individual surface waves and the corresponding antidunes appear to be moving against the flow, the whole series of waves is actually moving with the stream; because some waves disappear from the upstream end of the series and some others are generated at the downstream edge (Chien et al., 1998).

The crest lines of antidunes in plan are not quite parallel to each other; in most cases, they are similar to short and wide sea waves in which the length and width are the same order of magnitude. Thus, they usually occupy only a part of the width of a river. The lower Yellow River is quite wide, and antidunes that form along its course are generally either near the flood plain or at the confluences of channels. In transitional and wandering reaches of the Yellow River, especially in the straight sections downstream of bends, a special phenomenon, "Gan" occurs occasionally, and it is related to the formation of antidunes. For example, at the Tuchengzi section of the lower Yellow River, antidunes appear over the whole river cross section, (the width of the river is some 500–600 m), the height of the "Gan" corresponding to the antidunes is about 1 to 3 m, and its length is about 15 m. Figure 5.13(b) shows a general picture of antidunes and "Gan". "Gan" generally occurs during the falling stage of a flood. Initially, the river may appear calm and be flowing along gently, then suddenly, a series of waves, usually numbering between 6 and 10, but sometimes up to 20, appear on the water surface. These surface waves develop and increase rapidly in size; then, after about 10 minutes, they gradually decay and disappear. Sometimes they make a sound like thunder as they break. The wave appears not to move, but with observations related to a reference point on the bank, one can see that it actually moves slowly upstream.

From the foregoing discussion, the process of bed form development vis-à-vis an increasing flow velocity can be divided into two distinct stages. Ripples and dunes form in the first stage and antidunes in the

second. The transition between them is a flat bed stage or a bed with traces of dunes that are about to be washed out. In ordinary alluvial rivers, the most common bed features are ripples and dunes. Antidunes occur much less often.

In natural rivers, the process described previously may not occur in a normal progression; various types of bed forms can exist at the same time, and the process of development may differ from one instance to another. Even in flume experiments, different bed forms can co-exist in different parts of a flume; showing that a strong relation exists between the bed forms and the local turbulence structure. For certain combinations of flow and sediment, the initial flat bed can change directly into a dune or from a dune to an antidune without the usual transitional stages of ripples or a flat bed. Moreover, ripples and dunes may develop simultaneously on the riverbed, which was observed in the Liuhe River. The dunes are not well developed and ripples overlap on the dunes. Dunes need a certain water depth to develop but the flow in the river has high depth only in flood season, the flow discharge reduces sharply after the flood season and sometimes is cut off. Therefore, the development of the dunes is disturbed. Ripples are not affected by the flow depth very much and develop very well on the riverbed.   Similarly, ripples may develop on dunes in sand desert, as shown in Fig. 5.14.

The development of bed forms implies that a plane, cohesionless, granular surface is unstable where there is sediment transport (Knighton, 1998). Leeder (1983) envisaged a strong interplay between turbulence, sediment transport, and bed forms. Burst cycles are believed to be an inherent component of macro-turbulent flow responsible for the initiation of sediment transport, with sweeps exerting high instantaneous stresses against the bed and ejections carrying sediment away from the bed. Because bed disturbance is not uniform, such cycles have an important role in the initiation and maintenance of bed forms. Each bed element represents one "erosion-deposition" sequence with a wavelength dependent on the length of the burst process. Sediment transport rates vary across individual bed forms as a result of form-induced accelerations and decelerations, promoting scour in the troughs and deposition toward the crest.

Fig. 5.14   Ripples on sand dunes in the Kubiqi desert in northwest China, illustrating that the two bed forms may develop simultaneously on the sand bed

Bagnold (1956) showed theoretically that the formation of ripples and dunes is necessary if some degree of stability is to be achieved during sediment transport. Without the additional resistance provided by these bed forms, the channel could be destroyed as a coherent structure for the conveyance of water and sediment. However, there are few data to suggest how that resistance affects the turbulence structure.

The discussion on ripples, dunes and antidunes refers only to alluvial rivers with bed consisting of

sand and silt. For mountain rivers with gravel beds, no ripples, dunes and antidunes can develop, because the particles are too course. As discussed in Chapter 3 an important vertical structure of mountain stream bed is step-pool system.

5.1.4.2 Lower Regime and Upper Regime

Bed forms exert a drag on the flow in addition to that associated with the grains themselves. On the upstream side of an obstacle, the rising bed elevation causes an acceleration of the flow and a commensurate decrease in pressure. Beyond the crest of the obstacle, depth and pressure increase, and the flow decelerates. This effect, which produces pressure gradients, gives rise to form drag. This conclusion is only for ripples and dunes. The bed forms of ripples and dunes belong to the category of the lower flow regime, defined by Simons and Richardson (1966).

Bed forms of flat bed and antidunes are in the category of the upper regime. In the upper regime, the form drag reduces to nearly zero because the bed form and the water surface are in phase and grain roughness dominates in the flow. There is no pressure difference on the upstream and downstream sides of the antidunes. If a flow develops from lower regime to upper regime, the roughness n may reduce by 50% at the same flow discharge and the flow depth may reduce by 20%. Simons and Richardson (1966) measured the Weisbach friction factor $f\ (=8sgR/U^2)$ in their experiments, and found it varied with the type of bed form:

Lower flow regime:	Dunes:	$0.04 \leqslant f \leqslant 0.16$	
Upper flow regime:	Antidunes:	$0.02 \leqslant f \leqslant 0.07$	(5.19)

The transformation from the lower flow regime to the upper flow regime occurs if the stream power increases or the fall velocity reduces (Simons and Richardson, 1966). At a given discharge and sediment composition, if the water temperature reduces, the fall velocity of the sediment consequently reduces, and the bed form may develop from the lower regime into the upper regime. The resistance or roughness may abruptly reduce and the flow velocity may increase dramatically. Sediment transportation may greatly increase in a short time.

The same situation can also occur in natural streams. For the same slope and water depth, the bed may form dunes, or be flat without dunes, and the resistances for these two cases are quite different; correspondingly, the velocities are also different. As a result, different unit discharges can flow at the same slope and water depth. Figure 5.16 shows the relation between the hydraulic radius and velocity measured for the Rio Grande River in the U.S. (Culbertson and Nordin, 1960). For a hydraulic radius of
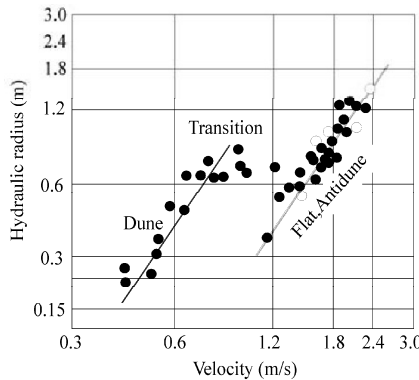
Fig. 5.16 Relation between hydraulic radius and velocity for the Rio Grade River, U.S. and the effect of bed forms from the lower flow regime to the upper flow regime (after Culbertson and Nordin, 1960)

about 0.7 m, the velocity changed from 0.8 to 1.5 m/s as the bed form developed from dunes to flat and antidunes, and the unit discharge, thus, changed correspondingly. Furthermore, since different discharges can occur for a given value of depth and slope, so also can different water depths occur for a given discharge and slope. Obviously, these phenomena are difficult to comprehend because they cannot be explained in terms of any of the existing formula for flow resistance.

In this situation, only after the intrinsic relation between the roughness and the flow has been determined, can one understand resistance in alluvial streams. The roughness of an alluvial stream has various components and each component has its own relation to the flow. Hence, a rational approach should be first to clearly demonstrate how each component functions for various conditions of flow, and then to determine how these components combine and function to provide a comprehensive picture of roughness for an alluvial stream. In the next section the resistance or roughness of various components in alluvial rivers is discussed.

Bed form adjustment represents a response to changing discharge and sediment load conditions during, for example, the passage of a flood wave, although there is always a lag between a change of flow and a corresponding change of bed form because of the redistribution of sediment involved. That lag, which has a spatial as well as a temporal dimension, will increase with the size of both the bed form and the river (Allen, 1983). Under certain conditions a given discharge can be transmitted at two or more different depths and velocities, depending on the type and size of bed form produced. Bed configuration in sand-bed streams is one of the most adjustable components of channel morphology, with the potential for regulating short-term interactions between hydraulic variables.

5.1.5 Resistance

Water flows in an open channel only if its energy gradient slopes downward in the direction of flow. For uniform flow, the water surface slope, s_w, and the channel bed slope, s, are the same and equal to the energy gradient, J, which denotes the energy loss per unit weight of water in overcoming resistance as it flows a unit distance in the channel. All the lost energy is finally transformed into thermal energy. To study the resistance in alluvial rivers is essentially to study the mechanism of the transfer of mechanical energy into thermal energy.

Figure 5.17 shows the forces acting on a water element in steady and uniform open channel flows. In this case, the mean velocity does not change from cross section to cross section. The flow energy comes totally from the potential energy. For the potential energy of each point in the water body, a small part transforms into thermal energy at any given location due to the viscosity of water, but most is transmitted to the boundary by the shear stress and transformed into turbulent kinetic energy. In the transformation, a portion of the energy is lost, and the rest is transformed into kinetic energy of eddies. The eddies leave the boundary, enter the main flow region and break up into smaller eddies. Then the energy of the smaller
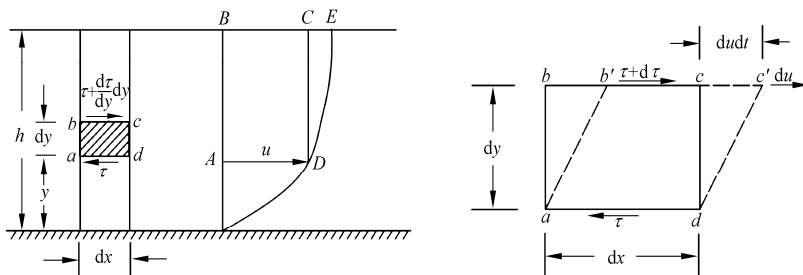
Fig. 5.17 Forces acting on the water element *abcd* in two dimensional open channel flow (after Qian and Wan, 1983)

eddies is dissipated locally into thermal energy due to the viscosity of water. These processes describe completely the way flow energy is transformed.

The energy taken in unit time from an element of water at y from the bed is given as follows

$$w_b = \gamma Ju = \gamma su \tag{5.20}$$

From the balance of the forces acting on the element abcd in Fig. 5.17, one can write

$$\left(\tau + \frac{d\tau}{dy}dy\right)dx - \tau dx + \gamma dxdys = 0$$

In reduced form

$$\frac{d\tau}{dy} + \gamma s = 0$$

Substituting this relation into Eq. (5.20), one gets

$$w_b = -u\frac{d\tau}{dy} \tag{5.21}$$

A part of the energy taken from the water body is lost in overcoming the resistance at a given location, as shown in Fig. 5.17(b). The water element deforms due to the forces acting on it; after a time step dt, the water body $abcd$ has deformed to $ab'c'd$. The work done during the deformation is equal to the product of the shear stress τdx and displacement $dudt = \frac{du}{dy}dydt$. Hence in a unit time step, the energy loss for a unit water body at the point y above the bed in overcoming local resistance is

$$w_s = \tau\frac{du}{dy} \tag{5.22}$$

The energy transmitted to the stream bed in a unit time is $\tau dxu - (\tau + d\tau)dx(u + du)$ if the high-order terms are neglected. If the terms in the equation are divided by the volume of the water body $dxdy$, the energy transmitted from a unit water body at the point y above the river bed to the bed in a unit time step is obtained:

$$w_t = -\frac{d}{dy}(\tau u) \tag{5.23}$$

In the main flow region, part of the energy taken from each layer is lost in overcoming the local resistance, and the surplus energy is transmitted to the boundary through the gradient of τu. However, the local energy near the boundary is not sufficient to overcome the local resistance, and must be supplemented from the main flow region. From the view point of the energy balance, it can be expressed as

$$w_b = w_s + w_t \tag{5.24}$$

or

$$-u\frac{d\tau}{dy} = \tau\frac{du}{dy} - \frac{d}{dy}(\tau u) \tag{5.25}$$

Equation (5.25) is the total differential of τu, and the above derivation shows that all terms in the equation have a definite physical significance.

The vertical distributions of w_b, w_t, and w_s are shown in Fig. 5.18. The maximum of the mechanical energies provided in all flow layers for overcoming the resistance occurs at the water surface, and the minimum value of zero occurs at the stream bottom. In contrast, the energy loss due to overcoming the local resistance is zero at the water surface and has its maximum value at the stream bottom. Thus, the energy of the flow is mostly in the main flow region, but the loss is concentrated near the boundary. The

energy transmission, w_t, is positive in the main flow region and negative in the bed region.

Bakhmeteff and Allan (1946) indicated that an inflection point M on the curve of the energy distribution divides the flow into two regions. The region above point M is called the main flow region; that below it is called the near-bed flow region. For natural streams, the near-bed flow region amounts to about 1/10 of the total water depth. Of the energy provided by the flow, 92% comes from the main flow region, and 90% of it is transmitted to the near-bed flow region and lost to resistance there. The local energy loss in the main flow region accounts for only 8% of the total.

The near-bed flow region is not only the region where most of the loss of flow energy is concentrated, but it is also the place where the exchanges between the bed material and bed load, and between the bed load and suspended load, take place. If the vertical distribution of sediment concentration has a gradient, this gradient normally reaches a maximum in this region. The existence of a gradient for the sediment concentration affects the local flow characteristics. Thus, from the viewpoint of sediment movement, the near-bed flow region is the most important region, unfortunately, however, it is also the most difficult region in which to take measurements.
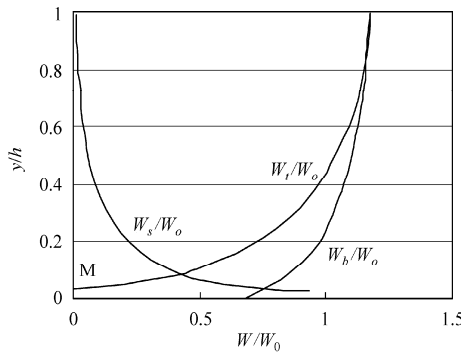
Fig. 5.18   Vertical distributions of the energy provided by flow, w_t, local energy loss, w_s, and energy transmitted to the boundary w_b, in a unit time step ($w_0 = \gamma s U$, where U is the mean velocity over the vertical) (after Qian and Wan, 1983)

In summary the complete process of energy transformation is simply described in Fig. 5.19.
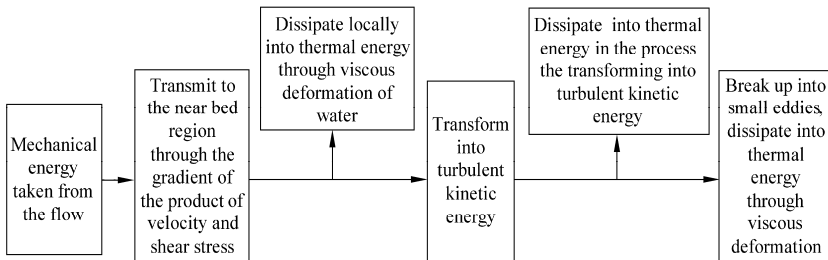
Fig. 5.19   Energy transformation in open channel flow (after Qian and Wan, 1983)

At any solid boundary, the sediment particles on an alluvial stream bed cause surface friction that is called the grain friction. Nikuradse glued uniform sediment particles to the inner surface of a pipe for his classical study of the resistance of flow through pipes. The particle diameter was taken as the size of the roughness in the pipe. For a natural stream with a nonuniform bed material, a representative particle size

of the bed material may be taken as the roughness size that characterizes the grain friction. The roughness size representing the grain friction may be larger even than the particles. Scientists have pointed out that even for a flat bed, the resistance of a movable stream bed may be quite different from that on a rigid bed.

In the previous section, the channel bed was shown to take various forms for various flow conditions. If ripples and dunes form, the flow separation at the peaks makes the pressure on the upstream face larger than that on the downstream face, and in this way causes form resistance. With antidunes, although the stream lines near the bed are almost parallel to the bed and are without separation, the water surface wave corresponding to the antidune can break and cause intensive local turbulence with an increase in the resistance loss. This kind of extra resistance is called form resistance (Rouse, 1965). The relation between grain friction and form resistance can be illustrated as follows. For flow passing over a piece of flat sand paper, the flow encounters only grain friction; if, however, the sand paper has a wavy shape, the flow encounters not only grain friction, but also form resistance.

The materials of river banks and floodplains are normally finer than the bed material. On the floodplains that are usually above the water level of normal floods, grasses and bushes often grow. The roughness due to them not only changes with their characteristics, density, stem height, and season, but it is also affected by the depth and velocity of the flow. In a shallow flow with a low velocity, the stems of grasses and bushes are erect, and they offer the maximum resistance to the flow. If the water depth and velocity are somewhat higher, the stems often bend down so that the flow area encountering resistance is less, and the bank and floodplain resistances are correspondingly less. At high flows, the grasses and bushes tend to lie flat on the bed, and the roughness is nearly constant and it changes very little with the discharge. If the bank is protected or lined, its roughness is unaffected by vegetation.

The friction loss is also affected by the shape of a channel. For channels with sand bars, the flow can be braided or meandering; the flow width is then variable and the resistance to flow is high. The resistance is proportional to the square of velocity for flow in an open channel with a regular shape. But if a river meanders and the flow Froude number exceeds a critical value, the resistance can be much higher and would no longer follow the square law. A low flow tends to be meandering, and a high flow tends to be straight. The channel form resistance for low flows, therefore, is higher than that for high flow.

Artificial structures built along a stream, like training and bank protection works, bridges, etc., tend to create local resistance. The magnitude depends on the shape, size, and orientation of the structure. Due to the complexity and variability of components of the friction loss in alluvial streams, and to the changeable property of resistance for flow carrying sediment, a unified understanding of resistance in alluvial streams does not exist at present.

Scientists use head loss and the Weisbach friction factor, f, to approach the resistance of open channel flows, in the following way

$$h_L = f \frac{U^2}{8gR} L \tag{5.26}$$

where L is the distance of the flow and h_L is the head loss for the flow over the distance. The energy slope is given by the ratio of $J = h_L/L$. For steady and uniform flows, the energy slope is equal to the bed slope, and the formula can be transformed into the expression of the Weisbach friction factor

$$f = 8sgR/U^2 \tag{5.27}$$

However, hydraulic engineers typically prefer the Manning roughness coefficient, n, to represent the resistance of flow. In the calculation of the average velocity the Manning formula has been widely accepted:

$$U = \frac{1}{n} R^{2/3} s^{1/2} \tag{5.28}$$

Manning's n is used in this book for the discussion of resistance.

For alluvial streams, especially sandy streams, the pattern of roughness is much more complex. The comprehensive resistance is the result of the joint action of the grain sizes, bed form, banks and floodplain, channel shape, and human structures. Among the factors contributing to the resistance, several depend on the flow condition, and not only on the boundary characteristics. In particular, the status of the bed configuration significantly affects the roughness. The roughness may increase by several hundred percent for streams with various bed configurations. In such cases, the roughness coefficient is surely not a constant.

In order to correctly understand the mechanism of resistance in alluvial streams, one must treat the resistance components individually, i.e. study the relation between them and the flow, and determine how the components combine together to produce the total resistance to flow in alluvial streams. Similarly, if the total resistance has been estimated from experimental data, one must also identify each component of the comprehensive resistance, especially the grain friction. Only then can one calculate the rate of sediment transport in alluvial streams through the mechanical relation between the grain friction and sediment movement.

For convenience, a simple river channel with a rectangular cross section of flow area A and wetted perimeter $P(=B+2h)$, where B is the width, is considered initially. In a unit distance, due to the boundary friction to flow, the resistance to the flow is $P\tau_0$, in which, τ_0 is the average shear stress on the boundary. For uniform flow, the energy slope, J, is identical to the bed slope, s, and the flow is not accelerating; hence

$$\tau_0 = \gamma R s \tag{5.29}$$

This flow resistance actually has two parts, one is the bank resistance acting on the two bank walls, expressed by τ_w, the other is the bed resistance acting on the bed, expressed by τ_b. The wetted perimeter of the former is $P_w = 2h$, and for the latter, $P_b = B$. Both parts can be expressed by a formula similar to Eq. (5.14) in which the variables correspond to the component parts of the resistance.

As shown in Fig. 5.20, the energy slope is taken as a constant but the hydraulic radius is divided according to the resistance components. For the above example, the expressions for the bed resistance and bank resistance are

$$\left. \begin{array}{l} \tau_w = \gamma R_w J \\ \tau_b = \gamma R_b J \end{array} \right\} \tag{5.30}$$
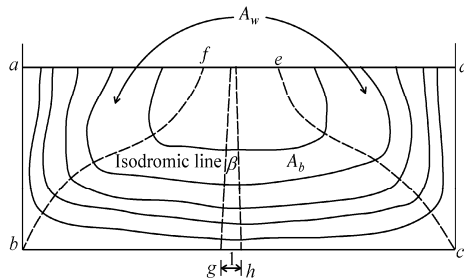
Fig. 5.20 Division of the energy and resistance. The energy consumed on the left wall ab is from the potential energy of water body abf. The energy consumed on the bed is from the potential energy of water body $bcef$. The energy consumed on the right wall cd is from the water body ced. (after Qian and Wan, 1983)

Because the energy slope is considered to be the same for both parts, the energy from a unit element of water transmits only in one direction: to the left wall, to the right wall, or to the channel bed. Thus, from the view of energy the whole flow section can be divided into three parts, as shown in Fig. 5.20. The energy concentrated on the left wall *ab* (for a unit thickness in the flow direction) is from the potential energy of water body *abf*, and the turbulent kinetic energy created by *ab* finally dissipates into thermal energy in the region *abf*. Similarly, the flow region *bcef* and the bottom *bc* combine together as one group in energy transmission, and the region *cde* and the right wall *cd* as another. No energy is exchanged across the faces *bf* and *ce*.

The energy components are not limited in number. For the area *gh* on a unit boundary perimeter (Fig. 5.20), the energy transmitted is taken from the water body with a volume β. If the total wetted perimeter is P, *pa* must equal to the whole volume of the flow, i.e. $A = P\beta$, or

$$\beta = \frac{A}{P} = R \tag{5.31}$$

Hence, the hydraulic radius itself does have a clear physical meaning. From the mechanism of the energy transformation of flow, the turbulent energy created on the area of a unit boundary element comes from the potential energy of a water volume, R; the turbulent kinetic energy created there finally dissipates into thermal energy in the same volume of water. The hydraulic radius, R, represents the water volume possessing this part of the energy (Einstein, 1934). Division or summation of the hydraulic radius only implies the division or summation of the volume of the water body, an understandable process.

In common alluvial streams, the roughness coefficients of the side walls and the bed are different, and the turbulence intensities there are different too. The energy taken from the flow by a unit area of the side wall is not equal to the one on the bed, hence the hydraulic radius, R_w, corresponding to the bank resistance is not equal to R_b, corresponding to the bed resistance, instead, the two are

$$R_w = \frac{A_w}{2h} \tag{5.32}$$

$$R_b = \frac{A_b}{B} \tag{5.33}$$

Here A_w is the sum of areas *abf* and *cde* in Fig. 5.20, and A_b is the area *bcef*.

The method of calculating the bank and bed resistances of a rectangular flow section according to the principle of division of energy is given as follows:

The following equations describe the relations between the flow energy and the partitioning of the hydraulic radius

$$A = A_w + A_b$$
$$AU = A_w U_w + A_b U_b$$
$$R_w = A_w / P_w = \frac{A_w}{2h}$$
$$R_b = A_b / P_b = A_b / B \tag{5.34}$$
$$U_b = \frac{1}{n_b} R_b^{2/3} J^{1/2}$$
$$U_w = \frac{1}{n_w} R_w^{2/3} J^{1/2}$$

There are 8 variables in the 6 equations: A_w, A_b, U_w, U_b, P_w, P_b, n_w, and n_b Usually n_w can be estimated from the bank composition, especially for rigid banks. We need one more equation to solve the problem. Different methods have been proposed but only the Einstein and Chien (1958) method is introduced for

illustration of the concept. Einstein and Chien assumed the additional condition that :

$$U = U_w = U_b \tag{5.35}$$

Then one may deduce:

$$n^{3/2} P = n_w^{3/2} p_w + n_b^{3/2} p_b \tag{5.36}$$

In this case, the resistances on different boundary elements are distributed according to the 1.5 power of the Manning coefficient.

In the study of flow resistance, the skin friction (i.e. grain friction) and form resistance (i.e. bed form resistance) often exist simultaneously. The principle of summation of resistance is tenable if the faces on which the resistance components act are fully separated, and if they partly overlap but have different heights, so that the resistance components do not affect each other.

Two different approaches are used in calculations based on the principle of summation of resistance. One is that under a certain velocity and flow depth without bed forms on the stream bed, the energy slope can be smaller; however, if bed forms also exist, the flow requires a larger energy slope. Thus, one can divide the energy slope into two parts corresponding to the grain friction and bed form, respectively (Meyer-Peter and Muller, 1948). Because the grain friction and bed form resistance occur on the same boundary, it is reasonable that an unit weight of water transmits energy simultaneously to the two resistance components. Also in dealing with the grain friction and bed form resistance, Einstein divided the hydraulic radius in the same way as for the bed resistance and bank resistance. Consequently, these two approaches are currently used for dividing the total resistance of alluvial streams into corresponding components in the following ways:
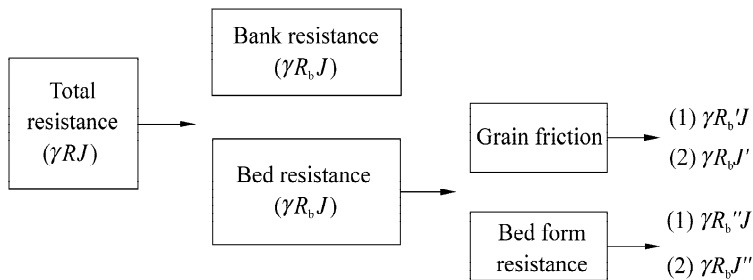
A similar approach can be used to combine bed form resistance and the resistance induced by artificial structures and other localized resistances. The floodplain resistance is discussed in the preceding sections. In the Three Gorges region of the Yangtze River, narrow and wide gorges alternate so that the cross-sectional geometry changes significantly in the longitudinal direction; the form resistance induced by these changes accounts for some 5 to 60% of the total resistance. In dealing with this issue, Hui and Chen (1981), using the approach of Einstein and Chien (1958), calculated the bed resistance and the bank resistance, and then divided form resistance induced by the sudden enlargement or contraction of the cross sections from the total resistance.

5.2 Sediment Transportation and Hyperconcentrated Flow

5.2.1 Fall Velocity

5.2.1.1 Fall Velocity
Fluvial process is a result of sediment deposition and erosion. To study sediment deposition and erosion

fall velocity and initiation velocity of sediment particles are the focal points, which have been studied for centuries.

The terminal velocity of solid particles settling in liquids, often called the fall velocity, is an important physical quantity that is used in characterizing sediment transport. The simplest case is a single sphere falling with a constant velocity in quiescent water of large extent. The force of gravity W that acts on a sphere with diameter D as it falls in water is

$$W = (\gamma_s - \gamma)\frac{\pi D^3}{6}$$

where γ_s is the specific weight of sediment particles. The resistance to the motion F is

$$F = C_D \frac{\pi D^2}{4} \frac{\rho \omega^2}{2}$$

in which ω is the fall velocity of the sphere and C_D is the drag coefficient.

At the beginning of the settling process, the velocity of the sphere is small, and the force of gravity is greater than the resistance. Hence, the sphere accelerates, and the resistance to the motion increases with the velocity. After a certain distance of travel, the resistance equals the force of gravity; and the sphere then falls with a constant velocity, called its fall velocity. That is, W and F are equal, and the equation for the fall velocity is

$$\omega^2 = \frac{4}{3} \cdot \frac{1}{C_D} \cdot \frac{\gamma_s - \gamma}{\gamma} gD \tag{5.37}$$

in which the drag coefficient is a function of the particle Reynolds number,

$$Re_p = \omega D / v.$$

During the settling process, the motion of a sediment particle causes the surrounding fluid to move also. If the inertia forces in the fluid are negligible, the Navier-Stokes equations can be linearized and solved. Early in 1851, Stokes obtained the following relationship in this way (Stokes, 1851):

$$F = 3\pi D \mu \omega \tag{5.38}$$

which is known as Stokes law. In this case, the drag coefficient is inversely proportional to the Reynolds number,

$$C_D = \frac{24}{Re_p} = \frac{24}{\dfrac{\omega D}{v}} \tag{5.39}$$

and it therefore follows a straight line with a slope of −1 as shown in Fig. 5.21. By substituting the Eq. (5.39) into Eq. (5.37), one obtains the fall velocity of the sphere in the form:

$$\omega = \frac{1}{18} \cdot \frac{\gamma_s - \gamma}{\gamma} \cdot \frac{gD^2}{v} \tag{5.40}$$

The condition for Stokes Law to apply is $Re_p < 0.4$, which in water at normal temperatures, corresponds to a limiting diameter of 0.08 mm.

For Reynolds numbers larger than 0.4, fluid inertia becomes more and more important as Re increases. The inertial force and the flow separation make the motion quite different from that characterized by Stokes Law. If the particle Reynolds number is larger than 1,000, the viscous force at the spherical surface is so small that compared with the form resistance, it can be neglected. The drag coefficient is then essentially constant, and, thus, independent of the particle Reynolds number, at $C_D = 0.45$, or

$$\omega = 1.72 \sqrt{\frac{\gamma_s - \gamma}{\gamma} gD} \tag{5.41}$$

In this range ($Re_p > 10^3$), the fall velocity of a sphere is linearly proportional to the square root of its diameter.
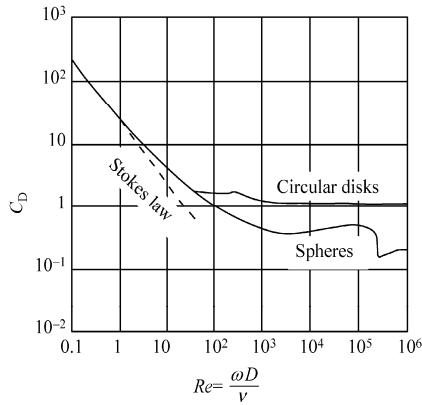
Fig. 5.21 Drag coefficient for settling of particles as a function of particle Reynolds number (Qian et al., 1998)

For particle Reynolds numbers between 0.4 and 10^3, the corresponding C_D value is available from Fig. 5.21, and by substituting it into Eq. (5.37), one obtains the fall velocity of a sphere with a given particle diameter and the specific gravity of the given liquid (Rouse, 1946). For a quartz sphere with specific gravity $\gamma_s / \gamma = 2.65$ settling in water, the fall velocities at different temperatures are presented in Fig. 5.22. Non-spherical particles can be regarded as a sphere because the particle settles with its surrounding liquid behaving similar to a sphere. The fall velocity for most natural sand can be determined with Fig. 5.22 because the main minerals composing of natural sand are quartz and feldspar, the later has a similar density and shape as the former.
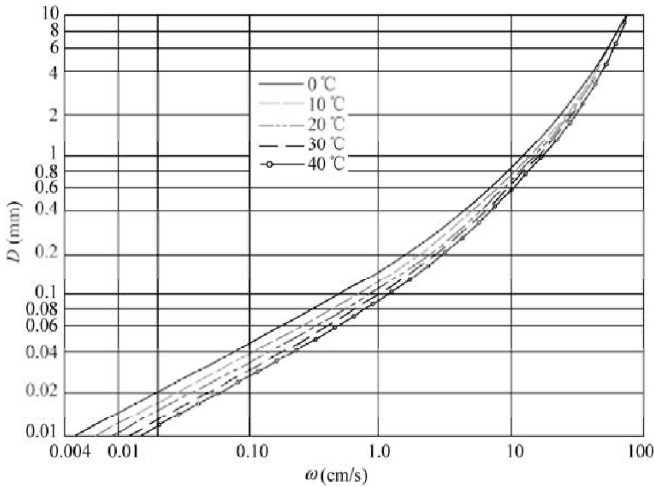
Fig. 5.22 Fall velocity of a quartz sphere in clear water (Qian et al., 1998)

5.2.1.2 Buoyancy Force and Group Fall Velocity

For a group of particles falling in a liquid the buoyancy may be different from that for a single particle

falling in the liquid. If an object is immersed in or floating on the surface of a liquid, the force acting on it due to liquid pressure is termed buoyancy. Archimedes found that the buoyancy is given by

$$F_{\mathrm{b}} = \gamma_{\mathrm{L}} V \tag{5.42}$$

where F_{b} is the buoyancy, γ_{L} is the specific weight of the liquid, V is the volume of the object or the volume of the fraction below the liquid surface. This is Archimedes law.

If, however, there are many suspended solid particles in the liquid, which have different densities from the liquid, the buoyancy of the object in the mixture of the liquid and solid particles is different.

Wang (1987) studied the problem and found that if the size of the object is much greater than the suspended solid particles, $L > 50\ D$, the buoyancy is given by

$$F_{\mathrm{b}} = \gamma_{\mathrm{m}} V \tag{5.43}$$

in which L is the size of the object, D is the diameter of the suspended particles, and γ_{m} is the specific weight of the mixture of the liquid and the suspended solid particles. If the size of the object is smaller than the diameter of the suspended solid particles, the buoyancy is the same as if the object was in the pure liquid,

$$F_{\mathrm{b}} = \gamma_{\mathrm{L}} V$$

If the size of the object is between D and $50D$, the buoyancy is given by

$$F_{\mathrm{b}} = V[\gamma + f\left(\frac{L}{d}\right)(\gamma_{\mathrm{s}} - \gamma)S_{\mathrm{v}}] \tag{5.44}$$

where S_{v} is the volume concentration of the suspended solid particles, $f(L/D)$ is a function of L/D.

Figure 5.23 shows the experimental setup of Wang (1987) and the curve of $f(L/D)$ he obtained from the experiment. If L/D is over 50, $f(L/D) = 1$, and eq. (5.44) reduced to eq. (5.43). If L/D is less than 1, $f = 0$ and Eq. (5.44) reduces to (5.42).
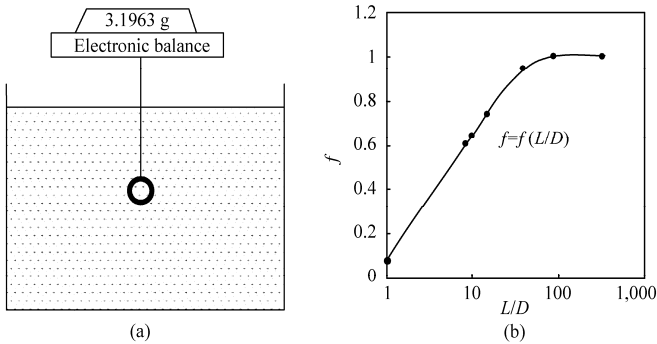
Fig. 5.23 (a) Experimental setup of Wang (1987), in which a copper ball with diameter, L, submerged in a suspension of solid particles is hung on an electronic balance, the figure shown on the balance is the difference of the weight of the ball minus the buoyancy force acting on the ball. (b) Buoyancy coefficient f versus the relative size L/D (after Wang, 1987)

In a special case of solid particles falling down in water, if all the particles have the same diameter, each particle is acted on by almost the same buoyancy as in pure water. Although the buoyancy is the same in this case the group fall velocity of the particles is smaller than that of a single particle falling in pure water. An empirical formula is

$$\omega' = \omega(1 - S_{\mathrm{v}})^{m} \tag{5.45}$$

in which ω' is the group fall velocity, ω is the fall velocity of a single particle in pure water, and m is a exponent varying within the range of 2–8 For fine sediment, m is large, e.g., $D=0.1$ mm, $m=8$; for coarse sediment, m is small, e.g. $D=2$ mm, $m=2$. Generally, m is a function of the particle Reynolds number, as shown in Fig. 5.24
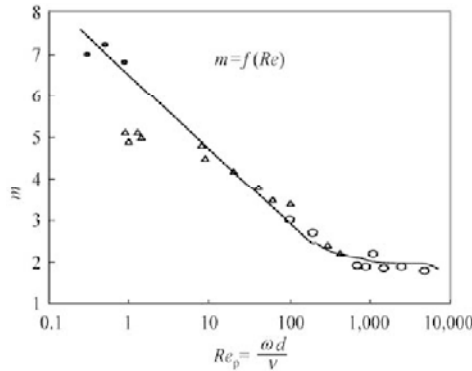
Fig. 5.24   The exponent m in the group fall velocity equation (5.45) as a function of particle Reynolds number, Re_p

5.2.2   Sediment Transportation

5.2.2.1   Initiation Velocity

Incipient motion is an important critical condition, under which sediment starts to move through the action of flow. In 1753, Brahms suggested that the velocity for incipient motion is proportional to the grain weight raised to the one-sixth power. This concept agreed quite well with the knowledge of incipient motion of sediment at that time. At the end of the nineteenth century, people began to study the problem from the concept of a balance of forces acting on the grains. In 1914, Forchheimer systematically summarized and evaluated the knowledge that had accumulated by that time, and he discussed the influence of sediment gradation, sorting, and armoring on the incipient motion of sediment. In 1936, Shields applied the method of dimensional analysis, prevalent at that time to sediment motion and developed the well-known Shields (1936) diagram, which is still used widely. In the 1950s, Lane (1953) applied the concept of drag force in canal design and proposed a design of regime canals that is more soundly based on theoretical grounds. More recently, investigations of the incipient motion of the sediment have focused on conditions for non-uniform and cohesive sediments. For the former, the armoring process at the bed should be included as part of the process of erosion, and for the latter, the sediment motion is related to the physico-chemical properties at the surface of fine grains. Both of these cases are quite complex. After long experience, people gradually began to conceive of incipient motion of sediment as a stochastic phenomenon. Its study must use an approach that combines the theories of probability and fluid mechanics if one is to understand the physical essence of the incipient motion of sediment.

The Shields (1936) equation for incipient drag force for non-cohesive uniform sediment can be used. Shields found that the dimensionless critical shear stress (Shields number) depends only on the grain Reynolds number, $Re_* = U_* D / v$.

$$\frac{\tau_c}{(\gamma_s - \gamma)D} = f\left(\frac{U_* D}{v}\right) \tag{5.46}$$

where τ_c is the critical value of shear stress needed to initiate sediment motion, and U_* is the shear

velocity.

Equation (5.46) is the formula Shields used for the drag force. In his original derivation he neglected the effect of uplift. Actually, the basic structure of the formula is not changed whether uplift is included or not. Hence, the formula shows that, when grains start to move, the ratio of the drag force acting on a grain to its weight is a function of the grain Reynolds number, as shown in Fig. 5.25.

After the work of Shields, a number of other researchers studied the incipient motion of sediment, these include White (1970), Mantz (1977), Tison (1948), and Li and Sun (1964). Their results are included in Fig. 5.25. A belt for the incipient drag force can be drawn to represent the data. This belt differs from the original Shields curve in two important ways.

(1) Shields concluded that if grain Reynolds number is less than 2, the curve would be a straight line with a 45° slope. However, he had no experimental data in that region. He may have relied on an analogy with the relation between the drag coefficient and the Reynolds number, and simply decided that $\tau_c/(\gamma_s-\gamma)D$ should be inversely proportional to the grain Reynolds number if the latter is sufficiently small. The later experiments, shown in Fig. 5.25, indicate that this concept does not agree with reality. In this range of Reynolds number, $\tau_c/(\gamma_s-\gamma)D$ is proportional to Re_* with an exponent of -0.3.

(2) If Re_* is quite large, Shields proposed that $\tau_c/(\gamma_s-\gamma)D$ would have the value 0.06. The results now available show that this value should be taken as an upper limit; and the lower limit should be about 0.04. In Fig. 5.25, most of the results fall within this range. From the experimental data of Paintal (1971), Miller et al. (1977) recommended that the ratio approaches the value 0.045, not 0.06, if Re_* is quite large.
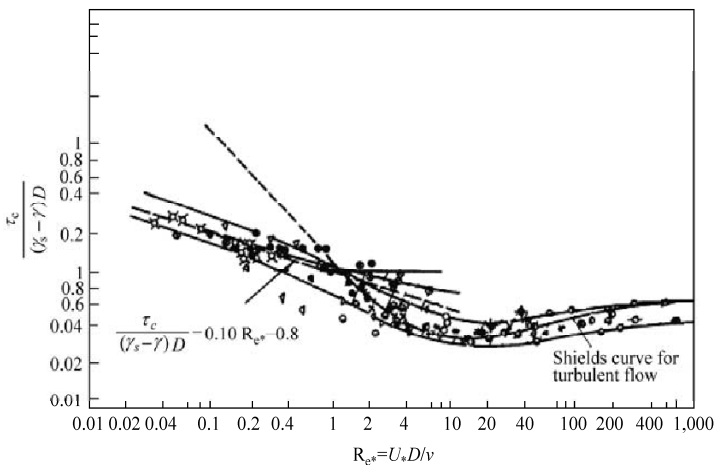
Fig. 5.25 Shields curve for incipient motion for non-cohesive sediment (Shields curve and its modification)

In the Shields diagram, the parameter $U_*(\tau_0=\rho U_*^2)$ occurs in both the abscissa and the ordinate. Hence, in determining the incipient drag force one must proceed by trial and error. To simplify the process, a set of lines for constant values of the parameter of $\dfrac{D}{\nu}\sqrt{0.1\dfrac{\gamma_s-\gamma}{\gamma}gD}$, with a slope of 2, has been drawn in Fig. 5.25. The intersections of these lines with the Shields curve are the corresponding drag forces for incipient motion.

5.2.2.2 Bed Load Transportation

In the last part of the 19th century, the French scientist DuBoys advanced a theory for bed load motion based on shear stress. Since then, many scientists have studied the phenomenon and they have proposed

a number of formulas for bed load transport and suspended load transport. These formulas are based on different modes of motion and use different parameters, including shear stress, flow velocity, and stream power. Although the formulas have been widely used in hydraulic engineering and numerical modeling of fluvial processes, the relative error is quite high. Several tens to thousand times difference between the calculated and measured rates of sediment transportation are found in some cases. Very briefly the Meyer-Peter and Muller (1948) formula for bed load transport and WIHEE (1961) formula for suspended load transport are introduced as examples.

Bed load is the sediment load that moves in the vicinity of the bed and at least intermittent contact with the bed. In many rivers, the bed load motion and deposition largely determines channel morphology. Bed load is critical in maintaining ecological diversity and habitat in stream channels. Therefore, bed load transport has become a focal point of research for a century, although bed load is only a very small portion of the total load. Since 19th century many scientists have studied the phenomenon and proposed a number of formulas for the rate of bed load transport. They used different parameters, including shear stress, flow velocity and stream power. The formulas of Meyer-Peter-Mullër, Einstein, Bagnold, Engelund and Yalin are the most widely applied (Chien et al., 1998). In the following the Meyer-Peter and Muller formula is introduced. Other formulas may be found in the literatures (Chien et al., 1998).

Since the 1970s, many researchers tested, analyzed and compared these formulas with measured data and flume experiments. All the bed load formulas can not accurately give the rate of bed load transport. For bed load motion in mountain streams, the relative error of the calculated results with all current formulas is too great to be applied and new approaches are needed, which is discussed in the last part of this chapter.

Meyer-Peter and Muller (1948) developed a simple empirical bed load formula by using a similarity law and data from their preliminary experiments. The formula involved only a few simple parameters. Then they applied the formula to more complex cases involving the variation of additional parameters and found a systematic difference between the measured data and the formula. They analyzed the difference and determined its cause. They studied the effect of each new parameter by separating it from the others in additional experiments and then incorporated the parameter into the formula. In this way, they studied the effects of density, size composition of the sediment, and bed form step by step and eventually obtained a comprehensive bed load formula. This approach required a long time to develop, but it is effective for studying problems involving numerous parameters.

For bed load motion in a steady and uniform flow, Meyer-Peter and Muller (1948) obtained the following formula:

$$g_b = 8g^{1/2}\gamma_s D^{3/2}\left[\left(\frac{K_b}{K_b{}'}\right)^{3/2}\left(\frac{\gamma}{\gamma_s-\gamma}\right)^{2/3}\frac{R_b J}{D}-0.047\left(\frac{\gamma_s-\gamma}{\gamma}\right)^{1/3}\right]^{3/2} \qquad (5.47)$$

where g_b is the rate of bed load transport per unit width in weight, D the diameter of the bed load and is usually represented by the median diameter, R_b is the hydraulic radius as affected by the bed resistance, $K_b{}'/K_b$ is the ratio of the roughness coefficient duo to grain resistance to that of the total resistance.

The Meyer-Peter and Muller Formula is based on a large quantity of experimental data. The main variables in their experiments varied within the following ranges:

Width of flume:	0.15 – 2 m
Flow depth:	0.01 – 1.2 m
Energy slope:	0.04% – 2%
Density of sediment:	1.25 – 4 g/cm^3

Diameter of sediment:　　　　　　　　　　0.40 – 30 mm

These data have quite a large scope, especially notable are those for gravel with a size of 30 mm. Therefore, the formula is more reliable than some of the others for rivers carrying coarse sand and gravel. The Meyer-Peter and Muller formula has been widely used in Europe, and the results obtained from it are generally satisfactory.

A point to note is that the flow velocities in the experiments were relatively high so that almost all of the sediment could be carried by the flows. For mountain rivers in China, however, many of the particles on the bed cannot be moved except in extreme events. The Meyer-Peter and Muller Formula predicts a larger bed load transport rate than is the observed in such cases (Du et al., 1980).

The Meyer-Peter and Muller formula was obtained from experiments with relatively uniform sediment. In natural streams with various sizes of bed material the flow selects different materials as bed load to meet its sediment demand for different flow discharges and the relation between the rate of bed load transportation and flow intensity is very different from the formula.

5.2.2.3　Suspended Load Transportation

Since suspended particles move with the same velocity as the local flow, u, the average transport rate of suspended load per width, q_s, can be solved as follows:

$$q_s = \int_a^h S_v u \, dy \tag{5.48}$$

in which "a" is the distance from the lower boundary of the suspension region to the bed, and S_v the volumetric concentration of suspended load at a distance y above the bed. The concentration distribution of suspended load in open channel flow is given by:

$$\frac{S_v}{S_{va}} = \left(\frac{h-y}{y} \frac{a}{h-a} \right)^z \tag{5.49}$$

in which

$$z = \frac{\omega}{\kappa U_*} \tag{5.50}$$

is a dimensionless number and is called the **Rouse Number**. With the Eqs. (5.48) and (5.49) one can calculate the transport rate of suspended load.

Nevertheless, an important problem is to determine the mean sediment concentration, S_{vm}, from known hydraulic parameters. Velikanov proposed the following formula (Chien et al., 1998),

$$S_{vm} = K \frac{U^3}{gh\omega} \tag{5.51}$$

in which K is a constant that must be determined and U is the average velocity. Equation (5.51) is the formula for the depth-averaged concentration of suspended load.

Researchers at the WIHEE (Wuhan Institute of Hydraulic and Electric Engineering) made an extensive analysis of field data collected from rivers and canals including the Yangtze River, Yellow River, Yongding River, People's Victory Canal, and Qingtongxia Irrigation System; and they concluded that Eq. (5.51) should be modified to the following (WIHEE, 1961)

$$S_{vm} = k \left(\frac{U^3}{gh\omega} \right)^m \tag{5.52}$$

in which the coefficients k and m are functions of ($U^3/gR\omega$) as shown in Fig. 5.26.
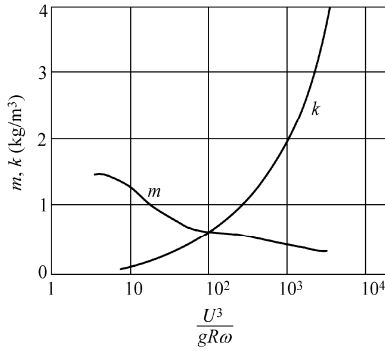
Fig. 5.26 Coefficient k and exponent m in the suspended load equation (5.52) as a function of $U^3/gR\omega$

5.2.3 Hyperconcentrated Flow

5.2.3.1 Hyperconcentrated Flows

Hyperconcentrated flow is defined as the flow carrying hundreds of kilograms of sediment (say > 200 kg/m³ or a volumetric concentration of about 8%). In the 1960s and 1970s hyperconcentrated floods occurred almost every year in the tributaries and the Yellow River. Locations where hyperconcentration of sediment were measured in the Yellow River basin are shown in Fig. 5.27. The concentration of a hyperconcentrated flood that occurred in 1964 in the Kuye River, which is a tributary of the Yellow River, was 1,500 kg/m³. A hyperconcentrated flood in 1974 in the Huangfuchuan River had a peak concentration of 1,570 kg/m³ (Qian, 1989). The sediment concentration of hyperconcentrated floods in the Yellow River also was high. The concentration reached 933 kg/m³ at the Longmen Station in 1966 and 911 kg/m³ at Sanmenxia in 1977 (Wan and Wang, 1994). Beginning in the middle of the 1980s, the sediment load and
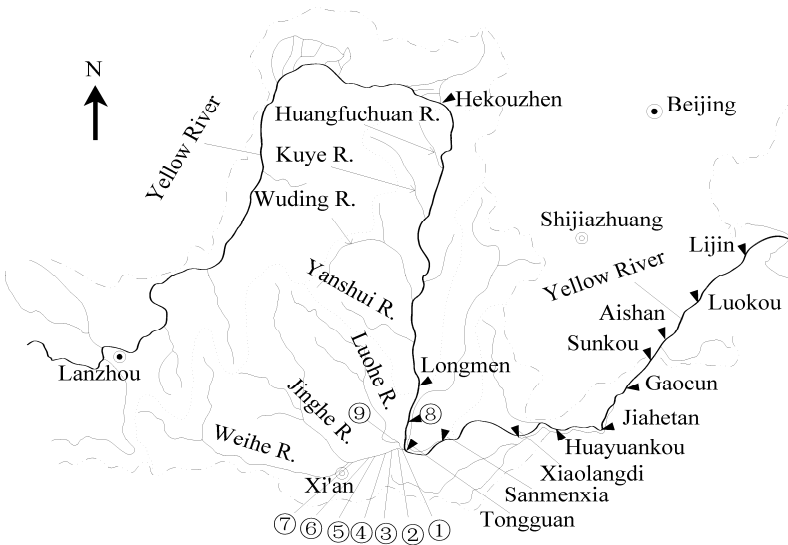
Fig. 5.27 The Yellow River and its tributaries on the Loess Plateau which have frequently experienced hyperconcentrated flow (Hydrological stations: ① Diaoqiao; ② Huayin; ③ Chencun; ④ Huaxian; ⑤ Shawang; ⑥ Jiaokou; ⑦ Lintong; ⑧ Shangyuantou; ⑨Chaoyi)

runoff began to reduce because of increasing water and sediment diversion and construction of numerous sediment trap dams in the upper and middle reaches of the river. In the 1990s and 2000s a few hyperconcentrated floods occurred in the Yellow River but the concentration was lower than before. Since the impoundment of the Xiaolangdi Reservoir, one hyperconcentrated flood has occurred in the lower Yellow River on Aug. 22–31, 2004. The highest sediment concentration and the crest discharge of the hyperconcentrated flood flowing into the Xiaolangdi Reservoir were 542 kg/m^3 and 2,960 m^3/s and the released concentration and discharge from the reservoir were 346 kg/m^3 and 2,690 m^3/s. The highest downstream concentration was to 358 kg/m^3 at Huayuankou (Zhengzhou), which then reduced to 179 kg/m^3 at Sunkou, 177 kg/m^3 at Aishan, and 146 kg/m^3 at Lijin.

Hyperconcentrated floods cause unique fluvial processes in the middle and lower reaches of the Yellow River. The high concentration and fluctuation in discharge cause some abnormal phenomena and problems in flood defense. The study of these phenomena and their mechanism may provide understanding of hyperconcentrated floods, which is essential for river training and flood defense strategies.

As early as the 1960s Chinese hydraulic engineers started field investigations of the hyperconcentrated flow occurring in the rivers on the Loess Plateau. In the first edition of their monograph published in 1983, Qian and Wan (1983) reported the basic characteristics of hyperconcentrated flows,. Qi and Zhao (1985) studied the fluvial process of hyperconcentrated floods. The first International Workshop on Hyperconcentrated Flow was held in Beijing in 1985. Chinese scientists reported on the hyperconcentrated floods in the Yellow River and its tributaries and the mechanism of hyperconcentrated flows (Qian et al., 1985; Wang and Qian, 1985) and American scientists reported on the sediment transportation by lahars and hyperconcentrated flows at Mount St. Helens (Scott and Dinehart, 1985; Janda and Meyer, 1985). Since then hyperconcentrated flow has attracted the concern of scientists and engineers. Qian (1989) summarized the main results on the development, flocculation, rheology, hydraulics, and application of hyperconcentrated flows. In the monograph with title of "Hyperconcentrated flow", Wan and Wang (1994) reported the unique features of hyperconcentrated floods, including the phenomena of ripping up the bottom, river clogging, roll waves and instability of hyperconcentrated flow, and the mechanism of these phenomena. Julien (1989), Julien and Lan (1991) and O'Brien and Julien (1995) performed laboratory studies on physical properties and mechanics of hyperconcentrated sediment flows. Wang et al. (1994, 1998) and Wang (2002) revealed the rheological properties of hyperconcentrated flows, mechanism of surface instability, and drag reduction.

Hyperconcentrated flow is complicated. The hydraulic features of hyperconcentrated floods are different from those for low concentration floods. The fluvial process induced by a hyperconcentrated flood is extremely rapid. The river morphology may be changed more by one hyperconcentrated flood than the changes that may be caused by normal flow and low concentration floods over a decade. The fluvial process during a hyperconcentrated flood also changes the propagation of flood waves and induces peculiar phenomena. This section provides a basic picture of these phenomena and mechanisms of these phenomena.

In hyperconcentrated flow, the presence of a large amount of solid particles remarkably influences or changes the fluid properties and flow behavior. In many cases of hyperconcentrated flow, sediment together with water, forming a pseudo-one-phase fluid, moves in its entirety and sediment can no longer be considered as material carried by the water. Hyperconcentrated flow occurs often in the Yellow River and its tributaries. In Table 5.1 the maximum and average monthly sediment concentrations of ten main tributaries in the middle reach of the Yellow River are listed. Hyperconcentrated floods may carry sediment, concentration higher than 1,500 kg/m^3. Hyperconcentrated floods cause rapid and severe erosion and deposition.

Table 5.1 Average monthly sediment concentration and maximum-recorded sediment concentration of ten main tributaries of the Yellow River

River	Gauging station	Period of record	Statistic	June	July	August	Sept	Annual load (10^6t)
Huangfuchuan	Huangfu	1953–1979	S_{av}	411	523	369	216	64.1
			S_{max}	1,370	1,570	1,480	1,240	
Gushanchuan	Gaoshiya	1953–1979	S_{av}	327	410	373	178	27.8
			S_{max}	1,300	1,190	1,090	829	
Kuye	Wenjiachuan	1953–1979	S_{av}	162	405	319	90.6	135
			S_{max}	1,400	1,700	1,500	970	
Wuding	Baijiachuan	1956–1979	S_{av}	12.5	352	323	90.8	106
			S_{max}	1,290	1,270	1,180	958	
Qingjian	Yanchuan	1954–1979	S_{av}	384	503	448	105	45.3
			S_{max}	1,150	1,080	970	881	
Yanshui	Ganguyi	1952–1979	S_{av}	287	454	368	119	54.6
			S_{max}	1,200	1,190	1,033	1,070	
Fenhe	Hejin	1943–1979	S_{av}	19	43	59.4	37.6	43.8
			S_{max}	174	386	227	143	
Weihe	Xianyang	1934–1979	S_{av}	37.1	71.4	80.2	28.5	168
			S_{max}	654	588	729	662	
Jinghe	Zhangjiashan	1931–1979	S_{av}	168	349	329	110	286
			S_{max}	906	1,430	984	946	
North Luohe	Zhuangtou	1933–1979	S_{av}	121	337	287	58.1	96.8
			S_{max}	987	1,150	1,190	1,340	

S_{av} = average monthly sediment concentration in kg/m^3; S_{max} = maximum recorded sediment concentration in that month in kg/m^3

A hyperconcentrated flow is non-Newtonian if the sediment consists of a certain amount of clay particles. The rheological curve of the hyperconcentrated flow approximately follows the following constitution equation (Bingham model):

$$\tau = \tau_B + \eta \frac{du}{dy} \tag{5.53}$$

where τ_B is the yield stress, and η is the rigidity coefficient.

Fine sediment in the flow can be supported by the yield stress and transported for long distance without deposition and exchange with the bed material. In such a case the concept of "sediment-carrying capacity" is meaningless. The amount of sediment transported by the flow depends only on the incoming sediment amount and boundary resistance. Dynamic characteristics of the flow depend on the rheological properties of the mixture, which in turn depend on the content of clay and silt.

Hyperconcentrated flow is often laminar because of its high viscosity. In the upper central part of an open channel flow where the shear stress is less than the yield stress, there is no velocity gradient. The mixture there moves entirely at a uniform velocity u_p and forms a flow plug. In wide and shallow rivers the velocity of the plug u_p and the plug zone are given by

$$u_p = \frac{\gamma_m J}{2\eta} \left(h - \frac{\tau_B}{\gamma_m J} \right)^2, \quad h - \frac{\tau_B}{\gamma_m J} < y < h \tag{5.54}$$

in which J is energy slope, which is equal to bed slope s if the flow is steady and uniform.

Figure 5.28 (a) shows the velocity profile and the plug zone. If the yield stress is high the plug velocity is approximately equal to the average velocity of the flow. Many rivers and gullies that frequently carry hyperconcentrated flows occur in the Loess Plateau in northwest China. The hyperconcentrated flows usually consist of clay and silt and have a very high yield stress. The scale of the plug zone reflects the magnitude of the yield stress. Witnesses described them as intermittent flows with larger waves between smaller waves. The flow plug can be also seen on the surface velocity distributions. Figure 5.28 (b) shows the surface velocity distribution of a hyperconcentrated flow in the Luohui Irrigation Canal, northwest China, through which hyperconcentrated floods were diverted from the North Luohe River for irrigation. About 80% of the width was in the plug zone and a velocity gradient existed only in zones close to the banks.
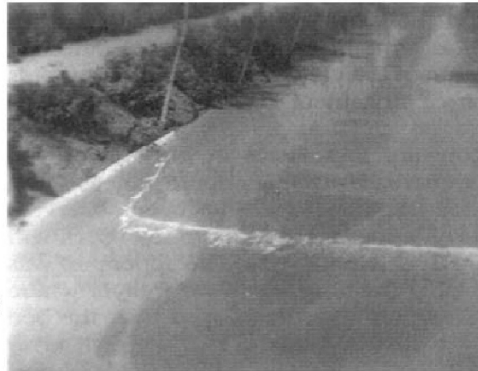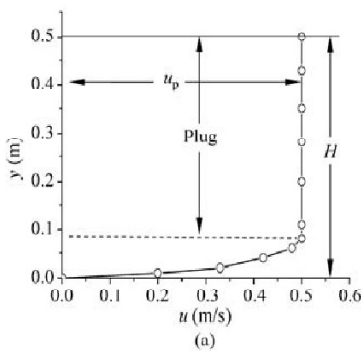
Fig. 5.28 (a) Velocity profile of hyperconcentrated flows; and (b) Surface velocity distribution of a hyperconcentrated flow in the Luohui Irrigation Canal (photo by Z.Wang)

5.2.3.2   Concentration Distribution and Resistance

In a hyperconcentrated flood, the fall velocity of sediment is nearly zero and the concentration distribution is uniform. Figure 5.29 shows the ratio of the concentration measured at $0.2h$ from the water surface ($S_{0.2}$) to the concentration measured at $0.8h$ ($S_{0.8}$), $S_{0.2}/S_{0.8}$, as a function of the average concentration of the flows, in which h is the flow depth. The numbers by the points in the figure indicate the median diameter of the suspended sediment in mm. When the concentration is lower than 200 kg/m3 the ratio is in the range of $0.4 – 0.9$; and when the concentration is higher than 200 kg/m3 the ratio is near 1.0. Even for the case of median sediment diameter around 0.1 mm, the concentration distribution of hyperconcentrated floods is quite uniform.

The resistance of hyperconcentrated flow can be represented by Manning's roughness coefficient, n, although hyperconcentrated flow exhibits higher viscosity than water flow or even becomes non-Newtonian (Qi and Han, 1991). Figure 5.30 shows the roughness coefficient n of hyperconcentrated floods and low concentration floods at the Xiaolangdi Hydrological Station on the Yellow River as a function of concentration, in which the points with concentrations higher than 200 kg/m^3 are regarded as hyperconcentrated. The discharge of the hyperconcentrated floods was in the range of $2,880 – 9,720$ m^3/s and the discharge of the low concentration floods was in the range of $4,150 – 9,400$ m^3/s. The resistance for the hyperconcentrated floods and low concentration floods is almost the same.
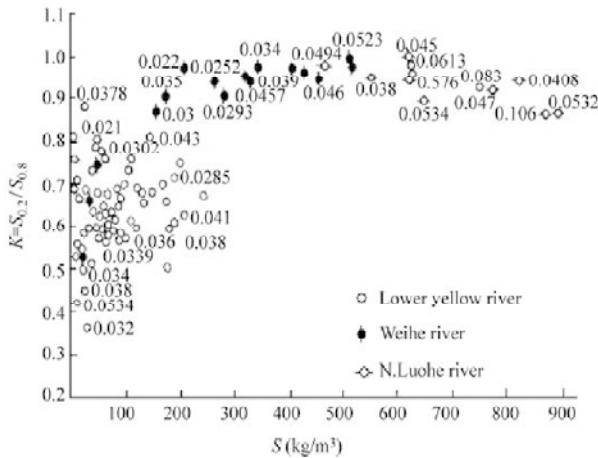
Fig. 5.29 Ratio of the concentration measured at 0.2h from the water surface ($S_{0.2}$) to the concentration measured at 0.8h ($S_{0.8}$), $S_{0.2}/S_{0.8}$, as a function of the average concentration, in which h is the flow depth (the numbers by the points in the figure indicate the median diameter of the suspended sediment in mm)
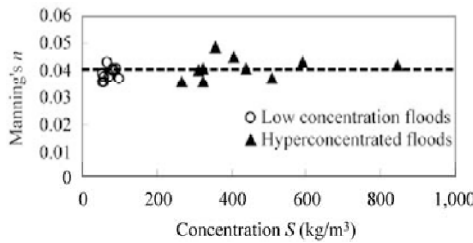
Fig. 5.30 Manning's roughness coefficient n of hyperconcentrated floods and low concentration floods at the Xiaolangdi Hydrological Station as a function of concentration

5.2.3.3 Wide and Shallow Channel and Narrow and Deep Channel

The river channel may be classified into three types according to the relation of the width/depth ratio, B/h, with discharge. The channel is wide and shallow if B/h increases with increasing discharge; is narrow and deep if B/h decreases with increasing discharge; and is transitional if B/h remains unchanged with increasing discharge. Figure 5.31 shows the relation between the width/depth ratio and the flood discharge for the lower Yellow River, the Weihe River, and the North Luohe River (Qi and Ru, 1995). The lower part of the Yellow River (Luokou station), the lower Weihe River (Huayin station), and the North Luohe River (Chaoyi station) have narrow and deep channels because the width/depth ratio decreases with increasing discharge. On the contrary, the upper part of the lower Yellow River (upstream of the Aishan station) has a wide and shallow channel (Huayuankou and Shangyuantou stations) and the width/depth ratio increases with discharge.

   Delivery ratio in narrow and deep channels—The delivery ratio is defined as the ratio of the amount of sediment load transported by a flood through a reach of river to the amount of sediment load coming into the reach from upstream. In narrow and deep channels, B/h decreases and the velocity increases with increasing discharge. Consequently the sediment carrying capacity and sediment delivery ratio increase with discharge. The sediment transportation in the narrow and deep channels exhibits the feature of "high incoming sediment load—high sediment delivery". For the lower part of the lower Yellow River (below the Aishan Station), the velocity may reach 2 m/s if the discharge is over 2,000 m³/s. The bed form

changes from the lower regime (dunes) into the upper regime (second flat bed and sometimes anti-dunes) and the sediment delivery ratio is high.
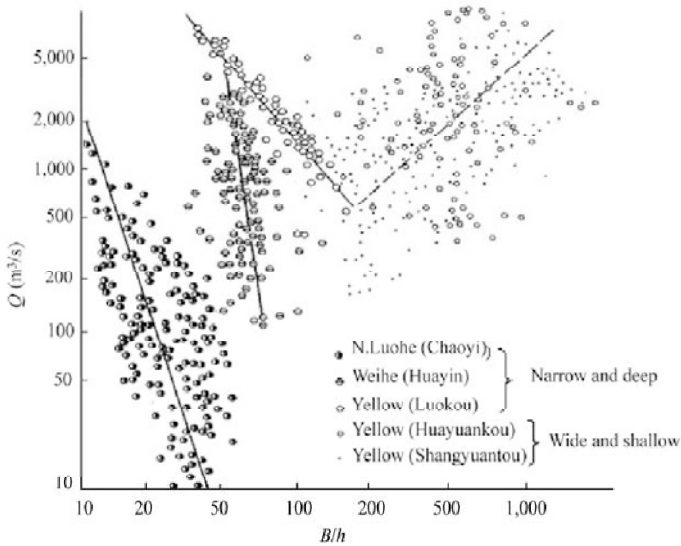
Fig. 5.31   Relations between the width/depth ratio, *B/h,* and the flood discharge, *Q,* for the lower Yellow River, the Weihe River, and the North Luohe River (after Qi and Ru, 1985)

Figure 5.32 shows the sediment delivery ratio as a function of the incoming sediment concentration for the reach from Aishan to Lijin, in which all data are for a flow discharge higher than 1,800 m^3/s. The Lijin station is the most downstream station on the Yellow River and the Aishan station is 270 km upstream of the Lijin station. In the figure the vertical axis is the sediment concentration measured at the Aishan station, and the horizontal axis is the ratio in percent of sediment concentration measured at the Lijin Station to the concentration measured at the Aishan station. For an inflow concentration higher than 50 kg/m^3, the delivery ratio is around 100%. For lower concentrations the delivery ratio varies in the range of 70% –150%,
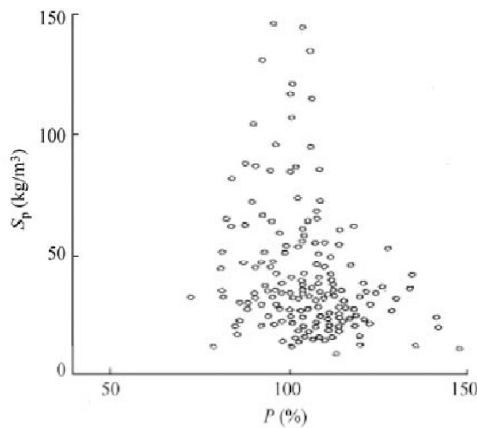
Fig. 5.32   Sediment delivery ratio (*P*) as a function of the incoming sediment concentration (*S*$_{up}$) for floods with a discharge higher than 1,800 m^3/s for the reach of the Yellow River from Aishan to Lijin

which means both erosion or sediment deposition may occur in the reach between Aishan and Lijin if the concentration is lower than 50 kg/m^3.

In general the sediment delivery ratio is high in narrow and deep channels. Figure 5.33 shows the relation of the sediment concentration at the downstream station with the concentration at the upstream station on rivers with narrow and deep channels. For hyperconcentrated floods with concentrations in the range from 100 to 800 kg/m^3, the delivery ratio is around 1 and the sediment concentration measured at the downstream stations is quite close to the concentration at the upstream stations. Hyperconcentrated floods may transport all of the sediment for more than 100 km although the riverbed slope is less than or equal to 10^{-4}. Hyperconcentrated flow may even deliver sediment in a channel with a slope as low as 0.3×10^{-4} (Qi and Ru, 1995). A hyperconcentrated flood has a much higher sediment carrying capacity than a normal flood.
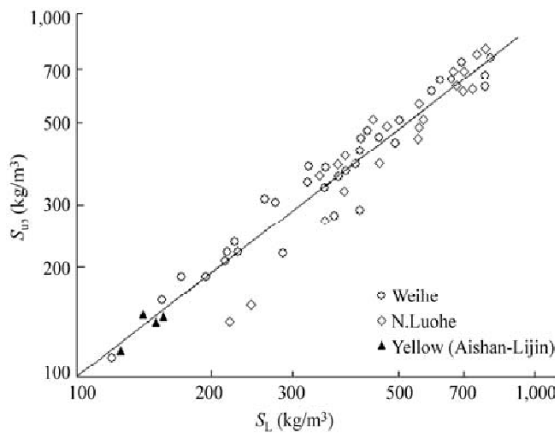
Fig. 5.33 Relation between the sediment concentration at the downstream station, S_L, with the concentration at the upstream station, S_{up} in narrow and deep channels

As shown in Fig. 5.29, the vertical concentration distribution is uniform if the average concentration is over 200 kg/m^3. When the average concentration of sediment is below 200 kg/m^3, the distribution may be quite non-uniform. In a reach downstream from the Aishan station the concentration near the surface is 130 kg/m^3, while the concentration near the bottom is 300 kg/m^3. The non-uniform sediment distribution caused a non-uniform velocity distribution. The velocity distributions in the lower Yellow River were measured during floods with different average sediment concentrations. K_v is defined as the ratio of the velocity at $y = 0.8h$ to the velocity at $y = 0.2h$ in each case measured from the bottom. For clear water flow, K_v=1.4.K_v increases with increasing sediment concentration from zero to about 200 kg/m^3. For an average sediment concentration of 200 kg/m^3, K_v reaches its maximum value of around 2. For further increases in concentration, K_v reduces and becomes smaller. For concentrations in the range of 300–900 kg/m^3, K_v reduces to 1.4. This phenomenon demonstrates that a sediment concentration around 200 kg/m^3 causes the greatest consumption of turbulent energy. Moreover, the critical discharge for non-siltation varies with concentration and reaches its maximum for a concentration around 200 kg/m^3. For instance, the non-siltation critical flow discharge in the lower Weihe River is about 500 m^3/s if the concentration less than 100 kg/m^3 or higher than 300 kg/m^3, and the critical discharge is 800 – 1000 m^3/s for concentrations around 200 kg/m^3. This fact illustrates that a sediment concentration around 200 kg/m^3 is the most difficult for the flow to transport.

Delivery ratio in wide and shallow channels—In wide and shallow channels, especially in the upper part of the lower Yellow River, the width of flow increases with discharge but the velocity does not increase with increasing discharge. Hyperconcentrated floods cause high sedimentation on the floodplain and the sediment delivery ratio is small. Figure 5.34 shows the sediment delivery ratio in percent as a function of the sediment concentration for the upper part of the lower Yellow River. For sediment concentrations higher than 50 kg/m^3, the delivery ratio is smaller than 100% and decreases with increasing sediment concentration. For hyperconcentrated floods with concentrations higher than 200 kg/m^3, the delivery ratio is only 40–60% and serious sedimentation occurs in the reach.
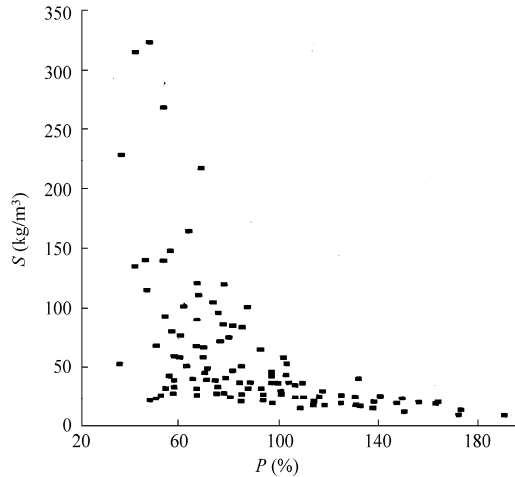
Fig. 5.34   Sediment delivery ratio (P) in percent as a function of the sediment concentration (S) for wide and shallow channels in the upper part of the lower Yellow River

Wang and Dittrich (1992) used the Rouse number Z to differentiate wash load and bed material load for hyperconcentrated flow and low concentration flow. The group fall velocity of the sediment in the Yellow River roughly follows the empirical formula given below, as shown in Fig. 5.35:

$$\omega = \omega_0 (1 - S_v)^7 \tag{5.55}$$
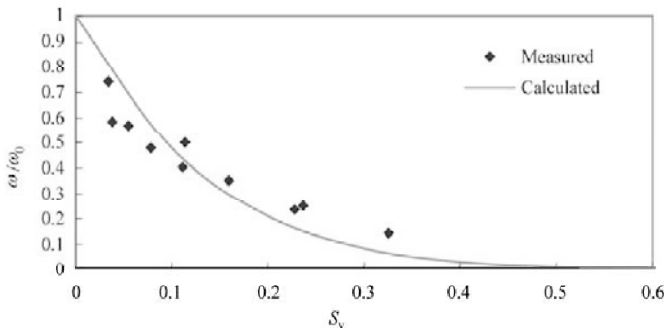
Fig. 5.35   The ratio of group fall velocity to the fall velocity of single particle, ω / ω_0, in hyperconcen-trated flows as a function of the volumetric sediment concentration, S_v

in which S_v can be estimated for Yellow River sediment by $S_v = S/2650$ (where S is in kg/m^3); ω_0 is the fall velocity of a single particle of diameter equal to D_{35}, the diameter for which 35 percent of the sediment is equal to or finer than.

The method of Wang and Dittrich (1992) for differentiating bed load, suspended bed material load and wash load has been introduced in Chapter 1:

$$\text{Bed Load} > Z = 3 > \text{Suspended Bed Material load}, > Z = 0.06 > \text{Wash Load} \qquad (5.56)$$

With this method and Eq. (5.55) a lot of relatively coarse sediment becomes wash load in hyperconcentrated flow because the fall velocity is very small and the value of the Rouse number is smaller than 0.06.

For hyperconcentrated flows in narrow and deep channels, the group fall velocity of sediment decreases quickly with sediment concentration and the Rouse number becomes very small. For instance, the fall velocity reduced by 50% compared to a single particle for a concentration of about 240 kg/m^3, and becomes 5 times smaller for a concentration of about 530 kg/m^3, 10 times smaller for 740 kg/m^3, and 30 times smaller for 1,000 kg/m^3. All sediment becomes wash load and the sediment delivery ratio is equal to one during hyperconcentrated floods. On the other hand, in a wide and shallow channel, especially on the floodplain, the shear velocity may be 10 times smaller than the main channel and the Rouse number is large, and, thus, the sediment becomes bed material load. The turbulence intensity is not sufficient to balance the fall velocity. Coarse particles settle down and the concentration reduces, thence the fall velocity of fine particles increases and these may settle as well. As a result, serious sedimentation occurs in a wide and shallow channel and the sediment delivery ratio is small.

The upper part of the lower Yellow River is wide and shallow and the channel is wandering. The Weihe River and the North Luohe River are narrow and deep and the channel is meandering. The sediment delivery ratio is high in a meandering channel and is low in a wandering channel, as shown in Fig. 5.36. Although the maximum daily-average discharge in the lower Yellow River is larger than that in the Weihe River and the North Luohe River, the sediment delivery ratio is much smaller than the later two.
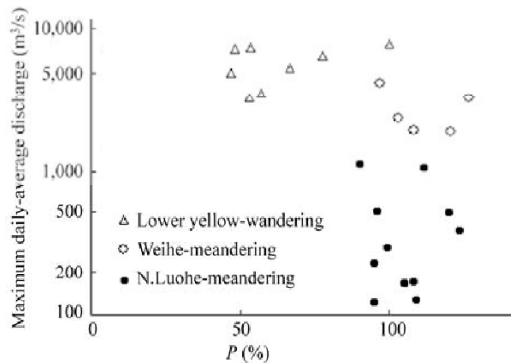
Fig. 5.36 Sediment delivery ratio (P) as a function of the maximum daily-average discharge for wandering and meandering channels (data from the Hydrological Data of the Yellow River, Yellow River Conservancy Commission)

5.2.3.4 Intensive Scour by Hyperconcentrated Floods

As the discharge of a hyperconcentrated flood is higher than the bank full discharge, the sediment suspension flows on the floodplain and serious sedimentation occurs on the floodplain because the roughness of the floodplain is high and the velocity is low. In the meantime the hyperconcentrated flood scours the main channel. Sometimes, a phenomenon of the so-called "ripping up the bottom" occurs (Wan and Wang, 1994). The peculiar phenomenon of 'ripping up the bottom' is described by local

witnesses as follows: as the flood passed, a block of the river bed, about one meter thick, was torn off by the flow; it turned around and stood up, towering over the water surface for several seconds. Then it collapsed with a great noise. After several minutes another block of the riverbed towered over the water surface and collapsed again. Such a fantastic phenomenon usually causes very quick erosion of the channel bed and has been recorded at Longmen and Tongguan on the middle reaches of the Yellow River, Lingtong on the Weihe River, and once on the lower reaches of the Yellow River upstream from Huayuankou. The phenomenon occurred at Longmen again during a hyperconcentrated flood in 2002, as shown in Fig. 5.36.

Fig. 5.36 "Ripping up the bottom" occurred near Longmen on the Yellow River during a hyperconcentrated flood in 2002

A hyperconcentrated flood may scour the channel bed down by several meters or even more than ten meters, in the form of "ripping up the bottom" or normal erosion. Figure 5.37 (a) shows the discharge, sediment concentration, stage, average elevation of the channel bed, and elevation of the deepest point of the channel measured at the Longmen station during a hyperconcentrated flood from August 1 to August 4, 1970; and Figure 5.37(b) shows the flood discharge, sediment concentration, average and deepest bed elevations, and the additional surface slope at the Chaoyi station on the North Luohe River during a hyperconcentrated flood from August. 6 to 9, 1977. In the two cases the sediment concentration was around 800 kg/m3 and the channel was scoured down by 6 – 9 m.

Intensive scour frequently occurs during the rising limb but siltation occurs during the receding limb of hyperconcentrated floods. Figure 5.38 shows the variation of discharge, sediment concentration, width, average elevation of the channel bed, and the elevation of the deepest point of the main channel measured at the Huayuankou station during a hyperconcentrated flood from August 10 to 21, 1992. As the discharge increased from 1,000 m^3/s to the crest discharge, the width and depth of the main channel increased and the flood conveyance capacity of the channel consequently increased. The deepest point of the channel was scoured down by 3 m in 12 hours. The flood stage was then reduced. In the receding limb of the flood, however, very quick siltation occurred in the channel, which made the deepest point of the channel rise to the elevation before the flood in only 1 – 2 days.

5.2.3.5 Stage Reduction Due to Scour

A hyperconcentrated flood may scour the main channel for a long distance and cause flood stage reduction. Table 5.2 shows the stage reduction at a discharge of 500 m^3/s due to bed erosion resulting from four hyperconcentrated floods in the Weihe River (Zhao and Ru, 1994). The four hyperconcentrated floods caused obvious bed erosion in the main channel in a reach of more than 100 km from Lintong to Diaoqiao. The stage for a discharge of 500 m^3/s reduced by 0.5 – 2 m. Measurement of the cross section after the floods proved that the deepest point had reduced by 0.4 – 3.7 m.
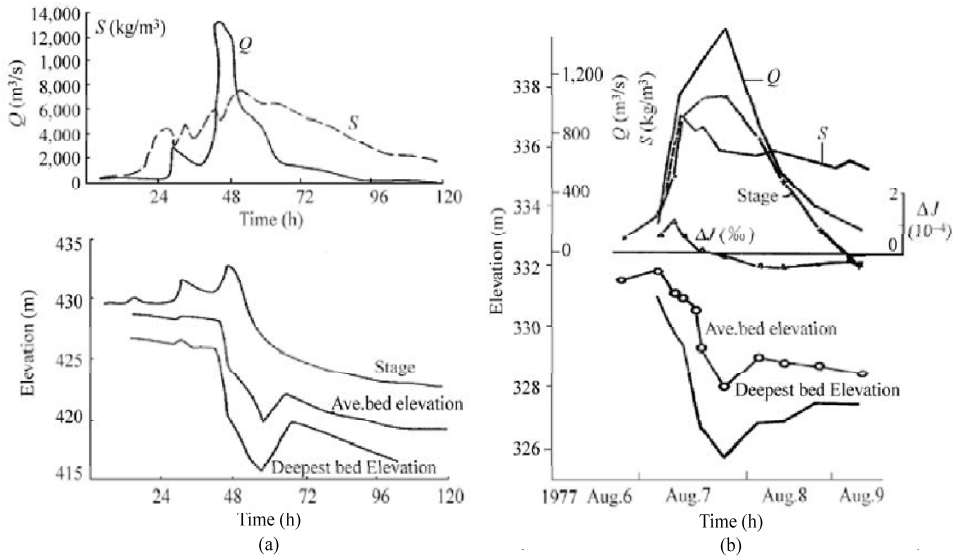
Fig. 5.37   (a) Flood discharge (Q), sediment concentration (S), stage and average and deepest bed elevation of the channel at the Longmen station during a hyperconcentrated flood from August 1 to 4, 1970; (b) Flood discharge, sediment concentration, average and deepest bed elevations, and the additional surface slope ($\triangle J$) at the Chaoyi station on the North Luohe River during a hyperconcentrated flood from August. 6 to 9, 1977
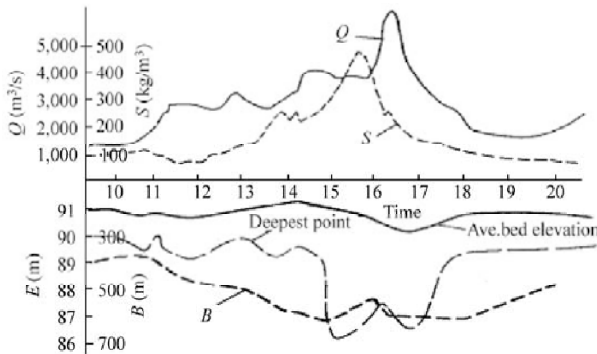
Fig. 5.38   Bed erosion process during a hyperconcentrated flood at the Huayuankou station in the lower Yellow River in August 1992 (where E is elevation, B is the channel width, Q is the flow discharge, and S is the sediment concentration)

Figure 5.39 shows the stage-discharge relation of hyperconcentrated floods at the Huayuankou station on the lower Yellow River. The stage was high in the rising limb of the floods and reduced by more than 1m in the falling limb of the flood for the same discharge, because the channel bed was scoured down by several meters during the hyperconcentrated floods. Figure 5.40 shows the stage-discharge relation of a recent hyperconcentrated flood in 2004 at the Aishan station on the lower Yellow River. The highest sediment concentration and the crest discharge of the hyperconcentrated flood flowing into the Xiaolangdi Reservoir were 542 kg/m^3 and 2,960 m^3/s and the released concentration and discharge from the reservoir were 346 kg/m^3 and 2,690 m^3/s. The flood consisted of two waves, the first one occurred from August. 22 – 25 and the second one from August. 25 – 31, with the crest discharge and maximum

Table 5.2   Stage reduction at a discharge of 500 m³/s due to main channel bed erosion resulting from four hyperconcentrated floods in the Weihe River (after Zhao and Ru, 1994)

Time	Stage reduction for Q =500 m³/s at the following stations (m)							Reduction in deepest point
	Lin-tong	Jiao-kou	Sha-Wang	Hua-yin	Chen-cun	Hua-xian	Diao-qiao	
12–17 Aug. 1964	0.50			0.40	0.70	0.60	0.10	
26–31 July 1966	0.90	0.60	1.20	0.50	0.80	1.40	1.40	0.4–3 m at 10 cross sections
02–10 Aug. 1970	0.30	0.45	0.60	0.32	0.80		0.70	0.6–3.7 m at 10 cross sections
06–10 July 1977	0.70		1.30	1.90		2.00		0.4–3 m at 19 cross sections

Note: Data from the Hydrological Data of the Yellow River, Yellow River Conservancy Commission. Jiaokou and Shawang stations are located between Lintong and Huayin stations and Chencun is located between Huayin and Huaxian stations
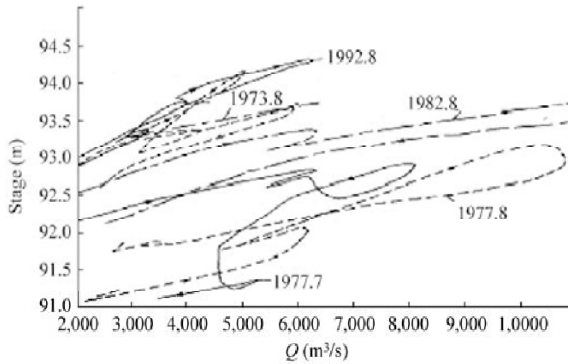
Fig. 5.39   Stage-discharge relation of hyperconcentrated floods at the Huayuankou station on the lower Yellow River
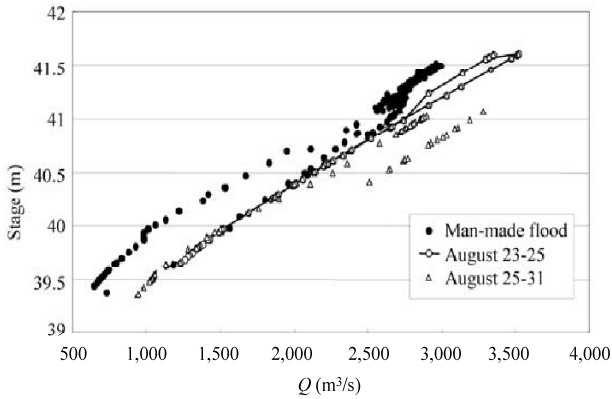
Fig. 5.40   Stage-discharge relation of the hyperconcentrated floods on August. 23 – 25 and August. 25 – 31, 2004 at the Aishan station on the lower Yellow River, in which the stage-discharge relation of a man-made flood (July 4 – 13, 2004) is shown in the figure for comparison

sediment concentration around 2,690 m^3/s and 2,450 m^3/s and 346 kg/m^3 and 156 kg/m^3, respectively. The sediment of the hyperconcentrated flood was fine and the median diameter was around 0.008 mm. The stage-discharge relation for a man-made flood is shown in the figure for comparison. The man-made flood was created with the Xiaolangdi Reservoir to scour the lower Yellow River, on July 4 – 13, 2004. The sediment concentration of the man-made flood was zero at Xiaolangdi and increased to 12 kg/m^3 at the Aishan station. The hyperconcentrated flood waves scoured the riverbed down and the stage had been clearly reduced by about half a meter.

5.2.3.6   Development of Narrow and Deep Channel

Hyperconcentrated floods change the channel to narrow and deep but low concentration floods cause collapse of the banks and make the channel wide and shallow. Figure 5.41 shows the comparison of the sedimentation and erosion along the course of the North Luohe River, which is a tributary of the Weihe River, after a hyperconcentrated flood and a low concentration flood. Sanmenxia Dam is located about 150 km downstream of the reach on the Yellow River. The horizontal axis is the distance to Sanmenxia Dam, which also shows the number of the measurement cross sections. ΔA, ΔB, and ΔH represent the changes in cross sectional area, width of the channel, and elevation of the deepest point of the channel due to sedimentation or erosion during the floods. A positive value of ΔA, means sedimentation and negative value means erosion, and positive values of ΔB and ΔH imply enlargement in width and depth, respectively, and negative values mean reduction in width and depth respectively. The upper diagram shows the changes in the cross sectional area after a low concentration flood and a hyperconcentrated flood. The low concentration flood caused no sedimentation on the flood plain, but the hyperconcentrated flood caused sedimentation on the floodplain in the lower section of the river. The cross sectional area of the main channel increased largely after the hyperconcentrated flood because the hyperconcentrated flood caused bed erosion in the main channel. The low concentration flood also increased the cross sectional area of the main channel but much less than the hyperconcentrated flood. The width of the main
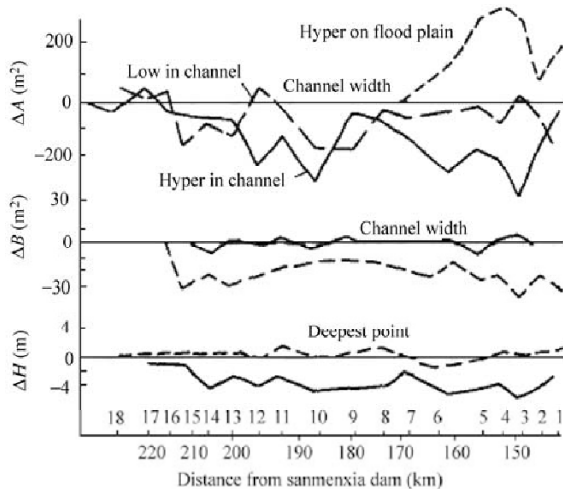
Fig. 5.41   Changes in the area of the floodplain due to sedimentation, and in the area, width, and elevation of the deepest point of the main channel resulting from sedimentation and erosion during a low concentration flood and a hyperconcentrated flood along the course of the North Luohe River. (Note: *A* positive value of ΔA means sedimentation and negative value means erosion; positive values of ΔB and ΔH imply enlargement in width and depth, respectively, and, negative values mean reduction in width and depth, respectively)

channel remained unchanged after the hyperconcentrated flood, but increased after the low concentration flood. The deepest point of the channel reduced by about 4 m after the hyperconcentrated flood but remained unchanged after the low concentration flood.

The width of the channel may reduce greatly during hyperconcentrated floods. For instance, the channel width at the Huayuankou station was 2,000 – 3,000 m in early 1977; and it reduced to 700 – 800 m after a hyperconcentrated flood in the summer (Qi and Zhao, 1984). The sediment delivery ratio may be enhanced due to the change of the channel from wide and shallow to narrow and deep. In the beginning of a hyperconcentrated flood, sediment deposits on the floodplain and at the two sides of the channel, the sediment delivery ratio is low and the channel becomes narrower. If the hyperconcentrated flood continues the channel bed is scoured deep and the sediment delivery ratio consequently increases. Table 5.3 lists the characteristics of consecutive hyperconcentrated floods in the Longmen-Tongguan reach and the Xiaolangdi-Jiahetan reach in 1977 and 1973, respectively. In the first hyperconcentrated flood at each location in July 1977 and August 1973, respectively, the sediment delivery ratio was only 78 and 66%, respectively. In the second hyperconcentrated flood in Aug. 1977 and Sept. 1973, respectively, the channel had been scoured deep and the delivery ratio increased to 101 and 124%, respectively.

Table 5.3 Characteristics of hyperconcentrated floods and variation of the sediment delivery ratio during consecutive hyperconcentrated floods on the Yellow River

Reach	Dates	Q_m (m³/s)	S_m (kg/m³)	D_{50} (mm)	Percentage of $D<0.01$mm (%)	Sediment delivery ratio (%)
Longmen-Tongguan	1977.7.6–7.8	14,500	690	0.04–0.05	14–20	78
	1977.8.5–8.8	12,700	821	0.08–0.13	11–15	101
Xiaolangdi-Jiahetan	1973.8.28–8.31	3,840	477	0.04–0.05	15–25	66
	1973.9.1–9.3	4,470	331	0.04–0.05	10–25	124

Note: Data from the Hydrological Data of the Yellow River, Yellow River Conservancy Commission

5.2.3.7 Impact on Hydraulic Characteristics

Morphological change of the river channel influences its hydraulic characteristics as well as the sediment transport capacity of the flow. It is found that the flood propagation speed is increased and the flood propagation time is shortened as a wide and shallow channel develops into a narrow and deep channel during the passage of a hyperconcentrated flood through the channel. As a result, the second wave may catch up with the first wave and cause enlargement of the crest discharge of the first flood wave in the downstream reaches.

The propagation speed of a flood wave, U_w, is a function of the channel shape and the average flow velocity, V:

$$U_w = KV \tag{5.57}$$

$$K = \frac{5}{3} - \frac{2}{3}\frac{R}{B}\frac{\partial B}{\partial z} \tag{5.58}$$

in which B is the width of the water surface, R is the hydraulic radius, and z is the elevation of water. For a U-shaped cross section, $\frac{\partial B}{\partial z}=0$ and K=5/3; for a V-shaped cross section, $\frac{B}{R}>\frac{\partial B}{\partial z}>0$ and K is between 1 and 5/3; for a wide and shallow channel, $\frac{\partial B}{\partial z}>\frac{B}{R}>0$ and K is smaller than 1.

Hyperconcentrated floods change the channel shape from wide and shallow to narrow and deep. The cross section becomes nearly U-shaped, and the value of K increases from less than 1 to nearly 5/3.

Moreover, the average velocity also increases due to the increase in the average depth or hydraulic radius. Thus, the second flood wave may travel much faster than the first flood wave. Table 5.4 lists three hyperconcentrated floods that occurred in 1977 and three hyperconcentrated floods that occurred in 1973. In 1977, the propagation speed of the first flood wave through the Longmen-Tongguan Reach was only 2.8 m/s and the speed increased to 3.61 m/s for the second flood wave and further to 4.81 m/s for the third flood wave. In the Xiaolangdi-Huayuankou reach in 1977, the propagation speed also increased from 1.25 m/s of the first flood wave to 2.26 m/s of the second flood wave. The same phenomenon occurred for the hyperconcentrated floods in 1973. The propagation speed through the Xiaolangdi-Huayuankou reach increased from 1.07 m/s for the first flood wave to 1.6 m/s for the second and third flood waves.

Table 5.4 Characteristics of hyperconcentrated floods and increase in propagation speed of hyperconcentrated flood waves in the Yellow River

Reach	Time	Q_m[1] (m³/s)	Q_{out}/Q_{in}	S_{ave}[1] (kg/m³)	S_m[1] (kg/m³)	Propa-Gation time (hours)	Propa-Gation speed (m/s)	Notes
Longmen-Tongguan	1977.7.6,17:00– 1977.7.7,6:00	14,500 13,600	0.93	575 615	690 616	13.0	2.80	Channel erosion and siltation on the floodplain
Longmen-Tongguan	1977.8.3,5:00– 1977.15:00	13,600 12,000	0.88	145 185	551 235	10.0	3.61	Channel erosion and siltation on the floodplain
Longmen-Tongguan	1977.8.6,15:00– 1977.23:00	12,700 15,400	1.21	480 911	821 911	7.5	4.81	Channel erosion and siltation on the floodplain S_m is 8.5 hr ahead of Q_m at the upstream station and 0 hr at the downstream station
Xiaolangdi-Huayuankou	1977.7.8,15:30– 1977.7.9,19:00	8,100 8,100	1.00	170 450	535 546	28.5	1.25	Channel erosion and siltation on the floodplain
Xiaolangdi-Huayuankou	1977.8.7,21:00– 1977.8.8,12:42	10,100 10,800	1.07	840 473	941 809	15.7	2.26	Channel erosion and siltation on the floodplain S_m is 1 hr ahead of Q_m at the upstream station and 3 hr ahead at the downstream station
Xiaolangdi-Huayuankou	1973.8.27, 1:42– 1973.8.28, 11:00	4,320 4,710[2]	1.10 (1.00)	110 120	110 150	33.3	1.07	Channel erosion and siltation on the floodplain
Xiaolangdi-Huayuankou	1973.8.30, 00:00– 22:00	3630 5020	1.38 (1.30)	360 230	509 450	22.0	1.60	Channel erosion and siltation on the floodplain S_m is 22 hr ahead of Q_m at the upstream station and 22 hr ahead at the downstream station
Xiaolangdi-Huayuankou	1973.9.2,12:00– 1973.9.3,10:00	4400 5890[3]	1.34 (1.27)	325 330	338 348	22.0	1.60	Channel erosion and siltation on the floodplain S_m is 2 hr ahead of Q_m at the upstream station and 2 hr behind at the downstream station

Note: 1) The upper figure is measured at the upstream station and the lower figure is measured at the downstream station. 2) The discharge flowing into the reach from tributaries during Aug. 27–28, 1973 was 400 m³/s; 3) The figure in the parentheses is Q'_{out}/Q_{in}, in which $Q'_{out} = Q_{out} - Q'_{in}$ and Q'_{in} is the discharge from the tributaries into this reach. The discharge flowing into the reach from tributaries during Aug. 30-Sept. 2, 1973 was 300 m³/s

The second consequence of the morphological process during hyperconcentrated floods is enlargement of the crest discharge in the downstream reaches. For low concentration floods, the crest discharge reduces

along the course and the hydrograph becomes flatter as flow propagates downstream. For hyperconcentrated floods, however, the crest discharge may increase along the course and the hydrograph may become steeper. Figure 5.42 shows the hydrographs of a hyperconcentrated flood at the Xiaolangdi, Huayuankou, and Jiahetan stations in August 1982. The crest discharge at the Xiaolangdi station was 4,570 m³/s, but increased to 6,260 m³/s at the Huayuankou station, and then reduced to 4,530 m³/s at the Jiahetan station. The inflow between the Xiaolangdi and the Huayuankou stations was only 100 m³/s.
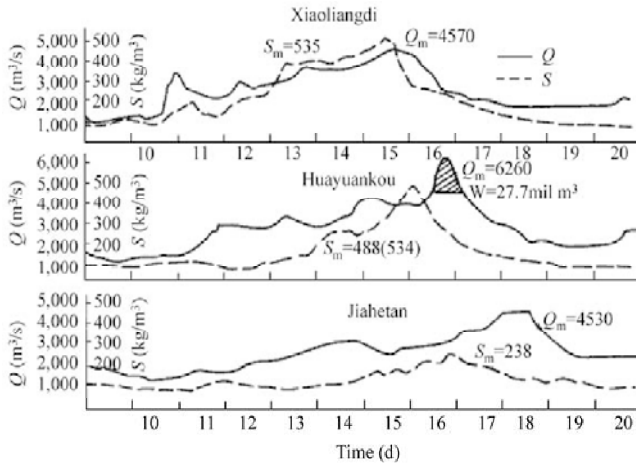
Fig. 5.42   (a) Hydrographs and sediment graphs of a hyperconcentrated flood at the Xiaolangdi, Huayuankou, and Jiahetan stations in August 1982

Enlargement of the crest discharge of the flood wave may be caused by ① inflow from tributaries between the two stations; ② scoured sediment from the channel increasing the volume of the flood wave; ③ measurement error; and ④ acceleration of the second flood wave and overlap of discharge of the two flood waves at the lower station. Generally speaking the measurement error is less than 5% and the inflow from the tributaries between the Xiaolangdi and Huayuankou stations was only several hundred cubic meters per second. The concentration at the downstream station was not higher than the concentration at the upstream station, therefore the enlargement of discharge was not due to scoured sediment. The enlargement of the peak discharge must be due to the acceleration of the second flood wave and overlap of the discharge of the two waves. Moreover, if the first flood wave is higher than the bank full discharge a part of the flood may be detained on the floodplain. The sediment may deposit on the floodplain because the flow turbulence is not sufficient to offset the fall velocity of the sediment. The floodplain becomes higher and the detained water becomes clearer, which flows back to the main channel and causes the higher discharge.

5.3   River Patterns

A channel pattern represents a mode of channel form adjustment in the horizontal plane, which is additional to but nevertheless linked with transverse and lengthwise modes. It influences flow and can be regarded as an alternative to slope adjustment when valley slope is treated as constant at short and medium timescales. The most important patterns of channels of alluvial rivers are meandering, braided, straight, wandering, and anastomosing channels.

5.3.1 Meandering Rivers

Leopold (1994) indicated that 90% of the alluvial rivers in the U.S. have meandering stream channels. A simple model of meander geometry is provided by the equation for a sine-generated curve:

$$\theta = \Theta \sin kx \tag{5.59}$$

where θ is the channel direction expressed as a sinusoidal function of distance x, Θ is the maximum angle between a channel segment and the mean down-valley axis, $k = 2\pi/\lambda$, and λ is the wavelength of the curved channel. However, it is much less applicable to non-regular bends or to lengthy meander traces in which a string of identical bends is unlikely.

It has long been recognized that consistent relations exist between the meander wavelength and radius of curvature and channel width (w), where the latter operates as a scale variable of the channel system. In particular, results from a variety of fluvial environments suggest that wavelength and radius of curvature are respectively about 10–14 and 2–3 times the channel width. Since width is approximately proportional to the square root of discharge, it is not unreasonable to expect that the meander wavelength will also be proportional to the square root of discharge. Thus, the following equation is proposed:

$$\lambda = 12w = KQ^{1/2} \tag{5.60}$$

In which K is a constant. This relation indicates a self-similarity of meander geometry over a wide range of scales and environmental conditions.

One important element of the meandering process is the flow pattern through the bends. In meanders, velocities are highest at the outside edge due to angular momentum (Fig. 5.43). The differences in flow
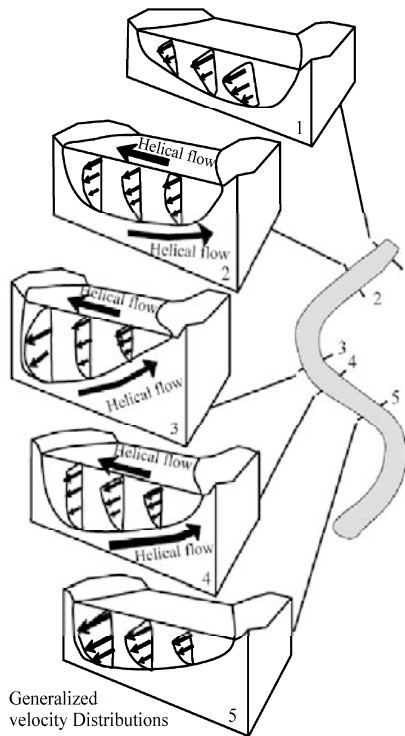
Fig. 5.43 Velocity distribution at a stream meander (flow direction is from the inner bank to the outer bank on the surface and in the opposite direction near the bottom) (after FISRWG, 1998)

velocity distribution in meandering streams result in both erosion and deposition at the meander bend. Erosion occurs at the outside of bends (cut banks) from high velocity flows, while the slower velocities at the insides of bends cause deposition on the point bar (FISRWG, 1998).

Second important feature of meandering river is the migration of the meanders. Migration can involve various types of movements: translation, when the bed shifts in position downstream without altering its basic shape; extension, when the bend moves predominantly in the lateral direction, increasing its amplitude and path length; rotation, when the bend axis changes in orientation. Figure 5.44 (a) shows the movement of a meander in the middle reaches of the Yangtze River.

The third feature of a meandering river is the cutoff of the channel. If the flow and bank material conditions are conductive to a continued increase in the amplitude and tightness of bends, a threshold sinuosity may be reached, at which the river can no longer maintain its shape and a cutoff develops. Figure 5.44(b) shows the cutoff of the Nianziwan Bend in the middle reaches of the Yangtze River. The cutoff occurred in 1950 but the bend extended again after the cutoff. Cutoff can be regarded as a response
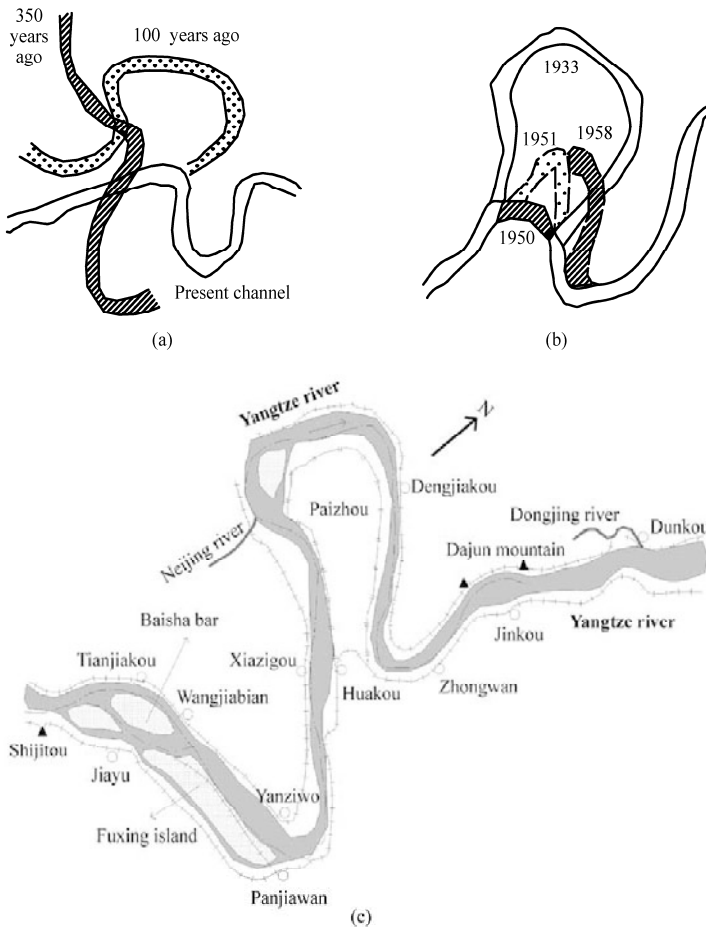
Fig. 5.44   (a) Movement of the Chibakou meander in the middle reaches of the Yangtze River; (b) Cutoff of the Nianziwan Bend in the middle reaches of the Yangtze River (after Qian et al., 1983); (c) Artificial cutoff at Huakou of the Paizhou Meander is suggested, which causes a big argument

to excessive sinuosity, which so lowers the channel gradient that the stream cannot transport the load supplied. Cutoff increases the channel gradient, and, therefore, the local transport capacity.

An artificial cutoff was started in the 19th century, when Hungarians cut 112 bends on the Tiso River and reduced the river length from 1,200 km to 745 km. In order to reduce the risk of bank failure at bends, the middle Yangtze River was artificially cutoff at 2 meanders and the river length was, therefore, reduced by 78 km in the 1960s. An artificial cutoff has been suggested at the Paizhou Meander, as shown in Fig. 5.44(c). The meander is located at the downstream of Tongting Lake and upstream of Wuhan City. There is a big argument between Tongting people and Wuhan people, the former supports the cutoff for reduction of flood risk. The later worries about that a flood may come to Wuhan quickly and threaten the safety of the city and is strongly against the cutoff. In general artificial cutoff causes intensive erosion in the new channel and siltation of the old channel. The new channel is not stable before the finish of an intensive fluvial process in, at least, several years.

Nowadays, engineers have begun to reconsider the strategy of artificial cutoff from the point of view of sustainable development and stream ecology protection. A flood wave may propagate through a shortened channel after cutoff but causes flooding problem to the downstream reaches. Moreover, meandering channel is better ecologically-sound than straight channel. Therefore, less and less artificial cutoffs have been implemented in the recent decades.

5.3.2 Straight Rivers

The longitudinal profile of a straight river is seldom constant, even over a short reach. Differences in geology, vegetation patterns, or human disturbances can result in flatter and steeper reaches within an overall profile. Riffles occur where the stream bottom is higher relative to the streambed elevation immediately upstream or downstream. These relatively deeper areas are considered pools. At normal flow, flow velocities decrease in pool areas, allowing deposition of fine sediment to occur, and increase atop riffles due to the increased bed slope between the riffle crest and the subsequent pool. In fact, the development of alternating pools and riffles is characteristic of both straight and meandering channels with heterogeneous bed material in the size range of 2–56 mm (Knighton, 1998)

A significant feature of riffle-pool geometry is the more or less regular spacing of successive pools or riffles at a distance of 5 to 7 times the channel width. The spacing distance is, thus, scale-related. It describes at best an average condition. The most extensive data-set has values of pool-to-pool spacing ranging from 1.5 to 23.3 channel widths, with an overall mean of 5.9 (Keller and Melhorn, 1978). Even in a channel disturbed by channelization schemes and the introduction of woody debris, the inter-riffle distance generally falls within the range of 5 to 7 channel widths (Gregory et al., 1994).

A complete explanation of riffle-pool formation needs to consider not only how they develop but also why they develop within the broader context of stream behavior. Basically, given a flat bed, a riffle-pool sequence through a combination of scour and deposition, organized spatially to give a more or less regular spacing between consecutive elements. The regular spacing of pool-riffle affect the bed form and a meandering thalweg develops within straight channels. Figure 5.45 shows a channelized stream in Yunnan, in which a regular meandering thalweg bed has formed.

Various mechanisms have been invoked to explain the development of riffle-pool sequences. Keller and Melhorn (1973) suggested that the regular pattern of scour and deposition required for the formation of a riffle-pool sequence may be the result of an alternation of convergent and divergent flow along the channel, combined with secondary circulation currents. Surface flow convergence at the pool induces a descending secondary current, which increases the bed shear stress and encourages scour, while surface flow divergence at the riffle produces convergence at the bed and thereby favors deposition. Thompson's (1986) diagrammatic representation of the process (Fig. 5.46) envisaged a repeated decay and regeneration

of the secondary cells in association with, and as a consequence of, the developing bed forms. With pool development alternating from one side of the channel to the other, a link to meander initiation is provided.

The riffle and pool sequence is linked with meandering based partly on the fact that the spacing of 5 to 7 times the channel width is approximately half the straight-line meander points in meanders, namely

Fig. 5.45 Regular meandering thalweg bed developed within a channelized stream in Yunnan, China (See color figure at the end of this book)
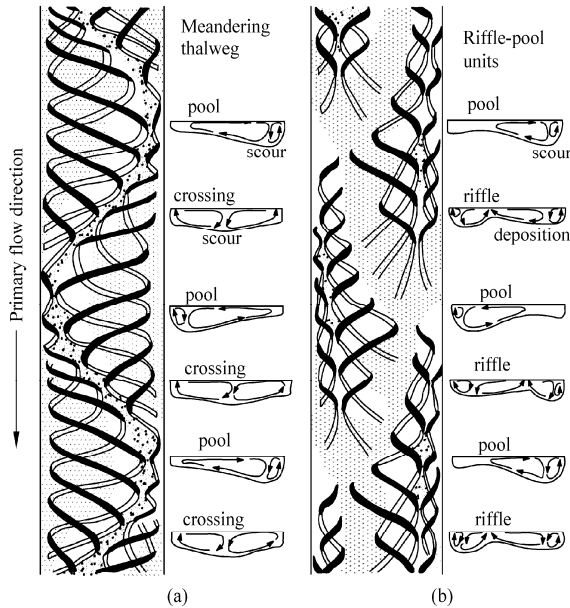
Fig. 5.46 Models of flow structure and associated bed forms in straight alluvial channels. (a) the Einstein and Shen (1964) model of twin periodically reversing, surface convergent helical cells; (b) the Thompson (1986) model of surface-convergent flow produced by interactions between the flow and mobile bed, creating riffle-pool units of alternate asymmetry. Black lines indicate surface currents, and white lines near bed currents (after Knighton, 1998)

points of inflection and pools at bend apices. Consequently several models of the transformation from a straight to a meandering pattern incorporate riffle-pool development as a significant element (Tinkler, 1970; Keller, 1972). The pattern of flow in meandering channels is regarded by Thompson (1986) as a natural development of that associated with riffle-pool units in straight channels.

5.3.3 Braided and Anabranching Rivers

Braiding develops in the middle and lower Yangtze River. In the 1,120 km reach from Chenglingji to Jiangyin, there are 41 braided sections with total length 799 km (71% of the total length of the reach). The braided channels are very stable because they meet the following conditions for braiding development.

The basic conditions for development of braided channels are: abundant bed load, erodible banks, highly variable discharge, and high stream power (Knighton, 1998). The availability of a large amount of sediment supplied from upstream or locally is regarded as a necessary condition for braiding. Where the load contains a wide range of size fractions, local inability to transport the larger sizes may induce the initial deposition from which the mid-channel bars evolve. Concentrated deposition in the form of bars diverts the flow against channel banks, and, thus, contributes to the bank erosion needed for the development of the wide, shallow channel commonly associated with bed load transport.

Figure 5.47 shows the braided Yalutsangbu River in Tibet. The river carries a large amount of gravel and fine sand from upstream tributaries and deposit in the middle reaches where the gradient is small. Many small mid-channel bars formed and they are not stable. The stream is bifurcated into two channels by one bar and bifurcated again by the second and third bars. Thus, a braided river developed with many unstable bars. If bars in a braided river are vegetated and stabilized, the braided river becomes anabranching river.

Fig. 5.47   Braided Yalutsangbu River in Tibet (See color figure at the end of this book)

In many mountain rivers flood carries cobbles and gravel and deposit them on the bed to form mid-channel bars. The bars create circumstances for silt and sand to deposit around the bars. Over time, vegetation develops on the bars, which become islands as if they are stabilized. In the meantime the islands continue to grow headward with more gravel deposit at the upstream end. Gravel deposit at the head end

of an island, while a complete vegetation develop with bamboos, shrubs and grass at the downstream end. Shrubs and grass grow in the middle part of the island and some pioneer plant species begin to colonize the new created land.

Banks composed of readily erodible material are an important source of sediment as well as being necessary for the channel widening characteristics of braided reaches. Without erodible banks, any incipient bar deposits would tend to be destroyed rather than added to. The Turandui River in New Zealand has changed over a period of years from a braided river to a meandering river as a result of the planting of willow shrubs at appropriate places.

Rapid fluctuation in discharge is often associated with high rates of sediment supply, bank erosion and irregular bed load movement, which are important for braided channel formation. High stream power is also a necessary condition for development of braiding. A river must be sufficiently powerful to erode its banks and achieve high bed mobility, which is a crucial requirement for braiding.

5.3.4   Wandering Rivers

A wandering river is defined as a river with unstable channels. A wandering river carries heavy sediment load and the discharge and sediment-carrying capacity are unsteady. A wandering river is usually associated with river aggradation. There are sand bars in the river channel but usually the stream flow remains in one channel during one period of time but flows in another channel during a second period of time. This is different from braided rivers, in which the stream flows in multiple channels simultaneously. One important feature of a wandering river is the high speed of migration of the mainstream channel. Migration of the main channel is due to the high sediment load and very erodible banks. Most of the wandering rivers have sediment composition in the bed and banks of sand, silt, and fine gravel.

There are many wandering rivers in the world. The lower reaches of the Brahmaputra River in India have a width of more than 10 km and moves at a speed of 70 m per year in the transverse direction. The Pudma River in Bangladesh widened at a rate of 200 m per year in the period 1984–1993. The Ganges River migrates consecutively resulting in many old mouths and deltas. It merged with the Brahmaputra River about 200 years ago and created the modern river delta. Such high-speed river migration and geomorphologic variation are closely related to the high sediment load and low erosion-resistance of the banks.

The Jiamura River in India also is wandering. Figure 5.48 shows the migration of the river channel near Bahadurabad with contour lines of water depth obtained by bathymetric survey. Fig. 5.48(a) is the result of the bathymetric survey done in August-September 1993 and Fig. 5.48(b) shows the contour lines in November 1993. At the fixed point cross 1, the so called Standard Low Water contour curve (the curve marked with "0") moved westward by about 400 m. At the upper fixed point cross 2 $(+^2)$, on the other hand, the Standard Low Water line migrated 520 m eastward.

Xu (1996) studied the wandering braided channel pattern of the Hanjiang River. Unlike the wandering channels of the lower Yellow River, which are due to the serious sedimentation resulting from the heavy sediment-laden floods, the wandering braided pattern of the middle Hanjiang River is caused by strong erosion of the riverbank initiated by the impoundment of the Danjiangkou Reservoir. Large quantities of sediment are supplied to the channel by bank erosion and deposited at many mid-channel bars during floods. Thence a wandering braided channel pattern with many unstable mid-channel bars developed under a condition of sediment transport equilibrium. Scientists place importance on erodible banks for a wandering braided channel (Knighton, 1984). It is striking that while the river was developing from a braided river into a wandering-braided river the sediment quantity measured at the upstream station was approximately equal to the that measured at the downstream station (Xu, 1996). This implies that a huge amount of sediment on the bed and banks was removed while a small amount of sediment was transported through

the channel. The river flow exhibited high sediment-removing capacity and low sediment-carrying capacity.
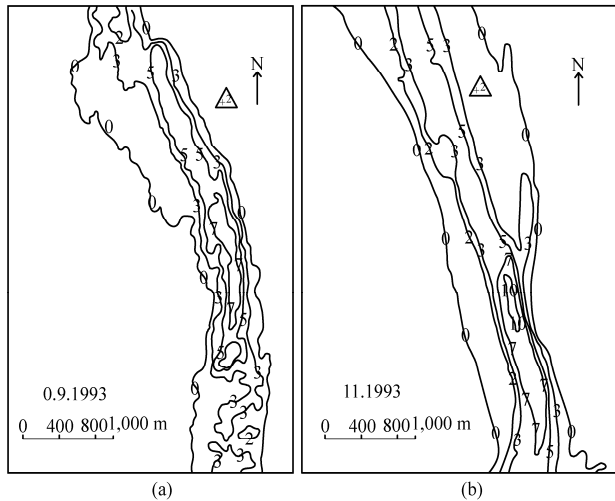
Fig. 5.48 Wandering of the Jamura River channel near Bahadurabad. (a) Contour lines of different water depths in September 1993; (b) Contour lines of different water depths in November 1993 (Barua et al., 1995)

The lower Yellow River is a wandering river with bed material mainly composed of silt and fine sand of median diameter about 0.02 mm. The sediment is very erodible. Bank erosion occurs at one side, while sediment deposition occurs at the other side of the channel. Although sedimentation dominates the long-term fluvial process of the river, short-term river adjustment is variable in time and space. The Yellow River flows out of the mountains at Xiaolangdi and develops a fluvial stream on the north China plain, which is indeed created by the river sedimentation. The stream, with a normal flowing width of only about 500 m, creeps within a 5–25 km wide river valley, defined by the grand levees.

The wandering channel was observed at many hydrological stations and measurements of the riverbed were performed at numerous cross sections. Table 5.5 lists the river motion distances at these sections and hydrologic stations. Table 5.5 illustrates that the maximum distance of the river motion is over 8 km and the motion distance in one year is over 5.6 km. The local farmers told the authors that the speed of the river motion could be as high as 100 m/day. A farmer watched his bicycle on the bank falling into the flowing water and had no time to rescue it when the flow assaulted the bank.

To stabilize the river channel, the local people have built many spur dikes along the main stream, like the Jiabu spur dyke built in 1973. Nevertheless, many of the spur dikes do not work well because the river channel moved far away from them after the spur dikes were completed. Figure 5.49(a) shows the spur dike at Kaiyi, a short distance upstream from Zhengzhou (Huayuankou). The spur dike controlled the river channel for a short period of time, then the channel migrated away from the spur dike, as shown in Fig. 5.49(b).

A wandering river is difficult to train. The capacity for channel motion is due to the high concentration of sediment and the unsteady discharge and unsteady sediment-carrying capacity. With regulation of the discharge and trapping of sediment by reservoirs, especially the recently completed Xiaolangdi Reservoir, both the unsteadiness and the sediment load released into the lower Yellow River have reduced. Therefore, the speed of channel migration will decrease.

Table 5.5   Migration of the lower Yellow River channel (Hu et al., 1998)

Cross Section	Average Wandering Distance (m)	Channel wandering Distance (m)	Maximum Distance of Channel Motion (m)		Maximum distance of channel motion in a year (m)	
			1955–1974	1975–1994	Right	Left
Tiexie	206	10–760	2,470	1,075	50	760
Xiagujie	507	5–2,000	3,620	2,060	1,220	2,000
Huayuan town	520	0–2,295	3,990	2,770	2,295	1,630
Mayugou	860	60–2,280	3,925	2,895	2,280	2,250
Peiyu	854	30–3,370	3,530	4,140	3,370	3,100
Luohe mouth	1,242	50–5,660	8,040	3,080	5,180	5,660
Gubaizui	468	50–1,250	1,470	1,180	1,250	1,230
Luocunpo	1,397	20–4,695	6,190	6,115	4,695	3,360
Guanzhuangyu	657	10–2,420	2,500	2,680	1,650	2,420
Qinchang	786	100–4,230	4,740	1,270	4,230	2,270
Huayuankou	873	40–3,980	4,080	2,375	3,980	2,330
Babao	1,249	50–4,100	4,000	3,670	4,100	3,800
Laitongzhai	923	10–3,440	3,950	2,030	3,440	3,130
Xinzhai	1,201	5–3,640	4,090	3,125	3,480	3,640
Heishi	1,375	30–4,570	5,650	7,750	4,570	3,925
Weicheng	1,784	5–5,130	6,010	4,965	5,130	4,380
Heigangkou	722	10–3,740	2,090	3,905	3,740	2,945
Liuyuankou	790	50–2,645	2,240	2,730	2,270	2,645
Gucheng	1,685	90–5,640	6,350	5,655	5,640	4,980
Caogang	602	0–1,800	2,000	1,380	1,790	1,800
Jiahetan	444	20–1,540	1,640	1,705	1,540	1,200
Dongbatou	594	6–2,780	3,050	890	2,450	2,780
Shanfang	909	30–3,100	5,570	1,285	2,560	3,100
Youfangzhai	1,270	20–3,470	4,800	5,790	3,080	3,470
Mazhai	669	0–3,000	3,350	2,630	3,000	1,680
Yangxiaozhai	854	35–2,820	3,020	3,630	2,820	2,160
Hedao village	488	10–1,410	2,710	2,350	1,410	1,200

(a)   (b)

Fig. 5.49   (a) The Kaiyi spur dike constructed on the lower Yellow River to stabilize the river channel; (b) The river moved far away from the dike only a few years after the spur dike was completed (See color figure at the end of this book)

5.3.5 Anastomosing Rivers

Anastomosing rivers are usually formed by avulsions, i.e., flow diversions that cause the formation of new channels on the floodplain. As a product of avulsion, anastomosing rivers essentially form in two ways: ① by formation of bypasses, while bypassed older channel-belt segments remain active for some period; and ② by splitting of the diverted flow, leading to contemporaneous scour of multiple channels on the floodplain. Both genetic types of anastomosis may coexist in one river system, but whereas the first may be a long-lived floodplain-wide phenomenon, the latter only represents a stage in the avulsion process on a restricted part of the floodplain. Long-lived anastomosis is caused by frequent avulsions and/or slow abandonment of old channels.

Avulsions (a kind of channel motion, which is discussed in Section 5.9.2) are primarily driven by aggradation of the channel belt and/or loss of channel capacity by in-channel deposition. Both processes are favored by a low floodplain gradient. Also of influence are a number of avulsion triggers such as extreme floods, log and ice jams, and in-channel aeolian dunes. Although some of these triggers are associated with a specific climate, the occurrence of anastomosis is not. A rapid rise of base level is conductive to anastomosis, but is not a necessary condition.

An anastomosing river is not very stable. If one of the parallel channels is scoured deeper all water may flow in this channel and abandon the others. Finally the anastomosing channels can change into a single thread channel. The lower part of the abandoned channels remain connected with the main channel and become channel-shape river connected lakes. Figure 5.50(a) shows the anastomosing channels of the Mudan River in northeast China, in which the abandoned old channels are still visible. Figure 5.50(b) shows the Hulan River near Harbin, which is a tributary of the Songhua River. The river had many anastomosing channels, but now most of the channels have been abandoned. The main part of the river has become a single thread, more or less meandering channel. The abandoned channels have separated or remain connected with the river, and some of them have become isolated or river-connected lakes. These lakes are different from the oxbow lakes resulting from development of a meandering river in shape and origin. Ice jam floods may be the main cause for development of anastomosing rivers. As a river channel

(a)   (b)
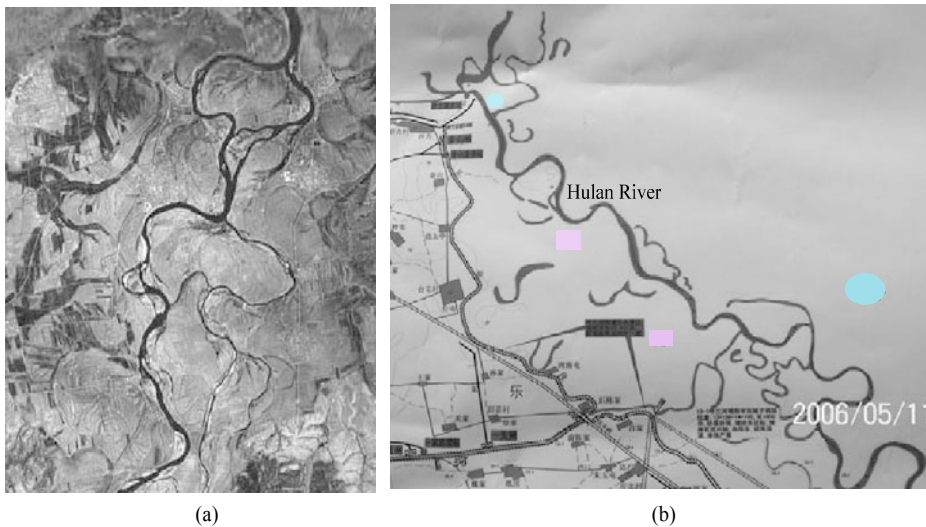
Fig. 5.50 (a) Anastomosing channels of the Mudanjiang River in northeast China; (b) The Hulan River near Harbin was an anastomosing river with many channels and is now a single thread, more or less meandering channel; Many isolated lakes are left after the anastomosing process

is blocked by a ice jam, the water stage rises, and the flooding water has to find a new channel. The new channel extends downstream and finally meet the original channel at a downstream point. Thus, a net of anastomosing channels develop. Ice jam floods occur very often in northeast China. This theory may explain why there are many anastomosing rivers in northeast China but very few in other areas in China.

5.3.6 Avulsion

Avulsion is a kind of non-continuous channel motion. Avulsion was defined by Allen (1965) as the abandonment of a part or the whole of a channel belt by a stream in favor of a new course. Avulsion is an inevitable result of river aggradation and is, therefore, closely related to the sediment load the stream carries. Avulsions are classified into nodal and random avulsions (Leeder, 1978). If, over time, more than 2 avulsions occur at approximately the same location this is called nodal avulsion. Random avulsion can occur from any point along the active channel belt. Field (2001) studied the channel avulsion on alluvial fans in southern Arizona. Channel avulsion invariably occurs where bank heights are low and often at channel bends. The action of aggradation during floods is critical in the avulsion process since the greatest amount of overland flow is generated where bank heights are lowest.

Avulsion is perhaps a final aspect of river behavior and concerns the large-scale movement of the river course. The process occurs in meandering, braided, and wandering rivers and is recorded by abandoned channel belts preserved on floodplains. The periodicity of avulsion appears to be on the order of 100–1,000 years. The diversion is actually gradual but can be considered instantaneous compared with the recurrence time of avulsions. Avulsions are common only where the streams are aggrading relative to their floodplain. In heavy sediment-laden rivers avulsion becomes the dominant mechanism of channel shifting on alluvial fans and river deltas.

Sediment-laden rivers undergo periodic shifts. Avulsion occurred in the Mississippi River Delta along the coast of Louisiana as successive channels searched for gradient advantages over their precursors (Leeder, 1983). The same story has occurred for the Kosi River in India. From 1730–1960, the Kosi River combed the Kosi River fan from east to west at a frequency of one avulsion per 23 years with the nodal apex around Jogbani (Gole and Chitale, 1966). Major avulsions or changes in channel direction and form occur regularly, particularly in semiarid areas and even in humid regions, during catastrophic, rare floods. A single rainstorm of 3 days duration in California in 1938 produced as much as 189 m^3/km^2 of sediment, primarily from cultivated land, and initiated about 700 new channels on an area of 162 km^2 (Leopold et al., 1964).

Slingerland and Smith (1998) studied the necessary conditions for a meandering river avulsion. They presented a 1-D model and showed that whether a crevasse heals, runs away to an avulsion, or reaches a steady state depends upon the ratio of crevasse to main-channel bed slopes, the height of the crevasse bottom above the bed of the main channel, and the bed grain size. For fine to medium sand, crevasse slopes greater than about eight times the main channel slope are predicted to capture all the main flow. The Yellow River carries sediment from the Loess Plateau in central China to the delta and caused the delta to expand by 2,000–3,000 ha per year in the period from 1855 to 1985. The extension of the river channel reduces the gradient and capacity of the channel resulting in avulsions. The length of the new channel is about 1/3–1/2 of the previous one and the gradient is 2–3 times higher.

As a comparison, the Mississippi River, transporting 240 million tons of sediment annually, extends into the Mexico Gulf at a speed of 150 m/year, and shifts its course once per 1,000 years (Fisk, 1944). The Danube River, carrying a much smaller sediment load, is quite stable with a frequency of channel shift once per 2,300 years (Panin et al., 1983). The Fraser River in Canada shifted its course in 1827, 1864, 1892, 1896, 1900, and 1912, with a frequency of about once per 17 years (Clague et al., 1983). The Po River in Italy shifted its delta channel 6 times in the past 3,000 years, about once per 500 years (Gandolfi

et al., 1982). The Gediz River in Turkey shifted 6 times in the last 10,000 years, with a frequency of about once per 1,600 years. The latest shift of the river occurred in 1980, and since then the river flows in the present channel, the Kirdeniz River (Aksu and Piper, 1983). The frequency of avulsion of the Rhine-Meuse River is very low because the river carries much less sediment load. Stouthamer (2001) studied the avulsions in the Holocene Rhine-Meuse Delta. Five avulsions occurred in the Rhine-Meuse Delta from about 6,500 yr BP to 1950 yr BP, when the Rhine-Meuse Delta experienced aggradation. The frequency of avulsion is about 1/800 years.

At present, an avulsion is occurring on the Mississippi River. Since the 1930s, the river gradually began shifting to the Atchafalaya River. Since 1950s the avulsion has been stopped by human hydro structures, which control the flow into the Atchafalaya at 1/3 of the discharge with 2/3 of the discharge remaining in the old Mississippi River channel to guarantee sufficient channel depth for navigation.

5.4   New Approaches

5.4.1   Rate of Bed Load Transport in Mountain Streams

Bed load motion in mountain streams is very complex and the bed load formulas available, including the formulas proposed by Meyer-Peter-Mullër, Einstein, Bagnold, Engelund and Yalin, are not applicable in many cases. Since the 1970s, researchers tested, analyzed and compared these formulas with measured data from mountain streams. The difference between the calculated and the measure rate of bed load transport were as large as on several orders of magnitude. It is because the disagreement of the bed load formulas and data that research on bed load transport theories and computing methods have never been stopped.

Barry et al. (1997, 2006) used bed load transport data measured from 24 gravel bed rivers in Idaho to compare the accuracy of eight different formulas and the results of this analysis showed substantial differences in performance of these formulas. Bathurst et al. (1987) tested the validity of bed load formulas for mountain rivers, and found that the Shields approach (based on constant dimensionless shear stress) failed for slopes $S \geqslant 0.01$ and the ratio of water depth/median diameter $\leqslant 10$.

The measured rate of bed load transport in mountain streams is sometimes much lower, or sometimes much higher compared with the calculated values from the bed load formulas. Carson and Griffiths (1987) evaluated the validity of bed load formulas using time-averaged transport measurements available for the Waimakariri River and other gravel-bed rivers in New Zealand. In particular, they focused on the ability of bed load equations, including the Bagnold formula, to estimate transport in braided rivers. They concluded that bed load formulas often under-predict transport rates by several orders of magnitude.

Martin (2003) evaluated the original and revised versions of the Bagnold formula, the Meyer-Peter-Mullër formula and a stream power correlation formula based on the data from Vedder River, a mountain stream in British Columbia. From the evaluations Martin found the formulas under-predict gravel transport rates by orders. Bagnold formula generally over-predicted bed load transport rates for braided rivers that were in equilibrium or aggrading. The Vedder River is situated on an aggrading alluvial fan, yet the original Bagnold formula under-predicted transport rates in the braided reaches.

Yu et al. (2009) measured the rate of bed load transport in the Diaoga River in Yunnan Province of southwestern China with a double-box sampler. The outer box was buried under the stream bed with the top edges of the box even with the local bed surface. Bed load particles were trapped, weighed and analyzed with sieves. Figure 5.51 shows the measured rate of bed load transport per width as a function of stream power, P, and the Shields dimensionless shear stress, Θ. For the same P or Θ, the rate of bed load transport varied with a range of three orders of magnitude. It also clearly shows that the rate of bed load transport before the first flood was 100 times higher compared with the rate after the flood.
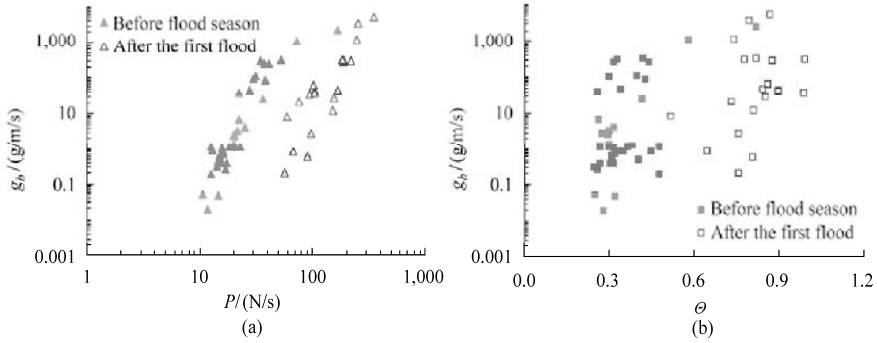
Fig. 5.51 Measured rate of bed load transport per width in the Diaoga River in 2007: (a) as functions of stream power P; and (b) as a function of Shields dimensionless shear stress Θ

Figure 5.52 shows measured rate of bed load transport as a function of flow discharge per width in 2006 and 2007. The rate of bed load transport differed by up to 1000 times for the same flow rate. Considering the sediment size and bed gradient were almost the same the great difference in the rate of bed load transport implies that the bed load transport in the stream can not be calculated with any formula based on the relation of bed load motion with water flow.
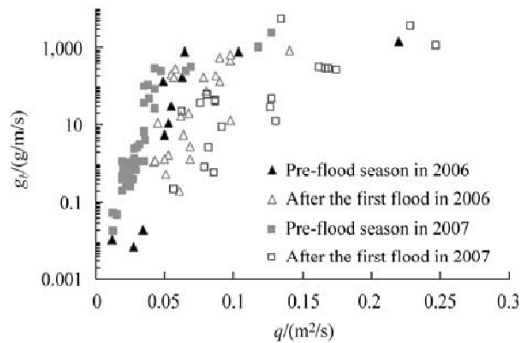
Fig. 5.52 Rate of bed load transport versus water discharge per width

Bed load motion in mountain streams is a complex process, which is influenced by many factors. Among these factors the incoming sediment load and bed structures are the most important. In Chapter 4 the bed structures, including cluster, ribbing structure and step-pools are discussed. These structures consume flow energy and prohibit sediment particles to be initiated from the bed. Moreover, the structures may be buried and the bed may be flattened if the incoming bed load is high. It is because the changing bed structure and varying incoming bed load the rate of bed load transport varies in several orders under the same flow conditions. Therefore, none of the bed load formulas can be used to calculate bed load transport, because these formulas were developed based on data from lab experiments with uniform sediment and simple boundary conditions.

To study the influence of bed structure and incoming bed load an experiment was carried out in the Diaoga River during non-flood season. Sediment was fed at a cross section 22 m upstream from the measurement section. The bed slope of the experimental reach was 0.05. During the experiment, the flow discharge ranged from 0.09 to 0.126 m^3/s. There was very low sediment transportation under the natural conditions due to a bed structure of cobbles clusters. Less than 1 kg of bed load were collected in 2 hours.

The median diameter of the bed sediment was about 60 mm and the median diameter of bed load was only 3 mm. The flow energy was dissipated by stream bed roughness, as shown in Fig.5.53 (a).

Sediment was taken from the flood plain of the stream and sieved into four groups: $D<2$mm, 2–5mm, 5–15mm and 15–42mm. The four groups of sediment were fed into the stream. The sediment was transported through the experimental reach and the bed structure was buried, as shown in Fig. 5.53(b). The bed roughness was greatly reduced and the energy consumption by the bed roughness was less than that of the stream power. A lot of bed load particles were initiated to move and collide with the bed to balance the extra stream power. The rate of bed load transport was measured at the measurement section.

(a)   (b)
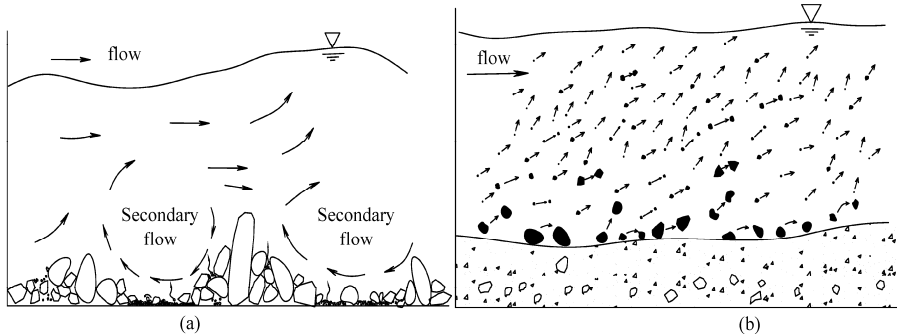
Fig. 5.53   (a) Almost no bed load motion under the natural conditions with a bed structure developed; (b) Incoming bed load buried the bed structure and intensive bed load motion occurred

Figure 5.54 show the process of sediment feeding at constant rates (rectangular pulses) and measured rate of bed load transportation for particle size groups of 2–5 mm and 5–15 mm (points and curves). The sediment of 2–5 mm was transported as bed load, which buried the bed structures and flattened the bed. This caused an intensive bed load motion to occur on the bed and approximately 35 min later the sediment moved to the measurement section and the measured bed load abruptly increased from nearly zero to a peak of 18 kg/min. The feeding of sediment of 5–15 mm also caused intensive bed load motion. Approximately 90 minutes after this intensive motion the bed load moved to the measurement section and the rate of bed load transportation increased from nearly zero to a peak of 7 kg/min. The integration of the measured bed load transportation curves was almost equal to the total feeding amounts for the two groups of sediment. The feeding of sediment of 15–42 mm did not cause intensive bed load motion. Most of the particles piled on the bed and there was no obvious increase in the measured bed load motion. Moreover, big particles piled on the bed, which created new resistance in the bed and, thus, further increased the bed roughness. It is only during flood season these particles can be transported along the channel.

Figure 5.55 shows the size distributions of sampled bed load sediment under natural conditions, feeding sediments of 2–5 mm and 5–15 mm, and the bed material of the channel. There is a critical diameter: sediment finer than the critical diameter may be transported through the channel. During the transportation the sediment buries the bed structure and changes the bed roughness. The portion of flow energy consumed on form drag reduced greatly and portion of flow energy for bed load transportation increased greatly. All incoming such fine bed load particles may be transported through the channel. The rate of bed load transport depends on the incoming amount rather than the flow intensity. Such a part of bed load is named travelling bed load. The critical diameter is defined as D_{b20}, where D_b represents the size of sediment on the surface of the channel bed. The critical diameter for the Diaoga River is about 15 mm.
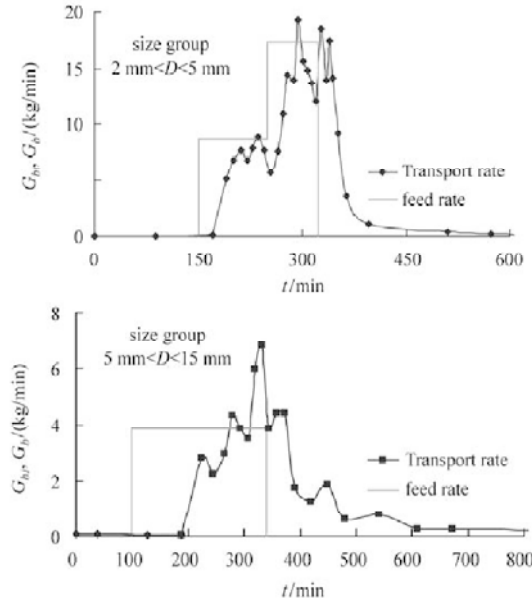
Fig. 5.54 Feeding and transportation processes of 2–5 mm and 5–15 mm sediment: Rectangular pulse—feeding rate; Points—measured rate of bed load transportation

The sediment coarser than the critical diameter can only be transported during the flood season. The particles stop motion and form mutually interlocking structures after the flood season. These particles of different sizes play different roles in the bed structures. Boulders and big cobbles are key stones in the bed structures and other particles surround these key stones. The particles larger than D_{b20}, are named structure bed load.
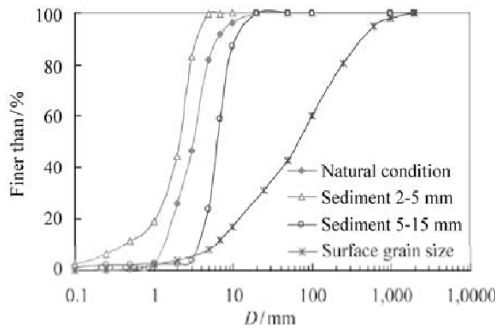
Fig. 5.55 Size distributions of feeding sediments and sediment on the bed surface before the experiment

The bed structure is dynamic during the experiment. A stronger bed structure results in a greater amount of flow energy consumption and thus resulting in a lower bed load transport rate. In Chapter 3 the development degree of bed structure S_p was introduced and measured with a specially-designed instrument. The value of S_p was measured before and during the experiment, and in the meantime the rate of bed load transport was measured. Figure 5.56 shows the ratio of the rate of bed load transport over the unit stream power, g_{b*}, as a function of the corresponding development degree of bed structure, S_p. The

value of S_p reduced to its minimum value when the rate of travelling bed load transport reached its peak. The bed structure gradually recovered and the value of S_p increased again after the feeding stopped. Following the increasing S_p more flow energy was consumed on the bed structure and the rate of bed load transportation decreased.

For the bed load motion in mountain streams the stream power, the bed structure and the rate of incoming bed load are the most important factors. A bed load formula may be expressed in the following form:

$$g_b = f(p, S_p, g_{bi}) \tag{5.61}$$

in which g_b is the rate of bed load transport per width; $p = \gamma q J$ is the unit stream power (stream power per width), in which q is unit flow discharge, J the energy slope; S_p is the development degree of bed structures; and g_{bi} is the incoming rate traveling bed load. The formula can not be established by normal laboratory experiments because the bed structure development can not be simulated in normal flumes. The formula may be established through experiments and measurements in mountain streams.
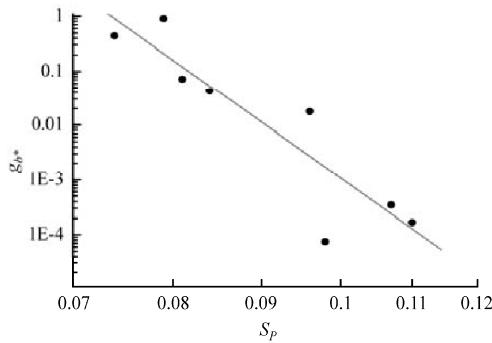
Fig. 5.56 Dimensionless rate of bed load transport as a function of the development degree of bed structure

5.4.2 River Motion Dynamics

5.4.2.1 River Motion

Flow and sediment transportation in a river always are unsteady and non-uniform, and, the river channel adjusts itself to fit the varying flow and sediment conditions. The adjustment of the channel is a kind of motion of the channel. If a section of river channel and the sediment-laden flow within it are treated as a moving body, the fluvial process is then the result of the motion of the deformable body, which is called river motion. The patterns of river motion are aggradation, degradation, widening, translation, rotation, wandering, bifurcation, and migration from one channel to another channel. Aggradation and degradation are vertical movement and the rest are horizontal movements. Avulsion and shifting of the channel are non-continuous motion and the rest are continuous motions (Wang et al., 1997). River motion dynamics studies the laws of river motion under the action of the unsteady river flow, which differs from the traditional mechanics of sediment movement. The latter studies the movement of sediment particles and the former studies the motion of the river channel in the space of the sediment deposit.

Wang and Wu (2001) studied unsteady flow in fluvial rivers, especially wandering rivers, and proposed a so-called river motion dynamics, which provides a new approach to fluvial processes. In their studies, the capacity of the flow to move sediment from one place to other places within a river section is called **sediment-removing capacity**. This differs from the well-defined **sediment-carrying capacity**. For instance, steady flow carries sediment through a reach of a fluvial river channel, but does not cause a considerable

volume of sediment to be scoured or deposited. The sediment-removing capacity of the flow is nearly zero in this case, but the sediment-carrying capacity may be high. The speed of motion of a river channel depends on the sediment-removing capacity of the flow. The higher the sediment-removing capacity, the faster the river channel moves.

The speed of channel motion depends not only on the sediment-removing capacity of the flow but also on the composition of the bed and bank material, which is characterized by the bed inertia (Wang, 1999). If the bed material is liable to be removed, or exhibits low bed inertia, the riverbed is quickly deformed to fit the changing discharge when a high flood occurs. On the other hand, if the inertia of the riverbed is high and the flow discharge sharply increases or decreases, the bed sediment cannot be quickly scoured and the channel does not move so much. For a given river section, if the sediment-removing capacity can be measured or calculated directly, the speed of motion of the channel can be obtained.

The channel motion is also controlled by restrictions of hardened banks and human built structures, like groins and spur dykes. In a channelized river or an artificial canal, considerable channel motion does not occur because there is no space for the channel to move. Therefore, the intensity of channel motion is a function of the sediment-removing capacity, riverbed inertia, and restriction caused by banks and human structures.

$$R_s = f(R_s^*, I_b, Bs) \qquad (5.62)$$

where R_s is the intensity of channel motion, R_s^* is the sediment-removing capacity of the flow, I_b is the riverbed inertia and Bs represents the restriction of hardened banks and human structures. The higher the sediment-removing capacity of the flow and the smaller the riverbed inertia, the higher will be the intensity of channel motion. The parameter of hardened banks and human structures, $Bs,$ confines the space of the channel motion.

The equation of motion (5.62) has not been developed and intensive work is needed to construct the equation of motion and validate it with sufficient data. In the following sections the work done by Wang and his colleagues on the intensity of channel motion, sediment-removing capacity, and riverbed inertia are presented, from which researchers may draw their inspiration for continued development of the subject.

5.4.2.2.　Sediment-Removing Capacity

Channel motion is a result of sediment deposition, bed scour, and bank erosion. The intensity of channel motion is defined as follows:

$$R_s = \frac{V_{scour} + V_{dep}}{LT} \qquad (5.63)$$

where R_s is the intensity of river motion, V_{scour} and V_{dep} are the sediment volumes scoured from the bank or the bed and deposited in the channel in the time period, T, respectively, L is the length of the measured river section, and T is the time interval of the measurements. In many cases the cross sections of the Chinese rivers are measured once a year, thence $T=1$ year. The measured R_s depends on the frequency of the measurement because the river motion in many cases is reciprocating.

Generally, channel motion is realized by bank erosion on one side and deposition on the other side of the channel, or vice versa. The speed of the channel motion is then given by

$$U_c = \frac{R_s}{2h} \qquad (5.64)$$

in which U_c is the speed of channel motion, and h is the depth of the channel. If the intensity of river motion is known, the speed of river motion can be calculated using Eq. (5.64).

If there is no restriction due to human structures, the intensity of river motion may reach its maximum

value, which is called sediment-removing capacity of the flow and is denoted as R_s^*. If the measurement frequency is high and the restriction of hardened banks and human structures are far from the channel, the measured R_s is equal to the sediment-carrying capacity.

The sediment-removing capacity is different from the well-defined sediment-carrying capacity. The sediment-carrying capacity is a feature of the mean flow, but the sediment-removing capacity is a feature of unsteady, non-equilibrium flow. The sediment-carrying capacity explains how much sediment load the flow can transport through the channel, while the sediment-removing capacity represents the capability of the flow to change the channel shape. The mathematical expression of the sediment-removing capacity is given as

$$R_s^* = R_{s\,max} = \left(\frac{V_{scour} + V_{dep}}{LT}\right)_{max} \tag{5.65}$$

In the period of 1979–1985 river motion was detected and measured at 12 cross sections in a 141 km long reach of the lower Yellow River near the Huayuankou (Zhengzhou) hydrological station with a frequency of 2 times a year. The volume of sediment removed is calculated from the measurements of the cross sections. Figure 5.57 shows the erosion and deposition at the Qinchang cross section, which illustrates the channel motion. The river channel moved to the right about 500 m from May to Oct. 1984 and moved back from Oct. 1984 to May 1985.
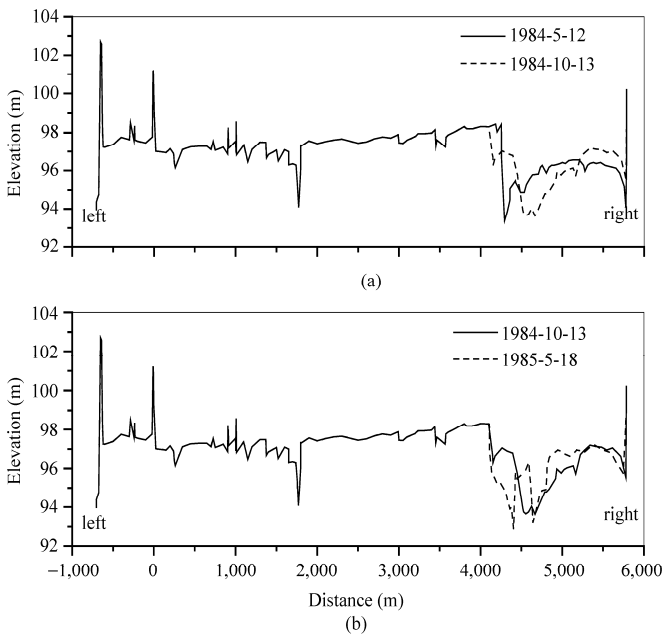
Fig. 5.57 Channel motion as a result of bank erosion, bed scour and sediment deposition at the Qinchang cross section (lower Yellow River near Zhengzhou): (a) the thalweg of the channel moved northward by about 500 m from May to October 1984. (b) The channel moved back in the period October 1984-May 1985

Table 5.6 presents the volumes of deposition and scour along the 141 km long channel, which are calculated by summing up for the 12 cross sections the products of the areas of the cross sectional changes (deposition and erosion) multiplied by the half way distances upstream and downstream. The intensity of channel motion calculated with the measured volumes of deposition and erosion is given in

the table. The flow discharge is a random process and is expressed as the sum of mean discharge, Q_m, and fluctuating discharge, Q':

$$Q(t) = Q_m + Q'(t) \tag{5.66}$$

The mean flow discharge, Q_m, mean sediment discharge, Q_{sm}, and the root-mean-square of the flow and sediment discharges, Q_{rms} and $Q_{s\text{-}rms}$, respectively are also listed in the table, which are defined by

$$Q_{rms} = \left[\frac{1}{T} \int_0^T (Q(t) - Q_m)^2 \, dt \right]^{1/2} = \left[\frac{1}{T} \int_0^T Q'(t)^2 \, dt \right]^{1/2} \tag{5.67}$$

$$Q_{s\text{-}rms} = \left[\frac{1}{T} \int_0^T (Q_s(t) - Q_{sm})^2 \, dt \right]^{1/2} = \left[\frac{1}{T} \int_0^T Q_s'(t)^2 \, dt \right]^{1/2} \tag{5.68}$$

where Q_s is the sediment discharge, Q_s' is the fluctuating sediment discharge, and Q_{rms} is the mean sediment discharge, Q_{rms} and $Q_{s\text{-}rms}$ are called the fluctuation intensities of the flow discharge and sediment discharge, respectively. The fluctuation intensity is on the same order or even larger than the mean values, demonstrating the flow is highly unsteady.

Table 5.6 Intensity of channel motion and fluctuation of flow discharge for the lower Yellow River near Zhengzhou

Time	V_{scour} $(10^6 m^3)$	V_{dep} $10^6 m^3$	$V_{scour} + V_{dep}$ $(10^6 m^3)$	Q_m (m^3/s)	Q_{rms} (m^3/s)	Q_{sm} (t/s)	$Q_{s\text{-}rms}$ (t/s)	R_s (m^2/yr)
1979.10 −1980.10	150.1	120.4	270.5	975.9	591.9	19.47	33.97	1907.8
−1981.10	219.4	193.9	413.3	1518.6	1703.4	41.87	70.59	2915.1
−1982.10	211.0	183.1	394.1	1330.5	1337.2	19.97	47.07	2779.7
−1983.10	227.2	239.1	466.3	1824.9	1506.7	26.7	39.30	3288.9
−1984.10	249.2	233.0	482.2	1402.2	1805.2	29.01	46.64	3401.0
−1985.10	256.6	194.0	450.6	1767.2	1501.2	24.9	47.60	3178.2

Note: The length of channel section of the measurements is 141.78 km, from the cross section at Guanzhuangyu to the cross section at Dongbatou.

Analysis of the data reviewed that the intensity of channel motion is proportional to the square root of Q_{rms}:

$$R_s = m\sqrt{Q_{rms}} \tag{5.69}$$

in which R_s is in m²/yr and Q_{rms} in m³/s, and m is a function of composition of bed sediment and constraint factor for channel motion.

The motion of the river channel is reciprocating because the motion is caused by the fluctuation of the flow discharge and the fluctuation is reciprocating. Some high frequency movement of the channel is not reflected in the measured values in Table 5.6, therefore, the measured R_s is smaller than the sediment-removing capacity, but it may be assumed proportional to the sediment removing capacity, given in the following formula:

$$R_s^* = kR_s \tag{5.70}$$

where k is a constant factor for a given river. Because the sediment-removing capacity results from the fluctuation of discharge, the factor, k, can be determined by the analysis of the spectrum of the discharge fluctuation. Using the daily-average discharge and performing an analysis of the spectrum of the discharge fluctuation, Wang et al. (1997) concluded that if the intensity of channel motion is measured with a measurement frequency of once a year the constant, k, is equal to 2 for the lower Yellow River.

5.4.2.3   Riverbed Inertia

Wang (1999) found from experiments that the riverbed deformation obviously lags behind the variation of flow and sediment carrying capacity. If the riverbed scour by flows is regarded as a kind of accelerating motion of the bed, the sediment carrying capacity of the flow is a "positive force" and the incoming sediment rate is a "negative force", and the idleness toward motion can be thought of as "inertia" of the bed. The "positive force" causes bed scour whereas the "negative force" causes siltation. Only if the "positive force" is balanced by the "negative force", the river bed does not change. For an open channel flow within hardened banks erosion and sediment deposition can only occur on the channel bed, and the equation of the bed motion can be expressed as

$$-I_b \frac{dZ}{dt} = g_{b*} - g_b \qquad (5.71)$$

in which Z is bed elevation, $-dZ/dt$ is the rate of bed degradation due to scour, I_b is called riverbed inertia, g_b is the rate of bed load transport, and g_{b*} is the bed load carrying capacity of the flow, or the rate of bed load transport by the flow when in equilibrium. Because the dimensions of g_b and $-dZ/dt$ are [Mass/(Time× Length)] and [Length/Time], respectively, the dimension of inertia of the bed is [Mass/Length^2].

For a flow carrying less sediment than its sediment-carrying capacity, channel bed scour occurs. The scour rate, S_r, is defined as the weight of sediment scoured from the bed per unit area per time, i.e.

$$S_r = W_s / A_b T_s \qquad (5.72)$$

where W_s is the weight of sediment scoured from the river bed, A_b is the area of channel bed subject to scour, and T_s is the time of scour. Scour occurs in unsteady flow and non-equilibrium sediment-laden flow. If a flow is stable and uniform, the sediment and flow are in equilibrium and the scoured sediment is balanced by the depositing sediment, which yields a zero scour rate. Wang (1999) has obtained an empirical formula for the scour rate under both conditions of clear water flow and sediment-laden flow. The rate of bed degradation is a function of the scour rate as follows:

$$-\frac{dZ}{dt} = \frac{S_r}{\gamma_s(1-p)} \qquad (5.73)$$

in which p is the porosity. Combining Eq. (5.73) with Eq. (5.71) yields a relation between the riverbed inertia and scour rate, which may be regarded as the definition of the riverbed inertia:

$$I_b = \frac{g_{b*} - g_b}{-dZ/dt} = \gamma_s(1-p)\frac{g_{b*} - g_b}{S_r} \qquad (5.74)$$

in which $\gamma_s(1-p)$ represents the dry weight of the bed material. For a given composition of bed material, the bed inertia should be a constant. Therefore, for different values of g_{b*} and g_b, calculation with the equation yields the same I_b value. Indeed, experimental results obtained by Wang (1999) showed that the values of inertia for each bed composition under different flow conditions and feeding rates of sediment load are the same. This proves that the river bed inertia is a physical property of the granular bed.

A small bed inertia implies that the bed deforms quickly with the change of flow and its capacity. If the bed inertia is large, the bed is slow to or does not respond to the flow changes, and it takes a long distance for the transport rate g_b to reach its equilibrium g_{b*}. If the bed material is composed of a wide range of sediment sizes, the inertia of the bed is large because an armoring layer will develop during the erosion process. In the experiments with sediment with a sorting coefficient larger than 15, the bed inertia is between 45 and 50 t/m^2. For mountain rivers, the bed material usually has a large sorting coefficient and the bed inertia can be roughly taken as 50 t/m^2 for convenience of calculation (Wang, 1999). For a riverbed composed with light grains, such as coal or other materials with small specific weight, the bed inertia is small. It seems that the inertia is proportional to the specific weight ratio $(\gamma_s - \gamma)/\gamma$.

Because only one kind of light grains has been tested a final conclusion can only be worked out after more experiments with various light bed materials are done.

There is still a lot of work to do to understand riverbed inertia and its application in fluvial processes. For a simple application I_b is introduced into the Exner equation and the partial differential equation is changed into a normal differential equation. The variation of bed elevation is related to the spacious variation of the sediment transport rate by the well-known Exner sediment-continuity equation

$$\frac{\partial g_b}{\partial x} + \gamma_s(1-p)\frac{\partial Z}{\partial t} = 0 \tag{5.75}$$

If g_b is smaller than the capacity g_{b*} the channel bed is scoured. Substituting Eq. (5.74) into (5.75) yields

$$\frac{dg_b}{dx} = \gamma_s(1-p)\frac{g_{b*}-g_b}{I_b} \tag{5.76}$$

The equation can be solved as follows

$$\frac{g_{b*}-g_b}{g_{b*}-g_{b0}} = \exp\left[-\gamma_s(1-p)\frac{x}{I_b}\right] \tag{5.77}$$

in which g_{b0} is the transport rate at $x=0$. The equation shows that if the bed inertia is large, the exponent is small and the flood has to travel a long distance for the transport rate to reach equilibrium. For instance, the bed load of mountain rivers has a large riverbed inertia, hence, the transport rate is often much less than the capacity. For a straight, plain riverbed composed of relatively uniform sand, the inertia is small and the transport rate responds to the flow variation quickly, therefore, the bed deforms following the rising and receding of floods.

The exponent in Eq. (5.77) is a dimensionless number,

$$A_r = \frac{\gamma_s(1-p)L_s}{I_b} \tag{5.78}$$

in which L_s is a specific length and can be represented by the distance that the flood travels in a channel with uniform flow and boundary conditions. The dimensionless number represents the ability of the channel to respond to the variation of the flow. The larger is the dimensionless number, the quicker the channel deforms following the flow variation.

5.4.3 Water-Sediment Chart

The Water-Sediment Chart is a diagrammatic expression of the distribution and variation of water and sediment load of a river in a period of time. The significance of the chart is discussed with the Yangtze River as an example. Figure 5.58 shows the water-sediment charts for the four main hydrological stations, i.e. Pingshan, Yichang, Hankou, and Datong Stations, along the main course of the Yangtze River. The long-term average ratio of sediment to water is 0.479 kg/m³ at Datong, which is the station between the river and the estuary. Then, the chart is drawn with the horizontal axis as the time of measurement, the left vertical axis as the annual water and the right vertical axis as the annual sediment load. Make the scale of the sediment load equal to the annual water volume with the sediment/water ratio, or 0.479 kg of sediment equal to 1 m³ of water. If the sediment curve is higher than water curve, the area between the two curves is black and represents an over load of sediment for the flow to carry into the ocean. If the water curve is higher than the sediment curve, the area between the two curves is gray and represents more water than is needed to carry sediment into the ocean.

At Pingshan Station flow is low and sediment load is high, which means that the drainage area upstream from Pingshan station is a sediment yield area. From Pingshan to Yichang both flow and sediment load increase but sediment load increases much more than flow, thence, the black area becomes larger.
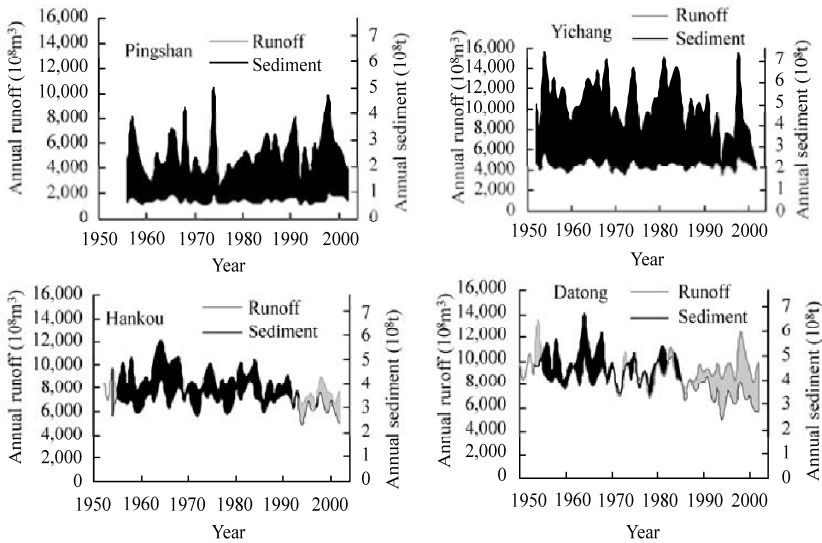
Fig. 5.58   Water-sediment charts of four main hydrological stations along the main course of the Yangtze River

From Yichang to Hankou, flow curve rises but the sediment curve decreases, which means a lot of sediment deposits in the reach between Yichang and Hankou. From Hankou to Datong, sediment load increases little but flow increases. The black area becomes very small and gray areas show up. Especially from 1980 to 2003, the sediment curve reduces below the flow curve and the black area changes into a gray area, which implies a trend of sediment reduction. The estuary is changing from a sedimentation area into an erosion area.

5.4.4   River Sediment Matrix

The river sediment matrix is composed of 3×3 components. The first row of the matrix represents sediment yield area—usually the upstream watershed, the second row means sediment transportation reaches—the river channel, and the third row stands for the sedimentation area—usually the delta and the estuary. The first column is sediment erosion from the local area, the second column means sediment transportation from upstream reaches, and the third column indicates sedimentation in the area.

For the Yellow River, the Loess Plateau is the main sediment yield area, therefore, the first row means the Loess Plateau, the second row represents the reach from Sanmenxia to Lijin, and the third row implies the sedimentation area in the estuary including the Yellow River delta and the river downstream from Lijin. Equation (5.79) is the Yellow River sediment matrix:

$$A_{\text{Yellow}} = \begin{pmatrix} 2.2 & 0.1 & 0.7 \\ 0.1 & 1.6 & 0.7 \\ 0.0 & 1.0 & 0.8 \end{pmatrix} \tag{5.79}$$

in which all the values are annual sediment amount in billion tons. The first row indicates that the annual sediment yield from the Loess Plateau is 2.2 billion tons, 0.1 billion tons of sediment are transported into the river from upstream areas, and 0.7 billion tons are deposited in the area. The second row shows that sediment erosion from the riverbed and banks in the reach between the Sanmenxia Dam and Lijin is 0.1 billion tons, 1.6 billion tons of sediment are transported into the reach from upstream reaches and 0.7 billion tons of sediment deposit in this reach. The third row shows that 1.0 billion tons of sediment are transported to Lijin from the lower reaches of the river and 0.8 billion tons of sediment are deposited in

the estuary and the neighboring coastal areas. It can be deduced that the remaining 0.2 billion tons is transported into the ocean.

For the Yangtze River the main sediment yield area is the drainage area between Panzhihua to Yichang, from Yichang to Datong is the sediment transportation channel, and from Datong to the river mouth is the estuary. Equation (5.80) is the Yangtze River sediment matrix:

$$A_{\text{Yangtze}} = \begin{pmatrix} 2.10 & 0.02 & 1.60 \\ 0.05 & 0.55 & 0.15 \\ 0.00 & 0.45 & 0.30 \end{pmatrix} \tag{5.80}$$

The explanation of the components is similar to that for Eq. (5.79).

Different rivers have different types of sediment matrix. For instance, a completely channelized river has a pseudo-diagonal matrix, because all sediment comes from upstream and is transported through the channel. There is no bank erosion and sedimentation on the channel bed.

$$\text{Sediment matrix for channelized rivers} = \begin{pmatrix} \otimes & & \\ & \otimes & \\ & \otimes & \otimes \end{pmatrix} \tag{5.81}$$

If the watershed is well-managed and there is no sediment yield from upstream reaches, the sediment-starved flow will scour the channel bed and banks, and waves and tidal currents will cause estuary erosion. In this case the sediment matrix becomes a lower triangular matrix, the Rhein River is an example of such a river.

$$\text{Sediment starved rivers} = \begin{pmatrix} \otimes & & \\ & & \\ \otimes & \otimes & \end{pmatrix} \tag{5.82}$$

Hyperconcentrated rivers have a matrix of the following type:

$$\text{Hyperconcentrated rivers} = \begin{pmatrix} \otimes & & \otimes \\ & \otimes & \otimes \\ & \otimes & \otimes \end{pmatrix} \tag{5.83}$$

The sediment matrix of the Yellow River is an example of this type.

River training engineering can be expressed with a matrix as well. For instance, a river suffering from delta erosion has the sediment matrix as follows:

$$A = \begin{pmatrix} 1 & 0 & 0 \\ 0 & 1 & 0 \\ 1 & 1 & 1 \end{pmatrix} \tag{5.84}$$

The inverse matrix of A is

$$A^{-1} = \begin{pmatrix} 1 & 0 & 0 \\ 0 & 1 & 0 \\ -1 & -1 & 1 \end{pmatrix} \tag{5.85}$$

Some engineering measures are taken to control coastal erosion in the estuarine area and make the river channelized. The sediment matrix after the training will be

$$\text{Channelized river matrix } B = \begin{pmatrix} 1 & 0 & 0 \\ 0 & 1 & 0 \\ 0 & 1 & 1 \end{pmatrix} \tag{5.86}$$

The engineering matrix is then

$$E = A^{-1}B = \begin{pmatrix} 1 & 0 & 0 \\ 0 & 1 & 0 \\ -1 & -1 & 1 \end{pmatrix}\begin{pmatrix} 1 & 0 & 0 \\ 0 & 1 & 0 \\ 0 & 1 & 1 \end{pmatrix} = \begin{pmatrix} 1 & 0 & 0 \\ 0 & 1 & 0 \\ -1 & 0 & 1 \end{pmatrix} \tag{5.87}$$

If the river sediment matrix is multiplied by the engineering matrix the river matrix will become the channelized river matrix, i.e.

$$AE = B \tag{5.88}$$

The engineering matrix has to be studied and physically explained.

Review Questions

1. Answer the following questions
   (a) What does "a 100-year flood" mean?
   (b) For an open channel flow, the depth is 1 m and the average velocity is 1m/s, calculate the Reynolds number and the Froude number. Is the flow laminar or turbulent? ($v = 10^{-6} m^2/s$) Is the flow supercritical (Fr>1) or subcritical (Fr<1)?
   (c) Explain the concepts of bed load, bed material load, suspended load, and wash load.
   (d) State the order of development of bed forms following increasing flow intensity.
   (e) What will happen if the bed configuration transforms from the lower regime into the upper regime?
   (f) What are the main features of hyperconcentrated flow?
   (g) What are the main river patterns?
   (h) State the features of meandering and straight rivers, basic conditions for development of braided, anabranching, wandering, and anastomosing rivers.
   (i) At what conditions may a meandering river transform into a wandering river?
   (j) What are the differences between sediment-carrying capacity and sediment-removing capacity of an open channel flow?
   (k) What is avulsion? Please give an example.
   2. A flood occurs in a river channel of irregular shape. The in-situ measurements give values of the average depth, $h = 2$ m, width, $B = 500$ m, the wet cross-sectional area, $A = 1,000$ m^2, and the energy slope, $J = 0.0001$. The bank roughness is $n_w = 0.025$. Calculate A_w, A_b, R_w, R_b, and the bed roughness, n_b.
   3. According to the minimum stream power theory, the morphology of fluvial rivers develops to reach the minimum stream power. Thus, the following equation is obtained:

$$\frac{dP}{dx} = \frac{d}{dx}(\gamma s Q) = \gamma\left(Q\frac{ds}{dx} + s\frac{dQ}{dx}\right) = 0$$

   (a) You are designing an irrigation canal. How can you design the canal slope? Please explain with the equation.
   (b) $dP/dx = 0$ can also be explained as constant stream power. What is your opinion, minimum stream power or constant stream power?
   4. Please describe the phenomena of hyperconcentrated flows. What are the main differences between hyperconcentrated flow and debris flow?
   5. Draw water-sediment charts for a river and explain the implications of the chart.
   6. For the Yangtze River the main sediment yield area is the drainage area between Panzhihua to Yichang, from Yichang to Datong is the sediment transportation channel, and from Datong to the river mouth is the estuary. The sediment matrix of the river is:

$$A_{\text{Yangtze}} = \begin{pmatrix} 2.10 & 0.02 & 1.60 \\ 0.05 & 0.55 & 0.15 \\ 0.00 & 0.45 & 0.30 \end{pmatrix}$$

Explain the physical meaning of the components of the matrix.

7. Why bed load formulas available, including the formulas proposed by Meyer-Peter-Mullër, Einstein, Bagnold, Engelund and Yalin, are not applicable to mountain rivers?

References

Aksu A.E. and Piper D.T.W., 1983. Progradation of the late quaternary dediz delta, Turkey. Marine Geology, 54(1/2), 1–25

Allen J.R.L., 1965. A review of the origin and characteristics of recent alluvial sediments. Sedimentology, 5, 89–101

Allen J.R.L., 1983. River bed forms: Progress and problems, in Modern and Ancient Fluvial Systems, Collinson, and Lewin. (eds.), Oxford, Blackwell, Special Publication of the International Association of Sedimentology

Bagnold R.A., 1956. Flow of cohesionless grains in fluid, Philos. Trans. actions, Royal Soc. of London, Series. B, 249, 235–297

Bakhmeteff B.A. and Allan W., 1946. The mechanism of energy loss in fluid friction, Trans. actions, American society of Civil Enginears,111, 1043–1102

Barry J.F., Biggs Maurice J., Duncan Steven N., Francoeur. and William D., Meyer., 1997. Physical characterization of microform bed cluster refugia in 12 headwater streams, New Zealand [J]. New Zealand Journal of Marine and Freshwater Research, 31,413–422

Barry J.J., Jeffrey J., Buffington John M., King John G., Goodwin Peter., 2006. Performance of bed load transport equations in mountain gravel-bed rivers: a re-analysis. Proceedings of the Eighth Federal Interagency Sedimentation Conference (8thFISC), Reno, NV, USA, 90–97

Barua D.K., Klaassen G.J. and Mahmood. 1995, On the adaption and equilibrium of Bangladesh rivers, 5th International Symposium on river Sedimentation, Central Board of Irrigation and Power, Oxford & IBH Publishing Co. PVT. Ltd, pp. 277–292.

Bathurst J.C., Graf W.H. and Cao H.H., 1987. Bed load discharge equations for steep mountain rivers. In: Thorne C.R., Bathurst J.C., Hey R.D. (eds.), Sediment Transport in Gravel-bed Rivers. John Wiley, Chichester, UK, 453–491

Carson M.A. and Griffiths G., 1987. A Bed load transport in gravel bed channels. Journal of Hydrology (New Zealand), 26(1), 1–151

Chien N., Wan Z.H. and McNown J., 1998. Mechanics of Sediment Movement, ASCE Press, New York

Chien, N., Wan, Z.H., and McNown, J. 1998, Mechanics of Sediment Movement, ASCE Press, New York.

Chin A., 1999. The morphologic structure of step-pool in mountain streams. Geomorphology, 27, 191–204

Clague J.J., Luternauer J.L. and Hebda R.J., 1983. Sedimentary environments and postglacial history of the Fraser delta and lower Fraser valley, British Columbia. Canadian Journal of Earth Science, 20(8), 1314–1326

Culbertson J.K. and Nordin C.F., 1960. Discussion of the paper-Discharge formula for straight alluvial channels, J. Hyd. Div., Proc. Amer. Soc. Civil Engrs., 86(Hy6), 98–102

Du G.H., Peng R.Z. and Wu D.Y., 1980. Reconstruction of the Dujiangyan Project and gravel bed load transportation problem. Sediment Research, 1, 12–22 (in Chinese)

Einstein H.A., 1934. Der hydraulische oder profil radius. Scherizerisch Bauzeitung, 103, (8)

Einstein H.A. and Shen S.W., 1964. A study of meandering in straight alluvial channels. Journal of Geological Research, 5239–5247

Einstein H.A. and Chien Ning., 1958. Discussion of the Paper-Mechanics of Streams with Movable Beds of Fine Sand, Trans., Amer. Soc. Civil Engrs, 123, 553–562

Field J., 2001. Channel avulsion on alluvial fans in southern Arizona. Geomorphology, 37, 91–104

Fisk H.N., 1944. Geological investigation of the alluvial valley of the Lower Mississippi River. Report of WAR

Department, Corps of Engineering, U.S. Army

FISRWG (Federal Interagency Stream Restoration Working Group), 1998. Stream Corridor Restoration: Principles, processes and practices The national technical information service, USA. (Available online at: Http://www.nrcs.usda.gov/techinica//stream-restoration)

Gandolfi G., et al., 1982. Composition and along-shore disposal of sand from the Po and Adige Rivers since the Pre-Etruscan Age, J. of Sed. Petrol, 52(3), 797–805

Gole C.V. and Chitale S.V., 1966. Inland delta building activity of Kosi River. Journal of the Hydraulics Division, ASCE, 92(HY2), 111–126

Grant G.E., Swanson F.J. and Wolman M.G., 1990. Pattern and origin of stepped-bed morphology in high gradient streams, Western Cascades, Oregon. Geological Survey of America Bulletin 102,340–352

Grass A.J., 1971. Structural features of turbulent flow over smooth and rough boundaries. Journal of Fluid Mechanics 50(2), 233–255

Gregory K.J., Gurnel A.M., Hill C.T. and Tooth S., 1994. Stability of the pool-riffle sequence in changing river channels. Regulated Rivers: Research and Management, 9, 35–43

Hu Y.S., Zhang H.W., Liu G.Z., Wang, K.C., Peng, R.S., Liu Y.L. 1998. River realignment for Wandering channels is lower Yellow River. Zhengzhou: Yellow River water Conservancy Press.

Hui Y.J. and Chen Z.C., 1981. Preliminary analysis of the roughness on the Three Gorges reaches of the Yangtze River. Research Report artment of Dept. of Hydraulic Engineering, Tsinghua University

Janda R.J. and Meyer D.F., 1985. Channel morphology changes caused by debris flow, hyperconcentrated flow, and sediment-laden streamflow, Toutle River, Mount St. Helens, Washington, Proceedings, International Workshop on Flow at Hyperconcentrations of Sediment, IRTCES (International Research and Training Center on Erosion and Sedimentation) Publication, Beijing, paper III–6

Julien P.Y., 1989. Laboratory analysis of hyperconcentrations, Proceedings. International Symposium on Sediment Transport Modeling, ASCE, New Orleans, 681–686

Julien P.Y. and Lan Y.Q., 1991. Rheology of hyperconcentrations. Journal of Hydraulic Engineering, ASCE, 115(3), 346–353

Keller E.A. and Melhorn W.N., 1973. Bedforms and fluvial processes in alluvial stream channels: Selected observations. In: Fluvial Geomorphology, Morisawa M. (ed.), Binghamton NY: Ney York State University Publications in Geomorphology, 253–283

Keller E.A. and Melhorn W.N., 1978. Rhythmic spacing and origin of pools and riffles. Geological Society of America Bulletin, 89, 723–730

Keller E.A., 1972. Development of alluvial stream channels: A five-stage model. Bulletin of the Geological Society of America, 83,1531–1536

Kim H.T., Kline S.J. and Reynolds W.C., 1971. The production of turbulence near a smooth wall in a turbulent boundary layer. Journal of Fluid Mechanics, 50(1), 133–160

Kline S.J., Reynolds W.C., Schraub F.A., Runstadler P.W., 1967. The structure of turbulent boundary layers. Joural of Fluid Mechanics, 30(4), 741–773

Knighton D., 1984. Fluvial forms and process. Edward Arnold, London

Knighton D., 1998. Fluvial Forms and Processes- A New Perspective, John Wiley and Sons, New York

Lane E.W., 1955. The importance of fluvial morphology in hydraulic engineering. Proceedings of the American Society of Civil Engineers 81(745), 1–17

Lane E.W., 1953. Progress report of studies on the design of stable channels by the Bureau of Reclamation. Proceedings, Amer. Soc. Civil Eengrs., 79(280)

Leeder M.R., 1983. Sedimentology-Process and Product. George Allen & Unwin Publishers Ltd

Leeder M.R., 1978. A quantitative stratigraphic model for alluvium with special reference to channel deposit density and interconnectedness, Fluvial Sedimentology, Memoir 5, Miall A.D. (ed.), Can. Soc. Petrol. Geol., 587–596

Leopold L.B., 1994. A view of the river. Harvard University Press. Cambridge, Massachusetts

Leopold L.B., Wolman M.G. and Miller J.P., 1964. Fluvial Processes in Geomorphology, W.H. Freeman and Company, San Francisco and London

Li C.H. and Sun M.X., 1964. Criteria for threshold shear stress and ripple formation, Proceedings. Nanjing Hydraulic Research Institute (River & Habour Division), (in Chinese)

Mantz P.A., 1977. Incipient transport of fine grains and flakes by fluids-extended shields diagram. Journal of the Hydraulies Divison, Proc., Amer. Soc. Civil Engrs, 103(HY6), 601–616

Martin Y., 2003. Evaluation of bed load transport formulae using field evidence from the Vedder River, British Columbia [J]. Geomorphology, 53, 75–95

Meyer-Peter E. and Muller R., 1948. Formulas for bedload transport. Proceedings, 3rd meeting of IAHR, Stockholm, 39–64

Miller M.C., McCave I.N. and Komar P.D., 1977. Threshold of sediment motion under uniderectional Currents. Sedimentology, 24(4), 507–527

O'Brien J.S. and Julien P.Y., 1995. Physical properties and mechanics of hyperconcentrated sediment flows, Proceedings, ASCE Specialty Conference on Delineation of Landslide, Flash Flood and Debris Flow Hazards in Utah, 1985. Utah Water Research Lab, Series UWRL/C-85103, 260–279

Offen G.R. and Kline S.J., 1974. Combined dye-streak and hydrogen-bubble visual observations of a turbulent boundary layer. Journal of Fluid Mechanics, 62(2), 223–339

Paintal A.S., 1971. A stochastic model for bed load transport. Journal of hydraulic research, 9(4), 527

Panin N., Panin S., Herz N. and Noakes J.E., 1983. Radiocarbon dating of Danube delta deposits. Quaternary Research, 19(2), 249–255

Qi P. and Han Q., 1991. The resistance of hyperconcentrated floods in the Yellow River. People's Yellow River, 3, 16–21 (in Chinese)

Qi P. and Ru Y., 1995. Sediment delivery capacity of the Yellow River channel downstream of the Aishan Station. People's Yellow River, 5, 5–11 (in Chinese)

Qi P. and Zhao A., 1984. Propagation and variation of the 1977's hyperconcentrated flood waves in the lower Yellow River. People's Yellow River, 4, 1–8 (in Chinese)

Qi P. and Zhao Y., 1985. The characteristics of sediment transport and problems of bed formation by flood with hyperconcentration of sediment in the Yellow River. Proceedings, International Workshop on Flow at Hyperconcentrations of Sediment, IRTCES Publication, Beijing, Paper III–3

Qian N. and Wang Z.Y., 1984. A preliminary study on the mechanism of debris flows. Acta Geographica Sinica, 39(1) (in Chinese)

Qian N. and Wan Z.H., 1983. Mechanics of sediment movement. Chinese Science Press, Beijing (in Chinese)

Qian N. (ed), 1989. Movement of hyperconcentrated flow, Tsinghua University Press, Beijing (in Chinese)

Qian N., Zhang R., Wan Z. and Wang X., 1985. The hyperconcentrated flow in the main stem and tributaries of the Yellow River. Proceedings, International Workshop on Flow at hyperconcentrations of Sediment, IRTCES Publication, Beijing, Paper III–4

Rantz S.E., et al., 1982. Measurement and computation of streamflow. USGS Water Supply Paper 2175, 2 vols. U.S. Geological Survey, Washington, DC Pp.347 165 Fig, 12 Tab, 82 Ref

Rouse H., 1965. Critical analysis of open-channel resistance. Journal of the Hydraulics Division, ASCE, 19(HY4), 1–25

Rouse H., 1946. Elementary Mechanics of Fluids. John Wiley and Sons

Schumm S.A., 1977. The fluvial system. John Wiley and Sons, New York

Scott K.M. and Dinehart R.L., 1985. Sediment transport and deposit characteristics of hyperconcentrated streamflow evolved from lahars at Mount St. Helens, Proceedings, International Workshop on Flow at Hyperconcentrations of Sediment, IRTCES Publication, Beijing, Paper III–2

Shields A., 1936. Anwendung der Aechlichkeitsmechanik und der Turbulenzforschung auf die Geschiebewegung, Mitt. Preussische Versuchsanstalt fur Wasserbau und Schiffbau, Berlin

Simons D.B. and Richardson E.V., 1966. Resistance of flow in alluvial channels. USGS Professional Paper 422–J

Slingerland R. and Smith N.D., 1998. Necessary conditions for a meandering-river avulsion. Geology, 26(5), 435–438

Stokes G.G., 1851. On the effect of the internal friction of fluids on the motion of pendulums. Transactions of Cambridge Philosophy Society, 9 Pt(2), 8–106

Stouthamer E., 2001. Sedimentary products of avulsions in the Holocene Rhine-Meuse Delta, the Netherlands. Sedimentary Geology, 145, 73–92

Thompson A., 1986. Secondry flows and pool-riffle units: A case study of the processes of meander development. Earth Surface Process and Landforms, 11, 631–641

Tinkler K.J., 1970. Pools, riffles and meanders. Bulletin of the Geological Society of America, 81, 547–552

Tison L.J., 1948. Etude des conditions dans lesquelles les particules solides sont transportees dans les courants a lit mobiles, Proc., Assoc. Intern. Sci. Hydro., Assemblee Generale d'Oslo, Tome 1, 293–310

Wan Z. and Wang Z.Y., 1994. Hyperconcentrated flow, monograph series of IAHR. A.A. Balkema Publishers, Rotterdam, the Netherlands

Wang Z.Y., 1987. Buoyancy force in solid-liquid mixtures. Proceedings, 22nd Congress. of IAHR, Lausanne, Switzerland

Wang Z.Y. and Qian N., 1985. A preliminary investigation on the mechanism of hyperconcentrated flow. Proc. of Intern. Workshop on Flow at Hyperconcentration of Sediment, IRTCESPublication, II4-1-16

Wang Z.Y., 1999. Experimental study on scour rate and channel bed inertia. Journal of Hydraulic Research, 37(1), 27–47

Wang Z.Y., 2002. Free surface instability of non-Newtonian laminar flows. Journal of Hydraulic Research. 40(4), 449–460

Wang Z.Y. and Dittrich A., 1992. A study on problems in suspended sediment transportation, Proceedings, 2nd International Conference on Hydraulics and Environmental Modelling of Coastal. Estuarine and River Waters, Ashgate, England, 467–478

Wang Z.Y., Larsen P. and Xiang W., 1994. Rheological properties of sediment suspensions and their implications. Journal of Hydraulic Research, 32(4), 495–516

Wang Z.Y., Larsen P., Nestmann F. and Dittrich A., 1998. Resistance and drag reduction of hyperconcentrated flows over rough boundaries. Journal of Hydraulic Engineering, ASCE, 121(1), 1–9

Wang Z.Y. and Wu Y.S., 2001. Sediment-removing capacity and river motion dynamics. International Journal of Sediment Research

Wang, Z.Y., Huang J.C. and Su D.H., 1997. Scour rate formula. International Journal of Sediment Research, 12(3), 11–20

Wanielista M., 1990, Hydrology and Water Quality Control. John and Wiley, New York. Water Resources and Power Press, 1–41

White S.J.,1970. Plain bed thresholds for fine grained sediments. Nature, 228, (5267), 152–153

WIHEE (Wuhan Institute of Hydraulic and Electric Engineerig), Hydraulics. Hydraulic and Electric Press, 1961, (in Chinese)

Xu J.X., 1996. Wandering braided river channel pattern developed under quasi-equilibrium: An example from the Hanjiang River, China. Journal of Hydrology, 181, 85–103

Yu G.A., Wang Z.Y., Zhang K. and Liu L., 2009. Impact of bed structure on bed load transport in a mountain stream. International Journal of Sediment Research, vol. 25 (in press)

Zhao A. and Ru Y., 1994. Causes of the development of narrow and deep channel in the lower Weihe River. People's Yellow River, (3), 1–4 (in Chinese)

6 Flood Defense and Water/Sediment Management—With Particular Reference to The Yellow River

Abstract

Management of the Yellow River is presented as a case study for alluvial river management. The river is difficult to manage because it carries a heavy sediment load and used to be the most disastrous river in China. The river has successfully been kept flowing within the Grand Levees for a half century. But new problems have attracted the attention of society, for example, the water diversion to meet increasing water demand has caused the river to run dry for parts of the year, and floodplain reclamation and sedimentation of the channel have resulted in historically high water stage. Integrated river management is more necessary than before to coordinate various efforts of river training and management.

Keywords

Yellow River, Water resources management, Flood defense strategies, Water diversion, Sanmenxia Reservoir, new management strategies.

6.1 Flood Disasters

6.1.1 The Yellow River Basin

The Yellow River shown in Fig. 6.1 has a drainage area of 795,000 km^2 and a length of 5,464 km making it the second longest river in China. The long-term annual sediment load at Sanmenxia Station was 1.6 billion tons before 1980, with a highest annual load of 3.9 billion tons. The river ranks first of all the world's rivers in terms of sediment load (Qian and Dai, 1980), although the sediment load has reduced
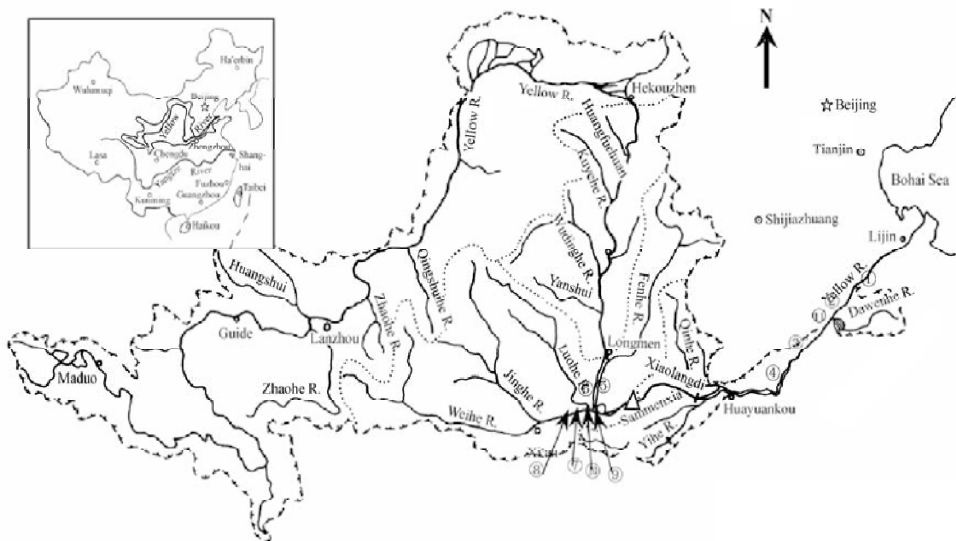
Fig. 6.1 The Yellow River and its tributaries (Note: Longmen, Sanmenxia, Xiaolangdi, Huayuankou, Lijin are shown on the map; Important hydrological stations are indicated in the map by numbers as follows: ①Luokou; ②Aishan; ③Gaocun; ④Jiahetan; ⑤Shangyuantou; ⑥Chaoyi; ⑦Huayin; ⑧Lintong; ⑨Tongguan; ⑩Diaoqiao; ⑪Sunkou)

greatly in the past 20 years. The long term (1950–1985) average sediment concentration was 40 kg/m^3 and the highest sediment concentration was recorded at 911 kg/m^3. The ratio of the highest annual runoff to the lowest is 3.4 and the ratio of the highest annual sediment load to the lowest is 10. More than 60% of the water and 85% of the sediment are transported in the flood season from July to October. The Yellow River, recognized as the cradle of Chinese civilization, is the most challenging river in the world. It carries the heaviest sediment load and often experiences erosion and sedimentation that make the river channel extremely unstable. The river watershed is mostly arid and semi-arid with a long term-average annual runoff depth of only 77 mm and total annual runoff 58 billion m^3. The water resource per capita in the watershed is only about 500 m^3, only one quarter of the average in China.

The sediment load of the lower Yellow River is mainly composed of silt; its mineral composition is quartz, feldspar, calcite, and illite. The sediment is readily suspended and no distinct bed load motion can be detected. Table 6.1 lists long term average values of water discharge and sediment load of the river; they are obtained by averaging over 39 years (1950–1989) of recorded values. Table 6.2 lists the discharge of floods of various recurrence periods for flood control design. The river deposits sediment at the river mouth and on the north China plain and has created more than 250,000 km^2 of fertile land forming the Pan Yellow River Delta with the apex at Zhengzhou.

Table 6.1   Average water and sediment load of the Yellow River in the period from 1950–1989

Hydrologic Station	Huayuankou (Zhengzhou)	Lijin (Dongying)
Annual Runoff	43 billion m^3	30 billion m^3
Annual Sediment Load	1.6 billion tons	1.0 billion tons
Average Sediment concentration	40 kg/m^3	33 kg/m^3
Median diameter of suspended sediment	0.019 mm	0.019mm
Maximum day-average discharge	6,860 m^3/s	5,400 m^3/s

Table 6.2   Flood features of the lower Yellow River (Chen, 1999)

Hydrological Station	Catchment (km^2)	Peak discharge (m^3/s)		5 days runoff (bm^3)		12 days runoff (bm^3)	
		100yrs	1000 yrs	100 yrs	1000 yrs	100yrs	1000 yrs
Huayuankou	730,036	29,200	42,100	7.13	9.84	12.5	16.4
Xiaolangdi	694,155	29,200	42,100	6.24	8.70	10.6	13.9
Sanmenxia	688,421	27,500	40,000	5.91	8.18	10.4	13.6

6.1.2   Flood Disasters in the History

Throughout the history of China, the Yellow River has been associated with floods and famine. The river carries sediment produced by soil erosion from the Loess Plateau, which deposits on the channel bed and in the estuary. Xu (1998) studied the sedimentation rate of the lower Yellow River applying map comparison, historical literature studies, modern data analysis, and ^{14}C dating. He divided the past 13,000 years into 4 periods, as shown in Fig.6.2: 1) from 11,000BC to 3,000BC is a period of low sedimentation with an average sedimentation rate of only 0.2 cm per year; 2) from 3,000BC to 600AD is a period with accelerated sedimentation due to climate changes. The sedimentation rate increased to about 0.5 cm per year in this period; 3) from 600AD to 1855 is a period with accelerated sedimentation caused by human activities. The average sedimentation rate increased to 1–3 cm per year; 4) since 1855 human activities have accelerated the sedimentation at an extremely high degree and the sedimentation rate has risen to 5–10 cm per year. The measured transverse riverbed profile at the Sunkou cross section in Fig. 6.3 shows that the sedimentation of the lower Yellow River raised the riverbed and floodplain by about 5 m in the

past 70 years. Sunkou is a typical cross section in the lower Yellow River, which is not very wide and not narrow and is located at the middle of the lower reaches of the river.
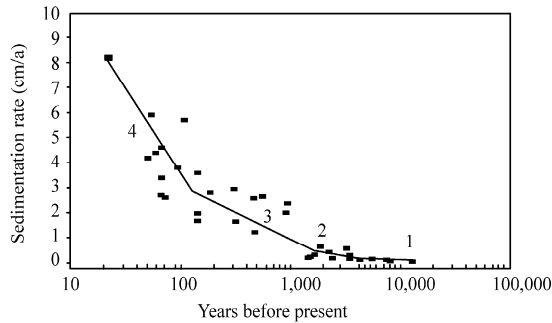
Fig. 6.2   Sedimentation rate in the lower Yellow River during the 4 historical periods: 1) geological sedimentation; 2) sedimentation due to climate change; 3) sedimentation due to human activities; 4) accelerated sedimentation due to human activities (after Xu 1998)
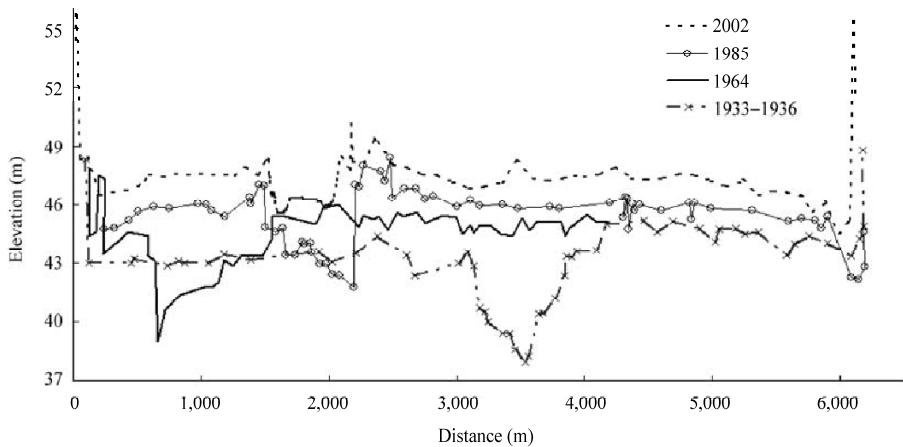
Fig. 6.3   Sedimentation caused changes in the riverbed at the Sunkou cross section during the period 1933–2002 (Sunkou is 300 km downstream from Zhengzhou and 440 km upstream from the river mouth)

Over time, a perched river formed that frequently breached its levees. From 602BC to 1949AD the river experienced 1,593 levee bursts, flooding vast areas in 543 years and claiming millions of human lives. The river shifted its major course (600–700 km long) by avulsion 26 times with the apex around Zhengzhou resulting in devastating calamities and numerous old channels, including 8 major shifts (5 natural and 3 human-caused) with the river mouth alternating between the Bohai Sea and the Yellow Sea. Because of its wild behavior, the lower Yellow River was dubbed "the sorrow of China". The 700 km long lower reaches have swept throughout the north China plain and left numerous old channels. Figure 6.4 shows the migration of the river from 602BC to 1855AD and the old channels and the land created by the river.

The most disastrous floods are briefly summarized as follows: (WUHEE and IWHR, 1985)

1117—A high flood occurred in the lower Yellow River due to heavy rainfall and the river levee was breached at many places. More than one million people were killed by the flood.
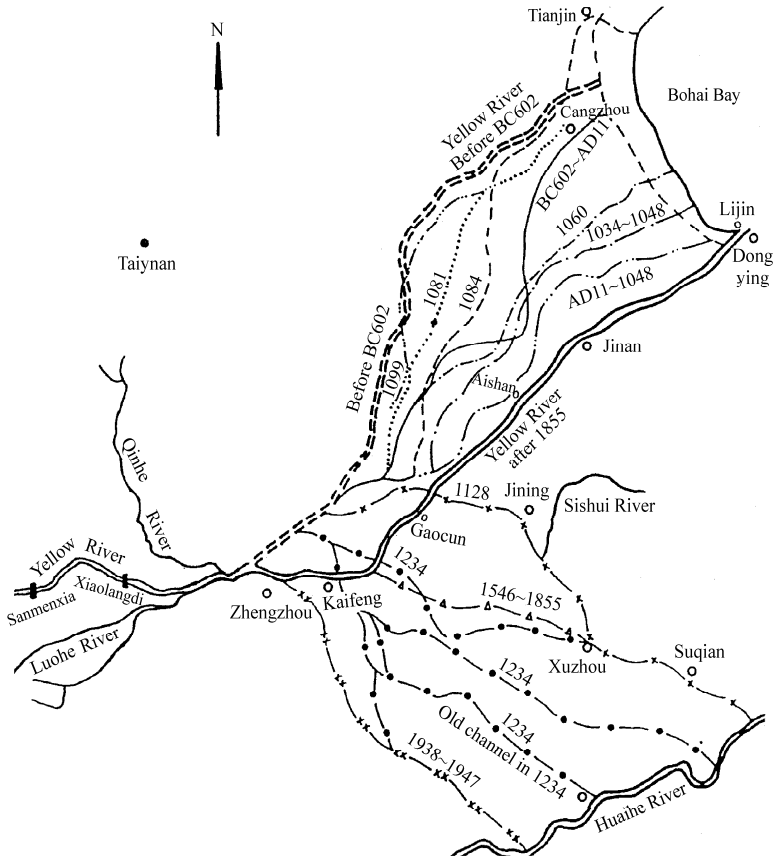
Fig. 6.4 Migration of the Yellow River and the abandoned channels

1761—Ten days of rainfall from August 9 to 18 resulted in 10 billion m^3 of runoff and caused a rare flood with a crest discharge of 32,000 m^3/s in the section from Xiaolangdi to Huayuankou. Twenty-six counties in Henan, Shandong and Anhui Provinces were flooded.

1843—A rainstorm occurred in the middle reaches of the Yellow River on August 6–8 and generated the biggest flood in recorded history (1000 yr reoccurrence). The crest discharge in the reach from Shanxian to Sanmenxia was up to 36,000 m^3/s and the total runoff in 12 days was over 11.9 billion m^3. The flood stage in the reach from Tongguan to Xiaolangdi (Fig. 6.1) was the highest in 1000 years of history. Twenty-seven counties and 15,000 villages were flooded and thousands of people were killed.

1855—From 1796 to 1855 the Grand Levees were breached 22 times and the major task for the river training was to close the breaches in this period. A flood from the upstream magnified by a heavy rainfall in the lower reaches breached the grand levee at Tongwaxiang on June 18, 1855. The river poured out and inundated 8 counties, and finally took over pirated the Daqing River Channel. Consequently, the Yellow River shifted its major course from south to north and flowed into the Bohai Sea. Thousands of people were killed by the flood and several million people lost their homes shelters and farmland.

1933—In 1933 the river swelled again by heavy rainfall during August 5–10. The 4 days of precipitation in the Qingjian River (a tributary of the Yellow River) watershed reached 255 mm. The crest discharge was recorded at 22,000 m^3/s at Shanxian Station. The flood caused 54 levee breaches, inundated 67

counties with a total flooded area of 8,637 km^2 and killed 18,293 people.

1938—On June 9, 1938 the embankment at Huayuankou was broken by the Chinese army attempting to stop invasion by the Japanese army. The river emptied itself through an inundated land area of about 50,000 km^2, and finally captured the Huaihe River channel. Consequently, the river shifted its major course from north to south and flowed into the Yellow Sea for 8 years, as shown in Fig. 6.5. More than 890,000 people were killed and 3.9 million people lost their homes and farmland. The river flowed on the plain without any fixed channel and levees and in the Huaihe River channel for 8 years. It brought about 10 billion tons of sediment deposition and created the Huangfan flooded area of 54,000 km^2, which is desert-like land with low productivity and poor vegetation. Figure 6.6 shows that people were escaping from their flooded homeland in 1938.

1958—A heavy rainstorm occurred in the drainage area between Sanmenxia and Huayuankou with 5 days of rainfall totaling 198 mm. The crest discharge at Huayuankou was recorded at 22,300 m^3/s and the
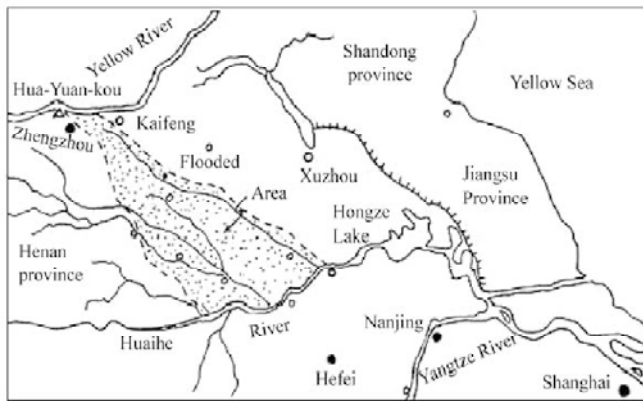
Fig. 6.5 Extent of the man-made flood caused by exploding the levee at Huayuankou in 1938. The flood water flowed on the plain and finally flowed into the Huaihe River, which created the 54,000 km^2 Huangfan desert

Fig. 6.6 About 890,000 people were killed and 3.9 million people lost their homes and farmland. This figure shows people escaping from their flooded homeland (after YRCC, 2001)

Dongping lake flood detention basin was used to reduce the threat to the lower reaches. The major levees were not broken but 1700 villages on the floodplain within the Grand Levees and in the flood-detention basin were flooded.

6.1.3 Training of the River

The flood defense history of China is essentially a history of the people's struggle against Yellow River floods because the floods were disastrous and training of the river is most challenging due to the heavy sediment load. Training of the Yellow River has a history of more than 3,000 years. Levee construction was the major strategy of flood control. The Qin Emperor united the country and linked the flood defense levees into an entire levee system about 2,200 years ago. The lower Yellow River was confined within the levees but sediment deposition raised the riverbed and made the river frequent shift its course. People developed many strategies to harness the river, among them the wide channel and narrow channel theories had the most influence. The wide channel theory is to confine the river within a wide river valley with levees and divert floods with diversion channels. Wang Jing—a minister of the Han Dynasty (206BC to 220AD)—was the major practitioner of the strategy. The second strategy is to narrow the river and confine the flood within the stem channel in order to raise the velocity and keep the high carrying capacity of the flow, preventing sediment from depositing and even scouring the bed. Pan Jixun—a minister of the Ming Dynasty (1368–1944)—was the most outstanding advocate and performer of this strategy.

In the Han Dynasty, Jia Rang proposed three river harnessing strategies: (1) widen the river channel and construct flood diversion basins to enhance the flood conveyance capacity of the river and mitigate flood disasters; (2) build gates and diversion channels, divert flood water through diversion channels into the Zhanghe River and other rivers; and (3) enhance and reinforce the levees every year. The main principle of Jia Rang was to give enough space for the river channel and flood flow. Any agricultural development should not occupy the flood plain, which was necessarily a flood way.

From 168BC to 69AD, the river was active; it flooded and changed its course several times. Wang Jing implemented a large-scale training project in 69AD. He completed and enhanced the levees and built many diversion channels and weirs. One of his strategies was to build inner levees parallel within the Grand Levees. Along the inner levees, he constructed many gates about 5 km apart. The inner levees were lower than the Grand Levees. During great events water flowed over the inner levees but was still controlled by the Grand Levees. As the flood receded, the gates were open allowing water to flow back to the inner channel. The channels were wide. Generally speaking the river was confined by the enhanced levees tens of kilometers apart. The riverbed silted up at a low speed of about 1-cm per year. In the meantime the major land use in the Loess Plateau changed from agriculture to husbandry, which reduced sediment yield and sediment load into the river. In the following 800 years the river was calmed and no big flood disasters occurred (Li, 1992).

From 850AD to 1500AD the river woke again and became very active. The Grand Levee was breached once per 2 years during the period (IWHR and WUHEE, 1985). Closing the breached levee was a hard job for the river training engineers and the technology of levee defence was developed. Xu Youzheng adopted the strategy of diverting floods with channels and weirs and implemented the Shawan Flood Diversion Projects in 1450–1456. Because of the population growth, the flood diversion strategy was more difficult to implement. Pan Jixun proposed the strategy of narrowing the river and confining the flood within the stem channel in order to raise the velocity and keep high the carrying capacity of the flood, preventing sediment from depositing and even promoting bed sediment scouring. He regulated the levee system, blocked many branches of the river and made the river flow in a single channel in the lower reaches in the period 1565–1592.

After Pan Jixun the sediment deposition in the lower Yellow River channel sped up to 5–10 cm per year. The river migrated from south to north and captured the Daqing River in 1855 due to the levee breach at Tongwaxiang. In the first 10 years after the major shift of the river course, the river flowed wildly and flooded frequently because there were no strong levee to accommodate the river water and the government hesitated to move the river back to the south or build a new levee system to stabilize the north channel. From 1864 to 1888 the new dyke system was constructed and since then the river has flowed into the Bohai Sea via Lijin.

Since the river was artificially shifted to the south in 1938 during the second World War, the river flowed over the plain without any levee between the Yellow River and the Huaihe River. It was disastrous and the local people appealed to the government to bring the river back to its north channel or to fix a channel between the Yellow and Huaihe Rivers. In 1945, the government and hydraulic engineers made an effort to close the breach and bring the river back to its north channel but failed. In 1946, hydraulic engineers finally closed the breach and made the river flow in the north channel across Shandong Province again. Figure 6.7 shows a photo of the closing of the breached south levee, which ended the 8 years flooding of the Yellow River water over the central China plain.

Fig. 6.7   The breached south levee of the Yellow River was finally closed in 1946, which ended the 8 years of flooding of Yellow River water over the central China plain. (after YRCC, 2001)

Since the 1950s the Yellow River Water Conservancy Commission (YRCC) has been the leading institute for river training. Wang Huayun, the chief of YRCC, proposed and implemented his training strategies in the period (Wang, 1989). The nation has spent $1 billion for flood control and saved $500 billion in flood losses (Chen 1999). The riverbed profile has remained stable for half a century, with only parallel rising following the extension of the river mouth into the sea (Zhang and Xie, 1985). The main strategies are to reduce flood discharge with reservoirs, enhance the capacity of the river channel by enhancing and reinforcing the levees, and retending floodwater with detention basins. These strategies are referred to in short as: *upper reaches storing, lower reaches discharging and two sides retaining.*

Three foreign names should be mentioned who worked on the training of the river: Engels, Freeman and Franzius (Yen, 1999). Freeman visited China in 1917 and proposed to build cross dikes extending

from the existing levees of the lower Yellow River, which were more than 6 km apart, and to build new levees near the tips of the dikes, 800 m apart (Freeman, 1922). Freeman's suggestion rekindled the century's debate on whether the levees should be close or far apart as they were at the time. Engles conducted physical model experiments, authorized by the Chinese National Economic Council in 1931–1934. The test results indicated that with the levees set far apart, a somewhat better scour was produced in the main channel than when the levees were close to the main channel edges (Engels, 1932). Franzius conducted another physical model experiment and obtained different results. Yen (1999) indicated that Franzius' experiments were conducted without tail gate regulation and the results are not reliable as those of Engels.

6.1.4   River Training Theories
Many river harnessing theories have been advocated. including:

(1) Naturalization theory proposed by Tian Fen (Han dynasty 2000 years ago)

It is the river's nature to move and people cannot harness it. The only way to reduce flooding losses is to evacuate the area at risk and freely allow river flooding over the land. A levee breach occurred and the river flowed over the north China plain for 23 years during Tian-Fen time, which caused disasters to the people but also created fertile land.

(2) Leveeless river valley theory

In this theory the river should flow over low ground without levees. It will shift to a new low land if the old one is silted up.

(3) Artificial migration theory

If the old channel is silted up, people may guide the river to a new channel. People may also utilize the river to resist an invading enemy army, which was practiced in 1112 and 1938.

(4) Flood diversion with branch channels

Flood diversion channels are necessary to reduce flood damages.

(5) Flood diversion basins

Build flood diversion basins to retain flood water in order to protect people in the lower reaches.

(6) Narrowing channel and enhancing sediment carrying capacity

Narrow the channel with levees and spur dikes, cut branch channels, and confine the flood in one channel to enhance the flow velocity and the sediment carrying capacity of the flow, to prevent sediment deposition and scour the channel bed (Pan Jixun).

(7) Upper reaches storing, lower reaches discharging and two sides retaining.

The theory which has guided the flood control practices in the past 50 years are: Reducing flood discharge with reservoirs in the upper reaches, enhancing discharge capacity of the lower reaches channel by enhancing and reinforcing the levees; and retaining rare flood water with detention basins on the two sides of the river.

6.2   Flood Defense Strategies

Many of the previously described theories were applied and people have developed many more flood control methods in the recent century. In the past 50 years, within which 10 major floods of discharge over 10,000 m^3/s occurred, the river has been controlled within the Grand Levees and no great disasters have occurred. The nation has spent $1 billion for flood control and saved $500 billion in flood loss (Chen, 1999). The main flood control practices are described in the following subsections.

6.2.1   Wide River Valley
The Yellow River flows from mountainous areas into the North China plain near Zhengzhou. A sharp

reduction in slope results in sedimentation and continuous silting up of the riverbed. The width of the river valley is 5–20 km controlled by Grand Levees in the Henan Province reach (about 200 km). Figure 6.8 shows the river and the Grand Levee and spur dykes controlling the flow. The channel is about 500 m wide and in most time the flow is kept in the channel. If a flood occurs the water is allowed to flow over the floodplain for reduction of flood losses in lower reaches. The wide river provides water detention capacity and space for sediment deposition. The wide river in the Henan reaches detained 2.4 billion m^3 of water during the 1958 flood and greatly reduced the flood discharge to the lower reaches (Wang, 1989). The capacity of the channel in the Henan reaches is 30,000 m^3/s. Nevertheless, the wide floodplain is rarely flooded and about 1.8 million people reclaimed the land and live in villages and towns within the Grand Levees nowadays.

To stabilize the channel and protect the villages and towns within the levees, numerous spur dykes have been constructed. The spur dykes were constructed at the bends of the channel to control the flow direction. Nevertheless, not all the spur dykes work well for channel stabilization. The river channel is very dynamic and often moves far away from the dykes, which makes the dykes abandoned. Statistically, about half of the spur dykes are effective for stabilization of the channel.
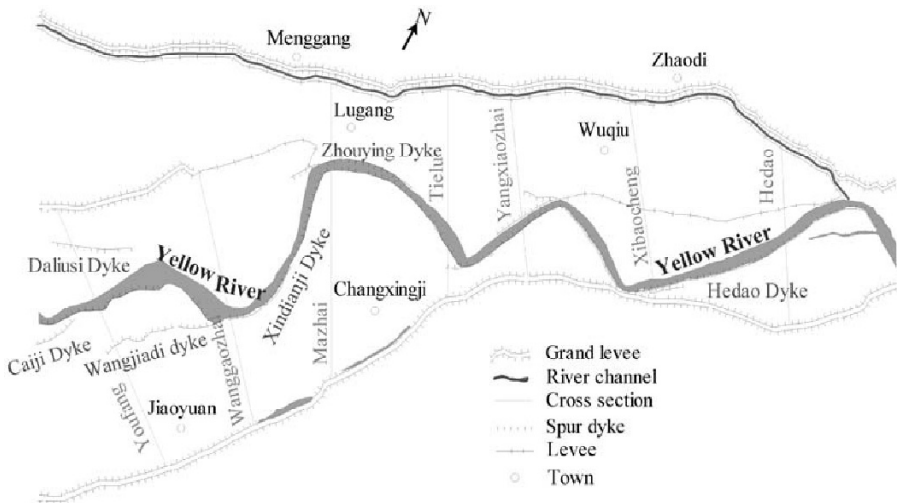
Fig. 6.8 Wide river valley defined by the Grand Levees in the reach in Henan Province

6.2.2   Narrow Channel

The most downstream reach of a length about 600 km of the Yellow River across the Shandong Province has a width of only 0.4–5 km. The narrow river favors a stable channel and high flow velocity and maintains high sediment carrying capacity, which is in accordance of the theory of narrowing the channel and enhancing the sediment carrying capacity developed by Pan Jixun. On the other hand, the capacity of the channel is limited, and can only accommodate floods of discharge less than 10,000 m^3/s. The Aishan Hydrological Station is the control point between the wide valley reach in Henan Province and the narrow channel reach in Shandong Province. The Aishan cross section has a width of only 275 m. The location of the Aishan station is shown in Fig. 6.1. The narrow section controls the flow into the Shandong Reach no more than 10,000 m^3/s. Therefore, it is named by the hydraulic engineers as "Aishan Lock". From Aishan to the river mouth the river is narrow. Figure 6.9 shows the Lijin cross section, which is the most downstream hydrological station of the river (the location of the Lijin station is also

shown in Fig. 6.1. As a comparison the Mazhai cross section is in the wide river reach near Huayuankou, as shown in Fig. 6.10.
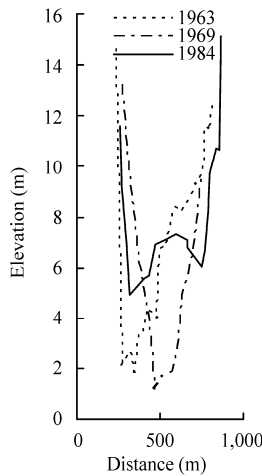
Fig. 6.9 The narrow Lijin cross section (upper, about 600 m wide), at which the most downstream hydrological station of the river Lijin Station is located
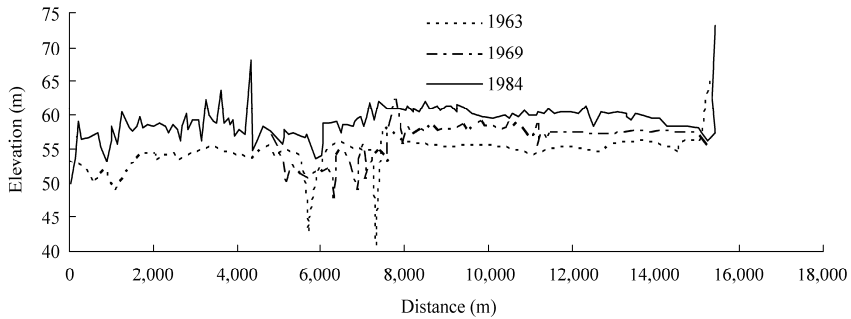
Fig. 6.10 Mazhai cross section in the wide river reach near Huayuankou

6.2.3 Reservoirs

In the past decades, the watershed experienced marvelous economic wonders. Eleven reservoirs were constructed in the Yellow River from 1957–2002, namely: Longyangxia, Lijiaxia, Liujiaxia, Yanguoxia, Bapanxia, Qingtongxia, Sanshenggong, Wanjiazhai, Tianqiao, Sanmenxia, and Xiaolangdi Reservoirs. The total capacity of the reservoirs is 55.8 billion m³, equal to the annual runoff of the whole watershed. Most of the upper floods (flood water comes from the watershed of the upper and middle reaches of the Yellow River) can be controlled with these reservoirs.

The Sanmenxia Dam is the first one built on the Yellow River, which was completed in 1960. Impoundment of the Sanmenxia Reservoir caused siltation of the Yellow River and the Weihe River and endangered Xian—capital city of Sha-anxi Province. The operation of the reservoir had to be altered from storing water and trapping sediment to retaining flood water and discharging sediment, and to storing clear water and releasing turbid water. Details of the management of the reservoir is presented in Section 6.5.

The reservoirs are also used to trap sediment. More than 10 billion tons of sediment has been trapped by the reservoirs reducing the total amount of sediment deposited in the lower Yellow River. Especially, the Xiaolangdi Reservoir was constructed with one purpose to trap sediment and control the siltation of the lower Yellow River. The total capacity of the Xiaolangdi Reservoir is 12 billion m^3 and the sediment-trapping capacity is 7 billion m^3. It is predicted that the sediment from the Loess Plateau can be trapped by the reservoir for at least 20 years, and, therefore, the lower Yellow River will be scoured down and the flood risk will then be eased.

6.2.4 Grand Levees

The flood discharge capacity of the lower Yellow River reduces following the siltation of the channel. People have continuously enhanced the levees in a race with the river sedimentation. A total length of 1, 320-km of levee along the lower Yellow River has been enhanced by about 9 m in the past 50 years, including three major levee enhancing projects and many local levee reinforcing projects, with a total amount of 400 million m^3 of earth work and 4 million m^3 of rock masonry work. Figure 6.11 shows the cross section of the levee at Taiqian in Henan Province and 9 times of enhancement (Zhu, 1991). An important strategy is to use heavy sediment-laden floods to reinforce the levees. Sediment suspensions are pumped warping on the lee side of the levee. Deposition of sediment by the levee makes it wider and stronger. Seepage and piping are often the direct causes of levee breach. Concrete anti-seepage walls has been built in the Grand Levees to control seepage and piping. Figure 6.12 (a) shows a machine cutting the land by the levee by 40 m and casting concrete, and Figure 6.12 (b) shows the anti-seepage wall which is 20 cm thick and 40 m deep.
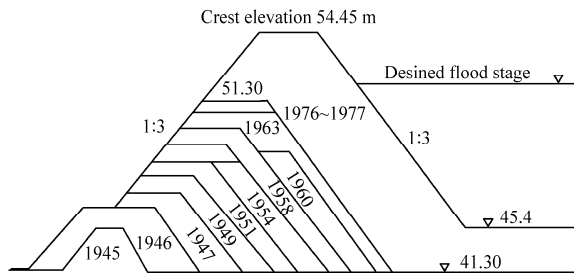
Fig. 6.11   Cross section of the Grand Levee at Taiqian in Henan Province showing 9 times of enhancement

6.2.5 Flood-Detention Basins

The capacity of the river channel in the Shandong reaches is only 10,000 m^3/s, less than that of the upstream Henan reaches (30,000m^3/s). Floodwater has to be detained in the wide valley in the Henan reaches, which will flood the villages on the floodplain if the discharge is over 10,000 m^3/s. For even higher discharge the flood detention basins must be used. There are 5 flood detention basins by the lower Yellow River, namely Dagong, Beijindi, Dongping lake, Beizhan, and Nanzhan. Among them the Beijindi and Dongping lake flood-detention basins are the most important. The Dongping Lake basin detained floods in 1954, 1957, 1958 and 1982 and effectively reduced the discharges to the lower reaches. Figure 6.13 shows the locations of the flood detention basins.

6.2.6 Reforestation and Sediment-Check Dams

Reforestation is a long-term strategy to reduce the river sedimentation. The strategy has been successfully applied in many small watersheds (less than 100 km^2). Figure 6.14 (a) shows the reforested Xizhao Gully on the Loess Plateau, northwest China. In the area the rate of soil erosion in the area is as
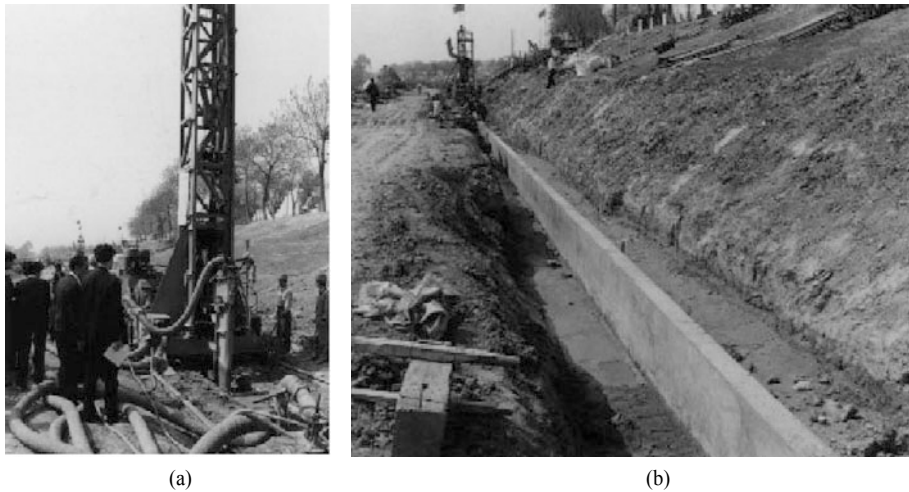
(a)   (b)

Fig. 6.12 (a) A machine cutting the land by the levee by 40 m and casting concrete; (b) The anti-seepage wall 20 cm thick and 40 m deep to control seepage and piping (See color figure at the end of this book)
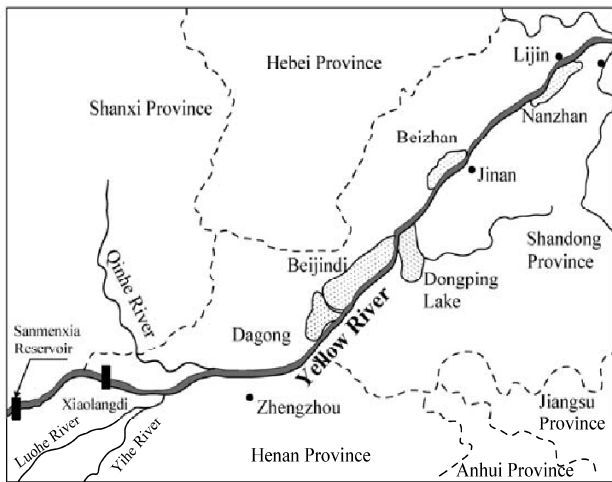
Fig. 6.13 Locations of the Dagong, Beijindi, Dongping Lake, Beizhan, and Nanzhan flood detention basins by the lower Yellow River

high as 10,000 t/km^{2}yr. Planted trees on the slope suffer from erosion and too low soil water. Only the trees in the gully may grow up and form a forest. The planted trees in the gully have trapped the most eroded sediment. Almost no sediment is transported out of the gully. In the southeast part of the Loess Plateau reforestation may be successful on hill slopes as well. Figure 6.14(b) shows the reforestation of the loess hill slopes in Shanxi Province, which effectively reduces soil erosion.

Sediment-check dams affect the river sediment load more directly. Farmers build the sediment-check dams under the encouragement of the government to create farmland, which is usually much more productive than the slope land. Figure 6.15(a) shows a sediment check dam on the loess plateau, which has trapped sediment and created fertile farmland. Figure 6.15(b) shows a new sediment check dam in the east part of the loess plateau, which has been just completed and begun trapping sediment. Reforestation

Fig. 6.14   (a) Planted trees in the Xizhao Gully on the Loess Plateau, northwest China trapped almost all of the eroded sediment from the slopes; (b) Reforestation of the Fengshenshan hill in Shanxi Province in the east side of the Loess Plateau

(a)   (b)

Fig. 6.15   (a) A sediment check dam in the Sha-anxi Province has trapped sediment and created fertile farmland; (b) A new sediment check dam in Shanxi Province has been completed and begun to trap sediment (See color figure at the end of this book)

and thousands of sediment-trapping dams on the Loess Plateau have resulted in a sharp reduction in sediment load to the lower Yellow River. Figure 6.16 shows the variation of annual sediment load transported to Lijin on the lower Yellow River. The average annual sediment load transported to Lijin was about 1 billion tons before 1985 and the value has been reduced 60% since 1985. It is estimated that about 300–500 million tons of the sediment reduction are due to reforestation and sediment-check dams on the Loess Plateau.

6.2.7   Artificial Flood

The recently impounded (2002) Xiaolangdi Reservoir is located about 800 km upstream of the Yellow River mouth and it is the most downstream gorge-type reservoir on the Yellow River. The multi-purpose reservoir is mainly for flood control and sediment retention to reduce siltation in the lower Yellow River. The total capacity of the reservoir is about 12 billion m^3, of which more than 7 billion m^3 will be used for trapping sediment. The sedimentation in the lower reaches of the river will be reduced after impounding

of the reservoir. In the first 8 years of the reservoir impoundment, coarse sediment will be trapped and clear water will be released to the lower reaches. It was calculated that 0.3 billion tons of sediment in the lower reaches channel will be scoured by the released clear water and transported to the ocean. The reservoir will be operated so as to trap coarse sediment and discharge fine sediment. Most of the fine sediment will be released with water discharges over 2,000 m^3/s or more. The sediment load will vary and can be roughly calculated as the incoming sediment load into the reservoir minus the fraction trapped in the reservoir, plus the scoured sediment from the lower reaches channel and the incoming sediment from the catchment below the reservoir. Most of the sediment load will be transported during the flood season and the sediment load transported will be more concentrated during floods.
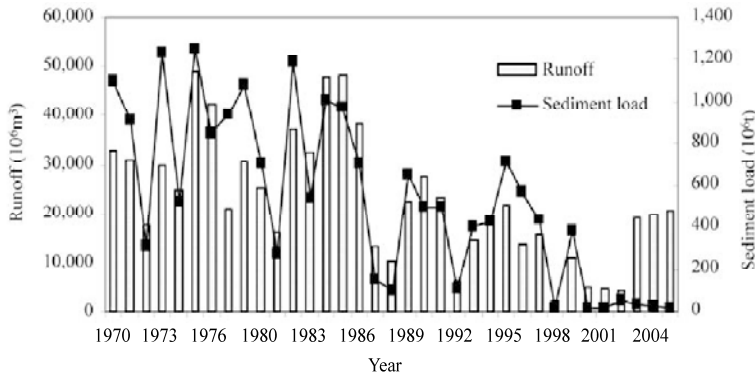
Fig. 6.16 Variation of water and sediment load at the Lijin Station in the lower Yellow River from 1970–2005

Because the coarse fraction of sediment is trapped by the reservoir, the rate of sedimentation of the lower Yellow River channel will be greatly reduced. According to numerical models, the Xiaolangdi Reservoir may control sedimentation of the lower Yellow River for more than 20 years. Nevertheless, the fine sediment will be released into the lower Yellow River to reduce the rate of sedimentation of the reservoir. Sediment finer than 0.02 mm in the river is mostly wash load and can be transported into the sea.

On July 4, 2002 the first experiment of an artificial flood created with the Xiaolangdi Reservoir was conducted to explore the possibility of scouring the lower Yellow River bed. The flood of peak discharge of about 2600 m^3/s was released from the reservoir and maintained about ten days. Figure 6.17 shows the

Fig. 6.17 Artificial flood created by releasing water from the Xiaolangdi Reservoir on July 04, 2002. Water was released from different elevations to control the sediment concentration. The released concentration from the bottom outlet is high dying the water yellow and red, and the water from the top outlet is clean and white

artificial flood created with the reservoir. The concentration of the released flow is planned at 10–20 kg/m^3. In order to control the concentration released sediment, the water is released from the bottom, middle, and top outlets. The released concentration from the bottom outlet is high dying the water yellow and red, and the water from the top outlet is clean and white. The flood scoured the river channel bed and the average concentration of suspended load increased from less than 20 kg/m^3 to 30 kg/m^3. From 2002 to 2004 three experiments were conducted to scour the lower Yellow River with artificial flood before the flood season. Each year 40–60 million tons of bed sediment were scoured by the artificial flood. Now the artificial flood has become a routine operation of the Xiaolngdi Reservoir before the flood season.

6.2.8   Dredging

The main flooding risk is due to the quick siltation and capacity reduction of the channel. Therefore, sedimentation control and increase of the water-conveying capacity of the channel is main aim of river training and the key criteria of the new strategies of river management. Besides the traditional strategies and regulation of sediment and water by using the Xiaolangdi Reservoir, Yellow River channel dredging has become an important auxiliary measure. Training of the river by human actions become much more common than before, and, therefore, people have begun to use dredging for controlling sedimentation. They dreamed that through dredging the river channel shrinkage at selected locations can be alleviated or stopped and a high capacity for carrying sediment, ice, and water can be preserved.

The functions of dredging are to: (a) widen and deepen the shrinking river channel at selected sections; (b) remove coarse sediment of diameter larger than 0.025–0.05 mm from main channel to the floodplain so to reduce the accumulative siltation of the main channel; (c) raise the elevation of the surrounding ground, reinforce dikes, improve soil quality, and create new wetlands at the river mouth with the dredged sediment.

Historically, the Yellow River channel was dredged many times, but the results were not satisfactory. On the one hand, annual sediment load was quite high and the dredged channel was soon resilted. On the other hand, dredging was not supported by advanced technology and suffered from lack of experiences. Today, the conditions and requirement for dredging are different. Many river training projects in China and other countries provide rich experience on dredging and the development of technology and dredgers has greatly improved the efficiency of dredging. Furthermore, there are less and less extreme events and the channel bed is rarely scoured. In the meantime economic development has enabled advanced dredgers to be used for river training. The Yellow River can be dredged by mechanical excavation and transportation, agitating with jets and explosion. Various dredgers have been used: dredge boat; agitating dredger; dipper dredger; hauling scraper; excavator and bulldozer; and trailer dredger (Zhang et al., 1997). Figure 6.18(a) and (b) show two types of agitating jet dredgers scouring sediment during flood season.

At the river mouth the width becomes larger, the depth also increases, the slope becomes gentler, and, therefore, the velocity here greatly reduces. The sediment carried by the flow is unloaded and a mouth bar is formed. The river mouth bar causes a resistance and results in higher flood stages in the upstream reaches. Sediment was, hence, deposited in the upstream channels before the 1980s, which was one reason for the frequent avulsion and channel shift. In the 1980s, dredging projects were implemented to remove the mouth bar. Different dredgers were used and the river mouth has been since then maintained free from a mouth bar. Because of the dredging of the mouth bar, the Qing-shui-gou channel has been used for much longer than the average life span of previous channels.

The success of dredging the mouth bar encouraged people to dredge the river channel as a solution of the channel sedimentation problem. A dredging test was conducted in a 11 km long section near the river mouth (35–46 km downstream of the Lijin Hydrological Station) in January to May 1998. An 11 km long, 200 m wide, 2.5 m deep ditch was dug in the almost flatted river bed and 5.48 million m^3 of sediment was

dredged to the lee side of the levee. Nevertheless, after the first flood in the year the dredged section was basically filled up by sediment deposition. Figure 6.19 shows 2 cross sections of the dredged reach. The cross sections were resilted after only one flood. The perspective of dredging the river channel as a general solution for channel sedimentation is not rather optimistic.

(a)   (b)
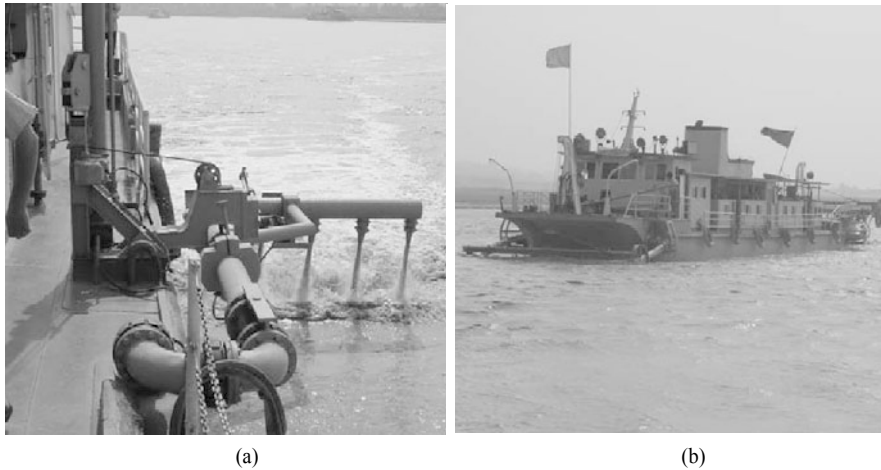
Fig. 6.18   Two types of agitating jet dredgers scouring sediment during flood season
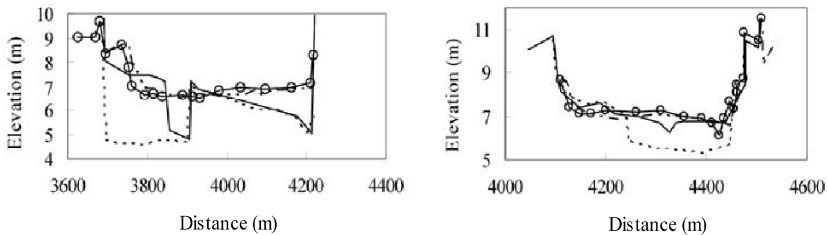
Fig. 6.19   Resiltation of the dredged sections after the first flood in 1998: (a) Wuqizha cross section; (b) Shibahu Cross section (——— Original bed, ········ Dredged ——○—— After the first flood)

6.3 Water Resources Management

6.3.1   General Conditions

The average precipitation on the Yellow River basin is 476 mm but the potential evaporation is 1,000–3,000 mm per year. The total runoff from the watershed is 58 billion m^3, about 2% of the total of the country. There is ground water of about 40.2 billion m^3 in the area but it must be recharged with surface water and rain water. Water resources per capita is 590 m^3 and the water resource per farmland is 4,850 m^3/ha. Moreover, the neighboring areas, such as the Haihe River basin and the Huaihe River basin, also divert water from the Yellow River because the two areas also suffer from water shortage and the lower Yellow River is higher than the surrounding ground and can be directly diverted to these areas. For instance, Tianjin has been supplied Yellow River water almost every year since the end of the 1990s. To supply 600 million m^3 of water more than 2 billion m^3 must be diverted from the Weishan water Diversion Station because more than 70% of the diverted water is consumed and diverted on the way from Weishan to Tianjin.

There are now 3,147 reservoirs in the whole basin with a total storage capacity of 57.4 billion m³. More than 4,500 water diversion projects have been completed and 29,000 pumping stations are working for irrigation and water supply. The irrigation area has increased from 0.8 million ha in 1950 to 7 million ha in 1995. The irrigated farmland is about 45% of the total farmland area but produces more than 70% of the grains. In the past 50 years people have invested $5.4 billion to develop water resources for agriculture and benefited by $57 billion in grain production, $8 billion for urban water supply, and industries benefited by $14.6 billion.

To transport sediment is an important job of Yellow River water. It is roughly estimated that at least 20 billion m³ are needed to transport 1 billion tons of sediment into the ocean. Figure 6.20 shows the average runoff and sediment load along the river course in the 1950s. The runoff remained unchanged from Huayuankou to the river mouth and the sediment load reduced slightly along the lower reaches course. Since 1985, however, the runoff has become less and less along the course from Huayuankou to the river mouth and the sediment carrying capacity reduces even more greatly. The reduced flow discharge is not able to carry the same amount of sediment, and, thus, results in quick siltation of the lower reaches channel.

(a) Annual runoff of the Yellow River

(b) Annual sediment transport of the Yellow River
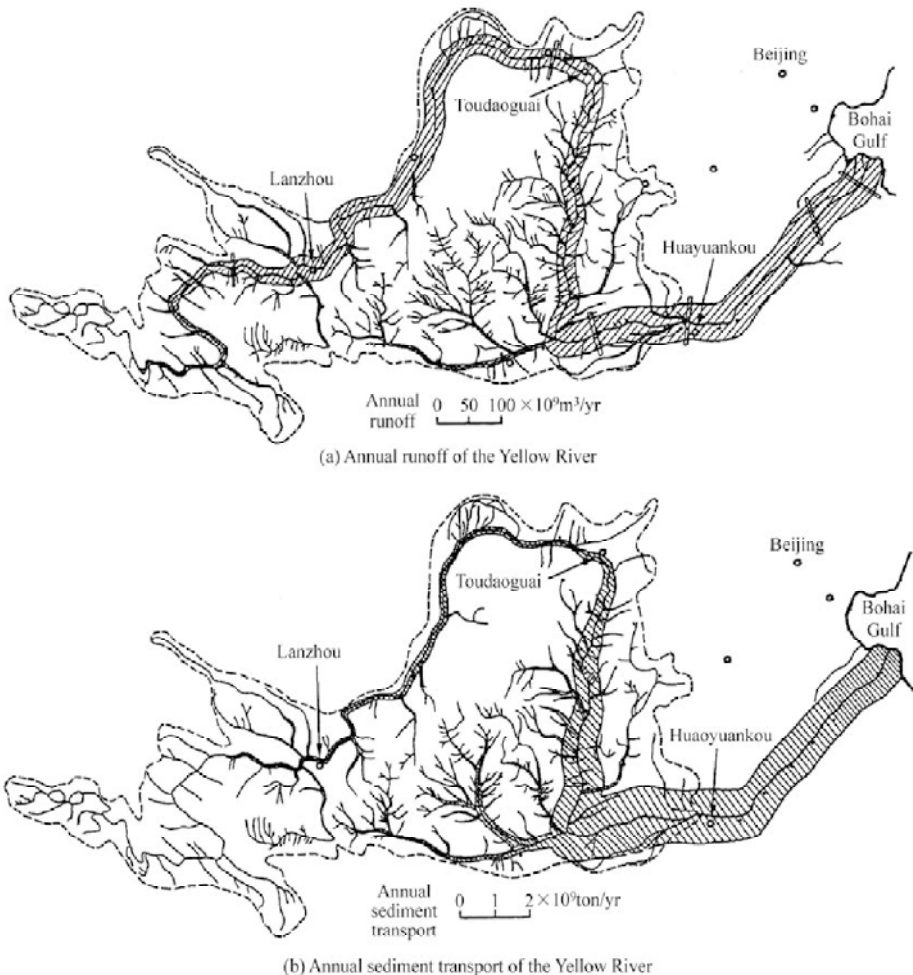
Fig. 6.20   Average runoff and sediment load of the Yellow River in the 1950s (after Qian and Zhou, 1964)

The Yellow River basin is one of the thirstiest areas in China and the economic development is plagued by more and more serious water shortages. All provinces have tried to use as much water as they can, which resulted in conflict between areas and provinces. The use of water resources needs central government coordination. Because the whole area of the Yellow River valley suffers from water shortage, the central government worked out an allocation scheme for use of the water resources in 1987. The quotas of water resources for the 11 provinces are listed in Table 6.3.

Table 6.3   Allocation of the Yellow River Water Resources

Provinces and autonomous regions	Quota (billion m^3)	Water consumption in the 1990s (billion m^3)
Qinghai	1.41	
Sichuan	0.04	
Gansu	3.04	1.76
Ningxia	4.00	3.70
Inner Mongolia	5.86	6.00
Shanxi	3.30	2.50
Shaanxi	4.81	2.00
Henan	5.54	3.50
Shandong	7.00	8.00
Hebei and Tianjin	2.00	0.50
Total	37.00	27.96

Note: The central government adjusted the quota in 1995 allowing the provinces to use 120% of the quota in wet years but only 80% in dry years

It is obvious that except for Shandong province and Inner Mongolia Autonomous Region the water consumption of most provinces and autonomous regions in the 1990s were less than the allocation quotas. It can be foreseen that water consumption of the upstream provinces and autonomous regions will increase following the development of the economy and increase in the ability to withdrawing water.

The allocation scheme was made based on the long-term average annual runoff of 58 billion m^3 in the whole Yellow River watershed. The allocation scheme has not worked well because not so much water was available while water demands of these provinces were more in dry years and increased water was available but less water was needed in wet years. Much less water was released from upstream reservoirs as the lower reaches was thirsty in dry years. The lower reach channel becomes completely dry from March to July during the 1990s. It is necessary to work out a more sophisticated allocation scheme in which the cases of dry and wet years must be taken into consideration.

6.3.2   A Case Study—the Yellow River Delta

6.3.2.1   The Yellow River Delta

The Yellow River Basin is too big to discuss all its water resources problems. To present more details of typical water resources problems the Yellow River delta in the mid 1990s is used as a case study. The location of the Yellow River Delta is shown in Fig. 6.1. It is located in the north-east part of Shandong Province. The majority of the delta is administrated by the city of Dongying, as shown in Fig. 6.21. Dongying is composed of 3 counties and 2 districts, namely, the Guangrao County, Kenli County, and Lijin County, and the Dongying District and the Hekou District. Since the Yellow River changed its course from the Huaihe River to the present river course in 1855, the main part of the course—upstream from the Lijin Hydrological Station—has been stabilized, but the most downstream part of the channel in
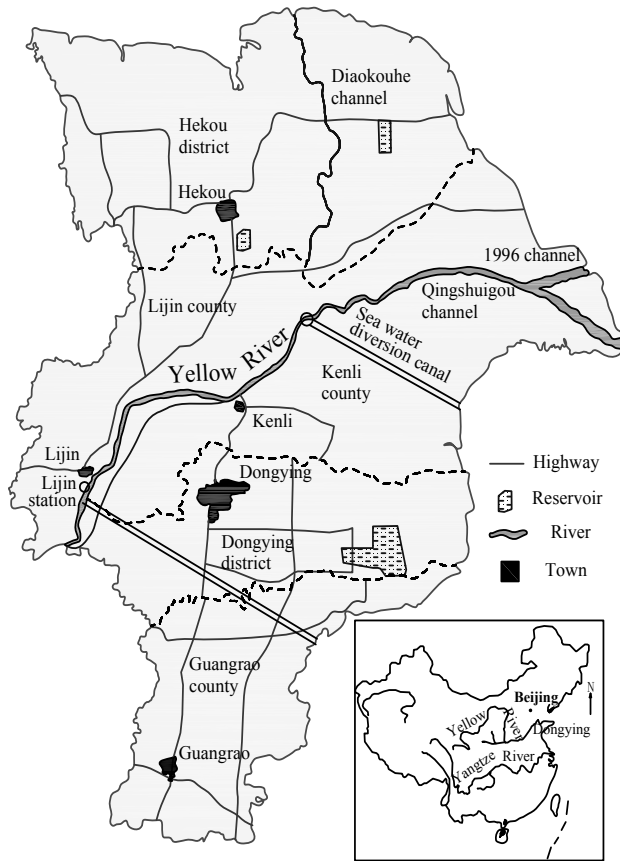
Fig. 6.21   Sketch of the administration of the Yellow River Delta (Dongying City)

the Yellow River delta has changed 11 times due to natural avulsions or human-controlled shifts of the channel. The delta land has become a valuable agricultural resource and beginning in the 1980s delta has seen considerable industrial development. Table 6.4 lists the main features of the Yellow River delta.

The Yellow River delta was created by rapid sediment deposition in the past century. Massive sediment transport, caused by serious erosion of the Loess Plateau in central China, brings fertile soil to the Yellow River delta and has made the delta expand by about 2,000 ha per year. The system is very dynamic and fluctuates with the fluvial regime, tide, and surges. The deposited sediment is composed mainly of silt of diameter about 0.02 mm, which is liable to be eroded and differs from large deltas elsewhere. Because of the high speed of siltation of the channel, the Yellow River shifted its course 11 times in the period from 1855 to 1996. The recent change of the flow course from Diaokouhe to Qing-Shui-Gou occurred in 1976 (Fig. 6.21). Since then the shape of the Yellow River delta changed remarkably. The deposited silt in the previous river (Diaokouhe) mouth was eroded and serious siltation took place in the new river mouth.

The Yellow River delta is mainly under the direct administration of the city of Dongying the Shengli Oilfield, the second largest oil-field in China, is located in the delta, with proved oil reserves of 3.2 billion tons and 25.7 billion m^3 of natural gas. The most important economic stimulus comes from the control, electricity, transportation and communication have rapidly developed. The new Dongying Port is

Table 6.4 Main Features of the Yellow River Delta based on conditions in the mid 1990s

Location	Northeast Shandong Province
Longitude	118°07'–119°10' East
Latitude	36°55'–38°12' North
Climate	Monsoon type continental climate
Temperature	$-19 - +39°C$ with mean value of 12.3 C
Frost-free period	211 days
Ice-free period	190 days
Coastal line	350 km
Marine tide	M2 type with average difference 0.8–1.5 m
Annual precipitation	601 mm
Annual evaporation	About 1,900 mm
Total population	1.62 million
Total land area	8053 km^2
Population density	190 p/km^2
Birth rate	1.033%
Death rate	0.544%
Rate of population increase	0.488%
Cultivated area	236,000 ha
Total grain production	870 million kg (1993)

Regional GNP
    1st industry (agriculture)
    2nd industry (industry)
    3rd industry (service)
	RMB 19.2 billion (1993)
	    RMB 2.13 billion
	    RMB 13.73 billion
	    RMB 2.06 billion

Regional GNP per capita	12,000 RMB (1993)
Water resources	The Yellow River and local water
Annual runoff	30.9 billion m^3
Usable water	3.8 billion m^3 (with sediment less than 30 kg/m^3)
Discharge in dry season (11–6)	0–100 m^3/s
Discharge in flood season (7–10)	2000–6000 m^3/s
Flood with 40 years recurrence interval	10,000 m^3/s
Annual sediment load	0.7–1.0 billion tons
Annual sediment deposition	0.5–0.7 billion tons
Annual created new land	20 km^2
Capacity of water storage	400 million m^3
Annual water consumption	1.7 billion m^3
Oil reserves	3.2 billion tons
Oil production	33 million tones per year
Natural gas reserves	25.7 billion m^3
Salt reserves	580 billion tons

Shengli Oilfield. Since the founding of Dongying in 1983, infrastructure for water supply and flood located at the Northwest coast of the delta. It is primarily used for supplies for the Shengli Oilfield and some passenger transport to Dalian, with 3,000–5,000 berths. Design depth for the harbor is 6 m after completion of the first phase and 10 m after completion of the second phase construction. The local governor is quoted as saying that the navigation line will be the fastest way from the Yellow River Valley Economic Belt to the North Eastern China Industrial Zone and will play an important role in the economic development of China.

6.3.2.2   Water Resources of the Yellow River Delta

The Yellow River is the main water resource of the delta. The distribution of runoff volume among the months at the Lijin Station and the monthly average sediment concentration are listed in Table 6.5. August and September are the wettest months with the highest runoff and sediment concentration. April and May are the driest months. Nevertheless, the clearest water flows in December, January and February with sediment concentrations less than 5 kg/m^3.

Table 6.5   Water distribution among months for the Yellow River at Lijin from 1973 to 1993

Month	1	2	3	4	5	6	7	8	9	10	11	12	Year-round
Long term average runoff (bi m^3)	1.270	0.980	1.124	0.783	0.788	0.868	2.911	4.897	5.151	4.741	2.448	1.554	27.52
With guarantee rate 75%	0.979	0.504	0.269	0.494	0.648	0.021	2.333	5.171	3.077	3.391	1.854	1.701	18.44
With guarantee rate 95%	0.391	0.108	0.129	0.144	0.041	0.000	0.076	2.989	2.629	1.808	1.517	0.912	10.74
Average concentration (kg/m^3)	2.65	2.99	6.51	5.78	5.72	7.74	30.66	41.96	31.33	18.92	9.72	4.30	25.33

Note: The guarantee rate stands for the probability of the runoff volume exceeding the given value. For instance, the probability of runoff volume in January over 0.979 billion m^3 is 75% and the probability of the water volume over 0.391 billion m^3 is 95%

The water resources from the Yellow River are changing and depend, to a great extent, on the economic development and water diversion from upstream reaches. According to the YRCC report "Development planning of the Yellow River Basin" in the 1990s, the coal production bases in Shanxi and Sha-anxi Provinces and Inner Mongolia Autonomous Region would divert 2.9 billion m^3 of water from the Yellow River, Tianjin would divert 2 billion m^3, and impoundment of the Xiaolangdi Reservoir would increase water diversion and evaporation. Therefore, the water resources from the Yellow River would continue to reduce.

The main water resource of the delta area is the Yellow River. Nevertheless, the number of days on which water diversion is allowed is constrained by:

(1) floods with discharge over 5,000 m^3/s cannot be diverted;

(2) water with sediment concentration over 30 kg/m^3 is not allowed to be diverted;

(3) during the ice cover period, water diversion may be carried out only 70% of the time; and

(4) the capacity of diversion canals does not match the capacity of diversion works, the maximum water conveyance is 270 m^3/s, or only 60% of the capacity of the diversion works.

As long as diversion works and canals have sufficient capacity and the sediment is properly disposed, water shortage in the delta area can be eased or solved. In other words, the water shortage in Dongying is due to inadequate water supply infrastructure rather than lack of resources.

6.3.2.3 Water Management

1) Water-Demand Reduction

The total area of irrigated farmland in the delta was 141,000 ha, of which only 3,333 ha, or 2.35% of the total, had been equipped with water-saving irrigation facilities. The average water use efficiency in irrigation was 0.46. The total length of canals in the area was 1,474 km, of which only 75 km, or 5.11% of the total, was lined. There were almost no sprinkler and drip irrigation and there was great potential for water-demand reduction in irrigation. For instance, in a small irrigation district, 64% of the water was lost due to seepage in irrigation canals and 17% was lost in conveyance canals. When the canals were lined for seepage prevention the percentages of water loss due to seepage was reduced to 35% and 6% for the two kinds of canals. The average water use efficiency of the Caodian irrigation district was increased to about 0.5.

Dongying plans to enhance the water use efficiency to 0.65. If the irrigation canals are replaced by pipelines, the conveyance water use efficiency in transportation can be up to 0.99 and the average water use efficiency can reach 0.7. The area with water conservation measures will also increase from 14,670 ha to 133,000 ha and the rate of water use will reduce from 8,310 m^3/ha to 5,580 m^3/ha.

Water conservation in industrial production has gotten attention since the 1980s. In the 1990s, the rate of water consumption is 272 m^3 per \$1200 and the rate of water reuse is about 20%. It is planned to reduce the rate of water consumption to 149–167 m^3 per \$1200 and to increase the rate of water reuse to 45%. Water for urban and industrial use is mainly supplied by the Genjing and Guangnan Reservoirs. In the 1990s, each of the reservoirs stored 165 million m^3 of water, and the amount of water supplied by each reservoir was 99 million m^3. Therefore, the water use efficiency of the two reservoirs is about 0.6, giving room for water conservation measures.

2) Utilization of Sediment-Laden Water

Water demand by agriculture is over 50% of the total. According to statistics, about 50% of the required amount of water for agriculture can be met by using sediment laden flood water from the Yellow River. The Yellow River delta is very flat. There is no place to construct desilting basins at the headwork of canals. At distances from the river there are saline spots, which can be used to construct plain reservoirs or develop agriculture after artificial siltation by using the Yellow River sediment. The canals have gentle slopes and are used to convey water and sediment for long distances. It is important to avoid siltation in the canals. In the Caodian Irrigation District, all canals are lined with concrete and stones. Low head pump stations are used to raise the water head and silty water with sediment concentrations up to 30-40 kg/m^3 has been transported in the canals for over 50 km without accumulated siltation. In the Mawan Irrigation District, the main canal is 26 km long fed by a pump station with a capacity of 30 m^3/s. Although it is an earthen canal without a desilting basin, the canal has been used to transport silty water for four years without serious siltation. These experiences are valuable and are going to be applied generally in the area.

3) Other Water Resources

Water resources other than the Yellow River in the delta include industrial waste water, urban sewage water, brackish ground water, local runoff, the Xiao-Qing River and the Zi-Mai-Gou River, water from South China via the east route of the South-North Water Transfer Project, and recovery of water lost due to seepage from the Yellow River. The total amount of these kinds of water is over 2 billion m^3 per year. These water resources may be exploited if the economic and environmental conditions allow.

6.3.2.4   Impacts of Water Resources Utilization on the Environment

Water utilization from the Yellow River affects the environment positively and negatively. The positive effects are: (a) promoting development of industry and agriculture, improving water supply, and enhancing the living standard of the local people; (b) developing forests and improving the environment in the area. To the south of the Xiao-Qing River, water diverted from the Yellow River promotes the recharge of local ground water and stops ground water depression. The seepage of surface and irrigation water desalinizes ground water and prevents salt water intrusion; (c) water diversion projects and reservoirs increase the water surface area and evaporation may increase the humidity of the air and change the local climate. The surface water may be used for recreation; and (d) utilization of highly silt-laden water from the Yellow River for land fill and ground level increase also improves soil quality and promotes agricultural development.

The negative effects are: (a) salinization induced by irrigation water percolation, and by seepage from canals and reservoirs; (b) occupation of land by water diversion works and reservoirs, and displacement of inhabitants from the by area submerged reservoirs; (c) reduction of water and sediment flowing into the sea may affect the species living in the waters and wetlands near the Yellow River mouth; and (d) desertification induced by deposition of sediment from diversion of heavily silt-laden flood water. Nevertheless, the negative effects on the environment can be reduced to the minimum by applying proper management strategies.

6.4   New Problems in the Yellow River Management

6.4.1   Power Generation Reduces the Channel Capacity

The 11 reservoirs on the Yellow River: Longyangxia, Lijiaxia, Liujiaxia, Yanguoxia, Bapanxia, Qingtongxia, Sanshenggong, Wanjiazhai, Tianqiao, Sanmenxia, and Xiaolangdi have a total capacity of 55.8 billion m^3, equal to the annual runoff of the whole watershed. The total installed capacity of power generation is 5,620 MW, of which 1,280 MW is at Longyangxia, 2,000 MW at Lijiaxia, and 1160 MW at Liujiaxia. These power plants generate 23 billion kw-hr per year, of which the 3 major power stations generate 6 billion kw-hr each. The reservoirs are operated mainly according to the requirements of power generation and water supply without consideration of the natural features of the river and maintenance of a high capacity for sediment transportation in the channel. The reservoirs store water the during flood season and release water in the non-flood season for power generation. Therefore, the flood peaks are flattened and much less water is transported at high discharges. Flows in the middle and lower Yellow River have changed remarkably.

The Sanmenxia Reservoir is the most downstream reservoir on the Yellow River about 1,000 km upstream from the river mouth. The Longmen Hydrological Station is about 230 km upstream from Sanmenxia Dam and the measured water and sediment at the station reflects the influence of human activities in the middle and upper watersheds. Figure 6.22 illustrates the runoff volume at different discharges at the Longmen Hydrological Station in the flood season (July to September). From 1950–1969 more than 7 billion m^3 of water, or 30% of the runoff in flood season, was transported at a discharge of about 3,000 m^3/s. In the period 1970–1985, the peak runoff-conveying discharge was still 3, 000 m^3/s but only 3.8 billion m of water flowed at that rate. In the period 1986–1995, however, the peak runoff-conveying discharge reduced to 1,500 m^3/s, which reflects the effects of discharge-regulation by the reservoirs, water diversion, and soil and water conservation works in the watershed (Pan and Li, 1998).

The average annual runoff and sediment load released from the Sanmenxia Reservoir to the lower reaches of the river in the period 1986–1994 were 30.7 billion m^3 and 0.8 billion tons which were 11.3

billion m^3 and 0.36 billion tons less than the long term (1950–1990) average values, and those to the river mouth were 17.2 billion m^3 and 0.42 billion tons, 23 billion m^3 and 0.58 billion tons less than the long term average values. The main causes for the remarkable changes are attributed to soil conservation projects and sediment trapping in the reservoirs in the upper and middle reaches, increasing water and sediment diversion, and sedimentation in the lower reaches (Zhang et al., 1997).
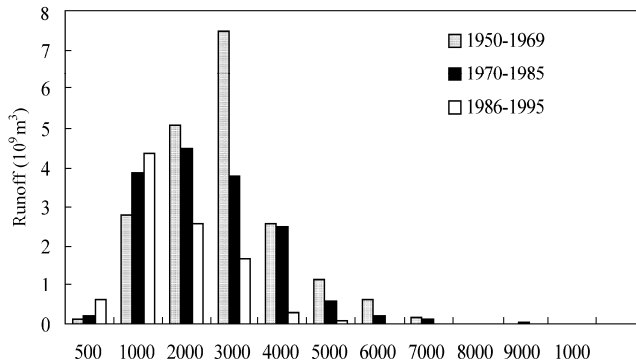
Fig. 6.22 Comparison of runoff volume in the flood season (July–Sep) at different discharges at the Longmen Hydrological Station for the periods 1950–1969, 1970–1985 and 1986–1995

In the past decade, the lower reaches changed rapidly in hydrological features. With the development of reservoirs and irrigation projects upstream, less water was released to the lower reaches. Only 700 million tons of sediment was transported to the lower reaches annually due to sediment trapping projects in the Loess Plateau and fewer rainstorms. Nevertheless, sedimentation in the lower reaches was not eased by the reduction of sediment load. Between 1985 and 1994 the average sediment accumulation in the lower reaches was 307 million tons during the non-flood season, of which 67 million tons were scoured during the flood season, resulting in a net sediment deposition of 240 million tons per year. In the meantime, on average 495 million tons of sediment were transported to the delta and into the Bohai Sea per year. The huge amount of sediment deposition caused serious aggradation of the riverbed and seabed. Table 6.6 lists the rise of the water stage at a discharge of 3,000 m^3/s at the main hydrological stations along the river in the period 1985–1994.

Table 6.6 Flood stage rise (at a discharge of 3,000 m^3/s) at the main gauging stations along the lower reaches of the Yellow River in the period 1985–1994

Hydrologic Station	Zhengzhou	Gaocun	Aishan	Jinan	Lijin
Distance from Lijin (km)	670	456	270	168	0
Stage rise (m)	0.99	0.93	1.13	1.35	1.62
Average rate of stage rise (m/year)	0.11	0.10	0.13	0.15	0.18

The stage rise is due to sediment deposition in the river channel. The important facts of sediment movement in the lower reaches of the Yellow River are: (i) siltation takes place in the low flow season and net scour occurs in the flood season; and (ii) scour occurs during the rising limb of a flood and siltation occurs during the receding limb of a flood. Analysis of the data from the lower Yellow River yield the following empirical formula relating the sediment load from scouring to the flow discharge:

$$\Delta Q_s = 0 \quad \text{if} \quad Q = 1,800 \text{ m}^3/\text{s} \tag{6.1}$$

in which ΔQ_s (in tons/s) is the increased sediment discharge due to scour in the section from Aishan to Lijin, Q is the water discharge in m³/s. In other words, $Q = 1800$ m³/s is the critical discharge for channel bed erosion and siltation. The bed is scoured if the flow discharge is greater than and sediment deposition occurs if the flow discharge is less than 1,800m³/s. Similar law was found by other researchers with the critical flow discharge at 1,500 m³/s (Qi, 1993). Figure 6.23 shows the average bed elevation at the Lijin Station corresponding to the discharge from July to November of 1977 (Yin and Chen, 1993). High discharge causes deep erosion of the riverbed, whilst flood recession and low flow were accompanied by aggradation.

Reservoirs have trapped a huge volume of sediment that resulted in a quick reduction in the sediment load to the lower reaches. The reservoirs also reduced water flow to the lower reaches, clipping peak flood discharges. Sediment carrying capacity of flow is proportional to the power of the discharge. Sediment used to deposit in the lower river channel in dry years and was scoured away in wet years when high discharge occurred. Reservoir regulation deprived the opportunities for bed scour and the channel accumulatively silted up.

Development of the economy and growth of the population lead to the reclamation of the river floodplain. Nowadays more than 1.7 million people are living on and plowing 270,000 ha farmland in the lower Yellow River floodplain within the Grand Levees. The people built levees by the main channel and prevented the floodplain from flooding, therefore, sediment mainly deposited in the main channel. In the 1950s, 80–100% of the deposited sediment was on the floodplain, whereas in the 1990s 74–113% of the sediment deposited in the main channel. Although the total amount of the annual sediment deposited in the lower Yellow River was less, the amount of sediment deposited in the main channel was much more than before, consequently, the channel shrank and the water conveying capacity of the river channel reduced greatly. Figure 6.24 shows the variation of the water discharge capacity of the river channel below elevation 93.5 m at Huayuankou in the period from 1958 to 1999. The capacity was about 18, 000 m³/s in 1960 and is now less than one tenth of that. In many sections the channel is silted up to an elevation higher than the floodplain and is therefore named the "perched channel" within the "suspended river".
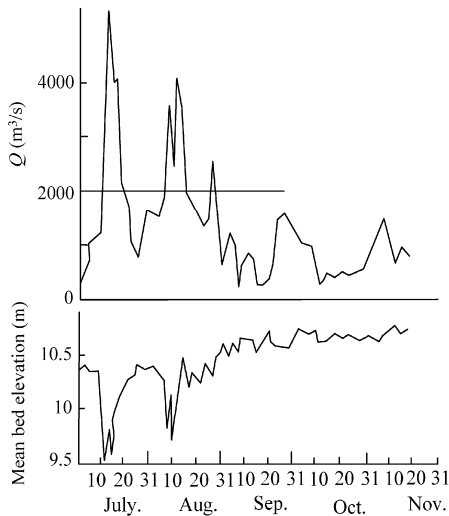
Fig. 6.23   Variation of bed elevation and the flood discharge at the Lijin Station during the flood season in 1977
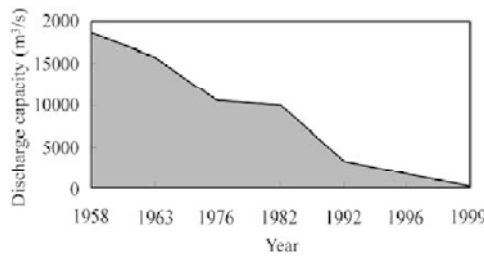
Fig. 6.24   Reduction of the discharge capacity of the Yellow River Channel below elevation 93.5 m at Huayuankou in the period from 1958 to 1999

6.4.2   Reclamation of the Floodplain Increases Flood Loss

Due to the high rate of population growth and the lack of land people reclaim the floodplain in the lower Yellow River valley. There are about 1.7 million people dwelling on the floodplain within the Grand Levees in the Henan and Shandong reaches of the river. They built levees within the river to protect their hometowns on the floodplain although the floodplain was used for retention of rare floods. They are not protected by the Grand Levees and exposed to high risk of flooding. When the inhabitants of a town near the Yellow River Changdong Bridge were woken by a muffled roaring sound August 5, 1996, some part of the town were already a meter under water. A flood of discharge 7,860 m^3/s washed through lower reaches of the river breaking levees and destroying 2,898 villages and 212 towns. About 2.41 million people were affected by the flood and $800 million were lost. The flood discharge was much less than the those of 1958 (22,300 m^3/s) and 1982 (15,000 m^3/s), but the flood caused the highest stage in historical records. Figure 6.25 shows the stage-discharge relations of the 1996 flood and those of 1958 and 1982 (Zhao and Liu, 1997). The recurrence period of the flood with peak discharge about 8,000 m^3/s is only 2 years according to 1950–1996 data. In other words 8,000 m^3/s or higher discharge occurred once per 2 years but such heavy loss never resulted prior to 1990.
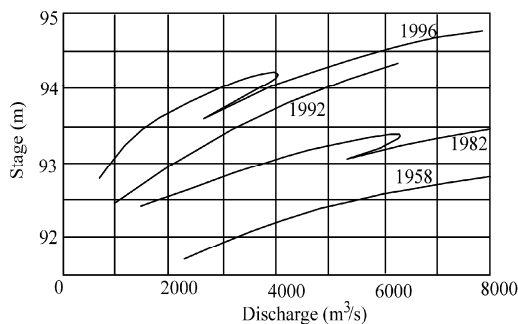
Fig. 6.25   Stage-Discharge relationships of 1996, 1992, 1982 and 1958 floods (after Zhao and Liu, 1997)

The high stage of the 1996 flood was due to the siltation of the main channel. Long term river evolution data demonstrate that sedimentation occurs at low discharge and the river bed is scoured if the discharge is over 1,800 m^3/s. With flow regulation by the reservoirs, trapping of water and sediment by thousands of warping reservoirs in the Loess Plateau, and diversion of huge amounts of water from the river, the peak discharge of floods was cut off and the total runoff of floods was remarkably reduced. It was estimated that if the 1996 rainstorm had occurred in 1950–1960, the peak discharge at Huayuankou would have been over 12,400 m^3/s (Zhao and Liu, 1997). Because the river channel now is rarely scoured by

turbulent floods, the main channel is silted up at high rate, 0.1–0.2 m/yr. Now the river bed is 6–10 m higher than the surrounding ground and is named the "suspended river". In many sections the main channel was flattened and was at the same elevation as the floodplain, therefore, the 1996 flood did not flow down the river in a well-defined channel but flowed randomly within an up to 10 km wide valley confined by the Grand Levees. In many sections the flow was directed to the levee and causing levee to burst. The propagation speed of the flood wave was much lower than normal, thus, the 1996 flood took 17 days to travel the 800 km from Huayuankou to Lijin although the average time for floods of the same discharge in 1950–1990 was only 7–8 days.

6.4.3   Water Diversion Causes Flow Cut-Off

The Yellow River watershed is a semi-arid area and the river is the main water resource for 150–200 million people in the middle and lower reaches. With the booming economy, demand for water has rapidly increased. Water diversion in the middle and lower reaches of the Yellow River has escalated. Because of the serious water shortages and the absence of a workable plan for distributing the valuable water to various provinces and regions, all localities on both banks of the river try to store and use water as much as they can. Not only low concentration water is diverted during the non-flood season, but also the high concentration flow in the flood season is diverted. As a result, less and less water is released to the lower reaches. The annual runoff and sediment load at Lijin (110 km from the river mouth) is shown in Figure 6.16. The annual water flow before 1985 was 40 billion m^3 but reduced to only 15 billion m^3 after 1985. Figure 6.26 shows the days and length of dried-up channels of the lower Yellow River from 1970 to 1998. In 1972, the Lijin Station in Shandong Province recorded a 15 day period when the river dried up. For the first time in known history, the mother river stopped flowing. The river suffered two major droughts, one from 1875–1878 and another from 1922 to 1932 without drying out, but it began to dry out in the 1970s. Flow cut-offs have occurred in 19 of 27 years in the period 1972–1998.
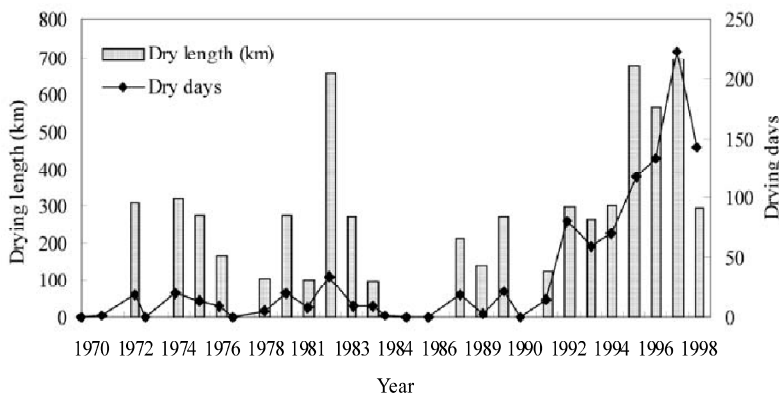
Fig. 6.26 Dry days and dry length of the lower Yellow River from 1972-1998

Before 1990, the drying out often took place in May and June. But after 1990, the drying up started early in February, and ended as late as October. In 1970s, the river only dried for about 10–20 days and the dry section was only 135 km long. The river remained dry for 80 days in 1994, 122 days in 1995, 133 days in 1996 and 226 days in 1997 and the dry section stretched to 700 km from the river mouth. The river flow was cut off in flood season because the floodwater was diverted for irrigation and drinking. Figure 6.27 shows that the river flow cut off and the dry river bed in the flood season in 1977. Boats were resting on the bed and the floating bridge was not so useful because vehicles may drive across the

(a)

(b)

Fig. 6.27 The cut off river flow and the dry river bed during the flood season in 1977: (a) A boat is resting on the bed; (b) A floating bridge is not useful because vehicles may drive across the riverbed at any place

riverbed at any place. The river is in danger of transforming into an inland river in the foreseeable future. Without prompt measures, China may someday find her mother river exhausted. No sediment and organic material were transported into the sea during the dry time, which cut off the food chain for some species. This will result in complex ecological problems, for instance, the fish in the estuary have been greatly affected and some precious species have vanished. The river is usually regarded as an "artery" of the country and the cut off of the river flow will seriously damage its "health". this is sounding a warning that water shortage is becoming a more serious problem than the need for flood control in northern China.

6.4.4 Collapse of Spur Dykes

To stabilize the channel in the wide river valleys in the lower Yellow River many spur dykes have been constructed. The spur dykes have, to a certain degree, fixed the channel and concentrated the flow and cause sediment deposition between the spur dykes. The channel, therefore, was deepened and relatively stabilized. A channelization degree is defined as the ratio of the total length of the spur dykes to the length of the channel, or the length of spur dykes per channel length. Figure 6.28 shows the distribution of channelization degree along the river downstream from Sanmenxia Reservoir. From the 1970s to 2002,

the degree has increased from 0.2–0.8 to 0.8–1.35. Nevertheless, the natural fluvial processes tend to break the constraint of the spur dykes, and the flow scours the dykes and causes them to collapse.
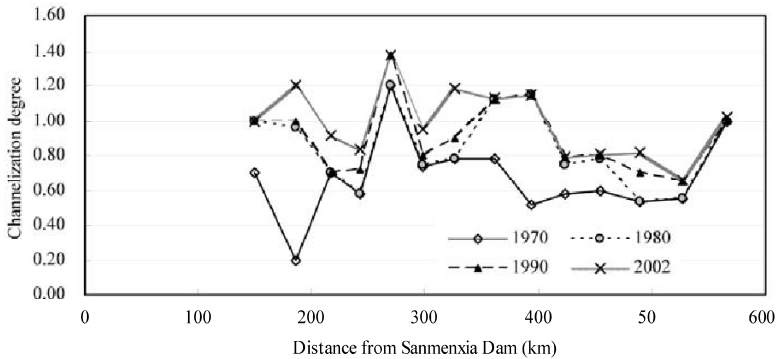
Fig. 6.28 Distribution of channelization degree (ratio of the length of the spur dykes to the length of the channel) along the lower Yellow River (Cheng et al., 2007)

Figure 6.29 shows the probability of collapse of each dyke as a function of the channelization degree. The probability is calculated with the total times of collapse per year over the number of spur dykes. The probability is low as if the channelization degree is lower than 0.8. For a channelization degree higher than 0.8, however, the probability of dyke collapse abruptly increases from 10% to 30%. The high probability of dyke collapse is due to the conflict between the natural fluvial processes and the constraint of channelization. In fact the strongest conflict occurs for channelization degrees in the range of 0.8–1.0, and, therefore, there is a corresponding high probability of dyke failure. Nevertheless, if the channelization degree approaches to 2 (the two sides of the channel are completely controlled with spur dykes), the channel motion will change from lateral to vertical. The channel will be deepened, resulting in an increase in the bank-full discharge. Figure 6.30 shows the probability of dyke failure against the bank full discharge. Following an increase in bank full discharge the probability of dyke failure decreases.
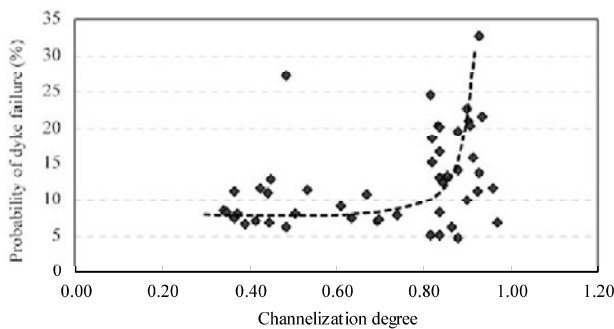
Fig. 6.29 Probability of dyke collapse as a function of the channelization degree

6.4.5   Water Diversion Changes Fluvial Process

The amount of water diversion from the lower Yellow River has been increasing in the past 50 years. Water diversion inevitably affects the fluvial processes. Water diversion may even change a section of a perennial stream to an ephemeral river section (Fogg and Muller, 1999). While water diversion projects have become a popular and important strategy to meet increasing water demand, the stream flow,

sediment transport and fluvial processes of rivers are increasingly affected.

Figures 6.31 (a) and (b) show the variation of the annual water and sediment load from 1960 to 1997 at Xiaolangdi and Lijin hydrologic stations, in which the horizontal lines represent the average runoff and sediment load. The differences between the figures at the two stations are due to the inflow from
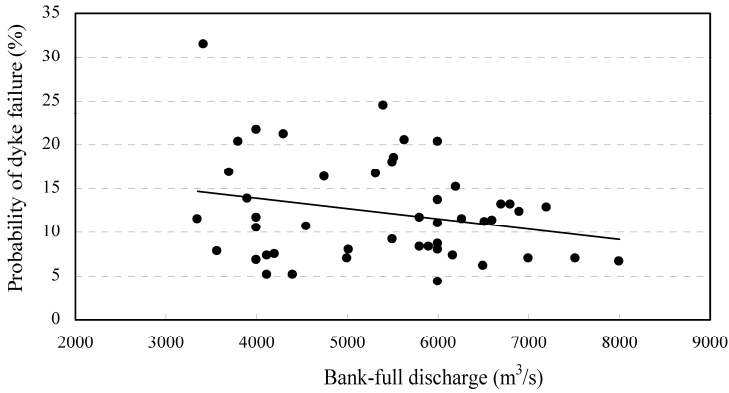
Fig. 6.30   Probability of dyke failure as a function of bank-full discharge
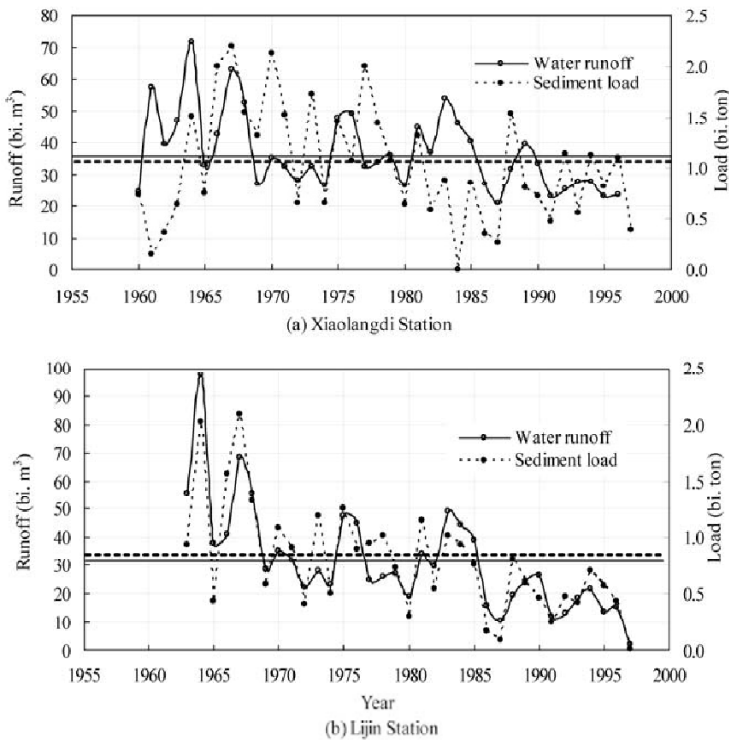
Fig. 6.31   Variation of annual runoff and sediment load in the period from 1960 to 1997 at (a) Xiaolangdi (130 km from Sanmenxia Dam) and (b) Lijin (900 km from Sanmenxia Dam). The differences between the two stations are due to the inflow from tributaries and water diversions

tributaries and outflow by water diversions along the course from Xiaolangdi to Lijin. From 1960–1969 there was more water flowing through Lijin than Xiaolangdi because the water diversion was less than the inflow from tributaries. From 1970–1985, the annual runoff at Lijin was equal to or slightly less than at Xiaolangdi because more water had been diverted. From 1986 to the present, however, the total volume of water diverted was much more than the inflow from tributaries, and the water runoff decreased along the course. The annual runoff was about 11 billion m^3 less at Lijin than at Xiaolangdi. The reduction in runoff over a long stretch of the river elicited a sharp reduction in the flow's sediment-carrying capacity. Therefore, the annual load was much less at Lijin than at Xiaolangdi during 1986 to the present.

From 1986, water and sediment load increases along the course and reach their maximum values at Huayuankou, and then reduce further downstream due to diversion. The sediment load at Lijin is less than that at Sanmenxia by more than 300 million tons, which must have deposited in the reach between Sanmenxia and Lijin and consequently changed the morphology of the river.

One of the impacts of the runoff reduction on the fluvial processes was the shrinkage of the channel. Figure 6.32 shows the bank full discharge of the lower Yellow River during different periods. Water diversion has reduced the discharge and sediment-carrying capacity, and sediment has been deposited in the channel, which has made the channel shallow and unstable. As a result, the bank full discharge has decreased steadily. The bank full discharge was about 9,000 m^3/s in 1958 and 1964; it decreased to about 6,000 m^3/s in 1985, and to only 3,000 m^3/s in 1999.
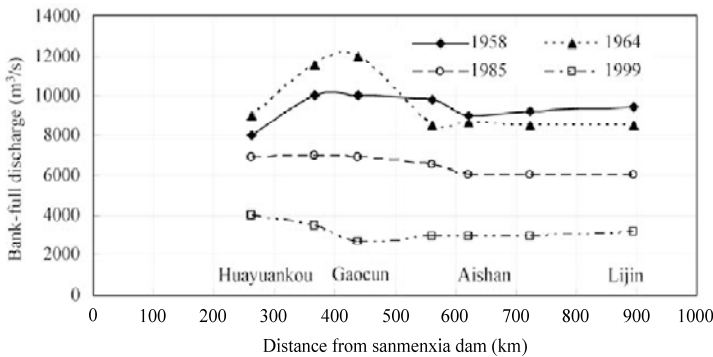
Fig. 6.32   Bank-full discharge along the lower Yellow River course during different periods

The second important impact of water diversions is the adjustment of the riverbed profile. Field evidence from natural streams shows that variations in successive processes and forms result from a system's tendency to minimize the rate of energy dissipation with time (Simon, 1992). For alluvial river with bed material consisting of sand and silt, no bed structures except for sand dunes can develop, the river morphology depends mainly on the stream power. According to the minimum stream power theory (Yang, 1996), the bed gradient develops to reach the minimum stream power, thus:

$$\frac{dP}{dx} = \frac{d}{dx}(\gamma s Q) = \gamma\left(Q\frac{ds}{dx} + s\frac{dQ}{dx}\right) = 0 \qquad (6.2)$$

in which P is the stream power in ton/s, γ is the specific weight of water in ton/m^3, s is the riverbed slope, x is the distance along the river course in km, and Q is the discharge in m^3/s. For most rivers, the discharge increases along the course due to the inflow from tributaries; thus, the term sdQ/dx is positive.

According to equation (6.2), the term Qds/dx must be negative, or the slope of the riverbed decreases

along the course; so that these rivers exhibit concave riverbed profiles. Equation (6.2) indicates the direction of morphological processes and equilibrium state of longitudinal river profile. Sediment load plays an important role in the speed of morphological process but does not change the direction and the final equilibrium of the profile. The higher is the sediment load the faster is the morphological process. For a low sediment load river the riverbed profile often does not meet Eq. (6.2) because it takes a very long time to reach the minimum stream power profile.

The Yellow River carries heavy sediment load and the morphological processes is fast. The large quantity of water diverted along the course of the Yellow River makes the term sdQ/dx negative. For instance, since 1986 the average discharge has decreased along the Yellow River course in the reach downstream of Huayuankou, i.e. $dQ/dx<0$. According to Eq. (6.2) the term Qds/dx must be positive. In this case, the riverbed profiles will develop toward a convex shape, which is different from the normal concave curve. Figure 6.33 shows the bed profiles of the lower Yellow River for 1977 and 1997. The mean bed elevation is the average bed elevation of the channel with a cross-section of wet area about 500 m^2. The figure shows that the lower section of the river is developing toward a convex profile. Because the profile of the upper section is concave, the river shows an "S-shape" longitudinal bed profile. The trend will continue and the turning point in the profile will move upstream because the water diversion is continuing and more water will be diverted in the foreseen future (Wang and Hu, 2004).
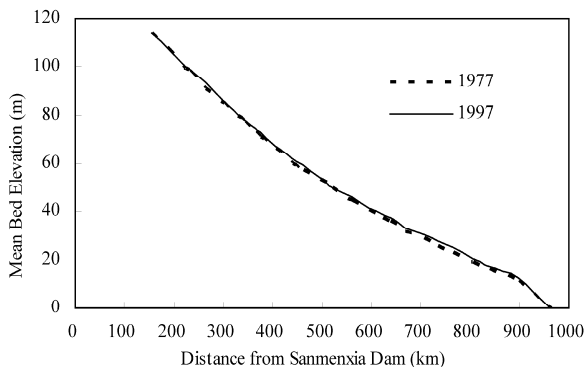
Fig. 6.33 Longitudinal bed profiles of the lower Yellow River in 1977 and 1997 (Wang and Hu, 2004)

6.4.6 Delta Channel Stability and Land Creation

The modern Yellow River flows into the Bohai Sea via Lijin since the river levee at Tongwaxiang (about 600 km from the present river mouth as shown in Fig. 6.1) was broken and flood water captured the Daqing River channel, in 1855. Thence the reaches upstream of Lijin have been densely populated and the levees in the reaches were enhanced and reinforced many times, and no avulsion and channel shift occurred in these reaches since 1855. The population density down stream from Lijin was low and the levees downstream of Ninghai were weak to resist the assault of flood. Therefore, nodal avulsions occurred around Ninghai (60–100 km from the mouth as shown in Fig. 6.34) and the river changed its delta channel 11 times between 1855 and 1976. The river channel swept over a fan-shape area of radius about 50 km. The present delta was created by rapid sediment deposition in the past 147 years, accompanied by frequent shifts of the channel in the area. The 12 old river channels are shown in Fig. 6.34 (Wang and Liang, 2000), that each has its own name. The present channel-Qing-Shui-Gou Channel- has been in use since 1976. A recent minor shift of the mouth channel (about 20 km from the mouth) to Chahe occurred in 1996, which is also shown in the figure. More detailed data on the channel shift and location of avulsions are presented in Table 6.7 (Yin and Chen, 1993, Zhang et al., 1997).
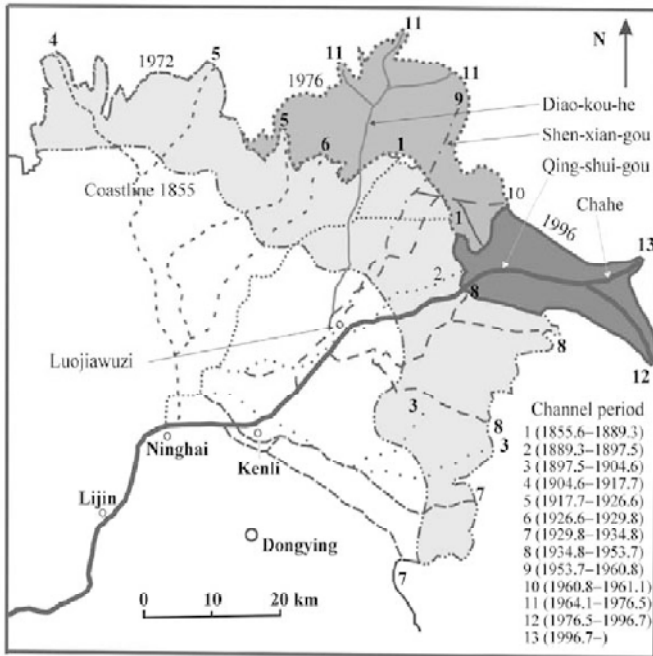
Fig. 6.34   Nodal avulsions and the abandoned Yellow River channels. The coastlines show the land created by the river in the periods between 1855–1972, 1972–1976, and 1976–1996

On average the delta channel changed once per 10 years. Before the 1950's, the change in the river course was triggered by overflow and levee breach at the diversion point. Since 1953, the river course has been artificially shifted 4 times. In the spring of 1964, an ice jam occurred and the safety of the Shengli Oil Field in the delta was threatened. The levee at Luo-jia-wu-zi was artificially broken, and the river shifted from the Shen-xian-gou channel to the Diao-kou-he channel. Before the recent diversion in 1976, people dug the Qing-shui-gou channel at a cost of $1 million. In May 1976, the river course was artificially shifted to the Qing-shui-gou and since then this river channel was safely used for more than 30 years (plus the Qing-shui-gou Channel period). During this period the river created land at a rate of 20–40 km²/year. It follows the routine of "channel siltation—high flood—broken levee—channel shift creation of new land."

In the early Qing-shui-gou period, the river channel was not well shaped. The sediment-laden flow built up its channel by depositing sediment in low velocity areas and scouring sediment in high velocity areas. During this process, seasonal variation of discharge and sediment deposition in the delta area has resulted in a high frequency of mouth migration, as shown in Fig. 6.35 (Ji et al., 1994). In the first 3 years (1976–1979), the channel was unstable and the new river mouth wandered in an area of a range of 30 km. The main stream flowed eastward into the sea in October 1977, but changed northward in October 1978. In the flood season of 1979 the river mouth moved from northeast to southeast again. The frequent shift of the mouth and channel is due to the floods with sediment high concentration in these years with a maximum sediment concentration up to 240 kg/m³. Since 1980, the main channel has moved east again and a relatively stable meandering channel formed. In 1986 the local people extended the guiding levees and the channel upstream from Q8 was not allowed to wander anymore (Fig. 6.35).

Table 6.7 Shift of the river course and the 11 river channels

No.	Year (AD)	Used time[*] (years)	Length[**] (km)	Diversion point	Name of the channel
0	1855	49		Tong-wa-xiang	
0	1881	71			
0	1889.4	32.5[***]	75		
1	1889.4	61		Xie-jia-yuan	
1	1897.6	5.10	71		
2	1897.6		59	Ling-zi-zhuang	
2	1904.7	5.9	65		
3	1904.7		57	Yan-wo	
3	1917.8	11	63		
4	1917.8		57	Tai-ping-ling	
4	1926.7	6.11	67		
5	1926.7			Ba-li-zhuang	
5	1929.9	2.11	65		
6	1929.9		73	Ji-jia-zhuang	
6	1934.1	3.4	65	Channel changed many times	
7	1934.1			Yi-Hao-Ba	
7	1950		75	Tian-shui-gou	
7	1953.7	9.6	85	Tian-shui-gou	
8	1953.7		75		Shen-xian-gou
8	1964.1	10.6	102		Shen-xian-gou
9	1964.1		70	Luo-jia-wu-zi	Diao-kou-he
9	1976.5	12.4	103		Diao-kou-he
10	1976.5		66	Xi-he-kou	Qing-shui-gou
10	1987		106		Qing-shui-gou
10	1996.7	20.2	112		Qing-shui-gou
11	1996.7		94	Cha-he	Qingshuigou-Chahe
11	1997.12	1.5	102		Qingshuigou-Chahe
11	1999.11	3.5	105		Qingshuigou-Chahe

[*] Used time = the time period the river flowed in a channel. Because the river often breaches the levees and water flowed outside of a channel sometimes, the used time of a channel is less than the time period from the river began to flow in the channel to its shifting to another channel

[**] Length = distance from the Lijin Hydrological Station to the mouth of the river

[***] 32.5 = 32 years and 5 months

A shift in the river course caused stage reduction in the upstream reaches. The new channels were shorter than their predecessors and had greater slope. Thus, the flow velocity was higher and stages at the same discharges were lower. Figure 6.36 shows the stages at Lijin and Aishan (locations of the two station in Fig. 6.1) for discharges of 1,000 and 3,000 m³/s in the period from 1950 to 1990. The stages decreased abruptly in 1953, 1964, and 1976, corresponding to the three shifts of the river course. The effect reached Aishan, which is more than 350 km from the river mouth. Following these short periods of stage reduction there was a sharp stage increase because of a quick extension of the new channel following the avulsion. Another stage reduction occurred in the 1980s, which is not due to a shift of the channel but to dredging of the river mouth.
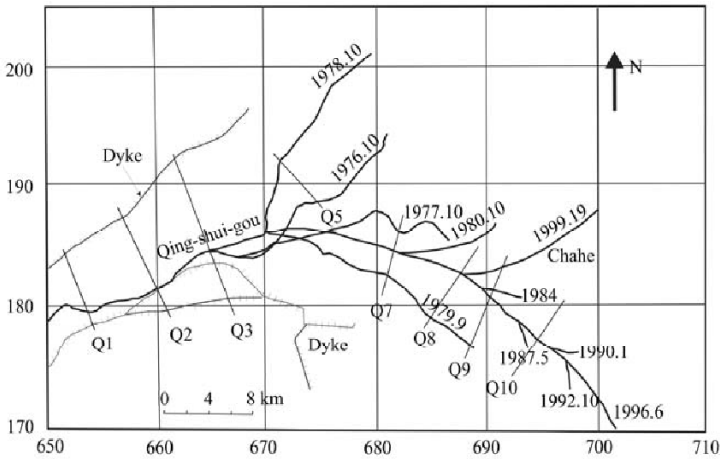
Fig. 6.35   Wandering of the Qing-shui-gou channel (Yellow River mouth) in the period 1976-2001 (Q1-Q10 are the cross sections for measurement)
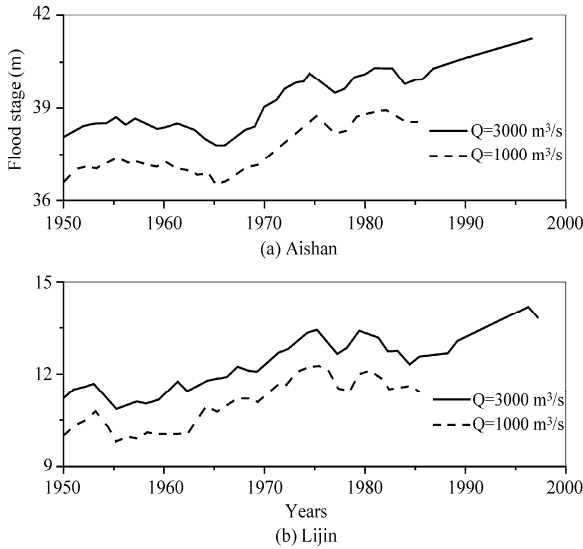
Fig. 6.36   Fluctuation of flood stage at (a) Aishan and (b) Lijin Stations at discharges of 1000 and 3000 m³/s due to avulsions (Stage reductions occurred in 1953, 1964, and 1976, which are coincidental with the avulsions)

   The delta is very dynamic and fluctuates in response to the alluvial regime, tide, and storm surges. The deposits in the delta consist mainly of silt ($d_{50} = 0.02$ mm), which is very erodible. The riverbed can be eroded and filled with several meters in one day during a flood (Wang, 1999). The Qing-shui-gou channel extends into the sea for over 40 km, and the shape of the Yellow River delta has changed remarkably since the river shifted to this channel in 1976. In the meantime, the silt deposited in the previous channel (Diao-kou-he) mouth was eroded. By comparing satellite images of the Yellow River Delta in 1976 and 1988, a map of topographic change in the two areas has been derived. The present river mouth was in the sea with a water depth of 10–20 m before the shift and the previous river mouths-Shen-xian-gou mouth and Diao-kou-he mouth were land of a few meters elevation. As shown in Fig. 6.37,

the new river mouth area (about 30 × 40 km) was silted up and emerged from the sea, with the maximum siltation of 14 m. In the meantime the old river mouths were eroded by waves and tidal currents. The maximum erosion depth is about 6 m (Zhang et al., 1997). The Qing-shui-gou channel extended by 11 km in 1976 and 5 km in 1977. The speed of extension decreased sharply in the succeeding years. The average speed of the river mouth moving into the sea was about 2.3 km/yr in the period from 1976–1994 and was zero in the period from 1994–1996. The rate of land creation is reduced because of the stabilization of the river mouth.
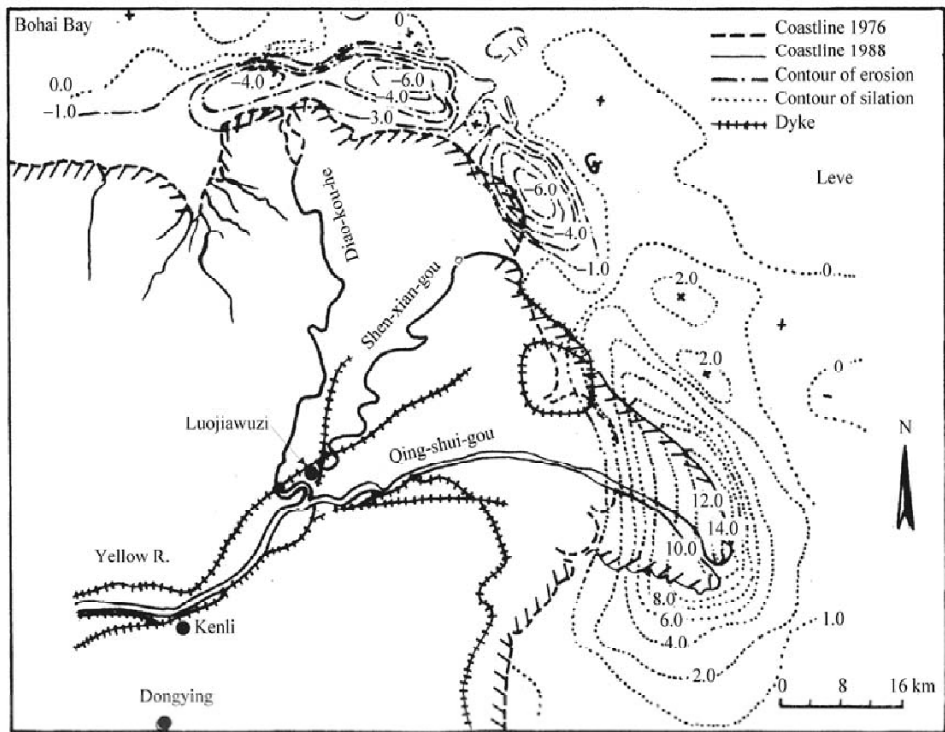
Fig. 6.37   Contours of siltation of the Qing-shui-gou mouth (1 to 14 m) and erosion of the Diao-kou-he and Shen-xian-gou mouths (-1 to -6m) from 1976–1988

The Yellow River delta is rich in oil and gas resources. The Shengli Oil Field, second largest in China, is developed on the delta. No long or medium term construction of oil fields can be planned if the channel cannot be stabilized. The Kendong Oil Field is located in the offshore area near the river mouth (the Chahe mouth in Fig. 6.35), with oil reserves of 257 million tons and could be developed into an oil field with an annual production of 5 million tons/year. The water depth in the area is in the range of 1–5 m. By utilizing sediment transported by the Yellow River to silt up the field, the cost of oil extraction can be reduced by $0.35 billion US.

The river was artificially switched to the Fork Channel in July 1996 for land creation (Zhang et al., 1997). When the first flood flowed through the Fork Channel in 1996, erosion took place and the channel became 3.5–4 m deep and 300–400 m wide. The new fork channel can be clearly seen from the satellite image shown in Fig. 6.38. The stage of 2,100 m³/s flood on August 5,1996, was recorded at 5.8 m at Ding-zi-kou and at only 5.81 m for a flood of 3, 860 m³/s on August 26, 1996, due to scouring of the

channel. Because the new channel was 16 km shorter than the previous one, the energy slope was higher and retrogressive erosion occurred in a section of 30 km from the river mouth. The shift to the new channel reduced the flood stage upstream to Lijin by more than 0.3 m. The peak discharge of the flood at Lijin was 4, 100 m³/s. The flow was kept in the main channel and no overbank flow occurred. Therefore, the 25, 000 ha of farmland and 4 oil fields on the floodplain were free from flood. More than 60 km² land were created at the new river mouth by the 1996 flood. According to the predicted sediment load and runoff, more than 200 km² of land could be created by the Yellow River sediment around the new river mouth in several years. The offshore oil field there would emerge. This was a successful operation integrating river mouth training and oil production. Fig. 6.38 is a satellite image in 2000, 5 years after the shift to the Qing-shui-gou-Chahe channel. The rate of land creation is less than the estimation because the sediment load and water to the river mouth in the past years were much less than the long term average. However, the new channel is stabilized quite soon. The original Qing-shui-gou channel bed is now covered with vegetation of shrubs and herbaceous.
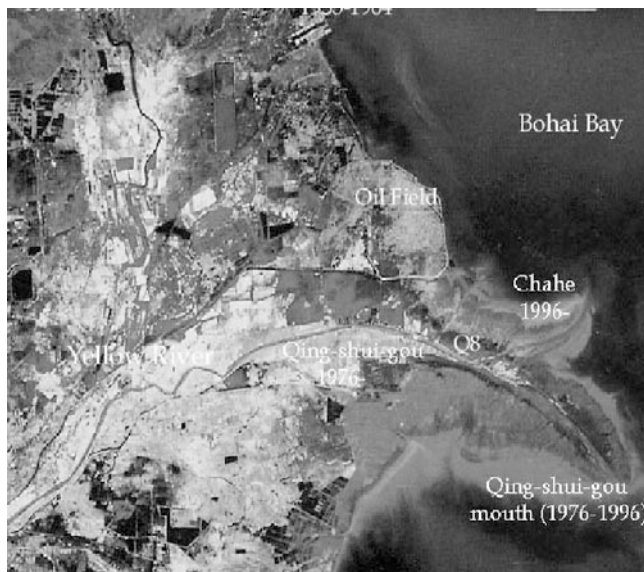
Fig. 6.38   Satellite image of the modern Yellow River delta and the Qing-shui-gou-Chahe channel in 2000 (See color figure at the end of this book)

6.5 Lessons From Sanmenxia Reservoir

Sanmenxia Reservoir demonstrates the perils of giving inadequate consideration to sediment management in the planning and design of a reservoir. Because the problems of siltation and induced flooding risk to the lower Weihe river have not been solved, decommissioning of the Sanmenxia dam has been under discussion for a long time as an alternative strategy to eventually solve the problem. The flooding disaster that occurred on the Weihe River in the fall of 2003 has rekindled the argument on decommissioning of the dam. The main cause for the disastrous high stage is the continuously increasing river bed and flood plain due to sedimentation. If there were no Sanmenxia Dam, the river bed would be much lower and the flood would cause no such disasters. Nevertheless, only 3 years ago when the Yellow River Conservancy Commission celebrated the 40 year anniversary of the Sanmenxia Reservoir, many

people spoke highly on the reservoir. Sanmenxia Reservoir was awarded as the great achievement in hydro-construction in China. It is a great practice in the training of heavy sediment load rivers. The half century of safety in the lower Yellow River and development of the river basin is attributed to the operation of the reservoir, which played an important role in flood control, ice-jam flood control, power generation, irrigation, and water supply. Moreover, scientists and engineers have accumulated experiences from the management of the reservoir for design and operation of dams on high sediment concentration rivers. Sanmenxia reservoir is a mistake or a great achievement? What we should learn from Sanmenxia Reservoir? The following section is attributed to the Sanmenxia Reservoir.

6.5.1 Sanmenxia Reservoir

The Sanmenxia Dam, 105-m high and 739-m long, was the first large dam on the Yellow River. The crest elevation of the dam is 353 m and the designed reservoir capacity is 35.4 billion m^3 with a normal pool level of 350 m. The main purposes of the dam are flood control, ice jam flood control, trapping sediment to reduce the downstream channel sedimentation, power generation, and irrigation. The reservoir controls a drainage area of 688,000 km^2 and 89% of the total runoff of the Yellow River basin. The reservoir area is shown in Fig. 6.39, in which the lower Weihe River is a part of the reservoir. Design of the dam and the reservoir was conduced by the Yellow River Conservation Commission (YRCC) under the guidance of Russian experts from the Soviet Union (ECASP, 1993).The heavy sediment load was considered and the designer planned a big part of the reservoir capacity for sediment deposition, which is mainly in the Yellow River.

The construction of the dam was initiated in 1957 and water impoundment commenced in September 1960. The reservoir area extends upstream a distance of 246 km to Longmen. The Yellow River flows
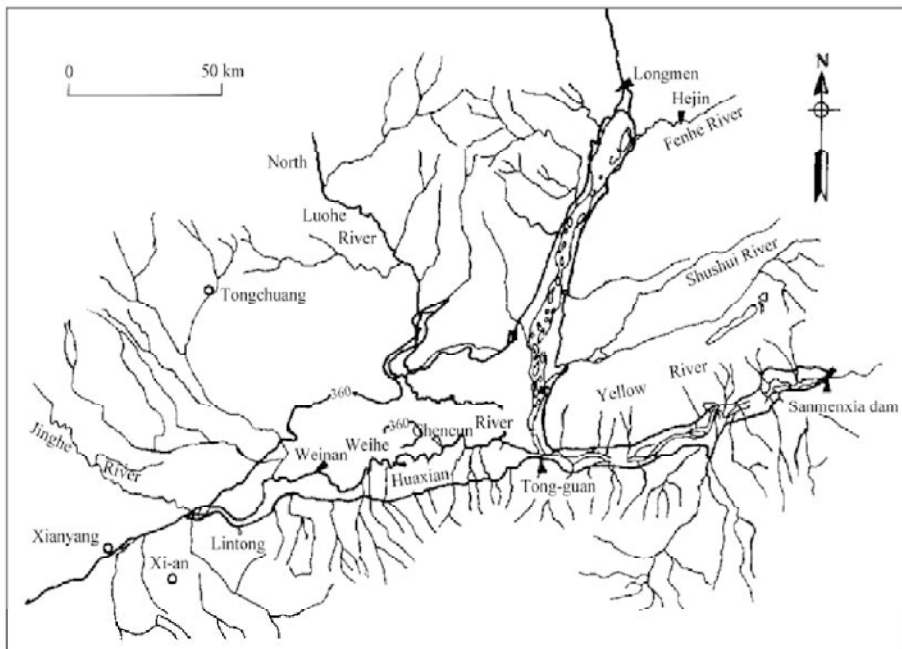
Fig. 6.39 Sanmenxia Reservoir area (enclosed by 360 m contour line) and the Weihe River, in which the Tongguan Hydrological Station on the Yellow River, and the Huaxian, Weinan, Lintong, and Xianyang stations on the Weihe River are indicated

south from Longmen to Tongguan, then makes a 90° turn and goes east. The Weihe River flows into the Yellow River at Tongguan.

To mitigate the sedimentation, the operation scheme of the dam was changed to detain only flood water in flood seasons. The primary function of Sanmenxia Dam was originally for flood control. For this purpose a capacity of 10 billion m^3 was reserved (even after the change in operations) to cope with floods that occur only once in a thousand years, such as the 1933 flood. However, the flood-releasing capacity of the outlet structures was limited. Though the reservoir was operated at a low level during flood seasons were with all the outlet structures fully opened, the reservoir stage was still high and serious sedimentation in the reservoir due to the detention of large amounts of flood water was still inevitable. The net accretion of sediment deposits amounted to $2.04 \times 10^9 m^3$ from April 1962 to May 1966. During this period, 16 floods lasting 89 days in the summer of 1964 caused 0.93×10^9 m^3 of sediment to be deposited in the reservoir area (Yang et al., 1994).

During the impounding period from September 1960 to March 1962, the "elevation of Tongguan," which indicates riverbed variations and is defined as the stage corresponding to a discharge of 1,000 m^3/s at Tongguan station, rose 4.5 m (Long and Chien, 1986; Long, 1996), finally reaching 327.2 m in March 1962. Backwater sediment deposition extended over Chishui in the lower Weihe River, about 187 km upstream of the dam, and extended 152 km in the Yellow River. After the mode of reservoir operation was changed, the backwater sediment deposition was still rapidly extending upstream, raising the bed elevation and flood levels in the Yellow River as far as 260 km upstream of the dam. This threatened the industrial and agricultural bases, and more importantly the capital city of Shanxi Province Xi'an, in the lower reaches of the Weihe River. In addition, it potentially required the relocation of an additional one million people. There was much pressure to improve the situation because of the dense population and the scarcity of farmland in China. In order to alleviate the serious reservoir sedimentation problem and to achieve a balance between sediment inflow and outflow, a special meeting was held in Xi'an City in December 1964 to find a solution to the sedimentation problem in the reservoir. The late Premier Zhou Enlai presided over the meeting, showing the high demand for a resolution to this problem. A policy was established to "ensure the safety of Xi'an City in the upstream as well as that of the lower Yellow River" and a decision was made on the reconstruction of outlet structures to increase the discharge capacity.

The reconstruction work was carried out in two stages. In the first stage, two tunnels at an elevation of 290 m were added on the left bank and four penstocks were remolded into outlets for the purpose of sluicing sediment, as shown in Fig. 6.40. After work on the first stage was in completed in August 1968, the discharge capacity had been increased from 3,080 m^3/s to 6,100 m^3/s at a water level of 315 m. The reconstructed outlets were put into operation one after another and played a definite role in reducing sediment deposition in the reservoir area below Tongguan. However, the sills of the outlet structures were too high and the capability of the reservoir to release floodwater was inadequate. The ratio of outflow-inflow sediment was 80%. The amount of backwater deposition was still high and the bed elevation at Tongguan continued to rise.

The work on the second stage commenced in December 1970. In this stage, 8 bottom outlets at an elevation of 280 m previously used for diversions were reopened to sluice sediment at the lower elevation and to generate stronger headward erosion. In order to suit power generation at a low altitude elevation by the river's current during the flood season, the intakes of penstocks No. 1–5 were lowered from an elevation of 300 m to 287 m, and 5 generation units with a total installed capacity of 250 MW were installed. The first generating unit started to operate at the end of 1973, and the rest were put into operation by the end of 1978. After the second stage of reconstruction, the release capacity of all the outlets increased to 10,000 m^3/s at an elevation of 315 m (Fig.6. 41). With this capacity, no significant backwater could accumulate immediately behind the dam in medium or minor flood conditions, and the
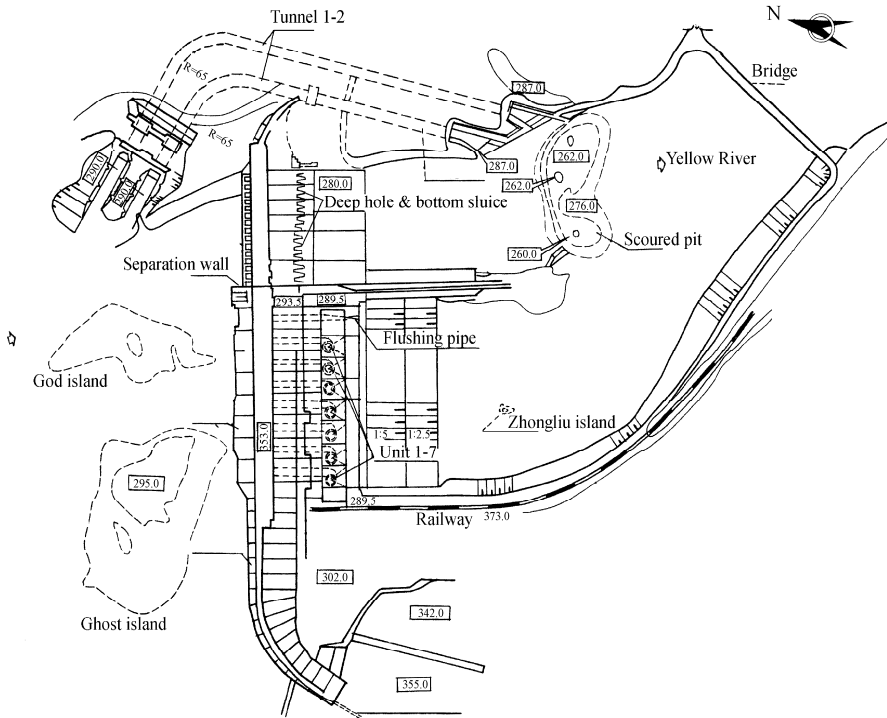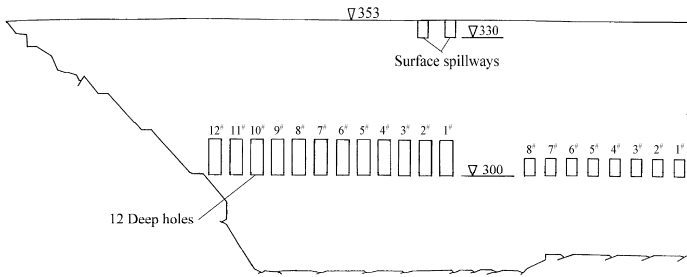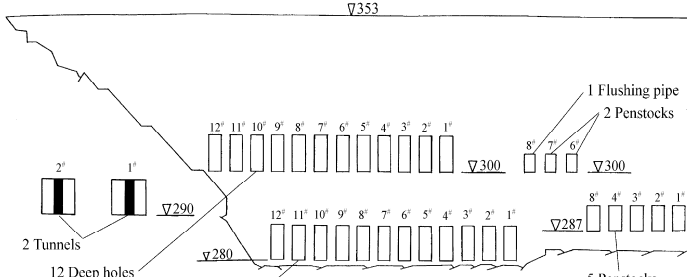
Fig. 6.40 General layout and outlet structures of Sanmenxia Dam: (a) Plan view; (b) Front view of original design; (c) Front view after reconstruction (Wu et al., 2006)
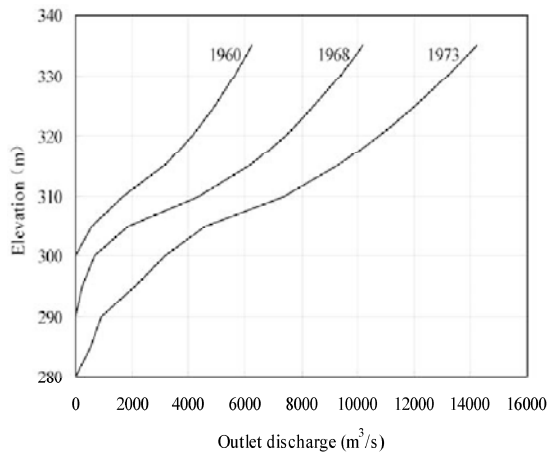
Fig. 6.41   Discharge capacity of the outlets of Sanmenxia Dam (Wu et al., 2005)

outflow and inflow ratio of sediment reached 105%. In the period from the beginning of the summer in 1970 to the end of the flood season in 1973, about 4.1 million m³ of sediment in the reach from the dam to Tongguan was scoured away, and a part of the reservoir capacity was restored. Correspondingly the bed elevation at Tongguan dropped by 2 m.

After these two stages of reconstruction, the dam can discharge sediment-laden water and causes no significant detention of large amounts of flood water. However, due to surface abrasion and cavitation, the bottom sluices were severely damaged, and, therefore, they underwent repairs from 1984–1988. As a result the total discharge capacity of bottom sluice openings No. 1 to 8 was reduced by about 471 m³/s due to compression. To compensate for the reduction resulting from bottom sluice repairs, two more bottom sluices, nos. 9 and 10, were opened in 1990. In an attempt to make the most of the dam by fully utilizing the potential for hydropower generation in the non flood season, penstocks nos. 6 and 7 were converted back to power generation in 1994 and 1997, respectively. Considering the effectiveness of sediment flushing by discharge at low levels, the last two bottom sluices, nos. 11 and 12, were also opened in 1999 and 2000, respectively. To date, there are 27 outlets in Sanmenxia Dam for discharging flood flows.

6.5.2   Management of Reservoir Sedimentation

Sedimentation in the reservoir depends on the incoming water and sediment, the discharge capacity, and the operational mode. Reconstruction of the outlet structures has significantly increased the discharge capacity, providing the dam with the necessary facilities for avoiding significant detention of flood water which is important for maintaining the sediment balance across the impounded reach in the reservoir. On top of this, the dam must be properly operated to maintain the reservoir level in order to increase the benefits of the project and to maintain the sediment balance. For this purpose, the Sanmenxia Reservoir has adopted three different modes of operation. The average pool levels corresponding to each operation mode are shown in Fig. 6.42.

(1) Storage. The mode was used during the initial period of reservoir impoundment, from September 1960 to March 1962, when the reservoir was operated at a high storage level throughout the whole year, according to the original project design.

(2) Flood detention. The mode was applied from March 1962 to October 1973, during which the reservoir was used for flood detention and sediment sluicing with the water being released without

restrictions. The reservoir was operated at a low storage level throughout the year, detaining floods only during flood seasons and sluicing sediment with the largest possible discharges.

(3) Controlled release. The mode has been used since November 1974, to store relatively clear water in non-flood seasons (November–June) and dispose of muddy water in flood seasons (July–October). In this period, the reservoir has been operated at a high water level in non-flood seasons, and at a low storage level during flood seasons, and all the outlets were to be opened in times of flood peaks to sluice the sediment as much as possible.
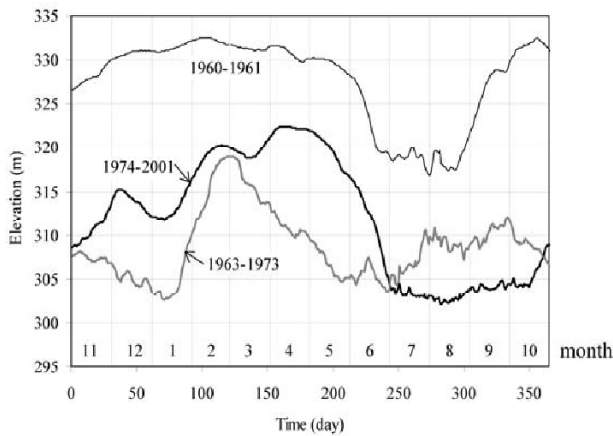
Fig. 6.42   Variation of average pool level of the Sanmenxia Reservoir in different time periods

Sedimentation in the reservoir is different corresponding to different operational modes and the outlet discharge capacities. Table 6.8 presents a summary of the amount of sediment deposited in the reservoir from Tongguan to the dam during the periods of different operation modes. The mean annual deposition volumes in the reservoir area are 620.38×10^6, -102.51×10^6, and 12.57×10^6 m^3 during the periods of storage, flood detention, and controlled release, respectively. Because the reservoir was operated at a low storage level and the discharge capacity was enlarged in the period of flood detention, the reservoir sediment was changed from accumulating to scouring. In the period of controlled release, deposition occurred during non-flood seasons while scouring occurred in flood seasons.

Figure 6.43a shows the accumulated volume of sediment deposition in different reaches in the reservoir area and Fig. 6.43b shows the variation of reservoir storage capacity. Within the range of operation levels

Table 6.8   Summary of sedimentation during different operation periods at Sanmenxia Reservoir

Time period	Mode of Operation	Maximum Discharge at 315 m (m^3/s)	Average Annual Runoff (10^9 m^3)	Average Annual Sediment (10^9 tons)	Mean Annual Deposition (10^6 m^3)		
					Non-flood season (Nov.-June)	Flood season (July-Oct.)	Year
9/1960 –10/1964	Storage	3,080	46.2	1.34	70.11	550.27	620.38
11/1964 –10/1973	Flood Detention	6,100	38.2	1.44	−63.61	−38.90	−102.51
11/1973 –10/2001	Controlled Release	10,000	31.6	0.86	129.02	−116.45	12.57

below 323 m, the capacity of 1.05 billion m³ is available for controlling medium floods in the flood season whenever necessary. About 3 billion m³ of the reservoir capacity below 330 m has been kept for use in the event of an extremely large flood. In the normal operation of the reservoir, the floodplain in the reservoir would be inundated only during extremely large floods; the major task of operation is the detention of such floods. The detained sediment would be eroded in the next several years. However, once the direct backwater effect reaches the confluence area above Tongguan during a flood event and lasts for a certain period of time, sediment deposition on the floodplain would be inevitable and a part of the reservoir capacity would become unavailable for use in the later periods. It is obvious that for preserving a usable capacity in the reservoir, one of the guiding principles of the reservoir's operation is to prevent the direct backwater effect from exceeding Tongguan as much as possible.
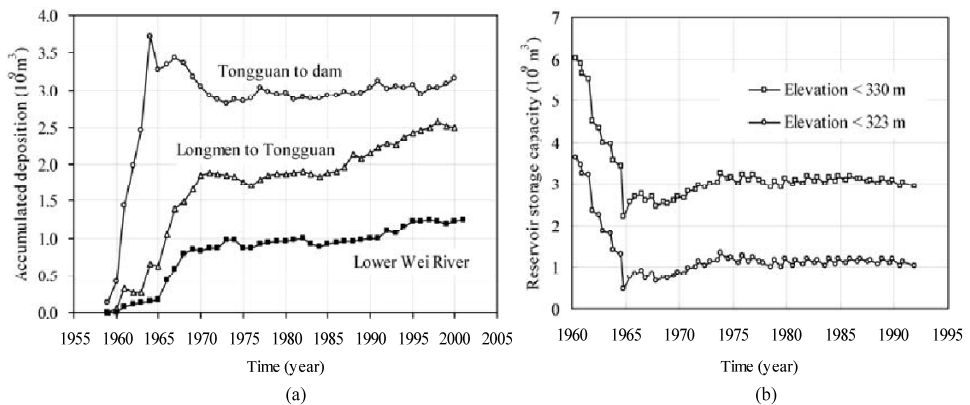
Fig. 6.43   Variations of accumulated deposition and reservoir capacity in Sanmenxia Reservoir: (a) accumulated deposition; (b) reservoir storage capacity

As shown in Fig. 6.44 the longitudinal and transverse profiles in the reservoir have been varied with the changes of operational conditions. The figures show that during the impoundment up to October 1961, i.e., the first year of operation, deposition was in the form of a delta with a topset slope of 0.00015 –0.00017, nearly half the original river bed slope, and a foreset slope of 0.0006–0.0009. The apex of the delta was near section 31, and the cross section was raised evenly in the transverse direction, making no distinction between the main channel and floodplain. During the wet year of 1964, the annual water and sediment inflows were 69.7 billion m³ and 3.06 billion tons, respectively. The reservoir was severely silted because the outlet capacity was too small and the sluice holes were located too high. About 1.95 billion tons of oncoming sediment was deposited in the reservoir during the flood season, which was 70% of the total incoming sediment. This was the most serious year of siltation. Longitudinal deposition was in the form of a cone, and a channel-floodplain configuration was formed. This can be seen from the transverse section, in which the floodplain rose simultaneously with the main channel. In 1973, the deposition occurred with the main channel being eroded because the reservoir was used for flood detention only during the flood season and the outlet discharge was enlarged after reconstruction. The figure reveals that the main channel had been lowered by erosion with basically no changes in the floodplain. The longitudinal bed slope of the main channel was 0.0002–0.00023 and that of the floodplain was 0.00012. A high floodplain and deep main channel had been formed; about one billion m³ of channel storage below Tongguan was recovered.

379
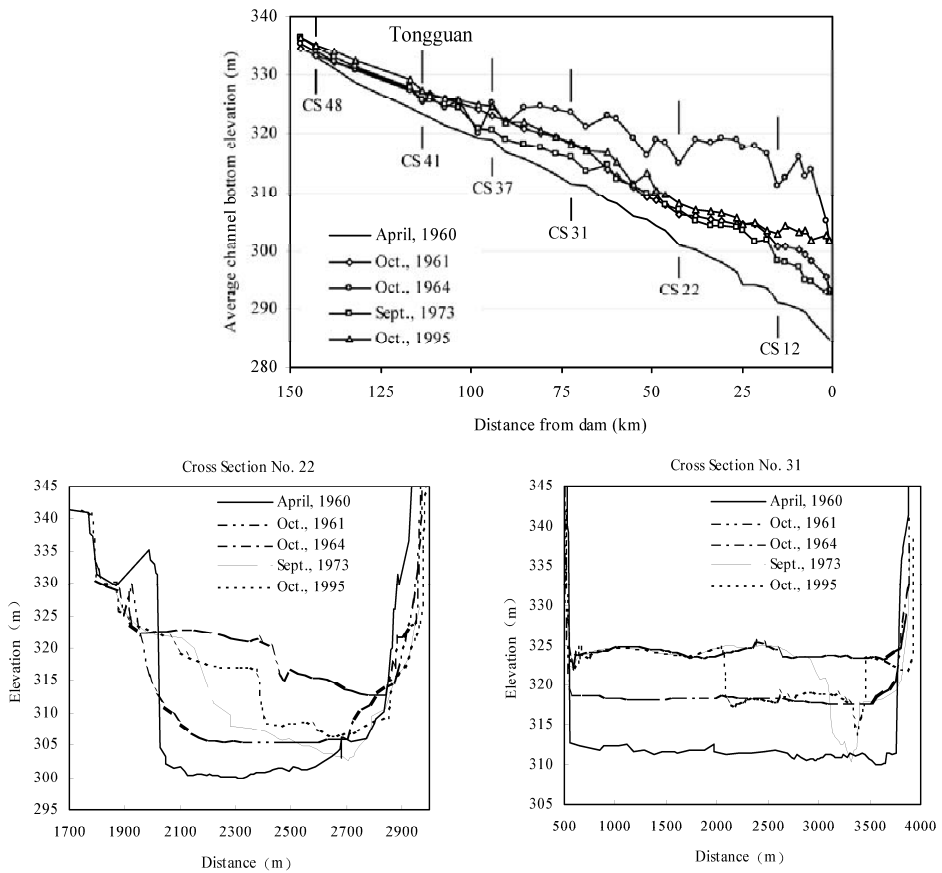
Fig. 6.44 Longitudinal (upper) and transverse (lower) profiles in the reservoir varying with the changes of operational conditions for the Sanmenxia Reservoir

6.5.3 Sedimentation of the Weihe River Induced by Sanmenxia Reservoir

The Weihe River is 818 km long and has a drainage area of 134,800 km^2 with more than 23 million people dwelling in the river basin. The river basin was known as the "800 li (1 li=0.5 km) fertile Qin Valley". The most serious adverse effect of Sanmenxia Dam is the unanticipated sedimentation in the lower Weihe River and consequently the high flooding risk to the lower Weihe Basin and Xi'an, an ancient capital of China. Sedimentation in the Weihe River has changed the valley into a swamp with a high ground water table. Local people complained and some officials and scientists suggest decommissioning the dam. The Weihe River has been experiencing a striking change in fluvial processes since the impoundment of Sanmenxia Reservoir. The river channel has been changing from meandering with a sinuosity of 1.65 to straight with a sinuosity of only 1.06 and slightly meandering with a sinuosity about 1.3.

The long-term average annual runoff of the Weihe River is 8.06 billion m^3 and annual sediment load is 386.6 million tons, which compose about 1/5 of the annual runoff and 1/3 of the annual sediment load of the Yellow River at Sanmenxia. In the past decades the water and sediment load in the Weihe River and the Yellow River have been reducing due mainly to human activities. Table 6.9 lists water and sediment load in the rivers in the periods 1960–2001 and 1986–2001. Water and sediment load in the two periods are less than the average values before 1980, but the ratios of water and sediment load from the Weihe

River to the Yellow River water and sediment load remain unchanged. The majority of the sediment load consists of silt with a median diameter of about 0.03 mm. Before the impoundment of Sanmenxia Dam the Weihe River carried 386.6 million tons of sediment into the Yellow River annually and the Weihe River itself remained a relatively stable longitudinal bed profile.

Table 6.9   Water and sediment load of the Yellow and Weihe Rivers

River/ Hydrologic station	Distance to the Yellow River mouth L (km)	Annual runoff (1960–2001) (bil. m³)	Annual sediment load (1960–2001) (mil. tons)	Average sediment concentration (1960–2001) (kg/m³)	Annual runoff (1986–2001) (bil. m³)	Annual sediment load (1986–2001) (mil. tons)
Weihe/ Huaxian	1177	6.79	312	46.04	4.66	248
Yellow/ Tongguan	1092	34.61	1043	30.13	25.16	722
Yellow/ Sanmenxia	996	34.69	1009	29.09	24.62	712
Yellow/ Huayuankou	734	37.44	910	24.20	25.88	610
Yellow/ Aishan	374	33.07	770	25.00	19.16	440
Yellow/ Lijin	100	28.56	700	36.80	13.56	350

The elevation of Tongguan or Tongguan's Elevation is defined as a flood stage corresponding to a discharge of 1,000 m³/s at the Tongguan Hydrological Station on the Yellow River, which acts as the base level of the bed profile of the Weihe River. Before Sanmenxia Dam Tongguan's Elevation was about 323.5 m. Since impoundment of Sanmenxia Reservoir, sediment has been depositing in the reservoir, which causes Tongguan's Elevation to increase. The energy slope and sediment carrying capacity of the flow in the Weihe River have been reduced. The sediment load could not be transported into the Yellow River and sedimentation occurred in the lower Weihe River. In other words, the rising Tongguan's Elevation has changed the lower boundary of the Weihe River, thence inducing a new cycle of fluvial processes.

Figure 6.45 shows the variations in Tongguan's Elevation over time from 1960 to 2001. There were three ascending periods, denoted by I, II, and III, and two descending periods, denoted by 1 and 2. The abrupt rise and fall in 1960 and 1962 were caused by the impoundment in 1960 and change of the operation mode from storage to flood detention. The time of high elevation (329 m in Fig. 6.45) was short and its influence on the Weihe River sedimentation was temporarily, although it caused an obvious flood stage rise in 1961. Therefore, the period of 1960–1962 is not separated from the ascending period I.

The ascent and descent of Tongguan's Elevation were results of reservoir sedimentation and erosion, which in turn were caused by variations in the pool level of the reservoir. Generally speaking, sedimentation in the lower Weihe River occurred during the periods when Tongguan's Elevation rose, and erosion occurred during the periods when it fell. The total volume of sediment deposited in the lower Weihe River up to the year 2001 was about 1.3 billion m³. The sedimentation was distributed mainly in a 100 km long reach from the confluence. The accumulated deposition volume per unit length was high near the confluence, reduced upstream, and to nearly zero near Xi'an. Figure 6.46 shows the transect of the profiles of the channel bed and floodplain in the lower Weihe River measured in 1960 and 2001 at the cross-sections WY-2 and WY-7, which are 21 and 59 km from Tongguan, respectively. The floodplain elevation had risen by 3 to 5 m due to sedimentation, and the main channel had shrunken and become

more unstable. The flood discharge capacity of the channel was thence reduced and the flood stage at the same discharge was substantially enhanced (Wang and Li, 2003).
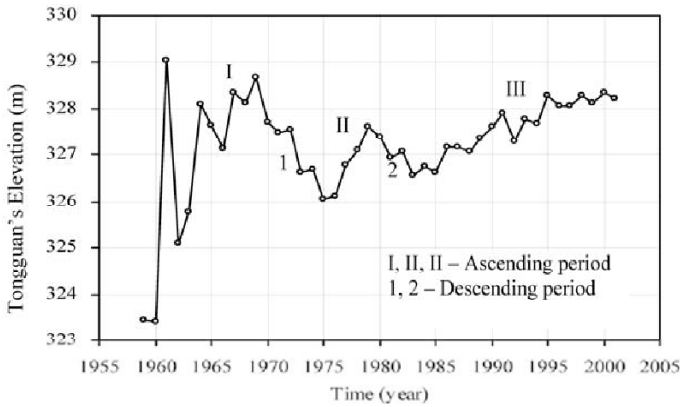
Fig. 6.45 Variation of Tongguan's Elevation (water-surface elevation at Tongguan for a flow of 1,000 m³/s)
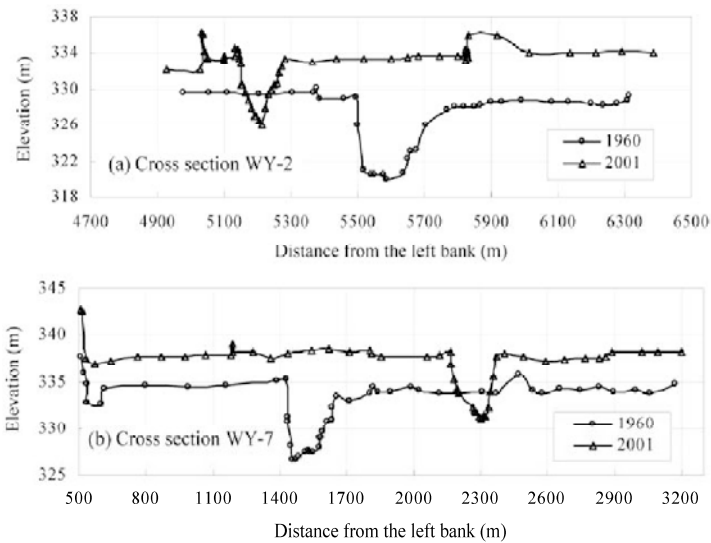
Fig. 6.46 Aggradation of the lower Weihe River measured at cross-sections WY-2 (21km from Tongguan) and WY-7 (59km from Tongguan) from 1960 to 2001

Simon (1989, 1996) studied channel response in disturbed alluvial channels and found that the changes imposed on a fluvial system tend to be absorbed by the system through several stages of channel adjustment and following exponential decay equations. The response of the Weihe River to the Sanmenxia Dam closure is more complex because the raised Tongguan's elevation is not stable and the effect has transmitted from the confluence to Xianyang Station (180 km upstream from Tongguan. Erosion and sedimentation caused by the ascending and descending of Tongguan's Elevation propagated upstream in retrogressive waves. Figure 6.47a–c shows the distribution of the deposition rate per unit river length in the periods 1960–1969, 1969–1973, and 1973–1980, respectively, in which the horizontal

axis is the number of the measurement cross-sections on the Weihe River; the average distance between the neighboring cross-sections is about 6 km. In the period from 1960 to 1969, Tongguan's Elevation rose abruptly from 323.5 to 328.5 m (see Fig. 6.45). As a result, sedimentation occurred in the reach around Huaxian at a rate of up to 2.5 million tons per km per year (Fig. 6.47a). The mark "I" indicates that the sedimentation corresponding to the first ascending period of Tongguan's Elevation. In the period from 1969 to 1973, the sedimentation wave moved upward to the reach between Huaxian and Lintong, but the rate of sedimentation decreased to about 0.75 million tons per km per year (Fig. 6.47b). In the meantime the first erosion wave occurred near the river mouth, which corresponded to the first descending period of Tongguan's Elevation, indicated by the mark "1". In 1973–1980 the first sedimentation wave had moved upstream to Lintong, the first erosion wave had moved to Huaxian, and the peaks had obviously decreased too. During this period, the second sedimentation wave occurred in the reach between the river mouth and Huaxian, indicated by the mark "II". This wave of sedimentation
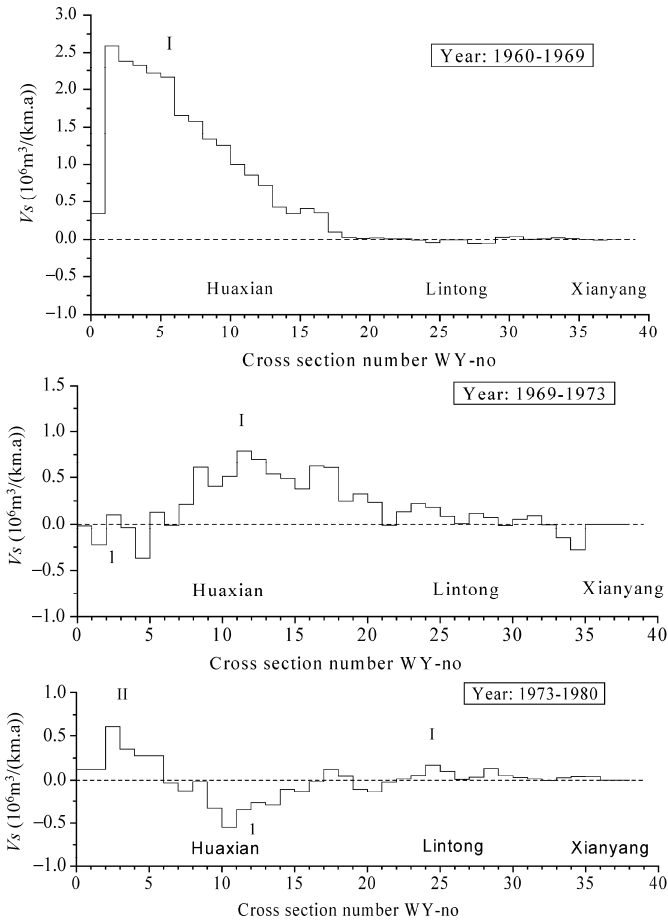
Fig. 6.47 Erosion (-) and sedimentation (+) per unit length per year showing retrogressive waves in the lower Weihe River, as a result of ascending and descending of Tongguan's Elevation. (The cross-sections are numbered from the river mouth. Huaxian, Lintong, and Xianyang are hydrological stations by the river and are about 50 km, 128 km and 180 km upstream from Tongguan. The distance between neighboring cross-sections is about 6 km.)

was associated with the second ascending period of Tongguan's Elevation. The ascending and descending of Tongguan's Elevation generated erosion and sedimentation waves, which propagated retrogressively along the Weihe River, at a speed of about 10 km per year.

Sedimentation has caused flood stage to rise escalating flood hazards in the lower Weihe River. Figure. 6.48 shows the stage rise at the Huaxian Hydrological Station for flood discharges at 250 and 3,000–5,000 m³/s. The stage rise is defined as the difference of the present flood stage minus the stage of the same discharge before the impoundment. For a discharge at 250 m³/s the flow is confined in the main channel and the stage rise reflects only the sedimentation and shrinking of the main channel. For a flood discharge in the range 3,000–5,000 m³/s the stage rise is due mainly to sedimentation on the floodplain. During the ascending periods of Tongguan's Elevation in the 1960s both the flood stage and low flow stage sharply increased by 4 m and 3 m respectively, because sediment deposition and channel reshaping increased the resistance. During Tongguan's Elevation descending periods 1970–1975 and 1980–1985, however, erosion occurred in the channel and the flood stage rise reduced by 1–2 m. In the mid 1990s the enhanced floodplain had been not flooded for several years and invasive and ruderal vegetation had developed, which increased the flow resistance greatly. As a result the flood stage rise increased sharply from 3–4 m to 6 m for floods flowing over the floodplain. At present the low flow stage is 4 m higher than that before the impoundment of Sanmenxia Reservoir and the flood stage is now 6 m higher, which poses a severe flood risk to the lower reaches of the Weihe River.
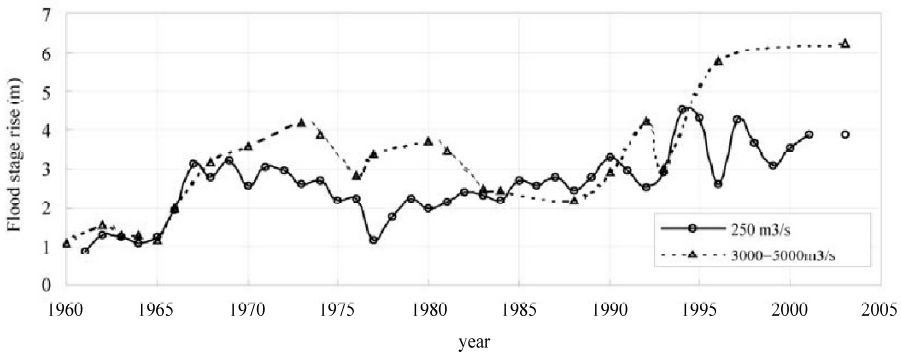
Fig. 6.48   Flood stage rise due to sedimentation at Huaxian station for discharges 250 m³/s and 3,000–5,000 m³/s

6.5.4   Equilibrium Sedimentation Model

Two questions to be answered about the fluvial processes in the Weihe River induced by Sanmenxia Dam are: Is there any equilibrium of sedimentation in the Weihe River? And whether the sedimentation has reached the equilibrium? The authors proposed a simple model to answer the questions (Wang et al., 2004). Assume there is an equilibrium sedimentation volume, V_e, for a given increment of Tongguan's Elevation. If the real sedimentation volume, V, is much less than V_e, the rate of sedimentation in the river is high. The rate of sedimentation is proportional to the difference between the equilibrium and real sedimentation volume:

$$\frac{dV}{dt} = K(V_e - V) \tag{6.3}$$

In which K is a constant with dimension of $[1/T]$. The solution of the equation is:

$$V = e^{-Kt}[\int KV_e e^{Kt} dt + const] \tag{6.4}$$

The equilibrium sedimentation volume V_e is proportional to the enhancement of Tongguan's Elevation ΔZ_t, which is given by $\Delta Z_t = Z_t - 323.5$, in which Z_t is Tongguan's Elevation at time t and 323.5 m is the Tongguan's Elevation before the dam. Simply the equilibrium sedimentation volume can be imagined to have a shape like a cone, then it may be assumed

$$V_e = A \Delta Z_t / 2 \tag{6.5}$$

In which A is a representative area of riverbed and floodplain on which sedimentation occurs. Substituting equation (6.5) into (6.4) yields,

$$V = \frac{1}{2} A K \mathrm{e}^{-Kt} \left[\int_0^t \Delta Z_t \mathrm{e}^{Kt} \mathrm{d}t - \Delta Z_t \right] \tag{6.6}$$

In which t is the time from 1960, when Sanmenxia Dam begin to fill and the Tongguan's Elevation began to rise. The parameters in the equation are determined from data as $A = 5.30*10^8 (\mathrm{m}^2)$ and $K = 0.15/yr$. Figure 6.49 shows the calculation result of the sedimentation volume (solid curve) in comparison with the real sedimentation volume (pyramids). The dashed curve in the figure is the calculation result with the value of ΔZ_t remaining unchanged at 5 m ($\Delta Z_t = 328.5 - 323.5 = 5$), which shows that the equilibrium sedimentation volume is around 1.3 billion m³.

As shown in Fig. 6.49 the model agrees well with the data of sedimentation, which proves that for a given Z_t, there is indeed an equilibrium sedimentation volume. If the increment in Tongguan's Elevation remains unchanged the sedimentation of the lower Weihe River may reach equilibrium in about 25 years. At present the sedimentation of the lower Weihe River is approaching to the equilibrium volume and there will be no great volume of accumulated sedimentation if Tongguan's Elevation stops rising. Nevertheless, the equilibrium sedimentation volume is dynamic and increases with rising lower boundary. If Tongguan's Elevation continues to rise the equilibrium sedimentation volume will be greater than 1.3 billion m³ and longer time is needed to reach the equilibrium (Wang and Li, 2003).
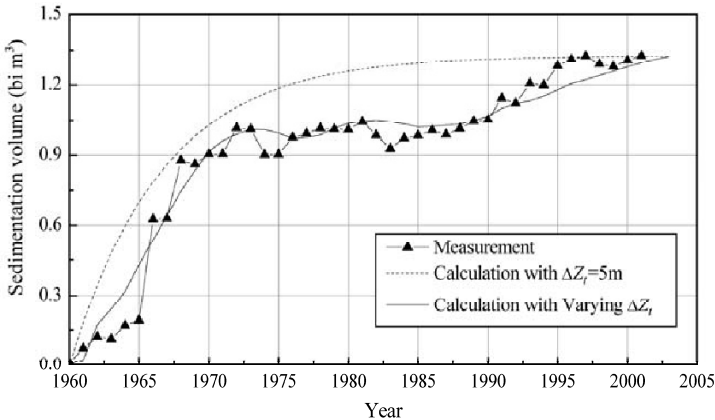
Fig. 6.49 Calculated cumulative sedimentation volume with Eq. (4) (solid curve) in comparison with the real sedimentation volume (pyramids). The dashed curve in the figure is the calculation result with the value of ΔZ_t remaining unchanged at 5 m

6.5.5 Changed River Patterns

Sanmenxia Dam not only caused retrogressive sedimentation and erosion in the lower Weihe River, but also changed the river patterns. Before the reservoir began to be used, the lower Weihe River was a meandering river, with a value of sinuosity of about 1.65, in which sinuosity is defined as the ratio of the

length of the channel to the length of the river valley. The closure of the dam reduced the sinuosity to 1.06 in 1968, as shown in Fig. 6.50a. Very quick sedimentation in this period buried the meandering channel. In the meantime a straight channel developed which was affected mainly by the reservoir operation. In the period from 1970 to 1975 the Weihe River experienced erosion and the channel developed gradually from straight to meandering. The sinuosity had gradually increased to 1.2. In the following period more and more meanders have developed and the lower Weihe River has been developing toward meandering with a sinuosity about 1.3.

Moreover, the river channel has become quite unstable since the closure of the dam. Figure 6.50b shows the migration distances of the stream channel measured at cross-sections WY5-35 during the first ascending and descending periods of Tongguan's Elevation. The migration distance was up to 1.8 km at the cross-sections near Huaxian (WY11). The dam had less effect in the reaches further upstream and the migration distance was less than 1 km at cross-sections WY18-35.
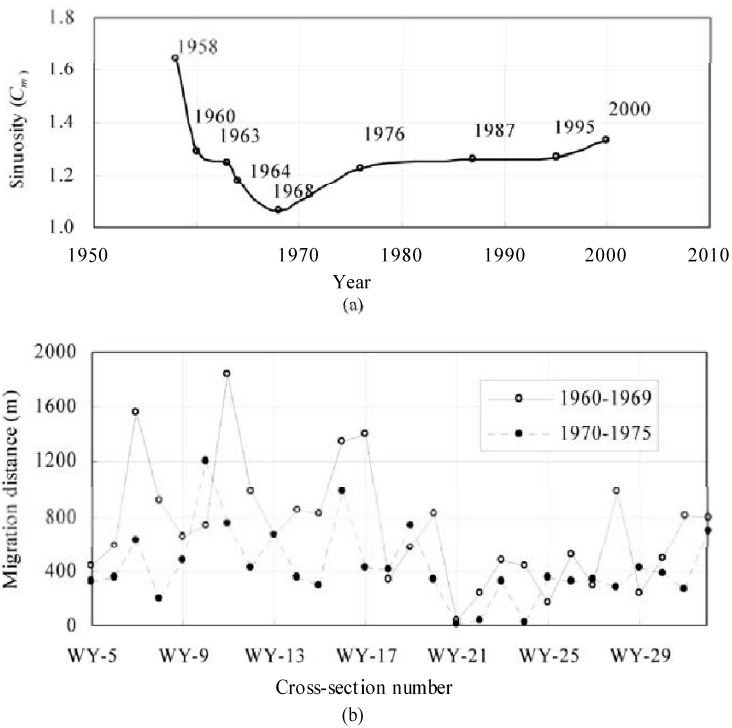
Fig. 6.50 (a) Variation of sinuosity of the lower Weihe River; (b) Migration distances of the stream channel measured at cross-sections WY5-WY35 during the first ascending and first descending periods of Tongguan's Elevation

6.5.6 Erosion and Resiltation Below Sanmenxia Dam

Sanmenxia Reservoir has trapped about 7.1 billion m^3 of sediment in 45 years, including the sedimentation volume in the Weihe River. The sediment load and runoff in the downstream reaches was then greatly reduced, especially in the first 4 years, which induced a complex morphological process downstream of the dam. The water and sediment released from Sanmenxia Dam varied with the operation modes of the reservoir. Consequently, erosion and resiltation occurred in the reaches downstream from the dam. The process of bed erosion and resiltation was very fast because the sediment load was high and the bed material was erodible. The erosion and resiltation occurred mainly in the reach about 180–600 km

downstream from the dam. About 2.31 billion tons of sediment had been eroded from the riverbed in the first 4 years since the closure of the dam. In the following 9 years, however, the reservoir changed its operation mode from storage to detaining flood water and sluicing sediment, and the downstream channel was resilted at a high rate, with a total volume of sediment deposition of about 3.95 billion tons (Yang et al., 1994). The erosion and resiltation occurred both in the stream channel and on the floodplain, with roughly 60% in the channel and 40% on the floodplain.

The lower Yellow River was a wandering river although it has been confined within the strong grand levees, which are on the two sides of the river 5–25 km apart from each other. The migration rate of the channel was quite high. The closure of Sanmenxia Dam did not change this situation. The river migrated at high speed with a maximum value of more than 5 km/yr. Even during the period immediately following the closure of the dam, when clear water was released into the reach, the channel migrated more than 3 km per year.

Generally, dams tend to cause a reduction in migration rates in the downstream reaches. For instance the closure of the Danjiangkou Dam on the braided Hanjiang River caused an initial reduction in bank erosion intensity from about 25 m/yr during 1955–1960 to about 7.0 m/yr during a period of 17 years immediately after the dam closure (Xu, 1997). The lower Yellow River did not respond the dam closure with reduced channel migration because of the specific features of reservoir operation.

Sanmenxia Reservoir has caused the lower Yellow River to change from a wandering-braided into a wandering-single thread channel. Figure 6.51 shows the channel morphology of the Tiexie-Peiyu reach, which is about 157–189 km downstream from Sanmenxia Dam, before and after the construction of the dam (Yang et al., 1994). There were many sand bars before closure of the dam; the number of bars had decreased 3 years after the dam was used for impoundment. The river had become a single thread channel by 1964.

(a) Date: 1960 8.27~29

(b) Date: 1963 7.24~26

(c) Date: 1964 11.17~22
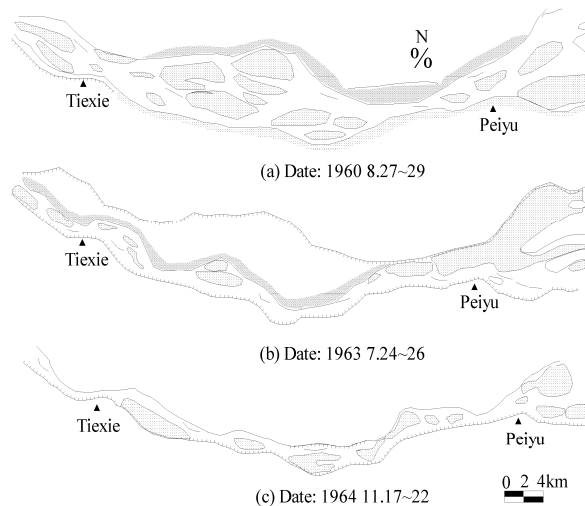
Fig. 6.51 Channel morphology of the Tiexie-Peiyu reach (157–189 km from Sanmenxia) pre- and post-Sanmenxia Dam

Meanders have generally developed after Sanmenxia Dam. The reach from the dam to Tiexie (0 to 157 km directly below the dam) is constrained by mountains and no meanders develop within it. A statistics is made for a 400 km long reach, from 150 km to 550 km below the dam, which was an active fluvial reach. Before the impoundment of the dam there were only 16 meanders in the 400-km long reach and

more meanders have generally developed after the impoundment. Figure 6.52 shows the numbers of meanders with different wavelength in the reach in the 1970s, 1980s, and 1990s.

The meander wavelength is defined as the distance from one turning point of the channel on one side of the valley to the next turning point at the same side. As shown in Fig. 6.52, there were 17 small meanders in the reach in the 1970s. Some meanders were separated by straight sections and some other meanders connected with each other and form small meandering sections. Between two small meandering sections was a section with straight channel. Late the reservoir operation became stable, more meanders developed and the meandering sections became longer. In the 1980s, however, 22 meanders with a wavelength from 3 to 30 km had developed in the reach. In the 1990s, the number of meanders continued increasing and the meanders became regular; 31 of them have meander wavelength within the range of 6–15 km. The river became more and more meandering. In the process, human constructed spur dykes affected, more or less, the development of meanders.
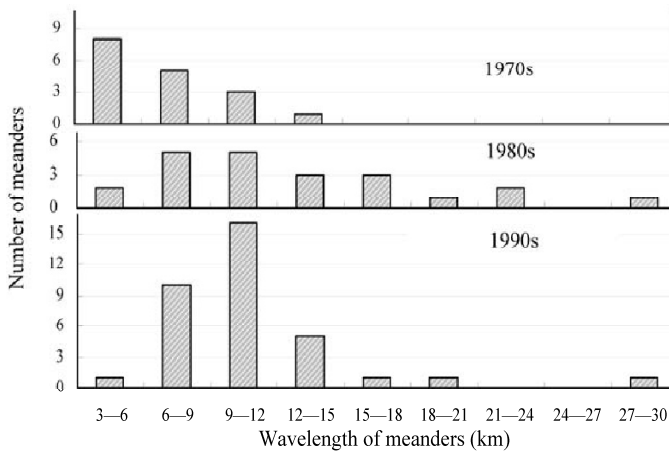
Fig. 6.52 Numbers of meanders with different wavelengths in a 400 km long reach downstream of Sanmenxia Reservoir in the 1970s, 1980s, and 1990s

6.6 Proposed New Strategies

6.6.1 Reclamation of the Floodplain

In general, most alluvial river valleys are narrowed and the channels are stabilized following social and economic development. The lower Yellow River was several tens of kilometers wide, which provided enough space for the channel to migrate and sediment deposition. Now it is much narrow and will be narrower. The Mississippi River valley was wide and has been narrowed for more than half century. Humans narrow the river valley for various purposes: urban development, land reclamation, flood control and navigation. In Europe, most large rivers, such as the Rhine, Rhone, Elbe and Danube, have been channelized, mostly for to gain land for development, to eliminate diseases such as malaria, to prevent floods, and to open waterways for shipping (Kern 1994). The Danube River near Vienna has been changed from a braided to a single-thread channel in 1859 (Humpesch, 1994), providing a large area of land for urban development. The river Rhone was channelized for shipping and land reclamation (Bloesch, 2002).

Ex-minister of water resources, Madame Qian paid a field trip to the wandering lower Yellow River and proposed to abandon the flood defense strategy with wide river valley, which has been applied as the main flood defense strategy for the safety of lower Yellow River since the 1950s (Qian, 2006). The wide river valley in the Henan reach of the lower Yellow River is too wide, more than 10-25 km. About 1.8 million people are now dwelling on the floodplain within the grand levees. The flood defense strategies for the people on the floodplain are mainly perched refuge platform and flood refuge building. The refuge platform and refuge building are effective for 20-years flood only and they are too expensive, about $1200 and $2500 per person. Nowadays, sediment load and flood volume have been remarkably reducing due to regulation of reservoirs. The 100-years flood has reduced from 33,000 m^3/s to 15,700 m^3/s and the 1,000-years flood has reduced from 45,000 m^3/s to 22,600 m^3/s. The wide river valley may be changed to relatively narrow river valley. Madame Qian proposed to narrow the river valley from 10-25 km to 3-4 km. A new grand levee should be built on the left side of the river and the floodplain between the new and old grand levees can be used for development of townships and industry. Modern infrastructures, such as highways, railways and power facilities, may be constructed for economic development. Figure 6.53 shows a picture of the narrow river valley and development of the floodplains.
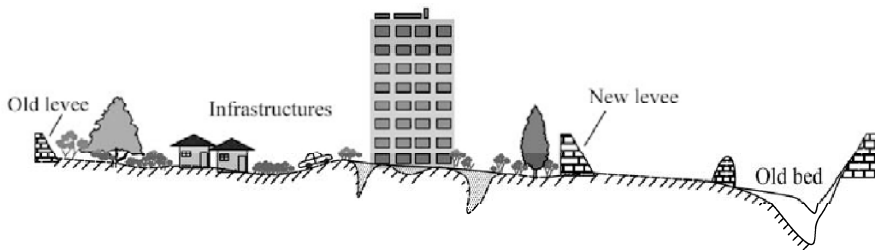
Fig. 6.53   A picture of the narrow river valley and reclamation of the floodplains in the lower Yellow River

6.6.2   Scouring the Yellow River Channel with Seawater

Lin et al. (1998) proposed to divert sea water from the Bohai Sea and pump it into the Yellow River to scour the river channel, because the river bed has been silting up quickly and there is less and less water to be used for scouring bed sediment. Two schemes have been studied: 1) divert sea water from Guangli Harbor and inject the sea water into the Yellow River near the Lijin Hydrological Station; 2) inject the sea water at Xihekou, as shown in Fig. 6.21. In the first scheme a canal is suggested to connect the Guangli Port and the Nanzhan Reservoir, which is now used as a flood detention basin. Sea water at discharge of 500 m^3/s will flow through the 48 km long canal and be pumped into the reservoir. It will then be released with peak discharge of 5, 000 m^3/s into the Yellow River (when the reservoir is fully impounded). The capacity of the reservoir is 50 million m^3. The reservoir can be draw down in 7 hours and impounded again in 28 hours. The 115 km long river channel downstream of Lijin would be scoured 251 times per year, for each time the river channel is scoured 7 hours.

The effect of seawater scour was calculated with a simple numerical model (Lin et al., 1998). The bed sediment was assumed to be 0.06 mm in diameter, and the sediment concentration in a flood is assumed to be 25.5 kg/m^3. The calculation demonstrated that the released seawater flood decreases as it moves down the river. The peak discharge of 5, 000 m^3/s at Lijin, reduces to 1,800 m^3/s at Xi-he-kou (47 km from Lijin) and to 1, 300 m^3/s at the river mouth. Because the sea water flow carries no sediment, the river channel is obviously scoured. The channel bed elevation at Lijin is scoured from 12 m to 6 m in the first year before the flood season and resilted to 10 m after the flood season. More than 170 million tons of bed sediment can be scoured and transported into the sea in five years.

Retrogressive erosion will occur because the stage reduction at Lijin increases the energy slope in upstream reaches. A 200–400 km long section upstream of Lijin can be affected by the retrogressive erosion and the accumulative siltation of the river channel can then be stopped. The high capacity of the river channel can be preserved by the strategy. Nevertheless, the injection of seawater in the Yellow River may cause salinization of the farmland and cause ecological problems to the areas downstream of the injection point.

To minimize the negative effect of the strategy, the second scheme is recommended. In the scheme, the injection point is Xihekou, 47 km downstream of Lijin. From Xihekou to the river mouth there is little agricultural land-use and the floodplain is now mainly used to plant shrubs and trees, and raise shrimp. The canal is only 24 km long to transport water from the sea to Xihekou (Fig. 6.21). The seawater will be directly pumped into the Yellow River at a rate of flow of 1,000 m^3/s. Figure 6.54 shows the result of numerical model studies for scheme 2—injection at Xihekou (Lin et al., 1998). After 10 years of seawater scour and retrogressive erosion, the thalweg at the injection point may be scoured down by 7–8 m but the flood stage (3000 m^3/s) may be lowered by 4.4 m.
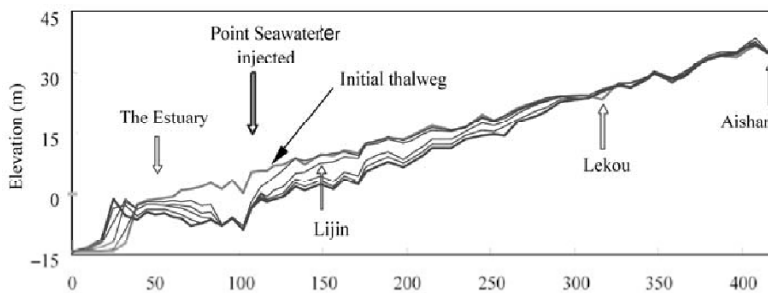
Fig. 6.54   The thalweg profiles of the river before and after 10 years of scouring with seawater and retrogressive erosion for scheme 2—injection at Xihekou (after Lin et al., 1998)

Difficulties are still likely in the implementation of the new strategy. For instance, the power needed for pumping water has a high cost input and the ecological impacts of pumping sea water into the river will be very complex. The following studies have to be conducted before the strategy is adopted: (1) the effects of the seawater scour should be further studied with physical scale model(s); (2) Impacts of seawater injection on the ecological system in the delta should be carefully studied. The maritime section of the Yellow River is only 20 km long because the tidal difference at the river mouth is only about 1 m. An artificial sea water flood in the river may cause alkalization of the riparian land. The riparian habitat, land use, fauna and animal population could be changed. (3) Comprehensive study is required on the riverbed scour with seawater, transportation of sediment by sea currents land creation at the river mouth, and the delta evolution and development. (4) Conduct a comparative study on seawater scour with dredging and other strategies.

6.6.3   Artificial Hyperconcentrated Floods

The main problem in the lower Yellow River is high sediment load and insufficient water flow. The average sediment concentration in the lower Yellow River is about 25–40 kg/m^3. Hyperconcentrated floods may transport sediment at concentration up to several hundred kg/m^3. Generation of artificial hyperconcentrated floods is suggested to transport sediment at high efficiency. Hyperconcentrated flow scours the main channel and causes sediment deposition on the floodplain. Therefore, hyperconcentrated flow can create and maintain a deep and narrow channel (Qi, 1993). Recorded data show that hyperconcentrated

floods can flow through a narrow and deep channel for a long distance without serious sedimentation. The sediment fall velocity for hyperconcentrated flow is much smaller than for low concentrations. Figure 6.55 shows a hyperconcentrated flood flowing in an artificial canal. The hyperconcentrated flood was diverted into a 50 km long irrigation canal without serious siltation of the canal.

Fig. 6.55 A hyperconcentrated flood in the North Luohe River is diverted into an irrigation canal and transported for over 50 km without serious sediment deposition

Much heavier sediment loads can be carried by hyperconcentrated flow than by low concentration flow. The Sanmenxia Reservoir was suddenly draw-drawn and emptied in 1963 before the flood season. Water carrying sediment was released to the lower reaches and the concentration was 300 kg/m^3. The artificial hyperconcentrated flow was maintained for 5 days (Zhao, 1996). Artificial hyperconcentrated floods can be generated by using the Xiaolangdi Reservoir to transport sediment at high efficiency through a narrow and deep channel to the sea. The total capacity and sediment trapping capacity of the Xiaolangdi Reservoir are larger than those of Sanmenxia Reservoir. Generation of hyperconcentrated flow using the Xiaolangdi Reservoir is feasible.

A difficulty for this strategy is how to narrow and deepen the lower Yellow River channel. Li (1992) suggested to dig a 800 km long deep and narrow channel with dredgers at a cost of $250 million over 3–5 years, then to initiate artificial hyperconcentrated floods by emptying the Xiaolangdi Reservoir and increase the sediment concentration by mechanical agitation along the river. In this way the average sediment concentration could be kept over 300 kg/m^3 and 8 billion m^3 water can transport more than 2.4 billion tons of sediment (three times the annual load) to the sea. Hence the problem of accumulative siltation of the channel could be solved. Wang et al. (1997) indicated that the following technical problems have to be solved before implementation of the project strategy:

(1) In order to create an artificial hyperconcentrated flow, the size composition and the ways to control the size composition have to be studied to make the size composition matches the flow intensity; (2) It takes at least 7–10 days for a hyperconcentrated flood to travel the distance from the Xiaolangdi Reservoir to the river mouth. How can an artificial hyperconcentrated flood be generated and maintained for more than 10 days? (3) The sediment carrying capacity of hyperconcentrated flow is high but very unstable. The fall velocity of sediment particles is proportional to the –4 to –7 power of sediment concentration. The fall velocity of coarse particles reduces sharply with increasing concentration, therefore, coarse particles can be carried in suspension by hyperconcentrated flow but if a part of the

coarse particles deposit, the concentration reduces and more particles will deposit because their fall velocity increases. A chain reaction may be triggered and serious deposition will occur (Wan and Wang, 1994). Maintaining a hyperconcentrated flow through the 800 km long channel without serious deposition is an arduous task for sediment engineers. (4) Hyperconcentrated flow transports 2.4 billion tons of sediment to the sea per year. A huge amount of sediment would accumulate in the mouth area and new retrogressive siltation will occur. How can the sediment at the river mouth be disposed of to avoid retrogressive siltation? 5) Zhou and Chen (1997) indicated that the sediment deposit in the Sanmenxia Reservoir is composed of fine material ($d_{50}=0.005$ mm) near the dam but of coarse sediment ($d_{50}=0.091$ mm) at 9 km or longer distance from the dam. It will be similar for the Xiaolangdi Dam in future. Fine sediment composes the matrix of the hyperconcentrated flow. Therefore, if the reservoir is successively drawn-down the fine material will be used up and the hyperconcentrated flow can not sustain for long time.

6.6.4 Interbasin Water Transfer Projects

The water shortage in the Yellow River basin was estimated to be around 7 billion m^3 in 2010 and 15 billion m^3 in 2030 (Chen, 1991). The main strategies to solve or ease the water shortage and save the river from dying out are reallocation of water resources and interbasin water transfer projects. Three routes of South–to–North Water Transfer Projects have been proposed and will be implemented. The West Route will transfer water from the Qinghai-Tibet plateau to the upper reaches of the Yellow River. The west route of water transfer project will transfer water from the Jinsha River (the Yangtze River), Yalong River, and the Dadu River to the upper Yellow River. About 1.95 billion m^3 water can flow to the Yellow River by building dams and tunnels. The water shortage problem of the Yellow River basin can be solved and the clear water may carry sediment into the sea, thence the siltation of the river channel can be stopped. Nevertheless, the ambitious project needs a lot of investment. The Jinsha, Yalong and Dadu Rivers are only 100–200 km from the upper Yellow River. The total annual runoff of three rivers is 120 billion m^3. The project can divert 19.5 billion m^3 water from the three rivers to the Yellow River. Nevertheless, the water diversion dams will constructed on tributaries of the three rivers, for instance, the Ake River, Duke River, Make River and Sequ River are tributaries of the Dadu River. The runoff of these tributaries are much less than the Dadu River. Water diversion will reduce the runoff by about 50%, which will impact the local ecology. It is necessary to study the impacts of water diversion on the local ecology and take measures to mitigate the impacts as the water diversion is implemented.

6.6.5 Liberate Flood Detention Basins

The pressure on land due to population growth and urbanization is increasing. It is proposed to use flood diversion channels to replace flood detention basins in order to liberate the basins for economic development and human habilitation (Li, 1999). The impoundment of the Xiaolangdi Reservoir has enhanced the flood defense capacity of the lower Yellow River from 100-years floods to 1000-years floods. It was suggested liberate the Beizhan flood diversion basins (Fig. 13) for construction of a water supply reservoir and an ecological park (Li, 2000)

Review Questions

1. What are the main theories for Yellow River training proposed in history?
2. What are the modern training strategies applied to the Yellow River?
3. What are the main factors that must be considered in the water resources development planning?
4. Why is the rate of the lower Yellow River channel siltation still so high although the total sediment load has reduced greatly in the past decades?

5. What are the main dynamic features of the Yellow River delta?

6. Please state the new strategies of Yellow River management.

7. The Yellow River is silted up at high rate and there is less and less water to be used for sediment transportation. Propose a management strategy to solve the problem.

8. What are the new problems in the management of the lower Yellow River? How to solve them.

9. What are problems and strategies of water resources management of the Yellow River basin?

10. What is your opinion on the proposed new strategies?

References

Bloesch J., 2002. The Danube River Basin—the other cradle of europe: the limnological eimension. Academia Scientiarum et Artium Europaea: Proceedings 1st EASA Conference The Danube River: life line of greater europe, budapest, Nov. 9–10, 2001. Annals of the European Academy of Sciences and Arts 34/12, 51–79

Chen J.Q., 1991. Water resources in China, in Qian Z.Y., (ed.), 1991. Water Conservancy in China. Water Resources and Hydro-Power Press, 1–42 (in Chinese)

Chen X.G., 1999. Flood control situation and strategies of the lower Yellow River. The Yellow River Water Conservation Commission (in Chinese)

Cheng D.S., Wang Z.Y. and Liu J.X., 2007. Relationship between dyke collapse and river discharge in the lower Yellow River. Journal of Hydraulic Engineering, 38(1), 74–78 (in Chinese)

ECASP (Editing Committee of the Annals of the Sanmenxia Project), 1993. Annals of Sanmenxia Project on the Yellow River. China Encyclopedia Press (in Chinese)

Engels H., 1932. Grossmodellversuche ueber das Verhalten eines geschiebefuehrenden gewundenen Wasserlaufes unter der Einwirking wechseln der Wasserstaende und verschiedenartiger Eindeichungen. Wasserkraft und Wasserwirschft, 27 (3&4), 25–31, 41–43

Fogg J.L. and Muller D.P., 1999. Resource values, instream flows and ground water dependence of an Oasis Stream in the Mojave Desert, Annual Summer Specialty Conference Proceedings. Science into Policy: Water in the Public Realm/Wildland Hydrology, Bozeman, Montana, June 30–July 2, 1999

Freeman J.R., 1922. Flood problems in China. Transactions ASCE, 85, 1405–1460

Humpesch U.H., 1994. Quantification of macro-invertebrates in the river bed of a free-flowing stretch of the Austrian Danube. In: Kinzelbach R., (ed.), Biologie der Donau. Limnologie aktuell, Band 2, G. Fischer Stuttgart, 109–125

IWHR. and WUHEE., 1985. History of Chinese Water Resources 1985. Water Resources and Hydro-Power Press (in Chinese)

Ji Z.W., Hu C.H., Zeng Q.H. and Yan Y., 1994. Analysis of recent evolution of the Yellow River Estuary by landsat images. J. of Sediment Research, 3, 12–22 (in Chinese)

Kern K., 1994. Basics in near-natural construction of waters. Geomorphological evolution of running waters (Grundlagen naturnaher Gewässergestaltung. Geomorphologische Entwicklung von Fliessgewässern). Springer, Berlin, Pp. 256

Li D.K., 1999. Jinanyan-a project benefit to the spring city (Jinan) and Shandong area, Bulletin of Shandong Academy of Social Sciences, 24, (in Chinese)

Li D.K. 2000. My opinion on the construction of Jinan Weir, Shandong Water Resources, (3) 90–01.

Li D.Y., 1992. Suggestion and discussion on the possibility to transport the Yellow River sediment to the sea by mechanical agitation, The People's Yellow River, 6, (in Chinese)

Li J.S., ed., 1992. Chinese flood control series-general introduction. Chinese Water Conservation and Hydropower Press (in Chinese)

Lin B.N., Zhou J.J., Zhang R. and Wang Z.Y., 1998. Scour by diverting sea water- A new approach to regulate the lower Yellow River. Journal of China Institute of Water Resources and Hydropower Research, 1(2), 1–10 (in Chinese)

Long Y.Q. and Chien N., 1986. Erosion and transportation of sediment in the Yellow River basin. International Journal of Sediment Research, IRTCES, Beijing, China, 1(1), 2–28

Long Y.Q., 1996. Sedimentation in the Sanmenxia Reservoir. Proceedings of the International Conference on Reservoir Sedimentation, Fort Collins, Colorado, III,1294–1328

Pan X.D. and Li Y., 1998. Comprehensive analysis on variation of Yellow River water and sediment, Report to the Yellow River Water and Sediment Variation Research Foundation (in Chinese)

Qi P., 1993. Laws of hyperconcentrated flows in the Yellow River and their applications. China Science Press (in Chinese)

Qian N. and Dai D.Z., 1980. The problems of river sedimentation and present status of its research in China. Proceedings of International Symposium on River Sedimentation, Guanghua Press (in Chinese)

Qian N. and Zhou W.H., 1964. Fluvial Process of the Lower Yellow River. Chinese Science Press (in Chinese)

Qian Z.Y., 2006. Speech on the training of the lower Yellow River, http://www.hwcc.com.cn, Oct. 18, 2006 (in Chinese)

Simon A. and Thorne C.R., 1996. Channel adjustment of an unstable coarse-grained stream: opposing trends of boundary and critical shear stress, and the applicability of extremal hypotheses. Earth Surface Process and Landforms, 21, 155–180

Simon A., 1989. A model of channel response in disturbed alluvial channels. Earth Surface Process and Landforms, 14, 11–26

Simon A., 1992. Energy, time, and channel evolution in catastrophically disturbed fluvial systems. Geomorphology, 5, 345–372

Wan Z.H. and Wang Z.Y., 1994. Hyperconcentrated flow, Monograph Series of IAHR, A.A. Balkema Publishers, Netherlands

Wang H.Y., 1989. My experiences of managing the rivers. Henan Science and Tecnology Press (in Chinese)

Wang Z.Y., 1999. Experimental study on scour rate and channel bed inertia. Journal of Hydraulic Research, IAHR, (1), 27–47

Wang Z.Y. and Liang Z.Y., 2000. Dynamic characteristics of the Yellow River Mouth. Earth Surface Process and Landforms, 25, 765–782

Wang Z.Y. and Hu C.H., 2004. Interactions between fluvial system and large scale hydro-projects. Keynote lecture. Proceedings of 9th International Symposium on River Sedimentation, 1, 46–64

Wang Z.Y. and Li C.Z., 2003. A study on the effect of Tongguan's elevation on sedimentation in the Weihe River, Research Report, Institute of River and Coastal Engineering, Tsinghua University (in Chinese)

Wang Z.Y., Cheng D.S., Li C.Z. and Zhou J., 2004. Analysis on fluvial processes and failure of spur dykes in the Lower Yellow River, research report. Institute of River and Coastal Engineering, Tsinghua University (In Chinese)

Wang Z.Y., Huang J.C. and Su D.H., 1997. Scour rate formula. International Journal of Sediment Research, 3, 11–20

Wang Z.Y., Lu X.Z., Zeng Q.H., 1990. Physical model experimental study on sedimentation in the Chongqing reach of the Yantze River for the Three Gorges Project- a report for the 175m scheme, in the Collection of Research Results on the Sedimentation in the Chongqing reach of the Yangtze River 195–1990, China Institute of Water Resources and Hydro-Power Research (in Chinese)

Wang Z.Y., Wu B.S. and Li C.Z., 2004. Has the sedimentation in the Lower Weihe River reached equilibrium? People's Yellow River, 5, (in Chinese)

Wu B.S. and Deng Y., 2005. Adjustment of longitudinal bed profile of riverbed in Sanemenxia Reservoir, Shuili Xuebao, 36(5), 549–552 (in Chinese)

Wu B.S., Xia J.Q. and Wang Z.Y., 2006. Delayed response of Tongguan's elevation to the sedimentation in Sanmenxia Reservoir. Journal of Sediment Research, 1, 9–16 (in Chinese)

WUHEE (Wuhan University on Hydraulic and Electrical Engineering) and IWHR (China Institute of Water Resources & Hydropower Research). 1985. China History of Water Conservancy. Beijing: China Water Power Press.

Xu J.X., 1998. Naturally and antjhropogenically accelerated sedimentation in the lwer Yellow River, China, over the past 13000 years. Geographika Annaler, 80A, 1, 67–78

Xu J.X., 1997. Evolution of mid-channel bars in a braided river and complex response to reservoir construction: an example from the middle Hanjiang River, China. Earth Surface Processes and Landforms 22, 953–965

Yang Q.A., Long Y.Q. and Miao F.J., 1994. Operational studies of sanmenxia project on the Yellow River. Henan People's Press (in Chinese)

Yang C.T., 1996. Sediment transport-theory and practice, The McGraw-Hill Companies, Inc., New York, St. Louis, San Francisco

Yen B.C., 1999. From Yellow River models to modeling of rivers. International Journal of Sediment Research, 2, 85–91

Yin X.L. and Chen J.R., 1993. The influence of the variation of water and sediment load on the evolution of the Yellow River Delta, Collective of Papers of Study on Variation of Water and Sediment Load of the Yellow River. The Research Foundation of the Yellow River, 5, 124–141 (in Chinese)

YRCC (Yellow River Conservancy Commission), 2001. Century Yellow River, Yellow River Press, Zhengzhou (in Chinese)

Zhang R. and Xie S.A., 1985. The depositional profile of the abandoned channel and the main cause of continuous aggradation of the Lower Yellow River. Sediment Research, 3, 1–10 (in Chinese)

Zhang S.Q., Cao W.H. and Dong J.Q., 1997. The Yellow River mouth sediment model. Supporting Report of UNDP Project No. CPR/91/144 (in Chinese)

Zhao Y.A. and Liu H.B., 1997. The 96.8 Flooding of the Lower Yellow River. The Yellow River Flood Control Press (in Chinese)

Zhao, W.L. 1996. Yellow River Sediment–Series of books on hydroscience & technology in the Yellow River. Yellow River Water Conservancy Press, Zhenzhou.

Zhou W.H. and Chen J.G., 1997. Discussion on the Yellow River Training strategy with hyperconcentrated flows, China Institute of Water Resources and Hydro-electric Power Research (in Chinese)

Zhu L.Q., ed., 1991. Series of picture albums of the Yellow River. Publication Center Yellow River Conservation Commission, China Environmental Science Press (in Chinese)

7   Dams and Impounded Rivers

Abstract

Construction of dams on numerous rivers throughout the world must be the greatest achievement of human beings in river development and the greatest disturbance to stream ecology. The dams impact the riparian vegetation, invertebrates and fish in both the reservoir and downstream reaches. Reservoir sedimentation has changed the fluvial processes. The downstream reaches are changed from aggradation to degradation, which causes ecological problems. Various strategies for reservoir sedimentation management have been applied, such as flushing, restoring clear water and releasing turbid water, and releasing turbidity (density) currents. The risk of dam failure is studied. The advantages and disadvantages of dam removal for habitat restoration are discussed. The Three Gorges Project on the Yangtze River has been the greatest hydro-project in China. The construction of the Three Gorges Dam and management strategies for the reservoir are also discussed in this Chapter.

Key words

Ecological impacts of dams, Reservoir sedimentation, Dam failure, Dam removal, Three Gorges Dam

7.1   Impacts of Dams on The Environment and Ecology

The Hoover Dam, an astonishingly graceful curve of concrete with a height of 221 m pushing back the Colorado River to fill its deep canyon on the Arizona–Nevada border, unleashed the big dam era. President Franklin D. Roosevelt spoke highly at the inauguration ceremony at Hoover Dam on 30 September 1935: "The power and the water, I came, I saw, and I was conquered." To many people, including leaders, engineers, and scientists, big dams have been potent symbols of both patriotic pride and the conquest of nature by human ingenuity. Providers of electric power, water, and food; tamers of floods; greeners of the desert; for most of the last century, dams, the largest single structures built by humanity, have symbolized progress. However, large dams also cause many problems, especially sedimentation in the reservoir, erosion in the downstream reaches, and disturbance to the stream and terrestrial ecology.

Impounded rivers change the flow conditions, and, therefore, change the water quality in the reservoirs and the downstream reaches, which affects the wildlife in the reservoir and downstream reaches (Petts, 1984). Freshwaters, because of a host of human assaults, but especially because of dams, are the most degraded among the major ecosystems. A dam tears at all the interconnected webs of river valley life. Swedish ecologists concluded in 1994 that nearly four-fifths of the total discharge of the largest rivers in the U.S., Canada, Europe, and the former USSR is 'strongly or moderately affected' by flow regulation, diversions, and the fragmentation of river channels by dams (Dynesius and Nilsson, 1994) The most extreme illustration of the downstream impacts of water diversions is the Aral Sea in Central Asia. Once the world's largest body of freshwater outside North America, the sea has shrunk to less than half its previous area and separated into three hypersaline lakes. The dams on the Yellow River in China have reduced the flow into the Bohai Sea and resulted in many cutoffs of flow in the lower reaches of the river (Chapter 6). With an increasing number of such kind of events the negative impacts of large dams on ecology have become a public concern.

7.1.1   Dam Construction

According to the estimates of the International Commission on Large Dams (ICOLD), the leading dam-industry association, the world's rivers had been obstructed by more than 40,000 large dams by the

end of 20th century, all but 5,000 of them built since 1950. A 'large dam' is usually defined by ICOLD as one measuring 15 m, or more from foundation to crest-(taller than a four-storey building), or with reservoir capacity greater than 1 million m³. According to ICOLD the total number of large dams in 2003 is 49,697 (Jia et al., 2004). There were only eight large dams in China in 1949. From 1950 to 1990 more than 19,000 large dams were constructed. In 2003 the country has 25,800 large dams, ranking first in the world. The U.S. is the country with the second highest number of large dams with some 8,724, followed by the ex-USSR, Japan, and India, as listed in Table 7.1. The U.S. is estimated to have around 96,000 small dams. If the proportion of small to large dams is similar in other countries, then at a rough estimate there are about 800,000 small dams in the world (McCully, 1999). Figure 7.1 shows the growth curves of the number of large dams of the world and China. From the 1970s to 2000 the number of large dams in the world and China increase parallelly, indicating that the dam construction occurred mainly in China in this period.

Table 7.1   The first 20 countries with the most large and major dams (as defined by ICOLD)

	Large dams (1986 data)		Large dams (2003 data)		Major dams (1994 data)	
Rank	Country	Number	Country	Number	Country	Number
1	China	18,820	China	25,800	U.S.A.	50
2	U.S.A.	5,459	U.S.A.	8,724	CIS	34
3	CIS	c. 3,000[*]	Japan	2,641	Canada	26
4	Japan	2,228	India	2,481	Brazil	19
5	India	1,137	South Korea	1,206	Japan	19
6	Spain	737	Spain	1,202	Turkey	11
7	South Korea	690	South Africa	923	China	10
8	Canada	608	Canada	804	Germany	9
9	UK	535	Brazil	634	Italy	9
10	Brazil	516	Albania	630	Switzerland	9
11	Mexico	503	Mexico	575	Argentina	8
12	France	468	Italy	549	India	7
13	South Africa	452	Turkey	521	France	5
14	Italy	440	UK	517	Mexico	5
15	Australia	409	Australia	474	Austria	4
16	Norway	245	Norway	336	Colombia	4
17	Germany	191	Germany	311	Iran	4
18	Czechoslovakia	146	Zimbabwe	244	Spain	4
19	Switzerland	144	Bulgaria	215	Australia	3
20	Sweden	141	Sandi Arabia	190	Pakistan	3

[*] The former USSR declared to ICOLD only the 132 large hydroelectric dams under the control of the Ministry of Energy and Electrification. If the dams built by the Ministry of Agriculture and local authorities were included, according to ICOLD, the number of large dams in the USSR should be 2,000–3,000

Source: ICOLD, 1988; International Water Power, 1995, Jia, et al, 2004

As the number of dams increased, so did their size and geographical distribution. Hoover Dam remained the world's highest dam for more than two decades until 1957 when it was overtaken by Mauvoisin in Switzerland. Four years later two more giants exceeded Hoover's height, Grande Dixence (also in Switzerland) and Italy's Vajont Dam. In 1968, Hoover Dam lost its position as the highest dam in the U.S. to California's Oroville Dam. Seven more dams in Canada, Colombia, the USSR, Mexico and Honduras overtook Hoover in the 1970s and 1980s. The dam, which is currently the world's highest, Nurek Dam, completed

in Tadjikistan in 1980, is an artificial mountain of earth and rock 300 m high, as tall as the Eiffel Tower (Tables 7.2–7.3).
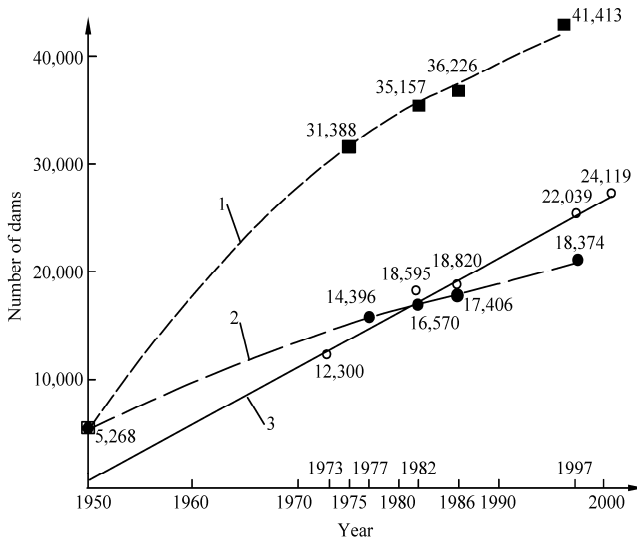
Fig. 7.1   Increasing number of large dams in the world and China: Curve-1 is the total number of large dams in the world; Curve-2 is the number of dams in the world except China; and Curve-3 is the number of dams in China (after Pan and He, 2000)

The industry defines a 'major dam' on the basis of either its height (at least 150 m), volume (at least 15 million m^3, reservoir storage (at least 25 km^3) or electrical generation capacity (at least 1,000 MW). In 1950, only 10 dams met these criteria; by 1995 the number had soared to some 305. The leading builder of major dams is the U.S., followed by the ex-USSR, Canada, Brazil and Japan. Table 7.1 lists the number of major dams in the countries ranking from 1 to 20. China was ranked 7 in 1994.

Most of the world's major river basins are now girdled with dams; many great rivers are now little more than staircases of reservoirs. A meagre 70 kilometres of the 2,000 kilometres of the Columbia River flows unimpeded by the slackwater of the 19 dams which cut across it. On the Yellow River in China, 11 dams have been constructed and the total capacity of the reservoirs is more than the annual runoff of the river. In the continental U.S., only the Yellowstone River remains undammed among rivers longer than 1,000 kilometres. In France, the only remaining free-flowing stretch of the Rhone River was impounded by a dam in 1986. Elsewhere in Europe, neither the Volga; the Weser, the Ebe nor the Tagus has a stretch more than a quarter its length which has escaped being turned into reservoir.

Worldwide, reservoirs are estimated to have a combined storage capacity of as much as 10,000 km^3, equivalent to five times the volume of water in all the rivers in the world (Chad, 1995). The weight of large reservoirs is so great that they can trigger earthquakes—scores of examples of so-called reservoir-induced seismicity have been recorded. Geophysicists even estimate that the redistribution of the weight of the earth's crust due to reservoirs may be having a very slight but measurable impact on the speed at which the earth rotates, the tilt of its axis and the shape of its gravitational field.

More than 400,000 km^2, the area of California, have been inundated by reservoirs worldwide (McCully, 1999). One of the world's largest impoundments, the 8,500 km^2 Volta Reservoir behind Akosombo Dam, flooded around 4% of the land area of Ghana. In the US, reservoirs have submerged an area equivalent to

Table 7.2 The world's highest dams (after International Water Power, 1995)

Rank	Dam	Country	Completed	Dam type	Height (m)
1	Nurek	Tadjikistan	1980	E	300
2	Grande Dixence	Switzerland	1961	G	285
3	Inguri	Georgia	1980	A	272
4	Tehri	India	U/C	E/R	261
5	Chicoasén	Mexico	1980	E/R	261
6	Mauvoisin	Switzerland	1957	A	250
7	Guavio	Colombia	1989	E/R	246
8	Sayano-Shushensk	Russia	1989	A/G	245
9	Mica	Canada	1973	E,/R	242
9	Ertan	China	2000	A	240
11	Chivor	Colombia	1957	E/R	237
11	Kishau	India	U/C	G	236
13	El Cajon	Honduras	1985	A	234
14	Chirkey	Russia	1978	A	233
15	Oroville	U.S.A.	1968	E	230
16	Bhakra	India	1963	G	226
17	Hoover	U.S.A.	1936	A/G	221
18	Contra	Switzerland	1965	A	220
18	Mrantinje	Yugoslavia	1976	A	220
20	Dworshak	U.S.A.	1973	G	219
21	Glen Canyon	U.S.A.	1966	A	216
22	Toktogul	Kyrgyzstan	1978	G	215

Dam types: A = arch; E = earth fill; G = gravity; R = rockfill; U/C = under construction

Table 7.3 Dams with largest capacity reservoirs (after International Water Power, 1995)

Rank	Dam	Country	Completed	Reservoir volume (10^9 m^3)
1	Owen Falls*	Uganda	1954	270.0
2	Kakhovskaya	Ukraine	1955	182.0
3	Kariba	Zimbabwe/Zambia	1959	180.0
4	Bratsk	Russia	1964	169.3
5	Aswan High	Egypt	1970	168.9
6	Akosombo	Ghana	1965	153.0
7	Daniel Johnson	Canada	1968	141.8
8	Guri	Venezuela	1986	138.0
9	Krasnoyarsk	Russia	1967	133.0
10	W.A.C. Bennett	Canada	1967	70.3
11	Zeya	Russia	1978	68.4
12	Cabora Bassa	Ozambique	1974	63.0
13	La Grande 2	Canada	1978	61.7
14	La Grande 3	Canada	1981	60.0
15	Ust-Ilim	Russia	1977	59.3
16	Boguchany	Russia	1989	58.2
17	Kuibyishev	Russia	1955	58.0
18	Serra da Mesa (São Felix)	Brazil	1993	54.0
19	Caniapiscau	Canada	1981	53.8
20	Bukhtarma	Kazakhstan	1960	49.8

*The major part of the lake volume (Lake Victoria) is natural. The 31 m high dam added 270 km^3 of storage to the existing capacity of the lake

New Hampshire and Vermont combined (Devine, 1995). The 0.3% of the global land surface which has been submerged represents a much greater loss than the raw statistic implies—the floodplain soils which reservoirs inundate provide the world's most fertile farmlands; their marshes and forests the most diverse wildlife habitats.

As listed in Table 7.4 the dams on the rivers provide a huge amount of power to the industries of the countries and serve as the engine of the economy. The dams also provide benefits of flood control, water supply and navigation facilities.

Table 7.4   Dams with largest capacity hydroplants (after International Water Power, 1995)

Rank	Dam	Country	Completed	Installed capacity (MW)
1	Itaipú	Brazil/Paraguay	1983	12,600
2	Guri (Raul Leoni)	Venezuela	1986	10,300
3	Sayano-Shushensk	Russia	1989	6,400
4	Grand Coulee	U.S.A.	1942	6,180
5	Krasnoyarsk	Russia	1968	6,000
6	Churchill Falls	Canada	1971	5,428
7	La Grande 2	Canada	1979	5,328
8	Bratsk	Russia	1961	4,500
9	Ust-Ilim	Russia	1977	4,320
10	Tucurut	Brazil	1984	3,960
11	Ilha Solteira	Brazil	1973	3,200
12	Tarbela	Pakistan	1977	3,046
13	Gezhouba	China	1981	2,715
14	Nurek	Tadjikistan	1976	2,700
15	Mica	Canada	1976	2,660
16	La Grande 4	Canada	1984	2,650
17	Volgograd	Russia	1958	2,563
18	Paulo Afonso IV	Brazil	1979	2,460
19	Cabora Bassa	Mozambique	1975	2,425
20	W.A.C. Bennet	Canada	1968	2,416

Note: The data are updated to 1995

7.1.2 Water Quality in Reservoirs

7.1.2.1   Thermal Stratification

The relatively small volume of water in any river section, together with turbulent mixing and the large surface-area in contact with the atmosphere, allows a rapid response of stream-water temperature to the prevailing meteorological conditions. In reservoirs, however, the increased mass of relatively still water allows heat storage to take place and this produces density differences. From spring through summer, a well-defined temperature gradient develops and highly stable summer stratification may become established in reservoirs (Fig. 7.2).

In the zone near the surface the temperature is roughly uniform because surface waves keep the water in the layer moving, this is the **epilimnion**. Whereas in the zone near the bottom, there is a layer also with a uniform temperature distribution, but much lower, which is called **hypolimnion**. An intermediate layer of maximum temperature-gradient may be established between the **epilimnion** and the cooler, denser, water of the **hypolimnion**. The rapid decrease of temperature with depth through the thermocline is associated with a rapid increase in density of the water. This density-discontinuity is poorly developed in spring, but becomes well defined in summer. At its full development, the thermocline commonly

exhibits a temperature gradient of up to 2℃/m. Within the hypolimnion, temperatures are typically low, and decrease only a small amount from the thermocline to the bed of the reservoir. Figure 7.3 illustrates the thermal stratification in different seasons in the Canyon Lake, Guadalupe River, U.S. (Hannan, 1979). The temperature distributes uniformly in January but a thermocline develops in July and the epilimnion and hypolimnion develop near the surface and near the bottom.
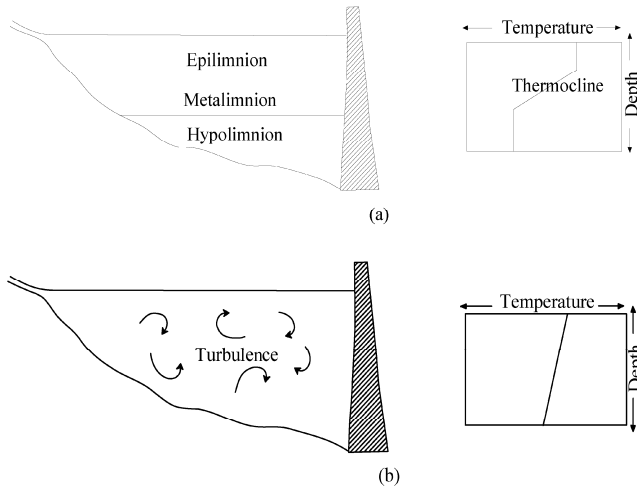
Fig. 7.2   Thermal stratification in reservoirs: (a) temperature stratification in summer; (b) homogeneous reservoir water because turbulence destroys the stratification
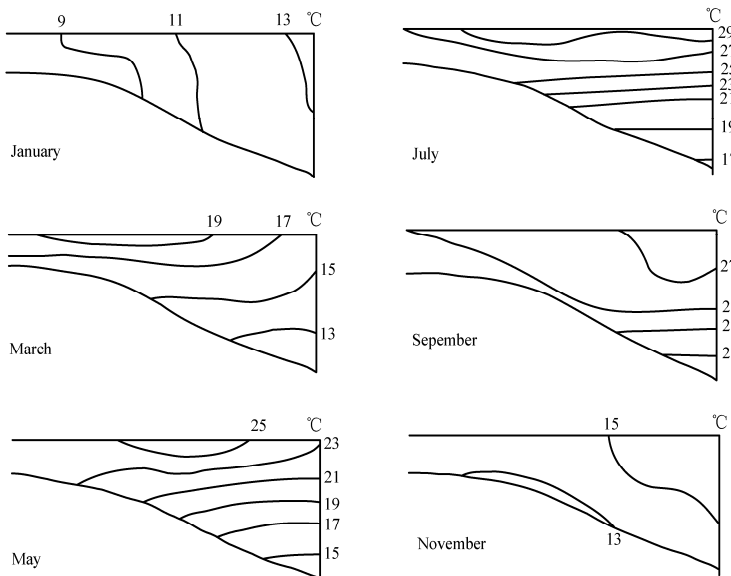
Fig. 7.3   Thermal stratification in different seasons in the Canyon Lake, Guadalupe River, U.S. (Hannan, 1979)

Water has its maximum density at about 4℃. It undergoes a normal thermal expansion—decreasing density with increasing temperature—from that point upwards and an inverse thermal expansion—

decreasing density with decreasing temperature—from that point downwards. In summer the higher-temperature, low-density, water layer 'floats' on top of the lower, cooler, water. In autumn and winter however, the temperature of the surface layer reduces to 4℃ and the density reaches its maximum and higher than that of the lower layer. The surface layer settles down and the lower layer overturns. The phenomenon is called **overturn,** which occurs two times a year in autumn and spring. Overturn occurs in the reservoirs in high latitude areas.

7.1.2.2   Chemical Stratification

The quality of natural river-water is controlled, predominantly, by the climatic and geological characteristics of the drainage basin. Water storage in open reservoirs induces physical, chemical and biological changes within the stored water. Natural river-water commonly contains four important **cations** (calcium, magnesium, sodium, and potassium), while chloride, sulfate and bicarbonate are the predominant **anions**. The relative importance of the different ions depends, in general terms, upon the geographical location (Gibbs, 1970). Soil disturbance, drainage and vegetation clearance, have increased concentrations of NO_3^-, SO_4^{2-}, and Mg^2 and urbanization can lead to the addition in stream-flows of phosphate, nitrogen compounds, and heavy metals.

The chemical composition of stream water that is released from a reservoir can be significantly different from that of the inflows—though, in some cases, releases can have a chemical composition, which reflects that of the inflows and any precipitation received. Chemical changes within reservoirs have been attributed to a variety of factors that are typically associated with their flow-dynamics and biological activity. Major, biologically induced, water-quality changes occur within thermally stratified reservoirs. Phytoplankton often proliferate in the warm epilimnion, releasing oxygen and maintaining concentrations at near-saturation levels for most of the year. Due to the settling of dead phytoplankton, and the presence of heterotrophic bacteria, oxygen will be consumed in the hypolimnion, often to exhaustion. Thus, the process of organic-matter decay becomes anaerobic; hydrogen sulphide gas is produced; carbon dioxide is released; PH decreases and the solution of iron and manganese occurs from the bottom sediments. The quality of the hypolimnial water becomes progressively worse, until the autumn overturn (Petts, 1984).

Some reservoirs may mature after as little as 3 or 4 years, but the trophic upsurge can take 6 years and in some reservoirs a period of more than 20 years may be required for the development of a stable water-quality pattern. A unique example of a reservoir maturing is given by Zhadin and Gerd (1963). The Dnieper Reservoir, USSR, built in 1934, was destroyed in 1941. During the intervening years considerable organic deposits, up to 4.0 m deep, accumulated and they subsequently were rapidly colonized by land vegetation. In 1947, the rebuilt hydroelectric power-dam was completed, the reservoir drowned the organic deposits and the decomposition of these deposits had an appreciable effect on the chemical and biological conditions of the new reservoir. During summer, a distinct stratification occurred, with the surface between 4.5 and 9.5°C warmer than the underlying layers and for the early years oxygen conditions were unfavorable. Above the decaying, flooded vegetation, oxygen was totally absent and the amount of free carbon dioxide approached 20 mg/L.

A dissolved-oxygen profile may demonstrate stratification even if the reservoir is not thermally stratified. In the epilimnial layer water-mixing, by wind and wave action, combined with photosynthesis by Algae, maintains dissolved oxygen (DO) concentrations at near-saturation. The rate of photosyntheseis in the upper layers of a reservoir will be limited by the supply of nutrients—particularly nitrogen and phosphorus- and by light-penetration, influenced partly by the algae themselves but also by suspended solids. Within Cherokee Reservoir, USA (Fig. 7.4), high dissolved-oxygen concentrations of 10 mg/L are related to dense concentrations of phytoplankton, of between 30 and 60 thousand per mL, near the surface. Below 10 m, however, conditions are unsuitable for phytoplankton and DO concentrations are reduced to

less than 1 mg/L, whilst between 6 and 10 m, the rapid reduction in DO concentration reflects the high number of zooplankton which graze on the phytoplankton (Churchill and Nicholas, 1967). A similar interrelationship was observed within the Boone Reservoir, Tennessee, although here the quantity of oxygen used in respiration by the zooplankton exceeds that produced by phytoplanktonic photosynthesis.
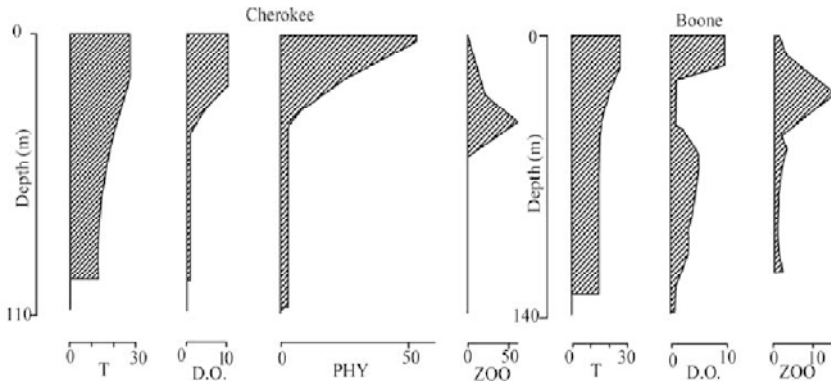
Fig. 7.4 Vertical water quality profiles for summer in Cherokee and Boone Reservoirs, Holston River, U.S.A.: T = temperature (°C); D.O. = dissolved oxygen (mg/L); PHY = phytoplankton (1000 cells/mL); and ZOO = zooplankton (number/L) (after Churchill and Nicholas, 1967)

7.1.2.3 Eutrophication

Lakes and reservoirs act as nutrient sinks and considerable attention has been directed to the eutrophication of natural and artificial lakes resulting from the accumulation of nutrients—particularly nitrogen and phosphorus, although potassium, magnesium, trace elements (such as iron, manganese, and copper) and organic materials also play a part. Figure 7.5 shows the blooming blue-green algae yano bacteria in the Dianchi Lake in southwest China. The lake has received increasing amounts of sewage water from towns and cities and suffers from increasing eutrophication in the past decades. The blooming blue-green algae produce an oil-like green surface layer, which causes a serious DO depletion. Many fishes have been killed.

Fig. 7.5 An oil-like green surface layer due to blooming blue-green algae in Dianchi Lake in southwest China, which causes serious DO depletion (See color figure at the end of this book)

Each lake and reservoir has a capacity for sustaining good water quality under a certain nutrient loading to avoid eutrophication. Although many studies have been done (Vollenweider, 1968 Pearl, 1988), more work is needed to find a method for estimation of the critical nutrient loadings to avoid eutrophication.

7.1.3   Water Quality Released from Reservoirs

Despite the range of parameters which control water quality, the thermal and chemical regimes of rivers will be moderated as a result of upstream impoundment: annual variations will be reduced, short-time extremes will be virtually eliminated and seasonal maxima and minima will be delayed. Long-retention reservoirs are often characterized by phyptoplankton assimilation of nitrate–nitrogen, and by the anaerobic metabolism of nitrate by bacteria in the hypolimnion (Petts, 1984). Nitrate loadings are reduced, whilst loads of ferrous iron can reach unusually high levels during stratification; the reduction of the insoluble ferric form of Fe to the soluble ferrous form is caused by high concentrations of CO_2, low pH, and the presence of organics within the anoxic hypolimnion (Hannan and Broz, 1976). In some cases, the effects of a reservoir may be limited to only 1 kilometer below the dam but often the effects have been transmitted for tens of kilometers downstream.

Where reservoir-discharge quality differs markedly from that of the natural discharges, thermal and chemical gradients may be established along the river and the downstream extent of any such gradient will reflect the relative discharges from the reservoir and tributary sources. For thermal gradients to be established, reservoir releases must be of sufficient magnitude to overcome gradients, produced by hypolimnial releases, have been reported below Cheesman Dam, South Platte River, Colorado, USA (Ward, 1974). The reservoir exerts a regulating effect upon temperatures immediately below the dam, so that the primary natural peaks, expected during August and April, are not experienced. Hypolimnial releases during reservoir stratification cause a thermal gradient to form between March and September, and temperatures increase downstream most rapidly in April and August. In October, uniform temperatures reflect the release of mixed water due to the autumn overturn.

The location of the outflow facility will determine the quality of releases from stratified reservoirs, because withdrawal will occur from a relatively narrow layer. Churchill and Nicholas (1967) showed that outflows from Cherokee Reservoir, Hoston River, USA, were withdrawn from a fairly narrow layer in the pool, located at the level of the intakes. However, within density-stratified reservoirs, vertical movements are suppressed whilst horizontal movements are enhanced (Wunderlich, 1971). Water will be drawn from all layers in the first moments of a release (Elder and Wunderlich, 1968), but once a steady rate of outflow has been achieved, a withdrawal layer of restricted vertical dimensions develops near the intake elevation and 'continuity' is satisfied by the establishment of secondary currents. Water from relatively narrow layer of approximately constant density will be withdrawn, so that the water quality of the outflow will vary considerably.

Reservoirs normally reach a condition of stability after between 5 and 10 years. After the initial effects produced by the submergence of vegetation and soils have disappeared, the water downstream from a nonpolluted reservoir improves to the point where only the yearly increment of leaves, dead algae, and other natural situations may arise to produce the short-time release of low-quality water. Low latitude reservoirs, in particular, can exert a pronounced cooling effect on streams via hypoliminial release (Pearson and Franklin, 1968). Oxygen depletion within the regulated Catawbe River, South Carolina, USA, was caused by the first reservoir release after a period of stable low-flows (Ingols, 1959). Reduced dissolved-oxygen concentrations occur because of the lower reaeration of the greater depth of water. Seasonal-pulses are climatically induced and may be caused by a major flood inflow which stirs the bottom sediments, releasing large quantities of orthophosphate into the water (Hannan and Broz, 1976), or by sudden destratification, which can produce extreme deoxygenation and the release of toxic water (Arumugam and Furtado, 1980).

Supersaturated water can be released into the river downstream from the epilimnion. The supersaturation of air gases can also be caused by the passage of water through turbines (Dominy, 1973) or by over-dam spillage (Beiningen and Ebel, 1970).

7.1.4 Water Quality Control

The impoundment of a river causes two major changes in the character of the water, both of which have a marked effect upon the water quality of the releases: firstly, the creation of a reservoir greatly increases the travel-time of the water through the system; and secondly, stratification may occur. Density stratification can have severe consequences for downstream water quality, particularly if the reservoir releases are large in relation to the cumulative volume of tributary discharge. The regulation of the physico-chemical quality of river-flows may prove beneficial, but reduced dissolved-oxygen concentrations, in particular, can be detrimental. The control of the quality of water released from impoundments, to maximize the inherent benefits and minimize the inherent detriments, is in all cases advisable and in many cases essential. Numerous operational techniques and structures of different design have been used to control the quality of reservoir releases and to minimize the adverse effects of reservoir stratification. These may be classified as selective withdrawal techniques and destratification techniques, and both have been recommended to maintain minimum-quality standards in the outflows.

7.1.4.1 Selective Withdrawal Techniques

Multiple-level intake points to facilitate selective withdrawal provides the simplest method of controlling water quality. Deoxygenated hypolimnial water, for example, can be drawn off slowly and blended with highly oxygenated water from the epilimnion. Furthermore, large discharges from outlets can generate mixing currents within the lake, which inhibit the development of anoxic conditions. The effectiveness of valve releases is well demonstrated by Gore (1978). Operational requirements of the Tongue River Reservoir Dam, Montana, USA, resulted in the control gates of the dam remaining open for most of the spring and summer of 1975. The continual high release of water prevented thermal stratification and the associated development of hypolimnial waters, so that the water quality of the release was near pre-impoundment conditions. Below the dam, discharges were observed to have temperatures only negligibly cooler than at the mouth of the river, approximately 150 km downstream, and the diurnal and monthly thermal fluctuations approached those expected for unregulated streams. The use of selected-depth release may, therefore, prove to be beneficial.

Selected releases of water from the epilimnion, through surface outlets, during times of stratification will provide high-quality discharges until the lake overturns, when the benefit may be lost. Releases from a number of outlets would dilute the hypolimnial waters over a longer period, and provide less extreme water quality conditions downstream. However, selective withdrawal has been considered by some authors (e.g. Brooks and Koh, 1969; Fruh and Clay, 1973) to provide only a limited solution for highly stratified lakes within which mixing is not induced by the releases themselves. Indeed, water-quality problems during summer below Stanley Reservoir, River Cauvery, India, related to two outflow sources which continued to flow as separate and distinct streams for about 2 km below the dam (Ganapati, 1973). Water released from the high-level sluice was relatively warm, well oxygenated, and contained low concentrations of phosphates, silicates, and nitrates. Tailrace water from turbines abstracted at a depth of 30 m (up to 3°C cooler, containing 50% less dissolved oxygen, lower pH and high phosphates, silicates, and nitrates) was released simultaneously but mixing and hence dilution did not occur. After the autumn overturn, uniform releases were discharged from both sources.

7.1.4.2 Artificial Destratification

Two approaches to artificially destratifying reservoirs have been commonly applied, namely air injection

and mechanical pumping. The maintenance of the reservoir storage in a nearly isothermal condition would permit continued water circulation and, therefore, an available supply of dissolved oxygen throughout the entire water-mass. Anaerobic conditions would be eliminated, along with many of the problems, which accompany them.

Artificial destratification and the mixing of epilimnial and hypolimnial waters during summer may often be desirable in order to obtain an improved and more uniform water quality within and, consequently, downstream from reservoirs. Indeed, the Quality Control in Reservoirs Committee in the USA recommend artificial destratification to water suppliers who are experiencing any water-quality deterioration in their reservoirs resulting from anaerobic conditions in the hypolimnion caused by thermal stratification (American Water Works Association, 1971).

Several investigators have attempted artificial destratification by injecting diffused air into a reservoir's hypolimnion. The mixing process, through interchange of heat from warmer to colder water, causes the water-mass to become nearly isothermal. Early attempts often failed to achieve sufficient circulation (e.g., Derby, 1956; Schmitz and Hasler, 1958). In Sweden, Lake Langsjon experienced severe stratification, with a hypolimnion devoid of oxygen (Heath, 1961); but compressed-air injections effectively eliminated stratification. Similar benefits of forced circulation have been reported by Riddick (1957) for the Ossining Reservoir, New York, U.S. and for Lake Wohiford, a subtropical reservoir in southern California (Ford, 1963). In the latter case, stratification was completely eliminated throughout the lake after 7 days of operation. During which air injections lasted for 9 hours on each of the first 6 days and for 24 hours on the last.

An air diffusion system has been successfully applied to the destratification of a medium-sized lake-Allatoona Lake, Georgia, USA, which, under normal conditions, begins to stratify in mid-March and achieves complete stability in mid-July, with overturn in early October (Rogers et al, 1973). In late summer, a maximum temperature difference of 17℃ is established between the surface and bottom of the lake, and dissolved oxygen may become exhausted below the upper 20% of the depth. During the summer of 1968, air was continuously supplied to the hypolimnion, and the reservoir was maintained in the destratified condition, with adequate dissolved-oxygen concentrations throughout the Lake. Improvement in the quality of reservoir releases is particularly noticeable if comparisons are made between the specific flow conditions. Under high flows, dissolved oxygen was slightly less during early summer in Allatoona Lake, but significantly higher during August and September under conditions of artificial hypolimnion aeration. Moreover, during low-flow conditions, levels of dissolved oxygen were generally maintained above 4 mg/L, whereas prior to air injection, concentrations of less than this value were experienced for most of the summer and temperatures were elevated by a maximum of 8˚C. Although air injection can be applied to a considerable area and a large amount of water can be set in motion, it is a relatively inefficient means of water transfer because it involves intermediate energy conversion for air compression.

Pumping cold water from the bottom of a water-body and discharging it at the surface has been suggested as an alternative method of control to air injection (Irwin et al., 1966). Symons et al. (1965) applied mechanical pumping to destratify a small lake, increasing the temperature and dissolved-oxygen concentrations in the lower layers; manganese and sulphide concentrations were reduced to zero and the ammonia nitrogen concentration resulting from anaerobic decomposition, was also reduced.

Pumping can be particularly useful if the operation is begun before a lake becomes stratified (Garton et al., 1976). An axial-flow pump was used in midsummer to transfer water at 0.674 m^3/s from the oxygen-rich epilimnion to the hypolimnion. Within 2 weeks the procedure had completely destratified water temperature in the lake, but a longer period of time was required to destratify dissolved-oxygen levels, as shown in Fig. 7.6. Significantly, the lake warmed uniformly at a particular depth, regardless of distance from the pump. Initially the dissolved-oxygen concentration of the surface water was markedly reduced, because

of mixing the water from an anoxic hypolimnion; but more significant was the rapid rise in dissolved-oxygen concentrations at depth. After 7 weeks, well oxygenated water was observed throughout the profile; the time-lag in relation to temperature probably resulted from large organic accumulation in the hypolimnion. The following year, pumping began before stratification had become established, although a 7°C temperature difference existed between the surface and bottom waters after only 2 days of pumping, an isothermal profile was developed and the dissolved oxygen concentration was stabilized.
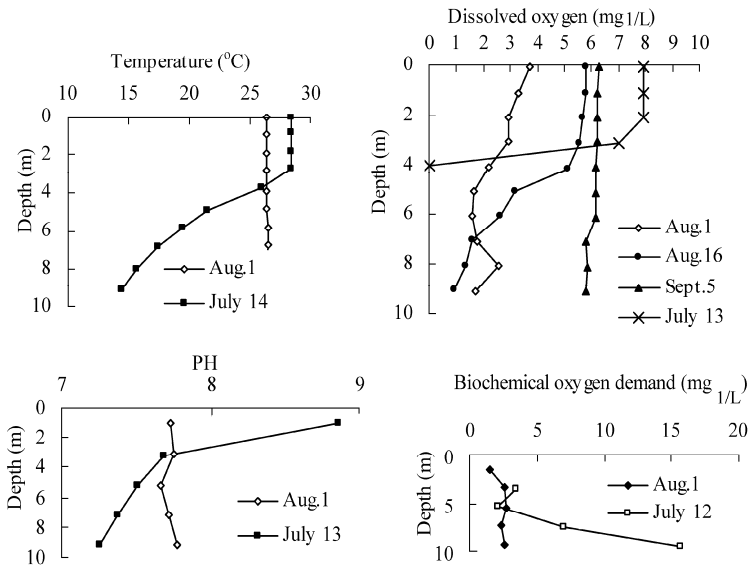
Fig. 7.6 Profiles of temperature, dissolved oxygen, PH, and biochemical oxygen for Ham Lake, Oklahoma, the USA before (July 12–14) and after destratification (after Garton et al., 1976)

7.1.5 Impacts on Ecology

Dams are one of the main reasons why one-fifth of the world's freshwater fish are now either endangered or extinct. The percentage rises even higher in the countries which have been most heavily dammed—to nearly 2/5 in the U.S. and 3/4 in Germany. Amphibians, molluscs, insects, waterfowl and other riverine and wetland lifeforms are similarly imperiled (World Resources Institute, 1994).

7.1.5.1 Phytoplankton

Impoundment of reservoirs favors the development of lentic plankton. Both zoo plankton and phyto-plankton require a minimum retention-time to allow development. The development time may be longer for the zooplankton than the phytoplankton (Brooks and Woodward, 1956). The quantity of lake plankton tends to be inversely proportional to the speed of water-flow, so that a general transition may be observed from a small, shallow reservoir receiving runoff from a large catchment area and having low primary production, to a large deep reservoir with a relatively small catchment, and supporting high primary production (Rzoska et al., 1955).

In all reservoirs, primary production is mainly derived from the activity of phytoplankton. Blue-green algae often dominate in numerical terms but they are often outweighed in biomass by diatoms. Three factors govern the contribution of lentic plankton to lotic systems: the rate of water replacement within the reservoir (the retention time or flushing time), the seasonal pattern of lentic plankton development, and the character of the outflows from the reservoir. Short retention-times are often associated with high

turbulence, a mixed water-body, and a lack of thermal stratification—such that, if rates of water movement through a lake exceed a few millimeters per second, little plankton will develop (Hynes, 1970). In the Pitlochry Reservoir, UK, the retention-time is never more than 4 days and only occasional planktonic organisms were found during a 4-year period of observation (Brooks and Woodward, 1956). In general, sediment concentration in the reservoir limits the concentration of phytoplankton and zooplankton.

In the first few years of impoundment, the amount of nitrogen and phosphorus in the reservoir water increase, as a result of the decay and mineralization of organic matter flooded by the lake, which may lead to blooms of blue-green algae (cyanobacteria). The plankton population of reservoirs constructed on a mountain stream or turbid lowland river, may require a long period of time to develop, whereas on a clean lowland stream, the process could be rapid. Some species will adapt to the lake conditions preferentially. It is these lentic species, which have significance for stimulating secondary production through invertebrates to fish etc., not only within the lake, but also within the river channel downstream. The impoundment of the River Niger in Nigeria, for example, has more than doubled the annual peak phytoplankton density to about 2500 algae/mL, and tripled the zooplankton peak within the river downstream (El-Zarka and El-Din, 1973).

Algal blooms occur in reservoirs if the concentrations of nitrogen and phosphorus in the lake water are high and high temperatures and sunshine are maintained for a long time. Hergenrader (1980) examined the eutrophication process as it occurred in a system of new reservoirs—the Salt Valley Reservoirs, Nebraska, USA. The intensively-cultivated prairie soils supply runoff to the reservoirs with high nutrient concentrations, and so promote eutrophication. All the reservoirs are shallow (maximum depth 10 m), and have large surface areas, which allow wind-induced mixing that prevents thermal stratification and provide a relatively homogeneous heat and nutrient distribution—conditions highly suited for vigorous algal growth. One of the reservoirs, dominated by high levels of inorganic turbidity, developed only a poor phytoplankton population within which diatoms persisted, whereas three 'clear' reservoirs produced dense standing-crops of phytoplankton and their surface-releases led to a continued increase in the nutrient pool, with a consequent increase in phytoplankton growth.

7.1.5.2   Vegetation Reaction

Beds of aquatic macrophytes play a significant role within river ecosystems (Turner and Karpiscak, 1980). Below deep-release dams, discharges may be oxygenated by plants during the day, and weed-beds provide a diverse microhabitat. Macroinvertebrates can have density values up to fifty times as great as in areas lacking macrophytes (Décamps et al., 1979). However, the development of aquatic plants is not always favorable. The lack of regular flushing by floods on the Zambezi, for example, has encouraged the development of dense aquatic macrophytes to the detriment of living-space for *Hippopotamus amphinius*, crocodiles, and wildfowl (Attwell, 1970). Similarly, stabilized flows on the Tuolumne River, California, U.S., have contributed to favorable conditions for luxurious growths of *Eichhornia crassopes* (Water-hyacinth) in some years, which can impair, and totally block the salmonid migration in extreme cases (Fraser, 1972).

Floating plants are of little importance in temperate latitudes, but in the tropics, where turbid water inhibits the growth of submerged species, floating plants are often important (Hynes, 1970). The elimination of high discharges to flush the problem species has allowed the extensive development of Eichornia crassipes and Salvinia molesta in both Africa (Jackson and Rogers, 1976) and Australia (Walker, 1979). Infestations of the floating plants caused deoxygenation of the water, clogged irrigation and water-supply intakes, provided breeding grounds for mosquitoes, and interfered with recreation.

Under natural conditions, flood discharges periodically submerge portions of the river-bank or floodplain. These flows rearrange sedimentary deposits, and can be key events in maintaining riparian habitats. An

important downstream manifestation of river impoundment is the loss of pulse-stimulated responses at the water–land interface of the riverine system (Gill, 1971). The species adapted to pulse-stimulated habitats are adversely affected by flow-regulation. The Eucalyptus forests (primarily eucalyptus camaldulensis) of the Murray floodplain, Australia, depend upon periodic flooding for seed germination, and regeneration has been curtailed by headwater impoundment (Walker, 1979). Artificial pulses generated by dam releases at the wrong time—in ecological terms—have also been recognized as a cause of forest destruction. Acacia xanthoploea, for example, is disappearing from the Pongolo system below Pongolapoort Dam, South Africa, as a result of mistimed high-flows (Furness, 1978).

For floodplain habitats, river impoundment and flow-regulation can have disastrous consequences. Periodic inundation is a vital component of wetland ecosystems, and the removal or altered timing of the annual flooding has changed, in many cases, highly productive habitats into unproductive scrub or, with further intervention by man, into vast areas of monoculture or industrial or urban uses. Within channels, the increased growth of macrophytes can support substantial numbers of invertebrates, but on floodplains, the elimination of the annual flood has devastated the often unique faunal assemblage. Moreover, the direct loss of annual silt and nutrient replenishment, consequent upon upstream impoundment, is thought to have contributed to the gradual loss of fertility of formerly productive floodplain soils (Attwell, 1970). However, the Aswan High Dam has increased productivity of the floodplain as a result of the provision of a reliable, all-year-round water-supply (Kinawy et al., 1973).

7.1.5.3   Macroinvertebrate Response to Upstream Impoundment

Within most natural rivers the pattern of flow, the temperature variations, the substrates and the bed stability are the dominant factors controlling macroinvertebrate distributions (Ward and Stanford, 1979). The life-cycles of many lotic species are related to the natural seasonal variations of discharge, and the biotic communities of streams are significantly affected by flow-velocity because of respiratory, physiological, and feeding requirements (Petts, 1984). In some of their habitats, most lotic species are limited in their preference of water-depth and the short-term magnitude and frequency of flow-variations can have a marked influence upon organisms of narrow depth-tolerance.

Many life-cycle phenomena, such as hatching, growth, and emergence, depend on thermal cues (Lehmkuhl, 1972) and the alteration of the thermal regime has been credited as a primary factor influencing community change (Gore, 1980). Substrate heterogeneity is a necessary requirement for the maintenance of a diverse number of macroinvertebrate species. Most aquatic insect adults are rheophilic and select upstream areas to colonize, reproduce, and deposit eggs (Hynes, 1955). A dam will act as a barrier to aerially colonizing adults as well as to the passive downstream drift of nymphs and larvae (Hynes, 1955; Minckley, 1964).

Most studies of impounded rivers utilize comparative data derived either from upstream or from adjacent or tributary rivers, because of the lack of reliable pre-dam data. Several responses can be recognized which are common to many impounded rivers in a review of twenty-three studies from USA, Europe, and South Africa. Stanford and Ward (1979) found that in all but three cases, species-diversity was reduced by river impoundment. However, even if the relative abundance does not change, the composition of each taxonomic group can be modified considerably. Table 7.5 lists some reported responces of macro-invertebrates to the impoundment (Petts, 1984).

Reservoir operations for hydroelectric power-generation, irrigation supply, or recreational or fishery demands, produce artificial discharge variations. These often involve extreme fluctuations of water depth and flow velocity, having unnatural rates of change, unnatural durations, and unnatural frequencies. Within natural rivers experiencing flows of high variability, a high level of production can be attained, provided that the community present is adapted to the frequency and magnitude of flow fluctuation

Table 7.5 Effects of impoundments upon benthic macroinvertebrates (after Petts, 1984)

River, reservoir, location	Macroinvertebrate changes	Source
River Elan, Craing Goch Reservoir, UK	Reduced abundance and diversity	Scullion (1982)
S. Saskatchewan River, Gardiner Dam, Canada	Marked reduction of macroinvertebrates downstream for over 100 km; 19 species of Ephemeroptera were probably eliminated	Lehmkuhl (1972)
Green River, Flaming Gorge Dam, USA	Number of taxonomic groups reduced and density of benthos increased for over 100 km downstream	Pearson and Franklin (1968)
Brazos River, Possum Kingdom Reservoir, USA	Increased zoobenthos diversity for 80 km below the dam	McClure and Stewart (1976)
S. Platte River, Cheesman Lake, USA	Reduced diversity but increased standing-crop for 32 km	Ward (1976)
Upper Colorado River, Navajo Dam, USA	Invertebrate densities increased from $820/m^2$ to $6727/m^2$ within a 13 km reach	Mullan et al. (1976)
River Tees, Cow Green Reservoir, UK	Reduced diversity and increased biomass for only 400 m below the dam	Armitage (1978)
Stevens Creek, Central California, USA	Biomass more than doubled	Briggs (1948)
River Svratka, Vir Valley Reservoir, Czechoslovakia	Numbers increased by up to 3.5 times and biomass by up to 2.8 times in comparison with the natural river	Peňáz et al. (1968)
Mill Creek, Wisconsin, USA	Many species disappeared and the fauna became dominated by a few species: *Simulium* sp., Chironomidae, and *Gammarus* sp.	Hilsenhoff (1971)
Tennessee Valley, South Holston Reservoir, USA	Increased numbers attributed to large population of simuliids, chironomids.	Pfitzer (1954)
Guadalupe River, Canyon Reservoir, USA	Diverse macroinvertebrate community established 24 km downstream 5 years after dam closure	Young et al. (1976)
Clinch River, Norris Dam, Tennessee, USA	Number reduced by 30%; Trichoptera and Ephemeroptera replaced by chironomids and gastropods.	Tarzwell (1939)

(Odum, 1969). However, such adaptations require a long time-period. Within impounded rivers, the fauna may become dominated by those species which can actively migrate into the substrate interstices for protection against rapid increases in flow velocity (Radford and Hartland-Rowe, 1971; Trotzky and Gregory, 1974; Ward and Short, 1978). In a reach immediately downstream of the Fengshuba Dam on the East River in south China, only one species—*Palaemonidae*—survived because power generation produces an artificial fluctuation of discharge and an abrupt increase and decrease of flow velocity. Excessive velocity appears to be the primary limiting factor. Thus, the depleted fauna of the main channel below Glen Canyon Dam, experiencing extreme flow-fluctuations, contrasts with the diverse benthic community found in adjacent quiet-water areas, which includes *gastropods, Diptera, Trichoptera, annelids, and amphi-pods* (Mullan et al., 1976).

Invertebrates, generally, are both sensitive to the environmental conditions in which they live, and able to colonize newly-available habitats by upstream migration of adults and downstream drift of nymphs and larvae. In an experiment the authors found that the taxa richness of macroinvertebrates increased from 17 species to 38 species and the number density increased from $60/m^2$ to $1700/m^2$ in just 20 days after establishing artificial step-pools in a mountain stream with relatively uniform width and depth. However, the community needs a longer time to reach an equilibrium adapting to the new environmental conditions after upstream impoundment. Young et al. (1976) considered that the successful reorganization of the benthic macroinvertebrate community to fill the new set of niches made available by changes of the environment, required 5 years on the Guadalupe River, Texas, USA, after the closure of the Canyon Reservoir.

Ward and Short (1978) grouped macroinvertebrates into four types, on the basis of observed responses to river impoundment: (1) Tolerant organisms having a ubiquitous distribution but forming large populations under certain types of river regulation; (2) Organisms present in unregulated streams, but favored by certain types of regulation; (3) Intolerant organisms present in unregulated streams, but reduced in, or eliminated from, regulated streams; (4) Indicator species not normally present in unregulated streams, but favored by regulation.

Considerable reorganization of the invertebrate community existing during and shortly after dam construction may, however, occur as the water quality, and thermal and discharge regimes, stabilize. For example, the impoundment of Mill Creek, Wisconsin, USA, had a dramatic effect upon the benthos (Table 7.6). Many species were eliminated, and the fauna became dominated by chironomid larvae and amphipods, while other benthos changed rapidly during, and after, impoundment (Hilsenhoff, 1971). Four general response-groups may be recognized: species that were common prior to impoundment but became reduced or eliminated after it (e.g., *Hydropsyche* and *Elmidae*); species that were common under pre-dam conditions, eliminated during dam construction or shortly after, but returned subsequently in limited numbers (e.g., *Baetis brunneicolor);* species that seemed largely unaffected by impoundment but experienced population explosions during, and immediately after, dam closure (e.g., *Chironomus* spp.); and species that showed an increase in abundance after dam completion (e.g., *Simulium vittatum*).

Table 7.6 Short-term macroinvertebrate changes during and shortly after dam construction at a riffle 300 m below the dam, Mill Creek, U.S. (after Hilsenhoff, 1971)

	Before	During	7–15 months after	19–27 months after
Ephemeroptera, Baetidae				
Baetis brunneicolor	21	0	0	10
Diptera, Chironomidae				
Chironomus spp.	0	508	345	3
Micropsectra spp.	5	80	239	41
Orthocladius spp.	74	54	66	210
Stictochironomus spp.	0	6	25	0
Diptera, Simuliidae				
Simulium vittatum	173	336	901	742
Diptera, Tipulidae				
Dicranota spp.	1	20	24	4
Amphipioda, Gammaridae				
Gammarus	34	-	50	132
Pseudolimnaeus				
Trichoptera, Hydropsychidae				
Hydropsyche betteni	177	81	0	2
Coleoptera, Elmidae	142	17	0	0
Summer total phosphorous (ppm)	0.08	-	1.24	0.58
Summer total nitrogen (ppm)	0.77	-	3.16	1.37

(Values = number per standard sample; - = Not measured)

7.1.5.4 Fish and Fisheries

Dam construction appears to have had a greater impact upon riverine fish than any other human activity. In 2 years after the completion of Lake Kainji, for example, catches of fish from the River Niger, Nigeria, were reduced by 30% (Lelek and El-Zarka, 1973). One immediate consequence of river impoundment is the conversion of naturally lotic environments to lentic habitats. The impoundment of relatively fast-flowing

rivers may totally preclude riverine fish, which are dependent upon flowing water for all their ecological requirements (Fraser, 1972), and species that are able to live only in running water can be eliminated (Zhadin and Gerd, 1963).

Many important 'commercial' fish migrate between the river-system and the sea, either for breeding or for feeding. Acipenseridae (Sturgeon) and salmonids, which breed in fresh water, have been particularly affected by impoundments. Reservoirs will inundate vast spawning-grounds, and great dams provide barriers to upstream and downstream migrations, but the effects of a single impoundment upon the discharge regime, water quality, and habitat structure, of rivers, may be transmitted for considerable distances downstream.

Fish species can become extinct as a result of river impoundment. Some of the native species which have disappeared from impounded rivers are listed in Table 7.7. Atlantic Salmon disappeared from the Dordogne River, France, soon after the first dams were built on the lower reaches between 1842 and 1904 (Décamps et al*.,* 1979). The extinctions have often been associated, not with the increased abundance of other native species, but with the introduction of exotics. Valuable fishes, such as *Salmo salar* and the Acipenseridae (Sturgeon family), have often been replaced by less valuable and slower-growing species: for example, *Rutilus rutilus* (Roach), and *Perca fluviatilis* (Perch).

Table 7.7   Selected examples of fish-fauna changes consequent upon river impoundment (after Petts, 1984)

Location	Native species disappeared	Introductions	Source
Australia	*Plectroplites ambiguus*	*Salmo* spp.	Walker (1979)
	Tandanus tandanus	*Perca fluviatilis, Carassius, auratus Tinca tinca*	
Scandinavia	*Salmo solar*	*Perca fluviatilis*	Henricson and Müller (1979)
	Salmo trutta	*Acerina cernua*	
	Thymallus thymallus	*Rutilus rutilus, Esox lucius*	Lillehammer and Saltveit (1979)
Central Europe	*Barbus* spp.	*Thymallus thymallus*	Peňáz et al. (1968)
	Perca fluviatilis	*Salmo trutta*	Lehmann (1927)
	Esox lucius	*Cottus gobio*	
Western Europe		*Salmo trutta, Cottus gobio*	Armitage (1979)
	Salmo salar	*Salmo trutta*	Décamps et al. (1979)
	Lampetra planeri	*Barbus barbus*	
	Petromyzon marinus Alosa alosa	*Anguilla anguilla*	
USSR	*Acipenseridae*	*Perca fluviatilis*	Zhadin and Gerd (1963)
		Acerina cernua, Rutilus rutilus	
India	*Hilsa ilisha, Puntius dubius*		Sreenivasan (1977)
USA	*Ptychocheilus lucius*		Minckley and Deacon (1968)
	Micropterus treculi	*Salmo gairdneri*	Edwards (1978)
	Ictalurus punctatus	*Notemigonus crysoleucas*	
	Hybopsis aestivalis	*Poecilia latipinna*	
	Cichlasoma cyanoguttatum	*Pimephales vigilax*	
	Notropis volucellues		

Dams may also have positive effects on some species. For fishes which spawn on inundated floodplains during the annual flood-season, the formation of shallow reservoirs with large surface-areas may enhance the spawning conditions. Such a change on the Kafue River, Zambia, benefits important species of *Tilapia,* which form a major part of the commercial catch, through improving growth-rate and the survival of juveniles (Dudley, 1974). Moreover, man-made lakes create good conditions for aquaculture.

After the completion of the Fenshuba Dam fish harvest has been much greater than the fishery within the river before the dam.

Assessments of impacts on fish, shortly after impoundment, may not provide an indication of the long-term effects, because the fauna will require time to readjust, and to recover after the initial impact of dam-closure and reservoir-filling. Post-impoundment studies of Lake Kainji, Nigeria, for example, suggested that the diverse, abundant and commercially important *Mormyridae*—highly specialized for lotic habitats—of the Niger system were radically affected by impoundment, being reduced from about 20% (Banks et al*., 1965; Motwani and Kanwai, 1970) to less than 5% (Lelek and El-Zarka, 1973; Lkwis, 1974) of the fish caught. Some species were wiped out, others adjusted rapidly to the change to lacustrine conditions, while yet others may recover but at a slower rate (Blake, 1977). For example, *H. pictus* increased in number to comprise over 70% of the total mormyrids caught, whereas *M. senegalensis* declined to 0.5%. Moreover, despite the sudden decline in total abundance during the first post-impoundment year, an increasing trend was subsequently apparent and as the species-composition adjusted to the changed conditions, the abundance of the Mormyridae recovered towards pre-impoundment levels.

7.2 Reservoir Sedimentation Management

7.2.1 Reservoir Sedimentation

7.2.1.1 Loss of Reservoir Capacity Due to Sedimentation

Sediment deposition always occurs in reservoirs, which causes not only loss of storage capacity but also environmental impacts. At the end of the 1950s, the United States made an investigation into the sedimentation in 1100 reservoirs. Of them, data from 66 representative reservoirs selected by L.G. Gotts are listed in Table 7.8. Table 7.9 lists the reservoir sedimentation in China (IRTCES, 1985).

A wide range of sedimentation related problems occur upstream of dams as a result of sediment trapping. Because of storage loss the functions of the reservoir reduce for flood control, power generation, and water supply. Sediment can enter and obstruct intakes and greatly accelerate abrasion of hydraulic machinery, thereby decreasing its efficiency and increasing maintenance costs. Sediment deposition in the delta region in the reservoir may affect navigation and impact the ecology. Dam construction is the largest single factor influencing sediment delivery to the downstream reaches. The cutoff of sediment transport by the dam can cause stream bed degradation, accelerate the rates of bank failure, and increase scour at structures such as bridge piers. Table 7.10 lists the main impacts of reservoir sedimentation on the environment.

Table 7.8 Reservoir sedimentation and capacity loss in the USA (after IRTCES, 1985)

Region	Number of reservoir	Number of years	Loss of storage capacity (%)
Northeast	3	30	24.7
Southeast	10	18.6	15.1
Middle West	11	16.5	14.0
Middle South	12	17.2	8.8
Northern Great Plain	9	23.1	29.6
Southwest	15	29.8	15.7
Northwest	6	23.1	7.0
Whole country	66	22.1	15.6

Table 7.9 Reservoir sedimentation in China (after IRTCES, 1985)

Reservoir	River	Drainage area (km^2)	Dam height (m)	Total capacity (10^6 m^3)	Years surveyed	Sedimentation (10^6 m^3)	Capacity loss (%)
Liujiaxia	Yellow	181,700	147	5,720	1968–78	580	10.1
Yanguoxia	Yellow	182,800	57	220	1961–78	160	72.7
Bapanxia	Yellow	204,700	43	49	1975–77	18	36.7
Qintongxia	Yellow	285,000	42.7	620	1966–77	485	78.2
Sansengong	Yellow	314,000	10	80	1961–77	40	50
Tianqiao	Yellow	388,000	42	68	1976–78	7.5	11
Sanmenxia	Yellow	688,421	106	9,640	1960–78	3,760	39
Bajiazui	Puhe	3,522	74	525	1960–78	194	37
Fengjiashan	Qianhe	3,232	73	389	1974–78	23	5.9
Heisonglin	Yeyu	370	45.5	8.6	1961–77	3.4	39
Fenhe	Fenhe	5,268	60	700	1959–77	260	37.1
Guanting	Yongding	47,600	45	1,270	1953–77	552	43.5
Hongshan	Xiliao	24,486	31	1,560	1960–77	475	30.4
Naodehai	Laoha	4,501	41.5	196	1942	38	19.5
Yeyuqn	Mihe	786	23.7	168	1959–72	12	7.2
Gangnan	Hutuo	15,900	63	1,558	1960–76	235	15.1
Gongzui	Dadu	76,400	88	351	1967–78	133	38
Bikou	Bailong	27,600	101	521	1976–78	28	5.4
Danjiangkou	Hanjiang	95,217	110	16,050	1968–79	897	5.6
Xinqiao	Hongliu	1,327	47	200	14 years	156	78

Table 7.10 Environmental impacts of reservoir sedimentation (after IRTCES, 1985)

Location	Impact	Description and illustration
Reservoir	1. Loss of storage capacity	1) Depletion of effective storage due to reservoir sedimentation. 2) Deposits plug up the mouth of tributaries, making part of the tributary capacity ineffective. For instance sedimentation in the Guanting Reservoir forms a bar of 5 m high at the mouth of Guishi River.
	2. Contamination of the environment	Chemicals absorbed on the surface of sediment particles enter the reservoir with the sediment. Water quality may deteriorate through ion exchange.
	3. Endanger the sluice structures and abrade the turbines	1) Abrasion of turbines due to passage of sediment particles. 2) Abrasion of gate and tunnel by high velocity current with heavy sediment concentration. 3) Sedimentation raises the reservoir bed to an elevation higher than the inlet of the power tunnel.
Upstream	4. Ecological effect	1) Sediment deposition in the spawning and breeding zone. 2) Siltation along lake perimeter and growth of aquatic weeds make the food rich lake bottom inaccessible to birds.
	5. Adverse effect on tourism	Advance of delta renders a part of the lake too shallow for boating and anchorage.
	6. Adverse effect on navigation	After draw down of the pool level, sand dunes with considerable height may form in the reach of fluctuating backwater region, bringing serious trouble to navigation (Lu, 1981).
	7. Extension of reservoir sedimentation upstream	The retrogressive deposition raises the flood stage, enlarges the zone of inundation, and enhances the flood risk in the reach upstream of the reservoir. Area of swamp and alkalization enlarged due to rise of the ground water table.

Stream morphology downstream of dams can be dramatically impacted by reduction in the supply of sediment. Clear water in the river channel, downstream of the dam tends to scour the stream bed causing it to coarsen, degrade, and become armored. Coarsening of the bed can make it unsuitable as an ecological habitat and spawning sites for both native and introduced species. Channel degradation can increase both bank height and bank erosion rates，increase scour at downstream bridges, lower water levels at intakes, reduce navigational depth in critical locations, and lower groundwater tables in riparian areas, adversely affecting both wetlands and agricultural areas. Sediment trapping by reservoirs reduces the suspended solids concentration downstream, which may have many beneficial effects. The suspended solids leve1s of many rivers have been dramatically increased due to upstream deforestation and development. Sediment trapping in reservoirs is beneficial to aquatic ecosystems sensitive to e1evated suspended solid levels, including coastal marine ecosystems such as grass beds and coral reefs harmed by sediment discharged from rivers draining disturbed landscapes.

7.2.1.2　Patterns of Reservoir Sedimentation

Patterns of reservoir sedimentation depend on the operational scheme of the dam, hydrologic conditions, sediment grain size, and reservoir geometry. In reservoirs with fluctuating water levels or that are periodically emptied, previously deposited sediments may be extensively eroded by processes such as downcutting by stream flow. Further complexity is added when there are significant sediment inputs from tributaries. Most sediment is transported within reservoirs to points of deposition by three process: (1) transport of coarse material as bed load along the topset delta deposits; (2) transport of fine sediment in turbid density currents; and (3) transport of fine sediment as suspended load (Morris and Fan, 1998).

The longitudinal sediment deposition exhibits five basic types depending on the inflowing sediment characteristics and reservoir operation, as shown in Fig. 7.7.
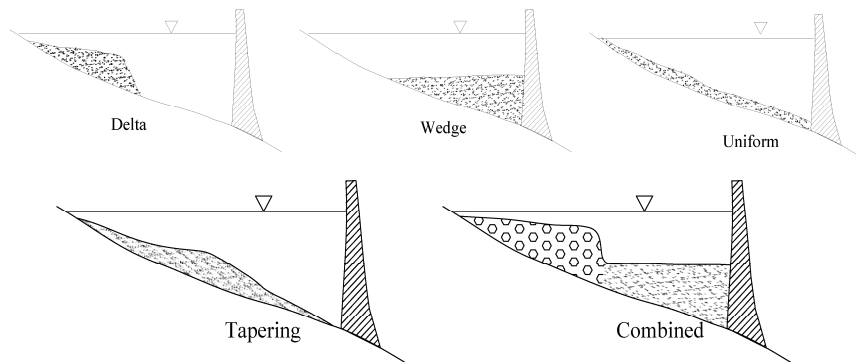
Fig. 7.7　Longitudinal patterns of sediment deposition in a reservoir

Delta—A delta shaped deposit is formed with the coarse fraction of the sediment load, which is rapidly deposited at the upper zone of the reservoir. It may consist of coarse sediment or may also contain a fraction of finer sediment such as silt. Such a deposition pattern occurs if the reservoir remains at high pool level for a long time.

Wedge—A wedge shaped deposit is a typical pattern of fine sediment deposition by turbidity currents. It occurs in small reservoirs with a large inflow of fine sediment and in large reservoirs operated at a low pool level during flood events, which causes most sediment to be carried to the vicinity of the dam. Figure 7.8 shows the profile of the Bajiazui Reservoir on the Puhe River as an example of the wedge shaped deposit.
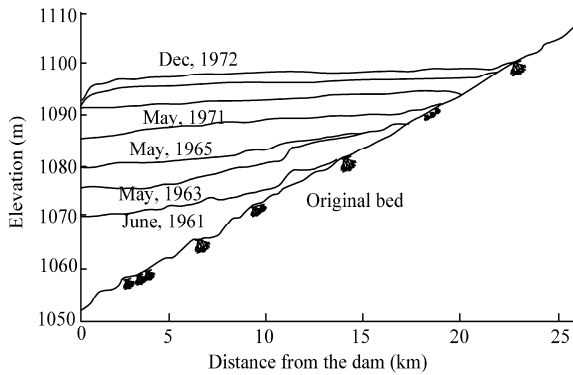
Fig. 7.8   Profile of the Bajiazui Reservoir on the Puhe River showing a wedge shaped deposit (after IRTCES, 1985)

Tapering deposit—A tapering deposit occurs in large reservoirs normally remaining at a high pool level, it is formed due to the progressive deposition of fine sediment from the flowing water moving toward the dam.

Uniform deposit—Uniform deposition occurs in narrow reservoirs with frequent water level fluctuation and a small inflow of fine sediment.

Combined patterns—Fine sediment deposits in the vincinity of the dam and form a wedge and coarse sediment deposits in the upper most part of the reservoir forming a delta. The Sakuma Reservoir in Japan exhibits such a complex depositional pattern, as shown in Fig. 7.9.
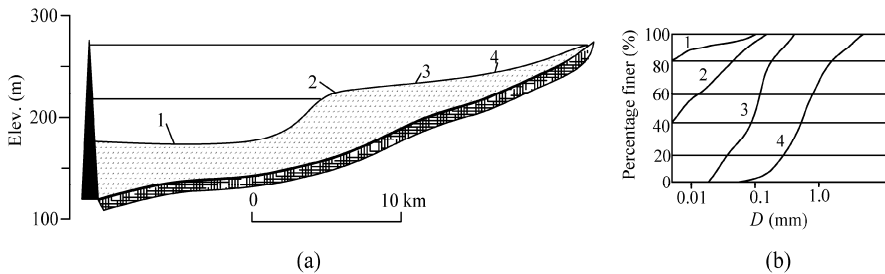
Fig. 7.9   (a) Complex longitudinal profile of the Sakuma Reservoir in Japan (after 24 years of operation); (b) Grain size distributions of deposits at different sites in the reservoir (after Okada Tsuyoshi and Baba Kyohei, 1982)

7.2.2   Sedimentation Management Strategies

Various strategies for reservoir sedimentation control have been studied and applied in reservoir management. Fan and Morris (1992 a and b) summarized the strategies with particular attention to turbidity currents. Garcia studied turbidity currents with poorly sorted sediment and sediment deposition in reservoirs (Garcia, 1994). Sediment bypassing is a method used to manage sediment by preventing it from entering the reservoir. An offstream reservoir can generate benefits in addition to a reduced rate of storage depletion (Morris et al., 2008). Empty flushing involves the opening of bottom outlets to completely empty the reservoir and allow stream flow to scour sediment deposits. The scouring of sediment by flood depends on the permeability, consolidation coefficient and the volume fraction of sand related to silt (Jacobs et al, 2007).

Wang and Hu (2009) summarized the reservoir sedimentation management strategies applied in China. Five strategies have been applied for reservoir sedimentation control: 1) Drawdown flushing or pressure

flushing; 2) empty flushing or free flow flushing; 3) releasing density currents; 4) storing the clear and releasing the turbid; and 5) dredging.

7.2.2.1 Empty Flushing

Fan (1985) has classified flushing into two general categories: (1) empty or free flow flushing, which involves emptying the reservoir to the level of the flushing outlet with riverine flow through the impoundment, and (2) drawdown or pressure flushing, which requires less drawdown but is also less effective. The second method is not commonly used. Empty flushing can also be classified according to whether it occurs during the flood season or the non-flood season. While both strategies have been applied successfully, flood season flushing is generally more effective because it provides larger discharges with more erosive energy, and flood borne sediments may be routed through the impoundment.

Flushing scours a single main channel through reservoir bed while floodplain deposits on either side are unaffected. Profile views of a flushing channel are shown in Fig. 7.10.

(a) (b)
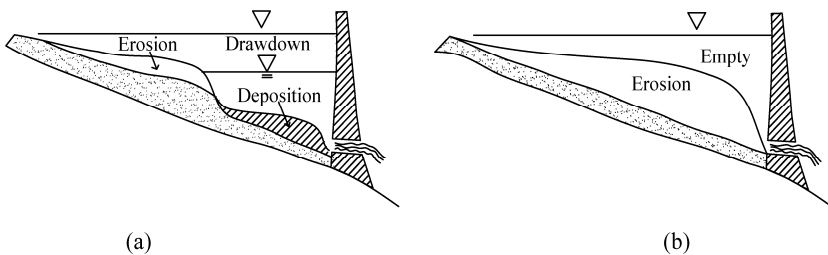
Fig. 7.10 (a) Drawdown flushing causes erosion in the upper part of the reservoir and redeposition near the dam, with pressure flow through the bottom outlets; (b) Empty flushing results in erosion in the whole reservoir, with free flow through bottom outlets

Some irrigation reservoirs with small capacity are emptied before flood season and flushed during the first part of the flood season. They are refilled during the latter part of the flood season. Because of the high sediment concentration that can be released during the flushing period, the downstream irrigation canals must be designed to be able to transport a high sediment concentration. Seasonal emptying is also feasible when water demand is seasonal.

Figure 7.11 shows the Sefid-Rud Reservoir in Iran being emptied for empty flushing. After the reservoir was emptied many fishes were left in the fluid mud layer on the reservoir bed. Local people row boats in the fluid mud and capture the fishes, as shown in Fig. 7.11(b). Figure 7.12 shows the sediment discharge and sediment concentration of the inflow and outflow of the Sefid-Rud Reservoir in Iran during the empty flushing. The sediment concentration and sediment discharge of the outflow was 40 times higher than those of the inflow due to flushing. Empty flushing is very effective for scouring sediment.

The Hengshan Reservoir on the Tangyu River (a tributary of the Yongding River) in Shanxi Province, China applied the empty flushing strategy to control sedimentation and restore the reservoir capacity. The Hengshan Dam is 69 m high with a reservoir capacity of 1.33 million m^3. From 1966 to 1974, 3.19 million m^3 of sediment deposited in the reservoir with a thickness of 27 m near the dam. To restore the capacity of the reservoir the reservoir was emptied to flush sediment in 1974 and 1979. During the empty flushing period from July 28 to September 4 in 1974, the inflowing sediment was 0.13 million t but 1.19 million t of sediment were flushed out of the reservoir (Guo et al., 1985). The reservoir was emptied and flushed again in 1979 from Aug. 9 to September 30, the inflowing sediment was 0.2 million t but 1.55 million t of sediment was flushed out of the reservoir. A mud flow with a maximum concentration of about 1370 kg/m^3

was created and flowed out of the reservoir. Figure 7.13 shows the sediment concentration and discharge of mud flow during the empty flushing. The flow cut a narrow yet deep channel in the reservoir sediment deposit. Guo et al. (1985) analyzed the empty flushing and noted that the channel can be deepened by using either small or large flows, but widening this channel can only be achieved by using large flows. It was found that the flushing effect is maximized if the reservoir is emptied immediately prior to the arrival of a flood because the flood flow exerts erosive force on deposits which have not yet had the time to fully dewater and consolidate. The phrase used to describe this strategy is "Deepen by small flow, widen by flood flow."

(a)

(b)

Fig. 7.11 (a) Sefid-Rud Reservoir in Iran is emptied for empty flushing; (b) Local people row boats in the fluid mud of the emptied reservoir and capture the fishes (after Forood and Ghafouiri, 2007)
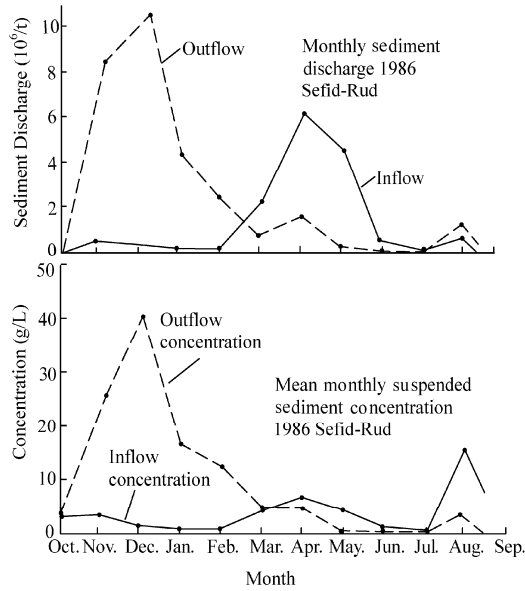
Fig. 7.12 Sediment discharge and sediment concentration of the inflow and outflow of the Sefid-Rud Reservoir in Iran during the empty flushing (after Forood and Ghafouiri, 2007)
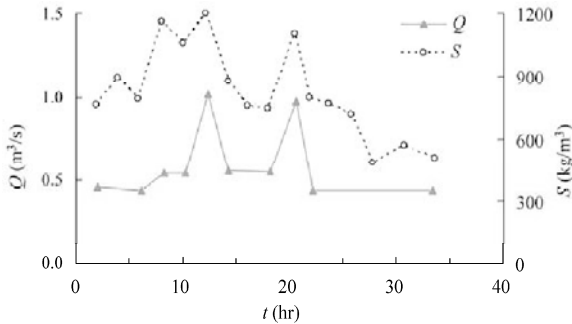
Fig. 7.13 Sediment concentration and discharge of mud flow during the empty flushing from the Hengshan Reservoir in 1979 (Data from Guo et al., 1985)

The Zhuwo Dam is on the Yongding River near Beijing, China, which is 33 m high with a reservoir capacity of 14.75 million m³. The reservoir began to store water in 1961 and lost 5.3 million m³ of reservoir capacity due to sedimentation after 25 years of operation. Most of the sediment deposit was cohesive sediment with a median diameter of 0.004 mm. A physical model experiment was conducted to study the efficiency of empty flushing of cohesive sediment from the reservoir (Wang and Zhang, 1989). Cohesive sediment may be carried downstream if the sediment is scoured from the reservoir. Figure 7.14 shows the critical velocity, U_c, for initial scouring of cohesive sediment from the reservoir as a function of the weight of sediment per unit volume in the deposit, γ_b, which followed the following formula:

$$U_c = 4.6\gamma_b^{\ 4} \tag{7.1}$$

Because the length and depth scale of the model was 1:50 then the velocity scale can be calculated from the Froude Number to be 1:7.07. The scale ratio for the critical velocity for scouring similarity is

then 1:1.63. The measured γ_b in the reservoir varied almost lineally from 0.55 g/cm^3 at the surface of the deposit to about 1.22 g/cm^3 at a depth of 20 m in the deposit. The modeling sediment is the cohesive sediment from the Zhuwo Reservoir and the value of γ_b was controlled, lineally distributed from 0.33 g/cm^3 at the surface of the deposit to 0.75 g/cm^3 at a depth of 40 cm in the model, which meet the requirement of scouring similarity.
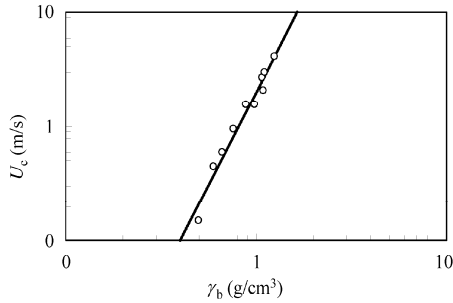
Fig. 7.14 Critical velocity for initial scouring of cohesive sediment from the Zhuwo Reservoir as a function of the weight of sediment per volume in the deposit

Figure 7.15 shows the sediment concentration and discharge of the mud flow stage of empty flushing during the model experiment. During the process a very small inflowing discharge, about 1 m^3/s, flowed to the reservoir and scoured the sediment. The sediment concentration varied in the range of 200 kg/m^3 to 700 kg/m^3 during the mud flow process. After 8 hours the mud flow stopped. Then the inflowing discharge of clear water increased to 12 m^3/s, which was controlled by the Guanting Reservoir. Retrogressive erosion occurred as a consequence of the inflowing discharge. Figure 7.16 shows the sediment concentration during the retrogressive erosion stage of the empty flushing. Because the sediment was very cohesive, the retrogressive erosion lasted only about 40 hours. Almost no more sediment could be scoured except if the inflowing discharge dramatically increase, which was not allowed because of the safety of water resources utilization for Beijing. The retrogressive erosion created many gullies on the reservoir bed, which formed a palm shape channel network. About 0.19 million m^3 of sediment deposit was discharged out of the reservoir during the empty flushing, of which 37% was released from the reservoir in the form of mud flow.
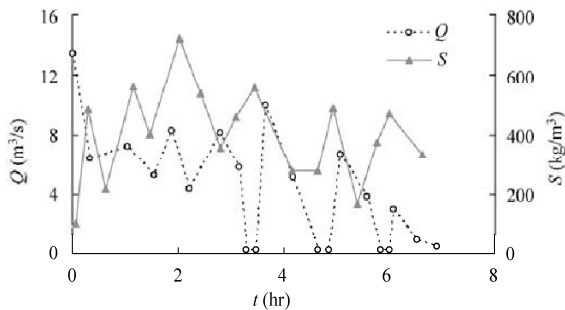
Fig. 7.15 Sediment concentration and discharge of mud flow during empty flushing of the Zhuwo Reservoir

7.2.2.2 Pressure Flushing

Hydraulic flushing involves reservoir draw-down by opening a low level outlet to temporarily establish riverine flow along the impound reach, flushing the eroded sediment through the outlet. Sediment entering

the reservoir during flushing periods is also released. In general a conical scour hole in front of the outlet is formed during the flushing. Sediment from the upper portion of the reservoir is transported towards the dam during draw down, but only material in the scour hole can be flushed out.
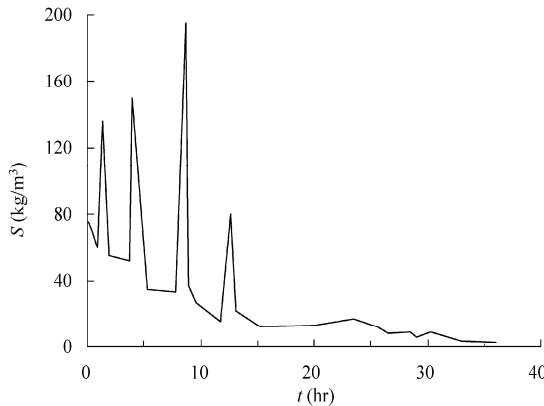
Fig. 7.16   Sediment concentration of mud flow during empty flushing of the Zhuwo Reservoir experiment

Draw-down flushing or pressure flushing was used to flush sandy bed material in the Tarbela Reservoir in Pakistan (Lowe and Fox, 1995). The Tarbela Dam is a 137 m-high embankment dam on the Indus River mainly used for hydropower (3,750 MW installed capacity) and irrigation. Its total capacity was 14.3 billion m^3 at closure in 1974 but it had decreased 17.4 percent due to sedimentation by 1992. The original project was designed for a 50-year economic life with no previsions for the eventual management of the inflowing sediment load of about 208 million tons per year. The inflowing sediment consists of 59% fine sand, 34% of silt, and 7% clay. Approximately 99% of the inflowing load is trapped and accumulates primarily in the form of a delta deposit which is advancing toward the dam (Fig. 7.17). Delta top-set beds have a slope of about s = 0.0006 to 0.0008. Most sediments are deposited on the top-set bed as the reservoir fills and levels rise during the wet season, but when the reservoir is draw down for irrigation deliveries, the river reworks and transports these deposits downstream, extending the delta toward the dam. Most sediment is transported to the face of the delta at the onset of the wet season when the pool level is still low but discharge increases from 1,500 to 4,500 m^3/s.
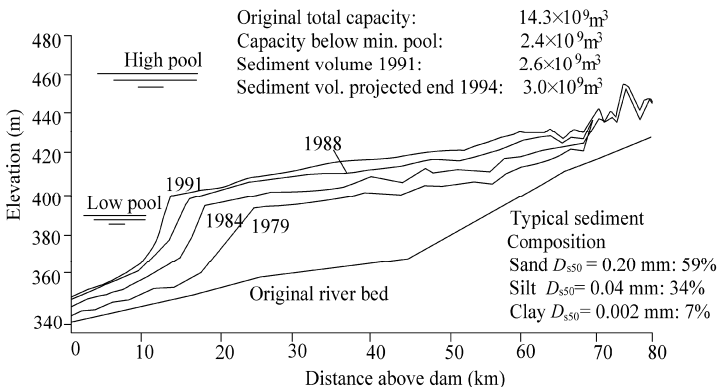
Fig. 7.17   Advancement of delta deposits toward Tarbela Dam, Indus River, Pakistan (after Lowe and Fox, 1995)

7.2.2.3   Storing the Clear and Releasing the Turbid

Sediment transportation in many Chinese rivers occurs mainly in 2–4 months of the flood season, that is, 80%–90% of the annual sediment load is transported with 50%–60% of the annual runoff. The Three Gorges Project on the Yangtze River is planned for flood control, power generation, and inland navigation. For these purposes, it is important to maintain adequate storage in the reservoir. The main strategy to control sedimentation is to draw down the pool level from 175 m to 145 m in the flood season from June to September when the sediment concentration is high and allow the turbid water to wash downstream through the reservoir. The reservoir starts to store water in October when the inflowing water becomes clear (i.e. has a lower sediment concentration). Figure 7.18 shows the typical variation process of sediment concentration at Yichang—the dam site—and the operation scheme of pool level for sedimentation control. By storing the clear water and releasing the turbid water, less sediment deposits in the reservoir while the reservoir is still able to store enough water for power generation in the low flow season. The details of the sedimentation management in the Three Gorges Reservoir are given in the Section 7.4.
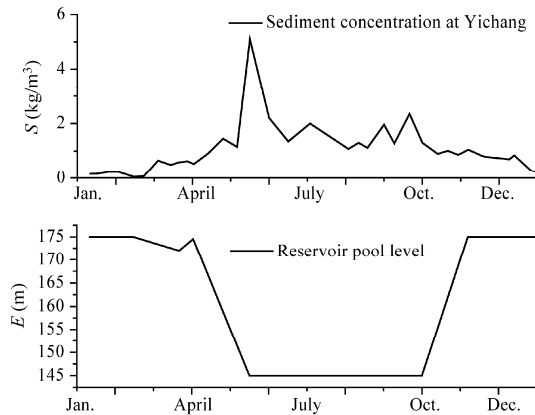
Fig. 7.18   Typical variation process of sediment concentration at the dam site of the Three Gorges Project and the operation scheme of pool level for sedimentation control

The strategy of storing clear water and releasing turbid water has also been successfully used in the management of sedimentation behind the Sanmenxia Dam on the Yellow River after several failures of other sedimentation management strategies. The Sanmenxia Dam, 105-m high and 739-m long, was the first large dam on the Yellow River. The crest elevation of the dam is 353 m and the designed reservoir capacity is 35.4 billion m^3 with a normal pool level of 350 m. The operation scheme of the Sanmenxia Reservoir has been substantially changed to achieve a balance between sediment inflow and outflow in the following three reservoir operation modes: (i) storage from September 1960 to March 1962, the reservoir was operated at a high storage level the whole year round; (ii) detaining flood water and sluicing sediment from March 1962 to October 1973, the reservoir was operated at a low storage level throughout the year, detaining floods only during flood seasons and sluicing sediment with the largest possible discharges; and (iii) storing the clear water and releasing the turbid water from November 1973 to the present, the reservoir has been operated at a high level (315–320 m) to store relatively clear water during non-flood seasons (November–June) and at a low level (302–305 m) to release high sediment concentrations during flood seasons (July–October). Serious sediment accumulation occurred during the first operation mode period. The operation pool level had to be changed to 303–318 m in 1962–1973, allowing flood water scoured sediment to flow through the reservoir. Sediment was sluiced out of the reservoir but at the

cost of power generation. The strategy of storing the clear and releasing the turbid was finally applied with the pool level very low during high sediment concentration period and high pool level during low concentration period for power generation.

The sedimentation has been controlled and the accumulated sediment deposition volume in two parts of the reservoir, comprising Tongguan to the dam and the lower Weihe River, remained unchanged since the operation mode changed to storing the clear water and releasing the turbid water in 1973. Only a slight increase of accumulated sediment occurred in the upper part of the reservoir extending from Longmen to Tongguan. The reservoir capacity has remained almost unchanged since 1973.

7.2.2.4 Dredging

Dredging has been used for a long time for sedimentation management in small reservoirs. Different dredging methods are applied in reservoir management, including mechanical dredging and dumping outside of the reservoir and agitating sediment with jets so that that sediment can be transported downstream of the reservoir by currents. Various dredgers have been used: dredge boat; agitating dredger; dipper dredger; hauling scraper; excavator and bulldozer; and trailer dredger. In general dredging is more expensive than other strategies of sedimentation control in reservoirs. Nevertheless, jets in combination with turbidity currents or flushing are more economically feasible and have been applied in large reservoirs.

The sediment in the Sanmenxia Reservoir was scoured by a jet or slurry pump, and it remains in suspension in the reservoir. Because the suspension has a slightly higher density than the water it flows to the dam along the reservoir bed in the form of a density current. The density current is released from the bottom outlet of the reservoir. Jet dredging was conducted in a reach near Tongguan from 1996 to 2003 during the flood season. Figure 7.19 shows the sediment amount scoured from the reservoir bed by jets. The sediment is composed mainly of silt and fine sand with 20% finer than 0.025 mm and about 40% finer than 0.05 mm. It is reported that the sediment finer than 0.05 mm may be transported by flow out of the reservoir but coarser sediment may settle again in the reservoir (Jiao et al., 2008).
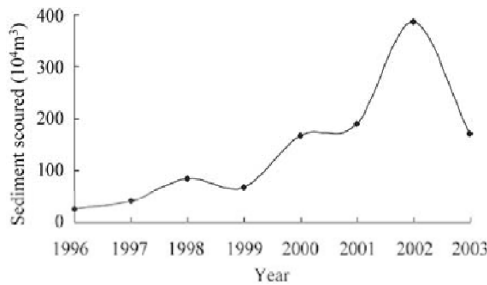
Fig. 7.19   Sediment amount scoured from the wake area of Sanmenxia Reservoir by jet dredging

Jet dredging was also used to create artificial turbidity currents to release sediment from the Xiaolangdi Reservoir. Since the Xiaolangdi Reservoir began to store water in 1999, about 1.5 billion m³ of fine sediment had deposited in a 40 km reach upstream from the dam in the reservoir by April 2005. The sediment is fine with a median diameter of about 0.01 mm. The reservoir sediment was scoured by jet, which resulted in fine sediment suspension in the reservoir. Because the suspension has a slightly higher density than the surrounding water, it flows to the dam along the reservoir bed in the form of a turbidity current. Most of the fine sediment is released from the bottom outlet of the reservoir with turbidity currents.

7.2.2.5 Density (Turbidity) Currents

A density current is the relative motion that takes place in a reservoir between two fluid layers that have

slightly different densities. At the end of the 19th Century, Swiss scientists noticed that after the River Rhone and Rhone River flowed into Lake Geneva and Lake Constance, respectively, the muddy and cold river water did not mix with the clear and warm lake water; instead, it dove to the bottom of the lake and continued to move as an entity. The same phenomenon was observed in Lake mead behind Hoover Dam on the Colorado River during the flood season when muddy water formed a density current and flowed the entire length of the reservoir. A density current may pass through the reservoir, without ever completely mixing with the epilimnial or hypolimnial waters, and may flow out of the reservoir if the bottom outlets are open.

Density current in reservoirs is caused by sediment, which is also called turbidity current. The turbidity currents in reservoirs generally involve only slight differences in the sediment concentrations of the upper and lower layers. Since the density difference is small, the reservoir water creates a large buoyancy effect within the inflowing liquid, so that the effective gravity of the flowing liquid is greatly reduced. Usually g' is defined as effective gravity given by:

$$g' = g\frac{\Delta\rho}{\rho} \tag{7.2}$$

in which g is the gravitational acceleration, $\Delta\rho$ is the density difference between the upper and lower liquids, and ρ is the density of the reservoir water. Many formulas describing open-channel flow apply also to density currents once g is replaced by g'. For example, the flow pattern in an open channel depends greatly on the Froude number of the flow; in a density current, the Froude number remains the key parameter but its form is modified as follows (Chien et al., 1998):

$$Fr' = \frac{U_r}{\sqrt{g'h'}} \tag{7.3}$$

in which U_r is the relative velocity between the two liquid layers and h' is the thickness of the density current.

Density currents usually flow near the reservoir bottom. Figure 7.20 is a schematic diagram of the transition from an open-channel flow with a high concentration of fine sediment to a well-defined density flow in a reservoir. After the flow enters the backwater region of the reservoir at point A, the velocity at the water surface gradually tends toward zero because of the increasing depth and the backwater effect of the dam. The reservoir water mixes with the inflow. Beyond point B, a distinct interface forms between lighter water near the surface and the heavier water below. From then on, two kinds of flows with different densities take place. Under the action of effective gravity, a density flow forms between point B and C. During the movement, the density flow drags some of the reservoir water above the interface along with it; other parts of the reservoir water in the upper region would then flow backwards, to maintain a water
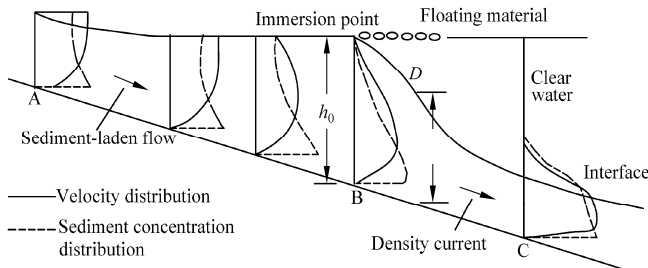
Fig. 7.20 Velocity and sediment concentration profiles varying along the reservoir during the transition from an open-channel flow to a density current (after Chien et al., 1998)

volume balance, and this flow pushes any floating material towards point B. The presence of such material is the most reliable signal that a density flow has formed. The concentration profiles change during the process due to the mixing of clear water at the interface and deposition of a part of the coarse sediment.

Data from both flume experiments and field observations show that the critical condition for the formation of a density current is (Fan, 1959):

$$\frac{q^2}{\frac{\Delta\rho}{\rho'}gh_0^3} = 0.6 \tag{7.4}$$

in which q is the discharge per unit width and h_0 is the depth at the immersion point. From the equation, if the water level upstream of the dam remains constant, an increase of the inflow discharge would cause the immersion point to move downstream; and an increase in the density difference between the inflow and the reservoir water would cause the point to move upstream.

The Xiaolangdi Reservoir is located 125 km downstream of the Sanmenxia Dam and about 860 km upstream of the river mouth. The reservoir is the most downstream gorge-type reservoir on the Yellow River. The multi-purpose reservoir is mainly for flood control, power generation and sediment retention for reducing siltation in the lower Yellow River. The total capacity of the reservoir is 12.65 billion m^3, of which more than 7.55 billion m^3 will be used for trapping sediment. The reservoir began to impound in October 1999. While the reservoir operates it traps coarse sediment and discharges fine sediment to the lower reaches. In the first 8 years, coarse sediment was trapped as clear water and a portion of fine sediment was released to the lower reaches mainly in the form of turbidity currents. Because a fraction of coarse sediment is trapped by the reservoir, the rate of sedimentation of the lower Yellow River channel is greatly reduced. Sediment finer than 0.02 mm was released to the lower reaches but it is mostly wash load and does not cause siltation of the lower reaches.

Since impoundment turbidity currents occurred every year, especially during hyper-concentrated floods, the turbidity currents flowed to the dam and were discharged out of the reservoir when the bottom outlets were open. Figure 7.21 shows the elevation of the interface between the turbidity currents and the upper clear water layer for five turbidity currents in 2001 (Hou and Jiao, 2003). The interface remained in a narrow range between 188 and 194 m in most parts of the reservoir, although the discharge of the turbidity currents varied in the range of 200 m^3/s–2800 m^3/s, the sediment concentration varied between 13 kg/m^3 and 530 kg/m^3, and the average velocity varied between 0.2 m/s to 1.2 m/s. The Froude number at the plunging point was measured at 0.5–0.61, which approximates the situation represented by Eq. (7.4) (Hou and Jiao, 2003).
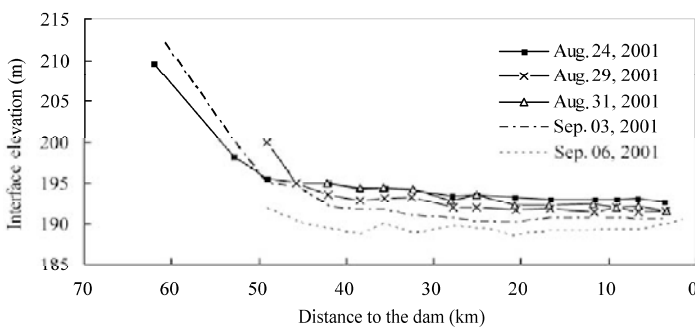
Fig. 7.21 Elevation of the interface between the turbidity currents and the upper clear water layer (data are from Hou and Jiao, 2003)

Maintaining a density flow needs a continuous supply of inflow sediment suspension and a force to overcome any resistance it encounters. If the inflow ceases to supply dense fluid so that it no longer forms a density current at the immersion point, the already formed density current downstream would soon stop moving. Since the energy to maintain the flow comes from the density difference and the slope of the reservoir bed, so a minimum density difference is clearly required. This density difference is much larger than that required to form a density current. According to field data from Shaver Lake in the U.S. (Bell, 1947), a density current will form if the sediment concentration is higher than 1.28 kg/m^3. However, the data from the Guanting Reservoir on the Yongding River in Chine indicates that only if the sediment concentration in a density current is more than 20 kg/m^3, can the current continue to flow and finally reach the dam (Chien et al., 1998).

A continuous turbidity current flowing to the dam is critical for sediment release, which depends on the inflowing discharge, sediment concentration and the portion of sediment particles finer than 0.01mm. Figure 7.22 shows the sediment concentration by weight, S, and discharge, Q, of turbidity currents in 2001–2004 (data from Wu et al., 2008). In the figure, the filled circles represent turbidity currents reaching the dam, in which the portion of sediment particles finer than 0.01 mm is between 25% and 75%; the black pyramids are turbidity currents moving to the dam but the portion of sediment particles finer than 0.01 mm is higher than 75%; the open triangles are turbidity currents not reaching the dam, although some of them consists of 90% fine sediment. The curve in the figure is given by:

$$SQ = 100,000 \,(\text{kg/s}) \tag{7.5}$$

For high sediment concentration and discharge, or the points above the curve, the turbidity currents flowed through the whole reservoir and arrived at the dam. For the points below the curve the turbidity currents stopped in the reservoir, failing to reach the dam.
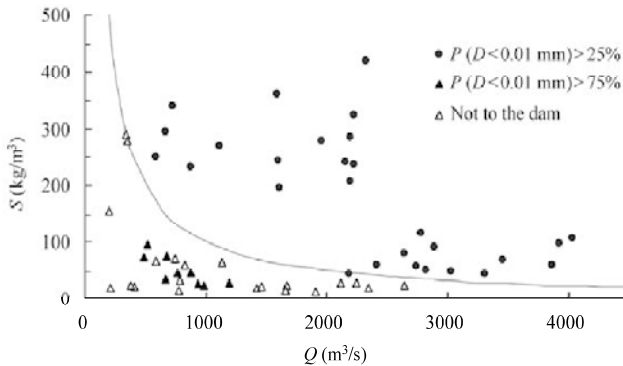
Fig. 7.22 Sediment concentration, S, and discharge, Q, of turbidity currents reaching and not reaching the dam occurred in 2001–2004 (data from Wu et al., 2008)

In general, the sediment releasing efficiency of turbidity currents is about 20%. Nevertheless, the turbidity currents in the Xiaolangdi Reservoir had low sediment releasing efficiency because the reservoir bed had not silted up to the low sill of the bottom outlets. Arriving at the dam the turbidity currents filled the reservoir and formed a muddy water reservoir. Only after the surface of the muddy water reservoir rose to the elevation of the bottom outlets, were the turbidity currents released from the reservoir. The average sediment releasing efficiency, or the ratio of the released sediment to the inflowing sediment load, was only 6% in the period from 2000 to 2004 (Hou and Jiao, 2003). In 2006, turbidity currents occurred again in the Xiaolangdi Reservoir by using Sanmenxia Reservoir to create high sediment concentration

flow (MWR, 2007). About 8.4 million tons of fine sediment, or 36% of inflowing sediment, was released during the turbidity currents because the sedimentation reservoir bed approached to the bottom outlets.

7.2.2.6 Sediment Releasing Efficiency

The sediment releasing efficiency, E, can be defined in two ways:

$$E = \frac{\text{volume} \sim \text{of} \sim \text{released} \sim se\dim ent}{\text{volume} \sim \text{of} \sim \text{income} \sim se\dim ent} \tag{7.6}$$

$$E = \frac{\text{time} \sim \text{needed} \sim \text{for} \sim se\dim entation}{\text{time} \sim \text{to} \sim \text{flush} \sim \text{the} \sim se\dim ent} \tag{7.7}$$

For the reservoir sedimentation management with pressure flushing, density current, and storing the clear and releasing the turbid the sediment releasing efficiency is calculated with Eq. (7.6). However, for empty flushing the sediment releasing efficiency is calculated by using Eq. (7.7). The sediment releasing efficiency is: 30%–100% for storing the clear water and releasing the turbid water, 6%–36% for turbidity current, varies in a range of several percent to more than 100% for pressure flushing. For empty flushing the sediment releasing efficiency may be as high as 2400%–5500%.

For the Hengshan Reservoir the efficiency was 24.7 during the empty flushing in 1974 and was 23.9 during the empty flushing in 1979. For the Zhuwo Reservoir, the efficiency was 55 during the empty flushing experiment. Empty flushing has the highest sediment releasing efficiency, but the flushing may cause high ecological stress on the downstream reaches. Suspended sediment adsorbs pollutants from flowing water in rivers and deposits in the reservoirs. A study showed that the concentration of heavy metals (Cr, Cd, Hg, Cu, Fe, Zn, Pb and As) were highest in the sediment and lowest in the water. Benthic invertebrates had higher concentrations of heavy metals in their tissues due to their proximity to contaminated sediments and fish had lower concentrations of heavy metals (Yi et al., 2008). Empty flushing might release the pollutants from the sediment and increase sharply the concentration of pollutants in water. The ecological system downstream of the Zhuwo Reservoir consists of numerous species of aquatic plants, benthic invertebrates and fish. Empty flushing can seriously impair the ecology. The Beijing government decided to dredge the Zhuwo Reservoir rather than implement an empty flushing technique. This had a higher economic cost but a much lower ecological cost.

In conclusion, density current has low sediment releasing efficiency; empty flushing may achieve very high sediment releasing efficiency but may cause a great disturbance to the stream ecology; dredging is used only as an auxiliary method for reservoir sedimentation management; the strategy of storing the clear water and releasing the turbid water is the best sedimentation management strategy because it may achieve relatively high releasing efficiency and only slightly affect the stream ecology.

7.3 Dam Failure and Dam Removal

7.3.1 Dam Failure

7.3.1.1 Dam Failure Events

Throughout history, dam incidents and dam failures have inflicted tremendous loss of lives, as well as great property damage. Dam failure has occurred to dams built according to accepted engineering standards of design and construction at the time and also to dams built without application of engineering principles. Dam failure may be caused by extreme events due to intense rainfall from thunderstorms and from extreme weather such as hurricanes, massive landslides, and landslide induced waves in the river, volcanic eruptions, and fires which could damage the outlet control structure and make the operation of the

spillways difficult. Regardless of the types of dam construction and direct causes, when a dam fails, huge quantities of water rush downstream with great destructive force.

In recent years the failure rate of dams has remained significant while the resulting costs have escalated. This is due largely to the increasing population of people settling and develop lands downstream from dams. In a general sense, the seriousness of the threat of dam failure is based on many variables: flash flooding, inadequate size of spillways, mechanical failure of valves and other equipment, rodent actions in earthen dams, freezing and thawing cycles, and earthquakes. Old age and neglect can intensify vulnerability to these same influences.

Table 7.11 The number of dam failure events in several countries and the failure rate, which is defined as the ratio of the number of dam failures to the number of dams and period of statistics. China, Spain, and the United States have a high failure rate.

Table 7.11 Number of dam failures and the failure rate in various countries

Country	Source	Number of dam failures	Number of dams	Time of statistics (years)	Rate of dam failure (1/dam·year)
U.S.	Gruner (1963; 1967)	33	1,764	40	5×10^{-4}
U.S.	Post-1940 dams	12	3,100	14	3×10^{-4}
U.S.	USCOLD (1975)	74	4,914	23	7×10^{-4}
U.S.	U.S. Bureau of Reclamation	1	4,500	1	2×10^{-4}
U.S.	Mark and Stuart-Alexander, 1977	125	7,500	40	4×10^{-4}
World	Middlebrooks, 1953	9	7,833	6	2×10^{-4}
Japan	Takase (1967)	1,046			4×10^{-5}
Spain	Gruner (1967)	150	1,620	145	6×10^{-4}
China	Nanking Institute of Water Resources and Hydro-power	3,462	85,120	47	8.65×10^{-4}
China	IWHR	3,481	85,153	50	8.18×10^{-4}

Table 7.12 lists numerous dam failure events in several countries. These events occurred mostly in the 1960s and caused casualties of 3 to 3,000 people and economic losses from 1 to 100 million US dollars. Table 7.13 lists the major dam failure events which have occurred in China. The dam failure events caused a total death toll of more than 30,000, damaged more than five million houses and more than one million ha of farmland (He et al., 2008).

Table 7.12 Typical dam failure events and loss of lives and property from countries around the world (Lou, 1981; He et al., 2008)

Dam	Country	Time of failure	Casualties	Economic loss (million dollars)
Puentes	Spain	1802-04-30	600	1.0
South Fork	U.S.	1889-05-31	2,200	100.0
Saint Francis	U.S.	1928-03-13	450	1.5
Veg de Tera	Spain	1959-01-10	144	
Malpasset	France	1959-12	421 (deaths)	68.0
Oros	Brazil	1960-03-25	50	
Babii Yar	USSR	1961-03	145	4.0
Hyokiri	North Korea	1961-07	250	
Quebrada La Chapa	Columbia	1963-04	250	

(Continued)

Dam	Country	Time of failure	Casualties	Economic loss (million dollars)
Vajont	Italy	1963-10-9	3,000	
Baldwin Hills	U.S.	1963-12-14	3	50.0
Mayfield	U.S.	1965		2.5
Vratsa	Bulgaria	1966-05-01	600	
Nanak Sagar	India	1967-09-08	100	
Sempor	Indonisia	1967-12-01	200	
Pardo	Agentina	1970		20.0
Buffalo Creek	U.S.	1974-02-26	118	65.0
Teton	U.S.	1976-06-05	6	70.0
Machhu II	India	1979-08-1	1,800 (deaths)	

Table 7.13 Major dam failure events in China

Dam/Province	Time of dam failure (Month-day-year)	Casualties (death toll)	Loss of properties	Data source
Lomngtun/Liaoning	07-21-1959	35,428 (707)	25,942 houses, 14,210 ha of farmland	Huang (1998)
Tiefosi/Henan	05-18-1960	1,662 (1,092)	7,102 houses	Huang (1998)
Liujiatai/Hebei	08-08-1963	(948)	67,721 houses, 1,587 ha of farmland	MWRC (1981)
Hengjiang/Guangdong	09-15-1970	(779)	66,600 ha of farmland	Huang (1998)
Lijiazui/Gansu	04-27-1973	(580)	1,133 ha farmland, 1,000 ha farmland	Huang (1998)
Shijiagou/Gansu	08-24-1973	146 (81)	298 houses, 40 ha of farmland	Huang (1998)
Banqiao and Shimantan/Henan	08-08-1975	10.155 million (26,000)	5.24 million houses, 1.13 million ha of farmland	Song (2000)
Gouhou/Qinghai	08-27-1993	(288)	18.5 million U.S. dollars	Huang (1998)

7.3.1.2 Periodicity

Figure 7.23 shows the number of dam failure events in the period from 1954 to 2003. There are two peaks of dam failure around 1960 and 1973. It seems that there are periodicities in the number of dam failure events. Treating the series of dam failure events in the same way as turbulent fluctuations and using the fast Fourier transformation a spectral density of dam failure events is calculated. Figure 7.24 presents the distributions of the spectral density of dam failure events. The distribution of spectral density has three peaks at frequencies of 0.04, 0.08, and 0.16 per year, which means periods of dam failure of 25 years, 12.5 years, and 6 years.

It seems that the periodicity of dam failure events is similar to the periodicity of solar activities. Figure 7.25 shows the distributions of the number of sunspots (maculas) and the number of dam failure events in the period from 1954 to 2005. The distributions exhibit similar periodicities with a phase difference of about $1/3\pi$. Peaks of dam failure events occur in the receding period of number of maculas. The dam failure events lag about 4 years behind the solar activity. Thus, it could be a factor causing dam failures.
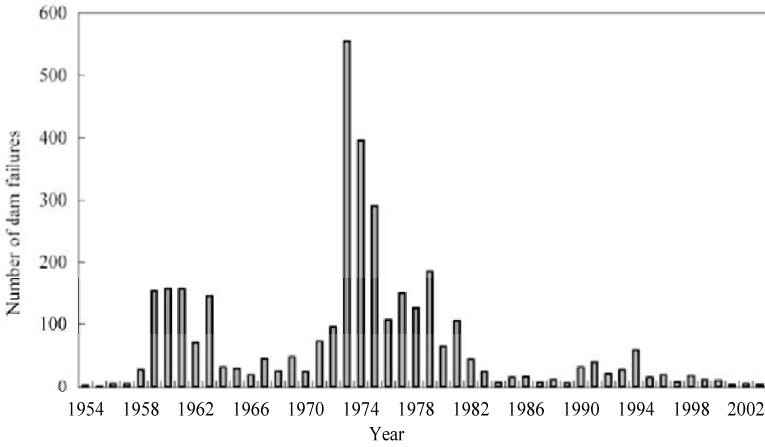
Fig. 7.23   Number of dam failures in the period from 1954 to 2003 in China (dams in Taiwan are not included)
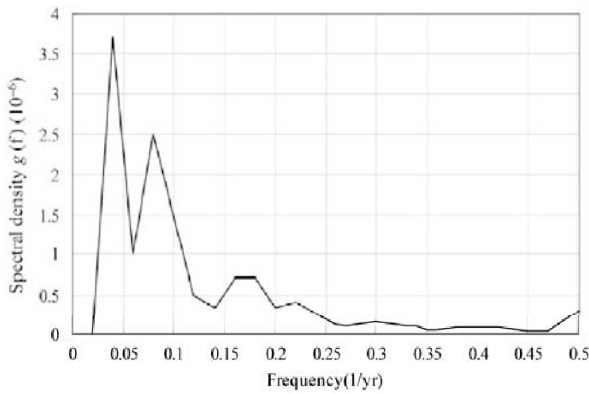
Fig. 7.24   Distribution of spectral density of dam failure events
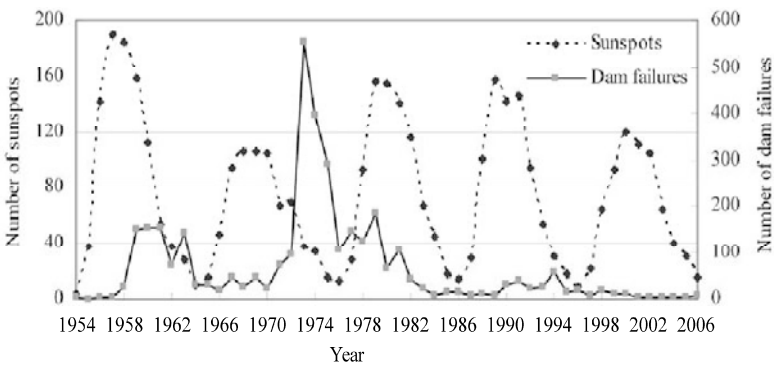
Fig. 7.25   Distributions of the number of the sunspots and the number of dam failure events in the period from 1954 to 2005

7.3.1.3 Infant Life

Dam failures occur at various ages. The dam failure events are grouped according to the age of failed dams into 0–1, 1–5, 6–10, 11–20, 21–30, 31–40, 41–50, 51–60, 61–70, 71–80, 81–90, 91–100, 100–200, and >200 years. Figure 7.26 shows the percentages of different age groups of failures of large dams (higher than 15 m) in China and throughout the world. The data on dam failures in China were collected in the period 1954–2003, and the data on other countries are from 50 countries including the U.S., UK, Australia, and India, including 900 dam failure events. About 60% of dam failures in China occurred within one year, in other words, the dams failed during the first flood or in the first time to impound water. A great many of these dams were constructed during the "Great leap" period in 1957–1962, a particular period in Chinese history of paying attention only to quantity but not quality. In the figure, the data on the world dam failures are collected from selected countries.
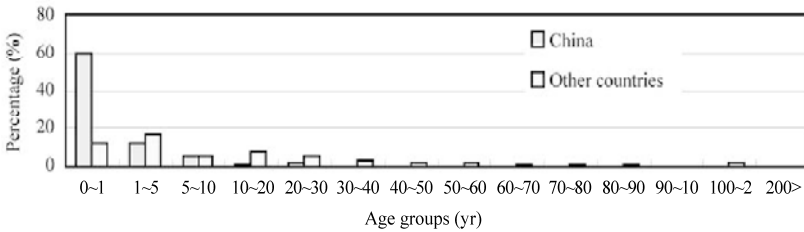
Fig. 7.26 Percentages of dam failures for different age groups in China and other countries

Similarly, Fig. 7.27 shows the percentage of different age groups of dam failures in Russia in comparison with the failures of world dams (He et al., 2008). The figures show that the dam failures mostly occur for the dams younger than 10 years. The dam failure probability reduces rapidly following with operation time.
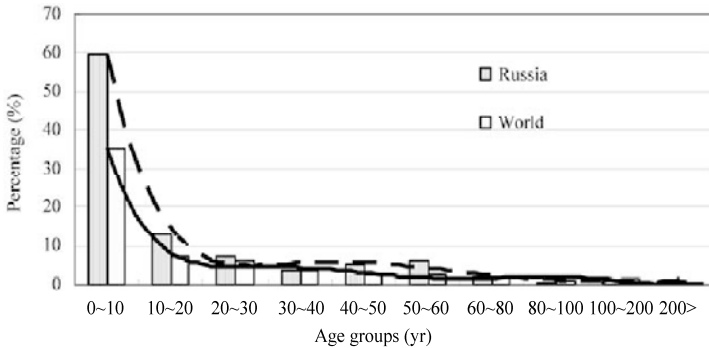
Fig. 7.27 Percentage of different age groups of dam failures in Russia in comparison with the failures of world dams

Many dam failures occur in arid and semi-arid areas. Figure 7.28 shows the spatial distribution of the dam failure rate in China, which was based on statistics of dam failure events in the provinces, in which the dam failure rate in each province is shown (He et al., 2008). The number in the figure is the failure rate $\times 10^4$. The dam failure rate is zero in Tibet, because there were no dams in the area. High dam failure rates occur in the north-west China, where the annual precipitation is low and rainfall intensity in summer is high. The figure shows a division line between provinces having a high dam failure rate ($>15 \times 10^4$) and a low dam failure rate ($<15 \times 10^4$), and also a contour of 400 mm precipitation. The division line and the

400 mm precipitation contour are very close, which illustrates that the distribution of dam failure events is closely related to the climatic zoning.

Fig. 7.28 Spatial distribution of the dam failure rate in units in China based on statistics of dam failure events in the provinces

7.3.1.4 Risk Analysis

The term risk is understood in different ways by different people. It is understood in the scientific community as the product of a hazard and its consequences (Kron, 2005). The authors of this book define risk of dam failure as the product of the probability and hazard of a dam failure. Per discussion in the previous section, dam failure has caused disasters, e.g., loss of human lives and damage of property. The risk of dam failure is given by:

$$\text{Risk or possibility of serious disasters} = \text{hazard} \times \text{probability of dam failure} \qquad (7.8)$$

In which hazard is defined as the number of people and property within a downstream area, which would be endangered in the event of dam failure; and the risk of dam failure is the probability of dam failure under various conditions. The most significant piece of dam safety is hazard rating of dams. Studies on the probability of dam failures are performed for estimation of dam safety. Event trees and other techniques are increasingly being used to determine the probability of failure of a particular component of a dam for a specific loading condition (e.g., earthquake, flood or, normal operational failure).

The Congress of the United States of America passed the Public Law 92-367—The National Dam Inspection Act in 1972. The program began with the preparation of an inventory showing all the dams in the United States. For instance, the Texas Natural Resource Conservation Commission (TNRCC) contracted the U.S. Army Corps of Engineers to accomplish the Texas inventory. The inventory lists contain a great amount of information on each of the over 7,212 dams in Texas (Hill et al., 2003). Dams are rated in three hazard levels: high hazard, significant hazard, and low hazard. The hazard rating has nothing to do with whether the dam is about to collapse immediately or will last forever. It does <u>not</u> relate to the condition or structure of the dam. Basically, it has to do with whether there are people living downstream in the floodplain area who would be endangered in the event of dam failure. Every dam is rated in this manner in the inventory. The following explains what the hazard classification means:

High Hazard—Dam failure would probably result in loss of life and major damage to property.

Significant Hazard—Dam failure could possibly cause some loss of life and property damage.

Low Hazard—Dam failure would be unlikely to cause loss of life or property damage.

A dam may be rated as high hazard but have low risk of failure. For instance, the Horsetooth Reservoir Dams in Colorado are rated as high hazard dams. The use of the term "high hazard" means that should the dam fail even though this possibility is remote, the failure could cause loss of life to downstream residents. On the positive side, these dams have a satisfactory rating when it comes to a structural assessment. Satisfactory is the highest of the three structural assessment ratings. The state of repair assessment has four ratings: excellent, good, poor, and unacceptable. The Horsetooth Reservoir Dams are rated in the good category (http://fcgov.com/oem/dam-failure.php). The excellent rating is only given to those dams which are maintained in essentially new or original condition.

Fell et al. (2000) summarized the methods for the estimation of dam failures for use in quantitative risk assessment. They recognize the following two broad categories of methods:

Historic Performance Methods—These methods use the historic performance of dams similar to the dam being analyzed to assess a historic failure frequency, and assume that the future performance of such dams will be similar. These methods do not directly account for the reservoir loading, nor do they allow for the detailed characteristics of the dam or for the particular intervention. Generally speaking, these methods are only applicable for initial or portfolio risk assessments, and for checking more detailed event tree methods, and should not be used alone for detailed assessments.

Event Tree Method—An event tree is a visual representation of all the events which can occur in a system. As the number of events increases, the picture fans out like the branches of a tree. **Event tree analysis** provides an inductive approach to reliability assessment as event trees are constructed using forward logic. Fault trees use a deductive approach as they are constructed by defining events and then use backward logic to define causes. Event tree analysis and fault tree analysis are, however, closely linked. Fault trees are often used to quantify system events that are part of event tree sequences (www.isograph-software.com, 2007).

Event trees can be used to analyze systems in which all components are continuously operating, or for systems in which some or all of the components are in standby mode—those that involve sequential operational logic and switching. The starting point (referred to as the initiating event) disrupts normal system operation. The event tree displays the sequences of events involving success and/or failure of the system components. A simple example of a dam failure event is shown in Fig. 7.29.
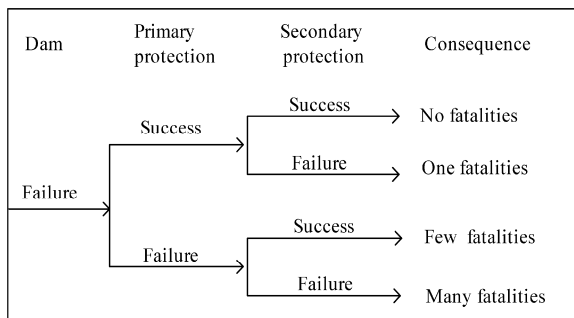
Fig. 7.29   An example of event tree describing the consequences of dam failure

The goal of an event tree is to determine the probability of an event based on the outcomes of each event in the chronological sequence of events leading up to it. By analyzing all possible outcomes, one can determine the percentage of outcomes which lead to the desired result. Event tree methods have the

advantage that the mechanics of the failure, from initiation to breach can be modeled; the details of the dam and its foundation and the ability to intervene to prevent breaching. However, sometimes there is little objective basis for estimation of the conditional probabilities within the event tree, and, therefore, it may be necessary to relate back to historic performance data as a "credibility check" on the answers.

7.3.2   Dam Removal

Dams have some negative impacts for while they provide power, water supply, navigation, and flood control capacity, they also obstruct river flows, alter nutrient cycles, block fish migration, and disrupt temperature regimes and dissolved oxygen concentrations favorable to aquatic life. Prime habitat is commonly lost, and exotic fish species are introduced. Dams also undermine the rights and livelihoods of affected communities. Increased international recognition of the high environmental and social costs of dams, along with numerous river restoration successes, are inspiring dam removal campaigns worldwide.

Numerous dams are now slated or proposed for removal. Many have simply outlived their purpose or sit abandoned, posing a danger to public safety. Other dams continue to operate, though with significant environmental and social consequences. Over a dam's lifespan, costs borne by damaged ecosystems and communities may outweigh other project benefits. With dam removal already outpacing dam construction in the U.S., decommissioning has significant implications for global river management.

7.3.2.1   Dam Removal in the U.S.

The American Society of Civil Engineers published the Guidelines for Retirement of Dams and Hydroelectric Facilities in 1997 (TCGRD, 1997). About 500 dams have been removed in the U.S., and most of them are less than 12-m high (Melching, 2006). The dam removal campaign is accelerating. Only 138 dams were removed before 1990; 177 dams were removed in the period from 1990 to 1999; and 185 dams have been removed in the period from 2000 to 2006. The dam removal campaign focuses on the removal of dams that do not make sense. In other words, these dams no longer serve their intended purpose or the dam's costs outweigh its benefits. Dam removal also involves those in a state of disrepair with no one to claiming ownership. Most of these dams were built decades ago and many have deteriorated due to age, erosion, damage, and for poor design.

Reasons for dam removal are: 1) ageing; 2) ecological restoration; 3) too expensive to repair and operate; and 4) nobody claims the ownership. In the U.S. there are more than 75,000 dams more than 2 m high, which obstruct 950,000 km of waterways. Firstly, safety is one of the reasons for dam decommission activities. About 1,800 dams in the U.S. are officially deemed unsafe. By 2020, 85% of all government owned US dams will be at least 50 years old, the typical design lifespan. Supporters of dam removal are calling attention to a serious lack of funding for dam safety programs.

Secondly, dam removal is an emerging option in relicensing proceedings, in which private hydropower dam owners seek to renew 30- to 50-year operation agreements with the Federal Energy Regulatory Commission (FERC). More than 500 FERC licenses will expire in the next decade. The dam relicensing process is forcing dam owners, government decision makers, river advocates, and affected communities to re-evaluate the costs and benefits of dams, especially in light of mandates to protect endangered species, recognize tribal fishing rights, and give "equal consideration" to fisheries, recreation, and environmental quality. In a growing number of cases, removal of unsafe or obsolete dams represents the best river management option. For instance, removal costs of 70 small dams in Wisconsin were found to be an average of 2–5 times less than estimated repair costs. The following are a few examples:

On the Baraboo River, Wisconsin, the cost of removing the 3-m high Oak Street Dam was $30,000, compared to repair estimates of $300,000;

In Maine, the removal cost for the 8-m high Edwards Dam was roughly one third of the $9 million price tag of upgrading fish ladders.

A few large dams have been and will be removed due to various reasons. On the White Salmon River in Washington State, the 38-m high Condit Dam is required to add modern fish ladders to mitigate its negative impacts on the eco-system. The fish ladders and other improvements would have cost more than $30 million. Dam removal is a better choice because the cost of dam removal is only $15 million.

The 32-m high Elwha Dam and 82-m high Glines Canyon Dam on the Elwha River were built in the early 1900s to power timber mills in the nearby town of Port Angeles, Washington State, as shown in Fig. 7.30 (http://www.irn.org/revival/decom/brochure/rrpt2.html). They are the highest dams ever slated for removal at government expense. The private dams, now within the Olympic Peninsula National Park, destroyed magnificent local runs of Pacific salmon, diminishing an important cultural symbol. Extinction of Elwha River sockeye salmon, and drastic declines in the river's ten other native species, undermines fishing rights of the Lower Elwha Klallam, a federally recognized Indian Nation. In 1992, the government finally heeded tribal demands to provide "full restoration" of the Elwha River, including dam removal. After 25 years of campaigning by the Lower Elwha Klallam Nation and conservation organizations, Congress approved funds in 1999 to purchase the dams. Once acquired, the government will begin dam removal activities estimated to cost at least $100 million. Restoration of the Elwha represents the last, best hope for resolution of Lower Klallam fishing rights and the return of a once spectacular salmon river.

(a)   (b)
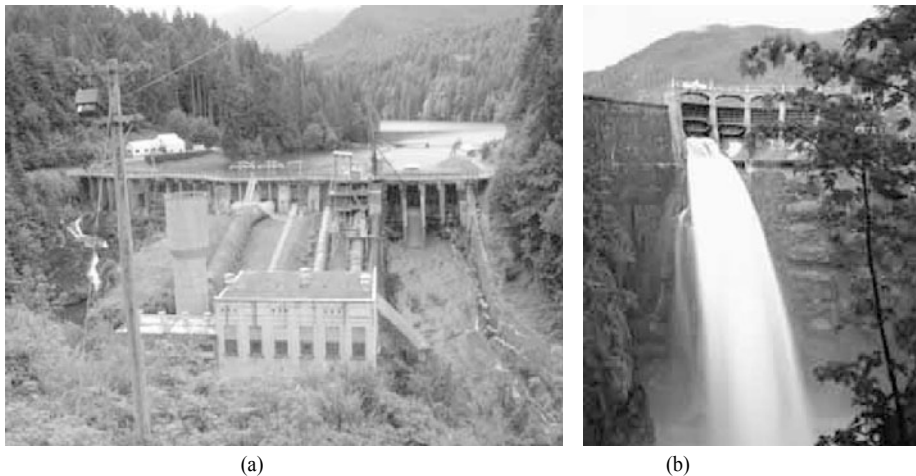
Fig. 7.30   The 32-m high Elwha Dam (a) and 82-m high Glines Canyon Dam (b) on the Elwha River, Washington, U.S. are going to be removed

Removal activities will start in 2008. Deconstruction of the Elwha Dam will be the most complex part of the three year project and will be undertaken in 6 phases, as shown in Fig. 7.31:

Phase 1 Open the four spill way gates on the south side of the dam to lower the level of the Lake Aldwell Reservoir 5.5 m in one month;

Phase 2 Remove the south gates and dig a diversion channel. Blast a 9.14×10.67 m plug of bed rock in five stages and reroute the river through the gap in 3 months;

Phase 3 Take out the north spillway and upper portion of the dam and install a 3.7 m wide road in order to access the penstock tubes in one month;

Phase 4 Remove steel penstocks and slide gates, the concrete intake structure and power house in 5 months;

Phase 5 Haul out 152,900 m^3 of rock, earth, concrete, and fir trees that were placed behind the gravity dam after a 1913 burst in a month.
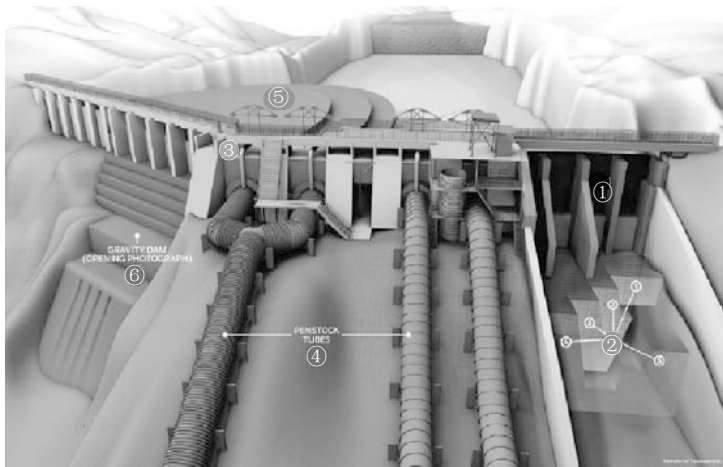
Fig. 7.31 Six phases of removal of the Elwha Dam

Phase 6 Remove the concrete gravity dam 2–3 m at a time using explosives and restore the natural river channel in 2 months.

7.3.2.2 Dam Removal in Other Countries

Internationally, grassroots campaigns are calling for dam removal to restore rivers and promote the rights of affected communities. Activists are targeting dams that continue to have significant negative social and environmental impacts and fail to live up to economic promises (http://www.irn.org/revival/decom/brochure/rrpt2.html, 2007).

France—Inspired in part by decommissioning efforts on the Elwha River in the U.S., the SOS Loire Vivante (Living Loire) network is working to remove old dams and restore France's only remaining river that supports native salmon. In 1998, two dams on tributaries of the Upper Loire were demolished to help protecting the last Loire salmon. First, the 12 m high Saint-Etienne-du-Vigan Dam on the Upper Allier was removed, marking the first case in which France's state-owned electricity utility destroyed a dam to restore the salmon habitat. The Vienne River, the second largest Loire tributary, also flows freely now after demolition of the 4 m high Maisons-Rouges Dam. A dam in Kernansquillec on the Leguer River was also dismantled, in 1996, after rapid sedimentation had reduced the reservoir capacity by 50%. Dam removal in France and the Loire River management plan reflect growing awareness across Europe, where concessions for thousands of dams built before 1950 are to be reviewed in the next decade.

Canada—In Canada, there is also growing interest in decommissioning dams and river restoration. Canada's regulatory regime differs from the U.S. system, especially in that dam licenses are issued in perpetuity. Of the 2,000 dams in British Columbia, 400 have either outlived their usefulness, provide only marginal benefits, or severely harm coastal fisheries. With the removal of nearly two dozen small dams in the province, support is growing for more ambitious decommissioning proposals.

On British Columbia's Theodosia River, a plan to revitalize lucrative commercial and sport salmon fisheries in the Georgia Straits is the basis for a plan to decommission a 35 year old water diversion dam. If removed, the 8 m high, 125 m long, Theodosia Dam would be the largest dam ever dismantled in Canada. Rather than dismantle the entire dam right away, stakeholders are pursuing other decommissioning options, including water diversion reductions. Save the Theodosia Coalition has attracted 140,000 people to join the coalition, they claimed that "No dam was meant to last forever- they do age and, eventually, outlive their usefulness. When that occurs, we have to look at the decommissioning or dismantling option in

an effort to restore habitat. It is a cautious, risk–averse approach to dam decommissioning and will do much to repair one of Georgia Strait's great salmon rivers." (http://www.irn.org/revival/decom/brochure/rrpt2.html, 2007).

Czech Republic—Since 1991, local NGOs and concerned citizens have campaigned to remove three small dams that flooded 1,300 acres of riparian and woodlands habitat along the Morava and Dyje rivers. The Ramsar Convention, which lists the affected area as a wetland of international importance, obliges the Czech Government to maintain the ecological character of the site. While conservation groups succeeded in securing a degree of restoration through partial draining of two reservoirs in 1995, the Czech Ministry of Agriculture may not support the ongoing restoration efforts. Czech conservation groups such as the Ecological Institute Veronica continue to demand decommissioning of the Nove Mlyny dams and further restoration efforts in the area.

Thailand—In Thailand, decommissioning campaigns have arisen as a result of social and ecological disruptions caused by dam construction on the Mun River, the largest tributary of the Mekong. The 135 MW Pak Mun Dam was funded by the World Bank and completed in 1994. As a direct result of the dam, more than 20,000 people have been affected by drastic reductions in fish populations upstream of the dam site, and other changes to their livelihoods. Villagers occupied the dam site and are demanded that dam gates be permanently opened to allow fish migration. The Rasi Salai Dam, the first project to be completed in a massive scheme to build 13 irrigation dams on the Chi and Mun rivers, is currently useless and likely to remain so. The reservoir overlays a geological salt dome that now makes the water too salty for irrigation. It also inundates the largest freshwater swamp forest in the Mun River basin, a source of food and traditional medicine for local villagers. More than 15,000 people lost farmland due to the reservoir, 60% of whom remain uncompensated.

7.3.2.3 Ecological Restoration After Dam Removal

In many cases dam removal is effective for ecology restoration. For instance, one year after the Edwards Dam removal in 1999, migratory fish returned in abundance to previously impounded parts of the Kennebec River. Fish diversity in the Baraboo River more than doubled, from 11 to 24 species, just 18 months after restoration of free-flowing conditions. Two years after removal of a dam on Tea Creek, the number of trout soared to more than 6 times the population necessary to reach "Class A" (the highest rating for recreational fisheries)

The state of Wisonsin leads the U.S. in dam removal. Over 130 dams have been removed in Wisconsin which is why Wisconsin has earned the reputation as a leader in selective dam removal internationally. Three major reasons for dam removals are: (1) removal of unsafe structure under chapter 31.19 of the state statutes; (2) removal of abandoned dams when either no owner is found or the owner is unable to fund repairs; and (3) removal of dams which have significant environmental impact.

In a few of cases, after a dam is removed, fisheries and hospitable habitat conditions return remarkably quickly. Dam removal alone may be insufficient to fully restore river systems, however, and may need to be accompanied by additional measures, such as protection of native fisheries, pollution abatement, restoration of riparian habitat, and stricter watershed management policies to increase the rate and extent of restoration. In France, the 1998 removal of two dams on Loire River tributaries is already revitalizing native shad, lamprey and salmon populations.

Technical Challenges in Dam Removal—Appropriate methods of dam decommissioning depend on project attributes (such as size, type, and location of dam), river characteristics, and intended objectives (such as fisheries restoration, land reclamation, and recreation). Dam decommissioning is, thus, highly site-specific. Careful planning minimizes public health and safety risks to downstream communities.

Dams trap immense quantities of river sediment. An estimated 5% of the world's total reservoir storage capacity is lost annually to sediment accumulation. In addition to creating problems for existing dams, sediment poses challenges during dam removal. Sediment removal is likely to represent the most costly and technically intensive aspect of decommissioning large dams.

Specific sediment removal techniques vary depending upon the amount of sediment, reservoir characteristics, project age and the effectiveness of periodical flushes, if at all feasible, to pass trapped sediment downstream. Sediment removal must be conducted carefully, as excessive release can damage sensitive downstream habitats. On Washington's Elwha River, for example, experts propose gradual, incremental drawdown to transport sediment without harming spawning habitats or juvenile salmon.

A potential result of sediment flushing is the release of accumulated contaminants into fisheries or water supplies. Following removal of a 9 m high dam on New York's Hudson River in 1973, tons of trapped toxins were suddenly exposed in the old riverbed or flushed downstream. Hazardous waste in sediment poses significant health risks, degrades water quality, and ultimately requires extensive cleanup efforts. Thus, thorough sediment an analysis and prior assessment of the foreseeable effects of releasing sediment must be included in decommissioning studies.

A key aspect of dam removal planning is early identification of alternative sources of hydropower, irrigation and public water supply, or other dam functions. Dam removal often entails trade-offs between competing river functions. However, American experience with dam removal demonstrates that replacement can often be accomplished with minimal difficulty. For example, a single hydropower dam may contribute only a fraction of a region's overall power—alternate sources are often available, and conservation measures can eliminate demand for this electricity altogether. In other cases, such as in the removal of 12 small dams on California's Butte Creek in 1998, dismantling the dams only had negligible effects on water supplies due to mitigation measures (e.g., improving efficiency of irrigation systems). Developing a comprehensive management plan that accounts for displaced dam functions minimizes the negative impacts of removal. Where changes or impacts are unavoidable, society may accept them as the price of long-term river restoration.

There are different dam removal methods: 1) Complete removal is often accomplished by first temporarily diverting the river, then using heavy equipment (e.g., wrecking ball, backhoe, and hydraulic hammer) to dismantle the dam. The removal of the 7 m high, 280 m long Edwards Dam on Maine's Kennebec River was accomplished in a matter of days using this technique. 2) Breaching of dams allows the river to flow around existing dam structures. Heavy machinery is typically used to breach earthen portions of dams located in relatively wide river corridors. Breaching is recommended for partial dam removal, such as the Lower Snake River dams, and represents a relatively inexpensive decommissioning option for larger structures, when feasible. 3) In the case of concrete dams, controlled explosives are occasionally used for demolition. Explosives were used to remove dams on the Clearwater (1963), Clyde (1996), Loire (1998) and Kissimmee (2000) rivers, among others. 4) A combination of explosives and heavy machinery may be required, especially with larger projects.

In summary, dam removal may be regarded as an option for the dams which have more negative impacts than benefit. Nevertheless, dam removal is not a good choice for many impounded rivers. Careful comparison should be undertaken before dam removal is used to end the life of the reservoir.

7.4   Construction and Management of the Three Gorges Project

The Three-Gorges Project (TGP) is well known due to its great scale and far-reaching influence in hydropower development and river management in China. The main purposes of the TGP are flood control, power generation and navigation. The construction and management of the TGP are discussed in this session.

7.4.1 Construction of the Three Gorges Dam

7.4.1.1 Purposes of the Project

The Yangtze River is the largest and longest river in China, with a drainage area of 1.80 million km². The Yangtze River basin has an elevation varying from 5,000 m to 0 m with latitude from N25° to N35°. The river flows through the Qinghai–Tibet Plateau, Yunnan–Guizhou Plateau, Sichuan Basin, Three Gorges, Jiang-Han Plain, Lower Yangtze Plain, and pours into the East China Sea at Shanghai. From the source to Yichang (Three Gorges Dam site) is the upper reach, from Yichang to Hukou (Poyang Lake mouth) is the middle reach, from Hukou to Datong is the lower reach, and below Datong is the estuary.

In China, the Yangtze River is called Changjiang (long river), with special names for different stretches: the lower reaches are called the Yangtze River, the middle reaches are called the Jingjiang River, the reach from Yichang to Yibin is called the Chuanjiang River, from Yibin to Zhimenda is called the Jinsha River, and from Zhimenda to the origin is called the Tongtian River (Heaven River). The river has become the most frequently flooding river in China since the 1950s, before which the Yellow River was the most disastrous river in China. The Jiang-Han plain is the most flood threatened area, because it is 10–15 m lower than the flood stage.

The Three Gorges Dam is constructed at Yichang, immediately upstream of the middle reaches of the river, allowing it to control floods from the upper reaches of the river. The Three Gorges Reservoir is a river type reservoir, as shown in Fig. 7.32.
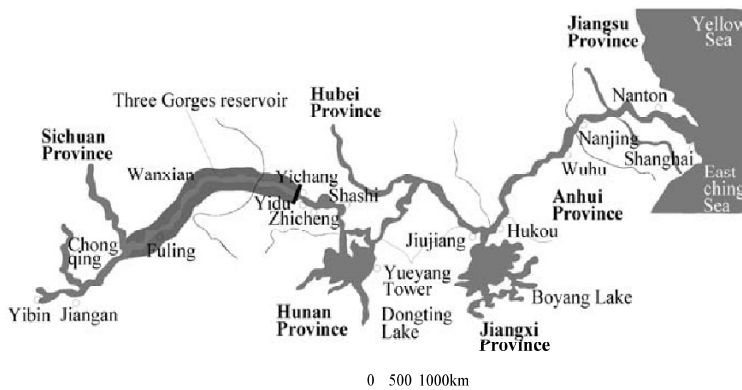
Fig. 7.32 Locations of the Three Gorges Dam and the Three Gorges Project reservoir

1) Flood Defense

The most important purpose of the project is to mitigate flood disasters. Historical records show that during the 2,000 years from the Han Dynasty (206 BC-220) to the late years of the Qing Dynasty (1644–1911), serious flooding occurred on the Yangtze River 214 times. The 20th century experienced three immense floods, two of which, one in 1931 and the other in 1935, flooded 3.4 million and 1.5 million ha of farmland and killed 145,000 and 142,000 people respectively. Although the 1954 floodwaters of the Yangtze failed to destroy the Jingjiang dyke and rush into the city of Wuhan, an area of 3.17 million ha of farmland was inundated, 18.88 million people became victims, and 30,000 others were killed. Direct losses from the flood reached more than 10 billion Yuan. In addition, the country suffered incalculable, indirect losses from the flood, such as the Beijing–Guangzhou railway line being unable to offer normal services for 100 days.

The floods of the Yangtze River mainly originate from the Jinsha, Minjiang, Jialing and Hanjiang Rivers, and the rivers tributary to the Tongting and Poyang Lakes. The main areas of flooding risk are in the

middle reaches of the river, especially the reach from Shashi to Jiujiang. Generally, the flood volume from the upper reaches (Yichang) accounts for 95% of the flow at the Shashi, 61%–80% of the flow at Chenglingji, 55%–76% of the flow at Wuhan (Hankou), and 54% of the flow at Datong. Floods from the major tributaries in the Sichuan–Chongqing Basin, such as the Minjiang and Jialing Rivers often meet with the floods from upstream of Chongqing exhibiting an obvious influence on the floods at Yichang and the middle reaches. The duration of a large flood is quite long, 30 days at Shashi, 50 days at Chenglingji, over 50 days at Wuhan (Hankou), Hukou, and Datong. Such a long duration of high water levels threatens the safety of the levees.

The floods on the Yangtze River may be classified into two basic types: floods resulting from heavy rainfall in the whole river basin and floods resulting from regionally heavy rainfall. The former is the result of consecutive heavy rainfalls in the upper and middle reaches of the Yangtze River, such as the 1931 and 1954 floods. As examples of the latter type, heavy rainfall in the upper reaches in 1870 and 1896 and that in the middle reaches in 1935 caused extreme floods (Luo and Luo, 1996; Zhou, 1999). In the 20th century the highest flood peak discharge occurred in 1954, but the most serious disaster was in 1931.

Flood protection of the middle reaches has a long tradition. The flood control system consists of the 3,570 km long grand levees, more than 30,000 km of levees along the tributaries, riparian lakes, and canals, on a local scale, protective walls built by municipalities, and Tongting and Poyang lakes and several man-made flood retention basins, as shown in Fig. 7.33. The retention basins protect cities and the grand levees. Most important is the portion of the river flooding stored in Tongting Lake. Flood water is diverted into the lake through the Songzi, Taiping, Ouchi, and Tiaoxuan diversion channels and flows back to the river at Chenglingji.
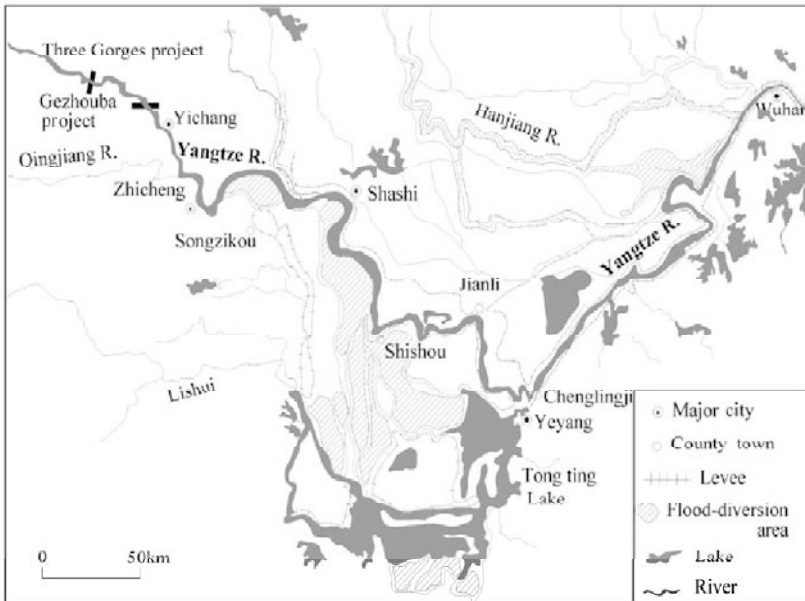
Fig. 7.33   Flood defense system of the middle and lower reaches of the Yangtze River (See color figure at the end of this book)

The flood control system protects 126,000 km^2 of flood plain on which 75 million people are dwelling and many industrial hubs like Wuhan, Nanjing, and Shanghai are located. Comprehensive flood control measures were taken after the 1950s, including raising and reinforcing the grand levees to prevent

overflows and the creation of flood diversion areas. Flood storage is increased through reservoirs on the tributaries and flood diversion basins, e.g., the Jingjiang and Dujiatai diversion basins. The most important flood diversion basin, the Jingjiang Polder with a surface area of 920 km^2 and storage capacity of 6 billion m^3, was built in 1952 and was inundated during the great flood of 1954.

In 1998 a flood occurred on the Yangtze River, which resulted in serious flood damages and affected 8 million people. Heavy rainfall occurred in the area in the summer of 1998 in the wake of the strongest El Nino phenomenon of the century, which reached its maximum at the end of 1997 and ended in May 1998. The rainfall caused floods on the Yangtze River and many of its tributaries. About three quarters of the flood volume at Wuhan was from the reaches of the river upstream of Yichang and the rest was from the Hanjiang River and Tongting Lake. The recurrence period of the 1998 flood is only 8 years in terms of the peak flood discharge. The runoff volume of the 1998 flood, however, was larger than that of 1931, but smaller than that in 1954. It was the second largest flood by volume in the 20th century, after the 1954 flood (Ministry of Water Resources, 1999). The flood stages in the middle reaches of the river were even higher than those in 1954 although the flood peak discharge and the total runoff volume were smaller (Zhou, 1999).

The 1998 flood caused the strategy of flood control for the river to be rethought. The new strategy rests on the following actions: construction of the Three Gorges Reservoir; reinforcing and increasing the height of the levees; back conversion of some polders into river channels; increasing the size of Tongting Lake by returning farmland to the lake area to increase its flood detention capacity; dredging the main channel of the river; moving people from flood detention polders; and reclamation and reforestation in the upper reaches of the catchment.

The main reason behind the serious flood threat in the middle and lower reaches of the Yangtze River is the high peak and large volume of the floodwater from torrential rainfall in the upper reaches when it exceeds the safe discharge capacity of the river. Currently, the safety limit for flow capacity along the Jingjiang section (including the flow towards Tongting Lake) is about 60,000 m^3/s, while for the Wuhan and downstream Hukou sections, it is 70,000 and 80,000 m^3/s, respectively. Materials gathered since 1877 show there have been 24 floods at Yichang with peak flows above 60,000 m^3/s. In the 850 years since from 1153, there were eight floods with peak flows larger than 80,000 m^3/s and five topped 90,000 m^3/s. During the 1860 and 1870 floods at the Zhicheng Station, the peak flows reached 110,000 m^3/s, obviously far exceeding the safe flow capacity of the river.

Presently Tongting Lake is still an important natural flood-detention basin in the middle reaches of the Yangtze River. During the flood season, floodwaters from the Jingjiang River account for one-third or one-fourth of the water entering Tongting Lake. The natural flood-detention lake can reduce the peak flow of the Jingjiang River by about 10,000 m^3/s. It is obvious that its role of regulation and detention remains of great significance for flood control. Tongting Lake, however, is shrinking quickly due to sedimentation and land reclamation. Based on the research of specialists, it is necessary to apply comprehensive flood mitigation measures to solve the serious flood control issues in the Jingjiang reach of the Yangtze River, including the heightening and reinforcement of levees, arrangement and setting up of flood diversion and detention areas, building reservoirs on the mainstream and tributaries, and realignment of rivers, as well as improved flood forecasts. The most crucial of these is the building of the Three Gorges Project.

The Three Gorges Project is sited at the place, where the Yangtze River's middle and upper reaches meet. Its unique location and topographical conditions as well as its reservoir with a flood control storage capacity of 22.15 billion m^3 will enable it to effectively control floods resulting from heavy rains in the upper drainage areas. The project's flood prevention role would be decisive in the Jingjiang reach, and it would also play a fairly good role in controlling floods originating over the whole valley and the middle-lower reaches. The Three Gorges Reservoir raises the flood control capacity, prevent breaches of the

Jingjiang grand levees and devastating destruction. Simultaneously, by effectively controlling upstream floods, it is possible to relieve threats to Wuhan, and reduce water and sand discharge into Tongting Lake.

2) Power Generation

Of the many benefits the Three Gorges Project promises, the most direct and most obvious will be its enormous ability to generate electricity. The hydroelectric station of the Three Gorges Project will be the biggest in the world, with an installed capacity of about 18,000 MW and an annual generation of 84 billion kwh. It will provide electricity mainly to central and east China and a small amount to the eastern Sichuan province. The electricity will provide an alternative to the consumption of 40 to 50 million tons of raw coal or to seven 2.4 million kw thermal power stations.

Coal resources along the Yangtze River are insufficient but water resources are rich. The huge amounts of energy it would generate could draw high profits and serve to repay loans. Even during the construction period, accumulated electricity output could reach 435.8 billion kwh and earn about 40 billion Yuan at a rate of 0.092 Yuan/kwh. After normal operation commences, the annual income of the project from sales of electricity alone will amount to 7.5 billion Yuan. After all loans are repaid, the project will be able to hand over 3.56 billion Yuan annually to the state with total profits and taxes turned over to the state treasury reaching 5.41 billion Yuan.

In addition, the replacement of thermal power stations by the Three Gorges Project will generate tremendous social benefits and good environmental effects. It will reduce the consumption of coal by 40 million or 50 million tons every year and cut carbon dioxide, sulphur-dioxide, carbon monoxide, and nitrogen-oxide emissions by 100 million tons, 2 million tons, 10,000 tons, and 370,000 tons, respectively. It will also greatly reduce the amount of industrial liquid waste and play a great role in cutting sources of environmental pollution, such as acid rain.

3) Navigation

The Yangtze River, with its mainstream and tributaries running through 18 provinces and municipalities, provides very favorable water transportation conditions and has always been China's main transport artery linking its eastern, central, and western regions. Its navigable mileage is more than 70,000 km, accounting for 70 percent of the nation's inland navigation mileage. Its annual freight volume accounts for 80 percent of the country's river-borne freight, earning the Yangtze River the name of the "Golden Waterway".

The reach of the Yangtze River to be flooded by the Three Gorges Reservoir includes 130 dangerous shoals and 46 one-way control sections, and it is not wide or deep enough for the passage of large ships. The Three Gorges Project will improve navigation conditions on the section from Yichang to Chongqing. After project completion 10,000-ton towboats will be able to sail unimpeded to Chongqing. With the construction of ports and modernization of ships, the annual shipping capacity may increase by 5 times and the transport costs may be cut by 35 to 37 percent.

The construction of the Three Gorges Project also plays a comprehensive role in fish breeding, city water supplies, and provision of adequate water supply for the transfer of water from the south to the north of China.

7.4.1.2   Design of the Dam

The Three Gorges Dam site is at Sandouping near Yichang in Hubei Province. A river shaped reservoir has appeared on the river as shown in Fig. 7.27. The dam is being built on a base of solid granite. Geological studies, including drilling at the dam site down to 100,000 m and 4,000 sets of rock mechanics tests, have been carried out, covering various aspects associated with the project construction for more than 3 decades. The design of the dam involves the dam, navigation facilities, and power houses.

1) Dam Structure

As shown in Fig. 7.34 the main buildings of the Three Gorges Project consist of the dam, hydroelectric station, and navigation structures. The Three Gorges Dam is a conventional concrete gravity type dam: 2,335m long and 175 m high, with its crest elevation at 185 m above sea level. The dam is constructed from right to left (in the picture) in order: right non-spillway section, ship lift, temporary ship lock (for construction period), non-spillway dam section, right power plant, right guiding wall, spillway, coffer dam section, left power plant, non-spillway section. The spillway is located at the central section of the river, composed of 27 dam blocks with 23 deep outlets (7×9 m, with a bottom elevation of 90 m), 22 bottom outlets (6×8.5 m, with a bottom elevation of 56 m) and 22 top outlets (8 m wide, with an elevation of 158 m) between them. The most striking feature of the project is its gargantuan scale. During the construction of the Three Gorges Dam, the casting volume of concrete was more than 4 million m^3 in the peak years.

Fig. 7.34   A model of the Three Gorges project on the Yangtze River- from right to left: five step ship locks including the upper and lower approach channels, the ship lift and its channel, the left power house, the spillway, and the right power house (See color figure at the end of this book)

2) Power House and Turbine

The two power plants with 26 sets of power generating units compose a total installed capacity of 18,200 MW and an annual output of 84.7 billion kwh. The hydroelectric station of the Three Gorges Project is huge and its total installed capacity ranks number one in the world. The installed capacity of each turbo-generator of the Three Gorges Hydroelectric Power Station is 680,000 kw. The Three Gorges Hydroelectric Power Station transmits 500-kV alternating current and –500 kV direct current. The profile of the turbo-generator is shown in Fig. 7.35. The left power house is 600-m long, 35.5-m wide, and 30-m high with 14 turbo-generator units. The center of the turbo-generator is at an elevation of 57 m. The turbine diameter is 9.5 m and the turbine weighs 3,350 tons. The generator is 23 m in diameter and weighs 3,800 tons. The rated revolution of the turbine is 71.4 revolutions per minute.

3) Navigation Structures

The navigation structure consists of two lines of five step permanent ship locks, a ship-lift, and a temporary ship lock. The total water head of the permanent ship locks is 113 m. The ship locks enable 10,000 t ships to pass through. The annual transportation capacity of the locks is 50 million t. The size of the permanent ship locks is $280 \times 34 \times 5$ m (length $\times$ width $\times$ the minimum depth over the sill). The upstream water stage of the ship locks is 135–156 m in the initial period and 145–175 m when the project is completed.

The lower stream stage is 62–78 m and the maximum flow discharge for navigation is 56,700 m³/s. The bottom level and the highest water level of the five step locks are 130–179 m, 119.25–161 m, 98.5–140.25 m, 77.75–119.50 m, 57–98.75 m, respectively.
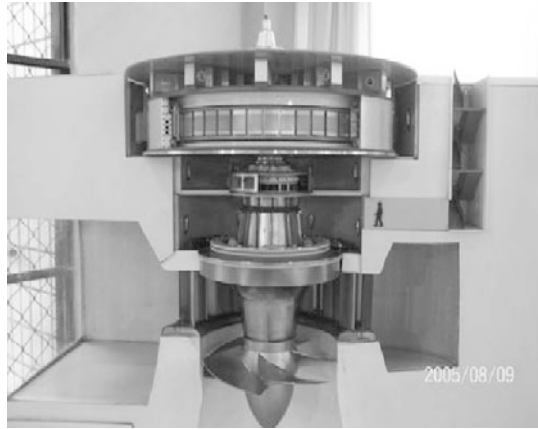
Fig. 7.35 Profile of a turbo-generator

The shiplift and the temporary ship lock use one approach channel, which connects to the lower approach channel of the permanent ship locks. The upstream approach channel of the ship locks is 2,113-m long and 180-m wide and the downstream channel is 2,722-m long and 180-m wide. One line of the ship locks is for navigation upstream and one line for downstream. For each step of the ship lock, only 12 minutes are needed to fill or empty water. The annual water consumption of the ship locks is 3.4 billion m³. The ship lift was used during the construction period and will be used as a fast channel to go through the dam after impoundment of the reservoir. The size of the lift cabinet will be is 120 × 18 × 3.5 m and may carry a 820 seat passenger ship and a 1,500 t freight ship. The bearing capacity is 11,800 t including the ship, 9000 t water and 2,800 t of its own weight. It takes 42 min for a ship to pass the dam through the ship lift. The ship lift can transport 5 million people and 6.26 million t of goods every year.

The temporary ship lock was used during the second phase of construction. As the flow discharge was less than 20,000 m³/s, ships navigated through the temporary open channel. Only a few kinds of ships with low navigation capability had to go through the temporary ship lock. If the flow discharge was higher than 20,000 m³/s, however, no ship could navigate through the open channel and all would have to use the temporary ship lock. The ship lock is 240-m long, and 24-m wide with water depth 4 m. Its working upstream water level is 65.7–75.5 m and the lower water level is 65.6–75.8 m. The maximum stage difference is 3.7 m. The annual transportation capacity is 9–11 million tons.

The temporary open channel on the right side was mainly for conveying flood flows and ship navigation during the second phase of construction phase. The open channel is able to discharge a 50-year flood flow, or a discharge of 79,000 m³/s. The open channel was 3,410-m long with minimum bottom width of 350 m.

7.4.1.3 Construction of the Three Gorges Project

Phase I (1994–1997)—The TGP is being constructed in three phases, as shown in Fig. 7.36. Preparations for construction of the dam were done in 1993 and 1994. Formal commencement was declared on Dec. 14, 1994. There was a small island, Zhongbao Island, at the dam axis, which divided the river into two branches. The right branch, Haohe branch, was dry in the low-flow season and floods flowed through it before the project. In the first phase, an earth coffer dam was built to enclose the right branch channel.

Along the right edge of the island a longitudinal dam was built within the coffer dam. The right channel was deepened and widened by excavation to form an open channel capable of conveying a discharge of 70,000 m³/s. The open channel was finished in 1997 and was put into use in May 1997. Ships started to navigate through the open channel in July, 1997. In the meantime, the temporary ship lock was built on the left bank of the main channel. The river was not substantially narrowed and floods passed through the river section smoothly. The permanent ship lock was put into use in this phase.

Phase II (1998–2002)—The beginning of the second phase was marked by the successful closure of the earth coffer dam on the main channel on Nov. 8, 1997. An enclosed area appeared in the river channel and the flood water flowed through the artificial open channel, as shown in Fig. 7.36(b). The main dam was constructed on the river bed within the area enclosed by the coffer dam in the period from 1998–2002. In the fall of 2002 the main dam and the five step ship locks were completed.

Phase III (2003–2009)—In 2002, the coffer dam on the main river channel was removed by explosion and water began to flow through the bottom outlets of the dam. The open channel was cut off by a coffer dam again, as shown in Fig. 7.36(c). On Nov. 7, 2002, the open channel coffer dam was closed. The new cofferdam was built from elevations of 50 to 140 m and constructed with rolled concrete. It formed a reservoir in conjunction with the main dam. The water level rose to 135–140 m and the turbo-generators began to generate electricity. The right part of the main dam was built within the coffer dam. Water flowed through the 23 bottom outlets of the spillway section. The permanent ship locks and the ship lift were used for ships to pass through the dam.
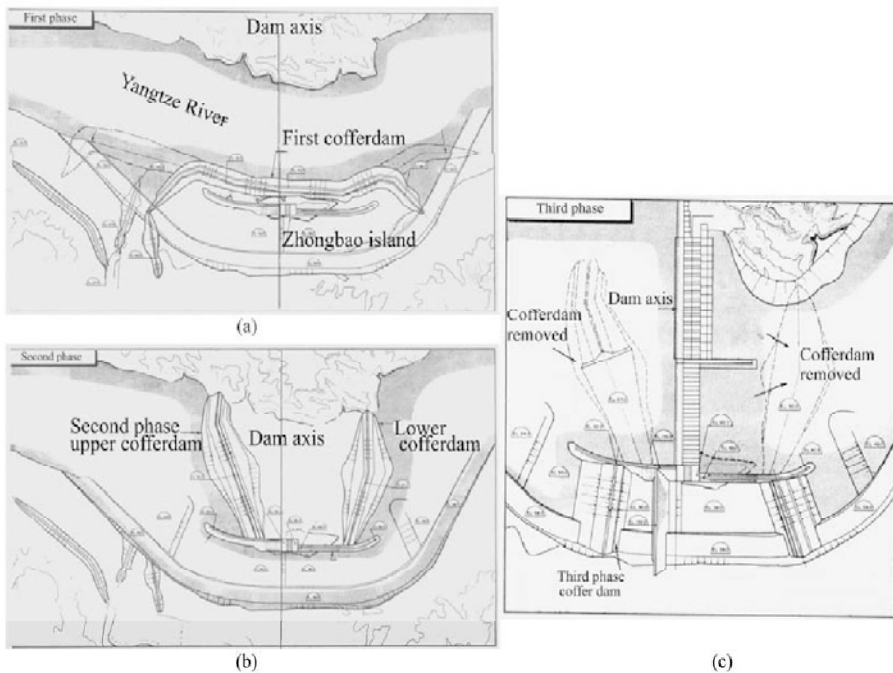
Fig. 7.36 Phasing of the TGP construction: (a) phase I—build coffer dam on the right channel, excavate the open channel and build the longitudinal dam along the right edge of Zhongbao island; (b) phase II—build coffer dam on the main channel of the river, construct the dam and permanent and temporary ship locks and ship-lift; floods flow through the open channel. (c) phase III—build coffer dam to close the open channel, construct the right part of the great dam, impound water to 135–140 m and begin to generate electricity, floods flow through the bottom outlets of the dam

7.4.2 Sedimentation and Management Strategies

The main sedimentation problems of concern in the TGP project are the following:

(1) Reservoir sedimentation and permanent use of the reservoir capacity for flood control;

(2) Sedimentation in the navigation channel in the backwater zone;

(3) Sedimentation in the vicinity of the dam;

(4) Degradation of the downstream reaches;

7.4.2.1 Reservoir Sedimentation and Permanent Use of the Reservoir

The normal pool level of the reservoir (NPL) is set at 175 m. Two other characteristic pool levels are considered, namely the flood control level (FCL), to which the pool will be drawn down at the beginning of the flood season, generally in June, and the low-flow season control level (LCL), to which the pool may be drawn down to satisfy the requirements of power generation and to provide adequate depths of flow, both up- and down-stream of the dam before the next flood season. The reservoir is impounded to the normal pool level after the flood season, usually from October. There are many alternative flood control levels for selection, such as 135, 140, 145, and 150 m. the FCL is the major factor affecting the amount of sediment deposition in the reservoir.

The hydrological station closest to the dam is the Yichang Station. The long term average annual runoff at Yichang is 450 billion m^3 and the annual sediment load is 532 million t, of which about 0.8 million t are gravel bed load. The median diameter of suspended load is 0.033 mm and the median diameter of bed load is 24 mm. More than 88% of the suspended load is finer than 0.1 mm. The long-term average discharge at Yichang is 14,300 m^3/s.

The Tsiantan station is located near Chongqing at the upstream end of the reservoir. The annual runoff, sediment load, and average concentration at Tsiantan are 350 billion m^3, 462 million t, and 1.32 kg/m^3, Only about 0.3 million t of the sediment load is bed load. The median diameter of suspended load is 0.037 mm and the median diameter of gravel bed load is 51 mm. Figure 7.37 shows the annual runoff, sediment load, and sediment concentration at Yichang and Tsiantan in the period from 1950–1985. The annual load at Yichang varies from 350 million to 750 million t and that at Tsiantan from 250 million to 700 million t.
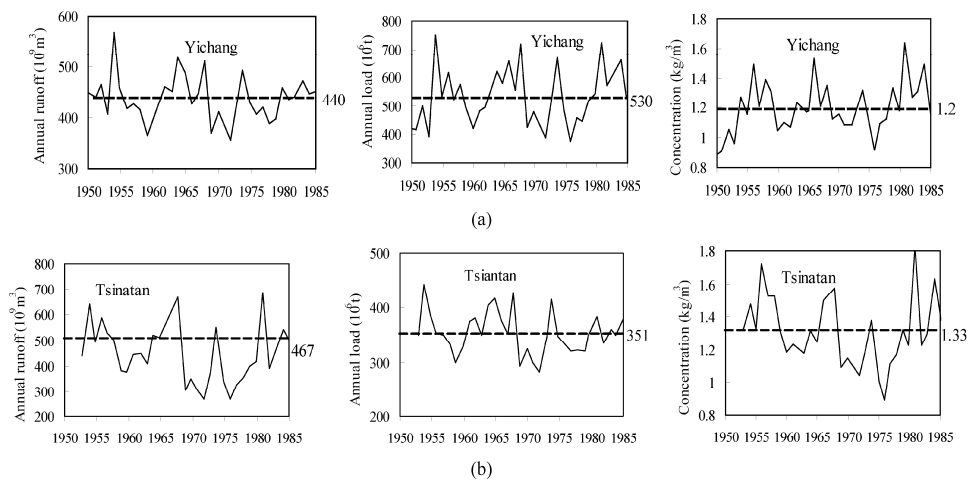
Fig. 7.37 (a) Annual runoff, sediment load, and sediment concentration at Yichang (1950–1985); (b) Annual runoff, sediment load, and sediment concentration at Tsiantan (1950–1985) where the dashed lines indicate the mean values

The main strategy to control sedimentation in the Three Gorges Reservoir is storing the clear water and releasing the turbid water. The Yangtze River transports about 90% of its annual sediment load with only 60% of its annual in the three months from mid June to mid September. The pool level is drawn down to 145 m from June to September allowing the turbid water wash through the reservoir downstream. The reservoir stores water beginning in October when the inflowing water becomes clear. By applying this strategy a permanent capacity of 22 billion m^3 can be preserved.

The 22 bottom outlets at an elevation of 56 m are used to discharge flood flow during the construction of the project and will be closed at the end of the third phase of construction. The 23 deep outlets will be permanently used for discharging flood flow. The elevation of the deep outlets is 90 m and the discharge capacity at pool levels 130, 140, and 150 m are 51,000, 60,000, and 64,000 m^3/s, respectively. If the flood discharge is not over 62,000 m^3/s, the reservoir is operated for **"storing the clear water and releasing the turbid water"** and the pool level is drawn down to 145 m to create a condition favorable for sediment flushing by letting a large discharge out of the reservoir. When the incoming flood exceeds this value, water will be stored in the reservoir and the release is adjusted according to a predetermined schedule aimed at keeping the flood damage in the downstream area to a minimum. After the flood peak has passed, the reservoir will again be drawn down to 145 m.

Drawing the reservoir down to 145 m during the majority part of the flood season in most years will keep the upper limit of deposition below the backwater curve with its lower end at the FCL (145 m), as shown in Fig. 7.38 (Curve 1). During the low-flow season, the river carries little sediment, but still conveys 39% of the annual runoff, i.e. 171 billion m^3 of water at Yichang. Water will then be stored in the reservoir for power generation and navigation. The amount of water needed to fill up the reservoir to its normal pool level varies with the scheme adopted but is generally less than 22 billion m^3, which is only a small portion of the runoff in the low flow season. Eventually a new alluvial channel will form in the reservoir under the backwater curve connecting the FCL at the dam and the natural flow upstream, shown as Curve 2 in Fig. 7.38. This part of the reservoir storage can be preserved indefinitely.
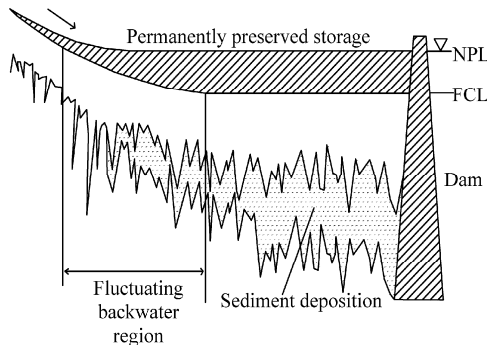
Fig. 7.38 Schematic diagram of the pool levels and deposition curve of the TGP reservoir: NPL—normal pool level (175 m); FCL—flood control level (145, 135, or 150 m); Curve 1 is the upper limit of sediment deposition and Curve 2 is the backwater profile for the case of the reservoir at the FCL

How much of the original flood regulating capacity can be preserved depends, among other things, on the morphology of the reservoir. The reservoir looks like a ribbon in the plan view. The 700-km long reservoir is quite uniform in width and is for the most part less than 1000-m wide. Since the estimated width of the equilibrium channel corresponding to the hydrological conditions of the reservoir is 1,300 m, little flood plain is expected to form along the main channel in the reservoir, Thus, large percentages of

both the flood control and low flow season regulation storage may be preserved indefinitely.

The sedimentation process of the TGP reservoir has been simulated by using one-dimensional numerical models. The computation was made for the reservoir operational levels schemes with hydrological time series. As the recurrence period of the 1954 flood is approximately 40 years, the stream record of 1954 was inserted into the hydrological series in such a manner that it appears three times in 106 years. The time series, thus, consists of the hydrological records of the flowing sequence of years:

2 cycles of 1961–1970 plus 1954, 1955;

2 cycles of 1961–1970 plus 1954, 1955;

4 cycles of 1961–1970 plus 1954, 1955 and

2 cycles of 1961–1970

Figure 7.39 shows the accumulation of sediment in the reservoir from 0 to 100 years for various schemes calculated by the Yangtze River Conservancy Commission, in which 160–135 means that the normal pool level is 160 m and the flood control pool level is 135 m. Curve 4 in the diagram is for the scheme with NPL = 175 m and FCL = 145 m (but in the first 10 years NPL = 156 m and FCL = 135 m). After 80 years of operation, the accumulated sedimentation amount is nearly in equilibrium and increases very slowly. The total sedimentation in 100 years is about 16 billion m^3.
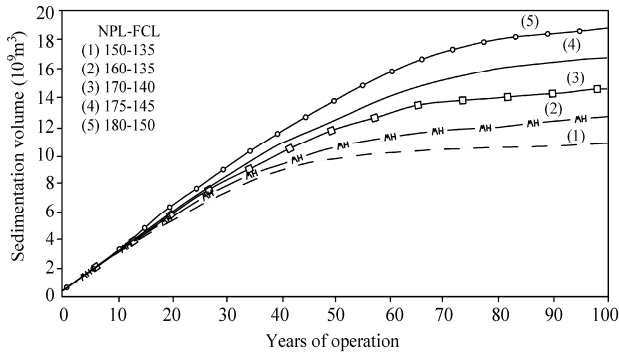
Fig. 7.39 Accumulated sedimentation in the reservoir during 0–100 years of operation of the reservoir for various reservoir operational level schemes (Sedimentation Panel for TGP, 2002)

In order to reduce the rate of sedimentation in the reservoir and develop the hydro-power of the river, the Xiangjiaba and Xiluodu Reservoirs will be constructed after the completion of the TGP reservoir. The Xiangjiaba Dam site is located 1,020 km upstream of the TGP dam with a capacity of 5.06 billion m^3. The reservoir can be used to trap sediment for 60 years before it reaches equilibrium. The Xiluodu Dam is located 1,180 km upstream of the TGP dam with a total capacity of 11.57 billion m^3. The reservoir can be used to trap sediment for 90 years before it reaches equilibrium. Bed load and coarse suspended load from upstream reaches of the Yangtze River can be trapped by the two reservoirs. Thus, the rate of sedimentation of the TGP reservoir can be reduced in the first 90 years. Figure 7.40 shows the accumulated sedimentation of the TGP reservoir for the three scenarios: Scheme 1 = without upstream reservoirs; Scheme 2 = with the Xiangjiaba Reservoir; and Scheme 3 = with the Xiluodu Reservoir. The operation of the Xiluodu or Xiangjiaba Reservoirs will reduce the sedimentation volume by 2–4 billion m^3 in the period of 30–80 years of TGP reservoir operation.

In the reality, the Three Gorges reservoir began to impound in June of 2003. Sedimentation in the first years of operation has received great attention. In the first ten years of operation the pool level rose gradually following the completion of the dam in the ranges of 135–141 to 145–156 and 145–175 m. From

January 2007 to January 2008 the pool level was controlled at around 156 m in non-flood season, and was drawn to 145 m from June to October, so high sediment concentration flood water flowed through the reservoir and released to the downstream reaches. Figure 7.41 shows the distributions of monthly runoff and sediment load at the Cuntan and Yichang stations in 2007, which represent water and load inflowing and out of the reservoir, respectively (MWR, 2008). The result shows that more than 30% of the incoming sediment load is discharged out of the reservoir during the flood season.
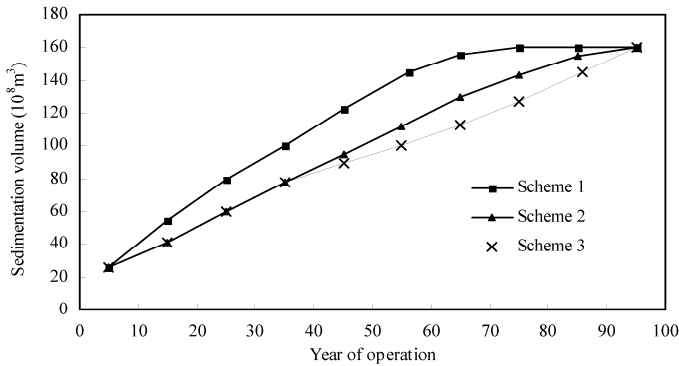
Fig. 7.40 Accumulated sedimentation of the Three Gorges Project reservoir for the three scenarios: Scheme 1 = without upstream reservoirs; Scheme 2 = with the Xiangjiaba Reservoir; and Scheme 3 = with the Xiluodu Reservoir
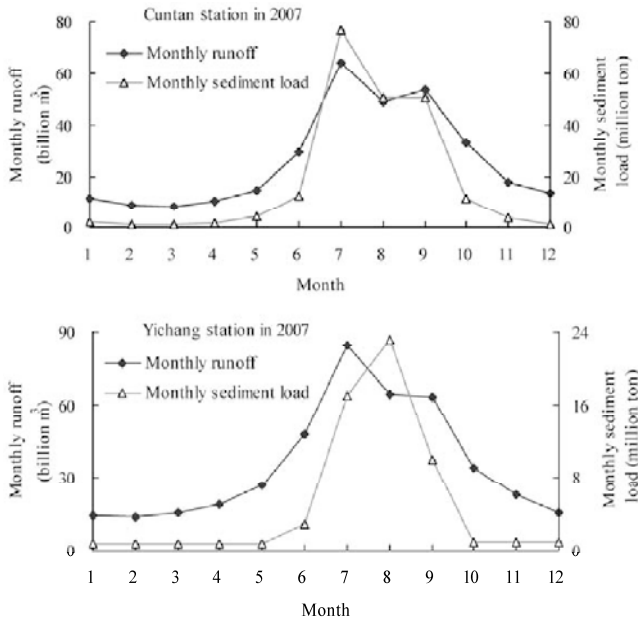
Fig. 7.41 Distributions of monthly runoff and sediment load at the Cuntan and Yichang stations, which represent water and sediment load flowing in and out of the reservoir, respectively (MWR, 2008)

Figure 7.42 (a)–(c) shows the measured cross sections in the reservoir in 2003, 2005, 2006 and 2007 at 5.6 km, 160 km and 356 km from the dam, respectively (MWR, 2007, 2008). Sediment accumulated in

the reservoir rapidly in the first two years (2003–2005) following impoundment, but from 2005 to 2007, the amount of sedimentation in the reservoir remained relatively constant. Comparing with the calculated sedimentation volume, the measured sedimentation volume in the first 4 years of operation was much less. The main reason was a dramatic sediment load reduction since the 1980s (Liu et al., 2008).
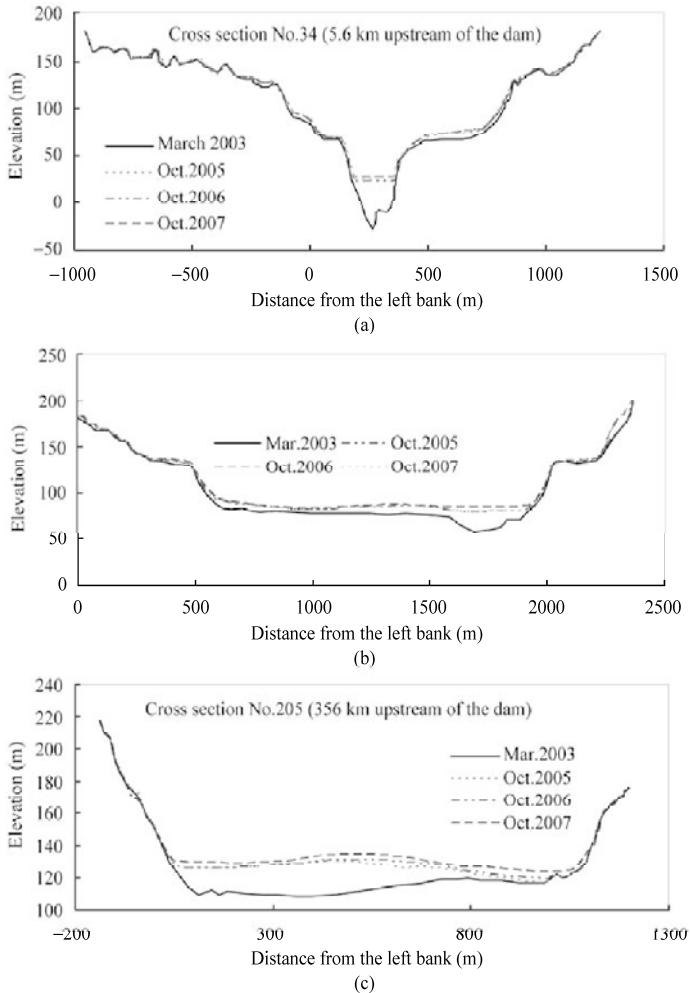
Fig. 7.42 Measured cross sections at the Three Gorges Reservoir in 2003, 2005, 2006, and 2007 at 5.6 km (a), 160 km (b), and 356 km (c) from the dam, respectively (MWR, 2008)

7.4.2.2 Sedimentation in the Fluctuating Backwater Region

The fluctuating backwater region is the river reach with a flood stage between the FCL and NPL, as shown in Fig. 7.38. The industrial hub of Chongqing is in the fluctuating backwater region, which is located at the confluence with the Jialing River—a major tributary of the Yangtze River. There is a passenger ship harbor—Chaotianmen Harbor and a freight ship harbor—Jiulongpo Harbor in Chongqing. The Chaotianmen shipping terminal at Chongqing is about 602 km from the dam, any small errors in the computation of the hydraulic gradient will result in sizable differences in stage elevations.

It is understood that for a 100-year flood (1% probability of exceedance in a given year) the city of Chongqing would not tolerate a stage higher than 200 m. This stage, however, would be reached only if a 100-year flood should occur after the reservoir had been in operation for about 100 years. The chance is rather remote. Moreover, during this intervening period of 100 years, the Xiangjiaba and the Xiluodu Reservoirs will be built upstream of the TGP. The operation of these reservoirs will have the permanent benefit of reducing peak discharges entering the TGP, which alone is sufficient to reduce the flood stages at Chongqing. In addition, following the commission of the reservoir, there will be a rather long period (10th–80th years of operation) during which the sediment influxes into the TGP will diminish. Reduction in deposition in the TGP reservoir will lead to a reduction in flood stages along the upstream reaches. The permanent storage capacity of the upstream reservoirs can regulate the flow in low flow season. This will result in an increase of the minimum discharge entering the TGP reservoir during the low flow season. With this increase more sediment will be scoured from the upper part of the backwater region, and for the same discharge lower flood stages at Chongqing may be expected.

Two major problems are to be addressed in the study of sedimentation in the fluctuating backwater region, namely: 1) whether sedimentation would result in a channel suitable for navigation of 10,000 t tows, and 2) whether the areas around the piers of shipping terminals at Chongqing could be free of deposition detrimental to shipping operations.

Regarding the first problem, studies were carried out with physical models. Five sections are critical for the influence of sedimentation on navigation. Nine physical models were built and scale model experiments were conducted. The results show that during the normal pool level period, the 660 km long navigation channel from Yichang to Chongqing would much improved. For all schemes investigated the minimum requirement of a channel 3.5-m deep, 100-m wide and with a radius of curvature of 1000 m for the passage of 10,000 t tows can generally be satisfied. Some dredging and training works may be needed here and there along the channel, but they will be generally of minor scale, because in May and June navigation problems may occur in a few broad and shallow sections when the pool level has been drawn down and sediment deposited in the channel has not yet been scoured away.

The problem of deposition around the shipping terminal—the port of Chongqing—is the center of attention. This deposition varies with the selection of the pool levels for the project and also with the operation schedule of the reservoir. Sediment will deposit at the apron of the Jiulongpo Harbor (Fig. 7.43), which is the biggest freight harbor in southwest China, and may even result in shifting the channel from left to right after 80 years of operation of the dam. Chaotianmen Harbor is the largest passenger harbor in Chongqing (Fig. 7.43).

Sediment accumulates in the Chaotianmen and Jiulongpo Harbors. After 50 years these harbors could not be used if dredging or other technical measures preventing sedimentation were not taken. The studies also proved that these problems can be solved by building spur dykes and groins to regulate the flow. The test demonstrated that the dykes and groins would narrow the channel and concentrate the flow, so that flow velocity in the navigation channel and harbor area can be enhanced to prevent sediment from depositing.

Some concern has been expressed regarding the possible consequences of deposition of gravel bed load in size range of 1–10 mm at the upper end of the fluctuating backwater region. Investigation shows that all the coarse sediment could be mined or dredged for building material and causes no accumulative sedimentation.

7.4.2.3 Sedimentation in the Vicinity of the Dam

Navigation in the TGP reservoir is unique in that the channel used by the ships is to be gradually shaped by the flow and sedimentation in a long reservoir. The initial equilibrium of the channel would come in
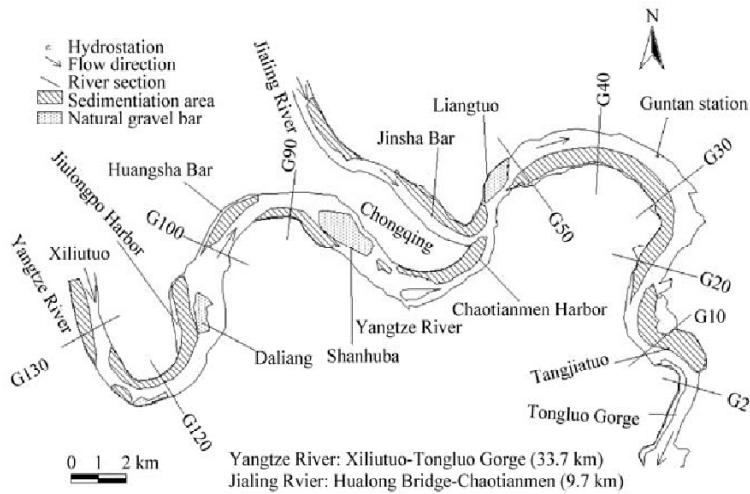
Fig. 7.43 Sedimentation in the Chongqing reach after 80 years of operation of the TGP reservoir. The shadowed areas indicate the places where cumulative sedimentation would occur. G2–G130 represent the measurement cross sections (after Wang et al., 1990)

80 to 100 years. During this period, the thalweg of the channel and the main current of flow would be shifting laterally as the bed rises and flood plains develop along the banks. Near the dam sediment deposits in the area by the right bank and the main flow channel shifts from the middle to the left (Zhou and Lin, 2002). The flow velocity in the approach channel will be affected by the main flow during the flood season after 80 years of operation. Sedimentation in the approach channel also poses a challenge to sediment management in the reservoir.

The layout of the approach channels has to suit a slowly changing flow during the sedimentation period of the reservoir. Due to the heavy deposition of sediment expected in the approaches, methods to clear the approaches are major issues in the selection of the approach layouts. The downstream lock approach is along the left bank and is protected by a dyke 3,550-m long on the right (Fig. 7.44). For the upstream approach, however, both the large tows using the locks and the smaller ships using the lift would share the same approach channel so that the sailing of all ships would be shielded.

Because the reservoir is about 700 km long, it will take a long period of time before the deposition in the vicinity of the dam will become significant. Thereafter, sedimentation would begin to be the factor dominating the morphology of the river reach in the vicinity of the dam, which affects the deposition in upstream approaches and the deposition of sediment in and around them. Great effort has been devoted to the estimation of deposition in the region. Both physical and mathematical models have been applied.

The model tests have shown that when deposition in the dam region increases, particularly when the flood plain at the convex bank on the right at a spot just a short distance upstream of the approach channel grows with time, the main current of the river in front of the dam would be pushed gradually to the left for a distance up to about 290 m. This means that the optimum location of the entrance to the approach channel would also change gradually as deposition in the reservoir proceeds. The optimum location of the entrance to the approach channel is, therefore, a rather important matter. Theoretically, one location of the entrance to the approach channel cannot suit the changing currents and that is why there is the possible need of rebuilding the entrance of the approach channel later at a certain stage of operation. As indicated previously, this is a unique problem arising from navigation in a channel molded in a deep and narrow reservoir by sedimentation.
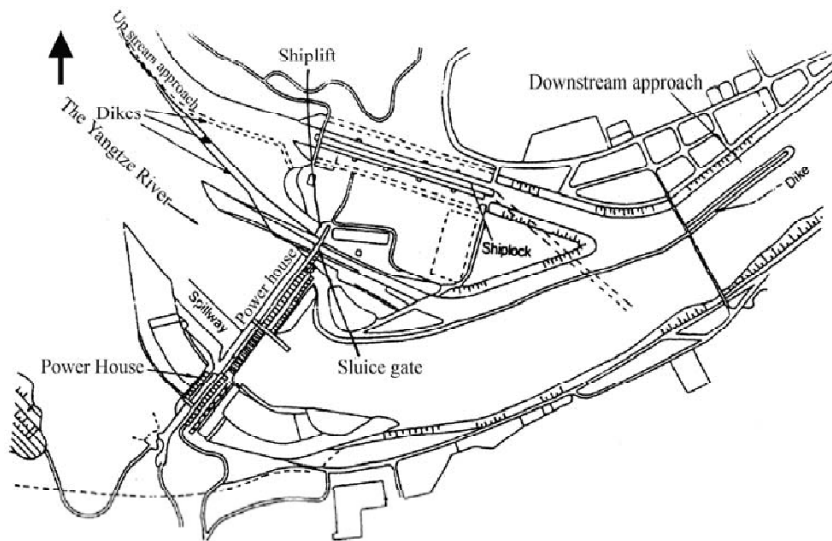
Fig. 7.44 Layout of the upper and lower approach channels, the shiplift, and sluice gate

Undesirable deposition in the approach channels could be cleared off by flushing, complemented by dredging. Regarding the possible hindering of navigation by deposition, the critical time for the upstream approach channel is the flood season, whereas that for the downstream approach channel is the dry season.

As to the downstream approach channel, the tailwater level during flood seasons ranges from 66.8 to 73.7 m, depending on the operation of the Gezhouba Dam, which is 38 km downstream of the Three Gorges Dam, while the bed elevation is 56.5 m. According to research, a part of the sediment flushed from the upstream approach channel would deposit in the downstream approach channel but would not encroach upon the minimum depth of 4 m required for navigation. At the end of the flood season, the water level may be lowered to around 63 m by operate the Gezhouba Dam. Under this low tailwater, deposition in the main parts of the downstream approach channel may be flushed out with the same discharge available for the flushing of the upstream approach channel. Dredging would then be applied to clear out the remnant deposition. Dredging is also required in a part of the river downstream of the lock approach.

7.4.2.4 Degradation of the Downstream Reaches

In the downstream reaches of the Three Gorges and Gezhouba dams, released clear water will scour the riverbed. The monthly mean discharge released from the Three Gorges Reservoir to the downstream reaches is higher than that before the dam from January to May but is less from October to November. In the flood season from July to September the released discharge will remain unchanged. Generally speaking, the sediment-carrying capacity of the flow does not change in the downstream reaches. Figure 7.45 shows the variation process of annual sediment load released from the reservoir to the downstream reaches compared with the annual sediment load at Yichang under natural conditions (recycle of the record in the period 1961–1970). The sediment load to the downstream reaches is greatly reduced by the trapping in the reservoir in the first 50 years. The load reduction must cause degradation of the downstream reaches.

Two 1-D numerical models, IWHR and YVPO, are used to calculate the amount of sediment scoured from the river bed in the reach from Yichang to Wuhan. In the first 40 years the two models yield the same results, about 2.5 billion t at the end of the 20th year and 4 billion t at the end of the 40th year. From the 50th year, however, the two models give different results. The YVPO model predicts the resiltation of
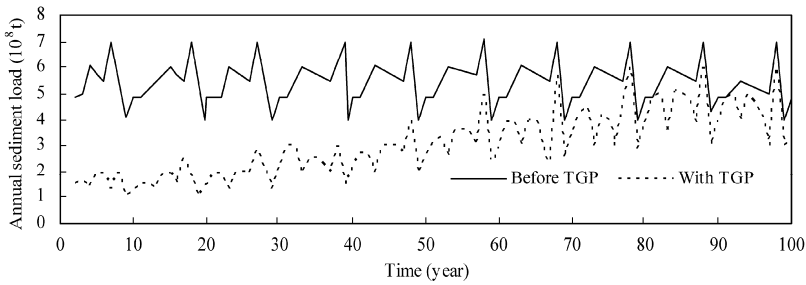
Fig. 7.45 Variation process of annual sediment load released to the downstream reaches from the reservoir compared with the annual sediment load at Yichang under natural conditions (recycle of the data in the period 1961–1970) (Sedimentation Panel for TGP, 2002)

the reach beginning from the 50th year but the IWHR result shows resiltation from the 70th year. The difference in the scoured volume in the period 70th–100th year of operation is about 1.2 billion t. The flood stage will reduce by 3 m at Shashi and 0.75 m at Wuhan for a flood of discharge 30,000 m³/s.

7.4.3 Environmental and Social Impacts

7.4.3.1 Earthquakes

Although human construction of large dams has a history of several thousand years the study of reservoir-induced earthquakes began only decades ago. To date, no one can give a complete and accurate answer to the question about the formation mechanism and the process of earthquakes since mankind's knowledge on the subject is limited. Nevertheless, some insight has been acquired into the general laws governing the formation of earthquakes and their potential damage.

Up to now the world has not witnessed the destruction of a dam caused by a reservoir-induced earthquake. Even the two most severe quakes set off in such circumstances, one in India and the other in China's Xinfengjiang River Reservoir, caused only slight damage to the dams. They had magnitudes of 6.5 and 6.1, respectively, on the Richter scale and an intensity of 8 at the epicenter. Following partial repairs and reinforcement, the dams resumed normal operation. Most other reservoir induced earthquakes have been under a magnitude of 4 on the Richter scale and all occurred soon after a reservoir was filled with water. With the gradual adjustment of stress on structures over time, the tremors have died away.

The salient point is that not every reservoir inevitably causes earthquakes. According to incomplete statistics, only about 100 reservoirs, or 0.1 percent of the world total, have brought about earth quakes. The figures from the United States Dam Committee indicate that only 0.7 percent of large reservoirs have the potential to cause earthquakes of any practical significance. China's statistics show that only 5 percent of its reservoirs each with a storage capacity of more than 100 million m³ of water have set off tremors. After the impoundment of the reservoir since 2002, no earthquake of practical importance has occurred.

7.4.3.2 Landslides

Impoundment of reservoirs often induces landslides. The Three Gorges Project may cause large-scale collapse of the reservoir banks. Studies on the stability of the reservoir slopes have been going on for several decades with various advanced ways and means, such as aerial remote sensing, surge wave model testing and calculations, analysis of stability, sensitivity and deformation monitoring. The studies have yielded similar results in terms of the number and magnitude of collapses and landslides. Landslides in the fluctuating backwater region may be initiated in the first 10–20 years of operation of the dam because the pool level varies in the range of 145–175 m. If the pool level is drawn down abruptly for flood control

the slope soil saturated with water has in sufficient time to dewater and may slide down to the river.

There are about 1,000 potential landslides in the Three Gorges area, of which 140 landslides and rockfalls each measure 1 million m^3 or more in size. Along the 1,300 km-long banks there are 22 large slopes that are unstable or may slide down once the reservoir is filled with water. These slopes vary in size from several million to 80 million m^3. However, after 10–20 years of operation, most of the potential landslides will become stable again. The overall stability conditions of the slopes of the Three Gorges Reservoir are basically firm.

Studies have indicated that any collapse of slopes that might occur after the Three Gorges Reservoir if silled, would not clog the Yangtze River nor form a blockage. The total mass of the 22 unstable slopes is only 380 million m^3. Even if the entire bulk slides into the reservoir, it will only fill up 2.2 percent of the reservoir at the 145-m water level.

7.4.3.3 Impact on Local Climate

It was estimated in the planning of the project that any change induced by the reservoir on the climate of the surrounding areas would be negligible. The average annual wind velocity would increase by 15%–40% and the relative humidity may rise by 2%–8% in the reservoir. Any impact on the frequency of foggy days, or volume and distribution of rainfall would be slight. Summer temperature might drop slightly by 0.9 to 1.2℃ on a monthly basis, but in winter the temperature might rise slightly by 0.3℃ to 1.3℃, with the minimum temperature up to 3℃.

In the first three years after the impoundment of the reservoir in 2002 there was no obvious climate change. In 2006, however, a severe drought, the worst in 100 years, occurred in Chongqing municipality and Sichuan Province. At least 14 million people and 15 million livestock suffered from a shortage of drinking water as continuous droughts and searing heat ravaged the area. Some scientists blamed the Three Gorges Project for the severe drought. The Sichuan and Chongqing Basin is enclosed by mountains and the main moisture flow path is the Yangtze River valley linking central China and the basin. The Three Gorges Dam has blocked the moisture inflow. Thus, the precipitation in the basin has been reduced greatly.

Meteorological experts said that there is no relation between the severe drought and the Three Gorges Project. The global greenhouse effect is the chief reason for droughts, especially in upper latitude regions of the northern hemisphere. Chongqing Municipality and Sichuan Province, the worst-hit areas, are located in these regions. According to the experts, the global greenhouse effect had led to rising temperatures, abnormal climate change and severe drought. The direct reason for the drought is the impact of abnormal air movements over the Qinghai–Tibet Plateau. Caused by booming human activities, deforestation and industrial projects in urban areas, the heat island effect around big cities also plays a role in producing the hot weather and rising temperatures. The heat island effect around Chengdu, capital of the Sichuan Province, and Chongqing has partly led to a dry summer and a lack of rainfall. According to experts at meteorological stations in Sichuan and Chongqing, constant typhoons, which landed in coastal areas in southern and eastern China in the summer in 2006, have prevented the entry of cold air fronts into the Sichuan Basin. Without cold air, the basin is covered solely by high-pressure currents and has no chance to produce rainfall.

7.4.3.4 Water Quality

The annual runoff at the dam is over 400 billion m^3; and the total wastewater discharged into the reservoir is about 1 billion tons. Now the water quality of the river, however, remains good, except for pollution belts along the banks near cities. Generally speaking, after impoundment the pollution in the reservoir worsened to some extent due to lower flow velocity and higher water level. Therefore, it is necessary to strictly control the discharge of wastewater from surrounding factories, mines, towns and cities, and to treat

wastewater before discharge into the river. At a press conference on June 5, 2003, the State Environment Protection Bureau reported that the impoundment of the TGP Reservoir would not obviously affect the water quality. The water quality in the reservoir is mostly still in Grade III in the Chinese water quality standards. Only in some places, the content of bacilli is high. A pollution control project was launched in 2002. All wastewater and sewage water will be treated after the completion of the project (Chinese Hydroweb, 2003).

Thermal stratification in the reservoir begins around April and ends in May. The water released from the bottom outlets in this period is colder than that before the dam, which may cause a 20 day delay in the temperature of downstream water rising to the spawning temperature of 18℃. On the other hand, the regulated flow is of benefit for control of snail fever. The area downstream of the dam, especially Tongting Lake and surrounding areas, has suffered from an infectious disease know as snail fever for which *oncomelania* is the intermediate host for a long time. With the impoundment of the reservoir, the artificial fluctuation of water levels makes it hard for such snails to breed. In addition, the alleviation of flooding along the river's middle and lower reaches makes it easier to eliminate the snails in swamp areas.

7.4.3.5　Fishes and Fishery

There are more than 300 fish species in the middle and lower Yangtze River, including catfish, bleak, and carp. After the impoundment, the freshwater fishes that thrive in rapids have to move upstream to find new habitats. The expanded water surface of the reservoir creates better conditions for aquatic farming in the river and its tributaries. The spawning grounds located in the reservoir section are inundated in part or in whole. The farm breeding of fishes has to be moved to the uppermost end of the reservoir or even farther.

There are four species of carp in the Yangtze River that have the most importance to the fresh water fishery. They are the black carp (Mylopharyngodon piceus), the grass carp (Ctenop haryngodon idellus), the silver carp (Hypophthal michthys molitrix), and the big-head carp (Aristichyths nobilis). Figure 7.46 shows 28 major spawning sites of the four carp species in the Yangtze River. Seven spawning sites have been inundated by the impoundment and the rest are affected by the regulated flow. Flood and stage rise are the main signals for the species to spawn (Yi and Liang, 1964).
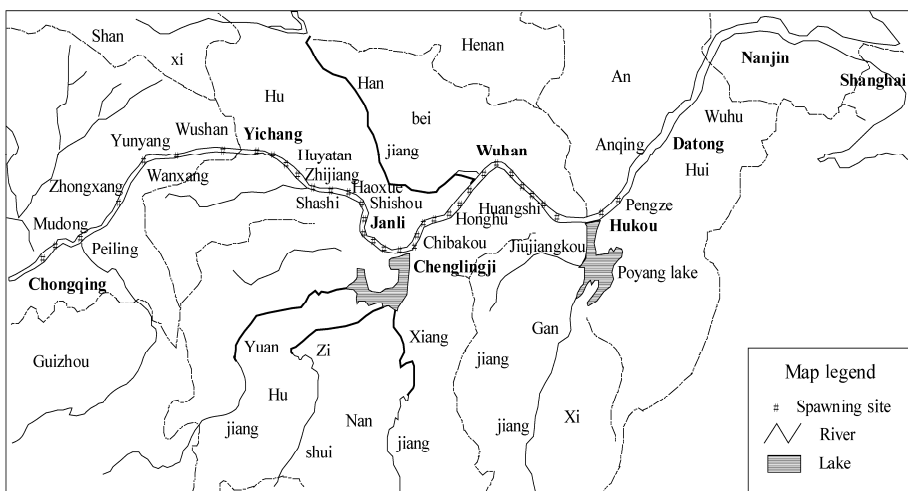
Fig. 7.46　Spawning sites of the four major Chinese carp species in the Yangtze River
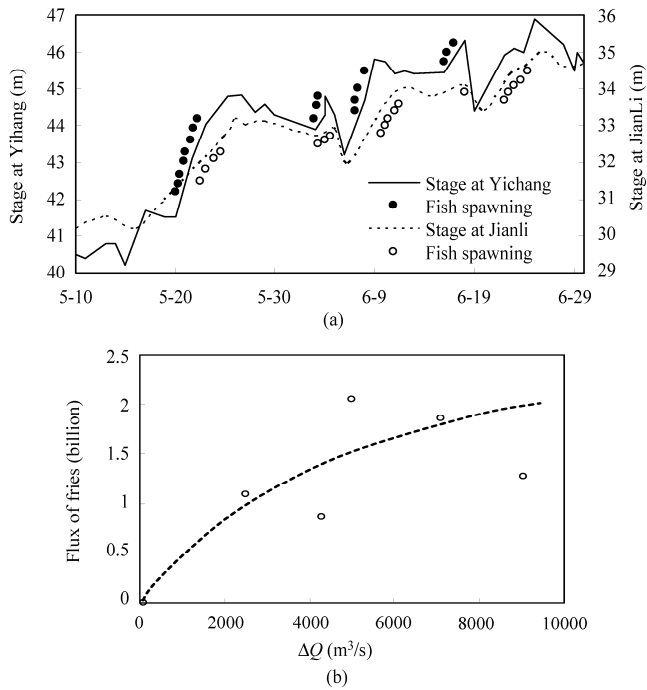
Fig. 7.47 (a) Stage variation at Yichang and Jianli under natural conditions and the spawning time of the Chinese carp; (b) Relation between the discharge increment and flux of fries (after Cao et al., 1987)

Figure 7.47(a) shows the stage variations at Yichang and Jianli and the time of fish spawning, in which the solid circles represent spawning of fishes (Cao et al., 1987). Figure 7.47(b) shows the relation between the discharge increment in a few to ten days and the flux of the fish fries, in which the flux of fries lags about 4–6 days behind the discharge increase. The figures demonstrate that the spawning of the fishes is excited by the stage and discharge increase. The higher the discharge increase, the higher the flux of fries will be. The TGP Reservoir regulates the runoff and especially moderates the stage rise and discharge increase in May, which affects the spawning of fishes and reduces the flux of fries. Now artificial spawning and hatching has successfully solved the problem. The effects of the impoundment on fisheries have been mitigated to a minimum.

7.4.3.6 Endangered Aquatic Species

There are several important species in the river, Chinese sturgeon, white-flag dolphin, Yangtze alligator, giant salamander, and the black finless porpoise are several among them. The reservoir has little impact on the living conditions of the Yangtze alligator, giant salamander, and black finless porpoise. Chinese sturgeon usually swim upstream to spawn and then return to their home grounds. The Gezhouba Dam has made it impossible for the fish to swim up and down the river during the spawning period. But the sturgeon has spawned naturally in the waters below the dam. Artificially induced breeding of fry has also been successful.

The white-flag dolphin usually lives in meandering and braided sections below the TGP Dam. Studies indicate that the species finds its best habitats in meandering and braided-meandering sections because it has been accustomed to the backwater zones created by the convex bank of meanders or the gravel and sand bars in the braided channels (Chen and Hua, 1987). The regulation of the flow by the reservoir and

the riverbed erosion resulting from the sediment-starved flow may change the fluvial processes and some meandering and braided sections of the river may become unstable, which may undermine the habitats of the species. More studies are needed for protection of the white-flag dolphin.

7.4.3.7 Resettlement

If the reservoir water level rises to 175 m, a total of about 1.2 million people in 19 counties have to be dislocated. Production facilities are inundated including 23,793 ha of farmland (paddy fields: 7,380 ha, and dry farmland: 16,314 ha), and 4,960 ha of citrus orchards. Moreover, 956 km of highways and 941 factories and mines are inundated as well. Eleven county towns and 107 towns have been moved to new sites.

Resettlement of the people in the submerged area started from 1989. The basic policy is to resettle most of these people in the surrounding areas. The submerged and surrounding areas are densely populated and poorly developed. In the areas to be settled the Gross Domestic Product (GDP) per capita is only 45% of the national average and the income per capita is only 53% of the national average. There is a lot of room to develop local industry and the tourism industry. More than 80,000 dams have been built in China and 10 million people have been dislocated. The government is carrying out a development resettlement policy. The basic point is to change over from one time compensation for settlers at once to overall arrangements for their production and living conditions for a long term.

There are about 2.7 million ha of barren hillside land within the territory of the 19 counties, more than 1% of which, or about 27,000 ha can be cultivated and utilized (Chen and Zhou, 1987). Experiments in the reservoir area indicate that the barren slope-land may be transformed into terraced citrus orchards, and then it is possible to produce an output value equal to as much as three times that of the original farmland. Thus, the surrounding area is able to support most of the resettled farmers. Moreover, the reservoir has a water surface of 67,000 ha for aquatic farming, which is a high production resource.

The resettled people are also encouraged to settle in other provinces at their choice. The State Council has made a decision that all provincial governments should provide assistance for emigration and resettlement. A number of economically developed provinces and municipalities have made agreements with the counties in the reservoir area to assist the resettlement. Many people have found their homes in lower reaches of the Yangtze River, Chongming Island at the river mouth, the Xinjiang Uygur Autonomous Region, Hainan, Heilongjiang, and other provinces.

Figure 7.48(a) shows the new houses in the area by the reservoir for the resettled people and Figure 7.48(b) shows the new county town of the Kaixian. Of the total population to be displaced, urban dwellers

(a)   (b)

Fig. 7.48 (a) New village constructed on the slope higher than 185 m around the reservoir for resettlement of people from the submerged area; (b) Newly constructed Kaixian county town (the old Kaixian town has been inundated by the reservoir water) (See color figure at the end of this book)

make up about 54 percent. Urban employees may continue in the same jobs. Working positions are needed for about 300,000 people who were from rural areas. Resettlement funds are to be allocated in advance to the settlement areas for construction and education. Losses from inundation are to be compensated by earmarking a proportion of the income to be derived from power generation after the project has yielded economic returns, which will be used as funds for economic development in the reservoir areas. Food supply for the affected people will be guaranteed and regularly subsidized to offset possible price differentials between state-rationed and marked-supplied food. Taxes are to be reduced or exempted, and enterprises will be allowed to retain a bigger share of their foreign exchange earnings. Loans, which can be repaid before taxes, will be granted for the reservoir area's economic development.

Review Questions

1. When thermal stratification occurs in reservoirs?
2. What is overturn? How does it affect reservoir ecology?
3. How do benthic invertebrates respond to impoundment?
4. What are effects of river impoundment on fish?
5. What are the five patterns of reservoir sedimentation?
6. What are the strategies for reservoir sedimentation management?
7. What are the factors affecting dam failure?
8. Why dams are removed in the USA?
9. What are the purposes of the Three Gorges Project?
10. What are the sediment problems in the TGP reservoir management?
11. What are the management strategies mitigating TGP reservoir sedimentation?
12. What are the environmental, ecological, and social impacts of the TGP project?
13. What measures can we take to mitigate the ecological impacts of the TGP reservoirs?
14. What are the impacts of dam removal on environment and ecology?

References

American Water Works Association, 1971. Quality control in reservoirs. Journal of the American Water Works Association, 63, 597–604

Armitage P.D., 1978. Downstream changes in the composition, number and biomass of bottom fauna in the Tess below Cow Green Reservoir and an unregulated tributary Maize Beck, in the first five years after impoundment. Hydrobiologia, 58, 145–156

Armitage P.D., 1979. Stream regulation in great Britain. in The Ecology of Regulated Streams, Ward J.V. and J.A. (eds)., Stanford Plenum Press, New York, 165–182

Arumugam P.T. and Furtado J.I., 1980. Physico-chemistry, destratfication and nutrient udet of a lowland eutrophicated Malaysian reservoir and its limnological implications. Hydrobiologia, 70, 11–24

Attwell R.I., 1970. Some effects of Lake Kariba on the ecology of a floodplain of the Mid-Zambezi Valley of Rhodesia. Biological Conservation, 2(3), 189–196

Banks J.W., Holden M.J. and McConnell R.H., 1965. Fishery report in The First Scientific Report of the Kainji Biological Research Team, WhiteE. (ed.), Unpublished report of the Ministry of Overseas Development, London, 21–42

Beiningen K.T. and Ebel W.J., 1970. Effect of John Day Dam on discharged nitrogen concentrations and salmon in the Columbia River. Transaction of the American Fisheries Society, 4, 664–671

Bell H.S., 1947. The effect of entrance mixing on the size of density currents in Shaver Lake. Trans actions, American. Geophysical, Union, 28(5), 780–791

Blake R.F., 1977. The effect of the impoundment of Lake Kainji, Nigeria, on the indigenous species of mormyrid

fishes. Freshwater Biology, 7(1), 37–42

Briggs J.C., 1948. The quantitative effects of a dam upon the bottom fauna of a small California stream. Transactions of the American Fisheries Society, 78, 70–81

Brooks A.J. and Woodward W.B., 1956. Some observations on the effects of water inflow and outflow on the plankton of small lakes. Journal of Animal Ecology, 25, 22–25

Brooks N.H. and Koh R.C.Y., 1969. Selective withdrawal from density stratified reservoirs. Journal of the Hydraulics Division, ASCE, 95, (HY4), 1369–1400

Cao W.X., Yu Z.T., Xu Y., Deng Z. and CaiM., 1987. Impacts of the three gorge project on aquatic ecosystems along the Changjiang River and possible countermeasures, in Environment and Ecology Panel of Chinese Academy of Sciences for the TGP Project (eds.), Impacts of the Yangtze River Three Gorges Project on Environment and Ecology, Chinese Science Press (in Chinese)

Chad B.F., 1995. Anthropological Impact on global heodymanics fue to teservoir eater impoundment

Chen H.Z. and Zhou H.Z., 1987. Effects of the Three Gorge Project on the land resources in the reservoir area and possible countermeasures, in Environment and Ecology Panel of Chinese Academy of Sciences for the TGP Project (eds.), Impacts of the Yangtze River Three Gorges Project on Environment and Ecology, Chinese Science Press (in Chinese)

Chen P.Z. and Hua Y.Y., 1987. Impacts of the Three Gorge Project on white-flag dolphin and species protection. Chinese Science Press, 31-34 (in Chinese)

Chien N., Wan Z.H. and McNown J., 1998. Mechanics of Sediment Movement, ASCE Press, United States

Chinese Hydro-Web, 2003. http://www.Chinawater.com, on March, 2, 2003 (in Chinese)

Churchill M.A. and Nicholas W.R., 1967. Effects of impoundments on water quality. Journal of the Sanitary Engineering Division, ASCE. 93, (SA6), 73–90

Décamps H., Capblancq J., Casanova H. and Tourenq J.M., 1979. Hydrobiology of some regulated rivers in the South-West of France. in The Ecology of Regulated Streams, Ward J.V. and Stanford J.A. (eds.)., Plenu, Press, New York, USA, 273–288

Derby R.L., 1956. Chlorination of deep reservoirs for taste and odor control. Journal of the American Water Works Association, 48(7), 775–780

Devine R.S., 1995. The Trouble With Dams. Atlantic Monthly, August 1995

Dominy C.L., 1973. Recent changes in Atlantic Salmon (Salmo salar) in the light of environmental changes in the Saint John River. New Brunswick, Canada. Biological Conservation, 5(2), 105–113

Dudley R.G., 1974. Growth of Tilapia of the Kafue floodplain, Zambezi: Predicted effects of the Kafue Gorge Dam. Transactions of the American Fisheries Society, 103, 281–291

Dynesius M. and Nilsson C., 1994. Fragmentation and flow regulation of river systems in the Northern third of the world. Science, 266, (5186), 753–762

Edwards R.J., 1978. The effect of hypolimnion releases on fish distribution and species diversity. Transactions of the American Fisheries Society, 107, 71–77

Elder R.A. and Wunderlich W.O., 1968. Evaluation of Fontana Reservoir field measurements. in Proceedings of the Specialty Conference on Current Research into the Effects of Reservoirs on Water Quality Elder R.A., Krenkel P.A., Thackston E.L., (eds.), Technical Report 17, Department of Environment and Water Resources Engineering, Vanderbilt University, Nashville, Tennessee, 221–286

El-Zarka. and El-Din S., 1973. Kainji Lake, Nigeria. in Man-Made Lakes: Their Problems and Environmental Effects Ackermann W.C., White G.F., Worthington E.R., (eds.), Geophysical Monograph 17, American Geophysical Union, Washington, Dc, 197–219

Fan J. and Morris G.L., 1992a. Reservoir sedimentation I: Delta and density current deposits. Journal of Hydraulic Engineering, 118(3), 354–369

Fan J. and Morris G.L., 1992b. Reservoir sedimentation II: Reservoir desiltation and long-term storage capacity. Journal of Hydraulic Engineering, 118(3), 370–384

Fan J.H., 1985. The reservoir sediment problem. Journal of Hydraulic Engineering, 24–31 (in Chinese)

Fan J.H. 1959. Experimental study of density currents. Journal of Hydraulic Engineering, (5), 30–48.

Fell R., Bowles D.S., Anderson L.R. and Bell G., 2000. The status of methods for estimation of the probability of failure of dams for use in quantitative risk assessment. Proc. International Commission on Large Dams 20th Congress, Beijing, (in Chinese)

Ford M.E., 1963. Air injection for control of reservoir limnology. Journal of the American Water Works Association,

55, 267–274

Foroods. and Ghafouiri M., 2007. Assessment of causes and effects of disastrous erosion and sediment flows and mitigation measures in Caspian Sea Watersheds-Iran, Proceedings of UNESCO Expert Meeting on Erosion in Arid and Semi-Arid Areas, Chalooz, Iran

Fraser J.C., 1972. Regulated discharge and the stream environment, in River Ecology and Man Oglesby R.T., Carlson C.A. and McCann J.A. (eds.)., Academic Press, New York, 26–85

Fruh E.G. and Clay H.M., 1973. Selective withdrawal as a water quality management tool for southwestern impoundments. in Man-Made Lakes: Their Problems and Environmental Effects Ackermann W.C., white G.F. and Worthington E.R. (eds.)., Geophysical Monograph 17, American Geophysical Union, Washington, DC, 335–341

Furness H.D., 1978. Ecological Studies on the Pongola River Floodplain. Working Document IV, Workshop on Man and the Pongolo Floodplain. C. I. S. R., Pietermaritzburg, South Africa, 14/106/7C

Ganapati S.V., 1973. Man-made lakes in South India. in Man-made Lakes: Their Problems and Environmental Effects Ackermann W.C., white G.F. and Worthington E.B. (eds.)., Geophysical Monograph 17, American Geophysical Union, Washington, DC, 65–73

Garcia M.H., 1994. Depositional turbidity currents laden with poorly sorted sediment. Journal of Hydraulic Engineering, 120, 1240–1263

Garton J.E., Rice C.E. and Steichen J.M., 1976. Modification of reservoir water quality by artificaial destratification. Annals of the Oklahoma Academy of Science, 5, 47–56

Gibbs R., 1970. Mechanisms controlling world water chemistry, Science, 170, 1088–1090

Gill D., 1971. Damming the Mackenzie: A theoretical assessment of the long-term influence of river impoundment on the ecology of the Mackenzie River Delta, in Proceedings of the Peace-Athabaska Delta Symposiu, Water Resources Centre, University of Alberta, Edmonton, Alberta, Canadg, 204–222

Gore J.A., 1978. A technique for predicting in-stream flow requirements of benthic macroinvertebrates. Freshwater Biology, 8, 141–151

Gore J.A., 1980. Ordinational analysis of benthic communities upstream and downstream of a prairie storage reservoir. Hydrobiologia, 69, 33–44

Guo Z.G., Zhou B., Ling L.W. and Li D.G., 1985. The hyperconcentrated flow and its related problems in operation at Hengshan Reservoir, Proc. Intern. Workshop on Flow at Hyperconcentrations of Sediment, 3-1

Hannan H.H. and Broz L., 1976. The influence of deep-storage and an underground reservoir on the physico-chemical limnology of a permanent central Texan river. Hydrobiologia, 51, 43–63

Hannan H.H., 1979. Chemical modifications in reservoir-regulated streams. in The Ecology of Regulated Streams Ward J.V. and Stanford J.A., (eds.), Plenum Press, New York, USA75-79

He X.Y., Wang Z.Y. and Huang J.C., 2008. An analysis on the temporal and spatial distributions of dam failures in China. International Journal of Sediment Research, 23(4), 398–405

Heath W.A., 1961. Compressed air revives polluted Swedish lakes. Water and Sewage Works, 108, 200

Henricson J. and Muller K., 1979. Stream regulation in Sweden with some examples from Central Europe. In: The Ecology of Regulated Streams, Ward J.V. and Stanford J.A. (eds.), Plenum Press, New York, USA, 183–200

Hergenrader G.L., 1980. Eutrophication at the Salt Valley Reservoir, 1968–1973. In: The effects of eutrophication of standing crop and composition of phytoplankton. Hydrobiologia, 71, 71–82

Hill P., Bowles D., Jordan P. and Nathan R., 2003. Estimating overall risk of dam failure: Practical considerations in combining failure probabilities. ANCOLD 2003 Risk Workshop, 1–10

Hilsenhoff W.L., 1971. Changes in the downstream insect and amphipod fauna caused by an impoundment with a hypolimnion drain. Annals of the Entomological Society of American, 64, 743–746

Hou S.Z. and Jiao E.Z., 2003. Analysis on turbidity currents in the Xiaolangdi Reservoir. Water Resources and Hydropower Engineering, 34(6), 11–14 (in Chinese)

http://www.irn.org/ revival/decom/brochure/rrpt2.html, 2007

Huang CT. 1998. Guidebook for flood control in China. Beijing: Liberation Army Press.

Hynes H.B.N., 1955. Distribution of some freshwater Amphipoda in Britain. Verandlungen Internationale Vereinigung fur Theoretische und Angewandte Limnologie, 12, 620–628

Hynes H.B.N., 1970. The Ecology of Running Waters, Liverpool University Press, Liverpool, England, UK

ICOLD (International Commission on Large Dams), 1988. World Register of Dams, Annual Report, Paris, 9, 21, 62, 109

Ingols R.S., 1959. Effect of impoundment on downstream water quality, Catawba River. S.C. Journal of the American Water Works Association, 51, 42–46

International Water Power, 1995. Dam Construction Handbook 1995, IWPDC, Sutton, UK, 1995

IRTCES (International Research and Training Center on Erosion and Sedimentation), 1985. Lecture notes of the training course on reservoir sedimentation. Series of publication, Beijing, China

Irwin W.H., Symons J.M. and Robeck G.G., 1966. Impoundment destratification by mechanical pumping. Journal of the Sanitary Engineering Division, ASCE, 92(6), 21–40

Jackson P.B.N. and Rogers K.H., 1976. Cabora Basin fish populations before and during the first filling phase. Zoologica Africana, 11(2), 373–397

Jacobs W., Van Kesteren W.G.M. and Winterwerp J.C., 2007. Permeability and consolidation of sediment mixtures as function of sand content and clay mineralogy. International Journal of Sediment Research, 3, 180–187

Jia J.S., Yuan Y.L. and Li T.J., 2004. China's and world's large dams in 2003. China Water Resources, 13, 25–33 (in Chinese)

Jiao E.Z., Miao F.J., Lin X.Z., 2008. Water and sediment management with reservoirs. Yellow River Press, 1–230 (in Chinese)

Kinawy I.Z., Wafa T.A., Labib A.H. and Shenouda W.E., 1973. Effects of sedimentation in the High Aswan Dam Reservoir, in Transactions of the Eleventh International Congress of Large Dams, Madrid, Spain, Vol.1. International Commission on Large Dams, Paris, France, 878–898

Kron W., 2005. Flood risk = hazard·values·vulnerability. Water International, 30(1), 58–68

Lehmann C., 1927. Uber den einfluss der talspeuen auf die unterhalb liegende bachand flussfischerei. Zeitschrift fur fischerei und deren Hilfswissenschaften, 25, 467–476 (in German)

Lehmkuhl D.M., 1972. Change in thermal regime as a cause of reduction of benthic fauna downstream of a reservoir. Journal of the Fisheries Research Board of Canada, 29, 1329–1332

Lelek A. and El-Zarka S., 1973. Ecological comparison of the pre-impoundment and post-impoundment fish fauna of the River Niger and Kainji Lake, Nigeria. in Man-Made Lakes: Their Problems and Environmental Effects, Ackermann W.C., White G.F., Worthington E.B. (eds.), Geophysical Monograph 17, American Geophysical Union, Washington, 655–690

Lillehammer A. and Saltveit S.J., 1979. Stream regulation in Norway, in The Ecology of Regulated Streams, Ward J. V. and Stanford J.A. (eds.), Plenum Press, New York, 201–214

Liu C., Sui J.Y. and Wang Z.Y., 2008. Sediment load reduction in Chinese rivers. International Journal of Sediment Research, 23(1), 44–55

Lkwis D.S.C., 1974. The effects of the formation of Lake Kainji (Nigeria) upon the indigenous fish population. Hydrobiologia, 45(2–3), 281–301

Lou W.C., 1981. Mathematical modeling of earth dam breaches, Ph.D. Dissertation, Colorado State University, Fort Collins, CO

Lowe J. and Fox I., 1995. Sediment management schemes for Tarbela Reservoir, USCOLD Annual Meeting 1995

Lu M.X., 1981. A preliminary investigation on the fluvial processes of the changing backwater effect reach of Han River in Danjiangkou Reservoir. Yangtze River Water Conservancy and Hydroelectric Power Res.Inst., Pp. 29 (in Chinese)

Luo C.Z. and Luo J.X., 1996. Major flood disasters in China, China Bookstore (in Chinese)

McClure R.G. and Stewart K.W., 1976. Life cycle and production of the mayfly Choroterpes (Neochoroterpes) mexicanus Allen (Ephemeroptera: Leptophlebiïdae). Annals of the Entomological Society of America, 69, 134–144

McCully 1999. Silenced Rivers-The Ecology and Politics of Large Dam, Zed Books, London

Melching C.S., 2006. Dam removal in the United States, Lecture notes for Ph. D. Students, Tsinghua University, Beijing

Minckley W.L., 1964. Upstream movements of Gammarus in Doe Run, Kentucky. Ecology, 45, 185–197

Minckley W.L. and Deacon J.C., 1968. Southwestern fishes and the enigma of endangered species, Science, 159, 1424–1432

Ministry of Water Resources of China, 1999. 1998 floods in China. Water and Hydropower Press (in Chinese)

Morris G.L. and Fan J.H., 1998. Reservoir sedimentation handbook: design and management of dams, Reservoirs, and Watersheds for Sustainable Use. McGraw-Hill, New York

Morris G.L., Annandale G. and Hotchkiss R., 2008. Reservoir sedimentation, in Garcia M.H. ed. Sedimentation Engineering, Published by American Society of Civil Engineering

Motwani N.P. and Kanwai Y., 1970. Fish and fisheries of the coffer-dammed right channel of the River Niger at Kainji. in Kainji Lake Studies, 1: (Ecology) Visser, S.A. (ed.), University of Ibadan press Ibadan, Nigeria, 24–48

Mullan J.W., Starostka V.J., Stone J.L., Wiley R.W. and Wiltzius W.J., 1976. In Instream Flow Needs, Vol. II, Orsborn J. F. and Allman C.H. (eds.), American Fisheries Society, Bethesda, Maryland, USA, 405–423

MWR (Ministry of Water Resources of China), 2007. China Gazette of River Sedimentation 2006. China Water Resources Press (in Chinese)

MWR (Ministry of Water Resources of China), 2008. China Gazette of River Sedimentation 2007. China Water Resources Press (in Chinese)

MWRC (Ministry of Water Resources of China). 1981. Lessons from "63.8" and "75.8" dam failure incidents, Report of Ministry of Water Resources of China.

Odum E.P., 1969. The strategy of ecosystem development. Science, 164, 262–270

Okada Tsuyoshi., Baba Kyohei., 1982. Sedimentation and slope stability.Technical and environmental effects. General Report, Q.54, Trans.14th ICOLD, 3, 639–669

Paerl H.W., 1988. Nuisance phytoplankton blooms in coastal, estuarine, and inland waters, Limnology and Oceanography, 33(4, Part 2), 823–847

Pan J.Z. and He J., 2000. China dam construction in the past 50 years. Chinese Water and Hydro-power Press, Beijing, China (in Chinese)

Pearson W.D. and Franklin D.R., 1968. Some factors affecting drift rates of Baetis and Simuiidae in large rivers. Ecology, 49, 75–81

Peňáz M., Kubícek F., Marvan P. and Zelinka M., 1968. Influence of the Vír River Valley Reservoir on the hydrobiological and ichthyological conditions in the River Svratka. Acta Scientiarum Naturalium, Academiae Scientiarum Bohemoslovacae-Brno, 2, 1–60

Petts G.E., 1984. Sedimentation within a regulated river: Afon Rheidol, Wales. Earth Surface Processes and Landforms, 9(2), 125–134

Pfitzer D.W., 1954. Investigation of waters below storage reservoirs in Tennessee. Transactions of the North American Wildlife Conference, 19, 271–282

Radford D.S. and Hartland-Rowe R., 1971. A preliminary investigation of bottom fauna and invertebrate drift in an unregulated and a regulated stream in Alberta. Journal of Applied Ecology, 8, 883–903

Riddick T.M., 1957. Forced circulation of reservoir waters. Water Sewage Works, 104(6), 231–237

Rogers H.H., Raynes J.J., Posey F.H. and Ruland W.E., 1973. Lake destratification by underwater air diffusion. in Man-made Lakes: Their Problems and Environmental Effects Ackermann W.C., White, G.F. and Worthington, E.B. (eds.), Geophysical Monograph 17, American Geophysical Union, Washington, DC, 572–577

Rzoska J., Brooks A.J. and Prowse G.A., 1955. Seasonal plankton development in the White and Blue Nile near Khartoum. Verhandlungen Internationale Vereinigung fur Theoretische und Angewandte Limnologie, 12, 327–334

Schmitz W.R. and Hasler A.D., 1958. Artificially induced circulation of lakes by means of compressed air. Science, 128 (3331), 1088–1089

Scullion I.J., 1982. Fish community structures and function along two habitat gradients in a headwater stream. Ecological Monographs, 52(4) 394–414

Sedimentation Panel for TGP, 2002. Comprehensive analysis on 9.5 sedimentation study results for the Three gorges Project on the Yangtze River. Intellectual Copyright Press (in Chinese)

Song, E.L. 2000. Reasons of several dam failures in China. Dam and Safety, (2), 41–44.

Sreenivasan A., 1977. Fisheries of the Stanley Reservoir (Mettur Dam) and three other reservoirs of Tamolnadu, India: A case history. Proceedings of the IPFC Symposium on the Development and Utilization of Inland Fishery Resources, Colombo, Sri Lanka, October 1976 J.A. (eds.), Dunn, I. (eds.), FAO Regional Office for Asia and the Far East, Bangkok, Thailand, 17, 27–79

Stanford J.A. and Ward J.V., 1979. Stream regulation in North America, in the Ecology of Regulated Streams, Ward J.V. and Stanford J.A. (eds.) Plenum Press, New York, USA: xi 398, 215–236

Symons J.M., Werbel S.R. and Robeck G.G., 1965. Impoundment influences on water quality. Journal of the American Water Works Association, 57(1), 51–75

Tarzwell C.M., 1939. Changing the Clinch River into a trout stream. Transactions of the American Fisheries Society, 68, 228–233

TCGRD., 1997. American Society of civil engineers published the guidelines for retirement of dams and hydroelectric facilities in 1997

Trotzky H.M. and Gregory R.W., 1974. The effects of water flow manipulation below a hydroelectric power dam on the bottom fauna of the upper Kennebec River, Maine. Transactions of the American Fisheries Society, 103, 318–324

Turner R.M. and Karpiscak M.M., 1980. Recent vegetation changes along the Colorado River between Glen Canyon Dam and Lake Mead, Arizona. U.S. Geological Survey Professional 1132, p.125

Vollenweider R.A., 1968. Scientific Fundamentals of the Autotrophication of Lakes and Flowing Waters with Particular References to Nitrogen and Phosphorus as Factors in Eutrophication. Technical Report OAS/CS1/68.27, OECD, Paris France, p.159

Walker K.F., 1979. Regulated streams in Australia: The Murray-darling River system. in The Ecology of Regulated Streams Wardm J.V. and Stanford J.A. (eds.), Plenum Press New York, 143–164

Wang Z.Y. and Hu C.H., 2009. Strategies for managing reservoir sedimentation. International Journal of Sediment Research, 24(4), 369–384

Wang Z.Y. and Zhang X.Y., 1985. Experimental study of empty flushing of cohesive sediment from a reservoir with a physical model. Journal of Sediment Research, 2, 62–69 (in Chinese)

Wang Z.Y., Lu X.Z. and Zeng Q.H., 1990. Physical model experimental study on sedimentation in the Chongqing reach of the Yangtze River for the Three Gorges Project-a report for the 175 m scheme, in the collection of research results on the sedimentation in the Chongqing reseach of the Yangtze Reiver, China Institute of Water Resources and Hydro-Power Research, Beijing (in Chinese)

Ward J.V., 1974. A temperature-stressed ecosystem below a hypolimnial release mountain reservoir. Archiv fur Hydrobiologie, 74, 247–275

Ward J.V., 1976. Effects of flow patterns below large dams on stream benthos. in Instream Flow Needs, Vol. II, Orsborn J.F. and Allman C.H. (eds.), American Fisheries Society, Bethesda, Maryland, USA, 235–252

Ward J.V. and Short R.A., 1978. Macroinvertebrate community structure of four special lotic habitats in Colorado. USA. Verhandlungen Internatonale Vereinigung Fur Theoretische und Angewandte Limnologie, 20, 1382–1387

Ward J.V. and Stanford J.A., 1979. Ecological factors controlling stream zoobenthos. in The Ecology of Regulated Streams, Ward J.V. and Stanford J.A. (eds.), Plenum Press, New York, 35–56

World Resources Institute, 1994. World Resources 1994–95. Oxford University Press, Oxford, p.184

Wu L.C., Zheng M.S. and Zheng H., 2008 Rising the sediment releasing efficiency and extending the life of the Xiaolangdi Reservoir, Proceedings of the Special Session for Comprehensive Utilization of Water Resources in the Middle and Lower Reaches of the Yellow River, 10th China Association for Science and Technology Annual Meeting. Zhenzhou, September, 17–19 (in Chinese)

Wunderlich W.O., 1971. The dynamics of density-stratified reservoirs. In reservoir fisheries and limnology. Special Publication No. 8, American Fisheries Society, Washington, DC, USA, 219–232

Yi B. and Liang Z., 1964. The natural conditions of the spawning ground and external factors affecting fish spawning in the Yangtze River. Journal of Hydrobiology, 5(1), 1–15 (in Chinese)

Yi Y.J., Wang Z.Y. and Lu Y.J., 2006. Habitat suitability index model of four major Chinese carp species in the Yangtze River. River Flow, Taylor and Francis Group, London, 2195–2201

Yi Y.J., Wang Z.Y., Zhang K., Yu G.A. and Duan X.H., 2008. Sediment pollution and its effect on fish through food chain in the Yangtze River. International Journal of Sediment Research, 4, 338–347

Young W.C., Kent D.H. and Whiteside B.G., 1976. The influence of a deep storage reservoir on the species diversity of benthic macro invertebrate communities of the Guadalupe River. Texas, Texas Journal of Science, 27, 213–224

Zhadin V.I. and Gerd S.V., 1963. Fauna and flora of the rivers, lakes and reservoirs of the USSR. Israel Program for Scientific Translations, Jerusalem, p. 625

Zhou J.J. and Lin B.G., 2002. Effect of DECL scheme on navigation conditions. China Three Gorges Construction, 6, (in Chinese)

Zhou Z.D., 1999. 1998 floods in the Yangtze River valley. International Research and Training Center on Erosion and Sedimentation, UNESCO Beijing Office

8   Estuary Processes and Managment

Abstract

Deltas are classified into river-, wave-, and tide- dominated deltas according to the dominant forces; or fan deltas and braided deltas according to their geomorphic settings. Large river deltas can also be classified into male deltas and female deltas. Estuary floods are due to 1) subsidence of the land or islands; 2) tsunamis, hurricanes and storm surges; and 3) heavy rainstorms. The flooding risk and flood defense strategies are discussed with the Venice Lagoon, Indian Ocean Tsunami, Hurricane Kartrina and New Orleans, and Hong Kong as examples. Human activities pose a serious threat to the health of estuaries and coastal waters. In particular, semi-enclosed estuaries are often under pressure to serve as wastewater disposal areas, leading to a high risk of eutrophication and algal blooms. Wastewater is flushed through repeated exchange of the intertidal water volume between the embayment and the open water body: clean water entering the embayment during flood tide fills the intertidal volume, mixing with the existing water in the embayment and, as the tide falls, the intertidal volume of water discharges out of the embayment, removing the dissolved substance. Tidal flushing time is taken as the time required for a tracer mass to reduce to a certain level of the initial mass. Wetlands along coastal shorelines serve as natural barriers against flood damage and erosion due to wind, waves and currents. Mangrove plants are capable of transferring oxygen from the atmosphere to the roots and creating an oxygenated zone for nitrification around the roots while the surrounding sediments are reduced thus favoring de-nitrification. Various techniques of wastewater outfalls, protection of wetlands, and prediction of algal blooms are also discussed in this chapter.

Key words

Deltaic process, Tsunami, Hurricane, Tidal flushing, Eutrophication, Algal bloom, Waste disposal

8.1   Deltaic Processes

8.1.1   Two Types of Delta Development

Many classification schemes have been used to organize the morphology of deltas through an understanding of sediment-transport dynamics (Syvitski and Saito, 2007). The processes of delta development depend largely on the ratio of sediment supply to sediment retention. Friedman and Sanders (1978) classified the morphology of the mouth of large rivers, according to concentration of suspended sediment load, as estuaries (<0.16 kg/m^3), deltas (>0.2 kg/m^3), and a transitional group (0.16–0.2 kg/m^3), based on data from 29 large rivers mouths across the world. The most cited classification scheme of deltas was introduced by Galloway (1975), where three main types of deltas were distinguished according to the dominant forces of the formation process: river-, wave-, and tide- dominated deltas. Mcpherson et al. (1987) classified deltas into different fan deltas according to their geomorphic and sedimentologic settings. Fan deltas are gravel-rich deltas formed where an alluvial fan is deposited directly into a standing body of water from an adjacent highland; and braided deltas are gravel-rich deltas that form where a braided fluvial system protrudes into a standing body of water. Factors affect deltaic processes include sediment load and grain size, quantitative wave and tide (Orton and Reading, 1993), sea-level variation (Dalrymple et al., 1992; Postma, 1995), and human activities (cannals, levees, dams, water diversion, etc), and these factors may vary in time and space (Correggiari et al., 2005).

Large rivers (with a length longer than 1000 km) carry no gravel to their mouths and their deltas are formed from sand, silt and clay. The gradient of these rivers in their estuarine reaches are mostly about or

less than 0.01%. The area of their deltas is very large, in a range of 10–10,000 km². The classification of large river deltas is different from that of small rivers. The dynamic, morphologic and ecological characteristics of the deltas are very different and can be classified into two types: male deltas and female deltas. In general, male deltas are not stable and have only one or two channels. Female deltas consist of complex channel network and numerous islands, which are relatively stable.

Male delta—Male delta develops if a river carries high sediment load and the tidal currents are weak. Sediment-laden rivers create land at high rate and extend into the ocean, forming a fan-shape delta. Such a process is accompanied with periodic nodal avulsions. The Yellow River carries sediment from the loess plateau in central China to the delta and causes the delta to expand by 2,000–3,000 ha per year. The present Yellow River delta has developed over the past one and half centuries as a consequence of channel siltation, flooding, and avulsions. Human activities have also changed the delta processes. Oil fields and a new city with a modern infrastructure have been developed on the newly created land. The river channel within the delta is unstable and avulsions often occur. The river mouth extends into the sea at a rate of about 2–3 km/yr, depending on the incoming sediment load. The details of the development history of Yellow River delta is described in Chapter 6. The extension of the river channel reduces the gradient and the sediment-carrying capacity, which results in avulsions occurring. In general, the length of the new channels are about 1/3–1/2 of the previous ones and the gradient is 2–3 times higher (Wang et al., 2003). Figure 8.1 shows the Yellow River delta in 1996, which had extended into the Bohai sea for more than 40 km in 20 years since the avulsion from the Diaokouhe channel to the Qingshuigou channel (Zhang et al., 1999).

Fig. 8.1 Yellow River delta is male, which has one or two channels and the channels are not stable

The Mississippi River in the U.S., the Luanhe River in China, the Ebro River in Spain and the Ural River in Russia are also male rivers. The basic features of these rivers are given in Table 8.1. The Mississippi River mouth extends deeply into the Mexico Gulf. Avulsions occurred in the Mississippi delta along the coast of Louisana as successive channels and searched for gradient advantages over their precursors (Leeder, 1983). The delta development is affected or partly controlled by humans. Upstream reservoirs, changes in agricultural practices and land uses, and bank stabilization measures have reduced average sediment loads in the lower Mississippi River by approximately 67% since the 1950s (Melching, 2006). The average concentration of suspended sediment has been reduced from 0.8 kg/m³ in 1950 to 0.24 kg/m³ in 2000.

Moreover, the natural avulsion from the present Mississippi River channel to the Atchefalaya channel is stopped by human structures. Consequently, the delta has a non-round fan-shape but a longer protrusion of river mouth.

Table 8.1   Basic features of male and female deltas

River	Yellow	Yangtze	Missi-ssippi	Ural	Luanhe	Irrawaddy	Pearl	Rhine-Meuse	Volga	Nile	Ebro
Length (km)	5464	6300	6021	2534	877	2714	2214	1320	3688	6670	927
Watershed (10^3km^2)	752	1800	3220	231	45	410	454	224	1380	2870	86
Runoff (10^9m3)	31.3 (1952-05)	903.4 (1950-05)	380.0	8.0	4.5	379.0	284.9	79.0	810.3	90.9	42.0
Annual load (10^6 t)	778 (1952-05)	414 (1951-05)	495	2.8	20.1	325	75.9	3.5	27	134	30
Load/water (kg/m^3)	24.856	0.458	1.303	0.350	4.514	0.858	0.266	0.044	0.033	1.474	0.714
D_{50} (mm)	0.019	0.009	0.010		0.065	0.0105		0.010		0.005	0.062
Delta area (km^2)	5450	50000	2108	671	82	32400	11300	35000	20000	23300	330
Tidal range (m)	1.30	2.67	1.20	0.01	1.4	2.71	1.35	2.00	0.01	0.43	0.10
Gender	**Male**	**Female**	**Male**	**Male**	**Male**	**Male**	**Female**	**Female**	**Female**	**M-F**	**Male**

Figure 8.2 shows the Ural and Ebro deltas. Both exhibit similar features with the Yellow River delta. The Ebro River is 928 km long and has a watershed area of 85,835 km^2. The Ebro watershed was a closed basin until its opening to the Mediterranean Sea 5.3 million years ago. In the following 1.6 million years the river extended into the sea and formed the ancient Ebro delta about 3.5 Million years BP, which was larger than the present Ebro delta. Canicio and Ibánez (1999) used ancient maps and reconstructed the revolutionary sequences of the delta in the past millennium. The river mouth was located to the southwest of the present mouth and the river flowed southeastward into the sea about 800 years ago. The river shifted its delta course and flowed northeastward into the sea before 1580. There are two delta lobs shown in the 1580 map because the new delta lob had been formed and the old one still existed. In 1750 the river shifted its channel to the present channel. In the following 100 years, the river extended into the sea for about 5 km and reached the present location of the mouth. Figure 8.2(b) shows the southern deltaic lobe and the northern deltaic lobe in the past and the present lobe and the river mouth (Maldonado, 1986). The present river mouth is receding due to sharp sediment load reduction in the past decades.

Female Delta—A female delta develops if a large river empties a huge amount of water into a sea with relatively strong tidal currents. The Yangtze River Estuary is an irregular semidiurnal tidal estuary, with a daily tidal range of 1.47 m between the daily mean higher high tide and the lower high tide (Shen and Pan, 1988). The thalweg of the ebb tidal current and river flow is directed to the right bank due to the action of the Coriolis force, forming the ebb tide channel, while the thalweg of the flood tidal current is directed to the left forming the flood tide channel. The main tide direction is nearly 305° progressing from the East China Sea toward the river mouth area while the ebb tide current direction is nearly 90°–115°. The ebb tide current is not in a direction opposite to the flood tide direction; there is a 10°–35° angle between the extension line of the flood and ebb tidal currents because of the Coriolis force. ebb tidal current is obviously diverted to the south, while the flood current is diverted to the north. Thus, between the flood and ebb tidal currents in the river mouth area there is a slack water region where sediment rapidly

(a)   (b)
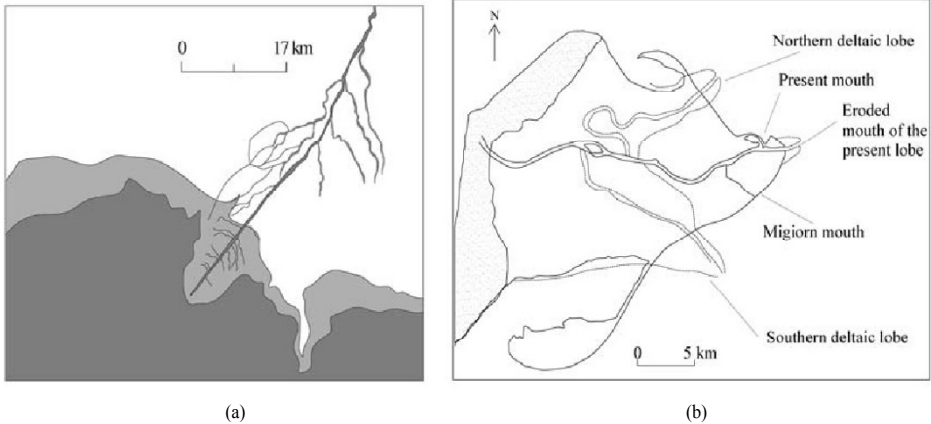
Fig. 8.2 Ural delta (a) and Ebro delta (b) extend into the sea, which show male delta features

deposits to form shoals that eventually coalesce to form estuarine islands. Consequently the river flow is bifurcated. Over time numerous islands develop in the estuary and a complex channel network forms. Figure 8.3 shows the channel network and the islands formed during the deltaic process of the Yangtze River (Xie et al., 2009).
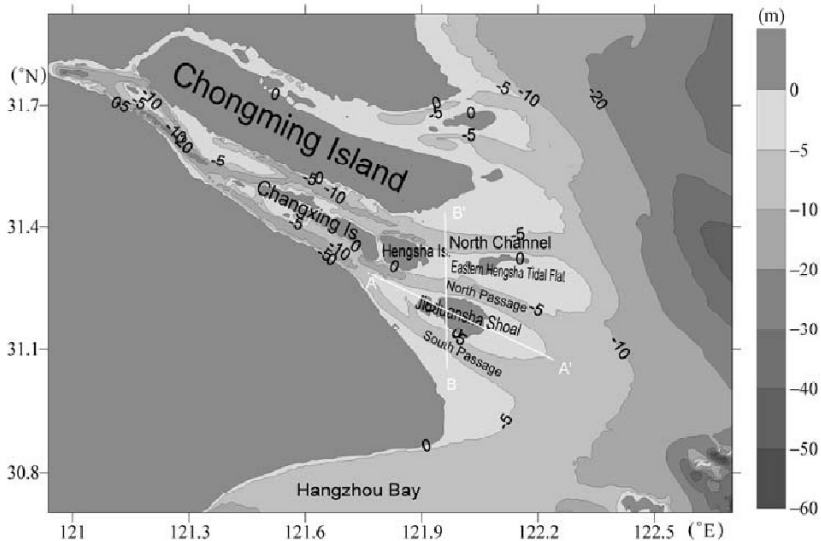
Fig. 8.3 Present Yangtze River estuary—Chongming Island divides the river into the North and South Branches; Changxing Island divides the South Branch into the North and South Channels; and Jiuduan Shoal divides the South Channel into the North and South Passages

The Yangtze River is characterized by a high flow discharge and a high sediment load (Table 8.1). The Yangtze River is the longest and largest river in China, and is also the third longest and third largest river in the world. The river is 6300 km long and has a drainage basin area of 1.8 million km². The Yangtze River carries large amounts of water and sediment into the East China Sea. In the history deltaic islands and shores develop continuously at the river mouth, leading to bifurcations of the channels. The Yangtze

River mouth has undergone significant geomorphological changes over the past 3,000 years. The river discharged into the East China Sea at Yangzhong some 2000 years ago (Chen et al., 1988). However, sedimentation has since moved the river mouth more than 200 kilometers downstream. The present location of the largest city of China—namely Shanghai—was located in the sea and emerged only in the 13th century. Chongming Island, a delta sand bar, appeared in the river mouth some 800 years ago and divided the river into the North Branch and South Branch. Shanghai is the largest industrial hub of China and land demand is increasing for urban construction and harbor expansion. In the past decades Shanghai has expanded by 11% by creating land in the river mouth and sea. The new created land was used for agriculture in the early period and since 1987 has been used mainly for industrial and urban development. An analysis of the deposits has shown that the Yangtze River mouth has been expanding for a long time, with 4,000 km^2 of land being created during the period from the 4th century to the 12th century and 3,000 km^2 from the 13th century to the 20th century (Wang et al., 2003).

Prior to the 18th century the North Branch was the main discharge channel; since then the main flow has shifted gradually to the South Branch and the North Branch discharge has decreased. The North Branch accommodated 25% of the river runoff in the 18th century and now only discharges river runoff during low tides in the flood season. The discharge ratio decreased to about 2% in the 1950s and is now about -8% since more tidal water flows upstream. Furthermore, the South Branch was bifurcated into the North Channel and the South Channel by Changxing Island, which emerged from the South Branch after the 100-year flood in 1860 (Le et al, 1998). A sand bar, namely Jiuduan Shoal, appeared after the 1954 flood and is now growing in the South Channel, and further divides the South Channel into the North Passage and South Passage.

Figure 8.4 shows the development process of the Jiuduansha Shoal, which is one of the shoals that have recently emerged from the water. The longitudinal section of the Jiuduansha Shoal forms a convex geomorphic pattern, which stands out on the link between the −10 m isobathic from the upper reach section to the lower reach section of the Yangtze River Estuary (Fig. 8.3 A–A').   In transverse section, the Jiuduansha Shoal is confined between the channels of the South Passage and the North Passage (Fig. 8.3 B–B'). The 1954-flood is a 100 years flood, having a period of 107 days with water discharge larger than 60,000 m^3/s. After the flood, the Jiuduansha Shoal was isolated from the Tongsha Tidal Flat and formed a new island in the Yangtze River Estuary, and then the Tongsha Tidal Flat was renamed the Eastern Hengsha Tidal Flat. The area of the Jiuduansha Shoal is the major place for the sediment deposition in the South Branch and South Channel. The sediment is deposited during the flood season and eroded during the dry seasons, with the sediment depositing at neap tides and eroding during spring tides under the action of runoff and the tidal current.

Figure 8.5 shows several female deltas: (a) Rhein-Meuse-Scheldt delta; (b) Irrawaddy delta; (c) Pearl delta; and (d) Volga delta. The Rhein-Meuse-Scheldt Delta and the Pearl River delta are female as well. The Rhein-Meuse-Scheldt delta consists of a very complex channel network, as shown in Figure 8.5(a). The Rhine River begins at the Rheinwaldhorn Glacier in the Swiss Alps and flows north and east approximately 1,320 km. At the Netherlands frontier, it divides into two parallel distributaries, the Lek and the Waal, as it crosses a wide, marshy plain and a great delta before entering the North Sea. The river Meuse links with the Rhine at the delta and forms a complex channel network. The Scheldt River also joins the channel network at the delta. There are many channels in the delta and many islands between the channels.

The Pearl River has a drainage area of 450,000 km^2, carrying 3.086 trillion m^3 of water and 87 million tons of sediment load annually into the South China Sea. The sediment load/water ratio is only about 0.03 kg/m^3, thus a female delta has developed in this location. The delta has a complex channel network
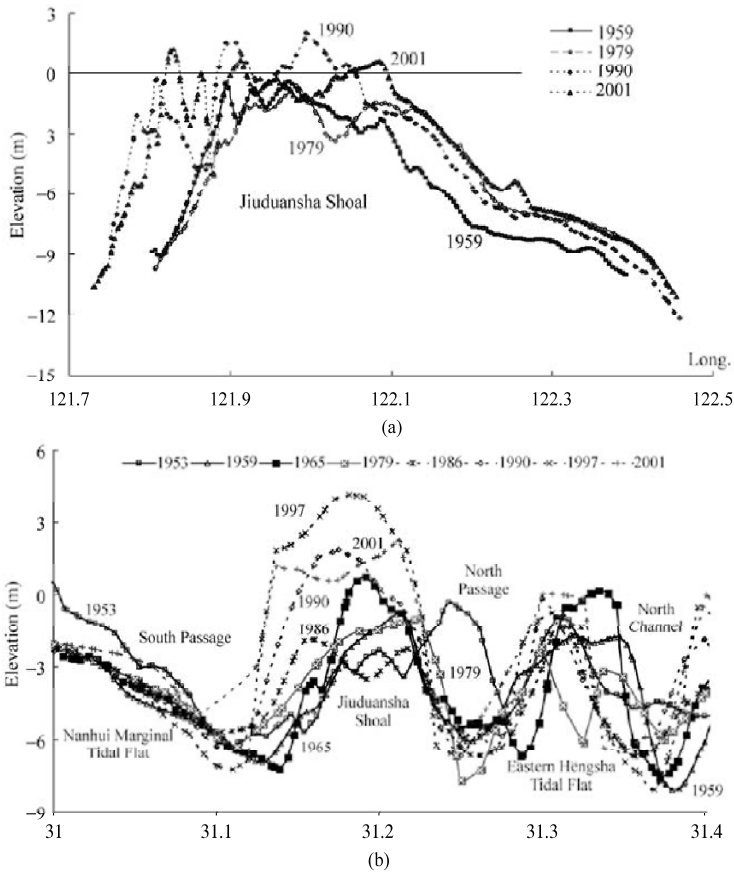
Fig. 8.4 Development of the Jiuduansha Shoal: (a) Longitudinal section of the Jiuduansha Shoal (121°35′E, 31°16′N–122°25′E, 31°5′N, Fig. 8.3 as A–A′) from 1959 to 2001; (b) Cross section of the Jiuduansha Shoal at 122°E (shown on Fig. 8.3 as B–B′) from 1953 to 2001

that consists of the West River, North River, East River, and Tanjiang, Suijiang, Liuxi, and Zengjiang Rivers. Sediment from these rivers has deposited at the bay and has formed many islands. Channels connect with each other like a spider web. The river water flows into the South China Sea through eight large mouths: Humen, Jiaomen, Hengmen, and Hongqili from the east, and Modaomen, Jitimen, Hutiaomen and Yamen from the west, as shown in Figure 8.5(c).

8.1.2　Effects of Human Activities

In general, male deltas develop if the sediment load/water ratio is high and the tidal current is weak, e.g. the Yellow River delta. If the load/water ratio is not high and tidal current is strong a female delta develops, e.g. the Yangtze River delta. Figure 8.6 shows the gender of the delta (thus gender of the river) as a function of sediment load/water ratio and tidal range. Points of female deltas are in the upper-left zone and points of male deltas are in the bottom-right zone. There is a transitional zone between the male and female areas. The impoundment of a river can cause the river to change genders because dam construction traps a lot of sediment,, resulting in a reduction of the load/water ratio by 70%–99%. The Nile River and the Ebro River are changing from male to female due to remarkably reduction in the sediment load transported to the deltas.
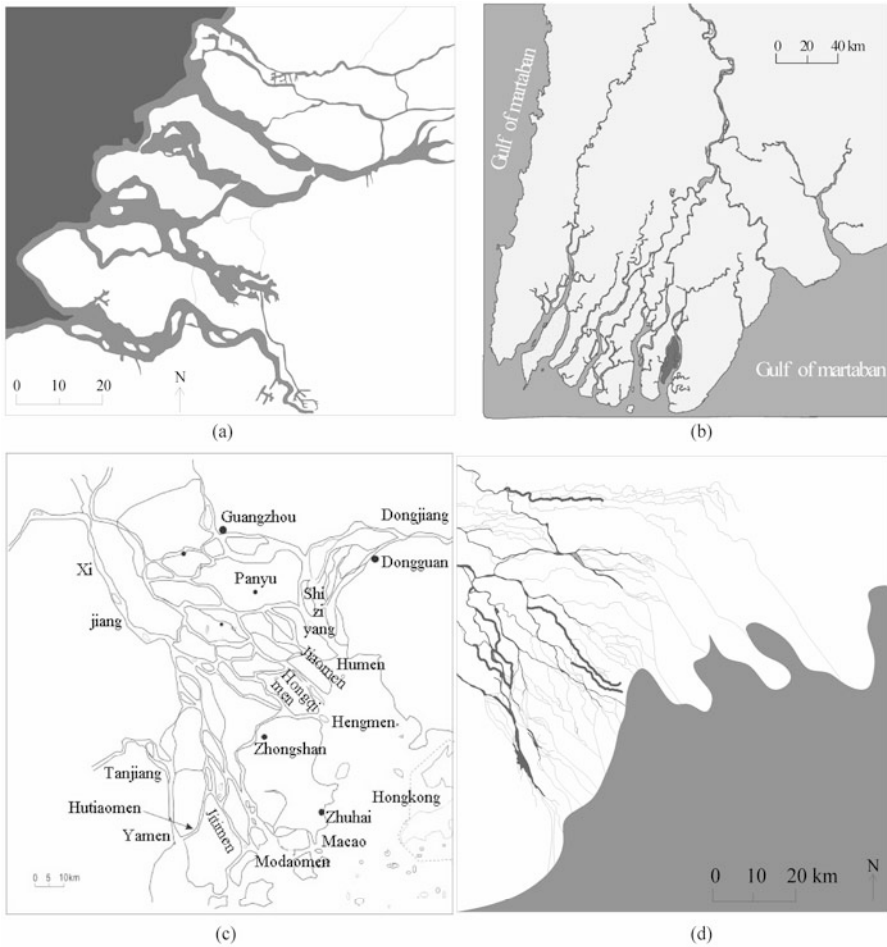
Fig. 8.5 Female deltas consist of numerous islands and spider-web like channels: (a) Rhine-Meuse-Scheldt delta; (b) Irrawadi delta; (c) Pearl River delta; and (d) Volga delta
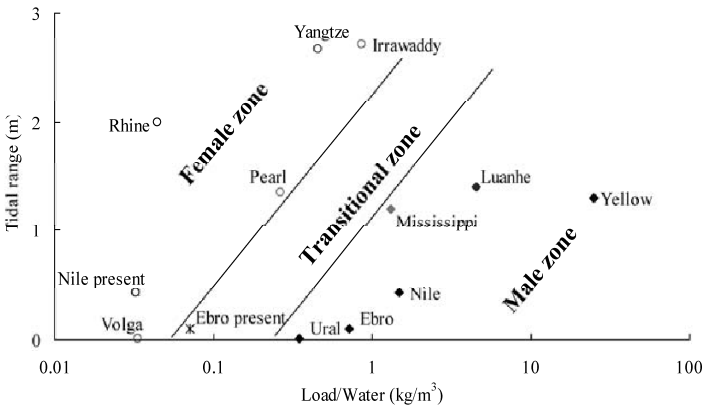
Fig. 8.6 Gender of the delta as a function of sediment load/water ratio and tidal range

The Mississippi River mouth extends deeply into the Mexico Gulf. Avulsions occurred in the Mississippi delta along the coast of Louisana as successive channels searched for higher gradient than their precursors (Leeder, 1983). Delta development is affected or partly controlled by humans. Upstream reservoirs, changes in agricultural practices and land uses, and bank stabilization measures have reduced average sediment loads in the lower Mississippi River by approximately 67% since the 1950s (Kesel, 1988). The average concentration of suspended sediment reduced from 0.8 kg/m^3 in 1950 to 0.24 kg/m^3 in 2000. Moreover, the natural avulsion from the present Mississippi River channel to the Atchefalaya channel has been stopped by human structures. The present delta is eroded by waves and tidal current. The delta lobe has become slender and thin.

The Nile River flows 6,825 km from central Africa to the delta and is the longest river in the world, which is the reason for the existence of Egypt and the great Egyptian civilization. It is an exotic river with no perennial-flow tributaries, but ephemeral wadis contribute sediment and water infrequently. In contrast to other large rivers, the Nile is straight, and appears to be relatively stable. The Nile today has been described as a "very low energy river with little capability to erode its banks (only 12% of its banks are experiencing erosion) or change its channel" (Mercer et al., 1992). In the past centuries the Nile River was a male river with annual sediment load about 160 million tons. The sediment concentration was as high as about 3.5 kg/m^3. A fan-shape delta developed with two channels extending into the red sea (Stanley and Winkley, 1994). The delta, with an area of about 23,300 km², has been formed through deposits over the course of tens of thousands of years on the originally shallow seabed. The area around the Nile has about 34 million inhabitants, which equates to half the entire population of Egypt. The coastline is about 400 km long, from Alexandria in the west to Port Said and the outlet of Suez Canal in the east. The construction of the Aswan Dam and the High Aswan Dam in addition to many barrages has changed the river remarkably. The river's long-term annual peak discharge of 8,430 m^3/s has been reduced to a maximum release of 2,550 m^3/s, while the suspended sediment concentration in flood season is now only about 0.1 kg/m^3 (Stanley and Winkley, 1994). These changes affect the delta development and coastal erosion of the delta. At the present, there are several brackish lagoons or lakes, of which Manzala and Burullus are the largest. The delta has two main channels: the Rosetta and Domietta rivers. The sediment load has been reduced by 99% due to dams and barrages. Thus, the delta has changed from male to female. A stable channel web consisting of numerous distributaries and canals has been formed.

The sediment load reduction also caused the Nile delta to change from a sediment deposition center into a man-altered coastal plain. The delta has stopped spreading out into the Mediterranean and locally is receding. It is no longer an active natural delta. Very little sediment is presently carried seaward to replenish the delta coast. The Nile has transformed from a seasonally fluctuating fluvial regime to a year-round storage and regulated flow system (Howell and Allan, 1994). The extended length of the river mouth has been shortened by 8 km in the past 80 years. The land loss was caused not only by wave current and dams and barrages, but also by retention of sediment on the delta plain due to channelization, irrigation and land reclamation on the delta proper (Stanley, 1996).

8.1.3 Ecology of Male and Female Rivers

In general, a river changes its gender from male to female due to sediment load reduction. Sharp sediment load reduction reduces land creation and causes problems to estuary management. For instance, sediment load reduction in the Yellow River has stopped land creation and resulted in land loss due to coastal erosion. In the Mississippi delta sediment load reduction has resulted in wetland loss. Nevertheless, if a gender change does not occur too fast and the delta has no severe pollution, the ecology may improve and the biodiversity of both fish and macro-invertebrates will increase after the gender change.

Female rivers provide stable habitats for both terrestrial and aquatic bio-communities and therefore have a higher biodiversity than that of male rivers. Benthic invertebrates and fish are main elements of aquatic ecology. Streambed sediment is one of the main factors affecting the biodiversity of benthic invertebrates (Duan et al., 2009). Samples of fish were taken from the lower reaches and samples of macro-invertebrates were taken from the beds of the lower reaches of the Yellow, Yangtze and Pearl rivers (Yi et al., 2008). Benthic macro-invertebrates were taken with a kick-net with holes of 420 μm and a weighted Petersen grab (1/16 m^2) and then sieved with a 420-μm sieve. Several sites were chosen for sampling for each river. Specimens were manually sorted out from sediment on a white porcelain plate and preserved in 75% ethanol. All species were identified under microscopes by experienced biologists. Fish samples were taken from the lower reaches of the Yangtze and Pearl rivers by hiring fishermen and using seine. For each river, four fishermen captured fish species for 3 days.

Table 8.2 lists the species of invertebrates and fish sampled from the lower reaches of the Yellow, Yangtze and Pearl rivers. The Yellow River is a male river and its channels are unstable. Erosion and sedimentation occurred occasionally. Samples of macro-invertebrates were taken from 6 sites selected from the lower reaches of the Yellow River. Only one species *Palaemonidae* (shrimp) was found from the river channels. Another eight species of invertebrates were sampled from a riparian wetland in the Yellow River delta. The extremely low biodiversity was caused by erosion, sedimentation of the river bed, and migration of the channel. There are only a few fish species in the lower Yellow River and the abundance of fish is low. Therefore, the Yellow River has no fisheries and no fisherman can be hired for fish sampling.

Female rivers have stable habitats and low sediment load, therefore, they have high biodiversity. The taxa richness and abundance of invertebrates and fish were much higher in the Yangtze and Pearl rivers than in the Yellow River. The results support the conclusion that habitat stability is the most important factor for high biodiversity (Wang and Xu, 2010). Fish samples were taken from six sites in the lower reaches of the Yangtze River. 43 species belonging to 11 families of fish were found from the 6 sampling sites. In the Pearl River, 70 species belonging to 29 families of macro-invertebrates were found from 18 sampling sites and 68 species belonging to 25 families of fish were found from 9 sampling sites.

The biodiversity in the female rivers are much higher than that of male rivers. In general, if a river changes its gender from male to female the biodiversity increases. Nevertheless, the causes of gender change (dam construction and water and sediment diversion) and the gender change itself are stresses on the bio-communities. Therefore, the ecology may be impaired during the gender change.

8.1.4   Parasitizing Rivers

Male rivers carry heavy sediment load to the lower reaches and deltas. Humans made continuous effort to control floods by constructing and enhancing grand levees. Overtime, the male rivers become perched rivers in their lower reaches and deltas. Over the course of time avulsions occurred and thus created many abandoned channels. Some abandoned channels have combined with other rivers and formed new river systems. Some abandoned channels have been cut into several depressions or wetlands, or totally disappeared due to human reclamation. Other abandoned channels still exist and rely on their father river. Moreover, male rivers have no tributaries in the perched reaches; instead, rainwater falling on the surrounding land of the river flows in new drainage channels parallel to the levees. These abandoned channels and new drainage channels are not tributary or distributary rivers, but their location and stability depend on their father rivers. These channels are parasitizing rivers of the male river.

The lower Yellow River is a perched river with its riverbed more than 10 m higher than the surrounding ground. The rain water can not flow into the river and water diversion from the river affects the fluvial process (Wang et al., 2008). Many drainage channels have developed on the levees and flow parallel with

Table 8.2 Species of invertebrates and fish in the lower reaches of male and female rivers

River (Gender)	Species of macro-invertebrates and fish
Yellow (male) Sampling sites: 6 for invertebrates	**Invertebrate (9 species, 7 families):** *Palaemonidae, Branchiura, Limnodrilus, Tipulidae, Planorbidae, Stenothyra, Lymnaeidae, Bithynia, Chironomidae sp.* **Fish (no samples):** *Few species and very low abundance*
Yangtze (Female) Sampling sites: 4 for fish; 0 for invertebrate	**Fish (43 species, 11 families):** *Mylopharyngodon piceus, Ctenopharyngodon idellus, Hypophthalmichthys molitrix, Cypriniformes carpio Linnaeus, Cypriniformes auratus auratus, Parabramis pekinensis, Silurus asotus Linnaeus, Pelteobagrus fulvidraco, Coreius heterodon, Distoechodon tumirostris, Misgurnus anguillicaudatus, Hemiculter leucisculus, Coilia ectenes, Coilia brachygnathus, Leptobotia Bleeker, Leiocassis longirostris Günther, Rhinogobio Bleeker, Saurogobio dabryi Bleeker, Channa argus, Odontobutis obscurus,Simiperca scherzeri steindachner, Lateolabrax japonicus, Erythroculter dabryi, Culter erythropterus Basilewsky, Pseudorasbora parve, Sarcocheilichthys nigripinnis, Hemiramphus kurumeus, Mystus macropterus*
Pearl (Female) Sampling sites: 18 for invertebratres 9 for fish	**Invertebrates (70 species, 29 families):** Nematoda, Nereididae, Nereididae, Spionidae, *Pseudopolydora paucibranchiata* (Okuda), Capitellidae, Naididae, *Dero digitata* (Müller), *Branchiodrilus semperi* (Bourne), *Slavina appendiculata* (d'Udekem), *Limnodrilus grandisetosus,* Nomura, *Limnodrilus claparedeianus* Ratzel, *Limnodrilus* sp., *Aulodrilus limnobius* Bretscher , *Aulodrilus pigueti* Kowalewski , *Aulodrilus pluriseta* (Piguet), *Branchiura sowerbyi* Beddard, *Glossiphonia* sp., *Helobdella* sp., *Erpobdella* sp., Bithyniidae, *Alocinma longicornis* (Benson), *Bithynia misella* (Greller), *Stenothyra glabra* A. Adams, *Bellamya purificata* (Heude), *Bellamya* sp., *Margarya* sp., *Rivularia globosa* Heude, *Pila* sp., *Semisulcospira cancellata* (Benson), *Semisulcospira libertina* (Gould), *Semisulcospira* sp., *Melaniodes tuberculata* (Müller), *Radix auricularia* (Linnaeus), *Radix lagotis* (Schrank), *Radix swinhoei* (H. Adams), *Galba* sp., *Hippeutis cantori* (Benson), *Hippeutis umbilicalis,* Mytilidae, *Limnoperna lacustris* (Martens), Unionidae, *Anodonta woodiana woodiana* (Lea), *Corbicula fluminea* (Müller),, Amphipoda, Acarina , *Baetis* sp. , *Ephemerella* sp. , *Lamelligomphus* sp. , *Megalogomphus* sp., *Leptogomphus* sp., *Parachauliodes* sp., *Neochauliodes* sp., Ceratopogonidae, Tipulidae, Dolichopodidae, Muscidae, *Clinotanypus* sp., *Nanocladius* sp., *Procladius* sp., *Tanypus* sp., *Cricotopus* sp., *Eukiefferiella* sp., *Parakiefferiella* sp., *Chironomus* sp., *Cladotanytarsus* sp., *Cryptochironomus* sp., *Cryptotendipes* sp., *Demicryptochironomus* sp., *Dicrotendipes* sp., *Endochironomus* sp., *Microchironomus* sp., *Polypedilum* sp., *Rheotanytarsus* sp., *Stictochironomus* sp., *Tanytarsus* sp.. **Fish (68 species, 25 families)** *Squaliobarbus curriculus, Channa maculate,,, Takifugu ocellatus, Erythroculter recurviceps,Pelteobagrus vachelli,Cranoglanididae bouderius bouderius, Pelteobagrus fulvidraco, Pseudogobio vaillanti vaillant, Clupanodon thrissa, Coilia grayi, Megalobrama terminalis, Cirrhina moitorella, Mugil cephalus Linnaeus, Xenocypris davidi, Sparus latus* Houttuyn, *Tilapia mossambica, Nemacheilus fasciolatus, Botia robusta, Acrossoch eilus parallens, Leiocassis virgatus, Squalidus argentatus, Garra orientalis, Culter erythropterus Basilewsky, Osteochilus salsburyi* Nichols et Pope, *Hemibarbus labe,Clarias fuscus, Ptychidio jordani, Saurogobio dabryi, Abbottina rivularis, Coilia grayi, Ptychidio jordani, Mystus guttatus, Varicorhinus gerlachi, Siniperca scherzeri, Parabotia maculosa, Plagiognathops microlepis, Saurogobio dabryi, Neosalanx taihuensis* Chen, *Siniperca kneri*
Notes	Fish samples were taken by hiring 4 fishermen and using seine for capturing different fish species for 3 days for the Yangtze and Pearl rivers. There is no fishery in the Yellow River and no fishermen to be hired for sampling.

the Yellow River into the sea. Some of these rivers are rather long, with a length of 600–800 km. These rivers were created by the Yellow River and originate from the grand levees of the Yellow River. Their persistence and stability depends on the stability of the Yellow River. Figure 8.7 shows the Yellow River and its parasitizing rivers. Although the drainage areas of the parasitizing rivers are not in the Yellow River basin, they are controlled by the Yellow River. Therefore, the drainage areas are called parasitizing drainage areas of the Yellow River. The boundary of the parasitizing drainage area and the divide of the watershed of the Yellow River meet at Zhengzhou, which forms an X-shape structure, as shown in Fig. 8.7.
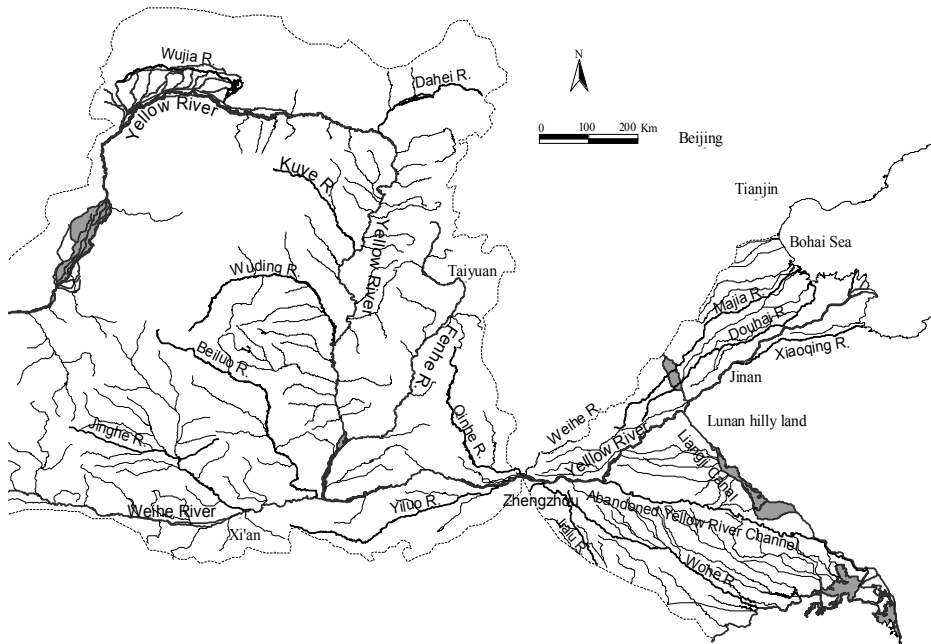
Fig. 8.7   The Yellow River and its parasitizing rivers

Small male rivers have their parasitizing rivers in their delta, which mostly developed from abandoned distributaries. Figure 8.8 shows the Luanhe River delta and its parasitizing rivers. The Luanhe River rises on the Mongolia Plateau, it travels through the Yanshan Mountains, and finally flows into the Bohai Gulf. The average annual runoff of the river is 4.56 billion m^3, but 70%–80% of it occurs in the flood season from June to September, and the flood season also transports 93% of the sediment load of 20.1 million tons. In 1915, the Luanhe River changed course to its present position, and has since developed its modern delta (Feng and Zhang, 1998). The delta land is 1–2 m above sea level. The sediment consists of mainly silt, fine sand and a small amount of clay. There are eight distributary courses. There is only one main drainage course for every period of development, the others tend to be abandoned gradually (Feng and Zhang, 1998). A few of them have developed into parasitizing rivers.

The parasitizing rivers on the Luanhe Delta become 300–500 m wide during a flood. The deposits in these channel beds are fine sand and sand. The upper reach is mainly composed of sand, but in the lower reach, there are many water pools, in which clays and silts are deposited. The dam construction and water and sediment diversion have caused the sediment load of the Luanhe River to decrease sharply to less than 1 million tons since 1980. The delta channel of the Luanhe River has become deep. As a consequence, the gender of river will change from male to female. The parasitizing rivers may finally link with their father-mother river and combine into a channel web like other female rivers.

Parasitizing rivers have no tributaries or mountainous watersheds. All runoff water comes from rain. Therefore, flow occurs only during rain season and the hydrograph of flow has only peaks and there is no flow between the peaks. Figure 8.9 shows the discharge hydrographs of the Majia River. The Majia River is a parasitizing river of the Yellow River, which is 425 km long and has a drainage area of 8,830 km^2. The river originates from the Beijindi Levee of the Yellow River. The river was once a channel dug by humans to drain the rainwater. Runoff is closely related to rainfall. In the past 20 years, discharge has increased faster than that of the period from 1956–1979 because urbanization and highway construction

have reduced the infiltration capacity of the ground surface (Zhang and Jiang, 2004). To store water during rain season humans constructed many locks. Nevertheless, the storage capacity of these locks is limited and these locks have to be open after rainstorms.
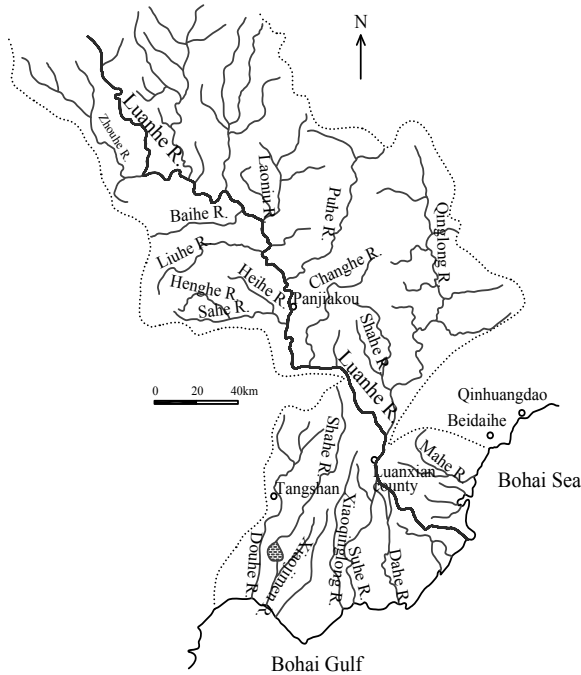
Fig. 8.8   The Luanhe River and its parasitizing rivers
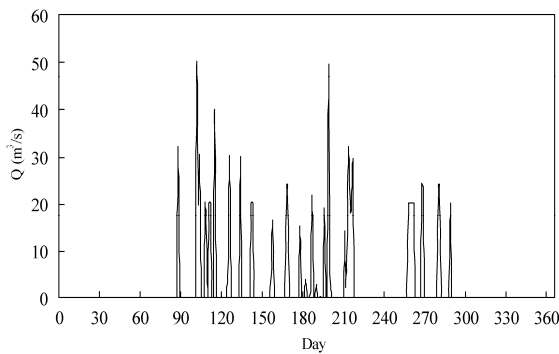
Fig. 8.9   Discharge hydrograph of Majia River at Liuqiao Station in 2008

Figure 8.10 shows the discharge hydrographs of the Shahe River. The Shahe River is 80 km long, which is a parasitizing river of the Luanhe River. The Shahe River was an abandoned channel of the Luanhe River after an avulsion of the delta channel. Flow occurs in the river only in July and August when rainstorms happen. Because the flood stage rises and falls very sharply and there is no water flow in the river during dry season the ecology in the river is poor. Weir and lock construction is the strategy to store water and improve the ecology.
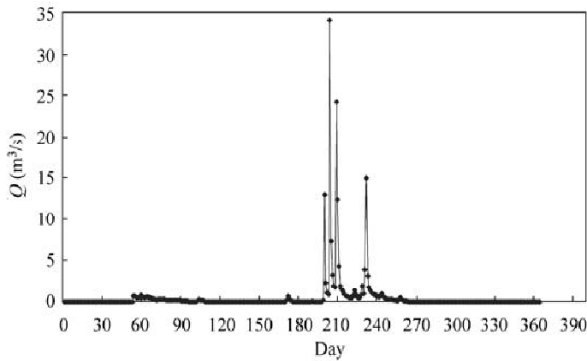
Fig. 8.10 Discharge hydrograph of Shahe River in 1963

8.2 Flooding Risk and Flood Defence Strategies

Large river deltas and coastal areas are densely populated and highly industrialized. Therefore, flooding risk and flood defense is an important issue for estuary management. Flooding risk, R, may be expressed as a function of flooding probability P_f and the number of people and value of properties threatened by a possible flood, N_v, i.e.

$$R = P_f N_v \qquad (8.1)$$

The flooding risk is very high in large river delta because both P_f and N_v are higher than other areas in the watershed. Flooding threat in large river delta is due to ① subsidence of the land, which is created by sedimentation from the river; ② tsunamis, hurricanes and storm surges; and ③ heavy rainstorm. The flooding risk and flood defence strategies are discussed with the Venice Lagoon, Indian Ocean Tsunami, Kartrina and New Olean, and Hong Kong as examples.

8.2.1 Flooding Due to Subsidence—Venice Lagoon

Venice Lagoon has 550 km² of surface area and is the largest wetland of the Mediterranean, as shown in Fig. 8.11. It is divided from the sea by a strip of barrier islands, that runs for about 60 km from the mouth of the Adige to the mouth of the Piave, interrupted by the lagoon inlets of Lido (800 m wide), Malamocco (400m wide) and Chioggia (380 m wide). Inside the lagoon basin are Venice, Chioggia, Murano, Burano Torcello and more than 50 islands; about 70 km² of salt marsh (low-lying areas which are covered with halophytic vegetation); a 1,580 km network of canals that ensures the propagation of the tidal currents up to the boundary with the mainland. In the northern and south-central lagoon, the lagoon boundary is defined by fish farms (areas that take up a surface area of about 90 km², are separated from the living lagoon and are equipped for fish farming). The average depth of the lagoon is 1.2 m.

The present drainage basin of Venice Lagoon has an area of about 2000 km² that pours about 2.8 million m³ of water a day into the lagoon. The drainage basin has a total of nearly 1.5 million inhabitants. The northern Adriatic governs the lagoon ecosystem with its tides that enter and exit the lagoon twice a day through the lagoon inlets, reaching two maximums and two minimums (semidiurnal tides). It has been calculated that the volume of water exchanged daily between the sea and the lagoon is about 400 million m³. The average range of tide heights in the lagoon is about 0.7 m. Nevertheless, the tidal level is subject to important variations, above all in relation to astronomical and meteorological factors.

In the history, rivers, including the Po River, carried sediment into the lagoon and resulted in a problem of sedimentation. In the 14–19 centuries, the rivers were deflected into the Adriatic bypassing the lagoon, which almost completely eliminated the "refurnishment" of sand and sediment from the hinterland. The

construction of the outer breakwaters at the inlets, which occurred between 1800 and 1900 with the aim of ensuring the passage of modern ships, also reduced the quantity of sediments brought in by the sea.

Fig. 8.11   Venice, Chioggia, Murano, Burano Torcello and more than 50 islands in the Venice Lagoon are threatened by tidal flooding due to subsidence (Source: http://www.salve.it/) (See color figure at the end of this book)

In the past 100 years, however, eustasy and subsidence have resulted in a loss of land level of more that 0.23 m. Although just a few centimeters, these are actually quite a lot for a city that rests on the surface of the water. When the tide grows to the point of provoking floods in the historic centers of the lagoon, the phenomenon of acquaalta is said to occur. The frequency and intensity of the floods have become progressively worse, so much so that today, in the autumn and winter, the lowest-lying zones of Venice undergo flooding almost daily, while the risk of a dramatic event, such as the one of Nov. 4, 1966, in which Venice, Chioggia and the other historic centers were completely submerged by water, is always present. Figure 8.12 shows that the San Marco square and the largest Church in Venice are floating on sea water. The beaches of the littoral have drastically reduced in width or have even disappeared, leaving the coastal areas ever more exposed to the violence of sea storms.

Fig. 8.12   The San Marco square and Basilica di San Marco a Venezia—the most famous of the city's churches and one of the best known examples of Byzantine archtecture in Venice are floating on sea water (See color figure at the end of this book)

The Venice Water Authority realizes the system of activities aimed at the physical and environmental safeguarding of Venice and the lagoon. The activities refer to a "General Plan of Interventions" that ties the defence of Venice and the lagoon ecosystem from high tides together with the environmental problems that for some time have been attacking the territory. The plan also outlines a series of activities for the resolution of the elements of crisis according to distinct but reciprocal and systemic lines of action: defence from high tides, defence from sea storms, and environmental defence.

As shown in Fig. 8.13 the high water defence system consists mainly of mobile barriers at the three outlets, which is combined with other measures have being underway for many years in the lagoon, tackling the various aspects of safeguarding Venice by means of a systematic approach. The mobile barriers automatically close the three outlets if the tidal water stage is higher than a critical level and automatically open if the tidal water stage reduces below the critical level.
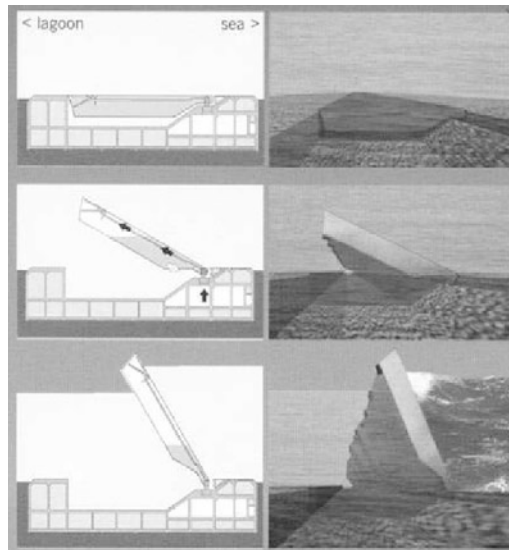
Fig. 8.13 High water defence system consists mainly of mobile barriers at the three outlets of the Venice Lagoon (Source: http://www.salve.it/)

The coastal strip, in the meantime, is protected by construction of new artificial beaches and the widening of eroded ones with sand. In the past, the coasts were protected by the construction of jetties, seawalls, groynes and offshore breakwaters, while today the most modern coastal engineering techniques attach ever greater importance to the role played by beaches for their ability to oppose and counteract the action of sea storms. Specific rock structures have been designed to protect the new beaches from erosion by "retaining" and stabilizing the sand spread or actually capturing part of the sand in transit suspended in the sea water. Depending on the area concerned, these consist in groynes (rock structures perpendicular to the coast) or "containment cells" (consisting of groynes and a submerged breakwater parallel with the beach) designed to take account of local coastal drift and current conditions, the characteristics of the section of coast concerned and the configuration of the sea bed. It is, however, impossible to completely eliminate erosive forces and the new beaches will therefore be subject to periodic maintenance. This will involve "reinforcement" with at least ten per cent every ten years.

Like Venice many cities on large river deltas and by the coast have the same problem of subsidence and increasing flooding risk, such as Shanghai, Tianjin, Los Angeles, Mexico City, New Orleans, and Osaka.

The subsidence is primarily caused by excessive groundwater withdrawal. Other reasons for the subsidence include the oil withdrawal and the neotectonic movement. The common characteristics of land subsidence are slow, accumulative, and irreversible. Adjustment of the aquifer exploitation practice is a subsidiary way to control land subsidence, but it cannot solve this problem completely (Xue et al., 2005).

Built on coastal sand and clay that lie 70 m below the ground surface, Shanghai is suffering from creeping subsidence. In addition to the overuse of underground water, the mushrooming of skyscrapers in central Shanghai has also contributed to the city's creeping subsidence. In the period 1957–1965, the city was sinking about 9 cm a year. At that rate, parts of the city would have been flooded by 1999. Control of ground water withdrawal and ground water recharging are effective measure to reduce subsidence. In the period 1966–1971, the subsidence was controlled and the ground level had been enhanced by a rate of 0.3 cm per year because of ground water recharging (China Daily, 2003). Nevertheless, the rate of subsidence increased again due to ground water withdrawal from the 1970s to 2000. The subsidence rate was 1.6 cm in the 1990s. Paying great attention to the problem, the city was installing subsidence and leakage monitors inside the many subway tunnels now under construction to keep track of the problem. The city reduced use of groundwater and is using increasing amounts of river water and pumping water back into depleted aquifers. These measures have been proved effective. The rate of subsidence for Shanghai City in 2000 was 1.21 cm and in 2006 was 0.75 cm.

8.2.2 Tsunami and Hurricane

Tsunami—The term tsunami comes from the meaning harbor and wave in Japanese. Tsunamis are common throughout Japanese history; approximately 195 events in Japan have been recorded. A tsunami has a very long wavelength (often hundreds of kilometers long), which is why they generally pass unnoticed at sea, forming only a slight swell usually about 300 mm above the normal sea surface. A tsunami can occur at any state of the tide and even at low tide will still inundate coastal areas if the incoming waves surge high enough (http://en.wikipedia.org/wiki/Tsunami). Tsunamis are among the most terrifying natural hazards known to man and have been responsible for tremendous loss of life and property throughout history. In the Pacific Ocean where the majority of these waves have been generated, the historical record shows tremendous destruction. In Japan tsunamis have destroyed entire coastal populations. There is also a history of tsunami destruction in Alaska, in the Hawaiian Islands in South America and elsewhere in the Pacific, although the historic records for these areas do not go back sufficiently in time. Historical records also document considerable loss of life and destruction of property on the western shores of the North and South Atlantic, the coastal regions of north-western Europe, and in the seismically active regions around the eastern Caribbean (George, 1985).

Tsunamis may be generated when an earthquake occurs causing the floor of the ocean to vertically displace the water column—one part "rises" whilst the other part "sinks". This occurs in seconds and huge volumes of sea water have incredibly large levels of energy transferred into them. This energy radiates outwards in a series of low frequency and therefore long wavelength waves which generally have an amplitude of about 300 mm above the normal swell of the ocean and are rarely observed as a result. It should be noted that the displacement forms a trough and a peak as it moves away from the zone of activation and will usually come ashore in the same manner. The trough causes "drawback" whilst the peak arrives as a sudden surge. Tsunami possible may be caused by landslides and explosive volcanic action, which rapidly displace large volumes of water, as energy from falling debris or expansion is transferred to the water into which the debris falls at a rate faster than the ocean water can absorb it.

Historically speaking, tsunamis are not rare, with at least 25 tsunamis occurring in the last century. Of these, many were recorded in the Asia—Pacific region—particularly Japan. On 1st April, 1946 a Magnitude 7.8 (Richter Scale) earthquake occurred near the Aleutian Islands, Alaska. It generated a tsunami which

inundated Hilo on the island of Hawai'i with a 14 m high surge. The 2004 Indian Ocean earthquake was an undersea earthquake (With a magnitude of between 9.1 and 9.3) that occurred at 00:58:53 UTC Dec. 26, 2004, with an epicentre off the west coast of Sumatra, Indonesia. The earthquake triggered a series of devastating tsunamis along the coasts of most landmasses bordering the Indian Ocean. The disaster, known as the Asian Tsunami or Boxing Day Tsunami, caused approx. 350,000 deaths and many more injuries (http://en.wikipedia.org/wiki/Tsunami), and inundation of coastal communities with waves up to 30 m. It was one of the deadliest natural disasters in history. Indonesia, Sri Lanka, India, and Thailand were hardest hit.

Mitigation of tsunami disasters relies mainly on early warning, disaster preparedness, vulnerability reduction and post-disaster relief and reconstruction (See http://lareef. blogspot.com/). There were no tsunami warning systems in the Indian Ocean to detect tsunamis or to warn the general populace living around the ocean. Tsunami detection is not easy because while a tsunami is in deep water it has little height and a network of sensors is needed to detect it. In the aftermath of the disaster, there is now an awareness of the need for a tsunami warning system for the Indian Ocean. The United Nations started working on an Indian Ocean Tsunami Warning System in 2005 (2004 Indian Ocean earthquake, http://en.wikipedia.org/).

The first warning sign of a possible tsunami is the earthquake itself. However, tsunami can strike thousands of kilometres away where the earthquake is only felt weakly or not at all. Because tsunami consists of a trough and a peak and the trough causes "drawback", in the minutes preceding a tsunami strike, the sea often recedes temporarily from the coast. Around the Indian Ocean, this rare sight reportedly induced people, especially children, to visit the coast to investigate and collect stranded fish on as much as 2.5 km of exposed beach, with fatal results. On Maikhao beach in northern Phuket, Thailand, a 10-year-old British tourist named Tilly Smith had studied tsunami in geography class at school and recognised the warning signs of the receding ocean and frothing bubbles. She and her parents warned others on the beach and saved many people. John Chroston, a biology teacher from Scotland, also recognised the signs at Kamala Bay north of Phuket, taking a busload of vacationers and locals to safety on higher ground (http://en.wikipedia.org/).

Hurricane—A hurricane is a type of tropical cyclone, which is a generic term for a low pressure system that generally forms in the tropics. The cyclone is accompanied by thunderstorms and, in the Northern Hemisphere, a counterclockwise circulation of winds near the earth's surface with a maximum speed about 120 km/h. Each year, about eleven tropical storms develop over the Atlantic Ocean, Caribbean Sea, and Gulf of Mexico and six of them become hurricanes. Hurricanes are categorized according to the strength of their winds using the Saffir-Simpson Hurricane Scale. A Category 1 storm has the lowest wind speed, while a Category 5 hurricane has the strongest. Hurricane and tropical storms produce significant damage and loss of life, mainly due to flooding (Source: http://www.nhc.noaa.gov/).

When the winds from these storms reach 63 km per hour, the cyclones are given names. An international committee developed names for Atlantic cyclones. In 1979 a six year rotating list of Atlantic storm names was adopted - alternating between male and female hurricane names. Storm names are used to facilitate geographic referencing, for warning services, for legal issues, and to reduce confusion when two or more tropical cyclones occur at the same time. Names are retired usually when hurricanes result in substantial damage or death or for other special circumstances.

The year 2005 is a year of hurricanes, in which 26 tropical storms occurred, 12 more than 2004 and the most for any year since records began in 1928. Fourteen of them reached hurricane strength and three of those made it to category 5. And hurricane Dennis, Emily, Rita, Katrina and Wilma destroyed lives, demolished houses and wrecked the land. They also smashed records. They were among the angriest, most violent hurricanes ever to rip their way across the North Atlantic and batter the Caribbean and the

Gulf coast. The most havoc hurricane was Katrina. On Aug. 29, 2005, hurricane Katrina made landfall on the Gulf Coast near New Orleans. A 6-metre storm surge smashed levees protecting low-lying New Orleans and much of New Orleans was flooded. The confirmed death toll (total of direct and indirect deaths) stood at 1,836, mainly from Louisiana (1,577) and Mississippi (238) and 705 people remain missing in Louisiana in 2006. Federal disaster declarations covered 233,000 km² of the United States. It is reported that Katrina's storm surge caused 53 different levee breaches in greater New Orleans submerging 80% of the city. Two-thirds of the flooding were due to levee breaches (Swenson and Marshall, 2005). The storm surge also devastated the coasts of Mississippi and Alabama, making Katrina the most destructive and costliest natural disaster in the history of the United States, and the deadliest hurricane since the 1928 Okeechobee Hurricane. The total damage from Katrina is estimated at $81.2 billion (2005 U.S. dollars) (USDC, 2006).

As shown in Fig. 8.14 the city of New Orleans is located between the Mississippi River and lake Pontchartrain. To its east is the Borgne Lake and Mexico Gulf. The lowest city ground is about –2 m (below the sea level), but the annual flood stage of the Mississippi River is 4.2 m and the normal water level in the Pontchartrain lake is 0.3 m. Hurricane Katrina brought heavy rain to Louisiana, with 200–250 mm falling on a wide swath of the eastern part of the state. As a result of the rainfall and storm surge the level of Lake Pontchartrain rose to 3.5 m and caused significant flooding along its northeastern shore. The city was flooded due to breaching of the levees and water poured into the city from the gulf, the lake and the river (http://en.wikipedia.org/wiki/Hurricane_Katrina).
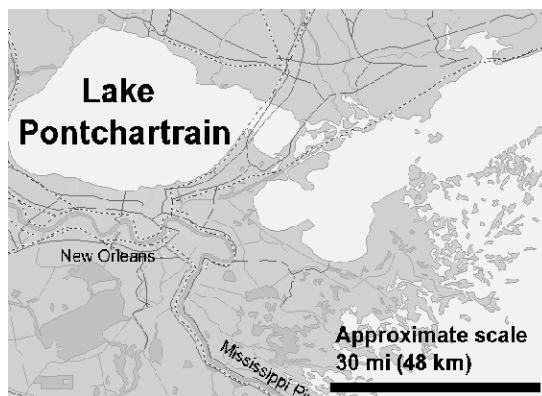
Fig. 8.14   New Orleans is located between the Mississippi River and lake Pontchartrain

The main strategy to mitigate the hurricane disasters is warning. Warnings and watches are two levels of alert issued by U.S. national weather forecasting bodies to coastal areas threatened by the imminent approach of a tropical cyclone of tropical storm or hurricane intensity. They are notices to the local population and civil authorities to make appropriate preparation for the cyclone, including evacuation of vulnerable areas where necessary. It is important that interests throughout the area of an alert make preparations to protect life and property. A hurricane warning is issued when a hurricane with sustained winds of 118 km/h or higher is expected in a specified coastal area in 24 hours or less. Maritime flags indicate this with two square red flags with a black square in the middle of each.

8.2.3   Rainstorm Flooding

Coastal areas and large cities at river mouths, such as Christchurch by the Waimakariri River, New York at the Hudson River mouth, Shanghai at the Yangtze River mouth, Tianjin at the Haihe River mouth and

Hong Kong at the Pearl River mouth are often hit by rainstorm flooding. Thunderstorms and lightning can damage electrical installations, start fires and cause death by electrocution. Waterspouts are rather more common and may capsize small boats in nearby waters and damaging coastal facilities. Hail sometimes forms in well-developed thunderstorm clouds. Hailstones are hard pellets of ice which are usually a few mm in diameter. Larger hailstones have alternate rings of clear ice and frost. Large hailstones can damage crops, particular young fruits and vegetables, and can break windows, glass houses and car windscreens. Flooding occurs when the rainfall rate is so large that natural or artificial drainage is insufficient to drain away the fast accumulating water on the ground. Floods are usually fairly transient in the urban area but may last longer in those rural areas with large catchment and gentle slopes.

Hong Kong is a harbor city and an international center of, finance, commerce and trade. The long term average annual rainfall in Hong Kong is 2,200 mm; about 80 percent of the rain falls between May and September. The wettest month is August, with an average monthly rainfall of 391 mm. The topography of drainage basins consists typically of steep upland terrain and relatively flat valley floor in the downstream semi-rural or densely populated "new towns" or metropolitan/urban areas. Over the past forty years, changing land use patterns (in particular the conversion of farm land to fish ponds and increasing urban areas) have resulted in the loss of flood plain storage and increased runoff. For example, agriculture land (cultivated and fallow) have decreased from 2830 ha in 1963 to 925 ha around 1990; on the other hand, the fish pond area increased from 665 ha to 990 ha, and developed urban area from 460 to 1465 ha respectively (Lee et al., 2002). In addition, the 1990s witnessed several unusally warm years, which seems to be correlated with record high rainfalls. For example, 1997 was the fourth warmest year on record, with an average temperature of 23.4℃; an extremely high annual rainfall of 3,343 mm was recorded, with extensive flooding in West Kowloon. The rainfall also exhibited significant spatial and temporal variability. In 2001 (the fourth wettest year), the annual rainfall was 3,091 mm; 1,368 mm of rain (62%) fell on the Northern New Territories in June 2001 alone, causing wide spread flooding (HKDSD, 2001).

A variety of measures have been developed to protect semi-rural areas, new towns, and metropolitan areas from flooding—including real time warning systems, village polder schemes, river training, storm-water diversion and storage schemes. Many of these flood control schemes share certain characteristics: high intense storms and inflows, the need to design conveyance systems under tight space constraints, proximity to densely populated areas and congested underground utilities, and enhanced backwater effect due to coastal reclamation. For instance the Yuen Long Bypass Floodway was designed under difficult land availability constraints—its success depends crucially on the use of the jet principle to lower water levels at a critical river junction, thus enabling the required flow diversion into the floodway (Lee et al., 1998). The design of these flood control schemes often involve highly complex three-dimensional flows: complicated subcritical-supercritical transitions, free surface, surcharged and two-phase flows, and spatially varied flow at 3D junctions.

The significant spatial and temporal variability of rainfall and rapid urbanization resulted in an insufficiency of drainage capacity and the solutions are very site-specified. For instance, as shown in Fig. 8.15, the upstream storm-water runoff from Tai Hang Road and Tat Chee Road are conveyed in underground storm drains; the combined flow passes through a steep culvert downstream to join with the Boundary Street Nullah in an open conduit. The total flow is discharged into a steep 1.5 km long culvert under Nullah Road leading to the Hong Kong Harbour. Due to rapid urbanization, the existing drainage system (designed for 10-years storm) failed to cope with severe rainstorms in recent years (Q_{max} = 110 m^3/s for 50-year storm); there are a number of flooding "black spots".

Rather than digging up roads and widening/adding existing sewers, which would be highly disruptive to the busy traffic and interfere with numerous existing underground structures and utilities, an upstream storage scheme is devised. The economic drainage improvement plan calls for the construction of a 100,000 m^3 underground storage underneath the Tai Hang Tung Recreation Ground. Part of the flood flow will be intercepted by a system of side weirs. The stormwater that overflows into the underground tank will be temporarily stored; the flow diversion serves to attenuate the flood peaks and prevent downstream flooding. The success of the scheme depends on the proper functioning of the side weir system and the hydraulics at the channel/weir junctions. For example, too early a spill into the storage tank may use up needed storage capacity for a later storm peak.
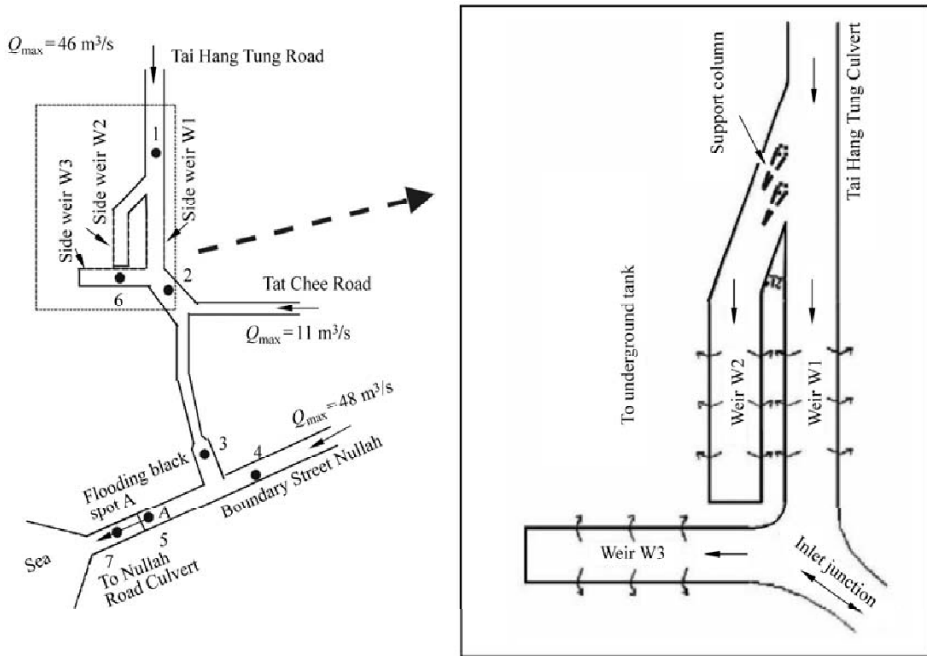
Fig. 8.15　Schematic diagram of Tai Hang Tung Storage Scheme and triple weir system (Lee et al., 2002)

Lee et al. (2002) conducted experiments to study the complicated turbulent flows in the stormwater drainage system and optimize the design of the side weir system and the inlet and hydraulic transition. The experimental results were also used for providing the side weir head-discharge characteristics for a 1-D numerical unsteady flow model developed to study the flow within the side weir system (Lee *et al* 2000, 2001a; Henderson 1966; Novak and Cabelka, 1983). The research results provided an understanding of the highly complex 3D junction flows for the successful design of these schemes. The Tai Hang Tung Storage Scheme and the Kai Tak Transfer Scheme enhanced the flood control capacity to cope with a 50 year rainstorm. The schemes are environmentally acceptable and ware built safely with minimal public disruption.

8.3　Estuarine Hydrography and Tidal Flushing

An estuary is a semi-enclosed coastal body of water which has a free connection with the open sea and within which sea water is measurably diluted with fresh water derived from land drainage (Cameron and

Pritchard, 1963). Along with the increase in population, human activities (e.g., industrialization, agricultural expansion, and livestock rearing) pose a serious threat to the health of estuaries and coastal waters. In particular, semi-enclosed estuaries are often under pressure to serve as wastewater disposal areas, leading to a high risk of eutrophication and considerable degradation of water quality. Because most of the living biomass and nutrients, contaminants, dissolved gases, and suspended particles are carried in the tidal flow, water quality studies of tidally influenced estuaries must include a thorough evaluation of the hydrodynamics of the estuarine system.

Influenced by saltwater-freshwater interactions and irregular geometry and bathymetry, hydrodynamic processes of estuaries are extremely complicated. The basic estuarine hydrodynamic characteristics (tides, currents, salinity structure, and tidal flushing) are illustrated using the Pearl River estuary (Fig. 8.16) and Hong Kong waters (Fig. 8.17) as an example. The Pearl River is China's third longest river and the second largest river in terms of discharge volume. It flows into the northern shelf of the South China Sea, near Hong Kong. Its average annual flow is approximately 10,500 m^3/s, and 80% of the total flow occurs in the wet season due to the high rainfall during this period (annual rainfall of 2100 mm). In the summer, river water moves into the western waters of Hong Kong due to the southwest monsoon winds. During the dry season, the northeast monsoon winds cause the surface river plume to move to the western side of the estuary, away from Hong Kong. An important feature of Hong Kong waters that lie on the eastern side of the Pearl River estuary is that they are shallow (mainly 10 to 20 m) and interlaced with hundreds of islands and inlets. This topography and bathymetry increases the complexity of the hydrodynamics (Lee et al., 2006).
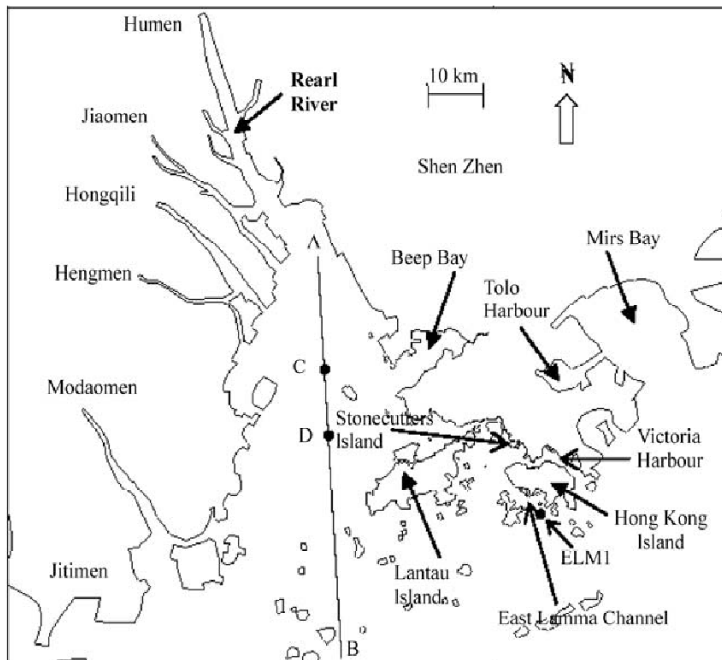
Fig. 8.16 Map of the Pearl River estuary and Hong Kong
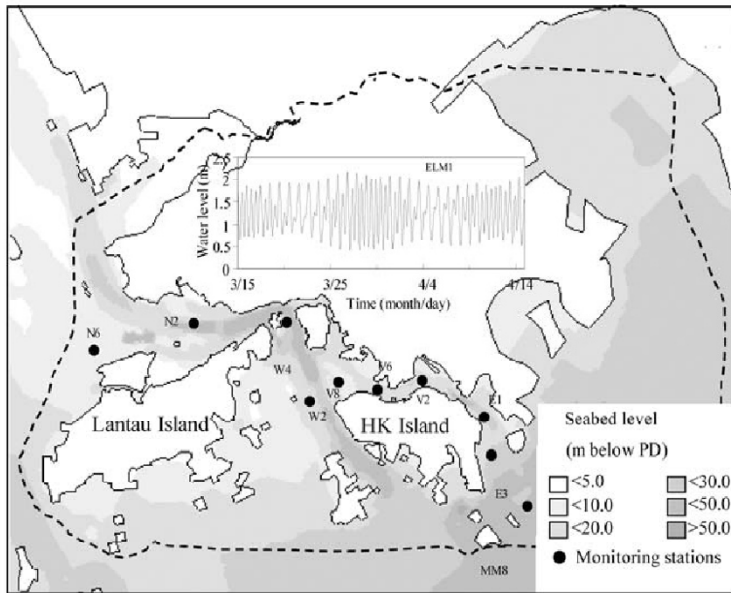
Fig. 8.17 Bathymetry of Hong Kong waters: the inset figure is the predicted water level during March to April 1998 at station ELM1 in East Lamma Channel

8.3.1 Tidal Currents

The water circulation in an estuary is mainly dominated by tidal exchange with the adjacent open sea. Astronomical tides, or simply tides—the regular rise and fall of the sea surface—are due to the relative motion of the earth-moon-sun system. In most regions, tides are semi-diurnal, meaning that during a typical day there are two high tides and two low tides. Depending on the location (latitude and topography), and time of the year, tides may be diurnal, meaning that there is only a single high tide and a single low tide in a day. A rising tide is termed a flood tide and a falling tide is termed an ebb tide. The moment when the water reaches its highest point at high tide (or its lowest point at low tide) is called the slack tide. The tidal range, defined as the difference in height between a high water and the following low water, also varies periodically with the phase of the moon in a given month. Tides of maximum range, known as spring tides, occur twice in 29 days, when the lunar and solar tide generating forces reinforce each other at around full and new moon. Likewise, tides of minimum range, known as neap tides, occur when the lunar constituent is opposed by the solar constituent—around the first and third quarter of the moon.

An accurate prediction of tides can aid the interpretation of water quality data and the planning of field surveys. In particular, it has been found that tide level is an important predictor for a few water quality parameters. Tidal prediction at a given location can be based on an extended harmonic analysis of a long term record (typically one year of hourly observations), in which tides are represented as the sum of a number of constituents of exactly known frequencies (derived from equilibrium tide theory, see e.g., Bowden, 1983). The harmonic analysis gives the standard amplitudes and phases of the tidal constituents—which can be used for prediction of tidal levels for that location. For example, Fig. 8.18 shows the comparison between predicted and observed tidal heights (based on 25 key tidal constituents) for typical tidal cycles in dry season. It is found that the tide level is well-predicted—in general with an average error of 0.1–0.2 m. Also shown are predictions based on tidal constituents derived from a calibrated three-dimensional (3D) hydrodynamic model (9 tidal constituents); with fewer harmonics the 3D model prediction is not as good, but still the phase is well-reproduced.
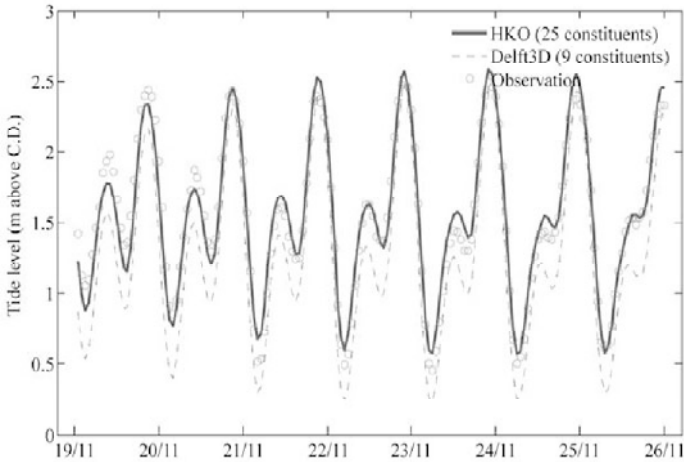
Fig. 8.18 Comparison of predicted tides (HKO and Delft3D model) with observations at Shek Pik for 19–26 November 2002 (dry season)

The general character of the tide can be expressed by the F-factor (ratio of tidal amplitudes for (K1+O1)/(M2+S2)). In general, tides would be considered semi-diurnal if $F < 0.25$ and diurnal if $F > 3.0$ (Bowden, 1983). In Hong Kong, F varies from 0.89 in Deep Bay (Tsim Bei Tsui) on the west to 1.27 in Mirs Bay (Kau Lau Wan) in eastern waters (Lee, unpublished; http://www.hko.gov.hk/tide/etide). Since $0.5 < F < 1.5$, tides in Hong Kong can be characterized as mixed and mainly semi-diurnal. The mean tidal range is 1.7 m; corresponding values for spring and neap tides are typically 2.0 and 1.0 m respectively. A typical spring-neap tidal variation in East Lamma Channel is shown in Fig. 8.17 (inset); it can be seen that the tide can vary from semi-diurnal tide (late March) to practically diurnal tide (early April) within a spring-neap cycle.

The hydrography of Hong Kong waters is mainly influenced by three factors: tidal currents, the Pearl River discharge, and monsoon-induced coastal currents. Tidal currents are determined by the interaction of ocean tides with the local topography and bathymetry; in general, the flow is from E/SE to W/NW through Victoria Harbor and East Lamma Channel which are deeper than the surrounding area, up towards the Pearl River estuary during flood, and from W/NW to E/SE during ebb. Figure 8.19(a) and (b) show the typical surface flow field during flood and ebb tides in the dry season. In the main tidal stream, significant peak surface velocities can be found in the northwestern waters north of Lantau Island (up to 2 m/s in narrow channels). During spring tide, the peak ebb velocity in Victoria Harbor is typically about 0.35 m/s near Stonecutters Island, 0.85 m/s in central Victoria Harbor, and increases to about 1.05 m/s at the eastern harbor entrance; the peak flood velocity is generally smaller at about 70%–90% of ebb velocities. During neap tide, the peak flood and ebb surface velocities are about 77%–86% of the spring tide values. The tidal velocity decreases towards the eastern waters; peak ebb velocity in Mirs Bay is about 0.2 m/s– 0.3 m/s near the entrance, and <0.1 m/s inside the bay. In some landlocked tidal inlets (e.g., inner Tolo Harbor), very weak currents of only a few cm/s are observed. Surface currents in the southern waters (south of Hong Kong Island, Lamma Island and Lantau Island) flow in accordance with the wind generated by the monsoon system. Fig. 8.19(c) and 8.19(d) show the surface flow field for the wet season. The predominant wind direction is E/NE in the dry season and W/SW in the wet season. In the wet season, during spring tide, the peak surface ebb velocity in Victoria Harbor is about 0.49 m/s near Stonecutters Island, 1.2 m/s in the central harbor, and increases to about 1.26 m/s at the eastern harbor

entrance; the peak flood velocity in the harbor is much smaller at about 30%–40% of ebb velocities. The peak flood and ebb surface velocities in neap tide are about 68%–75% of the spring tide values.

In Lema Channel at the entrance of the Pearl River Estuary, north-easterly residual currents of about 20 cm/s are observed during the wet season and south-westerly residual currents of similar magnitude are observed during the dry season. These support that besides the tidal induced residual flow, there are two seasonal Monsoons whose winds drive a strong additional residual current along the South China coast alternating in direction with the wet and dry season. In summary, the interaction of the freshwater runoff and the dominating oceanic currents determines the flow regime of the Hong Kong waters.
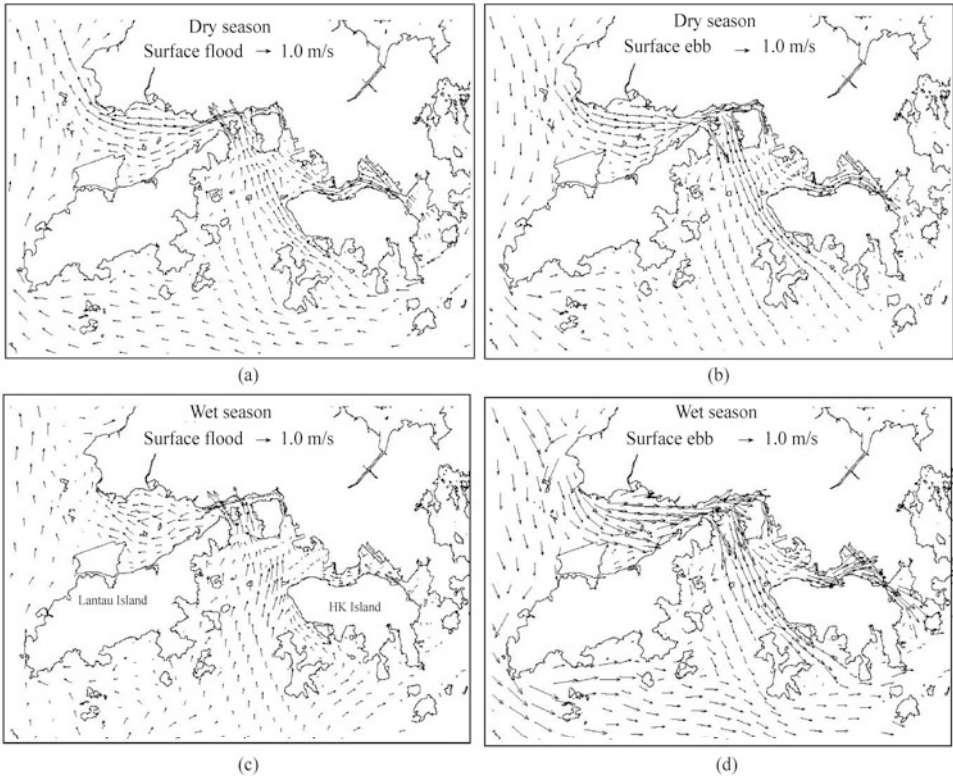
Fig. 8.19 General surface flow in Hong Kong waters during: (a) flood (HHW − 3 hr); and (b) ebb flow (HHW + 4 hr) in the dry season; and (c) flood (HHW − 3 hr); and (d) ebb flow (HHW + 4 hr) in the wet season (Lee et al., 2006) (Note HHW is higher high water)

8.3.2 Density Stratification

The hydrography is also intimately related to the salinity structure of the coastal waters. The coastal water is a mixture of fresh water derived from the river discharge (with low salinity) and oceanic shelf-water with relatively high salinity.

To illustrate the salinity transport in estuaries under the action of tide and freshwater runoff, the salinity intrusion in a rectangular estuary can be used as a simple test case. Ippen and Harleman (1961) have described the results of a series of salinity intrusion experiments conducted in a tidal flume. The channel is 327 ft. (99.67 m) long, 0.75 ft. (0.2886 m) wide and 1.5 ft. (0.4572 m) deep. The mean depth is kept at 0.5 ft. (0.1524 m) for all test runs discussed (Fig. 8.20(a). Tides are generated by means of a large

skimming weir in the tidal basin. Constant salinities are maintained at this end to represent the ocean end of the idealized estuary during each test run. Constant freshwater is discharged into the estuary at the other end of the channel. The flume is operated for a sufficiently long time to achieve mean steady state conditions for salinity intrusion.
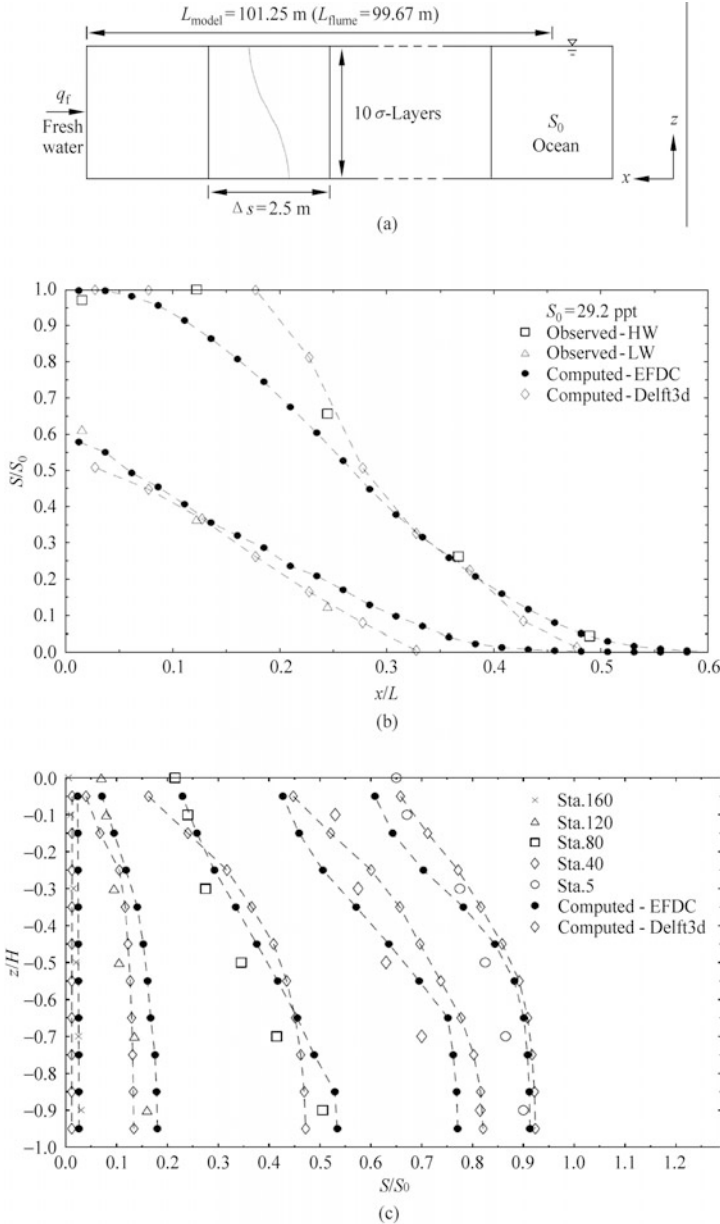
Fig. 8.20 (a) Schematic diagram of the numerical model for the tidal flume; (b) Comparison of experimental and computed instantaneous depth-averaged salinity distributions; (c) Comparison of experimental and computed tidally averaged salinity/ocean salinity vs. relative depth

A scenario with the following characteristics is selected: ocean salinity (S_0) = 29.2 ppt, freshwater discharge (per unit width q_f) = 0.929 × 10^{-3} m^2/s; tidal amplitude = 0.01524 m; tidal period T = 600 sec. The instantaneous depth-averaged salinity distribution is shown in Fig. 20(b). Figure 8.20(c) shows the tidally averaged vertical salinity profiles at selected locations. The observations are made at 5, 40, 80, 120, and 160 ft from the ocean boundary. The distance is used as the reference for the station as indicated in the figure. To reproduce the salinity transport in the estuary resulting from the salinity difference existing between the open sea and the freshwater inflow along the intrusion length, the results of two 3D hydrodynamic models (EFDC and Delft3D) are also presented.

In the dry season, Hong Kong waters are vertically well-mixed due to very low Pearl River discharge, strong tidal mixing and winds. The salinity (and temperature) is approximately vertically homogenous; salinities may vary from a low of around 15 ppt at the mouth of the Pearl Estuary to 34 ppt in the eastern waters (Fig. 8.21(a)). Salinity intrusions may reach to beyond Deep Bay (Fig. 8.21a), and Mirs Bay in the eastern waters is clearly unaffected by the Pearl River estuarine plume. In the wet season, however, the interaction of the Pearl River discharge and tidal currents creates significant vertical and horizontal salinity gradients (Fig. 8.21(b)). The western waters are strongly influenced by the Pearl River. For example, the surface salinity in the northwestern waters can be as low as 15 ppt, while the bottom salinity exceeds 32 ppt. By comparison, Victoria Harbor and East Lamma Channel are relatively more affected by tidal mixing, and the salinity differential is much less pronounced (< 7 ppt). The eastern waters are relatively sheltered from the Pearl River, and hence they are more oceanic with a typical salinity of 32-34 ppt and much weaker vertical salinity differentials. In the southern waters, the salinity differential is about 1 to 4 ppt, except for the fresh water main path in the deeper channels such as East Lamma Channel (with differentials in the range of 6-10 ppt).
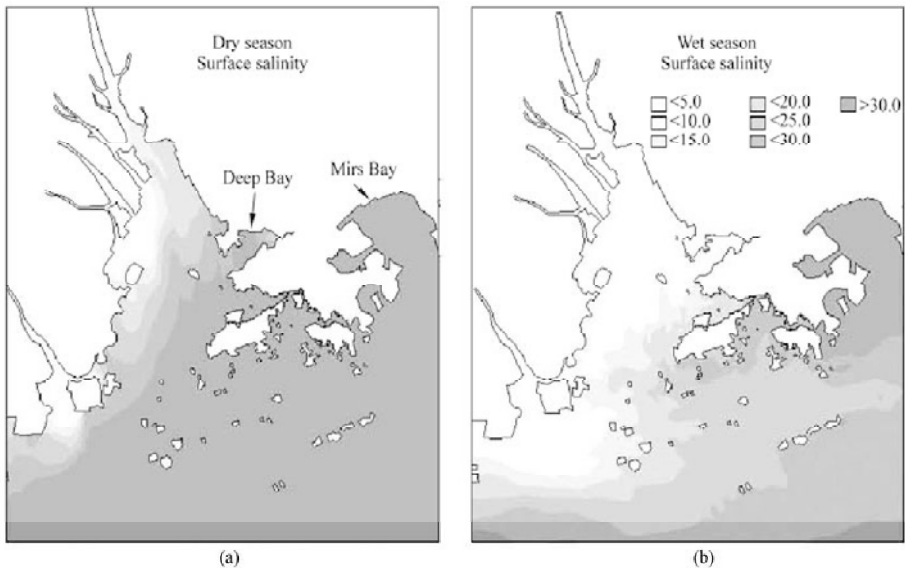
Fig. 8.21 General surface salinity field during flood at HHW−3 hr in (a) dry season and (b) wet season

In the wet season, the fresh river water spreads over the sea surface; the turbulent entrainment (mixing) of the more saline lower layer into the surface layer sets up a saline wedge intrusion which moves shoreward.

Figure 8.22(a) shows the salinity contours in a vertical section along a transect down the axis of the Pearl River, from A to B (Fig. 8.22a). Under an average wet season river discharge ($Q = 19,422$ m³/s), the bottom salinity of 18 ppt may intrude to the west of Deep Bay (point C, in Fig. 8.22(a) at higher high water (HHW), where the surface salinity is about 7 ppt. The bottom salinity of 18 ppt moves southward with the ebb flow, and reaches point D at lower low water (LLW), after a horizontal tidal excursion of about 12 km. At LLW, the vertical salinity distribution in the shallow estuary area is vertically well-mixed. Figure 8.22(b) shows the temporal changes in water level, salinity, and velocity at point C, where the salinity can change significantly within a tidal cycle. Pronounced vertical gradients can be observed around high tide, when the velocity is the weakest (high Richardson number and limited vertical mixing). In general, the vertical salinity gradients are much weaker in Victoria Harbor and adjacent waters.
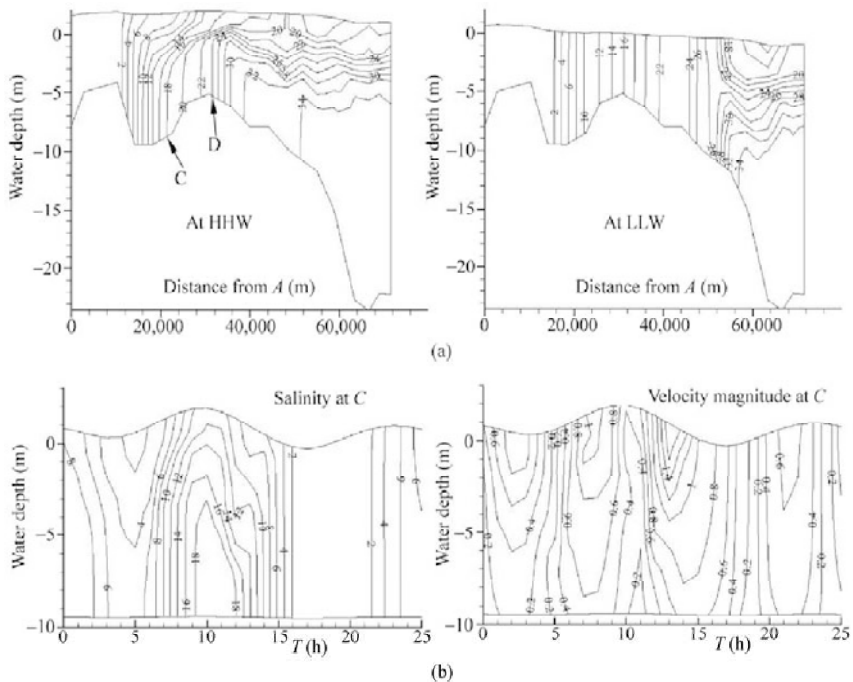
Fig. 8.22   (a) Computed salinity contours in a vertical section along a transect down the axis of the Pearl River estuary from A to B (see Fig. 8.17(a) at Higher High Water (HHW) and Lower Low Water (LLW) of a spring tide in the wet season for a Pearl River discharge of 19,422 m³/s; (b) Computed depth-time variation of salinity and velocity magnitude during a spring tide at location C in the wet season

8.3.4   Tidal Flushing

Wastes and pollutants released into the coastal environment are mixed and "flushed" by the highly variable estuarine hydrodynamic circulation as previously discussed. If the tide is the main forcing for the circulation, the flushing mechanism is then produced through repeated exchange of the intertidal water volume between the embayment and the open water body. Figure 8.23 presents a schematic illustration of the flushing mechanism for a semi-enclosed system: clean water (from the ocean or estuaries) entering the embayment during flood tide fills the intertidal volume, mixing with the existing water in the embayment and, as the tide falls, the intertidal volume of water discharges out of the embayment, removing the dissolved substance.

Time scales are often used to quantify the exchange and transport processes and to characterize the physical self-purification ability in an aquatic system. Tidal flushing time is a commonly used time scale, whose use can be traced back to the early 1950s. It is also known as residence time, total exchange time, turnover time, or detention time, but there is no unique agreed definition or method of determination. Very often, the flushing time is taken as the time required for a tracer mass to reduce to a certain level (such as e^{-1}, 50% or 10%) of the initial mass, so under certain assumptions it could be equivalent to such parameters as turnover time—the time taken for the mass level to fall to e^{-1} of the initial level (Prandle, 1984).
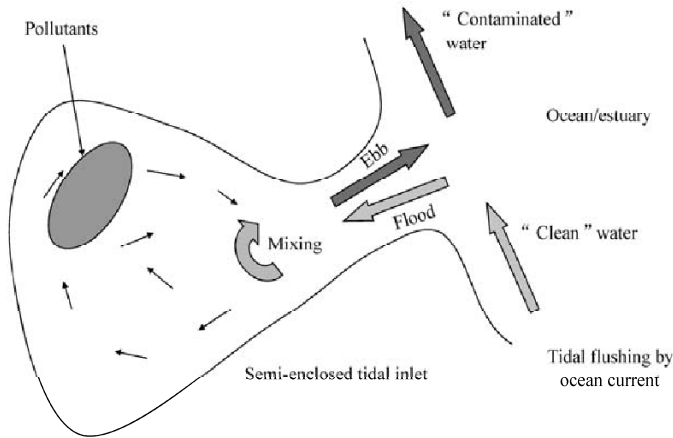
Fig. 8.23 Schematic illustration of tidal flushing mechanism for a semi-enclosed bay

In nature, the flushing time refers to the time needed for the entire volume of a specific water body to be removed through its open boundaries, but more often interest is focused on the removal of the dissolved substance in the water. For environmental management purposes, since many water quality processes occur at time scales much larger than that of tidal variation, hydrodynamic and water quality models can be effectively coupled by lumping all the tidal exchanges for a given system into a flushing rate. The main attractiveness of such a simplified approach is the immediate practical value of linking pollution input and ecosystem response in a tractable manner. For example, as a lumped measure of the effectiveness of hydrodynamic processes in removing any substance from the water body, the flushing time concept (or its inverse, flushing rate) is extremely important for ecosystem-scale nutrient budget assessment, or can be used to determine how much of a potentially harmful substance an embayment can tolerate.

A semi-enclosed embayment (e.g., fish farms or tidal inlets, or typhoon shelters) can be seen as a separate system within a larger water body connected to the outer sea. In general, the flushing time is governed by tidal exchanges between the system and the outer sea—which is a complicated function of the freshwater runoff, tidal range, topography and bathymetry, density stratification, and wind. Therefore, the exact value of flushing time is difficult to measure, but could be estimated from long term freshwater and salinity data when available, or alternatively be determined by hydrodynamic models.

The tidal flushing of a system can be studied with respect to a hypothetical tracer experiment. For a semi-enclosed system (Fig. 8.24) with a mean volume, V, and mean net flow, Q_e, a mass of tracer is instantaneously introduced into the system, and then the tracer mass in the system will decrease with time as tidal advection and dispersion act to remove the tracer through the open boundaries. If the system of water is initially labeled with a conservative tracer at initial mass, M_0, then assuming no mass return to
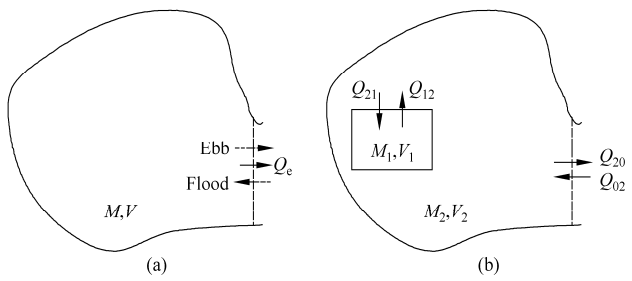
Fig. 8.24 Schematic diagram for flushing analysis of a semi-enclosed water body: a) one-segment system; b) two-segment system

the system from the exterior, the decrease of tracer mass due to tidal flushing is given by (Thomann and Mueller, 1987):

$$M = M_0 e^{-(Q_e/V)t} \tag{8.2}$$

In order to derive systematically the flushing time from numerical tracer experiments, we may adopt a definition of the flushing time as "the average lifetime of a particle in the given volume of water body" (Officer and Kester, 1991). For the tracer experiment, flushing time can be represented by the following equation:

$$T_f = -\frac{1}{M_0} \int_0^\infty t\, dM \tag{8.3}$$

Solving Eqs. (8.2) and (8.3) gives the flushing time:

$$T_f = \frac{V}{Q_e} \tag{8.4}$$

While the volume V can be readily obtained from field measurements, the net tidal exchange Q_e is affected by many factors including freshwater runoff, tidal flow, and salinity distribution, and cannot be directly measured. Hence, for a complex coastal embayment, traditionally, highly simplified methods based on readily available data (such as salinity or tide levels) are often applied – e.g., the "fraction of freshwater method" and "tidal prism method".

The tidal prism method is a classical approach to estimate flushing time in tidal systems when only basin geometry and tidal range information are available. By assuming that the flood flow entering the semi-enclosed inlet behaves like a jet, while the flow leaving the bay during ebb tide is a sink-type of flow (Ketchum, 1951; Stommel and Farmer, 1952), an analytical model of the tidal exchange characteristics between the inlet and its exterior can be obtained. Based on measurements of tidal cycles, the tidal prism method calculates the flushing time as:

$$T_f = \frac{VT}{(1-b)P} \tag{8.5}$$

where, V is the mean volume, T is the tidal period, P is the tidal prism equal to the difference in the volume of water between low and high tides, and b is the return ratio (fraction of ebb water returning to the embayment during the subsequent flood). The tidal prism method tacitly assumes complete mixing within the defined segments, and hence tends to produce overly optimistic flushing rates.

The tidal prism method cannot be applied to embayments with substantial freshwater inflow, because an increase of freshwater inflow leads to a decrease of the portion of the tidal prism volume. In such situations, the fraction of freshwater method is often used (Dyer, 1973; Fischer et al., 1979). Describing

the spatial variation as a linear mixing process, salinity is used to estimate the freshwater of the estuary over a pre-specified period:

$$V_f = \frac{S_o - S}{S_o} V \tag{8.6}$$

where V_f is the mean volume of freshwater in the embayment, V is the mean total volume of the embayment, S_o and S are the sea water salinity and the salinity in the embayment, respectively. The flushing time is then obtained by dividing the volume of fresh water (V_f) by the freshwater inflow (Q_f) to the estuary:

$$T_f = \frac{V_f}{Q_f} \tag{8.7}$$

This method provides a more realistic estimation of the flushing time, but can be used only when reliable detailed salinity and flow measurements are available. Moreover, the method is prone to error when salinity gradients along the coastal inlet are small (e.g., when most of the rainwater is routed to reservoirs, resulting in negligible freshwater inflow into the sea).

For environmental management purposes, it is necessary to define both local and system-wide flushing times to represent the effectiveness of the mass exchange with the surrounding water body and the open sea, respectively. The local flushing time is useful for estimating the local impact of any foreign substance or short-term effluent discharge from a small local region (e.g., a fish farm). However, for some water quality parameters such as nutrient level, the outer bay has a non-zero concentration due to the return of pollutants with the flood and ebb of tides. In this case, the system-wide flushing time needs to be considered by looking at mass removal from a much larger water body which is connected to an adjoining "clean" ocean. This definition takes into account the interactions between different parts of the water body which are not assumed to be clean and represents the long-term flushing efficiency of the region of interest. For this reason, it is often advantageous to model a semi-enclosed tidal region as a separate system within a larger water body connected to the open sea (Fig. 8.24b). We denote the tracer mass in the inner segment of volume V_1 as M_1 and the rest of the system (segment 2) of volume V_2 as M_2. Hence, the tracer concentrations are $C_1 (= M_1/V_1)$ and $C_2 (= M_2/V_2)$, respectively. Assuming the net tidal exchange flows between segments 1 and 2 are Q_{12} and Q_{21} and those between the system and the clean ocean are Q_{20} and Q_{02}, respectively, the following two equations can be obtained by tracer mass conservation (Choi and Lee, 2004),

$$\frac{dV_1 C_1}{dt} = -Q_{12} C_1 + Q_{21} C_2 \tag{8.8}$$

$$\frac{dV_2 C_2}{dt} = -Q_{20} C_2 + Q_{12} C_1 - Q_{21} C_2 \tag{8.9}$$

By applying different initial tracer distributions, both the local and system-wide flushing time can be computed from the tracer experiments. For example, assuming that a conservative tracer mass is instantaneously released into the fish farm (i.e., with the initial concentration of unity within the fish farm and zero elsewhere), the tracer mass reduction process is computed by solving Eqs. (8.8) and (8.9):

$$\frac{M}{M_o} = \gamma e^{-k_1 t} + (1 - \gamma) e^{-k_2 t} \tag{8.10}$$

where, the three coefficients γ, k_1 and k_2 are related to the segment volumes and tidal exchange flows. Using the definition in Eq. (8.3), the local flushing time is given by:

$$T_f = \frac{\gamma}{k_1} + \frac{1 - \gamma}{k_2} \tag{8.11}$$

Eq. (8.10) shows that the decrease in tracer mass follows a double-exponential curve described by

three flushing coefficients (i.e., γ, k_1 and k_2), and the local flushing time is solely dependent on the characteristics of the tracer mass removal curve. A similar relation is also found between the system-wide flushing time and its tracer mass removal process (Choi and Lee, 2004). With the advance of numerical hydrodynamic and mass transport models, the three flushing coefficients may be determined numerically from results of 3D numerical simulation, and then the flushing time can be determined subsequently. For estimating the local flushing time, the basic idea is that a mass of hypothetical conservative tracer is instantaneously introduced into a region of interest. A unit tracer concentration is prescribed initially inside that region, and the subsequent advective dispersion of this mass is then obtained by solving the mass transport equation numerically and the time-variation of the tracer mass inside the region is tracked. For estimating the system-wide flushing time, however, mass is released from everywhere inside the semi-enclosed water system.

As an example, the study for local flushing time and the system-wide flushing time in Yung Shue Au marine fish culture zone (FCZ), Three Fathoms Cove in Tolo Harbor is presented (Fig. 8.25). Figure 8.26(a) shows the tracer concentration distribution computed by a Lagrangian random walk method after 12 hours. It is found from Fig. 8.26(b) that the changes in tracer mass for both local flushing and system-wide flushing follow double-exponential curves (Choi and Lee, 2004).

Table 8.2 lists the flushing time and flushing rate of six representative fish culture zones (FCZs) in Hong Kong for the dry season and the wet season, respectively, including four FCZs in Tolo Harbor: Yung Shue Au, Lo Fu Wat, Yim Tin Tsai, and Yim Tin Tsai East (Fig. 8.25), and Sok Kwu Wan and Ma Wan. In general, assisted by the density-driven estuarine circulation, the flushing rate in the wet season is substantially greater than in the dry season.

Generally speaking, unlike the traditional approach of determining the flushing time using salinity or freshwater concentration, the numerical approach discussed herein is applicable even for cases when salt-balance methods cease to apply: negligible freshwater runoff and weak longitudinal salinity gradients, or when detailed salinity data are lacking (e.g., for new projects).
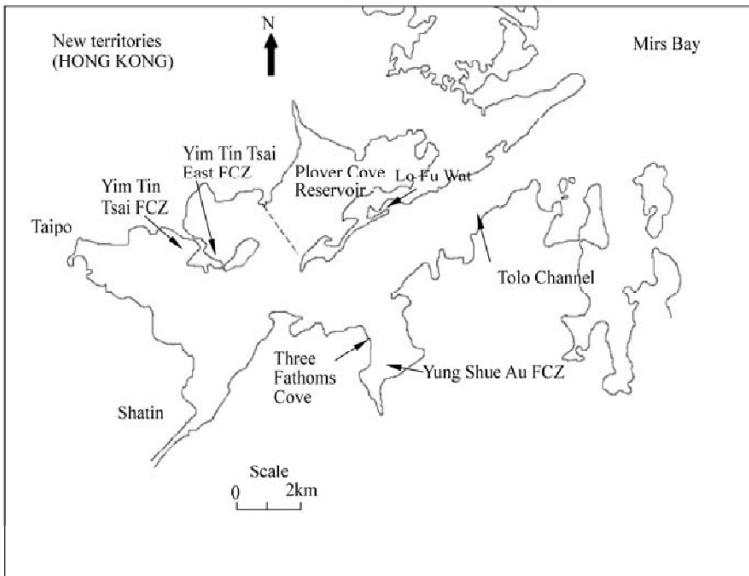
Fig. 8.25   Location of four marine fish culture zones in Tolo Harbor, Hong Kong: Yung Shue Au, Yim Tin Tsai, Yim Tin Tsai East and Lo Fu Wat

Table 8.2 Computed flushing time and flushing rate of six fish culture zones in Hong Kong

	Yung Shue Au		Lo Fu Wat		Yim Tin Tsai	
	Winter	Summer	Winter	Summer	Winter	Summer
Flushing time (day)	23.60	14.20	15.80	7.10	38.00	14.40
Flushing rate (d^{-1})	0.0424	0.0702	0.0632	0.1405	0.0264	0.0696
	Yim Tin Tsai East		Sok Kwu Wan		Ma Wan	
	Winter	Summer	Winter	Summer	Winter	Summer
Flushing time (day)	27.20	14.80	25.80	3.50	3.08	1.54
Flushing rate (d^{-1})	0.0368	0.0676	0.0387	0.2825	0.3247	0.6496
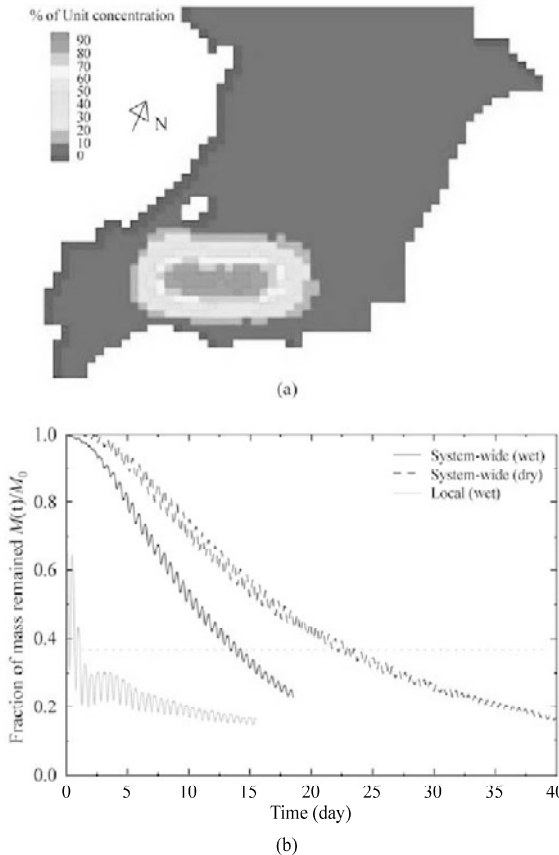
Fig. 8.26 (a) Computed tracer concentration distribution 12 hours after release of tracer mass in Yung Shue Au fish culture zone, Three Fathoms Cove, Hong Kong; (b) tracer mass variation with time for system-wide flushing and local flushing, for dry and wet season

8.3.5 Application for Estuarine Management

8.3.5.1 Third Shanghai Sewerage Project of the Yangtze River Estuary

Shanghai, the largest metropolitan area in China, is situated on the eastern boundary of the Yangtze River delta with the East China Sea in the east, Yangtze River in the north, Hangzhou Bay in the south, and

bordering the provinces of Zhejiang and Jiangsu in the west (Fig. 8.27). Rapid economic development and increase in population has resulted in serious surface water pollution problems due to large amounts of untreated wastewater being discharged into the rivers and other watercourses. It is estimated that the total sewerage flow from Shanghai will be 8.5 million m^3 per day in 2010, in which more than 7.0 million m^3 per day of wastewater will be discharged into the Yangtze River estuary (YRE) and Hangzhou Bay through outfalls after preliminary treatment; the other 1.0 million m^3 per day of wastewater or more will be discharged to the nearby inner rivers after intensive treatment.
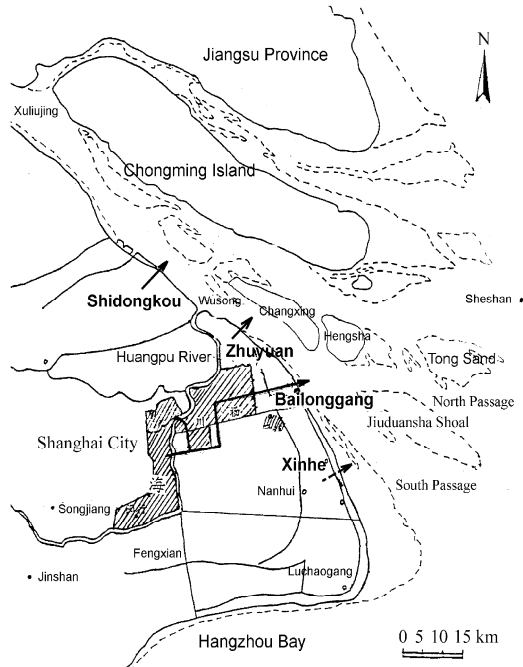
Fig. 8.27 Sketch map of Yangtze River estuary and the positions of the outfalls

Since the 1980s, great efforts have been devoted to improve the water environment in Shanghai by the provision of proper sewage treatment and disposal systems. The First Shanghai Sewerage Project (SSPI) was completed in 1993. In this project, the wastewater is conveyed and disposed to YRE at Zhuyuan through a submerged outfall after preliminary treatment. SSPII (completed in 2000) discharges wastewater into YRE through a submerged outfall at Bailonggang at the freshwater/saltwater interface and high turbidity mixing zone. Bailonggang is 38.5 km downstream of Wusong where the Huangpu River enters the Yangtze River, and 16.5 km downstream of Zhuyuan. For SSPIII (completed in 2008), a new Xinhe outfall (discharge 1.50 m^3 per day) has been established downstream of Bailonggang. Prior to SSPIII, the discharges of the Shidongkou, Zhuyuan and Bailonggang outfalls were 0.17, 1.45, and 0.79 million m^3 per day, respectively; for SSPIII projects, their loads are 0.8, 3.30, and 1.70 million m^3 per day.

Figure 8.27 shows a map of the YRE and the positions of existing outfalls and proposed outfall. The Yangtze River is bifurcated by Chongming Island into the south branch and north branch from Xuliujing, and almost all of the flow goes through the south branch while the flow in the north branch can be ignored. The south branch is divided into the south channel and north channel by Changxing Isle and Hengsha Isle, in which the flow distributes in close proximity to each other, and the south channel is bifurcated by

the Jiuduansha Shoal into the south passage and north passage.

During the period of SSPIII design, the importance of the YRE's hydrodynamic characteristics has been considered; a 2D hydrodynamic model based on Delft3D was developed to assess the effect of SSPI and SSPII so as to provide some reference for SSPIII (Lee et al., 2001b). The velocity vector fields, the water elevation, the trajectories of drogues, and the far field sewage dilution fields from the existing and proposed outfalls were studied for the spring/neap tide and the dry/wet season. In general, the modeling results show the hydrodynamic condition of the YRE is beneficial to sewage dilution and diffusion; however, it reveals the effluents discharged through outfalls at present have relatively little impact on the water environment of the YRE. For the SSPIII flow through 4 outfalls, the water quality of the YRE will significantly deteriorate in the absence of any treatment, especially during the neap tide of the dry season.

Based on the calibrated model, drogue tracks released from the 4 outfalls during wet and dry seasons have been simulated. Figure 8.28 shows the drogue trajectories after the sewage is released at different times from Bailonggang outfall. The drogues generally follow the tidal oscillation in a "to and fro" manner, progressively move downstream close to the shore, and eventually leave the computational boundary between Luchaogang and Dajishan towards Hangzhou Bay. As a whole, drogues released in spring tide move a little faster than when released between the spring and neap tide, while they move much faster in the wet season than in the dry season. The drogues released from Zhuyuan, Bailonggang and Xinhe outfalls can move out of the simulation boundary in 2 or 3 days in the wet season, while the drogues released from the more upstream Shidongkou outfall need 5 days or longer. It is found that the effluent from the four outfalls will be transported downstream towards Hangzhou Bay. The sewerage plan and SSPIII should hence consider the self-purification capacity of both the Yangtze River estuary and Hangzhou Bay.
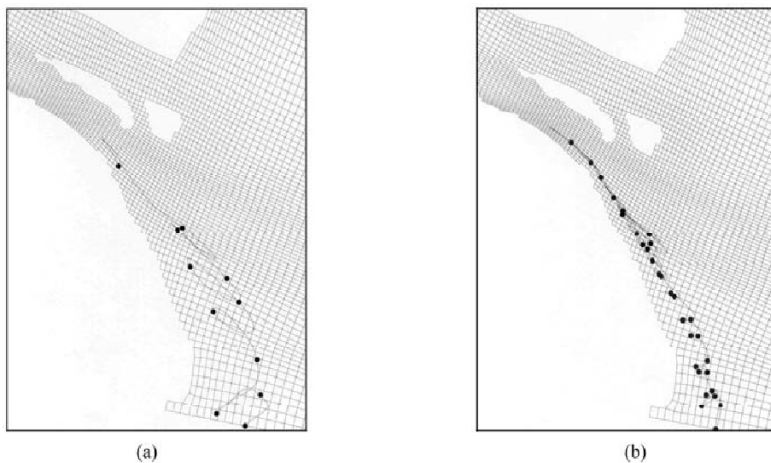
Fig. 8.28   Trajectories of drogues released from the Bailonggang outfall during the spring tide: (a) wet season; and (b) dry season

8.3.5.2   Impact of Land Reclamation on Victoria Harbor

The large scale land reclamation in Hong Kong was adopted to create land for urban development. By 2003, about 3200 hectares had been reclaimed in Hong Kong. Among these, 661 hectares are existing and committed reclamation areas in Victoria Harbor between Stonecutters Island and Lei Yue Mun (Fig. 8.29). Currently, Hong Kong is entering the final phase of land reclamation projects in Victoria Harbor. On Hong Kong Island, just two more projects are outstanding—the Central Reclamation Phase III (CRIII) and the Wan Chai Development Phase II (WDII). On the Kowloon peninsula side, reclamation is planned

for the South East Kowloon Development (SEKD) around the old Kai Tak airport. In recent years, the remaining two reclamations on the Hong Kong Island have been the focus of considerable public debate. The Hong Kong government has taken the initiative to review again the reclamations plans and the reclamation area of CRIII has been reduced to 18 hectares from the originally planned 32 hectares. It is of interest to study the effect of the drastic changes in coastal configuration and the proposed reclamation plan on tidal currents and water quality in the harbor.

Fig. 8.29 Existing and proposed large scale reclamation in Victoria Harbor, Hong Kong (yellow color: proposed reclamation, other colors: existing reclamation)

The effect of the existing large scale land reclamation and maximum possible Central and Wan Chai reclamation on tidal circulation and flushing in Victoria Harbor were computed by a calibrated three-dimensional hydrodynamic model for the Pearl River estuary (Kuang and Lee, 2004). In this study, this 3D hydrodynamic model with 10 uniform layers in the vertical direction was used to study the changes in tidal circulation and flushing in Victoria Harbor due to both existing reclamation and further Central and Wan Chai reclamation. The Pearl River Estuary Model was set up for studying the tidal circulation of Hong Kong coastal waters, and it uses a 230×159 boundary-fitted orthogonal grid, with a refined grid size of 45 m to 75 m around Victoria Harbor (Fig. 8.30).
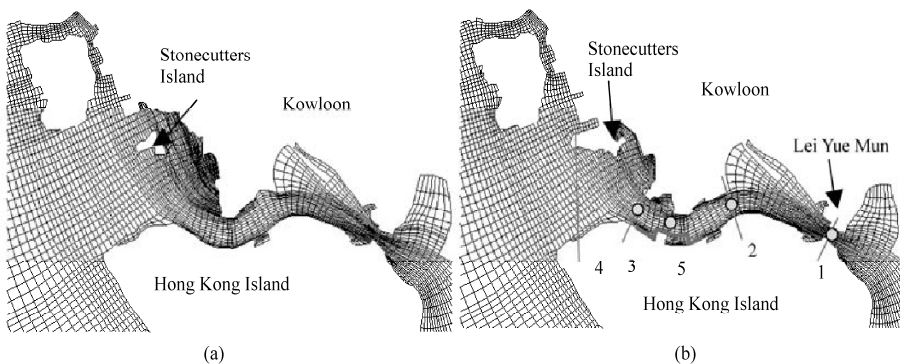
Fig. 8.30 Computational grid around Victoria Harbor with the coastline of year (a) 1975 and (b) 2003 the blue line: coastline after further maximum possible reclamation in central area)

Using this model, it was found that in the main tidal stream, peak velocities of the west-east ebb flow are found to be about 0.15 m/s near Stonecutters Island, 0.60 m/s in the central harbor, and to increase to about 1.05 m/s at Lei Yue Mun. The east-west flood flow is similar, with a little smaller peak flood velocities. The flow is qualitatively similar to that before reclamation, but there is a notable decrease of about 8%–17% with a mean value of 11.5% in peak discharge along the harbor channel. This leads to a decrease in tidal velocity in the east of section 2, but an increase in tidal velocity in the west of section 2 due to significant reduction in width after reclamation of a large area (Fig. 8.31). For example, the depth-average peak velocity decreases around 9.6% at point 1 and increases 19% at point 3; both will slightly increase by less than 1% after completion of the proposed reclamation (maximum possible Central and Wan Chai reclamation).
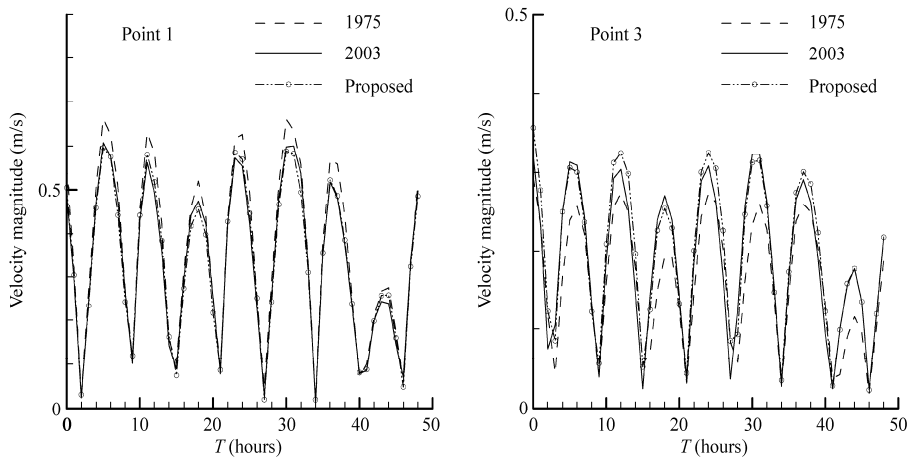
Fig. 8.31   Comparison of time variation of depth-averaged velocity magnitude at points 1 and 3 in the wet season with different coastlines ($T = 0$ at 0:00 on 5 August, 2003)

The computed flushing times in the wet and dry seasons for different coastlines are listed in Table 8.3. After reclamation of a large area, the self-cleansing capacity of Victoria Harbor is decreased by 30%–50%. Further Central and Wan Chai reclamation will slightly improve the flushing capacity in Victoria Harbor by 1%–1.5%. In present coastline, the flushing time in Victoria Harbor ranges from 1.5 to 2.5 days in the wet season and from 5 to 7 days in the dry season.

Table 8.3   Flushing time (days) in Victoria Harbor for different coastlines

Coastline	Wet season	Dry season
1975	1.10	4.85
2003	1.67	6.25
Proposed	1.65	6.16

8.4   Eutrophication and Algal Bloom

Eutrophication refers to the enrichment of a water body by nutrients—the chemical substances essential to the growth of plants—to a level that results in high biological productivity, deterioration in water quality, and undesirable disruption to the balance of aquatic ecosystem. Eutrophication can occur in rivers

and lakes, estuaries, coastal or marine waters, and has been recognized as an important and widespread global environmental problem.

Over very large time scales, eutrophication can be viewed as a natural process particularly in lakes and impounded waters. Young natural lakes are generally relatively barren bodies of waters. As ageing proceeds the materials retained by the lake gradually increase in the bottom sediments and, as a result of decomposition processes occurring there, nutrients are released to the lake water leading to an increase in biological productivity. This is also affected in part by the change in shape of the water body brought about by its filling; the increasing shallowness increases the re-cycling of available nutrients. As a result, the lake undergoes major changes gradually from the **oligotrophic** phase to **mesotrophic** phase and **eutrophic** phase (Table 8.4).

Table 8.4   Water quality impairment of lakes affected by nutrient enrichment

Limnological characteristics	Oligotrophic	Mesotrophic	Eutrophic
Nutrient	Low	Medium	High
Biomass	Low	Medium	High
Transparency	High	Medium	Low
Hypolimnetic oxygen content	High	Variable	Low
Impairment of multi-purpose use	Little	Variable	Great

The naturally slow eutrophication process can be greatly accelerated by human activities: intensive agricultural development, growth of human population, urbanization, and industrialization—all of which introduce excess nutrients into the receiving waters. For example, Fig. 8.32 shows a close relationship between the human population and the number of "red tide" occurrences from 1976 to 1986 in Tolo Harbor of Hong Kong (Lam and Ho, 1989). Human-induced eutrophication originally became the environmental focus in European and North American lakes and reservoirs in the mid-20th century (Rodhe, 1969). However, it has become more widespread, both in inland waters and coastal waters. For example, by the early 1990s, 54% of lakes in Asia were eutrophic; in Europe, 53%; in North America, 48%; in South America, 41%; and in Africa, 28% (ILEC, 1988).
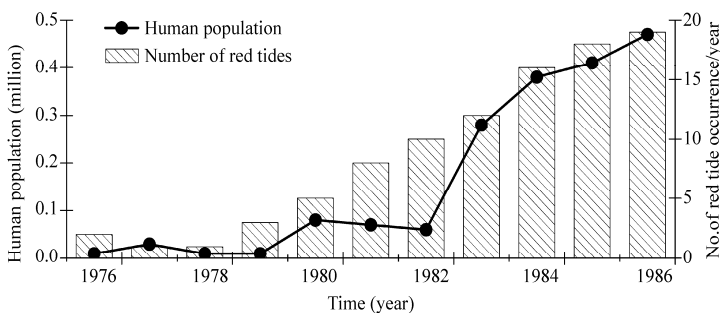
Fig. 8.32   Increase in human population and number of red tides occurrences in Tolo Harbor, Hong Kong

8.4.1   Symptoms and Environmental Impacts

Under favorable environmental conditions, excessive enrichment of nutrients in a eutrophic water body can lead to extremely rapid growth of microscopic algae or phytoplankton. When this happens the algae are said to have formed a bloom. High algal concentration gives the water a distinct greenish or brownish color in lakes ("pea soup"), while "red tides" are often observed in many estuaries and coastal waters. An

example of typical seasonal variation of environmental factors and algal bloom patterns in temperate climates is shown in Fig. 8.33 (Welch, 1980).
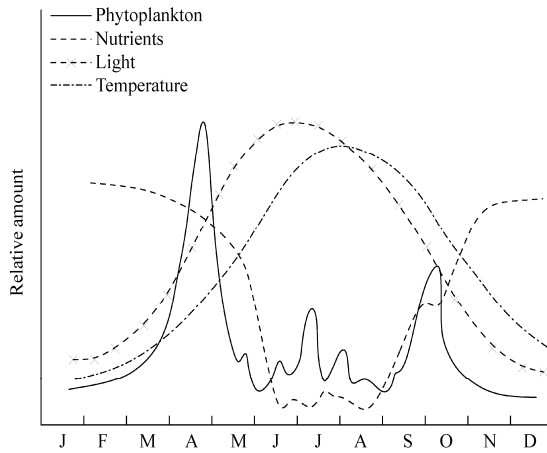
Fig. 8.33 Algal bloom patterns in temperate waters: general seasonal cycle of environmental forcing factors and phytoplankton biomass (modified from Welch, 1980)

Municipal effects—The excessive growth of phytoplankton can give rise to a variety of environmental problems: unsightly algal blooms, decreasing water transparency, and emission of noxious odors due to decomposition of algal scum; all these inevitably lead to deterioration of water quality and destroy the aesthetic and recreational uses of water bodies (e.g., swimming and boating activities). Some types of algae, e.g., cyanobacteria and filamentous species of chlorophytes may clog filtering systems in waterworks, making it difficult to treat drinking water for human consumption. Also, the treated water may have unacceptable taste or odor due to the secretion of organic compounds by microbes. Further, when water with high concentrations of dissolved organic carbon is disinfected by chlorination in the waterworks, several potentially carcinogenic and mutagenic byproducts may be formed.

Toxins—Harmful algal blooms (HABs) are caused not only by microalgae but also by cyanobacteria and protozoan agents that secrete toxins. Algal toxins can pose a grave health risk by damaging the liver, intestines, and nervous system. In inland waters, about half of all bloom species are toxic; in coastal waters, about 40 or 50 of the phytoplankton species may produce toxins. Drinking toxin-tainted water can cause vomiting, gastrointestinal disorders, headache, muscle pain, paralysis, respiratory failure, and even death. On the other hand, toxins from algae blooms may enter the food chain and become highly concentrated in various aquatic products which may become very dangerous for human consumption; for example, consumption of sea food contaminated by algal toxins can lead to Paralytic Shellfish Poisoning (PSP).

Hypoxia—Algal blooms and red tides can result in severe rapid oxygen depletion, especially in waters with poor hydrodynamic conditions—e.g., isolated lakes or semi-enclosed bays with poor flushing rates. Although phytoplankton can release oxygen to the water as a byproduct of photosynthesis during the day, water has a limited ability to store dissolved oxygen (DO). On the other hand, the respiration of phytoplankton and zooplankton, and the bacterial decomposition of organic matter (e.g., settled algal detritus) can consume large amounts of DO. The oxygen in the water can be rapidly depleted if the renewal processes of DO (at the free surface or with the open ocean) are very slow due to poor hydrodynamic conditions. Figure 8.34 illustrates the photosynthetic production of algae and bacterial consumption of oxygen in a stratified lake.
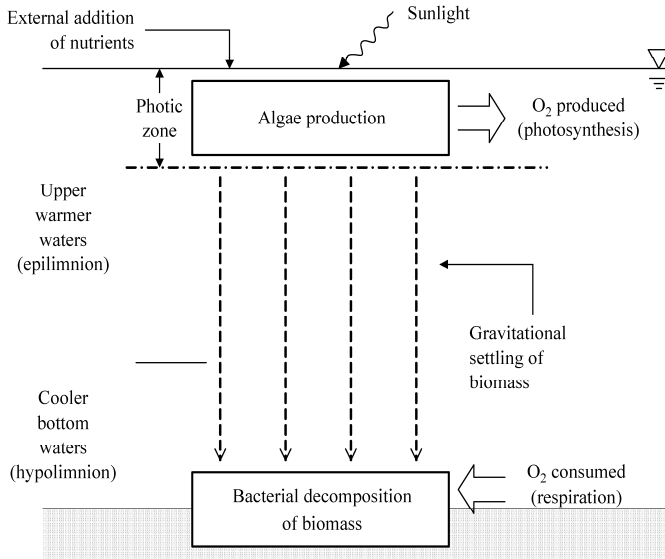
Fig. 8.34   Photosynthetic production and bacterial consumption of oxygen in a stratified lake

Biological effects—A number of biological changes may occur as a result of eutrophication: decreased biodiversity, adverse community reaction, and changes in biomass and dominant species. For instance, initially in an oligotrophic lake, the number of species of algae increases due to nutrient accumulation, causing temporary increase in diversity of primary producers; however, as eutrophication proceeds, specific bacteria become dominant, displacing many algal species. Some of these changes are indirect, e.g., increased turbidity significantly reduces the light penetration in the water column, which negatively impacts the survival of submerged plants relying on the sunlight for photosynthesis. Similarly, the fish community may be indirectly affected and becomes dominated by some surface-dwelling coarse fishes (e.g., cyprinid fish).

Fishkill—Algal blooms in lakes and coastal waters are often accompanied by massive fish kills, resulting in considerable economic loss and causing social concern and alarm. Extensive fish kills have been reported in many countries world wide (Fig. 8.35). The fish kills are often related to either toxic algal blooms or severe DO depletion. Although fishes can endure brief periods of reduced oxygen, they begin to die if DO concentrations fall below about 2–3 mg/L. In addition, adverse environmental conditions with low DO in the bottom waters results in the release of hydrogen sulphide (H_2S) from sediments, which is lethal to most fishes.

8.4.2   Causes of Eutrophication

Algal growth requires nutrients such as carbon, nitrogen, phosphorous, iron, manganese, boron, cobalt, vitamins, and others. However, the limiting nutrients mainly held responsible for cultural eutrophication are inorganic compounds of nitrogen or phosphorus. It is generally accepted that phosphorus is the limiting nutrient in most inland waters, and nitrogen has been proven to be the limiting nutrient in most coastal waters. Nitrogen and phosphorus come from many sources (Fig. 8.36): point sources of sewage and industrial discharge along tributaries, non-point sources from agricultural areas in the drainage basin or shores, pollution from aquaculture or mariculture zones, external loads from precipitation, and internal loads released from sediment bed.

Fig. 8.35 Global distribution of extensive fish kills recorded as of 2006 (Woods Hole Oceanographic Institution, http://www.whoi.edu)
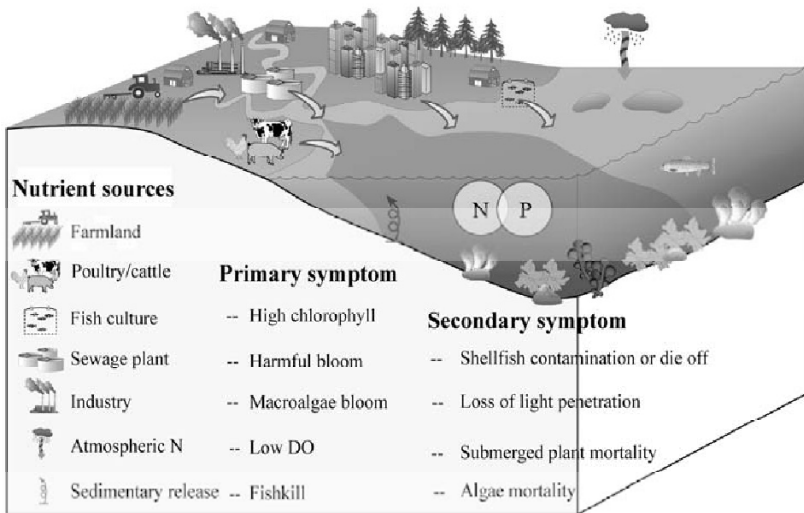
Fig. 8.36 Conceptual diagram of nutrient sources and eutrophication symptoms

Case study—Taihu Lake, situated in the Yangtze River delta (30º55'42"–31º33'50"N and 119º53'45"– 120º36'15"E), is the third-largest freshwater lake in China, with an average depth of 1.9 m and a surface area of 2,338 km^2 (Fig. 8.37). The lake is the source of drinking water supply for about 30 million people in the surrounding cities, and helps irrigate millions of hectares of grain and cotton fields in a lush agricultural region. In addition, it sustains one of China's most important fisheries for crab, carp, and eel. Even though the lake system is fed by over 200 streams in a river basin of 36,900 km^2, the discharges of most of these streams are very limited. For example, the mean discharge of the largest tributary is relatively small, only 26.8 m^3/s. Both field and modeling studies reveal that the circulation of this lake is primarily driven by wind, and its hydraulic retention time is around 300 days.
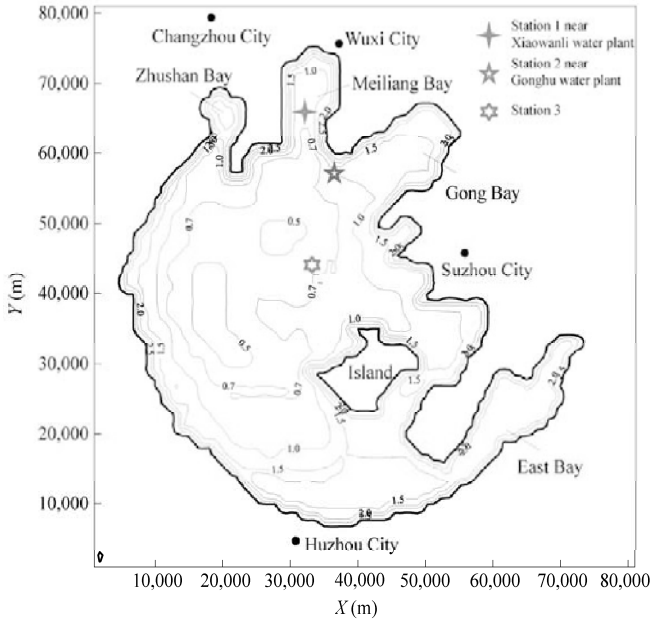
Fig. 8.37 Topographic overview of Taihu Lake (depth contour in MSL) (Mao, 2005)

Phosphorous is the limiting nutrient for Taihu Lake's eutrophication. Records show that Taihu Lake was oligotrophic as recently as the 1950s and 1960s, with chlorophyll-*a* concentrations of about 2 mg/m^3 and total phosphorus (TP) of about 10 mg/m^3 (Chen et al., 2003). However, since the late 1980s, the water quality of this lake has severely deteriorated and algal blooms have become a frequent nuisance. These blooms, which generally occurred in the summer and early fall, were considered to be the result of a combination of high nutrient loads and lengthened hydraulic retention times. Figure 8.38 shows the temporal variation of observed chlorophyll-*a* concentration at three representative sampling stations (see Fig. 8.37)—Station 1 near Xiaowanli water plant in the north, Station 2 near Gonghu water plant in the northeast, and Station 3 in the middle of the lake. It can be seen that from 1997 to 2002 the chlorophyll-*a* concentrations at these stations frequently exceeded 10–20 mg/m^3, with maximum values in excess of 100 mg/m^3.
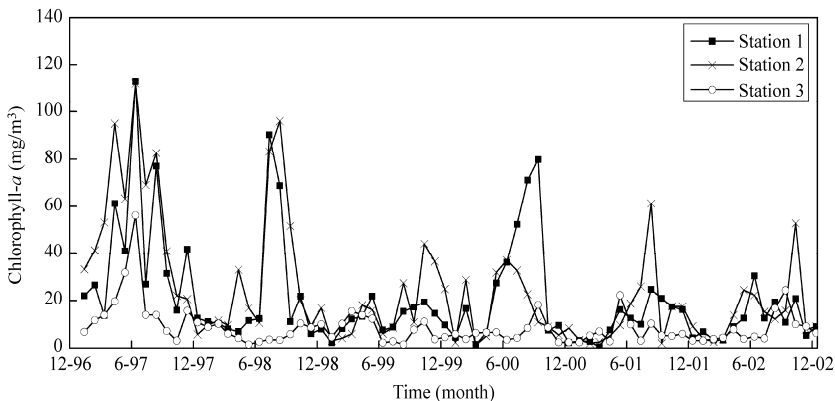
Fig. 8.38 Observed chlorophyll-*a* concentration at three sampling stations in Taihu Lake during 1997–2002 (Mao, 2005)
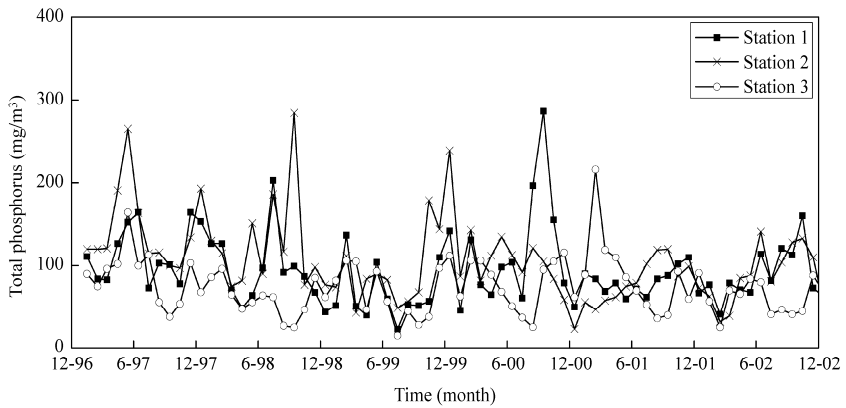
Fig. 8.39 Observed TP concentration at three sampling stations in Taihu Lake during 1997–2002

According to observation data, from 2000 to 2005, the averaged TP is up to 78 mg/m^3. Except for east and south parts, nearly 87% of the entire Taihu Lake was suffering from nutrients aggregation. As shown in Fig. 8.39, compared to the 1960s the concentrations of TP at these three stations have increased by 10–30 times due to high nutrient input from domestic sources and agricultural activities. For this reason, an algal bloom might break out without warning if the weather and physical conditions are favorable for algal growth. For example, in the early summer of 2007, a massive and wide spread bloom of cyanobacteria broke out in Taihu Lake, stimulated by extremely high concentrations of nutrients and unusually hot dry weather. This bloom covered about one-third of the lake and severely destroyed the water supply system (Fig. 8.40), and local residents of Wuxi, a city of 5 million, had to resort to bottled drinking water for several days. According to the Administration Bureau of Taihu Lake Basin, during the bloom, the chlorophyll concentrations at the water-supply sources of the north part of the lake all reached very high levels (Xiaowanli Waterworks, 259 μg/L; Gonghu Waterworks, 139 μg/L; and Xidong Waterworks, 53 μg/L). Consequentially, their DO concentrations declined to a very low level, almost to zero.

Fig. 8.40 A bloom of cyanobacteria at a water intake area of Wuxi, June, 2007 (Xinhua News Agency, http://www.xinhuanet.com) (See color figure at the end of this book)

8.4.4   Eutrophication Control and Management

Control of eutrophication is mainly affected by manipulating the nutrient input. So far many suggestions have been proposed to mitigate the effects of eutrophication, ranging from developing monitoring programs that provide early detection of algal blooms, to introducing potential pathogens to cure blooms. Because any action taken to control or cure blooms may have enormous impact on the environment, it is generally more cost-effective to take early preventive measures to control eutrophication than to develop curative strategies after the water quality has already deteriorated.

Common restoration methods mainly include diversion of nutrient input to another water body where the impact is less, and reduction of nitrogen or phosphorus by chemical and biological means (e.g., water treatment). It is usually sufficient to reduce only the most important limiting nutrient (Schindler and Fee, 1974). Control of point sources of pollution from municipalities and industries is usually given priority as it is the most cost-effective measure. In many cases, however, effective prevention of eutrophication, or restoration of eutrophic waters cannot be achieved without controlling non-point source pollution. Considering the difficulty for controlling non-point sources, the improvement in all aspects should be encouraged: ① control of agricultural practices contributing nutrients to water bodies, with special reference to waste from animal husbandry, irrigation, fertilizer application, and fish culture; ② integrated approaches to control urban runoff and storm overflows, which normally by-pass conventional treatment plants; ③ preserving natural buffer strips or constructing artificial wetlands to reduce the amounts of nutrients reaching water bodies from runoff, since they are based on the capacity of self purification of nature and are usually much cheaper to maintain and operate.

Considerable effort has been directed towards the development of tools for a better understanding of the causes and consequences of massive algal blooms. An interdisciplinary study is usually required for assessing the risks and impacts of eutrophication. In general, three approaches have been adopted: setting of thresholds based on available data and expert judgment, establishment of empirical cause-effect relationships, and development of numerical modeling (Nixon et al., 1996; OECD, 1982; Painting et al., 2007). An assessment standard may consider many environmental indicators of eutrophication, including primary production, nutrient, DO, turbidity, submerged vegetation, and macroalgae. Extensive research on empirical relationships has greatly improved our understanding of the causes and effects of eutrophication. Mathematical models that incorporate all the major interactions (growth kinetics, hydraulic transport, and environmental parameters) of the ecosystem have also proved to be useful in predicting trends of eutrophication and evaluating the effectiveness of alternative methods of control (e.g., waste reduction, flow augmentation).

Case study—Hong Kong is situated at the mouth of the Pearl River Estuary (Fig. 8.41) in southern China. The high incidence of red tides and algal blooms is a unique feature in the sub-tropical coastal waters around Hong Kong, which is believed to be related to the eutrophication caused by excessive and concentrated organic discharges. The reported number of red tides reached a peak of 88 outbreaks in 1988, but decreased to current frequencies of around 20 per year after the introduction of the Tolo Nutrient Export Scheme in the mid-1990s (Fig. 8.42). Hong Kong's population and organic sewage loads are centered around Victoria Harbor; before the Harbor Area Treatment Scheme came into operation in 2001, some 1.5 million m^3 of untreated sewage and industrial wastewater were discharged daily into Victoria Harbor. The annual non-point source pollution load into Hong Kong's coastal waters is estimated to be about 8000 tons of total nitrogen (TN) and 1500 tons of TP (Li et al., 2003). Besides, the background pollution is contributed by the organic load carried by the Pearl River estuary.

Fish kills are often associated with the observed red tides. The 1998 red tide (due to the dinoflagellate *Karenia digitatum*) was the most serious red tide in Hong Kong's history. It was recorded that 30 red tide
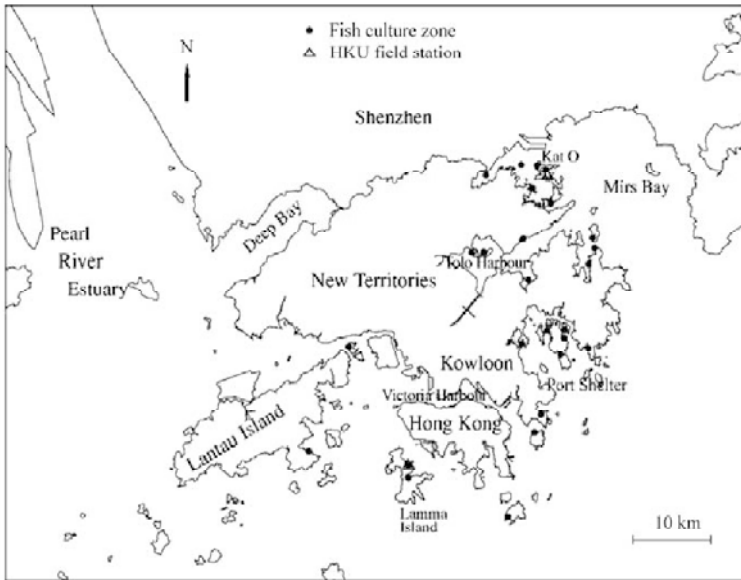
Fig. 8.41 Hong Kong and the Pearl River Estuary (locations of marine fish culture zones and algal dynamics field station indicated)
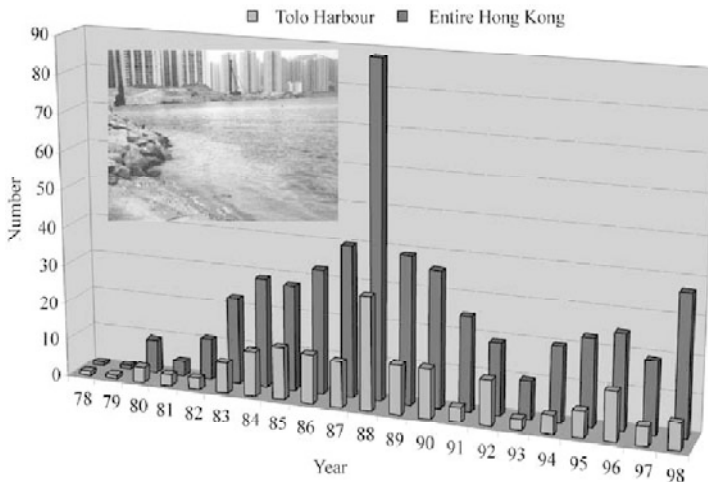
Fig. 8.42 Red tide occurrences in Hong Kong during 1978–1998

incidents appeared in the first six months of 1998 with the most serious events during the period 19 March to 17 April (Anderson, 1998). This unusually devastating red tide resulted in the worst fish kill in Hong Kong's history—it destroyed over 80% (3,400 t) of cultured fish stock, with an estimated loss of more than HK$312 million (Dickman, 1998; Yang et al., 2000). This massive red tide in Hong Kong's southern waters is related to algal bloom transport; it was reported that the algal bloom appeared first in the northeast Mirs Bay, and then appeared to be transported southward into Port Shelter, and further westward to Lamma Island, where the most severe fish kill occurred (Fig. 8.43).
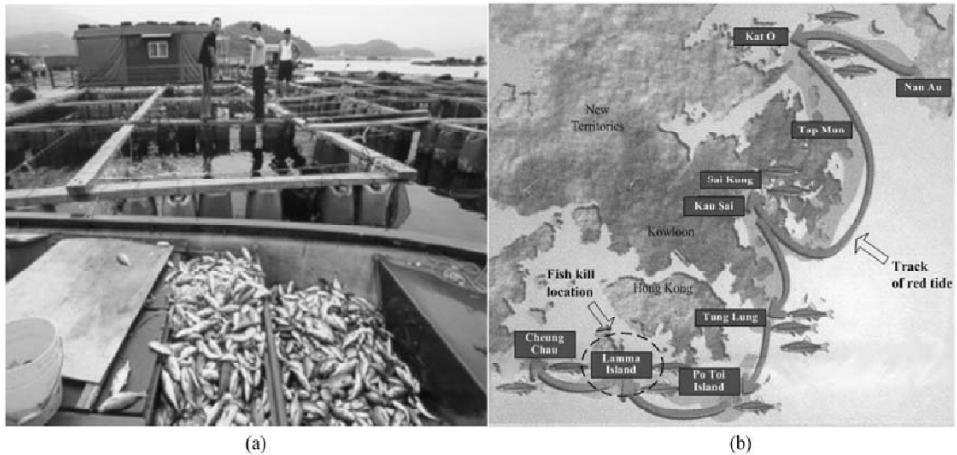
Fig. 8.43 The massive 1998 Hong Kong red tide: (a) severe fish kill at fish culture zone in Lamma Island (From Yang and Hodgkiss, 1999); (b) reported red tide movement

There is a genuine need to study bloom dynamics to provide a scientific basis for mariculture management. Long term field monitoring and modeling work in Hong Kong was initiated during 1987–1989; the emphasis was to understand the often perplexing observed DO variations in many of the 26 marine fish culture zones. It is of interest to understand the environmental factors and preconditions which lead to fish kills, and to predict the occurrence of severe DO depletion.

Field observations—The nature of DO and algal dynamics can best be illustrated by field observations. A total of seventeen 26-hour water quality field surveys were carried out in a weakly-flushed fish culture zone in Tolo Harbor (Lee et al., 1991a). The 26-hour field studies subsequently gave way to the development of a telemetry system to continuously monitor algal and dissolved oxygen dynamics (Lee and Lee, 1995). Since 2000 real time algal dynamics research stations have been deployed at two sites in Hong Kong, with the objective of developing a real time forecasting and warning system (Lee et al., 2000; Wong, 2004). Figure 8.44 shows the changes in the algal biomass (chlorophyll fluorescence) and DO recorded by real time monitoring at Kat O, Hong Kong. The measurements were recorded at three depths during a dinoflagellate (*Gonyaulax Polygramma*) bloom over the course of two weeks (Lee et al., 2000). It is seen that the diurnal DO fluctuations mirror the algal biomass; the difference between surface and bottom DO concentrations is also significant during the bloom period but relatively small on days without algal growth. This suggests the possibility of using DO data to gain insights into the algal dynamics—e.g., the vertical structure of a diatom bloom may be fundamentally different from the case when vertical migration of dinoflagellates can influence the DO consumption pattern.

Water quality modeling—Herein a summary is given of the elements of a water quality model that has been useful in practical application (Fig. 8.45). Phytoplankton growth and the associated nutrient and DO dynamics are governed by a number of interacting physical, biological, and chemical processes which vary in time and space: river inflows and tidally driven circulation, mass transport by advection and dispersion, algal growth as a function of environmental forcing (organic loads, solar radiation, rainfall and nutrient input), nutrient regeneration, deoxygenation, and reaeration. Phytoplankton dynamics and nutrient kinetics are based on a generally accepted framework (Bowie et al., 1985; Thomann and Mueller, 1987; Lee et al., 1991a,b; Ambrose et al., 1993). In order to simulate nutrient and DO exchange between the water column and the sea bed, an additional benthic layer is provided. Particulate organic nitrogen and phosphorus settle into the benthic sediment along with the respective nitrogen and phosphorus
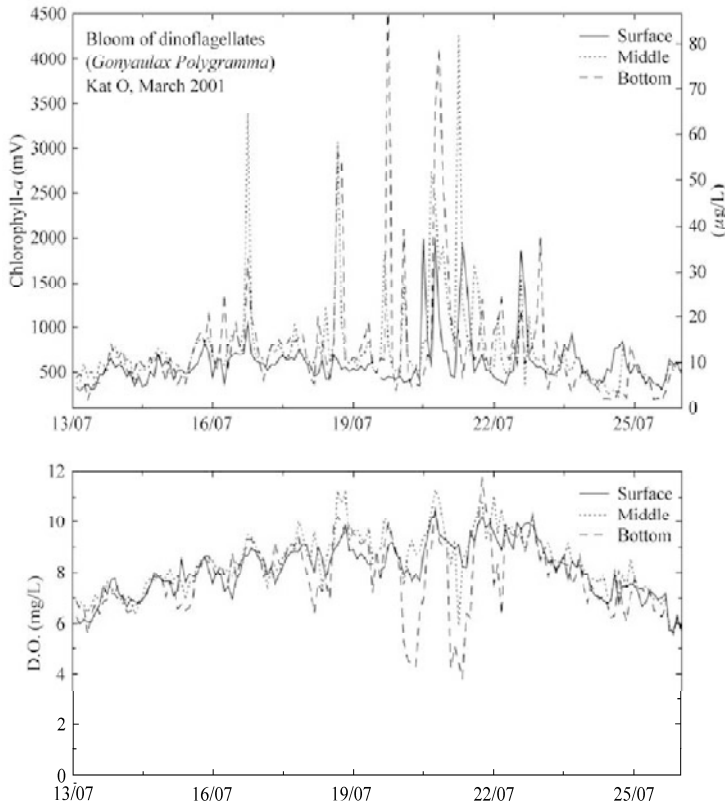
Fig. 8.44   Observed change of chlorophyll and DO during a dinoflagellate bloom at Kat O, Hong Kong

incorporated in the biomass of the settled algae. The benthic segment is assumed to be anaerobic, and organic, ammonia, and nitrate nitrogen, and biochemical oxygen demand are modeled in the sediment. In the reducing sediment settled non-algal particulate organic nitrogen is hydrolyzed to ammonia by bacterial action, and ammonia is also generated by the anaerobic decomposition of algal detritus. The ammonia nitrogen may then be exchanged with the overlying water column via diffusion. No nitrification occurs in the anaerobic sediment, while denitrification is modeled. Nitrate is present in the benthos due to diffusive exchange with the overlying water column. In the sediment, deoxygenation due to the anaerobic decomposition of carbonaceous and nitrogenous organic matter (CBOD and NBOD respectively) is used to determine the (negative) DO concentration. The flux of oxygen (sediment oxygen demand, SOD) and ammonium nitrogen across the sediment-water interface can then be computed from the respective water column and benthic layer concentrations using a Fickian diffusion approach. Further details and various versions of the model can be found elsewhere (Di Toro and Connolly, 1980; Ambrose et al., 1993; Lung, 1993; Arega and Lee 2000).

   The water quality model can be gainfully employed to interpret the observations of phytoplankton dynamics, and help unravel the causes and the environmental pre-conditions that would lead to severe DO depletion—and hence a potential fish kill. Figure 8.46 shows a hindcast of water quality variation over a two-week period in Three Fathoms Cove in July 1987. The daily variation of solar radiation, tidal range, water temperature, and Dissolved Inorganic Nitrogen (DIN) loading are also shown. The initial values at 00 hr, 21/7/87, are provided by measurements made on a hot sunny day, with Chlorophyll-*a* of
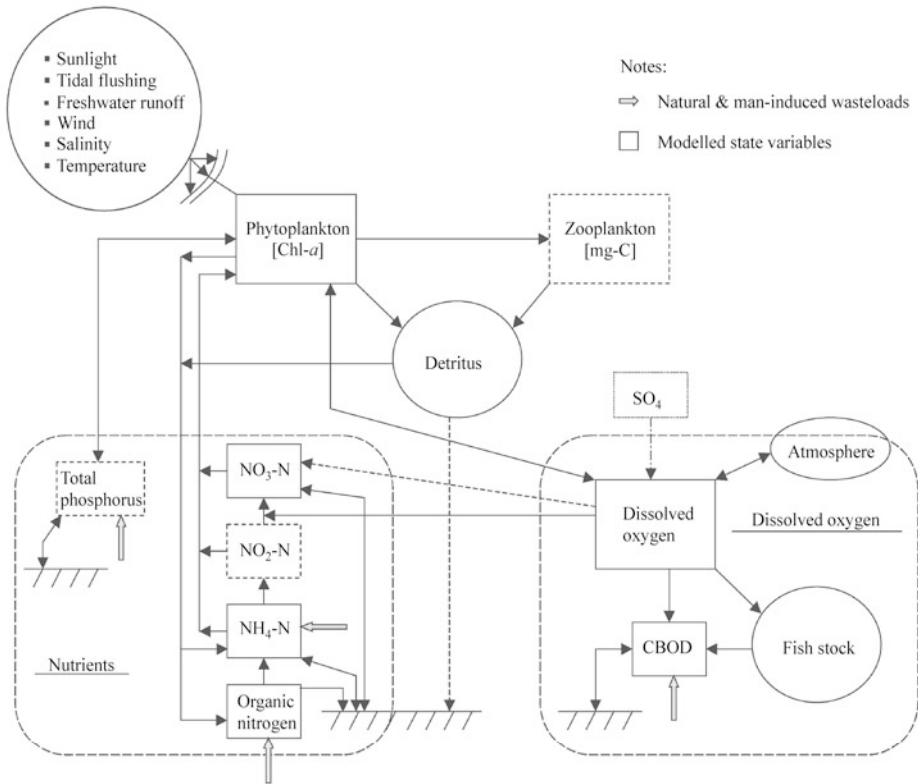
Fig. 8.45 Schematic of water quality model for dissolved oxygen and algal dynamics

around 12 mg/m³. A prolonged period of overcast skies, thunderstorms, and heavy rainfall then ensued. Water temperature was generally high in the summer, above 25℃. The computed DO stays fairly high for the first few days; the predicted range of DO is generally greater for sunny days. The model predicts a steady decline in DO down to a sustained period of critical low level, below 2 mg/L, around July 29. This coincided with a massive fish kill that occurred on July 29 during an unusual protracted (8 hours) period of slack tide. Observations of cell counts suggest that the causative species for this incident was the non-toxic dinoflagellate (*Peredinium faeroense*). The bloom developed from mid-July to a peak on July 28; peak cell counts went up to 0.5 million per mL; however, cell counts quickly decreased down to about 6300 per mL on July 29. The bloom subsided by July 31, with DO restored to high values on August 3 when the water was dominated by high densities of diatoms. This simulation demonstrates clearly the importance of hydro-meteorological conditions and the sediment oxygen demand on DO (due to decomposition of settled algae) in the fish culture zone.

In general, the DO predictions are often quite satisfactory; the same, however, cannot be said for predictions of algal biomass. Although general trends can be simulated, the model framework is limited in its description of the complicated growth and death patterns during an algal bloom. The prediction of bloom collapse under nutrient limited and oxygen depletion conditions remains a challenging task. For example, a more realistic sinking hypothesis (than an assumed constant algal sinking rate) may have to be adopted in order to correctly reproduce the timing of the bloom collapse; as the nutrients get depleted, laboratory experiments on algal cultures have revealed the sinking velocity of the algal cells (with changed structure) can increase by as much as six times.
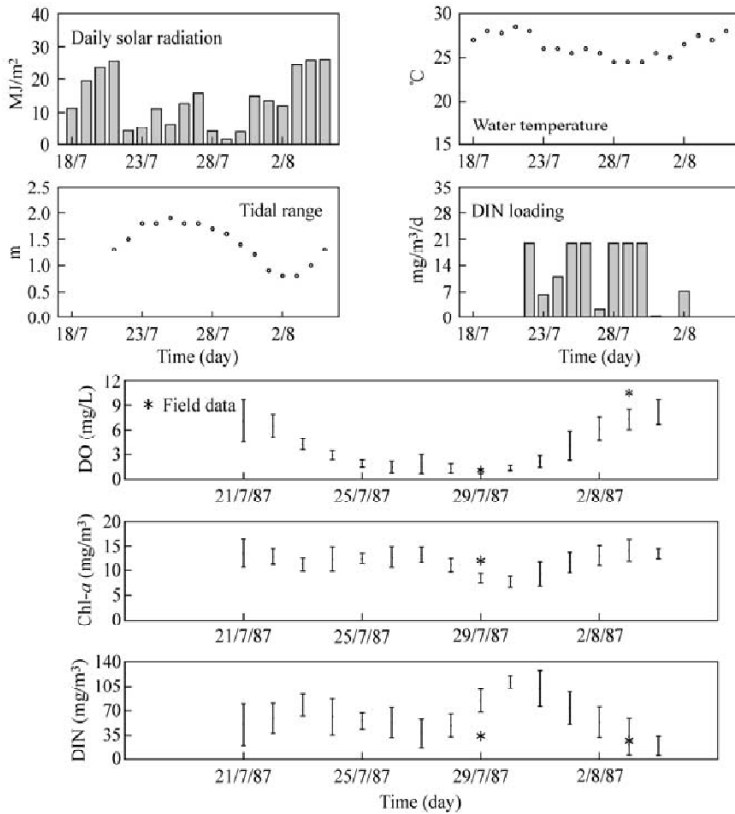
Fig. 8.46 Computed variation of DO, Chlorophyll-*a*, and DIN in Three Fathoms Cove, July 1987 (predicted daily range and field data shown)

To study seasonal and long term trends of eutrophication, a multi-segment dynamic eutrophication model (with the segments coinciding with the locations of routine biweekly water quality monitoring) has been formulated for Tolo Harbor (Lee and Arega, 1999). The modeling yields interesting insights about eutrophication dynamics, and provides useful information on the critical controlling factors: the relation between nutrient removal and water quality, and the effect of global climate change such as the greenhouse effect. Figure 8.47 shows the predicted variation of Chlorophyll-*a* levels in the surface and bottom layers at an inner and outer station in Tolo Harbor over an entire year (Arega and Lee, 2000); the median and range of monthly field measurements are also shown. It is seen that both the predictions and measurements indicate multiple blooms over the year. In the outer harbor, where flushing rates (more information can be found in Section 8.3) are much higher, much lower Chlorophyll-*a* levels are seen. Contrary to initial expectations, the modeling results indicate nutrients often are not the controlling factor; instead blooms are triggered by a combination of hydrologic and meteorological conditions. The sensitivity of bloom events to water temperature helps to explain why very low dissolved oxygen levels were observed in the harbor in 1998, even after substantial nutrient loads have been diverted into another catchment.

Environmental management of mariculture—The water quality model can be used for environmental management of marine fish culture (Lee et al., 2003). Figure 8.48(a) shows a typical fish culture zone (FCZ) in Hong Kong. The sustainable management of mariculture requires proper sites of the fish farms and stocking density control. Both of these are related to the carrying capacity (CC) of the water body
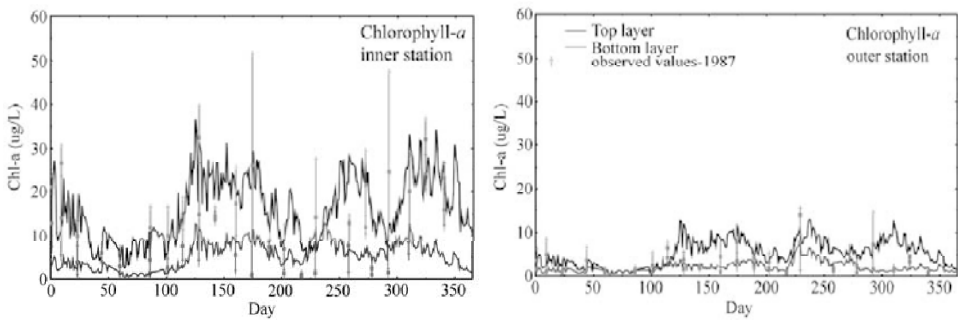
Fig. 8.47 Comparison of predicted and measured Chlorophyll-*a* at two stations in Tolo Harbor in 1987 (predicted values for surface and bottom shown against median and range of measurements)
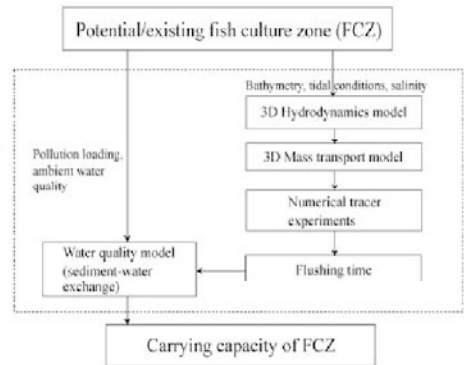
Fig. 8.48 (a) Yung Shue Au marine fish culture zone, Three Fathoms Cove, Tolo Harbor, Hong Kong; (b) Framework for modeling of carrying capacity of a fish culture zone

concerned, which is mainly governed by its flushing characteristics. The coupling of hydrodynamic and water quality models to assess the CC of a fish culture zone is schematized in Fig. 8.48(b). The fish culture zone is modeled as an ecosystem characterized by a number of key water quality variables (algal biomass, nutrients, and DO). The water quality and hence CC of the system is determined by the pollution loading, water temperature, and the tidal exchange with the outer ("clean") sea. The computed flushing rate is used in a quasi-steady seasonally-averaged water quality model that includes both the eutrophication kinetics in the water column and the sediment-water interactions (Lee and Wong, 1997). The CC of the fish farm can be assessed by reference to the key water quality indices: Chl-*a*, DO, organic nitrogen, and a potential lowest dissolved oxygen (PLDO) level.

The method has been successfully applied to six representative FCZs in Hong Kong with different hydrographic and fishfarm loading characteristics (Fig. 8.41). These consist of four FCZs in Tolo Harbor: Yung Shue Au (YSA), Yim Tin Tsai (YTT), Yim Tin Tsai East (YTTE), Lo Fu Wat (LFW); Sok Ku Wan (SKW) on Lamma Island, and Ma Wan (MW). Figure 8.49(a) shows the organic loading and computed flushing rate and key water quality variables at the FCZs for the summer and winter seasons. For a specified temperature and flushing rate, the maximum allowable pollution loading (or fish stocking density) in a FCZ can be obtained by ① prescribing a minimum level of DO (say 4 mg/L) or ② a minimum

level of Chlorophyll-*a* (say 20 mg/m^3); the minimum of the two allowable loadings can then be taken as the carrying capacity (Fig. 8.49(b)).
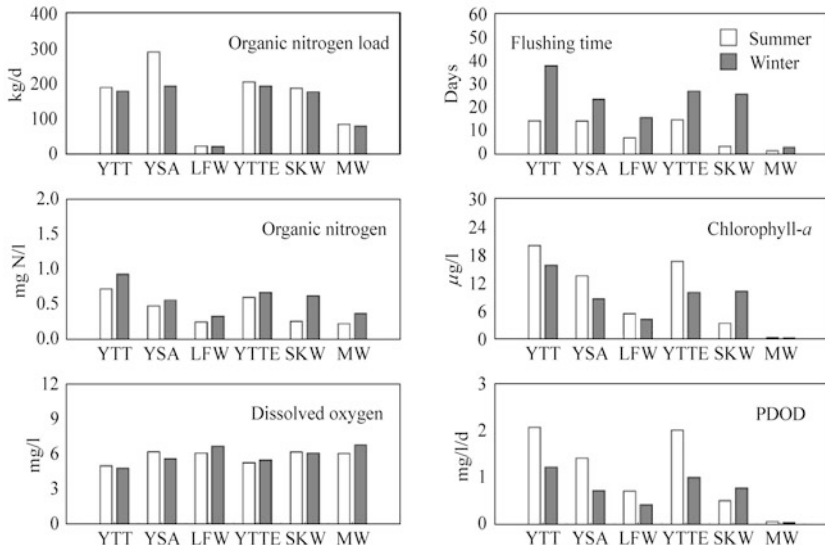
Nitrogen loads, flushing time and water quality indicators

(a)
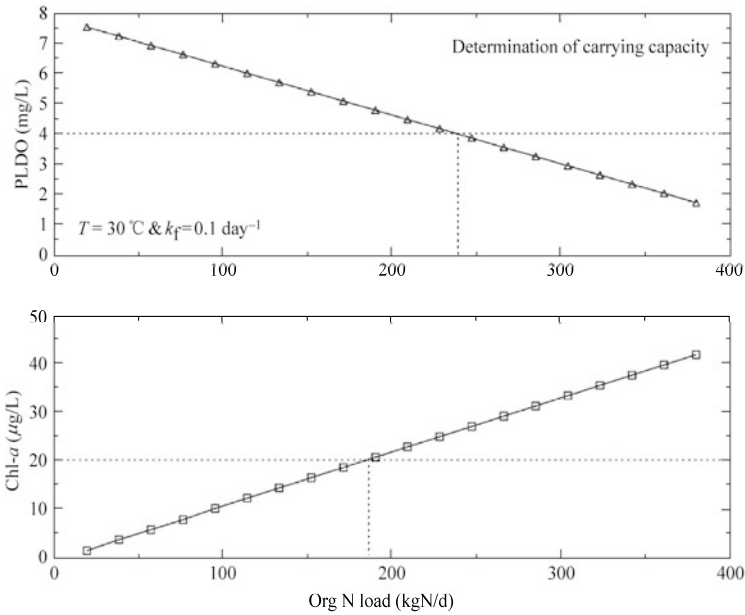
(b)

Fig. 8.49 Water quality model for determination of carrying capacity: (a) organic loads, flushing times and key water quality indicators at six FCZs; (b) allowable organic loading dictated by DO and algal biomass limits (PLDO—potential lowest dissolved oxygen)

8.5   Waste Disposal and Impact Assessment

8.5.1   Waste Disposal

The ocean has long been used as the ultimate sink of most pollutants owing to its enormous assimilative capacity. Nonetheless significant water quality problems may occur on a local or regional scale, as high concentrations of released substances can cause considerable harm and impact. Natural passive turbulent mixing can be rather slow, and visible "pollution belts" along a river bank can often be observed for many kilometers downstream of an industrial wastewater discharge (Fig. 8.50). In the coastal environment, domestic wastes issuing from the open end of a submerged discharge pipe may be poorly diluted, resulting in foul odors, visible sewage slicks, and high bacterial concentrations at the nearby shoreline. Typically, environmental regulations specify concentration limits or water quality standards that may not be exceeded outside of a "mixing zone". For example, for protection of public health the maximum *E.coli.* concentration at a bathing beach should not exceed 180 counts/100 mL and the average dissolved oxygen (DO) level should exceed 4 mg/L for protection of marine life (Hong Kong standards).

In general, the scientific management of water resources requires the ability to predict pollutant concentrations resulting from a given set of discharge and ambient conditions. Environmental impact assessment studies are required for any proposed infrastructure development and the pollution source must be controlled in such a way that the water quality objectives are achieved. There are two major sewage strategies: ① land-based sewage treatment; and ② advanced effluent diffusion technology to discharge partially-treated effluent through a submerged outfall diffuser system.

Fig. 8.50   Pollution belt resulting from discharge from a paper mill on the Yangtze River (See color figure at the end of this book)

For municipal discharges into inland rivers and lakes, a high degree of treatment is usually required; on the other hand, the use of sea outfalls in combination with a certain degree of land-based treatment may be appropriate for coastal or marine waters. Ultimately a rational decision on the appropriate level of treatment must be based on a consideration of environmental risks (damage to the ecosystem) and economic and public health costs. In many densely populated coastal cities, wastewater outfalls are often located in relatively shallow waters (e.g., 5–2 m depth), and not far (e.g., 5–10 km) from sensitive areas such as beaches or shellfisheries (Choi and Lee, 2007). The complex and highly variable hydrographic conditions present significant technical challenges for environmental impact assessment. In recent years, advances in environmental hydraulics and numerical modeling have enabled the proper determination of the risks associated with different sewage treatment and disposal schemes.

Sewage treatment—Normally there are three levels of sewage treatment: ① *primary treatment* typically removes at least 60% of suspended solids (SS) and 30% of biochemical oxygen demand (BOD) by means of sedimentation and filtration, but removes no nitrates, phosphates, salts, pesticides; ② *secondary treatment*, which removes at least 90% of SS and BOD, 70% of phosphorus (mostly as phosphates), 50% of nitrogen (mostly as nitrates), and 5% of dissolved salts through biological processes—mainly the activated sludge process (e.g., aeration of bacterial flocs) and bacterial biofilm process (e.g., biofilter tank); ③ *tertiary treatment*, which reduces the concentrations of inorganic nutrients and products of biological oxidation during secondary treatment (Miller, 2005). In the European Union, all communities with more than 15,000 people have been required to have secondary treatment since 2000, with all urban centers slated to have tertiary treatment by 2010. In developing countries like China, however, only about 10% (up to 2002) of municipal sewage receives secondary treatment (Ministry of Environmental Protection, China, http://www.sepa.gov.cn/cont/city)—the construction and operational costs of secondary treatment is 3–4 times higher than that of primary treatment. For small coastal communities located next to well-flushed waters, well-designed sea outfalls can provide an environmentally sound and economically attractive alternative to secondary treatment (Sharp, 1991).

Outfall optimization—As even state-of-the-art treatment plants cannot completely prevent pollution near coastal cities, there is a genuine need to develop better techniques for optimization of sewage discharge. There are two principal means to prevent, or at least mitigate, any harmful local effects of waste disposal impact (Jirka and Lee, 1994). First, through the choice and design of a **discharge structure**, we may control the amount of initial mixing and dilution that take place within a short time (typically within minutes to an hour) after the effluent enters the sea. Wastewater is commonly discharged via a submerged outfall system which consists of three sections (Fig. 8.51): onshore headwork (e.g., for gravity or pumped flow), a feeder pipeline section and the diffuser section that serves as the disposal terminal to release the wastewater. Second, through proper siting strategies and ambient transport predictions, we may assure that the discharged material is effectively and continuously removed from the discharge locality. From a fluid mechanics viewpoint, these two means involve the analysis of **near-field** processes and of **far-field** processes that affect the mixing and transport of the pollutant effluents.
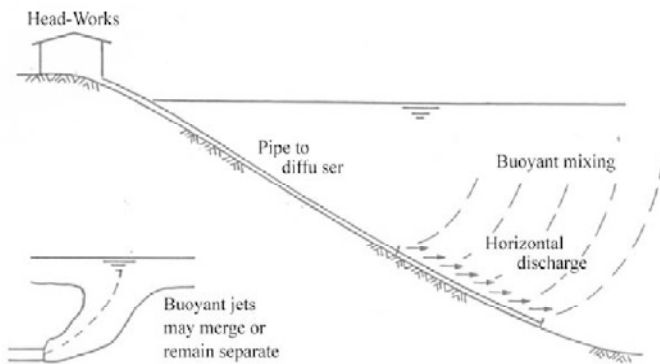
Fig. 8.51   Schematic diagram of sewage outfall diffuser

8.5.2   Initial Mixing

Mixing zones—The effluent discharge through a diffuser is mixed by the turbulent vortices in the environment, leading to a continuous and rapid reduction in pollutant concentration. Conceptually the mixing processes extend over two regions (Fig. 8.52). In the **near-field** (also called active dispersal region or initial mixing region), the region close to the discharge, the mixing is dynamically affected by

the discharge. The momentum and the buoyancy of the discharge modify the ambient flow pattern (mean and turbulent), and the discharge generates its own mean velocity and turbulence field. Rapid dilution of the effluent is achieved through jet entrainment, and the interaction of the jet momentum and buoyancy with the ambient current. The pollutant concentration can be reduced 100 times or more by the time the mixed effluent rises to the surface; when the ambient water is density-stratified (e.g., in the summer), the sewage plume may "find its own level of density" and be trapped beneath the surface (Fig. 8.53). The typical time scale in the near field is on the order of minutes, with length scale on the order of the water depth.
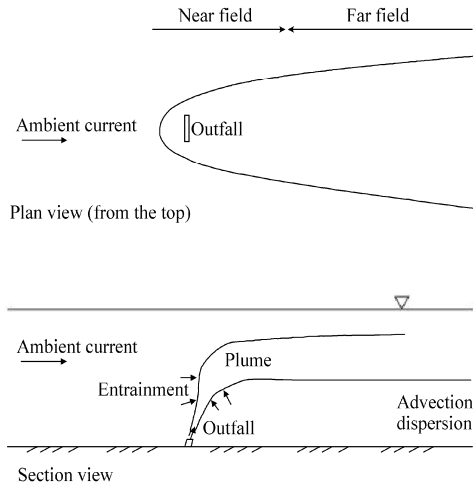
Fig. 8.52 Mixing and transport of submerged effluent discharge

Fig. 8.53 Buoyant jet trapped beneath the surface in stratified fluid

As the turbulent plume travels further away from the source, the detailed source characteristics become less important. The **far-field** (also called passive dispersal region) refers to the much larger region outside the near field in which the diluted waste field is mainly advected by the ambient current and undergoes passive turbulent diffusion by the ambient turbulence. The typical time and length scales in the far-field are on the order of hours and kilometers (Choi and Lee, 2007; Jirka and Lee, 1994).

Near-field—The near-field mixing characteristics of an effluent discharge can be discussed in relation to a typical single submerged port outfall (Fig. 8.52). From an orifice of diameter D laid on the sea floor, the effluent is discharged in the form of a buoyant jet with initial velocity U_0, relative density difference $\Delta\rho_0/\rho_a$, and reduced gravitational acceleration $g' = (\Delta\rho_0/\rho_a)g$. Provided that the jet Reynolds number $U_0 D/v$, in which v is the kinematic viscosity, exceeds about 2000—a condition that is always met in practice—the flow will be turbulent. The jet mixing is governed mainly by the kinematic momentum flux, $M = U_0^2 \pi D^2/4$, and kinematic buoyancy flux, $B = U_0 g' \pi D^2/4$ of the discharge. The volume flux $Q = U_0 \pi D^2/4$ plays a minor dynamic role and becomes important only for very shallow depths. Close to the point of discharge, the high velocity shear induces turbulent entrainment, and the source fluid mixes with the uncontaminated ambient water as it rises, gaining vertical momentum by buoyant acceleration. If C_0 is the concentration of a conservative substance in the discharge, then the local dilution at a given point can be defined in terms of its concentration $C(x, y, z, t)$ as $S = C_0/C$. The centerline or minimum dilution is defined as $S_c = C_0/C_c$, where S_c is the centerline concentration. The initial dilution—the minimum or centerline dilution at the surface – is often used as an outfall design parameter. For a buoyant jet in a stagnant fluid, the jet trajectory, the concentration, and velocity field are determined by two important governing parameters: a jet densimetric Froude number, $F_o = U_0/(g'D)^{1/2}$, the ratio of inertia to buoyancy forces, and the relative depth z/D. For $F_o \sim 1$, the discharge behaves like a pure source of buoyancy (plume), and for $F_o \to \infty$, the discharge resembles a pure momentum jet. For a buoyant jet, the flow is jet-like near the discharge and plume-like at large z/D where the initial source kinetic energy has been dissipated. Figure 8.54 shows examples of a jet and a plume in a laboratory experiment.
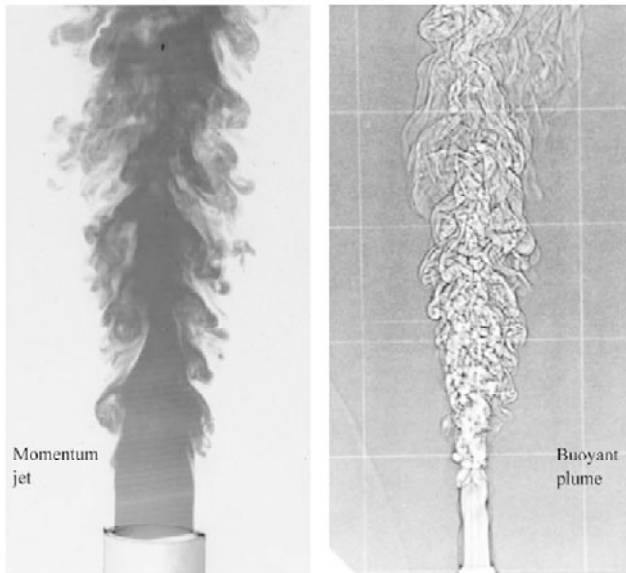
Fig. 8.54   Initial mixing of momentum jet and buoyant plume

Initial dilution prediction—A useful dilution formula for the initial dilution of a horizontal buoyant jet in stagnant ambient water has been given by Cederwall (1968).

$$S_c = 0.54 F_o \left(0.38 \frac{z}{DF_o} + 0.66 \right)^{5/3} \qquad \text{for} \quad z/D \geqslant 0.5 F_o \tag{8.12}$$

It is seen the initial dilution is dependent on the jet densimetric Froude number and the relative depth. Eq. (8.12) has been verified by numerical models and laboratory experiments. It can be used to estimate the initial mixing for the worst case of no ambient current.

When the effluent is discharged into an ambient current U_a, the interaction of the buoyant jet with the ambient current leads to the formation of a vortex pair (Fig. 8.55); the mixing is significantly enhanced from that in calm water. Field and theoretical studies have shown that the moving water dilution can be estimated by the following equations (Lee and Neville-Jones, 1987):

For buoyancy dominated near field:

$$S_m = 0.31 \frac{B^{1/3} H^{5/3}}{Q} \qquad \frac{HU_a^3}{B} < 5 \tag{8.13}$$

where, Q is the volume flux per time, B is the kinematic bouyancy flux and H is the depth.

For buoyancy dominated far field:

$$S_m = 0.32 \frac{U_a H^2}{Q} \qquad \frac{HU_a^3}{B} > 5 \tag{8.13}$$
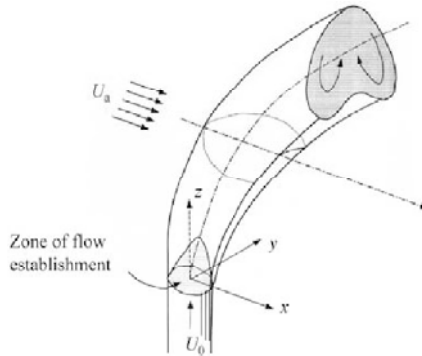
Fig. 8.55   Turbulent buoyant jet in a crossflow; the horse-shoe vortex pair in the bent-over jet leads to much greater dilution in moving water

Similar equations for estimation of initial dilution for asymptotic flow situations (e.g., pure jet or plume in uniform crossflow, linear stratification) can be obtained from experiments by dimensional analysis or from numerical models (Fischer et al., 1979; Lee and Chu, 2003).

For environmental risk assessment and outfall design, it is necessary to predict the impact of effluent discharges for a wide range of discharge and ambient conditions. Typically a general mathematical model is employed for prediction of initial mixing (e.g., Wei et al, 1998; Liu et al., 2002). The buoyant jet trajectory and mixing can be well predicted by a validated integral model that predicts the turbulent entrainment as a function of source characteristics, ambient velocity, and stratification. As a case study, a general interactive modeling system called VISJET (http://www.aoe-water.hku.hk/visjet/visjet.htm) is introduced. As can be seen in Fig. 8.56, VISJET is based on a robust near-field jet Lagrangian model JETLAG (Lee and Cheung, 1990; Lee and Chu, 2003) that is capable of predicting the mixing of an arbitrarily inclined

round buoyant jet in a stratified cross flow, with a 3D trajectory. JETLAG tracks the evolution of the average properties of a plume element by conservation of horizontal and vertical momentum, conservation of mass accounting for shear and vortex entrainment, and conservation of solute or tracer mass/heat. For a given set of ambient conditions (vertical profile of horizontal velocity, density, and tracer concentration), the jet trajectory, jet velocity and radius, and dilution (entrainment) can be predicted. The turbulent entrainment along the jet trajectory can then be obtained from the discharge point up to a terminal level (free surface, bottom, or trap level in the presence of ambient density stratification). In addition, the boundary conditions for the near-field model depend on the external (intermediate or far field) flow, which can be obtained from a 3D circulation model.
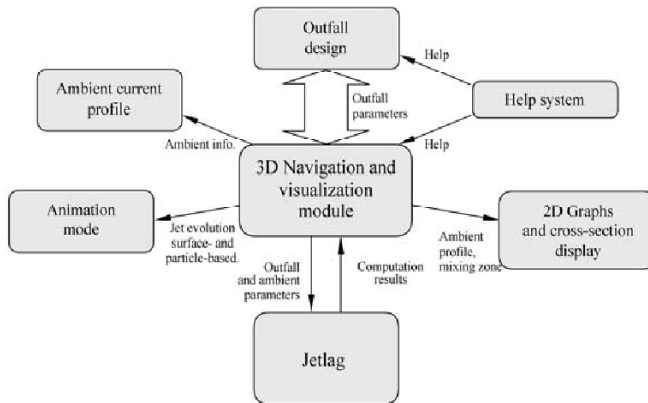
Fig. 8.56   Structure of the VISJET system

The simulation engine in the PC-based VISJET system is fully integrated with visualization technology, which makes it convenient for practical applications such as outfall design, impact assessment, and risk analysis of pollutant or natural environmental discharges. The jet trajectory data as output by the JETLAG module is readily available from the visualization results—e.g., the user may locate the point of interest to interactively retrieve the required data values. The realistic modeling and rendering of the surrounding environment, such as the sea bed and the sea surface in the case of an ocean outfall study, is used to enhance the user's sense of presence in a 3D environment so that the user can better understand the context of the simulated phenomena. Figure 8.57 shows an example of a jet trajectory computed by VISJET compared with the experimental observation for the Wah Fu Sewage Outfall, Hong Kong.

In many practical situations, the wastewater is discharged from an outfall riser in the form of rosette jet groups in the presence of a tidal current. A rosette jet group discharging into an ambient current is a complex flow involving mixing, merging and interaction of co-flowing, cross-flowing, and counter-flowing jets with three-dimensional trajectories. Figure 8.58 shows an example of VISJET simulation and experimental observation of multiple buoyant jets of such rosette buoyant jet groups from an ocean outfall riser. Figure 8.59 shows the near field jet mixing of a number of rosette risers mounted on a submerged ocean outfall; it is noted that the plumes from adjacent risers can interact and overlap significantly; the dilution of a jet group is, hence, less than that if jet interference is not present. The "composite dilution" of such jet groups can be determined from the degree of merging of these jet groups (Lai et al., 2007).

Near and far field coupling—Near-field models give predictions of pollutant concentrations in the initial mixing zone; while turbulent plume entrainment is properly modeled, important mixing characteristics such as the gravitational spreading layer and its coupling with plume entrainment cannot be predicted by
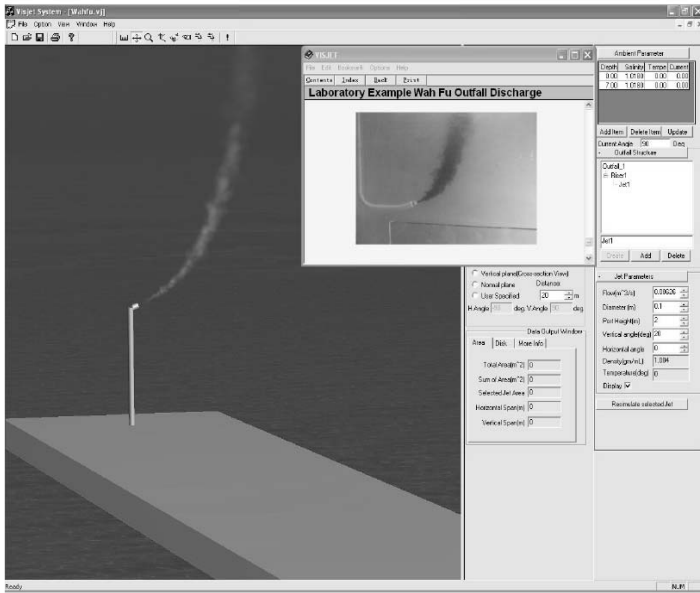
Fig. 8.57   VISJET modeling of the Wah Fu Sewage Outfall, Hong Kong and comparison with laboratory experiment

| (a) | (b) |
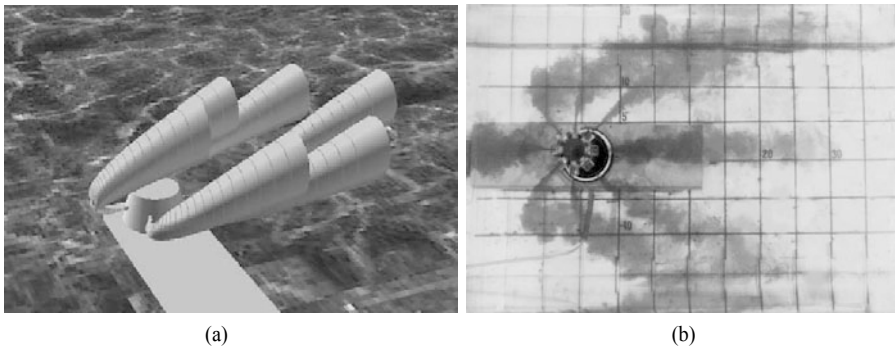
Fig. 8.58   Buoyant jet discharges from rosette-shaped diffuser: a) multiple jet trajectories simulated by VISJET; b) top view of experiment
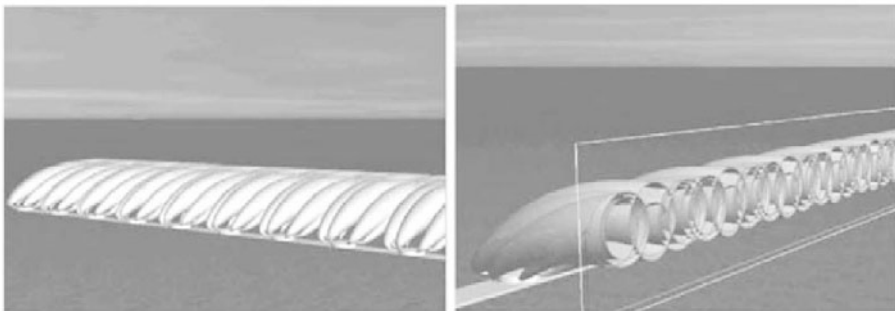
Fig. 8.59   VISJET Simulation of an eight jet group in nonlinear-stratified water

such integral type jet models. On the other hand, 3D shallow water circulation models are run on grids on the order of 100 m. Predictions tend to be overly optimistic as the impact is averaged over a region at least of the order of 100 m. And yet, predictions are often needed in the transition from the near to far field, or the intermediate field (Fig. 8.52). For example, the impact of a chlorinated wastewater discharge on a nearby beach located 3 km down current needs to be assessed. In general, the use of either the near field model or the far field model alone is highly unsatisfactory. Traditionally the near-far field coupling methods involve either "one-way coupling" or weak "two-way coupling", so the dynamic effects of the plume mixing cannot be satisfactorily represented in the far field model (Lee and Choi, 2008).

In the near-far field transition, the dynamics depends on the interaction of the near-field plume mixing and the ambient flow, gravitational spreading, and modifications in ambient stratification. In order to have a true two-way coupling for effective modeling of mixing and transport in the intermediate field, a dynamic coupling of the near field model and a 3D water circulation model can be achieved using a recently developed Distributed Entrainment Sink Approach (DESA, Choi and Lee, 2007). From the viewpoint of the surrounding water, the near-field flows are the bulk sink flows ("loss") due to the turbulent jet entrainment and the bulk source flows ("gain") due to the diluted discharges (mixed effluent). Therefore, the plume mixing can be represented as a series of distributed sinks along the jet trajectory. A source term representing the diluted source (total dilution) flow and the discharged pollution loading (tracer mass flux) is introduced at the terminal level.

In this coupling method, at any instant time, the ambient current $U_a(z)$, salinity $S_a(z)$, temperature $T_a(z)$, density $\rho_a(z)$, and tracer concentration $C_a(z)$ upstream of the outfall discharge is provided by the solution at the grid cells upstream of the source. Based on the ambient conditions, the embedded near-field jet model (e.g., JETLAG) can be run to compute the evolution of the average properties of the plume elements along the jet trajectory: average jet velocity and width, tracer concentration, location, density, and the total fluid mass entrained into the plume element as a result of shear and vortex entrainment, ΔM_k. Based on the location of the centre of the plume elements, the distributed entrainment sinks, Q^e, for each far field model grid cell can then be computed by summing the entrainment flows corresponding to all the plume elements within that cell:

$$Q^e = \sum \left(\frac{\Delta M_k}{\rho_a \Delta t} \right) \tag{8.15}$$

The diluted source flow at terminal height of rise, Q^d, is then given by:

$$Q^d = Q_o + \sum Q^e \tag{8.16}$$

which is applied as a source term to the corresponding far field model grid cell, where Q_o is the effluent discharge flow. Also, a source term representing the discharged pollution loading (tracer mass flux) is introduced at the terminal height of rise (i.e. the near field mixing is represented as fluid mass source in the continuity equation and tracer mass source in the tracer transport equation). Thus, a true two-way dynamic link can be established at the grid cell level between the near and far field models. The coupling captures the key physical mechanisms of ① turbulent jet entrainment; and ② 3D hydrodynamics with the hydrostatic pressure approximation in the intermediate field.

The accuracy of this method has been demonstrated for a number of complex 3D near-far field interaction problems including the interaction of a confined rising plume with ambient stratification, mixing of a line plume in cross-flow, and impact of an outfall discharge on a nearby beach. For example, the practically important problem of a finite "line plume" in a cross flow can be accurately predicted by using DESA. It is clearly shown in Fig. 8.60 that the DESA-predicted surface spreading is reasonably close to the observation especially in the near-to-intermediate field region where the effect of the rosette

jet configuration is still dominant. By contrast, the prediction using an actual source (AS) approach (with the volume and pollutant mass sources introduced at the point of discharge) results in significant over-prediction of upstream buoyant spread.

$F \sim 0.1$
(a)

$F \sim 1.0$
(b)

$F \sim 10.0$
(c)
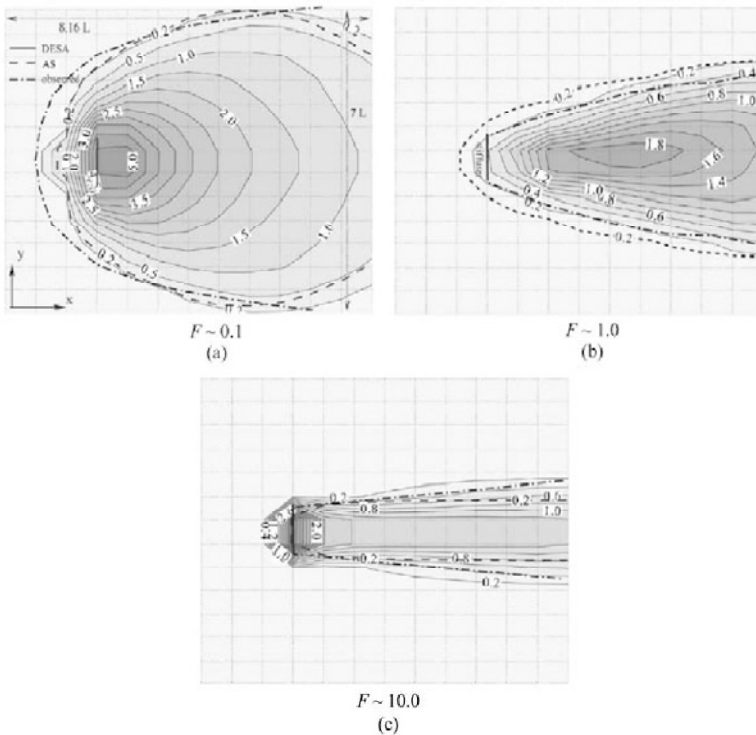
Fig. 8.60 Computed surface tracer concentration field (in units of 0.01 C_0) and observed surface field for a finite line plume in a perpendicular cross flow (F = Froude number, C_0 = effluent tracer concentration)

8.5.3 Diffuser Design

Initial dilution is determined by the choice of the outfall location and length. In addition, the impact on the receiving water is strongly affected by the diffuser configuration (number of jets and risers, jet orientation, riser geometry details, diffuser orientation and length). The optimal design of an outfall diffuser is an unavoidable step in the planning of a sewage disposal scheme. Theory and practice have shown that the multiport diffuser is an efficient device that is able to achieve rapid dilution of the effluent discharge through a large number of orifices with high flow rates (Jirka, 1982). The diffuser could have a simple port configuration installed in the wall of the pipe (Fig. 8.61(a)); some additional elements (e.g., duckbill-shaped elastomer valve, Fig. 8.61(b) could be installed to improve the performance of diffuser. If diffusers are covered with ballast, laid in a trench or even tunneled in the ocean floor, vertical risers (riser/port configuration, Fig. 8.61(c) need to be added. For deep-tunneled solutions rosette-like port arrangements (Fig. 8.61(d)) are often used to save on the number of costly riser installations (Bleninger, 2007).

Sea water intrusion into tunneled outfalls—Ocean sewage outfalls on exposed high energy coastlines are often most economically constructed by tunneling beneath the sea floor and discharging the sewage into the ocean through diffusers consisting of a series of vertical risers. Systems of this type have been constructed at Hastings, Weymouth, and Aberdeen (U.K.), San Francisco, Sydney, Shanghai, and Hong Kong.
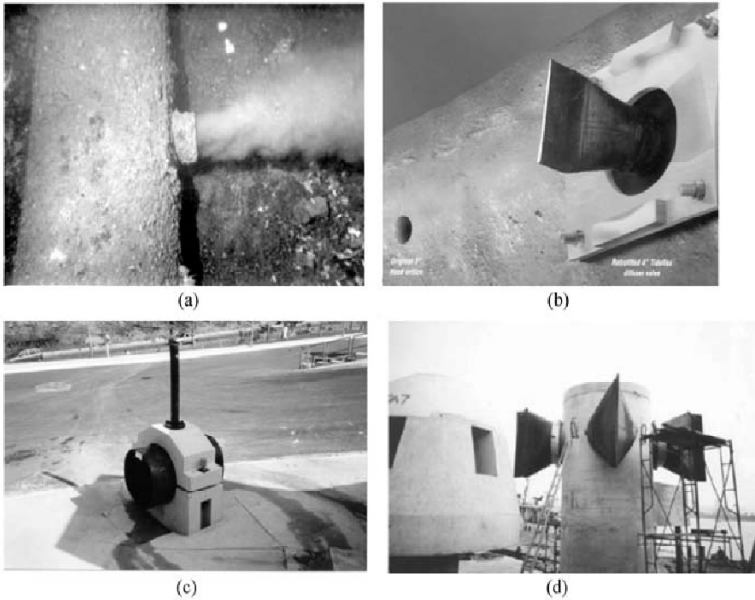
Fig. 8.61 Examples of diffuser configurations: (a) simple port; (b) variable-area duckbill valve; (c) riser/port configuration; (d) rosette like riser/port arrangement (after Lee et al., 2001b; Bleninger, 2007)

Outfall tunnels are typically 2 km–5 km in length and are located 30 to 100 m beneath the sea floor. The risers are often capped with multi-port heads to increase the initial dilution of the sewage plume. A schematic diagram of a tunneled ocean sewage outfall is shown in Fig. 8.62 (Wilkinson, 1984). Under certain conditions, it is observed that sea water from the ocean can intrude into the outfall tunnel, with the lighter sewage discharging through only some of the risers. The problem arises because the seawater has a greater density than the sewage and a pressure surcharge is required to purge the seawater from the tunnel. Figure 8.63 shows a tunneled outfall discharging through the landward risers, while sea water enters through the seaward risers, setting up a circulation.
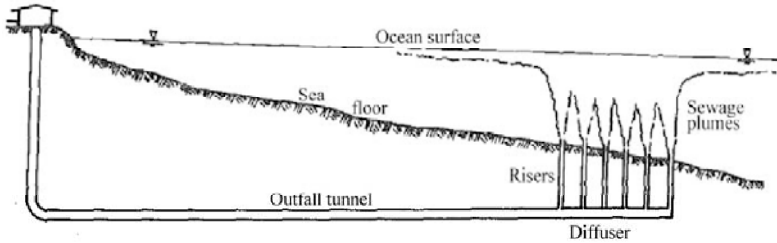
Fig. 8.62 Schematic diagram of tunneled sewage outfall (after Wilkinson, 1984)

This sea water intrusion is clearly hydraulically inefficient, and may lead to poorly diluted effluent and violation of water quality standards. In addition, silt and sand may settle out of the sea water and ultimately constrict the tunnel. The presence of circulating sea water will also promote marine growth on the tunnel walls which may also lead to tunnel blockage. The reason for the failure of some ocean outfalls to purge intruded sea water lies in the failure to account for the possible development of a salt water wedge within the outfall tunnel. In general, intrusion into a diffuser port will not occur if the jet densimetric Froude
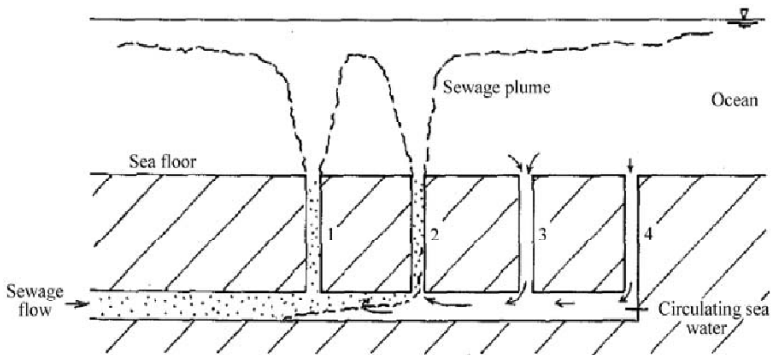
Fig. 8.63 Seawater intrusion into tunneled sewage outfalls; sea water intrudes into the tunnel through the seaward ports

number exceeds unity (Wilkinson, 1984; Yau, 1997). Outfalls are generally designed to ensure that this criterion is satisfied by a reasonable safety margin. However, at start-up, the tunnel is flooded with sea water and at low flow period (e.g., during breakdown) sea water may intrude into the outfall. Once this occurs, a discharge many times that required to prevent intrusion at the diffuser ports is needed to purge the sea water from the tunnel. In recent years, one-way non-return "Duckbill" valves have increasingly been used on riser heads as an effective means to prevent sea water intrusion into outfalls.

Hydraulics of duckbill valves—In this section more details about the duckbill valve (DBV) are presented to better demonstrate the optimal design of diffusers. Duckbill valves can be easily installed on wastewater effluent diffusers as well as stormwater outfalls and industrial flow systems (Fig. 8.64): ① a DBV is manufactured of neoprene flexible elastomer material reinforced with synthetic fabric, much like a car tire; ② it resembles a short piece of rubber hose that has been flattened at one end (the "bill"); ③ at the other end of the valve it is typically clamped onto an existing nozzle port (the "cuff"); ④ the transition between the bill and the cuff is termed the "saddle". Duckbill valves have been increasingly applied to submarine wastewater outfalls in many countries (Lee et al., 1998; Roberts et al., 1989). A case in point is the Urmston Road Outfall in Hong Kong—an outfall system consisting of dual 2.6 km long 1.8 m diameter steel and reinforced concrete submarine pipelines that discharge sewage into water 22 m deep; the last 600 m of the outfall contains 30 diffusers, each with four DBV discharge ports (Smith-Evans and Dawes, 1996).

Hydraulic characteristics—Conventional diffusers are often fitted with round nozzles or pipes with a fixed diameter; this is the easiest terminus to build and maintain. However, as the jet velocity in a constant diameter port varies linearly with discharge, intrusions of salt-water and sediment can occur at low discharge flows (Larsen, 1995). In contrast, experiments and theory show that the jet velocity through a duckbill valve varies nonlinearly with the discharge (Lee et al., 1997). A case with and without duckbill valves is shown herein to illustrate the effect of the duckbill valves on diffuser hydraulics (Lee et al., 1998). The most important hydraulic characteristic of this flow device is the relationship between pressure and flow, the so called "head–discharge" relationship. Figure 8.65(a) shows the computed variation of pressure with flow; it is seen that the relationship is very linear for all the thicknesses tested. On the other hand, Fig. 8.65(b) shows that the valve opening area (at the bill) varies nonlinearly with the discharge (Lee et al., 2004). Figure 8.66(a) shows the comparison of the best fit of the pressure-flow numerical results with the experimental data of a 305 mm valve. It is seen that the experimental data support the linear P–Q relation except at large flows, when the pressure measurement is probably affected by the size of the experimental setup; the high flow data also deviate somewhat from energy conservation checks. On the other hand, the comparison of the best fit numerical result with measured jet velocity (Fig. 8.66(b)) shows excellent agreement (the jet velocity for the highest flow was outside measurement range).
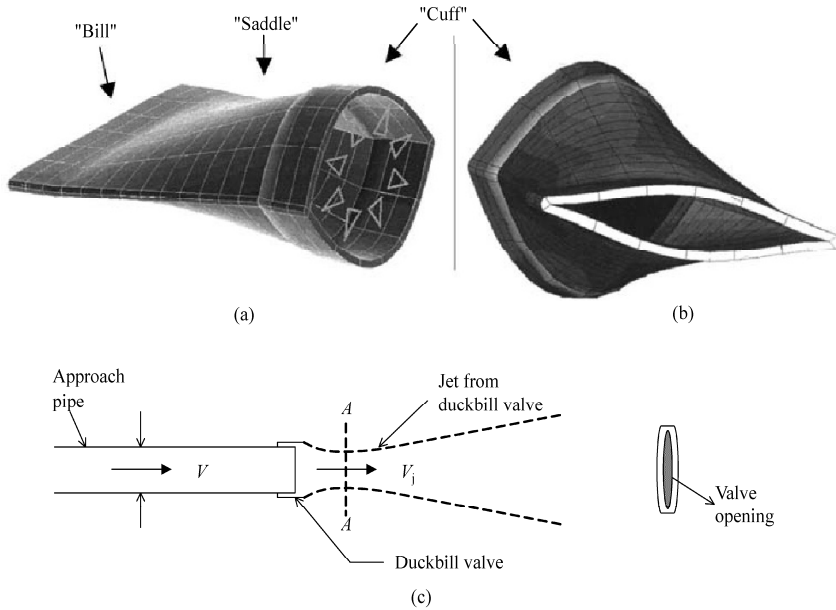
Fig. 8.64 (a) duckbill-shaped elastomer valve; (b) lip-shaped opening of duckbill valve; (c) definition diagram of duckbill valve jet characteristics
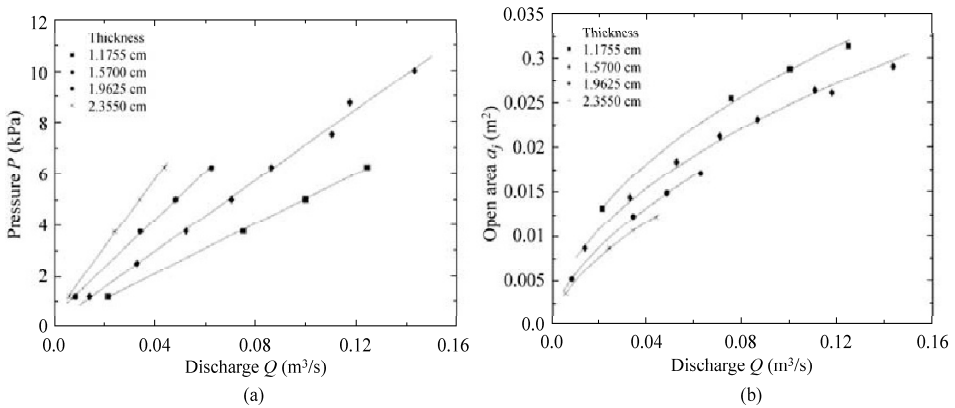
Fig. 8.65 Computed hydraulic characteristics of duckbill valve for different rubber thicknesses: a) pressure-discharge variation and b) opening area as function of flow rate (after Lee et al, 2004)

With its unique hydraulic characteristics, a duckbill valve may always maintain sufficiently high jet velocities (jet densimetric Froude number) and essentially permit flow only along one direction, which could prevent salt-water, sediment and aquatic life from entering submarine outfalls even during low flow periods. For example, at no flow condition, the flaps of the valve remain closed; as the discharge increases, pressure is exerted on the flaps of the valve, and the valve opens more. Compared with traditional diffusers with fixed diameters, experiments and turbulence modeling have shown that a duckbill valve may achieve optimal mixing of the underwater effluent discharge with the receiving water (Lee et al., 1997; Kuang and Lee, 2001).
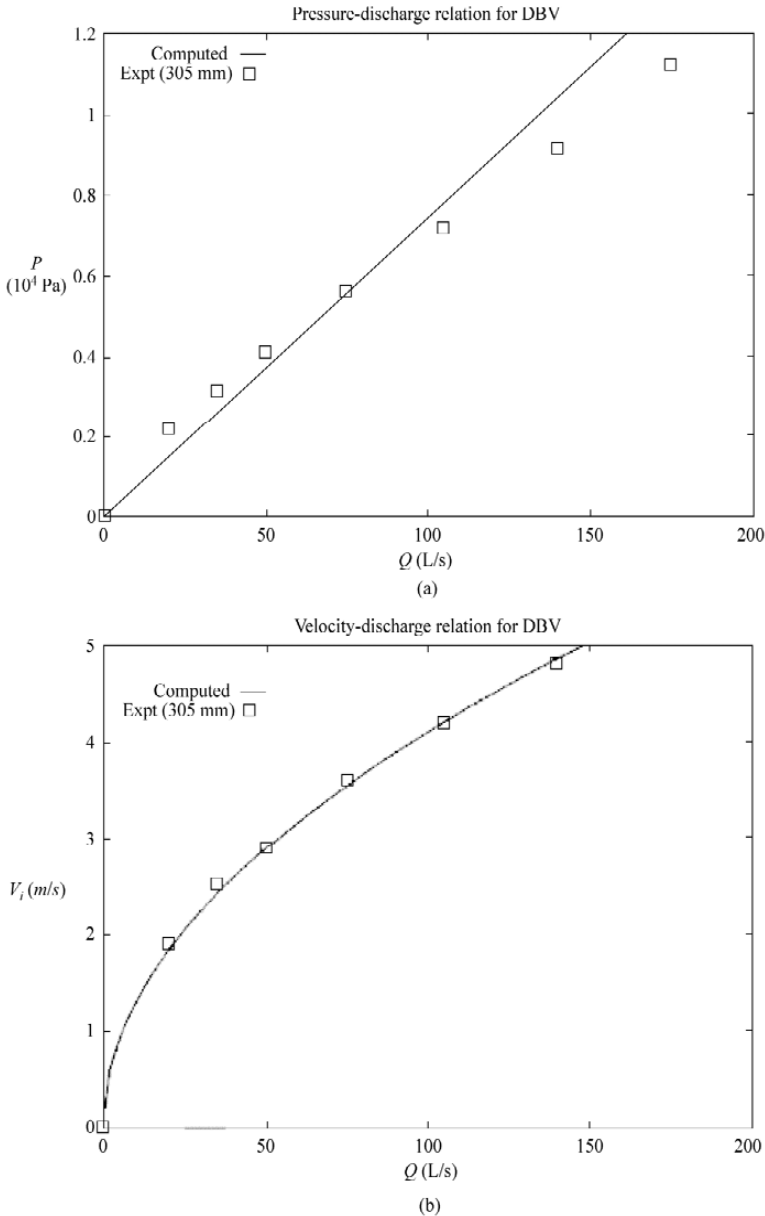
Fig. 8.66 Comparison of computed duckbill valve hydraulic characteristics (d_p = 305 mm, E = 7.32 MPa, t_0 = 1.57 cm) with experimental data: (a) pressure and (b) jet velocity as function of discharge. (d_p is pipe diameter, E is total energy head, and t_0 is rubber thicknesses)

8.5.4   Case Study: Hong Kong Harbor Area Treatment Scheme

The Harbor Area Treatment Scheme (HATS) is a major environmental infrastructure project that collects sewage from the densely populated urban areas of Kowloon and Hong Kong Island (via a 24 km long deep tunnel sewerage system) to a centralized sewage treatment works at Stonecutters Island (SCI) (Fig. 8.67). Stage I of HATS has been in operation since December 2001. The sewage receives Chemically Enhanced

Primary Treatment (CEPT) which removes about 70% of the organics, 80% of suspended solids, and 50% of bacteria. The treated effluent is discharged through a 1.2 km long submerged outfall diffuser into the western Victoria Harbor. The treatment works is designed for an average dry weather flow (DWF) of around 19 m³/s (peak flow 40 m³/s). The partially-treated effluent is discharged via a 1.1 km long submarine outfall into the western Victoria Harbor. The effluent is discharged into the tidal stream through 24 "rosette" risers installed along a 3.25 m diameter diffuser pipe, at a mean depth of around 12 m. Each riser has 8 discharge ports of diameter 0.25 m. The buoyant plumes from the risers are sufficiently separated and can be considered as independent of each other.
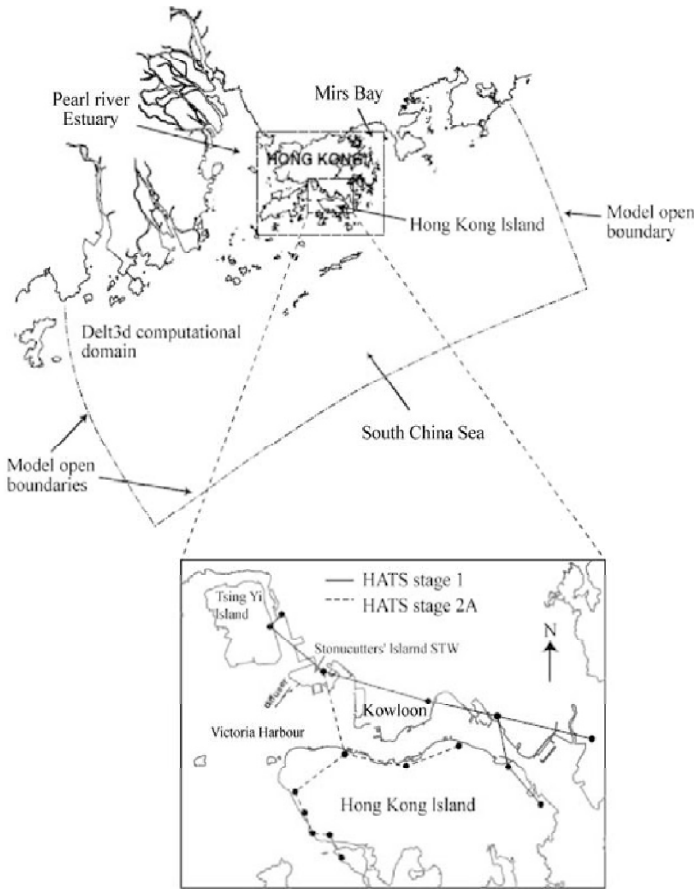
Fig. 8.67 Computational domain for Hong Kong waters model and Stonecutters Island sewage outfall

Ammonia is a principal pollutant in sewage effluent and one of the major pollutants in Hong Kong. At elevated concentrations, ammonia is toxic to aquatic organisms and its toxicity is mostly related to unionized ammonia NH_3. For example, fish exposed to an elevated NH_3 concentration may suffer a loss of equilibrium, hyperexcitability, coma, and even death. It is, therefore, important to consider the mixing zone based on NH_3, as it may pose threats to fisheries resources and marine bio-diversity in the vicinity of the sewage outfall. In addition, elevated bacterial (*E.coli*) levels at nearby beaches are also a major concern.

Several stages of HATS are being planned. In Stage 2A, the outfall will be used to carry additional sewage flows as more urban areas are connected to the sewerage system (Fig. 8.67), and the Chemically Enhanced Primary Treatment (CEPT) effluent will undergo chlorination. The dry weather flow will increase to 32 m³/s. In Stage 2B, secondary treatment will also be provided with a view to reducing the organic pollutant concentrations by 90%. Table 8.5 summarizes the treatment level, discharge flows, ammonia nitrogen concentration, and cost of the three different stages of HATS.

Table 8.5   Stages of Harbor Area Treatment Scheme (HATS) in Hong Kong

Stage	Sewage flow		Treatment level	Effluent NH₃ conc. (mg/L)	Cost (US$)
	(Mm³/d)	(m³/s)			
1	1.6	18.5	CEPT (advanced primary)	19.0	1.09 billion
2A	2.8	32.4	CEPT + disinfection	19.0	1.14 billion
2B	2.8	32.4	CEPT + biological + disinfection	1.90	1.52 billion

A three-dimensional hydrodynamic model with boundary-fitted curvilinear grid (8 uniform vertical layers for the present study) covering the entire Hong Kong Waters and Pearl River Estuary has been developed and calibrated to simulate the tidal circulation of Hong Kong Waters. The effect of effluent discharged from the HATS outfall have been computed for a typical 1 day spring-neap cycle using open boundary conditions derived from field data for ① the dry season; and ② the wet season. The HATS diffuser is represented by six 8 port rosette jet groups.

The Water Quality Objective (WQO) for NH₃ in Victoria Harbor is 0.021 mg/L; it can be used to define the boundary of the instantaneous mixing zone. Under different tidal stages and ambient density structures, the buoyant jets discharged from the sewage outfall may be trapped at different levels. Hence, the extent of the mixing zone also varies quite significantly with time. The predicted mixing zones (with NH₃ as the target pollutant) may be quite different under flood and ebb tide conditions. For environmental assessment purposes, it is more convenient to define a mixing zone in statistical terms. With the computed concentration time series for the simulated period, we can determine the 95 percentile of the concentrations at each grid cell. The mixing zone can then be meaningfully defined in terms of the 95 percentile concentrations and the WQO. The zone obtained will indicate the region outside which the WQO will be met 95% of the time. Figure 8.68 shows the mixing zone obtained for NH₃ in the wet season with HATS Stage 2A discharge. It can be seen that the mixing zone defined by unionized ammonia extends well into the western harbor towards Lantau Island.

E. coli is another key water quality indicator; the effluent concentration can be on the order of 10^7 counts/100mL. With initial dilution on the order of 100, the *E. coli* concentration at the end of the near field will be on the order of 10^5 counts/100mL—which is significantly greater than the regulatory allowable level of 180 counts/100 mL. Figure 8.69 shows the predicted mixing zone using *E. coli* as the target pollutant for the wet season under flood conditions. Even in the presence of bacteria decay, the extent of instantaneous impacted zones is much greater than that for the un-ionized ammonia, NH₃.

Environmental risks are best expressed in statistical terms. The methods of predicting the impact of waste discharges outlined in this chapter enables scientific determination of risks. An integrated risk assessment methodology has recently been proposed to quantify the ecological risks of HATS based on the target pollutant (Choi et al., 2009). The environmental risk is defined in terms of a hazard quotient (HQ); a HQ > 1 means that the organism is exposed to a pollutant concentration higher than the threshold value above which the marine organisms may possibly die. It is found that the probability of HQ > 1 for HATS Stage 1 is 0.11 for the wet season but just about 0.06 for the dry season. The risk increases to 0.08–0.13 with additional sewage loads of 0.8 million m³/day at the same level of treatment (HATS

Stage 2A). With an upgrade to secondary treatment (HATS Stage 2B), the probability will be reduced to 0.03–0.05. This type of quantitative analysis enables public engagement and policy decisions regarding the debate among alternative sewage treatment strategies.
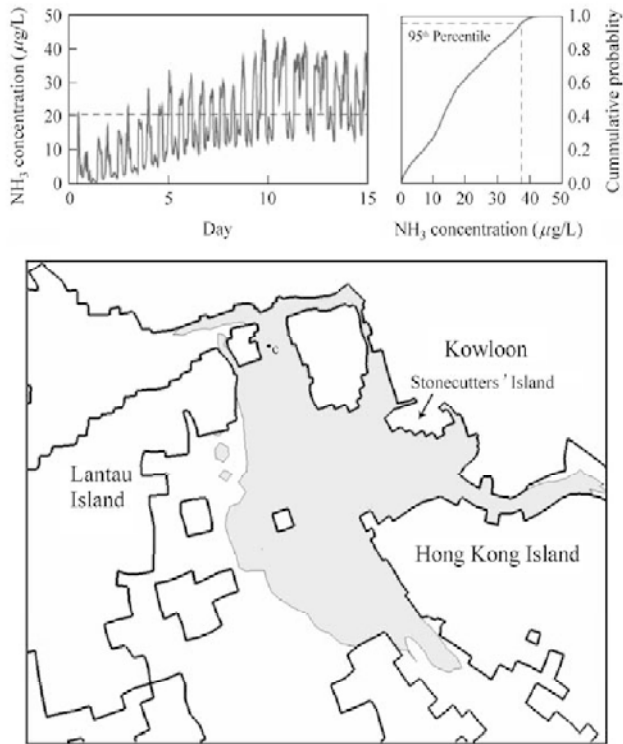
Fig. 8.68   Mixing zone based on predicted NH_3 concentrations for HATS Stage 2A in wet season
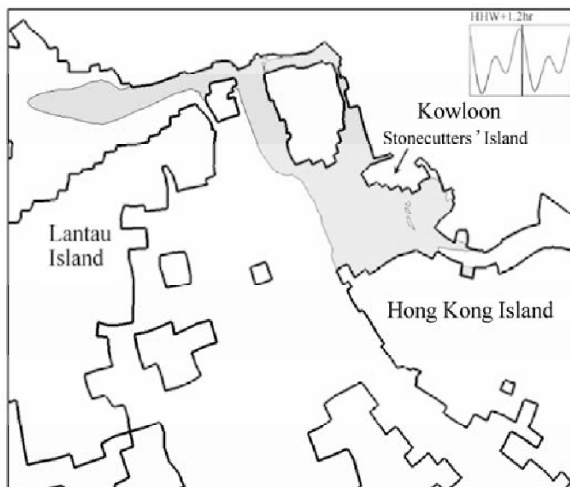
Fig. 8.69   Predicted impact of bacterial pollution for HATS Stage 2A scheme

8.6   Coastal Wetlands

Wetland is a generic term grouping together a wide range of inland, coastal and marine habitats that share a number of common features (Dugan, 1990). A representative definition has been suggested by the RAMSAR Wetland Convention (RAMSAR, www.ramsar.org): wetlands are "areas of marsh, fen, peatland or water, whether natural or artificial, permanent or temporary, with water that is static or flowing, fresh, brackish or salt, including areas of marine water, the depth of which at low tide does not exceed six meters."

Wetlands may be classified into 4 categories in terms of topography and geographic isolation: coastal (including deltas, tidal marshes, and mangrove swamps), riverine (wetlands along rivers and streams), wetlands associated with lakes, and inland wetlands. The coastal wetlands could be further classified into 12 sub-categories (RAMSAR, www.ramsar.org): permanent shallow marine waters, marine sub-tidal aquatic beds, coral reefs, rocky marine shores, sand/shingle/pebble shores, estuarine waters, intertidal mud/sand/salt flats, intertidal marshes, intertidal forested wetlands, coastal brackish/saline lagoons, coastal freshwater lagoons, and Karst/subterranean hydrological systems.

World wide, approximately 50% of the wetlands have been destroyed during the past century, largely due to human activities. Currently, the total global area of wetlands is estimated to be 2.9 million km^2 (Groombridge and Jenkins, 1998). Table 8.6 lists largest wetlands located along major river systems or coastal wetlands on terrestrial habitats that have little topographic relief.

Table 8.6   Some representative wetland habitats (source: Keddy, 2000 and www.ramsar.org)

Wetland Name	Location	Area (km^2)
West Siberian Lowlands	Eurasia	780,000–1,000,000
Amazon River	South America	800,000
Hudson Bay Lowlands	North America	200,000–320,000
Mississippi River	North America	86,000
Upper Nile Swamps	Africa	50,000–90,000
Chongming Dongtan Nature Reserve	Shanghai, China	3260
Yellow River Delta National Nature Reserve	Shandong Province, China	1530
Mai Po and Inner Deep Bay Nature Reserve	Hong Kong, China	15
Futian Nature Reserve	Shenzhen, China	3.7

8.6.1   Function of Wetlands

Historically, wetlands had been merely treated as areas that support agriculture, fishery, tourism or recreation. The importance of wetland's physical and ecological functions has been gradually understood in recent decades—often as a result of the drastic environmental degradation caused by loss of wetland habitats. The wetlands between the edge of a water body and the adjacent upland zone provide many environmental services that include: retaining and conveying flood waters, stabilizing the shoreline against wind and wave erosion, filtering contaminants and sediments, providing critical habitat and movement corridors for a wide variety of plants and animals. There is also increasing evidence of the important role that wetlands play in moderating global warming, by reducing the amount and rate of increase in atmospheric carbon dioxide and other greenhouse gases. In this section, we illustrate the beneficial functions of wetland ecosystems with several real-life examples that are particularly relevant to urban development and its impact on the natural environment.

8.6.1.1   Shoreline Protection

Coastal shorelines are critical interfaces between upland and the littoral zone of the adjacent sea, often

integrating influences from both the land and the sea in wetland areas. Wetlands along coastal shorelines serve as natural barriers against flood damage and erosion due to wind, waves and currents. In contrast to hardened structures such as riprap and seawalls, the construction and/or maintenance of native wetlands is often the most economical long term solution to shoreline stabilization problems. However, human activities within coastal shorelines have often removed the native wetlands and installed a variety of structures, causing problems of shoreline erosion and destabilization. In Louisiana, USA, it has been estimated that each kilometer of wetland reduces hurricane storm surges by 5 to 7 cm (Stokstad, 2005).

A representative example of the disastrous consequence of loss of wetland habitat can be illustrated by the well-known 2004 Indian Ocean tsunami. On 26 December 2004, an earthquake of magnitude 9.0 (on the Richter scale) occurred at the west coast of northern Sumatra, Indonesia, causing a catastrophic tsunami. A series of devastating waves attacked the coastal shorelines, severely damaging communities in Indonesia, Thailand, Sri Lanka, and India. The estimated tsunami death toll ranges from 156,000 to 178,000, with an additional 26,500 to 142,000 missing (Liu et al., 2005). Figure 8.70 shows the epicenter and the affected countries of this tsunami.

This earthquake is the largest ever recorded in the region and in the world since the 1964 Alaskan quake. Measurements of maximum tsunami wave heights, inshore inundation distances, eyewitness accounts and serendipitous observations suggest that human activities within coastal shorelines have likely modified the run-up behavior of the tsunami (Fernando, 2005). For example, coral reefs can provide shoreline protection in reduced erosion and wave damage; however, in some of the affected regions, coral is often illegally mined to provide souvenirs for tourists, which significantly increased the amount of destruction wrought by this tsunami (e.g., along Sri Lanka's coastline, Fig. 8.71). It is observed that the wave heights in narrow swaths where coral cover has been removed are as much as 5–10 times those with coral-reef protection. In an area where substantial coral mining had occurred, tsunami run-up in the area was nearly 8 m; a passenger train was derailed and overturned by the tsunami, killing more than 1,000 people (Liu et al., 2005).
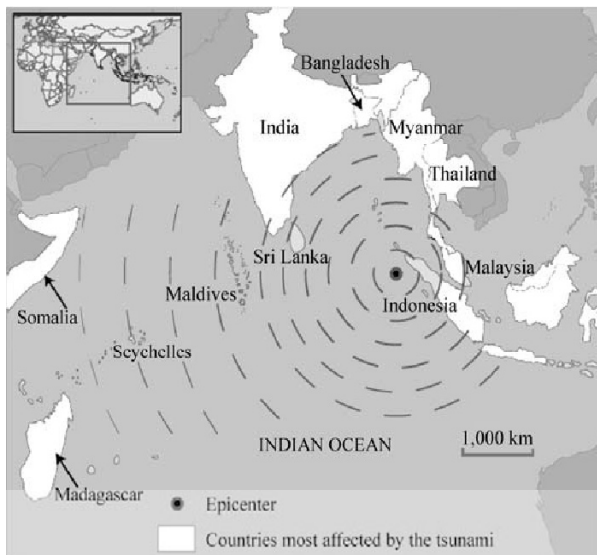
Fig. 8.70   The 2004 Indian Ocean tsunami driven by an oceanic earthquake (from Marris, 2005a)

Fig. 8.71   Tides of the Indian Ocean tsunami battering the coast of Sri Lanka (from Marris, 2005b)

The consequence of removing coral wetland habitats can be illustrated in laboratory experiments on wave propagation. Fernando et al. (2008) carried out a series of experiments in a long wave tank (32 m × 0.8 m × 1.8 m); wave-generated currents are measured in the presence of corals simulated using an array of submerged cylinders. A strip of solid vertical cylinders (1.25 cm diameter and 20 cm high) was attached to a bottom plate (Fig. 8.72) and placed on a sloping bed at a mean water depth of 30 cm. This array of cylinders acted as a submerged porous barrier to the oncoming waves. Two packing densities of rods were used, having porosities 20% and 50%. In some cases, the porous rod structure covered the entire width of the tank whereas in others the rods were removed to create a low resistance (i.e., low bottom drag) gap of width $W = 6.5$ cm in the middle of the canopy. This mimicked the local removal of corals in an otherwise uniform coral cover.
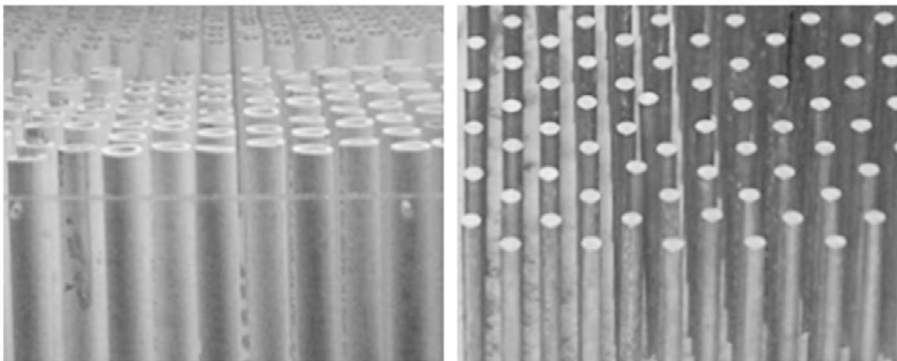
Fig. 8.72   Corals simulated by vertical cylinder arrays in laboratory experiment: left (high density, 20% porosity), and right (low density, 50% porosity)

Figure 8.73 shows mean velocity traces measured at the mid-height of the reef in the direction of wave propagation: without the reef, with the reef and with a gap in the reef. There is a clear reduction of velocity in the presence of the reef, indicating increased drag on wave motion; by comparison, the flow velocity is enhanced in the presence of the gap, with the magnitude of this enhancement decreasing with increasing porosity. Therefore, it can be concluded that: ① the flow velocity is substantially decreased in coral-laden areas due to the larger bottom drag coefficient, which is a strong function of the canopy porosity; ② if a stream-wise gap is created in the reef to create a low resistance path, then the approaching

535

flow can converge and rush through it in the form of a jet, thus enhancing the local height of the landward inundation.
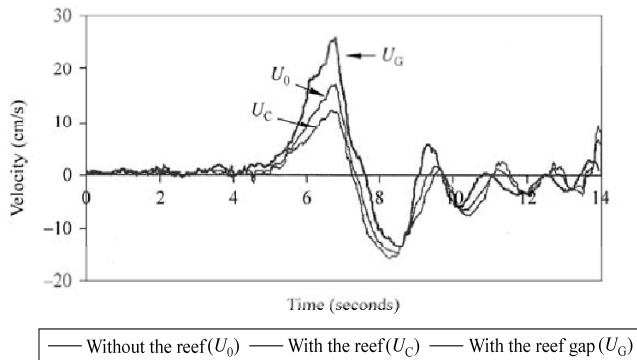
Fig. 8.73   Comparison of onshore velocity at $z/H = 0.5$ for cases without a reef, with a uniform reef (20% porosity) and a reef with a gap (wave amplitude to water depth ratio 0.09)

The abovementioned study has general implications on the presence of low resistance paths along beaches, which include removal of sand dunes, openings in beach reinforcements and the presence of natural flow passages such as estuaries. As such, construction of critical infrastructure and human habitat in such areas needs to consider all possible water inundation paths. A case of concern is shown in Fig. 8.74, taken in March 2006 during the height of post-tsunami reconstruction of beach defenses in Sri Lanka. Here the beaches are being reinforced with granite and sand barriers (Fig. 8.74(a)). Toward the end of the defense is an open area that creates conditions for a low resistance path for water in case of a surge (Fig. 8.74b). Although a clear warning sign (Fig. 8.74(b)) has cautioned the adverse impacts of coral removal, and that nearby area has been given additional protection by levees, the gap in the artificial barrier facing the ocean greatly increases risk of water inrush for the local inhabitants (Fernando, et al. 2008).

Fig. 8.74   (a) Post-tsunami reconstruction of beach defenses in Sri Lanka; (b) at the edge of a beach defense is an open area (arrow) that creates conditions for a low resistance path for water in case of a surge. (from Fernando, et al. 2008)

8.6.1.2   Pollutant Removal

Wetlands can prevent pollutants from entering an adjacent water body, by means of nutrient assimilation by

vegetation (e.g., removal of nitrogen and phosphorus) and removal of heavy metals by adsorption/precipitation reactions (e.g., aluminum, iron and calcium) in the soil. In view of the low cost and acceptable treatment efficiency, application of untreated or treated wastewater to wetlands is regarded as a simple, efficient and economical method for removal of wastewater pollutants. In addition, artificial wetlands—i.e. engineered wetlands that reproduce some of the natural functions of wetlands—are attracting considerable interest in river restoration and wetland compensation projects.

Mangrove wetlands are uniquely intertidal forested ecosystems, often found along the sediment-rich sheltered estuarine shores of tropical and subtropical regions (largely restricted to latitudes between 30°N and 30°S) that share some common characteristics: high temperature, fluctuating salinity, alternating aerobic and anaerobic conditions, periodically wet and dry, unstable and shifting sub-stratum (Tam, 2006). Mangrove communities are made up of diverse groups of plants and animals, but in general some mangrove associated plants (e.g., *Kandelia obovata*) dominate mangrove communities owing to their highly morphological and physiological adaptations to extreme conditions (Fig. 8.75). To survive in transition zones between terrestrial and marine environments, mangrove plants evolved two unique characteristics: ① they are physiologically tolerant of high salt levels through a combination of salt accumulation, excretion and exclusion—for instance, their root cell membranes can prevent the majority of salt from entering the plants, their leaves can store salt at medium level, and their glands can secrete excess salt; ② if the oxygen concentrations in soil become very low, mangrove plants can send forth pneumatophores—a kind of aerial root growing upwards from the root above the mud—to absorb enough oxygen for photosynthesis and metabolism.

Pollutants (e.g., nutrients and heavy metals) are apt to accumulate in mangrove ecosystems, because of their absorptive capacity or rapid microbial activities. Therefore, mangrove wetlands are often used as buffer zones to purify aquaculture wastewater prior to its entering the sea. For example, exchange of coastal waters with shrimp ponds in brackish estuarine waters is important to assure high yields; on the other hand, this will inevitably have a negative impact on the water quality of the coastal waters. Therefore, the environmental-friendly "integrated pond-mangrove farming system" is often used to strip nutrients from pond effluent. Ranges of "mangrove to pond area ratio" vary from 2 to 22 depending on the capacity for nitrogen removal by mangrove system (Robertson and Phillips, 1995), but could be reduced to a range of 0.04–0.12 if de-nitrification occurs in the mangrove system (Rivera-Monroy et al., 1999).

In addition, the feasibility of using mangroves to remove pollutants from municipal and livestock wastewater has also been studied. A 3-year field study in the Futian mangroves—a 370 hectare natural mangrove intertidal wetland in Shenzhen (Fig. 8.75)—showed that primary-treated domestic sewage could be purified if intermittently discharged to the landward region of the mangrove wetland during the low tide period; the tidal water was not contaminated and negative impacts on plant growth were not detected (Wong et al., 1997). Nitrification and de-nitrification processes are the most important pathways to remove nitrogen because mangroves are periodically flooded by tidal water with alternating aerobic and anaerobic conditions. Generally, the nutrient removal by wetland soils is most efficient at low nutrient loading rates, and removal efficiency falls off rapidly as loadings are increased. The percentage of nitrogen lost from the mangrove ecosystem is around 40% and the plant uptake varies from 12% to 68%, depending on the plant species and salinity, and the organic loading. In contrast, phosphorus and heavy metals in wastewater are mainly immobilized in sediments with little loss. At the end of the 3-year field study in Futian mangroves, the amounts of nitrogen retained in mangrove sediments were much less than that of phosphorus, despite the fact that more nitrogen was present in wastewater (Tam and Wong, 1995; Tam, 2006).

Mangrove plants are capable of transferring oxygen from the atmosphere to the roots and creating an oxygenated zone for nitrification around the roots while the surrounding sediments are reduced thus favor de-nitrification. The population sizes of various bacterial groups, in particular those related to the

nitrogen cycle, and the microbial activities in mangrove sediments can increase as a result of the addition of nutrient-rich sewage. With continuous losses of nitrogen from the system, mangrove ecosystems are maintained as a sustainable wastewater treatment facility without saturation. The Futian field study also showed that the species diversity and abundance of macro-algae and benthic invertebrates colonizing the mangrove floor were not affected by sewage discharge (Tam, 2006); only the surface sediments in the first two meters from the discharged points had 20% increases in total Kjeldahl nitrogen and 38% increases in phosphorus concentrations, while no significant change in nutrient concentrations was found in other sediments.
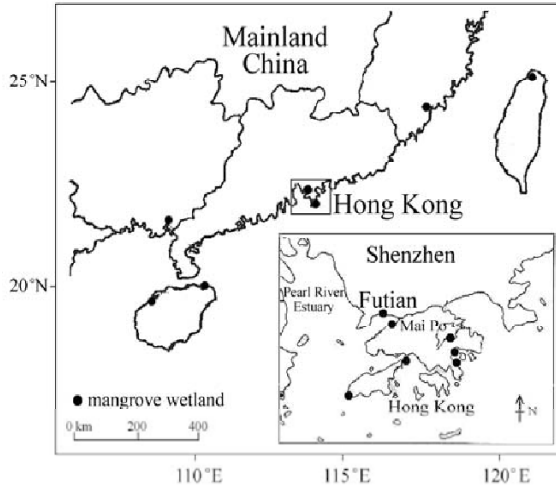
Fig. 8.75   Mangrove swamps in Hong Kong, Macau, Taiwan and Mainland China (from Tam, 2006)

Although the mangrove ecosystem has a high potential to act as a sink for organic pollutants, the long term capacity to assimilate pollutants depends on both the hydraulic and organic loading. For example, the Futian experiments involved application of sewage onto a 180 m × 10 m mangrove strip three times a week, and only 20 m^3 for each discharge—to allow the wastewater to be soaked into the sediment within 50 m of the discharge points. The dynamic nature of mangrove ecosystems is also strongly influenced by factors like tidal flow, wave action, climate, salinity, redox potential, and various biotic components—which may cause the retained pollutants to be re-suspended back to the aquatic environment. In general, coastal wetlands may offer practical and sustainable alternatives to wastewater treatment mainly for relatively small coastal communities that can provide the required mangrove area.

8.6.1.3   Bio-Diversity Conservation

Wetlands exhibit different characteristics that are influenced by freshwater flow, water level change, waves and tidal flow, salinity intrusion, sediment transport and the general climate. In general the rich variety of natural hydrologic and geologic environments lead to high biological diversity. Apart from serving as spawning and rearing areas and shelter for fish, wetlands support the food chain for the feeding, nesting and substrate of mammals, reptiles, amphibians and birds, including those endangered and threatened species. Healthy wetlands are of great importance for biodiversity conservation of coastal ecosystems—i.e., maintenance of the rich and balanced variety of plants, animals and microbes.

There are more than 300 species of birds in China's wetlands, accounting for one-third of the total number of birds found in China (Lu and Wang, 1995). The major wetlands in South China include the

Pearl River Estuary, with 418 species of zooplankton, 515 species of benthos and more than 302 species of main fishes (Chen et al., 2005). Similar bio-diversity is found in the wetlands in Guangxi Zhuang Autonomous Region (Hong, 1992) and Hainan Province (Zou et al., 1999). In particular, mangrove wetlands are of particular interest because they are the most productive ecosystems along the South China's coastlines. A healthy mangrove wetland is helpful to maintain coastal food webs and provide habitats for various living creatures. For example, the Mai Po mangrove wetland of Hong Kong (Fig. 8.75, 8.76) was listed as a 'Wetland of International Importance Especially as Waterfowl Habitat' under the RAMSAR Convention in September 1995, serving as an important area for internationally important numbers of wintering and migrating water birds. Over 200 bird species can be found in the Mai Po Nature Reserve; about 13 globally threatened species of birds and 17 species of invertebrates new to science are found in this site.

Fig. 8.76   Waterbirds (Black-faced Spoonbill and Egret) in Mai Po Marshes, Hong Kong (See color figure at the end of this book)

However, under increasing pollution threats and other anthropogenic influences (e.g., wastewater discharges, change of hydrology, coastal reclamation, sand mining), mangroves are among the most threatened wetlands with global loss exceeding 35% (mangrove ecosystems covered up to 75% of the tropical coastlines on earth in the 1990s). For instance, Deep Bay at the mouth of the Pearl River delta had the sixth largest mangrove forest in China (Fig. 8.75). However, since the 1980s, due to rapid industrialization and urbanization, mangroves around Deep Bay including Mai Po in Hong Kong and Futian in Shenzhen have suffered from excessive discharge of untreated domestic, livestock and industrial wastewater. At present, the mangrove in Shenzhen is the only one located in the heart of a modern city in China.

8.6.2   Wetland Evolution, Degradation and Restoration

8.6.2.1   Costal Wetland Evolution

Coastal wetland evolution is closely related to the dynamic interplay between natural erosion and accretion. The erosion factors are mainly from sea water, and the accretion factors are mainly from fresh water and sediment transportation by rivers. Wetlands will enlarge seaward if fresh water and sediment overwhelm erosion effects, and consequently a strong salinity gradient could be formed from fresh water at the landward end toward the coastal waters. For instance, the Yellow River is the second-longest river in

China, and is notable for the large amount of sediments it carries (around 1.4 billion tonnes to the sea annually). The wetland in Yellow River Delta is the largest wetland newly created in China, with a rate of 32.4 km^2 per year (Yue et al., 2003). Historic material, field investigation and remote sensing data all show that this vast neonatal wetland is attributable to its huge deposition of sand and mud transported by the Yellow River (Fig. 8.77).

Fig. 8.77   The Yellow River Delta Wetland

Human activities may have a very strong influence on wetland forms. The Chongming Dongtan Nature Reserve, China, located at the eastern end of the mouth of the Yangtze River, is a typical coastal wetland whose form is strongly suffering from human activities. This wetland has been re-marked as a representative wetland conservation zone by RAMSAR, because it is a staging and wintering site for millions of birds, as well as a spawning and feeding ground for 63 species of fish, including the endangered Chinese Sturgeon. Due to its extraordinary resources and its proximity to the city of Shanghai 45 km away, the site has become an attractive destination for eco-tourism and land development. For satisfying the need for farmland, fishponds, road systems and real estate, many parts of the new wetlands were reclaimed in a planned way by the construction of water conservancy works such as spur dikes (Fig. 8.78). Such human activities have severely changed the original wetland forms and ecosystems, forcing the sediment deposition to extend seaward, which could be reflected by the historical traces of farmland expansion shown in Fig. 8.79.

Fig. 8.78 Spur dikes established for reclamation of wetlands in the Chongming Island, China

Fig. 8.79   Effects of human activities on Chongming Island Wetland's form (See color figure at the end of this book)

Excessively irrational human activities can result in wetland **degradation**, by changing water quality/quantity, increasing pollutant inputs, and changing species composition as a result of exotic species invasion. Wetland degradation could be characterized by attributes such as reduction of coastal wetland area, pollution of seawater environment, degeneration of ecological environment, decrease of biodiversity. A comprehensive survey of 15 important coastal wetland ecosystems along the coastline of China showed that almost all of them had been in sub-health or unhealthy status (MWR, 2006).

Public **recognition** of significance for wetland restoration has become more and more active. Wetland restoration may be simply defined as those actions taken in a degraded wetland that result in the re-establishment of ecological processes, functions, and biotic/abiotic linkages and lead to a persistent and resilient system integrated within its landscape (Society of Wetland Scientists, 2000). In terms of restoration of biodiversity in a wetland, restoration specifically means the transfer of species composition towards a state more closely resembling a reference ecological community, often the historic indigenous community (Aronsen et al., 1993; Hobbs and Norton, 1996).

In view of the complexity inside a wetland system, restoration is rarely straightforward, and it often depends on reinstating ecological processes that have become disrupted or altered during previous degradation phases. In general, wetland restoration methods can be either passive or active. **Passive restoration** mainly relies on nature itself for completing the recovering work. Passive methods allow natural regeneration of wetland plant communities, natural re-colonization by animals, and re-establishment of wetland hydrology and soils. Passive approaches are most appropriate if the degraded site still retains basic wetland characteristics, and those factors causing degradation could be removed. For example, it has been commonly believed that, to restore a degraded wetland system caused by pollution, the waste discharge should be first controlled. **Active restoration** is necessary when a wetland is severely degraded or when restoration cannot be achieved through passive methods. Active restoration involves physical intervention in which humans directly control site processes to restore, create, or enhance wetland systems, e.g., re-contouring a site to the desired topography, changing the water flow by water control structures, intensive planting and seeding, intensive non-native species control, and bringing soils to provide the proper substrate for native species (USEPA, http://www.epa.gov/owow/wetlands/restore/). However, compared with passive restoration, active restoration usually needs more significant costs for design, engineering and construction work.

In summary, goals and performance guidelines for wetland restoration should include: improvement of hydrological environment, creation of equivalent wetland areas, replacement with the approximate ecological community, and restoration of flora and fauna. At present, however, there is no generally accepted comprehensive guideline for large-scale coastal wetland restoration. Despite hundreds of wetland restoration efforts in many countries, current efforts are largely more site-specific than scientific; experience gained in one case may not be generalized to other settings. In particular, in spite of many wetland models developed for wetland management, many of the hypothesized relationships used in the modeling are not confirmed. For example, little credible relationship has been found between natural-resource production activities and biodiversity loss. A better understanding of wetland dynamics and ecological processes is desirable. Wetland restoration efforts should also be accompanied by pre- and post-restoration monitoring and evaluation—including the collection of the necessary hydro-meteorological data and data on the status of vegetation, wildlife, fish, and macro-invertebrate.

8.6.2.2 Artificial Floods for Louisiana Wetlands Restoration

According to the United States Geological Survey (USGS), approximately half the original wetland habitats in the USA have been lost over the past 200 years. The wetland degradation in Louisiana is particularly serious; it accounts for 80% of wetland losses of USA. Between 1956 and 1990, nearly 3,460 km^2 of coastal wetlands reverted to open water, and more than 600 km^2 of wetlands have disappeared in the last decade (Stokstad, 2005). The wetland loss rate is about 65–91 km^2 per year, one of the highest rates of land loss in the world.

Human activities should be responsible for the degradation and loss of wetlands in Louisiana. Seasonal floods of Mississippi River are critical to the healthy growth of wetlands, since the infusion of fresh sediment from floodwater may offset soil subsidence in wetlands. Unfortunately, natural floods have been virtually eliminated by construction of massive levees, depriving wetlands of vital sediment. Cement-lined levees in South Louisiana prevent flood water in the Mississippi River from following the original flood route; the river sediment is transported into the Gulf of Mexico instead of allowing it to be distributed over the coastal wetlands. In addition, excessive construction of dredged systems and flood-control structures (for facilitating the development of recreation, residence, agriculture and industry) has aggravated the salt water intrusion from the Gulf of Mexico, creating an environment where wetland plants cannot survive. The US Environmental Protection Agency (USEPA) estimates that one-third of coastal wetlands in South Louisiana will vanish by 2050, if no efforts are made to halt this trend.

As part of efforts to halt the damage to wetlands and its huge impacts on coastal ecosystem, a series of restoration plans have been mapped out and carried out since the early 1970s. For example, 37 kilometers upstream from New Orleans, Louisiana, the Army Corps of Engineers (USACE) has constructed the USD 120 million Davis Pond Freshwater Diversion Structure (Fig. 8.80) to deliver water from the Mississippi River to help preserve some 130,000 hectares of Louisiana's endangered marshes of Barataria Bay, which are suffering from sediment loss like much of coastal Louisiana (Stokstad, 2005). However, this effort is just a tiny fraction of what is needed to restore the devastated Louisiana coastline; in reality it is difficult to mimic nature—to operate an artificial flood with proper water discharge and sediment in the right places. In addition, every wetland restoration project has its own impacts on the local environment and industry—e.g., a river diversion project may impact adversely on the oyster or shrimp habitat, thus affecting the local economy.

8.6.2.3 Kissimmee River Restoration

The Kissimmee River Restoration Program is a relatively successful example. Historically the Kissimmee River and its surrounding floodplain, located in Central Florida, USA, comprised a group of wetlands supporting diverse ecosystems and providing habitats to many unique species of plants and animals

Davis Pond diversion structure
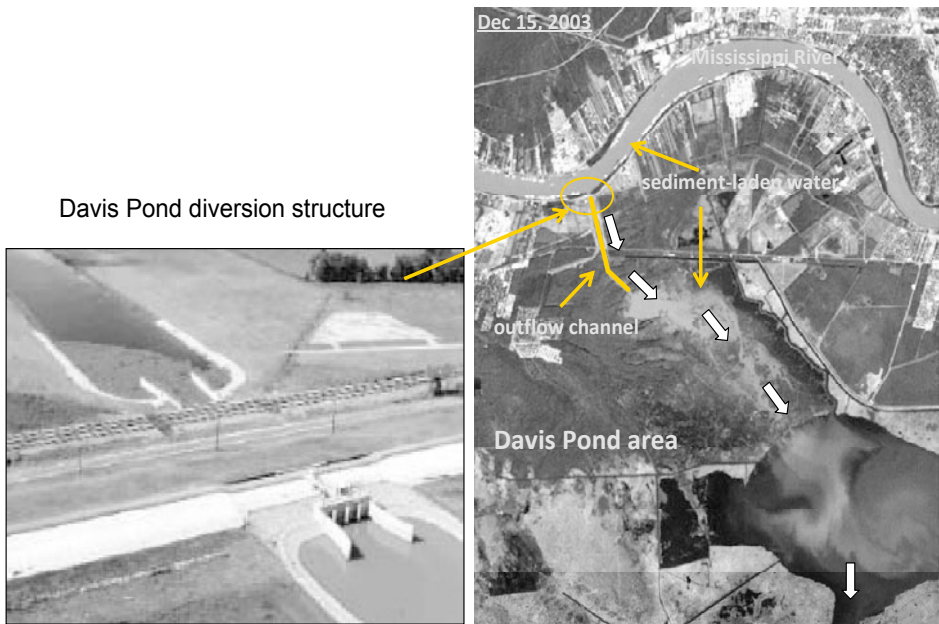
Fig. 8.80   Davis pond diversion structure in December 2003, two weeks after a full-capacity test-run. (Source: http://visibleearth.nasa.gov)

(waterfowl, migratory birds, and fish). The wetlands associated with the floodplain historically supported a diverse waterbird assemblage that included 17 species of wading birds and 19 species of waterfowl. However, as a result of intensive river training during 1962–1970, the Kissimmee River was channelized and transformed into a series of impounded reservoirs (Toth, 1993). Figure 8.81 compares the original Kissimmee River and channelized Kissimmee River. As a result, much of the adjoining floodplain was drained and many associated wetlands gradually disappeared, which severely impacted the Kissimmee's ecosystem, especially fish and other wildlife. For example, in the early 1970s wintering waterfowl populations decreased by 92%; lower dissolved oxygen levels led to the loss of largemouth bass; the stable water levels largely eliminated the fish spawning and foraging habitat (Perrin et al., 1982).

Fig. 8.81   Original Kissimmee River (left) and channelized Kissimmee River (right) (Hovey, 2000)

During the 1970s and 1980s, environmental concerns increased in the Kissimmee Basin. In 1991, the Kissimmee River Restoration Project was authorized by the U.S. Congress, with a total cost of $578

million. The goal of this project is to restore the physical form of the historical rivers and reestablish the natural functions. It is planned that once the hydrology is restored to approximate pre-channelized conditions, the water quality will improve, with return of native vegetation such as pickerel weed and other broadleaf marsh plant species. Once the habitat is restored, it will only be a matter of time before the wildlife communities rebound (http://www.dep.state.fl.us). Beginning in 1999, a number of activities associated with the project—including ecosystem restoration, restoration evaluation, aquatic plant management, land management, water quality improvement, and water supply planning—have been carried out. These restoration measures have produced good results—for example monitoring showed that the diversity of birds in the restored areas has increased tremendously (https://my.sfwmd.gov).

8.6.3 Wetland Construction and Protection

In this section, we introduce two examples in Hong Kong that illustrate the importance attached to wetland conservation in an urban environment. The engineered wetland constructed for the Yuen Long Bypass Floodway (YLBF) project is first introduced as an example of environmental compensation and enhancement for an engineering project. As a second example, the environmental litigation relating to the environmental impact assessment of the proposed Sheung Shui–Lok Ma Chau Spur Line in 2001 is presented to illustrate issues of ecological preservation against transport needs in urban development.

8.6.3.1 Engineered Wetland of Yuen Long Bypass Floodway, Hong Kong

Yuen Long town (population 341,000) is located in the northwestern part of the New Territories, Hong Kong; it is a satellite town developed in the middle 1980s. The runoff from the steep upstream catchment is drained into Deep Bay (Shenzhen Bay) through the Yuen Long town via three river channels: Yuen Long Main Nullah, the Sham Chung Channel, and the San Hui Nullah (Fig. 8.82). The concrete channel system built in the 1960s is not able to protect Yuen Long from serious flash floods at times of severe rainstorms. For example, during Typhoon Brenda in 1989 road links to the rest of Hong Kong were flooded, thus causing social and economic losses due to disruption of economic activities. The serious flooding in 1998 and 2000 had also caused major traffic disruptions to the Yuen Long Town, and in particular the Light Rail Train service was suspended.

The Yuen Long Bypass Floodway (YLBF) was designed to protect Yuen Long town from flooding (e.g., Arega et al., 2008). The concept was for the YLBF to intercept flows from the Sham Chung Channel, the San Hui Nullah, and part of the flow from the Yuen Long Main Nullah away from the town into the Kam Tin River (Fig. 8.82). The drainage capacity of YLBF is 385 m^3/s (200-year flood) (Wong et al., 2006); the HK\$470 million project was commissioned in 2006.

A number of river restoration features are built into this flood control project. Using an innovative "green channel, ecological channel" concept, the YLBF was designed to simulate a natural lively river system (Wong et al., 2006). First, the floodway meanders in the downstream, more rural sections of the Floodway, with bends and different flow regimes, e.g., shallow ponds (area 18,000 m^2) and wetland. Second, substantial greening work has been carried out to create a pleasant environment. The channel bottom and slope is paved by cellular reinforced concrete paving (52,000 m^2) which contains many pockets of soil on which vegetation of different species are planted. Third, as environmental compensation and to enhance the ecological value of the project, an engineered wetland (Fig. 8.82, 8.83) has been constructed from abandoned fields and fishponds near the downstream of YLBF and with an area of 7 hectares (i.e. the size of 10 standard football fields). The engineered wetland consists of sedimentation ponds, crusted brick fields, oyster shell fields, reed beds, 2 shallow ponds, 3 main ponds and 1 deep pond. The flow from the YLBF is naturally filtered on passage through the crusted bricks and oyster shells, and purified through the reed beds (nutrient uptake by plant growth), before it flows into the different ponds. The shallow

ponds and main ponds have been planted with 32 different species of herbaceous plants, bamboos, shrubs and trees. Young fishes have also been placed to the ponds to attract the visits of birds.
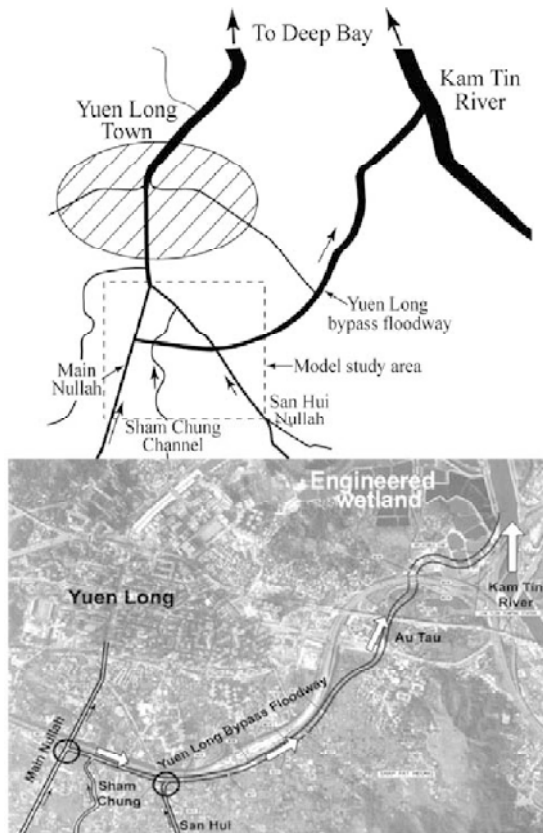
Fig. 8.82   Yuen Long bypass floodway—flood diversion and aerial view

Fig. 8.83   Engineered wetland of Yuen Long bypass floodway (See color figure at the end of this book)

With the above innovative designs, different kinds of ecological habitats are created. The engineered wetland has intrinsic ecological value for wetland birds, amphibian and invertebrates, and has improved the environment and ecology of the district. Post-operation environmental monitoring shows that: ① the

water quality objectives and standards have been achieved through the proper functioning of the sedimentation pond, the crushed brick field, the oyster shell field as well as the reed bed; ② a healthy wetland habitat frequented by precious wild life has been established, including rare species such as lesser whistling duck and pheasant-tailed jacana.

8.6.3.2 Long Valley Wetland Protection

In the 1990s the Kowloon Canton Railway Corporation (KCRC) of Hong Kong planned to build the Sheung Shui to Lok Ma Chau Spur Line (Fig. 8.84(a)). The 7.4 km long railway link is a key part of the Hong Kong's transport network, providing a second rail connection across the Hong Kong—Mainland China border into the Shenzhen Special Economic Zone. The HK$7 billion project was originally conceived as a fully-elevated rail extension, and involved a viaduct section that crosses the environmentally sensitive Long Valley wetland (Fig. 8.84(b)). However this proposal was met with strong opposition from a number of local environmental groups due to the possible ecological impact.
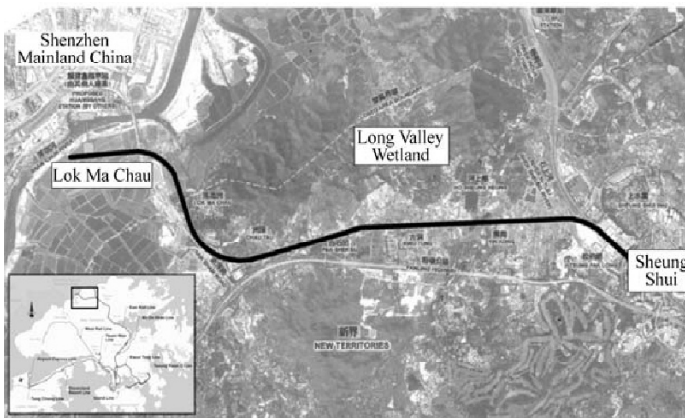
(a)
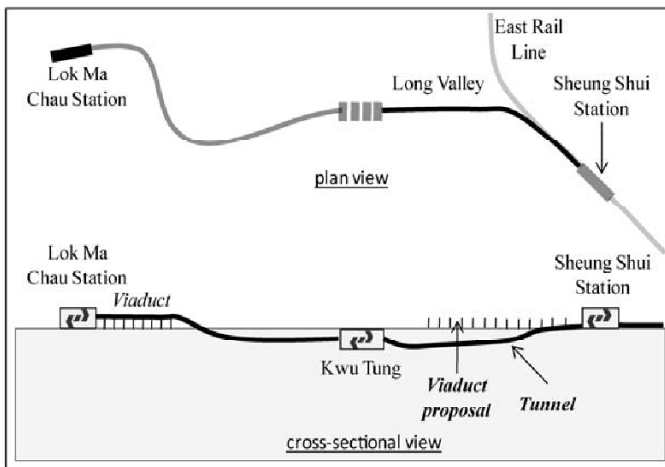
(b)

Fig. 8.84 (a) Sheung Shui to Lok Ma Chau Spur line, Hong Kong (source: KCRC); (b) the original viaduct proposal and the alternative tunnel scheme

Long Valley is the largest remaining area (33 hectares) of freshwater wetland in Hong Kong, bounded on the west and northwest by the River Beas and on the east by the River Sutlej (Fig. 8.85(a)). The settlement of Yin Kong is to the south; there is development to the southeast adjacent to the River Sutlej and the village of Ho Sheung Hueng is to the northwest on the opposite side of the River Beas. The ecological habitats of Long Valley Wetland are created by the agricultural activity, and the area as a whole can be regarded as un-fragmented (Fig. 8.85(b)).

This wetland is of high ecological importance with a high diversity of birds. Over 200 different species have been recorded, 29 of which are of conservation importance. Of particular concern is the Greater

(a)

(b)
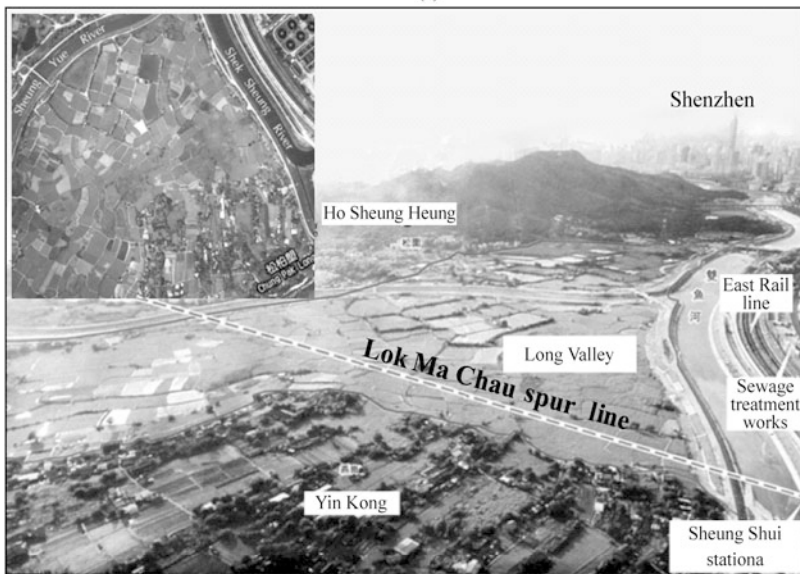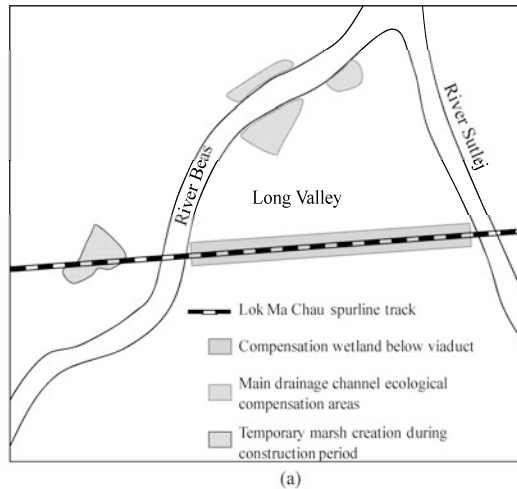
Fig. 8.85 (a) Predominantly agricultural Long Valley Wetland of high ecological value; (b) original proposed ecological mitigation areas during construction and operation of spur line viaduct within Long Valley. (source: Lands Department, Hong Kong and Mingpao News)

Painted Snipe which breeds in the summer in Long Valley. Both the active and inactive agriculture creates an attractive habitat for birds. This is in spite of disturbance by human activity both in farming and during extensive channelization work on both the River Beas and the River Sutlej. None of this has had any measurable adverse effect upon the ecology, which seems to be resilient. It is estimated that its ecological value depends upon the continuation of wetland agriculture; therefore, if this were abandoned for economical or any other reason the present eco-system may disappear.

In the original proposal, KCRC designed 700 meters of viaduct through the central part of the Long Valley Wetland to reduce adverse impacts on the wetland during operation (KCRC, 2000); some mitigation measures during construction are also provided, including the provision of a temporary freshwater wetland of 1.8 hectares as a roosting habitat (Fig. 8.85(a)). However, opponents pointed out that the viaduct construction would badly damage the landscape and biodiversity of the Long Valley Wetland; the environmentalists also questioned the effectiveness of the mitigation measures in making up for the possible ecological damage, based on the low success rates of man-made ecological environments abroad.

In July 2000, the Environmental Protection Department (EPD) rejected the environmental impact assessment (EIA) report of KCRC, and refused to issue an environmental permit for the construction work. It was the first time that the EPD rejected a EIA report since the Environmental Impact Assessment Ordinance came into effect in 1997. The reasons of rejection include: ① the lengthy fragmentation effect of the linear construction site; ② the mitigation proposed for fragmentation, silty run-off, hydrological disruption, concrete washing and other pollutants is unlikely to be practical or effective during construction, because of the poor drainage system in Long Valley, heavy rainfall, and flooding; ③ the 1.8 hectares of proposed temporary wetland is unlikely to be effective to compensate for habitat loss during construction.

The project sponsor lodged an appeal, on the grounds that the proposed rail link, which cuts through the Long Valley wetland, is the most appropriate one in balancing the needs of the environment, transportation and communities. After 27 days of hearing, the Environmental Impact Assessment Appeal Board maintained the original decision against allowing the KCRC to build the Long Valley Spur Line. Although the Appeal Board considered the viaduct to be a practicable solution, they considered that the KCRC had not sufficiently demonstrated that the mitigation would be successful and it required further studies to enable confidence to be given to this proposal.

Following the judgment, the KCRC developed an alternative scheme to construct a tunnel beneath Long Valley without disturbing the sensitive habitat (Musgrave and Plumbridge, 2007). Although this entailed an additional cost of around HK$ 2 billion, the tunnel scheme won the support of the environmentalists and the public. Fig. 8.84(b) presents a plan view and a cross-sectional view of the rejected viaduct proposal and the alternative tunnel scheme. The EIA report for the alternative scheme was approved by the EPD with conditions on 11 March 2002, and the project was commissioned in August 2007. The Sheung Shui—Lok Ma Chau Spurline case study serves as a good example of sustainable development, and a reminder that economic benefits must be carefully balanced against environmental costs.

Review Questions

1. What are the key factors for delta development?
2. What are the causes of flooding of estuarine and coastal areas?
3. How to calculate flushing time for a semi-enclosed bay?
4. What causes algal bloom and how to mitigate algal bloom?
5. What are the methods of waste disposal?
6. State the coastal wetland evolution, degradation and restoration strategies?

References

Ambrose R.B. et al., 1993. The Water quality analysis simulation program. WASP5, Environmental Research Laboratory, USEPA, Athens, Georgia

Anderson D.M., 1998. Study of red tide monitoring and management in Hong Kong: Literature review and background information. Technical Rep. No. 1, Agriculture and Fisheries Department, Hong Kong Government, Hong Kong

Arega F. and Lee J.H.W., 2000. Long term circulation and eutrophication model for Tolo Harbour, Hong Kong. Water Quality and Ecosystem Modelling, 1, 169–192

Arega F., Lee J.H.W. and Tang H.W., 2008. Hydraulic jet control for river junction design of Yuen Long Bypass Floodway, Hong Kong. Journal of Hydraulic Engineering, ASCE, 134(1), 23–33

Aronsen J., Floret C., Le Floc'h E., Ovalle C. and Pontanier R., 1993. Restoration and rehabilitation of degraded ecosystems in arid and semiarid regions. I. A view from the south. Restoration Ecology, 1, 8–17

Bleninger T., 2007. Coupled 3D hydrodynamic models for submarine outfalls: Environmental hydraulic design and control of multiport diffusers. Doctoral thesis, Universitätsverlag Karlsruhe

Bowden K.F., 1983. Physical Oceanography of Coastal Waters. Ellis Horwood, New York, Pp. 302

Bowie G.L., Mills W.B., Porcella D.B., Campbell C.L., Pagenkopf J.R., Rupp G.L., Johnson K.M., Chan P.W.H., Gherini S.A. and Chamberlain C.E., 1985. Rates, constants and kinetics formulations in surface water quality modeling. EPA/600/3-85/040, USEPA, Athens, Georgia

Cameron W.M. and Pritchard D.W., 1963. Estuaries. In M.N. Hill (editor): The Sea vol. 2, John Wiley and Sons, New York, 306–324

Canicio Antoni and Ibáñez Carles, 1999. The holocene evolution of the Ebre delta catalonia, Spain. Acta Geographica Sinica, 54(5), 462–469

Cederwall K., 1968. Hydraulics of marine waste disposal. Hydraulic Division, Chalmers Institute of Technology, Goteborg, Sweden, Report No. 42

Chen J.Y., Shen H.T., Yun C.X. 1988. Introduction In. Chen J.Y., Shen H.T. and Yun C.X. (eds.), Processes of hydrodynamics and geomorphology of the Changing Estuary. Shanghai: Shanghai Scientific and technical Publishers, 1–5 (in Chinese)

Chen G.Z., Lan Z.H. and Deng P.Y., 2005. The project reversing environmental degradation trends in the South China Sea and Gulf of Thailand—Special Report of Wetlands in China (in Chinese). Guangzhou: Zhongshan University Press, 6–9

Chen Y.W., Fan C.X., Teubner K. and Dokulil M., 2003. Changes of nutrients and phytoplankton chlorophyll-a in a large shallow lake, Taihu, China: an 8-year investigation. Hydrobiologia, 506, 273–279

China Daily, 2003. Shanghai puts up a fight to stop sinking, China Daily, 2003-07-16 07: 51

Choi D.K.W., Lee J.H.W., Kwok K.W.H. and Leung K.M.Y., 2009. Integrated stochastic environmental risk assessment of the Harbour Area Treatment Scheme (HATS) in HongKong, Environmental Science and Technology (accepted for publication, March 13, 2009

Choi K.W. and Lee J.H.W., 2004. Numerical determination of flushing time for stratified water bodies. Journal of Marine Systems, 50(3-4), 263-281

Choi K.W. and Lee J.H.W., 2007 Distributed entrainment sink approach for modeling mixing and transport in the intermediate field. Journal of Hydraulic Engineering, 133(7), 804–815

Correggiari A., Cattaneo A. and Trincardi F., 2005. Depositional patterns in the late Holocene Po delta system, in Giosan L. and Bhattacharya J.P. (eds.), River Deltas: Concepts, Models, and Examples: SEPM, Special Publication, 83, 363–390

Dalrymple R.W., Zaitlin B.A. and Boyd R., 1992. Estuarine facies models: conceptual basis and stratigraphic implications. Journal of Sedimentary Petrology, 62, 1130–1146

Di Toro D.M. and Connolly J.P., 1980. Mathematical models of water quality in large lakes, Part 2, Lake Erie. Manhattan College, Bronx, New York

Dickman M.D., 1998. Hong Kong's worst red tide. Proc., Int. Symp. on Environmental Hydraulics, Lee J.H.W. et al., (eds.), Balkema, Rotterdam, The Netherlands, 641–645

Duan X.H., Wang Z.Y., Xu M.Z. and Zhang K., 2009. Effect of streambed sediment on benthic ecology. International

Journal of Sediment Research, 134(9), 314–327

Dugan P., 1990. Wetland Conservation: A Review of Current Issues and Required Action. The World Conservation Union, IUCN

Dyer K.R., 1973. Estuaries: A physical introduction. John Wiley & Sons, New York

Feng J. and Zhang W., 1998. The evolution of the modern Luanhe River delta, north China. Geomorphology, 25(3–4), 269–278

Fernando H.J.S., McCulley J.L., Mendis S.G. and Perera K., 2005. Coral poaching worsens tsunami destruction in Sri Lanka. EOS, Transactions of the American Geophysical Union, 86(33)

Fernando H.J.S., Samarawickrama S.P., Balasubramanian S., Hettiarachchi S.S.L. and Voropayev S., 2008. Effects of porous barriers such as coral reefs on coastal wave propagation. Journal of Hydro-environment Research, 1(3–4), 187–194

Fischer H.B., List E.J., Koh R.C.Y., Imberger J. and Brooks N.H., 1979. Mixing in Inland and Coastal Waters. Academic Press, New York

Friedman G.M. and Sanders J.E. 1978. Principles of Sedimentology. New York, John Wiley & Sons, Pp. 792

Galloway W.E. 1975. Process framework for describing the morphologic and stratigraphic evolution of deltaic depositional systems. In: Broussard M.L. (ed.), Deltas, Models of Exploration. Houston Geological Society, Houston, Pp. 87–98

George Pararas-Carayannis, 1985. Tsunami: Forecasting. Preparedness and warning. Fifteenth Conference on Broadcast Meteorology of the American Meteorological Society, April 9–12, Honolulu, Hawaii

Groombridge B. and Jenkins M., 1998. Freshwater biodiversity: A preliminary global assessment. World Conservation Monitoring Centre (UNEP-WCMC)—World Conservation Press, Cambridge, UK

Henderson F.M., 1966. Open channel flow, Macmillan, New York. Mott MacDonald Hong Kong Ltd. (1990) Territorial land drainage and flood control strategy study—Phase I, Hong Kong Drainage Services Department, Vol. 2

HKDSD (Hong Kong Drainage Services Department), 2001. Investigation report on flooding in the New Territories and Tsuen Wan in June 2001, Report of Hong Kong Drainage Services Department, Hong Kong

Hobbs R.J. and Norton D.A., 1996. Towards a conceptual framework for restoration ecology. Restoration Ecology, 4, 93–110

Hong X A., 1992. Brief introduction on exploitation of tidal flat resources of Guangxi. Mar Info, 2, 34–36 (in Chinese)

Hovey C., 2000. Macrophyte communities within the channelized kissimmee river: expectations for restoration. Aquaphyte Newsletter, 20(1), 1–5

Howell P.P. and Allan J.A., Editors, 1994. The Nile: Sharing a Scarce Resource. Cambridge Univ. Press, Cambridge, Pp. 408

International Lake Environment Committee (ILEC) Lake Biwa Research Institute (eds.) 1988-1993. Survey of the State of the World's Lakes. Volumes I-IV. ILEC, Otsu, Japan

Ippen A.T. and Harleman D.R.F., 1961. One-dimensional Analysis of Salinity Intrusion in Estuaries. Technical Bulletin No. 5, Committee on Tidal Hydraulics, Corps of Engineers, U.S. Army

Jirka G.H. 1982. Multiport diffusers for heat disposal: a summary. Journal of Hydraulic Division, ASCE, 108(HY12), 1425–1468

Jirka G.H. and Lee J.H.W., 1994. Waste Disposal in the Ocean, in "Water Quality and its Control", Hino M. (ed.), Balkema, Rotterdam, 193–242

KCRC (Kowloon-Canton Railway Corporation), 2000. Sheung Shui to Lok Ma Chau spur line: environmental impact assessment report. Hong Kong. (http://www.epd.gov.hk/eia/register/report/)

Keddy P.A., 2000. Wetland Ecology: Principles and Conservation. Cambridge University Press, UK

Kesel R.H., 1988. The decline of the suspended load of the lower Mississippi river and its influence on adjacent wetlands. Environmental Geological Water Sciences, 11, 271–281

Ketchum B.H., 1951. The exchanges of fresh and salt waters in tidal estuaries. Journal of Marine Research 10(1), 18–38

Kowloon-Canton Railway Corporation (KCRC), 2000. Sheung Shui to Lok Ma Chau spur line: environmental impact assessment report. Hong Kong (http://www.epd.gov.hk/eia/register/report/)

Kuang C.P. and Lee J.H.W., 2001. Numerical experiments on the mixing of a duckbill valve jet. 3 rd International Symposium on Environmental Hydraulics, Arizona State University, Tempe, Arizona

Kuang C.P. and Lee J.H.W., 2004. Impact of reclamation and HATS Stage I on Victoria Harbour, Hong Kong. Proc. 14th IAHR-APD Congress, Hong Kong, Dec. 15–18, 1163–1168

Lai A.C.H., Yu D., Lee J.H.W., 2007. Near and intermediate field mixing of a rosette jet group. Proceedings of the fifth international symposium on environmental hydraulics, Tempe, Arizona, USA (CD-ROM), 4–7 December

Lam C.W.Y. and Ho K.C., 1989. Red tides in Tolo Harbour, Hong Kong. In: Okaichi T., Anderson D.M., Nemoto T., (eds.), Red Tides: Biology, Environmental Science, and Toxicology, Elsevier, New York, 49–52

Larsen T., 1995. Diffuser design for marine outfalls in areas with strong currents, high waves and sediment transport. Water science & technology, 32(2), 249–255

Le J.Z. et al., 1998. Analysis of the fluvial process of the Yangtze River mouth. Report of Shanghai Institute of Navigation Channel Survey and Design (in Chinese)

Lee H.S. and Lee J.H.W., 1995. Continuous monitoring of short term dissolved oxygen and algal dynamics. Water Research, 29, 2789–2796

Lee J. H.W., Townsend N.R. and Ng K.C. 2002. Urban flood control in Hong Kong-Chalenges and solutions, Keynote lecture, Flood Defence Wu et al. (eds.) Science Press, New York Ltd., ISSN 1-880132-54-0

Lee J.H.W. and Arega F., 1999. Eutrophication dynamics of Tolo Harbour, Hong Kong. Marine Pollution Bulletin, 39 (1–12), 187–192

Lee J.H.W. and Cheung V., 1990. Generalized Lagrangian model for buoyant jets in a current. Journal of Environmental Engineering, ASCE, 116(6), 1085–1106

Lee J.H.W. and Choi K.W., 2008. Real-time hydro-environmental modeling and visualization system for public engagement. Environmental Fluid Mechanics, 8, 411–421

Lee J.H.W. and Chu V.H., 2003. Turbulent jets and plumes - a Lagrangian approach. Kluwer Academic Publishers

Lee J.H.W. and Neville-Jones P., 1987. Initial dilution of horizontal jet in crossflow. Journal of Hydraulic Engineering, ASCE, 113, 615–629

Lee J.H.W. and Wong P.P.S., 1997. A water quality model for mariculture management. Journal of Environmental Engineering, ASCE, 123, 1136–1141

Lee J.H.W., Chai H., Arnold D., Lau P. and Kan F., 2001a. Hydraulics of a three-dimensional flow diversion structure for the Kai Tak Transfer Scheme, Proc. 6th Cross-Strait Symposium on Water Resources, Fuzhou, Sept. 13–15, 485–491

Lee J.H.W., Harrison P.J., Kuang C.P. and Yin K.D., 2006. Eutrophication dynamics in Hong Kong waters: Physical-biological interactions. The Environment in Asia Pacific Harbours. E. Wolanski, Editor, Springer, 187–206

Lee J.H.W., Karandikar J. and Horton P.R., 1997. Hydraulics of duckbill valve jet diffusers. Combined Australasian castal engineering and ports conference, Christchurch, 566–572

Lee J.H.W., Karandikar J. and Horton P.R., 1998. Hydraulics of "duckbill" elastomer check valve. Journal of hydraulics engineering, 124(4), 394–405

Lee J.H.W., Liu C. and Wei H.P., 2001b. Hydrodynamic simulation of the Yangtze Estuary for assessment of the Third Shanghai Sewerage Project, Proc. Third International Symposium on Environmental Hydraulics, Arizona State University, December 5–8 (CDROM)

Lee J.H.W., Lo S.H. and Lee K.L., 2004. Flow variation of duckbill valve jet in relation to large elastic deformation. Journal of Engineering Mechanics, ASCE, 130(8), 971–981

Lee J.H.W., Wong K.T.M., Huang Y. and Jayawardena A.W., 2000. A real time early warning and modelling system for red tides in Hong Kong, Proc. 8th International Symposium on Stochastic Hydraulics Wang Z.Y. and Hu S.X. (eds.), July 25–28, 2000, Beijing, Balkema, 659–669

Lee J.H.W., Wu R.S.S. and Cheung Y.K., 1991b. Forecasting of dissolved oxygen in marine fish culture zone. Journal of Environmental Engineering, ASCE, 117(6), 816–833

Lee J.H.W., Wu R.S.S., Cheung Y.K., and Wong P.P.S., 1991a. Dissolved oxygen variations in marine fish culture zone. Journal of Environmental Engineering, ASCE, 117(6), 799–815

Lee, J.H.W., Choi, K.W. and Arega, F., 2003. Environmental management of marine fish culture in Hong Kong,

Marine Pollution Bulletin, Vol. 47, Nos. 1–6, 202–210.

Leeder M. R. 1983. Sedimentology-Process and Product. George Allen & Unwin Publishers Ltd, Pp. 384

Li H.E., Lee J.H.W., Koenig A. and Jayawardena A.W., 2003. Nutrient load estimation of nonpoint source pollution for Hong Kong region, Proc. 7th IWA International Conference on Diffuse Pollution and Basin Management, August Dublin, 3(6), 88–93

Liu C., He Y., Lee J.H.W. and Wang Z.Y., 2002. Numerical study on environmental impact of the Third Shanghai Sewerage Project. International Journal of Sediment Research, 17(2), 165–173

Liu, P.L.F., Lynett, P., Fernando, H., Jaffe, B.E., Fritz, H., Higman, B., Morton, R., Goff, J. and Synolakis, C., 2005. Observations by the International Tsunami survey team in Sri Lanka. Science 308 (10 June), 1595.

Lu X. and Wang R., 1995. Study on wetland biodiversity in China. Chinese Geographical Science, 6(1), 15–23

Lung W.S., 1993. Water Quality Modeling: Application to Estuaries, CRC Press

Maldonado A., 1986, Sediment environment and evolution of the Ebro Delta, Thalassas, 4(1), 151–161

Mao J.Q., 2005. Study on assessment methods and numerical simulation of eutrophication in lakes and reservoirs. Ph.D. thesis, Tsinghua University, Beijing (in Chinese)

Marris E., 2005a. Inadequate warning system left Asia at the mercy of tsunami. Nature 433(7021), 3–5

Marris E., 2005b. Tsunami damage was enhanced by coral theft. Nature 436, 1072

Mcpherson J.G., Shanmugam G. and Moiola R.J., 1987. Fan deltas and braid deltas: varieties of coarse-grained deltas. Geological Society of America Bulletin, 99, 331–340

Melching C.S., 2006. Dam removal in the United States, Lecture notes for Ph.D. Students, Tsinghua University. Beijing

Mercer A.G. et al., 1992. Impact of future water resources projects on the Nile: Nile 2000. Conf. on protection and development of the Nile and other major rivers, 1, 2-8-1-2-8-6

Miller G.T. 2005. Living in the Environment: Principles, Connections, and Solutions. Thomson Brooks/Cole, Canada, 510–512

Musgrave J. and Plumbridge G., 2007. The Lok Ma Chau spur line tunnels: design and construction. The Arup Journal, 3, 48–54

NWR, 2006. A Survey of Aquatic Environmental Conservation and Restoration in China. The Ministry of Water Resources of People's Republic of China.

Nixon S.W., Ammerman J.W., Atkinson L.P., Berounsky V.M., Billen G., Boicourt W.C., Boynton W.R., Church T.M., Di Toro D.M., Elmgren R., Garber J.H., Giblin A.E., Jahnke R.A., Owens N.J.P., Pilson M.E.Q. and Seitzinger S.P., 1996. The fate of nitrogen and phosphorus at the land-sea margin of the North Atlantic Ocean. Biogeochemistry, 35, 141–180

Novak P. and Cabelka J., 1983. Models in hydraulic engineering, Pitman, London

Officer B.C. and Kester D.R. 1991. On estimating the non-advective tidal exchanges and advective gravitational circulation exchanges in an estuary. Estuarine, Coastal and Shelf Science, 32, 99–103

Organization for Economic Cooperation and Development (OECD), 1982. Eutrophication of Waters: Monitoring, Assessment and Control. OECD, Paris, France

Orton G. J. and Reading H.G., 1993. Variability of deltaic processes in terms of sediment supply, with particular emphasis on grain size. Sedimentology, 40(3), 475–512

Painting S.J., Devlin M.J., Malcolm S.J., Parker E.R., Mills D.K., Mills C., Tett P., Wither A., Burt J., Jones R. and Winpenny K., 2007. Assessing the impact of nutrient enrichment in estuaries: susceptibility to eutrophication. Marine Pollution Bulletin, 55, 74–90

Perrin L.S., Allen M.J., Rowse L.A., Montalbano III F., Foote K.J. and Olinde M.W., 1982. A report on fish and wildlife studies in the Kissimmee River Basin and recommendations for restoration. Florida Game and Fresh Water Fish Commission, Okeechobee, USA

Postma G., 1995. Sea-level-related architectural trends in coarse grained delta complexes. Sedimentary Geology, 98, 3–12

Prandle D., 1984. A modeling study of the mixing of ^{137}Cs in the seas of the European continental shelf. Philosophical Transactions of the Royal Society of London, 310, 407–436

Rivera-Monroy V.H., Torres L.A., Bahamon N., Newmark F. and Twilley R.R., 1999. The potential use of mangrove

forests as nitrogen sinks of shrimp aquaculture pond effluents: the role of denitrification. Journal of the World Aquaculture Society 30, 12–25

Roberts P., Snyder W. and Baumgartner D., 1989. Ocean outfalls. I. Submerged wastefield formation. II. Spatial evolution of submerged wastefield. Journal of Hydraulic Engineering, 115, 1–48

Robertson A.I. and Phillips M.J., 1995. Mangroves as filters of shrimp pond effluent: predictions and biogeochemical research needs. Hydrobiologia, 295, 311–321

Rodhe W., 1969. Crystallization of eutrophication concepts in North Europe. In: Eutrophication, Causes, Consequences, Correctives. National Academy of Sciences, Washington D.C., Standard Book Number 309-01700-9, 50–64

Schindler D.W. and Fee E.J., 1974. Experimental lakes area: whole-lake experiments in eutrophication, Fish J., Res. Board. Can., 31, 937–953

Sharp J.J., 1991. Marine outfalls for small communities in Atlantic Canada. Canadian Journal of Civil Engineering, 18, 388–396

Shen H.T. and Pan D.A., 1988. The characteristics of tidal current and its effects on the channel of the Changjiang Estuary, Processes of Dynamics and Geomorphology of the Changjiang Estuary, Chen H.T., Shen H.T. and Cai X.Y., (eds.), Shanghai Scientific and Technical Publishers, Shanghai, China, 80–90 (in Chinese)

Smith-Evans M. and Dawes A., 1996. Early experiences in monitoring the effects of Hong Kong's new generation of sewage outfalls on the marine environment. Mar. Pollut. Bull. 33(7–12), 317–327

Society of Wetland Scientists, 2000. Position paper on the definition of wetland restoration. Water Conservancy Science and Technology and Economy, http://www.sws.org

Stanley A.S. and Winkley B.R., 1994. The variability of large fluvial rivers, ASCE Press, New York

Stanley D.J., 1996. Nile delta: extreme case of sediment entrapment on a delta plain and consequent coastal land loss. Marine Geology, 129, 189–195

Stokstad E., 2005. Louisiana's wetlands struggle for survival. Science, 310, 1264–1266

Stommel H. and Farmer H.G., 1952. On the nature of estuarine circulation, Part II, Tech. Rep. WHOI-52-51, Woods Hole Oceanographic Institution, Woods Hole, MA

Swenson D.D. and Marshall Bob., 2005. Flash Flood: Hurricane Katrina's Inundation of New Orleans, August 29, (SWF). Times-Picayune, May, 14, 2005

Syvitski James P.M. and Saito Yoshiki, 2007. Morphodynamics of deltas under the influence of humans. Global and Planetary Change, 57(3–4), 261–282

Tam N.F.Y., 2006. Pollution studies on mangroves in Hong Kong and mainland China. The Environment in Asia Pacific Harbours. Springer, Netherlands

Tam N.F.Y., and Wong Y.S., 1995. Mangrove soils as sinks for wastewater-borne pollutants. Hydrobiologia, 295, 231–242

Thomann R.V. and Mueller J.A., 1987. Principles of surface water quality modeling and control. HarperCollins, New York

USDC (United States Department of Commerce) 2006. Hurricane Katrina Service Assessment Report (PDF). June 2006, http://en.wikipedia.org/wiki/Hurricane_Katrina

Wang Z.B, Wang Z.Y, de Vriend H.J., 2008. Impact of water diversion on the morphological development of the lower Yellow River. International Journal of Sediment Research, 23(1), 13–27

Wang Z.Y., and Xu M.Z., 2010. Habitat diversity and its relation with biodiversity, Proceedings of 8th IAHR International Symposium on Eco-hydraulics, Invited lecture, Seoul, South Korea, Sep. 2010

Wang Z.Y., Hu S.X., and Shao X.J., 2003. Delta processes and management strategies in China. Journal of River Basin Management. 1(2), 173–184

Wei H.P., Xu G.T., Lee J.H.W. and Choi D.K.W., 1998. Near field dilution study of Bailong Gang wastewater outfall of Stage 2 Shanghai Sewerage Project, Proc. 2nd International Symposium on Environmental Hydraulics, Hong Kong, Dec., Hong Kong, Balkema, 261–266

Welch E.B. 1980. Ecological effects of waste water, Cambridge University Press

Wilkinson D.L., 1984. Purging of saline wedges from ocean outfalls. J. Hydr. Engng., ASCE, 110(12), 1815–1829

Wong K.T.M., 2004. Red tides and algal blooms in subtropical Hong Kong waters: field observation and Lagrangian modelling, Ph.D. thesis, The University of Hong Kong

Wong C.K., Chan Y.Y. and Ip K.L., 2006. Yuen Long Bypass Floodway project for solving the flooding problem in Yuen Long town and surrounding areas. Proceedings of Mainland and Hong Kong conference on Urban Infrastructure Development and Construction Market Regulation, Urumqi, September 10–12, 2006

Wong Y.S., Tam N.F.Y., Lan C.Y., 1997. Mangrove wetlands as wastewater treatment facility: a field trial. Hydrobiologia, 352, 49-59

Xie X.P., Wang Z.Y. and Melching C.S., 2009, Formation and evolution of the Jiuduansha shoal over the past 50 Years. ASCE Journal of Hydaulic Engineering, 134(9), 741–754

Xue Y.Q., Zhang Y., Ye S.J., Wu J.C. and Li Q.F., 2005. Land subsidence in China. Environmental Geology, 48(6), 713–120

Yang Z.B. and Hodgkiss I.J., 1999. Massive fish killing by Gyrodinium sp. Harmful algae news. the Intergovernmental Oceanographic Commission of UNESCO, 18, 4–5

Yang Z.B., Takayama H., Matsuoka K. and Hodgkiss I.J., 2000. Karenia digitata sp. no., a new harmful algal bloom species from the coastal waters of west Japan and Hong Kong. Phycologia, 39(6), 463–470

Yau T.W.C., 1997. Studies of sea water intrusion and purging on the Hong Kong Oceanic Diffuser Model, MPhil thesis, The University of Hong Kong

Yi Y.J., Wang Z.Y., Zhang K., Yu G.A. and Duan X.H., 2008. Sediment pollution and its effect on fish through food chain in the Yangtze River. International Journal of Sediment Research, WASER, 23(4), 338–347

Yue T.X., Liu J.Y., Jørgensen S.E. and Ye Q.H., 2003. Landscape change detection of the newly created wetland in Yellow River Delta. Ecological Modelling, 164(1), 21–31

Zhang W. and Jiang R., 2004. Analysis on runoff change of the Majia River at Nanle Station. Hydrology, 24(5), 37–40 (in Chinese)

Zou F.S, Song X.J, Jiang H.S. and Chen K., 1999. Types and characteristics of the wetland of Hainan Island. Tropical Geography, 19(3), 204–207 (in Chinese)

9 Water Quality Management

Abstract

This chapter begins by describing some general water quality management problems and the definition of pollution from environmental and economic perspectives. The chapter then focuses on four of the major water pollution problems facing rivers throughout the world: dissolved oxygen (DO), nutrients, waterborne and water contact diseases, and sediment contamination. The DO relations are described through the simple Streeter-Phelps concept relating carbonaceous biochemical oxygen demand (BOD) to DO and the extensions of this concept to nitrogeneous BOD, benthic processes, and photosynthesis and respiration. Dispersion effects on BOD and DO are discussed and then the total, simplified DO balance is presented. Dissolved oxygen standards and the linkage between these standards and habitat are presented. Finally, remedial methods to improve low DO concentrations are discussed.

The discussion of nutrient problems includes eutrophication, methemoglobinemia, and ammonia toxicity in addition to effects of nitrogen on DO previously discussed. Methods of nutrient control also are discussed. The types of waterborne and water contact diseases are discussed. Because it is impractical to sample for all the pathogens that causes these diseases the need for and types of indicator organisms then are discussed. Simulation of indicator bacteria levels is presented, and microbial risk assessment is presented as an alternative or complement to the use of indicator bacteria. Finally, disinfection methods are reviewed. The discussion of sediment contamination focuses on the assessment of the sediment toxicity and the remediation/cleanup methods applied to contaminated sediment. Throughout the chapter examples from around the world are given to illustrate the fundamental problems.

Key Words

Water quality management, Dissolved oxygen, Nutrients, Waterborne diseases, Water contact diseases, Sediment contamination

9.1 Water Quality and Pollution

The water quality problems of rivers throughout the world are extensive and complex, and it is difficult to comprehensively describe all the problems in a single chapter. Nevertheless, this chapter strives to provide a useful overview of key problems and management solutions. The discussion begins with the definition of pollution and then focuses on the causes and solutions for low dissolved oxygen. The chapter then discusses nutrient loads and related problems, such as eutrophication. Pathogens and public health then are discussed. Finally, toxic pollutants and contaminated sediment are discussed. For more information readers should consult the useful textbooks that comprehensively discuss water-quality modeling and management, such as Thomann and Mueller (1987), Chapra (1997), or Novotny (2003).

9.1.1 Water Quality

High water quality in rivers is necessary for public health and ecosystems. Masters (1991) reports that "Water dissolves more substances than any other common solvent. As a result, it serves as an effective medium for both transporting dissolved nutrients to tissues and organs in living things as well as eliminating their wastes. Water also transports dissolved substances throughout the biosphere."

The ability of water to easily carry away wastes has been exploited by humans for many centuries as the primary means of sanitation. However, as waste loads overwhelmed the ability of rivers and streams to carry away and/or assimilate wastes, public health and ecosystem viability deteriorated. These problems

began to gain major attention in urban areas in the 19th Century. As a result of building sewers (initially combined stormwater and sanitary flow systems and later separate sanitary and stormwater systems) without treatment, many urban rivers became heavily overloaded and gave off an obnoxious stench, which was caused by anoxic decomposition of sewage and garbage in streamwater and muds. For example, Novotny (2003, p. 6) reported that every summer from the 19th Century to the middle of the 20th Century, the stench from the Thames River in London became so unbearable that the British Parliament recessed during the affected periods. Industrial pollution also placed a heavy load on urban rivers. In the 1950s, flammable waste discharges from the greater Cleveland-Akron industrial area caused the Cayahoga River in Ohio, U.S. to catch on fire. Whereas the burning Cayahoga River gained national and international fame similar fires were frequent in other U.S. rivers in the 1950s and 1960s such as the Chicago Waterway System and the Rouge River near Detroit. Finally, the untreated wastewater led to substantial public health problems in many cities because of pathogens. For example, lack of sanitation contributed to more than 1800 deaths due to typhoid in Chicago in 1892 (Engineering Board of Review, 1925) and over 3,000 deaths due to cholera in Brussels in 1866 (Archives D'Architecture Moderne, 1997).

As shown in the previous examples between the mid-19th and mid-20th Centuries, water quality in major urban rivers throughout the world had deteriorated to such an extent that the public and governments in many areas had to take strong steps. For example, the stench of the Milwaukee River in Milwaukee, U.S. was so bad that in 1880 the city government authorized the building of two flushing tunnels by which clean Lake Michigan water was delivered to two discharge points on the river and its tributary upstream from the city. These flushing tunnels are still in use during periods when low dissolved oxygen is detected in the river. Novotny (2003, p. 11) reported that the City of London applied a comprehensive wastewater treatment program, and by 1970, the Thames River in London was alive again, and fish have been caught there since. Chicago reversed the direction of flow of the Chicago River away from Lake Michigan (its water supply source) and toward the Des Plaines River in the Mississippi River basin, which together with the Pasteurization of milk lead to the virtual elimination of deaths due to typhoid in Chicago. Brussels covered over the Zenne River to relieve its public health problems and provide space for new modern squares and boulevards in the center of the city (Archives D'Architecture Moderne, 1997).

In the latter part of the 20th Century problems resulting from non-point source pollution from agricultural areas also became more pervasive and apparent. Novotny (2003, p. 21) reported that the Black Sea, Adriatic Sea, Chesapeake Bay, and Gulf of Mexico are examples of large bodies affected by transboundary and/or global inputs of non-point source pollution. These bodies suffer from one common symptom—excessive inputs of nutrients from farming operations and cities located thousands of kilometers upstream and brought in by large tributary rivers. The result of the high nutrient loads has been excessive algal development in the upper zone of the water body and anoxic (lack of oxygen) conditions in the deeper zone. Novotny (2003, p. 21) reported that 53% of U.S. estuaries experience hypoxia (reduced oxygen levels) or anoxia for at least part of the year. The most famous example of hypoxia in the U.S. is the hypoxic zone in the Gulf of Mexico that can reach an area as large as 19,000 km^2. In China, the overabundance of nutrients has resulted in a rapid increase in the size and frequency of toxic red tides from less than 10 in the 1960s (see Fig. 1.36) to 453 from 2001 to 2005. The China Daily (February 13, 2006) reported that among the 453 red tides between 2001 and 2005, 132 covered more than 100 km^2 each and 33 covered more than 1000 km^2 each. Most of these red tides occurred in areas adjacent to the Yangtze River estuary and the marine area south of Zhejiang Province.

Whereas the individual solutions in London, Milwaukee, Chicago, Brussels, and other locations resulted in improved local water quality, by the late 20th Century it was clear water quality problems needed to be solved in a comprehensive manner. The water pollution problems discussed in the foregoing paragraphs and many others led national and international bodies to develop laws and regulations for

water quality management or pollution control such as the U.S. Federal Water Pollution Control Act of 1972 (PL92-500), commonly known as the Clean Water Act (CWA), and the European Water Framework Directive (WFD). Full enactment of and compliance with these laws can greatly improve water quality, but it is a long and expensive process. The National Research Council (2001b) reported that nearly 30 years after enactment of the CWA and after the expenditure of billions of dollars for construction of domestic and industrial wastewater treatment and other mitigation projects and billions more for operation of these projects "there are about 21,000 polluted river segments, lakes, and estuaries making up over 300,000 river and shore miles (480,000 km) and 5 million lake acres (2 million hectares)" [parts in italics added]. Thus, a country like China that is just beginning to deal with water quality management in its rivers must be prepared for long, but worthwhile struggle to obtain improved water quality in its rivers and receiving lakes, estuaries, and seas.

In China, the current quality of some rivers is quite poor. According to the "Bulletin of Water Resources of China" for 2004, among the 412 monitored points of the 7 main rivers in China, the proportions of the Grades Ⅰ–Ⅲ, Grades Ⅳ–Ⅴ, and worse than Grade Ⅴ waters are 41.8%, 30.3%, and 27.9%. Waters of Grades Ⅰ–Ⅲ are suitable for use as water supply, Grade Ⅳ waters are suitable for industrial water use and non-contact recreation areas, and Grade Ⅴ waters are only suitable for agricultural water use and landscaping requirements. Thus, water at nearly 30% of all monitored river locations in China is not suitable for any use (below grade Ⅴ), but in the developed areas the percentage less than Grade V is far worse (based on data from 2000): Liao River –37.3%, Hai He River –58.7%, Huai He River 47.4%, and rivers in southeastern China –53.5%. In 2000 the quality of water in the Yantze River was generally good with more than 80% of the samples in Grades Ⅰ–Ⅲ, but this is misleading. The 27 billion m^3 wastewater load comprises only about 3% of the massive flow of the Yangtze River (980 billion m^3). Thus, the pollution is diluted such that Grades Ⅰ–Ⅲ are met, but when the flow discharges to the East China Sea the massive nutrient load leads to the red tide problems previously discussed.

9.1.2 Pollution

In the 1970s the definition of pollution most accepted by scientists was "unreasonable interferences of water quality with the beneficial uses of the resources" (Novotny, 2003, p. 25). However, the perception of beneficial use was different to different people, which was a problem. Clark et al. (1977, p. 242) noted "Acceptable water quality is dependent upon the requirements of many kinds of water consumers. Characteristics that make water unsuitable to one user may be unimportant or even desirable for another." Most substances that are considered "pollutants" occur in nature and have some beneficial properties for the environment. For example, Fair et al. (1971, p. 638) noted that if pollution is kept within bounds it contributes to the fertility of the receiving water and resultant aquatic population.

From an economist's viewpoint, pollution is the least expensive way for producers and consumers to get rid of wastes (Braden, 1988). Excessive waste loads arise and "pollution" as defined by interference with beneficial uses occurs when the waste disposal capacity of the environment is provided free of charge (Solow, 1971) and when producers and consumers do not incorporate into their products, consumption, and behavior the cost of damage resulting from pollution. An economic externality occurs when those who produce or consume goods are separated from those who suffer or bear adverse consequences caused by pollution generated by the producers and consumers (Novotny, 2003, p. 52). Upstream pollution causing downstream water-quality problems is a classic case of an economic externality. For example, research done at the University of Illinois in the 1970s indicated that the sedimentation related costs of on farm erosion were eight to ten times greater on downstream reservoirs and channels than the cost of lost productivity on the farm because of erosion (Gunetermann et al., 1975). It should also be remembered that pollution also has other non-economic costs, such as declining life expectancy, lost working hours due to

illness, loss of soil fertility, and loss of water resources for drinking (Novotny, 2003, p.56). Therefore, Novotny (2003, p. 55) concluded:

"Without regulation or enforcement, producers have no incentive to include social cost in their reasoning and the product would appear cheaper because the costs of those who have to cope with the pollution impact are not considered. With the cost of damage imposed (by regulation and/or a tax on the product) on the producer, the cost of the product will be increased. The amount of taxation should theoretically equal the amount of damage or recovery cost to the society."

For the case of agricultural pollution, farmers generally do not have the financial resources to compensate for the pollution resulting from farming, and, thus, society provides them financial incentives to apply soil conservation and other pollution mitigation practices. For example, Beck and Jeffrey (2007) described "Green Taxes" that are levied on individual water consumers (one set of stakeholders), to pay for farmers (another set of stakeholders) not to use land in ways that pollute water. "Green Taxes" are collected by municipalities (yet another stakeholder), taken by the central government (another stakeholder)—and generally used for purposes other than water or the environment.

Currently, developed countries put a high value on the protection of the environment that supersedes any economic savings that might be achieved by allowing injurious discharges of pollutants. Section 101(a) of the CWA states: "The objective of the Act is to restore and maintain the chemical, physical, and biological integrity of the nation's waters." In recent years "ecological integrity" has been taken as "biological integrity," and ecological integrity of a water body implies the ability of its ecological system to support and maintain "a balanced, integrated, adaptive community of organisms having a species composition, diversity and functional organisms comparable to that of natural biota of the region" (Karr and Dudley, 1981). Some of the methods used to evaluate biological diversity are described in Section 10.4. Novotny (2003, p. 26) defines physical and chemical integrity as follows:

Physical integrity implies habitat conditions of the water body that would support a balanced biological community. Chemical integrity means a chemical composition of water and sediments that would not be injurious to the aquatic biota.

In the CWA the Congress also established the goal of ensuring "water quality which provides for the protection of fish, shellfish, and wildlife, and provides of recreation in and on the water" (Davis and Masten, 2004, p. 266), the so-called "fishable" and "swimmable" requirements.

In the CWA the term "pollution" means the human-made or human-induced alteration of the chemical, physical, biological, and radiological integrity of water. In this regulatory definition of pollution it is important to note that "pollution" is differentiated from changes in the quality of the environment resulting from natural causes such as natural erosion, weathering of rocks, and natural elutriation of minerals; natural processes occurring in water bodies and sediments; and as a result of natural disasters such as volcanic eruptions or deposition of fly ash from (natural) forest fires (Novotny, 2003, p. 27). The alteration of the integrity is measured by the antidegradation principle. Strictly speaking antidegradation means no action should bring about worsening of water quality in water bodies that presently meet environmental standards, even if the action may not result in water quality that would violate standards. Novotny (2003, p. 66) notes that this strict definition of the antidegradation principle can make future economic development very difficult, if not impossible. In practice downgrading the water quality (but not the designated use and ensuing standards) is possible under the antidegradation rule. The quantity of potential pollutants that can be discharged into the receiving water body without altering its integrity is called the Waste Assimilative Capacity (Novotny, 2003, p. 29).

The U.S. Environmental Protection Agency (1999c) lists pollutants as "dredged spoil, solid waste, incineration residue, sewage, garbage, sewage sludge, munitions, chemical wastes, biological materials, radioactive materials, heat, wrecked or discarded equipment, rock, sand, cellar dirt, and industrial, municipal

and agricultural waste discharged into water." Included also are drinking water contaminants regulated under the Safe Drinking Water Act. Further, under the definition of human-made or human-induced alteration of the integrity of water any human action or alteration of a receiving water body that impairs its integrity could be considered pollution. Under this definition, cutting down trees along rivers, which increases temperature and impairs the habitat, straightening of channels and channel linings, hydraulic modifications, and reducing low flows below tolerable levels by excessive withdrawals would be pollution (Novotny, 2003, p. 27). Despite this broad definition of "pollution" this chapter focuses on the following pollutants of concern:

- ➢ Suspended solids and their organic (volatile) content
- ➢ Biochemical Oxygen Demand (BOD)
- ➢ Chemical Oxygen Demand (COD)
- ➢ Pathogenic Microorganisms
- ➢ Nutrients (nitrogen and phosphorus)
- ➢ Toxic Compounds (both organic—PAHs & PCBs—and inorganic—metals and salts)
- ➢ Algae

Section 10.4 discusses stream restoration strategies that can be applied to remediate some of the habitat modification forms of "pollution."

9.2   Dissolved Oxygen

9.2.1   The Basic Dissolved Oxygen Problem

Dissolved oxygen (DO) is the primary constituent needed for healthy aquatic ecosystems. In nature, clean waters are saturated with dissolved oxygen, or nearly so (Fair et al., 1971, p. 642). As DO concentrations drop, fish and other aquatic life are threatened and, in the extreme case, killed. In addition, as DO concentrations fall, undesirable odors, tastes, and colors reduce the acceptability of the water as a domestic supply and reduce its attractiveness for recreational uses (Masters, 1991, p. 107). Thus, maintenance of adequate DO concentrations is the key to the CWA's "fishable" requirement for water bodies. However, because water contains only about 0.8% oxygen by volume at normal temperatures (10˚C) the aquatic environment is inherently and critically sensitive to the oxygen demands of the organisms that populate it (Fair et al., 1971, p. 643). Thus, maintenance of adequate DO concentrations is a challenging problem.

Fair et al. (1971) provide an excellent summary of the life cycle of a discharge of biodegradable organic waste and its effect on receiving rivers that is reproduced as follows:

(1) When a single, heavy charge of biodegradable organic waste is poured into a clean body of water, the water becomes turbid, sunlight is shut out of the depths, and green plants, which by photosynthesis remove carbon dioxide from the water and release oxygen die off.

(2) Scavenging organisms increase in number until they match the food supply. The intensity of their life is mirrored in the intensity of the biochemical oxygen demand (BOD).

(3) The oxygen resources of the water are drawn upon heavily. In overloaded receiving waters the supply of oxygen may become exhausted. Further, Masters (1991, p. 127) noted in extreme cases, when anaerobic (without oxygen) conditions exist, most higher forms of life are killed or driven off, and noxious conditions including floating sludges, bubbling, odorous gases, black water, and slimy fungal growths, prevail.

(4) Nitrogen, carbon, sulfur, phosphorus, and other important nutritional elements run through their natural cycles, and sequences of microbic populations break down ① the waste matters that have been added, ② the natural polluting substances already within or otherwise entering the water, and ③ the food made available by the destruction of green plants and other organisms intolerant to pollution.

(5) Depending on the flow velocity of the receiving water, suspended matter is carried along or removed to the bottom by sedimentation. Bottom (benthic) deposits are laid down in thickness varying from a thin pollution carpet to heavy sludge banks.

(6) The decomposition of the bottom deposits differs from that in the supernatant waters. In the presence of oxygen dissolved in the overlying waters, benthic decomposition varies with depth of deposit from largely aerobic to largely anaerobic.

(7) In the course of time and distance, the energy values of the single charge of biodegradable organic waste are used up.

(8) The BOD is decreased, and the rate of absorption of oxygen from the atmosphere, which at first lagged behind the rate of oxygen utilization, falls into step with it and eventually outruns it.

(9) The water becomes clear. Green plants flourish in the sunlight and release oxygen to the water during photosynthesis.

(10) Other higher aquatic organisms, including game fish, which are notably sensitive to pollution, reappear and thrive in a balanced equilibrium.

(11) The waters have returned to normal purity. Self-purification is gradually completed.

Figure 9.1 shows the oxygen sag downstream of a waste discharge and its effects on the aquatic community. The natural purification of polluted waters described by Fair et al. (1971) and shown in Fig. 9.1 is never fast, and heavily polluted streams may traverse long distances during many days of flow before a significant degree of purification is accomplished.

The consumption of biodegradable organic matter is done by microorganisms, primarily bacteria, which break the matter down into simpler organic and inorganic substances. When this decomposition takes place in an aerobic environment, the process produces non-objectionable, stable end products such as carbon dioxide (CO_2), sulfate (SO_4), orthophosphate (PO_4), and nitrate (NO_3). When insufficient oxygen is available, the resulting anaerobic decomposition is performed by completely different microorganisms. They produce end products that can be highly objectionable, including hydrogen sulfide (H_2S), ammonia (NH_3), and methane (CH_4) (Masters, 1991).

Clean Zone	Decomposition Zone	Septic Zone	Recovery Zone	Clean Zone
Trout, perch, bass; mayfly, stonefly, and caddisfly larvae	Carp; blackfly and midge larvae	Fish absent; sludge worms; midge and mosquito larvae	Carp; blackfly and midge larvae	Trout, perch, bass; mayfly, stonefly, and caddisfly larvae
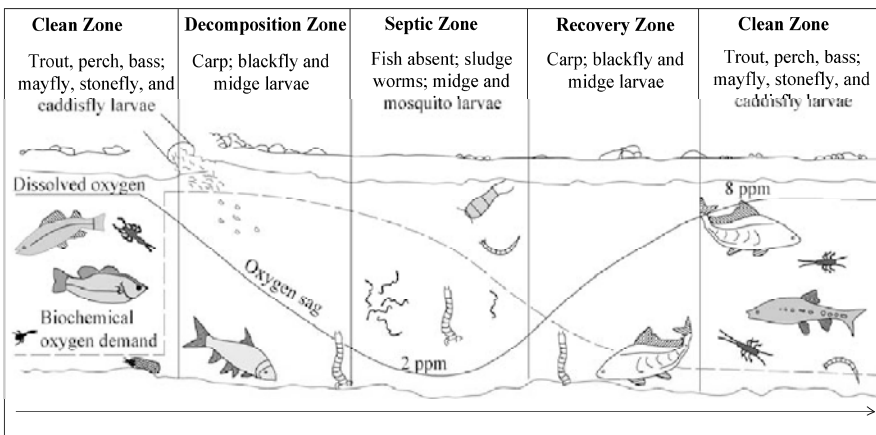
Fig. 9.1 Dissolved oxygen sag downstream from a source of biodegradable organic waste and its effect on stream biota (Davis and Masten, 2004)

Oxygen demand is exerted by three classes of matter: carbonaceous material, oxidizable nitrogen, and certain chemical reducing compounds. Clark et al. (1977) simply describes the oxygen demand process as

$$\text{waste organics} + \text{DO} \xrightarrow{\text{microorganisms}} CO_2 + \text{new cell growth}$$
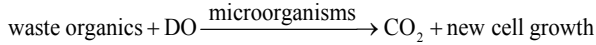
This relation is an oversimplification of the extremely complex biochemical reactions which take place. In the following subsections simple first-order and zero-order kinetics models describing the oxygen demand, stream reaeration, and photosynthesis processes are presented. These models are of the form of the Streeter-Phelps (1925) model and its modifications and extensions (O'Connor, 1967; Thomann, 1972). More complex and theoretically correct models are available, as described in books, such as Thomann and Mueller (1987), Chapra (1997), and Di Toro (2001), and are used in water-quality models, such as QUAL2E (Brown and Barnwell, 1987) and WASP (Ambrose et al., 1988). However, the extended Streeter-Phelps type models are presented here because they simply illustrate the overall DO balance for a river, can still be used for some DO analyses, and the concepts often are included in the fundamentally more complex models.

9.2.2 Streeter and Phelps Model

In streams, the interplay between deoxygenation resulting from the consumption of biodegradable organic wastes and reaeration produces a dissolved oxygen profile called the oxygen sag (Fig. 9.2). Streeter and Phelps (1925) approximated both the deoxygenation (related to the consumption of BOD) and reaeration processes as first-order processes.

Biochemical Oxygen Demand (BOD)—The first-order process describing the reduction of BOD concentration along a flowing stream has the following form:

$$L_x = L_0 e^{-(K_{11}/u)x} = L_0 e^{-K_{11}t} \tag{9.1}$$

where L_x = the BOD concentration at point x in milligrams per liter, L_0 = the initial BOD concentration at $x = 0$ in milligrams per liter, $t = x/u$ = travel time to point x in days, $K_{11} = K_1 + K_3$ = rate of BOD removal in 1/day, K_1 = the deoxygenation rate (i.e. rate of removal of BOD due to oxidation), also referred to as K_d in the literature, in 1/day, K_3 = rate of BOD lost due to sedimentation in 1/day, and u = average streamflow velocity in the reach in kilometers per day.

The distance x is measured in kilometers from the upstream end of the reach, typically a point of waste discharge. Streeter and Phelps (1925) assumed the rate of sedimentation was negligible, thus, the reduction in BOD along a flowing stream has the form:

$$L_x = L_0 e^{-K_d t} \tag{9.2}$$

which is directly related to the deoxygenation of the stream. This form is used for the purposes of illustration in this chapter.

As noted earlier both carbonaceous material and oxidizable nitrogen exert an oxygen demand and, thus, are part of BOD. The growth of nitrifying bacteria lags behind the growth of microorganisms which perform the carbonaceous reaction (Clark et al., 1977, p. 289). Further, Davis and Masten (2004, p. 281) note that few of the nitrifying organisms occur in untreated sewage, but the concentration in well treated effluent is high. Thus, at the time the Streeter-Phelps equations were developed most sewage was untreated and carbonaceous BOD (CBOD) dominated the BOD-DO relation, whereas today in the U.S. and other developed countries most effluent is well treated and both CBOD and nitrogeneous BOD (NBOD) are important. This section focuses on CBOD and the next section focuses on NBOD.

BOD is the amount of molecular oxygen required to stabilize the biodegradable organic (carbon or nitrogen) waste present in a water body by aerobic biochemical action. BOD and CBOD often are measured using a 5-day test resulting in the 5-day BOD or CBOD (BOD_5 and $CBOD_5$). The 5-day BOD was chosen as the standard value for most purposes because the test was devised by sanitary engineers in England, where the River Thames has a travel time to the sea of less than 5 days, so there was no need to consider oxygen
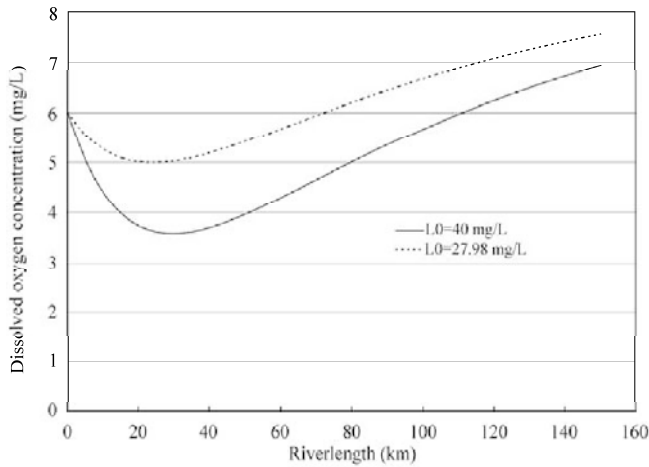
Fig. 9.2 Dissolved oxygen-sag curves for initial and allowable carbonaceous biochemical oxygen demand loadings for the Streeter-Phelps example problem

demand at longer times (Davis and Masten, 2004, p. 280). When measuring CBOD, chemicals are added to the sample to inhibit the nitrification process. Many water-quality models require information on the ultimate CBOD ($CBOD_U$), which may be computed from the $CBOD_5$ by reworking Eq. (9.2) as follows:

$$CBOD_U = CBOD_5 / (1 - e^{-5K_d})$$ (9.3)

where both $CBOD_5$ and $CBOD_U$ are in milligrams per liter. James (1993, pp. 123–126) shows that estimates of $CBOD_U$ and K_d derived from CBOD measurements over just 5 days may yield very poor results. He presented an example for which 59 measurements of CBOD were made over a 20 day period. The best nonlinear fit to these data yielded $CBOD_U$ = 10,100 mg/L and K_d = 0.217 d^{-1}. However, if just the 30 measurements from the first 5 days were used, $CBOD_U$-K_d pairs of 15,000 mg/L and 0.13 d^{-1} and 8,000 mg/L and 0.30 d^{-1} yielded nearly equal results as for the best fit to the full 20 days of data. Thus, James (1993, p. 123) recommended that some CBOD measurements at 15–20 days are needed to properly define $CBOD_U$ and K_d. Following this recommendation in the modeling of Salt Creek in the western suburbs of Chicago, U.S., CBOD was measured over a 21-day period and a linear regression was fit between time and the logarithms of oxygen demand to estimate $CBOD_U$ and K_d (Melching and Chang, 1996).

A related parameter to BOD is chemical oxygen demand (COD), which is the amount of oxygen needed to chemically oxidize wastes. The COD test is much quicker and less expensive than a BOD test, taking only a matter of hours. In a COD test, a strong chemical oxidizing agent is used to oxidize the organics rather than relying on microorganisms to do the job. Thus, because of its ease and cost many agencies measure COD rather than BOD. However, it does not distinguish between oxygen demand that will actually be felt in the environment due to biodegradation, and the chemical oxidation of inert matter (Masters, 1991, p. 126). Thus, the measured value of COD is higher than BOD, though Masters (1991, p. 126) speculates that for easily biodegradable matter the two will be quite similar. However, in the modeling of water quality in the Zenne River in Brussels, Belgium, Demuynck and Bauwens (1996) divided the COD concentrations measured in the combined sewer system of Brussels by Wollast et al. (1992) by 2.5 to compute the CBOD loads to the river. In general, the relation between COD and CBOD varies by location and type of water (sanitary sewage, treatment plant effluent, in-stream flow, etc.). Thus, if COD data are to be used as a surrogate for CBOD data in water quality modeling or analysis, some local CBOD data are necessary to properly convert COD to an equivalent value of CBOD for the given location and type of water.

Reaeration and dissolved oxygen deficit—A first-order process also is used to describe the reduction of DO deficit, D_x, along a flowing stream. The DO deficit is the difference between the saturated DO concentration, C_s, and the actual DO concentration at point x, C_x, or at travel time point, C_t. The saturation concentration of DO is a function of temperature, salinity, and barometric pressure. The effects of chlorides usually become significant only in estuarine and oceanic systems, whereas in freshwater systems, DO saturation is primarily dependent on water temperature (Thomann, 1972, p. 101). This dependence on temperature is given with sufficient accuracy by the following empirical nonlinear equation:

$$C_s = 14.652 - 0.41022T + 0.0079991T^2 - 0.000077774T^3 \tag{9.4}$$

where T is water temperature in degrees Celsius.

The reaeration and deoxygenation processes are coupled such that the deoxygenation process seeks to increase the DO deficit while the reaeration process seeks to decrease it. The resulting equation for the DO deficit derived by Streeter and Phelps (1925) is

$$D_t = \frac{L_0 K_d}{K_a - K_d}\left(e^{-K_d t} - e^{-K_a t}\right) + D_0 e^{-K_a t} \tag{9.5}$$

where K_a = the reaeration-rate coefficient in 1/day, and

D_0 = the initial dissolved oxygen deficit at $x = 0/t = 0$, in milligrams per liter.

The DO concentration at travel time point, t, may be computed as follows:

$$C_t = C_s - D_t \tag{9.6}$$

If the result of the calculation from Eq. (9.6) yields a negative DO concentration, it should be reported as zero because concentration values cannot be less than zero.

Equation (9.5) is applied to a reach of the river that has a single upstream inflow representing either the upstream flow of the main channel or a weighted average of the main channel flow and constituent concentrations and those of a single point source input (tributary stream or wastewater effluent). If several point sources are close together, they can be aggregated into a single point source. When moving downstream in the computations, when a new point source input is reached, a new mass balance must be computed to determine L_0 and D_0 for the new reach downstream from the new point source and Eqs. 9.2 and 9.5 are applied to the new reach. This is repeated until the end of river being studied is reached. A reach should be homogeneous in its physical conditions including channel shape, bottom composition, slope, and so on. New reaches can be defined because of changes in physical conditions of the river, and the downstream concentrations for the upstream reach become L_0 and D_0 for the downstream reach.

Several alternative formulations for the DO deficit are available in the literature.   One of the most useful relates the DO deficit, to the self-purification ratio, f, as follows:

$$D_t = \frac{L_0}{f-1}e^{-K_d t}\left[1 - e^{-(f-1)K_d t}\left(1-(f-1)\frac{D_0}{L_0}\right)\right] \tag{9.7}$$

where $f = K_a / K_d$. The minimum point in the oxygen sag curve (see Fig. 9.2) can be determined by setting the derivative of the DO deficit with respect to time equal to zero, i.e.

$$\frac{dD_t}{dt} = 0$$

and solving for the critical time, t_C. Doing this the following equation is obtained:

$$t_C = \frac{1}{(f-1)K_d}\ln\left[f\left(1-(f-1)\frac{D_0}{L_0}\right)\right] \tag{9.8}$$

The critical DO deficit, D_C, can then be computed using the following equation:

$$D_C = \frac{L_0}{f} e^{-K_d t_C} = \frac{L_0}{f \left\{ f \left[1 - (f-1)(D_0/L_0) \right] \right\}^{1/(f-1)}}$$

(9.9)

If Eq. 9.9 is reworked, the allowable upstream CBOD concentration, L_0^*, needed to keep the critical deficit below a specified value, i.e. the difference between C_s and the DO concentration standard, can be determined as follows:

$$L_0^* = D_C f \left\{ f \left[1 - (f-1)(D_0/L_0^*) \right] \right\}^{1/(f-1)}$$

(9.10)

Knowing the allowable upstream CBOD concentration, the allowable effluent discharge CBOD concentration can be determined by mass balance of flows upstream and downstream of the effluent discharge point. That is, L_0 is computed as follows:

$$L_0 = \frac{C_u Q_u + C_e Q_e}{Q_u + Q_e}$$

(9.11)

where C_u = the CBOD concentration in flow upstream of the effluent discharge point, $x = 0$, in milligrams per liter, C_e = the CBOD concentration in the wastewater treatment plant effluent in milligrams per liter, Q_u = flow discharge upstream of the effluent discharge point in cubic meters per second, and Q_e = wastewater treatment plant effluent discharge in cubic meters per second.

Reworking Eq. (9.11) the allowable CBOD concentration, C_e^*, in the effluent discharge may be computed as follows:

$$C_e^* = \frac{L_0^*(Q_u + Q_e) - C_u Q_u}{Q_e}$$

(9.12)

Streeter-phelps example—A stream has a reaeration-rate coefficient of 2.76 d^{-1} (representative of the 25th percentile of the U.S. Geological Survey (USGS) national reaeration-rate coefficient database (Melching and Flores, 1999)) and a deoxygenation rate of 0.5 d^{-1} (representative of raw sewage, see Table 9.1). The water temperature is 20℃. The initial oxygen deficit is 3 mg/L. Find (1) the DO deficit 48 hours later and the value of the critical time and critical deficit for an initial CBOD concentration of 40 mg/L, and (2) the allowable loading if a minimum DO concentration of 5 mg/L is required. If the mean stream velocity is 0.6 m/s, plot the DO sag curve versus distance along the stream.

Solution: In this example, the self-purification ratio form of the oxygen-sag curve (Eq. (9.7)) is used. The self-purification ratio, $f = K_a / K_d = 2.76\ d^{-1} / 0.5\ d^{-1} = 5.52$. Entering the appropriate values to Eq. (9.7) yields:

$$D_t = \frac{40\ \text{mg}/\text{L}}{5.52 - 1} e^{-0.5t} \left[1 - e^{-(5.52-1)0.5t} \left(1 - (5.52-1) \frac{3\ \text{mg}/\text{L}}{40\ \text{mg}/\text{L}} \right) \right]$$

which yields:

$$D_t = (8.85\ \text{mg}/\text{L})\, e^{-0.5t} (1 - 0.661\, e^{-2.26t})$$

For $t = 2$ days, $D_t = (8.85\ \text{mg}/\text{L})\, e^{-0.5 \times 2} (1 - 0.661 e^{-2.26 \times 2}) = 3.23\ \text{mg}/\text{L}$. For water with a temperature of 20℃, Eq. 9.4 yields the DO saturation concentration as 9.022 mg/L. Assuming a stream flow velocity of 0.6 m/s and using the above equation and Eq. (9.6), the oxygen-sag curve for the example problem was computed and is shown in Fig. 9.2.

The critical time is computed by entering the appropriate values into Eq. (9.8) as follows:

$$t_C = \frac{1}{(5.52-1)(0.5\ d^{-1})} \ln \left[5.52 \left(1 - (5.52-1) \frac{3\ \text{mg}/\text{L}}{40\ \text{mg}/\text{L}} \right) \right] = 0.573\ \text{days}$$

The critical deficit is computed by entering the appropriate values into Eq. (9.9) as follows:

$$D_C = \frac{40 \text{ mg} / \text{L}}{5.52} e^{-0.5(0.573)} = 5.44 \text{ mg} / \text{L}$$

For a minimum allowable DO concentration of 5 mg/L and a DO saturation concentration of 9.022 mg/L, the allowable DO deficit is 4.022 mg/L. The allowable upstream CBOD concentration then can be determined by entering the appropriate values into Eq. 9.10 yielding

$$L_0^* = (4.022)(5.52)\left\{5.52\left[1 - (5.52 - 1)(3 / L_0^*)\right]\right\}^{1/(5.52-1)}$$

$$L_0^* = 22.2\left\{5.52\left[1 - (13.56 / L_0^*)\right]\right\}^{0.2212}$$

Solving this equation by iteration yields $L_0^* = 27.98$ mg/L. The oxygen-sag curve for this case was also computed and is shown in Fig. 9.2.

Determination of the deoxygenation-rate coefficient, K_d—The value of K_d depends on a number of factors including the nature of the waste (some, such as simple sugars and starches, degrade easier than others, like cellulose), the ability of the available microorganisms to degrade the wastes in question (it may take some time for a healthy population of organisms to be able to thrive on the particular waste in the river), and the temperature (Masters, 1991, p. 126). This relation for K_d can be expressed as follows

$K_d = f$(nature of the waste, ability of organisms in the system to use the waste, temperature)

The effect of the nature of the waste is summarized in Table 9.1. The decrease in K_d from raw sewage to well-treated sewage and polluted river water probably results from differences in the ease of oxidation of the materials present, the rate decreasing as more easily oxidized substances are used up (Fair et al., 1971, p. 645).

Table 9.1 Typical Values for the Deoxygenation-Rate Coefficient (after Davis and Masten, 2004)

Sample	K_d at 20℃ (day^{-1})
Raw sewage	0.35–0.70
Well-treated sewage	0.12–0.23
Polluted river water	0.12–0.23

As shown in Table 9.1, the value of K_d usually is reported for a standard temperature of 20℃ and then adjusted to other temperatures as follows:

$$(K_d)_T = (K_d)_{20} \times 1.047^{(T-20)} \tag{9.13}$$

where T is the temperature of interest. However, Fair et al. (1971, p. 645) note that above 30℃ a decrease in rate with increasing temperature is observed, probably because of thermal inactivation of the enzymes responsible for oxidation of CBOD.

The value of K_d for use in river modeling and analysis may be determined by calibration of Eq. (9.1) or (9.2) using measured values of CBOD at several locations along the river of interest, and properly accounting for the settling of CBOD (which is easier said than done). It is generally assumed that the demands made on the oxygen resources of polluted waters by living organisms are the same as those observed in the laboratory when samples are mixed with convenient amounts of synthetic dilution water and incubated for the CBOD tests, so-called "bottle" estimates of K_d. Fair et al. (1971, p. 646) reported for large and passive streams, the correlation between ① laboratory observations of the BOD of polluted waters and ② field investigations of the reaction of such streams to pollution is usually high. Wright and McDonnell's (1979) study of measured in-stream values of K_d for 23 river systems primarily in the

eastern U.S. and one laboratory flume involving 72 K_d measurements confirmed this as they concluded "for a wide range of flow regimes, so-called "bottle" estimates of K_d adequately reflect corresponding rates that can be expected in receiving waters."

Masters (1991) reports that for turbulent, shallow, rapidly moving streams, the use of the bottle estimate of K_d is less valid because such streams have K_d values that can be significantly higher than the values determined in the laboratory. For example, Hamdy and Jatinder (1972) reported that the value of K_d under continuous mixing conditions is more than 10 times the value of K_d obtained under stagnant conditions. Finally, Wright and McDonnell (1979) reported that for shallow, low flow streams K_d falls consistently in the range 2.5 to 3.5 d^{-1} reflecting the turbulence in such mountain streams of the eastern U.S. (values as high as 4.24 d^{-1} are included in their database). Thus, if working in streams where turbulent flows are likely, field calibration of K_d based on in-stream CBOD measurements should be done.

Determination of the reaeration-rate coefficient, K_a—Reaeration is the physical absorption of oxygen from the atmosphere by water. It is the most important natural means by which rivers affected by waste inputs may recover DO. The reaeration-rate coefficient, K_a, typically is the dominant parameter affecting the uncertainty in the simulation of DO concentrations in streams (Brown and Barnwell, 1987; Melching and Yoon, 1996). Because the value of K_a can substantially affect waste load allocations derived with computer models, the value of K_a utilized in simulation models must be carefully determined.

The value of K_a can be measured accurately utilizing tracer-gas methods (Kilpatrick et al. 1989) and field measurement of K_a is strongly encouraged for reliable waste-load allocation (Melching and Flores, 1999). Extensive field measurements of K_a are, however, rarely done for waste-load allocation studies. K_a values typically are determined using one of three approaches for waste-load allocation studies.

(1) The concentrations of all key constituents in the river system are measured for a representative low-flow period, a simulation model is calibrated for this period, and the K_a estimation equation from the literature that results in the best fit to the data is used [e.g., New Jersey Department of Environmental Protection (1987)].

(2) A limited number of K_a values are measured for the river system in question utilizing the tracer-gas method, and the best K_a estimation equation from the literature for this river system is determined on the basis of these measurements [e.g., Schmidt and Stamer (1987)]. The example presented by St. John et al. (1984) illustrates an extrapolation problem with approach 2. St. John et al. (1984) applied 9 commonly used K_a estimation equations (listed in Table 9.2) to a hypothetical river for which the slope was 0.000985 and

Table 9.2 Summary of commonly used estimation equations for the reaeration-rate coefficient that were applied in the example of St. John et al. (1984)

Classification	Reference	Estimation equation
Velocity-depth	O'Connor and Dobbins (1958)	$K_a = 3.93 V^{0.5} / D^{1.5}$
	Owens et al. (1964)	$K_a = 5.32 V^{0.67} / D^{1.85}$
	Langbein and Durum (1967)	$K_a = 5.135 V / D^{1.33}$
	Churchill et al. (1962)	$K_a = 5.05 V^{0.97} / D^{1.67}$
	Bennett and Rathbun (1972) II	$K_a = 5.20 V^{0.61} / D^{1.69}$
Energy Dissipation	Tsivoglou and Neal (1976)	$K_a = 15,244 SV$
	Shindala and Truax (1980)	$K_a = 16,976 SV$
Others	Thackston and Krenkel (1969)	$K_a = 24.94(1 + F^{0.5}) u^* / D$
	Bennett and Rathbun (1972) I	$K_a = 32.47 V^{0.413} S^{0.273} / D^{1.408}$

Note: V = reach average velocity in meters per second, D = reach average depth in meters, S = energy slope for the reach in meter per meter, F = the Froude number = $V/(gD)^{0.5}$, g = the acceleration of gravity, u^* = the shear velocity = $(gRS)^{0.5}$, and R = the hydraulic radius, which approximately equals the reach average depth for a wide channel (assumed in computing Fig. 9.3)

the velocity, V, in meters per second and depth, D, in meters were given as functions of discharge, Q, in cubic meters per second as follows:

$$V = 0.05977Q^{0.5} \quad \text{and} \quad D = 0.6024Q^{0.4}$$

Figure 9.3 shows the values of K_a estimated for this river for a range of flows. If, for a discharge of 2.8 m³/s, the measured value of K_a was 1.45 d⁻¹, the O'Connor and Dobbins (1958), Owens et al. (1964), Bennett and Rathbun (1972), Tsivoglou and Neal (1976), and Shindala and Traux (1980) equations all would offer a good match to the measured value. However, if the design flow for waste-load allocation was 0.5 m³/s, the "good match" equations would estimate K_a values ranging from 0.6 to 3.2 d⁻¹. Thus, the waste-load allocation could be drastically different using different "good match" equations.
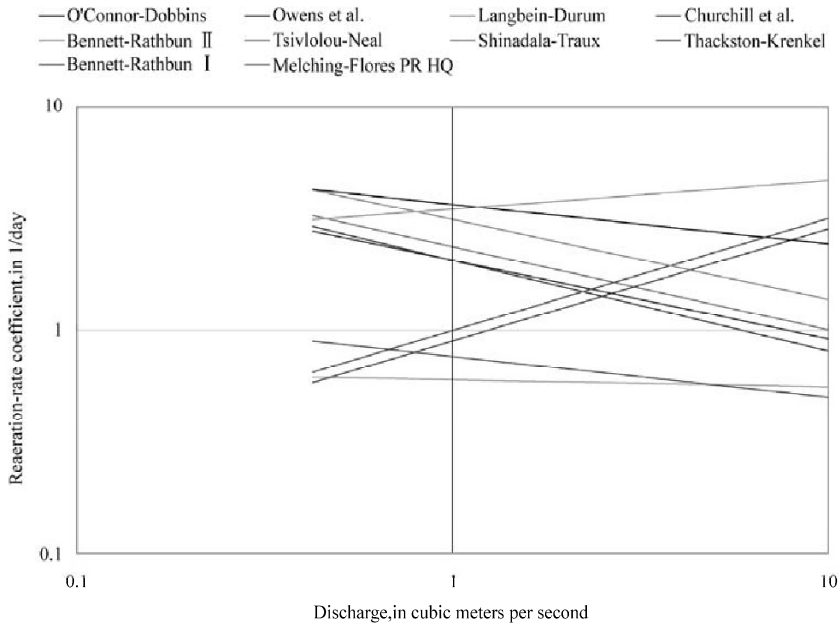
Fig. 9.3 Reaeration-rate coefficient values as a function of discharge computed using different estimation equations for the hypothetical river of St. John et al. (1984)

3) A set of K_a measurements is made for a group of rivers representative of a region or state, and these measurements are used to derive K_a estimation equations specific to that region or state, e.g., Cleveland (1989) for Texas and Hren (1984) for Ohio.

Generally, equations for estimation of K_a on the basis of stream hydraulic conditions are needed because either K_a measurements are not made or the low-flow conditions for which measurements are available may be substantially different from the low-flow conditions that must be considered for waste-load allocation. These equations provide a rational basis for estimation of K_a for unmeasured low flows. Furthermore, water-quality management often is done on the basis of continuous simulation of long periods—months or years—[e.g., Demuynck et al. (1997); Melching et al. (2004)]. In such cases, equations are needed to relate K_a to changing streamflow conditions throughout the year.

Reaeration varies with surface exposure and volume of water and the rate at which water is mixed by vertical and horizontal currents that distribute absorbed oxygen and bring fresh volumes of unsaturated water into contact with the atmosphere (Fair et al., 1971, p. 651). Considering the foregoing physical

concepts many researchers have developed equations for estimation of K_a. More than 30 equations are available in the literature for K_a estimation on the basis of stream hydraulic characteristics. Twenty nine of these equations and the data used to derive them are summarized in Flores (1998). Efforts in the literature to compare the various equations available prior to 1999, including the commonly used equations listed in Table 9.2, have identified the following problems with the equations:

(1) Most of the K_a estimation equations in the literature were derived from relatively small sets of laboratory or field data for a relatively localized group of steams. Wilson and Macleod (1974) applied 16 K_a estimation equations (eight empirical equations using flow velocity and depth and eight equations including an energy-dissipation term) to estimate K_a values for a large number of field and laboratory measurements (482 measurements for the velocity-depth equations and 382 measurements for the energy-dissipation equations). They found that each equation yielded accurate results for the data for which the equation was originally developed and yielded very poor results for almost all other data.

(2) Most of the K_a estimation equations in the literature developed using field data were derived from K_a measurements obtained by the DO-balance or disturbed-equilibrium methods. Considering the errors in measuring the various components of the DO-balance and disturbed-equilibrium methods, Bennett and Rathbun (1972) estimated that the expected relative standard error of these methods are 65 and 115%, respectively. Thus, the data on which these equations are based include potentially substantial errors. Gas-tracer methods have been reported to have accuracies on the order of 10% to 25% (Tsivoglou et al., 1968; Rathbun and Grant, 1978; Grant and Skavroneck, 1980; Melching, 1998). However, relatively few of the equations in the literature prior to 1999 were derived from gas-tracer data [e.g., Tsivoglou and Wallace (1972), Tsivoglou and Neal, (1976), Hren (1984), Parker and Gay (1987), Cleveland (1989), and Parker and DeSimone (1992)].

(3) The K_a values measured in the laboratory are accurate, but it is uncertain how well laboratory conditions reflect reaeration in the field.

In an effort to better understand the reaeration process and reaeration-rate coefficient the USGS complied a national database of K_a values measured throughout the U.S. by the USGS using gas-tracer methods. Through 1996 the USGS had completed nearly 50 studies in cooperation with state, county, city, and regional agencies that involved the in-stream measurement of K_a utilizing gas-tracer methods. In these studies, K_a values were measured for a total of 493 independent reaches on 166 streams in 23 states. The term independent reach refers to reaches that either are distinctly different in space along the stream or multiple measurements at the same locations but for different flow conditions. The compilation of measured K_a values also included the compilation of important stream hydraulic characteristics S, V (determined from reach length and measured travel time), D [$= Q/(VW)$], discharge (Q), and reach average top width (W), and also a classification of the flow regime in the reach as "pool and riffle" or "channel control." Channel control refers to prismatic streams with relatively uniform flow properties.

Comparison of the K_a estimation equations from the literature to the USGS K_a database yields very poor results, as would be expected from the foregoing discussion of the problems with these equations. For example, Gualtieri et al. (2000) showed that over the range of conditions used to derive the O'Connor and Dobbins equation, the estimated K_a values were, on average, one half the values measured by the USGS. Therefore, this chapter presents the K_a estimation equations derived by Melching and Flores (1999) on the basis of the USGS database as the best general-use equations available (i.e. region- or state-specific equations could be superior to the USGS national equations for use in that region or state).

The advantage of a large database is that data can be screened for quality and grouped into hydraulically relevant classes and the available data in each class still is sufficient to develop reliable equations. Kilpatrick et al. (1989) state that a low value of the product of the gas-transfer rate (K_T) and the measurement reach travel time, T_t, indicates that the gas desorption time between sampling sections

on a reach is insufficient for accurate measurement of the amount of desorption in the reach, and so the computed value of K_a may be inaccurate. Melching and Flores omitted all measurements for which $K_T T_t \leqslant 0.3$ from the analysis, essentially eliminating all K_T measurements with possible errors $\geqslant 33.3\%$. Using this criterion and other screening the number of data considered were reduced from 493 to 371 measured values of K_a.

The data then were subdivided into pool and riffle streams and channel control streams. Finally, nearly all the K_a measurements were made for low flow conditions on the respective rivers, thus, discharge was used a factor of scale to separate small and larger rivers. A flow of 0.556 m³/s was used as was done by Tsivoglou and Neal (1976). The following are the best-estimation equations for each subgroup (where K_a is in 1/day and all other variables are in metric units):

(1) Pool and riffle streams, low flow ($Q < 0.556$ m³/s) derived from 99 K_a measurements

$$K_a = 517(VS)^{0.524} / Q^{0.242} \tag{9.14}$$

(2) Pool and riffle streams, high flow ($Q > 0.556$ m³/s) derived from 130 K_a measurements

$$K_a = 596(VS)^{0.528} / Q^{0.136} \tag{9.15}$$

(3) Channel-control streams, low flow ($Q < 0.556$ m³/s) derived from 77 K_a measurements

$$K_a = 88(VS)^{0.313} / D^{0.353} \tag{9.16}$$

(4) Channel-control streams, high flow ($Q > 0.556$ m³/s) derived from 65 K_a measurements

$$K_a = 142(VS)^{0.333} /(D^{0.66} W^{0.243}) \tag{9.17}$$

A statistical summary of the quality of fit of these equations including the multiple correlation coefficient, the standard error of estimate of logarithms, and the coefficient of variation of the log transformed equations is listed in Table 9.3. If the estimated value of K_a obtained from the appropriate equation is considered the expected value of K_a for the streamflow conditions, the coefficient of variation gives the standard error of estimate in fractional terms. Thus, Eqs. (9.14)–(9.17) constitute overall best-estimation equations with estimation errors ranging between 44% and 61%. Scattergrams illustrating the overall fit quality of Eqs. (9.14) and (9.15) for pool and riffle streams and Eqs. (9.16) and (9.17) for channel control streams are shown in Figs. 9.4 and 9.5, respectively. For comparison Eq. (9.15) also was applied to the hypothetical stream of St. John et al. (1984) and the results are included in Fig. 9.3. In general, Eq. (9.15) yields higher K_a values than the other equations reflecting the higher reaeration in pool and riffle streams.

It is interesting that the empirical process of multiple linear regression resulted in best-fit estimation equations with an energy-dissipation form [i.e. Tsivolglou and Wallace (1972) reported that VS is a measure of energy dissipation in the reach]. Thus, based on a large data set for a wide variety of streams and flow conditions, it appears that a strong relation exists between energy dissipation and K_a. Further, from a conceptual viewpoint, the form of the fitted equations seems to indicate that the relation between the rate of energy dissipation and the reaeration-rate coefficient is regulated by stream scale. For channel-control

Table 9.3 Fit and verification statistics for K_a estimation equations developed from the U.S. Geological Survey database

Equation	Correlation coefficient	Standard error of logarithms	Coefficient of variation
Pool and riffle, Q < 0.556 m³/s	0.835	0.244	0.610
Pool and riffle, Q > 0.556 m³/s	0.900	0.183	0.441
Channel control, Q < 0.556 m³/s	0.690	0.238	0.591
Channel control, Q > 0.556 m³/s	0.845	0.241	0.601
Overall verification	0.900	0.300	0.782
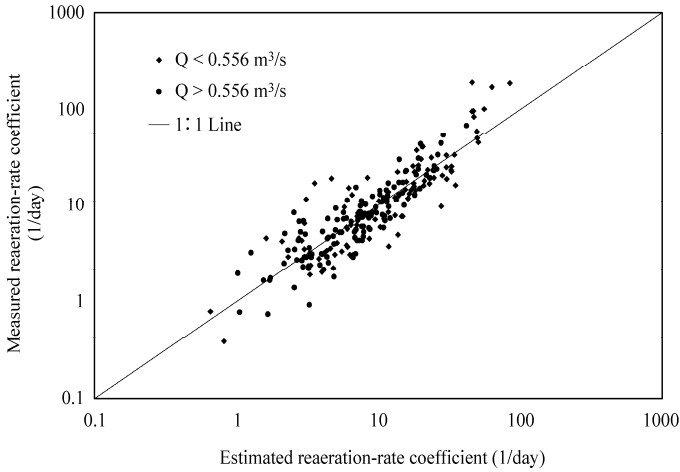
Fig. 9.4 Reaeration-rate coefficients measured and estimated with equations developed from multiple linear regression for pool and riffle streams in the USGS database (after Melching and Flores, 1999)
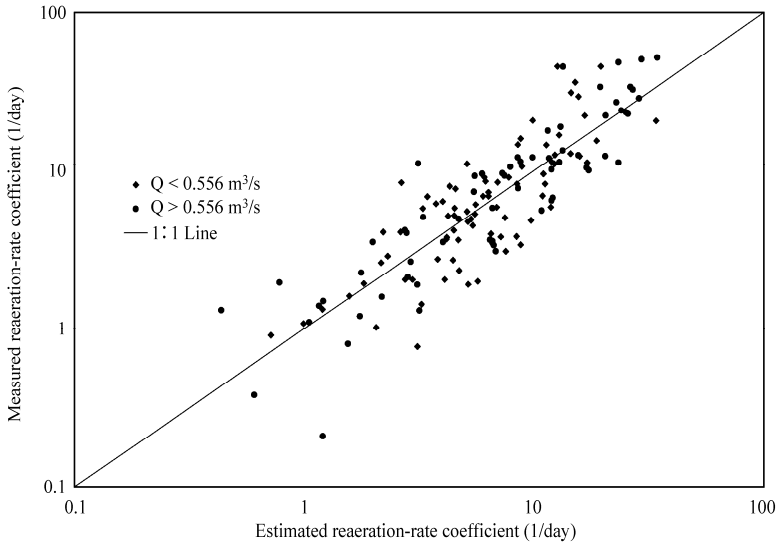
Fig. 9.5 Reaeration-rate coefficients measured and estimated with equations developed from multiple linear regression for channel control streams in the USGS database (after Melching and Flores, 1999)

conditions, the mean stream width and depth adequately describe stream scale, whereas for pool and riffle conditions, the mean stream width and depth are difficult to determine and, thus, discharge serves as a surrogate for stream scale.

For equation verification, a data set of K_a measurements made with tracer-gas procedures by other agencies was compiled from the literature. This compilation included 127 reaches on at least 24 rivers in at least 7 states. The streamflow regime was identified as pool and riffle for only about 30 reaches in the verification database, and for the other reaches streamflow regime was unspecified. Because the flow regime is unknown for most reaches, the best estimate of K_a from Eq. (9.14) or (9.16) and Eq. (9.15) or (9.17) was used for the unspecified reaches in the overall verification statistics in Table 9.3 and in the

scattergram of verification results in Fig. 9.6. The verification results are similar to the calibration results indicating the usefullnes of Eqs. (9.14)–(9.17).
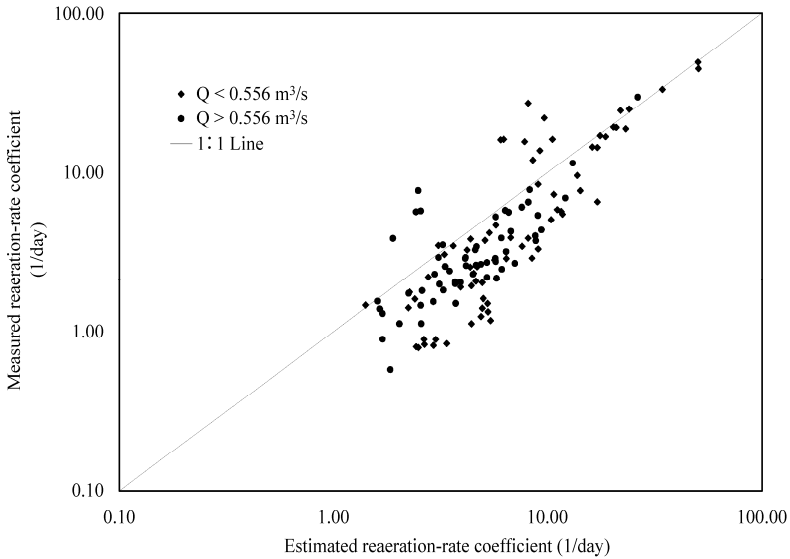
Fig. 9.6   For streams in the verification database, reaeration-rate coefficients measured and estimated with equations developed from multiple linear regression for pool and riffle or channel control streams (whichever is better) in the USGS database (after Melching and Flores, 1999)

As was true for K_d, the value of K_a is affected by temperature, and all the estimation equations yield values of K_a for a temperature of 20℃. The temperature adjustment for K_a is computed as follows:

$$(K_a)_T = (K_a)_{20} \times 1.024^{(T-20)} \tag{9.18}$$

Short comings of the streeter-phelps model—When Streeter and Phelps proposed their original model in 1925, relatively few municipal and industrial wastewaters were treated and CBOD concentrations were by far the dominant cause of low DO concentrations. However, as more and more treatment plants applying secondary treatment were built the importance of other dissolved oxygen demands became apparent. These include the following processes that need to be considered to overcome the short comings of the original Streeter-Phelps model.

(1) Removal of CBOD by sedimentation or adsorption [K_3 in Eq. (9.1)],

(2) Nitrogenous biochemical oxygen demand (NBOD),

(3) Addition of CBOD and NBOD along the reach resulting from local runoff,

(4) Addition of CBOD and NBOD along the reach resulting from the scour of bottom deposits or by diffusion of partly decomposed organic products from the benthic layer into the water column,

(5) Removal of oxygen from water by diffusion into the bethic layer to satisfy the oxygen demand of this layer's aerobic zone,

(6) Removal of oxygen from the water column by the purging action of gases rising from the benthic layer,

(7) Addition of oxygen by photosynthetic action of plankton and macrophytes,

(8) Removal of oxygen by respiration of plankton and macrophytes, and

(9) Continuous redistribution of CBOD, NBOD, and DO by longitudinal dispersion.

Processes (4)–(6) often are referred to as an aggregate process called sediment oxygen demand (SOD),

and process 1 is the source of the benthic deposits of organic material. In the following sections, processes (1)–(9) are discussed and simple models for their consideration are presented.

9.2.3 Biochemical Oxygen Demand

9.2.3.1 Nitrogenous Biochemical Oxygen Demand

The progressive exertion of the BOD of freshly polluted water generally breaks down into two stages: a first stage, in which it is largely the carbonaceous matter that is oxidized; and a second stage, in which nitrogenous substances are attacked in significant amounts and nitrification takes place (Fair et al., 1971). This occurs because the growth of nitrifying bacteria lags behind the growth of microorganisms which perform the carbonaceous reaction. In raw wastewater, the NBOD normally does not begin to exert itself for at least 5–8 days (Fig. 9.7), but for well treated waste the nitrifying bacteria are present in sufficient numbers to begin NBOD consumption.
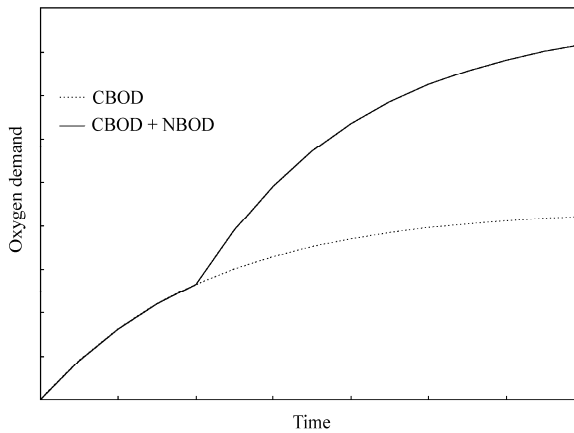
Fig. 9.7 General relation between carbonaceous and nitrogenous biochemical oxygen demand (CBOD and NBOD) in raw wastewater

Nitrogen is the critical element required for protein synthesis and, thus, is essential for life (Masters, 1991). The nitrogen cycle in water is as follows. When living things die, or excrete waste products, nitrogen that was tied to complex organic molecules (i.e. organic nitrogen) is converted to ammonium by bacteria and fungi. Then in aerobic environments Nitrosomonas bacteria (nitroso in relation below) convert ammonium to nitrite and Nitrobacter bacteria (nitro in relation below) convert nitrite to nitrate.

$$NH_3 + DO \xrightarrow[\text{bacteria}]{\text{nitroso}} NO_2 + DO \xrightarrow[\text{bacteria}]{\text{nitro}} NO_3$$
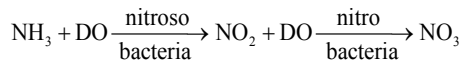
Nitrogen in the form of N_2 is unusable by plants and must first be transformed into either ammonium or nitrate in the process called nitrogen fixation. Under anaerobic conditions, certain denitrifying bacteria are capable of reducing NO_3 back into NO_2 and N_2, completing the nitrogen cycle.

The NBOD can be estimated by multiplying the sum of the organic nitrogen and ammonia nitrogen concentrations (known as total Kjeldahl nitrogen, TKN) by 4.57. Davis and Masten (2004, p. 281) report the actual NBOD is slightly less than the theoretical value due to the incorporation of some of the nitrogen into new bacterial cells, but the difference is only a few percent. The NBOD consumption can then be approximated using a first-order model in the same way as the CBOD as follows:

$$L_t^N = L_0^N e^{-K_n t} \tag{9.19}$$

where L_t^N = the NBOD concentration in milligrams per liter, L_0^N = the initial NBOD concentration at $x = 0$ ($t = 0$) in milligrams per liter, and K_n = NBOD removal rate due only to oxidation = normal range 0.1 to 0.6 d^{-1} (Thomann, 1972, p. 97).

The effect of the consumption of NBOD on DO can then be computed as follows:

$$D_{\text{NBOD}t} = \frac{K_n L_0^N}{K_a - K_n} \left[e^{-K_n t} - e^{-K_a t} \right]$$ (9.20)

where $D_{\text{NBOD}t}$ = equals the dissolved oxygen deficit resulting from NBOD. Because the Streeter-Phelps type functional models are linear system models, the results of Eqs. (9.5) and (9.20) may be summed to determine the deficit resulting from the combined effects of CBOD and NBOD.

9.2.3.2   Benthic Processes

Physical explanation—Fair et al. (1971) provide an interesting physical explanation of the processes in the sediment bed that result in sediment oxygen demand. Their explanation is relied on heavily in this subsection. Mud and sludge deposits are composites of settleable solids laid down, generally over the long periods of time during which currents were neither sufficiently fast to prevent sedimentation of suspended matter nor sufficiently erosive to encourage bottom scour. The sludge-water interface is by no means static. During periods of sedimentation, settling solids form new surface layers. During periods of scour, deposits are churned up. Some bottom-dwelling organisms, the sludge worms and insect larvae, for instance, ingest subsurface debris and cast their fecal pellets on the mud surface; other organisms burrow into the deposits and expose the spoil to flowing water. Gases of decomposition, principally CO_2, CH_4, and H_2S, are produced within the sludge. If they bubble up in sufficient volume, they may buoy some of the sludge into the supernatant water and even to the water surface. Scour may lift masses of sludge into supernatant water and exert sudden sometimes overpowering oxygen demand. In streams, the winter's accumulation of benthic materials may be washed away by spring floods. This spring housecleaning gives the waters a new start at the beginning of what is usually the most dangerous season, summer, when streamflows are low and rates of decomposition are high.

If the overriding waters contain DO, aerobic conditions are maintained at the interface between the accumulating organic debris and the water column. However, downward diffusion of oxygen into the deposits is normally too slow to carry it into the deeper strata and keep them from becoming anaerobic. Because the processes of decomposition in deep deposits are largely anaerobic, their rate of stabilization is normally slower than that of the suspended and dissolved pollution load. Finally, the previously mentioned gases of decomposition are one of the products of the anaerobic decomposition of the organic wastes in the sediments.

The most serious cases of organic matter in and on the river bed are the result of the discharge of domestic and industrial waste in slow flowing rivers. However, the oxygen demand of the river bed may not always be directly the result of sewage or industrial sludges. The death of floating and rooted aquatic plants and natural runoff may contribute to river bed organic material, which will also require oxygen for stabilization.

CBOD sedimentation and scour—As mentioned earlier the CBOD concentration in the water column can decrease both because of consumption of the organic matter by bacteria (deoxygenation) and by settling to the sediment bed and adding to the benthic deposit of organic matter. Thus, the removal of CBOD from the water column by sedimentation will result in the build-up of the benthic layer, and, in the worst cases, the formation of "sludge blankets" immediately below the waste outfall. Previously, the rate of CBOD lost due to sedimentation was defined by the symbol, K_3. Typically, the value of K_3 ranges between –0.36 and 0.36 d^{-1} (Brown and Barnwell, 1987). The negative value for K_3 allows for the resuspension (scour) of the benthic deposit. Taking CBOD sedimentation or scour into account, the Streeter-Phelps model

becomes Eq. (9.1) for CBOD and the following for the DO deficit:

$$D_t = \frac{L_0 K_d}{K_a - K_{11}} \left(e^{-K_{11}t} - e^{-K_a t} \right) + D_0 e^{-K_a t} \tag{9.21}$$

Rather than use a negative sedimentation rate, in some models resuspension, resulting from scour or from lifting by rising gases, is viewed as a distributed source of CBOD. This distributed source may be summed with overland runoff, baseflow, and contributions from minor tributaries as a line source of CBOD, L_{rd}. The effect of this CBOD source on DO can be computed as follows:

$$D_{rdt} = \frac{K_d L_{rd}}{K_a K_{11}} (1 - e^{-K_a t}) - \frac{L_{rd} K_d}{(K_a - K_{11}) K_{11}} \left(e^{-K_{11}t} - e^{-K_a t} \right) + D_0 e^{-K_a t} \tag{9.22}$$

where D_{rdt} = equals to the dissolved oxygen deficit resulting from a distributed source of CBOD. Again the results of Eqs. (9.5), (9.20), and (9.22) may be summed to determine the deficit resulting from the combined effects of CBOD, NBOD, and a distributed source of CBOD.

Combining Eqs. (9.22) and (9.1) allows for settling and resuspension to be modeled as occurring simultaneously in a reach, and, in reality, both removal and addition of CBOD to the flow can occur in a heavily polluted stretch of river that includes sludge deposits. However, depending principally on the velocity and temperature, either removal or addition will dominate. Further, in practical application of stream models to a reach where L_{rd} and K_3 are determined from in-stream CBOD measurements, where $L_{m,x}$ is the measured CBOD at point x, and K_d has been taken from a "bottle" estimate, either L_{rd} or K_3 will be set equal to zero as follows:

$$\text{if} \quad L_{m,x} > L = L_0 e^{-K_d t}$$

then CBOD is being added to the water column and L_{rd} will be determined such that the measured CBOD concentrations are matched and $K_3 = 0$ and $K_{11} = K_d$. Whereas

$$\text{if} \quad L_{m,x} < L = L_0 e^{-K_d t}$$

then CBOD is being removed faster than by the oxidation process and $L_{rd} = 0$ and K_3 equals the increment beyond K_d needed to match the measured CBOD concentrations. Thus, selection of computational reaches should consider which process dominates each section of the river.

Sediment oxygen demand (SOD)—SOD represents the combined effects of the oxygen diffusion into the benthic layer to satisfy the oxygen demand in the aerobic zone of this layer and the removal of oxygen by purging action of gases rising from the benthic layer. Di Toro (2001) has shown that the SOD is not restricted to just times when aerobic conditions are present in the surface sediments. Di Toro (2001, p. 167) proposed a model of SOD that dispenses with the complexity of the various processes that affect SOD by relating SOD to the flux of oxygen equivalents of all reduced substances in the benthic pore water without specific regard to the causing processes. Thus, SOD can be computed from a mass balance model of the oxygen equivalents in the sediment. The organic carbon and settled algae in the benthic layer are mineralized anaerobically. Both reactions are sinks for oxygen and quickly drive the oxygen in the benthic top layer negative. This negative concentration indicates a redox state that in the benthic layer that is reduced rather than oxidized. The calculated negative concentration is taken as the oxygen equivalence of the reduced intermediate products yielded by the mineralization reaction. The reduced carbon intermediates (expressed as oxygen equivalents) are assumed to be transported across the sediment interface and are oxidized to CO_2 and H_2O in the overlying water column. In this approach, the SOD is computed as the transport of oxygen and oxygen equivalents across the sediment water interface and is controlled by the decomposition of organic carbon in the sediment and the DO concentration in the overlying water (DUFLOW, 2000).

The SOD rate is typically assumed to be uniform along a reach. Therefore, the presence and magnitude of benthic deposits becomes another factor in reach selection.   The SOD rate, S_B, is typically specified in grams per square meter per day, and to convert this into a distributed sink of DO it is divided by the flow depth as follows:

$$S_b = S_B/D \tag{9.23}$$

where the units of S_b are in milligrams per liter per day. The effect on the DO deficit of this distributed sink of DO can be computed as follows:

$$D_{\text{SOD}t} = (1 - e^{-K_a t}) \frac{S_b}{K_a} \tag{9.24}$$

where $D_{\text{SOD}t}$ = equals to the dissolved oxygen deficit resulting from SOD.

SOD measurements—SOD rates can be measured in the laboratory and in the field (*in-situ*). The laboratory measurements are done by removing a sample of the river bed (preferably undisturbed) and placing the sample in a large container with oxygenated water. DO reduction over time is a measure of the uptake of the river bed. The *in-situ* measurements involve careful submersion of a sediment chamber that is sealed to the bed, minimally disturbing the sediments, and through which a gentle flow is water is introduced (Fig. 9.8). The DO concentration in the flowing water is measured over time to determine the SOD rate. If done carefully, the laboratory and *in-situ* methods for measuring SOD rates can yield similar results. For example, throughout the Passaic River, New Jersey, U.S. *in situ* measurements in 1983 ranged from nondetectable to 2.43 g/m²/day and laboratory measurements ranged from 1.46 to 4.03 g/m²/day both at 20℃ (New Jersey Department of Environmental Protection, 1987).

Fig. 9.8   The left photograph shows a cylindrical sediment oxygen demand (SOD) chamber being prepared for insertion in the sediment bed, and the right photograph shows the on-shore chamber to which water is pumped from the SOD chamber for continuous monitoring of the dissolved oxygen by the probe inserted in the top of the on-shore chamber (photos by Cheng Liu)

Several limitations are encountered when using SOD rate measurements in modeling for waste-load allocation. First, SOD rate measurements are point values, whereas SOD rates are applied reachwise in water-quality models. Second, there is a tendency to measure SOD at points where it is suspected to be high, i.e. field personnel are inclined to sample in sludge "banks" they can visibly identify. Third, SOD is a dynamic process that varies with time. Finally, disturbance of the bed during sampling can increase water-sediment interaction, and, thus, the measured SOD rates. All of these factors influence the reliability of using measured SOD rates in water-quality models applied to waste-load allocation. Measured SOD rates also can be useful in evaluating the long-term improvements in water quality in a river system. For example, Fig. 9.9 shows the reductions in SOD rates in the Chicago Waterway System from 1976 to

1991 reflecting the improvements in treatment processes at the 3 large waste water treatment plants discharging to the Chicago Waterway System. Similarly, for the Passaic River, New Jersey, U.S., SOD rates measured at Route 46 Bridge near Pine Brook reduced from 12 g/m^2/day in 1969 to near zero in 1983 (New Jersey Department of Environmental Protection, 1987).
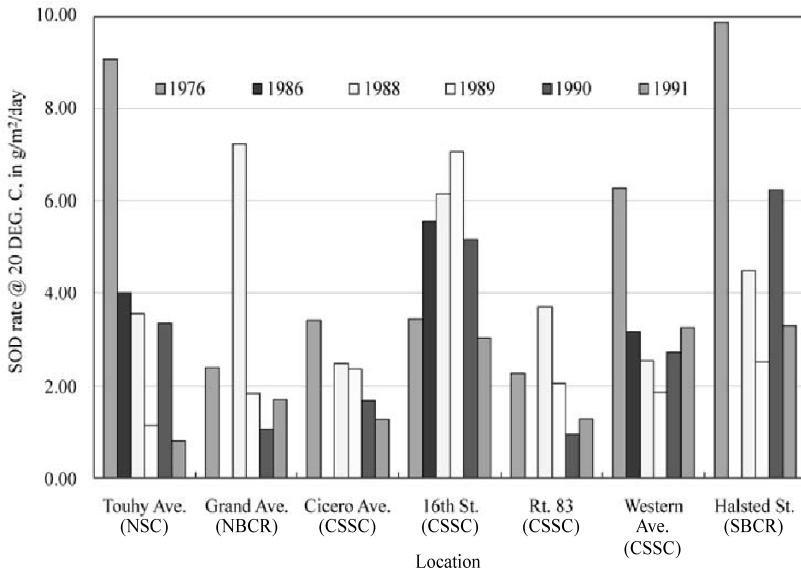
Fig. 9.9 SOD rates measured in the Chicago Deep-Draft Waterway System between 1976 and 1991 (data provided by the Metropolitan Water Reclamation District of Greater Chicago)

As previously noted, measured values of the SOD rate are expressed in terms of a common temperature of 20℃. Temperature effects on the SOD rate can be approximated in the 10-30℃ range by

$$(S_B)_T = (S_B)_{20} \times 1.065^{T-20} \tag{9.25}$$

Below 10℃ the value of S_B probably decreases more rapidly than indicated by Eq. (9.25) and approaches zero in the water temperature range of 0–5℃ (Thomann, 1972, p.105).

9.2.3.3 Photosynthesis and Respiration

Photosynthesis is the process by which plants convert water (H_2O) and carbon dioxide (CO_2) into glucose ($C_6H_{12}O_6$) and oxygen (O_2) is released as a by product. Photosynthesis is performed by chlorophyll using solar energy as follows:

$$6CO_2 + 12H_2O + 36ATP \rightarrow C_6H_{12}O_6 + 6O_2 + 6H_2O \tag{9.26}$$
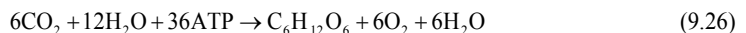
where 36 ATP is a measure of the photon energy required for the reaction. Photosynthesis releases pure oxygen into the water as compared to the reaeration process wherein the atmospheric source is only 21% oxygen. Thus, since all saturation values of DO are measured relative to equilibrium with standard atmospheric conditions, photosynthesis can result in supersaturated oxygen concentrations. Values as high as 150%–200% of the saturation DO concentration are not uncommon (Thomann, 1972, p. 105).

Although photosynthesis may make considerable amounts of oxygen available, oxygenation by green plants is confined to (Fair et al., 1971, p. 649):

(1) waters that are clean enough to encourage plant growth and (a) either not so heavily polluted that green plants die off or (b) sufficiently recovered to reestablish the growth of green plants;

(2) the hours of daylight;

(3) the warmer (growing) seasons of the year.

Thomann (1972, p. 105) notes that when dealing with photosynthesis a higher order biological system is involved relative to the CBOD, NBOD, and SOD relations. In large part this higher order results from the multiple types of plants in the aquatic system engaging in photosynthesis, including:

(1) phytoplankton or free floating aquatic plants with no motility of their own,

(2) aquatic weeds that may be attached to the river bed or free floating, and

(3) the attached algae (periphyton) clinging to rocks, stems, and other surfaces.

As indicated in Eq. (9.26), photosynthesis requires light energy, thus, during the night, aquatic plants respire consuming oxygen from the water and releasing CO_2 into the water. The production of DO during the day by photosynthesis and the consumption of DO at night by respiration leads to a diurnal cycle in the DO concentrations that can have a significant impact on the ability of a stream to meet dissolved oxygen standards (Section 9.3.8). Figure 9.10 shows the diurnal fluctuation in DO concentrations in Salt Creek in the western suburbs of Chicago, U.S., for June 27–28, 1995. It can be seen that during the daylight hours on June 27th, 5 mg/L or more of DO are present in the stream, but once the sun goes down the DO drops to unacceptably low concentrations (as low as 1.79 mg/L around midnight on the 27th). For this case the diurnal range in DO concentrations is a little less than 4 mg/L. However, for rivers that experience supersaturation during the day the nightly DO concentrations may be near zero and the diurnal range can be more than 10 mg/L.
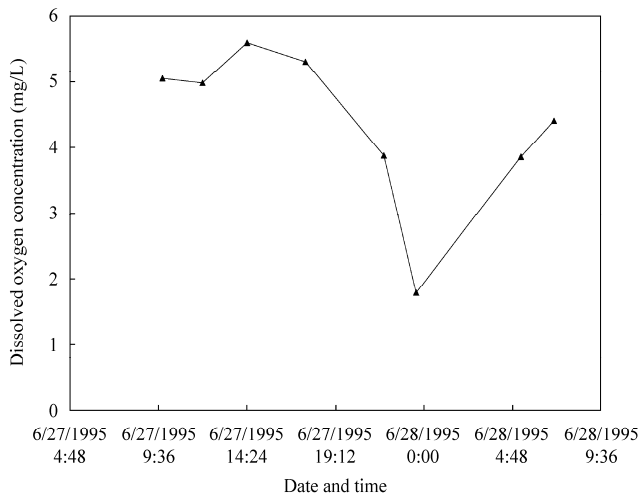
Fig. 9.10 Diurnal fluctuation in dissolved oxygen concentrations in Salt Creek at Elmhurst, Illinois, U.S., for June 27 and 28, 1995

As seen in Fig. 9.10, the photosynthesis-respiration process is very complex. With respect to the DO balance, net photosynethetic oxygen production (the difference between gross photosynthetic production, *P*, and respiration, *R*) primarily depends on:

(1) radiant light energy received at specific depths in the river,

(2) nutrient (particularly nitrogen and phosphorus) concentrations,

(3) dissolved oxygen, and

(4) water temperature.

Many complex models have been developed to relate growth, death (respiration), and photosynthetic activity to nutrient and light availability for a single algal species (e.g., Brown and Barnwell, 1987; Ambrose et al., 1988) and multiple algal species (e.g., DUFLOW, 2000). The details of these models are beyond the level of detail for the simple presentation of basic water quality problems and management solutions presented in this chapter. Instead this chapter takes what Thomann (1972, p. 105) refers to as the "naive" view that the inclusion of two terms, P and R in the mathematical model for the DO balance, can roughly represent the complexity of the photosynthesis-respiration process of aquatic plants. In this view, photosynthesis is modeled as a distributed source of oxygen, P, and respiration is modeled as a distributed sink of oxygen, R. The effect of the combined action of photosynthesis and respiration on the DO deficit, D_{PRt}, may then be computed as

$$D_{PRt} = (1 - e^{-K_a t}) \left[\frac{R}{K_a} - \frac{P}{K_a} \right]$$

(9.27)

Table 9.4 lists some average values of gross photosynthetic (P-R) production of DO as compiled by Thomann (1972). Thomann (1972, p. 107) noted that the values in Table 9.4 have many uncertainties including sunlight conditions, depths of samples, and method of determination. Nevertheless the values listed in Table 9.4 provide information on the order of magnitude from gross photosynthetic production to aid in starting the DO analysis. Finally, the values in Table 9.4 have the same units as distributed sources or sinks of DO like SOD, thus, like SOD the values in Table 9.4 must be divided by the flow depth before they can be used in Eq. (9.27).

Table 9.4 Some average values of gross photosynthetic (photosynthesis minus respiration) production of dissolved oxygen (after Thomann, 1972)

Water type and/or location	Gross production (g/m^2/day)
Truckee River, Nevada, U.S., – bed attached algae	9
Tidal Creek, U.S. – diatom bloom	6
Delaware River estuary, U.S. – Summer	3–7
Duwamish River estuary, Seattle, Washington, U.S.	0.5–2.0
Neuse River System, North Carolina, U.S.	0.3–2.4

The presence of algae and other aquatic plants varies throughout the year because of the complex combinations of the four previously listed factors. In particular, the total incoming light energy is a function of time of day and time of year. With intermittent or heavy cloud cover, random variations are imposed on the regular periodicity of incoming daily light energy. The combination of random hour to hour and day to day fluctuations and periodic fluctuations in light energy indicates that care must be taken in assigning photosynthetic input of DO as a steady-state source (Thomann, 1972, pp. 106–107). Thus, Fair et al. (1971, p. 649) note that as important as photosynthesis may be in the total oxygen economy of natural waters, it cannot be included in engineering calculations of the oxygen balance for waste-load allocation. Only oxygen absorbed from the atmosphere can be relied on to input oxygen at all times except when ice cover eliminates the air contact.

Normally, most water-quality managers think of DO problems in light of DO-BOD interactions, however, in some cases photosynthesis and respiration can be the primary cause of DO problems. For example, Manache and Melching (2004) found that for the Dender River in Belgium model parameters related to the simulation of algal growth had a dominating effect on the uncertainty in simulated DO concentrations. During the study period only 12% of the waste flow entering the Dender received treatment, thus, water

managers for the Dender thought it was suffering from the classical BOD-DO problem. However, for navigation purposes, the river has been channelized and regulated by several hydraulic structures. Thus, the Dender is a series of slow deep pools in which algal processes dominate DO concentrations despite the low levels of wastewater treatment.

9.2.3.4   Dispersion Effects on BOD and DO

For the case of steady-state flow and a downstream boundary condition of equilibrium between the rate of oxygen addition by reaeration and photosynthesis and the net rate of removal by oxidation and SOD, O'Connor (1967) derived a relation for how much error might be involved if the effects of longitudinal dispersion were neglected in computing the DO and BOD concentrations. He found that the ratio, R_R, between the deoxygenation (or reaeration) rate considering dispersion effects and that ignoring them can be computed as a function of reach average velocity, V, the longitudinal dispersion coefficient, D_L, and the reaction coefficient ($K_r = K_d$ or K_a as appropriate) as follows:

$$R_R = \left[\left(\frac{V^2}{2K_r D_L} \right) + 2 \left(\frac{V^2}{2K_r D_L} \right) \right]^{1/2} - \frac{V^2}{2K_r D_L} \tag{9.28}$$

Brown and Barnwell (1987) listed the D_L and V values for a wide variety of streams throughout the U.S. Assuming the 75th percentile value for K_a from the USGS database (Melching and Flores, 1999), Table 9.5 computes values of R_R for several rivers in Brown and Barnwell (1987). For four of six rivers the error is 1% or less, for the fifth river it is less than 4%, and even for the mighty Missouri River the error only is 7.6%. Further, these errors result for a relatively high value of K_a (although for the South Platte River the average K_a for 6 reaches in the USGS database is 12.9 d^{-1}), and the errors for deoxygenation would be far smaller because K_d will be far less than the K_a value used. In general, for steady-state conditions the effect of longitudinal dispersion in natural streams on BOD and DO is negligible.

Table 9.5   The ratio, R_R, between the reaeration rate considering dispersion effects and the reaeration rate ignoring them for several rivers in the U.S. [Dispersion and Velocity Data from Brown and Barnwell (1987)]

River	D_L (m^2/s)	V (m/s)	K_a (d^{-1})	$U^2/2K_a D_L$	R_R
Sacramento River	14.96	0.53	12.45	65.25	0.992
South Platte River	16.17	0.66	12.45	93.90	0.995
Missouri River	1486.	1.55	12.45	5.62	0.924
Copper Creek	19.97	0.27	12.45	12.78	0.964
Clinch River	47.01	0.80	12.45	47.07	0.990
Green-Duwamish River	6.77	0.43	12.45	93.29	0.995

9.2.4   Total Dissolved Oxygen Balance

9.2.4.1   Total DO Balance

Because the Streeter-Phelps type functional models are linear system models, the results of Eqs. (9.5), (9.20), (9.22), (9.24), and (9.27) may be summed to determine the deficit resulting from the combined effects of the initial DO deficit, CBOD, NBOD, a distributed source of CBOD, SOD, and photosynthesis and respiration. Further, the effects of a point source of DO such as an in-stream aerator (see Section 9.3.9) may be computed as follows:

$$D_{PS} = - \frac{W_D}{Q_l} e^{-K_a t} \tag{9.29}$$

where W_D is the load of oxygen delivered in milligrams per second, and Q_l is the flow rate in liters per

second. Combining Eq. (9.29) with Eqs. (9.5), (9.20), (9.22), (9.24), and (9.27) the total DO balance equation for a reach of river can be obtained. The following example illustrates the total DO balance for a stream reach.

Total DO balance example—This example will build on the previous Streeter-Phelps example. The stream reaeration-rate coefficient remains 2.76 d^{-1} (representative of the 25th percentile of the USGS national reaeration-rate coefficient database (Melching and Flores, 1999)), the water temperature remains 20℃, and the initial oxygen deficit remains 3 mg/L. However, the previous example showed that an initial CBOD load, L_0, of 40 mg/L is too high. Thus, it is assumed that as a result of the earlier computations, a 20 mg/L effluent standard for CBOD$_5$ was applied at a newly built wastewater treatment plant at the upstream end of the reach of interest. The wastewater flow is 1 m^3/s and the design river flow is 5.14 m^3/s and the river carries an upstream concentration of CBOD$_U$ of 5 mg/L. Further, since the waste flow now receives secondary treatment the deoxygenation rate, K_d, becomes 0.23 d^{-1}, which is representative of well treated sewage (Table 9.1). Using Eq. (9.3) the CBOD$_U$ in the wastewater treatment plant effluent may be computed as follows:

$$CBOD_U = CBOD_5 / (1 - e^{-5K_d}) = \frac{20 \text{ mg / L}}{1 - e^{-5 \times 0.23}} = 29.27 \text{ mg / L}$$

From the mass balance, then the upstream CBOD concentration, L_0, is computed as 8.96 mg/L, which is far below the upstream CBOD loading of 27.98 mg/L previously computed. But can the required DO concentration of 5 mg/L be met if the effects of NBOD, SOD, and photosynthesis and respiration are considered?

Thomann (1972, p. 16) reports that the approximate average NBOD concentration in untreated municipal wastewater is 220 mg/L, but about 10% of the ammonia and organic nitrogen will be taken up in the sludge at a wastewater treatment plant applying the activated sludge process to achieve secondary treatment. Thus, NBOD is assumed to be 200 mg/L. The NBOD concentration of the upstream flow is assumed to be 5 mg/L. The NBOD removal rate due only to oxidation, K_n, is assumed to be 0.3 d^{-1}. Further, since the stream has been subjected to years of untreated wastewater discharges, the average SOD rate for the Chicago Waterway System in 1976 (Fig. 9.9) of 5.24 g/m^2/day representing the result of the discharge of minimal treatment on the SOD in a reach is applied for the reach of interest. The gross photosynthetic production of DO for the reach will be taken as 1 g/m^2/day as per the middle of the range for the Neuse River System (Table 9.4) with P_{DS} and R_{DS} taken as 3 and 2 g/m^2/day, respectively, where the subscript *DS* means photosynthesis and respiration are being treated as a distributed source and distributed sink, respectively. Finally, the flow depth in the reach will be taken as 1 m.

<u>Solution:</u> Using the mass balance the upstream concentration of NBOD is computed as:

$$L_0^N = \frac{1 \text{ m}^3 / \text{s} (200 \text{ mg / L}) + 5.14 \text{ m}^3 / \text{s} (5 \text{ mg / L})}{1 \text{ m}^3 / \text{s} + 5.14 \text{ m}^3 / \text{s}} = 36.76 \text{ mg / L}$$

Using the previously defined rate constant and loading values the DO deficit component resulting from the initial deficit is computed as

$$D_{init} = D_0 e^{-K_a t} = 3 e^{-2.76t}$$

The DO deficit component resulting from CBOD is computed as

$$D_{CBOD} = \frac{L_0 K_d}{K_a - K_d} \left(e^{-K_d t} - e^{-K_a t} \right) = \frac{8.96 \text{ mg / L} (0.23 \text{ d}^{-1})}{2.76 \text{ d}^{-1} - 0.23 \text{ d}^{-1}} \left(e^{-0.23t} - e^{-2.76t} \right)$$

$$D_{CBOD} = 0.815 \left(e^{-0.23t} - e^{-2.76t} \right)$$

The DO deficit component resulting from NBOD is computed as

$$D_{\text{NBOD}} = \frac{K_n L_0^N}{K_a - K_n}\left[e^{-K_n t} - e^{-K_a t} \right] = \frac{36.76 \text{ mg / L} (0.3 \text{ d}^{-1})}{2.76 \text{ d}^{-1} - 0.3 \text{ d}^{-1}}\left(e^{-0.3t} - e^{-2.76t} \right)$$

$$D_{\text{NBOD}} = 4.483\left(e^{-0.3t} - e^{-2.76t} \right)$$

The DO deficit component resulting from SOD is computed as

$$D_{\text{SOD}} = (1 - e^{-K_a t})\frac{S_B / D}{K_a} = \left(1 - e^{-2.76t} \right)\frac{5.24 \text{ g / (m}^2\text{d)} / 1 \text{ m}}{2.76 \text{ d}^{-1}} = 1.90\left(1 - e^{-2.76t} \right)$$

The DO deficit component resulting from photosynthesis is computed as

$$D_{\text{Photo}} = (1 - e^{-K_a t})\frac{P_{DS} / D}{K_a} = \left(1 - e^{-2.76t} \right)\frac{3 \text{ g / (m}^2\text{d)} / 1 \text{ m}}{2.76 \text{ d}^{-1}} = 1.087\left(1 - e^{-2.76t} \right)$$

The DO deficit component resulting from respiration is computed as

$$D_{\text{Res}} = (1 - e^{-K_a t})\frac{R_{DS} / D}{K_a} = \left(1 - e^{-2.76t} \right)\frac{2 \text{ g / (m}^2\text{d)} / 1 \text{ m}}{2.76 \text{ d}^{-1}} = 0.725\left(1 - e^{-2.76t} \right)$$

The deficit components were computed and summed and then displayed in Fig. 9.11. The DO concentration then was computed corresponding to the total DO deficit in Fig. 9.11 and the saturation DO concentration at 20℃ of 9.022 mg/L and the result is shown in Fig. 9.12. From Fig. 9.12 it is clear that the required DO concentration of 5 mg/L cannot be met. Figure 9.12 also shows the computed DO concentration for the case that does not consider the net photosynthetic DO production as part of the DO balance for waste-load allocation as suggested by Fair et al. (1971, p. 649). For the case including photosynthesis the minimum DO concentration is 3.94 mg/L, whereas for the case not including photosynthesis the minimum DO concentration is 3.62 mg/L.
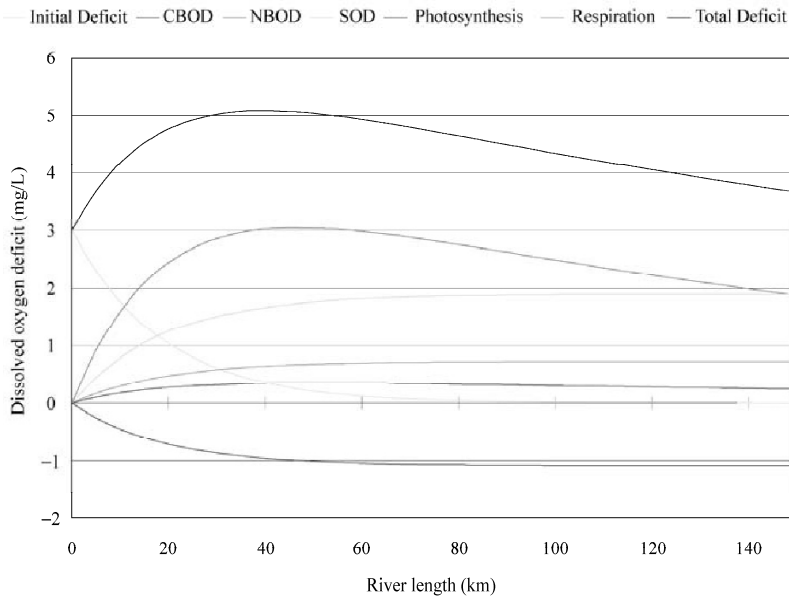
Fig. 9.11 Components of the dissolved oxygen deficit for the total dissolved oxygen balance example

Thus, it was decided to reduce the upstream NBOD concentration, L_0^N, until the 5 mg/L DO concentration could be met. It was found that L_0^N must equal 20 mg/L in order to achieve the 5 mg/L DO requirement

(Fig. 9.12). The corresponding effluent NBOD concentration was found to be 97.1 mg/L, which is more than a 50% reduction of the NBOD in the original effluent.
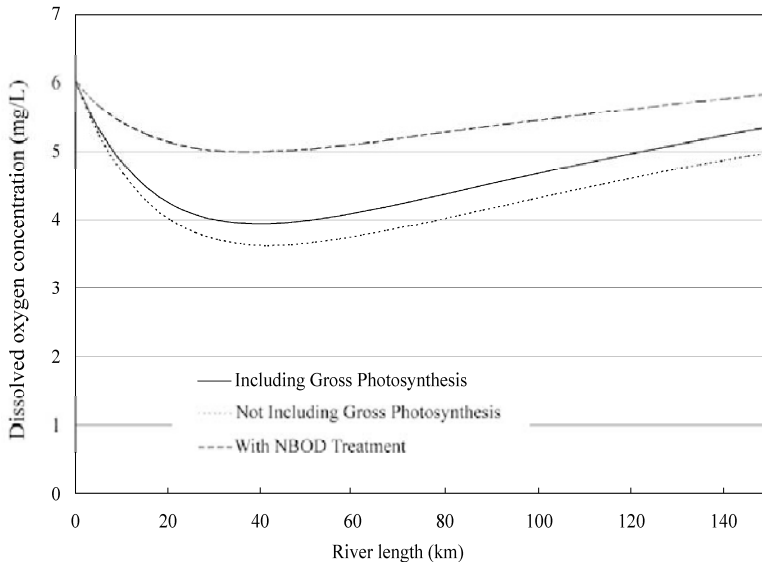
Figure 9.12 Dissolved oxygen (DO) concentration for the total dissolved oxygen balance example for cases considering gross photosynthetic DO production and not considering gross photosynthetic DO production with and without treatment to remove NBOD

9.2.4.2 Dissolved Oxygen Standards

Section 101(a) of the CWA states: "The objective of the Act is to restore and maintain the chemical, physical, and biological integrity of the nation's waters." However, in 1972 when the CWA was passed very little was known about the physical and biological integrity of rivers, lakes, and estuaries, but States still had to establish water-quality standards that met the goals of the CWA, particularly with respect to "fishable" and "swimmable" waters. Thus, in the absence of ways to assess physical and biological integrity, States adopted water-quality standards in the 1970s that had the sole goal of achieving chemical integrity, and it was assumed that if water-quality improved stream ecology also would improve and biological integrity would be achieved.

As noted earlier, maintenance of adequate DO concentrations is the key to the CWA's "fishable" requirement for water bodies. Many States have adopted minimum DO concentrations of 5 mg/L for maintenance of warmwater fish communities, e.g., Wisconsin's Warmwater Sportfish and Forage Fish Communities (Chapter NR 102.04(4) of the Wisconsin Administrative Code) and Ohio's Warmwater Streams (Ohio rule 3745-1-07). This 5 mg/L DO Standard for warmwater biological systems was proposed in 1968 by the National Technical Advisory Committee on Water Quality Criteria for Fish, Other Aquatic Life, and Wildlife (National Technical Committee of the Secretary of the Interior, 1968). However, on the basis of his research, Dr. Dominic Di Toro stated in a keynote speech to the TMDL Science Issues Conference of the Water Environment Federation on March 7, 2001 in St. Louis that the basis of the 5 mg/L DO standard was that fish farm operators reported no problems with their fish when DO concentrations were maintained at or above 5 mg/L.

By law the 5 mg/L DO standard used in Ohio, Wisconsin, and many other States must be met at all times. However, in practical applications, such as waste-load allocation, regional water quality planning, and

determination of impaired water bodies as per Section 303D of the CWA, allowance is made for the randomness in nature when assessing whether the DO (or other constituent) standard is met at all times. For example, in the waste-load allocation process compliance with the standard usually is assessed for a design low-flow condition. In the U.S., this condition is the 7-day, 10-year low flow, $Q_{7,10}$, which is the average flow over a 7-day period for which such average 7-day flows are smaller than $Q_{7,10}$ only once on average in 10 years. In the Regional Water Quality Management Plan Update for Southeastern Wisconsin if DO (or other constituent) concentrations met the appropriate standard at least 85% of the time, DO (or other constituent) was considered in compliance at that location (SEWRPC, 2007). Finally, in many States if DO (or other constituent) concentrations meet the appropriate standard at least 90% of the time, DO (or other constituent) is considered in compliance and the water body is not put on the 303D list of impaired waters for that constituent (Smith et al., 2001).

Biology-based criteria—By the mid-1980s the U.S. Environmental Protection Agency (USEPA) completed an exhaustive survey of the research on DO requirements for various, mainly "sportfish," fish species. This survey was used to develop National DO Criteria on the basis of DO requirements of fish that could be used by States as guidance for development of DO standards that could result in biological integrity of the fish community. The focus on sportfish resulted because the National DO Criteria were established to protect more sensitive species within the fish community. The National DO Criteria established by the USEPA (1986b) are listed in Table 9.6.

The National DO Criteria Document subdivides fish species into salmonid and nonsalmonid fish. Salmonid fish are coldwater fish. Nonsalmonid fish include many other coldwater and coolwater fish plus all warmwater fish (USEPA, 1986b, p. 2). The warmwater fish species are dominated by centrarchid fish. The National DO Criteria Document also notes that there is little published data on the DO requirements of most nonsalmonid species (USEPA, 1986b, pp. 2 and 12). The published data on the following DO sensitive species are the basis of the National DO Criteria recommended for nonsalmonid fish: largemouth bass, smallmouth bass, channel catfish, sunfish, black crappie, white sucker, white bass, northern pike, walleye, among others. The effects of various DO concentrations on the well-being of aquatic organisms have been studied more extensively for fish of the family Salmonidae (including various species of Salmon and trout) than for any other family of organisms (USEPA, 1986b, p. 4). Nearly all these studies have been conducted under laboratory conditions, simplifying cause and effect analysis, but eliminating or minimizing other possibly important environmental conditions, such as chemical and physical stresses associated with non-optimal water quality, as well as competition, behavior, and other related activities. These studies are the basis of the National DO Criteria for Salmonid fish.

Table 9.6 National water quality criteria for ambient dissolved oxygen concentration (after USEPA, 1986b, p. 34)

Time Period	Coldwater criteria		Warmwater criteria	
	Early life stages[1,2]	Other life stages	Early life stages[2]	Other life stages
30 day mean	NA[3]	6.5	NA	5.5
7 day mean	9.5 (6.5)	NA	6.0	NA
7 day mean minimum	NA	5.0	NA	4.0
1 day minimum[4,5]	8.0 (5.0)	4.0	5.0	3.0

[1] These are water column concentrations recommended to achieve the required intergravel DO concentrations shown in parentheses. The 3 mg/L differential is discussed in USEPA (1986b). For species that have early life stages exposed directly to the water column, the figures in parentheses apply.

[2] Includes all embryonic and larval stages and all juvenile forms to 30-days following hatching.

[3] NA means "not applicable".

[4] For highly manipulatable discharges, further restrictions apply (USEPA, 1986b, p. 37).

[5] All minima should be considered as instantaneous concentrations to be achieved at all times.

The Foundation for Water Research (1998) of the United Kingdom has proposed standards that specify allowable frequencies and durations of lower DO concentrations. These standards have been proposed for ecosystems suitable for ① sustainable salmonid fishery, ② sustainable cyprinid fishery, and ③ marginal cyprinid fishery. These standards are based on a literature survey of the DO requirements of the various types of fish communities (fisheries). These standards propose concentrations that may not be met for 1 hour, 6 hours, and 24 hours no more than once per month, once per 3 months, and once per year (Table 9.7). To account for changes in the toxicity of un-ionized ammonia under different environmental conditions and the synergistic effects of high un-ionized ammonia and low DO occurring together correction factors may be applied to the values in Table 9.7 as indicated in the notes to the table. For ① and ②, the standards provide protection to all life stages of all aquatic life (fish, invertebrates, plants) associated with the specified ecosystem type. For ③, the standards provide adequate protection for adult fish, with the exception of the most sensitive fish species and may not afford adequate protection to sensitive life-forms.

To interpret the standards in Table 9.7, it is important to understand the term return period. The return period of a particular set of conditions (e.g., 5 mg DO/L for six hours) is the average time over a sequence of years which elapses between two events when river conditions are equal to or worse than the stated conditions. Consider the river condition where DO is below 4 mg/L for one hour or longer. According to Table 9.7 for a cyprinid fishery, this condition has an allowable return period of one month and may be referred to as the 4 mg/L-one hour-one month standard. This means that the DO concentration at any given point in the river can occasionally fall below 4 mg/L for periods longer than one hour provided that the average interval between such events is not less than one month. Thus, there could be 12 such events per year on average. Continuing with this example, the durations of periods when DO is less than 4 mg/L for all but one of these 12 events must be less than 6 hours. That is, the standards allow for only one event per year on average to have a duration of DO less than 4 mg/L for more than 6 hours.

Table 9.7 Fundamental intermittent standards for dissolved oxygen concentration/duration thresholds not to be breached more frequently than shown (after Foundation for Water Research, 1998)

(1) Ecosystem suitable for sustainable salmonid fishery			
Return period	Dissolved oxygen concentration (mg/L)		
	1 hour	6 hours	24 hours
1 month	5.0	5.5	6.0
3 months	4.5	5.0	5.5
1 year	4.0	4.5	5.0
(2) Ecosystem suitable for sustainable cyprinid fishery			
1 month	4.0	5.0	5.5
3 months	3.5	4.5	5.0
1 year	3.0	4.0	4.5
(3) Marginal cyprinid fishery ecosystem			
1 month	3.0	3.5	4.0
3 months	2.5	3.0	3.5
1 year	2.0	2.5	3.0

Notes:
1. These limits apply when the concentration of un-ionized ammonia (NH_3-N) [See Section 9.4.3] is below 0.02 mg/L. The following correction factors apply at higher concurrent un-ionized ammonia concentrations:
   NH_3-N between 0.02 and 0.15 mg NH_3-N/L:
   correction factor = + (0.97 x ln(mg NH_3-N/L) + 3.8) mg O_2/L
   NH_3-N > 0.15 mg NH_3-N/L: correction factor = + 2 mg O_2/L
2. A correction factor of 3 mg O_2/L is added for salmonid spawning grounds.

In the U.S., the USEPA sets national criteria for various pollutants, such as the DO criteria in Table 9.6, but the individual States have to set and enforce the DO standards applicable in that State. Despite the USEPA (1986b) national criteria document indicating achievement of 3 mg/L of DO at all times may be sufficient to maintain a warmwater fish community, most States have retained their 1970s standards requiring 5 mg/L of DO at all times.

Linkage between habitat and standards—The DO standards like Wisconsin's Warmwater Sportfish and Forage Fish Communities and Ohio's Warmwater Streams are for aquatic life uses that meet the baseline regulatory requirements in line with the Clean Water Act "fishable goal". Many States have defined lower levels of aquatic life use for which lower DO concentrations are acceptable. The basis of these lower levels of aquatic life use typically is defined by physical habitat limitations on the potential aquatic community of the water body. These approaches attempt to link physical, chemical, and biological integrity, which is the original goal of the CWA. One of the best developed systems for defining alternate life uses and DO standards has been developed by the State of Ohio. Ohio's approach is described in the remainder of this subsection.

The Ohio Environmental Protection Agency developed the Qualitative Habitat Evaluation Index (QHEI) as a means to evaluate the quality of habitat features for support of diverse aquatic ecosystems. The QHEI considers and rates aspects of substrate, instream cover, channel quality, riparian/erosion condition, pool and riffle conditions, and gradient to obtain a total habitat quality score for a given location. The individual habitat metrics included in the QHEI are listed in Table 9.8, however, the details of the rating system are beyond the scope of this chapter and readers are directed to Ohio Environmental Protection Agency (1989).

Table 9.8 Component metrics and their score ranges in the qualitative habitat evaluation index of the ohio environmental protection Agency (1989)

Metric	Score
Substrate	**20 points**
(1) Type	0 to 20
(2) Quality	-5 to 3
Instream Cover	**20 points**
(1) Type	0 to 9
(2) Amount	1 to 11
Channel Quality	**20 points**
(1) Sinuosity	1 to 4
(2) Pool-Riffle Development	1 to 7
(3) Channelization	1 to 6
(4) Stability	1 to 3
Riparian/Erosion Condition	**10 points**
(1) Width	0 to 4
(2) Floodplain Quality	0 to 3
(3) Bank Erosion	1 to 3
Pool and Riffle Condition	**20 points**
(1) Maximum Depth	0 to 6
(2) Current Available	-2 to 4
(3) Pool Morphology	0 to 2
(4) Riffle/Run Depth	0 to 4
(5) Riffle Substrate Stability	0 to 2
(6) Riffle Embeddedness	-1 to 2
Gradient	0 to 10 points
Total Score	0 to 100 points

Rankin (1989) examined relations between the QHEI and the Index of Biological Integrity (IBI) (Section 10.4.2) in order to develop a procedure for relating stream potential to habitat quality that would provide some insight into how habitat might affect biological expectations in a given water body. The goal of his study was to provide guidance on the specification of aquatic life uses (i.e. potential aquatic ecological community) for water bodies that were impaired by pollution impacts. Rankin (1989, p. 2) noted that the procedure developed "needed to be useful enough to separate the relative effects of habitat versus water quality on fish community structure or at a minimum determine the baseline community that could be expected in a particular habitat." To develop the relations between QHEI and its subcomponent metrics and life uses Rankin (1989) considered data from a large number and wide variety of streams in Ohio including:

(1) streams that represent sites minimally impacted by chemical water quality or habitat,

(2) streams that contain areas that have relatively un-impacted water quality but have documented habitat impacts ("modified" reference sites), and

(3) within stream basins where the State of Ohio had used the QHEI in some water quality management decision.

In total, Rankin (1989) evaluated conditions for 471 reference sites throughout the State of Ohio.

Rankin (1989) found that for QHEI values less than 46, 72.5% of the waters evaluated had IBI values falling in the poor range, 23.5% falling in the fair range, and only 4% falling in the good range. When summarizing results such as these with respect to the relation between habitat, fish communities, and water-quality management Rankin (1989, p. 52) offered the following warning:

"It makes little sense to protect the biota by multimillion dollar improvements to a point source discharge while important biological uses are impaired by habitat modifications for reasons such as flood control, construction activities, and waterway improvements."

Hence, for cases where the QHEI is less than 46 a lower use standard (Modified Warmwater Stream), which must meet a lower DO concentration standard, is designated. Similarly, Rankin (1989) found that for QHEI values greater than 60, 26% of the waters evaluated had IBI values falling in the exceptional range, 54% falling in the good range, 17% falling in the fair range, and only 3% falling in the poor range. Thus, waters with QHEI values greater than 60 are designated Warmwater Streams for which the full CWA goals can be obtained. For QHEI values in the range 46 to 60, Rankin (1989) found 5% of the waters evaluated had IBI values falling in the exceptional range, 25% falling in the good range, 41% falling in the fair range, and 29% falling in the poor range. Thus, in this range waters are designated Warmwater Streams or Modified Warmwater Streams depending on the values of the individual QHEI component metrics. Table 9.9 indicates the key factors that determine whether a river is a Warmwater Stream or Modified Warmwater Stream. Finally, rivers with very low QHEI values less than 30 or 32 may be designated as Limited Resource Waters.

In the State of Ohio the DO criteria for Modified Warmwater Streams is a daily minimum of 3.0 mg/L and a daily average of 4.0 mg/L, and the minimum reduces to 2.5 mg/L in the Huron/Erie Lake Plain Ecoregion (Ohio rule 3745-1-07). Whereas for Limited Resources Waters the criterion for the daily minimum is 2.0 mg/L with a daily average of 3.0 mg/L (Ohio rule 3745-1-07). Such ecologically justified standards, tailored to the ecological conditions of a State or region, should be considered in all areas as a way to logically achieve the goals of the CWA.

9.2.4.3 Dissolved Oxygen Remediation

The best solution to the pollution problem is prevention—not to produce and discharge pollutants in the first place and to manage lands so that they do not result in degradation of receiving waters and other resources (Novotny, 2003, p. 50). Thus, the most effective means to improve DO concentrations in a river

Table 9.9 Habitat characteristics of modified warmwater streams and warmwater streams in Ohio. Superscripts for modified warmwater streams refer to the influence of a particular characteristic in determining the use (1 = High Influence, 2 = Moderate Influence). Characteristics apply to all ecoregions and types unless otherwise noted. [after Rankin (1989, p. 41)]

Feature number	Modified warmwater streams	Warmwater streams
1	Recent channelization[1] or recovering[2]	No channelization or recovered
2	Silt/muck substrates[1] or heavy to moderate silt covering other substrates[2]	Boulder, cobble, or gravel
3	Sand substrates[2-Boat], Hardpan origin[2]	Silt free
4	Fair-poor development[2]	Good-excellent development
5	Low-no sinuosity[2, 1-Headwater]	Moderate-high sinuosity
6	Only 1-2 cover types[2], cover sparse to none[1]	Cover extensive to moderate
7	Intermittent or interstitial[2-with poor pools]	Fast currents, eddies
8	Lack or fast current[2]	Low-normal substrate embeddedness
9	Maximum depth < 40 cm[1-Wading, 2-Headwater]	Maximum depth > 40 cm
10	High embeddedness of substrates[2]	Low/no embeddedness

Note: Development refers to pool and riffle development

system is to build and OPERATE wastewater treatment plants that remove CBOD and NBOD (mainly ammonia) by biological processes. The removal of CBOD and NBOD from the wastewater effluent will not only reduce the current oxygen demand in the water column, but will over time reduce the SOD as shown in Fig. 9.9. The operation of wastewater treatment plants is emphasized above because in China (and perhaps other countries) there has been an unfortunate tendency to build, but not fully and completely operate wastewater treatment plants. For example, on June 23, 2005, the *China Daily* reported

"Last week, a sewage disposal facility worth US$8 million was found lying idle, letting toxic water flow by to harm people downstream in Tongchuan in northwest China's Shaanxi Province In spite of worsening pollution there, the facility has never operated since being built about two years ago, allegedly because of lack of cash."

In the U.S. the CWA has established a system of regulations that force industries and municipalities to internalize the cost of pollution removal through treatment of their wastewater, however, for municipalities the CWA provided 75% cost share funding through 1987 and low interest loans beginning in 1987 to aid in the construction of wastewater treatment plants. The switch from cost share funding to low interest loans occurred because many communities delayed construction of or improvements to their wastewater treatment facilities because they were waiting to get to the head of the waiting list for federal cost share funds. Ackermann (1981, pp. 20–26) summarized the state of implementation of construction of municipal treatment plants nearly 10 years after the implementation of the CWA as follows:

"Only about $2.5 billion worth of municipal treatment works have been completed despite appropriations of $31.5 billion in construction grants. More embarrassing is that many treatment plants are not producing designed results. A recent study by the General Accounting Office found that 87 percent of the plants were in some violation of their effluent discharge permits. Failures were attributed to design deficiencies, operator problems, and equipment failures. Most damaging has been the delay in program progress because of ponderous regulations established by EPA. There are 11,240 municipal projects in the grant pipeline, 3840 of them worth $20.5 billion are under construction, and the remainder are 2–3 years away from groundbreaking."

Thus, from the experience of the U.S., countries seeking to aggressively construct and operate wastewater treatment plants can expect it will take a long time to fully get the plants on-line.

The tool for implementation of the pollutant clean up programs is the National Pollution Discharge Elimination System (NPDES) permit system, which requires industrial and municipal point source dischargers to obtain wastewater discharge permits that limit the quantity of pollution that can be discharged into the receiving water (Novotny, 2003, p. 12). The NPDES permit limit, in most cases, is based on the technological limitations of the available treatment technologies, the so-called "Best Available Technology Economically Achievable," and is unrelated to the waste assimilation capacity of the receiving water body. Failure to meet permit limits can result in high fines and even closure of a chronically offending facility.

Instream aeration—In the U.S., despite the fact that all industrial wastewater and nearly all domestic wastewater receives biological (secondary) treatment and a growing portion of the wastewater receives tertiary treatment. Many rivers still suffer from low DO concentrations. For example, the 2008 report to the USEPA on water body impairment in Illinois (the 303d report named after Section 303d of the CWA) indicated that 282 river reaches spanning more than 3000 river miles were impaired because of low DO. In these cases, it may be necessary to introduce additional DO to the river. Davis and Masten (2004, p. 293) note that often a relatively inexpensive method for improving stream quality is to add oxygen to the wastewater to bring it close to saturation prior to discharge. The Fox River Water Pollution Control Center in Brookfield, Wis., U.S., does this, and its NPDES permit limits require it to discharge effluent with DO concentrations at or above the following values throughout the year: 9.5 mg/L (January-February), 9.0 mg/L (March-May and November-December), 8.5 mg/L (June and October), and 8.0 mg/L (July-September).

Consideration of the addition of instream aeration stations to improve DO concentrations has been done since at least the late 1960s. The presumption, in the early studies, was strong that on any river where secondary treatment of effluents is insufficient to achieve desired DO concentrations, instream aeration will be a more economical means than advanced waste treatment to achieve desired dissolved oxygen levels (Whipple et al., 1970). A study done by the Metropolitan Water Reclamation District of Greater Chicago (MWRDGC) confirmed this as they found instream aeration was 7.5 times cheaper than advanced treatment for meeting DO standards in the Calumet-Sag Channel (Robison, 1994).Whipple et al. (1970) studied the possibility of using mechanical surface aerators and submerged diffuser aerators. They found the oxygen transfer rates of the diffuser aerators tested were only about two-thirds of those of the mechanical aerators, for comparable conditions. The costs of operation per horsepower-hour were almost the same for the two types of aerators. Thus, they concluded that, based upon the much lower transfer rate of diffusers, the mechanical aerator would be more economical by a wide margin. However, they also concluded there are certain other factors in favor of the diffuser aerators, particularly the lesser interference with boating, and the fact that the mechanical aerators must be serviced to remove heavy drift, and to adjust cables or remove the aerators in time of flood. Hence, mechanical surface aerators generally are not considered for practical applications of instream aeration.

A wide variety of devices have been used for aeration in wastewater treatment facilities, but a only a few different types of devices have been installed in rivers. The following subsections summarize devices that have been installed and/or are under consideration for use in the Chicago Waterway System.

Porous Ceramic Diffusers inject atmospheric oxygen supplied by blowers located on shore that travels trough a manifold system to the instream diffusers located near the bottom of the river. Figures 9.13 and 9.14 show a schematic diagram and a photograph of the operation of the Devon Avenue Instream Aeration Station in Chicago, which is one of two ceramic diffuser aeration stations operated by the MWRDGC since the early 1980s. The Oxygen Transfer Efficiency (OTE) of ceramic diffusers increases with depth and spacing of the diffusers and particularly with fineness of bubble. Fine bubble diffusers are subject to clogging, and, thus, coarse bubble diffusers are used in practice, such as at Devon Avenue. The North Branch of the Chicago at Devon Avenue is at least 3 m deep, which is a sufficient for a reasonable OTE.

However, for an example installation in the Passaic River in New Jersey, U.S., the diffuser headers were laid in a basin excavated 3 m deep at low water, in a channel which is normally 0.6–1.2 m deep (Whipple et al., 1970).
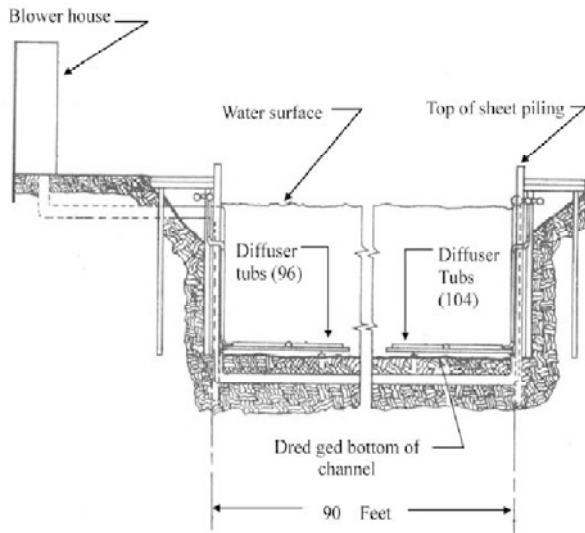
Fig. 9.13   Schematic diagram of the Devon Avenue Instream Aeration Station in Chicago, U.S. (figure provided by AECOM-CTE, Chicago, 2008)

Fig. 9.14   Operation of the Devon Avenue Instream Aeration Station in Chicago, U.S. (See color figure at the end of this book)

The MWRDGC aeration stations have been operating continuously for more than 25 years, and both have experienced operation and maintenance problems. The problems with ceramic diffusers include:

- Diffusers can clog due to sediment accumulation
- Periodic replacement of diffusers is required
- Significant shore area is required for blowers or pumps
- May not be applicable to areas where periodic dredging is required

Typically these fine bubble diffuser air systems have an OTE of 10–30 percent (CTE, 2007).

Membrane Diffusers inject atmospheric oxygen supplied by blowers located on shore that travels trough a manifold system to the instream diffusers located near the bottom of the river. There is no known use of membranes for waterway aeration, however, this technology is being considered for possible application in the Chicago Waterway System because they are generally very flexible and resist fouling because of the following characteristics (CTE, 2007):

- The membranes are normally closed until sufficient air pressure opens the units to begin operation.
- When the air is interrupted, the membranes close preventing liquid/solids entry.
- Membrane diffusers have only an exterior surface phenomena as the liquid and air interface is at the exterior surface of the membrane compared to the interior of a rigid material (such as ceramic diffusers).
- Operation of a membrane unit involves major flexing during on/off operation with major flexing even during normal airflows. This flexing tends to minimize the accumulation of surface inorganic materials.
- The surface of some membrane materials is quite smooth and slick. These smooth, slick surfaces minimize or eliminate calcium carbonate and other contaminant build up.
- Membrane diffusers also require relatively low electrical energy. Typically membrane diffusers have an OTE of 10%–30%.

Jet Ejectors mix air and water together using a Venturi and provide a jet of water containing air bubbles. The horizontal travel of the plume maintains a gas/liquid transfer interface for a much longer period of time than for conventional diffused aeration systems. The horizontally mixed plume is enriched with fine bubbles which will rise slowly to the surface providing for excellent oxygen absorption. Jet aerators have not been applied to waterway aeration, but this method of air diffusion has been proven to be reliable and effective in wastewater treatment tanks. Particularly because jet aerators are much less likely to clog compared to fine bubble diffusers this technology is being considered for possible application in the Chicago Waterway System (CTE, 2007). Typically jet aerators have an OTE of 10%–25%.

U-Tubes: The downward water velocity is designed to exceed the buoyant velocity of the air or oxygen bubbles that are released into the water column. Consequently, the bubbles are transferred downward and around the end of the baffle at the bottom, thus, the name U-Tube (Fig. 9.15). This process temporarily pressurizes the bubbles via the large increase in hydrostatic head within the U-Tube. This increases the saturation concentration which, in turn, increases the DO deficit thereby creating a greater driving force for the adsorption of oxygen into the water column. At sea level, a 34-ft head of water creates approximately two atmospheres of pressure inside a gas bubble (one due to air pressure and one due to water pressure). Typically U-tubes can produce OTE's as high as 90%.
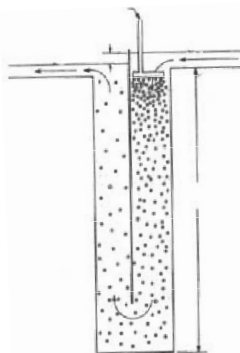
Fig. 9.15   Schematic diagram of a compressed air U-Tube contactor (figure provided by AECOM-CTE, Chicago, 2008)

The fact that DO concentrations in water can be significantly increased under pressurized conditions is not disputable, however, what is questionable is how much of this supersaturated gas remains in solution and remains usable upon exposure to normal atmospheric pressure (CTE, 2007). Shallow streams and rivers may not be capable of absorbing oxygen before it comes into contact with air and becomes lost as a gas into the atmosphere. Most applications of U-Tubes to date have been for deep water bodies including lakes, reservoirs, and deep running rivers, such as those found below high head hydropower dams. U-tubes have high capital costs and access for maintenance is difficult. However, compressed air U-tubes require relatively low electrical energy.

Free Fall Weirs and Cascades aerate water by rapid contact with the atmosphere on all sides as in a natural waterfall. Water flowing over dam spillways and waterfalls commonly achieves saturation DO concentrations in the course of falling through the atmosphere. The MWRDGC applied this principle on a large scale when they installed 5 Sidestream Elevated Pool Aeration (SEPA) stations along the Calumet River, Little Calumet River, and Calumet-Sag Channel on the south side of the Chicago area. The SEPA stations work by using screw pumps to lift water from the source waterway. The water then passes through a series of pools and over a cascade of weirs (see Fig. 9.16) through which DO concentrations at or even slightly above saturation are achieved in the final outflow (Butts et al., 2000). The SEPA stations have higher capital and operation and maintenance costs than ceramic diffusers and U-Tubes (CTE, 2007). They also require access to a significant stretch of land parallel and adjacent to the waterway, and have operational concerns, such as aquatic weed growth (see Fig. 9.16) and excessive sediment deposits in the pools. However, they have many substantial aesthetic benefits such as creating attractive park like conditions in the urban landscapes, such as the southern suburbs of Chicago.

Mobile (Barge-Mounted) Dispersion of Pure Oxygen can achieve OTEs as high as 90%. Such oxygen barges have been used in London and Shanghai (among other places) to combat transient events of low DO concentrations. However, this method does not seem practical to combat chronic problems of low DO concentrations.

Fig. 9.16 Sidestream Elevated Pool Aeration station number 5 discharging aerated water back to the Calumet-Sag Channel (See color figure at the end of this book)

9.3 Nutrient Effects

Nutrients are chemicals that are essential to the growth of living things, in this chapter the focus is on aquatic plants including algae. The main plant nutrients are carbon, nitrogen, and phosphorus each of

which is required in relatively large amounts and unless all three are available, growth will be limited. Plants acquire carbon from carbon dioxide in the atmosphere, and, thus, nitrogen and phosphorus typically are the limiting nutrients—with nitrogen typically limiting plant growth in seawater and phosphorus typically limiting plant growth in freshwater lakes and rivers (Welch, 1980). Nutrients are considered to be pollutants when their concentrations are sufficient to allow excessive growth of aquatic plants, particularly algae (Masters, 1991, p. 109).

The negative effects of phosphorus are primarily related to excessive and/or nuisance growth of aquatic plants. However, there are many negative effects associated with nitrogen compounds as follows:

(1) Conversion of ammonium to nitrate consumes large quantities of dissolved oxygen,

(2) Ammonia and nitrate serve as nutrients for excessive growth of algae,

(3) Nitrite and nitrate in the water have been linked to the disease methemoglobinemia,

(4) Ammonia in its unionized form is toxic to fish, and

(5) Chlorine and hypochlorus acid/hypochlorite can react with any ammonia present in the water forming chloramines, which are more toxic than either chlorine of hypochlorus acid/hypochlorite (Davis and Masten, 2004, p. 298).

The first effect has been discussed in a simplified way as nitrogenous biochemical oxygen demand in Section 9.3.3. The second through fourth effects are described in the following subsections of this chapter. The fifth effect is discussed relative to disinfection performance. This section closes with a discussion of methods to reduce nutrient loads in rural and urban non-point source/diffuse pollution.

9.3.1 Eutrophication

Eutrophication is a natural process that occurs in all lakes because of the gradual accumulation of silt and organic matter in the lake. As the accumulating silt and organic debris causes the lake to get shallower and warmer, more plants take root along the shallower edges, and the lake slowly transforms into a marsh or bog (Masters, 1991, p. 134). Cultural eutrophication is a process whereby water bodies, such as lakes, estuaries, or slow-moving rivers receive excess nutrients due to man's activities that stimulate excessive plant growth including algae, periphyton attached algae, and nuisance plants and weeds. The death of this excessive growth of plants and the settling of the dead organic matter greatly accelerates the natural eutrophication process. Throughout the rest of this discussion the term eutrophication refers to cultural eutrophication, which is a problem to be dealt with by Integrated River Management. Eutrophication is mainly associated with lakes, but it frequently occurs in impounded and slow moving rivers as shown in Fig. 9.17. A detailed discussion of general eutrophication problems and eutrophication management, focusing on examples for estuaries, is given in Section 8.4.

The enhanced plant growth often is referred to as an algal bloom. These blooms eventually die and decompose, and their decomposition removes oxygen from the water, potentially leading to concentrations of DO that are insufficient to sustain normal life forms. If anaerobic conditions result, hydrogen sulfide is formed in the bed sediments and metals such as iron and manganese, which are normally tied up as precipitates in sediments, are dissolved and released into the water column thorough a process called anaerobiosis. Algae and decaying organic matter add color, turbidity, odors, and objectionable tastes to water that are difficult to remove and that may greatly reduce its acceptability as a domestic water source (Masters, 1991, p. 109). Further, marginal amounts of chlorine, enough for disinfection but not enough for oxidation, may intensify algal odors and tastes in much the same way as they intensify phenolic tastes, whereas high concentrations of chlorine will destroy both the organisms and their odorous oils and cell matter (Fair et al., 1971, p. 670).

The decay of the excess organic matter is not the only water quality problem resulting from eutrophication. Clark et al. (1977, p. 276) note that oligotrophic (low in nutrients and primary productivity) surface

waters contain small counts of organisms but many different species of aquatic plants and animals, whereas eutrophic conditions create large numbers of plants and animals of fewer species. Eutrophication diminishes water quality because dissolved solids increase, transparency decreases, blue-green algae are more prevalent, rooted aquatic plants are more abundant, and finer fish are replaced by more tolerant species. In particular, the presence of blue-green algae (also known as cyanobacteria) results in nauseous odors and tastes, interference with stock watering, poisoned water fowl and cattle, poisoned mussels, shorter filter runs in water-purification plants, and interference with industrial water uses.

Fig. 9.17 Algal bloom in Rosenow Creek near Oconomowoc, Wis., U.S. (photo provided by Mike Hahn)

Masters (1991) notes the quickest way to control eutrophication is to identify the limiting nutrient and reduce its concentration. As previously noted, in eutrophic lakes the dominant species of algae are often blue-green (cyanobacteria), which are able to obtain nitrogen directly from the atmosphere (known as nitrogen fixation). Thus, to control blue-green algae phosphorus must be controlled. Fair et al. (1971, p. 664) note that from the mean stoichiometric relation for every milligram of phosphorus, 7 mg of nitrogen, and 41 mg of carbon enter into algal protoplasm. They further note that lake waters can usually obtain enough carbon dioxide from the atmosphere, decaying organic matter, and bicarbonate alkalinity to supply required amounts of carbon (Fair et al., 1971). The phosphorus source is orthophosphate and the nitrogen source is ammonia (typically preferred) or nitrate. Sawyer (1947) suggested that phosphorus concentrations in excess of 0.015 mg/L and nitrogen concentrations above 0.3 mg/L are sufficient to cause blooms of algae. Further, Thomann and Mueller (1987) suggest that nitrogen to phosphorus (N/P) ratios in a body of water over 20 generally indicate that phosphorus is the limiting nutrient, whereas N/P ratios of 5 or less reflect nitrogen limited systems. These recommendations suggest that phosphorus is typically is the limiting nutrient and that reductions to 0.015 mg/L are difficult to achieve considering that most current phosphorus effluent limitations based on the "Best Available Technology Economically Achievable" are around 1 mg/L. Further, complicating the control of phosphorus concentrations are the abundant natural sources. Phosphorus released from rocks can enter the water directly, but more commonly it enters the water in the form of dead plant matter (Davis and Masten, 2004).   It is extremely difficult to reduce the natural inputs of phosphorus.

In addition to nutrients, the major physical factors that influence aquatic-plant production are temperature, light, residence time of the water, and thermal stratification (Clark et al., 1977, p. 279). A very short residence time in a watercourse or impoundment seems to reduce the effects of eutrophication. Because of short residence times and blocking of light by turbidity due to high sediment loads, many major rivers are not subject to high algal production even though their nitrogen and phosphorus concentrations exceed

the minimum values required in a lake. On the other hand, slow moving clear-water streams are susceptible to eutrophication. In rivers, excessive plant growth can create a number of undesirable conditions, such as thick slime layers on rocks and dense growths of aquatic weeds (Fig. 9.18).

Fig. 9.18 Harvesting aquatic weeds in the Juma River west of Beijing, China

Methemoglobinemia—One of the most common forms of nitrogen in water is nitrate (NO_3), which is itself not particularly dangerous. Since the gastric juices of young infants lack sufficient acidity, nitrate reducing bacteria can grow in their upper intestinal tracts. When they ingest nitrate, the nitrate can be reduced to nitrite before the nitrate is completely absorbed in the bloodstream. Nitrites have a greater affinity for hemoglobin in the bloodstream than does oxygen, and when nitrites replace that needed oxygen, the nitrites react with the hemoglobin to form methemglobin. This condition, known as methemoglobinemia, results in ineffective oxygen carrying by the blood. The resulting oxygen starvation causes a bluish discoloration of the infant; hence, it is commonly referred to as the "blue baby" syndrome. In extreme cases the victim may die from suffocation. Usually after the age of about 6 months, the digestive system of a child is sufficiently developed that this syndrome does not occur.

Clark et al. (1977, p. 243) stated the evidence that links nitrates with methemoglobinemia and death in infants is not strong, but is widely cited in the literature. Despite this uncertainty of the link between nitrates and methemoglobinemia, most States in the U.S. have decided better safe than sorry and have set a 10 mg/L standard for nitrates in drinking water. Because of intensive use of fertilizers in agricultural areas in the Midwestern U.S. many communities, such as Bloomington and Decatur, Ill., have had to come up with innovative solutions to reduce nitrate concentrations in the drinking water supplies.

Ammonity toxicity—In natural water bodies total ammonia exists in two forms: the ammonium ion, NH_4^+, and the ammonia molecule, NH_3, also known as un-ionized ammonia. The un-ionized form of ammonia has been proven to harm aquatic animals. In the 1970s, concentrations above 0.05 mg/L were considered dangerous to fish and other aquatic life. Hence, most State standards from the 1970s through 1990s limit un-ionized ammonia concentrations to very low levels, e.g., Colorado = 0.02 mg/L and Illinois = 0.04 mg/L.

Generally, in natural water bodies, with low concentrations of background total ammonia the pH and temperatures are such that the ammonium ion is the dominant form. pH increases due to sewage wastes and eutrophication, and, thus, ammonia toxicity could be important in polluted water bodies. Normally models compute and monitoring programs measure the total ammonia concentration, whereas the State ammonia toxicity standards used to be (and in some cases still are) for un-ionized ammonia. Thus, to

detect an ammonia toxicity problem the un-ionized ammonia amount must be computed as

$$U = \frac{NH_4N}{0.94412(1+10^x)+0.0559}$$ (9.30)

Where U = the concentration of un-ionized ammonia in mg/L, and NH_4N = the concentration of total ammonia nitrogen in mg/L, and

$$x = 0.09018 + \frac{2729.92}{T+273.16} - pH$$

where pH = the pH of the water in standard units.

In the late 1990s, the USEPA (1998, 1999a) developed new criteria for ammonia toxicity on the basis of detailed toxicity studies of many key fish species. Different criteria were developed for acute toxicity and chronic toxicity, the presence or absence of salomonid fish, and the presence or absence of juvenile fish. The new criteria are for total ammonia with the conversion from un-ionized ammonia to total ammonia built into the criteria. These new USEPA standards have been incorporated into many State standards, such as those for Illinois.

Acute toxicity—The one hour average concentration of total ammonia nitrogen ($NH_4^+ + NH_3$) does not exceed, more than once in three years on average, the Criterion Maximum Concentration (CMC) that is calculated as follows:

Salmonid fish are present:

$$CMC = \frac{0.275}{1+10^{7.204-pH}} + \frac{39.0}{1+10^{pH-7.204}}$$ (9.31)

Salmonid fish are absent:

$$CMC = \frac{0.411}{1+10^{7.204-pH}} + \frac{58.4}{1+10^{pH-7.204}}$$ (9.32)

Chronic toxicity—The thirty-day average concentration of total ammonia nitrogen (in mg/L) does not exceed, more than once in three years on average, the Criterion Continuous Concentration (CCC) calculated as follows:

Early life stages are present:

$$CCC = \left[\frac{0.0577}{1+10^{7.688-pH}} + \frac{2.487}{1+10^{pH-7.688}}\right] \times min(2.85, 1.45 \times 10^{0.028(25-T)})$$ (9.33)

Early life stages are absent

$$CCC = \left[\frac{0.0577}{1+10^{7.688-pH}} + \frac{2.487}{1+10^{pH-7.688}}\right] \times 1.45 \times 10^{0.028(25-T)}$$ (9.34)

The 1999 update also included consideration of the 4-day average where the highest 4-day average within the 30-day period should not exceed 2.5 CCC.

Figure 9.19 shows a comparison of the new CMC standard and the old State of Illinois standard of 0.04 mg/L of un-ionized ammonia converted to the total ammonia concentration via Eq. (9.30) for three different pH levels. Except for temperatures less than 3℃ for a pH of 7, the new CMC standard is substantially less restrictive than the old State of Illinois standard. This example shows that through scientific research industry and municipalities can face reduced restrictions while still meeting the goals of the CWA.

The lower 51-km long reach of Salt Creek in the western suburbs of Chicago, U.S. presents an interesting example of the effects of ammonia toxicity on the aquatic community. During dry weather this reach of Salt Creek is a classic effluent dominated stream as it receives the effluent of 11 wastewater

treatment plants either directly or through its tributaries. In the 1970s and 1980s, these wastewater treatment plants operated as standard secondary treatment plants removing CBOD, but not ammonia. By the 1990s most of the plants applied nitrification to remove ammonia loads to Salt Creek.
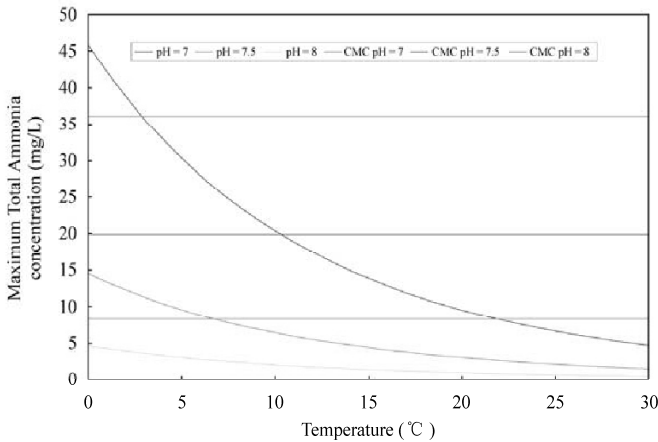
Fig. 9.19 Comparison of U.S. Environmental Protection Agency acute toxicity standard (Criterion Maximum Concentration, CMC) and the former Illinois un-ionized ammonia standard converted to total ammonia concentration

In Illinois the quality of the macroinvertebrate community in a stream is measured by the Macroinvertebrate Biotic Index, MBI (IEPA, 1987), which is a variation of the Hilsenhoff (1987) Biotic Index. The MBI is computed as follows:

$$\text{MBI} = \sum_{i=1}^{m} (n_i \, t_i) / N \tag{9.35}$$

where n_i is the number of individuals in each taxon, t_i is the tolerance rating assigned to each taxon, N is the total number of individuals in the sample, and m is the number of taxons. The MBI ratings are as follows: < 5 is very good; 5–5.9 is good; 6–7.5 is fair; 7.6–9 is poor; and $\geqslant 9$ is very poor. Figure 9.20 shows the changes in the MBI value over time for five sampling locations on Salt Creek. Station GL-10 is near the upstream boundary of the study reach and is minimally impacted by wastewater treatment plant effluent, hence the good to fair ratings at all times. Station GL-16 is at the confluence of Salt Creek and one of its major tributaries and is downstream from 3 wastewater treatment plants, hence it fair rating at all times. Stations GL-04 and GL-02 are downstream from 8 and 10 wastewater treatment plants, respectively, leading to the very poor ratings in 1975 and poor and fair ratings, respectively, in 1983. However, in 1995 once all of these plants applied nitrification and ammonia toxicity decreased the ratings moved into the good range. Station GL-09 is 14.3 km downstream from GL-02 and more than 17 km downstream from the last wastewater treatment plant. Thus, the fair ratings in 1975 and 1983 reflect the natural conversion of ammonia to nitrate (and consequent decreases in ammonia toxicity) as the water flows from GL-02 to GL-09, and the good rating in 1995 reflects both in-wastewater treatment plant and natural nitrification.

9.3.2   Nutrient Control

9.3.2.1   Best Management Practices (BMPs)

The primary sources of nutrients in surface waters are diffuse/non-point sources. For example, Goolsby and Battaglin (2000) reported that only 11% of the total nitrogen in the Mississippi River came from
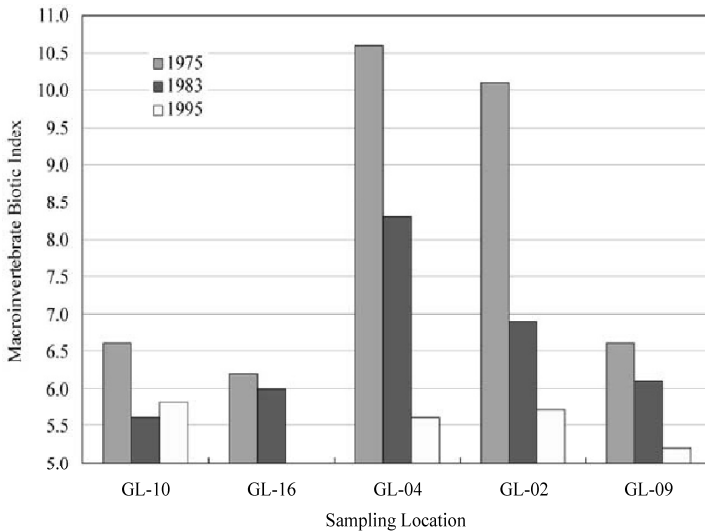
Fig. 9.20 Macroinvertebrate biotic index at five sampling locations along Salt Creek from upstream to downstream as a function of time (data provided by Howard Essig, Illinois Environmental Protection Agency)

municipal and industrial point sources, while Wang (2006) indicated that for Chinese rivers 67% of the load of total nitrogen and 63% of the load of total phosphorus came from non-point sources. Wang (2006) further noted the impacts of this pollution as more than 85% of China's lakes are at serious eutrophication stages and nearly 82% of 532 main rivers in China are contaminated by excessive nitrogen at various levels (the higher the stream order, the heavier the pollution). It is estimated that the economic loss resulting from non-point source water pollution in China is 0.5%–1.0% of GDP (Wang, 2006). Water bodies in the U.S. also are heavily impacted by non-point source pollution with non-point sources impairing 65% of U.S. streams failing to meet standards and 45% of estuaries (USEPA, 1997b). Thus, this section on nutrient control focuses on best management practices (BMPs) for the control of nutrients from non-point sources and the effectiveness of these BMPs.

9.3.2.2 Agricultural BMPs

In a broad sense, BMPs can be defined as any soil treatment, tillage practice, fertilizer-application procedure, crop rotation, structure, or other practices that achieve some watershed-management goal, such as the elimination or reduction of flooding, erosion, or transport of pollutants. In this section, however, the more traditional definition of BMPs as practices used for on-farm soil conservation is used. BMPs for soil conservation are often hypothesized to be a panacea providing reductions in flooding, erosion, and nutrient transport. However, the sediment-transport and nutrient-transport mechanisms are substantially different, and a review of observed nutrient-transport changes for soil-conservation BMPs, considering these differences, is very important.

This section discusses the principles and performance of one BMP not related to soil conservation, namely, nutrient management. Nutrient-management practices are included here because when these practices are carefully combined with soil-conservation BMPs, substantial reductions in nutrient loads may result.

Soil conservation BMPs include two broad classes: agronomic measures and structural measures. The agronomic measures can be further subdivided into contour-plowing, strip cropping and vegetative-filter-strips, and conservation-tillage methods. It is very important to consider that the agronomical and

structural practices discussed in this section are not alternatives but rather are complimentary practices. Similarly, for water-quality protection, nutrient-management methods are complimentary practices for agronomical and structural BMPs.

The effectiveness of agronomical practices is limited to lower slope regions. For example, Armstrong et al. (1980) found that contour plowing alone is effective in reducing erosion for slopes up to 8% for tropical conditions. Sheng (1981) notes that in the humid tropics heavy and frequent rains, as well as excessive runoff, limit the application of purely agronomical practices to slopes less than 12%. For areas with less intense rainfall, agronomical practices may be effective for steeper slopes (greater than 12%), but eventually some upper bound will be reached where agronomical practices must be supplemented with protective residue (mulch) or be abandoned for structural measures (Melching and Avery, 1990, p. 111).

There are three main types of structural protection measures: terraces, grassed waterways, and impoundments. The last two of these methods do not protect the key overland (agricultural) areas. As pointed out by Park (1981), the best way to eliminate or reduce problems resulting from erosion and sedimentation is to control erosion at or near sources. Thus, grassed waterways and impoundments should be considered only for cases where remedial action is necessary to deal with larger than expected sediment yields or floods. Terraces reduce erosion on-site not by protecting the soil itself but by preventing the eroded soil from leaving the field.

Factors that affect the nutrient reduction performance of agricultural BMPs—Processes that result in soil improvement and reduction in flow velocity at BMPs also result in increased infiltration and decreased surface runoff from agricultural areas where these BMPs are applied. Therefore, total runoff (surface plus subsurface) loads of nutrients are expected to decrease through the application of BMPs because of several processes ① reductions in sediment transport and, consequently, transport of constituents adsorbed to sediment, ② reductions in surface runoff and associated dissolved constituents, and ③increased immobilization and denitrification of nutrients in the soil resulting from higher soil-water content and microbial populations of protected soils (primarily results only for conservation tillage) (Doran, 1987; Levanon et al. 1993).

There are many limitations to the effectiveness of the processes described previously. Terstriep et al. (1982) reported typical sediment adsorption percentages for nutrients in urban runoff as 57%, 31%, and 0% for phosphorus, total Kjeldahl nitrogen (organic nitrogen plus ammonia), and nitrate plus nitrite, respectively. Further, fine particles have a higher adsorption potential because of their higher relative surface area. For example, Cooper and Gilliam (1987) found that finer particles contained a higher concentration of phosphorus than coarse particles. Because coarser materials are more likely to be deposited in filter strips, grassed waterways, impoundments, contour plowed fields, and terraces, while finer particles may leave the site, sediment removal efficiencies of BMPs are much higher than removal efficiencies for adsorbed constituents. Similar conclusions apply for urban BMPs that rely on sedimentation for pollutant removal such as grassed waterways, detention basins, vegetative buffer strips, among others.

Nutrient removal only results for the water that infiltrates into the soil if the nutrients transported into the soil are absorbed by plants or become trapped in or bound to the soil. The nutrients that are not immobilized are delivered to the receiving water by a subsurface route rather than a surface route (Casman, 1990). Ellis et al. (1985) reported that for various tillage practices, total nitrogen losses to ground water were 3.3 times greater than those in surface water and nitrate losses to ground water were 4.4–5.7 times greater than those in surface water. Alberts and Spomer (1985) reported that subsurface losses of nitrate exceeded surface losses by a factor of 10, whereas surface and subsurface losses of ammonia and dissolved phosphorus generally were of the same magnitude. Gaynor and Findlay (1995) reported that for various tillage practices, subsurface drainage accounted for 55–68 percent of the dissolved reactive phosphorus (orthophosphate) transported off-site. In general, Casman (1990) concludes that 5–20 times

more nutrients may be lost in subsurface runoff than in surface runoff. Thus, nutrients in the water that infiltrates must remain in the root zone long enough for plant uptake or fixation to soils by microbial activity.

The effectiveness of BMPs is dependent on complex, site-specific factors such as soils, slopes, crops, meteorology, and farmer diligence (Camacho, 1990). Therefore, available summaries of BMP efficiency studies (Casman, 1990; Camacho, 1990) report broad ranges of the effectiveness of BMPs. These ranges are presented here to provide information on the level of nutrient removal possible if the BMPs are properly applied and maintained. The actual removal efficiency of BMPs depends on site-specific factors. It should not be assumed that because a given BMP is applied that a favorable nutrient removal efficiency automatically results. In general, application of BMPs results in reduced nutrient loads leaving farm fields; however, examples where applications of BMPs resulted in increases in nutrient runoff are presented later for consideration.

9.3.2.3   Field Scale Effectiveness of Selected Agricultural BMPs

Strip cropping and vegetative filter strips—Factors affecting the effectiveness of vegetative filter strips (VFSs) include filter length, depth of flow, slope, cross slope, soil type, influent characteristics, clogging of filter with repeated use, and hydraulic loading rate (Casman 1990). Casman (1990) reported effectiveness ranges for nutrient removal utilizing VFSs based on several studies for near uniform, sheet inflow, as follows. The removal efficiency of total nitrogen and total phosphorus in surface runoff ranged from –17% to 71% and from 2% to 80%, respectively, whereas the removal efficiency of total nitrogen in all runoff ranged from –20% to 92%. Casman (1990) also stated that with all the variation in experimental design and results, it is clear that no single efficiency should be used to characterize VFS performance. However, based on these results, Casman (1990) estimated that for planning purposes the removal efficiencies for total nitrogen and total phosphorus in all runoff are approximately 30 percent and from 30 to 90 percent, respectively, for well designed and maintained VFSs.

The results of Dillaha et al. (1988) indicate that the nutrient removal efficiencies of VFSs determined by Casman (1990) are probably unrealistic. They reported that most VFSs on farms are ineffective because runoff tends to concentrate in natural drainageways before reaching the filter strip. They also found that filters that received such concentrated flows were from 40% to 69% less effective for sediment removal, from 70% to 95% less effective for phosphorus removal, and from 60% to 70% less effective for nitrogen removal than VFSs that received nearly uniform sheet flow.

Maintenance of the VFSs is an important factor in attaining high nutrient removal efficiencies. The sediment retention effectiveness of VFSs may decrease rapidly as the vegetation is covered with sediment. Further, in the long term, the sediment bound nutrients filtered out by grasses tend to wash back into the water (if allowed to build up); thus, decreasing removal effectiveness on a long-term basis. If the sediment deposited on the filter strips is regularly removed from the filter and incorporated in the surrounding soil, filter effectiveness may remain high.

Conservation tillage—The efficiency of tillage practices in reducing sediment and nutrient loads is greatly affected by soil properties; surface slope; the previous crop; the amount of residue removed; placement, type, quantity, and timing of fertilizer; harvesting practice; variety of crop; planter style; orientation of contour; and meteorologic conditions (Casman, 1990). Casman (1990) summarized the results of four studies on the removal effectiveness of conservation tillage for nitrogen. Subsurface losses of nitrate were higher for conservation tillage than for conventional tillage (removal efficiencies from –70% to 38% were reported, with three of the four studies reporting negative efficiencies). Higher subsurface losses of nitrate for conservation tillage compared to conventional tillage may result because plow tillage may produce higher nitrogen mineralization from the soil than conservation tillage (Levanon et al. 1993).

Subsurface losses of total nitrogen were reduced for conservation tillage from 7% to 36% relative to conventional tillage. Combined losses of nitrate in surface and subsurface runoff range from –208% to 35% for conservation tillage relative to conventional tillage. Casman (1990) indicated that a well designed and properly applied conservation tillage system could probably reduce total nitrogen by 35%.

Ellis et al. (1985) found that total phosphorus was reduced by 50% and increased by 9% for surface and subsurface runoff, respectively, for chisel tillage compared to conventional tillage practices. The removal efficiency for surface and subsurface runoff combined was 32%. Gaynor and Findlay (1995) found that average orthophosphate loss was 1.7–2.7 times greater for conservation tillage than from conventional tillage, and transport of total soluble phosphorus and total phosphorus increased 2.2 and 2.0 times, respectively. However, Gaynor and Findlay also reported that conservation tillage increased surface runoff 39% and decreased tile drainage 20% compared to conventional tillage. This was attributed to higher soil moisture content and decreased infiltration during spring storms. These unusual runoff results may have contributed to the poor phosphorus removal characteristics in this case. Casman (1990) indicated that a well designed and properly applied conservation tillage system probably could reduce total phosphorus by 35%. Casman (1990) also concluded that on the basis of the available data, conservation tillage practices alone do not consistently reduce nitrogen and phosphorus to surface and subsurface waters. However, Casman reported that conservation tillage in conjunction with nutrient management can be expected to reduce nutrient loss.

Structural best management practices—Kreis et al. (1972) analyzed the effect of passing runoff from a beef feedlot through a series of ponds and waterways. The runoff was held in detention ponds for several days before being discharged into a 2-mile long grassed waterway. The grassed waterway did not substantially reduce concentrations of total phosphorus, total organic nitrogen, and nitrate in surface flows. As discussed previously with respect to concentrated flows in vegetative-filter strips, sedimentation and nutrient transport are not appreciably reduced when vegetation is completely submerged. Thus, the primary function of grassed waterways is to stabilize ditches and reduce gullying, and they should not be considered a BMP for nutrient removal.

Langdale et al. (1985) studied the combined effects of a farm-management plan composed of conventional tillage with terraces, grassed waterways, and nutrient management (i.e. fertilizer level selected on the basis of soil tests). They found a 66% reduction in total phosphorus load relative to conventional tillage. Given that grassed waterways contribute little to total phosphorus reduction, it is clear that terraces can substantially contribute to total phosphorus reduction in runoff from agricultural areas.

Nutrient management—According to the Chesapeake Bay Nutrient Reduction Task Force, a nutrient-management plan is a management practice that provides recommendations on optimum nutrient-application rates, times, and methods based on soil- and manure-analysis results and expected crop yields (Camacho, 1990). These plans, when properly applied, contribute to the reduction of nutrient inputs to the land while maintaining or improving crop productivity. In practice, nutrient management is a composite of several practices including various degrees of reduced fertilizer application, split application, subsurface banding, and spring (and not fall) fertilization (Casman, 1990).

Each of the features of a nutrient-management plan is important in reducing nutrients in runoff and obtaining good crop yields, but the amount of fertilizer application is a particular concern. Farmers in many places follow a principle that "if 1 kg is good, 2 kg is better." For example, Casman (1990) notes that poultry farmers on the Delaware, Maryland, Virginia Penninsula, U.S., apply 2–4 times the recommended amount of manure with respect to N, and with respect to P manure is applied at even higher rates. In order to feed China's massive population fertilizer use in China is much higher than in the U.S. China's per hectare chemical fertilizer application grew rapidly from less than 10 kg in 1960 to

more than 800 kg in 2000. In 17 provinces, per hectare chemical fertilizer application is higher than the recommended level (225 kg) in the world (Wang, 2006).

Unfortunately, little is known on how a reduction of fertilizer and manure applications is translated into a reduction in nutrients in surface water, ground water, or at some point in the receiving water downstream from the field (Camacho, 1990). For example, in the Conestoga Headwaters Rural Clean Water Project, it was found that reducing the nitrogen application by 50% resulted in approximately a 10% reduction in nitrogen in runoff from a field with terraces. Similarly, Kanwar et al. (1987) found for field plots of no-till corn, a reduction in fertilizer of 30% resulted in a 15% reduction in subsurface nitrogen loss. Whitaker et al. (1987) studied the effectiveness of no-till in reducing total nitrogen in runoff and found that the total nitrogen reduction efficiency was 40%–60% whether the fertilizer nitrogen application was 7% or 166% of the recommended amount.

The other aspects of a nutrient-management plan also can be very important. For example, Shalit et al. (1995) stated that for structured soils, where preferential flow can be substantial, the BMP for reduction of dissolved constitutent loading to tile drains appears to be timing the fertilizer applications during drier soil conditions and mixing the fertilizer into the upper soil layer (subsurface banding). Subsurface banding of fertilizer is reported to reduce dissolved nitrogen and total phosphorus in surface runoff by 50 percent for several different types of conservation tillage (Casman, 1990). However, Casman notes that these results are more encouraging for phosphorus management than for nitrogen because most nitrogen is transported from the field in subsurface flow. Finally, Casman reports that the gross effect of fall fertilization on annual nutrient losses in runoff is to multiply losses observed from spring only fertilization by a factor of 1.5–2.

The problem with nutrient management is that well-trained people and substantial time are required to study the soils in each farm field and establish the optimum strategy for fertilization. For example, as of June 1993, only about 80,000 ha of the total 800,000 ha of farmland in the Chesapeake Bay watershed had nutrient managment plans despite several years of multi-State commitments to develop nutrient-management plans throughout the watershed.

Best management systems—When properly applied, BMPs may reduce nutrients in runoff 30%–40% relative to farming without BMPs, but proper application requires careful planning, implementation, and maintenance. A non-point source pollution problem is seldom eliminated or mitigated by application of a single BMP. Therefore, it should not be assumed that just because BMPs for soil conservation are implemented, substantial water-quality benefits (nutrient reduction) are obtained. Usually, a combination of BMPs that work together as a Best Management System (BMS) (Camacho 1993) is necessary to solve non-point source pollution problems. In particular, BMSs that utilize nutrient management in combination with agronomical BMPs such as strip cropping, conservation tillage, and winter cover crops (where appropriate) have been found to be cost effective management alternatives for nutrient reduction and are being implemented in the Chesapeake Bay, U.S., Nutrient Reduction Program (Camacho, 1993).

9.3.2.3   Watershed Scale Effectiveness of Agricultural BMPs

In the case of mixed land uses, a common assumption for non-point source pollution control is that constituent loads at the watershed outlet can be proportionally reduced if non-point source loadings from critical areas that substantially contribute to pollution are controlled. The effectiveness of BMPs applied to critical areas typically has been estimated utilizing information from field-scale tests (summarized previously) and/or non-point source pollution-model applications. It is not proven, however, that such applications actually reduce non-point source loadings from watersheds with complex land-use patterns.

Non-point source pollution-model-based estimates of watershed-scale nutrient reduction can often be grossly erroneous. For example, Garrison and Asplund (1993) compared model estimates with measured

phosphorus concentrations in White Clay Lake in Wisconsin, U.S. The watershed draining into White Clay Lake includes 1,215 ha of dairy farms and cropland. By 1981, 76 percent of farmers had installed animal waste controls and 50 percent had installed cropland BMPs. The cropland BMPs included grassed waterways (with and without tile drainage), vegetative-filter strips, and contour plowing. The slopes in the watershed generally are less than 12% and, therefore, the BMPs should be effective in reducing sediment and nutrient loads. A reduction in runoff phosphorus loads of 30 percent was estimated in model simulation. However, the phosphorus concentration of the lake has increased from 29 µg/L in 1977–1979 to 44 µg/L in 1986–1992. Garrison and Asplund attributed their results primarily to ineffectiveness of the BMPs. However, they attributed these results partly to the fact that the farms closest to water bodies did not participate in the watershed-management programs. The importance of farms close to water bodies participating in watershed-management plans has been demonstrated in a modeling study of nitrate concentrations in Lake Decatur, Ill. (Borah et al. 1996). The simulation results obtained by Borah et al. (1996) indicated that BMPs applied further away from the lake increased nitrate in the lake, whereas BMPs applied closer to the lake reduced nitrate in the lake.

Clausen et al. (1992) studied the effectiveness of a BMP program at a watershed scale for the 13,000 ha St. Albans Bay watershed in Vermont, U.S. They reported that after 10 years of comprehensive monitoring and extensive BMP implementation covering 74 percent of critical areas and 83 percent of animal units, a significant reduction in nutrient concentrations and mass exports was not observed in either tributary streams or the bay. They suggested that these results were obtained because the study ended before the changes in runoff quality could be detected at the watershed scale. This conclusion is supported by work in Germany done by Dannowski et al. summarized by Werner and Wodsak (1995). For the loose rock areas in the northeast of Germany, Dannowski et al. calculated time lags between nitrate transport from the top soil and nitrate arrival in surface waters via ground water between 2 and 10 years for source areas near rivers and between 50 and 500 years for retardation or retention source areas. On the basis of these findings, it may take more than 10 years for reductions in soluble constituents (e.g., nitrate) in the groundwater in fields to be detected in receiving waters. Therefore, implementation of BMPs cannot be considered a quick fix to pollution problems in a watershed.

9.3.2.4 Urban BMPs

The pollution potential of urban runoff carried by separate storm sewers is similar to that of treated sewage, while that of combined sewer overflows is between treated and untreated municipal wastewater (Novotny, 2003, p. 91). Therefore, many BMPs have been proposed to reduce pollutant loads in urban stormwater. BMPs for stromwater management and pollution control applied in urban areas are similar in nature and function to the BMPs applied agricultural areas, i.e. pollution is reduced by reducing sediment loads and/or by reducing runoff. Urban BMPs that remove pollution by removing contaminated sediment include wet and dry detention basins, storm water wetlands, grassed swales, vegetated buffer strips, sand filters, street sweeping, hydrodynamic devices (like Vortex separators that remove sediment from the flow), sediment traps, and sedimentation basins. Urban BMPs that reduce pollution by reducing runoff include infiltration trenches, infiltration basins, porous pavement and concrete grid pavement, biofilters, bioretention basins (rain gardens), and oil and water separators. Some of the BMPs in both groups provide both types of potential water quality benefits.

Parson et al. (2004) reviewed the data on urban BMP performance in pollutant removal in the International Stormwater BMP Database and summarized the performance of a number of BMPs for a variety of nutrients in runoff. Their results are summarized in Table 9.10. Parson et al. (2004) also included box and whisker plots of the measured removal efficiencies for total phosphorus, nitrate, and total nitrogen. From these figures it can be seen that the negative efficiencies for total nitrogen and total

phosphorus are rare, with the vast majority (more than 75% of cases) yielding reductions in load. For nitrate the vast majority of wetland and wet retention basin applications also yielded reductions in load, probably as a result of uptake of nitrate by aquatic plants. For nitrate 40% or more of the biofilter and filter applications resulted in increases in nitrate loads perhaps reflecting conversion of organic nitrogen and ammonia to nitrate in the course of passing through the filter.

   With respect to other urban BMPs, Novotny (2003, p. 91) notes that residential areas with natural swale drainage produced pollution loads that are approximately one order of magnitude lower than pollution loads from similar land with storm sewer drainage. Terstriep et al. (1982) found that mechanical street sweeping at frequencies as great as twice weekly is not effective in reducing the total loads of pollutants in urban storm runoff. Indications of increases in the loads of pollutants during sweeping were at least as strong as were indications of reductions. The fact that street sweeping mainly captures coarse materials while pollutants are attached to finer materials is the suspected cause of these results.

   The key conclusion from the data summarized by Parson et al. (2004) is that well designed and maintained urban BMPs can reduce nutrient loads in runoff as is the case for agricultural BMPs. However, if urban BMPs are not properly installed and maintained it is possible that nutrient loads can be magnified.

Table 9.10   Summary of Nutrient Removal Efficiency Medians and Ranges by Nutrient and BMP Type. (after Parson et al., 2004)

Pollutant		BMP Type						
		Biofilter-Grass Strip	Biofilter-Grass Strip	Detention Basin (dry)	Filter	Hydro-dynamic Devices	Retention Basin (wet)	Wetland
TP	Median (%)	34.0	26.0	34.0	51.0	15.5	80.5	43.5
	(Range)	(−107 to 80)	(−25 to 99)	(−156 to 100)	(−78 to 88)	(−9 to 66)	(14 to 97)	(−267 to 100)
	No. of studies	*n* = 11	*n* = 20	*n* = 27	*n* = 19	*n* = 8	*n* = 56	*n* = 40
OP	Median (%)						61.0	8.0
	(Range)						(−163 to 91)	(−527 to 79)
	No. of studies						*n* = 19	*n* = 14
TN	Median (%)			24.0	31.5		32.0	25.0
	(Range)			(−196 to 73)	(15 to 71)		(−12 to 76)	(−152 to 76)
	No. of studies			*n* = 13	*n* = 10		*n* = 22	*n* = 19
NO3	Median (%)	−5.5	9.0		−9.0		61.5	71.5
	(Range)	(−352 to 72)	(−40 to 99)		(−87 to 64)		(−85 to 97)	(4 to 99)
	No. of studies	*n* = 10	*n* = 11		*n* = 10		*n* = 20	*n* = 16

Note: TP = total phosphorus, OP = orthophosphate, TN = total nitrogen, NO3 = nitrate, blanks indicate insufficient data

9.4   Waterborne and Water-Contact Diseases

Waterborne diseases are caused by pathogenic microorganisms that are directly transmitted when contaminated fresh water is consumed. Dermal (skin), eye, and ear contact with pathogens in contaminated water also can lead to diseases and illnesses known as water-contact diseases. Waterborne diseases are one of the primary causes of death in children in developing countries and also cause substantial misery around the world. Diarrheal disease (including cholera) alone is responsible for the deaths of 1.8 million people every year, 90% are children under 5 (WHO, 2004). A significant amount of disease could be prevented especially in developing countries through better access to safe water supply, adequate sanitation facilities, and better hygiene practices.

   This section focuses on pathogens in rivers and their monitoring, control, and management, and, thus,

on providing better access to safe water supply. Types of waterborne and water-contact diseases are first reviewed. Then means of monitoring possible pathogen contamination and human health risk are discussed. Finally, methods to reduce pathogen loads reaching rivers are described.

9.4.1 Water-Contact Diseases and Indicator Organisms

9.4.1.1 Types of Diseases

Five categories of parasitic organisms infective to man are found in water: bacteria, protozoa, worms, viruses, and fungi (Fair et al., 1971, p. 283). Some of these complete their life cycle by passage through an intermediary aquatic host; others are merely transported by water from man to man. Masters (1991, p. 108) further details the disease producing organisms that grow and multiply through an intermediary aquatic host as follows:

- ➢ Bacterial causes of cholera, bacillary dysentery, typhoid, and paratyphoid fever
- ➢ Viral causes of infectious hepatitis and poliomyelitis
- ➢ Protoza which cause amebic dysentery and giardiasis
- ➢ Helminths (parasitic worms) which cause schistosomiasis and dracontiasis (Guinea worm)

The intestinal discharges of an infected individual, a carrier, may contain billions of these pathogens, which, if allowed to enter the water supply, can cause epidemics of immense proportions. Carriers may not even necessarily exhibit symptoms of their disease, which makes it even more important to carefully protect all water supplies from any human waste contamination (Masters, 1991, p. 108).

Giardia cysts and *Cryptosporidium* oocysts passed through feces of carriers pose an unusual threat to surface waters and even to municipal supply systems. Both of these are diarrheal diseases that can result in death. They can be carried by wild animals as well as humans, may survive for months in the environment, and are not easily destroyed by disinfection. In particular, dozens of species harbor *Cryptosporidium* oocysts, including mammals (e.g., cattle, horses, rodents, deer, dogs, cats, kangaroos), birds, reptiles, and fish. As such, there are many routes for this parasite to enter the environment, including natural runoff (non-point sources), runoff from agriculture, effluents from industries such as meat processors, wastewater effluents, and combined sewer overflows (Clancy et al., 2004).

Schistosomiasis is the most common water-contact disease in the world, affecting approximately 160 million people, and causing more than ten thousand deaths every year, mainly in sub-Saharan Africa (WHO, 2004). Schistosomiasis is spread by free swimming larva in water, called *cercaria*, which attach themselves to human skin, penetrate it, and enter the bloodstream. *Cercaria* mature in the liver into worms that lay masses of eggs on the walls of the intestine. When these eggs are excreted into water, they hatch and have only a few hours to find a snail host in which they develop into new *cercaria*. *Cercaria* exerted by snails, then, have a few days to find another human host, continuing the cycle. Continuation of the cycle requires continued contamination by schistosomiasis carriers in water that are still enough to allow snails to thrive. The effects of schistosomiasis can be controlled by monthly injections.

Shellfish can become toxic because they concentrate pathogenic organisms in their tissues, making the toxicity levels of the shellfish much greater than the levels in the surrounding water (Davis and Masten, 2004, p. 268). Diseases that can be transmitted through shellfish harvested from or stored in sewage—polluted water include typhoid, paratyphoid, bacillary dysentery, and infectious hepititus.

9.4.1.2 Indicator Organisms

The specific identification of pathogenic bacteria as pollution indicators would require extremely large samples and a wide variety of media and methods to exclude all the various pathogens that could be present (Clark et al., 1977, p. 259). To sample and measure for all these pathogens would be expensive if not impossible (i.e. measurement protocols have not been developed for some pathogens). Further, the

time required to complete a group of test procedures to identify many pathogens would greatly reduce the usefulness of the test results. Thus, such a group of test procedures is not applicable to the frequent routine sampling of water supplies and contact recreation (swimming, water skiing, kayaking, etc.) areas. Instead public health officials have tried to identify organisms that are indicative of human fecal matter and human pathogens. These indicator bacteria are monitored under the premise that if their concentrations are appropriately low the concentrations of pathogens also will be low and human health will be protected.

An ideal indicator organism should be associated with sources of human pathogens, unable to grow in aquatic environments, applicable to all types or water, and remain quantifiable after infectious levels of pathogens have disappeared (Oregon DEQ, 1994). The indicator organism also must correlate with the presence of human pathogens and the risk of disease.

In the U.S., in the early 1970s most states selected total coliforms or (primarily) fecal coliforms as the appropriate indicator of pathogen contamination. The typical fecal coliform standard is ① the log mean of five or more samples taken over a 30-day period should not exceed 200 MPN or CFU/100 mL, and ② no single sample should exceed 400 MPN or CFU/100 mL (where MPN is the most probable number, and CFU is colony forming units). Total coliforms and fecal coliforms are present in high abundance in the gastrointestinal tracts of most warm-blooded animals, and the detection of these organisms implies the presence of fecal contamination. The number of coliform organisms in human feces is very great, the daily per capita excretion varying from 125 to 400 billion (Clark et al., 1977, p. 261).

As a result of the Cabelli et al. (1982), Cabelli (1983), and DuFour (1984) epidemiological studies (study of disease in populations), the USEPA (1986a) recommended *E. coli* and *enterococci* spp. for monitoring the microbial quality of freshwaters. These epidemiological studies statistically correlated indicator organism concentrations and incidence of illness in swimmers exposed to the water, formulating a relationship between indicator organism concentrations and health effects. That is, regression results for illness versus either *E. coli* or *enterococci* were used to develop criteria for geometric mean levels of these indicators corresponding to the target acceptable illness rates. These studies were done from 1973 to 1982 on 6 ocean beaches and 5 fresh water beaches, four on Lake Erie in Ohio and one on Keystone Lake in Tulsa, Oklahoma. Some of these beaches were investigated two or three times, resulting in essentially 9 epidemiological trials (tests) for fresh water. Even though the criteria were determined from beaches they have been readily applied in rivers. The Ambient Water Quality Criteria for Bacteria adopted by USEPA (1986a) are as follows. For salt water, the $\log_{10}$ mean of five or more samples taken over a 30-day period of *enterococci* levels should not exceed 35 MPN/100 mL and no single sample should exceed 104 MPN/100 mL. For fresh water, the $\log_{10}$ mean of five or more samples taken over a 30-day period of *Escherichia coli* (*E. coli*) should not exceed 126 MPN/100 mL and no single sample should exceed 235 MPN/100 mL. Jin et al. (2004) also found that *enterococci* appeared to be a more reliable indicator than *E. coli* and fecal coliforms for brackish waters.

Despite the USEPA's publication of new standards in 1986 most states continue to use the conventional fecal coliform standard to assess compliance with establish standards for recreational water. State agencies have not switched to the new recommendations for the following reasons (Jin et al., 2004):

(1) There is no clear advantage in health risk assessment,

(2) Viral agents have different kinetics of inactivation,

(3) Parasitic disease organisms are not considered, and

(4) The fecal coliform group has been a fairly good indicator based on past experience.

Further, the regulated and scientific communities continue to question the validity of the 1986 Ambient Water Quality Criteria for Bacteria as discussed in the following paragraphs.

The draft "USEPA Guidance Document" (USEPA, 2003a) stated that the 1986 bacteria standards based on concentrations of *enterococci* and *E. coli* are scientifically more defensible than the old standards,

based on concentrations of total coliform and fecal coliform bacteria, because there are many environmental sources (e.g., soil, water, birds, sand, plants) for total coliform and fecal coliform. Therefore, the concentrations of these two groups of fecal bacteria in environmental waters often do not necessarily represent human fecal contamination. However, *enterococci* and *E. coli* also have environmental sources (soil, plant, and water), so the same argument the USEPA used to reject total coliform and fecal coliform could be used to refute the usefulness of *enterococci* and *E. coli* indicators (MWRDGC, 2006). These extraneous sources of indicator organisms best explain why even beaches in relatively undeveloped areas routinely exceed USEPA-recommended recreational standards, such as the beaches in Door County, Wisconsin monitored by Bower et al. (2005). In general, the position of the regulated community is that the 1986 USEPA criteria replaced an imperfect indicator with two other imperfect indicators, and that more studies are required (MWRDGC, 2006).

A main shortcoming of the 1986 USEPA criteria is that in the epidemiological studies, the strength of the association between swimming and illness at the freshwater sites was weak—only 2 of 9 trials showed statistically significant difference between swimmers and controls (non-swimmers) [MWRDGC, 2006]. This may be reflective of the insufficient power of the studies (too few subjects), or high levels of illness in the non-swimming control individuals in the studies. That is, in none of the epidemiological studies was a control group used that did not visit the beach, which can lead to bias in that the beach may have caused the illness not just direct contact with the water. Further, the focus of the epidemiological studies used by the USEPA in the development of criteria (and basically all such studies available) has been on gastrointestinal illness without considering water-contact diseases.

Another main shortcoming of the 1986 USEPA criteria is that they are not truly based on the human health risk posed by contact with the water. In the epidemiological studies, no attempt was made to evaluate the actual level of exposure (i.e. length of time in the water, extent of contact time with water, amount of water ingested, etc.) of each swimmer at the beaches studied, nor was any attempt made to evaluate the relationship between levels of indicators and actual pathogenic organisms at the study sites (MWRDGC, 2006).

More recently it has been found that the foundation of the indicator organism approach—namely, the implicit assumption that an approximate trend exists for human pathogens to be at higher levels whenever indicators are at higher levels—may be faulty. Recent studies indicate that there is poor correlation between indicator bacteria levels and levels of human pathogenic bacteria, viruses, and protozoa (Noble et al., 2006; Noble and Fuhrman, 2001; Hardwood et al., 2005; Jiang et al., 2001; Hörman et al., 2004). For example, Bower et al. (2005) found human specific Bacteroides spp. (indicative of human fecal contamination) when culturable *E. coli* levels were as low as 30 to 105 CFU/100 mL in nearshore Lake Michigan and 110 to 170 CFU/100 mL at a Lake Michigan beach following a combined sewer overflow in Milwaukee, U.S. However, Bower et al. (2005) also found that for surface runoff with high (> 10,000 CFU/100mL) *E. coli* levels Bacteroides spp. was present, but the human-specific genetic marker was negative. Results such as the former have led to concern regarding whether water body safety standards based on indicator bacteria adequately protect human health. Whereas results such as the latter have shown that proposals to disinfect urban stormwater runoff to meet fecal coliform or *E. coli* standards may be unnecessary. Such a proposal to disinfect urban stormwater runoff was included in a draft of the Southeastern Wisconsin Water Quality Management Plan Update (SEWRPC, 2007), but it was replaced by a program ① to sample for human specific Bacteroides in stormwater runoff and to remediate leaky storm sewers and ② complete a microbiological human health risk assessment (Section 9.4.4).

Human sources of fecal pollution constitute a serious health risk because of the high likelihood of the presence of human pathogens. Thus, if an indicator could be determined that is directly linked to human sources, it could be a powerful tool for determining which water bodies need remedial action with

respect to pathogens. Culture-independent, molecular methods detect genetic targets of organisms found in a specific host. These methods include detection of human enteroviruses and adenoviruses, host-specific species of Bacteroides, or virulence genes in *E. coli* (Bower et al., 2005). Fecal anaerobes, such as Bacteroides, have long been suggested as alternative indicators to the fecal coliform groups (Bower et al., 2005). Fecal anaerobes compose the majority of fecal bacteria in the gastrointestinal tract of humans and may be present at 1000 times higher densities than the fecal coliform group, making these organisms highly sensitive indicators of fecal pollution. The advent of molecular methods has made it more feasible to detect these organisms in contaminated waters. Certain species of fecal anaerobes have been identified as host specific, and PCR assays based on the 16S rRNA genes of certain species including the human-specific 16S gene, or closely related groups of species, allow the simultaneous detection of indicators and the source of the indicators (Bower et al., 2005). The research group of Dr. Sandra McLellan of the Great Lakes WATER Institute has been successfully using tests for Bacteroides to find sources of human fecal contamination throughout the rivers draining Milwaukee, U.S.

9.4.1.3 Simulation of Indicator Bacteria Levels

Even though indicator bacteria have many shortcomings for assessing human health impacts as described in the previous section, fecal coliforms and *E. coli* remain the parameters defining bacterial pollution in water bodies in most countries and their levels often are simulated using computer models. After discharge to a water body, fecal coliform and *E. coli* decay/loss is dominated by several factors such as sunlight, temperature, salinity, sedimentation, resuspension, predation, and aftergrowth. For example, Fair et al. (1971, p. 641) note the destruction of enteric bacteria is more rapid in:

(1) heavily polluted waters than in clean waters
(2) warm weather than in cold weather
(3) shallow, turbulent waters than in deep, sluggish water bodies
(4) in salt water than in fresh water.

A broad review of these factors can be found in Bowie et al. (1985) and Crane and Moore (1986). Wilkinson et al. (1995) and Jin et al. (2004) demonstrated that bed sediments also may be a significant source of fecal coliforms during sediment resuspension due to storms.

Crane and Moore (1986) reviewed several models that had been proposed to simulate fecal coliform concentrations in stream flow (similar models can be applied to *E. coli*). They noted that Mancini (1978) made an interesting effort to integrate the data found in other studies into a model that directly accounted for the effects of temperature, solar radiation, and salinity. Manacini's (1978) model generally is considered the most complete model of the fecal coliform decay/loss process (Thomann and Mueller 1987, p. 237), and it is given as follows:

$$k = \frac{(0.8 + 0.006 P_{SW})}{24} 1.07^{T-20} + \frac{\alpha I_0(t)}{K_e D} \left[1 - \exp(-K_e D) \right] + F_p \frac{v_s}{D} \tag{9.36}$$

where P_{SW} is the percent seawater, α is a proportionality constant, $I_0(t)$ is the surface solar radiation in cal/cm^2·h, K_e is the vertical light extinction coefficient in 1/m, F_p is the fraction of the bacteria attached to particles, and v_s is the settling velocity of particulate bacterial forms in m/day. When detailed data are available to parameterize this model and to define the fecal coliform or *E. coli* loads to the water body, this model may be used very effectively as shown by Connolly et al. (1999) in the simulation of pathogens in Mamala Bay, Hawaii.

In many modeling cases, the use of a simple model is justified by the fact that the uncertainty in the input loads is considerably high so that the use of a very detailed kinetic structure is impractical. Generally, a simple first-order kinetics decay model is used to characterize the change of the coliform

population in rivers or streams (Chick, 1908):

$$C_{ft} = C_{f0}e^{-kt} \tag{9.37}$$

where C_{ft} is the concentration of fecal coliforms or *E. coli* at time t (CFU/100 ml), C_{f0} is the initial concentration of fecal coliforms or *E. coli* at the outfall (CFU/100 ml), k is the decay rate (die-off) coefficient (1/day), and t is the exposure time (day). In this simple model, the overall net loss rate k is used as a measure of bacterial kinetics. Some researchers (e.g., Auer and Niehaus, 1993) have divided k into component parts of the death rate in the dark (that includes the effects of temperature, salinity, and predation), death rate due to solar radiation, and loss rate due to sedimentation. Because these factors may change with time use of a constant k in continuous modeling may result in problems. However, Elshorbagy and Ormsbee (2006) successfully simulated fecal coliform concentrations in streams draining rural watersheds in southeastern Kentucky using a constant k value throughout the simulation period. Also, Manache et al. (2007) determined constant k values by reach in the Chicago Waterway System on the basis of long term historical data and then tested these in continuous simulation modeling.

For a variety of situations, the simple exponential decay of fecal coliforms (i.e. first-order model) is a good representation of real data. For example, Fig. 9.21 shows the nearly constant relative decrease in fecal coliform concentrations between Diversey Avenue and Madison Street, 7.7 km downstream, in the Chicago Waterway System. Crane and Moore (1986) stated that the first-order model is appropriate for an environment that is totally unsuited to the indicator bacteria and decay is constant with time. On the basis of their literature review, they noted that the first-order model appears to accurately describe the decay of bacteria under all conditions, however, the decay rate coefficient is a highly variable parameter spanning several orders of magnitude for any given bacterial type. This highlights the need to use site-specific data to estimate the decay rate k. Finally, Crane and Moore (1986) noted that in many of the investigations reviewed, bacterial decay was not complete and residual populations at low levels were observed for time periods much longer than would be determined by use of a first-order model. Thus, the first-order model may only be appropriate for shorter travel times (residence times), and computational models applying the first-order approach should include several reaches so that the decrease in k farther downstream from point loads (Thomann and Mueller, 1987, pp. 239–241) can be properly accounted for.
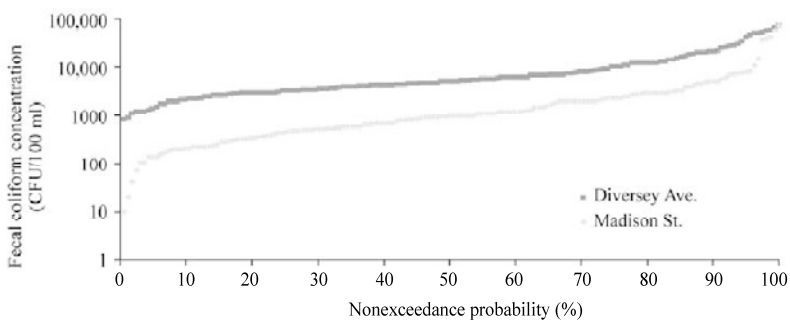
Fig. 9.21 Nonexceedence probability distribution of fecal coliform concentrations for 1990–2003 at Diversey Avenue on the North Branch of the Chicago River and Madison Street on the South Branch of the Chicago River 7.7 km downstream (after Manache et al., 2007)

9.4.2 Microbial Risk Assessment

Because of the questions regarding the uncertainty of the relation between indicator organism (fecal coliform or *E. coli*) and human health effects, over the last nearly twenty years a number of researchers

have advocated microbial human health risk assessment to determine the true threats to human health for cases when the indicator-based standards are difficult to achieve, such as in the case of surface runoff with *E. coli* levels greater than 10,000 CFU/100 mL but with no human sources documented by Bower et al. (2005). If the bacterial contamination does not pose a substantial risk even if the applicable standard is not met, is it worthwhile to apply extraordinary means to meet the standard if the change in risk is small? For example, human health risk assessment was recommended to assess the true extent of pathogen pollution before extraordinary means would be applied to reduce fecal coliform contamination in the recent Southeastern Wisconsin Water Quality Management Plan Update (SEWRPC, 2007).

Risk assessment methods for human health were first proposed in 1989 by the USEPA (1989) for guidance assessment for the Superfund program. Microbial risk assessment methods have been reviewed by the U.S. National Research Council (1994) and the Water Environment Research Foundation (2004), summarized in a book by Haas et al. (1999), and incorporated into the World Health Organization (WHO) Guidelines for Safe Recreational Waters (WHO, 2003). Further, many researchers and agencies are calling for microbial risk assessment before extraordinary measures are taken to meet indicator bacteria standards (Pitt, 2004; SEWRPC, 2007).

The steps in a microbial human-health risk assessment are as follows (National Research Council, 1994; USEPA, 1989):

(1) Hazard identification: Description of human health effects of the particular hazard

(2) Exposure assessment: Determination of the relevant pathways and nature of the exposed population along with quantitative estimates of the level of exposure.

(3) Dose-response assessment: Characterization of the relation between administered dose and incidence of health effects.

(4) Risk characterization: Integration of the information from the previous steps in order to estimate the magnitude of risks and to evaluate the variability and uncertainty.

Hazard identification—Recreational use of a water body may expose individuals through incidental ingestion, dermal, and inhalation pathways to disease-causing bacteria, viruses, and protozoa within the waters. For recreation, the most common illness is gastrointestinal upset (nausea, vomiting, and diarrhea), usually of moderate intensity and short duration. These illnesses were the focus of the epidemiological studies used to develop the USEPA 1986 Ambient Water Quality Criteria for Bacteria and they have been hazards considered in previous microbial human-health risk assessments (e.g., Geosyntec, 2008).

Exposure assessment—This assessment evaluates the duration, frequency, and magnitude of pathogen exposure by one or more pathways. The exposure parameters used in these assessments include incidental ingestion rates and exposure duration. These parameters typically are defined by probability distributions so that a probabilistic risk assessment is done. These parameters need to be evaluated for each exposure pathway. The pathways through which recreators are exposed to pathogens are incidental ingestion, inhalation, and eye or dermal contact. These pathways need to be evaluated for each recreational use of the water body. Recreational uses may include—Primary Contact: swimming, wading, jet skiing, and kayaking; and secondary contact: fishing, canoeing, and pleasure boating. For example, Fig. 9.22 shows the incidental ingestion rate and Fig. 9.23 shows the exposure duration distribution for canoeists on the Chicago Waterway System (Geosyntec, 2008).

The exposure assessment also needs to consider Secondary Attack Rates, which are the rates at which people who are infected through contact with water then infect other people. That is, the number of family members and possibly others that may be potentially exposed to illness by a person infected while recreating on the water body of interest must be determined and considered in the assessment.

Dose-response assessment—The dose-response is the mathematical relationship between the dose of a pathogenic organism and the probability of infection or illness in exposed persons. Biologically plausible
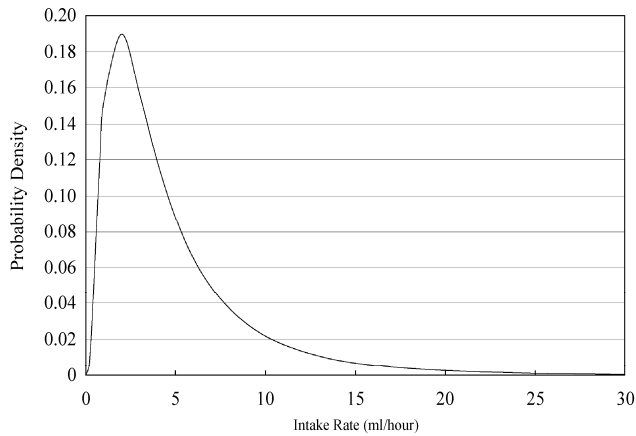
Fig. 9.22 Incidental ingestion rate distribution (lognormal with a mean of 5 and a standard deviation of 5) for canoeists on the Chicago Waterway System (after Geosyntec, 2008)
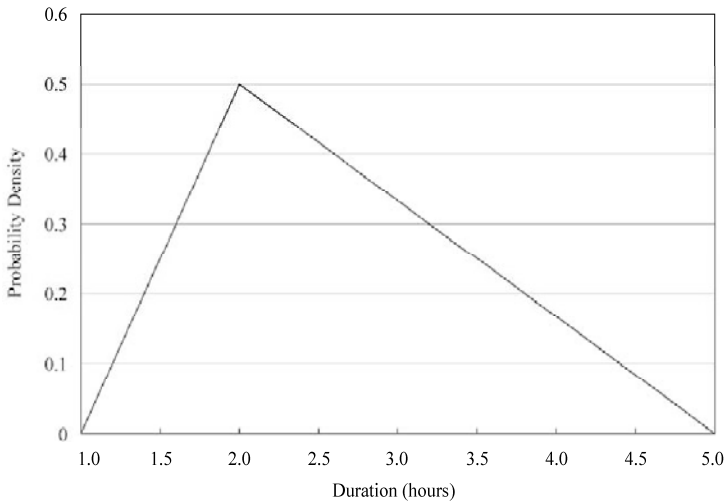
Fig. 9.23 Exposure duration for canoeists in the Chicago Waterway System [Mean = 2.67 hours] (after Geosyntec, 2008)

dose-response models must account for two conditional probabilities: the probability that an organism is ingested and the probability that once ingested an organism survives to infect the host (Haas et al., 1999). Dose-response models assume that even a single organism has a finite probability of initiating infection with an increasing number of pathogens resulting in an increasing probability.

The dose-response models normally take one of two forms: the Exponential Model and the Beta-Poisson Model. The Exponential Model assumes that all of the ingested organisms have the same probability of causing an infection. The Beta-Poisson Model is the current state-of-the-science for characterizing dose-response relationships where the probability of host-pathogen survival is governed by a probability distribution (Haas et al., 1999). Dose-Response Models Available for Poliovirus I, Echovirus 12, Coxsackie Virus, Rotavirus, *Cryptosporidium*, *Giardia*, *Salmonella*, *Shigella*, among others.

Risk characterization—The risk characterization normally is done probabilistically wherein probability distributions of the various model inputs (such as Figs. 9.22 and 9.23) are used, rather than point estimates,

to better represent the variability and uncertainty that exists for each input parameter (USEPA, 1997a). As is discussed in more detail in Section 9.5.5, the major wastewater treatment plants in the Chicago area currently do not disinfect their effluent so a microbial human health risk assessment for recreational use of the Chicago Waterway System was recently completed by Geosyntec (2008). For the Chicago Waterway System, 1,000,000 combinations of weather condition (wet or dry), pathogen concentration, recreation type, duration, ingestion rate, and dose-response were considered for each pathogen to determine health risks (Geosyntec, 2008). Table 9.11 lists the number of illnesses per 1000 exposures for combined wet and dry weather samples for different recreational uses downstream from the major wastewater treatment plants. For all designated recreational uses evaluated, the risks of developing illness were less than the proposed USEPA (2003a) limit of 14 illnesses per 1000 exposure events for freshwater recreational use including primary contact. This example shows the great potential value of microbial risk assessment in determining the true human health risks posed by pathogens in water bodies.

Table 9.11   Estimated illness rates for combined wet and dry weather samples assuming single recreational use with no effluent disinfection downstream from each major wastewater treatment plant in the Chicago Waterway System (after Geosyntec, 2008)

	Illnesses per 1000 exposures		
Recreational use	North Side	Stickney	Calumet
Canoeing	2.45	3.19	0.52
Fishing	1.42	1.90	0.31
Pleasure boating	0.66	1.05	0.14

9.4.3   Disinfection Methods

Pathogen sources include: faulty sewage disposal systems, combined and sanitary sewer overflows, wild and domestic animal waste, illegal discharges to drains and sewers, storm water runoff, and treated, but non-disinfected wastewater effluent. Among these the primary sources of human pathogens are those containing human waste that reaches rivers through urban sanitary sewers, combined sewers, groundwater leaching from septic fields, among other pathways. Therefore, the primary means of controlling pathogens is disinfection of wastewater. For example, once water disinfection by compounds of chlorine (1908 in the U.S.) and by chlorine itself (1911 in the U.S.) was added to wastewater treatment the incidence of waterborne typhoid fever was driven substantially to the vanishing point at less than 1 per million in communities of the U.S. and Europe (Fair et al., 1971, p. 283). While chlorination of effluent has greatly contributed to public health around the world it also has many potentially negative side effects, which led the USEPA in 1976 to delete the fecal coliform standard from its definition of secondary treatment, stating that the benefits achieved by disinfection by chlorine should be weighed against the environmental risks and costs. Further, other methods of disinfection—ultraviolet (UV) radiation and ozonation—were developed in the latter half of the 20th Century that have benefits over chlorine and should be considered for possible application to treated wastewater effluent.

The Water Environment Research Foundation (WERF, 2005) found because of post-disinfection regrowth of bacteria, relatively poor virucidal behavior, and generation of persistent disinfection by-products (DBPs), it is not clear that wastewater disinfection always yields improved effluent or receiving water quality. Most disinfectants are strong oxidants, and can generate oxidants, such as hydroxyl free radicals, as by-products that react with organic and inorganic compounds in water to produce DBPs. In applying any disinfectant, it is important to strike a balance between risks associated with microbial pathogens and those associated with DBPs. The following subsections describe the advantages, disadvantages, problems, and effectiveness of the various disinfection methods.

Chlorination—Done properly, chlorination following secondary treatment of wastewater will inactivate more than 99% of the pathogenic bacteria in the effluent. The chief elements in the use of chlorination have been its efficiency and economy compared to other means of disinfection. However, viruses and parasites found in municipal wastewater, whether primary or secondary, are characterized as being much more resistant and have different sensitivities to chlorination. Chlorine disinfection can inactivate some viruses in wastewater, but not as effectively as it does in drinking water because of interference by dissolved organics and suspended particles. Currently no data are available to demonstrate that *Giardia* cysts are inactivated during chlorine-based disinfection of secondary effluents (Geosyntec, 2008). Studies on infectivity of *Cryptosporidium* have found no inactivation due to chlorination of even highly treated wastewaters (WERF, 2005).

One of the primary problems with chlorination of wastewater effluent is that unless ammonia-nitrogen is removed from wastewater, the predominant form of chlorine will be chloramines, which are generally regarded as being less effective against viruses and parasites than free chlorine (WERF, 2005; USEPA, 1999b). There is very little inactivation of viruses with chloramines. Further, chlorination of secondary effluents produces insufficient virus reduction because suspended solids and turbidity in secondary effluents furnish a means by which particles may be mechanically protected from the inactivating effects of chlorine (Lue-Hing et al., 1976).

Other key problems with chlorine include (Lue-Hing et al., 1976):

(1) Residual chlorine and certain chlorine-based compounds formed as a result of the chlorination of domestic wastewater can be toxic to aquatic life in low concentrations.

(2) Chlorination may from carcinogenic compounds in secondary effluents.

Both the free and combined chlorine (chlorine available as chloramines) are toxic to fish and other aquatic organisms at concentrations down to 0.002 mg/L. Available scientific evidence indicates that 0.05 to 1.2 mg/L of chlorine as chloramines is toxic to aquatic organisms under average water quality conditions (Lue-Hing et al., 1976). In addition to toxicity, chlorine compounds can repel and deny spawning grounds to anadromous fish (Sedita et al., 1987). Studies have shown that dechlorination is capable of removing 87% to 98% of residual chlorine, but the remainder, which may exceed regulatory limits, was very slowly reduced (Geosyntec, 2008). Thus, in effluent dominated streams where little flow is available to dilute chlorine compounds in wastewater treatment plant effluent toxic conditions for fish may exist.

Sedita et al. (1987) documented large changes in fish communities after chlorination was ended at the wastewater treatment plants discharging to the Chicago Waterway System on April 1, 1984. For example, at Touhy Avenue (1.45 km downstream of the North Side Wastewater Treatment Plant) a grand total of only six species (20 individual fish) were collected in six collections during 1974 to 1980, whereas during one collection on November 5, 1984, nine species of fish and 115 individuals were collected. Further at Peterson Avenue (3.86 km downstream) only two fish species and nine individual fish were collected in six collections during 1974 to 1980, whereas during one collection on October 30, 1984, 11 species of fish and 366 individual fish were collected. Lue-Hing et al. (1976) noted the major wastewater treatment plants (Stickney, Calumet, and North Side) discharged, during dry weather, over 5.3 million m^3/day of chlorinated secondary effluent to the Chicago Waterway System, which at the state permissible level of 1 ppm residual chlorine represent a discharge of nearly 5 t of chlorine and chlorine compounds daily. The removal of this chlorine load was considered to be the reason for the recovery of the fish population.

Trihalomethanes (THM), mainly chloroform ($CHCl_3$), bromodichloromethane ($CHBrCl_2$), dibromo-chloromethane ($CHBr_2Cl$), and carbon tribromide ($CHBr_3$) account for the majority of chlorine DBPs on a weight basis. Most of these THMs are suspected carcinogens. Haloacetic acids are the next most significant fraction, accounting for about 25% of chlorine DBPs. Aldehydes account for about 7% of chlorine DBPs (USEPA, 1999b). More than 500 DBPs have been reported in the technical literature, but only a limited number of them have been studied for adverse health effects (Geosyntec, 2008).

Chlorinated effluents are particularly prone to the phenomenon of bacterial regrowth where effluents discharged with certain coliform levels quickly exhibit a marked increase in coliform levels. This phenomenon is believed to be caused by the "organic food" in the sewage which is sufficient to provide for a rapid growth of the coliform organisms. Lue-Hing et al. (1976) illustrated that coliform levels more than 20 km downstream from the three major wastewater treatment plants in the Chicago area were virtually the same before (1966) and after (1974) application of chlorination (Table 9.12). Further, Sedita et al. (1987) found the cessation of chlorination at the major wastewater treatment plants in the Chicago area on April 1, 1984, caused an increase in fecal coliform levels in the immediate downstream vicinity of the plant, but 16.9 to 27.8 km downstream the fecal coliform levels were not statistically different from those achieved prior to the cessation of chlorination.

Table 9.12 Fecal coliform levels before (1966) and after (1974) the application of chlorination at the three major wastewater treatment plants in the Chicago area

Wastewater treatment plant downstream location	River kilometer downstream	Geometric mean fecal coliform (counts/100 mL)	
		1966	1974
North side			
Touhy Avenue	1.45	30,190	125
Damen Avenue	25.43	2,844	3,041
Stickney			
Harlem Avenue	2.41	26,410	1,618
Upstream of Lemont Wastewater Treatment Plant	23.98	13,960	11,245
Calumet			
Ashland Avenue	3.70	44,500	2,464
Route 83	27.52	1,440	2,612

Ultraviolet (UV)—The effectiveness of UV disinfection is largely dependent on the applied UV dose, suspended solids content, UV transmittal, non-disinfected microbial concentration, and the degree of association of microorganisms with particles (USEPA, 2003b). UV radiation only is effective in destroying microorganisms if it reaches the microorganisms, thus, the wastewater must be relatively free of turbidity that can absorb UV energy and shield microorganisms. Nitrogenous compounds also can have an adverse effect on UV disinfection systems as UV-absorbing compounds (WERF, 2005). The advantages of UV versus chlorine disinfection are (Geosyntec, 2008):

(1) UV efficiency for protozoa of concern (*Cryptosporidium parvum* and *Giardia lamblia*) is significantly greater than chlorine efficiency.

(2) Proven ability to disinfect pathogenic bacteria and viruses. There are no significant differences between the efficacy of chlorine and UV radiation as a disinfectant for the reduction of fecal coliforms and *E. coli*.

(3) Formation of harmful by-products by UV is negligible at conventional UV doses.

(4) Increased safety compared to the storage and handling of chlorine.

(5) Increasing costs of chlorination due to regulation curbing chlorine discharge, thus, mandating dechlorination.

6) UV technology has become increasingly more reliable and predictable with regard to performance.

Ozonation—The high reactivity of ozone makes it useful for disinfection, color removal, the degradation or conversion of organic micropollutants, the reduction of chemical oxygen demand, and effluent oxygenation (Geosyntec, 2008). The effectiveness of ozone disinfection depends on the ozone dose, the quality of the

effluent, the ozone demand, and the transfer efficiency of the ozone system (USEPA, 2002). Ozone has been found to be very effective at inactivating a wide range of microorganisms and is generally believed to be more effective than chlorine. Ozone is particularly effective against viruses. For example, a 5 mg/L dose and a 5 min. contact time were sufficient to achieve a 5-log removal of the highly resistant virus, MS2 bacteriophage (Geosyntec, 2008). However, the heterogeneous nature of municipal wastewaters and the relatively high cost of ozone application make it unlikely that organic substances can be completely degraded (to carbon dioxide and water) by ozone treatment (Geosyntec, 2008). Finally, ozone may be unreliable when turbidity is high or variable, because viruses are protected in flocculated particles (Health Canada, 2004).

Because ozone dissipates rapidly and decomposes to oxygen, ozone residuals will normally not be found in the effluent discharged into the receiving water. However, some researchers have reported that ozonation can produce some unstable, toxic, mutagenic, and/or carcinogenic compounds (USEPA, 2002). By-products, such as aldehydes, ketones, acids, and other species, can be formed upon ozonation of wastewater (Geosyntec, 2008). The scarcity of information concerning the formation of ozonation by-products in wastewater effluents clearly indicates that further investigations are necessary on this subject (Paraskeva and Graham, 2002).

Bromate ion formation is an important consideration for waters containing more than 0.1 mg/L bromide ion. Even small residual ozone concentrations can cause mortality in fish and larvae (Paraskeva and Graham, 2002). Studies using fish and crustaceans as test organisms did not result in any changes in the toxicity of a secondary effluent after ozonation (Geosyntec, 2008).

Disinfection effectiveness—The effectiveness of disinfection is a complex function of several variables including type and dose of disinfectant, type and concentration of microorganisms, contact time, and water quality characteristics. The effectiveness of the various disinfectant methods for bacteria, protozoa, and viruses are summarized in the following paragraphs and in Table 9.13.

Bacteria—UV radiation and chlorination/dechlorination, when applied with the goal of complying with conventional effluent discharge regulations, are similar in terms of their ability to inactivate water-borne bacteria, although regrowth is more likely in chlorinated effluents than in UV radiated effluents. Bacterial spores are extremely resistant and many of the chemical disinfectants normally used will have little or no effect (WERF, 2005). Sporular bacteria forms are always far more resistant to ozone disinfection than vegetative forms, but all are easily destroyed by relatively low levels of ozone (USEPA, 1999b).

Protozoa—The resistance of *Giardia* cysts to chlorine has been reported to be two orders of magnitude higher than that of enteroviruses and more than three orders of magnitude higher than that of enteric bacteria (USEPA, 1999b). Chang et al. (1985) reported that the UV dose necessary to cause 99% inactivation of *Giardia* was within the operating range of many UV systems, but it was beyond the usual operating dose. According to Chang et al. (1985), the extreme resistance of *Giardia* makes it unlikely that normal UV radiation procedures would be sufficient to destroy cysts.

Cryptosporidium oocysts are resistant to chlorine-based disinfectants at the concentrations and contact times practiced for water treatment (Clancy et al., 2004). *Cryptosporidium* oocysts are approximately 10 times more resistant to ozone than *Giardia*. Ozone is very effective towards *Pseudomonas aeruginosa*, moderately effective toward *Giardia*, and substantially ineffective toward *Cryptosporidium* (USEPA, 1999b). Several recent studies have shown that UV is highly effective at relatively low doses (10 mJ/cm^2) for control of *Cryptosporidium* (Geosyntec, 2008).

Reactivation of *Giardia* and *Cryptosporidium* after ozonation is unlikely to occur (Paraskeva and Graham, 2002).

Viruses—Although viruses cannot replicate outside their host's cells and, therefore, cannot multiply in the environment, they can survive for several months in fresh water and for shorter periods in marine

water. Their survival in the environment is prolonged at low temperatures and in the sediments onto which they easily absorb (Jin et al., 2004). In contaminated surface water, levels of 1–100 culturable enteric viruses per liter are common. In less polluted surface water, their numbers are closer to 1–10 per 100 liters (Health Canada, 2004).

The conditions that are used to accomplish indicator bacteria inactivation based on chlorination/dechlorination are relatively ineffective for control of waterborne viruses, as compared to UV radiation (WERF, 2005), and viruses are one of the most resistant targets for UV disinfection. Adenoviruses are the most resistant to UV disinfection and are found in high concentrations in municipal wastewater (Geosyntec, 2008). While ozone is particularly effective against viruses, little information is available regarding the effectiveness of ozone on the inactivation of *Caliciviruses* and enteric adenoviruses (Geosyntec, 2008).

Table 9.13 Summary of pathogen disinfection efficiencies for the various disinfection methods

Pathogen	Ozonation	Ultraviolet	Chlorination/dechlorination
E. coli	4 log[a], 1.3 log–4.5 log[b]	4 log[h]	> 4 log[h]
Pseudomonas aeruginosa	2 log[b]	4 log[h]	> 4 log[h]
Salmonella	4 log[a]	3–4 log[j]	Not available
Enterococci	Not available	Not available	More resistant than *E. coli*[h]
Cryptosporidium	0.57 log–2.67log[b]	3 log[c]	0.2 log–3 log[a]
Giardia	1.57 log–2.7 log[b]	2 log[j]	0.5 log[a]
Total Enteric Viruses	5 log[b]	0.32 log–3.61 log[h]	5 log[d]
Calicivirus	2 log[e]	4 log[g]	2 log[e]
Adenovirus	4 log[i]	1 log–4 log[f]	2–4 log[k]

Note: A 1 log reduction is a 90% reduction, a 2 log reduction is a 99% reduction, and so on (after Geosyntec, 2008)
References: (a) USEPA (1999b); (b) Paraskeva and Graham (2002); (c) Clancy (2004); (d) Nelson et al., undated; (e) Health Canada (2004); (f) Gerba et al. (2002); (g) Thurston-Enriquez et al. (2003b); (h) WERF (2005); (i) Thurston-Enriquez et al. (2005); (j) Chang et al. (1985): and k) Thurston-Enriquez et al. (2003a)

9.5 Sediment Contamination

Most toxic heavy metals and complex hydrocarbons, such as petroleum hydrocarbons, Polycyclic Aromatic Hydrocarbons (PAHs), Polychlorinated Biphenyls (PCBs), and organochlorine pesticides, have a high affinity for sediments. For example, Terstriep et al. (1982) reported the following percentages of absorption to sediment in urban runoff for heavy metals: lead and nickel—100%, iron—98%, manganese —73%, and copper—68%; and Harremoes (1982) reported 95% of petroleum hydrocarbons adsorbed to sediment in urban runoff.

The list of toxic metals includes: aluminum, arsenic, beryllium, bismuth, cadmium, chromium, cobalt, copper, iron, lead, manganese, mercury, nickel, selenium, strontium, thallium, tin, titanium, and zinc (Masters, 1991, p. 114). The complex hydrocarbons either are toxic or carcinogenic, particularly the PCBs, PAHs, and organochlorine pesticides. The presence of these compounds can negatively impact the benthic community and then higher forms of life all the way to man through the food chain. The process of toxic or carcinogenic compounds moving through the food chain is known as bioaccumulation. For example, PCBs are efficiently adsorbed on phytoplankton, and, thus, the fate of PCBs is also strongly tied to the behavior of phytoplankton, which provide a direct route into the food chain. PCBs become progressively concentrated as they move up the food chain from phytoplankton to zooplankton, forage fish, and predator fish. As a result, many of the large fish in Green Bay (Lake Michigan, U.S.), such as lake trout,

walleye, and Chinook salmon have been found to bioaccumulate PCB concentrations 100,000 to one million times greater than the concentrations in surrounding waters (Smith et al., 1988). The No Observable Adverse Effect Level standard for Forster's Tern is 2,000,000 ppt. Harris and Kraft (1993) reported that in order to achieve this at the mouth of the Fox River (which feeds into Green Bay), the following biomagnifications would be needed: sediment—2 ppt, algae—20,000 ppt, forage fish—200,000 ppt, and Forster's tern egg—2,000,000 ppt. Since a typical goal for PCB clean-up/remediation is 0.25 ppm (e.g., Fox River cleanup in Wisconsin, U.S.), the current "State of the Art" in sediment remediation is not fully protective of wildlife health. In the following section one approach to evaluate the toxicity of pollutants in sediment is described.

9.5.1 Assessment of Sediment Toxicity

The Wisconsin Department of Natural Resources (WDNR, 2003) has established a system for evaluating the toxic effects of pollutants in sediment on the benthic organisms. The WDNR recommends the use of this system for establishing levels of concern for prioritizing sites for additional study and possible cleanup. This system uses three criteria based on the likely effects on benthic organisms as follows. The Threshold Effect Concentration (TEC) indicates contaminant concentrations below which adverse effects to benthic organisms are considered to be unlikely. The Probable Effect Concentration (PEC) indicates contaminant concentrations at which adverse effects to the benthic organisms are highly probable or frequently seen. The Midpoint Effect Concentration (MEC) is derived from the TEC and PEC values for the purpose of interpreting the effects of pollutant concentrations that fall between the TEC and PEC. Table 9.14 lists the TEC, MEC, and PEC values for some pollutants of concern commonly encountered in sediments, a more complete list of pollutants is included in WDNR (2003).

Table 9.14 Threshold Effect Concentration (TEC), Midpoint Effect Concentration (MEC), and Probable Effect Concentration (PEC) for selected contaminants that have commonly been found by the Wisconsin Department of Natural Resources (WDNR) at contaminated sites in Wisconsin

Substance	TEC	MEC	PEC
Metals			
Arsenic	9.80	21.40	33.0
Cadmium	0.99	3.00	5.0
Chromium	43.00	76.50	110.0
Copper	32.00	91.00	150.0
Mercury	0.18	0.64	1.1
Nickel	23.00	36.00	49.0
Lead	36.00	83.00	130.0
Zinc	120.00	290.00	460.0
Nonpolar organic compounds			
Total Polycyclic Aromatic Hydrocarbons (PAHs)	1610.00	12,205.00	22,800.0
Total Polychlorinated Biphenyls (PCBs)	60.00	368.00	676.0
Chlordane	3.20	10.60	18.0
Sum o,p + p,p DDT	4.20	33.60	63.0
Sum DDD+DDE+DDT	5.30	289.00	572.0
2,3,7,8-Tetrachlorodibenzo-p-dioxin (TCDD)	0.85	11.20	21.5

Note: TEC, MEC, and PEC values are from WDNR (2003), while the list of commonly found contaminants was provided by Dr. X. Zhang, WDNR. Metal values are in milligrams per kilogram, dry weight; nonpolar organic compound values are expressed on a dry weight basis normalized to a total organic carbon level of 1 percent and the units are micrograms per kilogram.

The system described in the foregoing paragraphs only estimates the effects of pollutants on benthic organisms. Where non-carcinogenic and non-bioaccumulative pollutants are considered, the foregoing guidelines should be protective of human health and wildlife concerns. For bioaccumulative pollutants, protection of human and/or wildlife health may require the use of more restrictive concentration levels.

The PEC values also are used to derive mean PEC-quotients for evaluation of the toxicity of mixtures of pollutants in sediments to benthic organisms. A PEC-quotient is computed for each pollutant in each sample by dividing the concentration of the pollutant in the sediment by the PEC concentration for that pollutant. The mean PEC-quotient then is computed by summing the individual PEC-quotients and dividing by the number of pollutants considered. This normalizes the value to provide comparable indices of pollution among samples for which different numbers of pollutants were analyzed. Mean PEC-quotients that represent mixtures of pollutants have been shown to be highly correlated with incidences of toxicity to benthic organisms in the sediments. The reliability of predictions of toxicity is the highest for mean PEC-quotients computed from total PAHs, total PCBs, and the metals arsenic, cadmium, chromium, copper, lead, nickel, and zinc. MacDonald et al. (2000) developed the following relation between the mean PEC-quotient value (*mPEC*) and the average incidence of toxicity (*TOX*), which is valid through an *mPEC* value of 4, beyond which the value of the average incidence of toxicity is 100%.

$$TOX = 101.48\left(1 - 0.36^{mPEC}\right) \tag{9.38}$$

9.5.2   Remediation/Cleanup of Contaminated Sediment

Typical remedial action objectives for clean-up of contaminated sediment include (Lue-Hing et al., 2001):

(1) Achieve surface water quality criteria, to the extent practicable, as quickly as possible.

(2) Protect human health by being able to remove fish consumption advisories as quickly as possible.

(3) Protect ecological receptors like healthy invertebrates, birds, fish, and mammals.

(4) Reduce the transport of PCBs from the river into downstream water bodies as quickly as possible.

(5) Minimize the downstream movement of PCBs during implementation of the remedy.

To achieve these objectives three methods of contamination remediation typically are applied either alone or in combination: natural attenuation, dredging, and capping.

The Committee on Remediation of PCB-Contaminated Sediments (the Committee) formed by the National Research Council did not believe that it is possible to state *a priori* whether natural attenuation, dredging, or caping is applicable, in general terms, to PCB-contaminated sediment sites (NRC, 2001a). The Committee believes that each PCB-contaminated site is unique, and selection of remediation options and determination of a risk-management strategy must be based on site-specific factors and risks. Therefore, each remedial option must be evaluated in the context of the specific contaminant distribution, hydrodynamic properties, and ecological conditions of each reach of a river system. These same conclusions apply to all forms of sediment contamination.

All remedial approaches leave residual contamination that must be managed and monitored (NRC, 2001a). Sampling and analysis of surface water, sediment, and fish; and physical measurements of the bottom of the river and the cap (if applied) are all components of the post-remediation monitoring system. If caps are applied, plans for monitoring and potential long-term maintenance of the cap are required to respond to potential design errors or changes in conditions.

As described in the following subsections each of the remediation methods has substantial disadvantages and problems. Further, these methods typically can only reach a PCB remediation goal of a Surface-area Weighted Average Concentration (SWAC) of 0.25 ppm, which, as noted earlier, often is substantially above the concentrations needed to protect wildlife, but is sufficient to reduce fish tissue PCB concentrations. Therefore, many projects to remediate contaminated sediment have been highly contentious, e.g., the

approximately $500 million project to remediate PCB contamination in the Fox River, Wis., U.S. (see the web site of the Fox River Watch [http://www.foxriverwatch.com/] for an example of the contention). At the present time (2009), the public needs to be patient as better methods are developed for and more experience with remediation are obtained. It must be remembered that a journey of a thousand miles begins with the first step.

Natural attenuation—The in-situ rate of biodegradation of PCBs, PAHs, and organochlorine pesticides in environmental systems is slow. Thus, natural attenuation relies on the natural deposition of clean sediments from upstream burying the contaminated sediments. The new sediments are "clean" because, in the U.S., the industrial sources of heavy metals and PAHs have been reduced by improved non-point source pollution control at factories, whereas production of PCBs was banned by the U.S. Congress in 1976 and by the Stockholm Convention on Persistent Organic Pollutants in 2001. In most harbors on the Great Lakes clean sediments have buried the heavily contaminated sediments, and navigational dredging is done very carefully to remove the clean sediments without disturbing the deeper contaminated sediments.

The natural attenuation process is very slow taking 30 to 40 years or more. For example, the slow rate of natural attenuation is evidenced by only partial recovery of the Fox River, Wis., U.S., despite the passage of 30 years after the bulk of the PCB loadings were discharged to the river (Lue-Hing et al., 2001). Thus, natural attenuation normally is used as complimentary to dredging or capping in the development of a remediation plan, and any remedial approach must be consistent with this natural attenuation process.

Dredging—Dredging involves the physical removal of the contaminated sediment from the river by mechanical or hydraulic means. Mechanical dredges remove material by scooping it from the bottom and then placing it on a waiting barge for transport to a designated Confined Disposal Facility (CDF). The two most common types of mechanical dredges are dipper dredges and clamshell dredges (a special version called a cable arm environmental clamshell often is used to dredge contaminated sediment). Figure 9.24 shows an environmental clamshell dredge removing PCB contaminated sediment from the Kinnickinnic River Great Lakes Legacy Act Cleanup in Milwaukee, U.S. Hydraulic dredges work by sucking a mixture of dredged material and water from the channel bottom. The amount of water sucked up with the material is controlled to make the best mixture. Too little water and the dredge will bog down; too much water and the dredge will not be efficient in moving sediment. Pipeline and hopper dredges are the two main types of hydraulic dredges.

Fig. 9.24 Environmental clamshell dredge removing PCB contaminated sediment from the Kinnickinnic River Great Lakes Legacy Act Cleanup in Milwaukee, U.S. and preparing to place it in a collection barge (photo provided by Dr. Xiaochun Zhang, Wisconsin Department of Natural Resources) (See color figure at the end of this book)

Dredging is most appropriate for exposed and accessible "hot spots" that pose significant risks. Dredging is very attractive conceptually to the public because the contamination removed and stored in a designed containment facility. However, there are many important problems with dredging.

First, dredging will leave a significant residue of contamination behind in the biologically available zone (approximately top 10 cm) that will require capping after completion of dredging activities or, absent such a post-dredging cap, will require repetitive dredging that may protract the recovery of the river by decades. Thus, dredging is far less certain than capping to achieve any given remedial design standard and will leave residual contamination in the biologically available zone (Lue-Hing et al., 2001).

Second, because of the disturbance to the bottom, dredging activities may be expected to result in higher contaminant concentrations in the water column and contact with exposed underlying contaminated sediments during and after cleanup completion until natural recovery processes isolate the residual contamination (Lue-Hing et al., 2001). That is, dredging will generally result in the interim exposure of sediments with higher contaminant concentrations that are not in equilibrium with the water column. Thus, significant contaminant releases into the water column can result during dredging operations.

Third, siting and permitting requirements of the requisite landfill/CDF may impose significant restrictions on the rate and productivity at which a river dredging project can proceed without further degrading the river's water quality. Some projects, such as the Kinnickinnic River Great Lakes Legacy Act Cleanup in Milwaukee may have access to an already designated CDF, however, for many others new CDFs must be developed and permitted before dredging can begin.

Fourth, wastewater and spoil management challenges associated with dredging are difficult to solve for large-scale projects. For example, Lue-Hing et al. (2001) reported that for the Fox River, Wis., U.S. treatment and disposal of the PCB contaminated sediments and the sediment-loaded wastewater will require development of a substantial infrastructure not currently in existence. For the Fox River the spoil management problem was solved by pumping the hydraulically dredged sediment water mixture into geotextile tubes (Fig. 9.25). The geotextile tube allows the water to flow out in response to hydrostatic pressure, which often is increased by stacking geotextile tubes (Fig. 9.25), while the vast majority of sediment is retained in the tubes. The water that "seeps" through the geotextile tubes is collected in a gravel-lined dewatering pad and is pumped to water treatment facilities. Once dewatered and dried in the geotextile tubes, the sediment may be removed and taken to the landfill/CDF.

Fig. 9.25 Geotextile tubes being filled by dredged sediment and water (left) and stack of geotextile tubes dewatering (right) at the Little Lake Butte des Morts project of the Fox River, Wisconsin, U.S. (photos provided by Steven Laszewski) (See color figure at the end of this book)

Fifth, treatment of dredge wastewater is very complex. Typical wastewater constituents requiring control include BOD, total suspended solids, PCBs, arsenic, cadmium, chromium, copper, lead, mercury, DDT and its metabolites, pentachlorophenol, dieldrin, and endrin. The simultaneous presence of PCBs,

mercury, arsenic, and other toxics in the wastewater poses a serious challenge to existing wastewater treatment technology (Lue-Hing et al., 2001). For example, Lue-Hing et al. (2001) noted Fox River demonstration dredging projects to date have not met the applicable pollution discharge limits, even at the demonstration scale. Care must be taken to ensure that the assimilative capacity of the river is not exceeded, otherwise both chronic and acute degradation of the river water quality could result. For the Little Lake Butte des Morts project of the Fox River remediation the wastewater treatment facility includes air floatation, sand filtration, and granular activated carbon in a fixed facility.

In summary, limited river access, high truck traffic density to haul away dewatered sediment to the CDF, residual sediment pollutant concentrations, and treatment requirements for dredged sediments and associated carrier water may make implementation of full-scale contaminated sediments dredging operations on rivers difficult, prolonged, and costly (Lue-Hing et al., 2001). Therefore, great care must be taken in planning large-scale dredging projects for cleanup of contaminated sediments in rivers.

Capping—Immediately upon construction a properly designed sub-aqueous cap will:

(1) Physically isolate contaminated sediment from organisms living at the sediment-water interface thereby substantially eliminating the bio-availability of pollutants.

(2) Attenuate chemical concentrations entering the overlying water.

(3) Provide protection from erosion for the underlying contaminated sediments (thereby preventing transport of contaminants down-river).

Capping is considered very effective for low-solubility and highly sorbed pollutants, like PCBs, where the principal transport mechanism is sediment resuspension and deposition. The effectiveness of a capping remedy is directly proportional to the area covered by the cap and isolated penetrations by individual organisms that extend through the cap will not significantly impact the cap area nor the remedy's overall effectiveness. Capping has one major short-coming that has limited its use in rivers, namely the fact that the contaminated sediment is still in the river, and, thus, is capable of being moved by a storm larger than the design storm. This condition is unacceptable to many environmental groups.

In comparison with dredging, capping would much more quickly isolate the contamination from biological availability and could substantially achieve a projected SWAC design standard upon installation. The reduction in SWAC is faster for capping because (Lue-Hing et al., 2001):

(1) the highest concentration areas can be remediated first,

(2) the benefits of natural attenuation are not sacrificed or deferred as a result of capping as they are with dredging, and

(3) the rate at which capping can proceed is dramatically faster than that for dredging due to the engineering and logistical constraints to which dredging is subject.

In addition to isolating polluted sediments, capping structures can be designed to repair and restore habitats and create new habitats and, by varying the capping material, can provide, promote, or encourage a particular type of habitat for the species for which improved habitat is desired (Lue-Hing et al., 2001). Capping provides the capability to design a diversity of habitats, through selective use of cobble, gravel, sand, and soft sediments as capping materials, to support wetlands, create fish spawning areas, and lower sediment loads, which could give rise to the most suitable environment for providing a diverse fish population. For the Fox River, Wis., U.S., likely opportunities for improved habitat include emergent wetlands, submerged vegetation, cobble-based spawning areas, and reduction of silt bottoms attractive to undesirable species such as carp (Lue-Hing et al., 2001). Placement of cap materials over existing sediment will, however, adversely impact the existing benthic community (as would dredging), and recolonization by benthic macroinvertebrates is slowed by lack of organic matter in the cap.

As an engineered structure, a cap can be designed to be stable in almost any flow regime although the armoring necessary in some environments may compromise other goals for the waterway (e.g., navigation).

The design of any cap material must take into account future stability under varying flow conditions, e.g., flood flow, ice scour, wind induced currents, navigational propeller wash, and potential hydraulic changes in the waterway. To account for these possible destabilizing conditions, the cap may need to be armored with an engineered layer (e.g., coarse gravel or cobble sized material). For the Fox River, Wis., U.S., remediation Lue-Hing et al. (2001) recommended that the cap be designed to be stable under all anticipated flow conditions, including the Standard Project Flood estimated by the U.S. Army Corps of Engineers, which is almost twice as severe as a 100-year flood (1.8 times the 100-year flood). To be effective, a conventional cap must remain in place until natural attenuation and/or fate processes eliminate the potential for exposure and risk from contaminants in the underlying sediments. Given the potential hydraulic difficulties in maintaining cap stability, Lue-Hing et al. (2001) noted that caps had primarily been applied in bays and harbors—Hiroshima Bay, Japan; Long Island Bight, U.S.; Akoni Bay, Japan; Hamilton Harbor, Canada: Pier 51 Ferry Terminal, Seattle, U.S.—and only a few rivers—St. Paul Waterway, Washington, U.S. and St. Lawrence River, New York, U.S. The final design for the remediation PCB contamination in the Fox River, Wis., U.S. will involve a combination of dredging and capping where caps will be used in areas with lower PCB contamination and lower flow energy.

A cap layer of only 5–15 cm will generally isolate the bulk of contaminants from the benthic community and overlying water. However, a minimum cap thickness of 15–30 cm is typical to provide a safety factor, to ensure that the cap layer remains stable even if there is significant heterogeneity in placement thickness, and to protect the overlying water from migration of water through the cap (Lue-Hing et al., 2001). A 15 cm cap with the upper 10 cm compromised by bioturbation will reduce the steady state flux (diffusion) to the overlying water by a factor of about 500, and a 30 cm cap with a 10 cm bioturbation layer gives a reduction factor of about 1500 (Lue-Hing et al., 2001). Sand is commonly used as cap material, however, other cap materials can also be used to satisfy specific objectives such as erosion protection and habitat enhancement. The cap design for the Little Lake Butte Des Morts project of the Fox River remediation is shown in Fig. 9.26. This design includes 17.8 cm (7 in.) of 2.5–3.2 cm (1–1.25 in.) angular stone (7.5 cm [3 in.] as an overplacement allowance) over 15 cm of medium sand (7.5 cm [3 in.] as an overplacement allowance).
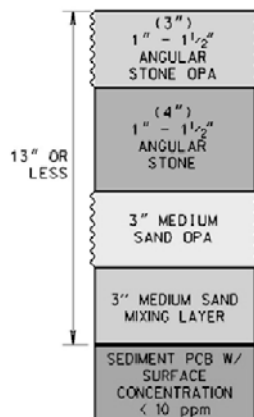
Fig. 9.26 Cap Design for the Little Lake Butte Des Morts project of the Fox River remediation project, Wisconsin, U.S. (figure provided by Steven Laszewski, Foth Infrastructure and Environment, Green Bay, WI)

If subaqueous capping is the selected technology (without dredging), the potential for cap loss and re-exposure of deeper sediments needs to be addressed (NRC, 2001a). Caps can be repaired if needed at relatively low cost.

Summary—The water quality problems discussed in this Chapter are some of the most important and difficult to solve water-quality management issues. Considerable time and money have been and will continue to be expended on the solution of these problems in developed countries, and these are key problems that must be dealt with as developing countries seek to improve their water environment. However, there are many other well-known water quality problems that were not discussed in detail here because of space limitations including: acid rain, acid mine drainage, pesticides, herbicides, heavy metals (away from the sediments), and temperature. Further, a number of new water-quality problems have emerged in recent years such as pharmaceuticals, personal care products, and endocrine disruptors. Despite these many water-quality problems, substantial improvement in the quality of rivers in the U.S. and Europe have been made particularly since the 1970s and the passage of the Clean Water Act. Thus, through societal dedication to solving these problems and the expenditure of the time and money needed to enact and maintain the solutions developing countries can similarly reduce water quality problems and consequently improve public and ecologic health.

Review Questions

1. Short Answer:
   a) What are the scientific, economic, and legal definitions of pollution?
   b) Define CBOD, NBOD, and COD.
   c) List the components of the dissolved oxygen balance of a stream.
   d) Why was the Streeter-Phelps equation acceptable in the early days of stream sanitation studies?
   e) In what ways can benthic deposits potentially affect stream dissolved oxygen?
   f) Why might field measured "SOD" values be much greater that the best reachwise average values?
   g) List the disadvantages of the well known equations for estimation of the reaeration-rate coefficient?
   h) Under what conditions are "bottle" estimates of the BOD decay rate representative of instream conditions?
   i) What has been the traditional complaint against the inclusion of photosynthesis in the consideration of allowable pollutant loads?
   j) List the key habitat features that define physical integrity for aquatic ecosystems.
   k) Describe the different aeration systems that could be applied to rivers.
   l) In what ways do nitrogeneous contaminants influence water quality, the aquatic environment, and public health?
   m) Define eutrophication and algal blooms.
   n) What problems are caused by algae?
   o) List agricultural best management practices (BMPs) for nutrient control. Which BMPs or combination of BMPs are most effective for nutrient management?
   p) Why have numerous water bodies experienced increasing pollutant concentrations even though extensive agricultural best management practices have been installed in the upstream watershed?
   q) List urban best management practices (BMPs) for non-point source pollution control.
   r) Name and describe three water borne diseases.
   s) Describe the problems with the indicator organism approach to detect and monitor pathogen contamination.
   t) List and describe the steps of microbial risk assessment.
   u) Discuss the effectiveness of the various methods for the disinfection of wastewater.
   v) Describe disinfection by-products.

w) Define TEC, MEC, and PEC.

x) Which pollutants are highly likely to adsorb to sediments?

y) List the advantages and disadvantages of the methods to remediate contaminated sediments.

2. a) For a river assume dissolved oxygen is lost to CBOD decay and sediment oxygen demand and it is replaced by atmospheric reaeration. Derive the equation for the stream critical time.

b) Determine the critical deficit for $K_a = 0.8$ day^{-1}, $K_d = 0.2$ day^{-1}, $S_B = 2$ mg/day/L, $D_0 = 1.5$ mg/L, and $L_0 = 10$ mg/L.

3. The Red River of the North in the vicinity of Fargo, North Dakota, receives wastewater flow from the Fargo Wastewater Treatment Plant (WWTP) and the Moorhead, Minnesota, WWTP. The population of Fargo was 73,000 in 1990 and at that time the WWTP was operating at full capacity of 0.42 m^3/s. By 2000 the population of Fargo had grown to 90,600, and the need for capacity expansion at the WWTP was obvious. Develop a Streeter-Phelps model of the Red River of the North to examine capacity expansion issues for the Fargo WWTP.

In the modeling the Red River of the North will be divided into 3 reaches as follows (note: data from Wesolowski (1994)).

Reach	Length (km)	Velocity (m/s)	Depth (m)	Slope	Comments
1	19.0	0.131	0.73	1.136×10^{-4}	Moorhead WWTP to Fargo WWTP
2	11.9	0.165	0.73	1.345×10^{-4}	Fargo WWTP to Sheyenne River
3	18.7	0.131	0.98	0.785×10^{-4}	Sheyenne River to end of study area

For the trial condition the following flows and characteristics should be considered.

Flow Source	Discharge (m^3/s)	BOD (mg/L)	DO (mg/L)
Upstream inflow	1.42	1.5	8.0
Moorhead WWTP	0.14	15.0	6.5
Fargo WWTP	1.07	25.0	5.0
Sheyenne River	0.45	5.7	8.5

The flow for the Fargo WWTP represents a capacity expansion to 1.14 m^3/s more than doubling the current capacity. The BOD concentrations for the WWTPs represent the current permit limits for a 7-day average. The upstream inflow on the Red River is substantially higher than the 7-day, 10-year low flow of 0.31 m^3/s and the flow of the Sheyenne River is double the 7-day, 10-year low flow of 0.23 m^3/s.

Step 1

Determine and plot the dissolved oxygen (DO) and BOD trajectories throughout the study reach. Can the North Dakota state DO standard of 5 mg/L be maintained with the new higher flow from the Fargo WWTP?

Temperature = 24.2℃, $K_d = 0.2$ day^{-1} at 20℃, and K_a is computed using the Tsivoglu and Neal (1976) equation.

Step 2

If the DO concentration does not meet the state standard, determine the allowable BOD discharge from the Fargo WWTP for the trial conditions.

Step 3

Determine and plot the DO trajectory throughout the study reach if the Langbein and Durum (1967) equation is used to determine K_a.

4. For the Red River of the North homework problem, suppose reach 1 also had a reach-wise uniform sediment oxygen demand, S_b, of 0.35 mg/L/day. Compute the dissolved oxygen concentration at the end of each reach.

5. It takes 18 days for 99.9 percent of the *E. Coli* bacteria to be removed (die, settle out) in the Ohio River. What is the appropriate first-order rate constant to describe this data? What can you conclude about the adequacy of the first-order assumption in this case?

Rerences

Alberts E.E., Spomer R.G., 1985. Nitrate movement in deep loess soils. ASAE Paper no. 85-2030. American Society of Agricultural Engineers, St. Joseph, MI

Ackermann W.C., 1981. Water Resources Policy, Class Notes. University of Illinois at Urbana-Champaign, IL

Ambrose R.B., Wool T.A., Connolly J.P. and Schanz R.W., 1988. WASP4, a hydrodynamic and water quality model-Model theory, user's manual, and programmer's guide, Report No. EPA/600/3-87-039. U.S. Environmental Protection Agency, Athens, GA

Archives D'Architecture Moderne, 1997. Brussels and the Senne, Brussels, Belgium

Armstrong C.L., Mitchell J.K. and Walker P.N., 1980. Soil loss estimation-Research in Africa—A review, in Assessment of Erosion, De Boodt M. and Gabriels D. (eds.), John Wiley and Sons, New York, 285–294

Auer M.T., Niehaus S.L., 1993. Modeling fecal coliform bacteria-I. Field and laboratory determination of loss kinetics. Water Research, 27(4), 693–701

Beck M.B., Jeffrey P., 2007. Sustainable standpoints-Embracing diversity of opinion, Water 21, August, 13–14

Bennett J.P., Rathbun R.E., 1972. Reaeration in open channel flow. U.S. Geological Survey Professional Paper No. 737. U.S. Geological Survey, Washington, DC

Borah D., Demissie M. and Keefer L., 1996. Effect of best management practice locations in the Upper Sangamon River Basin on nitrogen loading to Lake Decatur, in Proceedings, Rivertech '96: 1st International Conference on New/Emerging Concepts for Rivers, Maxwell W.H.C., Preul H.C., Stout G.E. (eds.), Chicago, IL, September 22–25, 665–672

Bowie G., Mills W., Porcella D., Campbell C., Pagenkopf J., Rupp G., Johnson K., Chan P., Gherini S. and Chamberlin C., 1985. Rates, constants and kinetics formulations in surface water quality modeling (2nd edition), Report No. EPA-600/3-85/040, U.S. Environmental Protection Agency, Athens, GA

Bower P.A., Scopel C.O., Jensen E.T., Depas M.M. and McLellan S.L., 2005. Detection of genetic markers of fecal indicator bacteria in Lake Michigan and determination of their relationship to Escherichia coli densities using standard microbiological methods. Applied and Environmental Microbiology, 71(12), 8305–8313

Braden J.B., 1988. Nonpoint pollution policies and politics: The role of economic incentives, in Nonpoint Pollution 1988: Policy, Economy, Management and Appropriate Technology, Novotny V. (ed.), American Water Resources Association, Bethesda, MD, 57–65

Brown L.C. and Barnwell T. O., 1987. The enhanced stream water quality models QUAL2E and QUAL2E-UNCAS: Documentation and user manual, Report No. EPA/600/3-87/007. U.S. Environmental Protection Agency, Athens, GA

Butts T.A., Shackleford D.B. and Bergerhouse T.R., 2000. Sidestream elevated pool aeration (SEPA) stations: Effect on instream dissolved oxygen. Illinois State Water Survey Contract Report 2000-02, Champaign, IL

Cabelli V.J., 1983. Health effects criteria for marine recreational waters, Report No. EPA-600-1-80-031, U.S. Environmental Protection Agency, Cincinnati, OH

Cabelli V.J., DuFour A.P., McCabe L.J. and Levin M.A., 1982. Swimming-associated gastroenteritis and water quality. American Journal of Epidemiology, 115, 606–616

Camacho R., 1990. Agricultural BMP nutrient reduction efficiencies: Chesapeake Bay watershed model BMPS. Interstate Commission on the Potomac River Basin Report 90-7, Rockville, MD, 24

Camacho R., 1993. Chesapeake Bay Program nutrient reduction strategy reevaluation: Report 8 financial cost effectiveness of point and nonpoint source nutrient reduction technologies in the Chesapeake Bay Basin. Interstate Commission

on the Potomac River Basin Report 92-4, Rockville, MD, 114

Casman E., 1990. Selected BMP efficiencies wrenched from empirical studies, second edition. Interstate Commission on the Potomac River Basin Report 90-10, Rockville, MD, 71

Chang J.C.H., Ossoff S.F., Lobe D.C., Dorfman M.H., Dumais C., Qualls R.G. and Johnson J.D., 1985. UV inactivation of pathogenic and indicator microorganism. Applied and Environmental Microbiology, 49(6), 1361–1365

Chapra S.C., 1997. Surface Water Quality Modeling, McGraw-Hill, Boston, 844

Chick H., 1908. An investigation of the laws of disinfection. Journal of Hygiene, 8(1), 92–158

Churchill M.A., Elmore H.L. and Buckingham R.A., 1962. Prediction of stream aeration rates. Journal of the Sanitary Engineering Division, ASCE, 88(SA4), 1–46

Clancy J.L., Linden K.G. and McCuin R.M., 2004. Cryptosporidium occurrence in wastewaters and control using UV disinfection. IUVA News, 6(3)

Clark J.W., Viessman W., Jr. and Hammer M.J., 1977. Water supply and pollution control. 3rd Edition, Crowell, Harper & Row, New York, 857

Clausen J.C., Meals D.W. and Cassell E.A., 1992. Estimation of lag time for water quality response to BMPS, Proceedings, The National RCWP Symposium, 10 Years of Controlling Agricultural Nonpoint Source Pollution: The RCWP Experience, September 13–17, Orlando, FL, 173–179

Cleveland K.D., 1989. Predicting reaeration rates in Texas streams. Journal of Environmental Engineering, 115(3), 620–632

Connolly J.P., Blumberg A.F. and Quadrini J.D., 1999. Modeling fate of pathogenic organisms in coastal waters of Oahu, Hawaii. Journal of Environmental Engineering, 125(5), 398–406

Consoer Townsend Envirodyne (CTE), 2007 Supplemental aeration of the North and South Branches of the Chicago River, Technical Memorandum 4WQ, report submitted to the Metropolitan Water Reclamation District of Greater Chicago, Chicago, IL

Cooper J.R. and Gilliam, J.W. 1987. Phosphorus redistribution for cultivated fields in riparian areas, Journal of the Soil Science Society of America, 51, 1600–1604.

Crane S.R. and Moore J.A., 1986. Modeling enteric bacterial die-off: A review. Water, Air, and Soil Pollution, 27, 411–439

Davis M.L. and Masten S.J., 2004. Principles of Environmental Engineering and Science, McGraw-Hill, New York, 704

Demuynck C. and Bauwens W., 1996. Modelling of the Water Quality of the River Zenne in the Brussels Region. Laboratory of Hydrology, Vrije Universiteit Brussel

Demuynck C., Bauwens W., De Pauw N., Dobbelaere I. and Poelman E., 1997. Evaluation of pollution reduction scenarios in a river basin: Application of long term water quality simulations. Water Science and Technology, 35(9), 65–75

Di Toro D.M., 2001. Sediment Flux Modeling. John Wiley and Sons, New York, 624

Dillaha T.A., Sherrard J.H., Lee D., Mostaghimi S. and Shanholtz V.O., 1988. Evaluation of vegetative filter strips as a best management practice for feed lots. Journal of the Water Pollution Control Federation, 60(7), 1231–1238

Doran J.W., 1987. Microbial biomass and mineralizable nitrogen distributions in no-tillage and plowed soils. Biology of Fertilized Soils, 5, 68–75

DUFLOW, 2000. DUFLOW for Windows V3.3: DUFLOW modelling studio: User's guide, reference guide DUFLOW, and reference guide RAM, EDS/STOWA, Utrecht, The Netherlands

DuFour A.P., 1984. Health effects criteria for fresh recreational waters, Report No. EPA-600/1-84-004, U.S. Environmental Protection Agency, Cincinnati, OH

Ellis B.G., Gold A.J. and Loudon T.L., 1985. Soil and nutrient runoff losses with conservation tillage, in A Systems Approach to Conservation Tillage, D'Itri F.M., ed., Lewis Publishers, Chelsea, MI, 275–291

Elshorbagy A. and Ormsbee L., 2006. Object-oriented modeling approach to surface water quality management. Environmental Modeling and Software, 21, 689–698

Engineering Board of Review, 1925. Report of the Engineering Board of Review of the Sanitary District of Chicago

on the Lake Lowering Controversy and a Program of Remedial Measures. Part II. The Technical Bases for the Recommendations of the Board of Review, Chicago, IL

Fair G.M., Geyer J.C. and Okun D.A., 1971. Elements of water supply and wastewater disposal. John Wiley & Sons, New York, 752

Flores H.E., 1998. Equations for estimating the reaeration-rate coefficient in natural streams developed from USGS national database, Thesis M.S., University of Illinois, Urbana, IL

Foundation for Water Research, 1998. Manual: Urban Water Pollution Management, 2nd Edition, October 1998, Buckinghamshire, United Kingdom

Garrison P.J. and Asplund T.R., 1993. Long-term (15 years) results of NPS controls in an agricultural watershed upon a receiving lake's water quality. Water Science and Technology, 28(3–5), 441–449

Gaynor J.D. and Findlay W.I., 1995. Soil and phosphorus loss from conservation and conventional tillage in corn production. Journal of Environmental Quality, 24, 734–741

Geosyntec 2008. Dry and Wet Weather Risk Assessment of Human Health: Impacts of Disinfection vs. No Disinfection of the Chicago Area Waterways System (CWS), Report submitted to the Metropolitan Water Reclamation District of Greater Chicago, Project No. CHE8188, Chicago, IL

Gerba C.P., Gramos D.M. and Nwachuku N., 2002. Comparative inactivation of enteroviruses and adenovirus 2 by UV light. Applied and Environmental Microbiology, 68(10), 5167–5169

Goolsby D.A. and Battaglin W.A., 2000. Nitrogen in the Mississippi Basin-Estimating sources and predicting flux to the Gulf of Mexico. U.S. Geological Survey Fact Sheet 135-00, Reston, VA

Grant R.S. and Skavroneck S., 1980. Comparison of tracer methods and predictive equations for determination of stream-reaeration coefficients on three small streams in Wisconsin. U.S. Geological Survey Water Resources Investigations Report No. 80–19, U.S. Geological Survey, Madison, WI

Gualtieri C., Gualtieri P. and Doria G.P., 2001. Discussion of Reaeration equations derived for U.S. Geological Survey database. Journal of Environmental Engineering, 126(12), 1159

Guntermann K.L., Lee M.T. and Swanson E.R., 1975. The off-site sediment damage function in selected Illinois watersheds. Journal of Soil and Water Conservation, 30(5), 219–224

Haas C.N., Rose J.B. and Gerba C.P., 1999. Quantitative Microbial Risk Assessment. John Wiley and Sons, New York, 449

Hamdy A. and Jatinder K.B., 1972. Effect of turbulence on BOD testing. Journal of the Water Pollution Control Federation, 44, 1798–1807

Hardwood V.J., Levine A.D., Scott T.M., Chivukula V., Lukasik J., Farrah S.R. and Rose J.B., 2005. Validity of the indicator organism paradigm for the pathogen reduction in reclaimed water and public health protection. Applied and Environmental Microbiology, 71(6), 3163–3170

Harremoës P., 1982. Urban storm drainage and water pollution, in Urban Stormwater Quality, Management and Planning, Yen B.C. (ed.), Water Resources Publications, Littleton, CO, 469–494

Harris H.J. and Kraft C., 1993. The State of the Bay: A watershed perspective the condition of the bay of green bay/lake Michigan. University of Wisconsin-Green Bay, Green Bay, WI

Health Canada, 2004. Guidelines for Canadian Drinking Water Quality: Supporting Documentation-Enteric Viruses, Ottawa, Canada

Hilsenhoff W.L., 1987. An improved biotic index of organic stream pollution, Great Lakes Entomology, 20, 31–39

Hörman A., Rimhanen-Finne R., Maunula L., Von Bonsdorff C.H., Torvela N., Hiekinheimo A. and Hänninen M.L., 2004. Campylobacter spp., giardia spp., cryptosporidium spp., noroviruses, and indicator organisms in surface water in southwestern Finland. Applied and Environmental Microbiology, 70(1), 87–95

Hren J., 1984. Determination of reaeration coefficients for Ohio streams, U.S. Geological Survey Water Resources Investigations Report No. 84-4139, U.S. Geological Survey, Columbus, OH

Illinois Environmental Protection Agency (IEPA), 1987. Quality Assurance and Field Methods Manual, Bureau of Water, Division of Water Pollution Control. Planning Section, Springfield, IL

James A. (ed.), 1993. An introduction to water quality modeling, 2nd edition. John Wiley & Sons, New York, 311

Jiang S., Noble R. and Chu W., 2001. Human adenoviruses and coliphages in urban runoff-Impacted coastal waters in southern California. Applied and Environmental Microbiology, 67(1), 179–184

Jin G., Englande A.J., Bradford H. and Jeng H.W., 2004. Comparison of E. coli, enterococci, and fecal coliform as indicators for brackish water quality assessment. Water Environment Research, 76(3), 245–255

Kanwar R.S., Baker J.L. and Baker D.G., 1987. Tillage and N-fertilizer management effects on ground water quality. ASAE Paper no. 87-2077, American Society of Agricultural Engineers, St. Joseph, MI

Karr J.R. and Dudley D.R., 1981. Ecological perspectives on water quality goals. Environmental Management, 5, 55–68

Kilpatrick F.A., Rathbun R.E., Yotsukura N., Parker G.W. and De Long L.L., 1989. Determination of stream reaeration coefficients by use of tracers. U.S. Geological Survey Techniques in Water-Resources Investigations, Book 3, Chapter A18, U.S. Geological Survey, Reston, VA

Kreis R.D., Scalf R.M. and McNabb J.F., 1972. Characteristics of rainfall runoff from a beef cattle feedlot, Report No. EPA-R2-72-061, Robert S. Kerr Environmental Research Laboratory, Ada, OK

Langbein W.D. and Durum W.H., 1967. The aeration capacity of streams, U.S. Geological Survey Circular 542. U.S. Geological Survey, Washington, DC

Langdale G.W., Leonard R.A. and Thomas A.W., 1985. Conservation practice effects on phosphorus losses from southern Piedmont watersheds. Journal of Soil and Water Conservation, 40(1), 157–161

Levanon D., Codling E.E., Meisinger J.J. and Starr J.L., 1993. Mobility of agrochemicals through soil from two tillage systems. Journal of Environmental Quality, 22, 155–161

Lue-Hing C., Lynam B.T. and Zenz D.R., 1976. Wastewater disinfection: The case against chlorination, Department of Research and Development Report No. 76-17, Metropolitan Sanitary District of Greater Chicago, Chicago, IL, 53

Lue-Hing C., Bhowmik N.G., Hayes D.F., Johnson M.L., Patterson J.W., Reible D.D. and Teal J.M., 2001. Ecosystem-Based Rehabilitation Plan: An Integrated Plan for Habitat Enhancement and Expedited Exposure Reduction in the Lower Fox River and Green Bay, Report prepared by the Johnson Company, Inc., Montpelier, VT

MacDonald D.D., Ingersoll C.G. and Berger T.A., 2000. Development and evaluation of consensus-based sediment quality guidelines for freshwater aquatic ecosystems. Archives of Environmental Contamination and Toxicology, 39, 20–31

Manache G. and Melching C.S., 2004. Sensitivity analysis of a water-quality model using Latin hypercube sampling. Journal of Water Resources Planning and Management, 130(3), 232–242

Manache G., Melching C.S. and Lanyon R., 2007. Calibration of a continuous simulation fecal coliform model based on historical data analysis. Journal of Environmental Engineering, 133(7), 681–691

Mancini J.L., 1978. Numerical estimates of coliform mortality rates under various conditions. Journal Water Pollution Control Federation, 50(11), 2477–2484

Masters G.M., 1991. Introduction to Environmental Engineering and Science, Prentice Hall. Englewood Cliffs, N.J., 460

Melching C.S., 1998. Accuracy of tracer measurement of gas-desorption rates, in Environmental Hydraulics, Lee J.H.W., Jayawardena A.W. and Wang Z.Y. (eds.), Balkema A.A. Rotterdam, The Netherlands, 481–486

Melching C.S. and Avery C.C., 1990. An introduction to watershed management for hydrologists, Vrije Universiteit Brussel Hydrologie Report 18, Brussels, Belgium, 128

Melching C.S. and Chang T.J., 1996. Simulation of water quality for Salt Creek in northeastern Illinois, U.S. Geological Survey Open-File Report 96-318, U.S. Geological Survey, Urbana, IL

Melching C.S. and Flores H.E., 1999. Reaeration equations derived from USGS data base. Journal of Environmental Engineering, 125(5), 407–414

Melching C.S. and Yoon C.G., 1996. Key sources of uncertainty in QUAL2E model of Passaic River. Journal of Water Resources Planning and Management, 122(2), 105–113

Melching C.S., Alp E., Shrestha R.L. and Lanyon R., 2004. Simulation of water quality during unsteady flow in the Chicago Waterway System, Proceedings CD-ROM, Watershed 2004, Dearborn, Michigan, July 11–14, 2004, Water Environment Federation

Metropolitan Water Reclamation District of Greater Chicago (MWRDGC), 2006. Expert review report regarding United States Environmental Protection Agency's water quality criteria-1986: Application to secondary contact recreation, Department of Research and Development Report No. 2006-38, Metropolitan Water Reclamation District of Greater Chicago, Chicago, IL, 27

National Research Council, 1994. Science and judgment in risk assessment. National Academy Press, Washington, DC

National Research Council (NRC), 2001a. A risk management strategy for PCB-Contaminated sediments. National Academy Press, Washington, DC

National Research Council (NRC), 2001b. Assessing the TMDL approach to water quality management, Committee to Assess the Scientific Basis of the TMDL Approach to Water Pollution Reduction, National Academy Press, Washington, DC

National Technical Committee of the Secretary of the Interior, 1968. Water quality criteria. Federal Water Pollution Control Administration, Washington, DC.

Nelson K., Sheikh B., Cooper R.C., Holden R. and Israel K., undated. Efficacy of Pathogen Removal During Full-Scale Operation of Water Reuse Facilities in Monterey, California

New Jersey Department of Environmental Protection, 1987. Passaic river water quality management study. Report, New Jersey Department of Environmental Protection, Trenton, NJ

Noble R.T. and Furhman J.A., 2001. Enteroviruses detected by reverse transcriptase polymerase chain reaction from the coastal waters of Santa Monica Bay, California: Low correlation to bacterial indicator levels. Hydrobiologia, 460, 175–184

Noble R.T., Griffith J.F., Blackwood A.D., Furhman J.A., Gregory J.B., Hernandez X., Liang X., Bera A.A. and Schiff K., 2006. Multi-tiered approach using quantitative PCR to track sources of fecal pollution affecting Santa Monica Bay, California. Applied and Environmental Microbiology, 71(2), 1604–1612

Novotny V., 2003. Water Quality-Diffuse Pollution and Watershed Management, 2nd Edition, Wiley, New York, 864

O'Connor D.J., 1967. The temporal and spatial distribution of dissolved oxygen in streams. Water Resources Research, 3(1), 65–79

O'Connor D.J. and Dobbins W.E., 1958. Mechanism of reaeration in natural streams. Transactions, ASCE, 123(2934), 641-684

Ohio Environmental Protection Agency, 1989. Biological Criteria for the Protection of Aqautic Life: Volume III: Standardized Biological Field Sampling and Laboratory Method for Assessing Fish and Macroinvertebrate Communities, Ecologic Assessment Section, Division of Water Quality Planning & Assessment, Ohio Environmental Protection Agency, Columbus, OH

Oregon Department of Environmental Quality (DEQ), 1994. Issue paper: Bacteria. Oregon Department of Environmental Quality, Portland, OR, 47

Owens M., Edwards R.W. and Gibbs J.W., 1964. Some reaeration studies in streams. International Journal of Air and Water Pollution, 8, 469–484

Paraskeva P. and Graham N.J.D., 2002. Ozonation of municipal wastewater effluents. Water Environment Research, 74(6), 569–581

Park S.W., 1981. Modeling soil erosion and sedimentation on small agricultural watersheds, Ph.D. Thesis, Department of Agricultural Engineering. University of Illinois at Urbana-Champaign, IL, 258

Parker G.W. and DeSimone L.A., 1992. Estimating reaeration coefficients for low-slope streams in Massachusetts and New York, U.S. Geological Survey Water Resources Investigations Report No. 91-4188, U.S. Geological Survey, Marlborough, MA

Parker G.W. and Gay F.B., 1987. A procedure for estimating reaeration coefficients for Massachusetts streams, U.S. Geological Survey Water Resources Investigations Report No. 86-4111. U.S. Geological Survey, Boston, Mass

Parson M.J., Morse C. and DePue M., 2004. Effectiveness of commonly used urban best management practices, Proceedings CD-ROM, Watershed 2004, Dearborn, Michigan, July 12-14, 2004, Water Environment Federation

Pitt R., 2004. Control of Microorganisms in Urban Waters. (http://unix.eng.ua.edu/~rpitt/Class/ ExperimentalDesignFieldSampling/MainEDFS.html, acce Pitt R., ssed 11/13/2009)

Rankin E.T., 1989. The Qualitative Habitat Evaluation Index [QHEI]: Rationale, Methods and Application, Ecologic Assessment Section, Division of Water Quality Planning & Assessment, Ohio Environmental Protection Agency, Columbus, OH

Rathbun R.E. and Grant R.S., 1978. Comparison of the radioactive and modified techniques for measurement of stream reaeration coefficients, U.S. Geological Survey Water Resources Investigations Report No. 784-68, U.S. Geological Survey, Madison, WI

Robison R., 1994. Chicago's waterfalls, Civil Engineering, 64(7), 36–39

Sawyer C.N., 1947. Fertilization of lakes by agricultural and urban drainage. Journal of the New England Water Works Association, 41(2), 109–127

Schmidt A.R. and Stamer J.K. 1987. Assessment of water quality and factors affecting dissolved oxygen in the Sangamon River, Decatur to Riverton, Illinois, summer 1982, U.S. Geological Survey Water Resources Investigations Report No. 87-4024. U.S. Geological Survey, Urbana, IL

Sedita S.J., Lue-Hing C. and Haas C.N., 1987. Effects of ceasing chlorination on selected indicator populations downstream of metropolitan Chicago's major wastewater treatment facilities, Department of Research and Development Report No. 87-17, Metropolitan Sanitary District of Greater Chicago, Chicago, IL, 15

Shalit G., Steenhuis T.S., Hakvoort H.M., Boll J., Geohring L.D. and van Es H.M., 1995. Subsurface drainage water quality from structured soil, Journal of Irrigation and Drainage Engineering, 121(3), 239–247

Sheng T.C., 1981. The need for soil conservation structures for steep cultivated slopes in the humid tropics, in Tropical Agricultural Hydrology: Watershed Management and Land Use, Lal, R. and Russell, E.W. (eds.), Wiley and Sons, New York, 189–200

Shindala A. and Traux D.D., 1980. Reaeration characteristics of small streams, Report No. MSSU-EIRS-CE-80-6, Mississippi State University, Engineering and Industrial Research Station, Mississippi State, MS

Smith P.L., Ragotzkie R.A., Andren A.W. and Harris H.J., 1988. Estuary rehabilitation: The Green Bay story. Oceanus, 31(3), 12–20

Smith E.P., Ye K., Hughes C. and Shabman L., 2001. Statistical assessment of violations of water quality standards under Section 303(d) of the Clean Water Act. Environmental Science and Technology, 35, 606–612

Solow R.M., 1971. The economist approach to pollution and its control. Science, 173, 497–503

Southeastern Wisconsin Regional Planning Commission (SEWRPC), 2007. A Regional Water Quality Management Plan Update for the Greater Milwaukee Watersheds. Planning Report No. 50, Waukesha, WI

St. John J.R., Gallagher T.W. and Paquin P.R., 1984. The sensitivity of the dissolved oxygen balance to predictive reaeration equations. In Gas Transfer at Water Surface, Brutsaert W. and Jirka G. (eds.), Reidel D., Publishing Company, Dordrecht, The Netherlands, 577–588

Streeter H.W. and Phelps E.B., 1925. A study of the pollution and purification of the Ohio River, III. Factors concerned in the phenomena of oxidation and reaeration. Public Health Bulletin 146, U.S. Public Health Service, Washington, DC

Terstriep M.L., Bender G.M. and Noel D.C., 1982. Final report. Nationwide Urban Runoff Project, Champaign, Illinois-Evaluation of the effectiveness of municipal street sweeping in the control of urban storm runoff pollution, Illinois State Water Survey Contract Report 300, Champaign, IL, 240

Thackston E.L. and Krenkle P.A., 1969. Reaeration prediction in natural streams. Journal of the Sanitary Engineering Division, ASCE, 95(1), 65–94

Thomann R.V., 1972. Systems Analysis and Water Quality Management, McGraw-Hill, New York, 286

Thomann R.V. and Mueller J.A., 1987. Principles of Surface Water Quality Modeling and Control, Harper and Row, New York, 644

Thurston-Enriquez J.A., Haas C.N., Jacangelo J. and Gerba C.P., 2003a. Chlorine inactivation of adevovirus type 40 and feline calicivirus, Applied and Environmental Microbiology, 69(7), 3979–3985

Thurston-Enriquez J.A., Haas C.N., Jacangelo J. and Gerba C.P., 2005. Inactivation of enteric adenovirus and feline calicivirus by ozone. Water Research, 39(15), 3650–3656

Thurston-Enriquez J.A., Haas C.N., Jacangelo J., Riley K. and Gerba C.P., 2003b. Inactivation of feline calicivirus

and adenovirus type 40 by UV radiation. Applied and Environmental Microbiology, 69(1), 577–582

Tsivoglou E.C. and Neal L.A., 1976. Tracer measurement of reaeration. III. Predicting the reaeration capacity of inland streams. Journal of the Water Pollution Control Federation, 48(12), 2669–2689

Tsivoglou E.C., Cohen J.B., Shearer S.D. and Godsil P.J. 1968. Tracer measurement of stream aeration. II. Field studies. Journal of the Water Pollution Control Federation, 40(2), 285–305

Tsivoglou E.R. and Wallace J.R., 1972. Characterizing stream reaeration capacity, Report No. EPA-R3-72-012, U.S. Environmental Protection Agency, Washington, DC

U.S. Environmental Protection Agency (USEPA), 1986a. Ambient water quality criteria for bacteria, Report No. EPA-440/5-84-002, Washington, DC

U.S. Environmental Protection Agency (USEPA), 1986b. Ambient water quality criteria for dissolved oxygen, Report No. EPA 440/5-86-003, Office of Water, Regulations and Standards Criteria and Standards Division, Washington, DC

U.S. Environmental Protection Agency (USEPA), 1989. Assessment guidance for superfund: Volume I-Human health evaluation manual (Part A), Interim Final, Report No. EPA/540/1-89/002, Washington, DC

U.S. Environmental Protection Agency (USEPA), 1997a. Guiding principles for Monte Carlo analysis, Office of Research and Development Risk Assessment Forum, Report No. EPA/630/R-97/001, Washington, DC

U.S. Environmental Protection Agency (USEPA). 1997b. The quality of our nation's water: 1996, Report No. EPA 841-S-97-001, Washington, DC

U.S. Environmental Protection Agency (USEPA), 1998. 1998 update of ambient water quality criteria for ammonia. Report No. EPA 822-R-98-008, Office of Water, Washington, DC. (Available online at http://www.epa.gov/ost/standards/nh3_rpt.pdf, accessed 10/29/09)

U.S. Environmental Protection Agency (USEPA). 1999a. 1999 update of ambient water quality criteria for ammonia. Report No. EPA 822-R-99-014, Office of Water, Washington, DC. (Available online at http://www.epa.gov/waterscience/criteria/ammonia/99update.pdf, accessed 10/29/09)

U.S. Environmental Protection Agency (USEPA). 1999b. Alternative disinfectants and oxidants guidance manual, Report No. EPA 815-R-99-014, Washington, DC

U.S. Environmental Protection Agency (USEPA). 1999c. Proposed revisions to the water quality planning and management regulations; Proposed Rule 40 CFR Part 130, Federal Register, 64(162)

U.S. Environmental Protection Agency (USEPA). 2002. The occurrence of disinfection by-products (DBPs) of health concern in drinking water: Results of a nationwide DBP occurrence study, Report No. EPA/600/R-02/068, Washington, DC

U.S. Environmental Protection Agency (USEPA). 2003a. Implementation guidance for ambient water quality criteria for bacteria, Report No. EPA-823-B-03, November, Draft

U.S. Environmental Protection Agency (USEPA). 2003b. Ultraviolet disinfection guidance manual, Report No. EPA 815-D-03-007, Office of Water, Wasington, DC

Wang X., 2006. Management of agricultural nonpoint source pollution in China: Current status and challenges. Water Science and Technology, 53(2), 1–9

Water Environment Research Foundation (WERF), 2004. Evaluation of Microbial Risk Assessment Techniques. WERF, Alexandria, VA

Water Environment Research Foundation (WERF), 2005. Effects of Wastewater Disinfection on Human Health, Report No. 99-HHE-l, WERF, Alexandria, VA

Welch E.B., 1980. Ecological Effects of Waste Water, Cambridge University Press, Cambridge, UK

Werner W. and Wodsak H.P., 1995. The role of non-point nutrient sources in water pollution-Present situation, countermeasures, outlook. Water Science and Technology, 31(8), 87–97

Wesolowski E.A., 1994. Calibration, verification, and use of a water-quality model to simulate effects of discharging treated wastewater to the Red River of the North at Fargo, North Dakota, U.S. Geological Survey Water Resources Investigations Report, 94–4058

Whipple W., Coughlan F.P. and Yu S.L., 1970. Instream aerators of Polluted rivers. Journal of the Sanitary Engineering Division, ASCE, 96(SA5), 1153–1165

Whitaker F.D., Heinemann H.G. and Burwell R.E., 1978. Fertilizing corn adequately with less nitrogen. Journal of Soil and Water Conservation, 33(1), 28–32

Wilkinson J., Jenkins A., Wyer M. and Kay D., 1995. Modelling faecal coliform dynamics in streams and rivers. Water Research, 29(3), 847–855

Wilson G.T. and Macleod N., 1974. A critical appraisal of empirical equations and models for the prediction of the coefficient of reaeration of deoxygenated water. Water Research, 8(6), 341–366

Wisconsin Department of Natural Resources (WDNR). 2003. Consensus-based sediment-quality guidelines: Recommendations for use and application, Publication No. PUBL-WT-732-2003, Madison, WI

Wollast R., et al., 1992. Réseau de Surveillance des Écoulements et des Charges Polluantes dans les Collecteurs D'Amenée à la Future Station D'Épuration de Bruxelles - Nord, Laboratorie de Traitement des Eaux et Pollution, Université Libre de Bruxelles, Belgium

World Health Organization (WHO), 2003. Guidelines for Safe Recreational Waters: Volume 1, Coastal and Fresh Waters, Geneva, Switzerland

World Health Organization (WHO), 2004. Water, sanitation and hygiene links to health, Fact Sheet, http://www.who.int/water_sanitation_health/publications/facts2004/en/print.html, accessed 11/12/2009

Wright R.M. and McDonnell A.J., 1979. In-stream deoxygenation rate prediction. Journal of the Environmental Engineering Division, 105(EE2), 323-335

10 River Ecology and Restoration

Abstract

The biological community of a river ecosystem is determined by the characteristics of both terrestrial and aquatic ecosystems. The terrestrial ecosystem depends mainly on the plant community and the aquatic ecosystem comprises aquatic plants, benthic invertebrates, and vertebrates. The main ecological functions of rivers are habitat, conduit, filter, barrier, source, and sink. Ecological stresses are defined as the disturbances that bring changes to river ecosystems. The ecological stresses are natural events or human-induced activities that occur separately or simultaneously. The structure of a system and its capability of carrying out important ecological functions may be changed by stresses, regardless of whether they act individually or in combination. Damming, gravel and sand mining, channelization, water diversion, habitat fragmentation, exotic species, landslides and debris flows, and intensive fluvial processes are the most common stresses on stream ecology.

For quantitative assessment of river ecology indicator species are selected, which are defined as a set of organisms whose characteristics are used as an index of attributes or environmental conditions of interest, which are too difficult, inconvenient, or expensive to measure for other species. Benthic invertebrates and fish are used as indicator species for most stream ecology assessment. The ecosystem can be assessed by monitoring the species richness (number of species) and the number density (or abundance) for each species. Many parameters representing biodiversity of river ecosystems have been proposed. Management and restoration of river ecosystems are based on an understanding of the relations between physical, chemical, and biological processes at varying time scales. Often, human activities have accelerated the temporal progression of these processes, resulting in unstable flow patterns and altered biological structure and function of stream corridors. Various strategies for ecological restoration are discussed in this chapter.

Key words

Stream corridor, Ecological stresses, Indicator species, Benthic invertebrates, Ecological restoration, Biodiversity

10.1 River Ecosystems

10.1.1 Spatial Elements of River Ecosystems

Ecosystems of rivers vary greatly in size. Taking a deeper look into these ecosystems can help to explain the functions of landscapes, watersheds, floodplains and streams, as shown in Fig. 10.1. In ecosystems movement between internal and external environments is common. This may involve movement of materials (e.g. sediment and storm water runoff), organisms (e.g. mammals, fish and insects) and also energy (e.g. heating and cooling of stream waters).

Many sub-ecosystems form a river ecosystem which, in turn, can also be part of a larger scale landscape ecosystem. The structure and functions of the landscape ecosystem are in part determined by the structure and functions of the river ecosystem. The river ecosystem may have input or output relations with the landscape ecosystem, thus, the two are related. In order to plan and design a river ecosystem restoration, it is vital to first investigate the relations between the ecosystems. Landscape ecologists use four basic terms to define spatial structure at a particular scale:

1. Matrix—the land cover that is dominant and interconnected over the majority of the land surface. Theoretically the matrix can be any land cover type but often it is forest or agriculture.

2. Patch—a nonlinear area (polygon) that is less abundant than, and different from, the matrix.

3. Corridor—a special type of patch that links other patches in the matrix. Usually, a corridor is linear or elongated in shape, such as a stream corridor.

4. Mosaic—a collection of patches, none of which are dominant enough to be interconnected throughout the landscape.
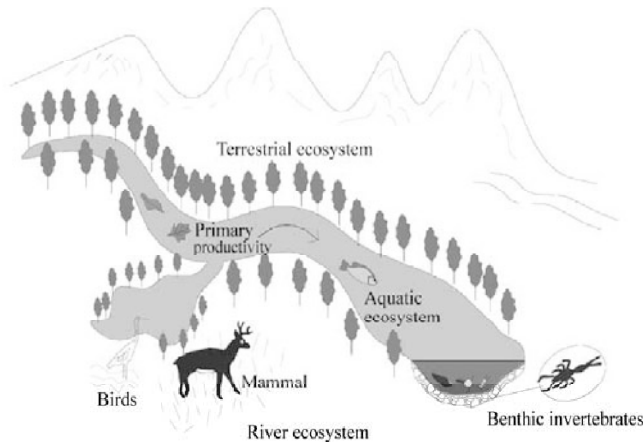
Fig. 10.1 A river ecosystem consists of the terrestrial ecosystem and the aquatic ecosystem, which is affected by and impacts on the landscape ecosystem through input and output (after FISRWG, 1997)

Figure 10.2 shows examples of a forest matrix, a city patch, a stream corridor, and a mosaic consisting of a lake, island, forest and hills. One may see a matrix of mature forest, cropland, pasture, clear-cuts, lakes, and wetlands on a landscape scale. However, on a river reach scale, in a matrix of less desirable shallow waters, a trout may perceive pools and well sheltered, cool, pockets of water as preferred patches and in order to travel safely among these habitat patches, the stream channel may be its only alternative. The matrix-patch-corridor-mosaic model is a very useful, basic way of describing structure in the environment at all levels. When planning and designing ecosystem restoration, it is very important to always consider multiple scales.

The stream corridor is an ecosystem with an internal and external environment (its surrounding landscape). Stream corridors often serve as a primary pathway for the aforementioned movement of energy, materials, and organisms in, through, and out of the system. This may be accomplished by connecting patches and functioning as a conduit between ecosystems and their external environment. Movement in, through, and out of the ecosystem may be dictated by spatial structure, especially in corridors; conversely, this movement also serves to change the structure over time. Thus, the end result of past movement is the spatial structure, as it appears at any point in time. In order to work with ecosystems at any scale it is paramount to understand the feedback loop between movement and structure.

Many of the functions of the stream corridor are strongly interlinked with drainage patterns. So, many people commonly use the term 'watershed scale', and it will also be used in this chapter. A *watershed* is defined as an area of land that drains water, sediment, and dissolved materials to a common outlet at some point along a stream channel (Dunne and Leopold, 1978). Watersheds, therefore, occur at many different scales, ranging from the watersheds of very small streams that measure only a few km^2 in size to the largest river basins, such as the Yangtze River watershed. The matrix, patch, corridor, and mosaic
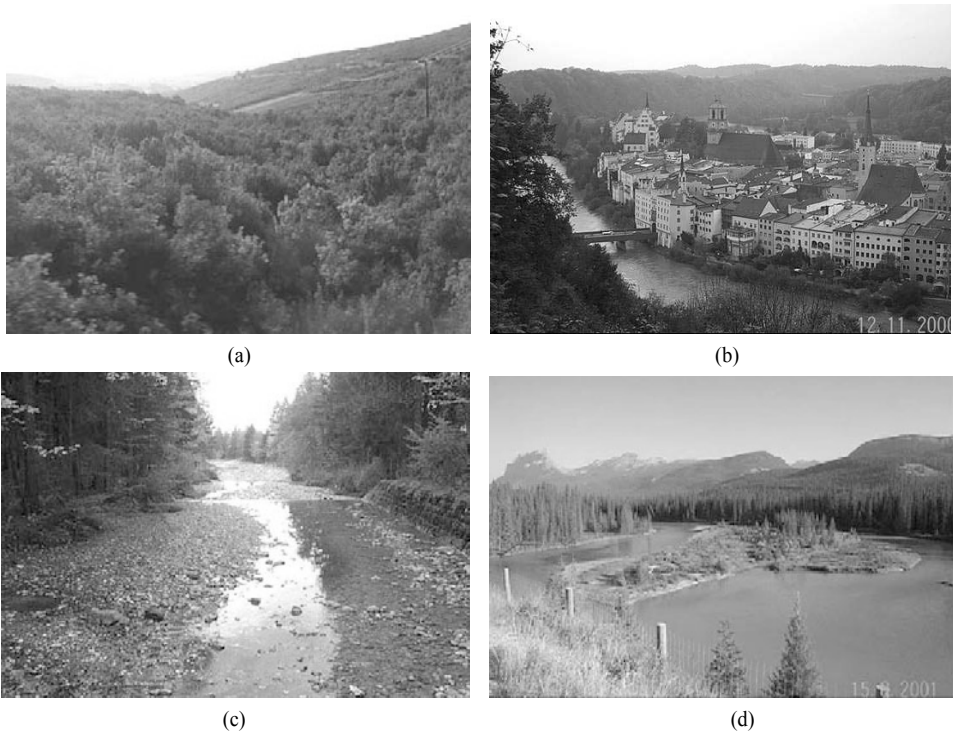
Fig. 10.2 (a) Forest matrix in the suburbs of Beijing, China; (b) A township patch and a surrounding stream corridor in Wasserburg, Germany; (c) Stream corridor (the Leinbach River in Germany) and riparian forest matrix; and (d) Mosaic consisting of forest, lake, island, and hills (Banff, Canada). (See color figure at the end of this book)

terms can still be used to describe the ecological structure within watersheds. However, one could further describe the watershed structure more meaningfully by also focusing on elements such as upper, middle, and lower watershed zones, drainage divides, upper and lower hill slopes; terraces; floodplains; estuaries and lagoons; and river mouths and deltas. Figure 10.3 displays examples of (a) the upper watershed (the Yangtze River at the Shennongjia Mountain); (b) a mountain stream the Yellow River Basin; (c) an alluvial river (the Blue Nile at the confluence with the White Nile River); and (d) an estuary (the Venice Lagoon at the Po River mouth).

The river corridor is a spatial element (a corridor) at the watershed and landscape scales. Common matrices in stream corridors include riparian forest or shrub cover or alternatively herbaceous vegetation. Examples of patches at the stream corridor scale are wetlands, forest, shrub land, grassland patches, oxbow lakes, residential or commercial development, islands in the channel, and passive recreation areas such as picnic grounds. Figure 10.4 shows a cross section of a river corridor. The river corridor can be subdivided by structural features and plant communities. Riparian areas have one or both of the following characteristics: (1) vegetative species clearly different from nearby areas; and (2) species similar to adjacent areas but exhibiting more vigorous or robust growth forms. Riparian areas are usually transitional between wetland and upland

10.1.2 Biological Communities

The biological community of a river ecosystem is determined by the characteristics of both terrestrial and aquatic ecosystems. The terrestrial ecosystem depends mainly on the plant community and the aquatic

ecosystem comprises aquatic plants, benthic invertebrates, and vertebrates (fish, reptiles, and amphibians).

(a)　　　　　　　　　　　　　　　　　　(b)

(c)　　　　　　　　　　　　　　　　　　(d)
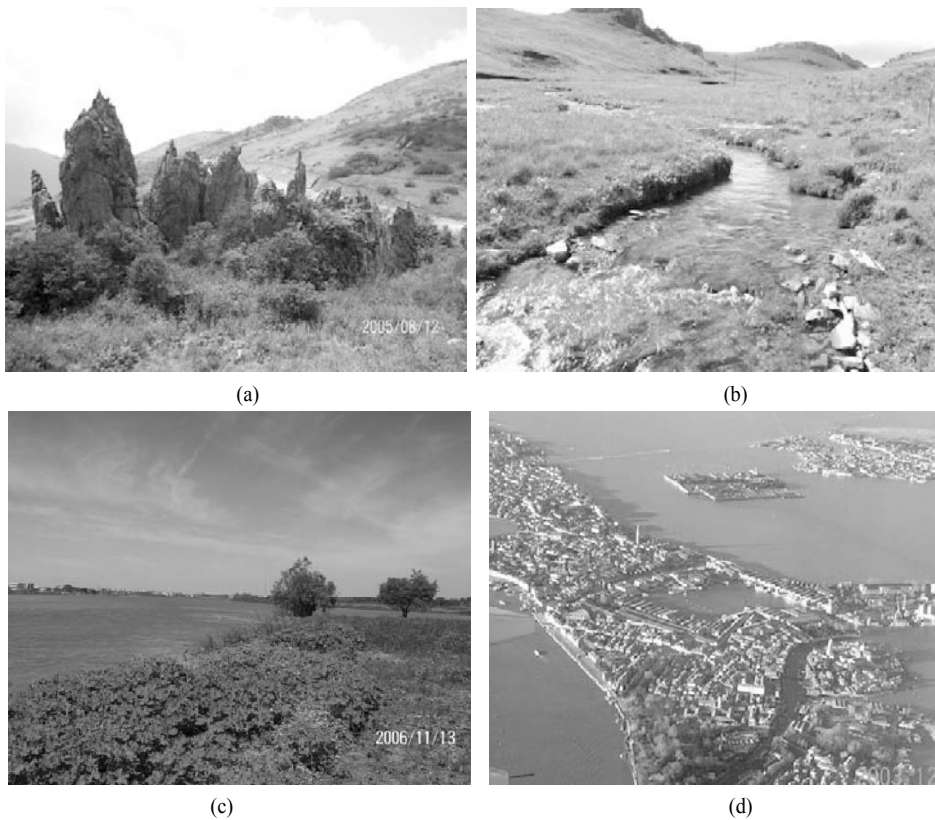
Fig. 10.3　(a) Upper watershed of the Yangtze River at the Shennongjia Mountain; (b) A small stream in the source area of the Yellow River; (c) the Blue Nile at the confluence with the White Nile in Sudan; and (d) the Venice Lagoon at the Po River mouth in Italy. (See color figure at the end of this book)
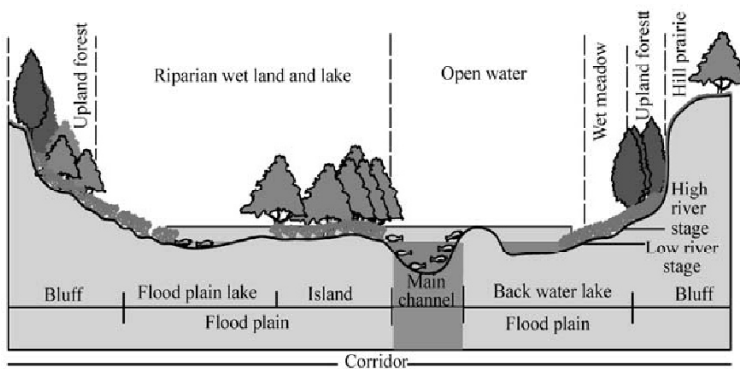
Fig. 10.4　A cross section of a river corridor, in which the river corridor is subdivided by structural features and plant communities (after FIRSWG, 1997)

10.1.2.1   Terrestrial Ecosystem

The terrestrial ecosystem comprises the plant community, amphibians, reptiles, mammals and birds. The plant community is an essential basic element for the stream ecology. The ecological integrity of a river is directly related to the integrity and ecological characteristics of the plant communities that make up and surround the river. The biological communities depend on these plant communities as a valuable source of energy. The plants also provide a physical habitat and moderate solar energy fluxes to and from the surrounding aquatic ecosystem. Figure 10.5 shows the terrestrial plant community by the upper Dadu River in Sichuan Province, China. The high density of vegetation develops in the valley and on the slopes, which provides the primary product for the aquatic ecosystem.

The primary product for ecology is provided by plant communities. Only a small amount of this organic material is stored as above- and below-ground biomass, while senescence, fractionation, and leaching to the organic soil layer in the form of leaves, twigs and decaying roots are the components of the annual loss of a significant fraction of organic matter. This annual loss of organic matter represents a major storage and cycling pool of available carbon, nitrogen, phosphorus and other nutrients, for it is rich in biological activity of microbial flora and microfauna.

The characteristics of the plant communities directly influence the diversity and integrity of the faunal communities. In general, complex floral community supports complex faunal communities. The faunal composition is a function of the following habitat features of river corridors: (1) permanent water; (2) high primary productivity and food availability; (3) spatial and temporal contrasts in cover types; (4) critical microclimates; (5) horizontal and vertical habitat diversity; 6) effective seasonal migration routes; (7) high connectivity between vegetated patches.

Following disturbances to the land, whether they be naturally occurring or resulting from human activity, plant succession occurs, in which pioneer species well-adapted to bare soil and plentiful light are gradually replaced by longer-lived species that can regenerate under more shaded and protected conditions. The most common natural sources of disturbance within a river valley are flooding and channel migration. Knowledge of natural succession in a stream corridor can be very useful for restoration practitioners and should be taken advantage of by planting hardy, pioneer species to stabilize an eroding bank, while planning for the eventual replacement of these species by longer-lived and higher-succession species.

Fig. 10.5   Terrestrial pant community by the Dadu River in Sichuan Province, China

In arid and semi-arid areas, water is vital for the fauna since the only naturally occurring permanent sources of water present are the streams. The high primary productivity and biomass of riparian areas is largely a result of these moist environments, for the food sources and cover types of the surrounding areas are very different from the riparian area. Stream corridors provide water, shade, evapotranspiration, and cover, thus, ameliorating the temperature and moisture extremes of uplands. Nearly all amphibians, many reptiles and mammals are found primarily in river corridors and riparian habitats.

10.1.2.2 Aquatic Ecosystem

Stream biota are often classified into seven groups—bacteria, algae, macrophytes (higher plants), protists (amoebas, flagellates, ciliates), micro-invertebrates (invertebrates less than 0.5 mm in length, such as rotifers, copepods, ostracods, and nematodes), macro-invertebrates (invertebrates greater than 0.5 mm in length, such as mayflies, stoneflies, caddisflies, crayfish, worms, clams, and snails), and vertebrates (fish, amphibians, reptiles, and mammals) as shown in Fig. 10.6. Undisturbed streams can contain a remarkable number of species. For example, more than 1,300 species were found in a 2 km reach of a small German stream, the Breitenbach, when a comprehensive inventory of stream biota was taken.

The most important elements of the aquatic ecosystem for river management are aquatic plants, benthic invertebrates, and vertebrates (fish, reptiles, and amphibians). Aquatic plants usually consist of mosses attached to permanent stream substrates and macrophytes including floating plants，such as *Eichoimia crassips*, submerged plants, such as *Potamogeton*, and emergent plants, such as *Phragmites communis trirn* (reed). These plants provide primary productivity for the faunal community, and play an important role in decontaminating the river water and providing multiple habitats for fish and invertebrates. Bedrock or boulders and cobbles are often covered by mosses and algae. Figure 10.7 shows microhabitats with moss on cobbles, submerged macrophytes species *Potamogeton*, floating plants species *Lemna minor L.*, and emergent plants species *Phragmites communis trirn* (reed). Rooted aquatic vegetation may occur where substrates are suitable and high currents do not scour the stream bottom. Luxuriant vascular plants may occur in some areas where water clarity, stable substrates, high nutrients, and slow water velocities are present.
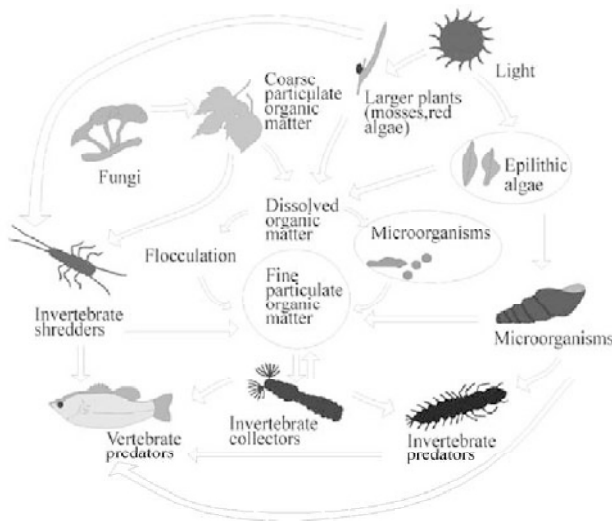
Fig. 10.6 Stream eco-system and bio-community (after FISRWG, 1997) (See color figure at the end of this book)
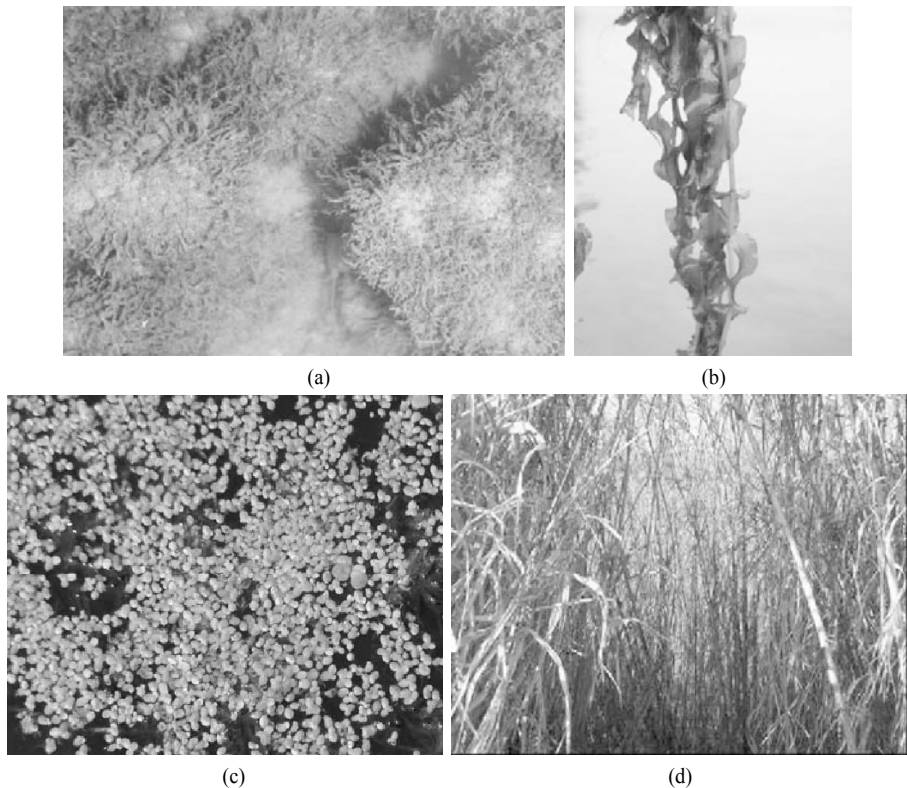
Fig. 10.7   Aquatic plants: (a) moss on cobbles; (b) *Potamogeton*; (c) *Lemna minor L*; and (d) *Phragmites communis trirn*

Benthic invertebrates collectively facilitate the breakdown of organic material, such as leaf litter, that enters the stream from external sources. Larger leaf litter is broken down into smaller particles by the feeding activities of invertebrates known as **shredders** (insect larvae and amphipods). Other invertebrates filter smaller organic material from the water, known as **filters** (blackfly larvae, some mayfly nymphs, and some caddisfly larvae); scrape material off the surfaces of bedrock, boulders, and cobles, known as **scrapers** (snails, limpets, and some caddisfly and mayfly nymphs); or feed on material deposited on the substrate, known as **collectors** (dipteran larvae and some mayfly nymphs) (Moss, 1988). Some macro-invertebrates are predatory, known as **predators**, such as dragonfly, which prey on small vertebrates. Figure10.8 shows typical species of the five groups with different ecological functions.

Fish are the apex **predator** in the aquatic system. Many restoration projects aim at restoration of fish habitat. From the headwaters to the estuaries the composition of fish species varies considerably due to changes in many hydrologic and geomorphic factors which control temperature, dissolved oxygen, gradient, current velocity, and substrate. The amount of different habitats in a given stream section is determined by a combination of these factors. Fish species richness (diversity) tends to increase downstream as gradient decreases and stream size increases. For small headwater streams, the gradient tends to be very steep and the stream is small and environmental fluctuations occur with a greater intensity and frequency, therefore, species richness is lowest (Hynes, 1970).

Some fish species are migratory and travel long distances to return to a certain site to spawn. They have to swim against currents and go up over waterfalls, thus, showing great strength and endurance. When
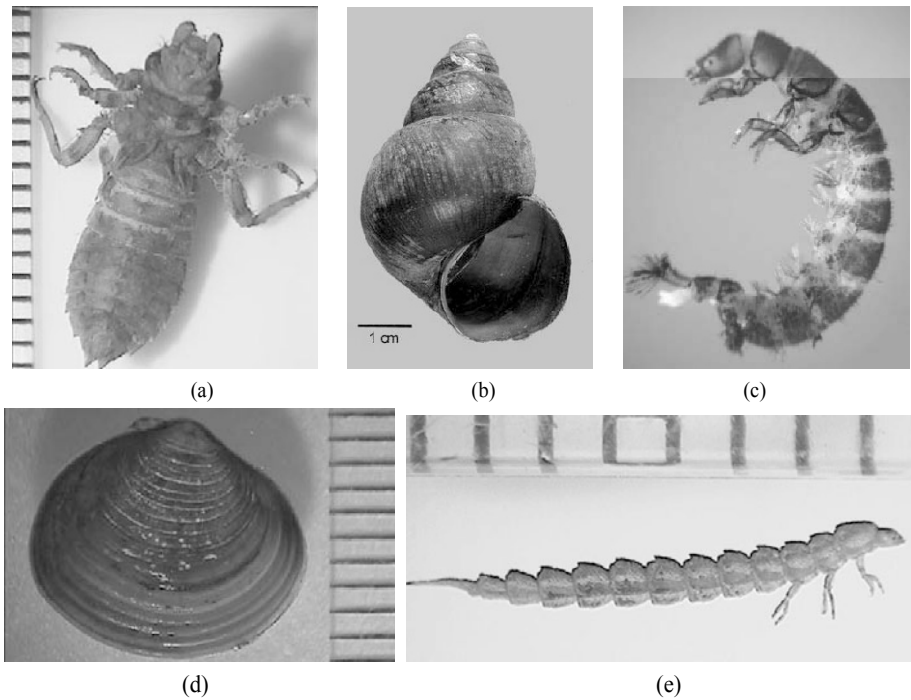
Fig. 10.8 Typical species of the five groups of benthic invertebrates with different functions in the food chain: (a) Gomphidae (Dragonfly-**predator**); (b) Viviparidae (**scraper**); (c) Hydropsychidae (**collector-filter**); (d) Corbiculidae (**filter-collector**); and (e) Haliplidae (**shredder**) (See color figure at the end of this book)

migrating they move between saltwater and freshwater, therefore, need to be able to osmoregulate efficiently (McKeown, 1984). According to their temperature requirements, species may also generally be referred to as cold water or warm water and gradations between. Salmonid fish prefer cold and highly oxygenated water, and, therefore, can generally be found at high altitudes or northern climes. Salmonid populations are very sensitive to change or deterioration of their habitat, including alteration of flows, temperature, and substrate quality. They tolerate only very small fluctuations in temperature and only reproduce under certain conditions. Their reproductive behavior and movements are affected by almost undetectable changes in temperature. Usually a salmonid spawns by depositing eggs over or between clean gravel, which remain oxygenated and silt free due to upwelling of currents between the interstitial spaces. Salmonid populations, therefore, are highly susceptible to many forms of habitat degradation, including alteration of flows, temperature, and substrate quality.

The general concern and interest in restoring habitats for fish by improving both quality and quantity, is due to the widespread decrease in numbers of native fish species. With ecological, economical, and recreational considerations in mind, the importance given to the restoration of fish communities is increasing. In 1996 approximately 35 million Americans went fishing for recreational purposes resulting in over $36 billion in expenditures (Brouha, 1997).

Since most recreational fishing is in streams, it is important to restore stream corridors. Restoration activities have often been focused on improving local habitats, such as fencing or removing livestock from streams, constructing fish passages, or installing instream physical habitat. However, the success of these activities, demonstrated by research, has been very small or questionable. Over its life span, a species needs many resources and has a great range of habitat requirements which were not considered

during the restoration.

Although the public are most interested in fish stocks, another goal of the stream restoration is to preserve other aquatic biota. Of particular concern are freshwater mussels, many species of which are threatened and endangered. Mussels are highly sensitive to habitat disturbances. Some of the major threats faced by mussels are dams, which lead to direct habitat loss and fragmentation of the remaining habitats, persistent sedimentation, pesticides, and exotic species like fish and other mussel species which are introduced into the habitat.

10.1.2.3   Habitat

The diversity of available habitats directly influences the biological diversity and abundance in streams. When a stream system is stably functioning, the diversity and availability of habitats is promoted. This is one of the primary reasons stream stability is always considered in river ecosystem restoration activities. Figure 10.9 (a) shows the gravel and cobbles bed of Juma River near Beijing, which is very stable even during flood events. The stable habitat is colonized by a biocommunity with high diversity. Figure 10.9 (b) shows the Dabai River in the upper Yangtze River basin, which channel bed has a very unstable due to high sediment load. There is few species in the Dabai River and the biodiversity is low. Under less disturbed situations, a narrow, steep-walled cross section provides less physical area for habitat than a wider cross section with less steep sides, but may provide more biologically rich habitat in deep pools. Habitat increases with stream sinuosity. A uniform sand bed in a stream provides less potential habitat diversity than a bed with debris dams, boulder cascades, rapids, step-pool sequences, pool-riffle sequences, or other types of "structures".

A river may be seen either as a single functioning entity or an ecosystem with components which interact and have numerous connections between them. In order to restore an ecosystem successfully, one must not forget these fundamental relations. Certain topographic settings may be more likely than others to be subject to periodic, dramatic changes in hydrology and related vegetation structure as a result of massive woody debris jams. The structural aspects of vegetation may affect the functions of the stream ecosystems. Vegetation and detritus influence the course of water in an undeveloped watershed. Balanced interactions between terrestrial and aquatic systems result from the mobilization and conservation of nutrients in complex patterns. Land uses such as agriculture and livestock grazing and the flow patterns of water, sediment, and nutrients cause the characteristics and distribution of vegetation to change.
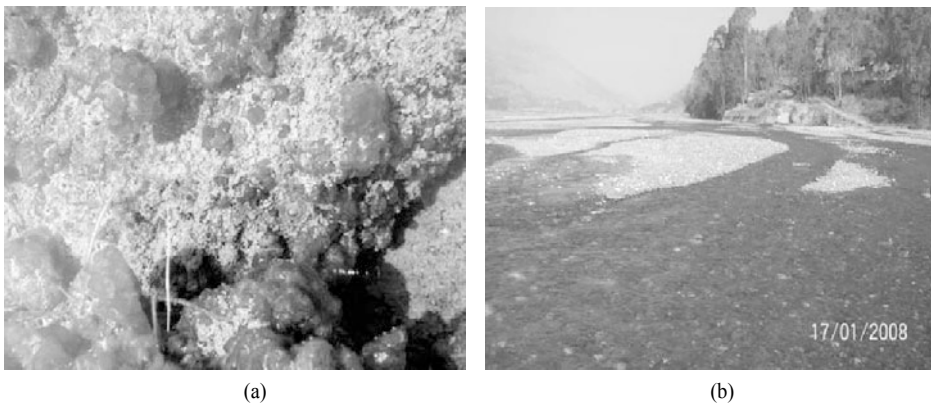
| (a) | (b) |

Fig. 10.9   (a) Gravel and cobbles bed of the Juma River near Beijing is stable, which is colonized by a biocommunity with high diversity; and (b) The Dabai River in the upper Yangtze River basin is very unstable due to high sediment load and has a very low biodiversity (See color figure at the end of this book)

The most obvious roles of plants are those that affect fish and wildlife. At the landscape level, the fragmentation of native cover types has had a negative impact on the wildlife needing large areas of ongoing vegetation. In some systems, small fractures in the continuity of corridors can greatly affect animal movement and can negatively impact the conditions in a stream which permit it to host certain aquatic species. Narrow stream corridors that are essentially edge habitat may encourage generalist species, nest parasites and predators, and where corridors have been established across historic barriers to animal movement, they can disrupt the integrity of regional animal assemblages (Knopf et al., 1988).

The conditions of nearby habitats must be taken into account when planning to restore riparian areas. Carothers (1979) found that non-riparian birds frequently use the edges of riparian areas as habitats. However, smaller riparian birds carry out activities within the riparian area during the breeding season and larger species often forage in nearby areas (Carothers et al., 1974). In fact although the larger species may forage many miles away from the riparian area, they would still depend on them critically (Lee et al., 1989).

If the conditions upstream of an ecosystem have been significantly altered by, for example, a dam or any other water diversion project, it will be impossible to restore that ecosystem to its natural, perfect condition. This stands even if complete restoration is a possibility. For example, the creation of areas of woody vegetation in the channel below several dams in the Platte River Valley in Nebraska has significantly decreased areas of wet meadow—an important habitat. The area has been declared a critical habitat for the Whooping Crane, the Piping Plover, and the Interior Least Tern (Aronson and Ellis, 1979).

10.1.3 Ecological Conditions

Flow—Streams are distinguished from other ecosystems by a flow of water from upstream to downstream. The micro-and macro-distribution patterns of many stream species are affected by the spatial and temporal characteristics of stream flow, such as fast versus slow, deep versus shallow, turbulent versus laminar, and flooding versus low flows (Bayley and Li, 1992: Reynolds, 1992; Ward, 1992). Flow velocity affects the deliverance of food and nutrients to organisms, however, it can also dislodge them and prevent them from remaining at a certain site. When a stream has a very slow flow, the fauna on the banks and the bed are similar in composition and configuration to those present in stagnant waters (Ruttner, 1963). High flows are cues for timing migration and spawning of some fish. When fish detect high flows, some will migrate and some will spawn.

Temperature—Water temperature can vary markedly in a stream system and between different stream systems. It is a very important factor for cold blooded aquatic organisms for it affects many of their physiological and biochemical processes. Stream insects, for example, often grow and develop more rapidly in warmer portions of a stream or during warmer seasons. Some species may complete two or more generations per year at warmer sites yet only one or fewer at cooler sites (Sweeney, 1984; Ward, 1992). This can also be applied to algae and fish for their growth rates increase with increased water temperature (Hynes, 1970; Reynolds, 1992). Some species are only found in certain areas due to the correlation between temperature and growth, development, and behavior.

Riparian vegetation—Decreased light and temperature in steams can be a result of riparian vegetation (Cole, 1994). When the flow of water is slow, direct sunlight can significantly warm up the water, especially in the summer. In Pennsylvania, the average daily stream temperatures increased by 12℃ when flowing through an open area in direct sunlight but then decreased significantly during flow through 500 m of forest (Lynch et al., 1980). However, during the winter, a lack of cover has the opposite effect and causes a decrease in temperature. Sweeney (1992) found that temperature changes of 2 to 6℃ usually altered key life-history characteristics of some species. It has been observed that riparian forest buffers help to prevent changes in natural temperature patterns and also to mitigate the increases in

temperature following deforestation.

Oxygen—Oxygen enters the water by absorption directly from the atmosphere and by plant photosynthesis (Mackenthun, 1969). Mountain streams that do not receive a lot of waste discharges are generally saturated with oxygen due to their shallow depth, constant motion, and large surface area exposed to the air. Aquatic organisms only survive because of the dissolved oxygen which, at appropriate concentrations, enables them to reproduce and develop and gives them vigor. When oxygen levels are low, organisms experience stress and become less competitive in sustaining the species (Mackenthun, 1969). Dissolved oxygen concentrations of 3 mg/L or less have been shown to interfere with fish populations for a number of reasons (Mackenthun, 1969). When the oxygen needed for chemical and biological processes exceeds the oxygen provided by re-aeration and photosynthesis, the fish will die. Dissolved oxygen concentrations will decrease and may even be depleted by slow currents, high temperatures, extensive growth of rooted aquatic plants, algal blooms or high concentrations of aquatic matter (Needham, 1969).

Pollution that depletes the stream of oxygen has a marked effect on stream communities (Odum, 1971). Major factors determining the amount of oxygen found in water are temperature, pressure, salinity, abundance of aquatic plants, and the amount of natural aeration from contact with the atmosphere (Needham, 1969). A level of 5 mg/L or higher of dissolved oxygen in water is the level associated with normal activity of most fish (Walburg, 1971). In streams filled with trout, the dissolved oxygen concentration has been shown, by analysis, to be between 4.5 and 9.5 mg/L (Needham, 1969).

pH-value—Aquatic biota survive best when the water has a pH of 7, i.e. nearly neutral hydrogen ion activity. If the pH changes, either becoming more acidic or more alkaline, the stress levels increase and eventually species diversity and abundance decrease. In streams under the stresses of various human activities, the pH often becomes more acidic and many species suffer, as shown in Fig. 10.10 (revised based on FISRWG, 1997). One of the main causes for changes in the pH of aquatic environments is the increase in the acidity of rainfall (Schreiber, 1995). Some soils have the ability to buffer pH changes; however, those which cannot neutralize acid inputs cause environmental concerns.

Substrate—Substrate influences stream biota. Within one reach of a stream, different species and different numbers of species can be seen among microinvertebrate aggregations found in snags, sand, bedrock and cobbles (Benke et al., 1984; Smock et al., 1985; Huryn and Wallace, 1987). The hyporheic zone is the area of substrate which is under the substrate-water boundary and is the main area for most benthic invertebrate species to live and reproduce. It may be only one centimeter thick in some cases or one meter thick in other cases. The hyporheic zone may form a large subsurface environment, as shown in Fig. 10.11.

Stream substrates are composed of various materials, including clay, sand, gravel, cobbles, boulders, organic matter and woody debris. Substrates form solid structures that modify surface and interstitial flow patterns, influence the accumulation of organic materials, and provide for production, decomposition, and other processes (Minshall, 1984). Sand and silt are considered to be the least suitable substrates for supporting aquatic organisms and provide for the fewest species and individuals. Rubble substrates have the highest densities and the most organisms (Odum, 1971). If woody debris, from nearby trees in forests and riparian areas, fall into the stream, the quantity and diversity of aquatic habitats is increased (Bisson et al., 1987; Dolloff et al., 1994).

Nutrients and eutrophication—Nitrogen, phosphorus, potassium, selenium, and silica, are needed for plant growth. However, nitrogen and phosphorus, if found in surplus, may cause an increase in the rate of growth of algae and aquatic flora in a stream. This process is called eutrophication. Eutrophication has been an environmental and ecological problem in China since the 1980s when the economy began to rapidly grow. If the excess organic matter is decomposed, it can result in oxygen depletion of the water, it

pH	6.5	6.0	5.5	5.0	4.5	4.0	3.5	3.0
Grass carp (*Ctenopharyngodon idellus*)								
Chinese sturgeon (*Acipenser sinensis*)								
Chinese river dolphin (*Lipotes Vexillifer Miller*)								
Rainow trout (*oncorhyncus mykiss*)								
Brown trout (*salmo trutta*)								
Brown trout (*salvelinus fontinalus*)								
Smallmouth bass (*micropterus dolomieu*)								
Fathead minnow (*pimephalus promelas*)								
Pumpkinseed sunfish (*lepomis gibbosus*)								
Yellow perch (*perca flavescens*)								
Bullfrog (*rana catesbeiana*)								
Wood frog (*r.sylvatica*)								
American toad (*bufo americanus*)								
Spotted salamander (*ambystoma maculatum*)								
Clam								
Crayfish								
Snail								
mayfly								

Fig. 10.10 Effects of acid rain on some aquatic species. As acidity increases (pH decreases) in lakes and streams, some species are lost as indicated by the lighter colors (revised on the basis of FISRWG, 1997)
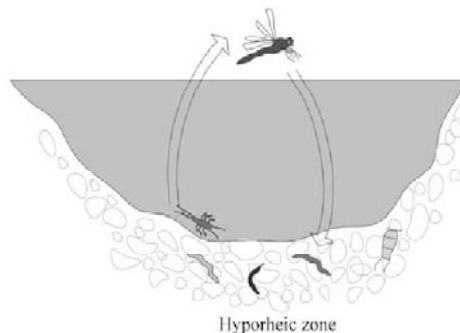
Hyporheic zone

Fig. 10.11 Schematic diagram of hyporheic zone

also can have terrible aesthetic consequences the worst of which is the death of fish. Eutrophication in lakes and reservoirs is indirectly measured as standing crops of phytoplankton biomass, usually represented by planktonic chlorophyll-a concentration. However, phytoplankton biomass is not generally the main component of plant biomass in smaller streams because the growth of periphyton and macrophytes, which live on the stream bed, is promoted by high substrate to volume ratios and periods of energetic flow. When there are decreased flows and high temperatures, excessive algal mats develop and oxygen is depleted due to eutrophication.

10.1.4   Ecological Functions of Rivers

The main ecological functions of rivers are habitat, conduit, filter, barrier, source, and sink. Ecological restoration is done in order to enable river corridor functions to be effectively restored. However, the goals of restoration are not only to reestablish the structure or to restore a particular physical or biological process. Section 10.1 emphasizes matrix, patch, corridor, and mosaic as the most basic building blocks of physical structure at local to regional scales. Ecological functions, too, can be summarized as a set of basic, common themes that reappear in an ongoing range of situations.

Two characteristics are particularly important to the operation of stream corridor functions:

(1) Connectivity—This is a measure of the dimensions of a stream corridor and how far it continues (Forman and Godron, 1986). This attribute is affected by breaks in the corridor and between the stream and adjacent land uses. Transport of materials and energy and movement of flora and fauna are valuable functions promoted by a high degree of connectivity in a stream between its natural communities.

(2) Width—In stream corridors, this refers to the distance across the stream and its zone of adjacent vegetation cover. Width is affected by edges, community composition, environmental gradients and disturbances/disruptions in adjacent ecosystems, including those with human activity. Average dimension and variance, number of narrows, and varying habitat requirements are some example measures of width (Dramstad et al., 1996).

10.1.4.1   Habitat Function

Habitat is a term used to describe an area where plants or animals (including people) normally live, grow, feed, reproduce, and otherwise exist for any portion of their life cycle. The important factors needed for survival such as space, food, water, and shelter are provided by the habitat. As long as the conditions are suitable, many species use river corridors to live, find food and water, reproduce, and establish viable populations. Population size, number of species, and genetic variation are a few measures of a stable biological community, which vary within known boundaries over time. Streams may positively affect these measures at different levels. Since corridors are linked to small habitat patches, they have a great value as habitats because they create large, more complex habitats with greater wildlife populations and higher biodiversity. In general, stream corridors are habitats for plants, fish, invertebrates, and amphibians. For instance, the Fazi River is an urban stream in Taichong City, as shown in Fig. 10.12. The river has gravel bed with alternative lentic and lotic waters. Although the river is seriously polluted in the upstream reaches several tens of species of macro-invertebrates, fish and birds are found in the river.

Habitat functions differ at various scales, and an appreciation of the scales at which different habitat functions occur will help a restoration initiative succeed. The evaluation of a habitat at larger scales, for example, may make note of a biotic community's size, composition, connectivity, and shape. To help describe habitat over large areas at the landscape scale, the concepts of matrix, patches, mosaics, and corridors can be used. Migrating species can be provided with their favorite resting and feeding habitats during migration stopovers by stream corridors with naturally occurring vegetation. Some patches are too small for large mammals like the black bear which need great, unbroken areas to live in. However, these patches may be linked by wide stream corridors to create a large enough territory for bears.

Assessing habitat function at small scales can also be viewed in terms of patches and corridors. It is also at local scales that transitions among the various habitats within the river can become more important. Two basic types of habitat structure: interior and edge habitat can be found in stream corridors. Connectivity and width greatly influence the functions of habitats at the corridor scale. A stream corridor provides a better habitat if it is wide and if it has greater connectivity. Changes in plant and animal communities can be caused by river valley morphology and environmental gradients, such as gradual changes in soil wetness, solar radiation, and precipitation. Species usually find ideal habitats in broad, unfractured, and diverse streams, rather than narrow and homogenous ones.

Fig. 10.12　The Fazi River, an urban stream in Taichong City, provides habitats for benthic invertebrates, fish and birds

Factors such as climate, microclimate, elevation, topography, soils, hydrology, vegetation, and human uses, cause the habitat conditions within a river to vary. When planning to restore a stream, its width is of great importance to wildlife. The size and shape of a stream corridor must be sufficiently wide for a species to populate. This must be considered when trying to maintain a certain wildlife species. If the corridor is too narrow, from the point of view of the species, it is as if there is a piece of the corridor missing.

Riparian forests provide diversity not only in their edge and interior habitats but also offer vertical habitat diversity in their canopy, sub-canopy, shrub, and herb layers. Within the channel itself, riffles, pools, glides, rapids, and backwaters all provide different habitat conditions in both the water column and the streambed. These examples, all described in terms of physical structure, yet again show that there is a strong correlation between structure and habitat function.

10.1.4.2　Conduit Function

To act as a route for the flow of energy, materials, and organisms is known as the conduit function, as shown in Fig. 10.13. A stream is foremost a conduit that was formed by and for collecting and transporting water and sediment. As well as water and sediment, aquatic fauna and other materials use the stream corridor as a conduit. Since there is movement across as well as along the stream and in many other directions, the corridor can be considered to have lateral and longitudinal conduit functions. If the stream corridor is covered by a closed canopy, then birds and mammals may cross over the stream through the vegetation. The food supply for fish and invertebrates may be enriched or increased by the movement of organic debris and nutrients from higher to lower floodplains.

Corridors can act as pathways and habitats at the same time for migratory or highly mobile wildlife. The migration of songbirds from their wintering habitat in the neo-tropics to a summer habitat further

north is made possible by rivers together with other, useful habitats. After all, birds can only fly a certain distance before they need to eat and rest. For rivers to function effectively as conduits for these birds, they must be sufficiently connected and be broad enough to provide the habitat required for migratory birds.

The migration of salmon upstream for spawning has been extensively investigated and is a well known example of the movement of aquatic organisms and interactions with the habitat. A conduit to their upstream spawning grounds is very important to the salmon which mature in a saltwater environment. In the case of the Pacific salmon species the stream corridor depends on the nutrient input and biomass of dying fish and plentiful spawning in the upstream reaches. So, not only are conduits important for the movement of aquatic biota but also for the transport of nutrients from ocean waters upstream.

Stream corridors are also conduits for the movement of energy, which occurs in many forms. Heat is transported with flowing water along a stream, as shown in Fig. 10.13. The potential energy of the stream is provided by gravity, which alters and carves the landscape. The corridor modifies heat and energy from sunlight as it remains cooler in spring and summer and warmer in the fall. Stream valleys move cool air from high to low altitudes in the evening, and, therefore, are effective air-sheds. The energy built up by the productivity of plants in a corridor is stored as living plant material and it moves into other systems by leaf fall and detritus.

Seeds may be carried for long distances by flowing water and then deposited. Whole plants may be uprooted, transported, and then deposited, still living, in a new area by strong floods. Plants are also transported when animals eat and transport their seeds throughout different parts of the river. Some riparian habitats depend on a continuous supply and transport of sediment, although many fish and invertebrates can be harmed by excess fine sediment.

Fig. 10.13   A stream is a flow pathway for heat, water, and other materials, and organisms as shown for a small tributary of the Songhua River in northeastern China (See color figure at the end of this book)

10.1.4.3   Filter and Barrier Functions

Stream corridors may act as filters, allowing selective penetration of energy, materials, and organisms, they may also act as a barrier to movement. In many ways, the entire stream corridor serves beneficially as a filter or barrier that reduces water pollution, minimizes sediment transport, and often provides a natural boundary to land uses, plant communities, and some less mobile wildlife species as shown in Fig. 10.14.

Fig. 10.14 A stream functions as a boundary of land uses, plant communities, and some less mobile wildlife species

Movement of materials, energy, and organisms perpendicular to the flow of the stream is most effectively filtered or barred, however, elements moving parallel to the stream corridor, along the edge, may also be selectively filtered. The movement of nutrients, sediment, and water over land is filtered by the riparian vegetation. Dissolved substances, such as nitrogen, phosphorus and other nutrients, entering a vegetated river valley, are restricted from entering the channel by friction, root absorption, clay, and soil organic matter.

Edges at the boundaries of stream corridors begin the process of filtering. Initial filtering functions are concentrated into a tight area by sudden edges. These edges tend to be caused by disruptions and usually encourage movement along boundaries while opposing movement between ecosystems. On the other hand, gradual edges promote movement between ecosystems and increase filtering and spread it across a wider ecological gradient. Gradual edges are found in natural settings and are more diverse (FISRWG, 1997).

10.1.4.4 Source and Sink Functions

Organisms, energy, and materials are supplied to the bordering area by rivers. Areas that function as sinks absorb organisms, energy, or materials from the surrounding landscape. A stream can act as both a source and a sink, as shown in Fig. 10.15. However, this is affected by the location of the stream and the time of year. Although they may sometimes function as a sink, when flooding deposits new sediment there, stream banks tend to act as a source, for example, of sediment to the stream. Genetic material throughout the landscape is supplied by and moves through corridors, which at the landscape scale, act as conduits or connectors to many different patches of habitats.

Surface water, ground water, nutrients, energy, and sediment can be stored in stream corridors, which then act as a sink and allow materials to be temporarily stored in the corridor. Friction, root absorption, clay, and soil organic matter prevent the entry of dissolved substances such as nitrogen, phosphorus, and other nutrients into a vegetated stream corridor. Forman (1995) offers three sources and sink functions resulting from floodplain vegetation: (1) decreased downstream flooding through floodwater moderation and/or uptake; (2) containment of sediments and other materials during flood stage, and (3) source of soil organic matter and water-borne organic matter.

Fig. 10.15 A stream functions as a source providing organisms, energy, or materials to the surrounding landscape, and also as a sink absorbing organisms, energy, or materials from the surrounding landscape

10.1.5   Dynamic Equilibrium

Even in the absence of human disruptions, the ecological characteristics of stream corridors, although consistent, are naturally and constantly changing in their structure, processes, and functions. Streams corridors show a dynamic form of stability. Stability is regarded as the capability of a system to prevail within a range of conditions. This phenomenon is referred to as *dynamic equilibrium*.

For a dynamic equilibrium to be preserved, the stream ecosystem must have an active series of self-correcting mechanisms. External disruptions and stresses may be moderated within a certain range of responses, by the ecosystem through these mechanisms, thus, preserving a self-sustaining condition. The threshold levels associated with these ranges are difficult to identify and quantify. If these levels are exceeded, the system can become unstable. A new steady state position may take a long time to become established, however this may be done if the stream is subjected to a series of adjustments.

Once the source of a disturbance is controlled or removed, a stream system can return to its working condition in a reasonable amount of time. The fact that ecosystems restore themselves after the removal of external stresses allows passive restoration. Removing the stress and allowing the ecosystem to recover by itself is an economical and effective method (see Chapter 9 for an example of ecosystem recovery after ammonia toxicity is reduced). However, following a profound disruption and alteration, the time needed for a stream corridor to heal itself could be several decades.

Even if a stream system does recover to equilibrium, it will be very different from before, and its ecological value may be greatly decreased. When an analysis by restoration practitioners shows that the recovery time will be long and questionable, they may decide that the use of active restoration techniques to reestablish a more operable channel form and biological community in a short time, may be viable. There are many difficulties with active restoration. Planning, designing, and implementing methods to regain the original state of dynamic equilibrium correctly are great challenges.

In some cases a disturbance may have such a great effect that the system may not be capable of recovery. In which case the stress must be removed and active restoration may be applied by repairing damage to the structure and function of the stream ecosystem. A stable ecosystem must have a combination of resistance, resilience, and capacity to recover. If it can keep its original form and functions, then it is resistant. The rate at which the ecosystem returns to its original form is known as its resilience. The

resilience of an ecosystem, r_e, may be measured with the ratio of the impairment of ecosystem after disturbances, τ, over the time needed for the ecosystem to return its original form, T:

$$r_e = \frac{\tau}{T} \qquad\qquad (10.1)$$

Recovery is the degree to which a system returns to its original condition after a disturbance. Natural systems are able to recover and restore stability following disruptions and disturbances.

A system may change yet still remain stable and in a good condition. When a large stable system has small, local changes within it, it is described as having mosaic stability. A good example would be a riparian system greatly disturbed by a 100-year flood. If this were to occur in an area which was urbanized, then it would become a dangerous gap in a habitat that is already rapidly decreasing and would separate and isolate cause populations of rare amphibian species. However, that same system, in a less urbanized area may not be harmful to amphibians but may just represent a mosaic of constantly shifting suitable and unsuitable habitats in a naturally functioning, unconfined system. A landscape with mosaic stability is not likely to need restoration, whilst one without would urgently need restoring.

10.2 Ecological Stresses

Ecological stresses are defined as the disturbances that bring changes to river ecosystems. The ecological stresses are natural events or human-induced activities that occur separately or simultaneously. The structure of a system and its capability of carrying out important ecological functions may be changed by stresses, regardless of whether they act individually or in combination. One or more characteristics of a stable system may be permanently changed by a causal chain of events produced by a stress present in a river. For instance, land use change may cause changes of hydrological and hydraulic features of the river, and these changes may cause chages in sediment transportation, habitat, and ecology (Wesche, 1985).

Disturbances are not all of equal frequency, duration, and intensity and they may occur anywhere within the stream corridor and associated ecosystems. A large number of disturbances of different frequency, duration, intensity, and location may be caused by one single disturbance. Once people understand the evolution of what disturbances are stressing the system, and how the system reacts to those stresses, people can decide which actions are needed to restore the function and structure of the stream corridor.

Disturbance occurs within variations of scale and time. Changes brought about by land use, for example, may occur within a single year at the stream or reach scale (crop rotation), a decade within the stream scale (urbanization), and even over decades within the landscape scale (long-term forest management). Despite the fact that wildlife populations, such as the monarch butterfly, remain stable over long periods of time, they may fluctuate greatly in short periods of time in a certain area. Similarly, while weather fluctuates daily, geomorphic or climatic changes may occur over hundreds to thousands of years.

Although it is not observed by humans, tectonic motion changes the landscape over periods of millions of years. The slope of the land and the elevation of the earth surface are affected by tectonics, such as earthquakes and mountain creating forces like folding and faulting. Streams may alter their cross section or plan form in response to changes brought on by tectonics. Great changes in the patterns of vegetation, soils, and runoff in a landscape are caused by the quantity, timing, and distribution of precipitation. As runoff and sediment loads vary, the stream corridor may change.

10.2.1 Natural Stresses
Climatic change, desertification, floods, hurricanes, tornadoes, erosion and sedimentation, fire, lightning, volcanic eruptions, earthquakes, landslides, temperature extremes, and drought are among the many

natural events that have a negative impact on the structure and functions of a river ecosystem. The relative stability, resistance, and resilience of an ecosystem determine their response to a disturbance.

Climate change may be illustrated with climate diagrams at meteorological stations. The climate diagram was suggested by Walter (1985). In the diagram, temperature is plotted on the left vertical axis and average total monthly precipitation on the right vertical axis. Temperature and precipitation are plotted on different scales. Walter (1985) used 20 mm/month as equivalent to 10℃ for the U.S. and Europe, but 100 mm/month is used as equivalent to 10℃ for a tropical rain forest. In this book, 30 mm/month equivalent to 10℃ for China. Very useful information, such as the seasonal fluctuation of temperature and precipitation, the duration and intensity of wet and dry seasons, and the percentage of the year in which the average monthly temperature is above and below 0℃, is summarized in this climate diagram. When the precipitation line lies above the temperature line then, in theory, there should be enough moisture for plants to grow. The potential evapotranspiration rate will exceed the precipitation if the temperature line lies above the precipitation line. The more the temperature line moves up and away from the precipitation line, the drier the climate will be.

Global climate change can be represented by the climate change in the Tibet Plateau, as it is the third pole of the earth. The distributions of decade average monthly temperatures and total monthly precipitation are shown in each diagram in Fig. 10.16. Between the 1960s and 1990s, the shape of the precipitation and temperature distributions has stayed the same. However, the average temperature has risen by about 1℃. The winter dry period which previously was from the beginning of October to the end of November, has extended from the beginning of October to the middle of December. The ecology of rivers around the world is affected by this climate change. As a consequence of global warming, continuous drought occurred in northern China. Figure 10.17 shows that many poplar trees in the Kuye River basin, which is a tributary of the Yellow River in northwestern China, were killed by continuous drought from 1997 to 2003.
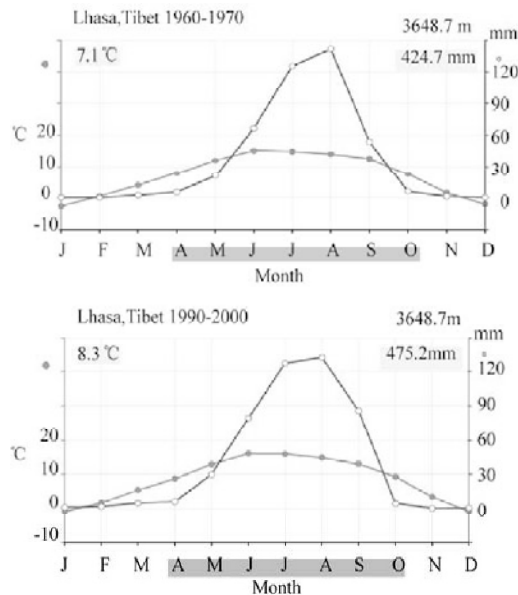
Fig. 10.16   Climate diagrams for the Tibet Plateau (at Lhasa), in which average monthly temperature is plotted on the left vertical axis and average total monthly precipitation on the right vertical axis (10℃ is equivalent to 30 mm of precipitation)

Fig. 10.17 A serious a drought that started in 1997 and lasted for 6 years killed many poplar trees in the Kuye River basin in Inner Mongolia Autonomous Region, China. The trunks and branches die but the root system is still alive. The roots sprouted and new branches grew after the climate became wetter after 2004 (See color figure at the end of this book)

The trunks and branches die but the root system is still alive. The roots sprouted and new branches grew after the climate became wetter after 2004.

Figure 10.18 shows that a sand dune in the Kubuqi desert in northwestern China is moving toward a seasonal stream. The riparian forest has been damaged and some reptiles and amphibians have suffered. Desertification has become an environmental problem, which may be a consequence of deforestation and climate change.

Fig. 10.18 A sand dune in Kubuqi desert in northwestern China is moving toward a seasonal stream (See color figure at the end of this book)

A huge landslide may totally destroy the terrestrial and aquatic ecosystem of a river. Figure 10.19 shows the Wenjiagou Landslide in Mianzhu City, Sichuan, China, which was induced by the Wenchuan Earthquake on May 12, 2008. The total volume of the sliding body was 81 million m^3. The stream and

Fig. 10.19 Wenjiagou Landslide in Mianzhu City buried the stream and vegetation

vegetation on slopes were buried underneath the 180 m thick landslide. Both faunal and floral communities have been totally destroyed and the restoration needs a long period of time.

Erosion and sedimentation often are the direct cause of ecology impairment. Figure 10.20(a) shows the high sediment concentration in a stream in Taiwan, southeastern China, which causes a strong stress on the aquatic biocommunity. The sediment results from intensive soil erosion caused by a rainstorm. The high concentration results in low transparency, low dissolved oxygen, and sediment coating the substrate. Benthic animals and fish may be killed during the high concentration event. Figure 10.20(b) shows the turbid seawater with a high concentration of sediment on the east coast of Taiwan. The sediment is transported into the ocean by debris flows and hyperconcentrated flows. Tidal current and waves bring the sediment onto the shore and bays, which impacts on fish and invertebrate communities.

Stream ecology is influenced by certain animal activities. For example, beavers build dams that cause ponds to form within a stream channel or in the floodplain. Figure 10.21(a) shows that a couple of beavers skillfully use natures building materials and construct a wood dam with tree branches on the Spring Pond in Pennsylvania; and Fig. 10.21(b) shows the 3 m high beaver dam forms a pond, which provides a good habitat for fish and birds. Without any machines the beavers transported so much building materials and built the dam within several months. The landlord of the Spring Pond, Mr. R. Devries pronounced that there is no way for humans "could ever match their dam skills, their dam resourcefulness, their dam ingenuity, their dam persistence, their dam determination and their dam work ethic".

Of course the dam construction by beavers disturbs the stream ecology. The pond kills much of the existing vegetation. Moreover, if appropriate woody plants in the floodplain are scarce, beavers extend their cutting activities into the uplands and can significantly alter the riparian and stream corridors. The sequence of beaver dams along a stream corridor may have major effects on hydrology, sedimentation, and mineral nutrients (Forman 1995). Silts and other fine sediments accumulate in the pond rather than being washed downstream. On the other hand the aquatic ecological conditions are improved by the beaver dams. Water from storm flow is held back, thereby affording some measure of flood control. Wetland areas usually form, and the water table rises upstream of the dam. The ponds combine slow flow, near-constant water levels, and low turbidity that support fish and other aquatic organisms. Birds may use beaver ponds extensively.

(a)

(b)

Fig. 10.20 (a) High sediment concentration in a stream in Taiwan, southeastern China, which results in low transparency, low dissolved oxygen, and sediment coating the substrate; (b) Turbid seawater with high concentration of sediment impacts on fish and invertebrate communities (See color figure at the end of this book)

The Pennsylvania Department of Environmental Quality found that "dams of this nature are inherently hazardous and cannot be permitted". The Department therefore orders "to restore the stream to a free-flow condition by removing all wood and brush forming the dams from the stream channel". The beaver dam and the life of beavers on fish in their "reservoir" is a part of the ecology, which increases the diversity of habitats. The landlord Mr. R. Devries pronounced on behalf of the beavers that "the Spring Pond Beavers have a right to build their unauthorized dams as long as the sky is blue, the grass is green and water flows downstream. They have more dam rights than humans do to live and enjoy Spring Pond. If the Department of Natural Resources and Environmental Protection lives up to its name, it should protect the natural resources (Beavers) and the environment (Beavers' Dams).

Riparian vegetation, in general, tends to be resilient. Despite the fact that a flood may destroy a mature cottonwood forest, the conditions it leaves behind are usually those of a nursery, so a new forest can be established, and, thus, the riparian ecosystem is increased (Brady et al., 1985). Having developed characteristics such as high biomass and deep established root systems, the riparian forest systems have adapted to many types of natural stresses. Due to this adaptation, small and frequent droughts, floods, and other natural disruptions are of little consequence to the systems. When an unexpected serious stress occurs like fire, then the effect is only local and does not affect the community on a larger scale.

However, the resilience of the system can be disrupted by widespread effects such as acid rain and indiscriminate logging and associated road building. Soil moisture, soil nutrients, and soil temperature can be critically changed by these and other disturbances, as well as other factors. Several tens of years are needed for the recovery of a system affected by widespread disturbance.

(a)

(b)

Fig. 10.21   (a) A couple of beavers began to construct a dam with tree branches on the Spring Pond in Pennsylvania, U.S.; (b) The 3 m high beaver dam forms a pond, which provides a good habitat for fish and birds

10.2.2   Human-Induced Stresses

Human-induced stresses undoubtedly have the greatest potential for introducing enduring changes to the ecological structure and functions of stream corridors. Physical disturbance effects occur at any scale from landscape and stream corridor to stream and reach, where they can cause impacts locally or at locations far removed from the site of origin. Activities such as flood control, road building and maintenance, agricultural tillage, and irrigation, as well as urban encroachment, can have dramatic effects on the geomorphology and hydrology of a watershed and the stream corridor morphology within it. The

modification of stream hydraulics directly affects the system, causing an increase in the intensity of disturbances caused by floods. Chemically defined disturbance effects, for example, can be introduced through many activities including discharging sewage and wastewater (acid mine drainage and heavy metals) into the stream. Ecological disturbance effects are mainly to the result of the introduction of exotic species. The introduction of exotic species, whether intentional or not, can cause disruptions such as predation, hybridization, and the introduction of diseases. For instance, bullfrogs have been introduced into the western U.S. They reproduce prodigiously and prey on numerous native amphibians, reptiles, fish, and small mammals and cause biological problems in the ecosystem. Altering the structure of plant communities can affect the infiltration and movement of water, thereby altering the timing and magnitude of runoff events.

Dams—Ranging from small temporary structures to huge multipurpose structures, human constructed barriers can have profound and varying impacts on stream corridors. The effect of disturbances resulting from barriers used for river impoundment on water quality, sediment transportation, and ecology are discussed extensively in Chapter 7. Barriers affect resident and migratory organisms in stream channels. Power plants may kill fish when they swim through the turbines. Figure 10.22 (a) shows that many birds are searching for dead fish at the outlets of a hydro-power plant in Korea, which were killed when they swam through the turbine; Figure 10.22 (b) shows that the Baozhusi Dam on the Bailong River in Sichuan Province has cut off the river flow. The stream ecology of the lower reaches has been greatly affected. The dam blocks or slows the passage and migration of aquatic organisms, which in turn affects food chains associated with stream ecological functions.
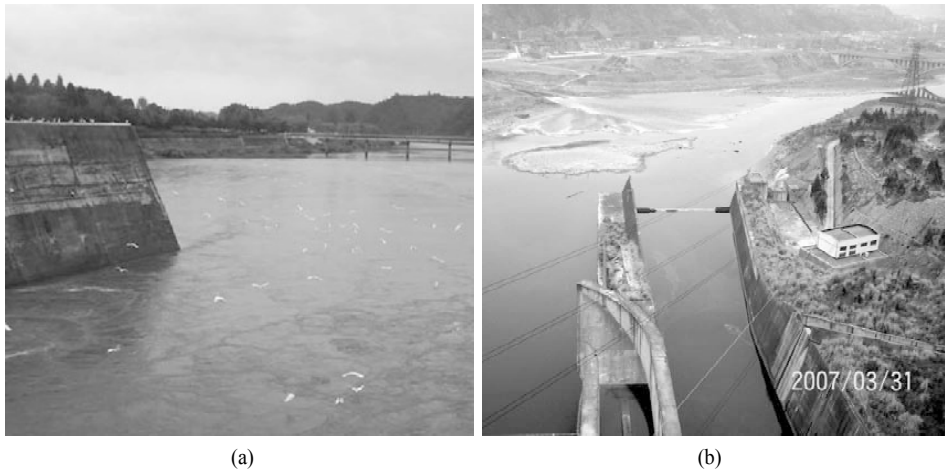
(a)   (b)

Fig. 10.22 (a) Birds are searching for dead fish at the outlets of a hydro-power plant at which fish are killed when they swim through the turbine; (b) The Baozhusi dam on the Bailong River has cut off the flow and greatly affects the stream ecology in the lower reaches (See color figure at the end of this book)

The Colorado River watershed is a 627,000 km^2 mosaic of mountains, deserts, and canyons. The watershed begins at over 4,000 m in the Rocky Mountains and ends at the Sea of Cortez. Many native species require very specific environments and ecosystem processes to survive. Under natural conditions, the basin's rivers and streams were characterized by a large stochastic variability in the annual and seasonal flow levels. This hydrologic variability was a key factor in the evolution of the basin's ecosystems. Today over 40 dams and diversion structures control the river system and result in extensive fragmentation of the watershed and riverine ecosystem.

Chanalization and water diversions—Like dams, channelization disturbs the stream ecology, by disrupting riffle and pool complexes needed at different times in the life cycle of certain aquatic organisms. The flood conveyance benefits of channelization and diversions are often offset by ecological losses resulting from increased stream velocities and reduced habitat diversity. Levees along rivers and diversion channels tend to replace riparian vegetation. The reduction in trees and other riparian vegetation along levees result in changes in shading, temperature, and nutrients. Hardened banks result in decreased habitat for organisms that live in stream sediments, banks, and riparian plants. Figure 10.23 (a) shows that the sediment banks of the lower Weihe River (the largest tributary of the Yellow River) have been replaced by stone walls in order to control floods and stabilize the channel. Figure 10.23 (b) shows that an urban stream in Beijing is reconstructed with concrete banks and channel bed for controlling seepage. Most of macro-invertebrates, reptiles, and amphibians have disappeared because the habitats for them have been covered with concrete.

(a)

(b)

Fig. 10.23   (a) Hardened banks of the Weihe River; (b) Concrete banks and bed of an urban stream in Beijing

Water diversion from rivers impacts the stream ecology, depending on the timing and amount of water diverted, as well as the location, design, and operation of the diversion structure. Figure 10.24 shows that

the water flow in the Minjiang River, which is a tributary of the Yangtze River, is cut off due to water diversion. To exploit the hydro-power at low cost many low dams have been constructed on the river and the river water is diverted through pipelines and tunnels to the hydropower plants, which are located at several tens of kilometers downstream. Because all water has been diverted the reaches between the dams and the power plants became dry and all aquatic life were killed or seriously impacted. There are many such hydro-power plants on the rivers in southwestern China, and, more hydro-power plants of such a type are being planned or are in construction. The management of stream ecology in southwestern China is facing a serious challenge.

Fig. 10.24 Water flow in the Minjiang River is cut off due to water diversion

Fragmentation of habitat—Some river training works result in the fragmentation and isolation of habitats. Figure 10.25 shows the Yangtze River and numerous riparian lakes with different sizes. Naturally these lakes connected with the Yangtze River and formed a huge habitat in the past. Humans cut the connection for flood defense and aquatic farming, thus, fragmenting the habitat. The fragmentation of habitat has resulted in deterioration of the ecology and extinction of some species.
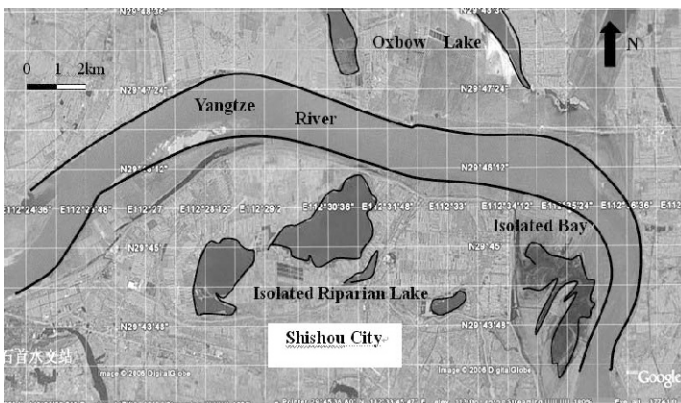
Fig. 10.25 Isolation of riparian lakes along the Yangtze River results in fragmentation of habitat (Satellite image from the web http://earth.google.com) (See color figure at the end of this book)

Cut-off of riparian lakes from the Yangtze River stressed the complex ecosystem in the lakes and the river. Figure 10.26 shows a comparison of species richness of aquatic plants and benthic invertebrates in isolated lakes and river-linked lakes in the middle and lower Yangtze River basin (Wang and Wang, 2008). The connection of the isolated lakes with the Yangtze River was cut off in the past decades, which has resulted in continuous reduction of species. The cut-off also caused reduction of fish species. There are 101 fish species in the river-linked Poyang Lake but only 57 and 47 fish species in the isolated Honghu Lake and Zhangdu Lake.

An experiment was conducted in the Juma River in the suburbs of Beijing. In a backwater area of the river two experimental plots, a large one with area of 100 m^2 and a small one with area of 4 m^2, were separated from the neighboring water by steel sheet walls. The impact on benthic invertebrates was monitored for 6 months. Figure 10.27 shows the variation of the total abundance and species richness in the two plots compared with those of the open water. In the first 40 days the differences between the three kinds of habitats are inconsistent. Nevertheless, it becomes clear after 40 days that both abundance and species number in the closed plots reduced greatly. The abundance and richness in the small plot
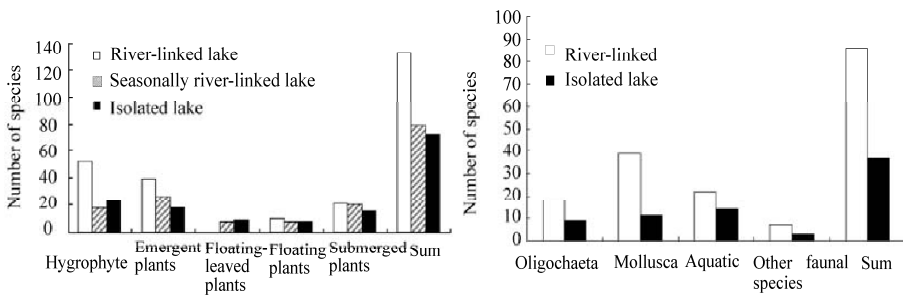
Fig. 10.26   Comparison of species richness of aquatic plants and benthic invertebrates in isolated lakes and river-linked lakes in the middle and lower Yangtze River basin (after Wang and Wang, 2008)
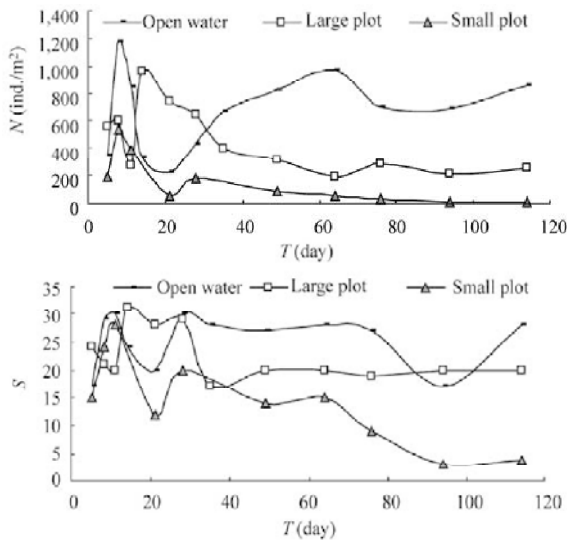
Fig. 10.27   The number density, N, and species number, S, of benthic invertebrates in fragmented habitats (large plot area = 100 m^2; small plot area = 4 m^2) varying with time (after Duan and Wang, 2008)

reduced to almost zero. In the large closed plot the abundance has reduced by two thirds and the species number reduced by one third (Duan and Wang, 2008). The results indicate that habitat fragmentation is a serious stress on the ecosystem and must be considered in ecological restoration of the river-lake complex system.

Mining—Gold placer mining in rivers has become an extreme intensive disturbance to the stream ecology in southwestern China. Figure 10.28(a) shows placer mining in the Bailong River, which is a tributary of the Jialing River in Sichuan Province. People are removing bed gravel from the river for placer mining. The benthic invertebrate community is completely disturbed. Moreover, mercury is used in the process, which has also resulted in water pollution. Compared with gold mining, gravel mining is much more wide-spread. Since the 1980s, gravel mining has become a serious ecological stress in many rivers throughout China, as shown in Fig.10.28(b). Gravel and coarse sand are mined for building materials. Gravel mining causes loss of habitat for benthic biocommunities and loss of spawning ground for many fish species. Lacking laws for controlling river sediment mining and attracted by great economic benefit, sediment mining has developed so quickly that almost all streams are stressed.

Surface mining also causes stresses on the river ecosystem. Exploration, extraction, processing, and transportation of coal, minerals, and other materials have had and continue to have a profound effect on

(a)

(b)

Fig. 10.28   (a) Gold placer mining in the Bailong River, a tributary of the Jialing River in Sichuan; (b) Gravel mining for building materials from the Qingjiang River, a tributary of the Yangtze River

stream corridors. Many rivers ecosystems remain in a degraded condition as a result of mining activities. Such mining activity frequently resulted in total destruction of the stream corridor. In some cases today, mining operations still disturb most or all of entire watersheds. Figure 10.29 shows a gold mine in the Henan Province in central China. Mercury was used to separate gold from the ore, therefore, mercury was also lost into streams. Present-day miners using suction dredges often find considerable quantities of mercury still resident in streambeds. Current heap-leaching methods use cyanide to extract gold from low-quality ores. This poses a special risk if operations are not carefully managed.

Fig. 10.29   A gold mine in the Henan in central China causes pollution of the Yihe River

Pollution—Point source pollution from industry and diffuse pollution from agriculture (pesticides and nutrients) have the potential to disturb natural chemical cycles in streams, and, thus, to degrade water quality and impact the ecosystem. Figure 10.30 (a) shows waste water from a factory discharged into the Jialing River, a large tributary of the Yangtze River in the Sichuan Province, and the seriously polluted river water. Riparian vegetation and animals near the outlet have been killed. The frog shown Fig 10.30 (b) has been killed due to the pollution. Heavy sewage discharge also causes stresses to the bio-communities. Figure 10.31 (a) show the pollution of a stream flowing through the Dalian City, which is caused by uncontrolled sewage discharge. Fish and many other animals in the stream have been killed by the pollution. Figure 10.31 (b) shows eutrophication of the Lijiang River at Guilin, a famous tourism attraction for its beautiful landscape and streams. Sewage discharge from the city causes pollution of the river water and blooming of phytoplankton and macrophytes.

Toxic runoff or precipitates can kill streamside vegetation or can cause a shift to species more tolerant of polluted conditions. This affects habitat required by many species for cover, food, and reproduction. Aquatic habitat suffers from several factors. Acid mine drainage can coat stream bottoms with iron precipitates, thereby affecting the habitat for bottom-dwelling and feeding organisms. Precipitates coating the stream bottom can eliminate places for egg survival. Fish that do hatch may face hostile stream conditions due to poor water quality.

Chemical disturbances from agriculture are usually widespread, nonpoint sources. Municipal and industrial waste contaminants are typically point sources and often chronic in duration. Secondary effects, such as agricultural chemicals attached to sediments, frequently occur as a result of physical activities (irrigation or heavy application of herbicides). In these cases, it is better to control the physical activity at its source than to treat the symptoms within a stream corridor.

(a)   (b)
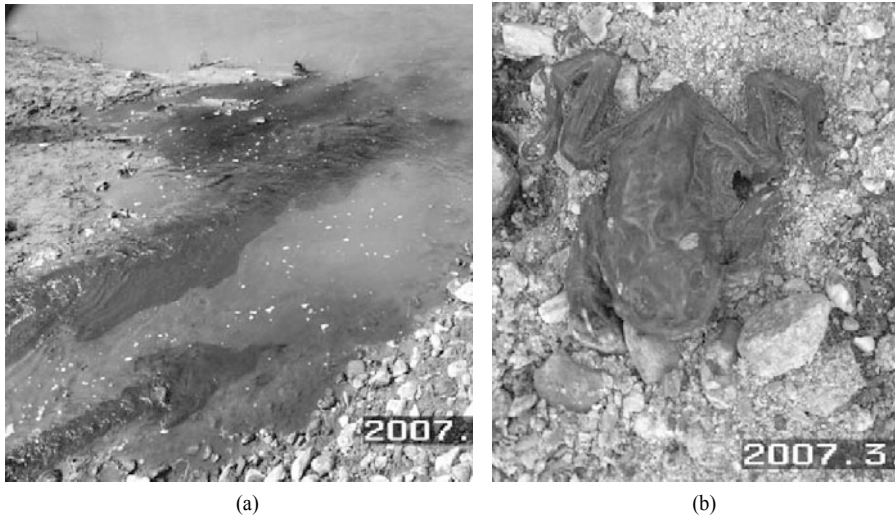
Fig. 10.30 (a) Waste water from a factory is discharged into the Jialing River and seriously polluting the river water; (b) A frog is killed due to the pollution

(a)   (b)
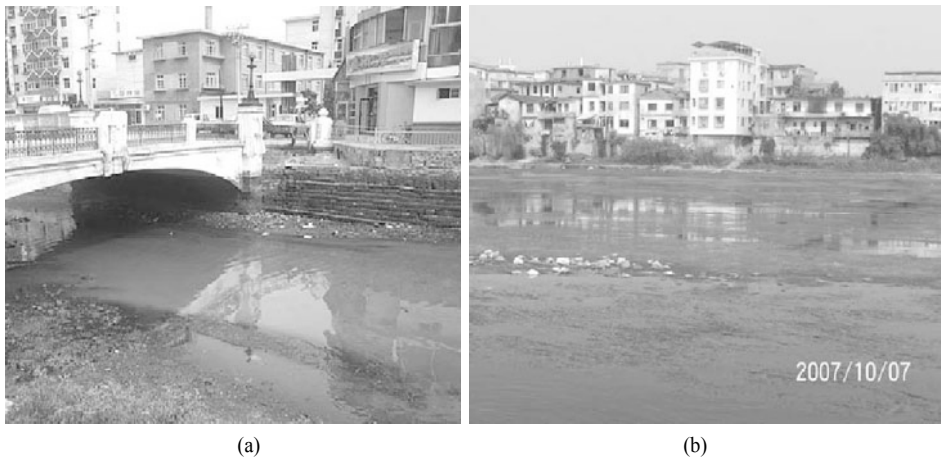
Fig. 10.31 (a) Urban sewage polluting a stream flowing through the Dalian in northeast China; (b) Eutrophication of the Lijiang River at Guilin, a famous tourism attraction for its beautiful landscape and streams

Urbanization—Urbanization in watersheds poses special challenges for stream ecological management. Recent research has shown that streams in urban watersheds have a character fundamentally different from that of streams in forested, rural, or even agricultural watersheds. Impervious cover directly influences urban streams by dramatically increasing surface runoff during storm events by 2 to 16 times, with proportional reductions in ground water recharge (Schueler, 1995). Figure 10.32 conceptually shows the effects of different amounts of impervious cover on the water balance for a watershed.

The unique character of urban streams often requires unique restoration strategies for the steam corridor. The peak discharge associated with the bankfull flow (1- to 2-year flood) increases sharply in magnitude in urban streams. Since impervious cover prevents rainfall from infiltrating into the soil, less flow is available to recharge ground water. Consequently, during extended periods without rainfall, baseflow

levels are often reduced in urban streams (Simmons and Reynolds, 1982). Another modification unique to urban streams is the installation of sanitary sewers underneath or parallel to the stream channel.
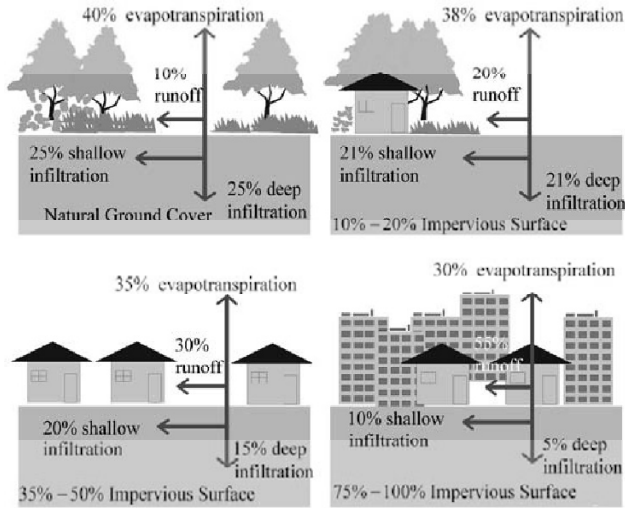
Fig. 10.32   Effects of different amounts of impervious cover on the water balance for a watershed (after FISRWG, 1997)

The water quality of urban streams during storm events is consistently poor. Urban storm water runoff contains moderate to high concentrations of sediment, carbon, nutrients, trace metals, hydrocarbons, chlorides, and bacteria (Schueler, 1987). Large woody debris is an important structural component of many small rivers, creating complex habitat structure and generally making the stream more retentive. In urban streams, the quantity of large woody debris found in stream channels is reduced due to the loss of riparian forest cover, storm washout, and channel maintenance practices (May et al., 1997). Many river crossings can become partial or total barriers to upstream fish migration, particularly if the streambed erodes below the fixed elevation of a culvert or a pipeline. The important role that riparian forests play in stream ecology often is diminished in urban watersheds since tree cover is often partially or totally removed along the stream as a consequence of development (May et al., 1997). Figure 10.33 shows a tributary of the Jialing River (a tributary of the Yangtze River) flowing through the Guangyuan that has been greatly affected by urbanization. Riparian forest has been replaced by residential buildings and the banks are hardened with concrete. The flow discharge in low the flow season has been reduced due to water diversion.

Agriculture and land-use change—Land-use change is the most common human-induced stress on the ecosystem. Agricultural activities have generally resulted in encroachment on stream corridors. Producers often crop as much productive land as possible to enhance economic returns; therefore, native vegetation is sacrificed to increase arable areas. As the composition and distribution of vegetation are altered, the interactions between ecosystem structure and function become fragmented. Vegetation removal from stream banks, floodplains, and uplands often conflicts with the hydrologic and geomorphic functions of stream corridors. These disturbances can result in sheet erosion, rill erosion, and gully erosion, reduced infiltration, increased upland surface runoff and transport of contaminants, increased bank erosion, unstable stream channels, and impaired habitat.

Fig. 10.33 Riparian forest has been replaced by buildings and the banks are hardened with concrete in Guangyuan, Sichuan

Tillage and soil compaction interfere with the soil's capacity to partition and regulate the flow of water in the landscape, increase surface runoff, and decrease the water-holding capacity of soils. Tillage also often aids in the development of a hard pan, a layer of increased soil density and decreased permeability that restricts the movement of water into the subsurface. Disturbance of soil associated with agriculture generates runoff polluted with sediment, a major nonpoint source pollutant in the world. Pesticides and nutrients (mainly nitrogen, phosphorous, and potassium) applied during the growing season can leach into ground water or flow in surface water to stream corridors, either dissolved or adsorbed to soil particles. Improper storage and application of animal waste from concentrated animal production facilities are potential sources of chemical and bacterial contaminants to stream corridors.

Tree removal decreases the quantity of nutrients in the watershed since approximately one-half of the nutrients in trees are in the trunks. Nutrient levels can increase if large limbs fall into streams during harvesting and decompose. Conversely, when tree cover is removed, there is a short-term increase in nutrient release followed by long-term reduction in nutrient levels. Removal of trees can affect the quality, quantity, and timing of stream flows. If trees are removed, from a large portion of a watershed, flow quantity can increase accordingly, and water temperature can increase during summer and decrease in winter.

Many of the potential effects of land use change are cumulative or synergistic. Restoration might not remove all disturbance factors; however, addressing one or two disturbance activities can dramatically reduce the impact of those remaining. Simple changes in management, such as the use of conservation buffer strips in cropland or managed livestock access to riparian areas, can substantially overcome undesired cumulative effects or synergistic interactions.

Domestic livestock—Stream corridors are particularly attractive to livestock for many reasons. They are generally highly productive and provide ample forage. Husbandry development in a watershed has applied a unique stress on the ecosystem. For instance, the riparian vegetation succession from herbaceous to shrubs has been delayed or even stopped by grazing of livestock along the Ake River on the Qinghai-Tibet Plateau, as shown in Fig. 10.34(a). On the other hand, the activities of livestock have become an important element of the river ecology. Excrement of cattle provides the main nutrient for the grassland. The positive and negative effects of grazing of domestic livestock must be considered in any restoration strategy. In many cases livestock swimming in a stream can result in extensive physical disturbance and bacteriological contamination, as shown in Fig. 10.34(b).

Recreation and tourism—The amount of impacts caused by the recreation and tourism industry depends on stream hydrology, soil type, vegetation cover, topography, and intensity of use. Various forms of foot and vehicular traffic associated with recreational activities can damage riparian vegetation and soil structure. All-terrain vehicles, for example, can cause increased erosion and habitat reduction. At locations, reduced infiltration due to soil compaction and subsequent surface runoff can result in increased sediment loading to the stream (Cole and Marion 1988). In areas where the stream can support recreational boating, the system is vulnerable to additional impacts. Propeller wash and water displacement can disrupt and resuspend bottom sediment, increase bank erosion, and disorient or injure sensitive aquatic species, as shown in Fig. 10.35.

(a)   (b)

Fig. 10.34 (a) Grazing pressure has been increased due to development of husbandry in the Tibet-Qinghai Plateau; (b) Livestock swimming in a stream can result in extensive physical disturbance and bacteriological contamination (See color figure at the end of this book)

Fig. 10.35 Recreational boating, cruise tours, propeller wash, and accidental spills can degrade stream habitat (See color figure at the end of this book)

Forestry—In addition to the changes in water, sediment, and nutrients loads to streams because of logging practices (i.e. land-use change), forestry may have other impacts of river ecosystems. Forest roads are constructed to move loaded logs to higher quality roads and then to a manufacturing facility.

Mechanical means to move logs to a loading area (landing) produce "skid trails." Stream crossings are necessary along some skid trails and most forest road systems and are in especially sensitive areas. Removal of topsoil, soil compaction, and logging equipment and log skidding can result in long-term loss of productivity, decreased porosity, decreased soil infiltration, and increased runoff and erosion. Spills of petroleum products can contaminate soils. Trails, roads, and landings can intercept ground water flow and cause it to become surface runoff.

10.3.3 Introduction of Exotic Species

Biologically defined disturbance effects occur within species (competition, cannibalism, etc.) and among species (competition, predation, etc.). These are natural interactions that are important determinants of population size and community organization in many ecosystems. Biological disturbances due to improper grazing management or recreational activities are frequently encountered. The introduction of exotic flora and fauna species can introduce widespread, intense, and continuous stress on native biological communities.

There are numerous examples worldwide of introduced species bringing about the extinction of native organisms. The most dramatic have involved predators. An extreme example is the deliberate introduction of the fish-eating Nile Perch *(Lates nilotica)* to Lake Victoria, in East Africa, causing the extinction of dozens of species of small endemic cichlid fish. Introduced cats, rats, and snakes have had a similar effect on island bird fauna (Dugeon and Corlett, 2004).

Exotic animals are a common problem in many areas in the U.S. and China. Species such as *Cambarus Clarkaij* have been introduced in many waters in south China. Without the normal checks and balances found in their native habitat in North America and Japan, *Cambarus Clarkaij* reproduces prodigiously and causes disturbance to the ecosystem. Figure 10.36 shows *Cambarus Clarkaij*. The species burrow in river levees and have caused many breaches and flooding disasters. The rapid spreading of the species has caused rice harvest reduction because the animals eat the rice paddies' root. In some places *Cambarus Clarkaij* has also caused prevalence of a disease.
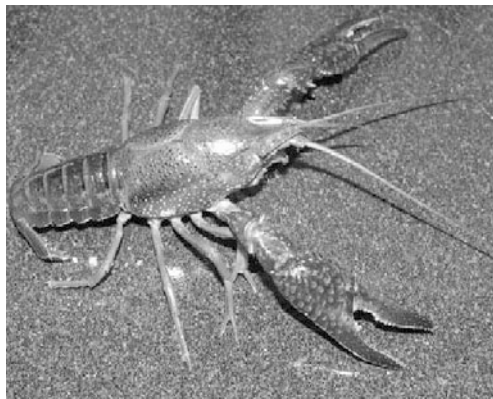
Fig. 10.36 *Cambarus Clarkaij* has been introduced in many waters in south China, resulting in ecological problems

Similarly introduction of the zebra mussel and bullfrog have imposed an intense stress on native biological communities in the western U.S. Without the normal checks and balances found in their native habitat in the eastern U.S., bullfrogs reproduce prodigiously and prey on numerous native amphibians, reptiles, fish, and small mammals.

Golden mussel (*Limnoperna fortunei*) is an invasive filter species of macro-invertebrate. Originally the

species comes from south China, which has spread to various regions, including Japan, Australia, Argentina, Thailand, India, Brazil and Europe (Darrigran *et al.,* 2003). The species colonizes habitats with water temperature between 8–35℃, flow velocity less than 2 m/s, water depth less than 10 m with or without sunlight, dissolved oxygen higher than 1.0 mg/L, and pH higher than 6.4 (Morton, 1982; Márcia, 2006; Darrigran and Damborenea, 2006). Golden mussels have unprimitive byssus threads, which allow them to attach onto solid walls, especially human constructed water transfer tunnels and pipelines. Dense attachment of golden mussels in drink water transfer tunnels and pipelines results in macro-fouling (Yamada *et al.,* 1997), causes high resistance to water flow and damage to pipeline walls. This along with dead mussels decay harms the surrounding water quality (Darrigran, 2002; Guan and Zhang, 2005).

Golden mussels have a high reproduction rate. Due to the favorable conditions in water diversion tunnels, cooling pipelines, pumps, and gate slots, golden mussel tends to colonize these habitats, ultimately leading to damage to these facilities. Figure 10.37 shows colonization of golden mussel in the water transfer tunnels in Shenzhen, southern China and attachment golden mussel on the surface of a concrete fragment. The density of golden mussel individuals is as high as to 20,000/m^2. Golden mussel invasion causes a serious challenge to water transfer projects that seek to solve issues such as the uneven distribution of water resources and the problem of water shortages in northern China. The presence of golden mussels results in quick and uncontrolled spread of the species.
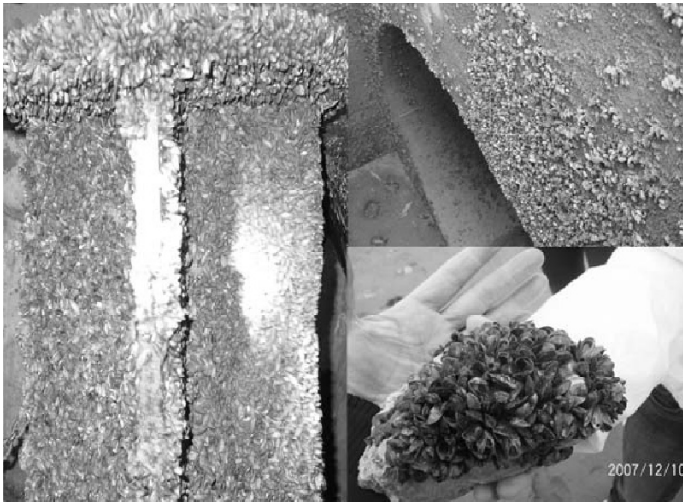
Fig. 10.37   Colonization of golden mussel on concrete walls in a water transfer tunnel and attachment of golden mussel on a concrete fragment with high density (See color figure at the end of this book)

Studies have been conducted to learn the golden mussels' biological characteristics in order to find effective and sustainable strategies to control its invasion (Morton, 1977b; Wang, 1997; Darrigran and Damborenea, 2006; Zhuang, 2006a; Liu et al., 2006; Li and Su, 2007). Many measures have been suggested to control golden mussels (Xu et al, 2009), such as filter screen at the entrance of the water transfer systems (Darrigran, 2002), sand filter by using proper size distribution of sand (Lou and Liu, 1958), adjustment of flow velocity to restrain the attachment (Xiang, 1985), smooth pipe walls with anticorrosive coat to stop attach (Luo, 2006; Zhuang, 2006b), temperature control, electromagnetic treating, and dissolved oxygen reduction (Morton, 1975; Mcennulty, 2001), hot and dry environment (Iwasaki, 1977; Darrigran, et al., 2004), sealing up the pipelines to block oxygen from entering (Liu et al.,

2006; Morton, 1977a), hot water spraying to kill golden mussels (Morton, 1975), medicaments to kill golden mussels rapidly (Yamada *et al*., 1997), culture species of fishes preying golden mussels, injecting certain steroids to disturb the normal spawning (John and Peter, 2001), and artificial or mechanical clearance during overhaul periods. Nevertheless, no effective and safe measures have been found to control the mussel. At present artificial or mechanical clearance during overhaul periods is the only effective and safe measure although it is expensive and causes intermittence of water supply.

Introduction of plant species may also cause stress on animal species. It was reported in the *China Daily* on Aug. 14, 2003, that the natural habitat of giant pandas, rare animals living mainly in China's Qinling Mountain range, is being threatened by larch forests (Fig. 10.38). The story is as follows: "In recent years farmers in Sha-anxi province introduced larch trees because of its low planting cost, high survival rate and quick maturation into useful timber. However, the blind introduction of larch trees into the panda protection zones has severely depleted the groves of bamboo, the food staple of pandas. Larch trees have large crowns which can cause plants growing beneath them to die from a shortage of sunshine and water. And larch seeds, spread by birds and the wind, grow quickly. This can seriously impact the growth of surrounding plants. The introduction of larch into Qinling Mountain areas started in the early 1980s. In Foping County, the major home of pandas, more than 1,333 hectares of larch trees have been planted and the damaged bamboo forest cannot be recovered. The situation is also worsening in other protection zones, such as Changqing and Yangxian. The corridor linking panda clans in Ningshan and Foping has now been destroyed by larches. The habitat was decreased and the animals will suffer from the lack of food. Experts warned that the pandas will lose their home if the larch is not put under control, and the local government is expected to take measures soon."

Fig. 10.38 Natural habitat of giant pandas is being threatened by the introduction of larch trees and rapid development of larch forests (See color figure at the end of this book)

Introduction of exotic species has inevitably occurred worldwide and this is accelerating following economic and ecologic globalization. Compared with faunal species, introduction of floral species is quicker and more intensive because humans pay less attention to the negative impacts of the introduction. The introduction of exotic species, whether intentional or not, can cause disruptions such as hybridization and the introduction of diseases. Nonnative species compete with native species for moisture, nutrients,

sunlight, and space and can adversely influence establishment rates for new plantings, foods, and habitat. In some cases, exotic plant species can even detract from the recreational value of streams by creating a dense, impenetrable thicket along the streambank.

Many exotic species have been introduced as consequences of human activities. For instance, at least 708 floral species and about 40 faunal species have been successfully introduced into China in the past century, among them several tens of species have caused ecological problems. A lot of money has been spent to remove these species. The most harmful species are *Eupatorium adenophorum*, *Eichoimia crassips*, Ambrosia artemisia L., and *Spartina alterniflora*.

Spartina alterniflora was introduced from the U.S. in 1980 to control coastal erosion and accelerate land creation in estuaries. The species may grow in salt marsh, because they tolerate periodical tidal inundation and resist wave erosion. The species colonize silt coasts very quickly and stabilize the coast with its dense roots. Nevertheless, the species dominate silt coasts and estuaries, resulting in a great reduction in biodiversity. Many invertebrates and fish cannot live in the shallow waters with *Spartina alterniflor*. The species has over to spread the neighboring coastal areas. Coastal areas and estuaries dominated by reed (*Phragmites communis trirn*) have been colonized and occupied by *Spartina alterniflor*. The fishery harvest has been significantly reduced. Figure. 10.39(a) shows *Spartina alterniflor* in the Yangtze River estuary.

Fig. 10.39   (a) *Spartina alterniflor* in the Yangtze River estuary; (b) *Eupatorium adenophorum* in southwestern China; (c) *Eichoimia crassip* in polluted waters; (d) Ambrosia artemisia L. in northeastern China. (See color figure at the end of this book)

Alien invasive species *Eupatorium adenophorum* originates from Mexico and was introduced into south China from south Asia in the 1940s. The species has spread quickly in southwestern China and eliminated local species. The species is toxic and many cattle and sheep have been killed. The area occupied by the species has increased to about 30 million ha (Li and Wang, 2003). To remove the species from grassland is very difficult. Millions of dollars have been lost due to husbandry loss and control of spreading of the species in Sichuan and Yunnan Provinces. Figure 10.39(b) shows the *Eupatorium adenophorum* in Yunnan Province in southwestern China.

Eichoimia crassip was introduced to control eutrophication in streams and lakes. The species adsorb pollutants and nutrients in the water and may enhance the purification capacity of the stream or lake. Nevertheless, the species spread too fast and fishery and water surface recreation have been affected. Humans have to remove them from waters, which has caused economic losses up to several tens of millions of dollars. Figure 10.39(c) shows *Eichoimia crassip* spreading quickly in a polluted stream in Beijing.

Ambrosia artemisia L. and *Ambrosia tritida* L. entered China in the 1930s and spread quickly since the 1980s and 1990s. The species produce a lot of pollen. In Shenyang in northeastern China the density of pollen in air in 1987 was 38 times of that in 1983 because of introduction of the species. About 1.5% of the local people suffer from pollinosis. Millions of dollars have been lost due to introduction of the species. Figure 10.39(d) shows the Ambrosia artemisia L. in northeastern China.

Introduction of exotic species is not always bad for the ecosystem. Hong Kong has become a paradise of exotic species and most of these species have been naturalized in the island. Hong Kong and the island of Dominica, in the Caribbean, probably had no inland plant species in common 500 years ago. Today they share more than a hundred weeds of human-dominated open habitats. The terms 'alien' is used to refer to species that originated elsewhere but have become established in Hong Kong. Although people have introduced many alien species by accident, others have been brought to a location deliberately, as crops, ornamentals, livestock, or pets. Not all introduced species are aliens. In fact, reintroduction of species to parts of their former range is an important conservation tool. Hong Kong's total vascular plant flora of approximately 2,100 species includes at least 150 naturalized aliens: that is, species introduced from other parts of the world which have run wild in Hong Kong (Dudgeon and Corlett, 2004). For faunal species, most of these aliens were brought to Hong Kong by people, but some have spread on their own. Some of these have established wild populations when they escaped, were abandoned or released.

In Hong Kong the majority of introduced species are confined to those areas where human influence is strongest and most persistent. Indeed, in most residential and industrial areas, as well as the few sites still used for intensive farming, alien species dominate the biota. In contrast, recognizable aliens are rare or absent in most upland streams and hillside communities. Thus, the majority of aliens are found in those places where the native flora and fauna has already suffered most as a result of human activities. At present, the impact of the numerous alien plant and animal species established in Hong Kong is, in most cases, hard to distinguish from the direct impact of human activities on the habitats they occupy (Dudgeon and Corlett, 2004).

The introduction of alien species into Hong Kong has increased the biodiversity and has resulted in no serious impacts on the local ecology. However, invasions by alien species are a potential conservation management problem that has received almost no attention in Hong Kong. Even if we ignore the risk posed by aliens to the ecology of Hong Kong, we have an obligation to ensure that the territory does not become a stepping-stone for invasion elsewhere.

10.3   Assessment of River Ecosystems

10.3.1   Indicator Species

Complete measurement of the state of a river ecosystem, or even a complete census of all of the species present, is not feasible. Thus, good indicators of the system conditions are efficient in the sense that they summarize the health of the overall system. The current value of an indicator for an impaired river ecosystem can be compared to a previously measured, pre-impact value, a desired future value, an observed value at an "unimpaired" reference site, or a normative value for that class of river ecosystems. For example, an index of species composition based on the presence or absence of a set of sensitive species might be generally correlated with water quality. If a river is polluted some species may be absent and the number of species may be less than that before the pollution. An index of indicator species itself provides no information on how water quality should be improved. However, the success of management actions in improving water quality could be tracked and evaluated through iterative measurement of the index.

An indicator species group is defined as a set of organisms whose characteristics (e.g., number of species, presence or absence, population density, dispersion, reproductive success) are used as an index of attributes or environmental conditions of interest, which are too difficult, inconvenient, or expensive to measure for other species (Landres et al., 1988). The 1970s–1980s is a peak interest period using aquatic and terrestrial indicator species for assessment of ecosystems. During that time, Habitat Evaluation Procedures (HEP) were developed by the U.S. Fish and Wildlife Service, and the use of management indicator species was mandated by law with passage of the National Forest Management Act in 1976. Since that time, numerous authors have expressed concern about the ability of indicator species to meet the expectations expressed in the above definition. Landres et al. (1988) critically evaluated the use of vertebrate species as ecological indicators and suggested that rigorous justification and evaluation are needed before the concept is used.

Indicator species have been used to predict environmental contamination, population trends, and habitat quality. The assumptions implicit in using indicators are that if the habitat is suitable for the indicator it is also suitable for other species and that wildlife populations reflect habitat conditions. However, because each species has unique life requisites, the relationship between the indicator and its guild may not be completely reliable. It is also difficult to include all the factors that might limit a population when selecting a group of species that an indicator is expected to represent.

10.3.1.1   Selection of Indicator Species

Several factors are important to consider in the selection process of indicator species (FISRWG, 1997):

(1) Sensitivity of the species to the environmental attribute being evaluated. When possible, data that suggest a cause-and-effect relation are preferred to mere correlation (to ensure the indicator reflects the variable of interest).

(2) Indicator accurately and precisely responds to the measured effect. High variation statistically limits the ability to detect effects. Generalist species do not reflect change as well as more sensitive endemics. However, because specialists usually have lower populations, they might not be the best for cost-effective sampling. When the goal of monitoring is to evaluate on-site conditions, using indicators that occur only within the site makes sense. However, although permanent residents may better reflect local conditions, the goal of many riparian restoration efforts is to provide habitat for migratory birds. In this case, residents such as cardinals or woodpeckers might not serve as good indicators for migrating warblers.

(3) Size of the species home range. If possible, the home range should be larger than that of other species in the evaluation area. Game species are often poor indicators simply because their populations

are highly influenced by hunting mortality, which can mask environmental effects. Species with low populations or restrictions on sampling methods, such as threatened and endangered species, are also poor indicators because they are difficult to sample adequately.

(4) Response uniformity in different geographic locations. Response of an indicator species to an environmental stress cannot be expected to be consistent across varying geographic locations or habitats. If possible, the response to a stress should be more uniform than that of other species in different geographic locations.

In summary, a good indicator species should be in the middle on the food chain to respond quickly and have relatively high stability, should have a narrow tolerance to stresses, and should be a native species (Erman, 1991). The selection of indicator species should be done through corroborative research.

10.3.1.2   Aquatic Macro-Invertebrates

Aquatic macro-invertebrates have been used as indicators of stream and riparian health for many years. Perhaps more than other taxa, they are closely tied to both aquatic and riparian habitat. Their life cycles usually include periods in and out of the water, with ties to riparian vegetation for feeding, pupation, emergence, mating, and egg laying (Erman, 1991). It is often important to look at the entire assemblage of aquatic invertebrates as an indicator group. Impacts of stresses to a stream often decrease biodiversity but might increase the abundance of some species (Wallace and Gurtz, 1986). Using benthic macro-invertebrates is advantageous for the following reasons: (1) they are good indicators of localized conditions; (2) they integrate the effects of short-term environmental variables; (3) degraded conditions are easily detected; (4) sampling is relatively easy; (5) they are in the middle of the food chain and provide food for many fish of commercial or recreational importance; and (6) macro-invertebrates are generally abundant (Plafkin *et al*., 1989).

Field sampling of macro-invertebrates usually requires a combination of quantitative and qualitative collection methods. The sampling may be performed for one site in a 100 m stretch with representative areas of flow velocity, water depth, substrata composition, and hydrophyte growth. For a segment of an investigated stream, collections were made in areas with different current velocity, water depth, and different substrate sizes. At least three replicate samples were collected at each sampling site at appropriate depths of 0.15 m of the substrate with a kick-net (1 m×1 m area, 420 μm mesh) if the water depth is less than 0.7 m. A D-frame dip net may be used to sample along stone surfaces and in plant clusters. If the water depth is greater than 0.7 m, samples may be collected with a Peterson grab sampler with an open area of 1/16 m². Replicate samples for each site are combined to form a composite sample, amounting to at least a minimum area of 1m² (Duan *et al*., 2007). The cobbles sampled are generally scrubbed by hand to remove invertebrates and then discarded. The debris and invertebrates are rinsed vigorously through a fine sieve with a 300 μm mesh. Then the macro-invertebrates are taken from the debris and are placed in plastic sample containers and preserved in 10% formaldehyde in the field.

Environmental parameters, including substrate composition, water depth, water temperature, average current velocity, and dissolved oxygen concentration, are usually measured and recorded *in situ*. Growth and cover proportion of aquatic hydrophytes are also described. All macro-invertebrates are picked out of the samples and then identified and counted under a stereoscopic microscope in the laboratory. Macro-invertebrates are identified most to family or genus level except early-instar insects (Liu *et al*., 1979), and each species is assigned to a FFG based on the literature (Plafkin *et al*., 1989; Barbour *et al*., 1999).

10.3.1.3   Fish

Fish are also used as indicator species. Some management agencies use fish species as indicators to track changes in habitat condition or to assess the influence of habitat alteration on selected species. Habitat suitability indices and other habitat models are often used for this purpose, though the metric chosen to

measure a species' response to its habitat can influence the outcome of the investigation. As van Horne (1983) pointed out, density or number of fish may be misleading indicators of habitat quality. Fish response guilds as indicators of restoration success in riparian ecosystems may be a valuable monitoring tool.

Hocutt (1981) states "perhaps the most compelling ecological factor is that structurally and functionally diverse fish communities both directly and indirectly provide evidence of water quality in that they incorporate all the local environmental perturbations into the stability of the communities themselves." The advantages of using fish as indicators are: (1) they are good indicators of longterm effects and broad habitat conditions; (2) fish communities represent a variety of trophic levels; (3) fish are at the top of the aquatic food chain and are consumed by humans; (4) fish are relatively easy to identify; and (5) water quality standards are often characterized in terms of fisheries. However, using fish as indicators is inconvenient because: (1) the cost of collection is high; (2) long term monitoring and a large number of samplings are needed to have reliable results and statistical validity may be hard to attain; and (3) the process of sampling may disturb the fish community.

Electrofishing is the most commonly used field technique. Each collecting station should be representative of the study reach and similar to other reaches sampled; effort between reaches should be equal. All fish species, not just game species, should be collected for the fish community assessment. Karr et al. (1986) used 12 biological metrics to assess biotic integrity using taxonomic and trophic composition and condition and abundance of fish. The assessment method using fish as indicator has been studied and applied in many large rivers (Plafkin et al., 1989).

10.3.1.4   Birds and Mammals

Birds and mammals are used as indicator species for both terrestrial and aquatic ecosystems. Croonquist et al. (1991) evaluated the effects of anthropogenic disturbances on small mammals and birds along Pennsylvania waterways. They evaluated species in five different response guilds, including wetland dependency, trophic level, species status (endangered, recreational, native, exotic), habitat specificity, and seasonality. The habitat specificity and seasonality response guilds for birds were best able to distinguish those species sensitive to disturbance from those, which were not affected or benefited. Edge and exotic species were greater in abundance in the disturbed habitats and might serve as good indicators there. Seasonality analysis showed migrant breeders were more common in undisturbed areas, which, as suggested by Verner (1984), indicate the ability of guild analysis to distinguish local impacts.

In general the advantages of using birds and mammals as indicator species are: (1) they are good indicators of long-term effects and broad habitat conditions, including terrestrial and aquatic ecosystems; (2) they are at the top of the food chain; (3) they are relatively easy to identify; and (4) some restoration projects aim at restoration of endangered birds and mammals. The disadvantages are: (1) the cost of collection is high; (2) long term monitoring is needed to have reliable results; and (3) they are not sensitive to aquatic habitat conditions (e.g., hydrological changes or water pollution). Birds have been used as indicator species for ecological assessment of wetlands.

10.3.1.5   Algae

Algae communities are also useful for bioassessment. Algae generally have short life spans and rapid reproduction rates, making them useful for evaluating short-term impacts. Sampling impacts are minimal to resident biota, and collection requires little effort. Primary productivity of algae is affected by physical and chemical impairments. Algal communities are sensitive to some pollutants that might not visibly affect other aquatic communities. Algal communities can be examined for species, diversity indices, species richness, community respiration, and colonization rates. A variety of nontaxonomic evaluations, such as biomass and chlorophyll, may be used and are summarized in Weitzel (1979). Rodgers et al. (1979)

describe functional measurements of algal communities, such as primary productivity and community respiration, to evaluate the effects of nutrient enrichment.

Although collecting algae in streams requires little effort, identifying for metrics, such as diversity indices and species richness, may require considerable effort. A great deal of effort may be expended to document diurnal and seasonal variations in productivity.

10.3.2　Metrics of Biodiversity

10.3.2.1　Richness and Abundance

If an indicator species group is selected, the ecosystem can be assessed by monitoring some variables of the indicator species group, including the species richness, S; the number density (or abundance), N, which is the total number of individuals per area; the biomass (the total weight of all individuals) per area; and the number of individuals per area for each species. Many parameters representing biodiversity of river ecosystems have been proposed. The species richness, S, is the most widely used index (Magurran, 1988) and the most important characteristic of biodiversity:

$$S = \text{total number of species in the samples from a sampling site} \qquad (10.2)$$

The ecological assessment and habitat conditions of streams may be mainly represented by the species richness. In general, the samples should be identified to species level for all species. Nevertheless, it is often not possible because to identity some species special instruments and experienced biologists are needed. In this case these species may be identified to genus level or family level. This does not affect the ecosystem assessment if the samples before and after the disturbance are examined by the same biologist and to the same level. A simple measure of richness is most often used in conservation biology studies because the many rare species that characterize most systems are generally of greater interest than the common species that dominate in diversity indices and because accurate population density estimates are often not available (Meffe et al., 1994).

In general there are more species within large areas than within small areas. The relation between species richness, S, and habitat area, A, follows a power function formula (Ricklefs, 2001) :

$$S = cA^z \qquad (10.3)$$

where c and z are constants fitted to data. Analysis of species-area relations revealed that most values of z fall within the range 0.20–0.35 for birds and fish, and within the range 0.05–0.2 for benthic macro-invertebrates. For example, for the land-bird fauna of the West Indies, species richness increases from only 16 within an area of 10 km^2 to about 100 within an area of about 100,000 km^2. The relation between S and A is then (Ricklefs, 2001)

$$S = 10A^{0.24} \qquad (10.4)$$

The species richness increases with habitat area because habitat heterogeneity increases with the size of the area (and resulting topographic heterogeneity) of islands in the west Indies, and larger islands make better targets for potential immigrants from mainland sources of colonization. In addition, the larger populations on larger islands probably persist longer, being endowed with greater genetic diversity, broader distributions over area and habitat, and numbers large enough to prevent chance extinction.

The fish community, like birds, also occurs in a large area of habitat and the sampling area must be large enough to a have reliable value of S. As a comparison, the macro-invertebrate community is more localized and needs much less sampling area for assessment of local ecosystems. If a river ecosystem with high heterogeneity of habitat is assessed with macro-invertebrates as indicator species, numerous sampling sites should be selected to represent different habitat conditions. For each sampling site the sampling area may be one or several m^2. The work load increases with the sampling area, therefore,

ecologists prefer small sampling areas as long as a sufficient number of species can be sampled. Figure 10.40 shows the relation of the number of species in a sample and the sampling area at each site (Duan et al., 2007). The sampling area at each site should be at least 1 m² for a relatively reliable value of richness.
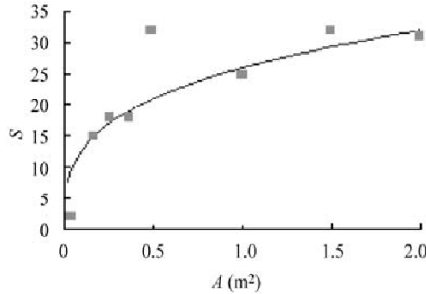
Fig. 10.40   Relation of the species richness in a sample and the sampling area at each site

The number density of individuals (abundance), N, is generally dynamic. If a bio-community colonizes a habitat at time t_0, the number density increases with time t and finally reaches equilibrium after a period of time. A differential equation describing the dynamic process of the number density growth is suggested (Ricklefs, 2001):

$$\frac{\mathrm{d}N}{\mathrm{d}t} = rN\left(1 - \frac{N}{K}\right) \tag{10.5}$$

in which r represents the intrinsic exponential growth rate of the population when its size is very small (that is, close to 0), and K is the carrying capacity of the environment, which represents the number of individuals that the environment can support. This equation is called the logistic equation. So long as N does not exceed the carrying capacity K, that is, N/K is less than 1, the number density continues to increase, albeit at a slowing rate. When N exceeds the value of K, the ratio N/K exceeds 1, $\mathrm{d}N/\mathrm{d}t$ becomes negative, and the density decreases. K is the eventual equilibrium size of number density growing according to the logistic equation. Integration of the logistic equation yields

$$N = \frac{K}{1 + \dfrac{K - N_0}{N_0}\mathrm{e}^{-rt}} \tag{10.6}$$

where N_0 is the number density of individuals at time $t = 0$. The logistic equation may be used for a species, e.g., black carp in Tongting Lake, or for a bio-community, e.g., benthic macro-invertebrates at a section of a stream.

The abundance (density number) of a particular species reflects the balance between a large number of factors and processes, variations in each of which result in small increments or decrements in abundance. Population distribution models account for the evenness (equitability) of distribution of species, which fit various distributions to known models, such as the geometric series, log series, lognormal, or broken stick. In a large sample of individuals, species often distribute themselves normally over the logarithmic abundance categories.

10.3.2.2   Diversity Indices

Not all species should contribute equally to the estimate of total diversity, because their functional roles in the community vary, to some degree, in proportion to their overall abundance. Ecologists have formulated

several diversity indices in which the contribution of each species is weighted by its relative abundance. Three such indices are widely used in ecology: Simpson's index, Margalef index and the Shannon-Weaver index. Simpson's index is

$$D = \left[\sum_{i=1}^{S} \left(\frac{n_i^2}{N^2} \right) \right]^{-1} \tag{10.7}$$

in which n_i is the number of individuals of the i-th species, and N is the total number of individuals in the sample. For any particular number of species in a sample (S), the value of D can vary from 1 to S, depending on the evenness of species abundances.

The Margalef index is defined as the total number of species present and the abundance or total number of individuals. The higher is the index, the greater the diversity. The Margalef index M is given by (Margalef, 1957):

$$M = (S-1)/\log_e^N \tag{10.8}$$

The Shannon-Weaver index, developed from information theory and integrating the species richness and evenness of the abundance distribution, is given by (Krebs, 1978):

$$H = -\sum_{i=1}^{S} \frac{n_i}{N} \ln \frac{n_i}{N} \tag{10.9}$$

The Shannon-Weaver Index provides no information on the total abundance of the bio-community. For instance, samples from two sites have the same number of species, the distributions are also the same but the density of individuals for site one is 10 ind/m^2 and for site two is 100 ind/m^2. Eq. (10.9) gives the same values of H. The difference in population density for the two cases is large, but it is not reflected by the values of H. Considering both the abundance and biodiversity, the following bio-community index is suggested (Wang et al., 2009):

$$B = H \ln N = -\ln N \sum_{i=1}^{S} \frac{n_i}{N} \ln \frac{n_i}{N} \tag{10.10}$$

Macro-invertebrates census data from 9 sites along the East River in south China can be used to illustrate these different methods of presentation, as listed in Table 10.1 (Wang et al., 2008). The East River is 562 km long and has a drainage area of 35,340 km^2. The river is one of the three major rivers of the Pearl River system—the largest system in South China. The Fenshuba Dam is a hydropower project on the river dividing the upper and middle reaches of the river and is 382 km from the river mouth. Figure 10.41 shows the variation of the species richness, S, number density of individual invertebrates, N, Shannon-Weaver index, H, and the bio-community index, B, from upper to lower reaches along the course. In general the richness, S, the density, N, Shannon-Weaver index, H, and the bio-community index, B, of benthic invertebrates reduce from the upper to the lower reaches. The Fenshuba Dam causes instantaneous fluctuation in flow discharge and velocity, which strongly impact the invertebrates. Therefore, only one species, *Palaemonidae*, which may survive the fluctuation, was found at the site downstream of the dam. The impact of velocity fluctuation becomes weak further downstream from the dam and exhibits no influence on the benthic invertebrates at a distance of 80 km from the dam.

In the lower reaches the channel has been regulated with relatively uniform width and the banks have been hardened with concrete and stones. Flow velocity in the channel is more uniform than the upper reaches and the substrate consists of only sand. The sand bed is compact, which provides no space for benthic animals to live and no shelter for the animals to escape current. The richness, number density, and biodiversity and bio-community indices in the lower reaches are very low or zero. Humans have reclaimed river bays, riparian lakes and wetlands, and sluggish and backwater zones, which caused loss

Table 10.1   Species of benthic macro-invertebrates at the sampling sites along the East River

Sampling site	Species and the number of animals of each species per area (Figure within the parentheses is the number of individual animals of each species per square meter)
Shang-Pingshui	*Baetidae (30); Melaniidae, S.libertine (23); Chironomidae (two species 16); Ceratopsyche sp.(7); Aphropsyche sp. (5); Elmidae (3); Corydalidae，Protohermes (3); Corbiculidae C.nitens (2); Polycentropodidae， Neureclipsis(2); Caenidae (1); Helobdella (1);*
Fengshuba Dam	*Palaemonidae (9)*
Yidu	*Leptophlebiidae，Paraleptophlebia(42); Chironomidae (21); Gomphidae (5); Siphlonuridae (4); Hydropsychidae (4); Leptophlebiidae, Leptophlebia (2); Decapoda (2); Hydrobiidae (2); Semisulcospira (1); Tipulidae, Hexatoma (1); Naucoridae (1); Corydalidae (1); Caenidae(1)*
Wuxing	*Natantia (44); Bellamya (10); Branchiura (3); Radix (2); Melanoides (2); Nepidae (1); Limnodrilus (1); Coenagrionidae, Pseudagrion (1); Leptophlebiidae, Traverella (1); Heptageniidae (1); Leptophlebiidae, Paraleptophlebia (1); Corbiculidae C.nitens (1); Noteridae (1); Whitmania (1); Hirudinea Sp1.(1)；*
Baipuhe	*Palaemonidae Sp1.(40); Palaemonidae, Palaemon modestus (12); Gomphidae (2); Macromiidae (2); Semisulcospira (2); Branchiura (2)*
Huizhou	*Chironomidae (3 species 11); Coenagrionidae (two species 6)；Branchiura (4); Paratelphusidae (1); Ilydrolus (1);Gomphidae (1); Platycnemididae (1); Ampullariidae (1)*
Yuanzhou	*0 (first sampling); Palaemonidae (9) (second sampling)*
Dasheng	*0 (first sampling); Palaemonidae (5) (second sampling)*
Yequ Creek	*Chironomidae(386); Simuliidae (18); Herpodellidae(4);Dytiscidae (3); Branchiura (3); Lumbriculidae (1); Psychodidae (1); Corduliidae, Epitheca marginata (1); Baetidae (1)*
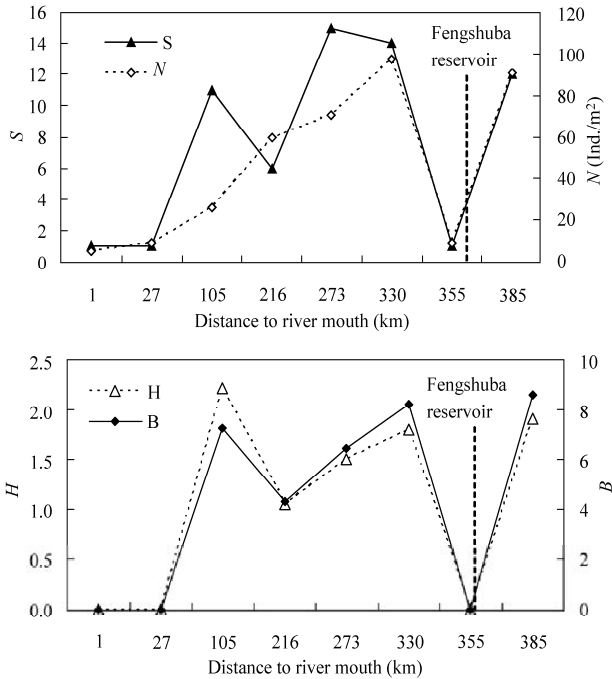
Fig. 10.41   Species richness, *S*, number density of individual invertebrates per area, *N,* Shannon-weaver Index*, H,* and the bio-community index, *B,* as functions of distance to the river mouth

of habitat and made formerly diversified habitats very uniform and unitary. In general, the biodiversity and bio-community indices are proportional to the diversity of habitats. The habitat loss and low diversity of habitats result in low biodiversity and bio-community.

As indicated in the previous section biological diversity refers mainly to the number of species in an area or region and includes a measure of the variety of species in a community that takes into account the relative abundance of each species (Ricklefs, 1990). When measuring diversity, it is important to clearly define the biological objectives, stating exactly what attributes of the system are of concern and why (Schroeder and Keller, 1990). Different measures of diversity can be applied at various levels of complexity, to different taxonomic groups, and at distinct spatial scales.

Overall diversity within any given level of complexity may be of less concern than diversity of a particular subset of species or habitats. Measures of overall diversity include all of the elements of concern and do not provide information about the occurrence of specific elements. For example, measures of overall species diversity do not provide information about the presence of individual species, such as Chinese sturgeon, or species groups of management concern. Thus, for a specific ecological restoration project, measurement of diversity may be limited to a target group of special concern.

3. Alpha and Beta Diversities

Diversity can be measured within the bounds of a single community, across community boundaries, or in large areas encompassing many communities. Diversity within a relatively homogeneous community is known as alpha diversity, or local diversity. Usually the diversity indices obtained by examining the samples taken from one site are referred to as alpha diversity. Diversity between communities in a region, described as the amount of differentiation along habitat gradients, is termed beta diversity, or regional diversity. For instance, the total number of species from numerous sites along a stream is the regional diversity of the stream. Beta diversity may be large in river-lake connected habitats with high heterogeneity, because some species colonize stream habitat and very different species may live in the riparian lakes.

Noss and Harris (1986) note that management for alpha diversity may increase local species richness, while the regional landscape (gamma diversity) may become more homogeneous and less diverse overall. They recommend a goal of maintaining the regional species pool in an approximately natural relative abundance pattern. The specific size of the area of concern should be defined when diversity objectives are established.

A beta diversity index is given by the following formula:

$$\beta = \frac{M}{\dfrac{1}{S}\sum_{i=1}^{S} m_i} \tag{10.11}$$

in which M is the number of sampled habitats in a region, e.g., the middle reaches of the Yangtze River; m_i is the number of habitats, in which the i-th species is found; and S is the total number of species found at all sampling sites in the region. If the species in all sites are the same, or $m_i = M$, the beta diversity index is 1. If all species occur at only one site, $m_i = 1$, the beta diversity index equals M. The total number of species, S, in the region is then the product of the average species richness by the beta diversity index.

The ecological implication of beta diversity may be seen from the example of preliminary assessment of aquatic ecology of the source region of the Yellow River. The benthic macro-invertebrates were sampled at 8 sites with different environmental conditions in the source region of the Yellow River from Aug. 7 to Aug. 15, 2009. Figure 10.42 shows the location of 8 sampling sites. Samples were taken from 5 sites from the Yellow River and riparian waters. In addition, samples were taken from a small stream on the plateau, the Eling Lake and the Qinghai Lake. The sampling method is as follows: In mountain streams
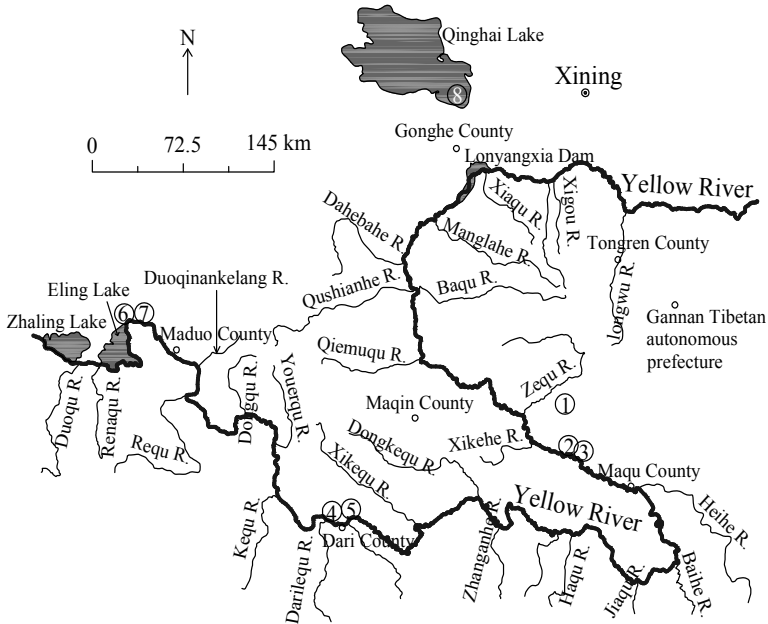
Fig. 10.42   Location of the 8 sampling sites in the source region of the Yellow River

with gravel beds, the gravels were washed and sieved with a kick-net with holes of 0.5 mm, and organic and inorganic detritus with macro-invertebrates collected. The detritus was subsequently placed on a white tray, and the invertebrates were collected. Invertebrate species were thereafter examined and identified to family or genus level under a microscope. The sampled area was 1.5 m² consists of three sub-sampling areas in order to reflect diversified ecological conditions. After sampling, macro-invertebrates and associated material were immediately preserved in ethanol and were subsequently processed and identified in the laboratory (Duan et al, 2010). There is little pollution and the water quality is very good.

In general, the community of benthic invertebrates is different if the environmental conditions are different. The main environmental factors for benthic invertebrates are stream substrate, water depth, flow velocity, and water quality (Wang et al., 2009). At the site ① the Zequ River is a tributary of the Yellow River with meandering channel. In its drainage area there are numerous swamps and rivulets with small but stable flow. The rivulets wriggle on vast meadows with grass coverage almost 100%. The site of streamlet represents the habitat type. Near the Yellow River by Kesheng town (site ②) there is an oxbow lake (site ③), which is abandoned channel of the Yellow River and has been cutoff from the river for a very long period of time. The site ④ is a riparian lake, which may connect with the Yellow River during high floods. The Dari bay ⑤ is a riparian wetland where the Yellow River flows from a normal channel to a very wide valley with shallow water. The main water flow has a deep channel, but plume of low sediment concentration drifts into the bay. The site ⑥ is a wetland by the Yellow River. The Eling Lake ⑦ is the source of the Yellow River with a capacity of 10 billion m³. The pool level in the lake is not stable depending on the incoming water and operation of a hydropower station just below it. The water level had been rising since a month before the field investigation. The Qinghai Lake ⑧ has brackish water with low concentration of salt. It is near by the source of the Yellow River and represents a type of habitat in the region.

Table 10.2 lists the species of macro-invertebrates identified from the samples of each site with the number density (ind/m²) of each species in the parentheses (Wang et al., 2010). The taxa richness, or the

number of species at each site, *S*, and the calculated biodiversity index *B* are listed in the table. Altogether 48 species of macro-invertebrates belonging to 24 families and 44 genera were identified. The average density and wet biomass of macro-invertebrates in the eight sampling stations were 360 ind/m^2 and 2.3934 g/m^2, respectively. Insects were predominant group, being 77.1% of the total in taxa number, 82.7% in density, and 88.6% in wet biomass. Figure 10.43 shows the representative species of macro-invertebrate in the sampling sites, which are dominant species or typical species at each site.

Table 10.2 Species composition of macro-invertebrates with densities (ind/m^2) in the parentheses

No.	Site	Species composition	*S*	*B*
1	Streamlet	*Limnodrilus grandisetosus* (2); Amphipoda (488); *Baetis* sp. (53); *Setodes* sp. (5); Tipulidae (1); *Eukiefferiella* sp. (9)	6	3.04
2	YR channel	Amphipoda (9); Acarina (2); *Baetis* sp. (3); *Cinygmula* sp. (4); *Ephemerella* sp. (30); *Leptonema* sp. (36); *Brachycentrus* sp. (3); Naucoridae (1); *Simulium* sp. (1); Culicidae (3); *Clinotanypus* sp. (1); *Eukiefferiella* sp. (9); *Orthocladius* sp. (2); *Cladotanytarsus* sp. (1); *Dicrotendipes* sp. (1); *Parachironomus* sp. (4); *Polypedilum* sp. (2)	17	9.86
3	Oxbow lake	Nematoda (300); *Aulodrilus pluriseta* (6); *Radix lagotis* (3); *Radix swinhoei* (12); *Hippeutis cantori* (9); *Hippeutis umbilicalis* (36); Amphipoda (93); Acarina (3); *Caenis* sp. (6); Dytiscidae (18); Elmidae (3); Corixidae (15); Pyralidae (336); *Procladius* sp. (15); *Chironomus* sp. (18); *Cryptochironomus* sp. (3); *Microchironomus* sp. (3); *Paratanytarsus* sp. (3); *Polypedilum braseniae* (3); *Xenochironomus* sp. (9)	20	11.84
4	Riparian lake	*Stylaria* sp. (1); *Limnodrilus* sp. (2); *Branchiura sowerbyi* (2); *Radix ovata* (4); Dytiscidae (8); Tipulidae (2); Culicidae (1); *Procladius* sp. (2); *Parametriocnemus* sp. (2); *Chironomus* sp. (10); *Cryptochironomus* sp. (1); *Endochironomus* sp. (1); *Paratanytarsus* sp. (17)	13	8.48
5	Dari bay	*Limnodrilus* sp. (3); Amphipoda (12); Tipulidae (1); *Psectrocladius* sp. (17); *Tvetenia* sp. (8); *Chironomus* sp. (10); *Polypedilum* sp. (13)	7	6.72
6	Eling Lake	no benthic animals	0	-
7	Riparian wetland	*Limnodrilus* sp. (1); Amphipoda (464); Culicidae (4); *Procladius* sp. (1); *Cricotopus* sp. (10); *Microchironomus* sp. (3); *Rheotanytarsus* sp. (75)	7	3.68
8	Qinghai Lake	Amphipoda (210); Culicidae (2); Ephydridae (2); *Cricotopus* sp. (105); *Eukiefferiella* sp. (19); *Chironomus* sp. (2)	6	5.32

The taxa richness *S* and the index *B* at each site are not high. In other words, the biodiversity of the sampling sites are not high. The streamlet and Qinghai Lake have only 6 species and both dominated by Amphipoda. The oxbow lake has the highest biodiversity, with 20 species and bio-community index about 12. In general, cobble, gravel and aquatic plants are the best substrates for benthic invertebrates. The oxbow lake, the isolated riparian lake at Dari, and the Yellow River channel at meanders have relatively stable environment and have multiple habitats with different substrates, therefore, they have high biodiversity. The Dari bay is an open shallow water connecting the Yellow River, its substrate consists of only fluid mud, and the sediment from the river drifting into the bay may change the fluid mud surface layer, thus it has relatively low biodiversity. Moreover, the species composition in the oxbow lake and riparian lake are quite different from the river and bay. These riparian waters are important in aquatic biodiversity.

The value of beta diversity was calculated for the source region of the Yellow River. The total number of sampled habitats is 8, so the value of *M* is 8 in Eq. (10.11). Calculation with the sampled species from the 8 habitats yields the beta diversity equal to 5.33, which is 66.7% of the maximum value. As a comparison, field investigations were paid to the Juma River in the suburbs of Beijing from Shidu to Yesanpo with a length of about 70 km. The river is a mountain stream with beautiful landscapes and
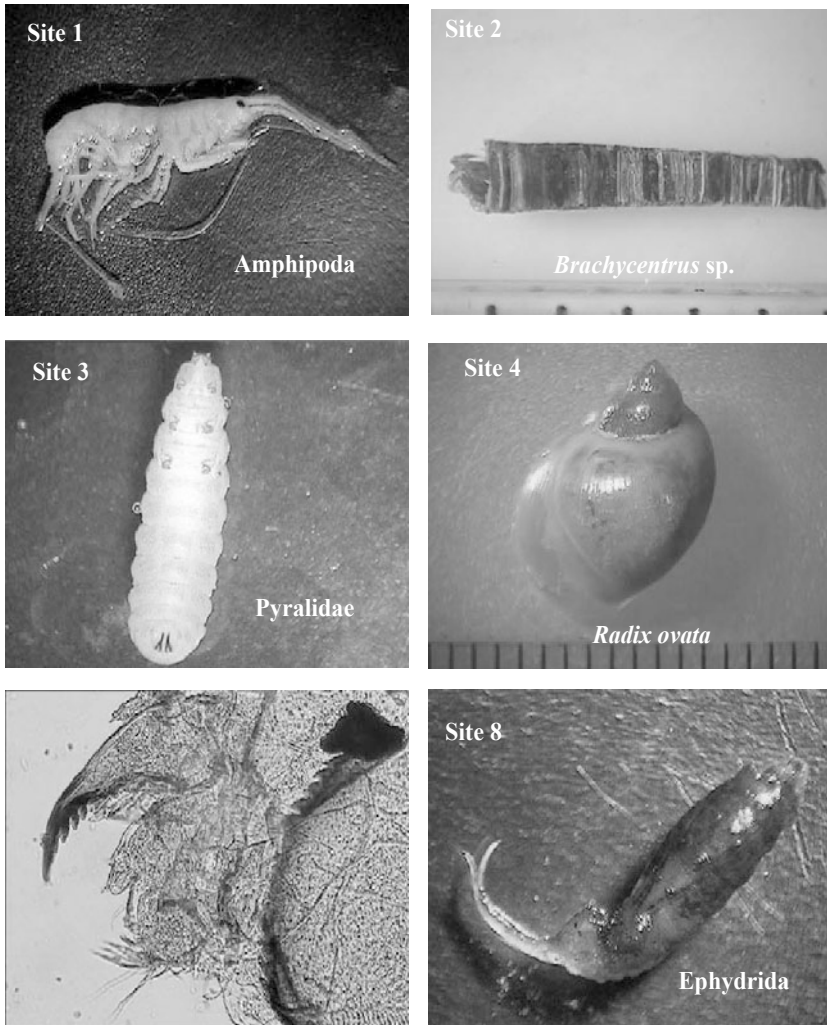
Fig. 10.43 Representative species of macro-invertebrate from the sites 1,2,3,4, 5 and 8 (See color figure at the end of this book)

good aquatic ecology. The river reach from Shidu to Yesanpo is a main tourist attraction for Beijing people. Samples of benthic invertebrates were taken from 8 sites with different habitats, including gravel bed with turbulent flow, riparian wetland with lentic water, branch channel with low velocity flow, and pool behind weir. The substrates at the sampling sites were different, varying from gravel, cobbles, sand and macrophytes. The average taxa richness for the 8 different habitats was 19.4 and the highest taxa richness was 28. The total number of species was 54. The average value of index B for the 8 habitats was 10 and the highest value of B was 16. All the 8 habitats have high local biodiversity (alpha biodiversity). Nevertheless, the species compositions at different sites were rather similar. The beta diversity for the Juma River was only 2.7. The beta diversity for the source region of the Yellow River is two times of the Juma River. Ecological management or restoration in the region must base on an overall consideration of various habitats in the region.

10.3.2.4 Indices of Biotic Integrity

1) Karr's IBI

Fish represent the top of the aquatic food chain, and, thus, the quality and composition of the fish community comprises the best measure of the overall health of the aquatic community. This is because the fish community integrates the effects of the entire suite of physical, chemical, and biological stresses on the ecosystem. A fish community index should include at least one metric for each of the five attributes of fish assemblages (Simon and Lyons, 1995): species richness and condition, indicator species, trophic function, reproduction function, and individual abundance and condition.

Considering the foregoing considerations, Karr (1981) proposed and revised (Karr et al., 1986) the Index of Biotic Integrity (IBI) to evaluate stream quality at the fish community level. The Karr's IBI is comprised of 12 metrics to define fish community structure. The index accounts for changes in fish community richness and allows for comparison of fish community composition with values for similar-sized streams. The applicability of the IBI concept has been demonstrated in a wide variety of streams types (Miller et al., 1988). As recommended by Karr et al. (1986), IBI metrics require adjustment for the region to which the index is applied. The basic components of Karr's index are listed in Table 10.3. It is recognized that stream size is an important factor when refining the IBI to a geographical region.

Table 10.3 Karr's Index of Biological Integrity (IBI) (after Karr et al., 1986)

Category	Metrics	Scoring criteria		
		5	3	1
Species richness and composition	1. Total number of fish species	Expectations for metrics 1–5 vary with stream size and region		
	2. Number and identity of darter species			
	3. Number and identity of sunfish species			
	4. Number and identity of sucker species			
	5. Number and identity of intolerant species			
	6. Proportion of individuals as green sunfish	<5%	5%–20%	>20%
Trophic composition	7. Proportion of individuals as omnivores	<20%	20%–45%	>45%
	8. Proportion of individuals as insectivorous Cyprinids	>45%	45%–20%	<20%
	9. Proportion of individuals as piscivores (top carnivores)	>5%	5%–1%	<1%
Fish abundance and Condition	10. Number of individuals in sample	Expectations vary with stream size and region		
	11. Proportion of individuals as hybrids	0%	0%–1%	>1%
	12. Proportion of individuals with disease, tumors, fin damage, skeletal anlmalies (DELT)	0%–2%	2%–5%	>5%

The definitions of the twelve metrics are described as follows (Karr et al., 1986, Lyons, 1992):

Total number of species—The total number of species collected at a site, excluding hybrids and subspecies. The number of fish species supported by streams of a given size in a given region decreases with environmental degradation, if other features are similar.

Number of darter species—The total number of darter species (family *Percidae*) collected, excluding hybrids. Darters are small benthic species that tend to be intolerant of many types of environmental degradation. They are mainly insectivorous, and for many of them riffles or runs are preferred habitats. These species are sensitive to degradation, particularly as a result of their need to reproduce and feed in benthic habitats. Such habitats are degraded by channelization, siltation, and reduction in oxygen content.

Number of sunfish species—The total of sunfish species (family *Centrarchidae*), including rock bass (*Amobloplites rupertris*) and crappies (*Pomoxis* species), but excluding hybrids and black basses

(*Micropterus salmoides*). Sunfish are medium sized, mid-water species, which tend to occur in pools or other shallow-moving water. Most, but not all, are tolerant of environmental degradation. All feed on a variety of invertebrates, although some larger adults may eat fish. Sunfish are included in the index because they are particularly responsive to the degradation of pool habitats and to other aspects of habitat such as instream cover.

Number of sucker species—The total number of sucker species (family *Catostomidae*) collected, excluding hybrids. Suckers are large benthic species that generally live in pools or runs, although a few species are common in riffles. Some species are intolerant of environmental degradation, whereas others are tolerant. Most species feed on insects, although a few also eat large quantities of detritus or plankton. Suckers are included in the index because many of these species are intolerant to degradation of habitat or chemical quality. Also, the longevity of suckers provides a multiyear integrative perspective.

Number of intolerant species—The total number of species, excluding hybrids, which are intolerant of environmental degradation, particularly poor water quality, siltation and increased turbidity, and reduced heterogeneity (e.g., channelization). Intolerant species are among the first to be decimated after perturbation to habitat or water quality, and the species identified in metrics 2–4 may be included in this group.

Proportion of individuals as green sunfish—In the Midwestern U.S., the green sunfish (*Lepomis cyanellus*) increases in relative abundance in degraded streams and may increase from an incidental to the dominant species. Thus, this metric evaluates the degree to which typically tolerant species dominate the community. In many other IBIs, tolerant species in the sample are listed and the proportion of tolerant individuals in the sample is computed and used as the metric in place of green sunfish.

Proportion of individuals as omnivores—The number of individuals that belong to species with an adult diet consisting of at least 25% (by volume) plant material or detritus and at least 25% live animal matter, expressed as a percentage of the total number of fish captured. By definition, omnivores can subsist on a broad range of food items, and they are relatively insensitive to the change in the food base of a stream caused by environmental degradation. Hybrids are included in this metric if both of the parental species are considered omnivores. The dominance of omnivores occurs as specific components of the food base become less reliable, and the opportunistic foraging habits of omnivores make them more successful than specialized foragers.

Proportion of individuals as insectivorous cyprinids—Cyprinids that belong to species with an adult diet normally dominated by aquatic or terrestrial insects, expressed as a percentage of the total number of fish captured. Although insectivorous cyprinids are a dominant trophic group in streams in the midwestern U.S., their relative abundance decreases with degradation, probably in response to variability in the insect supply, which in turn reflects alterations of water quality, energy sources, or instream habitat. In other regions the proportion of total insectivores to total individuals may provide better information for this metric with a resetting of the scoring criteria.

Proportion of individuals as piscivores (top carnivores)—The number of individuals that belong to species with an adult diet dominated by vertebrates (especially fish) or decapod crusteacea (e.g., crayfish, shrimp), expressed as a percentage of the total number of fish captured. Some species feed on invertebrates and fish as fry and juveniles. Hybrids are included in this metric only if both of the parental species are carnivores. Viable and healthy populations of top carnivores indicate a healthy, trophically diverse community.

Number of individuals in a sample—This metric evaluates populations and is expressed as catch per unit of sampling effort. Effort may be expressed per unit area sampled, per length of reach sampled, or per unit of time spent. In streams of a given size and with the same sampling method and efficiency of effort, poorer sites are generally expected to yield fewer individuals than sites of higher quality.

Proportion of individuals as hybrids—This metric is difficult to determine from historic data and is sometimes omitted for lack of data. Its primary purpose is to assess the extent to which degradation has altered reproductive isolation among species. Hybridization may be common among cyprinids after channelization, although difficulties in recognizing hybrids may preclude using this criterion with darters in addition to cyprinids. Sunfish also hybridize quite readily, and the frequency of their hybridization appears to increase with stream modifications.

Proportion of individuals with disease, tumors, fin damage, and skeletal anomalies (DELT)—The number of individual fish with skeletal or scale deformities, heavily frayed or eroded fins, open skin lesions, or tumors that are apparent from external examination, expressed as a percentage of the total number of fish captured. DELT fish are normally rare except at highly degraded sites.

Sampling of fish to determine these metrics is done on a reach basis. In Wisconsin, for example, a stream reach is defined as a minimum of 35 times the mean stream width based on at least 10 field measurements per site (Lyons, 1992). The results of the reach sampling are combined to define a sampling site.

2) IBI Examples

Karr's IBI concept has been adapted and modified from its midwestern U.S. beginnings for application throughout the world. Some IBIs simply adjust the scoring criteria as appropriate for their region of application, whereas other IBIs have combined new metrics with Karr's metrics. More than 40 fish metrics have been utilized in the various IBIs used in the U.S. (Limnotech, 2009).

The IBI developed for Taiwan (Hu et al., 2005) is an example, where the majority of Karr's original metrics (with slight modifications) were applied, but the scoring criteria were modified (Table 10.4). Other than the scoring criteria modifications, the main differences in the Taiwan IBI versus Karr's IBI are the use of all insectivores and consideration of numbers of hybrids or exotic species rather than the proportion of hybrids. Exotic species are species that are present in a region through introduction by man or have recent invasions that would not have been possible without human intervention. The total IBI scores then yield the following biological conditions categories: Non-impaired = 35 – 45, Slightly impaired = 23 – 34, Moderately impaired = 15 – 22, and Severely impaired = 0 – 14.

Table 10.4 Index of Biological Integrity (IBI) for Taiwan (after Hu et al., 2005)

Category	Metrics	Scoring criteria		
		5	3	1
Species richness and composition	1. Total number of fish species	≥10	4–9	0–3
	2. Number of darter species	≥3	1–2	0
	3. Number of sunfish species	≥2	1	0
	4. Number of suckers species	≥2	1	0
	5. Number of intolerant species	≥3	1-2	0
Trophic composition	6. Proportion of individuals as omnivores	< 60%	60%–80%	> 80%
	7. Proportion of individuals as insectivores	> 45%	45%–20%	< 20%
Fish abundance and condition	8. Number of individuals in sample	≥101	51–100	0–50
	9. Number of hybrids or exotic species	0	1	≥2

Karr's IBI and its many regional modifications for areas throughout the U.S. and around the world have generally been well calibrated to small "wadable" streams, but applications in larger rivers are less common (Lyons et al., 2001). Lyons et al. (2001) identified 7 IBIs developed for use in large rivers, and then developed IBIs for use in large rivers in Wisconsin. In this case large rivers are defined as having at

least 3 km of contiguous river channel too deep to be effectively sampled by wading. Lyons et al. (2001) used fish assemblage data from 155 main-channel-border sites on 30 large warmwater rivers in Wisconsin (including 19 sites on the Mississippi River) to construct, test, and apply a large river IBIs. Fourteen sites were sampled more than once for a total of 187 samples. Watershed drainage areas for these sites ranged from 349 to 218,890 km^2. Lyons et al. (2001) used some of Karr's original metrics while adding several different metrics. A main difference is that instead of just considering the proportion of individuals (i.e. numbers-based metrics) the large river IBI also considers the proportion of fish by weight (i.e. biomass-based metrics). Such biomass-based metrics best reflect the amount of energy flow across trophic levels and functional groups, whereas numbers-based metrics indicate the diversity of pathways that energy could follow and the potential for intra- and inter-specific interactions (Lyons et al., 2001).

The large river IBI for southern Wisconsin is listed in Table 10.5. Definitions of some of the "new" metrics are given as follows (Lyons, 1992; Lyons et al., 2001):

Weight per unit effort—Weight (biomass) to the nearest 0.1 kg of fish collected per 1600 m of shoreline, excluding tolerant species.

Total number of native species—The total number of species collected at a site, excluding hybrids (which are common among sunfish and certain minnow species) and exotic species.

Total number of riverine species—Number of species that are obligate stream or river dwellers not normally found in lentic habitats.

Table 10.5   Index of Biological Integrity (IBI) for large rivers in southern Wisconsin (after Lyons et al., 2001)

Metrics	Scoring criteria		
	10	5	0
1. Weight of fish per unit effort	> 25 kg	10–25 kg	0–9.9 kg
2. Total number of native fish species	>15	12–15	0–11
3. Number of suckers species	>4	3–4	0–2
4. Number of intolerant species	>2	2	0–1
5. Number of riverine species	>6	5–6	0–4
6. Proportion of individuals with disease, tumors fin damage, skeletal anlmalies (DELT)	<0.5%	0.5%–3%	>3%
7. Percent of individuals as riverine species	>20%	11%–20%	0%–10%
8. Percent of individuals as simple lithophilous spawners	>40%	26%–40%	0%–25%
9. Percent of insectivores by weight	>39%	21%–39%	0%–20%
10. Percent of round suckers by weight	>25%	11%–25%	0%–10%

Percent of individuals as simple lithophilous spawners—The number of individuals that belong to species that lay their eggs on clean gravel or cobble and do not build a nest or provide parental care, expressed as a percentage of the total number of fish captured. Simple lithophilous species need clean substrates for spawning and are particularly sensitive to sedimentation (embeddedness) of rocky substrates. Hybrids are included in this metric only if both of the parental species are simple lithophilous species.

The total IBI scores then yield the following biological conditions categories: Excellent = >80, Good = 60–79, Fair = 40–69, Poor = 20–39, Very Poor = <20. Lyons et al. (2001) found that the Wisconsin large river IBI was comparable to IBIs developed for use in large rivers in Ohio (including data for the Ohio River) and Indiana. The fact that the IBI metrics in Table 10.5 reflect conditions on the Mississippi River and Ohio River indicate that these metrics might be a good beginning point for developing IBIs for the other large rivers of the world.

3) Uses of the IBI

IBIs provide a valuable framework for assessing the status and evaluating the restoration of aquatic communities. IBIs encompass the structure, composition, and functional organization of the biological community. IBIs can be viewed as quantitative empirical models for rating the health of an aquatic ecosystem, providing a single, defensible, easily understood measure of the overall health of a river reach in question (Lyons et al., 2001). For example, IBIs can be used to quickly identify both high-quality reaches for protection and degraded sites for rehabilitation.

While total IBI scores can provide the user with an indication that a stream fish community is potentially degraded by environmental stressors, the total score cannot provide the ability to identify which individual stressors are causing the response. The same total IBI score can be reached by an infinite combination of individual metric scores, each with its own environmental stressor. Thus, several researchers have focused not on the final IBI score, but rather on how the individual metrics can be used to describe the effects of anthropogenic stresses on the fish community (e.g., Manolakos et al., 2007; O'Reilly, 2007; Novotny et al., 2008; Bedoya et al., 2009). If relations between stresses and the fish community can be found ways to reduce these stresses and efficiently improve the fish community can be derived.

10.3.3 Bioassessment

10.3.3.1 Rapid Bioassessment

Rapid bioassessment techniques are most appropriate when restoration goals are nonspecific and broad, such as improving the overall aquatic community or establishing a more balanced and diverse community in the river ecosystem (FISRWG, 1997). Bioassessment often refers to use of biotic indices or composite analyses, such as those used by the Ohio Environmental Protection Agency (Ohio EPA, 1990), and rapid bioassessment protocols (RBP), such as those documented by Plafkin et al. (1989). The Ohio EPA evaluates biotic integrity by using an invertebrate community index that emphasizes structural attributes of invertebrate communities and compares the sample community with a reference or control community. The invertebrate community index is based on 10 metrics that describe different taxonomic and pollution tolerance relations within the macro-invertebrate community. The rapid bioassessment protocols established by the U.S. Environmental Protection Agency were developed to provide states with the technical information necessary for conducting cost-effective biological assessments (Plafkin et al., 1989). The RBP are divided into five sets of protocols, three for macroinvertebrates and two for fish, as shown in Table 10.6.

The rapid bioassessment protocols RBP I to RBP Ⅲ are for macroinvertebrates. RBP I is a "screening" or reconnaissance-level analysis used to discriminate obviously impaired and unimpaired sites from potentially affected areas requiring further investigation. RBP Ⅱ and Ⅲ use a set of metrics based on taxon tolerance and community structure similar to the invertebrate community index used by the State of Ohio. Both are more labor-intensive than RBP Ⅰ and incorporate field sampling. RBP II uses family-level taxonomy to determine the following set of metrics used in describing the biotic integrity of a stream: (1) Species richness, (2) Hilsenhoff biotic index (Hilsenhoff, 1982), (3) Ratio of scrapers to filtering collectors, (4) Ratio of Ephemeroptera/ Plecoptera/Trichoptera (EPT) and chironomid abundances, (5) Percent contribution of dominant taxa, (6) EPT index, (7) Community similarity index, and (8) Ratio of shredders to total number of individuals. RBP Ⅲ further defines the level of biotic impairment and is essentially an intensified version of RBP Ⅱ that uses species-level taxonomy. As with the invertebrate community index, the RBP metrics for a site are compared to metrics from a control or reference site.

Table 10.6   Five tiers of the rapid bioassessment protocols (after Plafkin et al., 1989)

Level or tier	Organism group	Relative level of effort	Level of taxonomy/ where performed	Level of expertise required
I	Benthic invertebrates	Low; 1–2 hr per site (no standardized sampling)	Order, family/field	One highly-trained biologist
II	Benthic invertebrates	Intermediate; 1.5–2.5 hr per site (all taxonomy performed in the field)	Family/field	One highly-trained biologist and one technician
III	Benthic invertebrates	Most rigorous; 3–5 hr per site (2–3 hr of total are for lab taxonomy)	Genus or species/ laboratory	One highly-trained biologist and one technician
V	Fish	Low; 1–3 hr per site (no fieldwork involved	Not applicable	One highly-trained biologist
VI	Fish	Most rigorous; 2–7 hr per site (1–2 hr are for data analysis)	Species /field	One highly-trained biologist and 1–2 technicians

10.3.3.2   Comparison Standard

With stream restoration activities, it is important to select a desired end condition for the proposed management action. A predetermined standard of comparison provides a benchmark against which to measure progress. For example, if the chosen diversity measure is native species richness, the standard of comparison might be the maximum expected native species richness for a defined geographic area and time period. Historical conditions in the region should be considered when establishing a standard of comparison. If current conditions in a river are degraded, it may be best to establish the standard for a period in the past that represented more natural or desired conditions. In some cases historical diversity might have been less than current diversity due to changes in hydrology and encroachment of native and exotic riparian vegetation in the floodplain (Knopf, 1986). Thus, it is important to agree on what conditions are desired prior to establishing the standard of comparison.

For a hypothetical stream restoration initiative, the following biological diversity objective might be developed. Assume that a primary concern in an area is conserving native amphibian species and that 30 native species of amphibians have been known to occur historically in the watershed. The objective could be to manage the river ecosystem to provide and maintain suitable habitat for the 30 native amphibian species. River ecosystem restoration efforts must be directed toward those factors that can be managed to increase diversity to the desired level. Those factors might be the physical and structural features of the river ecosystem. Diversity can be measured directly or predicted from other information. Direct measurement requires an actual inventory of the element of diversity, such as counting the amphibian species in the study area.

Direct measures of diversity are most helpful when baseline information is available for comparing different sites. It is not possible, however, to directly measure certain attributes, such as species richness or the population level of various species, for various future conditions. Predicting diversity with a model is generally more rapid than directly measuring diversity. In addition, predictive methods provide a means to analyze alternative future conditions before implementing specific restoration plans. The reliability and accuracy of diversity models should be established before their use.

10.3.3.3   Classification Systems

The common goal of classification systems is to organize variation. Classification systems include (FISRWG, 1997):

(1) Geographic domain. The range of sites being classified varies from rivers of the world to local differences in the composition and characteristics of patches within one reach of a single river.

(2) Variables considered. Some classifications are restricted to hydrology, geomorphology, and aquatic chemistry. Other community classifications are restricted to biotic variables of species composition and abundance of a limited number of taxa. Many classifications include both abiotic and biotic variables. Even purely abiotic classification systems are relevant to biological evaluations because of the important correlations (e.g., the whole concept of physical habitat) between abiotic structure and community composition.

(3) Incorporation of temporal relations. Some classifications focus on describing correlations and similarities across sites at one, perhaps idealized, point in time. Other classifications identify explicit temporal transitions among classes, for example, succession of biotic communities or evolution of geomorphic landforms.

(4) Focus on structural variation or functional behavior. Some classifications emphasize a parsimonious description of observed variation in the classification variables. Others use classification variables to identify types with different behaviors. For example, a vegetation classification can be based primarily on patterns of species co-occurrence, or it can be based on similarities in functional effect of vegetation on habitat value.

(5) The extent to which management alternatives or human actions are explicitly considered as classification variables. To the extent that these variables are part of the classification itself, the classification system can directly predict the result of a management action. For example, a vegetation classification based on grazing intensity would predict a change from one class of vegetation to another class based on a change in grazing management.

Comparison of the degraded system to an actual unimpacted reference site, to the ideal type in a classification system, or to a range of similar systems can provide a framework for articulating the desired state of the degraded system. However, the desired state of the system is a management objective that ultimately comes from outside the classification of system variability.

10.3.3.4 Analyses of Species Requirements

Analyses of species requirements involve explicit statements of how variables interact to determine habitat or how well a system provides for the life requisites of fish and wildlife species. Complete specification of relations between all relevant variables and all species in a river system is not possible. Thus, analyses based on species requirements focus on one or more target species or groups of species. In a simple case, this type of analysis may be based on an explicit statement of the physical factors that distinguish good habitat for a species (places where it is most likely to be found or where it best reproduces) from poor habitat (places where it is unlikely to be found or reproduces poorly). In more complicated cases, such approaches incorporate variables beyond those of purely physical habitat, including other species that provide food or biotic structure, other species as competitors or predators, or spatial or temporal patterns of resource availability.

Analyses based on species requirements differ from synthetic measures of system condition in that they explicitly incorporate relations between "causal" variables and desired biological attributes. Such analyses can be used directly to decide what restoration actions will achieve a desired result and to evaluate the likely consequences of a proposed restoration action. For example, an analysis using the habitat evaluation procedures might identify mast production (the accumulation of nuts from a productive fruiting season which serves as a food source for animals) as a factor limiting squirrel populations. If squirrels are a species of concern, at least some parts of the stream restoration effort should be directed toward increasing mast production. In practice, this logical power is often compromised by incomplete knowledge of the species habitat requirements.

The complexity of these methods varies along a number of important dimensions, including prediction of habitat suitability versus population numbers, analysis for a single place and single time versus a temporal sequence of spatially complex requirements, and analysis for a single target species versus a set of target species involving tradeoffs. Each of these dimensions must be carefully considered in selecting an analysis procedure appropriate to the problem at hand.

10.3.4   Habitat Evaluation and Modeling

10.3.4.1   Habitat Diversity

Habitat evaluation is an important aspect of bioassessment. Habitat has a definable carrying capacity, or suitability, to support or produce wildlife populations (Fretwell and Lucas, 1970). The capacity depends, to a great extent, on the habitat diversity. A habitat diversity index is needed to represent this characteristic. The physical conditions of stream habitat are mainly (1) the substrate; (2) water depth; and (3) flow velocity (Gorman and Karr, 1978). Different physical conditions support different bio-communities and diversified physical conditions may support diversified bio-communities. A habitat diversity index, H_D, is proposed as follows (Wang et al., 2009):

$$H_D = N_h N_v \sum_i \alpha_i \tag{10.12}$$

where N_h and N_v are numbers for water depth diversity and velocity diversity, and α is the substrate diversity, which is different for different substrates. For water depth less than 0.1 m the habitat is colonized by species that like high concentrations of dissolved oxygen and plenty of light. For water depth larger than 0.5 m the habitat is colonized by species that like low light and dissolved oxygen. Many species may live in water with depths between 0.1–0.5 m. If a stream has three water areas: (1) shallow water, in which the water depth is in the range of 0–0.1 m; (2) mid depth water, in which the water depth is in the range of 0.1–0.5 m; and (3) deep water, in which water depth is larger than 0.5 m, and each of the three areas is larger than 10% of the stream water surface area, $N_h = 3$. If a stream has only shallow water and mid-depth water, and each of them is larger than 10% of the stream water surface area, $N_h = 2$. The value of N_h for other cases can be analogously obtained. For flow velocity less than 0.3 m/s the habitat is colonized by species that swim slowly. For velocity higher than 1 m/s the habitat is colonized by species that like high velocities. Many species live in the current between 0.3–1 m/s. If a stream has three water areas: (1) lentic area, in which the flow velocity is smaller than 0.3 m/s; (2) mid-velocity area, in which the flow velocity is in the range of 0.3–1 m/s; and (3) lotic area, in which the velocity is larger than 1 m/s, and each of the three areas is larger than 10% of the stream water surface area, $N_v = 3$. If a stream has only lentic and mid-velocity areas, and each of them is larger than 10% of stream water, $N_v = 2$. The value of N_v for other cases can be analogously obtained.

The selection of the critical values of water depth and velocity are determined by studying the habits of species, mainly of macro-invertebrates. It is found from field investigations that in the Yangtze River basin some species in the water depth between 0.1–0.5 m are different from those in shallower or deeper water. Similarly, some species living in the current range of 0.3–1 m/s are different from those in currents lower than 0.3 m/s or higher than 1 m/s. Beauger et al. (2006) reported that the highest species richness and density were found in various substrates where the velocity ranged between 0.3 and 1.2 m/s, and depths ranged from 0.16 to 0.5 m. Below 0.3 m/s the riverbed tends to be filled and not very productive, whereas above 1.2 m/s the current velocity acts as a constraint for most living material. Undoubtedly, at lower depths, vegetation and animals are disturbed by light, conversely at higher depths in which the primary productivity decreases, the bio-community is disturbed due to light attenuation. At lower and higher depths and velocities, only those species tolerant to the constraints may colonize the habitat.

Streambeds consisting of cobbles and boulders are very stable and provide the benthic macro-invertebrates diversified living spaces. Therefore, cobbles and boulders are associated with high habitat diversity. Stream flow over aquatic grasses has high velocity but the aquatic grasses generate a low velocity canopy, moreover, the aquatic grasses themselves are also habitat for some species. Thus, streams with aquatic grasses exhibit high habitat diversity. Some species may move and live within the fluid mud layer and consume the organic materials in the mud layer. The interstices in a fine gravel bed are small but sufficient for some species. A sand bed is compact and the interstices between sand particles are too small for big benthic macro-invertebrates to move and live within them. If sand particles are moving as bed load the bed provides no stable habitat for animals. Therefore, moving sand is the worst habitat for benthic macroinvertebrates. Based on this discussion and field investigations of 16 streams, the α-values for various substrates are listed in Table 10.7. It is well known that large woody debris can substantially contribute to habitat quality in streams (Gippel, 1995; Abbe and Montgomery, 1996), and, thus, a more generally applicable listing of α-values should also include a value for stream substrates with large woody debris. However, large woody debris does not often occur in Chinese streams, therefore, a rating for large woody debris has not been determined and is not listed in Table 10.7.

Table 10.7 Substrate diversity, α, values for different substrates (after Wang et al., 2009)

Substrate	Boulders and cobbles (D>200 mm)	Aquatic grass	Gravel (2–200 mm)	Fluid clay mud (D<0.02mm)	Silt (0.02 –0.2 mm)	Sand (0.2–2 mm)	Unstable sand, gravel, and silt bed (0.02–20 mm)
α	6	5	4	3	2	1	0

If a part of the streambed consists of one substrate and another part consists of the another substrate and both parts have areas larger than one tenth of the stream surface, the two α-values for the two kinds of substrates should be summed. However, if sand or silt fills the interstices of gravel the α-value should be taken as for the substrate of sand or silt. If a streambed has three parts with different substrates: boulders and cobbles, aquatic grasses, and fluid clay mud, and each of the three parts is larger than one tenth of the total stream area, the sum of the α-values for the stream is $\sum_i \alpha_i = 6+5+3 = 14$. If the streambed is covered by moving sand and gravel or the bed is very unstable, $\sum_i \alpha_i = 0$.

Gorman and Karr (1978) also developed a Habitat Diversity Index combining the effects of substrate, velocity, and depth. They showed that fish species diversity and richness were strongly related to a combination of the effects of substrate, velocity, and depth. Their substrate classification is similar to that proposed here with the main differences being in the divisions of sediment sizes into the various classes, but a similar ordinal ranking is applied to the substrate material. They also developed class ranges for velocity and depth throughout a reach determined by a weighting of point measurements. The index applied here takes a simpler approach to considering the diversity of velocity and depth.

The biodiversity of streams depends not only on the physical conditions but also is affected by food availability and water quality. Food availability is very different for different species and should be studied separately. Generally speaking, water pollution reduces the number of species but may not reduce the density of pollution-tolerant species. Water quality is not an inherent feature of a habitat and depends on human disturbances. Therefore, water quality is not taken in the habitat diversity index. Water temperature also is an important factor for stream ecology. However, the temperature does not vary much in a reach of a stream unless a thermal discharge is present and it is not necessary to consider it in the analysis of local habitat diversity. When habitat across different zones with great temperature differences is studied, then temperature difference has to be considered in the analysis.

High diversity of habitat supports high diversity of bio-community, which may be illustrated with the sampling results of macro-invertebrates in several mountain streams in the Xiaojiang River basin in Yunnan Province in southwestern China. Figure 10.44 shows the relations between the habitat diversity, H_D, and the species richness, S, the Shannon Weaver index, H, and the bio-community index, B, for these streams. In general, the higher is the habitat diversity, the higher are the species richness, the bio-diversity, and the bio-community index. However, the species richness, S, has the best relation with the habitat diversity clearly showing an increasing trend with habitat diversity. The bio-community index, B, also linearly increases with the habitat diversity. The Shannon-Weaver Index, H, increases with the habitat diversity, but the points around the $H_D \sim H$ curve is rather scattered. The results suggest that the species richness, S, and bio-community index, B, are suitable ecological indicators for good habitat in streams that are not impaired by poor water quality. Similar results also were obtained from a study on the East River basin in Guangdong Province. Figure 10.45 shows the relations of the habitat diversity, H_D, with the Shannon-Weaver index, H, and bio-community index, B, for the East River. The higher is the habitat diversity, the higher are the biodiversity and bio-community indices. The bio-community index, B, increases with habitat diversity, H_D, and the points of B-H_D relation are much closer to the curve than the relation of H-H_D.
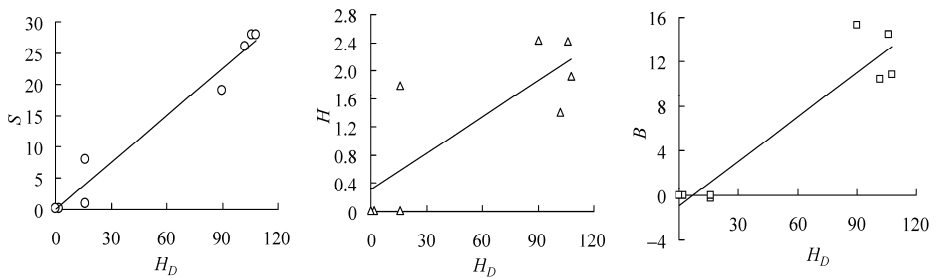
Fig. 10.44   Species richness, S; Shannon-Weaver Index, H; and the bio-community index, B, as functions of the habitat diversity index, H_D
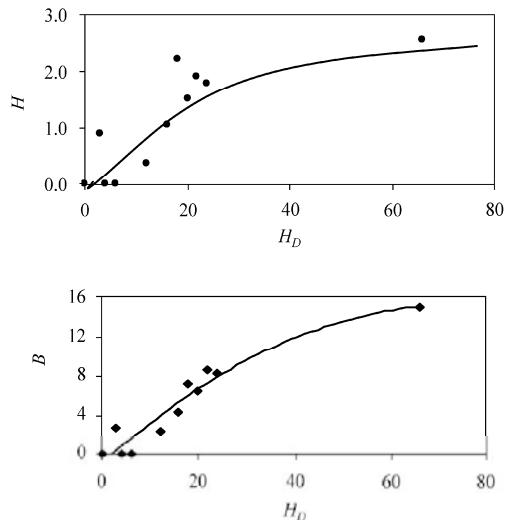
Fig. 10.45   Relation between habitat diversity, H_D, and Shannon-Weaver index, H (upper); and the relation between habitat diversity, H_D, and bio-community index, B (lower)

691

10.3.4.2 Habitat Evaluation Procedure

The Habitat Evaluation Procedures (HEP) can be used for several different types of habitat studies, including impact assessment, mitigation, and habitat management. The HEP provides information for two general types of habitat comparisons—the relative value of different areas at the same point in time and the relative value of the same area at different points in time.

The HEP is based on two fundamental ecological principles—habitat has a definable carrying capacity to support wildlife populations, and the suitability of habitat for a given wildlife species can be estimated using measurements of vegetative, physical, and chemical characteristics of the habitat. The suitability of a habitat for a given species is described by a habitat suitability index (HSI) constrained between 0 (unsuitable habitat) and 1 (optimum habitat). HSI models have been developed and published (Schamberger et al., 1982), the U.S. Fish and Wildlife Service (USFWS, 1981) also provides guidelines for use in developing HSI models for specific projects. HSI models can be developed for many of the previously described metrics, including species, guilds, and communities (Schroeder and Haire, 1993).

The fundamental unit of measure in The HEP is the Habitat Unit, computed as follows:

$$HU = AREA \times HIS \qquad (10.13)$$

where HU is the number of habitat units (units of area), AREA is the areal extent of the habitat being described (in km^2), and HSI is the index of suitability of the habitat (dimensionless). Conceptually, an HU integrates the quantity and quality of habitat into a single measure, and one HU is equivalent to one unit of optimal habitat. The HEP provides an assessment of the net change in the number of HUs attributable to a proposed future action, such as a stream restoration initiative. A HEP application is essentially a two-step process—calculating future HUs for a particular project alternative and calculating the net change as compared to a base condition.

10.3.4.3 Habitat Modeling

Many habitat evaluation models have been developed. The **Physical Habitat Simulation Model** was designed by the U.S. Fish and Wildlife Service primarily for instream flow analysis (Bovee, 1982). The model allows evaluation of available habitat within a study reach for various life stages of different fish species. The first component of the model is hydraulic simulation for predicting water surface elevations and velocities at unmeasured discharges (e.g., stage vs. discharge relations, Manning's equation, step-backwater computations). The second component of the model, habitat simulation, integrates species and lifestage—specific habitat suitability curves for water depth, velocity, and substrate with the hydraulic data. Output is a plot of weighted usable area against discharge for the species and life stages of interest.

Riverine Community Habitat Assessment and Restoration Concept Model is based on the assumption that aquatic habitat in a restored stream reach will best mimic natural conditions if the frequency distribution of depth and velocity in the subject channel is similar to a reference reach with good aquatic habitat. Study site and reference site data can be measured or calculated using a computer model. The similarity of the proposed design and reference reach is expressed with three-dimensional graphs and statistics (Nestler et al., 1993; Abt, 1995). The model has been used as the primary tool for environmental analysis on studies of flow management for the Missouri River and the Alabama Basin.

SALMOD (Salmonid Population Model) is a conceptual and mathematical model for the salmonid population for Chinook salmon in concert with a 12-year flow evaluation study in the Trinity River of California using experts on the local river system and fish species in workshop settings (Williamson et al., 1993; Bartholow et al., 1993). The structure of the model is a middle ground between a highly aggregated classical population model that tracks cohorts/size groups for a generally large area without spatial resolution, and an individual-based model that tracks individuals at a great level of detail for a generally small area. The conceptual model states that fish growth, movement, and mortality are directly related to

physical hydraulic habitat and water temperature, which in turn relate to the timing and amount of regulated stream flow. Habitat capacity is characterized by the hydraulic and thermal properties, which are the model's spatial computational units. Model processes include spawning, growth (including maturation), movement (freshet-induced, habitat-induced, and seasonal), and mortality (base, movement-related, and temperature-related). The model is limited to freshwater habitat for the first 9 months of life; estuarine and ocean habitats are not included.

10.3.4.4   Suitability Indices

Suitability Indices are the core for habitat modeling, which may be illustrated for the Chinese sturgeon (Yi et al., 2007). The life cycle of the Chinese sturgeon in the Yangtze River mainly comprises spawning, hatching, and growth of 1 yr juvenile sturgeon. Brood fish seek suitable spawning sites; fertilized eggs adhere to stone and hatch after about 120 to 150 h. Whelp sturgeon drift with the current, and grow slowly in the lower reaches of the Yangtze River and river mouth. Juvenile sturgeons swim to the East China Sea and stay there until they reach maturity. Therefore, analysis for the habitat quality of the Chinese sturgeon is based on basic requirements of spawning, hatching, and juvenile and adult sturgeon growth.

In habitat modeling variables which have been shown to affect growth, survival, abundance, or other measures of well-being of the Chinese sturgeon, are placed in the appropriate component. Ten aquatic eco-factors, which mainly influence the habitat of the Chinese sturgeon, are selected for the modeling as follows: (1) Water temperatures for adults and juveniles (V_1, ℃); (2) Water depth for adults (V_2, m); (3) Substrate for adults (V_3); (4) Water temperature for spawning (V_4, ℃); (5) Water depth for spawning (V_5, m); (6) Substrate for spawning and hatching (V_6); (7) Water temperature during hatching (V_7, ℃); (8) Flow velocity during spawning (V_8, m/s); (9) Suspended sediment concentration during spawning (V_9, mg/l); and (10) The amount of eggs-predating fish in the studied year in comparison to a standard year (V_{10}). The suitable ranges and the Suitability Index (*SI*) curves of the ten main eco-factors are determined based on biological research. By analyzing these eco-factors, a habitat assessment model is developed which combines these factors and can be used for assessing habitat changes caused by human activities and hydraulic processes. The habitat suitability function for the Chinese sturgeon mainly considered the suitability for juvenile and adult fish growth, spawning, and hatching.

Habitat Suitability Index:

$$HSI = \min(C_{Ad}, C_{Sp}, C_{Ha}) \tag{10.14}$$

in which C_{Ad} represents the suitability for juvenile and adult growth, given by

$$C_{Ad} = \min(V_1, V_2, V_3) \tag{10.15}$$

C_{Sp} represents the suitability for spawning

$$C_{Sp} = \min(V_4, V_5, V_6) \tag{10.16}$$

C_{Ha} represents the suitability for hatching

$$C_{Ha} = V_{10} \cdot \min(V_6, V_7, V_8, V_9) \tag{10.17}$$

where $V_1 - V_{10}$ are the ten factors. The SI curve quantifies physical habitat such as water temperature, flow velocity, and suspended sediment concentration. The habitat suitability ranges from unsuitable (0) to optimal habitat suitability (1). The intermediate values represent the suitability range based on a specified hydraulic variable.

Biological studies discovered that adult sturgeon distribution, spawning time, and spawning site selection by brood fish, are mainly influenced by water temperature (V_1, V_4), water depth (V_2, V_5) and substrate (V_3, V_6). The main eco-factors which influence hatching are water temperature (V_7), flow velocity (V_8), substrate (V_6), suspended sediment concentration (V_9), and the amount of the eggs-predating fish (V_{10}).

Water temperature is an essential factor for hatching; flow velocity influences the distribution of eggs and their cohesiveness on the river bed. Excessive suspended sediment concentration may cause sturgeon eggs to debond, which then affects fertilization and hatching. According to Chang (1999), 90% of sturgeon eggs suffer predation. The data sources used to develop the SIS are listed in Table 10.8, and the *SI* curves are shown in Fig. 10.46. The value of V_{10} (the ratio of estimated brood sturgeon to eggs-predatory fish) is not shown in the figure, because it depends on the physical conditions and the number of the eggs-predatory fish in the previous year. In the modeling the value of V_{10} is assumed equal to 1.0, i.e. the amount of eggs-predatory fish is the lowest in the record.

Table 10.8 Eco-factors for Chinese Sturgeon (after Yi et al., 2007)

Variables	Eco-factors	Results of previous research
V_1	Water temperature (adults and juveniles)	The Chinese sturgeon can survive temperatures between 0–37℃; 13–25℃ is suitable for growth, and 20–22℃ is optimum. The sturgeon becomes anorexic and stops growing when temperatures fall to 9–6℃ (NERCITA, 2004a). Research results indicate that the Chinese sturgeon grows well under a wide range of temperatures; feeding has been recorded from 8–29.1℃ (Guo and Lian, 2001). Yan (2003) found that Chinese sturgeon prefer tepid water, anorexia results and growth almost stops when temperatures are < 6℃ and > 28℃, growth rate slows when temperatures are near 10℃. 18–25℃ is an optimum range for growth; sturgeon will die when temperature is >35℃. The optimum temperature for juvenile sturgeon is 22–25℃ (Zhang, 1998).
V_2	Water depth (adults)	The Chinese sturgeon is distributed in areas with 9.3–40 m water depth; 90% of individuals are distributed at depths from 11–30 m; 11 Chinese sturgeons detected in the Yanzhiba to Gulaobei reach were distributed at depths from 9–19 m (Wei, 2005).
V_3	Substrate (adults)	Juvenile and adult Chinese sturgeons have similar substrate choices as with short-nose sturgeon in the US. Experiments show that juvenile short-nose sturgeon prefer habitat in sand-mud substrate or gravel substrate (Pottle and Dadswell, 1979). Chinese sturgeon prefer to cruise along river channels with deep trenches and sandy dunes, and are fond of resting in pools, backwaters, and places varied terrain (Guo and Lian, 2001).
V_4	Water temperature (spawning)	The spawning temperature for sturgeon is 17.0–20.0℃; spawning will stop when temperature < 16.5℃(Hu et al., 1992). The average temperature in the reaches downstream of the Gezhouba Dam during the sturgeon spawning period is 15.8–20.7℃. About 79.31% of fish are spread in the range of 17.5–19.5℃; the average temperature of the original spawning sites in the upper reaches of the Yangtze River is 17.0–20.2℃. Therefore, the suitable spawning temperature for Chinese sturgeon is 17.0–20.0℃ (Wei, 2005). Spawning occurs when temperature is 15.3–20.5℃; the suitable range is 17.0–20.0℃, and the optimum is 18.0–20.0℃ (Yang et al., 2007).
V_5	Water depth (spawning)	More than 20 years' of monitoring indicates that the length of new spawning sites is about 30 km from the tail water area of Gezhouba Dam to Gulabei, with 10–15 m water depth (Guo and Lian, 2001). The "stable spawning site of Chinese sturgeon" determined by Deng et al. (1991) has a water depth in a range from 4–10 m.
V_6	Substrate (spawning and hatching)	Gravel and pebbles are present in Chinese sturgeon spawning sites of (Li, 1999). The substrate of new spawning sites are composed of sand, grave with sand, gravel and stone, and gradually coarsen from left to right bank (Hu et al., 1992). The substrate of the original centralized spawning sites of Chinese sturgeon was mainly composed of stones and gravels (Xing, 2003).
V_7	Water temperature (hatching)	The suitable temperature for hatching is 16–22℃, the optimum is 17–21℃. The hatching rate decreases when at temperature < 16℃; deformity rate increases at temperature > 23℃. The temperature should be stable when zoosperms are hatching, abnormal fetation or death will occur with even small fluctuations in temperature of 3–5℃ (NERCITA, 2004b). Water temperature for cultivating fries should be between 12–29℃; the most suitable temperature is 16–24℃ (Wang et al., 2002).

(Continued)

V_8	Flow velocity (spawning)	Sturgeon prefer spawning areas with flow velocity of 0.08–0.14 m/s at the bottom, 0.43–0.58 m/s in the middle, and 1.15–1.70 m/s at the surface (Li, 2001). The surface flow velocity at spawning areas is 1.1–1.7 m/s (Li, 1999). The flow velocity of spawning areas during spawning season ranges from 0.82–2.01 m/s; 57.69% of fish are distributed between 1.2–1.5 m/s. When spawning occurs during periods when water levels are falling, the daily fluctuation range of flow velocity is 0.82–1.86 m/s, with an average of 1.24 m/s. The daily maximum fluctuation range is 1.20–2.33 m/s, with an average of 1.56 m/s. When spawning activity occurs during periods when water levels are rising, the daily fluctuation range of flow velocity is 1.17–2.01 m/s, with an average of 1.55 m/s (Wei, 2005). According to 31 records from 1983–2000, the average flow velocity on spawning day was between 0.81–1.98 m/s, and 81% took place in the range of 1.00–1.66 m/s (Yang et al., 2007).
V_9	Suspended sediment concentration (spawning)	The suspended sediment concentration in reaches downstream from the Gezhouba Dam is between 0.073–1.290 kg/m^3, with an average of 0.508 kg/m^3. About 66.67% of fish are distributed between 0.3–0.7 kg/m^3. When spawning activity occurs during periods of falling water level, the daily average suspended sediment concentration varies between 0.17–1.29 kg/m^3, with an average of 0.52 kg/m^3. When spawning activity occurs during periods of rising water levels, the daily average suspended sediment concentration varies between 0.41–1.02 kg/m^3, with an average of 0.61 kg/m^3 (Wei, 2005). The suitable range of suspended sediment concentration for Chinese sturgeon is 0.10–1.32 kg/m^3. From 1983–2000, 15 of 31 spawning events were in the range of 0.2–0.3 kg/m^3 (Yang et al., 2007).

10.3.4.5   Vegetation-Hydroperiod Modeling

Vegetation-Hydroperiod Modeling is a very useful tool for habitat evaluation. Hydroperiod is defined as the depth, duration, and frequency of inundation and is a powerful determinant of what plants are likely to be found in various positions in the riparian zone, as shown in Fig. 10.47. In most cases, the dominant factor that makes the riparian zone distinct from the surrounding uplands, and the most important gradient in structuring variation within the riparian zone, is site moisture conditions, or hydroperiod. Formalizing this relation as a vegetation-hydroperiod model can provide a powerful tool for analyzing existing distributions of riparian vegetation, casting forward or backward in time to alternative distributions, and designing new distributions. The suitability of site conditions for various species of plants can be described with the same conceptual approach used to model habitat suitability for animals. The basic logic of a vegetation-hydroperiod model is straightforward. It is possible to measure how wet a site is and, more importantly, to predict how wet a site will be. From this, it is possible to estimate what vegetation is likely to occur on the site.

The two basic elements of the vegetation-hydroperiod relation are the physical conditions of site moisture at various locations and the suitability of those sites for various plant species. In the simplest case of describing existing patterns, site moisture and vegetation can be directly measured at a number of locations. However, to use the vegetation-hydroperiod model to predict or design new situations, it is necessary to predict new site moisture conditions. The most useful vegetation-hydroperiod models have the following three components (FISRWG, 1997):

(1) Characterization of the hydrology or pattern of stream flow—This can take the form of a specific sequence of flows, a summary of how often different flows occur, such as a flow duration or flood frequency curve, or a representative flow value, such as bankfull discharge or mean annual discharge.

(2) A relation between streamflow and moisture conditions at sites in the riparian zone—This relation can be measured as the water surface elevation at a variety of discharges and summarized as a stage vs. discharge curve. It can also be calculated by a number of hydraulic models that relate water surface elevations to discharge, taking into account variables of channel geometry and roughness or resistance to
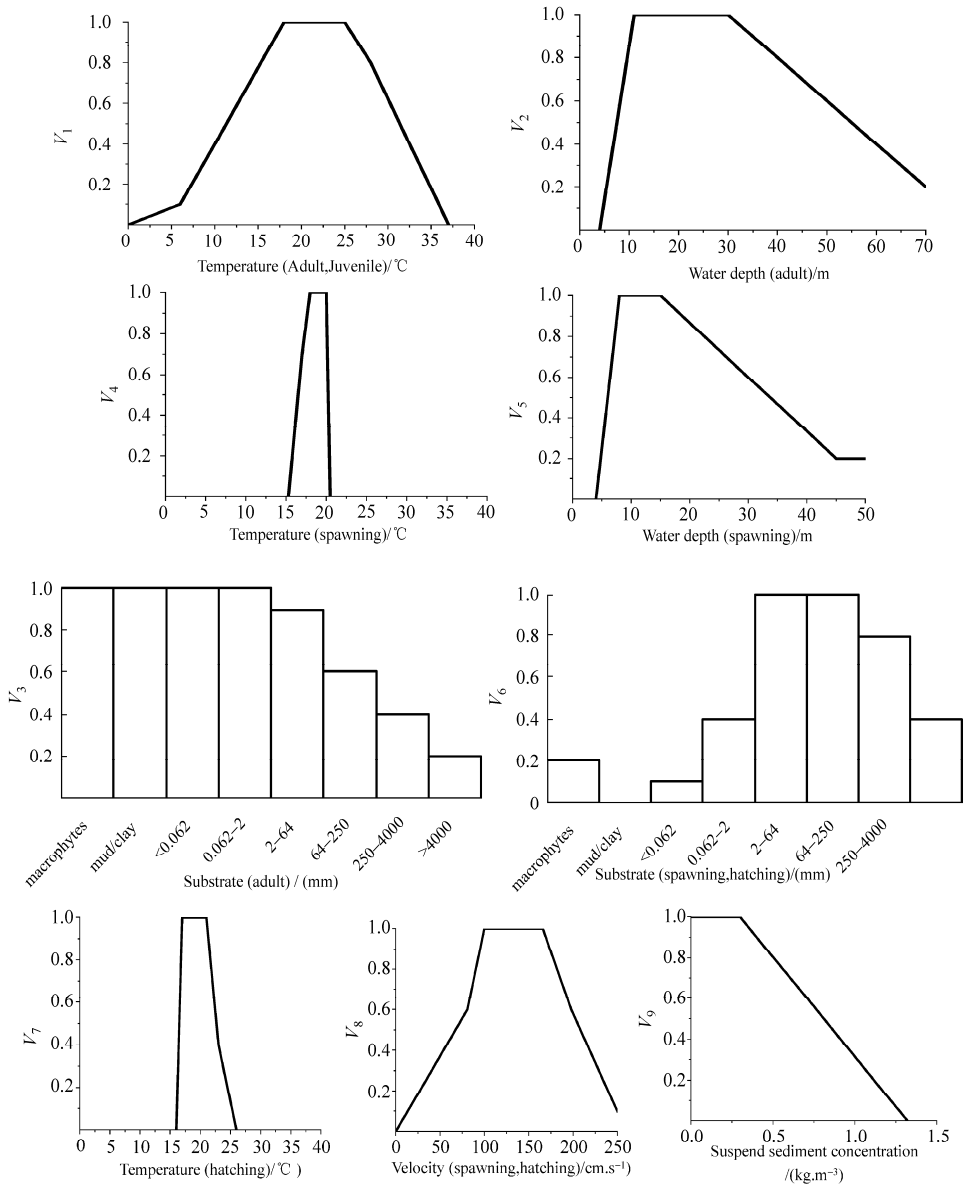
Fig. 10.46   Suitability Index curves for habitat of Chinese sturgeon

flow. In some cases, differences in simple elevation above the channel bottom may serve as a reasonable approximation of differences in inundating discharge.

(3) A relation between site moisture conditions and the actual or potential vegetation distribution—This relation expresses the suitability of a site for a plant species or cover type based on the moisture conditions at the site. It can be determined by sampling the distribution of vegetation at a variety of sites with known moisture conditions and then deriving probability distributions of the likelihood of finding a plant on a site given the moisture conditions at the site. General relations are also available from the literature for many species.

Fig. 10.47   Soil moisture conditions determine the plant communities in riparian areas of the Nile River in Sudan

In altered or degraded stream systems, current moisture conditions in the riparian zone may be dramatically unsuitable for the current, historical, or desired riparian vegetation. Several conditions can be relatively easily identified by comparing the distribution of vegetation to the distribution of vegetation suitabilities.

The hydrology of the stream has been altered, for example, if stream flow has diminished by diversion or flood attenuation, sites in the riparian zone may be drier and no longer suitable for the historic vegetation or for current long-lived vegetation that was established under a previous hydrologic regime. The inundating discharges of plots in the riparian zone have been altered so that streamflow no longer has the same relation to site moisture conditions; for example, levees, channel modifications, and bank treatments may have either increased or decreased the discharge required to inundate plots in the riparian zone. The vegetation of the riparian zone has been directly altered, for example, by clearing or planting so that the vegetation on plots no longer corresponds to the natural vegetation for which the plots are suitable.

Temporal variability is a particularly important characteristic of many stream ecosystems. Regular seasonal differences in biological requirements are examples of temporal variability that are often incorporated into biological analyses based on habitat suitability and time series simulations. The need for episodic extreme events is easy to ignore because these are as widely perceived as destructive both to biota and constructed river features. In reality, however, these extreme events seem to be essential to physical channel maintenance and to the long-term suitability of the riverine ecosystem for disturbance-dependent species.

Cottonwood in riparian systems in the western U.S. is one well understood case of a disturbance-dependent species. Cottonwood regeneration from seed is generally restricted to bare, moist sites. Creating these sites depends heavily on channel movement (meandering, narrowing, avulsion) or new flood deposits at high elevations. In some riparian systems, channel movement and sediment deposition on flood plains tend to occur infrequently in association with floods. The same events are also responsible for destroying stands of trees. Thus, maintaining good conditions for existing stands, or fixing the location of a stream's banks with structural measures, tends to reduce the regeneration potential and the longterm importance of this disturbance-dependent species in the system as a whole.

There is a large body of information on the flooding tolerances of various plant species. Summaries of this literature include Whitlow and Harris (1979) and the multivolume Impact of Water Level Changes on Woody Riparian and Wetland Communities (Teskey and Hinckley, 1978; Walters et al., 1978; Lee and

Hinckley, 1982; Chapman et al., 1982). This type of information can be coupled to site moisture conditions predicted by applying discharge estimates or flood frequency analyses to the inundating discharges of sites in the riparian zone. The resulting relation can be used to describe the suitability of sites for various plant species, e.g., relatively floodprone sites will likely have relatively flood-tolerant plants. Inundating discharge is strongly related to relative elevation within the floodplain. Other things being equal (i.e., within a limited geographic area and with roughly equivalent hydrologic regimes), elevation relative to a representative water surface line, such as bankfull discharge or the stage at mean annual flow, can, thus, provide a reasonable surrogate for site moisture conditions. Locally determined vegetation suitability can then be used to determine the likely vegetation in various elevation zones.

10.4   Restoration Strategies

"Leave it alone and let it heal itself." In some cases, the best solution to a river ecological problem might be to remove the stresses and "let it heal itself." Unfortunately, in many cases this process can take quite a long time. Therefore, the "leave it alone" concept is a difficult approach for people to accept (Gordon et al., 1992). Restoration of the impaired river ecosystem is necessary. According to the U.S. National Research Council (NRC, 1992), restoration should involve the return of a given ecosystem to a state approximating that in which it existed prior to disturbances.

10.4.1   Design of Stream Restoration

Design of instream habitat restoration can be guided and fine tuned by assessing the quality and quantity of habitat provided by the proposed design. It should be noted, however, that the best approach to habitat recovery is to restore a fully functional, well-vegetated stream corridor within a well-managed watershed. Man-made structures are less sustainable and rarely result in a stable channel. Over the long term, design should rely on natural fluvial processes interacting with floodplain vegetation and associated woody debris to provide high-quality aquatic habitat. Structures have little effect on populations that are limited by factors other than physical habitat.

Newbury and Gaboury (1993) and Garcia (1995) adapted the following procedures to restore instream habitat.

1) Select stream. Give priority to reaches with the greatest difference between actual (low) and potential (high) fish carrying capacity and with a high capacity for natural recovery processes.

2) Evaluate fish populations and their habitats. Give priority to reaches with habitats and species of special interest. Is this a biological, chemical, or physical problem? If a physical problem, do the following.

3) Diagnose physical habitat problems: **Drainage basin**—Trace watershed lines on topographical and geological maps to identify sample and rehabilitation basins. **Profiles**—Sketch main stem and tributary long profiles to identify discontinuities that might cause abrupt changes in stream characteristics (falls, former base levels, etc.). **Flow**—Prepare flow summary for rehabilitation reach using existing or nearby records if available (flood frequency, minimum flows, historical mass curve). **Channel geometry survey**—Select and survey sample reaches to establish the relation between channel geometry, drainage area, and bankfull channel-forming discharge. Quantify hydraulic parameters at design discharge. **Rehabilitation reach survey**—Survey rehabilitation reaches in sufficient detail to prepare channel cross section profiles and construction drawings and to establish survey reference markers. **Preferred habitat**—Prepare a summary of habitat factors for biologically preferred reaches using regional references and surveys. Identify multiple limiting factors for the species and life stages of greatest concern. Where possible, undertake reach surveys in reference streams with proven populations to identify local flow conditions, substrate, refuges, etc.

4) Design a habitat improvement plan. Quantify the desired results in terms of hydraulic changes, habitat improvement, and population increases. Integrate selection and sizing of habilitation works with instream flow requirements. Select potential schemes and structures that will be reinforced by the existing stream dynamics and geometry. Test designs for minimum and maximum flows and set target flows for critical periods derived from the historical mass curve.

5) Implement planned measures. Arrange for on-site location and elevation surveys and provide advice for finishing details in the stream.

6) Monitor and evaluate results. Arrange for periodic surveys of the rehabilitated reach and reference reaches, to improve the design, as the channel ages.

Evidence suggests that traditional design criteria for widespread bank and bed stabilization measures (e. g., concrete grade control structures, homogeneous riprap) can be modified, with no functional loss, to better meet environmental objectives and improve habitat diversity. Weirs are generally more failure-prone than deflectors. Deflectors and random rocks are minimally effective in environments where higher flows do not produce sufficient local velocities to produce scour holes near structures. Random rocks (boulders) are especially susceptible to undermining and burial when placed in sand-bed channels, although all types of stone structures experience similar problems. Additional guidance for evaluating the general suitability of various fish habitat structures for a wide range of morphological stream types is provided by Rosgen (1996). Seehorn (1985) provides guidance for small streams in the eastern U.S. Nowadays numerous design web sites are available (White and Brynildson, 1967; Seehorn, 1985; Wesche, 1985; Orsborn et al., 1992; Orth and White, 1993; Flosi and Reynolds, 1994). The use of any of these guides should also consider the relative stability of the stream, including aggradation and incision trends, for final design.

Hydraulic conditions at the design flow should provide the desired habitat; however, performance should also be evaluated at higher and lower flows. Barriers to movement, such as extremely shallow reaches or vertical drops not submerged at higher flows, should be avoided. If the conveyance of the channel is an issue, the effect of the proposed structures on stages at high flow should be investigated. Structures may be included in a standard backwater calculation model as contractions, low weirs, or increased flow resistance (Manning) coefficients, but the amount of increase is a matter of judgment or limited by National Flood Insurance Program ordinances. Scour holes should be included in the channel geometry downstream of weirs and dikes since a major portion of the head loss occurs in the scour hole. Hydraulic analysis should include estimation or computation of velocities or shear stresses to be experienced by the structure.

If the hydraulic analysis indicates a shift in the stage-discharge relation, the sediment-rating curve of the restored reach also may change, leading to deposition or erosion. Although modeling analyses are usually not cost-effective for a habitat structure design effort, informal analyses based on assumed relations between velocity and sediment discharge at the bankfull discharge may be helpful in detecting potential problems. An effort should be made to predict the locations and magnitude of local scour and deposition. Areas projected to experience significant scour and deposition should be sites for visual monitoring after construction.

Materials used for aquatic habitat structures include stone, fencing wire, posts, and felled trees. Priority should be given to materials that occur on site under natural conditions. In some cases, it may be possible to salvage rocks or logs generated from construction of channels or other project features. Logs give long service if continuously submerged. Even logs not continuously wet can give several decades of service if chosen from decay-resistant species. Logs and timbers must be firmly fastened together with bolts or rebar and must be well anchored to banks and bed. Stone size should be selected based on design velocities or shear stress.

10.4.2 Instream Structures for Habitat Restoration

Artificial instream structures have been used to modify fish habitat conditions from about the mid 1930s in the U.S. Since that time the use of these structures has gradually increased worldwide. Such techniques have been increasingly used to rehabilitate habitat in rivers impacted by channel works or adversely affected by regulation (Brookes and Shields, 1996). It appears that the techniques were initially used to improve rivers, which had a recreational value for salmonids, but more recently have been extended to degraded rivers also containing non-salmonid species. Instream structures are just one of the more localized methods of improving habitat. Common types of instream structures include weirs, deflectors, random rocks, bank covers, substrate reinstatement, fish passage structures, and off-channel ponds and coves. Habitat structures have been used more along cold water streams. In 1995, 1,234 structures were evaluated according to their general effectiveness, the habitat quality associated with the given structure type, and actual use of the structures by fish (Bio West, 1995). The study concluded that instream habitat structures generally provided increased fish habitat, but 18 percent of the structures need maintenance. Where excessive sediment delivery occurs, structures have a brief lifespan and limited value in terms of habitat improvement. The typical structures are listed in Table 10.9.

Table 10.9 Structural techniques used for instream habitat improvement (after Brookes and Shields, 1996)

Type	Functions
Deflectors	To direct flow and eliminate accumulated sediment or to narrow a channel, thereby increasing the velocity and creating a scour pool with a corresponding downstream riffle
Small weirs or sills	Diversify habitat by impounding a greater depth of flow above the structure and by increasing the velocity downstream to erode a scour pool
Substrate placement	Placement of new substrate to enhance the habitat for fish and macro invertebrates
Devices providing direct cover	Fixed to the bed or banks of a channel to float and adjust their level with varying discharge

Species-centered restoration—Many angling organizations have used instream structures to improve habitat for maximum production of salmonids and other game fish. In the U.S. there has also been Federal involvement through agencies such as the U.S. Forest Service and the U.S. Fish and Wildlife Service since the 1930s. There are a considerable number of publications, which demonstrate how effective such projects can be for increasing fish numbers and biomass. However, sometimes this type of work has been detrimental to other species, such as beaver (NRC, 1992). Gore (1985) argues that restoration of macro invertebrate communities is essential since they often form a substantial portion of the food supply for fish. Maximizing habitat value for any single species is not the same as recreating the biotic structure and function of a stream, involving consideration of a number of species (NRC, 1992).

A key characteristic of a productive stream is physical habitat diversity. It is essential that there are appropriate ranges of water depths, water velocities, and substrate types. Since cover is also important, consideration needs to be given to the riparian plant community (Hunt, 1988). Suitable depths and velocities are needed for spawning habitat, but if an appropriate substrate is absent then the habitat value is diminished for species, which spawn on the bed. Likewise, if substrate has been reinstated without consideration of holding pools for mature fish then the habitat value is again questionable. Many approaches have now been developed to quantify habitat value. The approaches are based on the concept that abundance of a particular species can be correlated with particular habitat requirements. For example, the U.S. Fish and Wildlife Service Physical Habitat Simulation System Model is useful for crude prediction and analysis of potential habitat improvement (Bovee and Milhous, 1978).

Deflectors—Perhaps the most widely used structures for habitat improvement are current deflectors. These function either to direct flow and eliminate accumulated sediment, or to narrow a channel, thereby locally increasing the velocity and creating a scour pool with a corresponding riffle downstream. Other effects include assisting the development of a meandering thalweg within a straightened channel, protecting stream banks from erosion, and encouraging the establishment of riparian vegetation through the formation of bars of sediment.

Deflectors are commonly angled in a downstream direction at approximately 45 degrees from the current (Wesche, 1985), although several different angles have been used depending on the local circumstances (Cooper and Wesche, 1976). Double wing deflectors, which consist of two current deflectors placed opposite each other at the same point in a reach, have also been used (Seehorn, 1985). Shape is another consideration and varies from single peninsular wing to a triangular wing (White and Brynildson, 1967). The latter shape has been successful in certain circumstances in regulating the tendency for erosion of the bed and bank behind the structure during high flows. The elevation of the water surface at low flow generally determines the structure height and it has been found that to avoid excessive damage to the structure itself during high flows the structure should not extend more than 0.15 to 0.30 m above the low flow elevation (Seehorn, 1985; Wesche, 1985). The distance that the deflector protrudes into the channel will vary from site to site and depends on the specific results desired. For example, in streams in the southeastern U.S., Seehorn (1985) found that to have any effect the channel would need to be narrowed to a width approximating the natural width. This width can be determined from adjacent or neighboring natural reaches with a similar slope, flow regime, and bed and bank materials.

Deflectors are very effective at manipulating flow and creating the diversity of habitat required for fish and other biota. Figure 10.48 shows a spur dike extension on the Lijiang River, to promote the formation of low velocity habitats. Patterns of scour and deposition are evident. Such structures can be built in series, alternating from one bank to the other, to create a meandering thalweg. Several authors have recommended a spacing of between five and seven channel widths, corresponding to the natural pool-riffle spacing of some natural streams (White, 1975; Everhart et al., 1975). This helps to formalize the low flow sinuous channel within a wide flood channel (Brookes, 1995). Many of these structures demonstrated marked improvement in fish population and the benthic macroinvertebrates. However, rarely have studies adopted a more integrated approach of objectively assessing the potential hydraulic and geomorphologic impacts at the outset, and most have been aimed at the restoration of single species.

An understanding of how deflectors typically function to provide habitat may aid in the selection of building material and design. Whilst deflectors by design, create and maintain pool-riffle sequences, they also provide zones of higher velocities. These areas are critical to some species of fish and macro invertebrates. Swiftly moving water transports food and oxygen into a river reach. To exploit these resources fish must either swim against the current at a rather high cost of energy to maintain their position, or they must find sheltered areas close enough to the fast water to derive the benefits of higher dissolved oxygen and food availability. Although many organisms typical of high velocity reaches are physically adapted to maintain position or spatial orientation, most species require ambush locations out of the direct flow of water. In unaltered streams, organisms use velocity shelters provided by undercut banks, boulders or large woody debris, but if these natural habitats are absent in degraded reaches, current deflectors may provide them. Studies in large rivers and small streams have shown that stone deflectors (groins, spur dikes) used for erosion control provide aquatic habitat superior to stone blanket revetment, which is not as effective in creating the juxtaposition of high and low velocity zones (Shields et al., 1995)

Fig. 10.48 Spur dikes on the Lijiang River in south China used to promote the formation of low velocity habitats

Weirs—Weirs also increase habitat diversity through creation of pool-riffle characteristics. Weirs constructed of locally derived material are relatively low cost, and can be built from a variety of materials, including logs, boulders, stones, and gabions. Wesche (1985) covers various designs in detail. Weirs can be placed to break up the flow of the river and increase turbulence downstream perhaps scouring a pool, whist impounding water upstream.

Figure 10.49 illustrates a weir placed on the Juma River in the suburbs of Beijing for creation and maintenance of a habitat with stable low current and high depth of water. In dry seasons the weir maintains a depth of water for fish and invertebrates to survive. Downstream from weirs sediment may be eroded to form a scour hole and the sediment may be transported for a distance and deposit to form a riffle-like feature. Weirs have been also used to impound flow to allow fish passage, to trap for gravel spawning moving along high gradient streams, to trap finer sediments, to aerate the water, and to slow

Fig. 10.49 A weir placed on the Juma River in the suburbs of Beijing for creation and maintenance of a habitat with stable low current and high depth of water. In dry seasons the weir maintains a depth of water for fish and invertebrates to survive

the flow, enabling organic debris to fall out and enhance invertebrate production (Wesche, 1985). Such structures extend across the entire width of the channel, although some incorporate a notch to locally concentrate flow. This type of structure is perhaps most effective for producing a pool-riffle pattern in low energy streams.

Habitat provided by weirs can be particularly valuable in channelized streams experiencing relatively high levels of erosion and deposition. Cooper and Knight (1987) compared fish catches from pools below weirs used as grade control structures and natural scour pools in unstable, channelized streams in Mississippi. U.S. Grade control pools produced greater catches by weight, more fish of harvestable size, and more stable length frequency distributions than natural scour holes. Cooper and Knight (1987) speculated that habitat created by grade control structures was more stable than natural scour holes, which undergo frequent cycles of filling and scouring. This stability resulted in more consistent successful spawning and recruitment and ultimately higher yields.

Weirs have been used successfully in many countries to increase fish population within relatively short periods of time (Gard, 1961; McCall and Knox, 1978; Carling and Kloslewski, 1981; Shields et al., 1995). Artificial pools created by weirs in New Mexico, U.S. were up to 70% greater by volume than natural pools and held 50% more trout with twice the biomass.

There are also many examples of failures (Wesche, 1985). The structure may fail in high-energy rivers, particularly at high flow and they tend to be unsuccessful in enhancing habitat where there is an excessively high sediment load (Keown, 1981). Structure failure may not necessarily equate to failed habitat improvement. For example, rock scattered from a failed deflector may provide substrate for invertebrates, resting areas, or ambush sites for stream fish. Other reasons for failure to enhance biological populations include the blockage of fish passage (Johnson, 1971) and the lack of an adequate food supply (Rockett, 1979).

Modification of substrate—Boulders have been placed in channels to provide cover for fish, to improve the pool-riffle characteristics, to provide additional habitat for rearing fish or to protect banks from erosion. Randomly placed boulders can enhance fish habitat substantially (Knox, 1982; Lere, 1982). Diamond-shaped clusters of four boulders are often used. A field experiment was conducted by replacing the substrate with gravel, stones, sand and silt. Figure 10.50 shows the experiment in the Juma River in the suburbs of Beijing. The highest species richness was obtained with gravel substrate, proving that replacing substrate with gravel may effectively improve the aquatic ecology.

In lowland streams where no endemic rock exists, large logs or wooden pilings may have ecological advantages over boulders. Woody debris is a key component of aquatic habitats in sand-bed rivers (Shields and Smith, 1992). Although woody structures do not last as long as rock, they provide a carbon source and may be more acceptable to organisms that have evolved to live on submerged woody debris. Wooden substrate may also be cheaper and more readily available.

From an ecological point of view the placement of more natural bed sediments may speed recovery (Gore, 1985). Placement of artificial materials such as crushed limestone and quarry rejects may also improve the habitat for fish and for macro-invertebrates (Stuart, 1960). For example, on the Afon Gwyfai in Wales decolonization of invertebrates on a reinstated gravel bed was a gradual process, taking about a year (Brookes, 1988). The stability of reinstated gravel is a key issue. If the gravel is unstable, then the diversity and abundance of species will be less than for a stable bed. In a high-energy environment it may be necessary to install structures to retain gravels in situ (Claire, 1980). Also, where sediment loads are too high due to upstream channel modification or land use change then spawning gravels may become smothered. This is a particular problem in low-energy lowland streams.

Devices Providing Cover—Under natural circumstances undercut banks and overhanging vegetation are important habitat features referred to as "cover". Fish utilize cover for shade and shelter. Figure 10.51

shows riparian trees and wood logs in the water that provide shade and shelter for aquatic wildlife in the Jiuzhaigou Creek in the upper Jialing River basin, which attract many fish in the river. Artificial devices may be fixed to the bed or banks to provide additional cover. They include log overhangs, overhanging platforms, felled trees, which have been anchored in place, and riprap (Claire, 1980). These have been demonstrated to be particularly effective at increasing the number of trout in a reach (White, 1975).

Fig. 10.50   Experiment of replacing substrate with gravel, stones, sand, and silt in the Juma River near Beijing

Fig. 10.51   Riparian trees and wood logs in the water provide shade and shelter for aquatic wildlife and attract many fish in the Jiuzhaigou Creek in upper Jialing River basin (See color figure at the end of this book)

Artificial "fish attractors" (a cover device made of brush, bundles of old tires) have been used and extensively tested in North American reservoirs, but less attention has been paid to rivers and streams. Wilbur (1978) found that materials used to construct the attractor determined which species exploited the created habitat. Brush and attractors made from the branches of trees were reported to be somewhat more successful in attracting fish than attractors constructed of other materials. Anecdotal evidence indicates that the spacing and configuration of branches may play an important role in attracting fish, so some consideration of plant species is needed when brush piles or tree reefs are used as cover in streams.

Engineered Log Jams—Woody debris within a stream can often influence the instream channel structure by increasing the occurrence of pools and riffles. As a result, streams with woody debris typically have less erosion, slower routing of organic detritus (the main food source for aquatic invertebrates), and greater habitat diversity than straight, even-gradient streams with no debris. Woody debris also provides habitat cover for aquatic species and characteristics ideally suited for fish spawning.

Reintroduction of woody debris, or log-jams, has been extensive, but limited understanding of woody debris stability has hampered many of these efforts. Engineered log jams can restore riverine habitat and in some situations can provide effective bank protection. Even in large alluvial channels that migrate at rates of 10 m/yr, jams can persist for centuries, creating a mosaic of stable sites that in turn host the large trees necessary to initiate stable jams (Abbe et al., 1997). Engineered log jams are designed to emulate natural jams and can meet management or restoration objectives such as habitat restoration and bank protection.

After learning about the uncertainty and potential risks of creating man-made log jams, landowners near Packwood, Washington, U.S. decided the potential environmental, economic, and aesthetic benefits outweighed the risks. An experimental project consisting of three engineered log jams was implemented to control severe erosion along 420 m of the upper Cowlitz River. Five weeks after constructing the log jams, the project experienced a 20-year return period flood (850 m^3/s). The engineered log jam remained intact and met design objectives by transforming an eroding shoreline into a local depositional environment (accreting shoreline). Approximately 93 tons of woody debris that was in transport during the flood was trapped by the jams, alleviating downstream hazards and enhancing structure stability (Abbe et al., 1997). Landowners have been delighted by the experiment.

10.4.3   stream Restoration

In some cases, it might be desirable to divert a straightened stream into a meandering alignment for restoration purposes. For cases where the designed channel will carry only a small amount of bed material load, bed slope and channel dimensions may be selected to carry the design discharge at a velocity that will be great enough to prevent suspended sediment deposition and small enough to prevent erosion of the bed. Increasing the sinuosity of a stream may create better habitats for faunal communities. Meanders can then be created with length ranges from 4 to 9 times the channel widths. Meanders should not be uniform. For instance, the incised, straightened channel of the River Backwater in the U.K. was restored to a meandering form by excavating a new low-level floodplain about 50 to 65 feet wide containing a sinuous channel about 16 feet wide and 3 feet deep (Hey, 1995). Preliminary calculations indicated that the bed of the channel was only slightly mobile at bank-full discharge, and sediment loads were low.

For small rivers restoration practices also involve change of the channel dimensions, in which the average values for width and depth of the channel were determined in the design. These determinations are based on the imposed water and sediment discharge, bed sediment size, bank vegetation, resistance, and average bed slope. However, both width and depth may be constrained by site factors, which the designer must consider once stability criteria are met. Perhaps the simplest approach to selecting channel width and depth is to use dimensions from stable reaches elsewhere in the watershed or from similar reaches in the region. A reference reach is a reach with a desired biological condition, which will be used as a target to strive for when comparing various restoration options. A reference reach used for stable channel design should be evaluated to make sure that it is stable and has a desirable ecological condition. In addition, it must be similar to the desired project reach in hydrology, sediment load, and bed and bank material. Often a stable reach upstream of or downstream from the reach to be restored is selected as the reference reach.

Stabilization of the bed and banks—Stabilization of the bed and banks is often required for ecosystem restoration. Plants may be established on upper bank and floodplain areas using traditional techniques for seeding or by planting bare-root and container-grown plants. However, these approaches provide little initial resistance to flows, and plantings may be destroyed if subjected to high water before they are fully established. Cuttings, pole plantings, and live stakes taken from species that sprout readily (e.g., willows) are more resistant to erosion and can be used lower on the bank (Fig. 10. 52). In addition, cuttings and pole plantings can provide immediate moderation of flow velocities if planted at high densities. Often, they can be placed deep enough to maintain contact with adequate soil moisture levels, thereby eliminating the need for irrigation. The reliable sprouting properties, rapid growth, and general availability of cuttings of willows and other pioneer species makes them particularly appropriate for use in bank revegetation projects, and they are used in most of the integrated bank protection approaches.
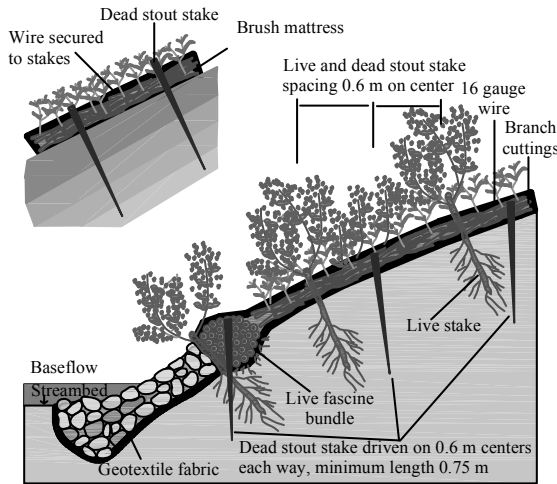
Fig. 10.52 The reliable sprouting properties, rapid growth, and general availability of cuttings of willows and other pioneer species re-vegetate the banks quickly (after FISRWG, 1997)

Geotextile systems—Geotextiles have been used for erosion control on road embankments and other upland settings, or with plants placed through slits in the fabric. In self-sustaining stream bank applications, only natural, biodegradable materials should be used, such as jute or coconut fiber (Johnson, 1994). The typical stream-bank use for these materials is in the construction of vegetated geo-grids, which are similar to brush layers except that the fill soils between the layers of cuttings are encased in fabric, allowing the bank to be constructed of successive "lifts" of soil, alternating with brush layers. This approach allows reconstruction of a bank and provides considerable erosion resistance. Natural fibers are also used in "Fiber-Schines," which are sold specifically for stream-bank applications. These are cylindrical fiber bundles that can be staked to a bank with cuttings or rooted plants inserted through or into the material. Vegetated plastic geo-grids and other non-degradable materials can be used where geo-technical problems require drainage or additional strength.

Tree Revetments—Tree revetments are made from whole tree trunks laid parallel to the bank, and cabled to piles or deadman anchors. Eastern red cedar (Juniperus Virginian) and other coniferous trees are used on small streams, where their springy branches provide interference to flow and trap sediment. The principal objective to these systems is the use of large amounts of cable and the potential for trees to be dislodged and cause downstream damage. Some projects have successfully used large trees in

conjunction with stone to provide bank protection as well as improved aquatic habitat cut into the bank, such that the root wads extend beyond the bank face at the toe (Fig. 10.53). The logs are overlapped and/or braced with stone to ensure stability, and the protruding rootwads effectively reduce flow velocities at the toe and over a range of flow elevations (Fig. 10.54). A major advantage of this approach is that it reestablishes one of the natural functions of large woody debris in streams by creating a dynamic near-bank environment that traps organic material and provides colonization substrates for invertebrates and refuge habitat for fish. The logs eventually rot, resulting in a more natural bank. The revetment stabilizes the bank until woody vegetation has matured, at which time the channel can return to a more natural pattern.
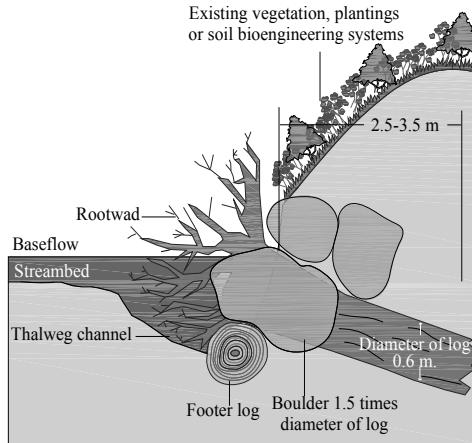
Fig. 10.53   Large trees and stone are used to provide bank protection (after FISRWG, 1997)

Fig. 10.54   The protruding rootwads effectively reduce flow velocities at the toe (after FISRWG, 1997)

10.4.4   Artificial Wetlands

Artificial wetlands have been created for ecological restoration. Wetland-loss has become a problem in many river systems as a result of sediment reduction, railway and highway construction, and drainage system development. The floral communities and faunal communities in the wetlands suffer from development and wetland-loss. To restore the wetland ecology artificial wetlands, for instance green tree

reservoirs, are applied. Greentree reservoirs are shallow, forested flood-plain impoundments usually created by building low levees and installing outlet structures. They are usually flooded in early fall and drained during late March to mid-April. Draining prevents damage to over-story hardwoods (Rudolph and Hunter, 1964). Most existing green tree reservoirs are in the southwestern U.S. The green tree reservoirs provide habitat for many animal species. The flooding of green tree reservoirs differs from the natural flood regime. Green tree reservoirs are typically flooded earlier and at depths greater than would normally occur under natural conditions. Over time, modifications of natural flood conditions can result in vegetation changes, lack of regeneration, decreased mast production, tree mortality, and disease. Proper management of Green tree reservoirs requires knowledge of the local system-especially the natural flood regime and sediment transport and deposition.

Figure 10.55 shows an artificial wetland in the suburbs of Seoul, South Korea. Many birds have colonized the new habitat just a few years after the artificial wetland was created. In the meantime the wetland also attracts tourists.

Fig. 10.55 An artificial wetland in the suburbs of Seoul, South Korea

Is it certain that the species richness, number density, and other biodiversity indices of benthic invertebrates and fish will increase if river-linked riparian lakes or wetlands are created? A comparative study was performed to answer these questions with samples taken from a river-lined lake—Zengjiang Bay, a low flow area of the Zengjiang River channel at Zhengguo, and an isolated riparian lake—Xizhijiang Oxbow Lake in the East River basin (Wang et al., 2008). Figure 10.56 shows the geographical locations of Zengjiang Bay, Zhengguo, and Xizhijiang Oxbow Lake. The Zengjiang River is a tributary of the lower reaches of the East River. Substrate in the main channel of the Zengjiang River consists of sand. No benthic invertebrates were found in the sample from the river at Zhengguo.

Zengjiang Bay is like a riparian lake with a 100 m wide outlet connecting the river. The river carries fine suspended sediment into the bay which is deposited there. A mud layer covers most of the bay, and some hydrophytes have colonized parts of the bay. The flow velocity and water depth in the bay vary in the range of 0–0.5 m/s and 0–3 m, respectively. Zengjiang Bay provides multiple habitats for benthic invertebrates. The species richness of samples taken from the bay is 31, and the abundance of individual invertebrates is 343 ind/m^2. The calculated Shannon-Weaver index and bio-community index are $H = 2.58$ and $B = 15.05$, both the highest value in the East River. There are many fish species in the bay.

Table 10.10 lists the species from the three sites, which shows that the river-lined riparian wetland has much higher species richness than those from the river and isolated riparian lakes.

Table 10.10 Species richness and abundance of macro-invertebrates from river-linked riparian lake Zengjian Bay, the main stem channel of the Zengjiang River at Zhengguo and a separated riparian lake – the Xizhijian Oxbow Lake

Zengjiang Bay	*Corbiculidae C.fluminea (113); Chironomidae (four species 44); Elmidae，Stenelmis (25); Ceratopogonidae Bezzia (25); Corixidae (21); Limnodrilus(23); Semisulcospira (20); Libellulidae (14); Ephemeridae (11); Bellamya B.Purificata (8); Macromiidae (6); Bellamya Sp1 (5); Branchiura (4); Coenagrionidae Pseudagrion (4); Gomphidae, Trigomphus (3); Ampullariidae (2); Psephenidae (2); Hydrophilidae Hydrobius (2); Tabanidae (2); Lepidoptera (1); Acariformes (1); Gomphidae, Sinictinogomphus (1)；Palaemonidae (1); Tricladida (1); Baetidae (1); Heptageniidae (1); Parafossarulus (1); Elmidae, Sp1.(1)*
Zhengguo	*0*
Xizhijiang Oxbow Lake	*Palaemonidae (13); Chironomidae (7); Hydrophilidae, Laccobius (2)*

The Xizhijiang Oxbow Lake was a section of the Xizhijiang River Channel, which flows into the East River at Huizhou, but became an oxbow lake since an artificial cutoff in the 1980s. It is separated from the Xizhijiang River by a highway, as shown in Fig. 10.56(b). Part of the lake has been converted into a fishpond. Because of the separation there is almost no flow velocity in the lake, while the separation also cut off the fine sediment supply to the lake. The substrate consists mainly of sand, which has remained unchanged for 20 years since the cut off. There is no mud layer in the lake. Analysis of samples from the lake indicates that the species richness is only 3 and the number density is 22 ind/m^2. The Shannon-Weaver index and biocommunity index are $H=0.89$ and $B=2.76$, which are much lower than those for Zengjiang Bay. To develop the oxbow lake into a good habitat for benthic invertebrates and fish, the lake should again be connected with the river, allowing fine sediment to be carried into the lake and a mud layer to form. The connection will also increase the flow velocity and exchange of lake water with river water.
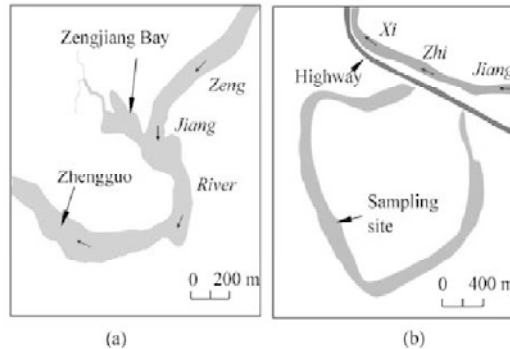
Fig. 10.56 Location and shape of (a) Zengjiang Bay and (b) Xizhijiang Oxbow Lake

In the lower East River if riparian waters are created similar to Zengjiang Bay the ecology in the river may be greatly improved. One example is to reconnect the Xizhijiang Oxbow Lake with the river. The lake water may exchange with the river water and fish and invertebrates may spend a part of their life cycle in the lake and other parts of their life cycle in the river.

10.4.5 Riparian Vegetation Restoration and Food Patches

Vegetation is a fundamental controlling factor for river eco-functions. Habitat, conduit, filter/barrier, and

source/sink functions are all critically tied to the vegetative biomass amount, quality, and condition. Restoration designs should protect existing native vegetation and restore vegetative structure to result in a contiguous and connected stream corridor. Numerous shrubs and trees have been evaluated as restoration candidates, including willows (Svejcar et al., 1992; Anderson et al., 1978); alder, serviceberry, oceanspray, and vine maple (Flessner et al., 1992); Sitka and thin leaf alder (Java and Everett, 1992); paloverde and honey mesquite (Anderson et al., 1978); and many others. Selection of vegetative species may be based on the desire to provide habitat for a particular species of interest. The current trend in restoration, however, is to apply a multi-species or ecosystem approach.

The large-scale restoration of forest in the U.S. was undertaken by the Tennessee Valley Authority in conjunction with reservoir construction projects in the southern U.S. during the 1940s. Roads and railways were relocated outside the influence of the maximum pool elevation, but they were placed on embankments. The Tennessee Valley Authority was concerned that the roads and railways would be subject to wave erosion during periods of extreme high water. To reduce that possibility, agricultural fields between the reservoir and the embankments were planted with trees. At Kentucky Reservoir, approximately 4 km^2 of trees were planted, mostly on hydric soils adjacent to tributaries of the Tennessee River. Because the purpose of the planting was erosion control, little thought was given to recreating natural patterns of plant community composition and structure. Trees were evenly spaced in rows, and planted species were apparently chosen for maximum flood tolerance. As a result, the studied stands had an initial composition dominated by bald cypress, green ash, red maple, and water tolerant species, but they did not originally contain many of the other common bottomland forest species, such as oaks.

In the middle reaches of the Yellow River to the north part of the Loess Plateau in China, a desert named the Maousu Desert extends over thousands of square kilometers. Very high rates of erosion occurred in the area, which impaired the terrestrial vegetation and caused detriment to the river ecology. Great efforts have been made for erosion control in this area. Figure 10.57 shows the reforestation of the desert land. As a result of reforestation the sediment yield has greatly reduced, a plant community has developed, and some animals find their habitats in the area. Finally, the river ecology has improved.

Plant community restoration—Non-native vegetation can prevent establishment of desirable native species or become an unwanted permanent component of vegetation. For example, kudzu can kill forest species planted on out pasture grasses and weeds. Restoration work should restore natural patterns of plant community distribution by comparing with a reference plant community (Brinson et al., 1981; Wharton et al., 1982).

Fig. 10.57   Reforestation of the desert in the middle reaches of the Yellow River

Large-scale restoration work sometimes includes panting of understory species, particularly if they are required to meet specific objectives such as providing essential components of endangered species habitat. However, it is often difficult to establish understory species, which typically are not tolerant to full sun, if the restoration area is open. Where understory species are unlikely to establish themselves for many years, they can be introduced in adjacent forested sites, or planted after the initial tree growth to create appropriate understory conditions. Understory species seeds are commonly broadcast by hydroseeding, requiring a special tank truck with a pump and nozzle for spraying the mixture of seeds, fertilizer, binder, and water (Fig. 10.58). A wider range of seed species can be planted more effectively with a seed drill towed behind a tractor (Haferkamp et al., 1985). Where access is limited, hand planting or aerial spreading of seeds might be feasible.

Fig. 10.58 Hydroseeding of a streambank for restoration of understory riparian vegetation. Special tank trucks carrying seed, water, and fertilizer are used in the revegetation efforts (after FISRWG, 1997)

In the past, stream corridor planting programs often included nonnative species selected for their rapid growth rates, soil binding characteristics, ability to produce abundant fruits for wildlife, or other perceived advantages over native species. These actions sometimes have unintended consequences and often prove to be extremely detrimental (Olson and Knopf, 1986). As a result, many local agencies discourage or prohibit planting of nonnative species within wetlands or prohibit planting streamside buffers. It may be feasible in some cases to focus restoration actions on encouraging the success of local seed-fall to ensure that locally adapted populations of vegetation are maintained on the site (Friedman et al., 1995).

Nest structures—Loss of riparian or terrestrial habitat in stream corridors has resulted in the decline of many species of birds and mammals that use associated trees and tree cavities for nesting or roosting. The most important limiting factor for cavity-nesting birds is usually the availability of nesting substrate (von Haartman, 1957), generally in the form of snags or dead limbs in live trees (Sedgwick and Knopf, 1986). Snags for nest structures can be created using explosives, girdling, or topping of trees. Artificial nest structures can compensate for a lack of natural sites in otherwise suitable habitat since many species of birds will readily use nest boxes or other artificial structures. For example, along the Mississippi River in Illinois and Wisconsin, U.S., where nest trees have become scarce, artificial nest structures have been erected and constructed for double-crested cormorants using utility poles (Yoakum et al., 1980). In many cases, increases in breeding bird density have resulted from providing such structures (Strange et al., 1971; Brush, 1983). Artificial nest structures can also improve nestling survival (Cowan, 1959).

Nest structures must be properly designed and placed, meeting the biological needs of the target species (FISRWG, 1997). They should also be durable, predator-proof, and economical to build. Design specifications for nest boxes include hole diameter and shape, internal box volume, distance from the

floor of the box to the opening, type of material used, whether an internal "ladder" is necessary, height of placement, and habitat type in which to place the box. Other types of nest structures include nest platforms for waterfowl and raptors; and tire nests for squirrels. Specifications for nest structures for riparian and wetland nesting species (including numerous Picids, passerines, waterfowl, and raptors) can be found in many sources including Yoakum et al. (1980), Kalmbach et al. (1969), and various state wildlife agency and conservation publications.

Food patches—Food patch planting is often expensive and not always predictable, but it can be carried out in wetlands or riparian systems mostly for the benefit of waterfowl. Environmental requirements of the food plants native to the area, proper time of year for introduction, management of water levels, and soil types must all be taken into consideration. Some of the more important food plants in wetlands include pondweed (*Potamogeton spp.*), smartweed (*Polyhonum spp.*), duckweeds (*Lemna spp.*), coontail, alkali bulrush (*Scirpus paludosus*), and various grasses. Two commonly planted native species include wild rice (*Zizania*) and wild millet. Details on these species can be found in Yoakum et al. (1980).

10.4.6 Restoration of Impounded and Channelized Streams

Damming of rivers may greatly change the hydrology, morphology and ecological conditions. Reservoir operation alters the flow of water, sediment, organic matter, and nutrients, resulting in both direct physical and indirect biological effects in tailwaters and downstream riparian and floodplain areas. Stream corridors below dams can be partially restored by modifying operation and management approaches. The modification of operation approaches, where possible, in combination with the application of properly designed and applied best management practices, can reduce the impacts caused by dams on downstream riparian and floodplain habitats. Partial restoration of stream corridors below dams can be achieved by designing operation procedures that mimic the natural hydrograph. Modifications include scheduling releases, and making seasonal adjustments in pool levels and in the timing and variation of the rates of drawdowns (USEPA, 1993).

Adequate fish passage around dams, diversions, and other obstructions may be a critically important component of restoring healthy fish populations to previously degraded rivers and streams. However, designing installing, and operating a fish passage facility and the flows necessary for operation are generally site specific. Figure 10.59 shows the fish ladder on the Bonneville Dam on the Columbia River, U.S. More than 1 million salmon swim through the fish ladder to pass the dam to upstream spawning grounds every year.

Fig. 10.59 Fish ladder on the Bonneville Dam on the Columbia River. More than 1 million salmon swim through the fish ladder to pass the dam to upstream spawning grounds every year.

Channelization and diversions represent forms of hydrologic modification commonly associated with most principal land uses, and their effects should be considered in all restoration efforts. In some cases, redesign of channel modifications to restore preexisting ecological characteristics is needed. All of the urban channels in Beijing have been channelized with concrete bed and banks. Riparian plant community and benthic invertebrates have lost their habitat and the water quality has become worse. It is planned to replace the concrete bed and banks with soil and stones, providing habitat for invertebrates. It is estimated that a high water quality may be maintained with only half of the water consumption.

Modifications of existing projects, including operation and maintenance or management, can improve some negative effects without changing the existing benefits or creating additional problems. Levees may be set back from the stream channel to better define the stream corridor and reestablish some or all of the natural floodplain functions. Setback levees can be constructed to allow for overbank flooding, which provides surface water contact with streamside areas such as floodplains and wetlands.

Instream modifications such as uniform cross sections or armoring associated with channelization or flow diversions may be removed, and design and placement of meanders can be used to reestablish more natural channel characteristics. In many cases, however, existing land uses might limit or prevent the removal of existing channel or floodplain modifications.

10.4.7   Restoration of Ecosystems Disturbed by Other Stresses

Exotic species—Restoration of ecosystems disturbed by exotic species is difficult. Some land uses have actually introduced exotics that have become uncontrolled, while others have merely created an opportunity for such exotics to spread. Again, control of exotic species has some common aspects across land uses, but design approaches are different for each land use. Control of exotics in some situations can be extremely difficult and may be impractical if large areas or well-established populations are involved. Use of herbicides may be tightly regulated or precluded in many wetland and streamside environments, and for some exotic species there are no effective control measures that can be easily implemented over large areas (Rieger and Kreager, 1990). Where aggressive exotics are present one should avoid unnecessary soil disturbance or disruption of intact native vegetation, and newly established populations of exotics should be eradicated.

Controlling exotics can be important because of potential competition with established native vegetation, colonized vegetation, and artificially planted vegetation, in restoration work. Exotics compete for moisture, sunlight, and space and can adversely influence establishment rates of new plantings. To improve the effectiveness of revegetation work, exotic vegetation should be cleared prior to planting; nonnative growth must also be controlled after planting. One must also understand the physical characteristics of the native vegetation for successful establishment. For example, native vegetation in the midwestern U.S. has learned to grow under conditions of low nutrient supply, and, thus, use of fertilizers often just promotes weed growth (Neal O'Reilly, Hey and Associates, personal commun). General techniques for control of exotics and weeds are mechanical (e.g., scalping or tilling), chemical (herbicides), and fire.

Agriculture—In agricultural areas when terraces and a waterway are installed in the nearby cropland, the scene depicts an ecologically deprived landscape. Nutrient and water flow, sediment trapping during floods, water storage, movement of flora and fauna, species diversity, interior habitat conditions, and provision of organic materials to aquatic communities are just a few of the functional conditions affected by these structural attributes.

Restoration design should establish functional connections within and external to stream corridors, landscape elements such as remnant patches of riparian vegetation, prairie, or forest exhibiting diverse or unique vegetative communities; productive land that can support ecological functions; reserve or abandoned land; associated wetlands or meadows; systems; ecologically innovative residential areas;

neighboring springs and stream systems; ecologically innovative residential areas; and fauna (field borders, windbreaks, waterways, grassed terraces, etc.) offer opportunities to establish these connections. An edge (transition zone) that gradually changes from one land use into another will soften environmental gradients and minimize disturbance.

Urbanization often is the strongest disturbance to river ecosystems. The development of residence areas may severely impair the riparian vegetation and aquatic biocommunities. Seven restoration tools can be applied to help restore urban streams (FISRWG, 1997; Schueler, 1987). The best results are usually obtained when the following tools are applied together.

Tool 1: Partially restore the predevelopment hydrological regime. The primary objective is to reduce the frequency of bankfull flows by constructing upstream stormwater detention ponds that capture and detain increased storm water runoff for up to 24 hours before release (i.e., extended detention).

Tool 2: Reduce urban pollutant pulses. A second need in urban stream restoration is to reduce concentrations of nutrients, bacteria, and toxics in the stream, as well as trapping excess sediment loads. Generally, three tools can be applied to reduce pollutant inputs to an urban stream: storm water retrofit ponds or wetlands, watershed pollution prevention programs, and the elimination of illicit or illegal sanitary connections to the storm sewer network.

Tool 3: Stabilize channel morphology. Over time, urban stream channels enlarge resulting in severe bank and bed erosion. Therefore, it is important to stabilize the channel, and if possible, restore equilibrium channel geometry. In addition, it is also useful to provide undercuts or overhead cover to improve fish habitat. Depending on the stream order, watershed impervious cover, and the height and angle of eroded banks, a series of different tools can be applied to stabilize the channel, and prevent further erosion. Bank stabilization measures include imbricated riprap, brush bundles, and soil bioengineering methods, such as willow stakes and bio-logs and rootwads.

Tool 4: Restore instream habitat structure. Most urban streams have poor instream habitat structure, often typified by indistinct and shallow low flow channels within a much larger and unstable storm channel. The goal is to restore instream habitat structure that has been blown out by erosive floods. Key restoration elements include the creation of pools and riffles, deepening of the low flow channels, and the provision of greater structural complexity across the streambed. Typical tools include the installation of log check-dams, stone wing deflectors and boulder clusters along the stream channel.

Tool 5: Reestablish vegetative banks and riparian cover. Vegetative banks and riparian cover are essential components of the urban stream ecosystem. They stabilize banks, provide woody debris and detritus, and shade the stream. Therefore, the fifth tool involves reestablishing the vegetative banks and riparian cover plant community along the stream network. Figure 10.60 shows an urban stream in Beijing where a layer of soil is placed on the hardened channel bed and banks, thus a vegetation bank and aquatic high plants have developed.

Tool 6: Protect critical stream substrates. A stable, well sorted streambed is often a critical requirement for fish spawning and secondary production by aquatic insects. The bed of urban streams, however, is often highly unstable and clogged by fine sediment deposits. It is often necessary to apply tools to restore the quality of stream substrates at points along the stream channel. Often, the energy of urban storm water can be used to create cleaner substrates—through the use of tools such as double wing deflectors and flow concentrators. If thick deposits of sediment have accumulated on the bed, mechanical sediment removal may be needed.

Tool 7: Allow for recolonization of the stream community. It may be difficult to reestablish the fish community in an urban stream if downstream fish barriers prevent natural recolonization. Thus, the last urban stream restoration tool involves the judgment of a fishery biologist to determine if downstream

fish barriers exist, whether they can be removed, or whether selective stocking of native fish is needed to recolonize the stream reach.

Fig. 10.60   A layer of soil is placed on the hardened channel bed and banks on an urban stream in Beijing, and a vegetation bank and aquatic high plants have developed

Review Questions

1. What are the main elements of ecosystems at various scales? Please explain with examples.
2. What is habitat? What is an aquatic habitat?
3. What is the relation between the animal communities and the plant communities?
4. What are the major ecological functions of rivers?
5. Explain the relation between the aquatic habitat and the physical attributes of rivers.
6. How are the stream biota classified?
7. What are the main factors characterizing the ecological conditions of a stream corridor?
8. What is substrate? What are good or bad substrates? Why?
9. What are the natural stresses on river ecology and how do they affect ecology?
10. Give some examples of human-induced stresses at several landscape scales.
11. What are biological indicator species and how should biological indicator species be selected?
12. What are the measures of biological diversity of a river ecological system?
13. How do you conduct a rapid bioassessment?
14. What is the Habitat Evaluation Procedure?
15. What is the vegetation-hydroperiod model? What can you do with the model?
16. What are the main strategies for the instream habitat restoration? Please explain the mechanisms.
17. How can you design instream habitat restoration?
18. What are the main strategies for restoration of river ecosystems?
19. What are the key tools for urban stream restoration design?
20. What are the restoration measures and their potential effects for the ecosystems disturbed by exotics?

References

Abbe T.B., and Montgomery D.R., 1996. Large woody debris jams, channel hydraulics and habitat formation in large rivers. Regulated Rivers. Research and Management, 12, 201–221

Abbe T.B., Montgomery D.R. and Petroff C., 1997. Design of stable in-channel wood debris structures for bank protection and habitat restoration: An example from the Cowlitz River, WA. In: Proceedings of the Conference on Management of Landscape Disturbed by Channel Incision, May 19–23

Abt S.R., 1995. Settlement and submergence adjustments for Parshall flume. Journal of Irrigation Drainage Engineering

Anderson B.W., Ohmart R.D. and Disano J., 1978. Revegetating the riparian floodplain for wildlife. In: Symposium on strategies for protection and management of floodplain wetlands and other riparian ecosystems, USDA Forest Service General Technical Report, WO-12, 318–331

Aronson J.G. and Ellis S.L., 1979. Monitoring, maintenance, rehabilitation and enhancement of critical Whooping Crane habitat, Platte River, Nebraska. In: The mitigation symposium: A national workshop on mitigating losses of Fish and wildlife habitats, tech. coord. Swanson G.A., 168–180. USDA Forest Service General Technical Report. RM-65. Rocky Mountain Forest and Range Experiment Station, Fort Collins, CO

Barbour M.T., Gerritsen B.D., Snyder B.D. and Stribling J.B., 1999. Benthic macroinvertebrate protocols. In Barbour M.T. Gerritsen B.D., Snyder B.D. and Stribling J.B. (eds.), Rapid Bioassessment Protocols for Use in Streams and Wadeable Rivers: Periphyton, benthic macroinvertebrates and Fish. EPA 841-B-99-002. U.S. Environmental Protection Agency; Office of Water, Washington, DC., 7.1–7.20

Bartholow J.M., Laake J.L. Stalnaker C.B., and Williamson S.C., 1993. A salmonid population model with emphasis on habitat limitations. Rivers, 4, 265–279

Bayley P.B. and Li H.W., 1992. Riverine fish. In: The Rivers Handbook, Calow P. and Petts G.E. (eds.), Blackwell Scientific Publications, Oxford, U.K. 1, 251–281

Beauger A., Lair N., Reyes-Marchant P. and Peiry J.L., 2006. The distribution of macro-invertebrate assemblages in a reach of the River Allier (France), in relation to riverbed characteristics. Hydrobiologia, 571, 63–76

Bedoya D., Novotny V. and Manolakos E., 2009. Instream and offstream environmental conditions and stream biotic integrity. Importance of scale and site similarities for learning and prediction purposes. Ecological Modeling, 220(19), 2393–2406

Benke A.C., Van Arsdall Jr., Gillespie D.M. and Parrish F.K., 1984. Invertebrate productivity in a subtropical blackwater river: The importance of habitat and life history. Ecological Monographs, 54, 25–63

Bio West, 1995. Stream Habitat Improvement Evaluation Project. Bio West, Logan,VT

Bisson R.A., Bilby R.E., Bryant M.D., Dolloff C.A., Grette G.B., House R.A., Murphy M.J., Koski K.V. and Sedell J.R., 1987. Large woody debris in forested streams in the Pacific Northwest: past, present, and future. In: Streamside Management: Forestry and Fishery Interactions, Salo E.O. and Cundy T.W., Institute of Forest Resources, University of Washington, Seattle, Washington, 143–190

Bovee K.D. and Milhous R.T., 1978. Hydraulic simulation in instream flow studies-theory and technique, Paper No.5, USFWS, OBS 78/33USGP Office, Washington DC, USA

Bovee K.D., 1982. A guide to stream habitat analysis using the instream flow incremental methodology. Instream Flow Information Paper No. 12, FWS/OBS-82-26. U.S. Fish and Wildlife Service, Biological Services Program, Fort Collins, Colorado

Brady W., Patton D.R. and Paxson J., 1985. The development of southwestern riparian gallery forests. In: Riparian Ecosystems and Their Management: Reconciling Conflicting Uses, R.R. Johnson et al., tech. coords. USDA Forest. Service General Technical Report RM-120, Rocky Mountain Forest and Range Experiment Station, Fort Collins, Colorado, 39–43

Brinson M.M., Swift B.L., Plantico R.C. and Barclay J.S., 1981. Riparian Ecosystems: Their Ecology and Status. FWS/OBS-81/17. U.S. Fish and Wildlife Service, Office of Biological Services, Washington

Brookes A., and Shields F.D. 1996. River Channel Restoration, John Willey & Sons

Brookes A., 1988. Channelized Rivers: Perspectives for environmental management. John Wiley and Sons, Ltd., Chichester, U.K

Brookes A., 1995. The importance of high flows for riverine environments. In: Harper D.M. and Ferguson A.J.D. (eds.), The Ecological Basis for River Management, John Wiley and Sons, Ltd., Chichester, U.K

Brouha P., 1997. Good news for U.S. fisheries. Fisheries 22, 4

Brush T., 1983. Cavity use by secondary cavity-nesting birds and response to manipulations. Condor, 85, 461–466

Carling R.F., and Kloslewski S.P., 1981. Responses of macroinvertebrate and fish populations to channelisation and

mitigation structures in chippewa creek and river styx, Ohio, Final Report on Project 761091/711102, The Ohio State University Research Foundation, Columbus,OH

Carothers S.W., 1979. Distribution and abundance of nongame birds in riparian vegetation in Arizona. Final report to USDA Forest Service, Rocky Mountain Forest and Range Experimental Station, Tempe, Arizona

Carothers S.W., Johnson R.R. and Aitchison S.W., 1974. Population structure and social organization of southwestern riparian birds. American Zoology, 14, 97–108

Chang J.B., 1999. Change trend of composition characteristic and number of Chinese sturgeon propagation colony. Ph.D. dissertation, Institute of Hydrobiology, Chinese Academy of Sciences, Wuhan (in Chinese)

Chapman R.J., Hinckley T.M., Lee L.C., and Teskey R.O., 1982. Impact of Water Level Changes on Woody Riparian and Wetland Communities, Vol. X. FWS/OBS-82/23. V.S. Department of Agriculture, Fish and Wildlife Service

Claire E.W., 1980. Stream habitat and riparian restoration techniques: Guidelines to consider in their use. In: Proceedings of Workshop for Design of Fish Habitat and Watershed Restoration Project, 761091/711102, The Ohio State University Research Foundation, Columbus, OH

Cole D.N., and Marion J.L., 1988. Recreation impacts in some riparian forests of the eastern United States. Environmental Management, 12, 99–107

Cole G.A., 1994. Textbook of limnology, 4th (ed.), Waveland Press, Prospect Heights, Illinois

Cooper C.M., and Knight S.S., 1987. Fisheries in man-made poolsbelow grade control structures and in naturally occurring scour holes of unstable streams. Journal of soil and water conservation, 42, 370–373

Cooper C.M. and Welsch T.A., 1976. Stream channel modification to enhance trout habitat under low flow conditions, Water Resources Series, No. 58, University of Wyoming, Laramie, WY

Cowan J., 1959. Pre-fab wire mesh cone gives doves better nest than they can build themselves. Outdoor California, 20, 10–11

Croonquist M.J., Brooks R.P., Bellis E.D., Keener C.S., Croonquist M.J. and Arnold D.E., 1991. A methodology for biological monitoring of cumulative impacts on wetland, stream, and riparian components of watershed. In: Proceedings of an International Symposium: Wetlands and River Corridor Management, July 5–9, 1989, Charleston, South Carolina, Kusler, J.A., and Daly, S. (eds.), 387–398

Darrigran G. and Damborenea C., 2006. Bio-invasión del mejillón dorado en el continente americano. Argentina (in Spanish)

Darrigran G. and Damborenea C., 2006. Bio-invasión del mejillón dorado en el continente americano. 156–160, Argentina

Darrigran G., 2002. Potential impact of filter-feeding invaders on temperate inland freshwater environments. Biological Invasions, 4, 145–156

Darrigran G., 2002. Potential impact of filter-feeding invaders on temperate inland freshwater environments. Biological Invasions, 4, 145–156

Darrigran G., 2004. Air exposure as a control mechanism for the golden mussel, Limnoperna fortunei, Bivalvia: Mytili- dae. Journal of Freshwater Ecology, 1–9

Darrigran G., Damborenea C., Penchaszadeh P., 2003. Reproductive stabilization limnoperna fortunei (Bivalvia Mytilidae) after ten years of invasion in the Americas. Journal of Shellfish Research, 22(1)1–6

Darrigran G., et al. 2004. Air exposure as a control mechanism for the golden mussel, Limnoperna fortunei, (Bivalvia: Mytilidae). Journal of Freshwater Ecology, 9

Deng Z.L., Xu Y.G. and ZhaoY., 1991. Analysis on Acipenser sinensis spawning ground and spawning scales below the Gezhouba Dam by means of examining the digestive contents of benthic fish. Bordeaux: CEMAGREF Pub, 243 (in Chinese)

Dolloff C.A., Flebbe P.A. and Owen M.D., 1994. Fish habitat and fish populations in a southern Appalachian watershed before and after Hurricane Hugo. Transactions of the American Fisheries Society, 123(4), 668–678

Dramstad W.E., Olson J.D. and Gorman R.T., 1996. Landscape ecology principles in landscape architecture and land-use planning. Island Press, Washington, DC

Duan X.H. and Wang Z.Y., 2008. Experimental study on effect of habitat isolation on river ecology, Accepted by Advances in Water Science (in Chinese)

Duan X.H., Wang Z.Y. and Cheng D.S., 2007. Benthic macroinvertebrates communities and biodiversity in various stream substrata, Acta Ecologica Sinica, 27 (4), 1664–1672 (in Chinese)

Duan X.H.,Wang Z.Y.and Xu M.Z., 2010，Benthic macroinvertebrate and application in the assessment of stream ecology,Tsinghua Press,Beijing, 1–180

Dugeon D. and Corlett R., 2004. The ecology and biodiversity in Hong Kong. Friends of the Country Park & Joint Publishing (HK) Company Ltd. Hong Kong

Dunne T. and Leopold L.B., 1978. Water in environmental planning. Freeman W.H., San Francisco Co

Erman N.A., 1991. Aquatic invertebrates as indicators of biodiversity. In: Proceedings of a Symposium on Biodiversity of Northwestern California, Santa Rosa,California. University of California, Berkeley

Everhart W.H., Eipper A.W. and Young W.D., 1975. Principles of fishery science, Cornell University Press, Ithaca, New York, USA

FISRWG (the Federal Interagency Stream Restoration Working Group), 1997. Stream Corridor Restoration. The National Technical Information Service, USA

Flessner T.R., Darris D.C. and Lambert S.M., 1992. Seed source evaluation of four native riparian shrubs for streambank rehabilitation in the Pacific Northwest. In: Symposium on Ecology and Management of Riparian Shrub Communities, USDA Forest Service General Technical Report INT-289. U.S. Department of Agriculture, Forest Service, 155–162

Flosi G. and Reynolds F.L., 1994. California Salmonid Stream Habitat Restoration Manual. 2nd ed., California Department of Fish and Game, Sacramento,CA

Forman R.T.T. and Godron M., 1986. Landscape ecology. John Wiley and Sons, New York

Forman R.T.T., 1995. Land Mosaics: The ecology of landscapes and regions. Cambridge University Press, U.K.

Fretwell S.D. and Lucas H.L., 1970. On territorial behavior and other factors influencing habitat distribution in birds. I. Theoretical development. Acta Biotheoretica, 19, 16–36

Friedman J.M., Scott M.L. and Lewis W.M., 1995. Restoration of riparian forests using irrigation, disturbance, and natural seedfall. Environmental Management 19, 547–557

Garcia D., Jalon D., 1995. Management of physical habitat for fish stocks. In: The Ecological Basis for River Management, Harper D.M. and Ferguson J.D. (eds.), John Wiley & Sons, Chichester,U.K. 363–374

Gard R., 1961. Creation of trout habitat by constructing dams, Journal of Wildlife Management, 25, 384–390

Gippel C.J., 1995. Environmental hydraulics of large woody debris in streams and rivers. Journal of Environmental Engineering, 121, 388–395

Gordon N.D., McMahon T.A. and Finlayson B.L., 1992. Stream Hydrology: An Introduction for Ecologists. John Wiley & Sons, Chichester, U.K.

Gore J.A., 1985. mechanisms of colonization and habitat enhancement for benthic macroinvertebrates in restored river channels, in: Alternatives in Regulated River Management, Gore J.A. and Petts G.E. (eds.), CRC Press, Boca Raton, FL

Gorman O.T. and Karr J.R., 1978. Habitat structure and stream fish communities. Ecology, 59, 507–515

Guan F. and Zhang X.H., 2005. Research on the oxygen consumption and ammonia excretion of invasive mussel Limnoperna fortunei in raw water transport pipeline. Water and wastewater engineering, 31(11), 23–26 (in Chinese)

Guan F., Zhang X.H., 2005. Research on the oxygen consumption and ammonia excretion of invasive mussel Limnoperna fortunei in raw water transport pipeline. Water & Wastewater Engineering, 31(11), 23–26 (in Chinese)

Guo Z.D. and Lian C.P., 2001. Experiment of Chinese sturgeon breed aquatics in small water body. Fishery Science, 20(2), 15–16 (in Chinese)

Haferkamp M.R., Miller R.F. and Sneva F.A., 1985. Seeding rangelands with a land imprinter and rangeland drill in the Palouse Prairie and sagebrushbunchgrass zone. In: Proceedings of Vegetative Rehabilitation and Equipment Workshop, U.S. Forest Service, 39th Annual Report, Salt Lake City, Utah, 19–22

Hey R.D., 1995. River processes and management. In: Environmental Science for Environmental Management. O'Riordan T. (eds.), Longman Group Limited, Essex, U.K. and John Wiley, New York, 131–150

Hilsenhoff W.L., 1982. Using a biotic index to evaluate water quality in streams. Department of Natural Resources, Madison, WI

Hocutt C.H., 1981. Fish as indicators of biological integrity. Fisheries, 6(6), 28–31

Hu D.G., Ke F.E., Zhang G.L. 1992. Investigation of Chinese sturgeon spawning sites in downstream of the Gezhouba Dam. Freshwater Fishery, 5, 6–10 (in Chinese)

Hu T.J., Wang H.W. and Lee H.Y., 2005. Environmental and ecological measures of river cooridor on Nan-Shih Stream in Taiwan, Proceedings (CD-ROM), 31st Congress of the International Association for Hydraulic Engineering and Research, Seoul, Korea, September 11–16, 2005

Hunt W.A., 1988. Management of riprap zones and stream channels to benefit fisheries, In: Integrating Forest Management for Wildlife and Fish, General Technical Report NC-122, USDA, North Central Forest Experiment Station, St. Paul, MN

Huryn A.D. and Wallace J.B., 1987. Local geomorphology as a determinant of macrofaunal production in a mountain stream. Ecology, 68, 1932–1942

Hynes H.B.N., 1970. The ecology of running waters. University of Liverpool Press, Liverpool, England

Iwasaki K., 1977. Behavior and tolerance to aerial exposure of a freshwater mussel, Limnoperna fortuner. Venus, 56,15–25

Java B.J. and Everett R.L., 1992. Rooting hardwood cuttings of Sitka and thinleaf alder, In: Symposium on Ecology and Management of Riparian Shrub Communities. USDA Forest Service General Technical Report INT-289. U.S. Department of Agriculture, Forest Service, 138–141

John W. and Peter P., 2001. Effects of the serotonin receptor ligand methiothepin on reproductive behavior of the freshwater snail biomphalaria glabrata: Reduction of Egg Laying and Induction of Penile Erection. Muscjhoaumrpn anl do fp. Pe.X Fpoenrgimental zoology, 289,202–207

Johnson R.R., 1971. Tree removal along southwestern rivers and effects on associated organisms. Amer. Phil. Soc. Yearbook

Johnson W.C., 1994. Woodland expansion in the Platte River, Nebraska: Patterns and causes. Ecological Monographs, 64, 45–84

Kalmbach E.R., McAtee W.L., Courtsal F.R. and Ivers R.E., 1969. Home for birds. U.S. Department of the Interior, Fish and Wildlife Service, Conservation Bulletin 14

Karr J.R., 1981. Assessment of biotic integrity using fish communities. Fisheries, 6(6), 21–27

Karr J.R., Fausch K.D., Angermeier P.L., Yant P.R. and Schlosser I.J. 1986 Assessing biological integrity in running waters: A method and its rationale. Illinois Natural History Survey Special Publication No. 5, Champaign, IL, 28

Keown M.P., 1981. Field investigation of the Fisher River channel realignment project near Libby, Montana, Inspection Report No. 11, U.S. Army Engineer Waterways Experiment Station, Vicksburg, MS

Knopf F.L., 1986. Changing landscapes and the cosmopolitanism of the eastern Colorado avifauna. Wildlife Society Bulletin, 14, 132–142

Knopf F.L., Johnson R.R., Rich T., Samson F.B. and Szaro R.C., 1988. Conservation of riparian systems in the United States. Wilson Bulletin 100, 272–284

Knox R.E., 1982. Stream habitat improvement in Colorado, In Proceedings of Rocky Mountain Stream Habitat Workshop, Wiley R. ed., Wyoming Game and Fish Department, Laramie,W.Y.

Krebs C.J., 1978. Ecology: The experimental analysis of distribution and abundance, 2d (ed.), Harper and Row, New York

Landres P.B., Verner J. and Thomas J.W., 1988. Ecological uses of vertebrate indicator species: a critique. Conservation Biology, 2, 316–328

Lee L.C. and Hinckley T.M., 1982. Impact of Water Level Changes on Woody Riparian and Wetland Communities, Vol. IX. FWS/OBS-82/22.U.S. Department of Agriculture, Fish and Wildlife Service

Lee L.C., Muir T.A. and Johnson R.R., 1989. Riparian ecosystems as essential habitat for raptors in the American West. In Proceedings of the Western Raptor Management Symposium and Workshop, Pendleton B.G., ed., 15–26. Institute for Wildlife Research, National Wildlife Federation. Sci. and Tech. Ser. No. 12

Lere M.E., 1982. The long term effectiveness of Three Types of Stream Improvement Structures Installed in Montana Streams, Masters Thesis, Montana State University, Bozeman, MT

Li A.P., 1999. Protection of sturgeon in the Yangtze River. Journal of Taiyuan Normal Collage, 4, 46–47 (in Chinese)

Li J.D. and Wang X.H., 2003. Harms caused by the main alien invasive species to China and the prevention and cure measures against them. Journal of Taishan University, 25(3), 82–86 (in Chinese)

Li M.J. and Su X.M., 2007. Reason Analysis and Countermeasure Study of the Seashell Problem in the Long Distance Water Transport Canal. Pearl river, 3, (in Chinese)

Li S.F., 2001. A Study on biodiversity and its conservation of major fish in the Yangtze River. Shanghai Science & Tecnolosy. Publication (in Chinese)

Limnotech, 2009. Review and selection of fish metrics for the Chicago Area Waterway System habitat evaluation and improvement study, Report Prepared for the Metropolitan Water Reclamation District of Greater Chicago, Ann Arbor, MI, 37

Liu L.J., Zhang J.S., Luo F.M., et al., 2006. Study on killing and removing mussels in pipeline by chlorine disinfectants. Water Purification Technology, 25(5), 25–27 (in Chinese)

Liu Y.Y., Zhang W.Z., and Wang X.Y., 1979. Economic fauna of china: Freshwater mollusk. Beijing, Science Press (in Chinese)

Lou K.H., Liu J., 1958. Study on prevention and extermination of mussel growths in pipelines. Oceanologia Et Limnologia Sinica, 1(3), 316–324 (in Chinese)

Luo F.M., 2006. Biology and prevention technology of Limnoperna fortunei in water transfer systems in the division of Shenzhen. Nanchang University, Nanchang, China (in Chinese)

Lynch J.A., Corbett E.S. and Sopper W.E., 1980. Evaluation of management practices on the biological and chemical characteristics of streamflow from forested watersheds. Technical Completion Report A-041-PA. Institute for Research on Land and Water Resources, The Pennsylvania State University, State College

Lyons J., 1992. Using The index of biotic integrity (IBI) to measure environmental quality in warmwater streams of wisconsin. U.S. Department of Agriculture, Forest Service, North Central Forest Experiment Station, General Technical Report NC-149, St. Paul, MN, 48

Lyons J., Piette R.R. and Niermeyer K.W., 2001. Development, validation, and application of a fish-based index of biotic integrity for Wisconsin's large warmwater rivers. Transactions of the American Fisheries Society, 130, 1077–1094

Mackenthun K.M., 1969. The practice of water pollution biology. U.S. Department of the Interior, Federal Water Pollution Control Administration, Division of Technical Support. U.S. Government Printing Office, Washington, DC

Magurran A.E., 1988. Ecological diversity and Its measurement. Princeton University Press, Princeton, New Jersey

Manolakos E., Virani H. and Novotny V., 2007. Extracting knowledge on the links between water body stressors and biotic integrity, Water Research, 41, 4041–4050

Márcia D., 2006. The limnological characteristics of aquatic environments which support the golden mussel (Limnoperna Fortunei, Dunker, 1857) and the potential of the golden mussel to further spread within the Paraguay River Basin, Brazil. 14th International Conference on Aquatic Invasive Species. Florida, 205

Margalef R., 1957. La teoria de la informacion en ecologia. Mem. Real Acad. Cienc. Artes Barcelona, 32, 373–499 transl. by Hall W., Gen. Syst. 3, 36–71

May C., Horner R., Karr J., Mar B. and Welch E., 1997. Effects of urbanization on small streams in the Puget Sound ecoregion. Watershed Protection Technique, 2(4), 483–494

McCall J.D. and Knox R.F., 1978. Riparian habitat in channelisation projects, In: Proceeding of the Symposium on Strategies for Protection and Management of Floodplain Wetlands and Other Riparian Ecosystems, Technical Report No. GTR WO-12, U.S. Department of Agriculture, Forest Seruice, Washington, DC

Mcennulty R., 2001. A review of rapid response options for the control of ABWMAC listed introduced marine pest species and related taxa in Australian waters. Centre for research on introduced marine pests. Technical Report No.23. Csiro Marine Research, Hobart

McKeown B.A., 1984. Fish migration. Timber Press, Beaverton, Oregon. B-18 Stream Corridor McLaughlin Water Engineers, Ltd. 1986. Evaluation of and design recommendations for drop structures in the Denver Metropolitan Area. A report prepared for the Denver Urban Drainage and Flood Control District by McLaughlin Water Engineers, Ltd

Meffe G.K., Carroll C.R. and Contributors. 1994. Principles of conservation biology. Sinauer Associates, Inc., Sunderland, Massachusetts

Miller D.L., Hughes R.M., Karr J.R., Leonard P.M., Moyle P.B., Schrader L.H., Thompson B.A., Daniels R.A., Fausch K.D., Fitzhugh G.A., Gammon J.R., Halliwell D.B., Angermeier P.L. and Orth D.J., 1988. Regional applications of an index of biotic integrity for use in water resource management, Fisheries, 13(5), 12–20

Minshall G.W., 1984. Aquatic insect-substratum relationships, In: The Ecology of Aquatic Insects, Resh V.H. and Rosenberg D.M., Praeger, New York, 358–400

Morton B., 1975. The colonization of Hong Kong's raw water supply system by Limnopema fortunei (Dunker,1857) (Bivalvia, Mytilidea) from China. Malacologia Review, 8, 91–105

Morton B., 1977a. The biology and functional morphology of Modiolus metcalfei (Bivalvia: Mytilacea) from the Singapore mangrove. Malacologia, 16, 501–517

Morton B., 1977b. The population dynamics of Limnoperna fortunei (Dunker1857) (Bivalvia, Mytilidea) in Plover Cove Reservoir, Hong Kong. Malacologia, 16, 165–182

Morton B., 1982. The reproductive cycle in Limnoperna fortunei (Dunker 1857) (Bivalvia: Mytilidae) fouling Hong Kong's raw water supply system. Oceanol. Limnol. Sinica,13(4), 312–324

Moss B., 1988. Ecology of fresh waters: Man and medium. Blackwell Scientific Publications, Boston

Needham P.R., 1969. Trout Streams: Conditions that Determine Their Productivity and Suggestions for Stream and Lake Management. Revised by C.F. Bond. Holden-Day, San Francisco

NERCITA (National Engineering Research Center for Information Technology in Agriculture). 2004a, Culture Technology of Chinese Sturgeon. http://www.nercita.org.cn/sturgeon_zzxt/ (in Chinese)

NERCITA (National Engineering Research Center for Information Technology in Agriculture), 2004b, Artificial Propagation of Chinese sturgeon. http://www.nercita.org.cn/sturgeon_zzxt/ (in Chinese)

Nestler J., Schneider T. and Latka D., 1993. RCHARC: A new method for physical habitat analysis. Engineering Hydrology, 294–99

Newbury R.W. and Gaboury M.N., 1993. Stream analysis and fish habitat design: A Field Manual. Newbury Hydraulics Ltd., Gibsons, British Columbia

Noss R.F. and Harris L.D., 1986. Nodes, networks, and MUMs: Preserving diversity at all scales. Environmental Management, 10(3), 299–309

Novotny V., Bedoya D., Virani H. and Manolakos E., 2008. Linking indices of biotic integrity to environmental and land use variables-Multimetric clustering and predictive models, Proceedings, IWA World Water Congress, Vienna, Sept. 2008, 8

NRC (National Research Council), 1992. Restoration of aquatic ecosystems: Science, Technology, and Public Policy. National Academy Press, Washington, DC

O'Reilly N., 2007. The development and evaluation of methods for quantifying environmental stress to fish in warm-water streams of Wisconsin using self-organized maps: Influences of watershed and habitat stressors, Ph.D. Dissertation, Marquette University, Milwaukee, WI

Odum E.P., 1971. Fundamentals of Ecology, 3d (ed.), W.B. Saunders Company, Philadelphia

Ohio Environmental Protection Agency (EPA.), 1990. Use of biocriteria in the Ohio EPA surface water monitoring and assessment program. Ohio Environmental Protection Agency, Division of Water Quality Planning and Assessment, Columbus, OH

Olson T.E. and Knopf F.L., 1986. Agency subsidization of a rapidly spreading exotic. Wildlife Society Bulletin, 14, 492–493

Orsborn J.F., Cullen R.T., Heiner B.A., Garric C.M. and Rashid M., 1992. A Handbook for the Planning and Analysis of Fisheries Habitat Modification Projects. Department of Civil and Environmental Engineering, Washington State University, Pullman,WA

Orth D.J. and White R.J., 1993. Stream habitat management. Chapter 9, In: Inland Fisheries Management in North America, Kohler C.C. and Hubert W.A. (eds.), American Fisheries Society, Bethesda, MD

Plafkin J.L., Barbour M.T., Porter K.D., Gross S.K. and Hughes R.M., 1989. Rapid Bioassessment Protocols for Use in Streams and Rivers. EPA444/4-89-001. U.S. Environmental Protection Agency, Washington, DC

Pottle R. and Dadswell M.J., 1979. Studies on Larval and Juvenile Shortnose Sturgeon. Report to Northeast Utilities Service Co. Hartford, CT

Reynolds C.S., 1992. Algae, In: The Rivers Handbook, Vol. 1, Calow P. and Petts G.E. (eds.), Blackwell Scientific Publications, Oxford, 195–215

Ricklefs R. E., 2001. The Economy of Nature, W.H. Freeman and Company, New York

Ricklefs R.E., 1990. Ecology. W.H. Freeman, New York

Rieger J.P. and Kreager D.A., 1990. Giant reed (Arundodonax): A climax community of the riparian zone. In: California Riparian Systems: Protection, Management, and Restoration for the 1990's, Abel D.L., tech. coord. Pacific. SW. Forest. and Range Experiment. Station, Berkeley, CA, 222–225

Rockett L.C., 1979. The influence of habitat improvement structure on the fish populations and physical characteristics of backtail creek, Crook County, Wyoming. Report on Proect 3079-08-7601, Wyoming Game and Fish Department, Cheyenne, WY

Rodgers J.H., Dickson K.L. and Cairns J., 1979. A review and analysis of some methods used to measure functional aspects of periphyton, In: Methods and Measurements of Periphyton Communities: A Review, Weitzel. R.L. (ed.), Special publication 690. American Society for Testing and Materials

Rosgen D.L., 1996. Applied river morphology. Wildland Hydrology, Colorado

Roy A.G. and Abrahams A.D., 1980. Discussion of rhythmic spacing and origin of pools and riffles. Geological Society of America Bulletin 91, 248–250

Rudolph R.R. and Hunter C.G., 1964. Green trees and greenheads, In: Waterfowl Tomorrow, Linduska J.P., (ed.), U.S. Department of the Interior, Fish and Wildlife Service, Washington, DC, 611–618

Ruttner F., 1963. Fundamentals of limnology. Transl D.G. and Frey F.E.J., Fry. University of Toronto Press, Toronto

Schamberger M., Farmer A.H. and Terrell J.W., 1982. Habitat suitability index models: Introduction. FWS/OBS-82/10. U.S. Department of the Interior, U.S. Fish and Wildlife Service, Washington, DC

Schreiber K., 1995. Acidic deposition (acid rain). In: Our living Resources: A report to the Nation on the Distribution, Abundance, and Health of U.S. Plants, Animals, and Ecosystems, LaRoe T., Ferris G.S. Puckett C.E., Doran P.D. and Mac M.J., U.S. Department of the Interior, National Biological Service, Washington, DC

Schroeder R.L. and Haire S.L., 1993. Guidelines for the development of community-level habitat evaluation models. Biological Report 8. U.S. Department of the Interior, U.S. Fish and Wildlife Service, Washington, DC

Schroeder R.L. and Keller M.E., 1990. Setting objectives: a prerequisite of ecosystem management. New York State Museum Bulletin 471, 1–4

Sedgwick J.A. and Knopf F.L., 1986. Cavity-nesting birds and the cavity-tree resource in plains cottonwood bottomlands. Journal of Wildlife Management, 50, 247–252

Seehorn M.E., 1985. Fish habitat improvement handbook. Technical Publication R8-TP 7. U.S. Department of Agriculture Forest Service, Southern Region

Shields F.D., and Smith R.H., 1992. Effects of large woody debrius removal on physical characteristics of a sand-bed river. Aquatic Conservation, Marine and Freshwater Systems, 2, 145–163

Shields F.D., Cooper C.M. and Knight S.S., 1995. Experiment in stream restoration. Journal of Hydraulic Engineering, 121, 494–502

Shields F.D., Knight S.S. and Cooper C.M., 1995. Use of biotic integrity to assess physical habitat degradation in warmwater streams. Hydrobiologia, 312, 191–208

Simmons D. and Reynolds R., 1982. Effects of urbanization on baseflow of selected south shore streams. Long Island, NY. Water Resources Bulletin, 18(5), 797–805

Simon T.P. and Lyons J., 1995. Application of the index of biotic integrity to evaluate water resources integrity in freshwater ecosystems, in Biological Assessment and Criteria: Tools for Water Resources Planning and Decision Making, Davis W.S. and Simon T.P. (eds.), Lewis Publishers, Boca Raton, FL, 245–262

Smock L.A., Gilinsky E. and Stoneburner D.L., 1985. Macroinvertebrate production in a southeastern United States blackwater stream. Ecology, 66, 1491–1503

Strange T.H., Cunningham E.R. and Goertz J.W., 1971. Use of nest boxes by wood ducks in Mississippi. Journal of Wildlife Management, 35, 786–793

Stuart T.A., 1960. Land drainage in Scotland and its effect on fisheries. Salmon and Trout Magazine, 158, 44–62

Svejcar T.J., Riegel G.M., Conroy S.D. and Trent J.D., 1992. Establishment and growth potential of riparian shrubs in the northern Sierra Nevada. In Symposium on Ecology and Management of Riparian Shrub Communities. USDA Forest Service General Technical Report INT-289. U.S. Department of Agriculture, Forest Service

Sweeney B.W., 1984. Factors influencing life-history patterns of aquatic insects. In: The Ecology of Aquatic Insects, Resh V.H. and Rosenberg D.M. (eds.), Praeger, New York, 56–100

Sweeney B.W., 1992. Streamside forests and the physical, chemical, and trophic characteristics of piedmont streams in eastern North America. Water Science Technology 26, 1–12

Teskey R.O. and Hinckley T.M., 1978. Impact of water level changes on woody riparian and wetland communities, Vols. I, II and III. FWS/OBS-77/58, -77/59, and -77/60. U.S. Department of Agriculture, Fish and Wildlife Service

USEPA (United States Environmental Protection Agency), 1993. Watershed Protection: Catalog of Federal Programs. EPA841-B-93-002. U.S. Environmental Protection Agency, Office of Wetlands, Oceans and Watersheds, Washington, DC

USFWS (United States Fish and Wildlife Service), 1981. Standards for the Development of Habitat Suitability Index Models (ESM 103). U.S. Department of the Interior, Fish and Wildlife Service, Washington, DC

Van Horne B., 1983. Density as a misleading indicator of habitat quality. Journal of Wildlife Management, 47, 893–901.

Verner J., 1984. The guild concept applied to management of bird populations. Environmental Management, 8, 1–14

Von Haartman L., 1957. Adaptations in hole nesting birds. Evolution, 11, 339–347

Walburg C.H., 1971. Zip code H2O. In Sport Fishing USA, Saults D., Walker M., Hines B. and Schmidt R.G. (eds.), U.S. Department of the Interior, Bureau of Sport Fisheries and Wildlife, Fish and Wildlife Service. U.S. Government Printing Office, Washington, DC

Wallace J.B. and Gurtz M.E., 1986. Response of Baetis mayflies (Ephemeroptera) to catchment logging. American Midland Naturalist, 115, 25–41

Walter H., 1985. Vegetation of the earth, 3rd (ed.), New York, Springer Verlag

Walters M.A., Teskey R.O. and Hinckley T.M., 1978. Impact of water level changes on woody riparian and wetland communities, Vols. VII and VIII. FWS/OBS-78/93 and -78/94. U.S. Department of Agriculture, Fish and Wildlife Service

Wang C.L., Teng Y., Liu C.L., ect. 2002. Propagation characteristic and development utilization of Chinese sturgeon. Fishery Science and Technology Information, 29(4), 174–176 (in Chinese)

Wang H.Z. and Wang H.J., 2008. Ecological impacts of cut-off of the connection of lakes with the Yangtze River and restoration strategies, in: Yangtze River Ecology and Optional Operation of Hydraulic Engineering, Wang Z.Y. (ed.), Chinese Science Press (in Chinese)

Wang Z.R., 1997. Fauna Sinica. Science Press, Beijing, China, (in Chinese)

Wang Z.R., 1997. Invertebrata, fauna sinica, vol. 12 Bivalvia: Mytiloida. Science Press (in Chinese)

Wang Z.Y., Lee J.H.W., Cheng D.S. and Duan X.H., 2008. Benthic invertebrates investigation in the East River and habitat restoration strategies. Journal of Hydro-Environment Research,accepted for publication

Wang Z.Y., Melching C.S., Duan X.H., Yu G.A., 2009. Ecological and hydraulic studies of step-pool systems. ASCE Journal of Hydraulic Engineering, 134 (9), 705–717

Wang Z.Y., Pan B.Z., Xu M.Z. and Yu G.A., Preliminary investigation of aquatic ecology in the source region of the Yellow River, in Brierley, Li and Chen (eds.), Landscape and Environment science and management in the Sanjiangyuan Region, Qinghai People's Publishing House

Wang Z.Y., Pan B.Z., Xu M.Z., Yu G.A., 2010. Community Characteristics of Benthic Macroinvertebrates in the Source Region of the Yellow River,Proceedings of 8th IAHR International Symposium on Eco-hydraulics, Seoul, South Korea.

Ward J.V., 1992. Aquatic Insect ecology. Biology and habitat. John Wiley and Sons, New York

Wei Q.W., 2005. Reproductive behavioral ecology of chinese sturgeon with its stock assessment [D]. Institute of Hydrobiology, Chinese Academy of Sciences, Wuhan (in Chinese)

Weitzel R.L., 1979. Periphyton measurements and applications. In: Methods and measurements of periphyton communities: A Review, ed. R.L.

Wesche T.A., 1985. Stream channel modifications and reclamation structures to enhance fish habitat. Chapter 5 in: The Restoration of Rivers and Streams, Gore J.A. ed. Butterworth, Boston

Wharton C.H., Kitchens W.M., Pendleton E.C. and Sipe T.W., 1982. The ecology of bottomland hardwood swamps of the southeast: A Community Profile. FWS/OBS-81/37. U.S. Fish and Wildlife Service, Biological Services Program, Washington, DC

White R.J. and Brynildson O.M., 1967. Guidelines for management of trout stream habitat in Wisconsin. Technical Bulletin 39. Department of Natural Resources, Madison, WI

White R.J., 1975. Trout population responses to stream-flow fluctuation and habitat management in Big Roch-A-Cri Creek, Wisconsin, Verhandlungen der Internationalen Vereingung fur Theretische und Angewandte Limonologie, 19, 2469–2477

Whitlow T.H. and Harris R.W., 1979. Flood tolerance in plants: A state-of-the-art review. Environmental and Water Quality Operational Studies, Technical Report E-79-2. U.S. Army Corps of Engineers Waterways Experiment Station, Vicksburg, MS

Wilbur R.L., 1978. Two types of fish attractions compared in lake tohopekaliga, Florida. Transactions of the American Fisheries Society, 107 (5), 689–695

Williamson S.C., Bartholow J.M. and Stalnaker C.B., 1993. Conceptual model for quantifying pre-smolt production from flow-dependent physical habitat and water temperature. Regulated Rivers: Research and Management 8, 15–28

Xiang Y.L., 1985. Study of the harm and prevention measures of Mussel growths in pipelines in power plant and generation. North China Electric Power, 4, 24–27 (in Chinese)

Xiang Y.L., 1985. Study of the harm and prevention measures of Mussel growths in pipelines in power plant and generation. North China Electric Power, (4), 24–27 (in Chinese)

Xing X.C., 2003. Rare Chinese sturgeon and Paddlefish in China. Bulletin of Biology, 38(9), 10–11 (in Chinese)

Xu M.Z., Wang Z.Y., Duan X.H., Zhuang M.Q. and Souza F.T., 2009. Ecological measures of controlling invasion of golden mussel (Limnoperna fortunei) in water transfer systems. Proceedings of the 33rd IAHR Congress, Vanconver,Canada. 1609–1616

Yamada Y., Kurita K. and Kawauchi N., 1997. Countermeasures for limnoperna fortunei in isojima intake facilities. Proceedings of the 24th Conference of Construction Technology, Osaka, Japan Water Works Association. 230–234

Yan Y.Y., 2003. Biological characteristic and culture methods for Chinese sturgeon. Fishery Science, 5, 14–16 (in Chinese)

Yang D.G., Wei Q.W., Chen X.H., etc. 2007. Hydraulic status and on the spawning grounds of Chinese sturgeon below the Gezhouba Dam and its relation to the spawning run. Acta Ecologica Sinica, 27(3), 862-869 (in Chinese)

Yi Y.J., Wang Z.Y. and Lu Y.J., 2006. Habitat suitability index model of four major Chinese carp species in the Yangtze River. River flow 2006, 1(2), 2195–2201

Yi Y.J., Wang Z.Y. and Lu Y.J., 2007. Habitat suitability index model of Chinese sturgeon in the Yangtze River. Advances in Water Science, 18(4), 538–543 (in Chinese)

Yoakum J., Dasmann W.P., Sanderson H.R., Nixon C.M. and Crawford H.S., 1980. Habitat improvement techniques. In: Wildlife Management Techniques Manual, 4th (ed.), rev., Schemnitz, The Wildlife Society, Washington, DC, 329–403

Zhang J., 1998. Technical points on sturgeon breed aquatics. Beijing Fishery, 1, 18–20 (in Chinese)

Zhuang M.Q., 2006a. Study of growth rhythm and controlling of mollusks in long distance water transfer pipelines (Report). The East River Water Source Project Management Division of Shenzhen, (in Chinese)

Zhuang M.Q., 2006b. Dongjiang water source project management diversion of shenzhen. Study of the Seashell Problem in the Long Distance Water Transport Canal (Report) (in Chinese)

11 Integrated River Management

Abstract

Traditional river management has usually been specific purpose-oriented to achieve water security, economic benefits, or habitat restoration and paid attention to only a short period, such as a few decades. Integrated river management aims for long-term stability and sustainable development, and coordination of various aspects of the river system, including morphology and landscape, river uses, and ecology. Four principles for river management are proposed: (1) extending the duration of water flowing in rivers, which may be achieved by extending the river course or reducing the flow velocity; (2) controlling various patterns of erosion and reducing the sediment transportation in rivers; (3) increasing the diversity of habitat and enhancing the connectivity between the river and riparian waters; and (4) restoring natural landscapes.

The limit velocity law and equivalency principle are presented. In alluvial rivers, the average velocity increases with an increase in discharge when the discharge is small. As the discharge exceeds the bank-full discharge, any further increase in discharge does not result in an increase in velocity. The average velocity approaches a limit, which is the so-called limit velocity. The limit velocity law has ecological importance because all fish and other aquatic species cannot survive at velocities higher than the limit velocity. Bed structures, such as step-pools system, dissipate flow energy as water flows through the structure. Bed load motion also consumes flow energy and plays a role to protect the bed from erosion. For mountain streams with the same stream power, strong bed structures are associated with low bed load transportation; and weak or no bed structures are associated with intensive bed load motion. Experiments have shown that for incised streams, the final bed profiles are the same if there is bed load motion or there are bed structures. Bed structures and bed load motion are mutually replaceable for flow energy consumption and streambed incision control. This is the principle of equivalency of bed load motion and bed structures, which may be applied for river training and management.

Two methods for computing the sediment budget are proposed. One method is based on the size distributions of sediment and sediment load in rivers, tributaries, and gullies in the sediment source area. The core of the second method is the sediment budget matrix. Case studies of integrated river management are presented with the Diaoga River, Wenjiagou Gully and Xiaojiang watershed as examples, in which step-pool system were used for controlling river bed incision and debris flows and for creation of habitat and increasing biodiversity.

Key words

Integrated river management, River morphology, Sediment budget, Bed structure, Energy dissipation, Habitat restoration.

11.1 Principles of Integrated River Management

11.1.1 Management of Rivers

River use has long been an important element in human activities and socioeconomic development. Water is used for domestic, industrial, and agricultural purposes. Hydropower is exploited to power the industry, the river channel is used for navigation, and the fresh water fishery is a traditional resource. Moreover, rivers and the riparian areas also are used for recreation and leisure. To achieve the economic benefits and meet other demands of humans, rivers have been dammed and channelized. The natural fluvial processes and ecological systems within the river and riparian areas have, thus, been disturbed to

a great extent. River regulation and river training have been performed for various purposes and negative effects have been shown in numerous cases. In some cases the negative effects are so serious that humans have to consider renaturalizing the regulated rivers. Only by using the strategies of integrated river management the diverse river uses and natural fluvial processes and ecological systems may be harmonized.

Until approximately 1750, the scale of river regulation worldwide was small, and engineering works modified or affected the natural dynamics of rivers. Subsequently, beginning in Europe, major schemes sought complete control of rivers from the headwaters to the mouth. In North America, Ellett proposed the control of the Ohio and Lower Mississippi Rivers by using both headwater storage reservoirs and channelization of the lower river (Gore and Petts, 1989). Complete control of rivers has been achieved during the 20th century with the development of dam-building technology and construction of numerous dams on rivers.

The reservoir index, RI, is defined as

$$RI = \text{total capacity of reservoirs/annual runoff} \tag{11.1}$$

Rivers can be grouped according to the degree of regulation by humans:

(1) Natural river, $RI < 10\%$;

(2) Half-natural river, $10\% < RI < 50\%$;

(3) Half-controlled river, $50\% < RI < 100\%$;

(4) Controlled river, $RI > 100\%$.

Figure 11.1 shows the RI and the total capacity of reservoirs on several rivers. The Yellow, Mississippi, Colorado, and Nile rivers have become human-controlled rivers and the Yangtze and Pearl rivers are half-natural rivers.
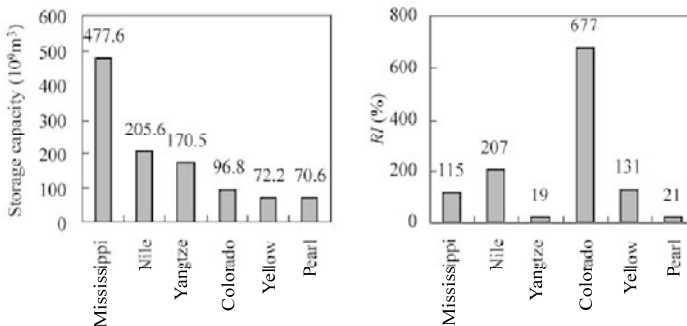
Fig. 11.1 Total storage capacity and reservoir index for several major rivers

Except for damming, channel alignment and levee construction are the most commonly practiced river training methods. The main aims of these methods are to control flood and enhance sediment-transport capacity. The fluvial processes are changed by these methods and most of the effects are obviously intentional, since natural rivers do not offer sufficient flood protection.

In river management projects factors including sediment transportation, fluvial processes, ecology protection and fish migration have been taken into consideration. Integrated river management comprises: (1) taking the watershed, including the tributaries, middle reaches, lower reaches, and the estuary as an integrated entity in planning, design, and management; (2) mitigating or controlling the negative impacts on hydrology, erosion and sedimentation, fluvial processes, land use, and environment while in achieving economic benefit, from water resources development, flood safety management, and hydropower

development; and (3) protecting, restoring, or improving the natural river ecology and landscapes. Rivers sustain ecological systems, which also have economic value, and in turn generate a healthy hydraulic system. People are able under stress conditions to make cautious use of water, thus, not preventing the next generation from having similar benefits from the same water system.

The necessity of integrated river management may be learned from the case studies for the Rhine, Yongding and Mississippi rivers. The Rhine River is the largest river in Germany and the second largest river in central and west Europe. In the past, the river changed its bed after each flood due to bed load transportation. The floodplain had a width of up to 10 km. In 1817, Tulla initiated the channelization of braided Alsatian section of the Rhine and his often quoted statement "As a rule, no stream or river needs more than one bed!" became general policy for hydraulic engineers (Gore and Petts, 1989). Tulla tried out techniques of cutting of bends and fortifying shorelines through levees and shore protection measures. Only when he convinced himself of the effectiveness of these measures did he set out to straighten the Rhine River in the whole upper Rhine valley. The Rhine training project was completed in 1872. The length of the river course was reduced by 23% and the channel was deepened and narrowed. Another project was set up to increase the capacity of the river as a waterway by increasing the depth of the navigable channel up to Strasbourg and Basel, and this was done under the leadership of Max Honsell (Gore and Petts, 1989).

After the river bank was hardened, the flow resistance was reduced greatly and the flow velocity increased. The time for the flood peak to pass from Basel to Karlsruhe was shortened from 64 hours to 23 hours. The Rhine flood peak then met with the flood peak from the Neckar River severely and threatened the downstream area. The area of swampland and bottomland flooded during the flood season decreased from 1,000 km^2 to 140 km^2. The capacity of the flood control facilities in the downstream reaches was reduced from guarding against a 200-year flood to a 50-year flood (Jiang, 1998). The channel was scoured several meters owing to the high velocity. Some reaches were scoured up to 7 m during the period 1860–1960. The lowering of ground water led to the deterioration of navigation channel, leaving the abstraction works and harbor constructions useless, and endangered the river bank and constructions along the river. To solve these problems engineers had to feed the Rhine with gravel at a high cost. Every year 170–260 thousand tons of gravels are added to the river downstream of Iffezheim Dam (Kuhl, 1992). The hardened banks also reduced the self-purification capacity of the Rhine and the increased flow velocity impacted the ecosystem of the river. The pollution in the Rhine stood out with social and economic development and the river ecology were deteriorated (Wang, 2002). The nations in the Rhine River basin restored the river primarily with a huge investment in the past 50 years.

The similar problems occurred in the Danube River after a series of river training projects, including meander cutoffs, bank hardening and dam construction. The regulated river channel is not as beautiful as the natural one and the flood wave propagates too fast and overwhelms the flood defense system in the downstream reaches. Many people have sought to renaturalize the Danube River.

The Mississippi River watershed, which drains 41% of the territory of the contiguous 48 states of the U.S., has undergone massive transformations in the last 200 years (Milliman and Meade, 1983). The main engineering projects were stepped dams and ship locks, which have increased the water depth for navigation. The middle and lower reaches were channelized with hardened banks and numerous spur dykes (Su and Wang, 1997; Hou and Xu, 2001). The bend cutoffs in the lower reach reduced the channel length by 30% (Xu, 2007; Izzo, 2004). The sediment transportation has been reduced and less than one third of the sediment carried by the river 100 years ago is transported to the estuary. As a consequence the Mississippi Delta and the coast lost more than 4,920 km^2 of wetlands over the past century. Restoration engineering has been proposed to stop the land loss and enable coastal Louisiana to become stable and self-sustaining.

In China, the Guanting Reservoir was built on the Yongding River in 1953 with main purposes of flood control and water supply to Beijing. At the time of construction about 2 billion m^3 of fresh water flowed into the reservoir annually. Since 1953 numerous dams have been constructed in the upper Yongding basin. All the river water is used before it flows into the Guanting Reservoir. Now, the Guanting Reservoir receives only 0.2 billion m^3 of sewage water discharged from upstream cities and towns. The ecology of the river has been impacted so seriously that there are almost no fish living in the river and the taxa richness of benthic invertebrates has been reduced from several tens of species to only a few species. Figure 11.2 shows the polluted water at the confluence of the Sanggan River and the Yanghe River, which is located at the upper end of the Guanting Reservoir. The figure also shows the two species of macro-invertebrates of *Oligochaeta* and *Chironomidae* found in the river bed. Both species are very tolerant and may live in heavily polluted water.

The three case studies show that integrated river management is needed. The river uses must be integrated with the management of hydrology, the ecological system, land use, and the fluvial processes. An integrated river management index, *I*, is introduced:

$$I = w_0 R - w_1 H - w_2 S - w_3 G - w_4 E - w_5 L \tag{11.2}$$

in which *H* is a hydrology management index; *S* is a sediment management index; *G* is a fluvial process and landscape management index; *E* is an ecological system management index; *L* is a land use management index; *R* is a river use index; and w_i is weight value for the *i*-th index.

Fig. 11.2 Polluted water of the confluence of the Sanggan River and the Yanghe River at the upper end of the Guanting Reservoir and two tolerant species of macro-invertebrates of *Oligochaeta* and *Chironomidae* (See color figure at the end of this book)

The index *R* is the sum of the economic benefit from power generation, navigation, water supply, tourism and recreation; *H* can be calculated as the relative change to the hydrological cycle; *S* is the intensity of complex influence on the sediment budget; *G* is the induced instability of the river channe and change of landscape; *E* can be measured as the reduction in number of species of floral and faunal communities; and *L* is the value of land use change. The weight values w_i must be determined from case studies. The assessment of integrated river management level of river management projects can be valued with the index *I*. The higher is the value of *I*, the better the river management system.

11.1.2 Stability of Rivers

The stability of rivers is the most important factor for river health. Mountain rivers and alluvial rivers are

grouped into stable streams, incised streams, aggrading streams, and streams with intensive bed load motion. The stable streams are the rivers with a stable channel bed with little bed load motion, examples are the Jiuzhai and Shengou creeks, and the Jialing and Ake rivers in the upper Yangtze River basin, the Chexi and Shennong creeks in the Three Gorges reach of the Yangtze River, the Balan and Songhua rivers in the northeastern China, Shangping Creek and the East River in the Pearl River basin, the Qingjiang River in the upper Weihe River basin, and the Juma River in the suburbs of Beijing. The incised streams are streams suffering channel bed erosion, such as the Duke, Marke, and Diaoga rivers. The aggrading streams are the rivers with accumulated sediment deposition, such as the lower reaches of the Yellow River, the middle and lower reaches of the Yangtze River, the Baishui and Bailong rivers in the upper Yangtze River basin, and the lower Fujiang River. The streams with intensive bed load motion include the Xiaobaini and Jiangjia ravines, and the Jinsha River.

Samples of macroinvertebrates were taken from these rivers and the biodiversity was assessed by identifying the species from these sampling sites. Figure 11.3 shows the rivers and locations of the sampling sites. The study was done before 2008 and a general relation between the biodiversity and the fluvial process was obtained. In 2008 and 2009 the rivers in the Qinghai-Tibet Plateau were also studied and samples were taken from 16 more sites in the source region of the Yellow, Yangtze, and Lancang rivers,
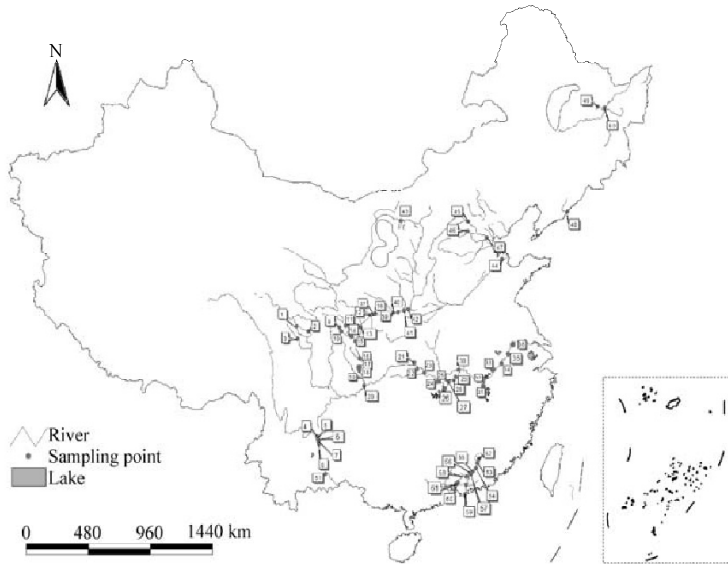
Fig. 11.3   Rivers and sampling sites
1 Marke R.; 2 Ake R.; 3 Duke R.; 4 Jinsha R.; 5 Jiangjia Ravine; 6 Shengou Ravine; 7 Xiaobaini Ravine; 8 Diaoga R.; 9 Jiuzhai Creek; 10 Baishui R.; 11 Bailong R. at Wudu; 12 Jialing R.-Source; 13 Jialing-Lueyang; 14 Bailong at Bikou; 15 Bailong R. at Baozhusi; 16 Jialing R. at Tingzikou; 17 Jialing at Nanchong; 18 Jialing at Lidu; 19 Fujiang R.; 20 Jialing at Chongqing; 21 Shennong Creek; 22 Chexi Creek; 23 Qing R. mouth; 24 Yangtze at Shishou; 25 Swan Island; 26 East Tongting Lake; 27 Honghu Lake; 28 Yangtze at Jiayu; 29 Yangtze at Paizhouwan; 30 Donghu Lake; 31 Poyang Lake; 32 Yangtze at Huanggang; 33 Yangtze at Anqing; 34 Yangtze at Datong; 35 Yangtze at Wuhu; 36 Yangtze at Nanjing; 37 Qingjiang R.; 38 Weihe R. at Baoji; 39 Weihe at Xianyang; 40 Weihe at Weinan; 41 Weihe at Huaxian; 42 Weihe mouth; 43 Yellow at Erdos; 44 Yellow R. mouth at Dongying; 45 Yongding R.; 46 Juma R.; 47 Haihe R.; 48 Yalu R.; 49 Balan R.; 50 Songhua R.; 51 Panlong R. at Kunming ; 52 Shangping Creek; 53 East R. at Fengshuba; 54 East R. at Longchuan; 55 East R. at Wuxing; 56 East R. at Heyuan; 57 Baipu R.; 58 Yequ Creek; 59 Xizhi R.; 60 Zengjiang Bay, Zengjiang at Zhengguo; 61 East R. at Yuanzhou

and the Yalutsangbu River and its tributaries. The new results from the Qinghai-Tibet Plateau agreed with the relation obtained from the rivers shown in Fig. 11.3.

Figure 11.4 shows the relations between the taxa richness (number of species per site) and abundance (number of individual animals per area) with the status of the fluvial process, in which "Stable" represents stable streams, "Incised" represents incised streams, "Silting" represents streams with continuous sediment deposition, and "Intensive ST" represents the streams with intensive bed load transportation. The biodiversity and density are high in stable streams, lower in degraded and aggraded rivers, but the lowest in streams with intensive sediment transportation. Compared with fluvial processes, pollution is of only any second importance on the river ecology. Bed stability is a precondition for stream ecology and is the most important factor for biodiversity.
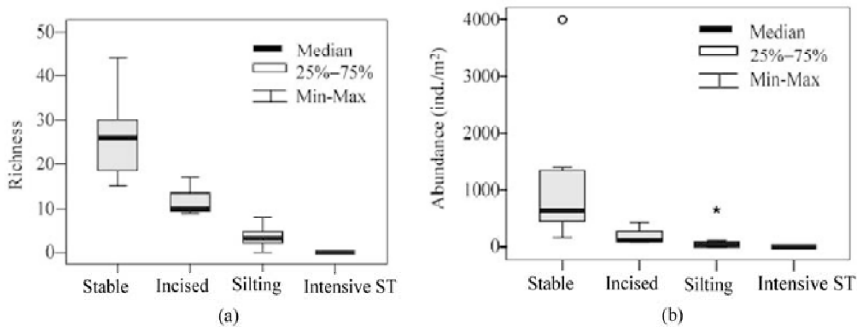
Fig. 11.4 (a) Relation of species richness of macroinvertebrates and status of the fluvial process of rivers; and (b) Relation of abundance of macroinvertebrates per area with status of the fluvial process

The stable streams provide stable and varied habitats for various species, and, therefore, support high diversity of aquatic bio-communities. The taxa richness is represented by *Ephemeroptera* (*Baetidae, Siphlonuridae, Ephemerellidae, Heptageniidae, Ephemeridae, Potamanthidae* and *Leptophlebiidae*), *Plecoptera* (*Perlidae* and *Nemouridae*), *Trichoptera* (*Hydropsychidae, Brachycentridae, Leptoceridae, Psychomyiidae, Hydroptilidae* and *Rhyacophilidae*), *Odonata* (*Gomphidae, Coenagrionidae* and *Euphaeidae*); *Diptera* (*Chironomidae, Tipulidae, Ceratopogonidae* and *Simuliidae*); *Coleoptera* (*Elmidae, Psephenidae, Hydrophilidae, Dytiscidae* and *Dryopidae*); *Gastropoda* (*Melaniidae, Hydrobiidae, Lymnaeidae and Planorbidae*), *Amphipoda* (*Gammaridae*) and *Hirudinea*. The species of the *Ephemeroptera, Plecoptera* and *Trichoptera* (EPT) imply natural conditions and very good water quality. Therefore, the number of species and density of the EPT are used as indicators of very good ecology. Figure 11.5 shows several representative species of *Ephemeroptera* and *Trichoptera* (Duan et al., 2010).

Incised rivers have V-shape cross sections and there is little or no floodplain. The substrate consists of cobbles, gravel, coarse sand, and bedrock. Flow velocity is high and only species which may clasp the bedrock or cobbles to resist the flow can live in incised streams. The taxa richness is lower than for stable streams. Species found in incised streams include: *Ephemeroptera* (*Baetidae, Heptageniidae, Siphlonuridae,* and *Ephemerellidae*), *Trichoptera* (*Hydropsychidae*), *Coleoptera* (*Elmidae, Haliplidae, Chrysomelidae, Curculionidae, Hydrophilidae,* and *Lightningbugs*), and *Diptera* (*Chironomidae, Ephydridae, Tipulidae,* and *Stratiomyiidae*). Figure 11.6 shows several representative species of *Placoptera* taken from incised rivers.

For rivers with continuous sediment deposition silt and fine sand cover the bed surface and fill in the interstices of large solid particles. The taxa richness and abundance of macroinvertebrates are lower than in stable and incised rivers. The biomass of invertebrates and volume of sediment deposition were
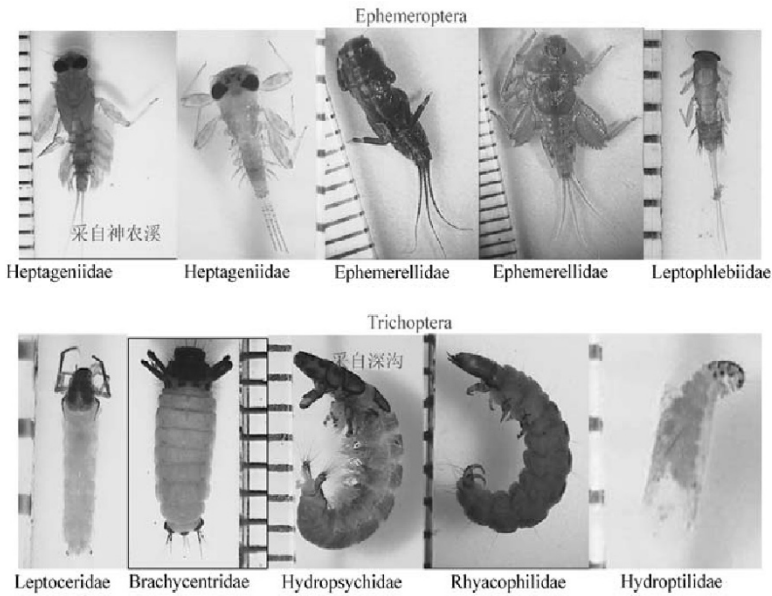
Fig. 11.5 Representative species of *Ephemeroptera* and *Trichoptera* taken from stable streams (See color figure at the end of this book)
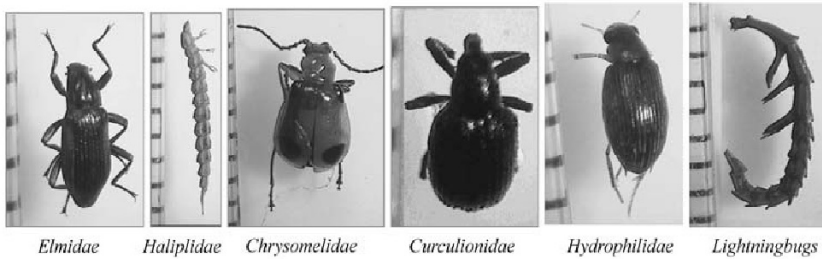
Fig. 11.6 Representative species of *Placoptera* taken from incised rivers (See color figure at the end of this book)

measured in a 100 m long section of the Diaoga River and the results are shown in Fig. 11.7 (Yu, 2008). The abundance of benthic macroinvertebrates (abundance) decreases with increasing sedimentation volume and increases again as the sedimentation volume reduces. Species found in the silting streams include: *Diptera* (*Chironomidae, Tipulidae,* and *Ceratopogonidae*), *Coleoptera* (*Dytiscidae, Hydrophilidae,* and *Elmidae*), *Ephemeroptera* (*Ephemeridae, Caenidae,* and *Ephemerellidae*), *Odonata* (*Gomphidae, Cordulegastridae,* and *Coenagrionidae*), *Oligocheata* (*Tubificidae*), and *Amphipoda*.

In the rivers with intensive bed load transportation there is no stable habitat for benthic animals. The taxa richness and abundance of macroinvertebrates are extremely low. For instance, in the Jiangjia Ravine the bed material is composed mainly of gravel but the bed load transport is intensive. Only three species were found in the samples from the Jiangjia Ravine and the abundance was extremely low (only 1 ind./m^2). In the Xiaobaini and Dabaini ravines and the lower Yellow River, the bed material consists mainly of coarse and fine sand and the rate of bed load transportation is high. Only one species was found from the samples and the abundance was nearly zero.

Stable streams provide stable habitats for diverse bio-communities. If the boundary of a stream remains stable even during extreme flood events the stream is in a state of **super-equilibrium**. The beautiful

Jiuzhai Creak is an example of such super-equilibrium. The average slope of Jiuzhai Creek is about 4%. Hundreds of landslides created landslide dams and formed 118 lakes. The lakes are filled with water, and are flat and smooth mirrors like surfaces. At the downstream end of the lakes the water flows over stones and forms waterfalls or steep rapids with step-pool systems. The waterfalls are normally several to several tens of meters high and the lakes are several meters to 80 m deep and have surface area of several hundreds to nearly one million m^2. The waterfalls and rapids are very stable and trees and shrubs have grown on them, as shown in Fig. 11.8.
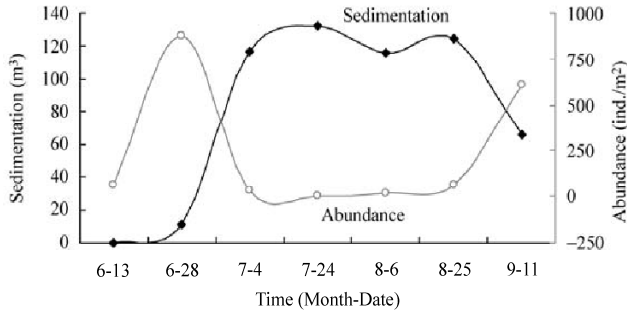
Fig. 11.7 Biomass per area of macroinvertebrates as a function of sediment deposition volume (Yu, 2008)

Fig. 11.8 Jiuzhai Creek in super-equilibrium

Another example of super-equilibrium is a mountain stream in the upper East River. As shown in Fig. 11.9, many boulders on the stream bed create high resistance and protect the bed from erosion. The stream is stable even during extreme flood events. Riparian vegetation develops very well. The biodiversity of benthic invertebrates and fish are quite high. Some shrub and herbaceous species have colonized the stream bed. Super-equilibrium involves high resistance and high biodiversity, and, therefore, is associated with good river health.

11.1.3   Principles For River Management

Principle I—Extending the Duration of Water Flowing in Rivers
The river is the carrier of lives and provides aquatic creatures with various habitats. The floodplain and

riparian wetlands are sites of high biodiversity that depend on flows from the river. Extending the duration of river water remaining on the continent may provide aquatic bio-communities larger and better habitats and provide humans longer time for river uses, e.g., flood water utilization and water surface recreation. There are two strategies for this purpose: (1) extending the river course; and (2) reducing the flow velocity (Wang et al., 2007).

Fig. 11.9   Large boulders create high resistance and protect the bed from erosion, which make the stream achieve super-equilibrium (See color figure at the end of this book)

Low velocity has important ecological implications. The stream and riparian waters are habitats for various species that depend on water flows. Most of aquatic animals live in lentic or low flow velocity waters. A suitability index, SI, is defined as the suitability of physiochemical conditions of the habitat for species to live and spawn. $SI=1$ represents the best conditions and $SI = 0$ means the worst conditions. In fact, $SI=0$ implies that the species prefer to not live in the habitat. Wang et al. (2007) studied the suitability index for most important vertebrate species in rivers and presented the distributions of the suitability index as a function of velocity for 36 fish species. Table 11.1 lists the values of critical velocities of U_{c1}, U_{c2}, U_{c3}, of which U_{c1} is the critical velocity when SI increases to 1; U_{c2} is the critical velocity when SI begins to reduce from 1; and U_{c3} is the critical velocity when SI reduces to zero. The value of SI equals to 1 for velocities between U_{c1} and U_{c2}.

The velocity range of SI for adult, fry, and juvenile fishes and spawning is different for different species. Figure 11.10 shows the statistical distributions of the three critical velocities for adult, fry, and juvenile fishes and spawning. The vertical axis is the percentage of the statistical species at which the critical velocity is smaller than U_c. The striped shaded area is the range for $SI=1$, or, the best range of velocity for the species to live and spawn. As shown in Fig. 11.10(a) and (b), 100% of the species have an SI value less than 1 and about 90% of the species prefer not to live in areas with velocity higher than 2 m/s for adults, and 100% of the species have an SI value less than 1 and about 85% of the species cannot spawn if the velocity is higher than 2 m/s. Figure 11.10(d) shows that 100% of the species have an SI value equal to zero for juvenile fishes if the velocity is higher than 2 m/s.

If the velocity is very low algal blooms may occur in rivers with eutrophication. According to field investigation very few algal bloom events occur if the flow velocity is higher than 0.3 m/s. Therefore, a flow velocity in the range of 0.3–2 m/s is the best for river ecology.

Table 11.1 Critical velocities defining when *SI* increases to 1, begins to reduce from 1, and reduces to zero for 36 fish species

Fish species	Adult			Spawning			References
	U_{C1} (m/s)	U_{C2} (m/s)	U_{C3} (m/s)	U_{C1} (m/s)	U_{C2} (m/s)	U_{C3} (m/s)	
Chinese sturgeon	0.15	0.45	1.52	1.15	1.5	2.6	Yi et al., 2007
Chinese carps (Black carp, grass carp, silver carp, and big head carp)				0.27	0.9	4.15	Yi et al., 2006
American Shad	0.2	0.9	1.5	0.3	0.9	1.3	Stier and Crance, 1986
Gizzard Shad	0	0.2	1.2	0	0.1	0.6	Williamson and Nelson, 1985
Arctic Grayling Riverine Populations	0.3	0.9	1.2				Hubert et al., 1985
Bluegill	0	0.09	0.43	0	0.08	0.36	Stuber et al., 1982a
Blacknose Dace	0	0.3	0.86	0.2	0.45	0.65	Trial et al., 1983a
Longnose Dace	0.45	0.65	1.23				Edwards, 1983a
Brook Trout				0.3	0.6	0.9	Raleigh, 1982
Brown Trout	0.2	0.2	1.8	0.2	0.5	1.2	Raleigh et al., 1986b
Cutthroat Trout				0.3	0.6	0.9	Hickman and Raleigh, 1982
Rainbow Trout	0.15	0.6	1.07	0.3	0.7	0.9	Raleigh et al.,1984
Common Shiner	0.15	0.2	0.5				Trial, et al., 1983b
Flathead Catfish	0	0.3	1.97				Lee and Terrell, 1987
Channel Catfish				0	0.15	0.43	McMahon, and Terrell, 1982
Chinook Salmon				0.3	0.85	1.15	Raleigh,et al., 1986a
Longnose Sucker				0.3	1	2.7	Edwards, 1983b
Green Sunfish	0	0.1	0.25	0	0.1	0.15	Stuber et al., 1982b
Redear sunfish	0	0.01	0.1				Beghart et al., 1984
Largemouth Bass	0	0.06	0.2	0	0.03	0.1	Stuber et al., 1982c
Smallmouth Bass	0	0	0.6	0	0.4	0.9	Edwards et al., 1983
Spotted Bass	0	0.06	0.85	0	0	0.3	McMahon et al., 1984a,
Inland Stocks of Striped Bass				0.5	1.2	4	Crance, 1984
Paddlefish	0	0.1	0.7	0.6	3.7	4.6	Hubert and Anderson, 1984
Yellow Perch	0	0.03	0.12	0	0.09	0.15	Krieger, et al., 1983
Pink Salmon	0	1.22	2.04	0.5	0.7	1.5	Raleigh and Nelson, 1985
Shortnose Sturgeon	0.16	0.45	1.52	0.3	0.76	1.52	Crance, 1983
Slough Darter	0	0.05	0.24				Edwards, et al., 1982a
Southern Kingfish	0.2	0.5	0.75				Sikora and Sikora, 1982
Walleye	0	0.06	0.9	0.76	0.9	1.1	McMahon et al., 1984b
Warmouth	0	0.06	0.25				McMahon et al., 1984c
White Sucker	0.1	0.15	0.4	0.3	0.6	0.9	Twomey et al., 1984
White Crappie	0	0.2	0.4				Edwards, et al., 1982b

Note: U_{c1} is the critical velocity when *SI* increases to 1; U_{c2} is the critical velocity when *SI* begins to reduce from 1; U_{c3} is the critical velocity when *SI* reduces to zero. The velocities between U_{c1} and U_{c2} is the best for the species. The species prefer live in waters with no velocities larger than U_{c3}.
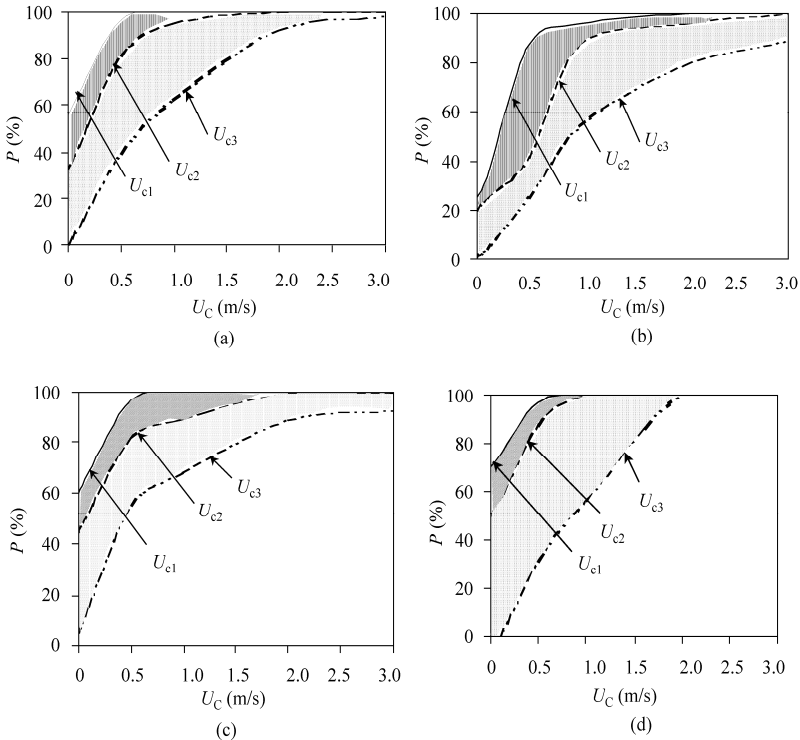
Fig. 11.10 Statistical distributions of the critical velocities when *SI* increases to 1 (U_{c1}), begins to reduce from 1 (U_{c2}), and reduces to zero (U_{c3}) for 36 species of adult fishes (a); spawning (b); fry fishes (c); and, juvenile fishes (d)

Dam construction on rivers reduces the flow velocity and extends the duration of water on the land, which is accordance with Principle I. On the other hand, dams have some negative impacts on the ecology mainly due to cutting off the path of migratory vertebrate species to their spawning sites. These negative effects may be offset by building fish ladders. However, channelization, hardening banks, cutting off meanders, and removing obstacles from the channel and floodplain to reduce the roughness are against Principle I. Such actions may damage the ecology, and cause the death or poor health of aquatic biota (Kingsford, 2000).

Meandering is natural for the nature stream channels. Artificial cutoff of meanders shortens the river course and is counter Principle I. After the cutoff the flow energy converges, which may result in intensive local scour and bank erosion, instability of the channel, and damage to aquatic habitats. Recently an artificial cutoff has been suggested at the Paizhou Meander on the Yangtze River. The meander is located downstream of Tongting Lake and upstream of Wuhan. There is a big argument between Tongting people and Wuhan people. The former support the cutoff for reduction of flood risk. The latter worries about that a flood may come to Wuhan quickly and threaten the safety of the city. A flood wave may propagate through a shortened channel more quickly after cutoff and cause flooding problems to the downstream reaches. Moreover, a meandering channel is more ecologicallysound than a straight channel. Therefore, the artificial cutoff of meanders is not a good strategy.

The term channelization encompasses all the procedures of river channel engineering which are used to control floods, improve drainage, maintain navigation, or restrain bank erosion. These procedures include enlargement, realignment, hardening, embanking, or protection of an existing channel, or the

construction of new channels. Other channelization procedures classified as river channel maintenance include dredging, cutting, or the removal of obstructions.

The application of conventional channelization methods can adversely affect the morphological and biological characteristics of river channels. In many rivers, the river banks are hardened and smoothened with concrete and stones, to enhance the flow velocity for quickly draining flood water. This practice is against Principle I and does not really provide better flood safety. The smooth banks have much smaller roughness than the natural vegetated banks, so high velocity current may directly assault the banks and break the levees. Figure 11.11(a) shows the concrete bank of the Lijiang River at Guilin, China. The hardened banks are too smooth so that the high flow velocity during flooding directly assaults the banks and has caused bank erosion and has broken the concrete bank. Figure 11.11(b) shows the hardened bank of the Blue Nile River in Sudan. The bank is roughened by sticking stones on the surface, thus the bank roughness is increased, which creates high resistance to the flow and moves high velocity current far from the banks. Figure 11.11(c) shows that channelization of the Zheduo River at Kangding resulted in high flow velocity and elimination of fish and aquatic plants. Only a few species of invertebrates live in the bed consisting of cobles and boulders.

Floodplain vegetation is a type of resistance against flood flow. Such vegetation behaves as an obvious obstacle to the flood propagation. A number of studies on flood flow and sediment transport in rivers with riparian vegetation have been conducted to understand the mechanical effects of riparian vegetation on river hydraulics and geomorphology (Ikeda and Izumi, 1990; Thorne, 1990; Ikeda et al., 1991; Thornton et al., 2000; Carollo et al., 2002). Riparian vegetation promotes geomorphic stability via increased flow resistance and reduced near-bank velocity (Andrews, 1984; Hey and Thorne, 1986). Riparian vegetation also increases the strength of bank and flood plain materials via buttressing, arching, and root reinforcement (Gray and Leiser, 1982). Communities of riparian vegetation can promote entrapment and deposition of fine sediment around the river bank and on flood plains (Abt et al., 1994; Lee et al., 1999; Elliott, 2000). In some places the floodplain vegetation is cleared for increasing flood velocity and reducing flood stage. This practice is against Principle I and should be abandoned.

Principle Ⅱ—Controlling Erosion and Reducing Sediment Transportation

Sediment is the core for the fluvial processes. Sediment movement starts from soil erosion. Therefore, erosion control is essential for stabilization of the river network. The sediment load of rivers comes from mountainous areas due to slope erosion, rill erosion, gully erosions and channel bed and bank erosions. Erosion is also the essential cause of the geological disasters of landslides and debris flows (Chapter 4). After the sediment is eroded from the upstream watershed and transported by the river flow, it will also be deposited somewhere in the river basin or at the river mouth. Erosion changes the upstream landscape and impairs or even destroys the vegetation, and sediment deposition changes the river morphology and buries the substrate of the aquatic habitat.

Construction of sediment trapping dams on the Loess Plateau of China is in accordance with Principle II. More than ten thousand sediment trapping dams have been constructed, which remarkably reduce the sediment load into the Yellow River. Most of the Yllow River's sediment load comes from the Loess Plateau. The reduction in sediment load also is mainly attributed to the reduction in sediment supply from the Loess Plateau. Figure 11.12 shows the variation of annual runoff and annual sediment load measured at the Tangnaihai station in the upper reaches on the Qinghai-Tibet Plateau, the Tongguan station in the middle reaches on the Loess Plateau, and the Lijin station on the Yellow River delta (Liu et al., 2008). No dams and very few human structures are in the watershed upstream of the Tangnaihai station. The runoff and sediment load at the Tangnaihai station have no reduction trend except for fluctuations due to variation in precipitation. The annual sediment load fluctuates with the variation of

(a)

(b)

(c)

Fig. 11.11   (a) Broken concrete bank of the Lijiang River at Guilin, China; (b) Roughened bank of the Blue Nile River in Sudan for protection against erosion; (c) Channelization of the Zheduo River at Kangding resulted in high flow velocity and elimination of species (See color figure at the end of this book)

737
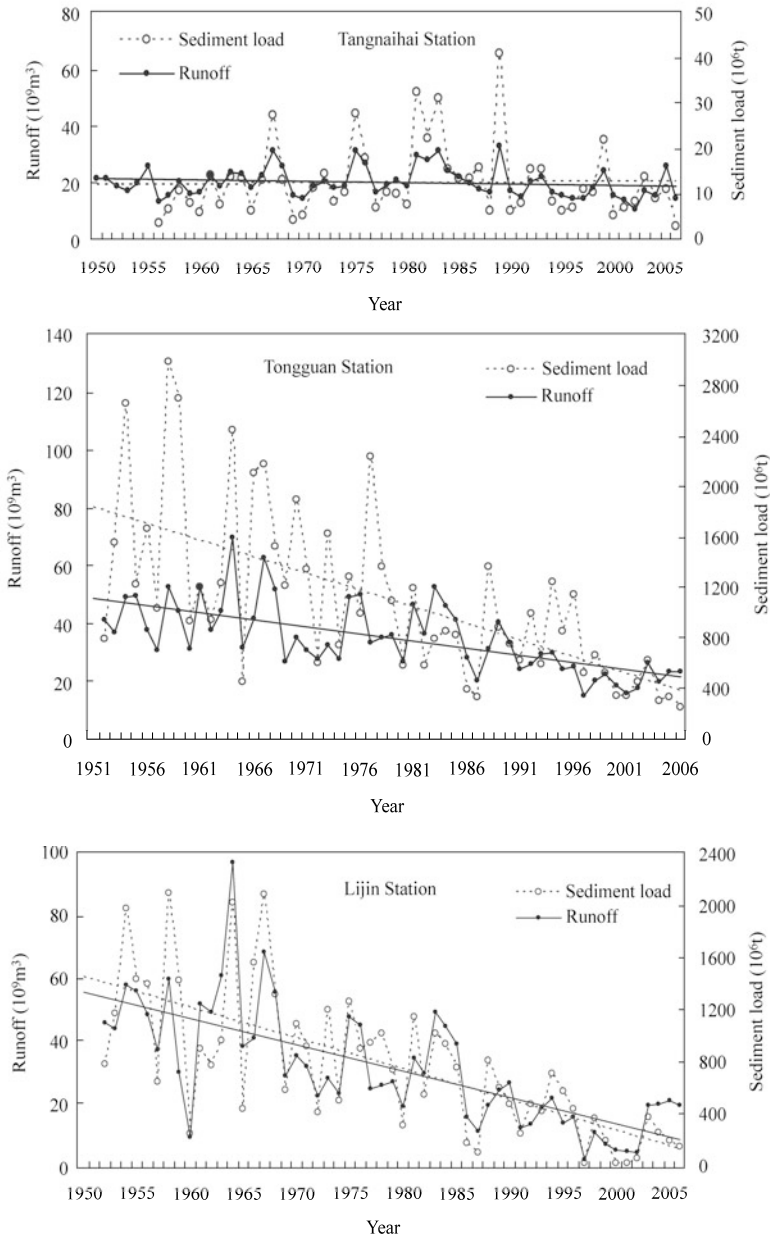
Fig. 11.12 Variation of annual runoff and annual sediment load measured at the Tangnaihai station in the upper reaches on the Qinghai-Tibet Plateau, the Tongguan station in the middle reaches on the Loess Plateau, and the Lijin station on the Yellow River delta (after Liu et al., 2008)

annual runoff. As a comparison, the Tongguan station has a remarkable reduction in sediment load and a slight reduction in runoff from the 1950s to 2006. The fluctuations of sediment load and runoff are out of phase. Numerous sediment trap dams on the Loess Plateau, about 3,000 reservoirs, and 9 large dams on

the river have regulated the flow and trap sediment load, thus, greatly changing the flow and sediment load. The Lijin station is the most downstream station on the Yellow River. The runoff and sediment load measured at the station represents the amounts of water and sediment transported into the sea. As shown in the figure, both runoff and sediment load have substantially reduced since the 1970s. The reductions of runoff and sediment reduce the flooding risk, wandering rate of the channel, and management difficulties. Nevertheless, the reduction in water flow has caused water shortages in the lower reaches, which have been discussed in Chapter 6.

It should be pointed out that gradual reduction of sediment transportation in rivers may improve the river health, but abrupt reduction may also cause stress on river management, land creation, and ecology.

Some river training projects have aimed to enhance sediment-transport capacity, which is against Principle Ⅱ. If sediment transportation in a reach is intensified, local sedimentation may be controlled but an abnormal stress is put on the downstream reaches. Moreover, high sediment-transport capacity can substantially fluctuate and is difficult to manage. In the Ming Dynasty, Pan proposed the strategy of narrowing the lower Yellow River and confining floods within the stem channel between the Grand Levees in order to raise the velocity and maintain a high sediment-carrying capacity, to prevent sediment from depositing and even promot bed sediment scouring (details are given in Chapter 6). He regulated the levee system, blocked many branches of the river and made the river flow in a single channel in the period 1565–1592. Nevertheless, the strategy of narrowing the channel was difficult to apply and soon after Pan's projects the sediment deposition in the downstream channel sped up to 5–10 cm per year.

Principle Ⅲ—Increasing Diversity and Connectivity of Habitats

The streams provide habitat for benthic macro-invertebrates and fish. The larger is the habitat area, the more species living in the habitat. According to research results, biodiversity is directly proportional to the stability and diversity of the habitats. The river management should increase the habitat diversity. To increase diversity two aspects must be met: (1) increase the water surface area in the river course and riparian waters and the connectivity between water bodies; and (2) increase the water area with low velocity and varied water depths, such as bays and lakes.

Some river training works result in the fragmentation and isolation of habitats. Figure 11.13(a) shows the concrete banks of an urban channel in Beijing, which have a bad effect on the ecology. The aquatic creatures living in the sediment bed lose their shelter and thus have disappeared from the channel. Only a very tolerant species of mosquito, which may survive in seriously polluted water, is found in the channel. Recently the Beijing government has decided to abandon the concrete channel bed and banks and to use the sediment bed and stone and vegetation banks instead for ecological improvement. It is reported that after the concrete banks and bed were replaced by a sediment bed and stone and vegetation banks the water volume needed to maintain good water quality has been halved.

Linkage of riparian wetlands with rivers is important for ecology. Fig. 11.13(b) shows a river-linked wetland by the Zengjiang River. The Zengjiang River is a tributary of the East River in south China. Substrate in the main channel of the river consists of quartz sand. No benthic invertebrates were found in the samples taken from the river bed because the sand bed is unstable. The wetland by the Zengjiang River is like a riparian lake with a 100 m wide outlet connecting the river. The river carries fine suspended sediment into the wetland which is deposited there. A mud layer covers most of the wetland, and some hydrophytes have colonized parts of the wetland. The flow velocity and water depth in the wetland vary in the range of 0–0.5 m/s and 0–3 m, respectively. The wetland provides multiple habitats for benthic invertebrates. The taxa richness in the sample taken from the wetland is 31, and the abundance of individual invertebrates is 343 ind/m^2. Many fish species are found in the wetland.

Dam construction and hydro-power exploitation cut off the migration of fishes from downstream to upstream for spawning and impair the ecology. Fish ladders have been built on many large dams to

mitigate the impact. The middle and lower reaches of the Yangtze River is a complex ecosystem with thousands of lakes and wetlands by the river. Naturally these lakes connected with the Yangtze River and formed a huge habitat in the past. Humans cut the connection for flood defense (i.e. levee construction) and aquatic farming, thus, fragmenting the habitat. Relinkage of the lakes and wetlands with the river will be an important restoration strategy for the ecosystem.

(a)   (b)
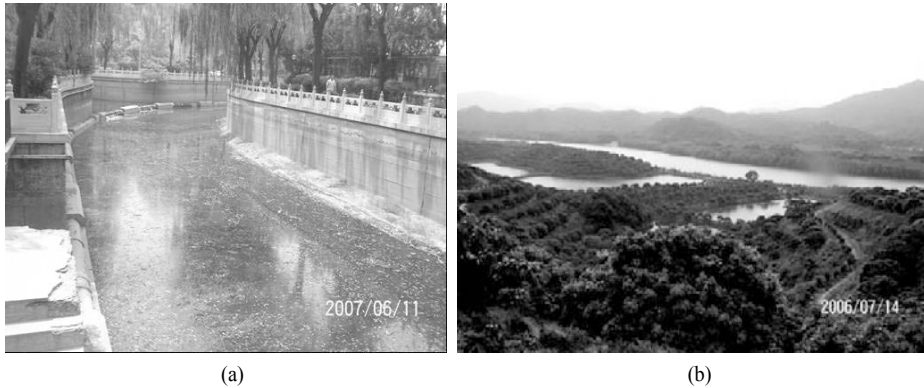
Fig. 11.13 (a) Concrete banks and bed of an urban channel in Beijing result in the disappediance of many species; and (b) a river-linked wetland by the Zengjiang River

Principle Ⅳ—Restoring Natural Landscapes
River flows through the continent and shapes all landscapes. Various river uses have changed the landscapes. Beautiful meanders have been changed into straight channels with hardened banks, waterfalls have been replaced by power stations, and the riparian forests have been changed into grand levees. Recently, people have realized that the landscapes are a wealth of nature presented to humans. Landscape restoration has become a public concern and projects have been performed to restore landscapes.

Cheongyechon in Seoul, South Korea was a beautiful stream in the past. Following rapid urbanization in the drainage area the river was clogged with rubbish and reshaped into a underground culvert. To restore the riverscape the government invested 360 million to reconstruct the urban stream. As shown in Fig. 11.14(a), now Cheongyechon has become a resort for urban residents, with clean water, a beautiful artificial step-pool system, bridges, riparian vegetation, and pedestrian paths, making the city more charming (Kyung and Zeng, 2007).

Jiuzhai Creek in southwestern China was a debris flow gully in the past. Landscape protection and restoration projects have been carried out. Check dams have been constructed to control debris flows but not affect the landscapes. The ecosystem in the creek has a high ecological resilience, which has been considered as an important element in the projects (Cui et al., 2003). Figure 11.14(b) shows the beautiful water falls on Jiuzhai Creek. The landscapes in the creek attract 1.5 million tourists every year. Economically, Jiuzhai Creek with its preserved landscapes is a better money-maker than hydro-power development. The annual tourism income is several times the hydro-power income from the Sanmenxia Dam on the Yellow River.

11.1.4   Limit Velocity Law
There is a noticeable phenomenon in natural streams: the flow velocity varies in a limited range, generally from zero to 2.5 m/s, while the discharge varies in a range of several orders, of magnitude from zero to thousands or several tens of thousands of m^3/s, depending on the size of the river. In alluvial

rivers the velocity varies within a small range, while the stream flow may spread over the channel and the floodplain. The limit velocity law is important for river management. In general, the average velocity increases with an increase in discharge when the discharge is small. As the discharge exceeds the bank-full discharge, any further increase in discharge does not result in an increase in velocity. The average velocity approaches a limit, which is the so-called limit velocity. The limit velocity, in most cases, is below 2.5 m/s.

(a)   (b)

Fig. 11.14   (a) Restoration of landscapes of Cheongyechon in Seoul, South Korea; (b) Beautiful Jiuzhai Creek in Sichuan Province in southwest China has become a tourist attraction because of its protected landscapes

Figure 11.15 shows the velocity-discharge relations for the Lalin River at the Caijiagou Station, the Huifa River at the Wudaogou Station, the Songhua River at the Jilin Station, and the Nenjiang River at the Ayanqian Station, in which Q is the daily average discharge and V is the average velocity over the cross section. The Lalin and Huifa rivers are tributaries of the Songhua River. With an increase in discharge, the average velocity approaches a limit velocity.
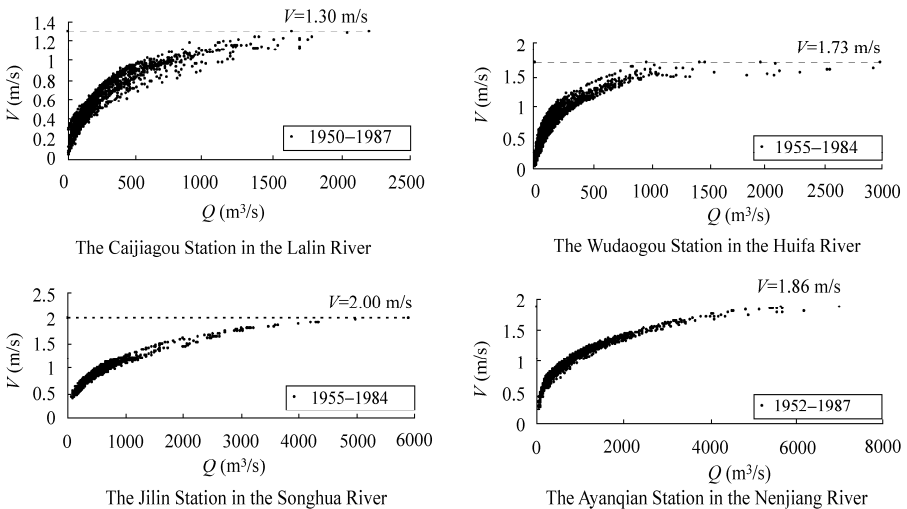
Fig. 11.15   Velocity-discharge relations for the Lalin, Huifa, Songhua and Nenjiang rivers showing a limit velocity

Figure 11.16 shows the velocity-discharge relations for the Yellow River at the Huayuankou and Gaocun hydrological stations (Liu, 2007). The Yellow River carries an extremely high sediment load, therefore, it is very dynamic. The cross sections vary every year and the bank-full wet areas consequently vary. In general the main channel has been shrinking in recent years due to sedimentation and less high flood events scouring the channel. The velocity increases with discharge faster in a small channel than in a large channel. Therefore, the points greatly scatter. Nevertheless, the velocity does not surpass a limit velocity between 2.5–3 m/s for channels with different bankfull areas.

(a) Huayuankou (1971−1990)

(b) Gaocun (1964 and 1996)
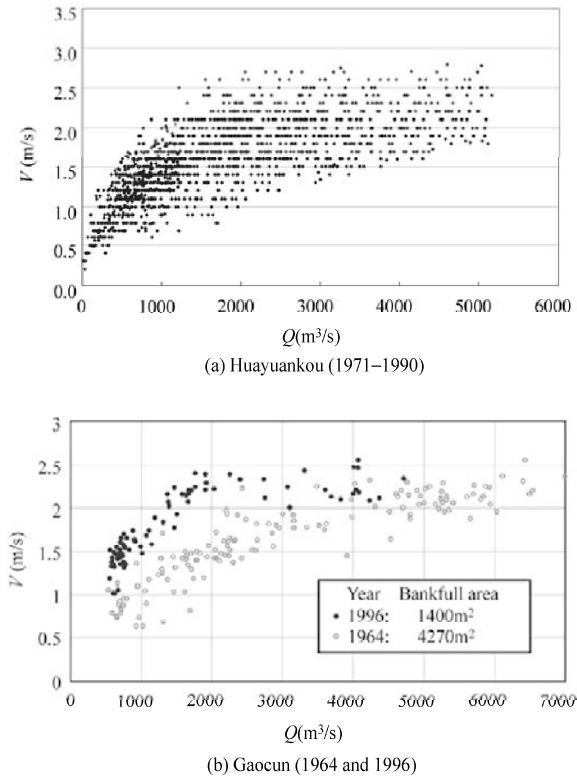
Fig. 11.16　Velocity-discharge relations for the Yellow River at the Huayuankou and Gaocun hydrological stations

In mountain rivers the development of the cross section is constrained by bed rock and bank rock. At a gorge section the velocity may be higher than 2.5 m/s during extremely high flood events. Nevertheless the high velocity sections are rather short. Figure. 11.17 shows the average velocity along the course from Yichang to Chongqing and Yibin on the Yangtze River at a discharge of 30,000 m³/s, which equals the normal flood discharge. The velocity was calculated with the discharge and cross sectional areas at narrow sections and wide sections. Although the velocity at a few locations is higher than 2.5 m/s, the average velocity for all reaches is well below 2.5 m/s.

The limit velocity law has both morphological and ecological implications. As listed in Table 11.1, all fish species cannot live in high flow velocities. River flow remains mostly within the velocity range of 0.3–2.5 m/s, which is the velocity most suitable for many fish species to live. On the other hand, natural rivers develop complex channels to reach the highest stability. In other words, the natural complex channel

shapes may accommodate the normal discharge variation and their channel chapes remain unchanged. During floods the discharge may be ten times higher than the average discharge. The complex channel shapes provide enough water conveyance capacity and keep the velocity below a critical value to prevent the banks from being eroded.
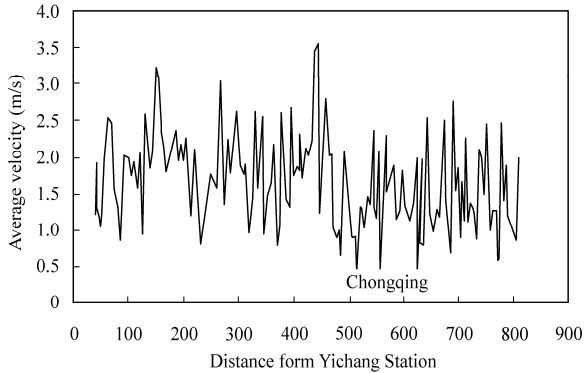
Fig. 11.17   Average velocity of the Yangtze River from Yibin to Yichang at a discharge of 30,000 m³/s

Figure 11.18 shows the typical complex channel shapes of channels and floodplains. Engineers consider the floodplain to be any part of the valley floor subject to occasional floods that threaten life and property. As flood discharge exceeds the bankfull discharge the wet area of the cross sections sharply increases with stage, thus, the flow velocity remains equal to or lower than the limit velocity. However, in many cases human structures constrain the channel within a narrow levee-defined valley and reclaim the floodplain for agriculture and residential development. Various channel improvements or impoundments are used to restrict the natural process of overbank flow. The limit velocity law is broken and the velocity during high floods is much higher than 2.5 m/s. In this case many organisms are stressed and the ecosystem is impaired. Moreover, high flow velocity scours the bed and banks, thus, the risk of bank failure is high. The limit velocity law should be taken into consideration when engineers design levees.
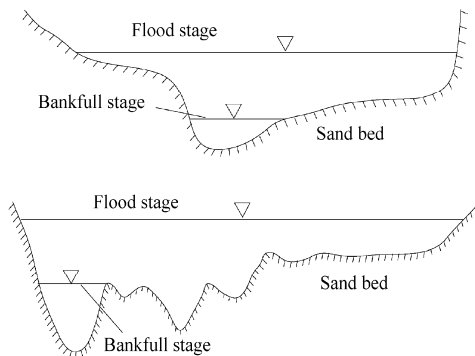
Fig. 11.18   Typical complex channel shapes of alluvial rivers

Figure 11.19 shows floodplain reclamation. Grand levees are constructed to constrain the flood water within a narrower valley. In order to control the flow velocity below the limit velocity, roughness elements,

such as trees and shrubs on the floodplain are useful to increase the resistance and control the flow velocity. With the roughness elements the overbank flood flow has higher stage but lower velocity, thus, the channel and floodplain may remain stable. One consequence of the high roughness is high flood stages, which may be solved by raising the grand levees. In general, high velocity rather than high stage poses a threat to levees.
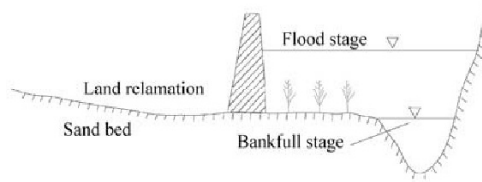
Fig. 11/19 Reclamation of floodplain with grand levees and narrowed flood channels with roughness elements

11.2 Sediment and River Morphology Management

A river system is a web of channels, of which all parts are mutually inter-affected. When considering the human role in relation to changing river channels, at least five challenges persist. First, because prediction of the nature and amount of likely change at a particular location is not certain, and because the contrasting responses of humid and arid systems needs to be considered, modeling is required to reduce uncertainty (Burkham, 1981). Second, feedback effects incorporated within the relation between changes at channel, reach, and network scales have considerable implications, especially because changes may have occurred, or have been initiated, under different environmental conditions. Third, consideration of global climate change is imperative when considering channel sensitivity and responses to threshold conditions. Fourth, channel design involving geomorphology should be an integral part of restoration procedures. Fifth, better understanding of the ways in which the perception of the human role in changing river channels varies with culture as well as varying over time should improve application of design for river channel landscapes.

11.2.1 River Networks

Horton's law (Horton, 1945) is regarded as the central principle of stream network research. Numerous investigations have shown that the linear rule of Horton's law is approximately valid in many natural drainage networks (Ciccacci et al., 1992; Kinner and Moody, 2005). Further, some artificial stream networks based on the random walk model also nearly obey Hortion's law in a similar manner (Shreve, 1966). Thus, many scholars believe that Horton's law is a universal description of stream networks. However, arguments about the Horton's law still persist.

Horton's ratios are defined by Eqs. (1.1)–(1.4) as follows:

$$R_B = \frac{N_\omega}{N_{\omega+1}} = e^B \tag{11.3}$$

$$R_L = \frac{L_{\omega+1}}{L_\omega} = e^D \tag{11.4}$$

$$R_A = \frac{A_{\omega+1}}{A_\omega} = e^H \tag{11.5}$$

where R_B is the bifurcation ratio; R_L is the length ratio; and R_A is the area ratio. If the ratios are constant, Horton's law may rewritten as:

$$N_\omega = R_B^{\,\Omega-\omega} \tag{11.6}$$

$$L_\omega = L_1 R_L^{\,\omega-1} \tag{11.7}$$

$$A_\omega = A_1 R_A^{\,\omega-1} \tag{11.8}$$

According to Horton's law the ratios R_B, R_A, and R_L are invariant with stream order and network structure. In other words, Horton's ratios are the same for different rivers and for different stream orders. Nevertheless, scientists doubt the universality of Horton's law. For instance, (Kirchner, 1993) argued that Horton's ratios may be not constant for different stream networks. Liu and Wang (2008) studied Horton's ratios for different rivers and found that the Horton's ratios are constant only for the stream orders higher than 8, or for rivers with a length over a thousand kilometers. For lower stream orders Horton's ratios vary with the stream order and are very different for different river networks.

Figure 11.20 shows the relations between Horton's ratios and stream order, in which the data were collected from Stankiewicz (2005) and Chinese rivers (Liu and Wang, 2008). For stream orders lower than 5, Hoton's ratios are very different for different rivers. Nevertheless, all Horton's ratios converge with increasing stream order. The bifurcation ratio, length ratio, and area ratio converge to 4, 2, and 4 for a stream order of 8, respectively. The law of 4-2-4 seems to be true only all drainage networks of high stream orders.

(a) Bifurcation ratio R_B

(b) Length ratio R_L

(c) Area ratio R_A
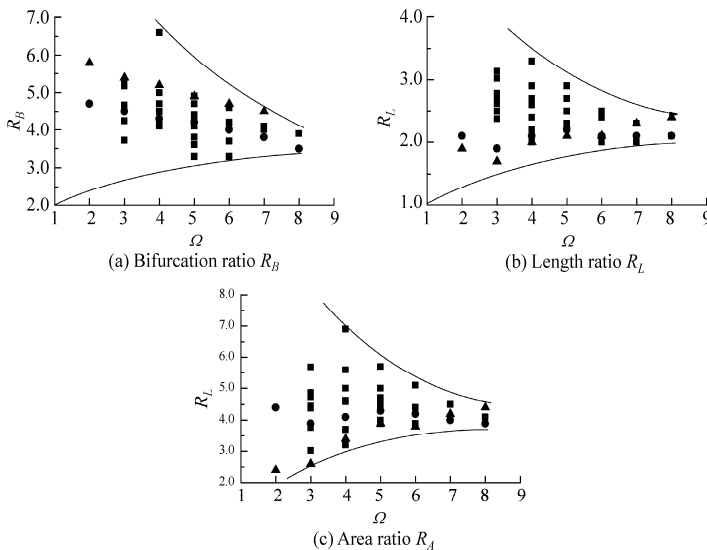
Fig. 11.20 Horton's ratios for Ω-order stream networks (■ data from Stankiewicz (2005); ▲ the Yanhe River; ● the Nuoming River both from Liu and Wang (2008))

For low stream orders Horton's ratios greatly vary. Howard (1967) classified stream networks into several types: Trellis network, Parallel network, and Radial network. Nevertheless, the classification sometimes divides networks with similar drainage structures into different categories. Also, this kind of classification lacks quantitative descriptions. Liu and Wang (2008) classified river networks into: plume network, vein network and dentritic network. They used GoogleEarth as the main data source, which provides global satellite images at varying resolutions by adjusting the "eye altitude" parameter. In their study the "eye altitude" was fixed for all data analysis. Thus, all data were collected in the same resolution.

Figure 11.21(a) shows a satellite image of a typical plume network on the Loess Plateau in western China; and Fig .11.21(b) shows a satellite image of a typical dentritic networks in northeastern China. Figure 11.22 shows the stream webs of the three types of drainage network. The plume network has a large number of first order streams flowing into a second order stream, forming a plume-like structure. The vein network has a main stream and its parallel tributaries, which looks like nervations. The dentritic network shows continuous bifurcation, which looks like tree branches.

Horton's ratios were calculated from the statistics for the three typical networks. Figure 11.23 shows Horton's ratios for the three types of network as functions of the stream order of the network. The bifurcation ratio of a plume type network is about 12 for stream orders less than 4, which is much greater than the value for a dentritic network (4) and a vein network (5). For stream orders higher than 4 the bifurcation ratio reduces and converges for all the three types of networks and approaches 4 for the stream order of 8. Other ratios have a similar trend. The ratios of dentritic networks are almost invariant for different stream orders, but the ratios for plume networks vary over a great range. In other words a dentritic network has the highest similarity between large watersheds and small watersheds; and a plume network is very different for small watersheds and from large watersheds.

(a)   (b)
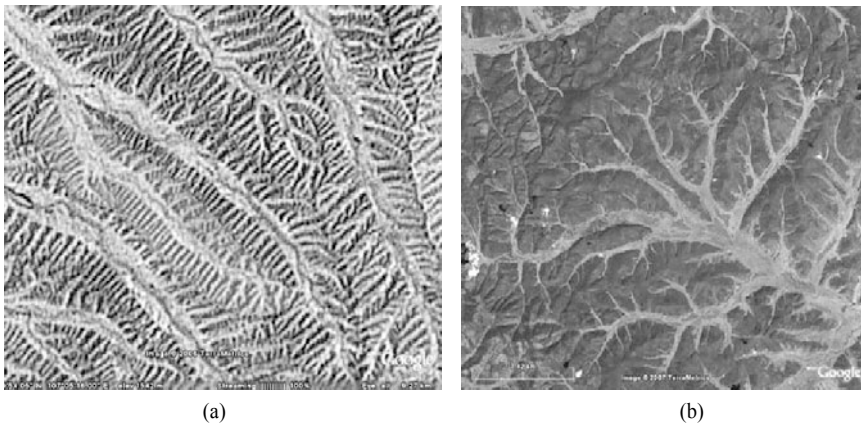
Fig. 11.21   (a) Satellite image of a typical plume network on the Loess Plateau in western China; (b) Satellite image of a typical dentritic network in northeastern China

(a)   (b)   (c)
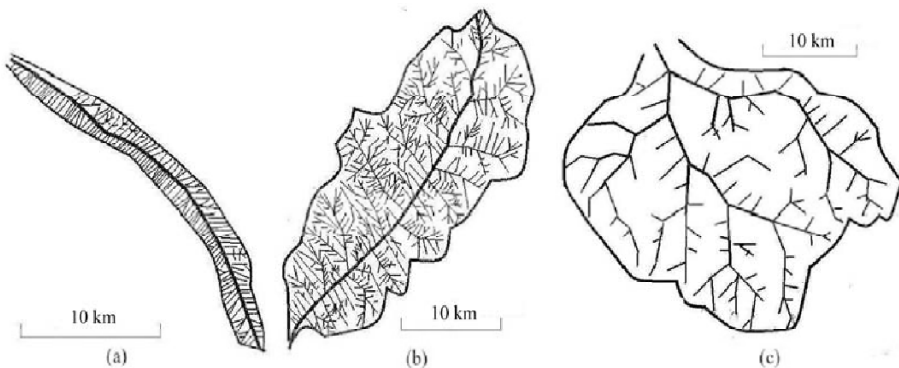
Fig. 11.22   Three types of drainage networks (a) Plume network (in the north part of the loess plateau); (b) vein network (the Yanhe River); and (c) Dentritic network (the Nuoming River)
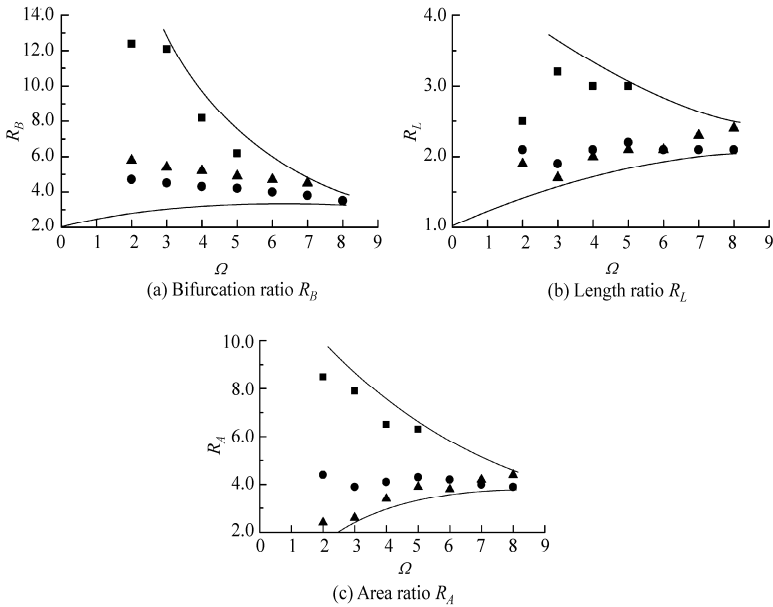
Fig. 11.23 Horton ratios of the three types of network as functions of the stream order of the networks (■ plume networks; ▲ vein networks; ● dentritic networks)

The three network patterns typically drain different in basin shapes. As shown in Fig. 11.24 the drainage area increases with stream length for the three types of networks. For the same channel length, the dentritic network has the largest drainage area, roughly following a square law with increasing stream length. The plume network has the smallest drainage area, which increases almost linearly with the stream length. Vein network is between the two. In general, plume networks develop in areas with annual precipitation around 200 mm, such as the north and west parts of the Loess Plateau in China. Dentritic networks develop in wet areas with annual precipitation higher than 800 mm. The bed sediment is non-uniform consisting of gravel, cobbles and boulders, sand, and silt. Vein networks develop in areas with precipitation between that for the plume and dentritic networks.
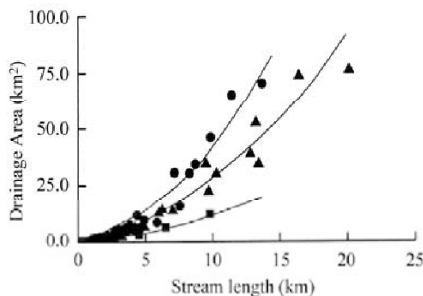
Fig. 11.24 Drainage area as a function of stream length for the three networks: (■ plume networks; ▲ vein networks; ● dentritic networks)

Among Horton's three ratios the bifurcation ratio is the most essential and most important. For dentritic networks of different orders, the bifurcation ratio is about 4. This is an important topological characteristic of stream networks. The 4-bifurcation law may be used to identify river networks. Figure 11.25(a) shows

the stream network of the Yalutsangpu River. The shape of the drainage area looks like that of a plume network and the drainage area increases with stream length almost linearly. Nevertheless, the stream network has 275 first order streams, 70 second order streams, 17 third order streams, 5 fourth order streams, and one fifth order stream. The bifurcation ratio is about 4, which means that the Yalutsangpu River network must be a dentritic network rather a than plume network. In general, the drainage area of a dentritic network is two dimensional. The Yalutsangpu River drainage area was two dimensional but was changed to almost one dimensional because the Indian Plate thrust against the Eurasia Plate, which changed the shape of the drainage area.
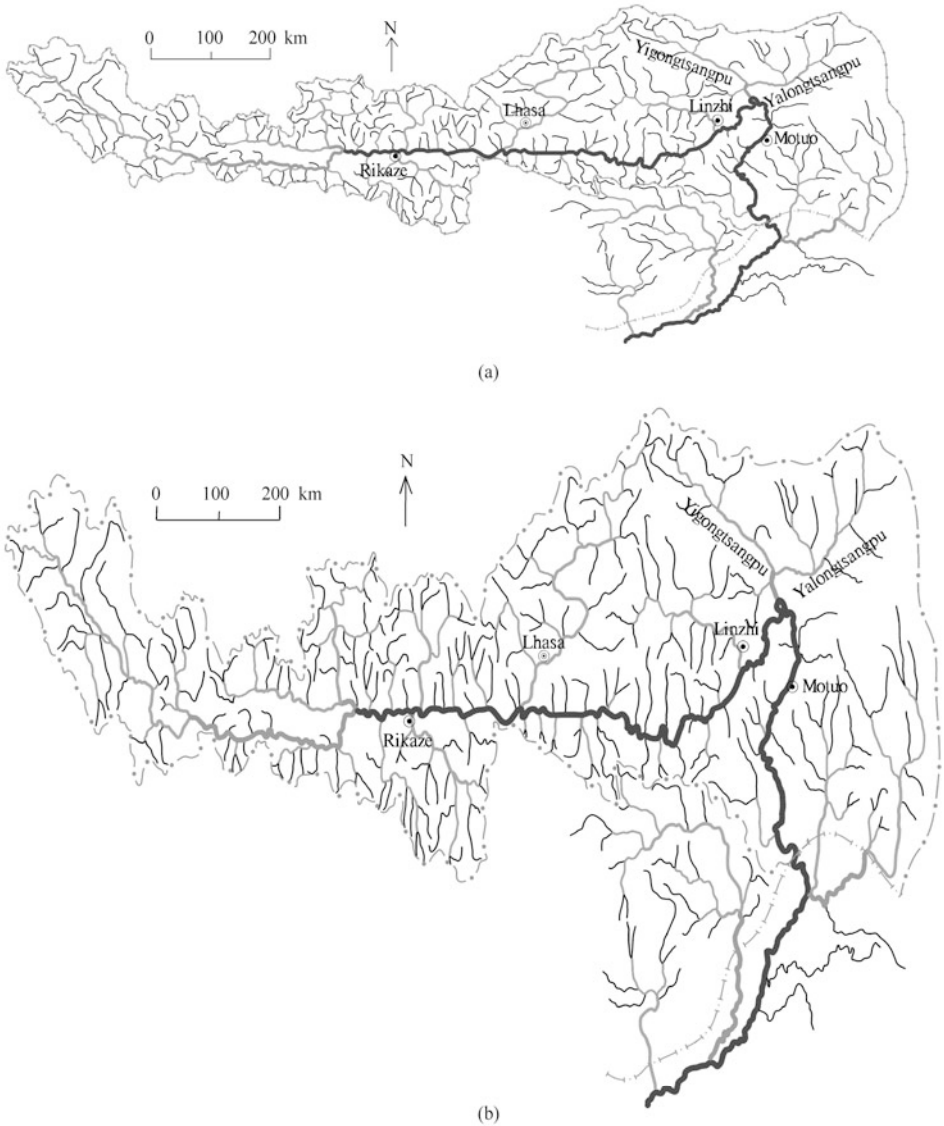
Fig. 11.25 (a) Stream network and drainage area of the Yalutsangbu River; (b) Conjectural drainage area of the Yalutsangpu River basin millions of years ago

The morphology of Yalutsangpu River watershed resulted from both geologic and morphologic processes. In the past millions of years the Indian continental plate was underthrusting the Himalayan crustal blocks in a relatively coherent and simple geometry (Ni and Barazangi, 1984). The Indian plate thrusts against the Eurasnia plate resulting in deformation of Yalutsangpu River watershed and uplift of the Himalaya Mountains. Figure 11.25(b) shows a conjectural drainage area of Yalutsangpu River millions years ago. The drainage area was not so narrow and slender but rather two dimensional, similar to a normal dentritic watershed. At present, the Yigongtsangpu and Yalutsangpu River flow in opposite directions and collide with each other at the confluence (Fig. 11.25(a)). Nevertheless, such a phenomenon of two rivers flowing in nearly the same valley but in opposite directions is by no means a result of morphological processes. Figure 11.25(b) shows the conjectural stream network, in which the two rivers (Yigongtsangpu and Yalutsangpu) flowed in different valleys. The thrust of the Indian Plate into the Eurasian Plate changed the flow directions and resulted in the present "opposite rivers."

11.2.2   Equivalency of Bed Structures and Bed Load Motion

Bed structures, such as step-pool systems, and bed load motion in rivers generate resistance to the water flow and consume energy. Bed structure and bed load motion are mutually replaceable in energy consumption and effect on fluvial processes. This is the law of equivalency of bed structures and bed load motion.

11.2.2.1   Energy Consumption by Bedload Motion and Bed Structures

Sediment particles carried by river flow have larger specific weight than water, and tend to settle down and stop motion. To maintain the movement of sediment particles, a force is needed to balance the submerged weight of the particles and prevent them from depositing. Bed load particles move in different ways depending on flow conditions and the size of the particles. One mode of bed load motion is by rolling and sliding on the bed, in which the submerged weight of particles is supported by the contact force. A second mode of bed load movement is by hopping or bouncing along the bed. Solid particles moving in this way is supported by dispersive force and is known as saltation load. Saltation load composes the major portion of bed load in intensive bed load motion.

The mechanism of the dispersive force is illustrated, in general, by the following example (Wang and Qian, 1985). As shown in Fig. 11.26, particle P located at point 1 at instant t_1 moves at a velocity, $\vec{V}$, relative to particle P_1, and it reaches point 2 at instant t_2 after collision with P_1 and its velocity changes to $\vec{V}'$. Such an abrupt change in velocity, both in magnitude and direction, because of collision, causes acceleration. The average acceleration during the time interval t_2-t_1 is

$$\vec{a} = \frac{(\vec{V}' - \vec{V})}{(t_2 - t_1)} = \frac{\Delta \vec{V}}{\Delta t} \tag{11.9}$$

According to Newton's second law, particle P must be subjected to action of a force. An average value of the force is given by

$$\vec{F} = M \vec{a} = \frac{M((\Delta \vec{V} \cdot \vec{i})\vec{i} + (\Delta \vec{V} \cdot \vec{j})\vec{j})}{\Delta t} \tag{11.10}$$

where M is the mass of the particle P, $\vec{i}$ and $\vec{j}$ are the basic vectors in the longitudinal and vertical directions, respectively. $\Delta \vec{V}$ and its two components are shown in Fig. 11.26. They represent the force $\vec{F}$ and two force components in the longitudinal and the vertical directions. The vertical component of the force is the dispersive force, which supports the particles and prevents them from depositing. The longitudinal component generates the resistance to the flow. The work done by the resistance is the energy consumption for the motion of one bed load particle:

$$e_P = \frac{M(-\Delta \vec{V} \cdot \vec{i})}{\Delta t} u_P \qquad (11.11)$$

in where u_P is the average velocity of the bed load particle, e_P is the energy consumption per time for one bed load particle. Because the horizontal vector component is against the flow direction, $-\Delta \vec{V} \cdot \vec{i}$ is positive. There are N bed load particles moving over the bed per area. The sum of e_P for all bed load particles, $N e_P$, is the total energy consumption of the water flow on bed load motion.
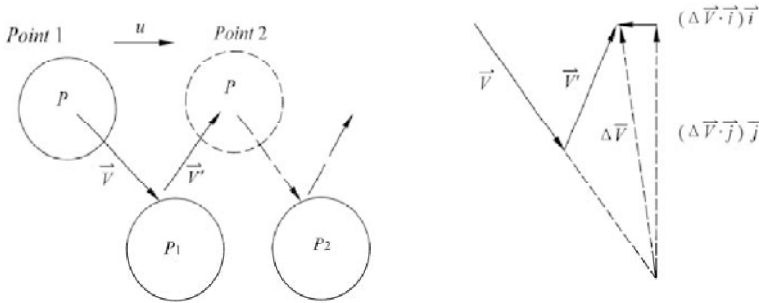
Fig. 11.26 The dispersive force as a result of collisions between moving particles

Almost all of the energy consumed during bed load motion comes from the water flow. The potential energy exerted on the bed by the water body is $P = \rho g h U s$, in which U is the average velocity of the water flow, ρ is the density of water, g is the gravitational acceleration, h is the water depth, and s is the bed slope. The bed load motion consumes a part of the water energy, thus

$$NM \frac{(-\Delta \vec{V} \cdot \vec{i})}{\Delta t} u_P = \beta \rho g h U s \qquad (11.12)$$

in which β is a coefficient. The equation may be rewritten as:

$$J_b = \beta s = \frac{NM}{\rho h} \frac{(-\Delta \vec{V} \cdot \vec{i})}{g \Delta t} \frac{u_P}{U} \qquad (11.13)$$

where J_b is the energy slope due to bed load motion. The rate of bed load transport per width is $g_b = g N M u_P$, thus J_b is proportional to the rate of bed load transport.

Bed load motion in river flow plays a role of protecting the bed from erosion. As shown in Fig. 11.27, particle P collides with the particles on the channel bed, which results in the dispersive force acting on the bed load particle. In the meantime the particles on the bed are acted upon by a reactionary force $\vec{F}$. The vertical component of the force, F_y plays an important role in protection of the bed from erosion. It is well known that the initiation of motion of sediment particles on the river bed is mainly related to the lift force of the flow. F_y counterbalances a part of the lift force, and, thereby, prevents the particles from entering into motion. With bed load movement increasing with increasing flow velocity, there comes an instant when the average value of F_y equals the lift force. The channel bed cannot be eroded further and the bed load motion reaches equilibrium. The bed load layer acts like a protective coating, which protects the bed against continuous erosion. The higher the flow velocity and the larger the tractive shear stress, the more the bed load and the thicker the protective coating, so that the channel bed can remain stable (i.e. not being continuously eroded) at different hydraulic conditions.

Bed structures create high resistance and consume flow energy. The energy consumption due to bed structures, such as step-pool systems, can be estimated using the formula of water head loss due to sand

dunes (Chien et al., 1998):

$$h_L = \alpha \frac{U^2}{2g}\left(\frac{\Delta}{h}\right)^2 \tag{11.14}$$

in which Δ is the height of the sand dune, and α is a coefficient. Chang (1970) found from his experiments that the coefficient α equals 1.9 and the exponent of (Δ/h) is not 2 but 1.8. If there are n sand dunes per length, i.e. $n = 1/\Lambda$, in which Λ is the wave length of sand dunes, the total water head loss per length is the energy slope due to sand dunes:

$$J_S = \frac{h_L}{\Lambda} = \alpha \frac{U^2}{2g\Lambda}\left(\frac{\Delta}{h}\right)^2 \tag{11.15}$$
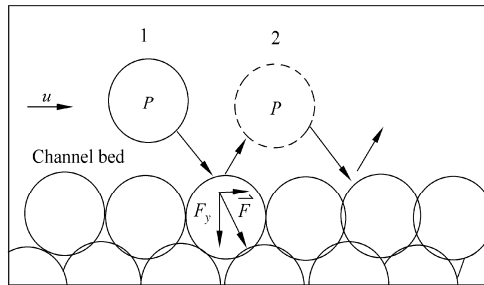
Fig. 11.27   Reactionary force on the bed particles resulting from bed load motion

For sand dunes in large rivers the ratio Δ/h is much smaller than 1. The water head loss, or the resistance, caused by the form drag of sand dunes is much larger than the resistance caused by the sediment on the bed. For instance, Simons and Richardson (1960) concluded from their experiments that the friction factor of ripples and dunes is 2–3 times the grain friction factor for sand of diameter of 0.28 mm, and the friction factor of ripples and dunes is 2–4 times the grain friction factor for sand of diameter of 0.45 mm.

In mountain streams with step-pool systems the resuistance reslting from the step-pools may be regarded as similar to that for sand dunes and Eq. (11.14) is applicable. The resistance resulting from step-pool systems, however, is much greater than that for sand dunes because the ratio of Δ/h is larger than 1. Most of the flow energy is consumed in the step-pool system. A step-pool system consumes the flow energy and also protects the bed sediment from erosion, which is similar to the protective action of bed load motion.

The potential energy exerted on the bed the water body is consumed to overcome the resistance created by bed structures and grain friction, and the remainder is consumed by bed load motion, thus

$$p = \rho g q s = \gamma q (J_S + J_b + J_g) \tag{11.16}$$

in which J_g is the energy slope due to skin friction of the sediment grains on the bed. In mountain streams, J_g is very small and often negligible. If a step-pool system develops well, such as the Jiuzhai Creek, the energy slope resulting from bed structures is so large as to be equal to the bed slope, s, and there is no bed load motion. If the bed structure is destroyed by a great flood or buried by sediment, J_b must be large enough to match the stream power. Therefore, intensive bed load motion occurs.

11.2.2.2   Relation of Bed Structures and Bed Load Motion in Rivers

Field measurements were performed in 15 tributaries of the Xiaojiang River during the flood season of

2008 and 2009 (Zhang et al., 2010). The rivers and measurement stations are shown in Fig. 11.28. Because the step height and step length are not regular, J_S cannot be directly measured. The development degree of the step-pool system, S_P, was used to reflect the effect of the step-pool system on the flow and bed load transportation. The rate of bed load transport per width of channel g_b, the stream power p, and the development degree of step-pool system S_P were measured at these stations. The rate of bed load transport was measured with a double box sampler, as shown in Fig. 11.29. The outer box was installed into the stream bed with its top edges even with the local bed surface. The size of the inner box was 0.5m×0.2m×0.2m. A steel-wire mesh was used at the bottom of the box to drain the water rapidly when the box was lifted out of the river. Wet weight of the collected bed load sediment was measured and the rate of bed load transport was calculated.

① Awangxiaohe R. ② Taojiaxiaohe R. ③ Xiaobaini R. ④ Dabaini R. ⑤ Xiaohaihe R. ⑥ Shengou Creek ⑦ Qingshui Gully ⑧ Hunshui Gully
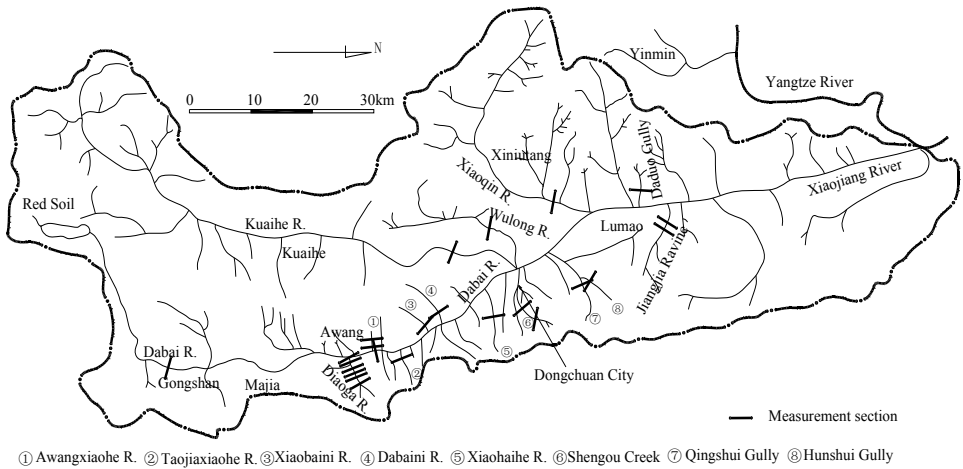
Fig. 11.28 Measurement stations on the tributary streams of the Xiaojiang River (in the upper Yangtze River basin)
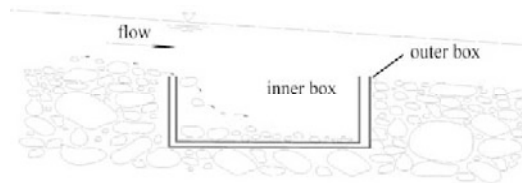
Fig. 11.29 Double box sampler of bed load

The development degree of the step-pool system, S_p, was defined in Chapter 3 and was measured with a specifically designed instrument shown in Fig. 3.28 and the value of S_p is calculated with Eq. (3.5). The energy slope resulting from bed structures, J_P, cannot be directly measured. Nevertheless, J_P may be represented by the measurable value of S_p. The larger is the value of S_p, the higher the energy slope resulting form bed structures J_P. Although the energy slope resulting form bed load motion is given by Eq. (11.7), the energy slope resulting form bed load motion, J_b, is not measurable as well, but is represented by the rate of bed load transport per width g_b. The higher is the rate of bed load transport, the larger is the energy slope resulting from bed load motion, J_b.

Figure 11.30 shows the Chaqing Gully, which flows into the Jiangjia Ravine, and the Hunshui Gully; which flows into the Daqiao River. The Jiangjia Ravine and the Daqiao River are both tributaries of the

Xiaojiang River from the river's right side. The measured stream power per width for the two streams were almost equal ($p = 9.2$ kg/ms for Chaqing Gully and $p = 10.16$ kg/ms for Hunshui Gully) and the sediments in the two rivers were from debris flow deposits. The sediments in the two streams had very similar size distributions, in which the median diameter in the Hunshui Gully was slightly larger, as shown in Fig. 11.31. Nevertheless, the rates of bed load transport in the two streams were extremely different. A step-pool system developed in the Chaqing Gully and the value of S_P was 0.155. The energy consumed by the step-pool system was quite high and the flow had no energy to carry bed load. Therefore, the rate of bed load transport was very low ($g_b = 0.0001$ kg/ms). Conversely, in Hunshui Gully where there was no step-pool system the measured value of S_p was small with a value of only 0.04. The flow energy was consumed mainly through bed load motion and the measured rate of bed load transport was $g_b = 18.9$ kg/ms, which was about 2×10^5 times higher than the value in the Chaqing Gully.

| (a) | (b) |

Fig. 11.30 Comparison of Chaqing Gully (a) and Hunshui Gully (b) (Chaqing Gully: $p = 9.20$ kg/ms, $S_p = 0.155$, $g_b = 0.0001$ kg/ms; Hunshui: $p = 10.16$ kg/ms, $S_p = 0.04$, $g_b = 18.9$ kg/ms) (See color figure at the end of this book)
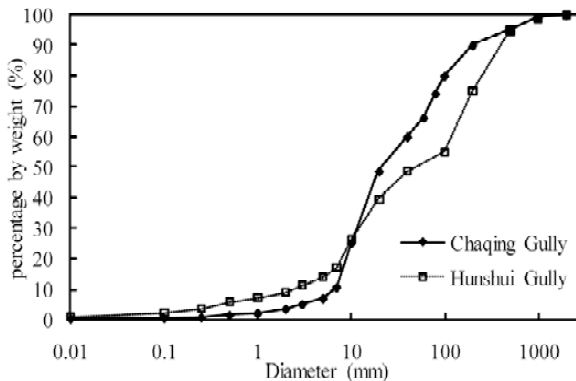
Fig. 11.31 Size distributions of bed sediment in the Chaqing and Hunshui gullies

A similar story occurred in the Awangxiaohe and Dabaini ravines. The measured stream power for the two streams was almost equal ($p = 2.6$ kg/ms for the Awangxiaohe Ravine and $p = 2.5$ kg/ms for the Dabaini Ravine). The sediment in both ravines was from debris flow deposits. A step-pool system had

developed for a long period of time in the Awangxiaohe Ravine, and therefore, the stream channel was stable and riparian vegetation developed well. The development degree of the step-pool system in the Awangxiaohe Ravine was measured at $S_p= 0.18$. Most of the flow energy was consumed by the step-pool system and the flow had no energy to carry bed load. Therefore, the rate of bed load transport was extremely low ($g_b= 0.00015$ kg/ms). On the contrary, there was no step-pool system in the Dabaini Ravine, and the measured value of S_p was very small ($S_p= 0.025$). The flow energy was consumed mainly through bed load motion and the measured rate of bed load transport was $g_b= 9.3$ kg/ms, which was about 60,000 times higher than the value in the Awangxiaohe Ravine.

Because the energy slope resulting form skin friction of sediment grains on the bed is negligible, for a given stream power a strong bed structure, or high value of S_P, is associated with low bed load transportation; and intensive bed load motion is associated with a low value of S_P. Figure 11.32 shows the measured rate of bed load transport as a function of S_P for different values of stream power. For a given stream power the rate of bed load transport reduced sharply with increasing S_P value. If the S_P value was smaller than 0.05, the bed load transportation was very intensive; and if the S_P value is larger than 0.35, the rate of bed load transport reduced to nearly zero.
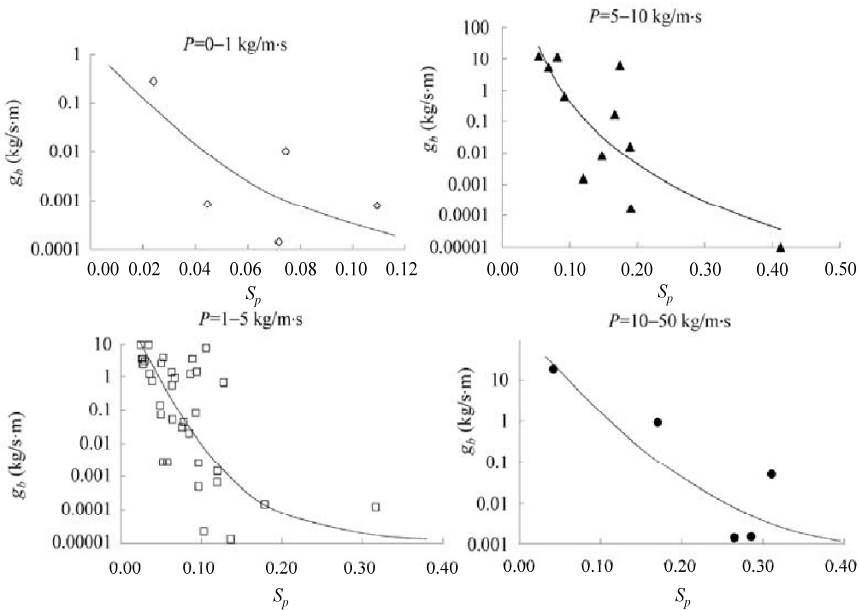
Fig. 11.32 Measured rate of bed load transport, g_b, in 15 rivers in the Xiaojiang River basin as a function of S_P for different values of stream power P

Equation (11.16) can be rewritten as

$$\frac{\gamma q J_b}{p} = 1 - \frac{\gamma q J_s}{p} \tag{11.17}$$

The energy slope resulting from bed load motion J_b is proportional to the rate of bed load transport, g_b, and the energy slope resulting from bed structures, J_S, is proportional to the development degree of the step-pool system, S_P. Although the relation between J_b and g_b and the relation between J_S and S_P are unknown, the ratio of bed load rate over stream power, g_b/p, may be expressed as a function of S_P. Figure 11.33

shows that the ratio of bed load rate over stream power, g_b/p, reduces with increasing S_P.
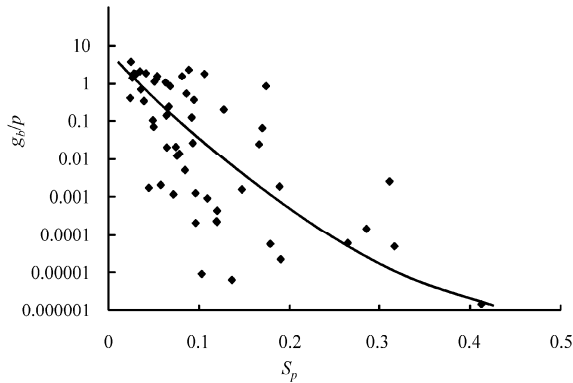
Fig. 11.33   The ratio of bed load rate over stream power, g_b/p, as a function of the development degree of the step-pool system, S_P

11.2.2.3   Experiment on Development of Bed Structures

Bed structures play a similar role as bed load motion in creating resistance, consuming energy of the flow, and protecting the bed material from erosion. Two kinds of experiments were done in the study. The first kind of experiments was done in the Jiangjia Ravine, in which three experiments were conducted (Liu and Wang, 2009, Liu et al., 2010). Figure 11.34(a) shows the experimental plot, which was on a debris flow deposit on the left side of the Jiangjia Ravine. Figure 11.34(b) shows the first experiment in which the water with loads flowed in the experimental channel and scoured the channel banks. After an intensive fluvial process the channel gradually became stable and reached equilibrium.
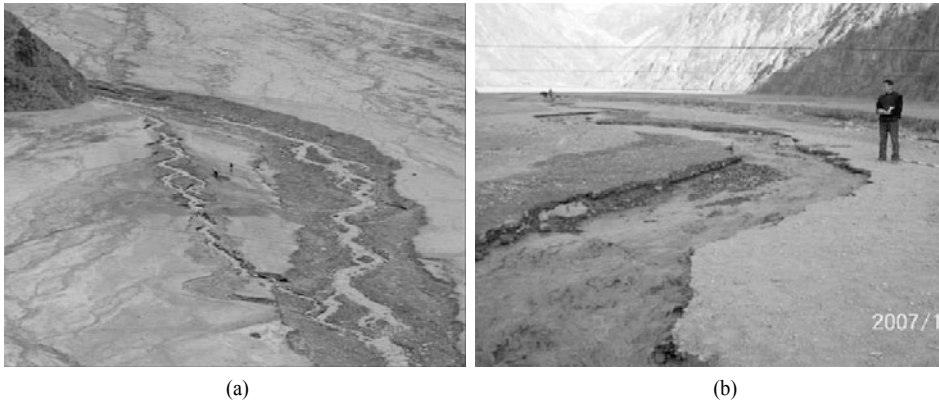
(a)   (b)

Fig. 11.34   (a) Experiment plot on the left side of the Jiangjia Ravine; (b) Water with loads flowed in the experimental channel and scoured the channel banks. (See color figure at the end of this book)

Figure 11.35(a) shows the original sediment size distribution of the experimental plot. The plot had various types of sediment including: silt, sand, gravel, cobbles, and boulders. Fine materials were mixed with cobbles and boulders, and, thus, the surface of the experimental plot looked smooth. The discharge was controlled by a small dam on the Jiangjia Ravine which consisted of boulders, cobbles and gravel. Figure 11.35(b) shows the flow discharge diverted into the experimental channel during the first experiment

(dashed line). The fluctuating discharge simulated the flood-low flow cycles. The duration of flood flow generally lasted 1–2 hours in the experiment. The rate of bed load transport was measured, which is also shown in Figure 11.35(b) (black pyramids). The total rate of bed load transport was very high during flood flow but low during low flow. The width of the channel varied in a range of 1–3 m along the course with an average of about 2 m. Therefore, the rate of bed load transport per width was about 3 kg/ms during flood flow, which was extremely high. The fluvial process and the bed deformation were very fast and generally reached a primary equilibrium after 6-10 hydro-cycles. The rate of bed load transport was still high in this case, which was equal to the incoming bed load. Because the incoming bed load was not controlled the measured rate of bed load transport fluctuated with fluctuation of discharge and incoming bed load.
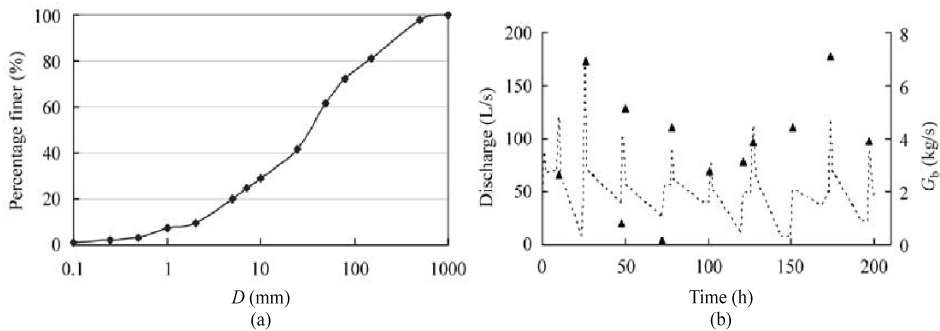
Fig. 11.35 (a) Original sediment size distribution of the materials in the experimental plot (debris flow deposit); (b) Flow discharge (dashed line) diverted into the experimental channel and measured rate of bed load transport (black pyramids) varying with time during the first experiment.

In the experiment, water was diverted from the Jiangjia Ravine and flowed back into the same ravine through the experimental channel. The experiment was conducted in a 60 m long lower section of the channel, on which 15 measurement cross sections were set. Between the experimental section and the upper section a 2 m long concrete flume was constructed for measurement of flow discharge with a velocimeter, which also acted as a base point for the measurement of the bed profiles. The bed structures, channel width and depth, erosion, sedimentation, and migration of the channel were measured at the 15 measurement cross sections.

Three experiments were done with different conditions. Figure 11.36 shows the bed profiles for the experiments. In the first experiment, bed load, suspended load and water were diverted though the concrete flume into the experimental section. The channel was scoured and widened but gradually reached equilibrium. The S_P value was measured at 0.08. The profile is shown in the figure marked with "With loads." In the second experiment, bed load was trapped in a pit at the upper end of the experimental channel and only water and suspended load flowed into the experimental channel. The channel bed was incised down until a bed structure similar to a step-pool system gradually developed. The bed incision finally stopped and the bed profile reached equilibrium (profile marked with "No bed load"). The S_P value was measured at 0.13 in this case. Before the third experiment, bed load again was allowed to transport into the experimental channel and the channel bed reaggraded because of bed load deposition. The S_P value reduced again to 0.08. The bed profile is shown in the figure marked with "Bed load". Then the third experiment started, no bed load was transported into the experimental section but the bed resistance was enhanced by constructing an artificial step-pool system. Artificial steps were constructed with cobbles 50–300 mm in diameter. The distance between two steps was 1–2 m. The S_P value was

measured at 0.11. No bed incision occurred in this case (profile marked with "Bed structure"). The bed profile with bed structure and the profile with bed load were almost the same, which implies that the bed structure played a similar role as bed load in affecting river morphology. Nevertheless, the artificial bed structure had different effects on cross sections compared with the effects that the bed load motion had on the cross sections. In the experiment with bed load motion the channel was not very stable and migrated slowly with moving meanders, but the experiment with artificial structures had relatively stable meanders.
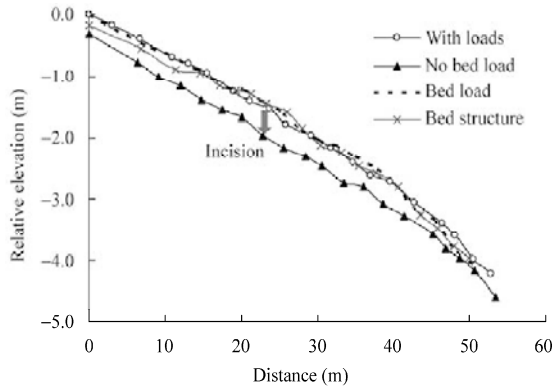
Fig. 11.36 Final bed profiles of the three experiments in the Jiangjia Ravine

In all three experiments, the suspended load was not controlled because it has little effect on the stream morphology. The concentration of suspended load at the beginning of the experiment was 16.7 kg/m^3 at the inlet of the experimental channel and 48.3 kg/m^3 at the outlet of the experimental channel, which implies that a lot of fine sediment was scoured and became suspended load during the channel development process. After the channel reached equilibrium the concentration was 22 kg/m^3 at the inlet and 25 kg/m^3 at the outlet, which implies that there was no intensive scouring in the experimental section.

11.2.2.4   Experiment of Destruction of Bed Structures

Development of bed structures, by nature or by humans, may control riverbed incision and reduce bed load transportation. Will the destruction of bed structures result in riverbed incision or intensive bed load motion? The second kind of experiment, conducted on the Diaoga River, Xiaobaini and Hunshui ravines, was designed to answer this question. It was very dry from January to May in 2010 and there was almost no rainfall in the Xiaojiang River basin. All flowing water in the streams was from ground water and spring water. There was no sediment supply from upstream reaches and tributaries because there had been no rain. The flow had to scour the bed and initiate bed load, or develop bed structures, to match the stream power. In April and May, bed structures, although not strong, have developed in all the streams and the bed load motion reduced to the minimum.

Before the second kind of experiment the *Sp* value of the bed structures, the stream power, the rate of bed load transportation and the size distributions of sediment were measured. Then, for each stream a 30 m-long section with a relatively regular structure and a generally low strength step-pool system, was selected. A few key stones for each step were removed and the structure was then destroyed. The flow velocity increased because of reduction in resistance. The bed sediment was scoured and the rate of bed load transport sharply increased. The diameter of the bed load particles also increased. The bed load motion and the bed structures were measured to compare with the values before the experiment. During the experiment the flow discharge

remained unchanged.

Figure 11.37(a) shows the size distributions of bed load before (B1-S and B2-S) and after (B1-R and B2-R) removal of key stones at two measurement sections, the size distributions of the mix bed sediment before (Bed material-M) and after (Bed material-R) removal of the key stones and the size distributions of the cobbles and boulder composing the steps (Bed structure). The mix bed sediment with the bed structures consisted of various sizes of sediment, including plenty of sand and fine gravel with diameter smaller than 10 mm, which was the main fraction of bed load. The sediment was stored in the pool sections and was protected by the steps, which consumed the flow energy and reduced the flow velocity. Figure 11.37(b) shows the size distributions of the bed load on the Xiaobaini Ravine (XB1-S and XB2-S) before the experiment at two measurement sections, the bed load after destroying the bed structures (XB1-R and XB2-R) at the two measurement sections, and the bed load on the Hunshui Ravine (HB-S) before the experiment and after removal of the key stones (HB-R). Similar to the results in the Diaoga River, the median diameter of bed load increased 2–20 times due to destruction of bed structures. Bed load coarsening was also caused by the destruction of bed structures.
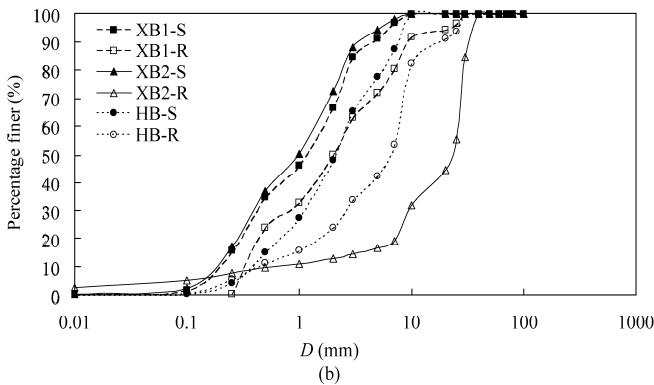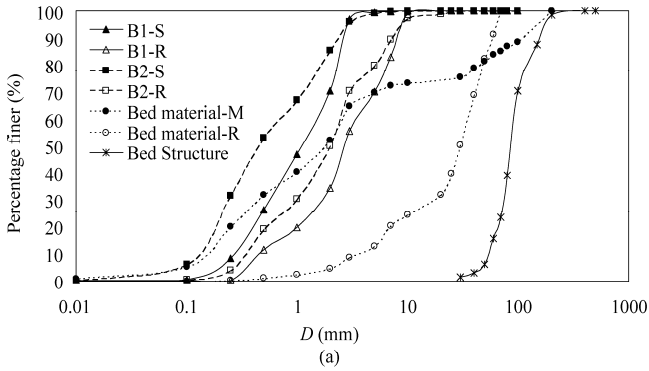
Fig. 11.37 (a) Size distributions of bed load before (B1-S and B2-S) and after (B1-R and B2-R) removal of key stones at two measurement sections, the size distributions of the mix bed sediment before (Bed material-M) and after (Bed material-R) removal of the key stones and the size distributions of the cobbles and boulder composing the steps (Bed structure) in the Diaoga River; (b) Size distributions of the bed load before (XB1-S and XB2-S) and after (XB1-R and XB2-R) destroying the bed structures on the Xiaobaini Ravine and Hunshui Ravine (HB-S and HB-R)

Figure 11.38 shows the changes in bed load transportation and S_p value after the removal of key stones of the bed structures on the Diaoga, Xiaobaini and Hunshui rivers. The S_p value decreased but the rate of

bed load transport increased about 100 times for the Hunshui and Xiaobaini ravines and about 10 times for the Diaoga River. The results prove that the effect of bed structures on the bed load transportation is reversible. In other words, the development of bed structures results in reduction in bed load motion and destruction of bed structure results in an increase of bed load motion. For a given stream power the functions of bed structures and bed load motion are mutually replaceable.
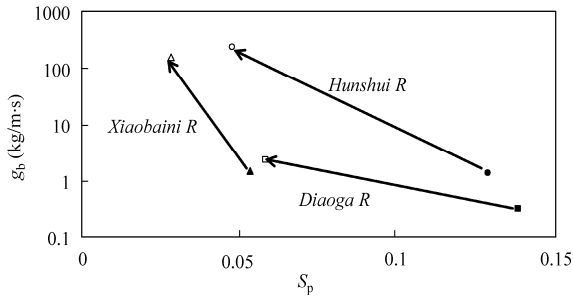
Fig. 11.38 Change of the rate of bed load transport g_b and the development degree of bed structures S_p due to destruction of the bed structures on the Diaoga, Xiaobaini and Hunshui rivers

11.2.2.5 Bed Structures Control Bed Load Motion

The Yalutsangbu Grand Canyon has the highest stream power p and strongest step-pool system. The step-pool system consumes most of the flow energy, therefore, there is no intensive bed load motion in the canyon. Figure 11.39 shows the bed profile of the Yalutsangbu River, in which five knickpoints are marked with numbers. The fourth and fifth knickpoints are the Grand Canyon, which is the deepest gorge in the world. Huge stones with diameter of 5–15 m overlapped and form huge step-pool systems.
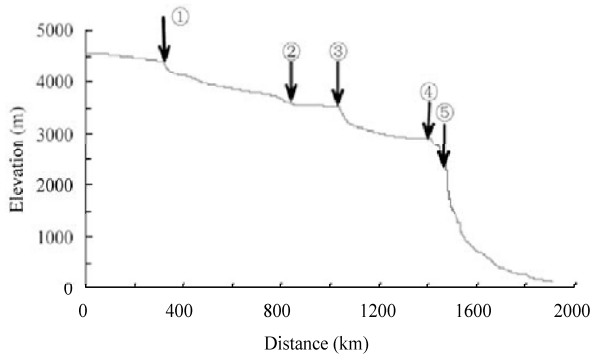
Fig. 11.39 Longitudinal bed profile of the Yalutsangbu River, in which numbers are knickpoints and Knickpoints 4 and 5 are the upper part of the Grand Canyon

The step-pool systems create high resistance to the flow and resulted in waves of height of several meters, as shown in Fig. 11.40(a). The waves consume a lot of energy and make great noise. The bed gradient is as high as 0.04–0.06, but the average velocity is only 3–4 m/s. Sand is carried by the flow as suspended load. Because the step-pool system balances the stream power there is no intensive bed load transportation. Therefore, no gravel and cobbles are transported through the grand canyon.

The plane view of the Yalutsangbu River upstream of the Grand Canyon looks like a lotus root, as shown in Fig. 11.40(b). Each narrow section is a gorge with high gradient bed consisting of step-pools.

Between the gorge sections are broad sections with gentle bed gradient. The authors studied the sediment in the broad sections and found that the sediment consists of gravel and fine sand. The maximum depth of the sediment is as large as 200–400 m. The gravel, with a diameter mainly from 10 mm to 200 mm, was not transported into the Grand Canyon but deposited in upstream broad sections. The step-pool systems in the canyon consumed the flow energy and protected the bed from erosion. Thus, the upstream sections are stable and a huge amount of gravel bed load is stored there. Figure 11.39(b) shows the Brahmaputra River in India, which is the downstream reach of the Yalutsangbu below the Grand Canyon. The riverbed consists mainly of sand rather than gravel, which proves that most of gravel bed load has been not transported through the canyon to India.

(a)

(b)

Fig. 11.40 (a) Huge step-pool system in the Grand Canyon (near knickpoint 4); (b) Brahmaputra River in India, which is downstream of the Yalutsangbu River below the Grand Canyon. (See color figure at the end of this book)

11.2.2.6   Application of the Equaivalency Law

The law of equivalency of bed load motion and bed structures is very useful. For instance bed load was

trapped by dams and weirs in the upstream reaches of the Rhine River and the river bed was incised by flood water. In order to prevent channel bed incision, German engineers have been feeding gravel to the river at a rate about 170,000 t/yr since 1978 (Kuhl, 1992). Nevertheless, engineers have difficulty to find enough gravel and the economic cost has become very high. According to the law of equivalency, the bed load may be replaced by bed structures. If a bed structure creates enough resistance the bed incision may be controlled and the water stage may remain stable.

The equivalency law may also be applied to control the riverbed incision of the Yangtze River resalting from the impoundment of the Three Gorges Reservoir. The middle and lower reaches of the Yangtze River have been scouring down by more than 10 m because most sediment has been trapped by the reservoir. The flood stage in these reaches has also been reducing. Figure 11.41 shows the measured bed cross sections of the middle Yangtze River at Baiyanghe, which is 88 km downstream from the Three Gorges Dam. The reservoir began to fill in 2003 and since then the middle reaches of the Yangtze River has been incising down. Compared with the cross section in 2002 the river bed has incised more than 10 m by 2008. The bed incision will continue if no measures are taken to control it.
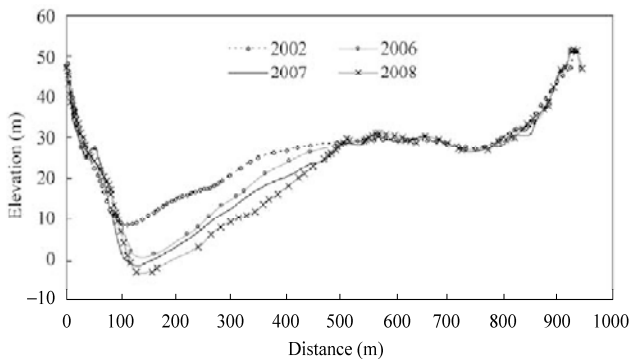
Fig. 11.41 Measured bed cross sections of the middle Yangtze River at Baiyanghe, 88 km downstream from the Three Gorges Dam (data from Sedimentation Panel, 2009)

A serious consequence of the riverbed incision in the middle reaches of the Yangtze River is the reduction of flood water diverted into Tongting Lake. The connection between the river and the Tongting Lake will be cut off or partly cut off, which may greatly impair the ecosystem. Tongting Lake has regulated the flood flow in the Yangtze River and has played an important role in flood control. Flood water flowed into the lake through Songzikou Channel, Taipingkou Channel, and Ouchikou Channel and flowed back to the river at Yueyang. Many fish species migrate from the great lake to the river for spawning and juvenile fish swim into the lake for feeding and growing. Nevertheless, the water and sediment diverted into Tongting Lake has been reducing due to riverbed incision, which was caused by cut-off of meanders in the 1960s, operation of the Gezhouba Reservoir since 1980, and filling of the Three Gorges Reservoir in 2003.

The problem riverbed incision may be solved by using bed structures. According to the law of equivalency of bed structure and bed load, the bed incision of the Yangtze River can be controlled by using roughness elements, such as tetrahedral frames. Tetrahedral frames were first introduced for protection of riverbanks against erosion. The tetrahedral frame is essentially hollow space frame consisting of 4 equilateral triangles. Experiments have showed that the velocity may be reduced by at least 50% around a tetrahedral frame in river flow, thus effectively controlling bed erosion (Tang et al., 2009). The velocity distribution can be changed and the velocity around the frame in the vicinity of the bed can be

greatly reduced. If enough such frames are put onto the river bed in the middle reaches of the Yangtze River, the flow energy consumption and bed protection effect of the frames is the same as if a lot of bed load is fed into the river. River bed incision will stop and flood stage will rise to the level before the dam. Therefore, the water diversion from the river into Tongting Lake will soon be regained and the migration of fish between the river and lake will be not affected. The effect of the human made "bed structure" on the navigation channel must be studied before application of this measure.

11.2.3   Sediment Budget—Size Distribution Method

The sediment budget studies the distribution of sediment in different parts of a river basin. The method deals only with the sediment amount without consideration of the transport mechanics. The International Association of Hydrological Sciences (IAHS) organized a symposium on the theme "Sediment Budget" in 1988. In selecting the theme, the organizers consciously chose a topic which draws on a wide range of research and which represents an important area of current interest (Bordas and Walling, 1988). As yet the study of the sediment budget is in its infancy and more research is required to develop the necessary monitoring and modeling strategies and to improve understanding of the processes involved. In the past many studies have focused on the erosion processes operating within a basin and sedimentation at its outlet. Now there is an increasing awareness of the need to integrate the two and to establish sediment budgets, which attempt to qualify the relations among the various components of the overall drainage basin erosion-transportation-deposition system.

Wang et al. (1997) studied the sediment budget and sediment demand of rivers. There are various demands for sediment, for instance, sediment mining for building material, land creation using sediment, maintaining river regime equilibrium, and preventing the channel bed from eroding. Both sediment yield and sediment demand need to be studied. Sediment budget studies balance between the yield and the demand and consider the disturbance to the balance by human activities.

11.2.3.1   Sediment Budget of The Yangtze River

Figure 11.42 shows the 6300-km long Yangtze River, which is the largest and longest river in China, with a drainage area of 1.80 million km². The figure also shows the locations of hydrological stations, meteorological stations, tributaries, riparian lakes, and debris flow areas. Below the map is the diagram of the water shed topography on an east-west line from Batang-to Chongqing-to Poyang Lake, showing the elevation of the basin from the origin in the west to the river mouth in the east. The Yangtze Basin has elevation varying from 5,000 m to 0 m with latitude from N25° to N35°. The river flows through the Qinghai-Tibet Plateau, Yunnan-Guizhou Plateau, Sichuan Basin, Three Gorges, Jiang-Han Plain, Lower Yangtze Plain, and pours into the East China Sea at Shanghai. From the source to Yichang (Three Gorges Dam site) is the upper reach, from Yichang to Hukou (Poyang Lake Mouth) is the middle reach, from Hukou (Wuhan) to Datong is the lower reach, and below Datong is the estuary.

In China, the Yangtze River is called Changjang (long river), with special names for different stretches: the lower reach and the estuary are called the Yangtze River; the middle reaches are called the Jingjiang River; the reach from Yichang to Yibin is called the Chuanjiang River, from Yibin to Batang is called the Jinsha River; and from Batang to the origin is called the Tongtian River (heaven river).

Investigation of the temporal and spatial variability of sediment transport within the upper Yangtze River catchment leads to the following paradox. There is evidence that the extent and magnitude of soil erosion across southern China has increased dramatically during the last 30–40 years (Smil, 1993; Wen, 1993; Lu and Higgitt, 1999; Edmonds, 1994). But there is no evidence of sediment load increasing at the Yichang Hydrological Station delivered from the upper Yangtze River catchment. Moreover, many studies have indicated that the total soil erosion from the upper reaches of the Yangtze River is around 2.2 billion

tons per year (Tang, 2004). But the sediment load measured at Yichang is only about 500 million tons per year. Thus, large volume of sediment is stored somewhere in the upper reaches.
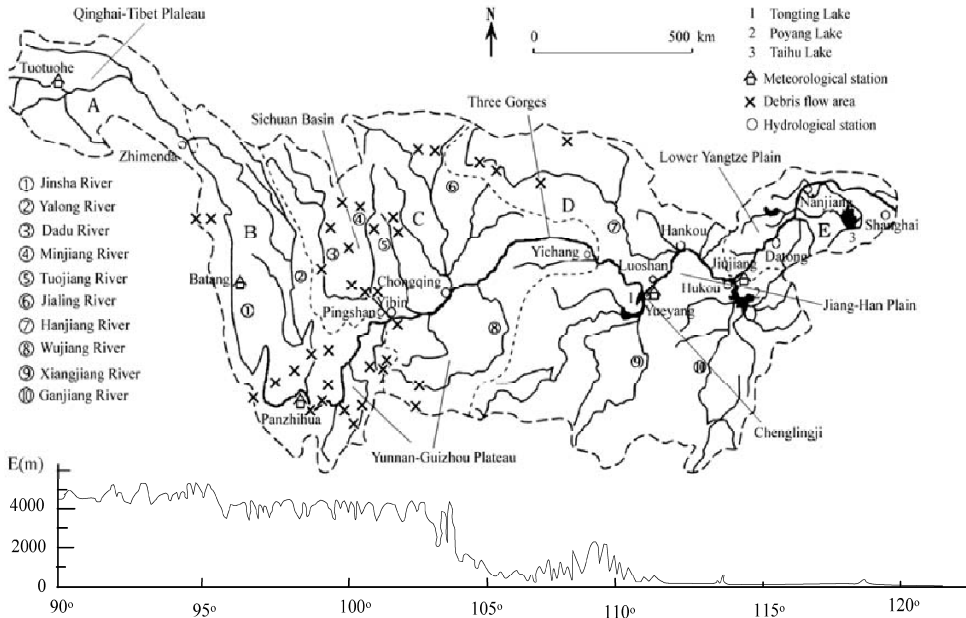
Fig. 11.42 The Yangtze River Basin, showing the locations of hydrological stations, meteorological stations, tributaries, riparian lakes, the debris flow areas; and the watershed topography on an east-west line from Batang through Chongqing and Poyang Lake to the East China Sea

Soil erosion, sediment load, and sediment storage have been measured and the data have been analyzed. There are many hydrological stations and numerous monitored cross sections and gauging stations on the river and its tributaries. Regular measurements are performed daily at the hydrological stations, including stage, velocity, discharge, suspended sediment concentration, and the rate of bed load transportation. The later is measured by using bed load samplers. Channel bed deformation is measured occasionally at all stations and at the monitored cross sections on the rivers, ravines, and gullies. The sediment load of the river is calculated with the flow discharge, suspended sediment concentration, and rate of bed load transportation. Because the bed load is less than 1% of the total load, the relatively large error in bed load measurement does not affect the accuracy of the total sediment load measurement. The volume of sediment deposition on the riverbed and reservoirs is calculated with the measured cross sections.

Soil erosion is measured in the following ways: (1) the soil erosion areas are determined by field investigations; (2) for each soil erosion area, the rate of sediment load transportation is measured at the downstream end of the small wartershed (generally several tens to a hundred square kilometers); (3) the rate of sediment erosion is calculated with the total load per year over the area of the watershed; or (4) the rate of soil erosion is directly measured by collecting the sediment eroded from a 100 m^2 sample plot, which is isolated by using low steel plate walls during rainfall; and (5) the amount of soil erosion from all small watersheds is summed to obtain the total amount of soil erosion from the basin.

The total amount of soil erosion from the upper Yangtze River Basin is reported at 1.6–2.24 billion tons per year, depending on the statistics. (Yu et al., 1991) evaluated the statistics and reported the total

soil erosion from the upper Yangtze River basin as 1.6 billion tons per year. (Tang, 2004) presented the value of 2.24 billion tons per year. Yu (2003) adopted the value at 2.179 billion tons per year. The Ministry of Water Resources reported the total soil erosion determined by remote sensing performed in 1990, which agrees with the value around 2.2 billion tons (ACRS, 1990). Table 11.2 lists the rates of soil erosion from different drainage areas of the upper Yangtze River basin presented by Yu (2003), in which the rate of soil erosion per area is the average value over the area of soil erosion but not over the whole river basin. The Jinsha and Jialing river basins are the main sediment sources for the Yangtze River. This book uses the figure of 2.179 billion tons per year as the total soil erosion for the Yangtze River basin.

Table 11.2   Rate of soil erosion from different drainage areas of the upper Yangtze River basin (after Yu, 2003)

Watershed	Area (km^2)	Area of soil erosion (km^2)	Soil erosion (mil·t/yr)	Percentage in total soil loss (%)	Rate of soil erosion per area (t/km^{2}yr)
Jinsha River (upper Yangtze)	488,900	223,800	829	38.04	3704
Jialing River	159,900	92,400	559	25.65	6043
Tuojiang River	27,800	14,800	92	4.22	6216
Minjiang River	135,400	5,800	253	11.61	4362
YangtzeRiver Pingshan-Cuntan	45,700	24,400	107	4.97	4385
Wujiang River	86,600	46,300	191	8.77	4125
Three Gorges Reservoir (Cuntan-Yichang)	61,100	36,500	148	6.79	4055
Total	1,005,400	496,300	2179	100	4390

11.2.3.2   Sediment Storage in the Upper Yangtze River Basin

The total soil erosion from the upstream reaches of the Yangtze River is 2.179 billion tons per year. But the long-term average suspended load at Yichang before the completion of the Gezhouba Dam- the first dam on the river—in 1980 was 514 million tons, with an additional sum of bed load of 9.54 million tons (sand bed load 8.78 million tons plus gravel bed load 0.758 million tons) (TGP Water Survey, 2005). The difference between the volumes of the total soil erosion from the upper Yangtze River basin and sediment load at Yichang is 1.655 billion tons. Thus there must be a huge amount of sediment stored in the upper river basin.

The Jinsha River basin is the main sediment source of the Yangtze River, with total soil erosion of more than 800 million tons per year. As shown in Fig. 11.42, there are many debris flow areas in the basin and the slope in the basin is quite high. Table 11.3 lists the sediment yield from several debris flow gullies measured at the downstream end of the gullies. The sediment yield per area from the debris flow

Table 11.3   Sediment yield per area from debris flow gullies in the upper Yangtze River basin

Debris flow Gully	Area (km^2)	Sediment yield per area (t/km^2·yr)	Period of measurement	References
Guxiang Gully	26.00	470,020	1964–1965	Wang and Zhang, 1985
Liuwan Gully	1.97	124,970	1963	Yang, 1985
Huoshao Gully	2.03	126,100	1973	Yang, 1985
Niwan Gully	10.30	65,500	1965	Yang, 1985
Hunshui Gully	4.50	374,240	1976–1978	Zhang and Liu, 1989
Jiangjia Ravine	48.60	142,200	1965–2002	MWRC, 2000

gullies is generally more than 40 times higher than the basin average. For example, the Xiaojiang River is a tributary of the Jinsha River (as shown in Fig. 11.28), which is 138 km long and has a drainage area of 3043 km^2. There are 107 debris flow gullies in this small river basin, among which the Jiangjia Ravine is the most well-known because of its high frequency of debris flow events, and they transport huge amounts of sediment into the Xiaojiang River every year. The sediment yield from the Jiangjia Ravine is 142,200 t/km^2.yr, of which only 2% can be transported downstream by the Xiaojiang River.

The sediment storage in the upstream watershed was studied by comparing the size distributions of sediments particles sampled from numerous tributaries, debris flow gullies, and the upper and middle reaches of the Yangtze River (Wang et al., 2007). Bed load is a main type of sediment transportation in mountain streams, which consists of coarse sand, gravel, cobbles, and even boulders. The size distribution of bed load from the Diaoga River, a tributary of the Xiaojiang River, is shown in Fig. 11.43. Measurement of the bed load and suspended load in the Diaoga River in the flood season from June to September 2006, demonstrated that the ratio of bed load to the suspended load in the four months was 21% to 79%, much greater than the ratio in the Yangtze River (2% to 98%). In fact, bed load transportation reduces from mountain streams to tributaries and from tributaries to the main stem of the Yangtze River. In other words, coarse particles are transported from mountains in low order streams and stop moving in high order streams because the bed slope reduces with increasing stream order.

Figure 11.43 shows the size distributions of sediment deposits in debris flow gullies and tributaries in the upper Yangtze River basin in comparison with the size distributions of suspended load at the Yichang and Datong Hydrological Stations (Kang et al., 2004; Xu, 2005; Wang et al., 2001; Xie et al., 2004; Wan et al., 2003). All the size distribution curves are averages of several tens of samples. Dividing the sediment into n-fractions with diameter in the ranges $D_1 \sim D_2, D_2 \sim D_3, D_3 \sim D_4,$ …in which the subscripts 1, 2, 3,… are the order numbers, let ΔP_i be the percentage of diameter within the range $D_i \sim D_{i+1}$. The amount of sediment depositing in the upper reaches, S_{di}, is given by:

$$S_{di} = S_{up}(\Delta P_i)_{up} - S_{down}(\Delta P_i)_{down} \qquad (11.18)$$

in which the subscripts up and $down$ represent the upper Yangtze River basin and the Yichang Station, e.g. S_{up} is the total sediment eroded from the watershed upstream from Yichang, and S_{down} is sediment load at the Yichang station.

A representative size distribution of the original sediment eroded from the upper Yangtze River basin can be roughly estimated in the following way: (1) Make an average for the size distributions of sediment deposits from the river beds and gully beds in the upstream basin, and denote it as Sa; (2) Because a part of the fine sediment has been transported as suspended load into the Yangtze River (23.6% of the total eroded sediment), the representative size distribution of original eroded sediment, Sm, should be given by taking this part into account and may be given by:

$$Sm = 0.764 Sa + 0.236 S12 \qquad (11.19)$$

where the coefficients are the ratios of sediment deposited and transported into the Yangtze River to the total eroded sediment, and $S12$ is the size distribution of suspended load at the Yichang station.

Figure 11.43 shows the representative size distribution curve Sm. At the Yichang station, gravel bed load composes only 0.15% and sand bed load 1.7% of the total load, the size distribution curve of suspended load can be approximately regarded as the size distribution of the total load. The amount of sediment storage of different size fractions in the gullies and tributaries can be calculated by using Eq. (11.18) and taking figures for the upper watershed from Sm and for the downstream section from the size distribution at Yichang:

For the fraction coarser than 0.5 mm, $S_d = 2179*0.528 = 1151$ million tons

For the fraction in the range $0.05 \sim 0.5$ mm, $S_d = 2179*0.226 - 514*0.35 = 313$ million tons

For the fraction finer than 0.05 mm, S_d = 2179*0.246 – 514*0.65 = 202 million tons

In other words, almost all the sediment coarser than 0.5 mm eroded from the watershed deposits in the gullies and tributaries of the upper Yangtze River basin; 313 of the 492 million tons of sediment of diameter in the range of 0.05~0.5 mm and 202 of the 536 million tons of sediment finer than 0.05 mm deposit in the gullies and the tributaries of the upper Yangtze River basin.
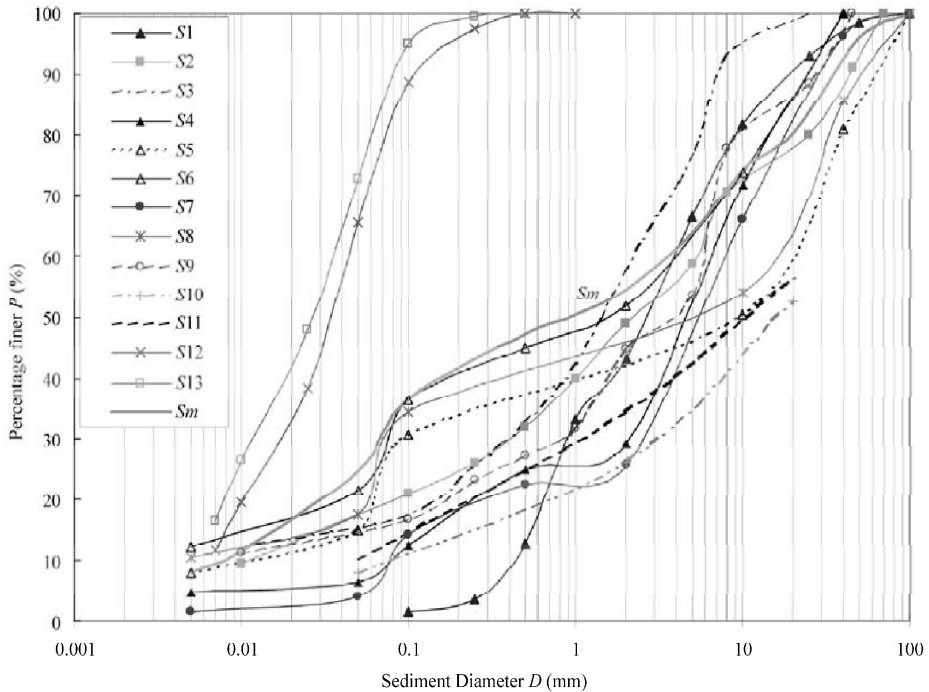
Fig. 11.43 Comparison of the size distributions of sediment deposits in debris flow gullies and tributaries in the upper Yangtze River basin with those of suspended load at the Yichang and Datong stations. (S1—bed load in the Diaoga River; S2—S11 are sediment deposits in gullies and tributaries: S2—Xiaobaini Ravine; S3—Dabaini Ravine, S4—Tongchangqing Gully; S5—Dade Gully; S6—Xiaohai River; S7—Jiangjia Ravine; S8—Daduo Gully; S9—Xiaojiang River; S10—Sunshui River; S11—Niuri River; S12—suspended load at Yichang; S13—suspended load at Datong; Sm—representative size distribution of eroded sediment from the upper Yangtze River basin)

Figure 11.43 also shows the size distribution of bed load from the Diaoga River, which is an average of 18 samples weighted with the rate of bed load transportation. The rate of bed load transportation in the Diaoga River is as high as 100 kg/m.min in flood season, which is much higher than that in the Yangtze River. Nevertheless, most of the bed load cannot be transported to Yichang but deposits in the gullies and tributaries in the upper Yangtze River basin.

11.2.3.3 Sediment Transported in the Yangtze River

Figure 11.44 shows the annual runoff and sediment load in the Yangtze River along its course. The annual runoff increases from upstream to downstream but the annual sediment load increases from the source to Yichang (the Three Gorges Dam site) reaching its highest amount of 514 million tons/year. Between Yichang and Luoshan the river flows out of the mountains and enters its alluvial reaches. The sediment load reduces from Yichang to Hankou (Wuhan) due to deposition.
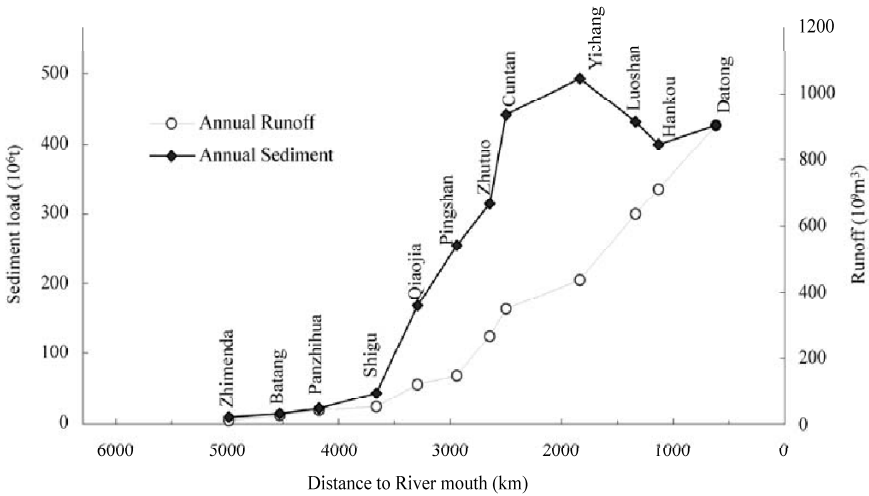
Fig. 11.44   Distribution of annual runoff and sediment load along the course of the Yangtze River (The points are the average value for the period of 1950–2000 with data measured at the stations)

The middle and lower reaches of the Yangtze River are alluvial and the sediment load varies in accordance with the sediment carrying capacity of the flow. Figure 11.45 shows the relations between the total sediment load and water discharge at the Yichang, Hankou, and Datong stations in different seasons. At Yichang (upper reaches), the sediment load is always proportional to the flow discharge because both sediment and water are from the upper reaches. At Hankou and Datong (middle and lower reaches), however, the sediment load is proportional to the flow discharge in the low flow season from October to June, but the load is not related to the discharge in the flood season from July to September. In the middle and lower reaches, sediment consists mainly of bed material load in the low flow season. The higher the flow discharge, the more sediment is eroded from the channel bed, and, therefore, the higher the sediment load. In the flood season, however, a lot of sediment is transported from upstream reaches but half of the water is from the middle and lower reaches. Sediment and water are from different reaches and a huge amount of sediment load is wash load, therefore, the sediment load is not strongly related to the flow discharge.
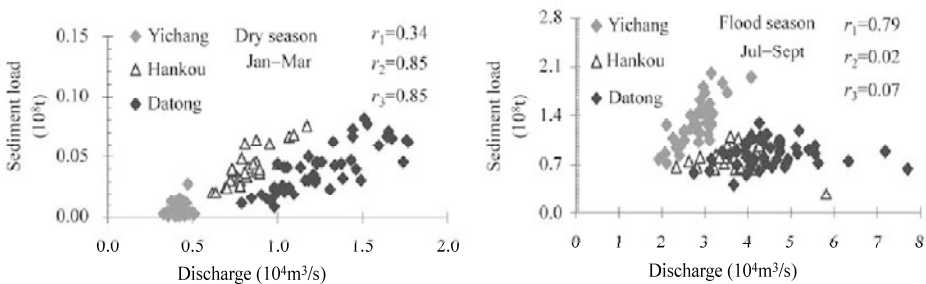
Fig. 11.45   Relations between the monthly sediment load and monthly average flow discharge at Yichang, Hankou and Datong in the low flow season (January to March) and the flood season (July to September) (r_n is the correlation coefficient of these relations)

11.2.3.4 Sediment Demand

The sediment demand in the Yangtze River consists of three components: (1) sediment needed for fluvial processes; (2) sediment mining for building material; and (3) sediment utilized for land creation. The fluvial process and lateral movement of the channel is now constrained by the grand levees in the middle and lower reaches of the river. Sediment deposition and erosion mainly affect the longitudinal profile of the river. In alluvial rivers there are no bed structures and natural knickpoints and the bed material consists mainly of sand. According to the minimum stream power theory, the morphology of alluvial rivers develops to reach the minimum stream power (Yang, 1996). This can be described by the following equation:

$$\frac{\mathrm{d}p}{\mathrm{d}x} = \frac{\mathrm{d}}{\mathrm{d}x}(\gamma s Q) = \gamma\left(Q\frac{\mathrm{d}s}{\mathrm{d}x} + s\frac{\mathrm{d}Q}{\mathrm{d}x}\right) = 0 \tag{11.20}$$

where Q is the annual discharge, γ is the specific weight of water, s is the bed slope and x is the distance down the river. The equilibrium bed slope can then be calculated with the following formula:

$$s_{n+1} = \frac{s_n}{Q_n}\left[Q_n - \frac{\Delta Q_n}{\Delta x_n}(x_{n+1} - x_{n-1})\right] \tag{11.21}$$

For the fluvial reaches of the Yangtze River (downstream from Yichang), the discharge increases along the course due to the inflow from tributaries; thus, the equilibrium slope decreases along the course. The river exhibits a concave downward riverbed profile, as shown in the measured profiles in 1971 and 1982 in Fig. 11.46. The fluvial process is developing toward the calculated profile (dashed curve). The inflow of water from the tributaries in the middle and lower reaches is reducing due to water diversion for economic development and agriculture. Assuming a reduction in the reach of about 10%, the equilibrium riverbed profile will be different as shown in Fig. 11.46 (solid curve). It is clear that the measured bed profile is developing toward the equilibrium profile.
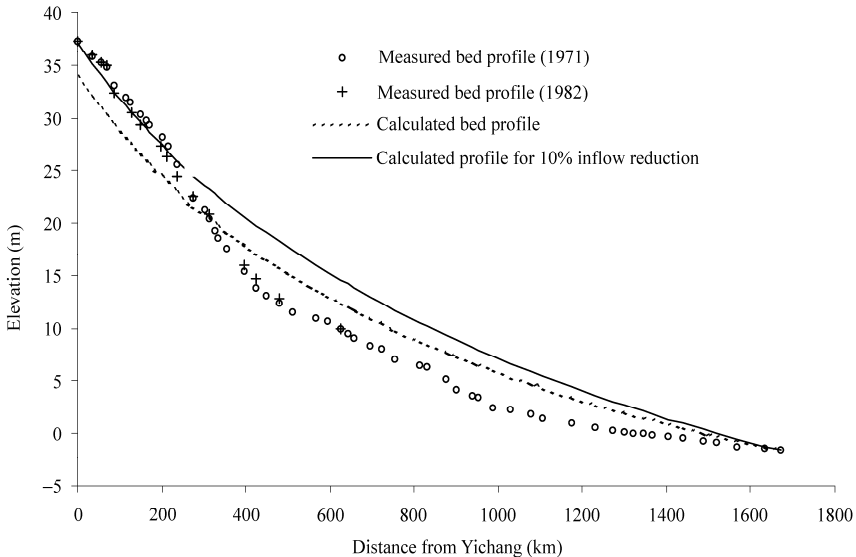
Fig. 11.46 Longitudinal bed profiles of the middle and lower Yangtze River in comparison with the equilibrium bed profile required to reach the minimum stream power. [Bed profile data from NDN-PLA (1983)]

The equilibrium bed profile is higher than the present profile and sedimentation dominates the fluvial process of the middle and lower reaches. Still a huge amount of sediment is needed for the riverbed to reach the equilibrium profile. Nevertheless, the volume of annual sedimentation in the middle and lower reaches depends on the incoming load. Figure 11.47 shows the relation between the net sedimentation (the volume of sedimentation minus erosion) and incoming sediment load from the upper reaches (measured at Yichang) and the Hanjiang River, in which the sedimentation in Tongting Lake is not included in the net sedimentation. The sediment load from Yichang and the Hanjiang River is more than 95% of the total sediment transported into the middle and lower reaches of the Yangtze River, to which the total incoming load refers in the following text. The net sedimentation in the middle and lower reaches increases linearly with the total incoming load. If the total incoming load is more than 280 million tons, sedimentation occurs in the river; if the total incoming load is around 500 million tons, 100 million tons of the sediment will deposit in the river. If there were no interruption by human activities, the fluvial process to reach the minimum stream power would continue for a long period of time because the present bed profile is still far from the equilibrium profile.
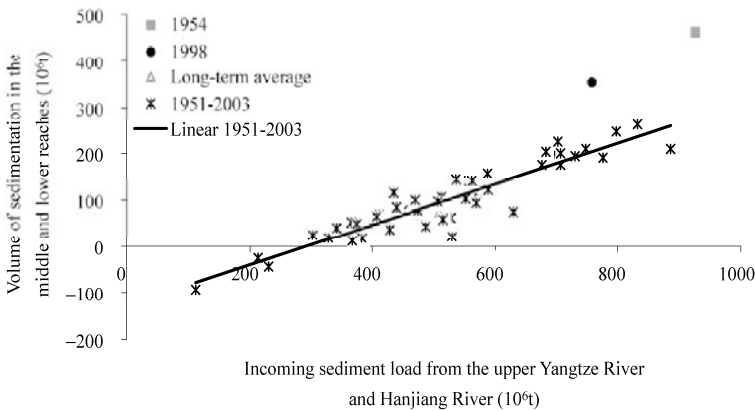
Fig. 11.47   Relation of the net sedimentation in the middle and lower Yangtze River with the incoming sediment load from the upper Yangtze River (measured at Yichang) and the Hanjiang River

Tongting Lake is between Yichang and Wuhan, and is used as a flood diversion basin in the flood season. If the sediment load at Yichang is more than 100 million tons, a part of the load will be carried into Tongting Lake and deposit in the lake. The amount of sedimentation in the lake is proportional to the incoming sediment load from Yichang. The sediment budget for the middle and lower reaches can be summarized in the following formulas:

$$S_Y + S_H = S_F + S_T + S_E \tag{11.22}$$

$$S_F = k_1(S_Y + S_H - S_{c1}) \tag{11.23}$$

$$S_T = k_2(S_Y - S_{c2}) \tag{11.24}$$

where S_Y is the annual sediment load at Yichang; S_H is the annual sediment load from the Hanjiang River; S_F is the amount of sediment depositing in middle and lower reaches in the fluvial processes, which may be positive (sedimentation) or negative (erosion); S_T is the amount of sediment depositing in Tongting Lake; S_E is the annual sediment load at Datong, which represents the sediment load entering the estuary; S_{c1} and S_{c2} are the minimum incoming sediment load for initiation of sedimentation in the middle and lower Yangtze River and Tongting Lake, respectively; and k_1 and k_2 are dimensionless coefficients. Statistical

analysis resulted in the values of k_1 and S_{c1}, and S_{c2} and k_2 as follows:

$$k_1 = 0.4316; \qquad S_{c1} = 285 \times 10^6 \, \text{t}$$

$$k_2 = 0.2905; \qquad S_{c2} = 105 \times 10^6 \, \text{t}$$

From Eqs. (11.22–11.24) and using the values of k_1, S_{c1}, k_2, and S_{c2} the following formula is obtained for the sediment load entering the estuary:

$$S_E = 0.2779 S_Y + 0.5684 S_H + 153.8 \times 10^6 \, \text{t} \qquad (11.25)$$

If the sediment load from Yichang and Hanjiang reduce to zero, about 150 million tons of sediment may be transported into the estuary and all the sediment is eroded from the middle and lower reaches.

Sediment mining has become an increasing sediment demand. In the 1990s, Yibin, Luzhou, and Chongqing (Wanxian City not included) mined 5.16 million tons of gravel and 10.14 million tons of sand from the Yangtze River for building material per year (Yi, 2003). It is estimated that the other cities on the upper Yangtze River including Panzhihua, Wanxian, and Yichang mined roughly the same amount of sediment from the Yangtze River. The total sediment mining from the upper Yangtze River is around 30 million tons per year. More sediment has been mined from the middle and lower reaches. In the early 1980s the annual mining from the middle and lower Yangtze River was about 40 million tons, this figure increased to 80 million tons in the late 1990s (Chen, 2004). The Yangtze River Conservation Commission issued a regulation in 2003 that the total sediment mining from the middle and lower Yangtze River is limited to 34 million tons per year (Shen et al., 2003). The amount of sediment mining has not really been reduced. The total capacity of sediment mining is about 6 times of the limit. Illegal mining is active. The amount of sediment mining from the middle and lower reaches is not less than 80 million tons. At present the total sediment mining from the upper reaches and the middle and lower reaches is estimated at 110 million tons per year.

The third sediment demand is for land creation in the Yangtze River estuary. According to the data from 1951–2002, about 433 million tons of suspended load are transported into the Yangtze River estuary annually, of which 45 million tons deposit in the reach between Datong and Xuliujing, 28 million tons deposit in the north branch (north of the Chongming Island), 4 million tons deposit south of the Chongming Island, 138 million tons deposit in the river mouth and increase the shelf, 180 million tons are transported into the Qiantang River estuary and deposit there, the rest is transported into the ocean, as shown in Fig. 11.48 (Wu, 2001).

Figure 11.49 shows the size distributions of sediment deposits (deposit-1 and deposit-2) at the Yangtze River mouth and the suspended load measured at Datong. The comparison between the size distributions shows that the percentage of sediment finer than 0.01 mm of the suspended load at the Datong Station is about 10% higher than those of deposits at the river mouth. In other words, about 10% of the fine sediment in the suspended load transported to the estuary does not deposit in the river mouth but is transported away into the ocean by tidal currents. In summary, of the total sediment transported to the estuary 45% deposits in the Yangtze River mouth for land creation, 45% are transported into the Qiantang River mouth and deposit there forming a sediment sill, and, only about 10% are transported into the ocean.

Land creation in the Yangtze River estuary is essential for the development of Shanghai. In the past 50 years the Yangtze River has created 800 km^2 of new land in the river mouth (Jin et al., 1997). The natural land creation speed has slowed down and does not meet the increasing demand for land. Various engineering measures have been and will be applied to accelerate land creation. The Shanghai government has an ambitious plan to create 1,000 km^2 land in the Yangtze River mouth in 20 years by using the sediment load. It is estimated that 300 million tons of sediment is needed every year for land creation.
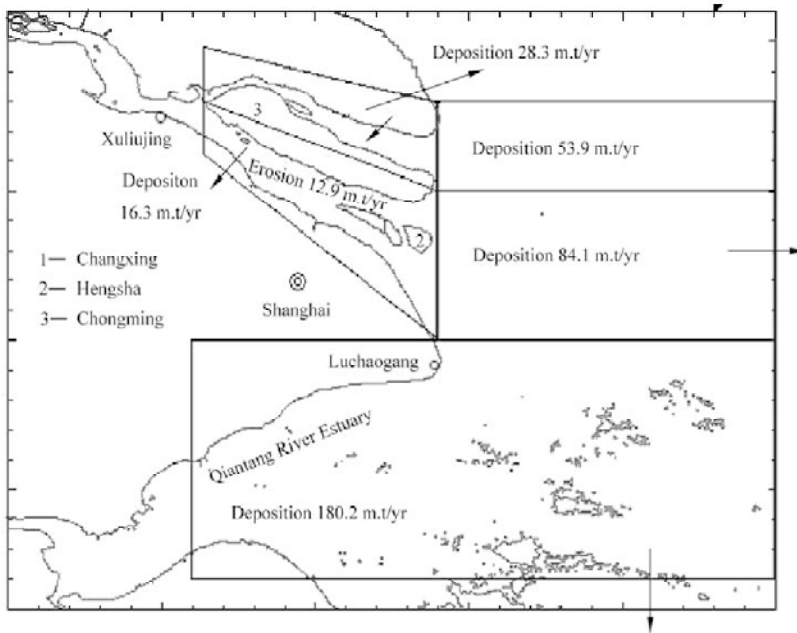
Fig. 11.48   Distribution of sediment deposition in the Yangtze River estuary
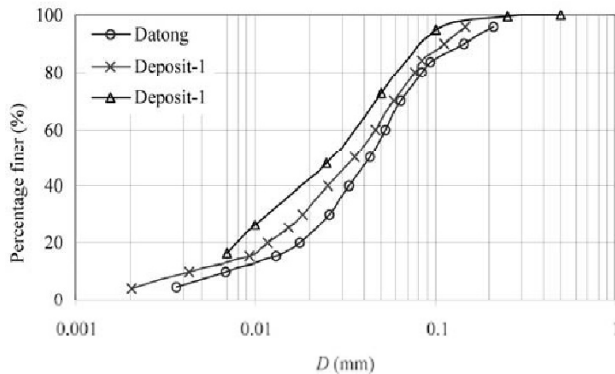
Fig. 11.49   Size distributions of sediment deposits at the Yangtze River mouth and suspended load measured at the Datong hydrological station

Sediment transported to the lower reaches and the river mouth is remarkably reduced and cannot meet the sediment demands of the river. Sediment shortage has become a new challenge to river engineers and sediment managers. The annual sediment load at Yichang has reduced from a long-term average of 514 million tons to 392 million tons since the mid 1980s and further has reduced to about 100 million tons in 2003–2004, and sediment load at Datong has reduced from 427 million tons to 327 million tons since the mid 1980s and further reduced to less than 200 million tons in 2003–2004. On the other hand, the total sediment demand is more than 300 million tons for land creation and building materials. There is a sediment shortage of about 100 million tons in the Yangtze River (Wang et al., 2007).

11.2.4 Sediment Budget Matrix

The difference between the amount of sediment erosion and sediment yield (sediment transported by river flow per drainage area) is great. Most of the newly eroded material from overland ares is deposited in the upstream gullies. A part of the deposited sediment may be eroded again. Therefore, erosion is a multiple event process and the amount of sediment erosion can be counted multiple times. A sediment budget matrix can be used to clearly show the amount of sediment in consecutive erosion processes:

$$B = \begin{bmatrix} E_1 & D_1 & T_1 \\ & E_2 & D_2 \\ & & E_3 \end{bmatrix} \tag{11.26}$$

in which E_1 is the annual amount of erosion due to landslide and avalanches per unit area, D_1 is the sediment deposited in the gullies after landslides and avalanches, T_1 is the portion of sediment transported by flowing water after landslides and avalanches, E_2 is the eroded sediment amount due to bank failure and gully erosion, D_2 is the sediment deposited in the gully and on the riverbed after bank failure and gully erosion, E_3 is the soil erosion from slopes. The total amount of erosion is given by:

$$E = E_1 + E_2 + E_3 \tag{11.27}$$

The sediment yield from a drainage area is defined as the annual sediment load over the drainage area. The sediment yield can be measured at the hydrological stations. The amount of sediment yield is much smaller than the amount of erosion because only the fine portion of the eroded sediment is able to be transported for a long distance by flowing water. In general, the sediment yield may be given by

$$S = f_1 T_1 + f_2 (E_2 - D_2) + f_3 E_3 \tag{11.28}$$

where f_1, f_2 and f_3 are sediment delivery ratios with values less than 1. The factors f_1, f_2 and f_3 can be determined by using the following formulas:

$$f_1 = F_1 (D < D_{84}) \tag{11.29}$$

$$f_2 = F_2 (D < D_{84}) \tag{11.30}$$

$$f_3 = F_3 (D < D_{84}) \tag{11.31}$$

in which $F_1(D < D_{84})$ is the sediment fraction in E_1 with diameter smaller than D_{84} of the suspended sediment sampled from the stem river at hydrological stations; $F_2(D < D_{84})$ is the sediment fraction in E_2 with diameter smaller than D_{84} of the suspended sediment sampled from the stem river at hydrological stations; $F_3(D < D_{84})$ is the sediment fraction in E_3 with diameter smaller than D_{84} of the suspended sediment sampled from the stem river at hydrological stations; and D_{84} is the diameter of the sediment particles which is larger than or equal to 84% of the sediment. Moreover, if f_1 and f_2 are known, f_3 may also be determined with Eq. (11.28).

In general, E_1 is much greater than E_2 and E_3 by an order of magnitude or more difference. Nevertheless, E_1 is extremely high in some individual years, but is zero in most years, as shown in Fig. 11.50. E_3 is continuous and fairly stable. E_2 fluctuates but is not intermittent, like E_1.

The values of the components in the matrix B may be determined by field investigation, measurement and analysis of satellite images and digital topographical maps. Selection of a typical small watershed is important, it should be one of the high soil erosion watersheds. The scale of the watershed is large enough to have all types of erosion. Figure 11.51 shows a small watershed in the upper Jialing River basin—the Liujia Gully watershed. The Liujia Gully is 6.82 km long with a drainage area of 11.76 km². The Liujia Gully is a second order stream and flows into the Yanzi River, which flows into the Xihanshui River. The Xihanshui River is in fact the upper Jialing River (the second largest tributary of the Yangtze River).
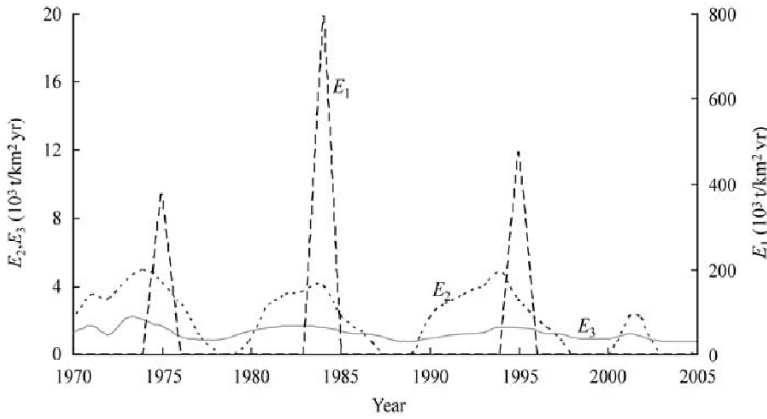
Fig. 11.50   Series of E_1, E_2 and E_3
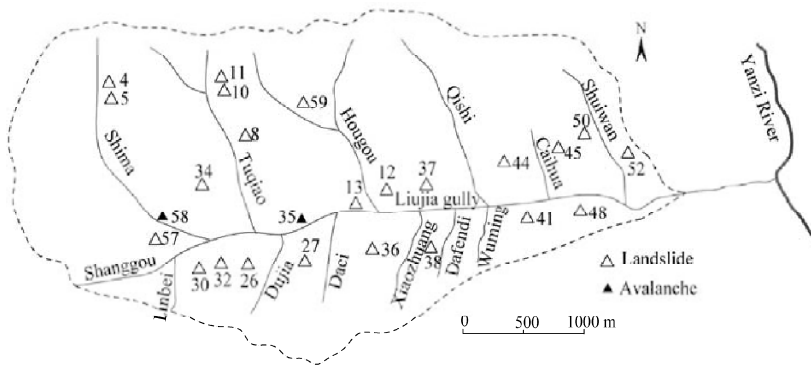
Fig. 11.51   The Liujia Gully watershed and the locations of landslides and avalanches in the period from 1960 to 2009

Field investigations and measurements were conducted in the Liujia Gully in 2008–2009. Twenty three landslides and 2 avalanches were found in the small watershed. These events occurred in the period from 1960 to 2009. The occurrence time of the events were determined by local records and talks with local residents. The volume of the landslides and avalanches was measured with laser rangefinders. The largest landslide had a volume of 9.9 million m^3 and the smallest landslide had a volume of 0.1 million m^3. The avalanches had volumes of 6800 and 900 m^3. The total volume of landslides and avalanches was 34.7 million m^3. Thus, the value of E_1 is 60,218 m^3/km^2yr. Only 4% of the deposits of the landslides and avalanches have been transported by flowing water, which means the value of T_1 is 2400 m^3/km^2yr.

The value of E_2 was determined by comparing the digital maps for 1984 and 2005. The eroded sediment amount due to bank failure and gully erosion was determined as 0.97 million m^3. Thus, the value of E_2 is 3900 m^3/km^2yr, of which a major fraction deposited on the river bed (D_2).

The value of E_3 was determined by using the fallout ^{137}Cs technique (Jia and Wang, 2010). More than 100 samples were taken from 10 sites and 20 hillslopes with a 10 cm diameter hand-operated core driller, each sample was 60 cm long and about 10 kg in weight. The ^{137}Cs activity was analyzed by gamma spectrometry using a BE5030 detector. The simplified mass balance model and the profile distribution model were used in calculating the soil erosion and deposition rates. The local ^{137}Cs reference inventories range from 1600 to 2402 Bqm^{-2}, and the average reference inventory is 2022 Bqm^{-2}. This indicates an

exponential decrease of mass concentration and inventory with depth down an undisturbed soil profile. The soil erosion in the watershed is moderate or intensive in cultivated land with the annual erosion rate in the range of 2000–6000 t/km²yr. In general ultra-intensive or intensive soil erosion occurs at the upper section of slopes, intensive or moderate soil erosion occurs at the middle section of slopes, and moderate or slight soil erosion occurs at the lower section of slopes. On the slopes with vegetation consisting of herbaceous and wood species the erosion rate is much lower or zero. On the lower section of slopes with well-developed vegetation, however, no erosion but deposition occurs with a deposition rate higher than 1000 t/km²yr. The slope gradient and vegetation cover affect soil erosion and deposition rates, and in general, the rate of soil erosion is proportional to the slope gradient and inversely proportional to the vegetation cover. On average the erosion rate from slope or the value of E_3 is about 2000 t/km²yr.

The values of $F_1(D < D_{84})$ and $F_2(D < D_{84})$ were found to be around 0.1, and the value of $F_3(D < D_{84})$ was about 0.8. The specific weight of the deposits was about 1.4 t/m³, therefore, the total sediment yield is:

$$S = 0.1T_1 + 0.1(E_2 - D_2) + 0.8E_3 = 2482 \text{ t / km}^2\text{yr}$$

The measured sediment yield per area from hydrological stations is about 2500 t/km².yr. On the other hand the total amount of erosion is

$$E = E_1 + E_2 + E_3 = 91,765 \text{ t / km}^2\text{yr}$$

The sediment yield is only a very small portion of the eroded sediment. The major portion of the eroded sediment is stored on the hill slopes and gully bed. Most of the total erosion is to the result of gravitational erosion and gully erosion, which play the most important role in the morphological process in upper river basins. The sediment load in rivers is only a small portion of the fine sediment. The annual load per area is the sediment yield, of which two thirds are from the slope soil erosion. The sediment load is the main driver of the fluvial process of the alluvial river section in the lower reaches.

The method of sediment budget matrix can be used for small watersheds and the results may be used to estimate the total erosion in the whole river basin. It may be derived that the total erosion in the Yangtze River basin is much more than 2.2 billion tons. The total erosion in the Liujia Gully is about 30 times higher than the sediment yield. If this conclusion is used for estimating erosion from the whole Yangtze River basin the total erosion would be more than 15 billion tons. The present estimation of the total soil erosion from the upper Yangtze River basin is only 2.2 billion tons because the erosion due to landslides and avalanches (E_1) is not included and the soil erosion is estimated by analyzing satellite images which is calibrated with direct measurement for small tributaries. For the calibration, measurements are performed at the downstream end of small watersheds and the amount of soil erosion from all small watersheds is summed to obtain the total amount of soil erosion from the tributary basins.

11.3 Methods of Integrated River Restoration

Integrated river management strategies are needed to achieve sustainable ecosystems that integrate hazard mitigation, power generation and social development. There are various river management issues: riverbed incision, and induced landslides and avalanches, soil erosion and debris flows, water diversion and pollution, dam construction and habitat loss, urbanization and flood hazard, sediment transportation and land creation, reservoir operation and ecological stresses, and fluvial processes and morphological development. On incised mountain rivers a well planned cascade of dams may effectively control riverbed incision while achieving power generation and habitat stabilization. A good habitat for benthic invertebrates should have stable streambed consisting of boulders, cobbles, or gravel. Mud and aquatic plants are also good substrate for invertebrates. Typical habitats for benthic invertebrates include mountain

streams with boulders and cobbles, bays by the river, riparian lakes and wetlands, and backwater and sluggish flow zones. Artificial step-pool systems may be used for integrated mountain stream management to achieve incision control, hazard mitigations and ecology improvement or restoration. Reforestation with selected wood species and diverse local understory species is beneficial both for soil erosion control and terrestrial ecology. If the pollution is controlled below a critical level, a river ecosystem consisting of diverse aquatic plants and benthic faunal communities may consume nutrients and organic pollutants and purify the water.

11.3.1   Hazard Mitigation, and Ecology Restoration With Artificial Step-Pool System

River bed incision causes bank failures, landslides, and debris flows on many rivers in southwestern China. The stream ecology is also seriously impaired due to lack of stable habitats. The Diaoga River is a tributary of Xiaojiang River, which is an upstream tributary of the Yangtze River (Fig. 11.52). It originates from Huangcaoling Mountain (elevation 2708 m) on Yunnan-Guizhou Plateau in southwestern China, prior to joining the Xiaojiang River (elevation 1490 m). The average gradient of the river bed is about 9.6%. This small mountain stream has a main channel length of 12 km and a drainage area of about 54 km^2. The basin lithology is generally comprised of shales, siltstones, and sandstones and the dominant plants includes eucalyptus, pine tree, sisal, chestnut and walnut tree.
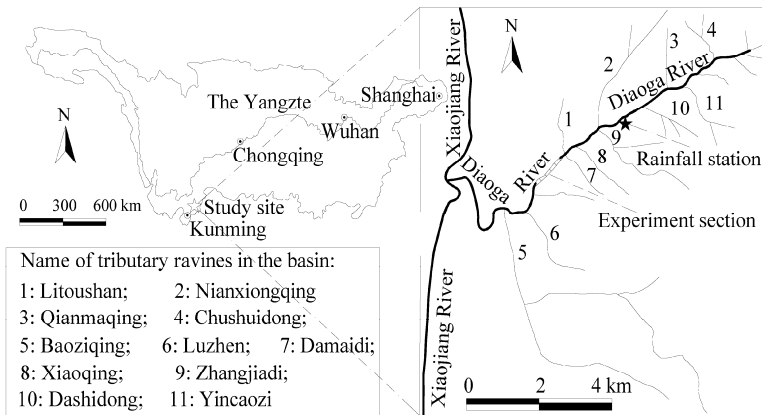
Fig. 11.52   Experiment location on the Diaoga River

The Diaoga River is seriously incised because of the high bed gradients. Bed incision has caused serious bank failures, slope and rill erosion, and induces landslide and debris flow events. The stream ecosystem is impaired and the aquatic habitats are frequently damaged or destroyed by landslides, debris flows, and intensive bed load transportation. The environment of the mountain stream has gradually degraded in recent decades. The average annual sediment yield is around 3000 t/km^2·yr (Lv, 2000). The annual average precipitation is about 1000 mm. Most of this falls as rain during the flood season mainly between July and August. Localized thunderstorms with precipitation intensities greater than 35–55 mm/day are common in summer. Sediment transportation in the stream is intensive because plenty of sediment is fed into the stream by landslides and debris flows. Human activities also increase soil erosion to some extent. In most river sections, there are no natural step-pools. The relatively uniform and homogenous stream habitat and bed instability provide poor habitats for benthic bio-communities and the stream has quite low biodiversity.

An experiment was conducted on the river for incision control, mitigation of landslides and debris

flow hazards and restoration and improvement of ecology with an artificial step-pool system (Yu et al., 2010). Step-pool systems are effective in dissipating flow energy and stabilizing riverbeds (Wilcox et al., 2006). This is achieved by increasing flow resistance (Aberle and Smart, 2003). In some instances, step-pool systems comprise more than 90% of the resistance, with grain resistance and channel form drag making up less than 10% of the total resistance (Curran and Wohl, 2003). A step-pool system on mountain streams is ecologically sound. Some studies have found that the richness and abundance of macro-invertebrates species are much higher in streams with step-pool systems than other streams without step-pools (Cereghino et al., 2001; Wang et al., 2009). Development of a step-pool system has become an important strategy for incision control and ecological restoration. A restoration project in Kleinschmidt Creek, Montana, USA, took steps to restore the aquatic habitat of trout and salmon (http://fwp.mt.gov/habitat/). Recent research has examined the design criteria and effects on ecology of step-pool system (Lenzi, 2002; Lenzi and Comiti, 2003; Todd and Mike, 2003; Weichert, 2005; Weichert et al., 2009). Field experiments found that morphological alterations, even if slight, may affect biological diversity and the presence of some specific taxa (Bona et al., 2008). Hence, artificial step-pools seem to provide a good trade-off between the need to limit channel incision whilst maintaining the functionality of aquatic ecosystems (Comiti et al., 2009).

The experiment was conducted in June 2006 on a 260 m long reach of the Diaoga River. The experimental reach is located at the middle of the river, controlling a drainage area of about 18 km^2. Design and construction of 24 artificial steps were based on the results of field investigations and flume experiments on step-pool systems. The artificial steps mimic the structure configuration and planform feature of natural steps developed in ecologically-sound mountain streams. The distance between these steps is about 5–12 m and the height of each is about 1 m. Large stones of diameter ranging from 0.2 to 1.5 m were laid overlapping with each other to act as a framework tightly interlocking the step structure with considerable stability. The experimental reach of the river and the constructed step-pool system are shown in Fig. 11.53.
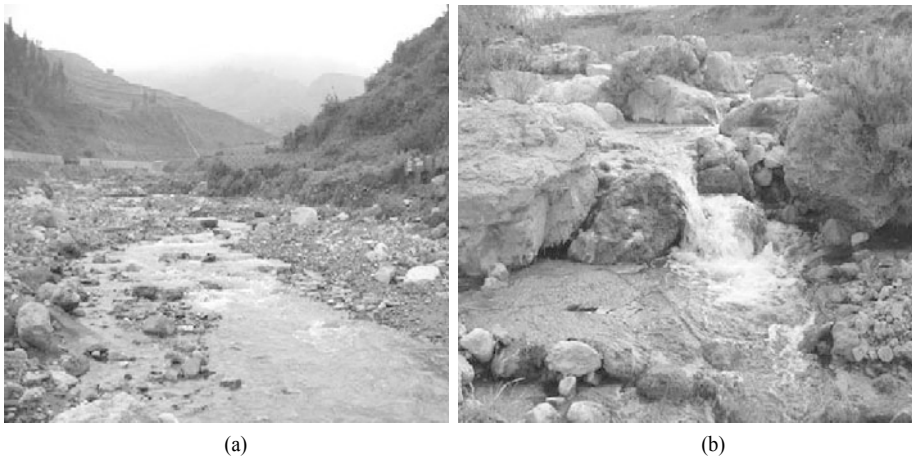
<div align="center">(a)   (b)</div>

Fig. 11.53 (a) Experimental reach on the Diaoga River (May 2006); (b) Constructed step-pool system on the river bed (March 2007) (See color figure at the end of this book)

The topography of the stream bed (the longitudinal profile and cross sections) and aquatic habitat environment (water surface area, substrate, flow velocity, and water depth) were monitored before and after the construction of the artificial step-pool system. In total, 46 cross sections were placed upstream of

steps, downstream of steps in the pools, and in the backwater zones, enabling the monitoring of siltation or erosion in the test reach. The cross sections and longitudinal profile were surveyed by an electronic theodolite. Figure 11.54 shows the monitoring reach on which 12 artificial steps are constructed.
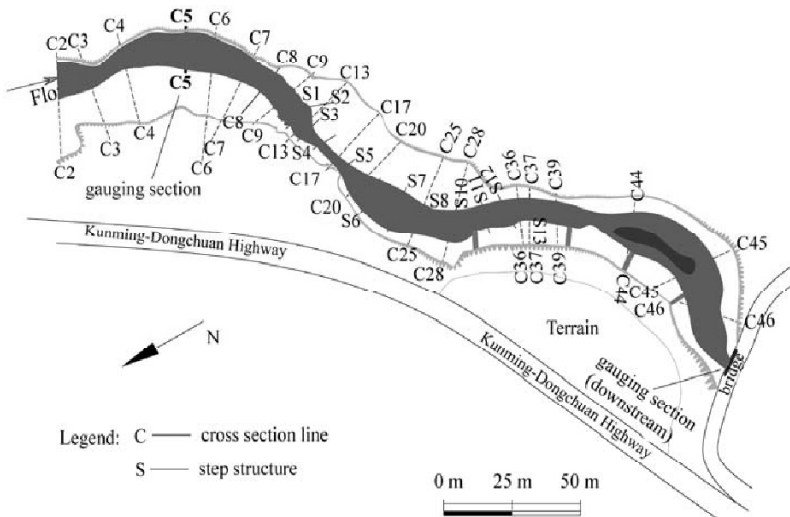
Fig. 11.54 Sketch of experimental reach and location of measurement cross sections

The long-term average rate of bed incision was estimated at 5 cm/yr before the experiment. A bridge was constructed 40 years ago and the bottom sill of the bridge became by 2.2 m over the river bed in 2006. Incision and scouring have been especially pronounced in some sections, not only inducing bank failure, landslides, and debris flow, but also causing damage to local infrastructure and aquatic ecosystems. After installation of the artificial step-pool system the streambed incision was effectively controlled (Fig. 11.55). At the initial stage the stream bed rose about 20 cm. In general, the most intense aggradation occurred upstream of steps, where the depth of siltation was 20 to 50 cm. This was mainly affected by the elevation difference between the stream bed and the crest of the step lip. Subsequently, the streambed gradually became stable. As a comparison, the reach downstream of the test reach continued to incise (Fig. 11.55(b) to (e)).

Figure 11.56(a) shows the bed elevation variation of a typical crosssection in the experimental reach before and after the installation of the artificial step-pool system. The crosssection was incised for about 0.7 m from June 2003 to June 2006, and threatened the road bed of the newly-built Kunming-Dongchuan highway on the right channel bank. After the artificial step-pools were installed, incision was stopped and a part of the channel bed silted up. Subsequently, the streambed gradually became stable. As a comparison the bed elevation of a cross-section located downstream of the test reach continued to incise as shown in Fig. 11.56(b).

The resistance caused by the step-pool system composes the main flow resistance. Manning's roughness coefficient, n, increases with the development degree of step-pool systems, S_P (Wang et al., 2009). In this experiment, S_P increased from 0.13 for the natural channel to 0.21 after construction of the artificial steps. The increasing S_P represents high dissipation of flow energy, thereby reducing bed-load transport, and protecting the bed from erosion. Figure 11.57 shows the velocity profiles upstream of an artificial step, on the step lip, and in a pool downstream of the step. Strong turbulence occurred in the pool, which acted as an energy dissipation pool. The flow energy was dissipated, and, thus, the flow could not scour
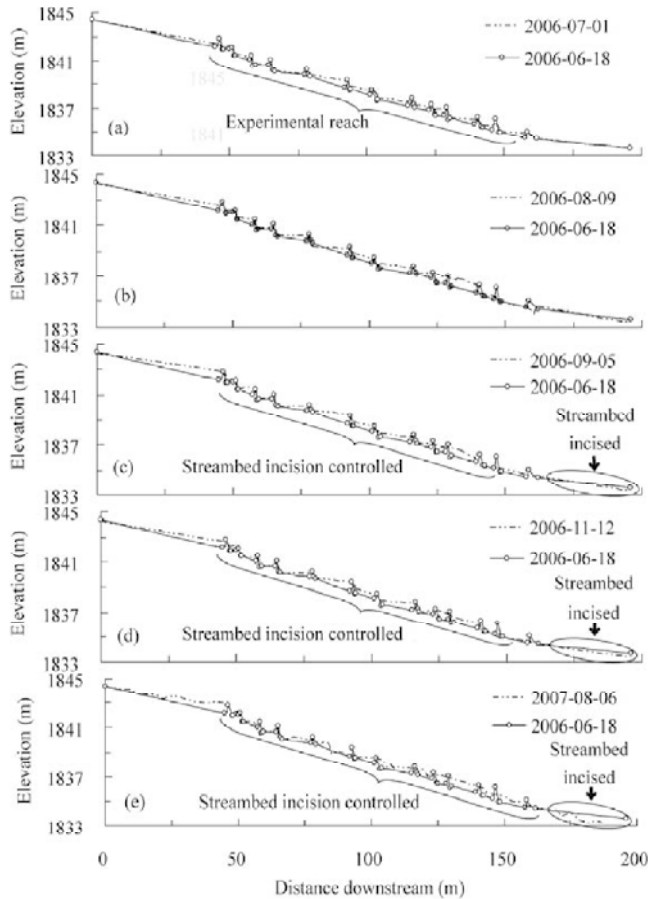
Fig. 11.55 Longitudinal bed profiles before and after the artificial step-pool system experiment in 2006 (a, b, c, d) and 2007 (e)
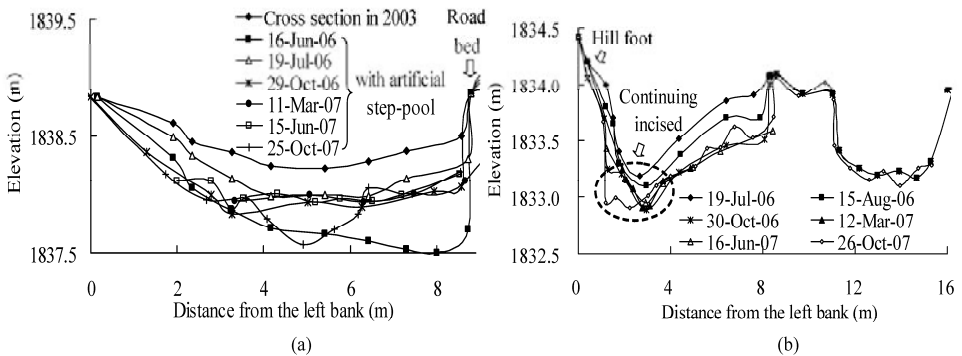
Fig. 11.56 (a) Bed elevation variation of a cross-section in the experimental reach with an artificial step-pool system; (b) Bed elevation variation of a cross section downstream from the experimental reach
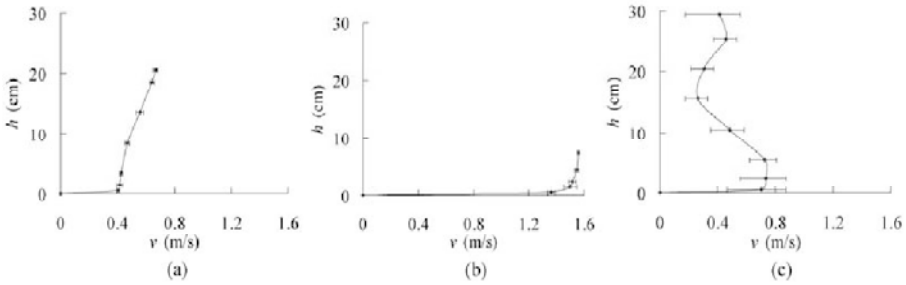
Fig. 11.57 (a) Velocity profile uppstream from a step, where flow depth was 0.22 m; (b) Velocity profile at the steplip, where the step was 0.8 m high and the flow depth was only 0.08 m; (c) Velocity profile in a pool which was 0.5 m downstream of the step with a flow depth of 0.3 m.

the channel bed (Wohl and Thompson, 2000; Wilcox and Wohl, 2007). Several debris flow events occurred after the artificial step-pool system was instand, but the debris flows have been reduced to hyperconcentrated flows when they passed the experimental reach. The high resistance created by the artificial steps caused great velocity reduction and sediment deposition. The pools were filled with the debris flow deposits. Nevertheless, the pools were partly restored after floods with low sediment concentrations.

Artificial step-pool systems create stable and diverse aquatic habitats. The habitat diversity index H_D (Table 11.4) distinct increased because of three primary aspects: (1) Water surface area is increased relative to the natural channel, enlarging the area of aquatic habitat (2) streambed substrate became diversified. Besides boulders, cobbles, and gravels in the natural condition, other substrates, such as silt, mud, and even organic debris and water moss also appeared on the bed, and (3) the range of flow velocity expanded. Before the artificial step-pool system the flow velocity was relatively uniform, typically from 0.4 to 1.0 m/s. After the installed artificial step-pool system, flow velocities differed much more in various zones. Surface flow velocity is low (0–0.2 m/s) in the sluggish water zone upstream of the steps. Near the step crest, velocity rises to 1.5 m/s, or even higher. Flow velocity in pools fluctuates intensively, as the water body entrains air bubbles, thereby increasing the concentration of dissolved oxygen. The biodiversity was greatly increased after the artificial step-pool system installed. The taxa richness, S, increased from 17 under natural conditions to 22–37 after the artificial step-pool system installed. The abundance increased from 62 ind/m^2 to 5217 ind/m^2 only nine months later, and the biodiversity index, B, also rose.

Table 11.4 Biodiversity and habitat diversity before and after the artificial step-pool system was installed

	Sampling date	H_D	S	Abundance (ind/m^2)	B	Dominant species (Density of individual invertebrate)
Natural channel	Jun 13, 2006	12	17	61.5	9.5	*Hydropsychidae (17), Baetidae (9), Haliplidae, Haliplus sp (7)*
With artificial step-pool system	Jun 28, 2006	22	37	881.5	11.3	*Baetidae (492), Simuliidae (150), Tipulidae, Antocha (65)*
	Sep 11, 2006	12	28	612.8	10.8	*Baetidae, Baetis (330), Baetidae, Baetiella sp. (70), Chironomidae sp 1 (57), Chironomidae sp 2 (48)*
	Nov 12, 2006	30	35	1087.5	11.7	*Baetidae, Baetis (445), Baetidae, Baetiella sp (257), Heptageniidae, Iron sp. (139), Hydropsychidae, Ceratopsyche sp. (66)*
	Mar 11, 2007	42	22	5217	10.4	*Baetidae, Baetis (3280), Chironomidae sp. 1 (1394), Chironomidae sp 2 (186), Chironomidae sp 3 (124), Baetidae, Baetiella sp (78), Grouvellinus sp (39)*

The artificial step-pool system provided stable habitat, therefore, some aquatic plant species colonized the stream bed, which made the stream green, as shown in Fig. 11.58. Under natural conditions before the artificial step-pool system was installed, the main species of benthic invertebrates sampled in the Diaoga River were *Hydropsychidae, Baetidae,* and *Haliplidae*. After the artificial step-pool system was installed, the dominant species were *Baetidae, Simuliidae,* and *Hydropsychidae*. Some species, such as *Caenis, Perlidae,* and *Limnephilidae,* which were not found in the stream before the artificial step-pool system was installed, colonized the habitat. Baetidae species feed mostly by scraping algae and fine particulate detritus from solid surfaces (Gui, 1994). Simuliidae often develop in running-water habitat and play an important role in the diets of other aquatic organisms, such as fish (Peter and Wang 1994). Hydropsychidae feeds by collecting organic detritus from running water (Glenn, 1994). The change of taxa richness and abundance of the dominant benthic invertebrates indicates that the aquatic habitat environment was more favorable to invertebrate development. Hence, the aquatic ecosystem of the experimental reach had been improved.

Fig. 11.58   The stream became green two years after the artificial step-pool system was installed

Artificial step-pool systems have been used for ecological restoration in many streams. However, the experiment on the Diaoga River was perhaps the first time a system was used integrating incision control, hazard mitigation, and ecology restoration. An artificial step-pool system on a mountain stream represents a return toward a more 'natural' condition that previously had a relatively heterogeneous physical structure that had been transformed to more homogenous conditions in response to accelerated rates of sediment flux induced by incision and land-use changes (Fryirs and Brierley, 2009). Alterations to the physical structure of the river modified process-forms relationships and associated sedimentation patterns, enhancing retention of pools along the study reach. Enhancement of physical conditions is a critical step in improving ecological relationships along the river (Brierley and Fryirs, 2008). Creation of step-pool sequences resulted in greater heterogeneity in the physical river structure, thereby providing multiple habitats for different species. This, in turn, resulted in obvious ecological improvements. Aquatic biodiversity has increased, with more species of benthic macro-invertebrates observed following construction of step-pools.

11.3.2   Debris Flow Control With Artificial Step-Pool System

11.3.2.1   Wenjiagou Landslide and Debris Flow in 2008
Artificial step-pool systems may also used to stabilize new drainage systems on landslides and control debris flows. The Wenjiagou Landslide, which was triggered by the Wenchuan Earthquake on May 12,

2008, buried the Wenjiagou Ravine and its tributaries underneath a thick landslide debris with a thickness of 20–180 m (read the disasters chains induced by landslides in Chapter 4). Figure 11.59 shows the area of Wenjiagou landslide deposit, the old Wenjiagou channel before the landslide and the new Wenjiagou channels developed during debris flows. The landslide deposit consisted of loose solid materials with different sizes, varying from huge boulders of several meters to clay of less than 0.01 mm in diameter. The boulders were mostly on the top layer of the landslide. The deposit had a porosity of about 30% and was liable to be eroded. Because the high porosity of the landslide deposit low intensity of rainfall water infiltrated into the loose material, and rainfall intensities higher than 30 mm/day triggered debris flows in 2008. A debris flow with a total volume of 0.9 million m^3 was triggered by a high rainfall intensity of 88 mm/day on September 23, 2008. The debris flows incised the landslide deposit and formed a 50 m deep channel, which was named new Wenjiagou. The debris flows transported solid material to the gully mouth and buried many farmers' houses. The new Wenjiagou was 1,400 m shorter and about 100 m higher than the old Wenjiagou, but the new channel was not directly above the old channel and about 150 m to the right of the old channel.
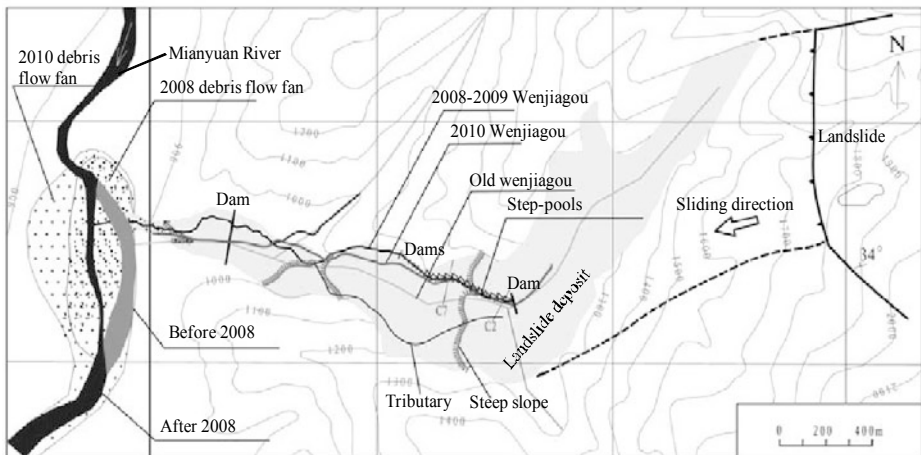
Fig. 11.59   Wenjiagou landslide deposit and old and new Wenjiagou channels (See color figure at the end of this book)

Figure 11.60 shows a cross section of the Wenjiagou valley before and after the landslide in 2008 at a distance of 1,500 m from the gully mouth. The thickness of the landslide deposit was more than 150 m. The central part of the deposit was higher than the two sides. Thus, two new channels formed after several debris flows in the wet season in 2008. The elevation of the landslide deposit on the right hand side (face from upstream to the downstream) was much lower than the central part and the left hand side. The main rainfall runoff flowed at the right hand side, and, thus, a deep and large channel formed on the right hand side, which became the new Wenjiagou channel. The new Wenjiagou had a drainage area of 4.50 km^2 and an average bed gradient of 0.18. It was 50m deep with bank slopes of 40~50°.

Figure 11.61(a) shows the longitudinal bed profiles of the old and new Wenjiagou channels and the profile of the landslide deposit. Figure 11.61(b) shows the new Wenjiagou channel after the debris flows in 2008, which was about 50 m deep. The banks had slopes at the repose angle of the loose solid materials. If a runoff in the new channel incised the channel bed, the loose solid material might slide down from the banks into the flow and form debris flow. Therefore, the new Wenjiagou gully was not stable. All water infiltrated into the loose solid bed for small rainfall intensity and debris flows occurred for rainfall intensity larger than 30 mm/day in 2008.
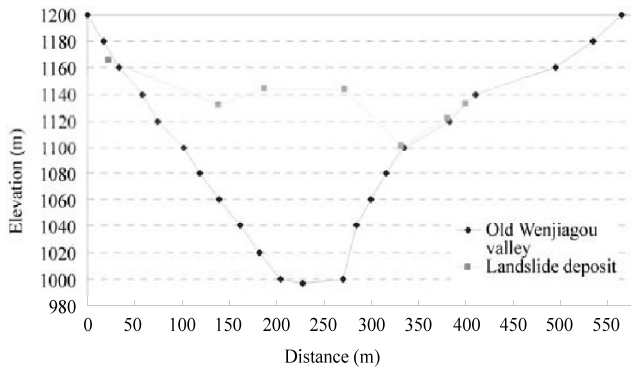
Fig. 11.60 A cross section of the Wenjiagou valley and the landslide deposit in June 2008
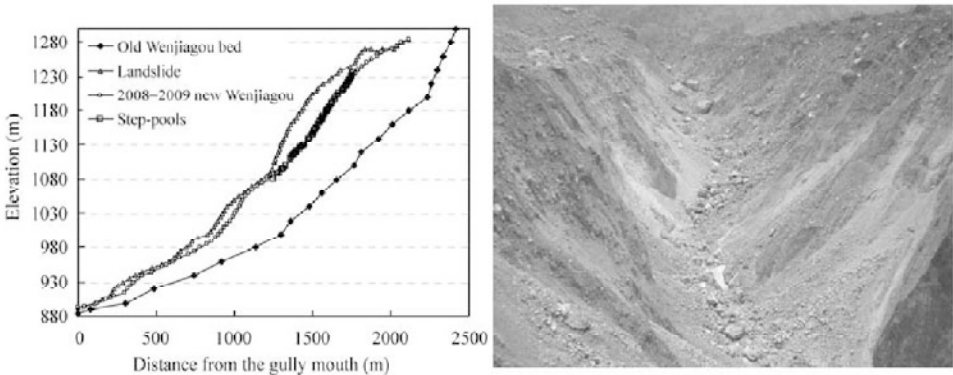
Fig. 11.61 (a) Bed profiles of the old and new Wenjiagou channels and the landslide deposit in 2008; (b) New Wengjiagou gully developed during debris flows on the landslide deposit (See color figure at the end of this book)

11.3.2.2 Artificial Step-Pool System in 2009

To stabilize the new Wenjiagou and mitigate debris flow hazard 33 artificial step-pools were constructed in a 400 m long section of the new Wenjiagou channel at a construction cost of only $ 0.03 million US dollars from May to June of 2009. Figure 11.62 shows the design of the steps with 2–4 keystones on the bed to form a step. Boulders and cobbles were placed interlocking with the keystones for high stability. Steel wire nets with cobbles and boulders inside were used to form two wings for protection of the two
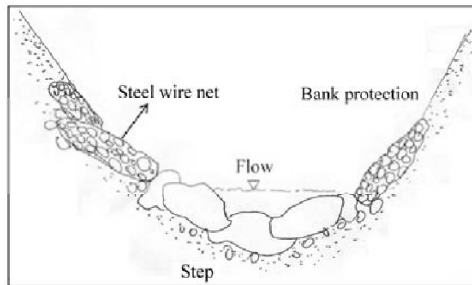
Fig. 11.62 Artificial steps with keystones on the bed and steel wire nets with cobbles inside to form two wings for protection of bank slopes

banks. There were no roads on the landslide deposit for any vehicles and machines. Only human labors could be used for construction of the step-pool system. There were many large boulders on the bank slopes of new Wenjiagou and they were moved from the slopes to the channel bed to become the keystones of steps, as shown in Figure 11.63 (a). Several huge boulders of more than 500 tones in weight were left on the channel bed after debris flows in 2008. Using the huge boulders as keystones more boulders of 0.5–1.5 m in diameter were placed around the huge boulders to form large steps of 2–4 m in height, as shown in Figure 11.63 (b). Although the rainfall intensity in 2009 was higher than 2008 only a small debris flows occurred and did not cause any loss of life and properties.

(a)   (b)

Fig. 11.63   An artificial step-pool system was constructed in June 2009 for stabilization of the new drainage system on the Wenjiagou Landslide: (a) Large stones with diameters larger than 1 m were removed from the banks of the new gully for construction of steps; (b) Large stones were placed together to form the artificial steps. (See color figure at the end of this book)

Step-pool system created high resistance and dissipated most of the flow energy in water falls on the steps and hydraulic jumps in pools. The flow was very turbulent with standing but broken waves and air bubbles. The turbulence intensity and fluctuation of flow were intensive but the mean flow velocity was not high because the kinetic energy of the flow had been transformed into turbulence. A lot of energy was consumed at hydraulic jumps. The dissipation ratio of the total energy (the sum of potential energy and kinetic energy) due to hydraulic jump may be calculated with the following formulas (Ni and Liu, 2008):

$$\eta_{hj} = 1 - \frac{h_d + \dfrac{q^2}{2gh_d^2}}{z_1 + h_1 con\alpha + \dfrac{q^2}{2gh_1^2}} \tag{11.32}$$

The parameters h_d, h_1, z_1, and α are given in Fig.11.64. q is the flow discharge per width, and g is gravitational acceleration. No measurement was performed in the step-pool system, which was too difficult and too dangerous. For torrential flood the parameters may be estimated based on observations:

$$q = 2 \text{ m}^2/\text{s}, \ h_d = z_1 = 1.5 \text{ m}, \ h_1 = 0.5 \text{ m and } \ \alpha = 30^\circ$$

Thus, the energy dissipation ratio of each hydraulic jump is equal to 0.42.

As shown in Fig. 11.65 the flow energy dissipated at the steps as well. Very strong turbulence occurs at the steps and generates a lot of bubbles and turbulent eddies. The energy dissipation at the steps was

similar to the energy dissipation at stepped spillway, which has been applied for energy dissipation at dams and has been studied by many scientists and engineers. The stepped spillway is designed to increase the rate of energy dissipation (Chanson, 2001) and the design engineer must predict accurately the energy dissipation. Following increase in discharge the flow on the stepped spillway develops from nappe flow into skimming flow. A characteristic feature of the skimming flow is the high level of free-surface aeration (Rajaratnam, 1990). Through the air-water interface, air is continuously trapped and released, and the resulting two-phase mixture interacts with the flow turbulence yielding some intricate air-water structure associated with complicated energy dissipation mechanisms (Chanson and Toombes, 2002, Carosi and Chanson, 2008).
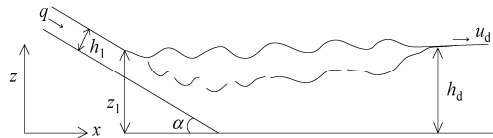
Fig. 11.64　Defination of parameters for hydraulic jump for flow from slope to horizontal channel
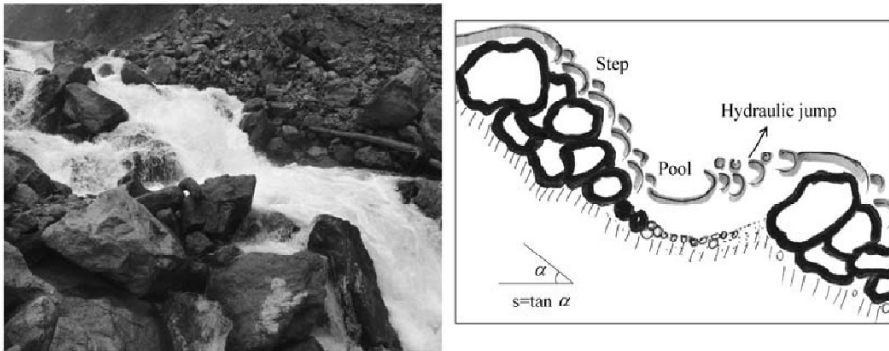
Fig. 11.65　Step-pool system dissipated flow energy in hydraulic jumps and steps and the energy was transformed into turbulence

The energy dissipation ratio at the stepped spillway η_{st} is given by

$$\eta_{sp} = \frac{E_0 - E_b}{E_0} \times 100\% \tag{11.33}$$

$$E_0 = H + \frac{u_0^2}{2g} \tag{11.34}$$

$$E_b = h_b \cos\alpha + \frac{u_b^2}{2g} \tag{11.35}$$

where E_0 is the total specific energy of the flow at the top of the stepped spillway relative to a reference plane; H is the height of the water surface on the top of the spillway relative to the reference plane; u_0 is the average velocity at the top of the spillway; α is the slope of the tangent of the spillway to the horizon; E_b is the total specific energy of the flow at the bottom of the stepped spillway relative to the reference plane; h_b is the water depth at the bottom of the stepped spillway; u_b is the average velocity at the bottom of the spillway. Experimental studies have been done by scientists (Shvainshtein, 1999; Lu et al., 2006).

An empirical formula was proposed for the dissipation ratio (Lu et al., 2006)

$$\eta_{sp} = 0.97 \exp\left(-4.08\frac{h_k}{h_t}\right) \times 100\% \tag{11.36}$$

in which h_k is the critical flow depth, and h_t is the total height of the stepped spillway or the sum of heights of the all steps of the spillway. For the case of the step-pool system, h_k/h_t was the ratio of the critical flow depth to the height of the steps, which was estimated at around 0.25. Then, the energy dissipation ratio on the steps was about 0.35.

The total energy dissipation ratio at step-pools η_{sp} is given by:

$$\eta_{sp} = 1 - (1 - \eta_{hj})(1 - \eta_{st}) \tag{11.37}$$

The total energy dissipation ratio at step-pools was calculated at 62.3%. Because the flow energy also consumed at boundary friction it may be deduced that less than one third of the flow energy could be used to carry solid particles. In other words at least three times high flow discharge was needed for initiation of debris flows after a step-pool system was constructed. In Wenjiagou, almost all rainfalls with intensity higher than 30 mm/day triggered debris flows in 2008. The step-pool system stabilized new Wenjiagou in 2009, and only a small debris flow with a volume of 0.02 million m^3 was triggered by a rainfall of intensity of 91.2 mm/day on July 17. It seems that the critical rainfall intensity for triggering debris flows was enhanced by 3 times by the step-pool system, which coincidently agreed with the conclusion from the energy dissipation ratio by step-pools.

Because the flow energy was dissipated by the step-pool system almost no bed incision occurred in 2009. Debris flows and sediment laden flows carried sediment from the upstream reaches unload the sediment in the step-pool section because the flow energy was not enough to carry the sediment further downstream. Thus, debris flows reduced to normal torrential floods with no any catastrophe. The pools were filled with the sediment. Nevertheless, low sediment load flows and clear water flows during the receding part of floods scoured fine sediment from the pools and partly recover the pools, as shown in Fig.11.66.

Fig. 11.66 Pool filled with sediment by the debris flows from upstream and partly recovered during low sediment load and clear water flows

Five rainstorms with rainfall intensity higher than 30 mm/day occurred in 2009, which were recorded by a rainfall meter in Wenjiagou. The step-pool system was partly damaged after each rainstorm. The research team repaired the damaged steps after the rainstorms. Only a small debris flow, with a volume of only 0.02 million m^3, occurred on July 17, 2009 triggered by a rainfall intensity of 91.2 mm/day. The small debris flow occurred at the downstream reach of the step-pools and caused no consequences.

As a comparison more than 20 debris flow events occurred in the gullies with no step-pool systems near Wenjiagou in 2009. Two debris flow events, each with a volume of more than 0.30 million m³, were triggered at the Heidongya Gully (7 km upstream of Wenjiagou) by rainstorms. The two debris flows dammed the Mianyuan River for two times. Another two debris flow events, each with a volume of 0.15 million m³, were triggered at the Yongjiagou Gully (2.5 km upstream of Wenjiagou) by rainstorms. Six debris flows occurred in the Xiaogangjian Gully (7 km downstream of Wenjiagou) dammed the Mianyuan River six times and cutoff the transportation from Mianzhu county to Qingping town to in 2009.

11.3.2.3 Check Dams in 2010

In 2010, however, the step-pool system was replaced with 20 check dams, of which two were main dams at the lower and upper end. The dams were constructed on the new Wenjiagou from Feberary to July in 2010 with a budget of $1.42 million US dollars. The keystones of the 2009 step-pool system were broken into small pieces of less than 0.5 m and used as building materials for the dams. The locations and lengths of the dams are shown in Figure 11.59. Most of the dams have a height of 6 m except for one main dam of 8 m high and two small dams of 3 m high. The base of the dams in the gully bed was 3 m. Figure 11.67 shows the design and construction of the dams. The lengths of the lower and upper main dams were 220 m and 84 m, respectively, and other dams had lengths of 20–27 m depending on the width of the channel. The distances between small dams were 20–40 m and the distance from the lower main dam to nearest small dam was 867 m and from the upper main dam to the nearest small dam was 68 m. The locations of the dams are shown in Figure 1.
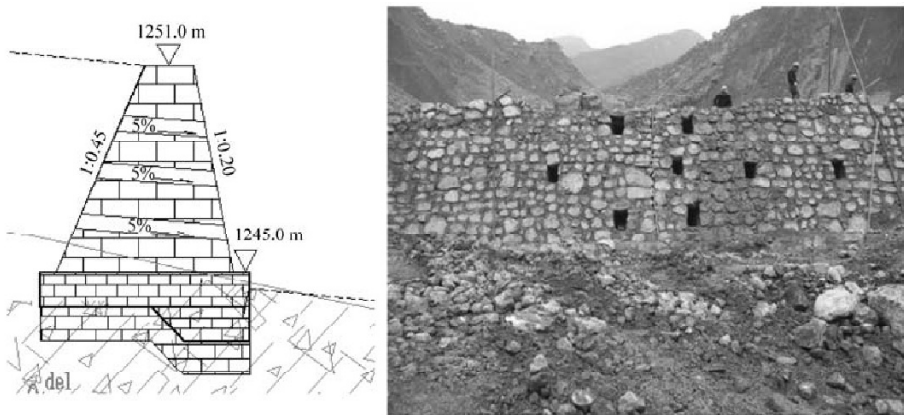
Fig. 11.67 Design and construction of the dams.

The dams were completed on July 28, 2010. On Aug.13 a rainstorm of intensity 98.5 mm/day at Wenjiagou initiated a debris flow with a volume of 4.5 million m³. All the 20 dams failed and the gully bed was incised by 50 m. The new Wenjiagou channel extended 130 m due to headwater erosion. As shown in Fig. 11.68, the flow energy was not dissipated but concentrated at the dams. Water flowed over the dams and scoured the base of the dams. Because the stones on the bed were removed and used for construction of dams, the bed was scoured down by torrential flood, which resulted in suspension of dams and caused dam failures. The bank slopes of the gully were at the repose angle of the loose solid materials. Bed incision increased the slope angle and resulted in bank failures. A lot of solid materials fell into the flow and mixed with water, and, thus, formed debris flows. Because the right bank of the gully was near the rocky mountain slope. The flow scoured the left bank while incised the bed, and the main

channel moved to the left side by about 80 m. The debris flow caused a great disaster, 14 people were killed and many new houses were buried.

There were different reports on the rainfall intensity triggering the large volume debris flow on Aug. 13, 2010, mainly because the rainfall intensity differed greatly in short distances. No systematic rainfall data at Wenjiagou were recorded, instead, several rain storms were measured with a rainfall meter installed on the roof of a farmer's house. It was reported on Aug. 13, 2010 that the rainfall was 98.5 mm at Wenjiagou, 227 mm at Xiaogangjian (7 km south of Wenjiagou), and 163 mm at Nanmugou (8 km, south of Wenjiagou) (Yu et al, 2010). Systematic rainfall data were obtained from the Mianzhu rainfall station, which were provided by the Mianzhu Weather Bureau. The distance from Mianzhu to Wenjiagou is about 50 km, but the rainfall at Mianzhu was only 6 mm on Aug. 13, 2010. Some people used 227 mm/day as the rainfall intensity for triggering the large volume debris flow in Wenjiagou.
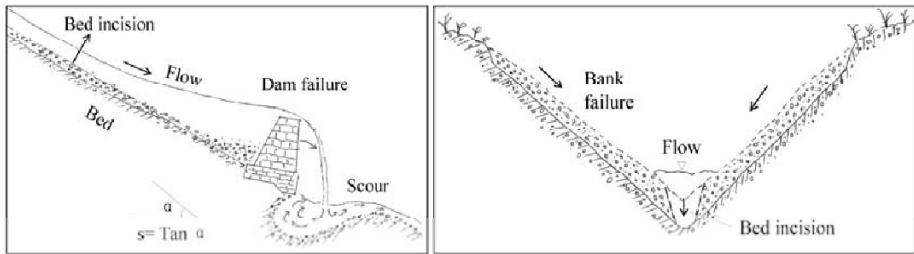
Fig. 11.68 (a) Water flowed over the dams and scoured the base of the dams causing dam failure; (b) Bed incision increased the slope angle and resulted bank failures, which resulted in debris flow

Let E_k denote the kinetic energy of a column of water flowing in the gully with a unit length in the flow direction. The height of the column is the water depth h, and the width is the channel width B. As shown in Fig. 11.68(b), the flow scours the channel bed and the loose solid materials on the two banks slide into the flow. Assume there is no sediment in the water column at position 1. As the flow travels a distance Δx to the position 2, h and B increase because a lot of solid materials have entered into the column. The kinetic energy of the flow column increases (or decreases) by ΔE_k :

$$\Delta E_k = \frac{1}{2}(M_2 u_2^2 - M_1 u_1^2) \tag{11.38}$$

in which M_1 and M_2 are the total mass of the water-sediment mixture in the column at position 1 and position 2, respectively; u_1 and u_2 are the velocity of the water-sediment mixture at position 1 and position 2, respectively. The kinetic energy increases due to release of potential energy of water e_1, and decreases due to the friction at the channel bed and banks e_2; the kinetic energy also increases due to the release of potential energy of solid materials e_3, and decreases due to the energy consumption in solid particles collisions during the transportation e_4. Thus,

$$\Delta E_k = e_1 - e_2 + e_3 - e_4 \tag{11.39}$$

The released potential energy of water flowing from position 1 to position 2 is

$$e_1 = \rho g h B S \Delta x = \rho g S h B u \Delta t = \rho g S Q \Delta t \tag{11.40}$$

in which ρ is the density of water, S is the bed gradient, Q is the discharge of water, and Δt is the time needed for the water flows from position 1 to position 2. The energy consumption due to friction at the channel bed and banks is given by

$$e_2 = \tau_0 (p_B + p_w) \Delta x = \tau_0 (p_B + p_w) u \Delta t \tag{11.41}$$

in which τ_0 is the average shear stress of the flow at the channel bed and banks; p_B and p_w are the wet perimeter at the bed and banks, respectively; and u is the velocity of the flowing column.

The released potential energy of solid materials is

$$e_2 = \rho_s gS(B\Delta h + d_L L_L + d_R L_R)\Delta x = \rho_s gSQ_s\Delta t \tag{11.42}$$

in which ρ_s is the density of sediment; Δh is the depth of the channel bed incision; d_L and L_L are the thickness and length of the sliding layer from the left bank, respectively; d_R and L_R are the thickness and length of the sliding layer from the right bank, respectively; and Q_S is the sediment discharge at position 2.

According to Bagnold (1988), collisions between the solid particles create a dispersive stress on the channel bed T:

$$T = 0.013\rho_s(\lambda D)^2\left(\frac{\partial u_p}{\partial z}\right)^2 \tag{11.43}$$

in which D is the diameter of particles; u_p is the velocity of particles; λ is the linear concentration defined by Bagnold (1954):

$$\lambda = \frac{1}{\left(\dfrac{C_{v*}}{C_v}\right)^{1/3} - 1} \tag{11.44}$$

where C_{v*} is the maximum concentration for sediment when the particles compactly piled, which is equal to 0.73 for uniform round particles (Bagnold, 1954).

The energy consumption due to collision of solid particles is given by

$$e_4 = TB\Delta x = TBu\Delta t \tag{11.45}$$

Substituting Eqs. (11.40–11.42) and Eq. (11.45) into Eq. (11.39) yields

$$\frac{\Delta E_k}{\Delta t} = \rho gSQ - \tau_0(p_B + p_w)u + \rho_s gSQ_s - TBu \approx \frac{\partial E_k}{\partial t} \tag{11.46}$$

In general, the released potential energy of water balances the friction at the wet perimeter. If the third term in the equation, or the released energy from the solid materials, is large or equal to the fourth term, or the energy consumption due to collision of solid particles, the kinetic energy increases or remain constant. The flow may continuously scour the channel bed and banks and more and more sediment enters the flow, and finally, the flow develops into a debris flow. If the gradient of the gully is high the third term is larger than the fourth term. Development of debris flow depends on the incision of the bed and collapse of banks. In this case the bed structure of step-pools becomes the key for debris flow control. If there are no bed structures or bed structures are destroyed, the gully bed can be scoured by torrential flood, which in turn causes bank collapses. The sediment entering into the flow does not cause reduction of the kinetic energy of the flow. Thus, a disastrous flow of water and high concentration of solid materials occurs. The debris flows occurring in Wenjiagou in 2010 illustrated the theory. If the solid materials consist of a lot of large stones, the fourth term in the equation may slightly larger than the third term because T is proportional to the square of the diameter D^2. The kinetic energy may reduce until the velocity becomes small.

Figure 11.69 shows the longitudinal bed profile of the new Wenjiagou Gully after the debris flow in 2010. The bed profiles in 2008 and 2009 are shown as a comparison, on which locations of the 20 dams are indicated. For the gully reach of 1,300 m–1,800 m from the gully mouth the landslide buried the gully with a thickness of about 150 m. In 2008 debris flows scoured the landslide deposit by about 50 m and formed the new Wenjiagou channel. In 2009 the step-pool system controlled debris flows and stabilized the channel bed. The bed profile remained the same as in 2008. In 2010 the new channel bed was again

incised by more than 50 m because the step-pools were destroyed but the constructed dams could not control incision and debris flows. The channel bed was still higher than the old Wenjiagou channel by about 50 m. Nevertheless, the gradient of the channel bed became larger and the bank slopes became larger and deeper than in 2009.
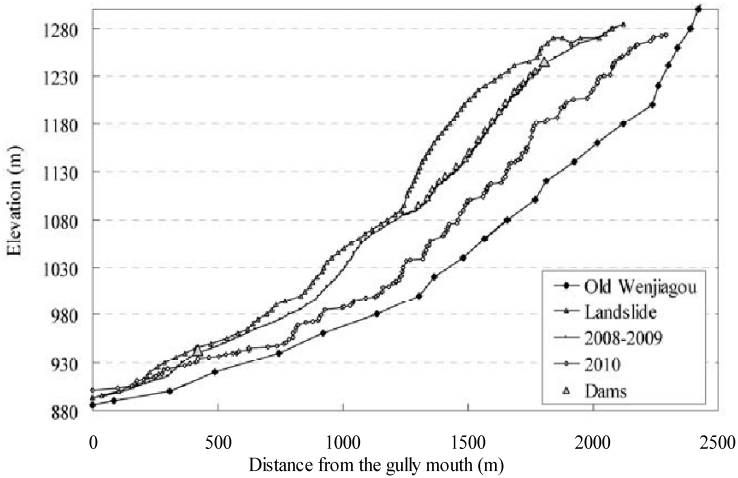
Fig. 11.69   Bed profile of Wengjiagou after the 2010 debris flows in comparison with the bed profiles in 2008 and 2009

As shown in Fig. 11.70, the remaining parts of failed dams were suspended on the banks. The upper main dam was completely removed by the debris flows and the gully extended upward by 130 m. Figure 11.71 shows two cross sections of Wenjiagou in 2009 and 2010. The locations of the cross sections are shown in Figure 11.59. The cross section 2 remained unchanged in 2009 because the step-pool system protected the bed from erosion. Nevertheless, the bed was scoured down by 16 m and the gully was widened by 90 m in 2010 because the dams were not able to control the incision and slope erosion. At cross section 7, the bed was scoured slightly in July, 2009 because the step-pools were partly damaged. The bed aggraded again in August and September 2009 after the steps were repaired. The whole cross section remained stable in 2009. In 2010, however, the bed was incised by 45 m and the gully was widened by 70 m.
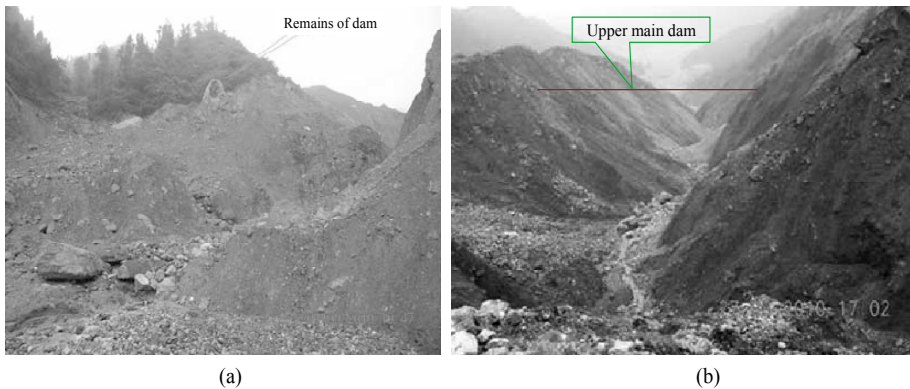
Fig. 11.70   (a) Suspended remaining part of a failed dam after bed incision; (b) The upper main dam was completely removed and the gully extended due to headwater erosion. (See color figure at the end of this book)
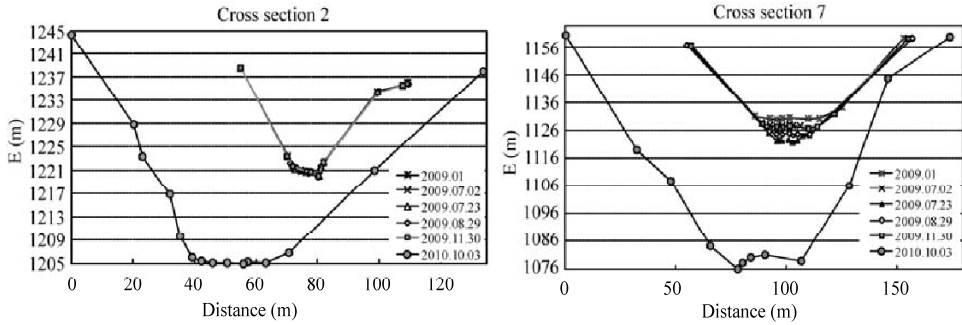
Fig. 11.71 Variation of cross section 2 and cross section 7 in 2009 and 2010

Figure 11.72 shows the size distributions of the solid materials on the gully bed and bank slopes in 2009 and 2010, which were the average of size distributions from 6 sites along the gully. The size distributions of debris flow deposits in 2008 and 2010 are shown in the figure as well. The solid materials in the gully in 2009 and debris flow deposits in 2008 were coarser than the solid material in the gully and debris flow deposit in 2010. A lot of large stones were on the top layer of the Wenjiagou landslide deposit. The debris flows in 2008 were two-phase debris flow because the particles were very coarse. After the debris flows in 2008 many large stones were left on the gully bed and bank slopes, which were used for construction of step-pools. In 2010, however, all large stones were exploded into small pieces and used for construction of 20 dams. The dams were removed by torrential floods. The solid materials were not very coarse and the debris flows were not two-phase, but more or less, pseudo-one-phase, debris flows. Therefore, the debris flows in 2010 were killing and disastrous. After the debris flows in 2010, the solid materials on the gully bed and slopes became much finer than in 2009 and 2008.
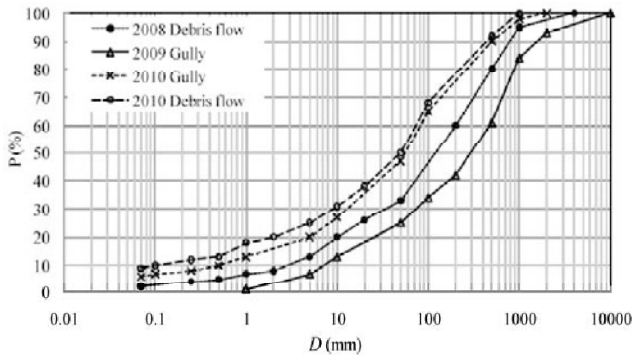
Fig. 11.72 Size distributions of solid material on the gully bed and slopes and in debris flow deposits

The failure of dams does not mean that the dams are not effective for debris flow control. In many cases check dams have successfully controlled normal debris flows. The focal point of designing check dams should be energy dissipation rather than restoration. Although the check dams on Wenjiagou had many windows the flow could not flow through the dam freely because stones carried by the debris flow closed the windows. Water restored in the reservoirs, which resulted high pressure on the dam and caused a high rising of ground water table. The loose solid materials were saturated with water and very unstable, which was one reason for the large volume debris flow disaster. The check dams should have a low sill allowing water flowing through but trapping large solid particles. Moreover, combination of check dams

and step-pool system may be the best effective for controlling various types of debris flow, in which the dams trap sediment and the step-pool system dissipate the flow energy and protect the bed against incision.

11.3.3 Reforestation and Terrestrial Ecosystem Management With Selected Wood Species

Vegetation is the most effective form of erosion control. No man-made products can approach it in long-term durability and effectiveness. Vegetation shields the soil surface from the impact of falling rain, slows the velocity of runoff, holds soil particles in place, and maintains the soil's capacity to absorb water. These plant communities in the watershed are a valuable source of energy for the biological communities, provide physical habitat, and moderate solar energy fluxes to and from the surrounding aquatic and terrestrial ecosystems. The characteristics of the plant communities directly influence the diversity and integrity of the faunal communities. Plant communities that cover a large area and that are diverse in their vertical and horizontal structural characteristics can support far more diverse faunal communities than relatively homogenous plant communities, such as meadows. The terrestrial ecosystem and part of the aquatic ecosystem depend on the internal complexity of vegetation, including the number of layers of vegetation and the species comprising each layer; competitive interactions among species; and the presence of detrital components, such as litter, downed wood, and snags. Species and age composition of vegetation structure also can be extremely important.

However, a lot of natural vegetation has been damaged or destroyed due to agriculture, husbandry, urbanization, and mining. The natural process of the vegetation restoration will take about 100 years in semitropical zone (Zhuang, 1997), yet reforestation will shorten the course of restoration (Wang et al., 2006). So planting is the most effective measure for accelerating vegetation restoration and erosion control. Selected wood species are planted on deforested mountains, which provide habitats for native species in the forest canopy. Both the fauna community and herbaceous vegetation with complex community composition have developed in the understory habitats. Planting has accelerated the vegetation succession process (Wang et al., 2006). From the 1980s, "returning farmland to forest" and other reforestation projects were implemented to restore the ecological environment in the upper Yangtze River basin. Many fast-growing native and alien trees were planted to increase the tree coverage and control erosion. Nevertheless, different planted wood species provided different habitats for understory communities and have different ecological effects, although they have the same function of erosion control.

The Xiaojiang River is a tributary of the Yangtze River. The Xiaojiang River basin has been experiencing serious soil erosion because of deforestation and mining in the past centuries. The river basin includes 107 debris flow gullies, where numerous debris flow events occur every year. The climate in the basin has distinct vertical zoning. The Xiaojiang River valley with elevations below 1500 m is a typical hot and dry valley, which has an average annual precipitation of about 700 mm, brown-red soil, and savanna shrub and grass vegetation. The surrounding area on the mountain slopes with elevations between 1500–3000 m is a temperate semiarid zone, which has an average annual precipitation of about 900 mm, yellow-red soil, and mountainous needle and broad-leaved mixed evergreen forest vegetation. On the top of the mountains with elevations above 3000 m is cold-temperate zone, which has average annual precipitation of about 1200 mm, brown and meadow soil, and alpine shrub and meadow communities (Zhang et al., 2006). It is wet from May to October during which rain falls accounting for 88% of the annual precipitation (Du and Kang, 1990).

As discussed in Chapter 2 reforestation and multiple-drop check dams are effective for erosion control in the basin. The rate of soil erosion may be reduced from 13,000 t/km^{2}yr to nearly zero if the fraction wood vegetation cover increases from 0.1 to 0.65. Nevertheless, the effects of wood species on the canopy ecology are very different, which has been studied by sampling and analyses (Yang et al., 2009).

The sampled plots arelocated in a region of elevation between 1600-2200 m. This region is the main source of solid material for debris flows, where rainstorms and severe soil erosion occurs in the wet season. Reforestation projects have been conducted and different wood species have been planted since the 1980s. In general one species was planted on one mountain slope and different wood species were planted on different mountain slopes.

Samples were taken from selected sites on the reforested slopes, where four wood species were planted: *Eucalyptus spp.*, *Acacia mearnsii*, *Leucaena leucocephala* and *Pinus yunnanensis*. The selected sites were consistent in slope steepness, soil type and soil texture, and water content. At each site 2 tree plots, each with an area of 10 m×10 m, were sampled. In each tree plot 3 herb plots with an area of 1 m ×1 m were selected randomly. The time of plantting was obtained from the records of the forest managers, which was further confirmed with tree-rings. Table 11.5 lists the features of the selected sites and sampled plots.

The wood species were planted in the 1980s during a national project to return farmlands to forests. Before the reforestation project the mountain slopes had been reclaimed for agriculture for many years and there was no native vegetation. The slope steepness was higher than 10º and serious soil erosion occurred on the slopes. Nutrient cups with one year old saplings of *Eucalyptus spp.* and *Acacia mearnsii* were planted for quick reforestation. *Leucaena leucocephala* and *Pinus yunnanensis* were planted by direct seeding methods. The reforested slopes were closed after plantation.

Table 11.5 Features of selected sites and sampled plots

Site	Wood species	Location of plots	Elevation (m)	Azimuth (°)	Slope gradient (°)	Tree age (yr)
1	*Eucalyptus spp.*	E103°09.311' N26°14.737'	1635	NW 6	30	3
		E103°16.155' N25°54.110'	1914	ES 23	22	8
		E103°16.045' N25°53.981'	1825	SE10	35	14
2	*Acacia mearnsii*	E103°16.095' N25°54.154'	1999	SE 50	10	4
		E103°16.191' N25°54.329'	1957	SE59	27	7
		E103°16.197' N25°54.106'	1914	SE 52	24	8
3	*Leucaena leucocephala*	E103°07.994' N26°14.733'	1635	NE4	31	4
		E103°13.228' N26°06.881'	1645	SE65	16	10
		E103°12.431' N26°06.300'	1587	SE7	17	20
4	*Pinus yunnanensis*	E103°16.097' N25°54.086'	1934	SE 37	17	4
		E103°17.633' N25°54.730'	2176	SE 49	40	14
		E103°17.612' N25°54.827'	2152	NW 23	35	20

Figure 11.73 shows the forest cover as a function of tree age for the four species. In general the forest cover increased with the age of the trees. *Acacia mearnsii* had the fastest growing speed, and the forest cover reached 80% at an age of 7 to 8 years. *Leucaena leucocephala* yielded a large amount of seeds and had a high rate of germination and regeneration (Zong et al., 2007). The two species reforested the slopes very quickly. The forest cover with 10 year old *Leucaena leucocephala* had reached 80%. Nevertheless, cover declined for 20 year old of *Leucaena leucocephala* mainly because the number density of the species was too high, which led to rarefaction of the crown of trees. The forest cover of *Pinus yunnanensis* increased with age at a steady but slow rate. The forest cover of 20 year old *Pinus yunnanensis* was about 65%, less than that of 8 year of *Acacia mearnsii* and 10 year *Leucaena leucocephala*. The forest cover of *Eucalyptus spp.* was low and increased very slowly with tree age. *Acacia mearnsii* and *Leucaena leucocephala* had the highest forest cover, and, therefore, were very effective for soil erosion control.

The planted wood species provided special habitats for understory communities to develop. Table 11.6 lists the average height, *H*, cover, number of species, *S*, and number of shrubs and herb species in the canopy habitats. There were only a few shrub species in the canopy habitat of *Leucaena leucocephala* forest. *Rhododendron sp.* and *Jatropha curcas* appeared after 10 in years *Leucaena leucocephala* forest, but only one shrub species *Ricinus communis* was found after 20 years in *Leucaena leucocephala* forest. As a comparison, 12 shrub species was found in the canopy habitat of *Pinus yunnanensis* forest. Dominant shrub species were *Qnerous*, *Hypericum acmosepalum*, *Neolitsea aurata*, and *Kerria japonica*. Figure 11.74 shows the comparison of the understory communities after 20 years *Leucaena leucocephala* forest and 20 years *Pinus yunnanensis* forest. The *Pinus yunnanensis* forest had developed into three layers vegetation with 12 shrub species and 22 herb species. The *Leucaena leucocephala* forest consisted of only 1 shrub species and 4 herb species.
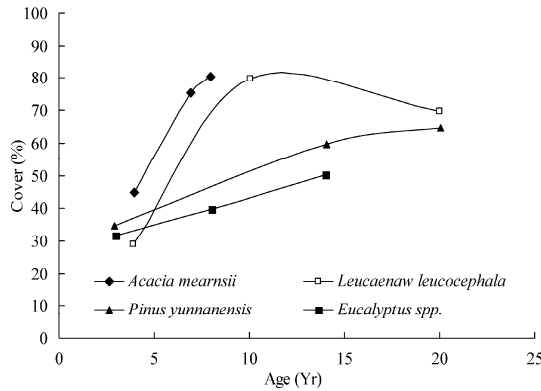
Fig. 11.73   Forest cover as a function of tree age for four planted species of trees

Table 11.6   Understory communities of the four planted wood species

Planted wood species	Age (yr)	Tree layer				Shrub layer				Herb layer		
		H (m)	D (cm)	Cover (%)	Density (n/hm²)	H (m)	N	S	Cover (%)	H (m)	Cover (%)	S
Eucalyptus spp.	3	3.1	1.4	32	2600	0.3	5	2	6	0.10	25	7
	8	21	16.4	40	1000	1.5	18	5	10	0.45	93	12
	14	22	18.5	50	1100	1.3	23	6	15	0.45	93	14
Acacia mearnsii	4	9.2	2.6	40	5600	0.25	20	1	4	0.10	20	11
	7	11	8.3	75	3200	1.1	31	4	7	0.05	6	9
	8	11.5	9.1	80	2900	0.6	23	5	6	0.15	9	7
Leucaena leucocephala	4	5.5	1.9	30	3700	0	0	0	0	0.10	22	5
	10	14	3.64	80	2200	1.5	10	2	4	0.50	88	8
	20	16	4.5	70	6000	1.4	2	1	2	0.05	0.7	4
Pinus yunnanensis	4	3	1.93	35	3400	0.2	7	2	1	0.15	30	8
	14	4.5	5.63	60	2000	0.5	94	7	11	0.15	18	13
	20	15.2	17.8	65	1400	2.5	136	12	26	0.20	46	22

Note: *H* is the average height of plants; *D* is the average diameter of trees; *N* is the number of shrub at eachs site in 200 m², and *S* is the number of species of shrubs or grasses

(a)

(b)

Fig. 11.74 (a) 20 years after planting of *Pinus yunnanensis* the forest had three layers with 12 shrub species and 22 herb species; (b) In the canopy habitat of 20 years after planting *Leucaena leucocephala* forest there were only 1 shrub species and 4 herb species (See color figure at the end of this book)

The results indicate that different planted species have very different effects on soil erosion control and understory floral communities. Because complex floral communities support complex faunal communities the wood species used for a watershed reforestation affect the whole terrestrial ecosystem, which in turn affects the aquatic ecosystem. According to the vegetation-erosion dynamics (see section 2.3.2) the Xiaojiang River basin may develop into a forest with a certain capacity for self-restoration. Selection of the wood species may effectively control erosion and in the mean time restore the terrestrial ecology.

Review Questions

1. Why river stability is important for stream ecology?
2. What are the principles for river management?
3. What are the implications of limit velocity law?
4. Explain the application of the theory of equivalency of bed structure and bed load motion with an example.
5. Explain the difference between the amount of erosion and sediment yield.
6. Why step-pool systems can mitigate geological hazards and improve stream ecology?
7. How can step-pool system dissipate flow energy and control debris flows?

References

Aberle J. and Smart G.M., 2003. The influence of roughness structure on flow resistance on steep slopes. J. Res. 41(3): 259–269

Abt S.R., Clary W.P. and Thornton C.I., 1994. Sediment deposition and entrapment in vegetated streambeds. J. Irrig, Drain, Eng., 120(6): 1098–1111

ACRS., 1990. Statistics of soil erosion by using remote sensing. Application Center of Remote Sensing Technology, Ministry of Water Resources of China (in Chinese)

Andrews E.D., 1984. Bed-material entrainment and hydraulic geometry of gravel-bed rivers. Geol. Soc. Am. Bull., 95: 371–378

Beghart G., Maughan O.E., Twomey K.A. and Nelson P.C., 1984. Habitat Suitability Index Models and Instream Flow Suitability Curves: Redear sunfish. Report to National Ecology Center Division of Wildlife and Contaminant Research, Fish and Wildlife Service. Washington, DC

Bona F., Falasco E., Fenoglio S., Iorio L. and Badino G., 2008. Response of macroinvertebrate and diatom communities to human-induced physical alteration in mountain streams. River Res. and Appl, 24(8): 1068–1081

Bordas M.P. and Walling D.E., 1988. Sediment Budgets. International Association of Hydrological Sciences, Publication No. 174

Brierley G.J. and Fryirs K.A., (eds.), 2008. River Futures: An Integrative Scientific Approach to River Repair. Island Press, Washington, DC

Burkham D.E., 1981. Uncertainties resulting from changes in river form. Journal of the Hydraulics Division, ASCE 107 (HYS): 593–610

Carollo F.G., Ferro V. and Termini D., 2002. Flow velocity measurements in vegetated channels. J. Hydraul. Eng., 128(7): 664–673

Carosi G. and Chanson H., 2008. Turbulence characteristics in skimming flows on stepped spillways. Canadian Journal of Civil Engineering, 35(9): 865–880

Cereghino R., Giraydel J.L. and Compin A., 2001. Spatial analysis of stream invertebrates distribution in the Adour-Garonne drainage basin (France), using Kohonen self organizing maps. Ecol. Modell. 146(1–3): 167–180

Chang F.M., 1970. Ripple concentration and friction factor. J. of Hyd. Div., ASCE, 96(2): 417–430

Chanson H. 2001. The Hydraulics of Stepped Chutes and Spillways. Balkema, Lisse, The Netherlands

Chanson H. and Toombes L., 2002. Experimental investigations of air entrainment in transition and skimming flows down a stepped Chute. Canadian Journal of Civil Engineering, 29(1): 145–156

Chen X.Q., 2004. Sand extraction from the mid-lower Yangtze River channel and its impacts on sediment discharge into the sea, Proceedings, 9th International Symposium on River Sedimentation, Tsinghua University Press, 3: 1699–1704

Chien N., Wan Z.H. and McNown J., 1998. Mechanics of Sediment Movement, ASCE Press, New York

Ciccacci S., D'Alessandro L., Fredi P. and Lupia P.E., 1992. Relation between morphometric characteristics and denudation processes in some drainage basins of Italy. Zeitschrift fuer Geomorphologic, N.F. 36(1): 53–67

Comiti F., Mao L., Lenzi M.A. and Siligardi M., 2009. Artificial steps to stabilize moun tain rivers: A post-project ecological assessment. River Res. and Appl, 25(5): 639–659

Crance J.H., 1983. Habitat suitability index models and instream flow duitability curves: Shortnose Sturgeon. Report to National Ecology Center Division of Wildlife and Contaminant Research, Fish and Wildlife Service, Washington, DC

Crance J.H., 1984. Habitat suitability index models and instream flow duitability curves: Inland Stocks of Striped Bass. Report to National Ecology Center Division of Wildlife and Contaminant Research, Fish and Wildlife Service. Washington, DC

Cui P., Liu S.Q., Tang B.X. and Chen X.Q., 2003. The management model of debris flow in famous scenery. Science in China Series E: Technological Sciences, (1): 1–9

Curran J.H. and Wohl E.E., 2003. Large woody debris and flow resistance in step-pool channels, Cascade Range, Washington. Geomorphology, 51(1–3): 141–157

Du R.H. and Kang Z.C., 1990. Humid-desertification process and regulation in Xiaojiang drainage basin. In: Annual Report of Dongchuan Debris Flow Observation and Research Station, Chinese Academic of Sciences, 22–33 (in Chinese)

Duan X.H., Wang, Z.Y. and Xu, M.Z., 2010. Benthic invertebrates and river ecological assessment. Tsinghua

University Press, Beijing (in Chinese)

Edmonds R.L., 1994. Patterns of China's lost harmony: A Survey of the Country's Environmental Degradation and Protection. Routledge, London

Edwards E.A., 1983a. Habitat suitability index models and instream flow suitability curves: Longnose Dace. Report to National Ecology Center Division of Wildlife and Contaminant Research, Fish and Wildlife Service, Washington, DC

Edwards E.A., 1983b. Habitat suitability index models and instream flow suitability curves: Longnose Sucker. Report to National Ecology Center Division of Wildlife and Contaminant Research, Fish and Wildlife Service, Washington, DC

Edwards E.A., Bacteller M. and Maughan O.E., 1982a. Habitat suitability index models and instream flow suitability curves: Slough Darter. Report to National Ecology Center Division of Wildlife and Contaminant Research, Fish and Wildlife Service, Washington, DC

Edwards E.A., Gebhart G.. and Maughan O.E., 1983. Habitat suitability index models and instream flow suitability curves: Smallmouth Bass. Report to National Ecology Center Division of Wildlife and Contaminant Research, Fish and Wildlife Service, Washington, DC

Edwards E.A., Kriger D.A., Gebhart G. and Maughan O.E., 1982b. Habitat suitability index models and instream flow suitability curves White Crappie. Report to National Ecology Center Division of Wildlife and Contaminant Research, Fish and Wildlife Service, Washington, DC

Elliott A.H., 2000. Settling of fine sediment in a channel with emergent vegetation. J. Hydraul. Eng., 126(8): 570–577

Fryirs K.A., Brierley G.J., 2009. Naturalness and place in river rehabilitation. Ecol. and Soc., 14(1): 20

Glenn B.W., 1994. Trichoptera-Aquatic Insects of China Useful for Monitoring Water Quality, 260, John C.M., Yang L.F. and Tian L.X., (eds.), Hohai University Press, Nanjing

Gore J.A. and Petts G.E., 1989. Alternatives in regulated river management. CRC Press, Boco Raton, FL

Gray D.H. and Leiser A.T., 1982. Biotechnical Slope Protection. Van Nostrand-Reinhold. New York

Gui H., 1994. Ephemeroptera, Aquatic insects of china useful for monitoring water quality, John C.M., Yang L.F., Tian L.X., (eds.), Nanjing, 124. Hohai University Press

Hey R.D. and Thorne C.R., 1986. Stable channels with mobile gravel beds. J. Hydraul. Eng., 112(8): 671–689

Hickman T. and Raleigh R.F., 1982. Habitat suitability index models and instream flow suitability curves: Cutthroat Trout. Report to National Ecology Center Division of Wildlife and Contaminant Research, Fish and Wildlife Service. Washington, DC

Horton R.E., 1945. Erosional development of streams and their drainage basins: Hydrophysical approach to quantitative morphology. Geological Society of America Bulletin, 56: 275–370

Hou L.S. and Xu X.G., 2001. Treatments and inspiration of Mississippi Basin. Yellow River, 23(1): 39–41 (in Chinese)

Howard A.D., 1967. Drainage analysis in geological interpretation, A summation. Bull. Amer. Assoc. Petroleum Geologists, 51: 2246–2259

Hubert W.A. and Anderson S.H., 1984. Habitat suitability index models and instream flow suitability curves: Paddlefish. Report to National Ecology Center Division of Wildlife and Contaminant Research, Fish and Wildlife Service, Washington, DC

Hubert W.A., Helzner R.S., Lee L.A. and Nelson P.C., 1985. Habitat suitability index models and instream flow suitability curves: Arctic Grayling Riverine Populations. Report to National Ecology Center Division of Wildlife and Contaminant Research, Fish and Wildlife Service, Washington, DC

Ikeda S. and Izumi N., 1990. Width and depth of self-formed straight gravel river with bank vegetation. Water Resour. Res., 26(10): 2353–2364

Ikeda S., Izumi N. and Ito R., 1991. Effects of pile dikes on flow retardation and sediment transport. J. Hydraul. Eng., 117(11): 1450–1479

Izzo D., 2004. Reengineering the Mississippi. Civil Engineering, 74(7), 39–45

Jia Y.H. and Wang Z.Y., 2010. Estimation of soil erosion in the Xihanshui Watershed by using of 137Cs technique. International Journal of Sediment Research (accepted)

Jiang J.G., 1998. Re-naturalize the Rhine River. People's Daily (980904, 7th version)

Jin Z.X., Shi G.P. and Zhou, J.D., 1997. Shanghai municipal planning of reclamation of beach and shoals in the Yangtze River mouth, Deptortment. of Water Resources of Shanghai (in Chinese)

Kang Z., Li Z., Ma A. and Luo J., 2004. Debris Flow Studies in China. Science Press, Beijing (in Chinese)

Kingsford R.T., 2000. Ecological impacts of dams, water diversions and river management on floodplain wetlands in Australia. Australian Ecology, 25 (2): 109–127

Kinner D.A., Moody J.A., 2005. Drainage networks after wildfire. International Journal of Sediment Research, 20(3): 194–201

Kirchner J.W. 1993. Statistical inevitability of Horton's laws and the apparent randomness of stream channel networks. Geology, 21: 591–594

Krieger D.A., Terrell J.W. and Nelson P.C., 1983. Habitat suitability index models and instream flow suitability curves: Yellow Perch. Report to National Ecology Center Division of Wildlife and Contaminant Research, Fish and Wildlife Service, Washington, DC

Kuhl D., 1992. Fourteen years of artificial grain feeding in the Rhine downstream of the barrage Iffezheim, Proceedings 5th International Symposium on River Sedimentation, Karlsruhe, Germany, 1121–1129

Kyung S.L. and Zeng L., 2007. The restoration and protection of Cheongyechon in the city of Seoul, South Korea. Chinese Landscape Architecture. 7: 30–35

Lee L.A. and Terrell J.W., 1987. Habitat suitability index models and instream flow suitability curves: Flathead Catfish. Report to National Ecology Center Division of Wildlife and Contaminant Research, Fish and Wildlife Service, Washington, DC

Lee S., Fujita K. and Yamamoto K., 1999. A scenario of area expansion of stable vegetation in a gravel-bed river based on the upper Tama River case. J. Hydraul. Eng., JSCE, 43: 977–982 (in Japaneses)

Lenzi M.A. and Comiti F., 2003. Local scouring and morphological adjustments in steep channels with check-dam sequences. Geomorphology, 55(1–4): 97–109

Lenzi M.A., 2002. Stream bed stabilization using boulder check dams that mimic step-pool morphology features in northern. Italy Geomorphology, 45: 243–260.

Liu C., Sui J. and Wang Z.Y., 2008. Changes in runoff and sediment yield along the Yellow River during the period from 1950 to 2006, Journal of Environmental Informatics, ISEIS 12 (2): 129–139

Liu H.X. and Wang Z.Y., 2008. Relationship between river network pattern and environmental condition. Journal of Tsinghua University, 48(9): 1408–1412 (in Chinese)

Liu H.X. and Wang Z.Y., 2009. Field experimental study on development of mountain streambed structures. Journal of Hydraulic Engineering, 40(11): 1339–1344 (in Chinese)

Liu H.X., Wang Z.Y. and Yu S.Y., 2010. Growth distribution of the riverbed structures in mountain area. J. Tsinghua Univ. (Sci & Tech), 50(6): 857–860 (in Chinese)

Liu X.Y., 2007. Discussion on several problems related to the river health. www.waterscience.cn, April 29

Lu F.C., Shi B. and Bao Z.J. 2006. Study on energy dissipation characteristics of stepped spillway. Journal of Yangtze River Scientific Research Institute, 23(1): 9–11

Lu X.X. and Higgitt D.L., 1999. Sediment yield variability in the Upper Yangtze, China. Earth Surface Processes and Landforms, 24: 1077–1093

Lv T.N., 2000. Countermeasures for vegetation recovery in Dongchuan Region with serious soil erosion. Research of Soil and Water Conservation, 7(3): 134–137 (in Chinese)

McMahon T.E. and Terrell J.W., 1982. Habitat suitability index models and instream flow suitability curves: Channel Catfish. Report to National Ecology Center Division of Wildlife and Contaminant Research, Fish and Wildlife Service, Washington, DC

McMahon T.E., Beghart G., Maughan O.E. and Nelson P.C., 1984a. Habitat suitability index models and instream flow suitability curves: Spotted Bass. Report to National Ecology Center Division of Wildlife and Contaminant Research, Fish and Wildlife Service, Washington, DC

McMahon T.E., Gebhart G., Maughan O.E. and Nelson P.C., 1984c. Habitat suitability index models and instream flow suitability curves: Warmouth. Report to National Ecology Center Division of Wildlife and Contaminant Research, Fish and Wildlife Service, Washington, DC

McMahon T.E., Terrell J.W. and Nelson P.C., 1984b. Habitat suitability index models and instream flow suitability curves: Walleye. Report to National Ecology Center Division of Wildlife and Contaminant Research, Fish and Wildlife Service, Washington, DC

Milliman J.D., Meade R.H., 1983. World-wide delivery of river sediment to the oceans. J. Geol. 91: 1–21

MWRC (Ministry of Water Resources of China), 2000. China sediment gazette-2000. Ministry of Water Resources of China (in Chinese)

NDN-PLA (Navigation Department of Navy of People's Liberation Army), 1983. Atlas of Changjiang navigation channels. Navy of People' Liberation Army (in Chinese).

Ni H.G. and Liu Y.K., 2008. Shock wave hydraulic jump plunge energy dissipation. Dalian University of Technology Press, Dalian (in Chinese)

Ni J. and Barazangi M., 1984. Seismotectonics of the Himalayan Collision Zone: Geometry of the Underthrusting Indian plate beneath the Himalaya, J. Geophys. Res., 89(B2): 1147–1163

Peter H.A., Wang Z.M., 1994. Simuliidae. Aquatic insects of China useful for monitoring water quality, 478, John C.M., Yang L.F., Tian L.X. (eds.), Hohai University Press, Nanjing

Rajaratnam N., 1990. Skimming flow in stepped spillways. J. Hydr. Engrg. ASCE, 116(4): 587–591

Raleigh R.F. and Nelson P.C., 1985. Habitat suitability index models and instream flow suitability curves: Pink Salmon. Report to National Ecology Center Division of Wildlife and Contaminant Research, Fish and Wildlife Service, Washington, DC

Raleigh R.F., 1982. Habitat suitability index models and instream flow suitability curves: Brook Trout. Report to National Ecology Center Division of Wildlife and Contaminant Research, Fish and Wildlife Service, Washington, DC

Raleigh R.F., Hickman T., Solomon R.C. and Nelson P.C., 1984. Habitat suitability index models and instream flow suitability curves: Rainbow Trout. Report to National Ecology Center Division of Wildlife and Contaminant Research, Fish and Wildlife Service, Washington, DC

Raleigh R.F., Miller W.J. and Nelson P.C., 1986a. Habitat suitability index models and instream flow suitability curves: Chinook Salmon. Report to National Ecology Center Division of Wildlife and Contaminant Research, Fish and Wildlife Service, Washington, DC

Raleigh R.F., Zuckerman L.D. and Nelson P.C., 1986b. Habitat suitability index models and instream flow suitability curves: Brown Trout. Report to National Ecology Center Division of Wildlife and Contaminant Research, Fish and Wildlife Service, Washington, DC

Sedimentation Panel, 2009. Impoundment of three gorges reservoir-brief results of measurement of water and sediment. Sediment Panel for the Three Gorges Project, China Science and Technology Press (in Chinese)

Shen T., Yang C., Wu Z.G., Li J. and Zhao Y., 2003. Review of the planning of the sediment mining in the middle and lower Yangtze River. People's Yangtze River, 34(6), (in Chinese)

Shreve R.L., 1966. Statistical law of stream numbers. J. Geol. 74: 17–37

Shvainshtein A.M., 1999. Stepped spillways and energy dissipation. Hydrotechnical Construction, 33(5): 275–282

Sikora W.B. and Sikora J.P., 1982. Habitat suitability index models and instream Flow suitability curves: Southern Kingfish. Report to National Ecology Center Division of Wildlife and Contaminant Research, Fish and Wildlife Service, Washington, DC

Simons D.B. and Richardson E.V., 1960. Resistance of flow in alluvial channels, J. of Hyd. Div., Proc., ASCE, 86(5): 73–99

Smil V., 1993. China's Environmental Crisis: An inquiry into the limits of national development. Sharpe M.E., New York

Stankiewicz J., 2005. Fractal river networks of Southern Africa. South African Journal of Geology, 108: 333–344

Stier D.J. and Crance J.H., 1986. Habitat Suitability Index Models and Instream Flow Suitability Curves: American Shad. Report to National Ecology Center Division of Wildlife and Contaminant Research, Fish and Wildlife Service, Washington, DC

Stuber R.J., Gebhart G. and Maughan O.E., 1982a. Habitat suitability index models and instream flow suitability curves: Bluegill. Report to National Ecology Center Division of Wildlife and Contaminant Research, Fish and Wildlife Service, Washington, DC

Stuber R.J., Gebhart G. and Maughan O.E., 1982b. Habitat suitability index models and instream flow suitability curves: Green Sunfish. Report to National Ecology Center Division of Wildlife and Contaminant Research, Fish and Wildlife Service, Washington, DC

Stuber R.J., Gebhart G. and Maughan O.E., 1982c. Habitat suitability index models and instream flow suitability curves: Largemouth Bass. Report to National Ecology Center Division of Wildlife and Contaminant Research, Fish and Wildlife Service, Washington, DC

Su Y. and Wang Z.Y., 1997. The management experiences and evaluation of Mississippi River. Journal of Sediment Research, 1: 1–8 (in Chinese)

Tang H.W., Ding B., Chi Y.M. and Fang S.L., 2009. Protection of bridge piers against scouring with tetrahedral frames. International Journal of Sediment Research, 24(4): 385–399

Tang K.L., Editor, 2004. China Soil Conservation. Chinese Science Press, 264 (in Chinese)

TGP Water Survey, 2005. Introduction about the Yichang hydrological station. The Three Gorges Hydrology and Water Resource Survey Bureau (in Chinese)

Thorne C.R., 1990. Effects of vegetation on river bank erosion and stability. In: Vegetation and erosion, Thornes J.B. (ed.), Wiley, Chichester, U.K., 125–144

Thornton, C.I., Abt S.R., Morris C.E. and Fischenich J.C., 2000. Calculating shear stress at channel-overbank interfaces in straight channel with vegetated floodplains. J. Hydraul. Eng., 126(12): 929–936

Todd M. and Mike L., 2003. Natural channel design of step-pool watercourses using the "key-stone" concept [J]. ASCE conference process, 18: 1–11

Trial J.G., Stanley J.G., Batcheller M., Gebhart G., Maughan O.E. and Nelson P.C., 1983a. Habitat suitability index models and instream flow suitability curves: Blacknose Dace. Report to National Ecology Center Division of Wildlife and Contaminant Research, Fish and Wildlife Service, Washington, DC

Trial J.G., Wade C.S., Stanley J.G. and Nelson P.C., 1983b. Habitat suitability index models and instream flow suitability curves: Common Shiner. Report to National Ecology Center Division of Wildlife and Contaminant Research, Fish and Wildlife Service, Washington, DC

Twomey K.A., Williamson K.L. and Nelson P.C., 1984. Habitat suitability index models and instream flow suitability curves: White Sucker. Report to National Ecology Center Division of Wildlife and Contaminant Research, Fish and Wildlife Service, Washington, DC

Wan X., Li J., He Q., Xiang W. and Wu H., 2003. Variation of the sediment flux in the middle and lower Yangtze River. Sediment Research, 4: 29–35 (in Chinese)

Wang F.X., Wang Z.Y., Yang Z.M. and Ji X.N., 2006. Vegetation succession processinduced by reforestation in erosion area. Acta Ecologica Sinica, 26(8): 133–140 (in Chinese)

Wang T.S., 2002. Water resources protection and management in Rhine Basin. Water Resources Protection, 4: 60–62 (in Chinese)

Wang W.R. and Zhang S.C., 1985. Characteristics of debris flow in the Guxiang Gully in Tibet, Research Paper Corpus, No. 4, Research Institute of Glaciology and Cryology (in Chinese).

Wang Y., Zhan Q. and Yan B., 2001. Structure and rheological properties of debris flows. Hunan Science Press, Changsha (in Chinese)

Wang Z.Y. and Qian N., 1985. Experimental study of motion of laminated load. Scientia Sinica, Ser. A, 28(1): 102–112

Wang Z.Y., Lin B.G. and Nestmann F., 1997. Prospect and new problems of sediment research. International Journal of Sediment Research, 12(1): 1–15

Wang Z.Y., Melching, C.S., Duan X.H. and Yu G.A., 2009. Ecological and hydraulic studies of step-pool systems. ASCE Journal of Hydraulic Engineering, 134(9): 705–717

Wang Z.Y., Tian S.M., Yi Y.J. and Yu G.A., 2007. Principles of river training and management. International Journal of Sediment Research, 22(4): 247–262

Weichert R., 2005. Bed morphology and stability in steep open channels, PhD dissertation, No. 16316. ETH Zurich. http://ecollection.ethbib.ethz.ch/eserv/eth:28455/eth-28455–02

Weichert R.B., Bezzola G.R. and Minor H.E., 2009. Bed erosion in steep open channels. J. Hydraulic Res. 47(3): 360–371

Wen D.Z., 1993. Soil erosion and conservation in China. In: Pimental D. (ed.), World Soil Erosion and Conservation, pimental D., ed., Cambridge University. Press, Cambridge, UK, 63–85

Wilcox A., Nelson J.M. and Wohl E.E., 2006. Flow resistance dynamics in step-pool channels 2: Partitioning between grain, spill, and woody debris resistance. Water Res. Res. 42, W05419, doi:10.1029/2005WR004278

Wilcox A.C., Wohl E.E., 2007. Field measurements of three-dimensional hydraulics in a step-pool channel. Geomorphology, 83(3–4): 215–231

Williamson K.L. and Nelson P.C., 1985. Habitat suitability index models and instream flow suitability curves: Gizzard Shad. Report to National Ecology Center Division of Wildlife and Contaminant Research, Fish and Wildlife Service, Washington, DC

Wohl E.E., Thompson D.M., 2000. Velocity fluctuations along a small step-pool channel. Earth Surf. Processes Landforms 25(4): 353–367

Wu H.L., 2001. Evolusion process of Changjiang estuary and its sediment flux, Ph.D. Thesis. East China Normal University, 200062 Shanghai, China (in Chinese)

Xie H., Zhong D., Li Y. and Wei F., 2004. Characteristics of debris flow disasters in the upper Yangtze River basin, Resources and Environment of the Yangtze River Basin, 13(1): 94–99 (in Chinese)

Xu G.B., 2007. Canalized regulation of the lower Yellow River. Journal of Sediment Research, 1: 1–7 (in Chinese)

Xu J.X., 2005. Variation of the suspended sediment size in the upper Yangtze River in the past 40 years and its relationship with human activities, Sediment Research, 3: 8–16 (in Chinese)

Yang C.T., 1996. Sediment transport-theory and practice. McGraw-Hill, New York.

Yang J.S., Wang Z.Y., Yu G.A., Zhang K. and Liu H.X., 2009. Community structures and erosion control ability of different plantations in the Xiaojiang Basin. Acta Geologica Sinica, 29(4): 1921–1930 (in Chinese)

Yang Z.N., 1985. A discussion on the velocity formulae of rainfall debris flows, Research Paper Corpus, No. 4. Research Institute of Glaciology and Cryology (in Chinese)

Yi Y.J., Wang Z.Y., Lu Y.J., 2006. Habitat suitability index model of four major chinese carp species in the Yangtze River. River Flow, 2195–2201

Yi Y.J., Wang Z.Y., Lu Y.J., 2007. Habitat suitability index model of chinese sturgeon in the Yangtze River [J]. Advances in Water Science (in Chinese)

Yi Z.W., 2003. Sediment in the Yangtze River. Sichuan Shuili, 15 (in Chinese)

Yu B., Ma Y., Wu Y.F., 2010. Investigation of severe debris flow hazards in Wenjiagou gully of Sichuan province after the Wenchuan Earthquake. Journal of Engineering Geology, 18(6): 827–836 (in Chinese)

Yu G.A., 2008. Experimental study of the effects of bed structures on bed load transportation and river bed incision, Ph. D. Thesis. Department of Hydraulic Engineering, Tsinghua University (in Chinese)

Yu G.A., Wang Z.Y., Zhang K., Duan X.H. and Chang T.C., 2010. Restoration of an incised mountain stream using artificial step-pool system. IAHR Journal of Hydraulic Research, 48(2): 178–187

Yu J.R., Shi L.R. and Feng M.H., 1991. Soil erosion and river sediment in the upper stream reaches of the Yangtze River. Bulletin of Water Resources, 11(1): 9–17 (in Chinese)

Yu X.G., 2003. Research on the sustainable development of the Yangtze River Basin. Chinese Science Press, 280 (in Chinese)

Zhang K., Wang, Z.Y., Liu L. and Yu G.A., 2010. The effect of riverbed structure on bed load transportation in mountain streams. IAHR-River Flow 2010- International Conference on Fluvial Hydraulics. 8–10 September 2010, Braunschweig, Germany

Zhang X.B. and Liu J., 1989. Debris flows in the Dayingjiang Basin in Yunnan. Chengdu Atlas Press (in Chinese)

Zhang Z., Shi X. and Xu X.Q., 2006. Approx-natural form in urban river landscape eco-environment improvement. Journal of Zhejiang Forestry College, 23(2): 202–206 (in Chinese)

Zhuang X.Y., 1997. Rehabilitation and development of forest on degraded hills of Hong Kong. Ecol. Manage. 99: 197–201

Zong Y.C., Zheng Y.Q., Zhang C.H., 2007. Natural regeneration of Leucaena leucocephala in Yuanmou dry-hot valley. Chinese Journal of Ecology, 26 (1): 135–138 (in Chinese)

Subject Index

Color Figures Index

(a)

(b)

Fig. 1.7 C-type channel networks in the upper reaches of the Yangtze River in Yunnan Province: (a) Developing network; (b) Developed network

(a)

(b)

(c)

Fig. 1.9 (a) Weathering of granite produces quartz, feldspar and mica particles in the upper reaches of the East River in Guangdong in South China; (b) Weathering of metamorphic rocks in the Xiaojiang watershed produces various particles from clay to boulders; (c) Weathering of limestone produces few granular particles in Dali in Yunnan

Fig. 1.29 Soil erosion in the Loess Plateau of central China bring a huge amount of sediment to the lower reaches of the Yellow River

Fig. 1.30 The silt drifting from the Yellow River mouth under the action of tidal currents is deposited at the New Ziya River mouth. The channel is silted up by 6 m and the discharge capacity of the channel has reduced by 60%

Fig. 1.34 Pollution causes the bad odor the Weihe River water and kills all fish

Fig. 2.1   The Hailuo Gully glacier on the Gongga Mountain on the east margin of the Qinghai-Tibet Plateau has eroded the gully bed and carries a lot of solid material on its surface

Fig. 2.6   Channel erosion and collapse of vegetative banks and hardened banks on the Charlooze River in Iran, which was caused by floods

<table>
<tr><td>(a)</td><td>(b)</td></tr>
</table>

Fig. 2.9   (a) Tile structure on the slope in the Xiaojiang River basin in southern China; (b) Vegetation cover protecting the soil from various erosion

Fig. 2.11 (a) Grain flow in the Xiaobaini Ravine scoured the bank slope to form a 2 m-deep 42° slope channel; (b) Several grain erosion sites along the Minjiang River near Wenchuan; (c) Grain erosion on the north bank of the upper Jiangjia Ravine, in Yunnan, China; (d) Grain flow on the slope of Jiuzhai Creek, which has killed many trees

Fig. 2.15 Grain erosion occurs on the south-facing bank (a) while rill erosion (water erosion) occurs on the north-facing bank (b) of a small stream

811
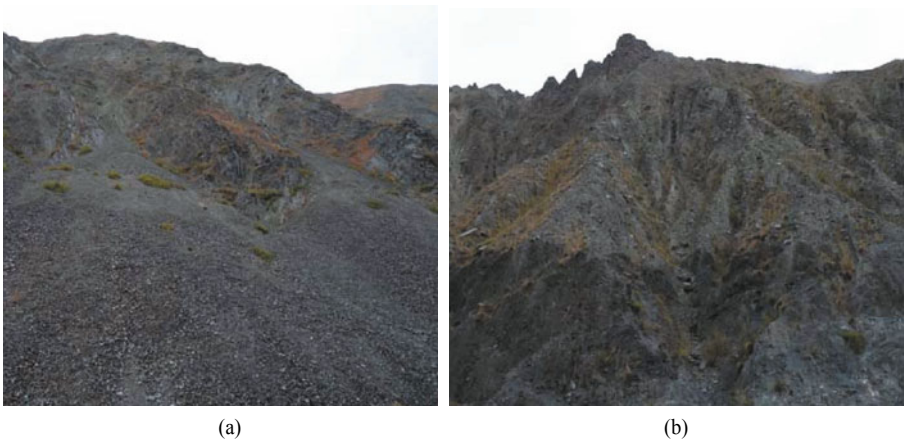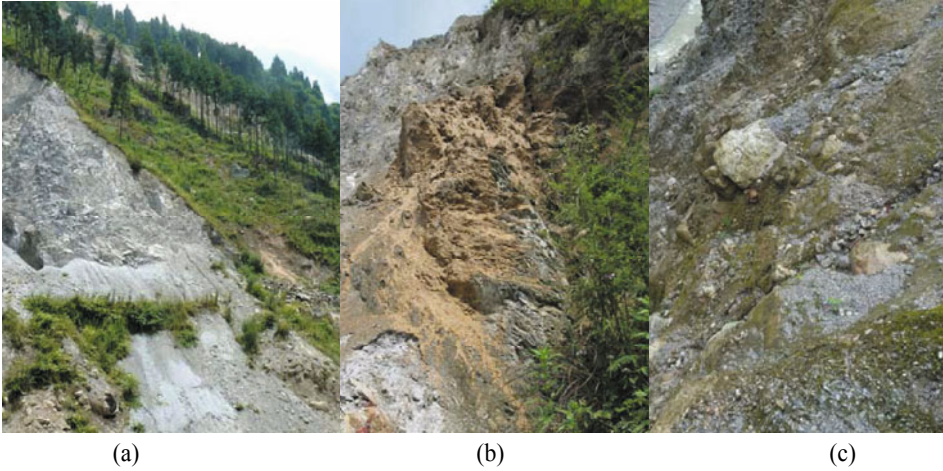
Fig. 2.17 (a) Grain erosion site at Xiaomuling on the Mianyuan River, Sichuan; (b) Clay suspension with moss spores was splashed on the Xiaomuling grain erosion rock; (c) Two months later the rock surface was green and grain erosion was controlled

Fig. 2.24 Trees on the gully banks used to estimate the rate of gully erosion

Fig. 2.25 Various natural stresses on vegetation: (a) Soil erosion damages the vegetation on a slope of the Yunnan-Guizhou Plateau of China. (b) Soil salinization has resulted in the mortality of shrub vegetation on the Yellow River delta; (c) An earthquake-induced landslide destroyed the vegetation in Taiwan, China in 1999; (d) Insects killed trees; (e) Heavy snow broke trees on Zhangjiajie Mountain; and (f) A forest fire cleared the vegetation in the upper reaches of the East River in southern China

Fig. 2.29 Vegetation and erosion may reach an equilibrium state, if the circumstances remain unchanged for a long period of time

Fig. 2.31 A slope suffers from accelerating soil erosion because the top soil is removed in a red soil area in southern China

(a)

(b)

(c)

(d)

Fig. 2.32 (a) Herbaceous vegetation on the Qinghai-Tibet Plateau controls splash and sheet erosions but not gully erosion; (b) Herbaceous vegetation in the Xiaojiang River basin controls rill erosion; (c) Shrubs and trees on the Loess Plateau control gully erosion; (d) Channel erosion caused bank failure on the Chenyoulan River in Taiwan, China

(a) (b)

Fig. 2.50 Comparison of the vegetation consisting of woods, grasses, shrubs, liana, and bamboo in an experimental plot by planting Acacia Mangium (a) with the vegetation in a closed plot consisting of only herbaceous and some shrubs species (b)

Underflow jam
$L > W$
Local bed & bank scour
limited backwater
sedimentation

Dam jam
$L = W$
Backwater pools and
log-steps.
Sediment wedge formation,
and plunge scour

Deflector jam
$0.5W < L < W$
Flow deflection, bed
scour and bank erosion.
Local channel widening
bar developoment in the
lee of jams

Parallel/bar head jam
$L < 0.5W$
Bank toe protection
sepecially in apex of bends.
Accelerates incipient bar
growth

Increasing watershed ared/discharce

pool

bar

bank

bar
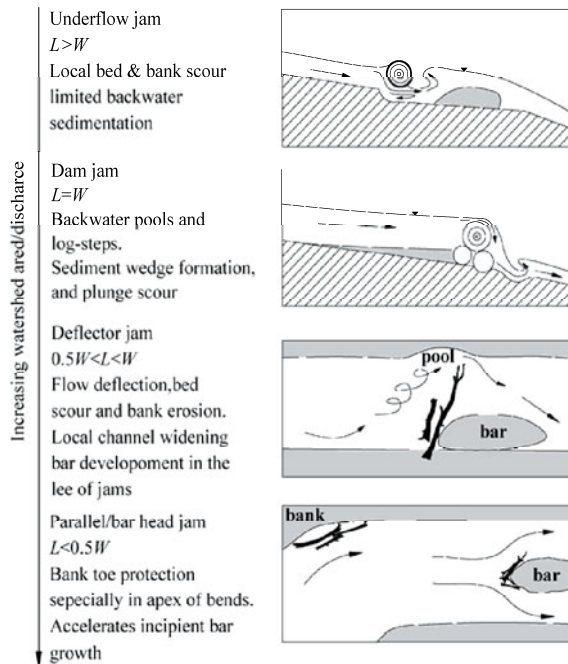
Fig. 2.54 Impacts of the large woody debris on fluvial processes (after Wallerstein et al., 1997) (L is the length of the woody debris; and W is the channel width)
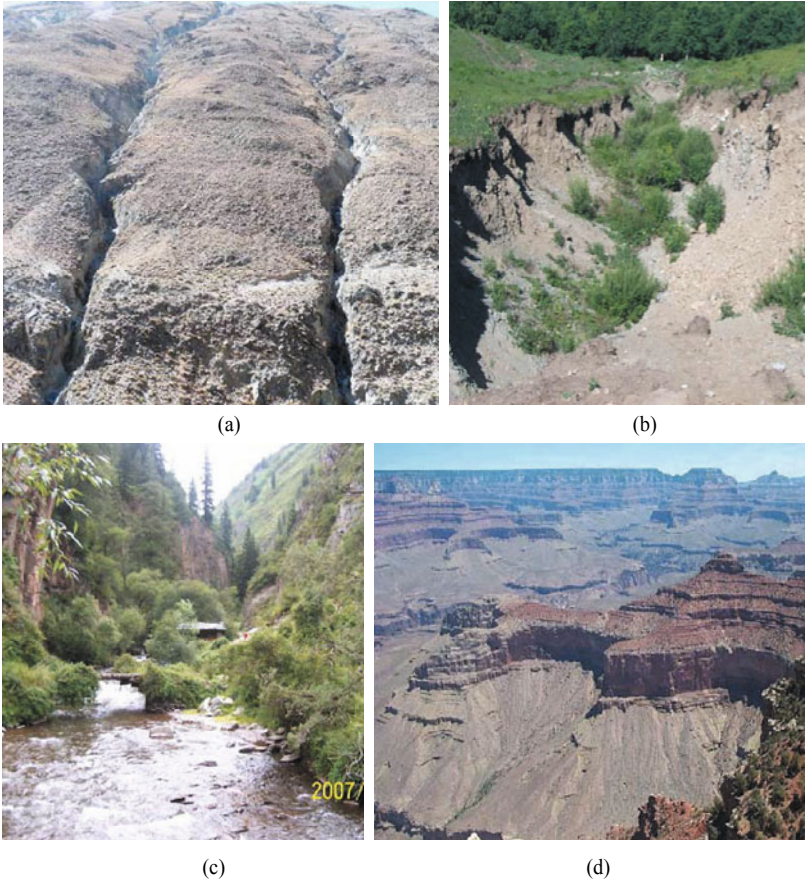
815

Fig. 3.1 (a) Rills developed on slope by erosion on the bank slope of the Yalutsangbu River; (b) A gully developed from rills in the Yongding River basin; (c) A stream in the upper Yangtze River basin in Sichuan Province developing into an entrenched stream in a process of channel incision; (d) The Grand Canyon of the Colorado River, U.S. is a composite incised channel

Fig. 3.3 (a) The upper reaches of the Liwu River in Taiwan, China; (b) Bank failure due to incision on a small stream in Sichuan

Fig. 3.9 Bank failure during the process of stream bed incision of the Liujia Gully in Lixian, Gansu

Fig. 3.11 (a) A tributary of the Minjiang River in the rapid degradation stage; (b) the Dajinchuan River in the degradation and widening stage; (c) the Kuaihe River in the upper Yangtze River basin in the aggradation and widening stage; (d) an upstream reach of the Dahu River in the equilibrium stage

(a)   (b)

Fig. 3.14 (a) Bed rock channel in the middle reaches of the Yellow River; (b) Bed rock channel of the Jinghe River with a V-shaped cross sections

(a)

(b)   (c)

Fig. 3.17 The bedrock channel of the Lijiang River is eroded by corrasion induced by gravel movement on the bed; (b) Bedrock channel of a tributary of the Jinsha River has been incised down by about 20 m mainly due to corrasion; (c) Parallel corrasion slots on bedrock of the Jinsha River

Fig. 3.23 (a) A step-pool system develops in a high gradient stream channel- Shenggou Creek; (b) Step—pool causes hydraulic jumps; (c) No step-pool system in the Jiangjia Ravine, which is about 16 km from Shengou Creek; (d) No step-pool system in the Xiaobaini Ravine (8 km away from Shengou Creek)
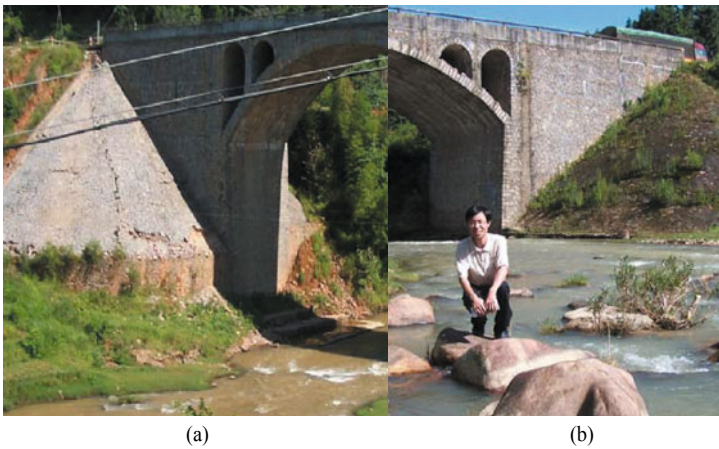
Fig. 3.37 (a) In a section of a tributary of the East River without ribbing structures the channel bed is eroded down by about 2 m and the bridge is endangered by the incision; (b) In a section of the same stream with ribbing structures the channel bed remains stable

(a)   (b)
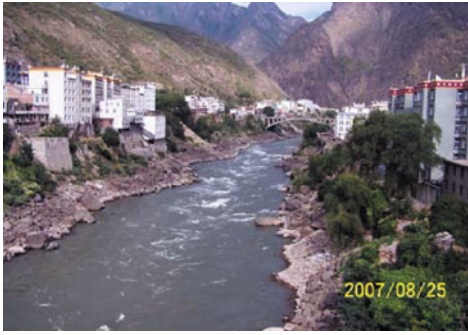
Fig. 3.40 (a) Bank stones structure on the Dadu River, which protects the Danba County Town; (b) Bank stones structure on the Jialing River

(a)   (b)

Fig. 3.44 (a) Incised upper Jiangjia Ravine; (b) Bank failures and landslides destroyed the pine forest at the upper end of the Jiangjia Ravine

(a)   (b)

Fig. 3.50 (a) Hutiaoxia barrier lake; (b) Part of the step-pool system on the Hutiaoxia landslide dam

Fig. 4.1   Different types of mass movements: (a) topple; (b) rockfall; (c) avalanche; (d) landslide

Fig. 4.4   A large scale landslide occurred on the Huoshigou Gully in Chongzhou County, which was triggered by the Wenchuan Earthquake on May 12, 2008: (a) A flood flow scoured the landslide deposit by 30–40 m and developed into a debris flow; (b) The debris flow carried sediment into the Anzi River and resulted in 4–9 meters of sedimentation on the bed

Fig. 4.12 (a) Wenjiagou landslide (after Sichuan Geological Engineering Corporation, 2009); (b) New Wenjiagou Gully is developing on the deposits of the landslide

Fig. 4.24 (a) Bed profiles of the Shenxi Ravine, showing three landslide dams and filled lakes; (b) Tilted and broken highway along the Shenxi Ravine during the Wenchuan Earthquake

Fig. 4.25 (a) Spillway channel on the Diexi landslide dam, and the upper and lower lakes on the Minjiang River; (b) Half-preserved Shibangou landslide dam on the Qingzhu River in Qingchuan County

Fig. 4.28 Yujunmen barrier lake on the Mianyuan River in Sichuan (left) and a step-pool system on the spillway channel on the Yujunmen landslide dam (right)

Fig. 4.31 (a) Deposits of a pseudo-one-phase debris flow in the Jiangjia Ravine on the Yunnan-Guizhou Plateau of China; (b) Pseudo-one-phase debris flow mixture looks like concrete; (c) Deposits of a two-phase debris flow in the Doufu Ravine; (d) Deposit of a two-phase debris flow in the Zoumaling Gully in the Mianyuan River basin in Sichuan in 2008. A building in the gully was not destroyed by the debris flow because the velocity was low

(a)   (b)

Fig. 4.52 (a) Viscous debris flow deposits in the Dabaini Ravine in the Xiaojiang watershed; (b) Viscous debris flow deposits in a debris flow gully in the Bailong River basin in Gansu Province

(a)

(b)

Fig. 4.56 Comparison of the bed surfaces before (a) and after (b) the bed paving process. The bed surface is much smoother after the bed paving process and the resistance is, therefore, reduced

(a)   (b)

Fig. 4.59 (a) Gangue deposit of a gold mine on a mountain slope in Lixian County, Gansu Province; (b) A slope debris flow on the gangue deposit which was initiated by heavy rainfall

(a)   (b)

Fig. 4.61 (a) Slope debris flow at Xiaogangjian along the Mianyuan River; (b) Slope debris flow at Xiaomuling along the Mianyuan River

(a)   (b)

Fig. 4.73 (a) Debris flow control dam cascade on the Houshan Ravine of Heishui County, Yunnan Province, China (after Kang, 1996); (b) Comb frame dam on a debris flow gully in Taiwan, China
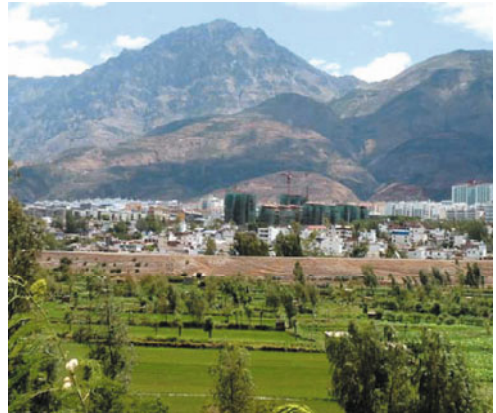
Fig. 4.79 (a) Agriculture and village on a landslide deposit by the Xiaojiang River; (b) The Dongchuan city town on a huge landslide deposit in Yunnan, China

Fig. 4.80 A new town developed on the Awangxiaohe debris flow fan in the Xiaojiang River basin
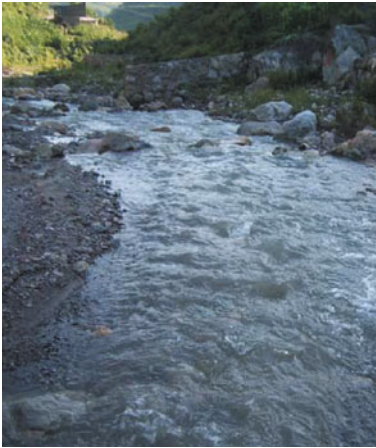
Fig. 5.6 (a) Supercritical flow in a mountain stream, in which there are some standing waves; (b) Subcritical flow in the Jinsha River, in which waves generated by a navigating boat are moving on the water surface

Fig. 5.11 Sand dunes (0.5–1 m high and 10–30 m long) on the bed of the Songzi River in the middle reaches of Yangtze River basin

Fig. 5.12 Sand dunes (10 m high and 50 m long) in the Kubuqi Desert in northwest China

Fig. 5.45 Regular meandering thalweg bed developed within a channelized stream in Yunnan, China

Fig. 5.47 Braided Yalutsangbu River in Tibet

(a)	(b)

Fig. 5.49 (a) The Kaiyi spur dike constructed on the lower Yellow River to stabilize the river channel; (b) The river moved far away from the dike only a few years after the spur dike was completed

<div align="center">(a)   (b)</div>

Fig. 6.12 (a) A machine cutting the land by the levee by 40 m and casting concrete; (b) The anti-seepage wall 20 cm thick and 40 m deep to control seepage and piping

<div align="center">(a)   (b)</div>

Fig. 6.15 (a) A sediment check dam in the Sha-anxi Province has trapped sediment and created fertile farmland; (b) A new sediment check dam in Shanxi Province has been completed and begun to trap sediment
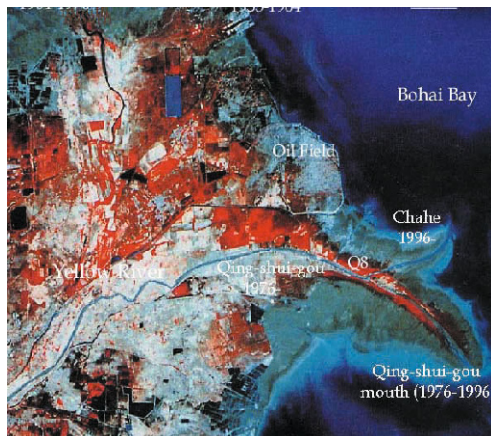
Fig. 6.38 Satellite image of the modern Yellow River delta and the Qing-shui-gou-Chahe channel in 2000

Fig. 7.5 An oil-like green surface layer due to blooming blue-green algae in Dianchi Lake in southwest China, which causes serious DO depletion
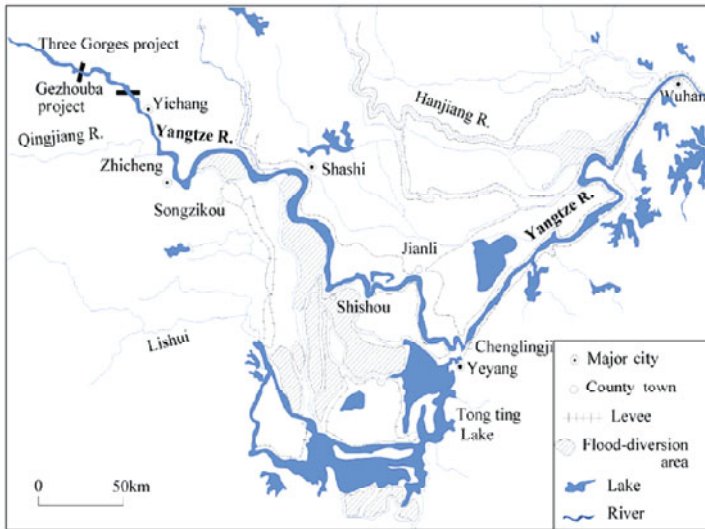
Fig. 7.33 Flood defense system of the middle and lower reaches of the Yangtze River

Fig. 7.34 A model of the Three Gorges project on the Yangtze River- from right to left: five step ship locks including the upper and lower approach channels, the ship lift and its channel, the left power house, the spillway, and the right power house

(a)   (b)

Fig. 7.48 (a) New village constructed on the slope higher than 185 m around the reservoir for resettlement of people from the submerged area; (b) Newly constructed Kaixian county town (the old Kaixian town has been inundated by the reservoir water)

Fig. 8.11 Venice, Chioggia, Murano, Burano Torcello and more than 50 islands in the Venice Lagoon are threatened by tidal flooding due to subsidence (Source: http://www.salve.it/)

Fig. 8.12 The San Marco square and Basilica di San Marco a Venezia—the most famous of the city's churches and one of the best known examples of Byzantine archtecture in Venice are floating on sea water

Fig. 8.40 A bloom of cyanobacteria at a water intake area of Wuxi, June, 2007 (Xinhua News Agency, http://www.xinhuanet.com)

Fig. 8.50 Pollution belt resulting from discharge from a paper mill on the Yangtze River

Fig. 8.76 Waterbirds (Black-faced Spoonbill and Egret) in Mai Po Marshes, Hong Kong

Fig. 8.79 Effects of human activities on Chongming Island Wetland's form

Fig. 8.83 Engineered wetland of Yuen Long bypass floodway

Fig. 9.14 Operation of the Devon Avenue Instream Aeration Station in Chicago, U.S.

Fig. 9.16 Sidestream Elevated Pool Aeration station number 5 discharging aerated water back to the Calumet-Sag Channel

Fig. 9.24 Environmental clamshell dredge removing PCB contaminated sediment from the Kinnickinnic River Great Lakes Legacy Act Cleanup in Milwaukee, U.S. and preparing to place it in a collection barge (photo provided by Dr. Xiaochun Zhang, Wisconsin Department of Natural Resources)

Fig. 9.25 Geotextile tubes being filled by dredged sediment and water (left) and stack of geotextile tubes dewatering (right) at the Little Lake Butte des Morts project of the Fox River, Wisconsin, U.S. (photos provided by Steven Laszewski)

Fig. 10.2 (a) Forest matrix in the suburbs of Beijing, China; (b) A township patch and a surrounding stream corridor in Wasserburg, Germany; (c) Stream corridor (the Leinbach River in Germany) and riparian forest matrix; and (d) Mosaic consisting of forest, lake, island, and hills (Banff, Canada).

Fig. 10.3 (a) Upper watershed of the Yangtze River at the Shennongjia Mountain; (b) A small stream in the source area of the Yellow River; (c) the Blue Nile at the confluence with the White Nile in Sudan; and (d) the Venice Lagoon at the Po River mouth in Italy.

Fig. 10.6 Stream eco-system and bio-community (after FISRWG, 1997)
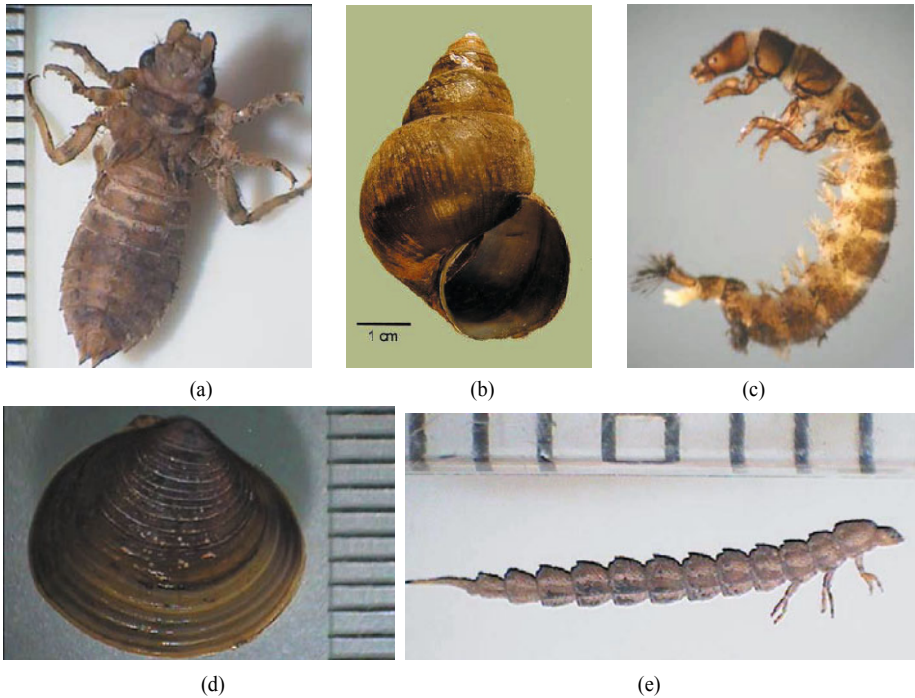
| (a) | (b) | (c) |

| (d) | (e) |

Fig. 10.8 Typical species of the five groups of benthic invertebrates with different functions in the food chain: (a) Gomphidae (Dragonfly-**predator**); (b) Viviparidae (**scraper**); (c) Hydropsychidae (**collector-filter**); (d) Corbiculidae (**filter-collector**); and (e) Haliplidae (**shredder**)

(a)　　　　　　　　　　　　　　　　　　(b)

Fig. 10.9 (a) Gravel and cobbles bed of the Juma River near Beijing is stable, which is colonized by a biocommunity with high diversity; and (b) The Dabai River in the upper Yangtze River basin is very unstable due to high sediment load and has a very low biodiversity

Fig. 10.13 A stream is a flow pathway for heat, water, and other materials, and organisms as shown for a small tributary of the Songhua River in northeastern China

Fig. 10.17 A serious a drought that started in 1997 and lasted for 6 years killed many poplar trees in the Kuye River basin in Inner Mongolia Autonomous Region, China. The trunks and branches die but the root system is still alive. The roots sprouted and new branches grew after the climate became wetter after 2004

Fig. 10.18   A sand dune in Kubuqi desert in northwestern China is moving toward a seasonal stream

(a)

(b)

Fig. 10.20   (a) High sediment concentration in a stream in Taiwan, southeastern China, which results in low transparency, low dissolved oxygen, and sediment coating the substrate; (b) Turbid seawater with high concentration of sediment impacts on fish and invertebrate communities

<p style="text-align:center">(a)   (b)</p>

Fig. 10.22 (a) Birds are searching for dead fish at the outlets of a hydro-power plant at which fish are killed when they swim through the turbine; (b) The Baozhusi dam on the Bailong River has cut off the flow and greatly affects the stream ecology in the lower reaches

Fig. 10.25 Isolation of riparian lakes along the Yangtze River results in fragmentation of habitat (Satellite image from the web http://earth.google.com)

<p style="text-align:center">(a)   (b)</p>
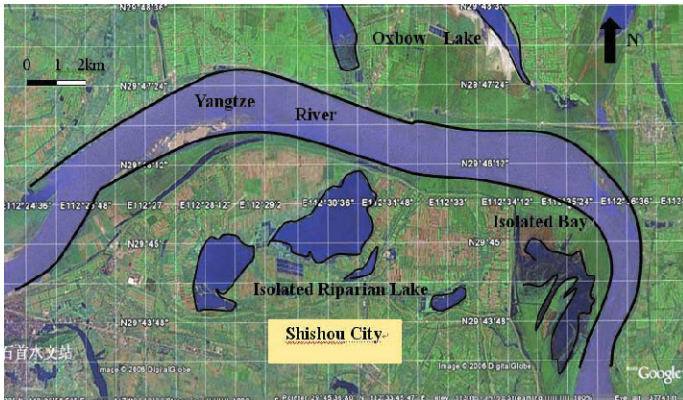
Fig. 10.34 (a) Grazing pressure has been increased due to development of husbandry in the Tibet-Qinghai Plateau; (b) Livestock swimming in a stream can result in extensive physical disturbance and bacteriological contamination

Fig. 10.35 Recreational boating, cruise tours, propeller wash, and accidental spills can degrade stream habitat

Fig. 10.37 Colonization of golden mussel on concrete walls in a water transfer tunnel and attachment of golden mussel on a concrete fragment with high density

Fig. 10.38 Natural habitat of giant pandas is being threatened by the introduction of larch trees and rapid development of larch forests

Fig. 10.39 (a) *Spartina alterniflor* in the Yangtze River estuary; (b) *Eupatorium adenophorum* in southwestern China; (c) *Eichoimia crassip* in polluted waters; (d) Ambrosia artemisia L. in northeastern China.
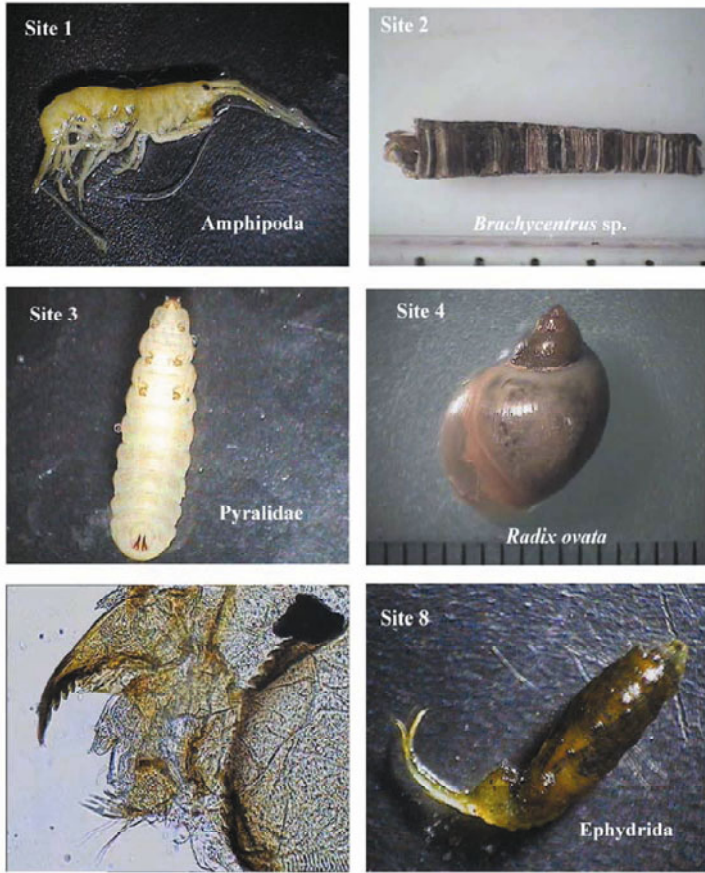
Fig. 10.43 Representative species of macro-invertebrate from the sites 1,2,3,4, 5 and 8

Fig. 10.51 Riparian trees and wood logs in the water provide shade and shelter for aquatic wildlife and attract many fish in the Jiuzhaigou Creek in upper Jialing River basin

Fig. 11.2 Polluted water of the confluence of the Sanggan River and the Yanghe River at the upper end of the Guanting Reservoir and two tolerant species of macro-invertebrates of *Oligochaeta* and *Chironomidae*
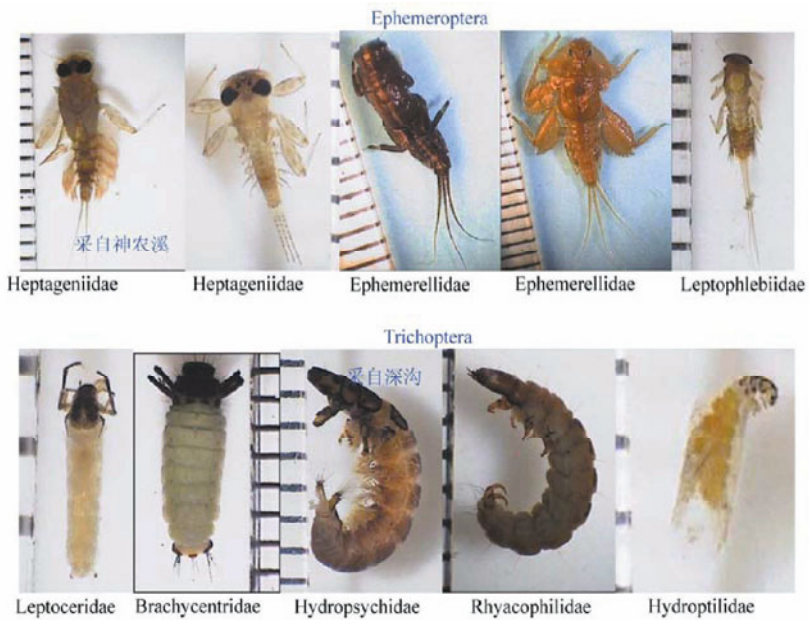
Fig. 11.5 Representative species of *Ephemeroptera* and *Trichoptera* taken from stable streams
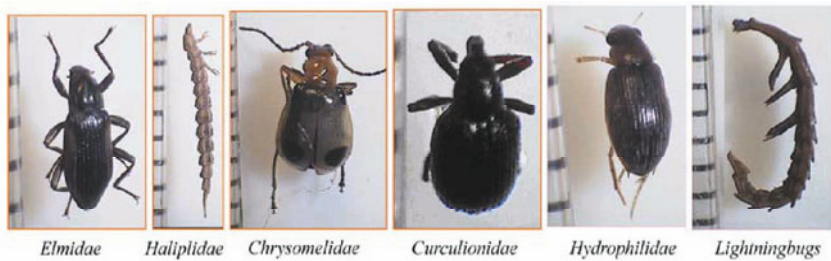
Fig. 11.6 Representative species of *Placoptera* taken from incised rivers

Fig. 11.9 Large boulders create high resistance and protect the bed from erosion, which make the stream achieve super-equilibrium

(a)

(b)

(c)

Fig. 11.11 (a) Broken concrete bank of the Lijiang River at Guilin, China; (b) Roughened bank of the Blue Nile River in Sudan for protection against erosion; (c) Channelization of the Zheduo River at Kangding resulted in high flow velocity and elimination of species

<p align="center">(a)   (b)</p>

Fig. 11.30 Comparison of Chaqing Gully (a) and Hunshui Gully (b) (Chaqing Gully: $p = 9.20$ kg/ms, $S_p = 0.155$, $g_b = 0.0001$ kg/ms; Hunshui: $p = 10.16$ kg/ms, $S_p = 0.04$, $g_b = 18.9$ kg/ms)

<p align="center">(a)   (b)</p>

Fig. 11.34 (a) Experiment plot on the left side of the Jiangjia Ravine; (b) Water with loads flowed in the experimental channel and scoured the channel banks.

<p align="center">(a)   (b)</p>

Fig. 11.40 (a) Huge step-pool system in the Grand Canyon (near knickpoint 4); (b) Brahmaputra River in India, which is downstream of the Yalutsangbu River below the Grand Canyon.

Fig. 11.53 (a) Experimental reach on the Diaoga River (May 2006); (b) Constructed step-pool system on the river bed (March 2007)
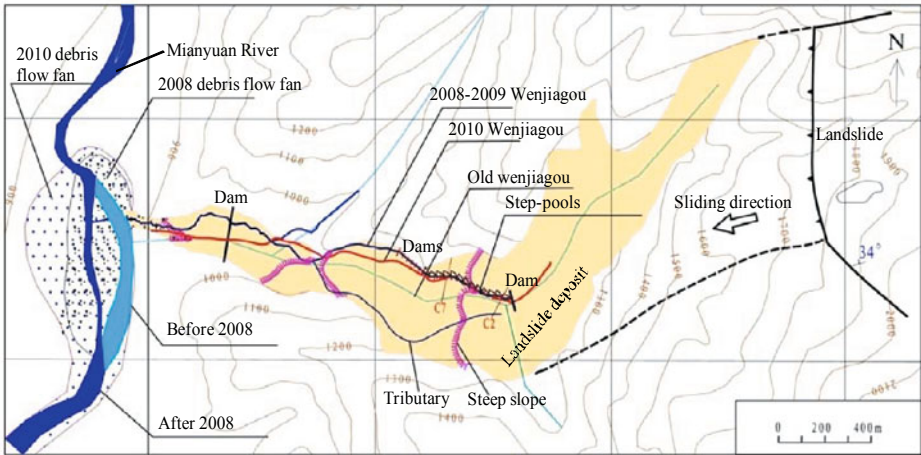
Fig. 11.59 Wenjiagou landslide deposit and old and new Wenjiagou channels
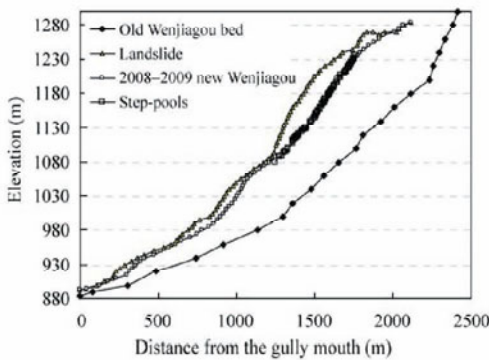
Fig. 11.61 (a) Bed profiles of the old and new Wenjiagou channels and the landslide deposit in 2008; (b) New Wengjiagou gully developed during debris flows on the landslide deposit

(a)	(b)

Fig. 11.63 An artificial step-pool system was constructed in June 2009 for stabilization of the new drainage system on the Wenjiagou Landslide: (a) Large stones with diameters larger than 1 m were removed from the banks of the new gully for construction of steps; (b) Large stones were placed together to form the artificial steps.

(a)	(b)

Fig. 11.70 (a) Suspended remaining part of a failed dam after bed incision; (b) The upper main dam was completely removed and the gully extended due to headwater erosion.

(a)	(b)

Fig. 11.74 (a) 20 years after planting of *Pinus yunnanensis* the forest had three layers with 12 shrub species and 22 herb species; (b) In the canopy habitat of 20 years after planting *Leucaena leucocephala* forest there were only 1 shrub species and 4 herb species